SYSTEM CALIBRATION, GEOMETRIC ACCURACY TESTING AND VALIDATION OF DEM AND ORTHOIMAGE DATA EXTRACTED FROM SPOT STEREO-PAIRS USING COMMERCIALLY AVAILABLE IMAGE PROCESSING SYSTEMS

BY

NAIEF MAHMOUD Al-ROUSAN

Volume I

A Thesis Submitted for

the Degree of Doctor of Philosophy (Ph.D.)

of the Faculty of Science at the University of Glasgow

in Photogrammetry and Remote Sensing

Topographic Science, July 1998

ProQuest LLC.
789 East Eisenhower Parkway
P.O. Box 1346
Ann Arbor, MI 48106 – 1346

ACKNOWLEDGEMENTS

The author would like to express his sincere gratitude to his supervisor, **Prof. G. Petrie,** for suggesting this research topic and for his continuous advice, help and supervision throughout the period of this study. Indeed without this continuous help, this project would have never come to its present form. I will never forget his efforts with the system suppliers to resolve the problems resulting from the flaws that were discovered in the systems as a result of my experimental work.

The author is also extremely grateful to his second supervisor, **Mr D. A. Tait,** for his encouragement and his valuable advice.

Prof. J. Briggs, Head of the Department, has to be thanked for all his various kindnesses and support, especially when he authorized the purchase of the stereo-pair of Level 1A SPOT images for comparison purposes, which helped to overcome the initial difficulties experienced with the testing of the systems. He also played an important part in ensuring that the author was able to undertake his research work in Jordan within the Badia Project.

The help received from the other Staff members of the Topographic Science section of the Department is gratefully acknowledged, in particular that obtained from **Dr. J. Drummond**; **Mr. J. Shearer** and **Mr. M. Shand.**

Thanks are also due to the following individuals and organizations outside the Department:

Special thanks to **Dr. P. Cheng** of PCI in Canada for his help throughout the period of testing the EASI/PACE system and for his quick response in solving the rather fundamental problems experienced with the system. Also **Dr. Th. Toutin** of CCRS in Canada for his assistance in this same matter.

Prof. R. Welch and **Mr. T. R. Jordan** from University of Georgia in USA for their continuous help during the testing of the DMS system and their contribution in solving the initial shortcomings of the DMS system.

Dr. D. Miller from the Macaulay Institute for Land Use Research (MLURI) in Aberdeen for his help in providing all the facilities needed to test the ERDAS OrthoMAX system and the necessary expertize to run the system.

Mr. J. McCreadie of Survey & Development Services and **Mr. R. Chiles** of NPA Ltd for loaning their VirtuZo and TNT-mips systems - even if the results were unsuccessful.

Dr. P. Bjerke from Norwegian Defence Research Establishment for his cooperation in using his FFI system to test the Badia data.

Mr. M. Shahbaz of the HCST in Jordan and **Dr. R. Dutton** of the University of Durham (the two Co-Directors of the overall scientific programme of the Badia Project) for their help in providing the block of five stereo-pairs of SPOT imagery.

Brigadier Saleem Khalifah and the **Staff** of the Royal Jordanian Geographic Centre (RJGC) for their excellent cooperation and their help in establishing the Badia Test Field and for providing the digitised map and GPS profile data used as reference data sets for validation purposes.

Mu'tah University in Jordan, for the financial support received during the period over which this research has been conducted.

Research colleagues in the University of Glasgow for their help and support, especially **Dr. Gurcan Buyuksalih** and **Dr. Valadan Zoej**.

Finally, the author is extremely grateful to his spouse and his son and daughter for their patience during the long absences from home that were necessary to complete his research work and dissertation.

ABSTRACT

This thesis covers the system calibration and the geometric accuracy testing and validation of the data produced by the photogrammetric modules of a number of digital image processing systems that have been developed recently to produce DEMs and orthoimages from SPOT 1B stereo-pairs. This work has been carried out over a high accuracy test field that has been established in the Badia, a desert area in North East Jordan. The reference data comprises 130 points whose positions and elevations have been established using high precision GPS sets, supplemented by digitized contours from existing maps and elevation profiles measured using kinematic GPS techniques.

After a initial review of previous research work in this area, the mathematical modelling and the analytical photogrammetric solutions used by the tested systems are discussed at some length, including the algorithm employed in the automatic image matching procedures used to extract a dense DEM from the SPOT digital images. The results of extensive tests of the geometric accuracy of planimetry and height obtained by these systems and the many problems encountered with these systems are reported in detail, as are the solutions that have been devised in collaboration with the system suppliers to overcome these problems - to the benefit of the whole mapping community. The results from tests of the planimetric accuracy obtained from the modified 3-D systems show a sub-pixel accuracy and correspond to the accuracy specifications of 1:50,000 scale topographic mapping. In the case of the height accuracy, the results obtained at both the control points and check points mostly lie in the range between ± 5 to 8m and show that it is now possible with digital systems to reach accuracies comparable with those previously achieved with analytical plotters.

On completion of the accuracy tests using the ground control points, DEMs of the test area were generated by each of the systems from the SPOT Level 1A and 1B stereo-pairs using automatic matching techniques. These DEMs have then been merged and validated. Four different methods of validation have been applied to test the accuracy of the elevation data in the DEMs using the reference contour and profile data sets. The results of the extensive series of height accuracy tests correspond to the requirements of contouring at 20 to 30m interval which may meet the specifications of 1:50,000 scale

topographic maps in certain areas but more often those at smaller scales. The final orthoimages produced by these systems are of a high quality in radiometric terms, while a check of their geometric accuracy reveals sub-pixel accuracy with planimetric accuracy varying slightly from one system to another.

The geometric accuracy tests and the validation of the DEMs carried out in the present research have been analyzed and compared with the geometric accuracy tests and validations of the DEMs reported by several previous researchers over different test areas. These comparison show that the results obtained in the tests carried out over the Badia test field are among the best that have been achieved using digital photogrammetric systems and indeed are superior to most of the accuracy tests reported by other researchers. After the systems had been modified as a result of the author's work, the results of this highly automated all-digital photogrammetric procedure are of especial relevance to those concerned with the topographic mapping of extensive areas of arid and semi-arid terrain. The test field with its network of high accuracy ground control points and its reference data sets has shown its worth and is available and suitable for the calibration and testing of the images from the forthcoming high-resolution Earth Observation satellites.

CONTENTS

1. Introduction

1.1 Introduction. 1
1.2 Mapping in the Red Sea Region. 3
1.2.1 Mapping in North-East Africa. 3
1.2.2 Mapping in South-West Asia. 6
1.2.2.1 Mapping in Jordan. 7
1.3 Justification for the Research Study. 8
1.3.1 Need for Test Sites and Data Sets to Calibrate Satellite Imaging Systems and Validate DEMs Being Generated on a Global Scale. 9
1.3.2 The Photogrammetric Dimension of the Research Project 10
1.4 Research Objectives. 11
1.5 Provision of Test Data. 12
1.6 Outline of the Thesis. 13

2. Published Results on the Geometric Accuracy of Data Acquired from SPOT Images. 16

2.1 Introduction. 16
2.2 Geometric Accuracy Tests Carried out for Single Stereo-pairs. . . . 16
2.2.1 Accuracy Tests over the South France Test Area by IGN. 17
2.2.1.1 South France Test Reported by Rodriguez. 18
2.2.1.2 Accuracy Tests over the Aix-en-Provence Area by UCL. 19
2.2.1.3 Accuracy Tests over the Marseilles Area by the University of Hannover. 21
2.2.2 Accuracy of Stereo-models of South West Cyprus. 23
2.2.2.1 South West Cyprus Tests Reported by Gugan and Dowman. 23
2.2.2.2 South West Cyprus Test Reported by Ley. 24
2.2.3 Accuracy Tests Carried out on SPOT Stereo-models in Canada. 26
2.2.3.1 Ottawa, Sherbroke, Grenoble Tests Reported by Kratky. 26
2.2.3.2 Ottawa Test Reported by Toutin and Carbonneau 27
2.2.3.3 Irvine Test Reported by Cheng and Toutin. 28
2.2.3.4 Test in British Columbia Reported by Toutin and Beaudoin. 30
2.2.4 Stereo-model Accuracy Achieved During Mapping from SPOT Stereo-pairs in North-East Yemen. 31
2.2.5 Accuracy Tests of Stereo-model of South-West Sinai. . . . 32
2.2.5.1 Initial South-West Sinai Tests Reported by Diefallah. 32
2.2.5.2 Later Test Reported by Diefallah. 33
2.2.6 Accuracy Tests Carried out in China on Various Stereo-images. 35

2.2.6.1 Test over the Tangshan Area (China) Reported by Zhong. 36
2.2.7 Sor Rondane Mountains Test. 37
2.2.8 Geometric Accuracy Test Reported By Yeu. 36
2.3 Strips of SPOT Stereo-models Measured by Space Triangulation. . 39
2.3.1 South France Test Reported by Veillet. 39
2.3.2 OEEPE Test Reported by Dowman. 40
2.3.3 Djibouti Test Reported by Veillet. 42
2.4 Summary and Analysis of the Published Results. 42
2.5 Conclusion 44

3. Published Results on Validation of DEMs Extracted from SPOT Stereo-Pairs. 46

3.1 Introduction. 46
3.2 Tests Carried out in the UK. 46
3.2.1 South-West Cyprus Test Reported by Ley. 46
3.2.2 Validation of DEMs Reported by Theodossiou and Dowman. 49
3.3 Validation of DEM Reported by Diefallah. 50
3.4 Tests Carried out in Australia. 51
3.4.1 Validation of DEM of Australia Stereo-pair Reported by Priebbenow. 51
3.4.2 Sydney Test Reported by Anglerand et al. 53
3.4.3 Validation of DEMs of Sydney and Other Areas Reported by Trinder et al. 53
3.5 Tests Carried out in Germany. 56
3.5.1 Heidelburg and Priorat Tests Reported by Heipke et al. . . 56
3.6 Tests Carried out in North America. 58
3.6.1 Validation of DEM Reported by Brockelbank and Tam. . . 58
3.6.2 Validation of DEM Reported by Sasowsky et al. 59
3.6.3 Validation of DEM Reported by Bolstad and Stowe. . . . 61
3.6.4 Validation of DEM Reported by Giles and Franklin. 61
3.7 Tests Carried out in Japan. 62
3.7.1 Validation of DEM Reported by Fukushima. 62
3.7.2 Validation of DEM Reported by Akiyama. 65
3.8 Summary and Analysis of the Published Results. 66
3.9 Conclusion. 68

4. Status of Topographic Mapping in Jordan 70

4.1 Introduction. 70
4.2 World Mapping. 70
4.2.1 Mapping in South West Asia. 71
4.2.2 Mapping in Jordan. 72
4.3 Background to Mapping in Jordan. 73
4.4 The Establishment of the Royal Jordanian Geographic Centre (RJGC). 76
4.4.1 Cooperation Agreement with IGN. 77

4.4.2 RJGC Training Centre. 77
4.5 Geodetic Network. 79
4.6 Current Capabilities of RJGC. 80
4.6.1 Equipment and Facilities. 80
4.6.2 Photogrammetric Operations. 82
4.6.3 Status of Topographic Mapping in Jordan. 82
4.6.4 Tourist Maps. 87
4.6.4.1 Amman Maps. 87
4.6.4.2 Other Cities and Sites. 87
4.6.5 Map Accuracy. 88
4.6.5.1 Accuracy of 1:50,000 Scale Topographic Maps. 88
4.5.5.2 Accuracy of 1:250,000 Scale Maps. 90
4.7 Conclusion. 90

5. Overview and Characteristics of the Systems Tested 93
93
5.1 Introduction. . . . . .
5.2 Digital Photogrammetric Techniques Applied to Remotely Sensed Imagery. 94
5.3 Classification of DPWs 95
5.3.1 DPWs Using SPOT Images. 97
5.4 Main Characteristics of the Systems Tested. 99
5.4.1 PCI EASI/PACE Package Characteristics. 100
5.4.1.1 Photogrammetric Solution. 101
5.4.1.2 Rectification and Resampling to Epipolar Geometry. 102
5.4.1.3 Image Matching. 102
5.4.1.4 DEM Editing Tools. 103
5.4.1.5 Ortho-Image Generation. 104
5.4.1.6 Mosaicing DEMs and Orthoimages. 104
5.4.1.7 Contour Generation and Mosaicing. 105
5.4.1.8 Perspective Generation of Views. 105
5.4.2 ERDAS OrthoMAX Package Characteristics. 105
5.4.2.1 Photogrammetric Solution. 107
5.4.2.2 Image Matching (stereocorrelation). 107
5.4.2.3 DEM Editing. 108
5.4.2.4 Ortho-Image Generation. 108
5.4.2.5 Mosaicing of DEMs and Orthoimages. 109
5.4.2.6 Contour Generation. 109
5.4.3 Desktop Mapping System (DMS) Characteristics. 109
5.4.3.1 Photogrammetric Solution. 110
5.4.3.2 Image Matching (Stereocorrelation). 110
5.4.3.3 DEM Editing. 111
5.4.3.4 Ortho-image Generation. 111
5.4.3.5 Mosaicing DEMs and Ortho-images. 112
5.4.3.6 Contour Generation. 112
5.4.4 FFI System. 112
5.4.4.1 Image Data and Ground Coordinate Requirements. 113

5.4.4.2 Photogrammetric Solution. 113
5.4.4.3 Rectification and Resampling to Epipolar Geometry. 114
5.4.4.4 Image Matching (Stereocorrelation). 114
5.4.4.5 Contour Generation. 114
5.4.4.6 Ortho-image Generation. 115
5.5 Summary. 115
5.6 Conclusion. 117

6. Mathematical Models and Photogrammetric Solutions Applied in the Tested Systems. 119

6.1 Introduction. 119
6.2 SPOT Image Formats. 121
6.2.1 SPOT Level 1A Imagery. 121
6.2.2 SPOT Level 1B Imagery. 122
6.2.3 SPOT Level 2A and 2B Imagery. 123
6.3 Geometric and Mathematical Modelling. 124
6.3.1 Orbital Parameter Data. 125
6.3.2 Coordinate Systems. 128
6.3.3 Collinearity Equations. 130
6.4 EASI/PACE Mathematical Model. 131
6.4.1 Introduction. 131
6.4.2 Reference Systems. 132
6.4.3 Collinearity Equations and the Parameters to be Determined. 134
6.4.4 Epipolar Geometry. 137
6.5 ERDAS OrthoMAX Mathematical Model. 137
6.5.1 Introduction. 137
6.5.2 Reference Systems. 138
6.5.3 Collinearity Equations and Parameters to be Determined. 140
6.5.4 Inverse Transformation of SPOT Level 1B Image to Level 1A Form. 141
6.5.5 Computational Procedure. 142
6.5.6 Bundle Adjustment. 143
6.6 DMS Mathematical Model. 145
6.6.1 Introduction. 145
6.6.2 Polynomial Approach. 145
6.7 FFI System Mathematical Model. 149
6.7.1 Introduction. 149
6.7.2 Reference System. 150
6.7.3 Procedure for Determination of the Orientation of the Individual SPOT Image. 151
6.7.4 First Algorithm. 153
6.7.4.1 Determination of the Position and Elevation Coordinates of Points on the Ground. 153
6.7.5 Second Algorithm. 155
6.7.5.1 Determination of the Position and Elevation Coordinates of Points on the Ground. 157

6.8 Conclusion 157

7. Overall Strategy, General Considerations and Experimental Procedures Used in the Tests 160

7.1 Introduction 160
7.2 Overall Strategy and Experimental Requirements 160
7.2.1 Test Material and Data 162
7.2.1.1 SPOT Stereo-images 162
7.2.1.2 Digitised Maps 163
7.2.2 Establishment of the Badia Test Field 163
7.2.3 Systems to be Tested 165
7.3 Experimental Procedures 166
7.3.1 Geometric Accuracy Tests 166
7.3.2 Validation of DEMs 168
7.3.3 Geometric Accuracy Tests of Orthoimages 170
7.4 Conclusion 170

8. Field Survey Work Carried Out for the Badia Project Area 172

8.1 Introduction 172
8.2 Requirement for Control Points for the SPOT Stereo-Pairs 173
8.2.1 The Nature of the Field Work 173
8.2.2 The Study Area 173
8.2.2.1 Geology of the Project Area 176
8.2.2.2 Geomorphology of the Project Area 178
8.2.3 Field Work Planning 183
8.2.3.1 Reconnaissance and Selection of the Ground Control Points 184
8.2.3.2 Selection of the Ground Control Points 184
8.2.3.3 Final Location of the Ground Control Points 185
8.2.3.4 Problems 186
8.2.4 GPS Instrumentation and Software 188
8.2.4.1 GPS Instruments 189
8.2.5 GPS Observation 191
8.2.5.1 System Set Up Used for the Rapid Static Technique 192
8.2.5.2 Observation (Operating the Receivers) 193
8.2.5.3 GPS Processing and Adjustment 201
8.2.6 Observation Accuracy Assessment 202
8.3 Profiles Along the Major Old Roads 202
8.4 Conclusion 203

9. Geometric Accuracy Tests of the EASI/PACE System 205

9.1 Introduction 205
9.2 Ground Control Measurements on the Images 205
9.3 Space Resection 208
9.3.1 Results of Initial Processing Using SMODEL 209

9.3.2 Investigation into the Source of Errors. 209
9.3.3 Solution to Level 1B Processing Problem. 211
9.3.3.1 University of Glasgow Solution. 211
9.3.3.2 PCI Solution. 213
9.4 Space Resection Accuracy Tests. 217
9.5 Absolute Orientation Accuracy Tests. 219
9.5.1 Accuracy Tests of the Level 1B and 1A Stereo-pairs of the Badia Test Area Using Absolute Orientation and All the Available Ground Control Points. 220
9.5.2 Accuracy Tests of the Level 1B Stereo-pairs of the Reference Scene 122/285 Using Combinations of Control Points and Check Points. 221
9.5.3 Accuracy Tests of the Other Level 1B Stereo-Models for Scenes 123/ 285, 123/286 and 124/285. 222
9.5.4 Accuracy Tests of the Level 1A Stereo-pair of the Reference Scene 122/285. 223
9.5.5 Vector Plots of Errors Values at the Control and Check Points for Model 122/285. 224
9.6 Conclusion. 227

10. Validation of DEMs, Contours and Orthoimages Produced by the EASI/PACE System 229

10.1 Introduction. 229
10.2 Rectification and Resampling to an Epipolar Geometry. 229
10.3 Digital Elevation Model (DEM) Extraction. 230
10.3.1 DEM Editing. 231
10.3.2 Geocoding the DEM. 233
10.4 Generation of Orthoimages. 233
10.4.1 Orthoimage Printed Output. 235
10.5 Contour Generation. 238
10.5.1 Contour Output. 238
10.6 Generation of a Wire Mesh Perspective View. 242
10.7 Mosaicing of DEMs, Contours and Orthoimages. 243
10.7.1 Mosaicing of DEMs. 243
10.7.2 Merging the Contour Line Plots. 246
10.7.3 Mosaicing of the Orthoimages. 247
10.8 Experience with EASI/PACE. 250
10.9 Accuracy Test of the DEMs of the Badia Test Area. 251
10.9.1 Comparison of Superimposed Contours 251
10.9.2 Comparison of Height Given by the Contours from the Reference Map with the Corresponding Value given by the DEM. 259
10.9.2.1 Comparison of DEM Heights with 50m Contours 259
10.9.2.2 Comparison of DEM Heights with 10m Contours 260
10.9.3 DEMs Accuracy at the GCPs. 261
10.9.4 Accuracy Tests Using the GPS Profiles. 265
10.10 Planimetric Accuracy Test of the Orthoimages Produced from the Level 1A and 1B Stereo-pairs for Scene 122/285. 266

10.11 Conclusion. 267

11. Geometric Accuracy Tests and Validations of DEMs, Contours and Orthoimages Using DMS Software. 270

11.1 Introduction. 270
11.2 Initial Accuracy Test of the Level 1B Stereo-Pair for Reference Scene 122/285. 270
11.2.1 DMS Problems. 273
11.2.2 DMS Modified Version. 275
11.3 Tests of the New Image Processing Procedures for Registration and DEM Extraction. 277
11.3.1 Measurement of the GCPs. 277
11.3.2 Merging the CP Files. 277
11.3.3 Registration. 277
11.3.3.1 Planimetric Accuracy and Vector Plots of Stereo-Pair 122/285. 279
11.3.3.2 Accuracy Test of Planimetry and Vector Plot of the Other Stereo-Pairs. 281
11.3.4 Stereocorrelation. 283
11.3.5 Orthoimage Generation. 285
11.3.6 Mosaicing of DEMs and Orthoimages. 286
11.4 Accuracy Tests of the DEMs of the Badia Test Area. 288
11.4.1 DEMs Accuracy at the GCPs. 289
11.4.1.1 Accuracy of the Elevation Data at the GCPs Extracted from the Level 1B Stereo-pair for Scene 122/285. 289
11.4.1.2 Accuracy of the Elevation Data at the GCPs Extracted from Other Stereo-Pairs of the Badia Area. 291
11.4.2 Accuracy of Fit of the Contours Derived from DEMs Superimposed over the Digitised Contours Extracted from Existing Topographic Maps. 296
11.4.3 Comparison of Heights Given by the Contours from the Reference Map with the Corresponding Values Given by the DEM. 302
11.4.3.1 Comparison of DEM Heights with 50m Contours 302
11.4.3.2 Comparison of DEM Heights with 10m Contours 303
11.4.4 Accuracy Test of the DEMs Using the Profiles Measured by GPS. 303
11.5 Accuracy Test of the Orthoimage of the Reference Stereo-model. . 304
11.6 Conclusion. 305

12. Geometric Accuracy Tests and Validation of DEMs, Contours and Orthoimages using OrthoMAX Software 307

12.1 Introduction. 307

12.2 Procedures Used in ERDAS OrthoMAX for the Photogrammetric Processing of SPOT Stereo-Pairs 307
12.2.1 Pre-processing Procedures 308
12.2.2 Ground Control Point Measurements on the Images 308
12.2.3 Bundle Adjustment Procedures 309
11.2.3.1 Interpretation of the Result 310
12.2.4 DEM Extraction (Stereocorrelation) 314
12.2.4.1 DEM Stereo Editing in the Professional Version of OrthoMAX 315
12.2.4.2 Accuracy Test of the Reference Level 1B Stereo-model by Superimposed Contours 316
12.3 Accuracy Tests of the Other Four Stereo-Pairs 318
12.3.1 Problems in Bundle Adjustment for Stereo-Pairs 123/285 and 123/286 320
12.4 Accuracy Tests of the Level 1A and 1B Stereo-models of the Reference Scene 122/285 321
12.5 New Format of SPOT Stereo-Pairs 123/285 and 123/286 323
12.6 Contour Generation 323
12.7 Accuracy Test of Heights Contained in the DEM of the Badia Test Area 324
12.7.1 Accuracy Tests of Height at Selected Check Points in the DEM 331
12.7.2 Comparison of Superimposed Contours 331
12.7.3 Comparison of Heights Given by the Contours from the Reference Map with the Values Given by the DEM 337
12.7.4 Accuracy Test of the Level 1B DEM of the Reference Stereo-model 122/285 Using GPS Profiles 338
12.8 Overall Summary and Comparison of the Various Tests of Elevation Accuracy 339
12.9 Orthoimage Generation 340
12.9.1 Orthorectification Procedures Within OrthoMAX 341
12.9.2 Orthoimage Mosaic 342
12.9.3 Planimetric Accuracy Test of Orthoimages Produced by OrthoMAX 346
12.10 Conclusion 347

13. Geometric Accuracy Tests and Validation of DEMs, Contours and Orthoimages Generated By FFI Software 350

13.1 Introduction 350
13.2 Test Material and Data 350
13.3 Orientation and Geometric Accuracy Tests of the Level 1A SPOT Stereo-pair of Scene 122/285 of the Badia Area 351
13.3.1 Accuracy Tests of the Space Resection of the Individual SPOT Images 351
13.3.2 Accuracy Tests of Absolute Orientation 352
13.3.3 Accuracy Tests of Absolute Orientation with the New Algorithm 355
13.4 DEM Extraction from the Level 1A Stereo-Model of the

Reference Scene 122/285. 359
13.5 Reading the DEM File. 359
13.6 Contour Generation. 359
13.7 Orthoimage Generation. 360
13.8 Accuracy Tests of Height in the DEM Produced by the FFI System 360
13.8.1 Accuracy Test of Height Values Given by the FFI Produced DEM at the Ground Control Points. 360
13.8.2 Accuracy Tests of Height by Superimposition of Contours. 365
13.8.3 Accuracy Tests of Comparison of the DEM Elevation Values with the Elevation Values Given by the RJGC Topographic Map Contours. 367
13.8.4 Accuracy Tests of Heights Produced Using the FFI System Against GPS. 367
13.9 Accuracy Test of Orthoimage. 367
13.10 Tests of the Orientation and Geometric Accuracy of the SPOT Level 1A Stereo-Pair of the Oslo Test Area Using the FFI System. 368
13.10.1 Accuracy Test of Space Resection of the Individual SPOT Images Using the FFI System. 368
13.10.2 Accuracy Tests of Absolute Orientation Using the FFI System. 369
13.10.3 Accuracy Tests of Absolute Orientation with the New Algorithm of the FFI system. 374
13.11 Geometric Accuracy Tests of the Oslo Stereo-model Using the EASI/PACE System. 374
13.11.1 Space Resection of the Individual SPOT Images of the Oslo Stereo-Model Using EASI/PACE. 376
13.11.2 Accuracy Tests of Planimetry and Height of Absolute Orientation of the Oslo Stereo-Model Using EASI/PACE 376
13.11.3 Accuracy Tests of Height in the DEMs Produced by Stereocorrelation Using EASI/PACE. 379
13.12 Contours Generated from the Oslo DEM by EASI/PACE. 379
13.13 Orthoimage Generation Using EASI/PACE. 380
13.14 Conclusion. 380

14. Comparison of Geometric Accuracy Tests and Subsequent Analysis 382

14.1 Introduction. 382
14.2 Limitations in Comparing the Results from Different Systems. . . . 382
14.3 Accuracy of the Level 1A and 1B Stereo-pairs of the Reference Scene 122/285. 383
14.3.1 An Overall Comparison of the Results for Level 1A and 1B Stereo-Pairs Obtained by the EASI/PACE and OrthoMAX Systems. 383
14.4 Accuracy Results of Other Level 1B Stereo-Pairs of the Badia Area.. 385
14.5 General Remarks about the Results of the Geometric Accuracy Tests in the Context of Topographic Mapping. 387

14.6 Comparative Accuracy Tests of SPOT Level 1B Stereo-Pairs..... 389
14.6.1 Comparison of Planimetric Accuracy Results..... 390
14.6.2 Comparison of Height Accuracy Results..... 391
14.7 Comparative Accuracy Tests of SPOT Level 1A Stereo-Pairs..... 392
14.7.1 Comparison of Planimetric Accuracy Results..... 393
14.7.2 Comparison of Height Accuracy Results..... 395
14.8 Conclusion..... 396

15. Comparative Accuracy Tests and Validation of the DEM Data and Orthoimages Produced by Different Systems 398

15.1 Introduction..... 398
15.2 Comparative Height Accuracy Tests of the DEM Data Produced by the Different Systems..... 398
15.2.1 Comparative Height Accuracy of the DEM Data at the Control and Check Points of the Level 1A and 1B Stereo-Pairs for the Reference Scene 122/285..... 399
15.2.1.1 Comparison of the Level 1A Data..... 399
15.2.1.2 Comparison of the Level 1B Data..... 400
15.2.2 Comparative Height Accuracy Tests of the DEM Data of the Other Level 1B Stereo-Pairs Covering the Badia Area Produced by Different Systems..... 401
15.3 Comparison of Accuracy of the Heights Given by the Contours Digitised from 1:250,000 Scale Topographic Map with the Height Values Given by the DEMs Produced by Different Systems..... 402
15.3.1 Accuracy of Height Data in the Level 1A and 1B DEMs of the Stereo-model for the Reference Scene 122/285 as Compared with the Heights Given by the Contours of the 1:250,000 Scale Map..... 402
15.3.2 Accuracy of Height Data of the DEMs Produced from the Other Level 1B Stereo-Pairs as Compared with the 50m Contours of the 1:250,000 Scale Map..... 404
15.3.3 Comparison of the Heights Given by the Contours at 10m Interval Digitised from the 1:50,000 Scale Topographic Map with the Corresponding Values Given by the Level 1A and 1B DEMs of the Stereo-Pair for Reference Scene 122/285..... 405
15.4 Accuracy Tests of Height in the DEMs Produced by the Different Systems Through Comparison with the GPS Profiles..... 405
15.5 General Remarks about the Results of Accuracy Tests of Height Values of the DEM Data..... 406
15.6 Overall Comparison of the Height Accuracy of DEMs Investigated and Reported by Different Researchers Using Different Systems Compared to the Height Accuracy of the DEMs of the Badia Test Area..... 410
15.6.1 Comparison with Results Obtained Using Analytical Plotters..... 410
15.6.2 Comparison with Results Obtained Using Digital Photogrammetric Systems..... 416

15.6.2.1 Comparison with the Results of Trinder et al (1994) 417
15.7 Planimetric Accuracy Results of the Ortho-images of the Level 1A and 1B Stereo-models of the Reference Scene 122/285 of the Badia Test Field 420
15.8 Conclusion 422

16. Conclusions and Recommendations 425

16.1 Introduction 425
16.2 Research Summary 426
16.3 Overall Conclusions and Recommendations 427
16.3.1 Badia Test Field 427
16.3.2 Calibration of the Systems Using SPOT Level 1A and 1B Stereo Models 430
16.3.3 Geometric Accuracy Test Results of Planimetry and Height of Level 1A and 1B SPOT stereo-pairs of the Badia Test Area Using Different Systems 432
16.3.4 Validation of DEMs and Orthoimages 436
16.3.5 DEM Extraction and Generation of Digital Orthoimages and Contours for the Badia Project 439
16.3.6 The Potential Contribution of SPOT Images and Other Satellite Images to Topographic Mapping in Jordan 440
16.4 Final Remarks 441

APPENDIX A: CONTROL POINTS AND PROFILE DATA
APPENDIX B: RESULTS FROM TESTS OF THE EASI/PACE SYSTEM
APPENDIX C: RESULTS FROM TESTS OF THE DMS SYSTEM
APPENDIX D: RESULTS FROM TESTS OF THE ORTHOMAX SYSTEM
APPENDIX E: RESULTS FROM TESTS OF THE EASI/PACE SYSTEM OVER THE OSLO TEST AREA

CHAPTER 1: INTRODUCTION

1.1 Introduction

Every country in the world faces an increasing demand for maps to meet the various different requirements of sustainable development, adminstration and defence. Furthermore, for many users, the measurement, study, management and conservation of the Earth's resources have become an urgent challenge besides using these resources to satisfy the continuously increasing demands of human kind. All of these activities should be based on accurate and readily available topographic maps. These maps should be continuously updated, due to the rapid and dynamic changes of both the physical landscape and its man-made or cultural features, as well as the exponential changes of the users' needs. Most recently, the monitoring and planning of the environment has became important: the nations of the world have committed themselves to cooperate in a spirit of global partnership to conserve, protect and restore the health and integrity of the Earth's ecosystem. By doing so, knowingly or unknowingly, they have also committed themselves to the development and use of more comprehensive and more accurate mapping systems both in the developing world and in the more technically advanced nations.

Consideration of the current status of world mapping shows that much needs to be done to complete the task, especially in the developing countries, some of which still do not have any substantial coverage of basic medium-scale topographic maps. In particular, some developing countries have very substantial deficiencies in coverage at the standard scales of 1:50,000, 1:100,000 and 1:200,000 used for nation-wide topographic mapping. This is due to various factors mostly relating to their poor economic situation and chronic political and military conflicts, but it is also due to the vast area of many individual countries, much of which comprises desert, dense forest or mountainous terrain and which is either uninhabited, inaccessible or sparsely inhabited. Almost invariably, Africa is quoted as the most poorly mapped continent, followed by South America. While the situation in the more advanced countries is much better, even there, the pace of development in many areas has caused the existing maps to became out-of-

date. Thus the need for up-to-date maps becomes a necessity. One of a number of possible solutions that are being investigated to try and satisfy such needs, especially in the developing countries, is to try to make efficient use of space images. In this respect, the need for topographic mapping in developing countries to be carried out using such imagery receives quite a lot of attention both in the scientific literature and at a political level - though the actual use of the method is quite low.

To help rectify the situation and increase the rate of mapping and map revision at medium and small-scales, it seems that one way of doing this is to utilize the capabilities of modern remote sensing technology. Among the spaceborne platforms currently being operated is the French SPOT satellite with its stereoscopic imaging capability. At the moment, in the context of satellite mapping capabilities, SPOT can be considered to be the most important space imaging system. Indeed, seen from the purely mapping point of view, currently it is the only fully operational satellite imaging system - though the Indian IRS-1C and 1D satellites (which are in many ways similar to SPOT) are now begining to compete with SPOT. However it will take some considerable time before these IRS satellites achieve the complete coverage and the archive that has been built up with SPOT.

Using and exploiting these SPOT and IRS satellite images with their cross-track stereo-coverage for topographic mapping and map revision purposes requires the availability of expensive high-tech solutions and systems such as analytical plotters or digital photogrammetric workstations which need to be equipped with specialized software if the extraction of heights and contours is required and accurate results are to be achieved. From the economic point of view, fewer images are required to cover a given area with SPOT or IRS imagery as compared with small-scale aerial photography, and consequently there will be a reduction in the ground control point requirements. The negative side till now has been the shortcomings in the ground resolution of the satellite images. Nevertheless there is still much interest in trying to carry out topographic mapping from SPOT stereo-imagery. However, in spite of much effort on the part of researchers and system suppliers, the results have not been as satisfactory as had been hoped. This has sometimes been due to poor ground control but it has also been caused by shortcomings in the software that has been available for topographic mapping

operations from SPOT imagery. Recently a new generation of digital photogrammetric systems has come on to the market replacing the previous generation of analytical plotters that have been used for the purpose up till now. These new systems are now becoming available with software allowing them to carry out mapping from SPOT stereo-imagery, including the automated extraction of DEMs and the generation of ortho-images - operations that were difficult to implement on an analytical plotter.

1.2 Mapping in the Red Sea Region

The area of North East Africa and South West Asia bordering the Red Sea and Gulf of Aden is one of special interest to the mapping community in general and to the author (who is Jordanian) in particular. It is mostly a harsh and sparsely populated land, comprising extensive areas of sandy and stony desert and rugged mountainous terrain, within which communications networks are poorly developed. This poses special difficulties for those concerned with mapping of its topography and geology, access to the many remote areas requiring mapping often being very poor. Over the last 25 to 30 years, the situation has changed gradually and quite extensive topographic map coverage now exists for a number of countries in the region - though there are still some major areas where the coverage is either seriously deficient or does not exist at all. While the primary method of mapping has been based on the use of aerial photogrammetric techniques, a considerable amount of topographic mapping has been carried out using satellite imagery. Indeed up till now, more satellite mapping has been conducted in this region than in any other part of the world and interest in the technique remains high.

1.2.1 Mapping in North-East Africa

On the African side of the Red Sea region, the situation regarding topographic map coverage is very mixed. Some countries such as Egypt have extensive coverage, although substantial parts need revision. Somalia has 100% coverage - though it is now 25 years old - while, in other countries, the situation is mostly one of poor coverage, more especially in the Sudan (with only 10% cover), Ethiopia (40%), Eritrea (5%), etc. Looking at Sudan as an example, it is the largest country in Africa and has huge areas of desert and semi-desert in the north and central parts of the country and dense tropical

rainforest in the south. In addition, it has some high, rugged mountain areas such as the Red Sea Hills. Settlement is mostly sparse and very widely distributed, the transport and communication networks are poorly developed, and many areas are not readily accessible. During the period 1970-1976, the 1:250.000 series of the early Anglo-Egyptian period was revised by adding changes to administrative boundaries and the positions and names of new settlements (Petrie & El Niweiri, 1994). Since the 1:250,000 scale series did not provide enough detail for many purposes, it was decided that a new 1:100,000 scale series with contours should be produced with the support of a UNDP programme. At this scale, 920 sheets would be required to cover the country.

During the late 1970s and early 1980s, a number of joint projects to fulfill this requirement were carried out under a British aid programme by the Directorate of Overseas Surveys (DOS) in collaboration with the Sudan Survey Department (SSD). These produced 136 sheets, extending through the Red Sea Hills and the area along the Ethiopian border, but later the work was stopped due to the civil war in Southern Sudan which also resulted in a chronic lack of foreign currency and shortage of skilled, trained personnel. In this situation, almost inevitably, attention has been focused on the possibilities of using space imagery for mapping purposes. Since most of the Sudan comprises desert and semi-arid land, over which the weather is often cloud free, so the problems of acquiring optical images from space are less likely to occur than in the cloudy areas of the tropics. Furthermore it would be possible to produce several image maps, photo maps or line maps from a single space image or stereo-model. This would result in a drastic reduction in the photogrammmetric operations required for mapping. It would also lead to a reduction in the provision of the control points needed for this mapping, which is a major consideration in the context of the large areas with very poor accessibility. With all this in mind, several researchers from European universities and mapping agencies have investigated the possibilities of mapping from space imagery for the Sudan. Indeed the Department of Geography and Topographic Science has been heavily engaged in this work, as evidenced by the work of Abdalla (1980), El-Niweiri (1988), Valadan Zoej (1997) and others (Petrie and El-Niweiri (1992 and 1994); Petrie et al (1998)).

As noted above, in Ethiopia, only 40% of the country has been mapped using conventional aerial photogrammetric methods. An initial pilot project to assess the possibilities of utilizing SPOT stereo images was carried out in the Asela area by a Swedish team using advanced digital photogrammetric techniques, to produce a digital elevation model (DEM) and ortho-images (Kihlblom, 1992). Since then, SPOT stereo-images have been adopted by the Ethiopian Mapping Authority (EMA) to continue the 1:50,000 scale mapping of the country (Petrie, 1997). This uses hard-copy SPOT Pan images in a Wild BC-2 analytical plotter. The final output of a DEM and the corresponding ortho-images are produced at 1:50,000 scale using a Wild OR-1 analytical orthophoto printer. In addition to the 1:50,000 scale mapping, EMA is also using monoscopic Landsat TM and SPOT XS images to revise the 30 sheets most in need of the 1:250,000 scale map series (93 sheets in total) covering the whole country which was originally produced under a U.S. aid programme (Petrie, 1997).

Djibouti has also been mapped from SPOT stereo-images by the French IGN using Matra analytical plotters at 1:200,000 scale, covering the whole country, while the more developed and populated part was covered by 1:50,000 scale mapping. During the same period, a very similar mapping project was undertaken in Yemen by Ordnance Survey International (OSI) to produce maps of North East Yemen at 1:100,000 scale. Hard copy SPOT stereo-images were used to produce the required map information, and around 18 stereo-models were plotted at 1:100,000 scale with a 40 m contour interval using a Kern DSR analytical plotter.

In spite of this quite considerable activity, there have also been a number of drawbacks to the methods that have been used. Essentially a very classical type of photogrammetric operation has been adopted by all the agencies concerned with these space mapping projects with manual/visual measurement of the planimetric detail and contours by an operator. Even in the EMA work producing ortho-images, the measurements of the DEM are carried out manually by an operator using profiling techniques. So far, no mapping agency in the area has adopted the new all-digital photogrammetric systems with their highly automated methods for extracting digital elevation models (DEMs) and ortho-images. Yet there is much interest in the possibilities offered by this new technology; though this attitude is tempered by some uncertainty as whether it would

work well in the arid and mountainous terrain of North East Africa. Research into this matter is an obvious pre-requisite if the new technology is to be adopted in the region - especially when financial resources (in the shape of foreign currency) are scarce. The technology must be proven before it will be purchased and used.

1.2.2 Mapping in South-West Asia

By contrast, in the countries of South West Asia lying on the eastern side of the Red Sea, there is extensive existing map coverage of good quality, e.g. in Jordan, Syria, Iraq, Yemen, Saudi Arabia and Israel. While there is often complete or extensive cover, the major problem is that of the revision of a very large number of maps, e.g. 2,300 individual sheets at 1:50,000 and 1:100,000 scales in the case of Saudi Arabia. Recently attempts to revise the 1:250,000 scale topographic mapping of the sensitive border areas of Saudi Arabia from satellite imagery have been carried out by its Military Survey Department (MSD). So yet again, there is much interest throughout the region in the possibilites for map revision offered by SPOT stereo-imagery and, now, the similar IRS stereo-imagery - though, at the moment, the IRS vertical coverage is still not complete for the region and the acquisition of the corresponding stereo-coverage has only just begun.

In general, the most unfortunate aspect of mapping in certain of these developing countries in the Red Sea region such as Sudan and Ethiopia is that the coverage of topographic maps increases very slowly; and even where the coverage has been completed, the pace of change that is taking place in some parts of these countries occurs at a higher speed than the increase in topographic map coverage or the rate of map revision. For the more developed countries in the region, especially those in South West Asia, the revision of existing maps is now the major task facing national mapping organisations. In both of these situations, mapping from satellite stereo-imagery is a matter of great interest, but it is, as yet, unproven in a production environment - especially if it is to be carried out using the newly developed capabilities of digital photogrammetric systems to exploit and utilize such imagery.

1.2.2.1 Mapping in Jordan

Concerning Jordan, the mapping situation is somewhat akin to that of Saudi Arabia in that the basic topographic mapping has been completed at 1:50,000 scale and the main concerns are now the continuous revision of this series and the extension of new coverage at 1:25,000 scale for the more developed western part of the country bordering the Jordan Valley. For the map revision requirement, again the possibilities of undertaking the task using satellite mapping techniques is a matter of great current interest.

Within Jordan, the Badia is a vast arid area of 72,000 square kilometres occupying the eastern part of the country. It covers over four-fifths of the country but contains only about one-twentieth of the population and, for too long, it has been regarded as a separate part of Jordan's living space. For hundreds of years up until the end of the First World War, the Bedouin tribes, inhabiting large areas of Syria, Iraq, Jordan and Saudi Arabia, moved freely about this area with their herds of livestock. Since the end of the First World War, many changes have affected the traditional situation. These include the creation of international borders, changes in land tenure, the advent of road networks and vehicles, and the spread of settlements. Some of these changes have undoubtedly brought material benefits to the communities of the Badia as they face a transition from a truly nomadic to more settled existence.

The Royal Geographical Society (RGS) in the U.K. has been invited by the Jordanian Government to collaborate and participate in an ambitous joint three year research project located in the north-east part of the Badia region. The Badia Project's objective is to undertake inter-disciplinary research both in the field sciences (geology, ecology, hydrology, soils, agriculture, etc) and in the social sciences (demography, sociology, etc.) which will lead to development activities, environmental improvement and beneficial economic change. The setting up of a Field Centre at Safawi was the first major achievement of the Badia Programme, giving a base from which all of the initial surveying and fieldwork could take place. A wide-ranging multi-disciplinary study of a regional environment of this type requires the close integration of the vast amount of data collected by researchers both on the ground and through the use of aerial and

satellite imagery. All of these data must then be assimilated into a computerised database with facilities for spatial analysis and mapping. The resulting geographical information system (GIS) is intended to be an essential part of the Project management structure, located at the Safawi Field Centre. The Project's research management team was determined also to utilize remote sensing imagery and technology to help build the database and, to this end, it has been acquiring large data sets for the purpose, including continuous NOAA AVHRR coverage at the macro-scale and SPOT coverage at the other end of the resolution scale (for optical imagery) and ERS SAR coverage (for microwave radar imagery). This provided an obvious opportunity for a research project into mapping from space imagery using the latest technology to be devised and incorporated into the Project's programme.

To the author's knowlege, satellite images have never been used for the production or revision of topographic mapping in Jordan. However financial problems now face the national mapping organisation and there is insufficient financial support to cover the country with new aerial photography and to carry out map revision. Indeed, the progress of map production and revision by this method is still too slow having regard to the demands of users for up-to-date topographic information. An investigation into the matter of whether satellite images can be used for topographic mapping and map revision in Jordan is therefore timely since it would not be too difficult for the national mapping agency to acquire the capability to do so in terms of equipment and trained personnel.

1.3 Justification for the Research Study

Researchers have considered satellite imagery as a solution for world wide mapping problems for some time. Indeed Petrie (1970) had pointed out this possibility even before the launch of the first American civil Earth Observation satellite in the Landsat series - namely that there could be economic advantages to be gained from using satellite imagery for topographic mapping purposes, especially where there is the potential for a large reduction in the cost and time required for the mapping of a large area at small scales. Nowadays it can be taken virtually for granted that projects in any field of science that cover a large area of terrain will try to make use of the data

provided by remote sensing devices. The image data can be utilised for land cover/land use mapping and for scientific studies concerned with geology, hydrology, landforms, vegetation, agriculture, etc. This is the case with the Badia area, and is one of the reasons underlying its selection by NASA as one of its Pathfinder sites forming part of its Global Land Cover Test Site Project: indeed the Badia Project area is the only site short-listed from the Middle East. This will result in the regular supply of the image data acquired by the satellites launched by NASA, e.g. that from Landsat (TM), NOAA (AVHRR), etc. needed for the continuous monitoring of the area. Of course, satellite image data from other sources can be used to supplement the NASA data and SPOT imagery is an obvious example which will provide better ground resolution than that of the NASA products.

1.3.1 Need for Test Sites and Data Sets to Calibrate Satellite Imaging Systems and Validate DEMs Being Generated on a Global Scale

Quite apart from the generation of all this useful data for scientific purposes within the Badia Project, there is also a substantial photogrammetric research component that can usefully be undertaken within the scope of this research project. In particular, currently there is a considerable interest world-wide in the validation of DEM data derived from satellite stereo-imagery and in the calibration of the systems used to create such DEMs. This forms part of the effort to create a worldwide or Global DEM for geophysical work and for other scientific activities such as environmental monitoring and global change research, including the correction of satellite data for the effects of topography. Thus, for example, the multi-national Committee on Earth Observation Satellites (CEOS) has formed a special Working Group on Calibration and Validation (WGCV) to coordinate international activities in this area (Lauritson, and Howard 1993). This Working Group has a sub-group on Terrain Mapping which is trying to establish a series of controlled test sites in different parts of the world, each with different topographic and land cover characteristics. These should have a network of very accurate control points and accurate reference data sets available which will allow the

(i) validation of the terrain height data contained in the DEMs produced from space;

(ii) the testing of different algorithms and matching techniques used to produce DEM data; and

(iii) the inter-comparison of different types of imagery and systems used to produce these DEMs (Dowman, 1993).

The ISPRS Commision IV Working Group (IV/2) on mapping from high-resolution space imagery has also been encouraging this type of investigation. However, so far, only a few test sites have been established and there is a pressing need for further sites to be established. It was hoped therefore that, in the course of establishing the extensive network of very accurate ground control points (GCPs) needed to generate the DEM required for the Badia Project, the area can also be established as an international test site, supplementing and enhancing its existing status as a NASA Pathfinder site.

1.3.2 The Photogrammetric Dimension of the Research Project

In this context, it is also worth mentioning that there have only been one or two independent studies (e.g. that by Trinder et al (1994)) which attempt to assess the quality of the elevation data that can be derived automatically from satellite images using the newly developed digital photogrammetric workstations (DPWs) based on the use of an image processing system. In spite of all the discussion of the possibilities of using such automated systems that has taken place in the scientific and technical press, very few actual results have been obtained using such systems and indeed most of the published results apart from those of Trinder have been very disappointing. Furthermore most of the good results that have been published on the accuracy of the planimetric detail and height data obtained from satellite imagery have been based on the use of analytical plotters in conjunction with manual/visual measurements of hard copy SPOT stereo-images.

In this context, over the last three or four years, there have been noticeable moves by several well-known commercial suppliers of software to the remote sensing community to enter the field of DEM production and ortho-image generation in competition with the well established mainstream photogrammetric system suppliers. This is the result of the rapid convergence of two technologies - those developed for photogrammetry and remote sensing respectively - which were previously quite separate and distinctive.

These new systems utilize a variety of geometric and algorithmic approaches and employ a variety of quite different image matching techniques. It is a matter of considerable interest to both the remote sensing and photogrammetric communities to try to establish the quality of the DEM data and ortho-images that can be generated from satellite imagery using these new systems. Till now, few have used commercially available systems and attempted to verify the quality of the data that is generated by these systems. This matter is a main concern of the present research project.

A further concern has been to investigate the suitability and potential of SPOT Level 1B imagery for topographic mapping. Up till now, both researchers into the use of SPOT stereo-imagery and the actual users of the imagery for topographic mapping have concentrated on the use of Level 1A imagery in hard-copy form, usually carried out using analytical plotters. By contrast, most users in the geoscience, geophysical and geoexploration communities have tended to use Level 1B imagery in digital form because of its more map-like geometry which makes it easier to correlate with digitized maps in raster format of the area being covered. So formerly there has been a clear division between the types of image and the technologies used by the respective communities. However the suppliers of the new digital photogrammetric systems have now introduced the capability of carrying out photogrammetric operations on Level 1B imagery - clearly to allow geoscientists to produce DEMs and ortho-images from SPOT stereo-pairs using automated methods. The investigation of this new capability will also be a major concern of the author's research study.

1.4 Research Objectives

So far, the importance of mapping from space has been discussed; in addition, the justification of carrying out this research project has also been presented. Based on the above discussion, the main research objectives can be stated to be as follows:

1. Establishing a test area capable of being recognised as an international test field of the highest quality suitable for geometric accuracy testing and the validation of DEMs and ortho-images generated from satellite imagery of all types.

2. Calibration of the software packages from each of the main remote sensing system suppliers with a particular emphasis on the use of SPOT Level 1B stereo-pairs.

3. Carrying out geometric accuracy tests of the planimetry and heights after absolute orientation of the SPOT stereo-pairs, based on different mathematical models and using different software packages and different numbers of control points and check points.

4. The execution of tests to validate the DEMs and ortho-images generated from SPOT stereo-pairs by the various systems by comparison with the reference data sets given by aerial photogrammetry and GPS profiles.

5. The production of a digital terrain model and ortho-image mosaic for the whole of the large area covered by the Badia Project. This is intended to form part of the topographic database for a GIS covering the Project area. The DEMs generated would also be made available to other researchers in some British universities and other researchers in Jordanian Universities who are studying the geology, geomorphology, soils and hydrology of the Badia area. In this respect, it was also hoped to carry out a terrain analysis of the area in collaboration with a geomorphologist from the University of Durham.

6. The results of the research work would also provide important information as to the possibilities of undertaking medium and small-scale topographic mapping and map revision in Jordan from satellite imagery.

1.5 Provision of Test Data

To achieve these objectives, certain test materials needed to be made available to the present author. A block of five SPOT Pan Level 1B stereo-pairs with a pixel size of 10m covering the Badia Project area was provided by the Higher Council of Science and Technology (HCST) in Amman. All of these scenes are of a good image quality, being free from the dust and haze which spoils many satellite images. Also, the individual images comprising each stereo-pair had been taken with only a small time gap between them, so there are no difficulties arising from changes in the appearance of the vegetation or hydrology of the area which might affect the image matching operation. Furthermore, all of these SPOT stereo-pairs possess an excellent base-to-height ratio

(0.86 to 0.98). Originally, it was also hoped to include the testing of pairs of ERS-1/-2 radar images using interferometric techniques to generate DEM data of the area. Unfortunately, due to an oversight on the part of the principal investigator from another university who was supposed to arrange for this data to be acquired, this was not possible.

Obviously, the close cooperation of Jordan's national surveying and mapping organisation, the Royal Jordanian Geographic Centre (RJGC), was essential for this proposed research programme to take place. Indeed, in collaboration with the present author, the RJGC has made a massive contribution towards his research project by first establishing a dense network of highly-accurate ground control points (GCPs) in the area, and by agreeing to carry out the digitizing of the existing 1:50,000 scale topographic maps of the area produced by photogrammetric techniques, including the contours. The RJGC also agreed to establish very accurate GPS profiles crossing the Badia area along the old main roads by measuring more than 15,000 GPS points for validation purposes. This work has been executed under a special agreement for cooperation within the Badia Project made between the Higher Council for Science and Technology (HCST) and the RJGC.

1.6 Outline of the Thesis

Apart from this introductory chapter, the rest of this thesis is organized as follows:-

Chapter 2 gives a review, summary and analysis of the previously published results of geometric accuracy testing of SPOT stereo-pairs. This includes the results of testing individual stereo-models that have been measured singly and strips of SPOT stereo-model that have been measured by space triangulation. **Chapter 3** comprises a similar review of the published work concerned with the generation and validation of DEM data from SPOT stereo-pairs that has been carried out either by an operator or using automatic image matching and using different types of hardware and software. Through these two initial review chapters, the reader is given the background to the accuracy testing and validation work that has been carried out to date, which hopefully will help to place the author's research project in its proper context. **Chapter 4** discusses the status of topographic mapping in Jordan since again this constitutes part of the

background and context within which the research project has been conducted. This includes a historical review of the development of mapping in Jordan and a summary of its present situation.

In Chapter 5, an overview and the main characteristics of the systems that have been tested in the present research are given. The discussion includes the overall system requirements for the application of digital photogrammetric techniques to SPOT stereo-pairs; a classification of digital photogrammetric workstations in the specific context of their ability to handle this type of imagery; and descriptions of the main characteristics of the four main systems employed during the research project. This leads on directly to **Chapter 6** which analyzes the various geometric and mathematical models and photogrammetric solutions that have been adopted in the tested systems.

The overall strategy, the general considerations and the actual experimental procedures used in the author's tests are outlined in **Chapter 7**. This discussion includes the overall experimental requirements to be able to carry out the geometric accuracy tests of the stereo-models; the validation of the DEMs; and the geometric accuracy testing of the ortho-images generated during the project. Following directly on from these more general considerations, **Chapter 8** describes the field survey work carried out to establish the test field within the Badia Project area. This includes a short general description and discussion of the terrain and landscape of the study area, followed by a detailed account of the field work planning, the selection of the control points, and the instrumentation used. This is followed by an account of the observational procedures and a discussion of the problems encountered during the field work phase of the research project. Also a short account of the processing and adjustment of the observed data is given.

Chapters 9 to 13 give a detailed account of the extensive programme of experimental work carried out by the author, with each individual chapter being devoted to a different set of tests carried out on a different system The procedures used, the problems encountered and the solutions devised and implemented to overcome these problems are all described and discussed and the results achieved during each stage of the experimental work are described and discussed in some detail. In **Chapters 14 and 15,**

an overall comparison and analysis of the results achieved in the geometric accuracy testing is provided together with a detailed review of the results of the validation of the DEMs generated by the different systems that have been tested. In both chapters, comparisons are made with the results published by other researchers working in this field. Finally **Chapter 16** forms the conclusion to this dissertation, giving an overall summary of the results of the author's research project and the conclusions reached, together with recommendations for future work.

CHAPTER 2 : PUBLISHED RESULTS ON THE GEOMETRIC ACCURACY OF DATA ACQUIRED FROM SPOT IMAGES

2.1 Introduction

In this chapter, the geometric accuracy of the data that has been obtained from SPOT imagery will be presented. In later chapters, the results of these tests will be compared with the author's own results using the new software-based digital photogrammetric systems. It is important to mention that most of the test results presented here relate to the accuracy of photogrammetric measurements carried out on plan and height control points derived using analytical plotters. Till now, very few results have been published on tests carried out on digital stereo-plotters or image processing systems using PC's. Generally speaking, it will be seen that, from the results published in the scientific literature, SPOT imagery is capable of providing plan and height accuracy of up to 5m at best. However, many results are much poorer than this, the actual results varying from one test to another due to many factors - including base-to-height ratio, image quality, the number and distribution of the ground control points and the instrumentation or software packages that have been used. In this context, another important matter is the degree of pre-processing carried out on the SPOT images which results in various image processing levels (1A, 1B, 2A, 2B, etc) and products.

In this Chapter, the discussion will comprise a review, summary and analysis of the main published results of tests of SPOT stereo-pairs where

(i) individual stereo-models have been measured singly; and

(ii) strips of SPOT stereo-models have been measured by space triangulation.

Later, in the next Chapter (3), a similar review will be conducted for

(iii) DEM generation that has been carried out using either an operator or by automatic image matching.

2.2 Geometric Accuracy Tests Carried out for Single Stereo-pairs

After the advent of the SPOT satellite into operational service in 1986, there was a great deal of research activity during the three or four years that followed. This resulted in quite a number of papers being published giving the results of tests of the geometric

accuracy of the data that could be obtained from the SPOT imagery. Other tests were conducted in parallel with these accuracy tests to establish the interpretability of the imagery and the content that could be extracted from it for topographic mapping applications. From all these tests, it then became clear that there were some fundamental difficulties about using SPOT stereopairs for mapping purposes. In particular, because of cloud, it was often difficult to acquire stereo-pairs with a good base-to-height ratio. Furthermore, even when this was achieved, the two component images making up the stereo-pair often had a very different appearance as a result of seasonal changes in vegetation, land use and hydrology. This often made measurement difficult and automatic image matching impossible. On the top of this, there also was the matter of the limited resolution of the SPOT imagery - in practice, the 10m ground pixel of the SPOT Pan imagery translated to 15 to 18 m in ground resolution terms (Petrie and Liwa, 1995). This resulted in a real shortfall in the detail that could be measured and extracted from SPOT stereo-pairs used for small-scale topographic mapping

2.2.1 Accuracy Tests over the South France Test Area by IGN

Quite a number of these initial investigations into the amount and the quality of the data that could be obtained from SPOT imagery took place in the south-eastern part of France where the various French agencies that were involved in the SPOT satellite project - e.g. the Centre National d'Etudes Spatials (CNES) and the Institut Geographic National (IGN) - made available a block of SPOT stereo-imagery and the appropriate ground control points (GCPs) to allow tests of geometric accuracy (and of interpretability) to be carried out by a number of photogrammetric organizations. Thus, although the titles used for the test areas were varied - Marseilles, Aix-en Province, Grenoble, etc - essentially they are referring to different parts of the same general area. The ground control points provided for these tests were gathered over the area from field survey and existing topographic maps. The test materials used in this early work mainly comprised film diapositives supplied by SPOT Image on an 18 x 18cm format at 1:400,000 scale for use in analytical plotters. Because of the very limited development of digital photogrammetric systems in the late 1980s, only a few of the images were provided in digital form.

For the tests, 31 good scenes were obtained over the area from which sixty stereo-pairs could be formed from various combinations of these scenes. Of these, 14 stereo-pairs could be formed with a base:height ratio = 1.0 (i.e. with viewing angles +27°/-27°); 42 stereopairs had a base:height ratio = 0.5 (with viewing angles 0°/± 27°); and 4 stereopairs had a base:height ratio of 0.5, (with viewing angles +13°/ -13°). Around 177 control points were identified on aerial photographs. The ground coordinates of these points were measured and defined by the Photogrammetric Service of the IGN in 1985 with an estimated accuracy of under 3m in planimetry and less than 1.5m in height

2.2.1.1 South France Test Reported by Rodriguez

First Galtier (1986) reported the initial results obtained by IGN during the in-flight assessment period of SPOT between March and May 1986. Then a much more detailed account of these IGN tests was given by Rodriguez et al (1988). As mentioned above, the main test areas were located in the south eastern part of France. The investigations involved the modelling of the SPOT viewing geometry; the measurement of the ground control points and check points on the SPOT images; and the calculation of the deviations of the photogrammetrically determined values of the positions and elevations of the ground control points (GCPs) from their correct positions and heights as determined on the ground. As noted above, the test stereopairs comprised Level 1A images produced as film diapositives at 1:400,000 scale. These were measured using a Matra Traster analytical plotter and processed using IGN's own software. The main results obtained are presented in Table 2.1.

The results given at the foot of the table are related to the use of two different base-height (B:H) ratios (1.0 and 0.5). These specific results should be noted - especially the improvement in the Z coordinates with the use of larger B:H ratios. The term filtering as used in the table refers to the removal of these points having residual errors greater than 2.7x the standard deviation; it was thought that the poor results at these points were due to mis-identification or to poor measurements of the control points.

	Raw Residuals			Filtering Per Modelling		Overall Filtering	
	No. of Points Measured		RMSE (m)	No. of Pts.	RMSE (m)	No. of Pts.	RMSE (m)
Modelling residuals (Control Points)	X Y Z P	561 (on 73 GCPs)	±4.5 ±4.1 ±4.1 ±2.8				
All stereo-pairs restitution (Check Points)	X Y Z P	631 (on 86 GCPs)	±8.0 ±6.6 ±7.1 ±4.6	559 587 584 613	±4.8 ±4.5 ±5.3 ±4.2	557 589 593 618	±4.6 ±4.4 ±5.3 ±4.1
Northerly region, all stereo-pairs	X Y Z	245	±9.8 ±8.8 ±8.8				
Southerly region, all stereo-pairs (Excluding 4 points)	X Y Z	386	±6.5 ±4.7 ±5.8				
B/H = 1 Configuration +27° /-27° All regions	X Y Z P	215	±8.1 ±5.5 ±4.3 ±4.0	179 205 206 212	±3.9 ±4.4 ±3.5 ±3.9	180 205 209 214	±3.8 ±4.2 ±3.4 ±3.9
B/H =0.5 configuration 0°/± 27° All regions	X Y Z P	394	±7.8 ±7.2 ±8.3 ±4.9	360 360 360 360	±5.2 ±4.5 ±6.2 ±4.4	352 360 379 384	±4.6 ±4.4 ±6.7 ±4.4

(P = minimum parallax distance between rays)

Table 2.1 Accuracy results (Rodriguez et al, 1988).

The RMSE values of the residual errors from the 561 measured points - apparently utilising multiple measurements of the 73 GCPs used as control points - were ± 4.5m in X and ±4.1m in Y and in Z. It was found that six to eight GCPs were sufficient to obtain a reliable modelling and small values of the residual errors for the stereo-pairs. Eighty-six points were used as check points; four of these showed high residual errors and therefore were eliminated. The RMSE values of the residual errors obtained for the 631 check points were ± 8.0m in X, ± 6.6m in Y, and ± 7.1m in Z. These results can be regarded as quite excellent, though whether they can be regarded as really representative is an open question - since they appear to have been acquired from multiple measurements of the GCPs.

2.2.1.2 Accuracy Tests over the Aix-en-Provence Area by UCL

Other results of geometric accuracy have been published relating to the Aix-en-Provence stereo-model made available to researchers as a part of the Preliminary Evaluation Programme for SPOT (PEPS). In particular, a group of researchers at University College London (UCL) also played a strong part in these initial tests. A

preliminary report on their results was given by Dowman et al (1987) and Gugan (1987) and a more detailed one appeared in Gugan and Dowman (1988). They reported that this model had been measured both in a Kern DSR-1 analytical plotter and on an I^2S model 75 image processing system re-programmed to perform as a digital stereoplotter. The appropriate software had been written and implemented to run on these systems by Gugan at UCL, and both systems were then used for tests of stereoscopic measurement and mapping on SPOT stereo-pairs. The total of 12 different panchromatic film SPOT images used by UCL consisted of three Level 1A scenes and two Level 1P scenes for the Aix-en-Provence area in addition to three Level 1A scenes of the Marseilles area. The Marseilles stereo-pairs appear to have been little used, since 65% of their area covered sea. Later, two Level 1A scenes and two Level 1B scenes of south west Cyprus have been measured and assessed with the Kern DSR-1. The results from these latter tests will be discussed later in Section 2.2.2.

For the Aix-en-Provence Level 1A model, 10 control points provided by IGN were used for the test to establish the orientations of the images; of these, nine points had been measured photogrammetrically while the remaining point had been measured from a 1:25,000 scale map sheet of the area. A further 20 check points were also measured from map sheets at the same scale. The control and check points have been selected to be well distributed over the whole model (Gugan, 1987). A summary of some of the main results are given below in Tables 2.2 (a), (b) and (c).

No. of Parameters	Image Residuals at Check Points (mm)		Ground Residuals at Check Points (m)	
	x	y	Plan X/Y	Height Z
10	±0.023	±0.022	±18.1	±8.5
7	±0.021	±0.024	±17.7	±8.1
5	±0.037	±0.030	± 26.1	±16.6

Table 2.2 (a) Overall results of stereo-model accuracy showing the effects of using different parameters in Gugan's modelling.

Table 2.2 (a) presents the residual errors in terms of the RMSE values at the 20 check points using images with mirror tilt angles of -17°.5 and +22°.6 respectively. From this, it can be seen that the RMSE values for the residual errors at these check points were ± 18m in planimetry (X/Y) and ± 8m in height. These results were somewhat poorer than those obtained by IGN given in Table 2.1.

Images used	B:H ratio	No. of check points	Height residuals at check points (m)
01-6-86/18-5-86	0.73	62	± 5.4
12-5-86/18-5-86	0.41	64	±8.4
01-6-86/12-5-87	0.32	53	±8.0

Table 2.2 (b) Effect of base-to-height ratio on heighting accuracy.

Table 2.2 (b) shows the effects of varying the base-to-height ratio on heighting accuracy. The results were obtained from a test of a large number of spot heights over the whole model area (Gugan, 1987). The results indicate that the heighting accuracy of the stereopair with the largest base:height ratio of 0.73 (with tilt angles of 17.5° and 22.6°) is ± 5.4m in terms of the RMSE value.

No. of Control Points	10 Parameters		7 Parameters		5 Parameters	
	RMSE (m)		RMSE (m)		RMSE (m)	
	Plan	Height	Plan	Height	Plan	Height
10	±15.3	±8.2	±18.4	±7.4	±25.4	±21.9
9	±15.3	±8.6	±16.4	±7.0	±25.7	±21.8
8	±15.8	±8.5	±17.1	±6.8	±26.8	±20.9
7	±16.0	±8.4	±17.2	±6.8	±27.0	±20.2
6	±18.7	±9.8	±17.7	±8.1	±28.5	±22.6
5	±25.0	±9.8	±18.2	±10.2	±28.8	±21.5
4			±112.9	±90.0	±27.2	±20.5
3					±32.5	±30.9

Table 2.2 (c) Stereomodel accuracy related to the number of control points and the number of parameters used in the orientation (Gugan and Dowman, 1988).

The results in Table 2.2 (c) at 20 check points show the effects on the orientation of reducing the number of control points to find a solution. With varying numbers of parameters used in the modelling and photogrammetric solution, the effect of the number of ground control points did not appear to be particularly significant. However the use of the different sets of parameters in the solution developed by Gugan obviously had a significant effect on the results, especially when only 5 parameters are used. Overall, it will be seen that the results in planimetry achieved at UCL were markedly poorer than the IGN results. The reasons for this are not clear and were not discussed by Gugan.

2.2.1.3 Accuracy Tests over the Marseilles Area by the University of Hannover

Konecny et al. (1987) and Picht (1987) of the University of Hannover presented the results for a test carried out over the Marseilles area - having measured the appropriate

SPOT stereo-pair on a Zeiss Planicomp analytical plotter. To implement this test, a suitable real time program was produced for the analytical plotter based on the well-known BINGO bundle adjustment program originally developed for use in close-range photogrammetry. Obviously, this program required substantial changes to be made to be able to handle SPOT imagery, since each line of the image has its own perspective centre and - at least potentially - a different orientation. The actual changes in orientation are taken care of through the use of additional parameters - much as is done in conventional bundle adjustment programs.

The Marseilles model that was tested at Hannover consisted of panchromatic images with a base-to-height ratio of 1.0. For this model, 83 ground points were digitised from the 1:25,000 scale IGN maps. Some of these points were used as control points in several adjustments; the other points have been treated as independent check points. In the first processing, all of the points were introduced as control points. These were then reduced to the 18 control points which were necessary to stabilize the geometry of the model. As noted above, a great disadvantage was that 60% of the Marseilles model was covered by water. Obviously this water covered area contained no information for the determination of the unknowns, especially the additional parameters. The accuracy obtained from the stereo-model gave an RMSE value for the planimetric positional error of ± 18.0m and an RMSE value for the elevation error of ± 6.5m in terms - see Table 2.3. It is clear that the accuracy in height improved with an increase in the number of control points used.

Number of Adjusted Points	**Number of Control Points**	**Add. Par. Left/Right**	**Internal Accuracy**				
			θ_o	θ_{xy}	θ_{xy}	θ_z	θ_z
86	18	4/3	8.4	8.7	5.2	10.9	8.5
86	34	3/3	7.9	6.1	4.5	8.8	7.1
89	83	4/5	6.1	4.5	3.0	5.6	5.0
Number of Control Points	**Number of Independent Check Points**	**Mean Differences**			**Mean Square Differences**		
		X (m)	**Y (m)**	**Z (m)**	**X (m)**	**Y (m)**	**Z (m)**
18	68	±7.9	±10.4	±4.8	±10.9	±13.7	±6.5
34	52	±8.3	±10.5	±4.5	±11.3	±13.8	±6.2

Table 2.3 Representative results of the accuracy test using the BINGO bundle adjustment program with additional parameters.

2.2.2 Accuracy of Stereo-models of South West Cyprus

Further accuracy tests were undertaken by two British organisations - UCL and Military Survey - for a test area located in the south west of Cyprus.

2.2.2.1 South West Cyprus Tests Reported By Gugan and Dowman

In addition to the test described above is Section 2.2.12 which had been carried out on Level 1A stereo-pair of Aix-en-Provence, Gugan (1987) gave details of the results achieved with tests of orientation and geometric accuracy achieved with a Level 1A stereo model of the south western part of Cyprus. This area is typical of a mountainous terrain, with the landscape rising from a coastal plain to mountains that are 2,000m high. These tests were performed on stereo-imagery that had mirror look angles of -23.77° and +21.18° respectively giving a base:height ratio of 0.82. The estimated accuracy for the ground control points taken from the Military Survey 1:50,000 scale map sheet of the area compiled in 1973 was around 20m in plan and 7m in height. A well distributed set of 10 GCPs were used to set up the model and a further 19 points were used as check points. Table 2.4 shows the results in terms of the RMSE values for the residual errors in planimetry and height after orientation, using different numbers of parameters in the orbital model.

No. of Parameters	Image Residual Errors at Check Points (mm)		Plan and Height Ground Residual Errors at Check Points (m)	
	x	y	Plan	Height
10	±0.032	±0.038	±29.2	±8.8
7	±0.031	±0.038	±28.8	±8.9

Table 2.4 Cyprus stereo model orientation results in terms of RMSE values of the residual errors.

Gugan (1987) and Gugan and Dowman (1988) reported the results of another test that had been carried out with the Level 1B stereomodel covering south-west Cyprus. In spite of the fact that the software which had been used in the test mentioned above had been designed originally for the orientation of raw Level 1A imagery; the widespread use of Level 1B imagery encouraged them to assess its suitability for orientation and model formation by modifying the software developed for Level 1A imagery.

No. of Parameters	Level 1A Ground Residuals		Level 1B Ground Residuals	
	Plan (m)	Height (m)	Plan (m)	Height (m)
10+3 1B Parameters 10	±28.2	±11.1	±35.8	±15.9
7+2 1B Parameters 7	±27.8	±9.4	±31.6	±18.9

Table 2.5 Comparison of Level 1A and Level 1B image orientation and accuracy test of Cyprus stereomodel (Gugan and Dowman (1988)).

The results are given in Table 2.5 for a comparison of the respective Level 1A and 1B image orientation and accuracy tests. Ten control points were used and the results were reported for 15 check points. The results showed very high residual errors in terms of the RMSE values in plan and in height in the order of ± 30m and ±19m respectively. This was thought to be due to the quality of the ground control points which had been taken from the 1:50,000 scale map sheets and had an estimated accuracy of ± 20m in plan and ± 7m in height. The results have been improved for the Level 1B stereo-pair after removal of those points having residual errors greater than 2.5 times the standard error and allowing for the control point accuracy. But still, the published results for the Level 1B imagery lying between ± 16 and 19m were rather poor. As will be seen later, these results for the Level 1B stereo-pair are of special significance in the context of the work carried out by the present author - which has mostly been concerned with the testing of Level 1B stereo-pairs.

Gugan and Dowman (1988) also reported the results of a test of the accuracy of height measurement of a digital elevation model (DEM) for a small area of a distinctive feature which has been carried out on the Cyprus Level 1A imagery. A 108 point grid DEM was measured and compared with a reference DEM produced from the contours of the 1:50,000 scale map. The accuracy of the results obtained in terms of the RMSE value in elevation was ± 9.9m, reduced to ± 8.6m when the error of ± 4.8m inherent in the reference DTM was removed.

2.2.2.2 South West Cyprus Test Reported by Ley

Ley (1988) from the UK Military Survey's Mapping and Charting Establishment (MCE) presented comparative results from tests of the same SPOT imagery of south western

Cyprus obtained from three different systems, namely the Kern DSR-1 analytical plotter and the I^2S image processing system available at UCL, and the Meridian software package from MacDonald Dettwiler and Associates Ltd (MDA). The MDA Meridian system is completely digital in that height extraction is undertaken within a digital photogrammetric environment incorporating image matching (i.e. stereocorrelation) routines. An outline of the MDA approach is given in the paper by Swann et al (1988). The two UCL systems utilise the same routines devised by Gugan despite employing different hard copy and digital formats of the same imagery. However the UCL and MDA approaches are broadly similar in that they utilize a model which is based upon the modelling of the position and attitude of the SPOT sensor as a function of time. The MDA approach relies upon the rectification and resampling of the imagery into an epipolar projection, with about six to eight GCPs needed to derive an accurate satellite orbital model. In the UCL solution, the orientation and compilation of the imagery is undertaken purely in the geocentric coordinate system.

Fifteen ground control points derived from the existing 1:50,000 scale mapping of the test area were used to set up the SPOT stereo-model in the DSR-1 and I^2S systems. The RMSE values of the residual errors at the GCPs after the orientation had been completed were ± 15.7m in Easting and ± 9.2m in Northing (±18.1m in planimetry) and ± 7.2m in height. In the MDA test, six trigonometric points with an accuracy of about 1m were identified on the RAF photography and were used to set up the stereo-model. The RMSE values of the residual errors at the control points after orientation were ±5.6m in planimetry and ± 4.2m in height. Another test had also been carried using the MDA using 6 ground control points taken from 1:50,000 scale map to set up the SPOT model. The RMSE values in the orientation were ± 8.8m in planimetry and ± 6.4m in height. Table 2.6 gives a comparison between the DSR-1 analytical plotter and the digital MDA Meridian system. The test results showed that the model utilising the triangulation data provided a more accurate stereomodel than that using map derived control.

System	Source of GCPs	Number of GCPs	Residual Errors (RMSE)	
			Plan (m)	Height (m)
DSR-1	Mapping at 1:50,000 Scale	15	±18.1	±7.2
MDA	Mapping at 1:50,000 Scale	6	±8.8	±6.4
MDA	Trigonometric Points and Photography	6	±5.6	±4.2

Table 2.6 Ground control and model accuracy (Ley, 1988).

It will be noticed that these tests simply indicate the fit of the stereo-model to control points. No independent check points were used to verify the results. As will be seen later, Ley's tests were mainly concerned with the extraction of DEMs from SPOT stereo-pairs.

2.2.3 Accuracy Tests Carried out on SPOT Stereo-models in Canada

Canadian agencies and institutions have always been active in developing the use of remotely sensed imagery for mapping using both optical and radar imagery. Thus quite a lot of tests of geometric accuracy of SPOT imagery have been carried out by these organisations. A representative sample and summary of these is given below.

2.2.3.1 Ottawa, Sherbroke, Grenoble Tests Reported by Kratky

Kratky (1988) of the Canada Centre for Mapping (CCM) presented the results shown in Table 2.8 for three test areas (Ottawa, Sherbrooke, Grenoble) using SPOT stereo imagery. His method utilized a rigorous photogrammetric reconstruction of the three-dimensional stereomodel from SPOT images based on a bundle adjustment modified to operate in a time-dependent mode, with additional constraints derived from the known orbital parameters. The tests were carried out on the NRC Anaplot I analytical plotter supported by a DEC PDP 11/45 minicomputer on which the method had been programmed.

The Ottawa test was based on two SPOT images taken four orbits apart in August 1987 with view angles of $+27.89^{\circ}$ and $+7.31^{\circ}$ and with a quite poor base-to-height ratio of 0.4. As shown in Table 2.7, the results demonstrated the practical effect of using certain parameters to model the orbital path in the solution. The first two tests, computed without using a calibration correction, showed that there was no need to use quadratic terms for the attitude model. When the linear model of attitude variation was applied, the realisation of the quadratic formulation was in fact preserved. In the third example, an improvement in the accuracy of elevation was obtained arising from the correction for sensor misalignment.

In the Sherbrooke test, with a better base-to-height ratio of 0.61, while an improvement was obtained in elevation, the results in planimetry were comparable to those achieved in the Ottawa test. In this test, the number of check points that were available was very high compared to those used in the other tests. These were used to experiment with the number of control points needed to achieve a reasonable solution and to find the effects of the selection and the number of control points on the accuracy of the reconstructed geometric model. From Table 2.7, it is clear that the number of control points did not affect the solution; even with only five control points, a good solution was achieved.

For the Grenoble test, three individual scenes that were available for space triangulation experiments were processed independently in order to check the quality of identification of the ground control points. A single model was formed with a base-to-height ratio of 0.94. The RMSE values listed in Table 2.7 correspond to the discrepancies at the control points after adjustment. One set of RMSE values also reflected the fit at the check points.

Test Area	Attitude Mode	Unknown Parameters	Control Points	Check Points	Standard Error of Unit Weight (μm)	RMSE at the Check Points E (m)	N(m)	H (m)
Ottawa	Quadratic	26	6	65	±12.0	±4.8	±6.0	±12.9
	Linear	20	6	65	±9.0	±4.9	±6.3	±12.2
	Linear	22	5	62	±9.7	±4.6	±5.3	±8.4
Sherbrooke	Linear	22	16	237	±6.8	±4.9	±5.1	±7.3
	Linear	22	9	244	±6.1	±5.2	±5.8	±7.9
	Linear	22	7	246	±6.8	±5.3	±6.1	±7.9
	Linear	22	5	248	±8.8	±5.6	±5.3	±7.5
Grenoble	Linear	22	17	0	±7.6	±5.5	±4.4	±2.3 GCP
	Linear	22	5	12	±3.7	±8.1	±5.8	±3.3 CHK
	Linear	22	12	0	±8.6	±5.8	±5.1	±3.5 GCP
	Linear	22	10	0	±7.1	±2.0	±5.7	±3.5 GCP

Table 2.7 Accuracy Results (Kratky, 1988).

2.2.3.2 Ottawa Test Reported by Toutin and Carbonneau

The tests carried out by Kratky were followed by a further series of tests carried out by Toutin of the Canada Centre for Remote Sensing (CCRS) and various collaborators which utilized both the Ottawa area and other test areas located in different parts of North America. Unlike Kratky, who used an analytical plotter, Toutin's tests have involved the use of digital photogrammetric systems.

Toutin and Carbonneau (1990) utilized the so-called CARTOSPOT system developed by Toutin and the DIGIM company in a test of three SPOT Level 1A Pan scenes of the Ottawa area covering view angles of +2.30°, 28.6° and -20° respectively. The ground control point (GCP) data had been produced through the aerial triangulation of 130 aerial photographs at 1:40,000 scale to give coordinate data with an estimated accuracy of 1 to 2m. The measurements of the GCPs were carried out monoscopically on each image. Using 6 control points, the RMSE values of the residual errors at 92 independent check points out of the initial set of 235 GCPs obtained by aerial triangulation were as shown in Table 2.8.

No. of Images	RMSE - ΔX (m)	RMSE - ΔY (m)	RMSE - ΔZ (m)
3	±3.9	±3.9	±3.2
2 (B:H =1.0)	±4.1	±4.4	±3.5
1 (±28.6°)	±4.7	±4.6	-

Table 2.8 Accuracy results for 92 check points (Toutin and Carbonneau 1990).

Using the 72 best defined check points, these already remarkably good figures were improved still further to give the values shown in Table 2.9.

No. of Images	RMSE - ΔX (m)	RMSE - ΔY (m)	RMSE - ΔZ (m)
3	±3.2	±2.8	±2.9
2 (B:H =1.0)	±3.5	±3.1	±2.8
1 (±28.6°)	±4.0	±3.8	-

Table 2.9 Accuracy results for 72 check points (Toutin and Carbonneau 1990)

2.2.3.3 Irvine Test Reported by Cheng and Toutin

Cheng and Toutin (1995) carried out a test comparing the accuracy of simple polynomial methods and full photogrammetric methods of data reduction using four different satellite images for the comparisons. The satellite DEM extraction and orthorectification package from PCI was used for this test: this package had been developed by PCI on the basis of Toutin's mathematical modelling of satellite imagery and a pre-operational software package developed at CCRS. The four test images were SPOT 1A Pan and Multiband HRV images with viewing angles of L21.6 degrees; a Landsat TM image; and an ERS-1 SAR image. Obviously the test concerned the use of single images instead of overlapping stereo-pairs. The test was conducted over the area located around Irvine, California in the USA. GCPs were obtained using the USGS 1:24,000 scale maps covering the test area. The DEM was obtained from USGS at 30 metre grid interval with an accuracy of ± 10 metres. For each image, a total of ten

control points was available; a further ten independent check points (ICPs) were collected which were not used in the solution.

Method	SPOT Pan (10m)		SPOT (20m)	
	ΔX (m)	ΔY (m)	ΔX (m)	ΔY (m)
Photogrammetric	±3.3	±2.6	±5.0	±2.8
Polynomial Ist order	±81.0	±4.2	±93.2	±7.2
Polynomial 2nd order	±77.3	±3.7	±86.6	±4.4
Polynomial 3rd order	±23.5	±1.6	±66.8	±4.0

Table 2.10 (a) RMSE values of the residual errors at the control points.

Method	**SPOT Pan (10m)**		**SPOT (20m)**	
	ΔX (m)	**ΔY (m)**	**ΔX (m)**	**ΔY (m)**
Photogrammetric	±3.4	±3.2	±3.0	±4.5
Polynomial Ist order	±80.2	±2.9	±96.0	±10.8
Polynomial 2nd order	±74.7	±2.6	±83.8	±9.6
Polynomial 3rd order	±704.6	±45.8	±940.0	±55.0

Table 2.10 (b) RMSE values of the residual errors at the check points.

Tables 2.10 (a) and (b) show the results obtained at the control points and check points respectively using the photogrammetric method (employing space resection and rectification) devised by Toutin and the simple 2D polynomial transformation method. The results given are restricted to those obtained using the SPOT Pan Level 1A (10m) and the SPOT Multispectral (20m) images only. In these tables, the RMSE values of the residual errors obtained at the control points and at the check points are given for different tests using polynomials of various degrees and the more exact photogrammetric method.

Starting with the polynomial method, as shown in Table 2.10 (a), the third order polynomial gave the smallest RMSE value for the residual errors in planimetry at the control points of ± 23.6m, whereas those resulting after the application of the second order and first order polynomial were ± 77.4m and ± 81.1m respectively. When comparing the errors at the check points given in Table 2.10 (b), the RMSE value for the residual errors for the third order polynomial was very high compared with those resulting from the use of the second and first order polynomials. The RMSE value obtained with the third order polynomial at the check points was ± 706m in planimetry compared with the RMSE values of ± 74.7m and ± 80.3m resulting from the use of the second and first order polynomials respectively. In fact, this indicates that the occurrence of smaller residual errors at the control points does not lead to an

improvement in accuracy elsewhere in the image. With a fixed number of GCPs available to solve the larger number of unknowns in a higher order polynomial, the degree of freedom in the least squares adjustment is smaller, and this causes the reduction in the size of the residual errors at the control points.

The comparison with the photogrammetric method indicated that the latter gives by far the best results. The RMSE value of the residual error obtained in planimetry for the SPOT Level 1A image was ± 4.2m at the control points, while, with the SPOT multispectral image, it was ± 5.7m - as shown in Table 2.10 (a). At the check points - as shown in Table 2.10 (b) - for the SPOT Level 1A image, the RMSE value obtained in planimetry was ± 4.7m - which was only a little higher than that on the measured control points. The results obtained in terms of the RMSE value of the residual error in planimetry on the SPOT multispectral image was ± 5.4m - which is again only a little higher than that on the SPOT Level 1A Pan image.

2.2.3.4 Test in British Columbia Reported by Toutin and Beaudoin

Most recently, Toutin and Beaudoin (1995) have reported the results of the extraction of planimetric and altimetric features from digital SPOT Pan data used in stereoscopic mode on the DVP - which is a low-cost PC-based digital photogrammetric workstation developed at Laval University in Canada. Again the DVP-SPOT software module is based on the mathematical model devised by Toutin. In this project, two aspects of data extraction were studied. The first concerned the planimetric accuracy of those features that could be obtained from the stereo model through the geometric correction process; the second concerned the accuracy of the digital elevation model and the contour lines derived from the stereo-model. After the stereo-model had been set up and the feature extraction carried out using the DVP-SPOT package, the measured features were transferred to the ARC/INFO system to be compared quantitatively with the reference digital topographic data set.

The study area was located in British Columbia (Canada). The two SPOT images which were used were raw Level 1A images recorded in panchromatic mode, with a base-to-height ratio of 0.74. The topographic data were obtained from the Canada Centre for Mapping (CCM). This data set was originally stereo-compiled from 1:50,000 scale

aerial photographs taken in 1981. Twelve ground control points (mainly road intersections) were first identified and their ground coordinates (X Y Z) were extracted from the aerial photographs of the test area using measurements made on a Wild STK-1 stereo comparator. Using the ground control point coordinates, and the attitude and orbital parameters from the SPOT header file, the geometric modelling was then computed using the full photogrammetric solution of the DVP-SPOT module. Using a least-squares adjustment, the residual errors at the 12 GCPs gave RMSE values of ± 6.4m, ± 8.6m, and ± 5.5m in X, Y, and Z respectively. Further improvements to the DVP system resulted in an increase in the zoom factor used in the measurement and acquisition of image coordinates from two to four. This improved the accuracy achieved during the orientation process. Using the same combination of GCPs and tie points, the residual errors became smaller with RMSE values of ± 4.7m, ± 4.0m, and ± 3.7m in X, Y, and Z respectively. These are quite remarkable figures to say the least - especially considering the very simple stereo-viewing and measuring facilities of the DVP. The results achieved with map compilation and DEM extraction via operator-controlled measurements from the SPOT stereopair showed a planimetric accuracy of ± 12m for well identifiable features and an altimetric accuracy for the DEM of ± 30m in terms of the respective RMSE values.

2.2.4 Stereo-Model Accuracy Achieved During Mapping from SPOT Stereo-Pairs in North-East Yemen

A number of papers by Hartley (1988), Murray and Farrow (1988), Murray and Newby (1990) and Murray and Gilbert (1990) have been published concerning the preparation of a series of topographic map sheets at 1:100,000 scale from SPOT stereo-pairs by the Overseas Survey Directorate (OSD) of Ordnance Survey (OS) covering 25,000 km^2 of north-east Yemen. Map compilation was carried out in early 1988 and the work was completed in March 1989, first using a Kern DSR-11 and later a Kern DSR-15 analytical plotting instrument. The Kern SPOT software suite developed by University College London (UCL) was purchased by the Ordnance Survey (OS) and installed on the DSR-11 analytical plotter for use in this mapping project.

Most of the published papers were concerned with the mapping side of the project and are not of concern to this review of geometric accuracy. However some information was also given regarding the accuracy of setting up the SPOT stereo-pairs in the DSR instruments. The ground control points (GCPs) had been obtained mostly using satellite doppler methods in the field with additional GCPs acquired from adjacent blocks of aerial photos to the west established from previous surveys within that area. The distribution of the GCPs was not good, especially in the eastern part where much of the area in the scenes fell outside the extent of the control points. Additional difficulties were encountered in setting up the stereo-models caused mainly by GCP identification - in spite of utilising surveyor's sketches and RAF aerial photography acquired in 1973. Each model was set independently using approximately 12 GCPs per model requiring an average setting time of 12 hours. Of the 16 models used, the average RMSE value of the residual errors at the control points was ± 10.2m in Easting, ± 9.4m in Northing and ± 9.4m in height in the UTM system. From this account, it will be seen that this is not a formal test, but the results given are those achieved during the actual production of topographic maps from SPOT imagery.

2.2.5 Accuracy Tests of Stereo-models of South-West Sinai

2.2.5.1 Initial South-West Sinai Tests Reported by Diefallah

Diefallah 1992 (a) first carried out an investigation to assess the planimetric accuracy of two SPOT Level 1A images and to test different mathematical models. A single stereo-pair which covers the desert area of south west Sinai with limited cultural features was used as the test area. The image coordinates of the identified control points were measured on a Wild BC-2 analytical plotter used in comparator mode, with a standard deviation of ± 5μm. In this particular investigation, a series of 2D polynomial transformations were then used to transform the measured image coordinates into ground coordinates. Ground control points (GCPs) were derived from the Egyptian Military Survey 1:50,000 scale topographic maps; the coordinates of 150 GCPs were measured on the maps and digitised using the plotting table of the Wild BC-2.

The accuracy obtained after applying different transformation models to the best 25 reference points for the first test image was an RMSE value of ± 35.1m in planimetry

when applying the 2-dimensional similarity (linear) transformation; an RMSE value of ±32.0m in planimetry when applying the affine transformation; and ±27.2m in planimetry when applying the second order polynomial transformation.

For the second test image, applying different transformations to the best 36 reference points and with all the GCPs used as control points, the respective RMSE values of the planimetric vector errors were ±58.1m for the 2-dimensional similarity (linear) transformation; ±30.3m when applying an affine transformation; and ±27.3m when applying the second order polynomial. The results obtained indicated that, when using the full set of 68 ground points, the best RMSE values of the planimetric vector errors achieved with the second order polynomial are ± 45.2m and ± 50.2m respectively on the two images. The results also indicated that an affine transformation, with 4 to 6 well-identified ground control points is sometimes quite sufficient for SPOT image rectification. Analysis of the residual errors revealed that, when applying polynomials with more than three parameters, a large number of ground control points are needed and the control points must be well distributed, including some placed near the image corners.

2.2.5.2 Later Test Reported by Diefallah

Diefallah (1990, 1992 b) also reported on his second investigation into the accuracy of the height information that can be extracted from a SPOT stereo-pair utilising two different photogrammetric methods. For these studies, he again used the SPOT stereo-pair of south-west Sinai with the Wild BC-2 used as measuring device. In the first method that was used, a stereoscopic model was formed by analytical relative orientation. The model coordinates were then fitted to the coordinates of the control points using three dimensional affine and polynomial transformations. In the second method, the ground coordinates of the check points were computed via space resection and intersection.

Regarding the first method it is far from clear from the two papers how a seemingly conventional orientation procedure used with aerial photography can be modified and utilised as the basis for the computation of planimetric and elevation coordinate values

from measurement on SPOT images. A variable number of ground control points has been used to determine the orientation and transformation parameters. The ground control points were classified according to their identification qualities into two groups. The first was formed from 23 well-identified points. The second was formed by adding another 9 points of moderate identification quality to first group making a total of 32 reference points. The RMSE values of the residual errors of the coordinates of the control points after use of the modified orientation method are computed and shown in Table 2.11

No. of Reference Points	RMSE (Metres) Affine Transformation			RMSE (Metres) Second-order Polynomial		
	ΔX	ΔY	ΔZ	ΔX	ΔY	ΔZ
32	±55	±58	±19	±38	±39	±18
23	±40	±47	±17	±24	±29	±13

Table 2.11 RMSE of residuals at reference points using three-dimensional affine and second order polynomial transformations.

In the second method, the RMSE values of the residual errors at the control points were computed after applying the space resection-intersection method; these results are shown in Table 2.12. It will be noted that Diefallah's figures all relate to the use of control points : in spite of the large number of GCPs available, no attempt was made to use some of them as check points.

No. of Control Points	No. of Orientation Elements	No. of Control Points	RMSE (metres)			
			ΔX	ΔY	ΔZ	ΔZ*
32	4	06	±61	±85	±21	-
		10	±45	±77	±26	-
		15	±59	±89	±13	±14
		20	±52	±81	±10	±20
		32	±50	±81	±09	±09
	6	10	±45	±40	±15	-
		15	±34	±46	±13	±13
		20	±35	±43	±12	±10
		30	±34	±37	±10	±12
		32	±33	±25	±09	±09
23	4	06	±50	±67	±20	-
		10	±52	±65	±21	±28
		15	±43	±60	±20	±22
		23	±42	±58	±19	±20
	6	06	±48	±24	±22	±10
		10	±45	±23	±18	±2.3
		15	±27	±20	±15	±1.7
		20	±27	±19	±14	±1.7
		23	±25	±19	±14	±1.6

Table 2.12 RMSE values of residuals at reference points (Diefallah, 1992).
ΔZ* Root Mean Square Error in Height after Reducing the Effects of the Observation Errors.

It is quite difficult to see the value of Diefallah's tests when the stereo-model has not been formed in the analytical plotter which was simply used in comparator mode.

2.2.6 Accuracy Tests Carried out in China on Various Stereo-images

Chen (1992) from the Xian Research Insitute of Surveying and Mapping in China reported the results of accuracy tests carried out using three different stereo pairs, labelled STF (France), STC (China) and STU (USA). He had developed a group of programs for the simultaneous bundle adjustment of SPOT scenes using orbital data and a few ground control points. In the tests accompanying the description of his mathematical modelling and photogrammetric solution, Chen mainly concentrated on the effects of using or not using ephemeris data with his solution. No details are given in the paper regarding the location of the test areas or source of the ground control point data. It was clear from the tests that the errors due to Earth rotation should be removed before adjustment in order to ensure the reliability of the solution. The effect of using the ephemeris data was clear in those cases where the number of GCPs is small, resulting in an improvement in accuracy. The results of the various tests carried out by Chen are given in Table 2.13.

Scene	Status	No. of Points		RMSE at Control Pts.(m)			RMSE at Check Pts.(m)		
		Control	Check	X	Y	Z	X	Y	Z
STF Incidence	With the rotation correction	34	50	±6.2	±8.5	±1.5	±10.5	±15.1	±5.0
		18	66	±5.6	±7.1	±1.2	±11.8	±14.7	±6.2
		9	75	±1.9	±4.1	±1.0	±11.4	±15.4	±6.2
L: 25.0 R:26.2 B/H = 0.95	Without the rotation correction	34	50	±9.9	±8.9	±1.7	±12.7	±16.0	±9.1
		18	66	±9.0	±7.9	±1.6	±13.0	±16.5	±9.4
		9	75	±5.1	±6.2	±1.0	±16.1	±22.1	±11.9
STC Incidence	With the ephemeris data	25	32	±5.2	±6.1	±2.0	±13.2	±14.3	±7.8
		15	42	±4.8	±6.9	±1.5	±14.5	±14.6	±7.9
		5	52	±0.8	±1.4	±0.7	±14.6	±16.0	±8.8
L:14.8 R:16.5 B/H = 0.56	Without ephemeris data	25	32	±4.9	±5.7	±1.5	±13.9	±15.5	±8.5
		15	42	±4.7	±5.9	±1.2	±15.7	±15.4	±8.9
		9	48	±3.5	±4.1	±1.2	±16.7	±17.5	±9.9
STU Incidence L:12.9 R:8.9	With the ephemeris data	25	23	±5.1	±8.7	±1.7	±16.1	±16.2	±7.1
		15	33	±4.7	±8.8	±1.4	±15.5	±16.1	±7.2
		9	39	±2.2	±5.3	±1.7	±16.4	±17.4	±8.1
		5	43	±0.9	±1.2	±0.4	±16.0	±17.7	±8.9
	Attitude	0	48				±221.5	±250.2	±36.2
B/H = 0.38	With the ephemeris data	25	23	±4.7	±7.9	±1.5	±15.9	±18.1	±18.2
		15	33	±4.7	±8.8	±1.4	±17.2	±16.3	±7.9
		9	39	±2.0	±5.3	±0.8	±16.0	±19.6	±13.3

Table 2.13 Accuracy tests of different stereoimages in different areas.

In the STF test, the orbital data were not included. The results demonstrated the practical effects of Earth rotation: it is obvious from Table 2.13 that the smaller the number of GCPs, the more important the correction for Earth rotation. The test indicated that the error due to Earth rotation can be removed if the coordinates of the image points had not been corrected previously. It is also clear from the results of the STC and STU tests included in Table 2.13, that, when the orbital parameter data is used, the accuracy is improved. Even with a small number of control points (5 to 9), the accuracies achieved are comparable to those from 18 to 34 points. In the STU test, the attitude drift rates were employed. Chen believed that the result of his tests indicate that it is possible to process SPOT scenes without GCPs at a "special level of accuracy" - which is rather difficult to believe. The other conclusion from this test reached by Chen was that the accuracy of his solution would be improved with the improvement in the accuracy of the orbital data - which - to say the least - is a rather obvious conclusion.

2.2.6.1 Test over the Tangshan Area (China) Reported by Zhong

An accuracy test of a stereopair of SPOT images of the Tangshan area in China has been reported by Zhong (1992) of the Research Institute of Survey and Mapping in Beijing. The SPOT Level 1A stereopair had an overlap area of 90%, and a base-to-height ratio of 0.5. Ground control points and check points were acquired from 1:10,000 and 1:50,000 scale maps. Seventeen ground control points were used to compute the exterior parameters of the images, while 80 check points were used for a comparison of the ground coordinates acquired from the orientated stereoscopic model with the corresponding values extracted from existing maps. The test was performed on the Chinese-built JX-3 analytical plotter using software designed and written by Zhong and based on the use of a quadratic polynomial to model the attitude values of the individual lines of the SPOT image. The RMSE values obtained for the 40 check points obtained from the 1;10,000 scale maps were ± 8.1m in X; ± 8.2m in Y; and ± 5.7m in Z. For the other 40 check points obtained from the 1:50,000 scale maps, the RMSE values were ± 11.9m in X; ± 12.7m in Y and ± 6.9m in Z. These are truly remarkable figures given the accuracy of control data acquired from 1:50,000 scale maps, where an RMSE of ± 0.3mm in planimetry on the map is equivalent to 15m on the ground.

2.2.7 Sør Rondane Mountains Test

Pattyn (1992) of the Free University of Brussels in Belgium presented the results achieved during a project concerned with mapping from a Level 1A stereo-pair having a base-to-height ratio of 0.75, and covering the central part of the Sør Rondane Mountains in Antarctica (located at 72°S, 25°E). The software used appears to have been developed by Pattyn himself based on various models previously published elsewhere. For his test, eight geodetic points were used as control points for the geometric correction model, and 28 check points were collected from an existing topographic map of the area at 1:50,000 scale. To test the geometric correction accuracy using the digital image processing system, the stereoimages were geocoded using the control points. Parallaxes were calculated for the control points, from which three-dimensional coordinates were obtained. The results of the accuracy test is shown in Table 2.14.

Check Points	RMSE		
	X (m)	Y (m)	Z (m)
28	±18.3	±11.5	±19.9

Table 2.14 Model accuracy for the Sør Rondane images

2.2.8 Geometric Accuracy Test Reported by Yeu

Another study was carried out by Yeu et al. (1992 a, b) from South Korea to improve the accuracy of the three-dimensional model through analysis of the optimum polynomial used with the exterior orientation for each processing Level. This improvement was made through the introduction of additional parameters in the geometric adjustment of image distortion, and through the elimination of gross errors in the input data. Tests were carried out for three different processing levels - Levels 1A, 1AP and 1B - of the satellite images. Hard copy Level 1AP and 1B transparencies were used where image coordinates were acquired using a Zeiss P2 Planicomp analytical plotter, while the Level 1A data was used in digital format where the image coordinates of the GCPs were obtained using the ERDAS image processing package. All the images used were for an area located near the west coast of South Korea acquired from different orbits, with a base-to-height ratio of about 0.57. The total number of the ground control points (GCPs) used was 23; 13 of these were used as control points and 10 acted as

check points. These points were acquired by ground survey using EDM instruments and by digitising from 1:25,000 scale and 1:50,000 scale topographic maps.

The exterior orientation parameters employed for each pre-processing level indicated that for Level 1B, a 15 parameter polynomial was optimal, while for Level 1A and 1AP, a 12 parameter polynomial was best. The results of the bundle adjustment for each case with the optimal polynomial as shown in Table 2.15 indicated that the Level 1AP photogrammetric film products are more accurate in positioning than Level 1B due to their geometric stability; indeed they are even more accurate than those achieved using Level 1A imagery. To design a logical adjustment system for positioning, appropriate additional parameters were introduced to the polynomial.

Exterior Orientation Parameters	Processing Level	RMSE at Control Points (m)		RMSE at Check Points (m)	
		ΔPl	ΔZ	ΔPl	ΔZ
15	1B	±10.0	±18.4	±14.0	±13.8
12	1AP	±7.1	±12.0	±10.1	±11.3
12	1A	±10.3	±15.0	±10.8	±6.4

Table 2.15 3-D Positioning Accuracy with different processing levels.

Also, a simultaneous adjustment method for the detection and elimination of gross errors was developed for studying the effects of different adjustment methods. For comparing accuracies according to adjustment method, two cases were studied. The first case involved the use of the Level 1AP stereo-pair with GCPs collected by ground survey; the second case utilised the Level 1A stereo-pair with GCPs taken from 1:50,000 scale maps. This second case was intended to represent the situation where mapping had to be carried out for an inaccessible area. For this analysis, a self-calibration bundle adjustment with 18 variables was selected, and a simultaneous adjustment method for the detection and elimination of gross error was developed. After adjustment, the accuracy of the check points improved uniformly to less than 10m, while the accuracy of the second case was improved by 10% for height and about 5% for the planimetry - see Table 2.16 .

Case	**Without Additional Parameters**				**With Additional Parameters**			
	Control Points (m)		**Check Points (m)**		**Control Points (m)**		**Check Points (m)**	
	ΔPl	**ΔZ**	**ΔPl**	**ΔZ**	**ΔPl**	**ΔZ**	**ΔPl**	**ΔZ**
1	±7.1	±12.0	±10.1	±11.3	±6.2	±9.8	±9.0	±9.5
2	±16.6	±36.1	±38.3	±26.1	±16.6	±31.5	±38.0	±20.6

Table 2.16 Accuracy analysis with additional parameters in terms of RMSE values.

2.3 Strips of SPOT Stereo-models Measured by Space Triangulation

Besides the tests of individual SPOT stereo-pairs, a few results have been published for the accuracy of space triangulation of SPOT stereo-pairs

2.3.1 South France Test Reported by Veillet

Veillet (1990) of IGN reported the results of carrying out a triangulation and block adjustment of SPOT stereo-pairs with the aim of lowering the number of the GCPs required. The test area used by her for the evaluation of space triangulation was that located in the south-east of France previously used for tests of individual stereo-pairs by IGN, UCL, etc. It consisted of four strips of SPOT stereo-image data, each of them comprising four images. This area was selected due to the availability of a large amount of control and check point data. In total, about 560 ground control points had been acquired from aerial photogrammetric measurements, topographic maps and field survey. The triangulation and block adjustment software had been written in-house by IGN for experimental use and ran on a Vax 3200 computer. The SPOT images were in film form generated in-house by IGN from a Level 1A CCT. The measurements were made with a Matra Traster analytical stereoplotter. This equipment can handle strips with controls distributed widely over them. A preliminary adjustment was computed using all the available points as control points to check their quality. After eliminating the points with high residual errors, the results of the computation were stored as a reference set. The RMSE values of the differences between the adjusted and the known coordinates of ground points were ± 7.9m in planimetry and ± 3.9m in altimetry.

The result of tests carried out on a single stereo strip in terms of the RMSE values of the residual errors at the control points were ± 15 m in planimetry and ± 10m in altimetry using only two control points, one located on the west edge and the other on the east edge of the strip. This was done to evaluate the minimum number of GCPs required to control a single stereo strip. With three points, the accuracy achieved was around ± 12m in planimetry and ± 6m in altimetry. With four points, the accuracy became still better. For the whole block using four control points located at the four corners, the RMSE values on 520 check points were ± 8.6m in planimetry and ± 5.3m in altimetry; with six

points, the accuracy reached was ± 7.9m in planimetry and ± 4.3m in height. These are quite remarkable figures in that they are as good as the best figures for the accuracy of a single stereo-model and better than most achieved with individual stereo-models.

2.3.2 OEEPE Test Reported by Dowman

Dowman (1991) reported on the results achieved with a test of triangulation of SPOT data which had been carried out under OEEPE auspices by six centres that participated fully in the test; while two additional organisations (UCL (O'Neill) and Trifid) also contributed to it. The OEEPE organised this test over IGN's test area in south eastern France to establish the accuracy that could be achieved when determining a set of control points from a strip of stereo SPOT data, and to determine the number of control points that would be necessary for the purpose. Also it aimed to investigate the way in which the information provided by satellite tracking and on-board measurement of the attitude and positional values can be used in the triangulation of SPOT data. Finally the intention was to compare the different methods that were available for the triangulation of SPOT data at that time.

The data consisted of two strips of stereoscopic images, each of four models, for which 255 ground control points were provided by IGN: these were used both to control the strips and to check the accuracy of the triangulation. A 10 control point configuration was specified by the organisers of the test. The participants were provided with the SPOT data and the ground control point information to carry out the triangulation and to determine the coordinates of the check points. However UCL (O'Neill) and Trifid carried out their own evaluation and did not use the specified control point configurations and their results were therefore treated separately. The SPOT images were supplied to the participants either in the form of a Level 1A CCT, or as second generation Level 1A film diapositives. In fact, all of the participants used hard copy film transparencies in analytical plotters from different system suppliers.

The basis of all the mathematical models is similar except for the UCL (O'Neill) method (which employs an orbital model with relaxation using conjugate points) and that from Hannover using additional parameters. All use a model which describes the orbit in

terms of orbital parameters or coordinates with constraints, and attitude values in terms of a polynomial, and relate object space to image space with collinearity equations. This can be described as a special form of bundle adjustment. The majority - except UCL (Gugan), which could only deal with a single image or individual strip - use conjugate points in the solution but the methods differ in the use of constraints and the method of determining the initial values of the unknowns. By contrast, the University of Hannover used a bundle adjustment that is based on the BINGO block adjustment for use with close-range photographs and the use of additional parameters to allow for the different geometry of SPOT. Finally the UCL (O'Neill) method uses the SPOT header data and conjugate points only to carry out a relative orientation.

The coordinates of the check points provided by the main participants after carrying out the triangulation were compared with the given ground coordinates determined by IGN. The RMSE values of the residual errors in planimetry and height achieved by each of the participants using 10 ground control points are shown in Table 2.17.

Research centre	**Mathematical model**	**RMSE values in metres**	
		ΔP	**ΔH**
Milan	Orbital parameter model developed by De Haan (1991)	±16.5	±11.5
CCM	Multi-projection centre model developed by Kratky (1988)	±21.1	±6.7
Hannover	Additional parameter model developed by Konecny et al (1987)	±13.5	±6.4
Queensland	Orbital parameter model developed by Priebbenow (1991)	±13.3	±6.8
IGN	Bundle adjustment with orbital constrains (unknown)	±7.6	±4.9
UCL	Orbital parameter model developed by Gugan (1987)	±16.1	±7.3

Table 2.17 RMSE values obtained from the OEEPE accuracy tests of a common SPOT scene using different mathematical models (Dowman, 1991).

In fact, the 10 control point configuration was specified using 20 control points. The various configurations that were used involved 20, 10, 6, 4 and 2 points arranged in different distributions. Table 2.17 gives the results for one case of the control point configuration using 10 ground control points. The CCM and UCL (Gugan) solutions did not produce results for all control point configurations, because their models could not obtain a solution without a minimum number of control points. For UCL, this is because single image space resection was used without support from conjugate points. While, in

the case of the CCM method, the solution failed due to the ill conditioning and singularity of the solution. The results for 20, 10 and 6 GCPs respectively were all very similar except in the case of CCM where the results using 10 control points was worse than those using 6 points. It was also found that a big difference occurred between the UCL and IGN results in those cases where more control points were being used. The best result was obtained by IGN with 10 ground control points, even better than the results with 20 GCPs. The RMSE values of the residual errors with the IGN method were ± 7.6m in planimetry and ± 4.9m in height, followed not too closely by these from Hannover and Queensland with RMSE values of around ± 13.5m in planimetry and ±6.5m in height. Once again the results achieved by IGN are quite remarkable.

2.3.3 Djibouti Test Reported by Veillet

As a follow-on to her test of the south-eastern France data, Veillet (1990) reported the results of the triangulation undertaken by IGN for the Djibouti project to produce maps at 1:200,000 scale over the whole of that country and 1:50,000 scale over one-fourth of the area. The whole country was covered by 16 SPOT stereo-pairs. The field survey operations were undertaken in late 1988 using GPS sets to establish the positions and heights of 30 ground control points, supplemented by additional height points located on hill tops and along the coast. This was followed by a spatial triangulation and block adjustment of the SPOT stereo-pairs. The measurements were made on a Matra Traster analytical plotter, and much the same results were got as for the French tests. Using 24 planimetric and 49 height control points, the RMSE values of the residual errors at the control points after block adjustment were ± 5.7m in X; ±6.2m in Y; and ±4.9m in Z; and ±6.8m at 80 independent check height points. Another test based on the use of 6 ground control points gave ± 7m in both X and Y for 18 plan check points, and ± 6.5m for the 123 check height points used. These are again quite astonishing figures, especially given well defined cultural features found in metropolitan France.

2.4 Summary and Analysis of the Published Results

By far the best results that have been published both for single models and space triangulation of SPOT Pan stereo-pairs are those achieved by IGN and by Dr. Toutin of

CCRS (who carried out his original research into the modelling of SPOT imagery at IGN). RMSE values of ±10m in planimetry (equivalent to one pixel) and ±3.5 to 5m (less than half of pixel) have been reported in their various tests. Presumably this is the result of having optimum conditions for the tests, including an excellent modelling of the SPOT orbital track; good geometry in terms of the base-to-height ratio used; very high quality ground control points for use both as control points for orientation and as independent check points; and first class measurements of the image coordinates (including discarding any slightly suspect points).

By contrast, most of the results published by other researchers are somewhat poorer. This is noticeably the case in terms of planimetric accuracy where many of the results achieved by reputable photogrammetric institutions such as these at UCL, Hannover, etc. are noticeably greater, with RMSE values mostly in the range ±12 to 15m. Similarly with the corresponding RMSE value in elevation - at best, these tend to be in the range ±5 to 8m. It must be presumed that the conditions under which these tests have been conducted have not been optimised to quite the same degree as these carried out by IGN and in Canada.

It is also quite noticeable how few results have been published regarding the accuracy that can be achieved using SPOT Level 1B stereo-pairs. This is quite surprising given the fact that this type of imagery is very popular and is in widespread use among the geoscience, geophysical and geoexploration communities. The reasons for this popularity arises from the fact that Level 1B images have had substantial geometric processing applied to them, including these for Earth rotation, Earth curvature, tilt angle, etc. This results in an image whose geometry approximates to that of a map, though it still contains the displacements due to terrain relief. With the few tests carried out on Level 1B stereo-pairs, the results have been markedly poorer than these achieved with Level 1A stereo-pairs. Thus, in the comparative tests involving both Level 1A and Level 1B stereo-pairs reported by Gugan and Dowman (1988), both the planimetric accuracies (±28 v. 33m) and height accuracies (±10m v. ±17m) obtained at the check points were considerably poorer. Poorer results were also published by Yeu et al (1992) both for planimetry (±11 v. ±14m) and height (±6.4 v. ± 13.8m). There appears to be no good

reason for such differences or discrepancies. Thus this particular matter is one that will be addressed in the work carried out by the author.

It can be seen from the previous studies reviewed in this chapter that most of the tests have been carried on analytical plotters using different kind of hardware and software and different kinds of mathematical models for SPOT orientation. Comparatively few studies have been carried out using the photogrammetric modules provided with digital image processing systems. Again this is a matter that will be addressed in this dissertation.

2.5 Conclusion

In this chapter, the published work on tests of the geometric accuracy achieved with the orientation of single stereo-pairs and with strips of SPOT stereo-models measured by space triangulation have been reviewed. Quite different results have been achieved in the various tests with the orientation of SPOT images and the accuracy of the final coordinates at control and check points. These depend largely on the quality of the control points; the base-to-height ratio; the quality of the images; the nature of the terrain; and the mathematical models used. The best results obtained from stereo-pairs occur when the GCPs have been acquired by ground survey or from precise measurement on aerial photographs, in conjunction with the use of a rigorous mathematical model. The number of test fields having good quality control points is limited and indeed many of the more significant experiments carried out in the test field located in south eastern France set up by IGN.

It must also be noted, that apart from IGN and CCRS, most of the geometric accuracy tests for SPOT orientation have been carried out in universities and research organisations and most of the systems and software used for experiments were developed by these universities. Till now, few have used commercially available systems and only one or two have attempted to verify the quality of the data that is generated by these systems. This is a matter that will be investigated by the present author.

As mentioned above, the main concern in this chapter has been to review a representative sample of the previous published research into the geometric accuracy of SPOT images treated either as a single stereo-pair or as strips of SPOT stereo-pairs measured by space triangulation. In the next chapter, the published results of the previous studies into the validation of digital elevation models (DEMs) will be presented and discussed.

CHAPTER 3: PUBLISHED RESULTS ON VALIDATION OF DEMs EXTRACTED FROM SPOT STEREO-PAIRS

3.1 Introduction

Following on from the results of the geometric accuracy tests of SPOT stereo-pairs published by a number of researchers that have discussed in the previous chapter, a review of the tests previously carried out to validate the DEMs that can be extracted from SPOT stereo-pairs will be given in this chapter. This matter is of especial importance in the context of the author's experimental work carried out over the Badia area - since this involved the extraction and validation of the DEMs produced by the systems that are currently available from commercial remote sensing system suppliers. In this context, it is quite noticeable how few tests have been carried out into the accuracy of the elevation data that can be extracted from SPOT stereo-pairs. Of course, part of the problem in carrying out such tests is the difficulty in doing so over the large area (60 x 60 km) covered by a single SPOT stereo-pair and in finding elevation data of a high enough density and quality to act as a reference data set to allow the validation of the DEM data to be achieved.

3.2. Tests Carried Out in the UK

Most of this work has utilized the systems and software developed by Gugan at UCL for use with SPOT stereo-pairs.

3.2.1 South -West Cyprus Test Reported by Ley

The same stereo-model and systems that were used by Ley (1988) and reported in Section 2.2.2.2 were also used for DEM extraction. The film diapositives used with the analytical plotter suffered from atmospheric haze, whereas the digital images derived from the data gave much sharper features after enhancement. Once the stereomodel had been set-up, the role of the operator was very different. In both UCL methods using the Kern DSR-1 analytical plotter and the I^2S-based digital stereo-plotter in conjunction with UCL's own software, the program was used to drive the measuring mark through the model to the successive positions of the nodes of the final DEM at a grid interval of

100 m. At each node, the operator then measured the height of the terrain manually by placing the floating mark on the ground and recording the X, Y, Z coordinates. For this work, an inexperienced operator was employed to give a worse case result. The smoothness of the operation on the DSR-1 using the KERN MAPS package was in contrast to that of the I^2S system where some problems were encountered with the software. The result of these problems was that the nodes on the DEM derived from the SPOT imagery did not coincide with those of the reference DEM.

By contrast, the MDA Meridian software allowed the extraction of height information automatically via image matching. This system employs an hierarchical approach using low to high frequency filters so that the boundaries of large features are matched initially. Thus the boundaries are matched through correspondence of shapes (i.e. by feature based matching) and not by the correlation of pixels. The coordinates of these matched boundaries from each image were then subtracted to produce the stereoscopic parallax. These parallaxes were transformed through an epipolar projection into the X, Y, and Z coordinates of the map projection and coordinate system. Interpolation routines were included in the software to allow for the production of a gridded DEM. In this case, a 25m gridded DEM was produced to permit a comparison with the reference DEMs. These had been produced from the 1:50,000 scale maps having a 20m contour interval (with some 10m supplementary contours) to cover the whole area of the stereo model. Also a DEM (area number 10 in Table 3.1) had been produced from 1:25,000 scale maps covering some areas with a contour interval of 5m.

In fact, 20 individual small areas were chosen within the SPOT stereo-overlap for test purposes. However, six of these were affected by cloud, so only 14 areas were actually tested. The heights for the 14 grid elevation matrices were measured in the photogrammetric systems, nine being 1x1 km in area, while four areas were 1 x 2 km in area and one was 3 x 3 km in size. The figures given in Table 3.1 were derived from the three different systems being tested. The measured height values were then compared with those in the same positions derived from the 1:50,000 scale maps after a interpolation from their contours.

Area	Size (km)	DSR-1		I^2S		MDA	
		Mean (m)	σ (m)	Mean (m)	σ (m)	Mean (m)	σ (m)
1	1 x 1	7	±16	7	±18	-19	±17
2	2 x 1	3	±16	18	±22	-	-
3	2 x 1	7	±12	20	±14	-26	±9
6	1 x 1	2	±15	8	±9	-15	±11
10	2 x 1	1	±8	14	±5	-16	±4
12	1 x 1	16	±24	1	±21	-17	±22
13	1 x 1	20	±29	1	±23	-26	±21
14	1 x 1	15	±11	14	±9	-22	±13
15	1 x 1	20	±12	21	±10	-26	±11
16	1 x 1	4	±12	28	±18	-23	±11
17	1 x 1	16	±11	33	±11	-23	±11
18	1 x 1	16	±11	26	±12	-22	±10
19	2 x 1	23	±10	36	±13	-19	±12
20	3 x 3	20	±8	-	-	-22	±6
Overall		**11**	**±15**	**17**	**±15**	**-21**	**±13**

Table 3.1 Differences in height between the reference DEMs and SPOT derived DEMs (Ley, 1988).

It should be stressed that the three systems are not directly comparable because of the differences already outlined above. For example, the DSR-1 system provides the heights of each node directly from the imagery whereas both digital systems involve an interpolation step. Also the MDA Meridian system used automatic image matching while, in the other two systems, the DEM measurements were made manually and visually by an operator. Table 3.1 shows the differences in height between the reference DEMs and the SPOT derived DEMs. In the three tests, the systematic error was highly significant and was made up of a number of component errors. Later, the DEM measurements had been carried out again on the DSR-1 by an experienced operator, when the systematic error was very much reduced. This meant that much of the systematic error present in the test with the hard copy images on the DSR-1 was due to operator inexperience either in setting up the model or in not placing the floating mark consistently on the ground. The second matter that came to light in Ley's analysis was the location of the GCPs relative to the mid-point of the test area or chip. It was found that the systematic error in the model increased as a result of increasing remoteness from any control point.

The MDA system created elevations at a 25m grid interval, whilst the other two systems produced the elevation data on a 100 m grid. The results from the MDA and the I^2S systems were said to reflect the error of the entire model, whereas those of the DSR-1

system were confined to the collected points only. The interpolation error produced by the MDA system was estimated to be about 8m, whilst the I^2S system introduced about 10m. This is probably due to the density of the collected points rather than the algorithms used. In general, overall RMSE values of ± 13m to ± 15m in elevation were recorded for the 14 areas tested. Errors were greatest in the steepest terrain with poor contrast. The two digital systems produced slightly better results than those produced by the DSR-1.

3.2.2 Validation of DEMs Reported by Theodossiou and Dowman

As a follow-up to the work by Gugan and Dowman reported in Section 2.2.1.2, further work was carried out at UCL on the accuracy of DEMs produced by manual and visual observations with the Level 1A stereo-model of the Aix-en-Provence area having a base-to-height ratio of 0.84 (Theodossiou and Dowman 1990). The hard-copy film transparencies were again set up and measured on UCL's Kern DSR 1 analytical plotter using 10 ground control points supplied by IGN. The same instrument was also used for the triangulation and the generation of elevation data from two strips of 1:30,000 scale aerial photographs amounting to 10 stereo-models. These operations produced a digital elevation matrix at a 30m grid spacing amounting to 95,865 points; this data was considered to be error-free for the purpose of the DEM accuracy evaluation. The test area covered by the SPOT stereo-model was divided into 16 blocks for this evaluation. Later a second SPOT stereo-model for the same area with a base-to-height ratio of 0.91 was acquired and measured on the basis of 15 ground control points derived from the aerial triangulation of 1:60,000 scale aerial photography. Six DEM blocks amounting to 5,400 points with a 100m grid interval were measured on this second stereo-pair.

The fit of the first SPOT stereo-model after exterior orientation gave an RMSE value in terms of vector error of ± 8.7m at the control points, while the RMSE value of the planimetric vector error at 20 check points was ± 15.3m. For the second model, the corresponding RMSE value for the vector error was ±7.8m at the control points. The results of the comparison between the elevation data derived from the aerial photographs and the SPOT elevation data are given below in Tables 3.2 and 3.3.

DEM Block	No. of Compared Points	Mean (m)	RMSE (M)	SD (m)	Average slope (%)
1	183	-3.9	±11.2	±10.5	26.1
2	514	4.8	±16.9	±16.2	35.5
3	514	-4.6	±15.8	±14.4	41.7
4	218	3.5	±16.2	±15.8	27.3
5	252	-3.8	±9.7	±8.9	30.3
6	708	4.3	±19.4	±18.9	43.3
7	708	16.0	±28.2	±23.2	64.6
8	300	4.6	±12.6	±11.7	35.4
9	249	-1.3	±6.0	±5.9	28.5
10	708	-3.5	±8.8	±8.1	36.4
11	708	11.8	±27.5	±24.9	66.4
12	301	9.4	±18.0	±15.3	38.6
13	185	3.0	±5.7	±4.8	7.6
14	531	6.0	±8.6	±6.1	11.9
15	531	0.3	±12.9	±12.9	58.3
16	223	0.8	±10.0	±10.0	31.6

Table 3.2 Comparison of elevation data from aerial photography and first SPOT stereo-pair.

Data Set	No. of Compared Points	Mean (m)	SD (m)	Minimum-Maximum Elevation Differences		Average Slope (%)
1	177	-3.8	±6.9	-17.84	10.08	26.2
2	640	4.2	±10.8	-26.65	58.53	35.5
3	650	4.9	±10.7	-37.90	42.62	41.7
5	157	-6.2	±7.5	-46.94	11.14	30.3
6	664	0.1	±12.2	-95.64	55.98	43.3
7	648	9.8	±18.1	-29.86	82.57	64.6

Table 3.3 Comparison of elevation data from aerial photography and the second SPOT stereo-pair.

3.3 Validation of DEM Reported by Diefallah.

As mentioned already in Section 2.2.5.2, Diefallah (1990) has also reported on the accuracy of the heights derived from SPOT stereoscopic data of south-west Sinai dated 1987, and forming a base-to-height ratio of 1.0. The two images had been supplied in the form of prints and diapositives with an approximate format size of 18cm x 18cm and were measured in a Wild BC2 analytical plotter. A total of 20 ground control points (GCPs) had been derived from the Egyptian Military Survey 1:50,000 scale topographic maps having a 10m contour interval. The image coordinates of points on the SPOT images were measured on the BC-2 in grid mode with a spacing of 1km. Ground coordinates for these points were then determined by applying a space intersection method and, from these values, contour lines were interpolated at a contour interval of

20m using the Wild CIP (Contour Interpolation Program) available with the software package of the BC2. When the elevation points used are 1km apart, the quality of the resulting contours cannot be expected to be very high.

For the DEM accuracy test, 66 check points were used. These points were identified and measured on the 1:50,000 scale topographic map and in the SPOT stereomodel. The RMSE values of the residual errors in height obtained at the 66 check points were ±14.5m and ±11.0m before and after filtering respectively. Using 56 check points, by removing the check points with big errors, the RMSE values in height were ± 12.0m and ±9.4m before and after filtering respectively. Essentially - in terms of the small sample of points used - this test is really more like a test of the geometric accuracy of a single stereo-model (like these described in Chapter 2) than a true DEM test.

3.4 Tests Carried out in Australia

A first test of the accuracy of a DEM from a SPOT stereo-pair was carried out by Priebbenow and Clerici (1988) in Queensland. Afterwards a number of tests have been carried out by Professor Trinder and his colleagues and collaborators at the University of New South Wales (UNSW). These tests have concerned both the use of the SATMAP software produced at UNSW and the use of several software packages for the extraction of DEMs from SPOT stereo-pairs that have been produced elsewhere by other organisations.

3.4.1 Validation of DEM of Australia Stereo-pair Reported by Priebbenow

Priebbenow and Clerici (1988) reported their investigation into the suitability of stereoscopic SPOT imagery for the production of digital terrain models, orthoimages and conventional topographic line maps from SPOT stereoscopic imagery in Australia. This project was carried out jointly by members of the Australian Key Centre in Land Information Studies located in Queensland. The project was carried out using two overlapping SPOT panchromatic images covering the Brisbane metropolitan area, and extending westwards into relatively rugged, forest terrain, and southwards into a rural

area. The images were acquired 19 days apart in July and August 1986, with view angles of 22.6° L and 25.4°R. Aerial photography was used to derive the data against which the SPOT-derived DEM could be compared.

A Zeiss Planicomp C 100 analytical plotter was used to carry out the measurements on film images of both the aerial photographs and the SPOT images. For the latter, the mathematical modelling and the software package were both produced locally. A set of 210 points that could be identified both in the SPOT images and in the existing controlled aerial photography over the test area were selected and measured from the photography and the SPOT imagery. 22 points from this set were rejected, having been classified as poor points. 27 good ground control points that were well distributed over the images were selected as control points. The 3D coordinates of the remaining 161 points were then calculated using the measurements made on the SPOT image. For all 188 points, the differences between the ground coordinates derived from the SPOT images and those from the photography were calculated. The RMSE values of the residual errors in Easting, Northing and Planimetry were ±4.2m, ±4.0m and ±6.2m respectively, while the RMSE value of the residual errors in height was ±3.1m. Essentially this can be considered to be an extended geometric accuracy test, with results that fall in the same top-class category as those from IGN and Toutin discussed in the previous chapter.

For the DEM accuracy test, profiles covering the area of a 1:25,000 scale map sheet were measured at a 100m interval using the SPOT imagery. Elevations at a 25m grid interval were then interpolated from these measurements using the HIFI DEM package. A grid of heights at 50m spacing was measured over the same area using the controlled aerial photography and again elevations were interpolated at a 25m interval using the HIFI package. The accuracy of the SPOT-derived DEM was then assessed by calculating the height differences between the two data sets for every point within the interpolated grid. The RMSE values derived from these differences in height was ±5.4m - which is a startlingly good result.

3.4.2 Sydney Test Reported by Anglerand et al

The paper by Anglerand et al (1992) concentrated first on the SATMAP modelling and software package produced at UNSW for use with a Wild BC2 analytical plotter both for mapping and for the production of DEMs from SPOT stereo-pairs using automatic image matching techniques. The latter involved the measurements of 10 GCPs for the orientation of the two images followed by a Delaunay triangulation of these points (which provided predictive information on the area that should be matched) and the actual image matching of these areas. This used feature-based matching followed by area-based matching for the determination of the final parallaxes or disparities from which the elevation values were calculated.

For the accuracy test, a DEM was observed manually on the Wild BC-2 instrument using the SATMAP package to produce 55,000 elevation points at a 250m interval over the area around Sydney covered by a Level 1A stereo-pair with a base-to-height ratio of 1.0. When tested against the elevation data provided by maps at a scale of 1:4,000, the accuracy in terms of the RMSE value of the elevation differences was ±5 to 6m. A further comparison was made between 1,700 points in the manually observed DEM and 9,000 points over the same area produced by image matching. The comparison of the two sets of values gave an RMSE value for the elevation values of ±9m, after all those values having differences greater than three times the RMSE value (equal to ±27m) had been discarded - amounting to 5% of the total number of points that were sampled.

3.4.3 Validation of DEMs of Sydney and Other Areas Reported by Trinder et al

Trinder et al (1994) reported further on the process of DEM determination from SPOT digital images using five software packages available for this operation and they presented the results of tests of the accuracy of the DEMs extracted from these packages. The software packages included the Helava and Associates Inc. (HAI) package; the University College London (UCL) package; the ERDAS OrthoMAX module; the software produced by the Joanneum Research Centre of the University of Graz in Austria; and that developed by the University of New South Wales (UNSW).

Thus the HAI and OrthoMAX packages were from commercial suppliers; the others were from universities. The test of the ERDAS OrthoMAX system was undertaken by the staff in the office of the ERDAS agent in Australia. The test of the HAI package was carried out by staff at the Sydney office of Leica, while the test on the Joanneum package was made by the authors of the package in Austria. Finally the tests of the UCL and UNSW packages were carried out at the University of New South Wales (UNSW).

Two areas in Australia were used for the tests of the accuracies of the DEMs. In the Albury area, the locations and heights of 12 ground control points had been fixed by GPS for the earlier SPOT-1 pair of images covering the test area, but the later SPOT-2 pair of images supplied for this test were displaced from the original pair so that only 7 ground control points were available for use. These points were supplemented by additional points observed on the Wild BC2 analytical plotter on the original SPOT-1 pair with an accuracy in the order of ±5m. The accuracy of the orientation using the combined set of control points, as measured by the RMSE values of the residual errors was of the order of ±5m in E, N, and elevation. The results of the tests on two of the packages (those from UCL and UNSW) for this area are shown in Table 3.4. For the purpose of validating the DEM, 98 additional check points were measured on 1:80,000 scale aerial photographs using the BC2 analytical plotter. The standard deviation values comparing the elevation values from the SPOT stereo-pairs with those from the aerial photographs at these 98 check points were ±11m for the UCL package and ± 14m for the UNSW package. Again the relatively small sample of check points and made this more like the geometric accuracy tests reviewed in Chapter 2.

The Sydney scenes were acquired in 1986 from SPOT-1, when the column noise that affected the system in the early days of its operation had not been corrected. Therefore the images suffered from degraded quality. As mentioned above in the previous Section (3.4.2), the control points had been determined from 1:4,000 scale maps in the metropolitan area and from 1:25,000 scale maps in the rural area. The orientation of the stereo-model resulted in RMSE values for the residual errors at the control points of ±5m to ± 7m in planimetry and less than ±5m in elevation. The check data for the DEMs was derived from the digitised 1m and 2m contours available on 6 complete

1:4,000 scale orthophotomaps. The mean has been computed from the mean of the errors and therefore is the estimated elevation of the datum, while the standard deviation has been computed with the respect to that mean.

The Sydney test comprised 4 different areas (labelled Men, Terry, Badg/Lond, and Regent) lying within the overall stereo-model. Each of these areas was covered by a DEM with several thousand elevation values. The two easiest areas to extract elevation data from the SPOT stereo-pair were Badg/Lond and Regent since they are gently undulating and contained little vegetation. For the Regent area, the standard deviations determined from the various software packages were generally around ±5m or better, but for Badg/Lond area - which includes more vegetation and is steeper - there was some deterioration in the results which varied with standard deviations between ±4m to ±21m. For the two most difficult areas, Men and Terrey, the accuracy in terms of standard deviation values varies from ±7.4m to ±15m in Men and from ±14 m to ±30m in Terrey.

Test area and Type of Ground Cover	Terrain Slope	UNSW Std. Dev. Mean Elev. No. of Points %>30m	UCL Std. Dev. Mean Elev. No. of Points %>30m	HAI Std. Dev. Mean Elev. No. of Points %>30m	ERDAS Std. Dev. Mean Elev. No. of Points %>30m	Joanneum Std. Dev. Mean Elev. No. of Points %>30m
Albury Light to heavy tree cover	Undulating to steep, mean slope 10-15%	**±13.9m** 7.5m 98	**±11.0m** 8.3m 98	-	-	-
Men - Little cover with few trees; freeway	Undulating to steep, average 10-15%	**±7.4m** 5.2m 24,505 0.7%	**±15.1m** 5.3m 4,614 4%	**±5.2m** 3.6m 7,131 0.6%	**±8.9m** -3.2m 24,523 1.1%	**±12.1m** -2.8m 5,950 ≈4%
Terrey - 5% heavy vegetation cover	Very steep, ranging, 10%-50%, mean 30%	**±20.3m** -4.4m 14,880 15%	**±19.5m** -3.2m 2,753 11.7%	**±14.8m** 15.8m 9,247 11%	**±30.0m** 2.4m 14,367 27%	**±14.0m** 4.0m 3,956 ≈7%
Badg/Lond open farmland, sparse trees	Slopes from 0% to 15% mean 5%	**±3.8m** 1.6m 32,083 0.1%	**±21.1m** -0.2m 6,141 4.0%	**±8.6m** 7.6m 29,005 0.55	**±10.5m** 0.7m 32,043 2.3%	**±7.6m** 1.7m 9,508 ≈1%
Regent Suburban, residential	slopes <5%, mean 3%	**±2.4m** -3.9m 15,612 0%	**±2.3m** -4.1m 2,969 0%	**±5.4m** 5.8m 15,199 0%	**±4.6m** -2.7m 15,108 0%	**±4.4m** 0.3m 5,073 0%

Table 3.4 Results from DEM accuracy tests of different packages

All of the packages showed considerable variations in their results. The highest accuracies were obtained from these packages that used the least squares method of image matching. A comparison revealed that generally speaking, except for the Terrey area, with its steep slopes and heavy vegetation cover, the UNSW, HAI, ERDAS, and Joanneum packages gave fairly consistent results. In addition, those packages that are based on the use of image pyramids tended to be more robust than the others. As will be seen later, the work carried out by Trinder and his associates is that which is closest to that carried out by the author - though the latter's project was also concerned with extensive testing of Level 1B stereo-pairs and covered a much larger test area than that used by the UNSW group.

3.5 Tests Carried out in Germany

Curiously, in view of the interest in the development of image matching techniques and terrain modelling in Germany which have resulted in widespread use of software packages such as Match-T (for image matching) and HIFI and SCOP (for terrain modelling), these has been relatively little work published by German organisations of the validation of DEM data from SPOT stereo-pairs.

3.5.1 Heidelburg and Priorat Tests Reported by Heipke et al

Heipke and Kornus (1991) and Heipke et al (1992) of the Technical University of Munich reported the results of two test projects carried out over the Heidelberg area in Germany and the Priorat area in Spain. Software with the aim of automatic derivation of digital elevation model (DEM) data and orthoimages had been developed at the University and the procedures that had been adopted were evaluated by these two practical test projects.

For the Heidelberg area, the images had been acquired in 1988 with a base-to-height ratio of 0.4; a few clouds covered some parts of one of the images. 834 GCPs derived from high altitude aerotriangulation were used as test data in the Heidelburg test. They were assessed to have an accuracy of ±3 m in planimetry and ± 5m in height. These points were first measured stereoscopically on a Zeiss Planicomp P1 analytical plotter

using film hard copies provided by SPOT Image. For the subsequent image matching, 10 GCPs were selected as starting points. The size of the template matrix used for the matching process was set to 19 x19 pixels; 0.6 was selected for the minimum correlation coefficient; 0.1 pixel was defined as the maximum semi-major axis of the error ellipse; 2.5 pixels was the value for the maximum difference to the initial values; and a maximum of 10 iterations was allowed in the adjustment. The results of the point determination are given in Table 3.5.

Number of GCPs	RMSE of Object Coordinates (metres)		
	X	Y	Z
5	±13.1	±21.5	±7.0
6	±13.6	±17.4	±5.5
10	±12.9	±16.2	±6.2
5	±12.8	±15.5	±4.3

Table 3.5 Result of accuracy determination at the control points.

These results showed that the use of five to six GCPs was sufficient in order to obtain accurate results in planimetry for many mapping purposes. The accuracy in Z in terms of their RMSE values lies between ± 5m and ± 7m; obviously the planimetric accuracy is worse by factor 2 to 3 - indeed this is a feature of most tests of SPOT stereo-pairs. According to Heipke et al (1992), this is probably due to the fact that most of the check points were located at the centres of road crossings which lay in relatively flat areas. If a point is measured by accident at the border of the road rather than in the middle, the resulting height will still be correct, although the corresponding X, Y coordinates are not. It is clear also that the accuracy in X is better than Y, due to the fact that, with the linear array sensor used in SPOT, the parallel projection in the flight direction is less stable than the central perspective in the direction perpendicular to the flight path.

From the results, it is also clear that the accuracy is not improved in planimetry but it is improved in height with the use of an increased number of GCPs. With the elements of exterior orientation determined from six GCPs, an intersection was performed for each pair of conjugate points obtained from the image matching. A DEM was then generated using the HIFI program package. In order to determine the DEM quality, heights for the 834 check points were interpolated from the derived DTM and compared with the known values; in this way, an empirical standard deviation of ± 10.8m was obtained.

In the second project, a SPOT stereo-pair with a base-to-height ratio of 0.6 covering the Priorat area in South Catalonia was available, provided by the Institut Cartografic de Catalunya. The image coordinates of nine conjugate points were measured in both images. Additionally about 30 GCPs were provided which were identified and measured in the images; however the measurements were performed in either the left and right image. Image matching was performed as in the Heidelberg test using the 9 control points as starting points. For the bundle adjustment, about 1,300 equally distributed points were selected such that the correlation coefficient of each point is a local maximum. These points were processed, together with seven GCPs in each of the two images and the XYZ coordinates of the projection centres. The heights of the 1,300 check points derived from SPOT stereo-model were then checked against the DTM database of Catalonia having an accuracy of approximately 1 to 2m. The RMSE value of the residual errors at the check points resulted in $Z = \pm 8.8$m.

3.6 Tests Carried out in North America

The results of the tests of the elevation values extracted from SPOT stereo-pairs carried out in North America are of considerable interest in that they all report on the DEMs extracted either by individual commercially available packages (HIVIEW and LANDSCAN) or from a commercial bureau (STX) offering a service to its clients.

3.6.1 Validation of DEM Reported by Brockelbank and Tam

A detailed report on research into the use of different image matching techniques (including feature-based, area-based and hybrid techniques) with SPOT stereo-pairs was published by Brockelbank and Tam (1991). The work formed part of a joint effort by the Alberta Research Council, the University of Calgary and a private company, Applied Terravision Systems, to enhance the LANDSCAN package developed by the company by providing it with the capability of extracting DEMs from SPOT stereo-pairs. While much of the paper is devoted to comparison of the relative efficiencies of the different image matching techniques, it also gave the results of practical tests to validate the resulting DEMs.

The two test areas used were Dinosaur National Monument (DNM) in Colorado in the USA and Red Deer, Alberta, Canada. The former comprised rough undeveloped terrain with an elevation range of 1,230m and few features; the latter is a comparatively flat area with 205m elevation range and comprised a rural area with a patchwork of fields and roads. The DNM area was covered by a SPOT stereo-pair with a base-to-height ratio of 0.88, while the Red Deer area was covered by a stereo-pair having a base-to-height ratio of 0.97.

With regard to the results in terms of accuracy, the DNM stereo-model utilized 8 control points and 39 check points, the RMSE values of the residual errors at the check points being ±12.8m in X; ±13.3m in Y and ±11.7m in Z. The corresponding results for the Red Deer stereo-model where 9 control points and 88 check points were used, were ± 8.5m in X; ±9.6m in Y and ±8.2m in Z at the check points. The DEMs were formed for only a portion of each of the two models - an area of 1,001 x 990 pixels in the case of the DNM model and 3,263 x 2,654 pixels in the case of the Red Deer model. In case of the Red Deer model, the DEM data was tested against elevation data extracted from the 1:50,000 scale map of the area and Alberta survey control point data. The best results were obtained using the area-based image matching technique and gave rise to RMSE errors in elevation for the DEM points tested of ±16.8m for the DNM stereo-model and ± 11.8m for the Red Deer stereo-model

3.6.2 Validation of DEM Reported by Sasowsky et al

Sasowsky et al (1992) from Penn State University reported on the evaluation of the accuracy of a portion of a SPOT DEM relative to reference DEMs and the accuracy of certain derivative products, specifically slope and aspect. Their study area was located on the North Slope of Alaska near the Kuparuk River in the northern foothills of the Brooks Range, approximately 120 km south-west of Prudhoe Bay and is moderately diverse in topographic terms. The test area was around 25 km^2 so it only covered a very small part of the 3,600km^2 of a single SPOT scene.

In this study, a Level 1A SPOT panchromatic stereo-pair was used with a base-to-height ratio of 0.48. The DEM of the area had been purchased from the STX Corporation and consisted of a 211,128 -cell data set. Each cell of this subset of the STX DEM was compared with two reference data sets: one derived from the 1:63,360 scale U.S. Geological Survey topographic map of the area with a 50 foot (15.2m) contour interval, while the other had been derived from a photogrammetrically produced topographic map at 1:6,000 scale with a 5m contour interval. The contour lines of both maps were digitised, and a DEM extracted using a grid interval of 10m. The DEM created from the 1:63,360 scale map had been interpolated from the digitised points on the contours using a search radius of 400m; a 200m radius was used with the 1:6,000 scale map. Both DEMs were created using a linearly decreasing weight for the interpolated points as distance increased from the node. Obviously the data set derived from the 5m contour interval was assumed to be much more accurate due to the higher resolution of the original source map.

Residual errors were generated as the differences of the elevation at each of the 211,128 nodes between the two reference data sets (i.e. the 1:63,360 scale and 1:6,000 scale DEMs) and the test data set of the SPOT DEM. The accuracy obtained in terms of the standard deviation of the differences between the STX DEM and the DEM generated from the 5m contour interval was ±18.5m - which is hardly believable!!. The corresponding accuracy obtained between the STX DEM and the DEM generated from the 15m contour line data was ±13.5m. Thus the STX DEM is in error by 3 to 4 contour intervals compared with the DEM derived from the 5m contour data and less than one contour interval when compared with DEM produced from the 15m contour data. The difference between the elevations given by the two reference DEMs was ±14.1m. It must be said that, to an outside observer if not to the authors of this particular paper, these results were somewhat disappointing. Indeed those relating to the comparison with the DEM derived from 1:6,000 scale DEM are inexplicable.

3.6.3 Evaluation of a DEM Reported by Bolstad and Stowe

Interestingly, a further test of a SPOT DEM produced by the STX Corporation was carried out by Bolstad of the Virginia Polytechnic Institute (VPI) and Stowe (1994). This comprised a comparison of USGS and SPOT-derived DEMs for the area around Blacksburg, Virginia where VPI is located. The USGS DEM had been produced from 1:40,000 scale aerial photography using a Gestalt Photomapper I (GPM) equipped with an automatic stereo correlation unit. The SPOT DEM was produced by the STX Corporation from a SPOT stereo-pair with 16.5° and 17° inclinations respectively using its own image matching algorithm and software package. A total of 42 accurate control points fixed by GPS or available from existing control networks were also identified.

Unfortunately the results given in the paper were not reported in the familiar form of RMSE or standard deviation values. However the range of error experienced at the 42 test points measured by ground survey lay in the range -12 to +7m, whereas that for the STX/SPOT DEM lay in the range -12 to +18m. A comparison was also made between the two DEMs, in which 63% of the differences were between 10m or less; and 90% were less than 22m. Individual differences of up to 82m were found. Much of the test of the comparison involved the analysis of errors in slope and aspect. Nevertheless the two tests undertaken by Sasowsky et al and by Bolstad and Stowe are two of the very few studies of the accuracy of commercially produced DEMs generated from SPOT stereo-pairs. The results cannot be said to be outstanding.

3.6.4 Validation of DEM Reported by Giles and Franklin

Giles and Franklin (1996) of Department of Geography, University of Calgary, Alberta, Canada reported on the test of a digital elevation model (DEM) derived from SPOT satellite imagery for its accuracy both in elevation and in three of its derivative topographic surfaces: slope gradient, incidence value and profile curvature. Their study area is called the Three Guardsmen Upland, and is located in the south-west of the Yukon Territory in Canada. An area of approximately 21 km by 21 km was selected for the test; it comprises moderate to high relief with an elevation range of 1,300m, with steep slopes greater than 55° in some parts of the area.

A SPOT multispectral stereo-pair with a base-to-height ratio of 0.63 was utilised with around one year separation between the overlapping scenes. An automated DEM generation software package called HI-VIEW was employed to generate the elevation data. This uses an area matching technique, with the user controlling the window size. The planimetric resolution (i.e. the grid interval) of the DEM was 20m with elevation values recorded with a step size of 0.15m. The elevation data used for evaluation was extracted from the 1:50,000 scale Canadian National Topographic Survey maps of the area. A total of 122 points were selected randomly throughout the study area. The results of the elevation data accuracy assessment were obtained by calculating the differences between the values from the SPOT DEM and the comparison values from the maps. The RMSE value of these differences in elevation that was obtained was ±21.6m.

3.7 Tests Carried out in Japan

Two validation tests of SPOT-derived DEMs have been undertaken by the Geographical Survey Institute (GSI) which is the national mapping organisation of Japan. Both of these utilized SPOT coverage of Mount Fuji to carry out these tests.

3.7.1 Validation of DEM Reported by Fukushima

In his paper, Fukushima (1988) reported on the accuracy of a DEM generated by digital image correlation methods using three Level 1A SPOT images over the area surrounding Mt. Fuji by applying three different methods for this purpose. Each of the three test areas used for the validation of the elevation data generated by the image correlation were 2 x 4 km in area. The first test area is mountainous with very steep slopes and some areas covered slightly by snow; the second area is flat and is surrounded by a mountainous area; while the third area is covered by coniferous forest and has slopes that are changing gradually.

The accuracies obtained at the ground control points after exterior orientation expressed as RMSE values were ±9.5m in planimetry and ±11.5m in height respectively. For comparison of the DEMs generated by correlation from the SPOT stereo-pairs, grid spaced DEM's were derived from the digitised contour lines of the 1:25,000 scale

topographic maps to form reference data sets. Before undertaking the image correlation process, the y-parallaxes of the three images were eliminated after the parameters of exterior orientation had been determined. The image correlation process was applied to two stereo-pairs with base-to-height ratios of 0.2 and 0.52 respectively. The first pair consisted of the centre and left images of the triplet covering the area giving the base-to-height ratio of 0.2, while the second pair consisted of the centre and right images giving the base-to-height ratio of 0.52. The left and right images with a base-to-height ratio of 0.72 were not used due to the distortion of the two images.

The use of the triplet of images was also employed to improve the accuracy of the DEM by eliminating mismatches and comparing the heights obtained from the two stereo-pairs. The three image correlation methods were applied. The first method employed image matching of the individual stereo-pair. The second method of triplet matching was used, in the first instance to eliminate mismatching using the two stereo-pairs. In the second instance, the method employed the condition of having a common intersection point for the rays from all three images.

A preliminary test was applied to find the specific window size which would gives a good accuracy in image matching for a part of test area in addition to the use of a median filter. Table 3.6 summarizes the results from preliminary tests of the discrepancies between the height extracted from DEM using image correlation with different window sizes and the heights from the DEM extracted from the contours - without use of a filter, while Table 3.7 shows the results using the median filter. The overall results are very poor in terms of both the RMSE and standard deviation values. In general, the use of smaller windows gave better results.

Size of Window	Maximum Errors on Plus (m)	Maximum Errors on Minus (m)	Bias (m)	RMSE (m)	Standard Deviation (m)
5	143	-187	-26.5	±35.8	±24.1
7	137	-165	-26.6	±33.0	±19.6
9	118	-178	-27.4	±33.1	±18.6
11	132	-169	-27.1	±33.1	±19.1
13	62	-187	-27.1	±33.6	±19.9
15	29	-166	-27.4	±34.5	±20.9
19	118	-144	-27.1	±36.4	±24.3
21	94	-170	-27.3	±37.4	±25.5
25	122	-164	-27.6	±40.7	±29.7
29	158	-165	-27.4	±43.5	±33.8
33	161	-198	-26.8	±46.1	±37.5

Table 3.6 Preliminary test results of a comparison of the residual errors between the DEM extracted from stereo-pair using correlation and the DEM extracted from digitised contours.

Table 3.8 presents the results obtained using the condition of having the same intersection points from different images and using a median filter. It was found that the highest accuracy of ±12.3m was obtained from the use of the second method for a 5 x 5 window size.

Size of Window	Maximum Errors on Plus (m)	Maximum Errors on Minus	Bias (m)	RMSE (m)	Standard Deviation (m)
5	41	-133	-27.0	±30.9	±15.0
7	26	-94	-27.2	±30.5	±13.7
9	25	-92	-27.5	±31.0	±14.3
11	33	-124	-27.4	±31.3	±15.1
13	58	-99	-27.6	±32.1	±16.4
15	38	-96	-27.9	±33.0	±17.6
17	46	-118	-27.5	±33.4	±18.9
19	77	-117	-27.4	±34.7	±21.3
21	100	-142	-27.8	±36.1	±22.9
25	109	-144	-28.2	±39.2	±27.2
29	136	-177	-27.5	±41.7	±31.3

Table 3.7 Preliminary test results of a comparison of the residual errors between the DEM extracted from stereo-pair using correlation and the DEM extracted from digitised contours using a median filter (accuracy improved 30% by using median filter).

Size of Window	Maximum Errors on Plus (m)	Maximum Errors on Minus (m)	Bias (m)	RMSE (m)	Standard Deviation (m)
5	34	-83	-23.5	±26.5	±12.3
7	34	-73	-24.1	±27.1	±12.3
9	30	-80	-24.7	±28.3	±13.8
11	43	-83	-25.5	±29.6	±15.0
13	47	-87	-25.6	±30.5	±16.7
15	51	-95	-25.7	±31.6	±18.5
17	56	-108	-26.1	±33.0	±20.2
19	65	-120	-25.2	±33.7	±22.5
21	64	-117	-24.9	±34.5	±23.9
25	81	-136	-24.3	±36.9	±27.8
29	98	-140	-23.5	±38.7	±30.7

Table 3.8 Accuracy results of the residual errors in height in the DEM at different window size compared with the DEM produced from digitised contours employing method 2 (that of triplet - matching) using the condition of the same intersection point from different images and using a median filter.

Also it was found that the accuracy in Case 1 of the first method for the stereo-pair of base-to-height ratio 0.2 is better than the accuracy obtained from the stereo-pair having the base-to-height ratio of 0.52 due to the quality of the right image.

Taking the window size of 7 x 7 pixels and applying digital image correlation for the areas covered by the three test sites, the results that were obtained are summarized in Tables 3.9 and 3.10.

Test Area	Case	Maximum Errors on Plus (m)	Maximum Errors on Minus	Bias	RMSE (m)	Standard Deviation (m)
1	1-1	192	-189	-23.8	±32.9	±22.7
	1-2	153	-868	-38.7	±101.62	±94.0
2	1-1	304	-226	-27.3	±30.23	±29.0
	1.2	291	-237	-29.0	±23.4	±21.6
3	1-1	226	-248	-31.0	±38.6	±23.0
	1-2	128	-237	-28.0	±34.5	±20.1

Table 3.9 Accuracy results of the residual errors in height using the 7 x 7 window size generated for the three test areas using the first method of an individual stereo-pair and using a median filter.

Test Area	Method	Maximum Errors on Plus (m)	Maximum Errors on Minus	Bias	RMSE (m)	Standard Deviation (m)
1	2-1	144	-864	-32.9	±83.7	±77.1
	2-2(filter)	47	-91	-22.3	±26.2	±13.7
	2-2	195	-291	-21.8	±27.4	±16.6
2	2-1	155	-181	8.8	±16.8	±14.4
	2-2 (filter)	119	-74	6.6	±13.3	±11.5
	2-2	278	-133	7.2	±17.0	±15.4
3	2-1	96	-158	-28.3	±32.0	±15.0
	2-2 (filter)	43	-111	-28.2	±30.3	±11.1
	2-2	112	-162	-28.2	±32.2	±15.5

Table 3.10 Accuracy results of the residual errors in height using the 7 x 7 window size generated for the three test areas using the second method of triplet matching.

It must be said that the results achieved in these tests are not particularly good when compared with many of the others reviewed in this chapter.

3.7.2 Validation of DEM Reported by Akiyama

In a paper by Akiyama (1992) of GSI, Japan, there is a short account of the further verification of the DEMs extracted from SPOT stereo-pairs carried out for two small test sites, each 3 x 3km, located in the Mount Fuji area in Japan using a Zeiss Planicomp analytical plotter and the modified BINGO software from the University of Hannover. The SPOT stereo-imagery comprised three images with +24.1° (Left), -4.0° (Centre) and -15.7° (Right). 32 GCPs were obtained from the 1:25,000 scale GSI topographic maps of the area. On this occasion, the elevation values were measured manually and visually at a 100m grid interval on the oriented SPOT stereo-pairs of the different combinations

of the overlapping images and were compared with the corresponding DEMs extracted from aerial photographs.

The orientation accuracy using the 32 GCPs gave RMSE values for the residual errors in planimetry of ± 5m both for the Centre/Right pair and the Left/Right pair with height accuracy figures (in terms of RMSE values) of ±5m and ± 4m for the respective stereo-pairs. For the DEM accuracy tests, two small test areas - classified as (a) flat and (b) mountainous respectively - were used. Table 3.11 sets out Akiyama's results for the errors in elevation in the SPOT DEM compared with the corresponding values given by the aerial photography.

Area	Stereo-pair	B:H Ratio	RMSE (m)	Max. Error (m)
Flat	C/R	0.52	±5.5	-24.7
Flat	L/R	0.72	±5.8	22.4
Mountain	C/R	0.52	±9.6	62.7
Mountain	L/R	0.72	±6.9	31.1

Table 3.11 Accuracy results of the residual errors in height in the two test areas.

These RMSE figures appear to be astonishingly good - especially compared with those achieved by his GSI colleague (Fukushima) for the same areas discussed in the previous section. Furthermore they hardly equate with the statement made by Akiyama that the results after constructing contours from the DEM and comparing them with these of 1:50,000 scale map, were somewhat disappointing. Thus he gave the opinion that the results were really compatible with 1:100,000 scale mapping with a 40m contour interval.

3.8 Summary and Analysis of the Published Results

With some of the papers published on the validation of the DEMs from SPOT stereo-pairs, the number of points that have been measured and validated is relatively small (50 to 200 points). This tends to occur in those cases where the measurements have been made visually and manually in an analytical plotter. In these cases, the tests are essentially extensions of the geometric accuracy tests that have been discussed and analyzed in Chapter 2. However, in other cases, the DEM data has been acquired through the use of automated digital image matching techniques, in which case, the data

sets available for verification purposes is very large. For example, if an elevation value was to be extracted for every 10m pixel in the stereo-model formed from a pair of SPOT Pan images, then the total number of elevations available from a single stereo-pair would be 6,000 x 6,000 = 36,000,000 individual values. With a 20m grid interval, the data set would amount to 3,000 x 3,000 = 9,000,000 individual height values: even with a 100m grid interval, this gives rise to 600 x 600 = 360,000 individual values.

With such large data sets, it then becomes a problem to carry out the validation of the data and to assess the data quality. In the first place, it is difficult to find a reference data set of an adequate quality with which to carry out the validation. To extract high quality elevation data from aerial photographs - e.g. with an accuracy of ± 1m to act as a reference data set, - would require a huge effort in terms of providing ground control points and carrying out measurements for an equivalent size of data set from a large block of such photography. Thus most validation exercises and studies that have been carried out up till now have been applied to small samples of the total data set, e.g. by testing small representative sub-areas of 1 x 1km to 3 x 3km in area or by sampling at a relatively wide grid interval over the whole area of the SPOT stereo-model. As the review has shown, much of the validation has been carried out using data that has been interpolated from digitized contours - which immediately calls into question the quality of the reference data set, especially when the contours that have been used have (inevitably) been those taken from 1:50,000 scale maps covering the test area. As will be seen later, this has also been partly the case with the author's project where the reference data set has been extracted from 1:50,000 scale maps. However this has also been supplemented by high accuracy GPS profiles measured on the ground.

With regard to the accuracy figures that have been obtained in the relatively few studies that have been published, there is a huge range from the astonishing ±5.4m of Priebbenow and Clerici (1988) through the ±10m to 12m of Ley (1988) and Heipke et al (1992) to the ±20m to 30m of some of the less good results. The results from Theodossiou and Dowman (1990) and Trinder et al (1994) are especially interesting in that they show the variation in accuracy with slope and other terrain parameters. In the context of the author's project, the work of Trinder and his group at the University of

New South Wales is particularly relevant since it gave, for the first time, a comparison of the results achieved with different systems and packages over the same test area, including two of the recently developed systems offered by commercial suppliers. However, till now, no one has reported on the accuracy that can be achieved with DEMs extracted from SPOT Level 1B stereo-imagery.

3.9 Conclusion

It can be seen from the previous studies reviewed in this chapter that most of the validation tests have been carried on analytical plotters using different kinds of hardware and software. Comparatively few studies have been carried out using digital image processing systems.

The accuracy of the DEMs obtained from SPOT stereopairs using digital image processing systems and rigorous mathematical models is very varied. From the results of the DEM accuracy tests reported by different researchers, one can say that the accuracy of the DEM as given by the RMSE values will fall in the range between ±7m to ± 30m which correspond to topographic maps having 20m to 100m contour intervals according to American national mapping standards. It is an open question still as to whether data of this quality is acceptable to users or not. For unmapped or poorly mapped areas, it can be argued that the DEM data of this quality produced from SPOT stereo-pairs would be quite invaluable. But for small-scale topographic mapping produced to current accuracy standards, the data might be regarded as barely adequate or even quite inadequate and unacceptable.

The validation of the DEMs extracted from SPOT stereo-pairs has been mainly restricted to two different methods. The first method has been the validation of the DEMs at a comparatively small number of check points. The second method has been to compare the height values extracted by the DEMs at a large number of grid points over a relatively small area with the corresponding height values extracted from the DEMs generated from contours at the same grid interval. There is still a need for further studies to be taken, especially in this period where a lot of remote sensing systems from commercial suppliers have appeared on the market recently, using different

mathematical models and incorporating quite different approaches to the photogrammetric solution.

In the next chapter, the status of topographic mapping in Jordan will be reported and discussed since this will place the author's research project in its proper context. This account will include the background to mapping in Jordan, followed by a discussion of the country's geodetic network; the current status of topographic mapping in Jordan, including the facilities, hardware and software available in the Royal Jordanian Geographic Centre (RJGC) and the work of the Training Centre in RJGC. Finally an assessment of the accuracy of the small-scale topographic maps that are available for the author's test area in Jordan will be given.

CHAPTER 4 : STATUS OF TOPOGRAPHIC MAPPING IN JORDAN

4.1 Introduction

Since the author's project has been carried out in Jordan and he has made extensive use of its maps and survey data throughout his project, it seems appropriate to review the situation regarding surveying and mapping in the country. This is particularly the case since the author hopes that the results of his project will be of value to the mapping of Jordan. Furthermore he has made considerable use of the existing topographic map coverage of Jordan to verify the data that he has extracted from the SPOT stereo-coverage. Thus the coverage and quality of the existing maps is another matter of considerable importance to the research project undertaken by the author.

4.2 World Mapping

At the present time, every country in the world faces a big challenge in satisfying the various requirements associated with its economic development. In turn, such a development also requires each country to carry out the monitoring of its environment to plan and manage its natural resources in a sustainable fashion. Furthermore, since topographic maps are considered to be the basic prerequisite for the planning, development and effective management of the natural resources of any nation (Atilola, 1992), there is an increasing demand for maps to help meet these requirements. In certain parts of the world, such as the Middle East, defence requirements are a further major incentive for countries to fund mapping programmes. All of these maps should be accurate and up-to-date.

The current status of world mapping shows that much needs to be done. Recent surveys conducted by the United Nations Organization (UNO) and reported by Jacobsen (1990, 1993) and Konecny (1994) have revealed that the coverage of topographic mapping is still rather inadequate in the developing continents. The most highly developed countries of the world in Western Europe, North America, Australia and Japan are those that are best mapped, while, at the other end of the scale, in a number of developing countries in Africa (Petrie and Liwa (1995); Petrie (1997)) and South America, the

situation is quite bleak, due to factors relating to their poor economic situation and to wars and political conflict. Of course, other terrain-related factors may play a part, e.g. those related to the vast area of many individual countries, much of which comprises desert, tropical forest or rough terrain and is therefore inaccessible and uninhabited. Furthermore, world wide, the progress in updating maps in areas already mapped is also poor. According to the UN, it is 2.3% per annum for 1:50.000 scale and 4.9% for 1:25.000 scale, with an average age of over 40 years for maps at 1:50.000 scale.

4.2.1 Mapping in South West Asia

By contrast, in South West Asia, there is extensive existing map coverage of good quality, e.g. in Jordan, Syria, Iraq, Saudi Arabia, Yemen and Israel. Most of these countries have complete cover either at 1:100,000 scale or 1:50,000 scale and even parts at 1:25,000 scale. The major problem is that of map revision of very large numbers of maps - 2,300 individual sheets in the case of Saudi Arabia's basic topographic map series at 1:50,000 and 1:100,000 scales. In the case of Jordan, the whole of the country is covered by a topographic map series at 1:50,000 scale. Of the total coverage of 174 sheets, 60 of these need map revision at short intervals due to the fast changes taking place in the landscape. Furthermore, the 47 sheets at 1:100,000 scale covering the whole country need to be updated all the time for specific military tasks.

The use of SPOT stereopairs as an economic method of topographic map production and map revision at small scales for the vast areas of arid or semi-arid land that exist in the region is a matter which needs to be considered carefully by national mapping organizations in South West Asia. However, there is already some experience of carrying out topographic mapping from SPOT stereo-pairs within the South West Asian region. This has been carried out largely using analytical plotters in conjunction with hard copy film transparencies and manual operator-controlled measurements resulting in the production of the classical type of vector line maps - rather than the use of all-digital systems with the highly automated extraction of DEMs and orthoimages that are the principal concern of the research project reported in this dissertation. Thus, for example, the mapping of North East Yemen at 1:100,000 scale with a 40m contour interval was carried out in the late 1980s under a British aid programme by Ordnance Survey

International (OSI) - as described in the papers by Hartley (1988), Murray and Farrow (1988), Murray and Newby (1990) and Murray and Gilbert (1990). These maps were compiled and plotted from 18 SPOT Pan stereo-models using a Kern DSR-1 analytical plotter, supplemented by a thorough field completion of those villages, buildings, minor roads and tracks that could not be plotted due to the shortfall in the ground resolution of the SPOT images.

SPOT stereo-pairs have also been used in Saudi Arabia for the revision of the 1:250,000 scale Joint Operation Graphic (JOG) maps used mainly for air navigation. This work has been carried out for the sensitive border areas with Yemen, Oman, Iraq, Jordan, etc. where "no fly" zones operate and the use of aerial photography is not practicable. Again this has been carried out using Intergraph IMA analytical plotters, though more recently, the new Intergraph IMD digital stereo-plotter, based on the company's Image Station, has also came into use for this task - but again using vector line plotting techniques.

4.2.2 Mapping in Jordan

As noted above, maps of all kinds are a basic requirement of any development project. Thus the demand for maps has been increasing in Jordan over the past few years as a direct result of the country's national development plans and it is anticipated that this demand will accelerate as the current five-year development plan is implemented. Every project - of whatever nature - requires accurate and up-to-date mapping at a particular scale; these scales will vary from one project to another. Thus it is foreseen that the volume of work needed to meet the increasing demand for maps will become larger as the planning and execution of various projects proceeds, since any delay in commencing mapping activities will cause a bottle-neck in the development activities being carried out in Jordan and will lead to economic losses.

In recent years, Jordan has suffered from the fast growth of its major cities, especially the capital, Amman, due to the migration of people from villages in the rural areas and

from the Badia desert area, and the influx of refugees from neighbouring countries caused by the wars in the Middle East. This latter kind of migration - especially after the Arab-Israel wars - caused a lot of pressure on the country's infrastructure, obliging the government to cope with these problems. Even before this, it was considered imperative to establish a national mapping organization which would use the most modern technological and scientific methods available to provide Jordan with the capabilities - human and material - needed to produce the required mapping for the various needs of the country at the time when they are needed. The Royal Jordanian Geographic Centre (RJGC) is the mapping organization that was set up to deal with and to respond quickly to the demands of government planning and development projects and to cope with the army's requirements by supplying up-to-date maps. Since its foundation, the demand for maps has increased rapidly. This has resulted in acute financial problems within the RJGC as it has tried to satisfy all these demands. As a result, some government Departments have carried out their projects with little help from RJGC to provide their basic mapping requirements - even though official agreements between the two sides exist, through which direct payment of the cost of the work that has to be done could be made.

4.3 Background to Mapping in Jordan

After the First World War, and following the collapse of the Ottoman Empire, the country was formed in 1923 under the title of Trans-Jordan, at first, largely under the control of the British government acting under a mandate from the League of Nations. At the same time, Palestine was also under a mandate of the British government. The geodetic network of any country forms the basis of all the triangulation and control networks of lower orders and the basis from which all survey and cadastral works are undertaken. Initially since Trans-Jordan had no survey and mapping capability, the primary triangulation network was based on work carried out by the Survey of Palestine in the 1920s and 1930s and only covered the more developed western part of Jordan adjacent to Palestine. This network was extended by survey units from the armed forces of Australia, New Zealand and the U.K during the Second World War. Thus, it was made under wartime conditions and by different teams which had limited co-ordination, the result of which was that many points had two or more different coordinate values.

This network sufficed for urgent military purposes, but a new control network needed to be established to serve the pressing need for more accurate information.

During the period when Jordan came under the Ottoman Empire, there were only a few land registration offices located in the main cities. Under the British mandate, the main survey authority that existed in that period was called the Department of Survey and Government Lands, renamed later to be the Lands and Survey Department. Its main concern was land registration. In this situation, cooperation with British mapping organizations was necessary to provide topographic maps of Jordan. In this way, some parts of Jordan were covered by topographic maps at 1:50,000 scale and 1:100,000 scale, and a strip of maps at 1:25,000 scale extended from north to south covering the area adjacent to Palestine. Small scale mapping was also carried out to provide full coverage at 1:250,000 and 1:50,000 scales. Much of this topographic mapping was carried out during the period from 1946 to 1948 by the military survey units of the British Middle East Land Forces (MELF).

In 1928, Trans-Jordan became largely self-governing, though full independence was only achieved in 1946. The first years of this independence were to a large extent dominated by the wars with Israel and the huge influx of refugees from Palestine. During this period, the old geodetic network was almost completely destroyed. In 1956, the Jordanian Army established a Military Survey Branch which was attached to the Military Intelligence Branch. The army used all the various editions of topographic mapping produced by the United Kingdom until 1961, after which, a new edition of 1:50,000 scale maps based on the UTM coordinate system became available. This had been prepared for the Ministry of Economy by the United States Agency for International Development (USAID). It was produced by the Aero Service Corp in the United States, being compiled by photogrammetric methods from aerial photography taken in 1961, and from existing data furnished by the Jordan Department of Lands and Surveys. A later edition of this 1:50,000 scale map series was produced in 1974 by the Directorate of Military Survey in the U.K using aerial photography from 1972.

In the late 1960s, the Military Survey Branch was transferred and attached to the Royal Engineering Corps. New equipment was bought, including offset litho printing machines, photographic labs and the capability to enlarge or reduce the size of maps. With this equipment, the Military Survey Branch became capable of producing and reprinting old maps, though without undertaking any revision of the maps due to a lack of trained people. With regard to large-scale mapping, the early edition of the 1:5,000 scale series for Amman city was produced by Hunting Surveys in 1956.

In 1975, the Military Survey Branch was separated from the Royal Engineering Corps. and became an independent unit called the Directorate of Military Survey. Also in 1975, Jordan started its formal plans for its economic growth and the development of its natural resources. During the 30 years after the first Arab-Israeli war, there had been substantial and widespread changes in the landscapes of Jordan and the rapid and often uncontrolled growth of many towns and cities. In particular, the man-made cultural landscape in the form of settlements, communication networks, etc. had been altered drastically. Many of these changes related to the effects of the third Arab-Israel war of 1967 in which Israel took over the West Bank of Palestine and caused a further flood of refugees which drastically affected the distribution of population in Jordan. Later came a rapid growth in the economy due to both the financial help of the governments of the Gulf States, and the income sent back to Jordan by Jordanians and Palestinians working in the Gulf States. To meet these changes, existing maps had to be revised. In addition to topographic maps, new types of city maps, tourist maps and road maps were required.

The Directorate of Military Survey (DMS) was quite unable to meet these requirements. In the topographic mapping field - which was the main responsibility of DMS - the most pressing problem was revising and bringing up-to-date the planimetric detail of the very large number of existing topographic maps in the more developed areas. Thus DMS had to face numerous problems and an acceptable solution to these had to be found. The government faced two choices, the first being to expand DMS and train military people abroad which was difficult to achieve. The second choice was to create a new civilian agency and to train civilian people both at home or abroad. The latter appeared to be a

more reasonable solution and easier to achieve. Therefore to meet the mapping requirements of the country, in 1975, a civilian department was also established, called originally the Jordan National Geographic Centre (JNGC), later renamed as the Royal Jordanian Geographic Centre (RJGC), with staff and equipment from the DMS forming the initial nucleus of the RJGC.

4.4 The Establishment of the Royal Jordanian Geographic Centre (RJGC)

In the late 1970s, work started on the construction of a new purpose-built building to a French design at an estimated cost of 1.5 million dollars. In late 1983, some departments of RJGC occupied their places in the new building, and it became fully occupied in 1984.

The RJGC was given the following duties:

- Establishing and updating a national geodetic network and triangulation with first to third order control points covering the whole of the country.
- Providing the necessary data to the Lands and Survey Department for the making of cadastral maps.
- Producing thematic and base maps for the specific use of different ministries, government bureaux and institutions.
- Performing aerial photography according to the scales required by the different ministries.
- Offering advice relating to the training of technicians and the purchase and use of the various instruments needed for surveying and map production.
- Training enough technicians to meet the needs of the RJGC, ministries, government bureaux and national institutions.
- Keeping in touch with the advanced techniques being used in map production, remote sensing and digital mapping, as well as the establishment of a comprehensive geographic information system.

4.4.1 Cooperation Agreement with IGN

During the period after its establishment, it was foreseen that the RJGC would be unable to carry out its duties fully. Thus, in 1975, a cooperation agreement was signed between the French national mapping organization, the Institut Geographique National (IGN), and the RJGC, covering training, the production of topographic maps of some parts of Jordan, and the establishment of a new geodetic network of Jordan. The obligations of IGN under the agreement were:

(i) to train 104 Jordanian engineers and survey technicians in France for periods from two to six years: in fact, only 23 engineers and 28 assistant engineers graduated under this programme;

(ii) to train 162 to 200 Jordanian survey technicians locally in Jordan and to provide two permanent experts for local training throughout the period of the agreement: IGN was also to provide up to 25 French experts for short periods of three or four months throughout the period of the agreement;

(iii) to execute all the projects needed in Jordan for the production of all types of maps, with the co-operation of JNGC;

(v) to make use of all available personnel and equipment at JNGC in order to lower the cost of these projects and to provide an additional opportunity for training Jordanian students locally; and

(iv) to carry out various mapping projects at the same prices agreed upon for the mapping of southern Jordan in 1973.

4.4.2 RJGC Training Centre

The most important items in the agreement concerned training. Besides the more advanced training given in France, the following educational programmes and training courses have been implemented in-house in RJGC's Training Centre between 1975 and 1990, supervised by French experts in topographic science:

- Assistant engineers having undertaken courses amounting to 115 credit hours which are equivalent to 3 years of academic study. The student's specialisation could be in topographic survey, photogrammetry or cartography. This programme still runs, now given by Jordanian staff, and usually commences on the first of October each year.

- Technician programme at 74 credit hours which is equivalent to 2 years of academic study. Specialisation can again be in topographic survey, photogrammetry or cartography, in addition to which, printing and map reproduction are also offered - see Table 4.1. The students first utilised all the facilities available in the DMS, and later the new equipment provided by RGJC.

In 1990, the RJGC Training Centre became an intermediate community college, and from then on, it adhered to and followed the regulations of the Ministry of Higher Education in Jordan. The duration of the programme is two years, distributed over 4 semesters. Graduates have to pass the comprehensive exam conducted by the Ministry of Higher Education. Specialisation can be in one of three fields - topographic surveying; photogrammetry and cartography; and printing and map reproduction. These programmes amount to 71 credit hours for surveying; 72 credit hours for cartography and photogrammetry; and 64 hours for printing and reproduction. In addition to the regular courses, special training courses are also held. These short courses vary in their duration and technical levels. They are usually agreed upon with the requesting agency and can cover a variety of topics such as: topographic surveying, cartography, digital mapping, remote sensing, geodesy, printing and reproduction and other fields within these domains suggested by the requesting area. The number of students graduating from the college reached around 166 during the period 1990 to 1996 - see Table 4.2.

Courses / Years	Assistant Engineers (FT)		Assistant Engineers (dP)		Technician (DPT)		Technician (AFT)		Technician (PP)	
	Local	Others	Local	Others	Local	Others	Local	Others	Local	Others
1977	19		17				19			
1979	26				13				20	
1980	16				18					
1981	21		17		20				17	
1983	22		19		22				3	9
1984	24		18							
1985	12	2	18		4	4	2	2		
1986	10	1	14	1		9		9		
1987	4	9								
1988	1	13	14			2				
1990	5	1								

Table 4.1 Graduated Students from the RJGC Training Centre, 1977-1990

Courses / Year	Assist. Eng FT	Assist. Eng DP	Technicians PP
1990	7	7	8
1991		7	
1992		7	
1993	7		
1994	10		
1995	14	10	
1996	40	27	22
Total	78	58	30

Table 4.2 Graduated Students from the RJGC College, 1990-1996

Now the RJGC is trying to convert its community college to a university college, supervised by the University of Jordan. If RJGC succeeds in this step, this university college could attract many students from Jordan and from other Arabic speaking countries. This would also provide RJGC with the opportunity to receive additional financial resources which could be employed to buy more hardware and software to be able, for example, to handle satellite imagery for topographic mapping purposes and remote sensing applications.

4.5 Geodetic Network

The second priority for the RJGC in the period after its foundation was to establish the geodetic network for the whole country. Part of the agreement with the French IGN was to help RJGC to carry out this task. Gradually, over a period of time, the RJGC was able to share in the execution of this work, especially after the first groups of technicians had graduated from the Training Centre. The field work involved in establishing the first order geodetic network which started in July 1978 and lasted one year. The field work used conventional triangulation techniques and was fully supervised by the French survey experts, while the computation and adjustment of the network also carried out by French experts in France. The total number of first order points that were established was 87; of these, 14 were Doppler points and 17 astronomic points. At the same time as the geodetic network was being established, other teams of surveyors were carrying out

precise levelling along the main roads. Nowadays three teams of surveyors are working on maintenance of the geodetic points.

For the second order network, field work was started in 1979 and lasted until 1983. More field surveyors from RJGC shared in the survey work, while, at the same time, the number of French surveyors was reduced. The computation work was done in Jordan with the help of French experts. The total number of points established in this second order network was 529; of these, 10 were astronomic points. The field work for the third order network finished in 1988. This work was carried out fully by RJGC technicians; the total number of points established in this network was 2,002. For the fourth order network, it was left to the Lands and Survey Department to carry out this kind of survey.

4.6 Current Capabilities of RJGC

Basically the RJGC is well equipped and able to produce almost any type of survey and cartographic data or product - although, at present, it is not well equipped to carry out photogrammetric and topographic mapping operations from space imagery.

4.6.1 Equipment and Facilities

Surveying equipment of various types is available for control purposes, including measuring angles and distances; carrying out astronomical observations and levelling; and drawing up maps and plans. Most recently, high quality dual-frequency GPS sets have been purchased for control purposes. A wide range of analogue photogrammetric instruments such as the Wild B8S, A8, A10 and AG1 and the Kern PG2 have been installed, several of which are equipped with encoders to allow data to be generated in digital form, so allowing the use of computer systems for storing and manipulating digital data. The latest development has been to carry out modifications to some of these analogue photogrammetric machines to convert them to be analytical plotters. In addition to the analogue instruments, one Wild BC2 analytical plotter is available which can only be used for conventional aerial photography - i.e. it does not have software to allow it to be used with SPOT stereo-pairs. For digital image processing for photogrammetric applications the software that is available is PCI EASI/PACE running on an HP UNIX workstation; according to the author's knowledge, this software is not complete. Other software such as MicroStation version 5 from Bentley Systems is

available for data collection, editing and drafting. Moreover, the photogrammetric section has other software available such as the PROSD, PROABS, PRO600 (PROCART) programs from Leica, and Terra Modeler from Terrasolid.

A full suite of conventional cartographic and appropriate equipment is available, including computer-based typesetting systems. Photographic labs allow the processing of coloured and black and white films and prints and have the ability to enlarge or reduce the size of maps, plans, and photographs.

For digital mapping operations, the RJGC possesses modern equipment such as digitizers and plotters, and it deploys various software packages which drive screens for verifying and editing data. ARC/INFO is the software package that has been used as the basis of digital mapping and GIS activities since 1988. The hardware used in the digital mapping unit includes:-

(1) an HP server acting as a host computer;

(2) two X-terminals and two HP graphics workstations running ARC/INFO;

(3) a 600 dpi raster scanner attached to a Sun workstation running ArcScan software;

(4) two pen plotters; and

(5) one inkjet plotter.

The RJGC also possesses remote sensing systems, equipped with a variety of hardware devices - including a scanner to convert aerial photography to digital image data; and workstations for correcting and analysing images through digital processing. There are three software systems available for remote sensing work. The first is the French Pericolor system running on a MicroVAX-II host computer. This system is already out-of-date and it serves for training purposes only. The second and third systems are from Dipix from Canada. These were installed in late 1989 and have been running since then without any upgrading. The hardware components of this system comprise the following items:-

(1) a MicroVAX-II serving as the host computer for the two systems;

(2) two graphics workstations equipped with array processors and adequate display capabilities;

(3) one medium quality raster scanner (resolution < 300 dpi);

(4) one Versatec electrostatic plotter; and

(5) a mag tape unit.

4.6.2 Photogrammetric Operations

As mentioned above, the photogrammetric section in RJGC has a lot of conventional photogrammetric instuments. For any mapping task, the appropriate instument - either analogue or analytical - will be selected according to the required scale. Subsequent operations are quite conventional. The operator first carries out the relative and absolute orientation. Of course, the operator is provided with a number of control points to define the coordinates and the height of all points contained in the stereomodel. After the operator has set up the stereo-model, he then starts to plot the contours on a separate sheet. After plotting the contour lines, his other task is to plot the planimetric details such as roads, drainage, buildings, etc. on a separate sheet. In the case of good operators, the plotting can be done directly on scribecoat. Field completion is then carried out to provide the missing details and to record new changes within the area together with the names and locations of settlements and other relevant objects falling within the map sheet. After the photogrammetric operator and field topographer have plotted all the planimetric details and altimetry of the area of interest, the plotting sheets will be taken to the cartographic section to carry out the final drawing and scribing and putting on the names and symbols before the reprographic work and printing of the final map.

3.6.3 Status of Topographic Mapping in Jordan

At the moment, the coverage and status of the topographic mapping of Jordan can be summarised as follows:

(i) the 1:1,000,000 scale Operational Navigational Chart (ONC) covering Jordan and some other neighbouring countries is produced by the USA.

(ii) 1:500,000 scale series

(a) Tactical Pilotage Charts (TPC) are also provided by the USA. They comprise several sheets covering Jordan and the surrounding countries.

(b) The Unified Arabic System series. This consists of 6 sheets covering the whole area of Jordan in addition to full coverage of Syria. This series was originally produced in Syria and the Jordan coverage has been updated by RJGC.

(iii) 1:250,000 scale Series. This consists of many different editions: two use English text, the others are in Arabic.

(a) The English Edition dates from 1978 and consists of 13 sheets printed in three colours. The original version of this series was compiled from an older edition made by British Middle East Land Forces (MELF). A recent revision of this series was made by RJGC in 1992.

(b) The Joint Operation Graphic (JOG) with English names and text consists of 13 sheets covering the whole area of Jordan that have been provided by the USA.

(c) The Arabic edition consists of 14 sheets which give complete coverage of the whole country. Most of these sheets are printed in 4 colours. The maps of this series are the products of a recent revision of a series originally produced in Syria.

(d) The Palestine road map (Arabic) series published by RJGC in 1982.

(e) The Service map (Arabic) series. These maps are prepared in a such a way that various services could be added and shown on any of these maps. Such services could be administrative, educational, medical, agricultural, etc. according to the specific needs of the requesting party.

(iv) 1:100,000 scale series. This series comprises the following editions:

(a) The Arabic edition consists of 19 sheets. This series is an old version and only a limited number of sheets had been produced. It does not give complete coverage of the country - only the heavily populated areas are covered. The edition has been reprinted several times without making any revision. This series was taken from the old edition that had been made by MELF.

(b) The English edition consists of 47 sheets based on the Palestine grid and printed in four colours. These sheets give complete coverage of the whole country. These sheets have been reprinted several times and some limited revision was done to a certain number of sheets. This series was taken from the old version of the English edition which was made by MELF.

(c) The Unified Arabic System series dating from 1988 consists of 47 sheets. which give complete coverage of the whole country. Full revision of the complete coverage was carried out for this series. These sheets can only be made available to government users.

(v) 1:50,000 scale Series This consists of two editions:

(a) The UTM edition with English text consists of 174 sheets. which give complete coverage of the whole country. These sheets were originally produced in 1961, having been prepared for the Ministry of Economy of Jordan through an aid programme provided by the United States Agency for International Development (USAID). These sheets have been reprinted several times without any revision being made.

(b) Arabic edition Currently this is constructed on the JTM (Jordan Transverse Mercator) projection and dates from 1993. It consists of 174 sheets which give complete coverage of Jordan in six colours. This series is now the base for all topographic mapping in Jordan. The sheet size is the same as the UTM sheets and the altimetry is taken from the UTM sheets.

During the 1970s, the 1:50,000 scale series was first produced with two grid systems - the Palestine and UTM grids - overprinted on it. No revision was made for this series which was produced on the basis of the US maps. In 1984, it was decided to carry out the revision of a limited number (60) of these sheets, due to the increased demand for this scale, both for military reasons and for the planning of development projects under the five year plans announced by the government. This limited number was governed by the economic situation prevailing at that time. Therefore, important areas in which investigations needed to be carried out for various Earth resources and development projects, were selected and given priority. Changes contained in this revised edition included the change to the use of the JTM (Jordan Transverse

Mercator) projection and Palestine grid. Aerial photography and photogrammetric methods were used to provide a quick and easy means for the production of the maps. In the late 1980s, it was decided to extend the map revision programme to include the coverage of this series for the whole country. In 1993, this coverage was completed (see Figure 4.1).

(vi) 1:25,000 scale Arabic series The full production process has been carried out by RJGC for this series. It is not appropriate to produce full coverage of the country at this scale, since this would require around 700 sheets. Thus coverage at this scale is confined mostly to the western part of the country. The work has been carried out in a number of stages:

(a) The first stage started in 1978, only three years after the establishment of RJGC. At this stage, RJGC was unable to work alone and without any help due to lack of sufficient technical resources. At the same time, there was a government requirement that the mapping at this scale should be related to specific development projects contained in the country's five year plans. Therefore, it was quite appropriate at that time to fulfil this demand through cooperation with IGN to produce maps of the main areas of interest according to the agreement between the two parties. At this stage, a full cooperation between the RJGC and the French team was implemented to carry out the production. Priority was given to the Amman governorate. The area and the size of the sheets was defined by the present author, the maps being produced in France with the field completion being carried out by RJGC surveyors. Full coverage of the Amman governorate was produced in this way.

(b) The second stage started at the beginning of the 1980s. During this stage, priority was given to the Irbid Governorate which contains 1/3 of the whole population of Jordan, and is the second most heavily populated governorate in Jordan. The production of this series comprising 35 sheets has been carried out wholly by RJGC and was completed in the mid 1980s.

(c) The third stage was started in the second half of 1980s to produce maps at the same scale to cover the Karak governorate. Full coverage consists of 40 sheets: the production was completed at the beginning of the 1990s.

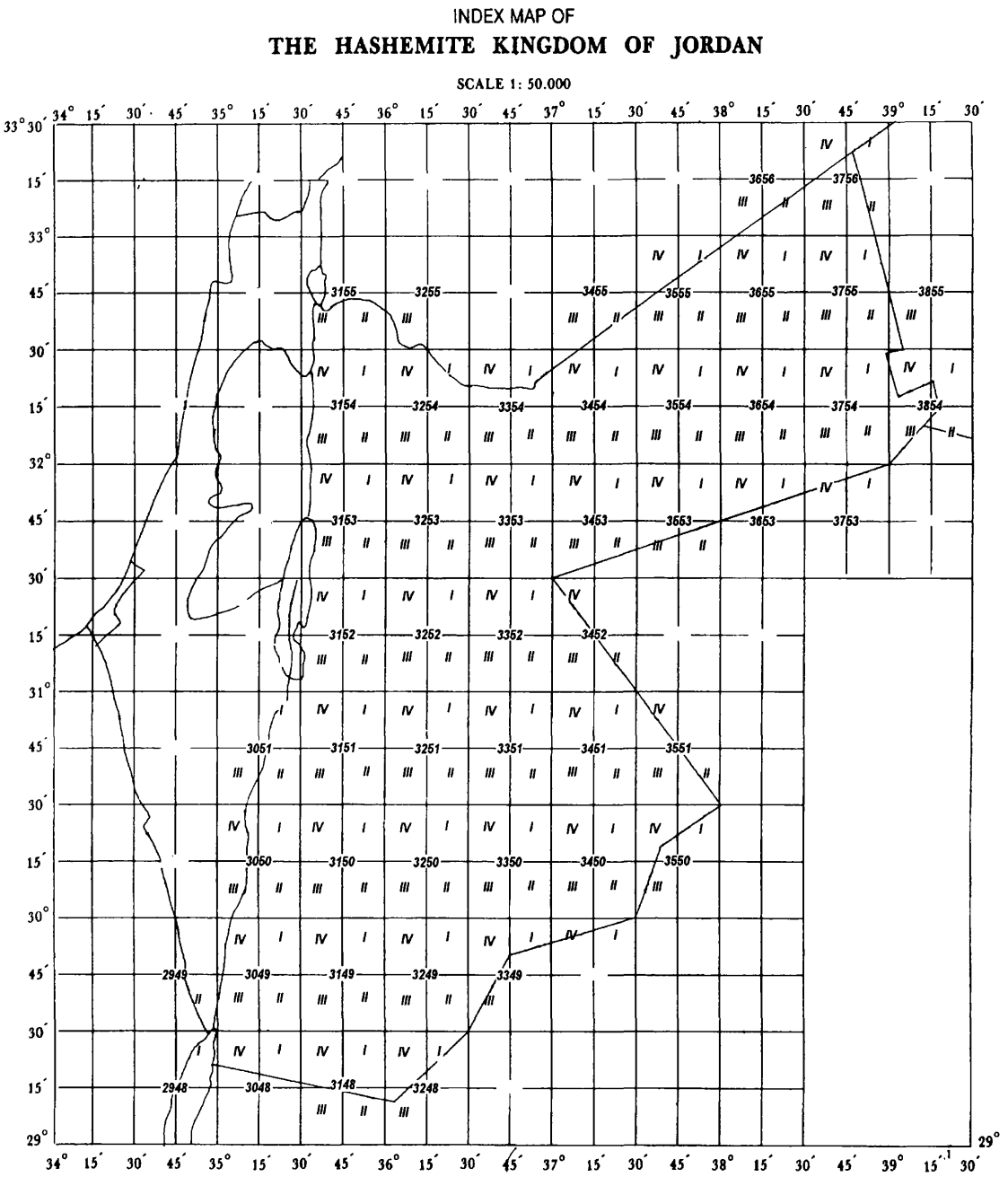

Figure 4.1 Index of UTM 1:50,000 scale topographic Maps

(d) The Jordan-Iraqi boundary series consists of 26 sheets that were produced after the agreement between the two governments in 1986 to modify the boundary.

4.6.4 Tourist Maps

In addition to the regular topographic map series, in recent years, the RJGC has expended quite some effort to produce tourist maps - especially for those areas in Jordan that are well known for their archaeological sites. The production included all the major cities and all historical sites as discussed below.

4.6.4.1 Amman Maps

(a) The Amman tourist map at 1:20.000 scale was published in 1989, in both Arabic and English versions. The map contains all the information that a tourist may need, including details of hotels, roads, theatres, hospitals, banks, cultural and sports centres, museums, etc.

(b) Maps at 1:10.000 scale were published in 1984 and consisted of 16 sheets.

(c) A further series at 1:10.000 scale was published in 1988.

(d) The current map series of Amman at 1:5,000 scale was produced in UK in 1974 in two editions. One gave full topographic details, including contours and grid, while the second covered the same area but excluding contours and grid.

4.6.4.2 Other Cities and Sites

A map of Irbid at 1:10.000 scale was published in the early 1980s; a map of Jarash at 1:5,000 scale was published in 1989 which shows the old city of Jarash and the main archaeological sites; while a map of Petra at 1:5,000 scale was published in 1989 which indicates the location of the various archaeological sites in this famous rocky rose-red city. Other similar maps that have been produced include these of Ajlun at 1:5,000 scale in 1990; Aqaba at 1:5,000 scale in 1990; Madaba; and Al Karak at 1:5,000 scale published in 1991; and Rum published in 1992 at 1:38,000 scale.

4.6.5 Map Accuracy

Since the 1:50,000 and 1:250,000 scale maps of the test area used by the author have been used to validate the data generated from SPOT stereo-pairs, it is important to consider the accuracy specification for these two series.

4.6.5.1 Accuracy of the 1:50,000 Scale Topographic Maps

The 1:50,000 scale topographic maps based on the UTM projection covering the whole country have been produced originally by Aero Service Corp. in the USA by photogrammetric methods using aerial photographs which had been taken in 1961. These maps are considered to be the basic map coverage of the country and form the basis for the maps of Jordan at smaller scales. The full production of these maps was undertaken in the USA and paid for by USAID. The field completion and the provision of other related data, control points, etc. was carried out by the Lands and Survey Department in Jordan. These maps were constructed to US National Map Accuracy Standards.

The aerial photographs are believed to have been taken at 1:40,000 scale with a wide angle (f = 15cm) camera from 20,000ft (6,000m). The commonly used yardstick for heighting accuracy in terms of measured spot heights in a production environment is 1/5,000 of the flying height. Thus for flying height of 6,000m, the RMSE value for spot height accuracy = ± 1/5,000 x 6,000 = ± 1.2m.

For the plotting of the planimetric details at the scale of 1:25,000 used for compilation of the final map at the 1:50,000 scale, the accuracy of these details according to the US National Map Accuracy Standard (NMAS) is specified as a standard error of ± 0.3mm x map scale number. In which case, the accuracy at the plotting scale will be: $\sigma\rho$ = 0.3mm x 25,000 = ± 7.5m on the ground.

For contour accuracy, again according to the US National Map Accuracy Standards, 90% of the points tested on the ground should be within one-half of the contour interval.

For the contour interval of the Jordanian maps, this interval is 20m; thus 90% must lie within 10m, this is equivalent to a standard error of M_h of 68/90 x 10 = ±7.5m. For an accuracy of 1/4 of the contour interval 68/90 x 5 = ± 4m.

According to the alternative approach used by Imhof (1982) that takes into account the slope of the ground, the height accuracy of contours in high-quality mapping is:-

$M_h = \pm (1.5 + 10 \tan \alpha)$ for 1:50,000 scale with contour interval of 20m.

If the contour accuracy is calculated according to this formula, then the accuracy of the 1:50,000 scale maps with a contour interval 20 m and with an average slope of 5° will be M_h = ± 2.4m. On the basis of this alternative approach, the standards for M_h in current use in USA for 1:50,000 scale appear to be: $M_h = \pm (1.8 + 15 \tan \alpha)$

For the Badia test area used in the author's research project, the terrain surface is largely covered by basalt with some isolated volcanic hills. It is dipping from the north west to the south with a relatively smooth slope but with quite a rough surface of boulders in many places. Other areas, such as the salt encrusted pans, are quite flat. The area can be divided roughly according to slope into 5 zones. The vertical accuracy of the five different landscape types found in the maps covering this area, taking slope into account, is shown in Table 4.3 for each of the five zones.

Area	Characteristic of the Area	Slope in Degrees	Vertical Accuracy
1	Flat terrain in the Pans or Qaa	0°- 0.5°	± 1.9 m
2	Gently sloping area comprising an almost flat sheet of basalt located in the Harra area and the Al-Hammad area in eastern part of the test area.	0.5° - 1°	± 2.1 m
3	Undulating surfaces which prevail in three zones in the western part and in the east of the area associated with the lava flow in the Al-Harra area.	1°-3°	± 2.6 m
4	Foothills and rolling topography	3°-5°	± 3.1 m
5	Isolated volcanoes; some steep slopes also occur along the valleys.	10°-12°	± 5.0 m

Table 4.3 Vertical accuracy of the contours on 1:50,000 scale topographic maps in different parts of the Badia taking slope into account.

4.6.5.2 Accuracy of the 1:250,000 Scale Maps

Regarding the maps at 1:250,000 scale with a contour interval of 50m, the source of the data is the 1:50,000 and 1:100,000 scale topographic map series. The data is produced via the 5 or 2.5 times reduction and subsequent generalisation of the 1:50,000 or 1:100,000 scale maps. According to the US National Map Accuracy Standard, the accuracy of these maps in terms of their RMSE value in planimetry would be expected to be ± 75m. Information received from Royal Jordanian Geographic Centre (RJGC) indicates that the accuracy of these maps is ± 40m in planimetry. Regarding height accuracy, as has been mentioned above, the source of data is the 1:50,000 and 1:100,000 scales with an accuracy of the contours in terms of RMSE value of ±7.5m according to the US National Map Accuracy Standard is in the range ± 2 to 5m if the alternative approach is adopted. Thus the accuracy of the contours shown on the 1:250,00 scale map should fall in this range with some diminution in accuracy due to the generalization process.

4.7 Conclusion

In this chapter, the status of topographic mapping in Jordan has been discussed. It can be seen from this discussion that Jordan is well covered by topographic maps at different scales. The RJGC is the only mapping organisation in Jordan which has the capability in terms of personnel and equipment to produce maps at any scale. Up till now, no commercial survey and mapping industry has been allowed to develop in the manner seen in highly developed countries - largely due to the exclusive conditions contained in the RJGC's charter.

Arising from the development process that covers most parts of Jordan, the efforts made by the Royal Jordanian Geographic Centre (RJGC) to support the demands made on it have been considerable. It is clear from what has been written above that, while Jordan is well covered with small, medium and large-scale topographic maps, the distribution of these maps - especially those at 1:50,000 and larger scales to the general public and even to other Government Departments is limited for security reasons. At the same time,

the fast growth of the Jordanian population and the considerable economic growth and development of the recent years is reflected in the widespread changes in the landscapes of Jordan. These really require continuous map revision to meet the consequences of these changes. Unfortunately the RJGC does not have its own aircraft to carry out aerial photography when it is needed - in spite of the fact that it has its own photogrammetric camera. The latter is still not used because RJGC does not have the financial means to buy a suitable aircraft. Furthermore, even if it could buy such an aircraft, it could not support the associated operational, maintenance and licensing costs. Thus, throughout its existence, the RJGC has had to bring in foreign contractors to undertake its aerial photography.

However, the RJGC does have the capability in terms of the personnel and the equipment needed to deal with satellite imagery. With the quite moderate investment needed to buy software to handle satellite imagery, this could result in a dramatic reduction in the costs involved in working with the conventional aerial photogrammetric methods used currently for the revision and production of small-scale topographic maps. In particular, data could be produced in the form of image maps or orthoimage maps, especially for the boundary areas and the vast areas in the desert, at a lower cost compared with those necessary to prepare conventional line maps from aerial images. With regard to the deficiencies - especially in ground resolution - of current satellite images for topographic mapping, it is apparent that the high resolution images that should become available in the future from the new American commercial satellite imaging companies such as Earthwatch (with its Early Bird and Quick Bird systems), Space Imaging (with its IKONOS-1 sensor) and OrbImaging (with its OrbView satellite) - in addition to the Russian space reconnaissance photographs - will be of great interest to RJGC. In particular, the high ground resolutions of these images could be useful for both planimetric mapping and map revision. If the cost of purchasing this imagery are reasonable, this might revolutionise certain aspects of data acquisition for mapping and would almost certainly attract more mapping organisations to use the satellite imagery for mapping at 1:50,000 scale or even larger. In particular, it should have great potential especially in the arid and semi arid areas that constitute such a large part of Jordan. For Jordan, much of the land is a desert area where the weather is cloud free most of the year. This factor should also help Jordan in the acquisition and use of satellite imagery

for the map revision of its small scale topographic maps. This does not mean that the use of aerial photographs will stop. They will still be needed for the production of larger scale maps where the needs for high resolution are such that they cannot be met by the new commercial satellites.

CHAPTER 5 : OVERVIEW AND MAIN CHARACTERISTICS OF THE SYSTEMS TESTED

5.1 Introduction

During the past decade, (i) the developments and improvements in the speed and affordability of computer technology in general and of image data processing in particular, and (ii) the increasing availability of high quality and lower cost digital image data, have led to new ways of processing this type of data. In parallel with this development has come an increasing need and demand for digital topographic and thematic data both for mapping purposes as well as input to geographical information systems. In turn, this has led to a considerable expansion in the availability and application of digital image processing systems within the context of photogrammetry and topographic mapping.

The advent of the SPOT satellite offered the first practical possibility for the acquisition of data that can be used for small-scale topographic mapping from satellite imagery. In particular, the off-nadir imaging capabilities of the SPOT system made it possible to create three-dimensional models from stereo-pairs of images overlapping in the cross-track direction. Up till now, analytical plotters have mostly been used to extract spatial data from these models using hard copy images; however digital image processing techniques are now beginning to be used with SPOT digital image data having overlapping stereoscopic coverage.

Moving first from the individual pioneering systems devised by research groups in certain European Universities, and the specialised systems produced for military mapping agencies in the United States, the last fifteen years have also been seen the gradual development of digital photogrammetric systems. The first commercially marketed digital photogrammetric workstation (DPW) - the Kern DSP 1 - was shown at the ISPRS Congress in Kyoto in 1988. Since then, a wide range of systems with different capabilities have appeared from a variety of suppliers. The importance of these developments first became apparent at the ISPRS Congress held in Washington in 1992,

and have quickly grown to a dominant extent - as became obvious at the latest ISPRS Congress held in Vienna in 1996.

In this chapter, first of all, the application of digital photogrammetric techniques to SPOT stereo-pairs will be presented. This will be followed by a classification of digital photogrammetric workstations, and by a description of the main characteristics of the three commercial systems and one devised for military mapping purposes that have been used in this research project to carry out tests of SPOT stereo-pairs over a high-precision test field.

5.2 Digital Photogrammetric Systems Applied to Remotely Sensed Imagery

A digital photogrammetric system is defined as an integrated hardware and software configuration that produces 2D or 3D coordinate data and map-related products from digital imagery using photogrammetric procedures employing both manual and automatic techniques. The output from such systems may include three-dimensional object point coordinates, restructured terrain surfaces, extracted feature data for mapping, and ortho-images. While the principles of photogrammetry have not changed, the tools have. Creating a digital photogrammetric system suitable for production purposes requires thoughtful integration of the latest technologies with respect to a fairly traditional photogrammetric workflow and output (Madani, 1996).

Over the last few years, there has been a noticeable trend for suppliers of image processing systems for use with remote sensing imagery to became involved with digital photogrammetry. In parallel with the development of similar systems by the traditional mainstream photogrammetric system suppliers, they have developed systems to handle SPOT stereo-imagery. However this approach has been substantially different to that using manual measurements of hard copy SPOT images for feature extraction in an analytical plotter. By contrast, it usually involves the use of digital image data in conjunction with automatic image matching techniques to produce DEMs and ortho-images to act either as direct input to a GIS system or as the basis for the production of hard-copy image maps or line maps using manual feature extraction techniques. This

development has been aimed not only at national mapping agencies but also at the geoscience, geophysical and geoexploration communities which have needs for the rapid generation of DEMs and ortho-images in remote areas, for which either no map exists or access to them is restricted by security considerations.

In this context, it has been noticeable that initially the systems produced by the remote sensing system suppliers have not had stereo-viewing or measuring facilities - features that are regarded as essential by photogrammetrists. However recently this situation has changed and these capabilities are now recognised by the suppliers as being essential both for feature extraction and for data editing purposes. So they are now beginning to appear in the workstations produced by the remote sensing system suppliers.

5.3 Classification of DPWs

The Digital Photogrammetric Workstation (DPW) consists of a graphics workstation with enhanced image processing, memory and display capabilities, including, in most cases, but not all, a stereo-viewing facility, and with appropriate software to allow photogrammetric operations to be undertaken - see Figure 5.1 (Petrie, 1997).

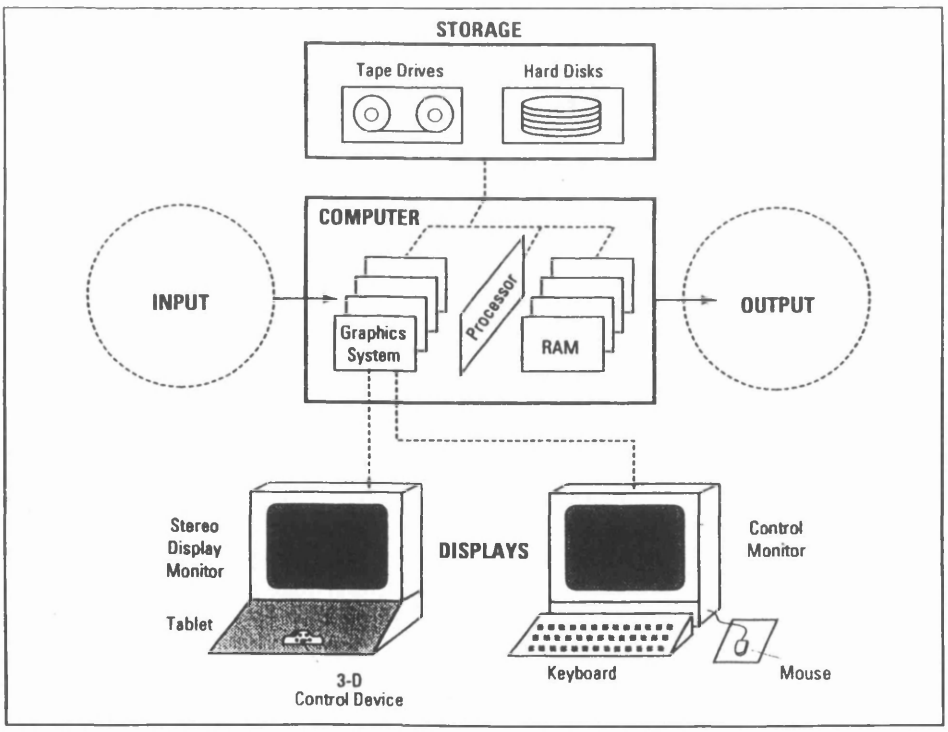

Figure 5.1 Main Elements of Digital Photogrammetric Workstation

The main features of the computer hardware utilized in a DPW are that it comprises a very powerful processor with very large memory [- 32 Mbytes of RAM is the minimum, typically 64 MB of RAM is used, while up to 128 Mbyte is not uncommon (Walker and Petrie, 1996)]. In addition, a very large data storage is essential to deal with very high resolution digital image data. This can be achieved through the use of hard disks of multi-gigabyte capacity and having high transfer rates to and from the RAM. Generally the host computer is supplied with at least one internal hard disk of 2 to 4 GB and, often, one or more external hard disks of 9 GB each. However, in the context of remotely sensed image data, these disks are usually supplemented by CD-ROM drives since this data is commonly supplied on CDs. Graphic accelerators may be used to assist with the implementation of stereo-viewing, especially in those systems employing alternating imaging on the display screen where rapid refresh rates have to be achieved, and for roaming over the stereo-model. In association with this feature, a high - resolution display monitor is necessary for all DPWs, with 1,024 x 1,024 pixels being the minimum size needed to display image data on the screen. Some DPWs are supplied with two monitors - one for image display and stereo-viewing; the other for the display of the system information.

A 3-D measuring device is also required to allow the precise positioning of a measuring mark or cursor and its use in height measurement. A wide range of devices are in use currently to enable the operator to execute the various mensuration tasks. These include the P-cursor used by Zeiss; Intergraph's multi-button cursor; a common 3-D mouse which is in use by Leica/Helava, DAT/EM and KLT Associates; the tracker ball utilized by Matra and ISM; and the hand wheels and foot disk used in analogue and analytical stereo-plotters that are now found on many DPWs. The required movements of the measuring mark or cursor relative to the images can be implemented in one or other of two ways - the first with moving image and fixed cursor, the second method with moving cursor and fixed image.

While most DPWs provide a stereo-viewing capability, initially this has not been the case with some of the systems emanating from companies that specialize in the remote

sensing field, e.g. the EASI/PACE system from PCI. Various methods are in current use to give 3D viewing on a DPW as discussed below:-

(i) The use of a mirror stereoscope with either split screen viewing on a single monitor or twin-screen viewing with two monitors. These have not been used much in the DPWs handling remotely sensed satellite image data, though they are utilized in various DPWs (from Topcon, Galileo, etc.) restricted to the use of aerial photos. However the DVP stereo-plotter which does handle SPOT stereo-pairs uses split-screen viewing.

(ii) The use of anaglyphic viewing with complementary (red/blue) filters. This method is used both in the R-WEL DMS system and in the TNT-mips system originating from a remote sensing system supplier.

(iii) The use of alternating screen images viewed either using active (shuttered) glasses or passive (polarising) glasses. These methods have been used in the DPWs from Leica/Helava, ERDAS, etc. that can handle SPOT stereo-pairs. Further details are given in the paper by Petrie (1997).

As noted above, while all DPWs are able to handle aerial photography, only a certain number are also designed to handle satellite imageries. Furthermore, it should be noted that, while some of the DPWs are able to handle the stereo-pairs generated by SPOT, the software is often not available in many mapping organizations and academic institutions due to the substantial extra cost involved in purchasing the additional modules.

5.3.1 DPWs Using SPOT Images

The different combinations of hardware elements mentioned above to form a DPW have been used to form a great variety of systems with different capabilities and a wide range of cost. Walker and Petrie (1996) and Petrie (1997) divided DPWs into three main categories. These comprised (i) Unix-based systems running on graphics workstations; (ii) PC-based systems; and (iii) systems produced by remote sensing system suppliers. Even in the short period since the publication of these recent papers, the situation has changed, e.g. Leica/Helava and Intergraph now have PC- based systems as well as those based on graphics work stations. Furthermore, since Walker and Petrie made their classification, some of the mainstream photogrammetric suppliers such as Leica/Helava

have expanded their coverage to include modules to handle SPOT and IRS stereo-imagery, while all of the remote sensing system suppliers now offer the capability of handling aerial photographs using classical photogrammetric techniques. Also they now offer stereo-capabilities which were not available even a year ago.

Since, in this research, the main concern is with those DPWs that are capable of handling SPOT stereo-images, the further discussion in this Section will be confined to such systems. These can be divided into two categories on the basis of the hardware and the operating system under which they are running - see Table 5.1.

Category A. Based on Graphics Workstations Running Under Unix OS

Supplier	LH Systems	Intergraph	VirtuoZo	Vision Int.	PCI	PCI	ERDAS	Micro-Images
System	SOCET SET	Image Station	Classic	SoftPlotter	EASI/ PACE	Ortho-Engine	OrthoMAX	TNT-mips
Computer	Sun Sparc	Inter 6000	Silcon Gr.	Sun Sparc	Sun/SGI	Sun/SGI	Sun/SGI	Sun Sparc
Stereo-viewing	Polarizing or Alt. Shutter	Alt-Shutter	Alt-Shutter	Alt-Shutter	None	Alt-Shutter	Alt-Shutter	Anag-lyph
Measure	3D Cursor	3D Cursor	Mouse	Mouse	Mouse	Mouse	Mouse	Mouse

Category B. Intel-Based PCs Running Either Under DOS or Microsoft Windows

Supplier	LH Systems	Intergraph	R-WEL	Leica	PCI	PCI	MicroImages	
System	SOCET SET	Image St Z	DMS	DVP	ImageWorks	OrthoEngine	TNT-mips	
Stereo-viewing	Polarizing or Alt. Shutter	Alt-Shutter	Anaglyph	Split Screen	Polarizing or Anaglyph	Alt- Shutter or Anaglyph	Anaglyph	
Measure	3D cursor	3D Cursor	Mouse	Digitising Tablet	Mouse	Mouse	Mouse	

Table 5.1 Digital Photogrammetric Workstations Applied to SPOT Stereo-images

(a) The first group of systems comprises those DPWs that are running on graphics workstations under the Unix operating system. These include DPWs such as those available from mainstream photogrammetric suppliers, e.g. from Leica/Helava, Intergraph, VirtuoZo and Vision International, and from remote sensing suppliers such as PCI with its EASI/PACE and OrthoEngine products, and MicroImages with TNT-mips. The ERDAS OrthoMAX module (licensed from Vision International) may also be placed in this category.

(b) The second category comprises systems which are based on Intel-based PCs running either under DOS or some version of Microsoft Windows (either 3.1, 95 or NT). These comprise systems from Leica/Helava, Intergraph, R-WEL, DVP, PCI and MicroImages.

The main concern of the present research has been to test as many systems as possible of those that can handle SPOT stereo-pairs but inevitably some limitations have been

encountered. In this respect, two systems - the Intergraph InterMap Digital (IMD) system installed in BGS and the Leica/Helava SOCET SET system installed in this Department - have not been tested due to the need for additional funding for the first one (IMD) and the failure to provide the promised key for the second one. Two other systems have been tested but did not work at all during the period when they were being tested by the author. The first of these was the TNT-mips system which was loaned by the U.K agents, Nigel Press Associates. The second one was the VirtuoZo system that was available in the SDS company. It should be noted, that, at the time of writing this chapter, the TNT-mips and VirtuoZo systems have recently been modified to overcome the difficulties experienced by the author. However these changes have come too late for the author to carry out further tests on them. Thus only four systems were available. However these constitute a representative group that have been tested rigorously in the present research project undertaken by the author.

5.4 Main Characteristics of the Systems Tested

Three commercially available systems have been tested with the SPOT stereo-pairs while a fourth one that has been developed for military mapping purposes has also been tested. These four are the following:-

(i) PCI EASI/PACE (Canada);

(ii) ERDAS OrthoMAX (U.S.A.);

(iii) R-WEL DMS (U.S.A.); and

(iv) FFI System (Norway)

As noted above, two of these systems - EASI/PACE and OrthoMAX - come from suppliers (PCI and ERDAS) that have been engaged principally in the remote sensing field and are relative newcomers to the field of digital photogrammetry. The third system - DMS - originates from the research activities of the well established Centre for Remote Sensing and Mapping Sciences (CRMS) of the University of Georgia. The fourth system - FFI - has been developed by Dr. Bjerke, a research scientist in the Norwegian Defence Research Establishment.

The first two of the systems - EASI/PACE and OrthoMAX - employ a full spatial (3-D) solution. They utilize mathematical modelling of the satellite orbital track in conjunction with classical analytical photogrammetric methods based on the use of collinearity equations - albeit modified for use with the SPOT images acquired using its linear array scanners. The third system - FFI - uses a unique 3-D solution which employs surface mapping functions to model the satellite orbital track in conjunction with 3D vectors to achieve the spatial intersection of the ground points. The fourth system - DMS - uses a 2-D polynomial procedure to fit the individual SPOT images to the terrain system followed by the derivation of heights using simple parallax heighting formulae. With all four systems, the SPOT images are first fitted to a group of ground control points. This is followed by the rectification of the images which removes tilt from them but not the relief displacement. Next a digital elevation model (DEM) is produced using automatic image matching techniques, the resulting elevation values forming the basis for the corresponding production of the ortho-images from the SPOT image data. Some more detailed discussion of the main characteristics of the four tested systems will be given below.

5.4.1 PCI EASI/PACE Package Characteristics

PCI is a Canadian company that was founded in 1982. Essentially PCI is a software house, i.e. it does not manufacture or supply hardware. Its software is used primarily for resources analysis and thematic mapping applications of remotely sensed data. Typical areas of its applications include forestry, geology, agriculture, ecology, geography, etc. that are traditionally associated with such packages. Only recently has it entered the field of digital photogrammetry, first with air photo and satellite modules attached to its EASI/PACE package and now with its newly introduced OrthoEngine product line.

EASI/PACE is a well established image processing package from PCI that features the radiometric and geometric pre-processing of a wide variety of remotely sensed images. It is available on a wide range of computing platforms and operating systems including PCs (running Windows 3.1, 95 or NT or OS/2), Unix-based graphics workstations (e.g. from, SGI, DEC, HP, IBM, and DG), DEC VAX/VMS systems and Apple Macintosh.

5.4.1.1 Photogrammetric Solution

For the geometric correction of satellite imagery using the EASI/PACE system, the mathematical model developed by Dr. Toutin of CCRS - which forms the basis of the analytical photogrammetric solution - has been used in the development by PCI of a satellite orthorectification and DEM extraction module within the main software package (Cheng and Toutin, 1995). In addition, a separate and complementary module implements the orthorectification of aerial photographs using a DEM, which can either be extracted from the overlapping pairs of photographs or is supplied from some other source such as an existing DEM derived from contoured maps (Cheng and Stohr, 1996).

The so-called **SMODEL** (satellite model) forms an essential part of the Satellite Ortho and DEM package. SMODEL carries out the orientation and the rectification of the individual SPOT images utilizing the satellite orbital data and the sensor attitude data as well as the GCPs for this purpose. It also gives the user the option to examine and modify the GCPs interactively if required. In the initial stages, each of the two linear array images making up the SPOT stereo-pair is handled separately using SMODEL. This means that the measurements of the GCPs are made monocularly on each of the images. Then each SPOT image is fitted individually to the ground control points using a separate space resection based on the available GCPs. On completion of this stage, the fit of the individual image to the GCPs after carrying out this analytical rectification procedure using SMODEL is then declared in terms of the residual errors for the planimetric coordinates only (either ΔX, ΔY or ΔE, ΔN) both for the control points and any available check points. From these results, the software gives the option for the user to delete any of the control points exhibiting such large residual errors that they can be regarded as gross errors or blunders. Alternatively it can be used to modify any points that show high residual error values or to designate some points as check points. The software guides the user through all of these operations via a series of prompts to which the user has to respond.

In response to a specific request from Professor Petrie and the author, PCI has now added an absolute orientation module to allow the formation of a stereo-model and to declare the residual errors in both planimetry and height (ΔX, ΔY, ΔZ) for the stereo-model. Thus the two images are fitted to the GCPs first via a special form of space resection followed by a space intersection to give the absolute orientation of the stereo-model.

5.4.1.2 Rectification and Resampling to Epipolar Geometry

After completion of the orientation procedures, EASI/PACE performs the rectification and resampling of the right image through the **SEPIPRO** routine. By this means, the right image is rectified, transformed and resampled to give it a quasi-epipolar geometry. This ensures that the left and right images are offset only in the horizontal direction. SEPIPRO rectifies the uncorrected SPOT satellite image and produces the epipolar projected image. Using the rectified epipolar image, the y-parallax between the left and right stereo-images is reduced to just one single image line. Hence, during the subsequent extraction of the digital terrain model (DEM), the matching procedure can be reduced to a search only in the x-direction, which will improve the speed and reliability of the DEM extraction.

5.4.1.3 Image Matching

To extract a DEM from a stereo-pair, it is necessary to match points on the one image with the corresponding points on the other image. For this purpose, the EASI/PACE system employs an area-based image matching technique. As a first step, the image matching technique implements a hierarchical or pyramidal approach (Dr. Cheng - personal communication). In this first step, the image is reduced to a low resolution on which a coarse matching is carried out and an approximate DEM calculated. This is useful for the next step to estimate the matching position, in which the image is enlarged to twice the resolution used in the first step and the DEM is calculated again. Again, these results will be used to estimate the matching position for the third step in which

the full resolution of the image will be used in the matching operation and the elevation values calculated.

The automated image matching procedure used to produce the DEM is carried out through a comparison of the respective grey values along the corresponding epipolar lines using the **SDEM** module. This procedure utilizes a neighbourhood matching method to match the pixels in the left image and the rectified right image. Matching is performed by considering the neighbourhood surrounding a given pixel in the left image (which constitutes a template) and moving the template within a search area on the epipolar image until a position is found which gives the best match. The actual matching method employed generates correlation coefficients between 0 and 1 for each matched pixel, where 0 represents a total mismatch and 1 represents a perfect match. A second-order surface is then fitted around the maximum correlation coefficients to find the match position to a sub-pixel accuracy. The difference in location between the centre of the template and the best matched pixel position is the disparity or parallax arising from the terrain relief, which an analytical photogrammetric solution using space intersection then converts to absolute elevation values above the local mean sea level datum. The elevation values at each of the ground control points resulting from this image matching process are then compared with the corresponding given elevation values of these points to produce the residual errors in ΔH at each point.

5.4.1.4 DEM Editing Tools

As a result of the representations made by Professor Petrie and the author, stereo-viewing has just now been implemented as part of the new OrthoEngine package. However, during the period of the author's tests of EASI/PACE, it had no stereo-mensuration capabilities to allow the 3-D measurement of GCPs or the correction of erroneous elevation values in the DEM. However, the package did contain a number of editing tools that can carry out noise removal; interpolation of missing values; filtering; etc. As will be seen later, these have been used by the author in the course of DEM generation and testing.

5.4.1.5 Ortho-Image Generation

The **SORTHO** module from the Satellite Ortho and DEM package can be run to produce ortho-images using the elevation data from the DEM. In this process, the DEM is used in the differential rectification and correction of one of the SPOT images in the stereo-pair to give it the geometry of a map. After the differential rectification has been completed, resampling of the grey level values in the output image is carried out using one of the commonly used resampling methods (nearest neighbour, bilinear or cubic).

5.4.1.6 Mosaicing DEMs and Orthoimages

The results of generating both the DEMs and ortho-images are high accuracy data sets for individual stereo-models which are in the form of separate files. Since, for a given area covered by several SPOT stereo-pairs, the original satellite images and stereo-models may have been acquired at different dates, the final individual ortho-images can differ quite significantly from one another in terms of their radiometry and appearance. Thus it is necessary to try to ensure that they have as far as possible a common scale grey level values so that there are no abrupt changes in appearance when they are mosaiced together. On top of this, the various DEMs and ortho-images produced from adjacent SPOT stereo-pairs may have substantial lateral and longitudinal overlaps with in which the corresponding elevation and grey level values from the adjacent models may differ.

In order to produce a single homogeneous mosaic from these different data sets, the variations in information content in the overlapping regions of adjacent scenes have to be resolved - both for the grey level values of the ortho-image mosaics and for the elevation values of the DEM. These then need to be merged together to form seamless ortho-image mosaics or DEMs. For the mosaicing of the ortho-images, EASI/PACE has a variety of tools to carry out automatic contrast matching and the feathering of overlap areas without any obvious joins being visible between the individual component images. Assistance with these operations being carried out on the ortho-image data is given to the user through the use of histograms of the grey level values which can be calculated

for each double set of information. Weighting can be assigned to the image data depending on its distance from the cutline between images. A similar set of tools is provided to resolve the differences in the elevation values in the overlapping areas to produce a seamless DEM.

5.4.1.7 Contour Generation and Mosaicing

The **CONTOUR** module which forms part of the vector utilities application packages within EASI/PACE can be used to generate contours from a DEM at a required contour interval. Contours can be generated by the program using a simple linear interpolation method. For the mosaicing or merging of the contours generated from different DEMs having a common overlap, the **VECMERGE** program within EASI/PACE can be used. This program merges the overlapping contours generated from different DEMs. The success of this merging depends largely on the accuracy of the component DEMs. Another simpler way of obtaining contours is by generating them from the already mosaiced DEMs.

5.4.1.8 Perspective Generation of Views.

Once the elevation values have determined correctly for the whole stereo-model, EASI/PACE provides additional routines that can be used to generate perspective views to present the terrain relief.

5.4.2 ERDAS OrthoMAX Package Characteristics

OrthoMAX is a software package that was developed originally by Vision International, a division of Autometric Inc. This is a well established American photogrammetric system supplier which has constructed many analytical plotters that have been used by U.S. government agencies. More recently, it has entered the digital photogrammetric field, first with its Pegasus DPW and later with its SoftPlotter DPW. The OrthoMAX package forms part of the software of the Vision SoftPlotter DPW that can be used to generate DEMs and ortho-images from stereo-pairs of aerial photographs and satellite

images. It runs primarly on Unix-based graphics workstation such or those from SGI and Sun

ERDAS is a remote sensing system supplier based in Atlanta, Georgia that has licensed OrthoMAX from Vision International and integrated it into its Imagine software package. ERDAS Imagine is a comprehensive and highly customizable image processing and raster-based GIS package which provides extensive tools for land cover classification and an interface for object-based spatial modelling. The Imagine OrthoMAX products are add-on modules to the baseline ERDAS Imagine image processing package. OrthoMAX has the capability of working with both standard aerial photography and SPOT satellite data.

OrthoMAX can be used to produce digital elevation data by extracting it automatically from stereo-imagery. OrthoMAX can also perform orthorectification to remove the inherent geometric distortions and the effects of terrain relief displacement that are present in aerial photographic or satellite imagery. Two versions of OrthoMAX are available; these are OrthoMAX Basic and OrthoMAX Professionals. The main features available in these two versions are given below in Table 5.2.

Type	**Triangulation and Orthorectification**	**Elevation Extraction**	**Stereo Viewing and Editing**	**Surface Modelling**	**Vector Module**
OrthoMAX Basic	Standard	Optional	Not Available	Optional	Optional
OrthoMAX Professional	Standard	Standard	Standard	Optional	Optional

Table 5.2 Availability of Modules for OrthoMAX Basic and Professional

In this research, OrthoMAX Basic has been used. It will be seen that this does not have the capability for stereo-viewing and editing. In this case, for the measurements of ground control points and tie points, the photogrammetrist has to carry out monocular measurements. However, the system shows the two images on the screen side-by-side for comparative purposes and to increase the speed of measurement of the control points.

5.4.2.1 Photogrammetric Solution

In many ways, this system is similar to the EASI/PACE system in that OrthoMAX uses a mathematical modelling of the satellite orbital track in conjunction with classical photogrammetric space resection and space intersection procedures in the form of a bundle adjustment program that has been suitably modified for use with linear array imagery. Using this program, the system is capable of carrying out the space triangulation and adjustment of a block of SPOT stereo-imagery. The bundle adjustment program can be used too for the orientation and rectification of individual stereo-pairs of SPOT images utilizing the satellite orbital data (and attitude data) available in the imagery header information as well as the GCPs for this purpose. The bundle adjustment process is started with the space resection followed by space intersection. Essentially the bundle adjustment process is applied to the imagery such that points in the ground space are first mapped accurately into image space and then the orientation data and measured control point data from the two overlapping images are used to form the model using space intersection. At the end of the first iteration in the bundle adjustment process, the pattern of residual errors can be reviewed. If necessary, an update can be applied to change the bundle adjustment parameters or to alter the number or pattern of control points used. Then a second bundle adjustment run can be implemented using the results from the previous bundle adjustment to give the initial starting values. The process continues in this iterative fashion until a satisfactory result is achieved.

5.4.2.2 Image Matching (Stereocorrelation)

As with EASI/PACE, the Vision International automatic image matching or stereo-correlation procedure uses an area correlation algorithm in which patches of pixels from the source images are correlated (compared) during the matching process. The primary correlation measure is to employ normalized cross-correlation which takes into account the overall differences in contrast and brightness between the image patches. Again, as with the EASI/PACE procedure, the particular algorithm used in this package employs a hierarchical or pyramidal approach in which correlations are performed successively at

increasingly higher resolutions of the imagery. This approach is useful both to speed up the computational process and to compensate for any large changes in elevation that may be present in the DEM - since it constrains any movement between resolutions to prevent "false fixes" at largely disparate elevation values. However, as far as can be seen from using the system, it does not carry out a pre-rectification of the individual images to allow searches for matches to be carried out along epipolar lines (as is done with EASI/PACE).

The unique aspect that is claimed for the Vision algorithm is the simultaneous derivation and use of orthorectified patches of the imagery in the matching process. By using results from both the current resolution and the previous resolution, increasingly accurate local models of the terrain around a point are used to orthorectify patches; the matching is performed to judge the correlation of the patches from the two images.

5.4.2.3 DEM Editing

Following the collection of the elevation data at each resolution, elevation values for those points which were not successfully correlated during the automatic process are interpolated by using suitable groups of successfully correlated points in the neighbourhood about each of these points.

5.4.2.4 Ortho-Image Generation

In the orthorectification process, the effects of relief are removed from the image. The user can select one of the images used in the bundle adjustment process along with the corresponding DEM. The orthorectification algorithm works in ground space; thus the 3D coordinate data for each point is projected back from the ground up to the image. In other words, a target set of horizontal ground coordinates is used to interpolate the associated height from the DEM. Then the ground point defined by this 3D coordinate set is projected back into the corresponding position in image space. Bilinear interpolation using the grey level values of the surrounding pixels is used to determine the best intensity value to be assigned to the resulting output pixel. The final output is an

ortho-image geocoded to the reference coordinate system with an accuracy that is the result of both the triangulation process and the resolution and the accuracy of the DEM.

5.4.2.5 Mosaicing of DEMs and Orthoimages

This system uses much the same method of mosaicing that has been implemented in the EASI/PACE system. Using the individual ortho-images and DEMs, this system creates seamless mosaics using automatic contrast matching, feathering of overlap areas and user defined cutlines.

5.4.2.6 Contour Generation

The user is also able to generate contours from the DEM using the built-in facilities of OrthoMAX. Much the same methodology applied in the EASI/PACE system is used in OrthoMAX to generate contours. The system is normally used with a simple linear interpolation method to generate the required contours.

5.4.3 Desktop Mapping System (DMS) Characteristics

The DMS package originates from research and development carried out by Professor Welch (1989) and his colleagues at the Center for Remote Sensing and Mapping Science (CRMS) at the University of Georgia in the U.S.A. The first appearance of this package was in 1987 at the ASPRS-ACSM Conference held in Baltimore, Maryland. The package is marketed commercially by a spin-off company called R-WEL.

DMS is a photogrammetric software package for use on personal computers that is designed to carry out digital mapping operations from stereo and monoscopic image data in digital format, including scanned aerial photographs and satellite images. The package is designed to work on standard, off-the-shelf Intel 486 or Pentium-based personal computers (PCs) operating under MSDOS 6.x, Windows 3.1/3.11 or Windows 95. The minimum recommended configuration is an IBM-compatible 486DX-66Mhz (or faster) computer with at least 8 Mbytes RAM (16 Mbytes for Windows 95).

Additional memory (giving a total of 16 to 32 Mbytes RAM) is recommended for use as a disk cache, while a 500 + Mbyte hard disk is a minimum with 1 to 2 Gb as the recommended size.

5.4.3.1 Photogrammetric Solution

This system can use only Level 1B SPOT images which have been pre-processed to include geometric corrections such as Earth curvature and rotation and which have been partly rectified since the effects of the tilts imparted by the off-nadir viewing mirror have been removed during the generation of the Level 1B image. As has been indicated in Section 5.4, the DMS system employs a quite different photogrammetric solution to that utilized in the previous two systems (EASI/PACE and OrthoMAX). The photogrammetric solution is carried out in two steps. In the first step, a minimum of 5 ground control points (GCPs) are identified on each image for use as registration points. The left image is designated as the reference image to which the right image is to be registered. After this registration has been completed, the second stage is to planimetrically rectify each of the two images forming the stereo-model using all available GCPs. This operation is based on the use of 2D polynomial equations which carry out a planimetric transformation of the individual SPOT images to fit the GCPs based on a least-squares solution. This will yield a set of correction coefficients for each image and determine a root mean square error (RMSE) value in planimetry indicating the degree of fit between the transformed image and the locations of the ground control points (GCPs). No space resection or absolute orientation is carried out in the photogrammetric solution as was the case with the two previously discussed systems. After the subsequent rectification of the individual images, a stereo-model can be formed and stereoplotting performed, where the height values can be measured manually in stereo by the operator using anaglyphic spectacles.

5.4.3.2 Image Matching (Stereocorrelation)

Alternatively the DMS program can create a DEM automatically using image matching techniques on the left and right image files created in the previous stage during the

registration and rectification process. No attempt is made to use epipolar geometry in the search operations carried out during image matching which is carried out on a patch-by-patch basis. For the actual matching, an area-based procedure is used based on the use of cross-correlation which determines the disparities or parallaxes resulting from the terrain relief. These values are then converted to the differences in height from the given elevation values at the surrounding GCPs using a simple parallax formula to give the final DEM elevation values.

5.4.3.3 DEM Editing

After DEM extraction, DMS provides filters for the elimination of large spikes or errors occurring in the DEM. The stereoimage can also be viewed in 3D for checking and editing purposes with the DEM overlaid on the top of the stereo-model as a grid of floating dots which allow the individual DEM elevations can be compared visually in 3D with the actual stereo-model. Erroneous points in the DEM will then be apparent; i.e. they will appear to lie either above or below the ground model surface. The user has to use the zoom facility to magnify the required area to be able to view the stereo-model and edit the DEM in 3D using the anaglyphic glasses.

5.4.3.4 Ortho-Images Generation

The orthorectification process in the DMS system is somewhat different to that undertaken by the other systems. In the DMS system, the ortho-image is produced via two separate processing stages. During the first stage, the DEM produced from the stereocorrelation process is used for the correction of the relief displacements that are present in the image. In the second stage, the final ortho-image is produced through the further rectification of the image, going from image coordinates to the ground coordinate system and using one of usual resampling methods (nearest neighbour, bilinear and cubic) to generate the corresponding grey level values.

5.4.3.5 Mosaicing DEMs and Ortho-images

The DMS software also has the capability to mosaic adjacent DEMs and ortho-images automatically with no interface with the user. The individual images can be joined and merged together to form a single ortho-image or DEM mosaic. If radiometric correction or enhancement of the whole composite ortho-image needs to be carried out, then a third-party image processing package such as Adobe Photoshop has to be used for the purpose.

5.4.3.6 Contour Generation

Contours cannot be generated from the DEM within the DMS system. In order to overcome this problem, the DEM has to be exported to third party software such as SURFER or EASI/PACE to generate contours.

5.4.4 FFI System

This system has been developed as a result of a research programme into mapping from satellite imagery carried out at the Norwegian Defence Research Establishment during the early 1990s by Dr. P. Bjerke, a research scientist working in the remote sensing section of this Establishment. It is not available commercially, but came to the notice of Professor Petrie through his connections with the Norwegian mapping and remote sensing community. It has been used for research and internal mapping projects within the Establishment. The system has only been implemented on PCs running under Microsoft Windows.

The system was selected for testing by the author as an alternative to the TNT-mips package, when problems started to appear with the latter system in fitting the stereo-model to the ground control points, and it was obvious that there was no quick solution to these problems.

5.4.4.1 Image Data and Ground Coordinate Requirements

This system is able to process and handle SPOT Level 1A data only. Also the system is has been devised and implemented on the basis that the ground control points (GCPs) must be given in geocentric coordinates within the WGS84 system. Thus, a number of separate transformations and reverse transformations have been developed between the WGS84 geocentric coordinate system and other well established coordinate systems, e.g. geographic latitude and longitude and the UTM projection, and between the geocentric values and the associated heights above either the reference ellipsoid or the geoid.

5.4.4.2 Photogrammetric Solution

The FFI system employs completely different methods of geometric modelling and of generating 3D coordinate data to those commonly used in space photogrammetry that have been applied in the EASI/PACE and OrthoMAX systems. A highly original solution has been devised by Dr. Bjerke which is not based on the conventional analytical photogrammetric theory or the algorithms normally used with SPOT stereo-pairs. Instead, it makes extensive use of surface mapping functions for the modelling of the orbital path of the SPOT satellite. Initially the orbital parameters for each of the individual images making up the stereo-pair are modelled and determined separately. For this analysis, the raw satellite ephemeris data contained in the SPOT header file is used as basic information in conjunction with (i) measurements of the positions of the GCPs on the image and (ii) the GCP terrain coordinates to generate a set of correction parameters for an individual image based on these special mapping functions. Essentially these functions take the place of the modified space resection technique using collinearity equations which is normally used with SPOT stereo-imagery to generate the individual positions and heights of the satellite and the attitude values of its sensor at each successive perspective centre (corresponding to each individual line of the image) along its orbital path. Once the analysis and generation of the mapping functions has been completed separately for each image, they are used as corrective values to generate the 3D coordinates of any point lying within the stereo-model. These

can be computed from the intersection of the two 3D vectors generated from the image coordinates of that point measured on each of the individual images making up the stereo-pair.

5.4.4.3 Rectification and Resampling to Epipolar Geometry

After the determination of the sets of surface mapping functions and the fitting of the stereo-model to the GCPs, each of the two images forming the stereo-pair is rectified and resampled to give a quasi-epipolar geometry. In this operation, the orientation and offset of the corresponding lines in each image is altered and a relatively simple transformation can then be used to produce the corresponding quasi-epipolar lines. This operation is supplemented by an appropriate resampling of the grey level values of the data along each of these lines.

5.4.4.4 Image Matching (Stereocorrelation)

The actual image matching operation is undertaken with a search for matching points along the quasi-epipolar lines. In the FFI system, an area-based correlation procedure is employed. In order to speed up the search, the system uses image pyramids with matching first carried out using a coarse resolution which speeds up the correlation between the two images; then a much more accurate correlation is carried out at a series of different levels using increasing resolution on each occasion. The system employs correlation and re-sampling in small patches, which result in a large number of individual files that later have to be merged together. A unique aspect of this system of generating the DEM is that it utilizes a fixed grid interval or post spacing of 10m.

5.4.4.5 Contour Generation

As the case in DMS system, contours can only generated from the DEMs using third party software.

5.4.4.6 Ortho-image Generation

The FFI system employs much the same procedure for ortho-image generation as that which has been employed in the EASI/PACE and OrthoMAX systems. Since the DEM generated by this system has a fixed grid spacing of 10m, so the ortho-image generated by this system is also based on a 10m pixel size.

5.5 Summary

In this chapter, the application of digital photogrammetric techniques to SPOT stereo-pairs and the classification of digital photogrammetic workstation, have first been presented and discussed. These have been followed by a description of the main characteristics of the systems that have actually been tested in this research project. Table 5.3 summarises the main characteristics of the four systems employed in the present research project.

System	EASI/PACE	OrthoMAX	DMS	FFI
Vendor	PCI	ERDAS	R-WEL	Dr. Bjerk (NDRE)
System Product	EASI/PACE	Imagine	DMS	FFI
Operating Systems	Unix, DOS, Windows	Unix	DOS,Windows	DOS, Windows
Year of Introduction	1991	1992	1987	Early 1990s
Imagery Handled				
Aerial Photographs	Yes	Yes	Yes	No
SPOT Processing Levels	1A and 1B	1A and 1B (old format)	1B only	1A only
GCP Measurements				
Single Image Measure	Yes	Yes	Yes	Yes
Two Images (side by side)	No	Yes	Yes	No
Stereo Measurements	No	No	No	No
Stereo				
Viewing	None	Alter.shutter (Professional only)	Anaglyph	None
Measure	No	Yes (Professional only)	Yes	No
Feature Extraction	Yes only x, y from Ortho-image	Yes (X,Y, Z) (Professional only)	Yes (X,Y, Z)	No
Orbital Modelling	Yes	Yes	No	Yes
Photogrammetric Solution	Collinearity	Collinearity	Polynomial	Surface Mapping Functions
Search and Matching				
Epipolar Lines	Yes	Yes	No	Yes
Pyramidal Approach	Yes	Yes	No	Yes
Image Matching	Area-based (Cross Correlation)	Area-based (Cross Correlation)	Area-based (Cross Correlation)	Area-based (Cross Correlation)
DEM and Orthoimages	Yes	Yes	Yes	Yes
DEM Editing Tools	Yes	No (Professional only)	Yes	No
Contours	Yes	Yes	No	No
Perspective View	Yes	Yes	Yes	Yes
Profiles	No	Yes	Yes	No
Mosaicing	Yes	Yes	Yes	No
Reports (RMSE X,Y,Z)	Yes	Yes	Yes (x,y only; Z later)	Yes
Map File Output	Yes	Yes	Yes	Yes

Table 5.3 Characteristics of the systems employed in the present research

(1) Three of these systems (EASI/PACE, OrthoMAX, FFI) employ a full 3-D solution, two of them (EASI/PACE, OrthoMAX) utilizing classical photogrammetric methods based on the use of collinearity equations as applied to linear array imagery, while the third (FFI) employs surface mapping functions. The fourth system (DMS) uses a 2-D polynomial solution which is applied to each image separately as a rectification procedure.

(2) With regard to the rectification and resampling methods that are used, the DMS system rectifies and resamples both of the images forming the stereo-model. With EASI/PACE, the system rectifies and resamples the right image only to produce it with epipolar geometry. For the FFI system, both of the images forming the stereomodel can be rectified to produce epipolar geometry. In the case of OrthoMAX, no prior rectification and resampling to epipolar geometry is carried out.

(3) For image matching, all of the systems employ area correlation based on cross-correlation. Three of these systems (EASI/PACE, OrthoMAX, and FFI) employ image pyramids to assist the image matching procedure. As noted above, the EASI/PACE and FFI systems also employ epipolar lines for search purposes to speed up the correlation process, while in OrthoMAX and DMS the correlation is carried out on a patch-by-patch basis.

(4) The elevation values for the DEM are calculated from the disparity or parallax values arising from the terrain relief, employing an analytical photogrammetric solution using space intersection in the case of the three systems employing a 3D solution. In the case of the DMS system, the differences in x-parallax are used to derive relative elevations or height differences utilizing a simple parallax equation. When referenced to one or more ground control points of known elevation, these height differences give the absolute elevation values required to form a DEM. Two of the systems (EASI/PACE and OrthoMAX) interpolate the heights at different grid intervals according to the user input, while in the DMS system, the minimum grid interval appears to be 100m. In the FFI system, the heights are generated at a 10m grid interval.

(5) For ortho-image generation, basically all of these systems employ the same differential rectification and resampling method.

(6) With regard to the respective editing facilities provided for use with the DEMs, two systems (EASI/PACE and DMS) can provide fairly full editing facilities. For the other

two (OrthoMAX and FFI) systems, few editing tools are provided except for the OrthoMAX Professional version.

(7) Mosaicing facilities are provided by three of the systems (EASI/PACE, OrthoMAX and DMS). Two systems (EASI/PACE and OrthoMAX) provide an interface with the user to radiometrically match the mosaiced images, while no interface with the user is provided by the DMS system.

(8) Using simple linear interpolation methods, contours can be generated from only two of the systems (EASI/PACE and OrthoMAX), while the other two systems require third-party software to generate contours.

5.6 Conclusion

From the information and discussion given above in this Chapter, it can be seen that these now exists a substantial capability to undertake photogrammetric operations on SPOT stereo-imagery in digital form using DPWs. Previously such operations could only be undertaken on two or three specific models of analytical plotter using hard-copy images. Furthermore data extraction from SPOT stereo-pairs was largely confined to the manual stereo-plotting of the planimetric features visible in the stereo-models and to the manual measurement of spot heights and contours by operators in the classical manner. Needless to say, these characteristics restricted the use of SPOT stereo-pairs for topographic mapping purposes to a very considerable extent. As a result, only a very few national mapping organisations have attempted to use SPOT imagery in this way; other organisations simply did not have the knowledge or expertize to do so.

However, over the last few years, the advent of DPWs has allowed many more systems to be developed with the capability of conducting photogrammetric operations on SPOT stereo-pairs. These have now come on to the market. Thus more organisations can exploit their potential for small-scale topographic mapping and the generation of spatial data for use in GIS and geophysical systems. As discussed above in this Chapter, this development has come both from the mainstream photogrammetric system suppliers and from the remote sensing system suppliers. Indeed, in this respect, it is very interesting to note the convergence of the two previously quite separate groups of suppliers with their

different interests, markets and technologies. Now, in this particular area, they have come together developing powerful systems with features that previously were unique to only one group. Thus, for example, analytical photogrammetric procedures, stereo-viewing and accurate 3D measuring techniques have come from the one side, while radiometric enhancements and geometric pre-processing has come from the other side. Developments in image matching procedures appear to have come from both sides. The resulting systems are notable for the high degree of automation that they offer, especially in the generation of DEMs and ortho-images.

Much of this development to handle SPOT stereo-pairs in this way has only come to fruition or maturity over the last three or four years. Indeed the developments in this area during the period of the author's project have been quite marked. It is therefore very timely to conduct research into the geometric accuracy of the data that can be generated from SPOT stereo-pairs by a representative group of these systems and to validate the products such as DEMs and ortho-images that they can generate using highly automated techniques.

Since, in this chapter, the application of digital photogrammetric techniques to SPOT stereo-pairs has been introduced and discussed in fairly general terms and has been followed by an overview of the main characteristics of the systems that implement these techniques, in the next chapter, the mathematical models and algorithms employed by the various systems will be explained in more detail.

CHAPTER 6: MATHEMATICAL MODELS AND PHOTOGRAMMETRIC SOLUTIONS APPLIED IN THE TESTED SYSTEMS

6.1 Introduction

Accurate mapping of the terrain from any form of remotely sensed imagery requires the correct geometric relationship to be established between the image and the ground. This requires both a model that describes the exact sensor geometry and a model that describes the variation in the position and attitude of the imaging sensor with time. The latter requirement arises from the fact that the remotely sensed imagery produced by scanners, radar etc. is built up as a continuous strip image through the forward motion of the airborne or spaceborne platform on which the sensor is mounted. Thus an image such as that produced by the SPOT scanner's linear array sensor is exposed from a continuous series of exposure stations in space. For photogrammetric work, the positions and heights of each of these stations (i.e. the perspective centres) have to be established together with the corresponding set of attitude (tilt) values - since these will also be varying continuously as the image is being acquired. Thus the situation experienced during the exposure of a single SPOT image is very different to that of an aerial or space photograph, where the exposure of the whole image is made from a single exposure station and a single set of attitude (tilt) values applies to the whole image.

By contrast, the SPOT HRV sensor is a pushbroom scanner that employs a linear array of CCDs (charged-coupled devices) as its imaging sensor. The projection of this linear array on the ground forms a very narrow rectangular strip with its longer-side oriented perpendicular to the flight line of the SPOT satellite. This produces a single line of the strip image. Successive lines are exposed to build up the complete image through the forward motion of the satellite with the linear array exposing each new line as a unit simultaneously (see Figure 6.1). Thus a continuous two-dimensional (2D) image is constructed by the SPOT sensor as a long strip covering the ground located under the satellite flight line and lying within the angular coverage of the HRV sensor.

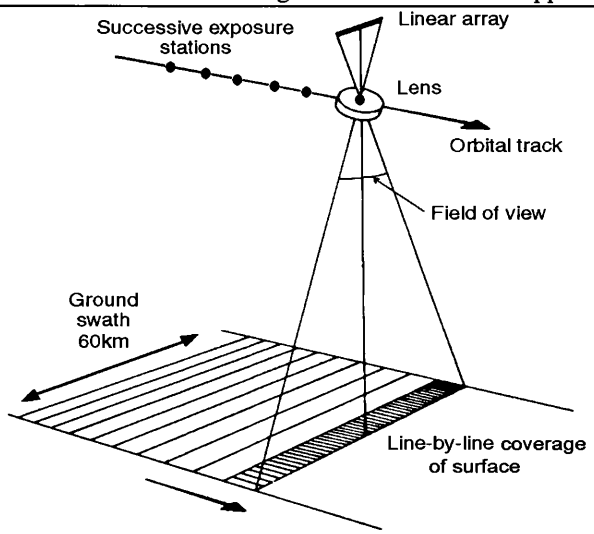

Figure 6.1 The pushbroom scanner

Linear array scanners such as those used in the SPOT and IRS-IC satellites acquire their stereo images cross-track from adjacent orbits using their off-nadir viewing capabilities which offer different base-to-height ratios up to 1.0 (see Figure 6.2). However the differences in time for image acquisition (often amounting to several months) can cause some problems arising from seasonal climatic differences resulting in changes in the appearance of the land covered by the image (Petrie, 1996). This gives rise to difficulties in the formation of the model of the ground, especially with the automatic image matching procedures often used to extract DEMs from SPOT stereo-pairs and in the image interpretation carried out during stereoplotting with extraction of the features that have to be mapped from the stereo-model.

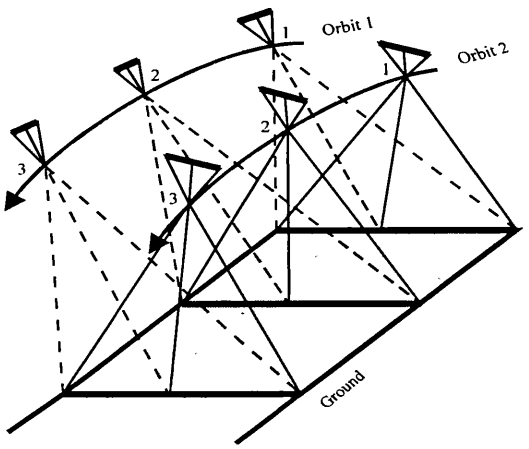

Figure 6.2 Formation of SPOT stereo-model from overlapping cross-track images

6.2 SPOT Image Formats

Consideration has also to be given to the fact that the image data can be ordered and supplied by the various SPOT processing facilities in a variety of formats with widely differing degrees of processing and accuracy. These may alter the basic geometry of the SPOT image, so requiring modifications to be made either to the modelling or to the photogrammetric procedures used in mapping from these images. The two most commonly supplied are the so-called Level 1A and Level 1B formats.

6.2.1 SPOT Level 1A Imagery

With Level 1A imagery, no geometric corrections are applied, only radiometric corrections. In particular, detector normalization is performed using a linear model which equalizes the differences in sensitivity between individual CCD detectors. The image comprises 6,000 x 6,000 pixels in panchromatic mode, or 3,000 x 3,000 pixels in each band when the sensor is used in multispectral mode. The image appears as a square (see Figure 6.3), irrespective of the mirror inclination that produces the tilt required to give the cross-track coverage of a SPOT stereo-pair.

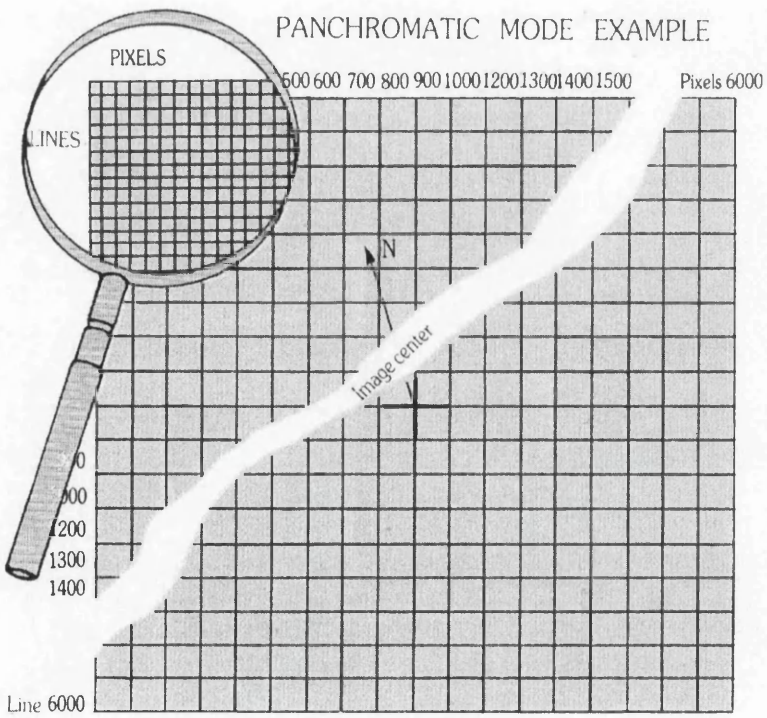

Figure 6.3 SPOT Level 1A format

In this case, the number of pixels remains constant, but the area covered by each pixel will vary in the cross-track direction according to the viewing angle. In this case, every pixel could be 10 m or more depending on the viewing angle of the sensor. However the geometry of this Level of SPOT image is relatively simple and easy to understand: so most of the photogrammetric solutions that have been developed for use with SPOT imagery are based on the use of Level 1A imagery.

6.2.2 SPOT Level 1B Imagery

In Level 1B imagery, the basic geometry of the SPOT images has been altered during their processing in the SPOT facility. The radiometric corrections are in fact the same as those applied to Level 1A images. However the geometric corrections that are applied to them during processing are much more extensive and take into account the systematic distortions of the raw image due to Earth rotation and curvature; the sensor viewing angle; and desmearing. Since the tilt of the off-nadir viewing is compensated for, so the image is partially rectified and approximates to an orthographic view of the Earth - though it still contains the displacements produced by the terrain relief and the displacements caused by small changes in the attitude (tilt) of the sensor during flight (Valadan Zoej and Petrie 1998). After this rectification, every pixel has the same size - 10 or 20 metres according to the spectral mode used - while the number of pixels varies from 6,400 to 8,500 in panchromatic mode and from 3,200 to 4,240 in multispectral mode, depending on the viewing angles which can reach ± 27°. While the dimension of the image is altered (i.e. increased) in the cross-track direction, the dimensions in the along-track direction stay fixed. This gives an image size of between 60 to 80 km in the cross-track (East-West) direction and 60 km in the along-track (North-South) direction. The non-image areas of the overall image are generated by adding zero values to the pixels (Figure 6.4).

For SPOT Level 1B images produced before September 1995, SPOT Image utilized a third-order polynomial to carry out the required geometric corrections, while for images produced after this date, a fifth-order polynomial has been used.

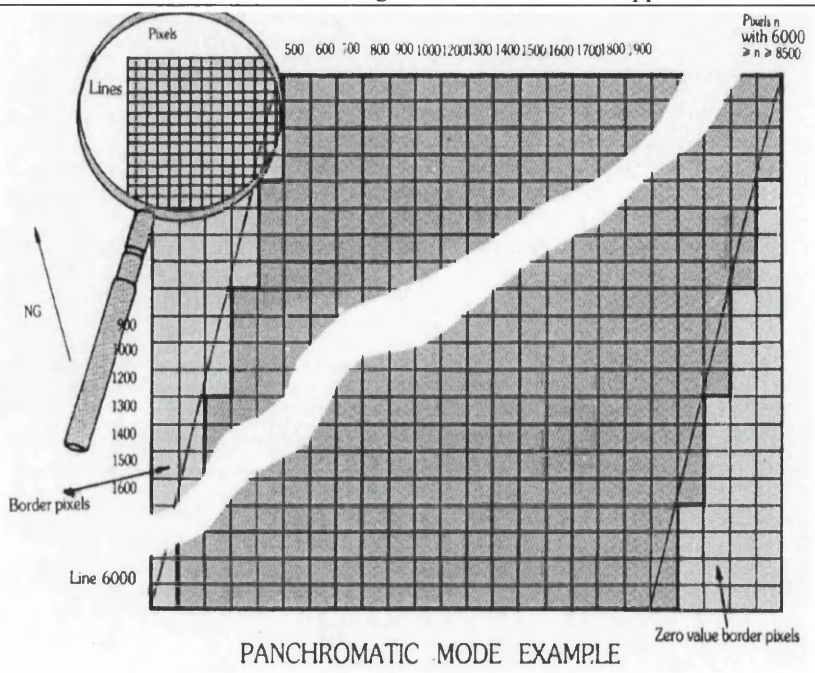

Figure 6.4 SPOT Level 1B format

Because of the near-orthographic geometry, Level 1B images are very popular with many users - since they are more easily correlated with existing map coverage of the imaged area. In view of this, the software packages devised by the system suppliers need to be able to handle both commonly used Levels of SPOT imagery. However, only a few packages can actually do so. The usual approach taken by most suppliers is to standardize on a Level 1A solution and to convert the Level 1B images back to their equivalent Level 1A format so that they can utilize the same photogrammetric solution.

6.2.3 SPOT Level 2A and 2B Imagery

Other Levels of processing such as Levels 2A and 2B can be supplied by the SPOT processing facilities. Level 2A is a precision image which includes both the radiometric corrections performed in Level 1A and certain bi-directional geometric corrections carried out without the use of ground control points. The SPOT scene is rectified in a comparatively simple manner to fit a given cartographic projection (e.g. Lambert Conformal, UTM, Oblique Mercator, Polar Stereographic, Polyconic, etc.). The image is also rotated and aligned with true north. These corrections are performed using only the satellite attitude data (i.e. the variations in the satellite attitude recorded during imaging) and the basic imaging geometry without using ground control points. By contrast, a

Level 2B image is a higher-precision product which includes both the radiometric corrections performed in Level 1A and additional bi-directional geometric corrections involving the use of ground control points. Again the scene is rectified to fit a given cartographic projection. Level 2B products are aligned with true north which also involves resampling the image. To perform Level 2B processing, maps of sufficient accuracy are required for the acquisition of the ground control points (preferably at a scale of 1:25,000 to ensure sufficient accuracy). These maps must be provided to the SPOT processing facility by the customer. If no map is available, control points will have to be acquired on the ground, e.g. by a GPS survey. The processed image is then directly registerable with a map at these control points. However there will still be discrepancies between the two products, since the displacements due to relief have not been removed from the images. These can only be removed through the availability of a DEM which is used in a further differential rectification procedure to produce an ortho-image.

6.3 Geometric and Mathematical Modelling

The CCD line scanner geometry can be recovered to a satisfactory level using one of various mathematical models of varying complexity and employing different approaches. In this respect, it should be realised that, whereas there is only little variation possible in the mathematical modelling of aerial photography, with SPOT imagery, many valid alternatives exist, especially for the modelling of the satellite's orbit and the attitude of the platform and its HRV sensor (De Hann 1992). Quite a number of researchers have investigated the geometry and developed mathematical modelling suitable for use with cross-track stereo scanner images. As a result of these investigations, quite a number of different mathematical models have been devised for the photogrammetric orientation, rectification and exploitation of these images. These different mathematical models can be divided into three main groups (Valadan Zoej 1997) as follows:

- A two-dimensional interpolative approach using polynomials of various degrees;
- A two-dimensional projective transformation; and

- A three-dimensional approach developed from a rigorous geometric analysis of linear array imagery.

Only the three-dimensional approach can give an exact photogrammetric solution. As noted above, most of the mathematical models that have been applied to SPOT imagery using this approach are based on the use of collinearity equations. Various alternative methods using orbital parameters have been devised by different researchers such as Guichard (1983), Toutin (1985, 1986, 1990), Gugan (1987), Westin (1990, 1991), Priebbenow (1991), De Haan (1991, 1992), Radhadevi and Ramachandran (1994). Some others have used an alternative approach - that of the multiple projection centre model: these include the methods devised by Kratky (1987, 1988a, 1988b), Granguly (1991), Shibasaki et al. (1988), Deren and Jiayu (1988). Still others such as Konecny et al (1987) and Kruck (1987) have used an additional parameter model. Recently El-Manadili and Novak (1996) have developed a mathematical model for the geometric correction of stereo linear array imagery based on the well-known Direct Linear Transformation (DLT) model, originally developed by Karara and Abdel Aziz (1979). A detailed account of all of these different approaches has been given in the Ph.D. dissertation of Dr. Valadan Zoej (1997).

With regard to the various software packages used in the author's tests, three of them - the PCI EASI/PACE, ERDAS OrthoMAX and FFI systems - use a three-dimensional approach, while the fourth - R-WEL DMS - uses a two-dimensional interpolative approach. The two-dimensional projective transformation has not been used in any commercial system to date, though the basis of a such a system has been indicated by Novak (1992).

6.3.1 Orbital Parameter Data

The auxiliary data that is generated by the SPOT satellite comprises a set of position, height, velocity and attitude (tilt) values that have been measured by the package of measuring instruments (gyroscopes, accelerometers and tilt sensors) installed in the satellite. The measured values of these parameters are first recorded on-board the SPOT satellite and then telemetered back to the ground receiving station along with the actual image data. The orbital parametric data is processed at the ground station where it is

supplemented by information got from ground tracking and is then issued as a header file accompanying the image data supplied to users. This orbital parameter data has only been measured with a certain limited accuracy in terms of achieving a photogrammetric solution that can provide accurate terrain data in the form of a map, an orthoimage or a DEM. Nevertheless this orbital data, however limited it is in accuracy terms, serves as the starting point for many of the photogrammetric solutions that have been adopted and implemented in the systems that are currently available on the commercial market. This data is used initially to give a first solution which is then corrected and refined through the use of ground control points (GCPs) until a correct orientation of the overlapping stereo-images has been achieved. When this situation has been reached, it allows a stereo-model to be formed and the appropriate terrain coordinate data can then be measured and determined to the accuracy limits that are inherent in the particular pair of SPOT images being used for the purpose. In this particular respect, the base:height ratio of the particular pair of overlapping cross-track images plays an important role in the accuracy of the final coordinate values.

As noted above, the accuracy of the positional data given by the SPOT orbital navigation system is somewhat limited - in the order of ±50m to 100m after post-processing at the ground receiving station. These positional values can be given in terms of the geocentric coordinate values (X_S, Y_S, Z_S) of the satellite in space, where S is the instantaneous position of the satellite and can be regarded as the perspective centre through which all the rays from the ground pass to form the image of the individual line of the SPOT image. Closely associated with these coordinate values are the velocity vectors (V_X, V_Y, V_Z) which are measured along the three coordinate axes by the on-board sensors.

Values of both sets of these parameters are measured by the system at time intervals of one second. Since the speed of the SPOT satellite over the ground is 6.4 km/sec, this means that, for an individual scene covering 60 x 60 km, only 8 or 9 directly measured sets of values of these parameters are available for each image of the stereo-pair and for the orbital modelling and photogrammetric solution. With regard to the attitude of the platform and its HRV sensor, this is continually measured by a set of gyroscopes on-board the satellite which provide data on the rates of change in the tilts as measured

around the pitch, roll and yaw axes. These values are recorded at intervals of 1/8th second (0.125s) (De Hann 1992). Thus there are 70 sets of tilt values available for a single SPOT image. So the values of the orbital parameters for all the intermediate positions of the satellite at which an individual image line has been acquired have to be generated by interpolation.

To do this, the relationship of each line on the SPOT image with respect to time must be accurately known. The time value (t_{3000}) for the centre point of a SPOT Pan scene is given by the header file to the nearest millisecond in the absolute time reference system of Julian days, hours and seconds used in the orbital tracking. The exact time interval between lines is 1.504 millisecond - which means that, for the acquisition of a complete image of 6,000 lines, the elapsed time is approximately 1.5 millisecond x 6,000 lines = 9,000 milliseconds = 9 seconds. With sampling of the positional and velocity vectors being carried out at one second intervals, this means that this information is only available at intervals of 6,000 lines ÷ 9 = 667 lines along the image in the flight direction. In the case of the attitude data, this is only available at intervals of 6,000 lines ÷ 70 = 86 lines. Hence the need for interpolation.

During the time over which the image data and the associated orbital parameter data is being collected, the SPOT satellite remains relatively stable in terms of its attitude. This results from the fact that the satellite is moving in the near-vacuum of space; this is in great contrast to the atmospheric turbulence which affects imaging sensors mounted on airborne platforms. Thus space imagery is not subjected to the unpredictable tilts and shifts of the type commonly experienced with the images produced by aerial cameras and airborne scanners. Instead changes in attitude take place quite slowly and in a relatively predictable manner. This allows space scanner imagery to be modelled mathematically to a good accuracy using quite simple interpolative functions.

In the first instance, each single line of the SPOT image can be regarded as an individual image (equivalent to an individual photograph) with its own perspective centre defined by its X_S, Y_S and Z_S coordinates and with its own set of attitude values. Of course, in practice, these values are highly correlated with the corresponding values of the adjacent

image lines with only very small changes in their respective attitude values. This greatly aids the modelling.

6.3.2 Coordinate Systems

Figure 6.5 shows the Keplerian elements (Ω, ω_p, f and i) - in which the satellite orbital positions are commonly expressed during tracking. Those exterior orientation parameters which depend on the satellite position and velocity vector can be modelled by consideration of these Keplerian elements. If required, the geocentric coordinates of the perspective centres (X_S, Y_S, Z_S) can be derived from the Keplerian orbital parameter data as follows (Valadan Zoej, 1997).

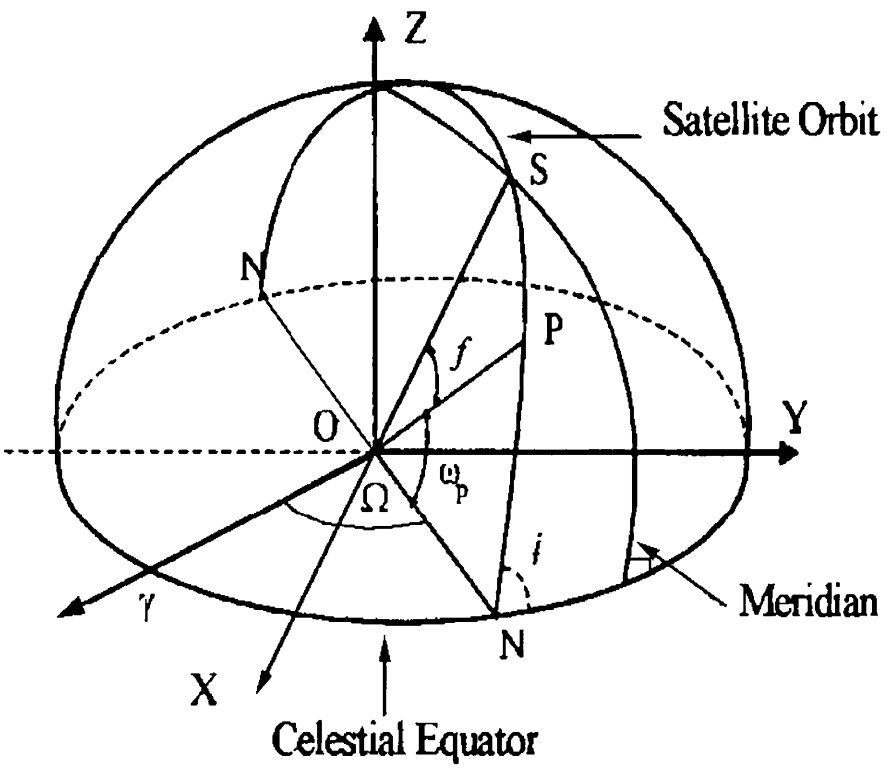

Figure 6.5 Keplerian parameters in space related system.

$$\begin{bmatrix} X_S \\ Y_S \\ Z_S \end{bmatrix} = r \begin{bmatrix} \cos\Omega\cos(f+\omega_p) - \sin\Omega\sin(f+\omega_p)\cos i \\ \sin\Omega\cos(f+\omega_p) + \cos\Omega\sin(f+\omega_p)\cos i \\ \sin(f+\omega_p)\sin i \end{bmatrix} \tag{6.1}$$

where, r = a $(1-e^2) / (1 + e \cos f)$; in which a is the semi-major axis of the satellite orbit;

e is the orbit eccentricity;

f is the so-called true anomaly (the angular distance of the satellite after passing perigee)

ω_p the argument of perigee;

Ω the right ascension of the ascending node; and

i orbital inclination.

Thus the coordinates of the satellite itself can be expressed in terms of the X, Y, Z coordinates of a geocentric coordinate system such as GRS 80 (used by SPOT Image) or WGS 84. For mapping purposes (– as distinct from satellite tracking or geodetic purposes -) neither of these systems is convenient, so usually a terrain related system such as UTM will be used instead. So the availability and use of transformations between these different coordinate systems in object space are a necessity in most space photogrammetric work.

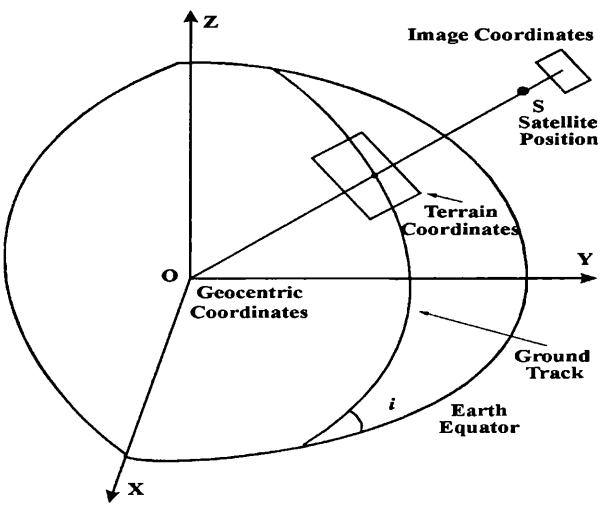

Figure 6.6 Relation between geocentric, terrain and image coordinate systems in Earth-related terms.

Finally an image coordinate system will be used to define the coordinates of points measured on the images. It should be pointed out that there is absolutely no standardisation in the various coordinate systems that are used in space photogrammetry. Each researcher defines his set of own coordinate systems in his own particular way and may select quite a different set of parameters to be used in the photogrammetric solution to those used by other researchers. These characteristics are reflected both in the articles that they have published in the scientific literature and in

the actual systems from commercial suppliers that have been based on their published work.

6.3.3 Collinearity Equations

The image coordinates of a point located along a particular line of the image are related to the object coordinates of the corresponding point on the terrain via the well known collinearity equations of analytical photogrammetry. Each ray from the terrain will pass through the appropriate perspective centre to be imaged in the corresponding point in the image plane.

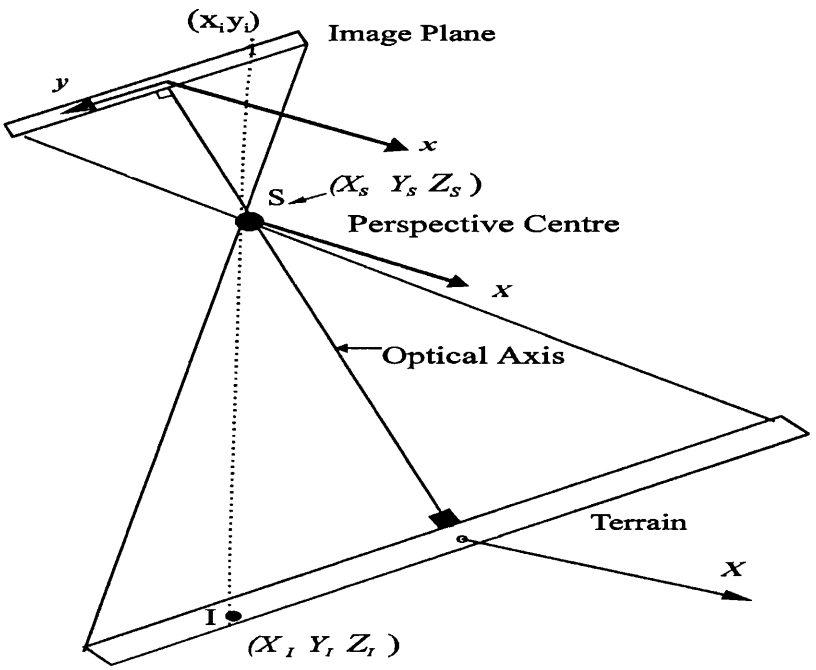

Figure 6.7 Cross Section for a single line of the SPOT image.

As mentioned above, a separate set of collinearity equations can be generated for each line linking the image points (i) with the corresponding ground points (I) and passing through the perspective centre (S). These will have the general form (Valadan Zoej 1997):-

$$\begin{vmatrix} x_i - x_0 \\ y_i - y_0 \\ -c \end{vmatrix} = \lambda R_1(\beta).R_3(\kappa).R_2(\varphi).R_1(\omega)R_2\left[\left(f+\omega_p\right)-\frac{\pi}{2}\right]R_1\left(\frac{\pi}{2}-i\right).R_3(\Omega-\pi)\begin{vmatrix} X_I - X_S \\ Y_I - Y_S \\ Z_I - Z_S \end{vmatrix} \quad (6.2)$$

Where β = the viewing angle (mirror inclination angle for cross-track coverage);

x_i y_i = image coordinates of the image point i;

x_0, y_0 = image coordinates of the principal point of the image;

X_S, Y_S, Z_S = object coordinates of the perspective centre S;

X_I, Y_I, Z_I = object coordinates of ground point I;

ω, φ, κ = the tilt values at the time of exposure; and

λ = the scale factor.

It will be seen that, unlike the classical form of collinearity equation used with aerial photographs where the rays pass from ground to image through a single perspective centre for all positions on the image, the solution used with scanner images is constrained to a single (Y/Z) plane with its own individual perspective centre and containing the image line and the corresponding line on the terrain. It will be seen also that any displacement of the image due to relief will also be constrained in a similar manner - i.e. it can only occur in the y-direction on the SPOT image.

6.4 EASI/PACE Mathematical Model

6.4.1 Introduction

The mathematical model which underlies and forms the basis of the analytical photogrammetric solutions adopted in the EASI/PACE package is based on the work originally carried out by Guichard (1983) and Toutin (1985) and since developed further by Toutin (1995) at the Canada Centre for Remote Sensing (CCRS). It follows the three-dimensional approach based on the use of collinearity equations which relates corresponding points in the image space and object space via the perspective centre of the imaging sensor. As discussed above in Section 6.3.3, these equations have been adapted and formulated to suit the geometry of linear array (pushbroom) scanners such as SPOT in which each line of the scanner image has an individual and different perspective centre, instead of the single perspective centre for a whole image which exists with the frame photographs generated by aerial or space cameras.

Besides the need to estimate and reconstruct the 3-D coordinates of the individual perspective centre for each individual line of a linear array image, it is also necessary to take account of the changing attitude of the satellite and its sensor over the time period during which the SPOT image has been acquired. Again, as discussed above, this is achieved through the modelling of the satellite orbital path in space by combining the satellite's positional and velocity vectors with the changing attitude of the platform to generate the exterior orientation parameters for the linear array image. Thus Toutin's model takes into account both the displacements due to the dynamically changing platform and sensor motion and orientation and those arising from the sensor geometry due to the physical characteristics of the Earth (rotation, curvature, and ground relief) (Toutin, 1985). His model has also been developed to take into consideration the geoid and the ellipsoid used in the area over which the image has been acquired and the relevant cartographic projection system such as UTM or a national variant (such as the JTM used in Jordan).

6.4.2 Reference Systems

The different spaces with their reference coordinate systems that are considered by Toutin in his mathematical representation for connecting the two-dimensional image coordinates to the three-dimensional object coordinates are as shown in Figure 6.8. The definition of these systems are as follows:

(a) Image coordinate system x, y (Figure 6.8a)

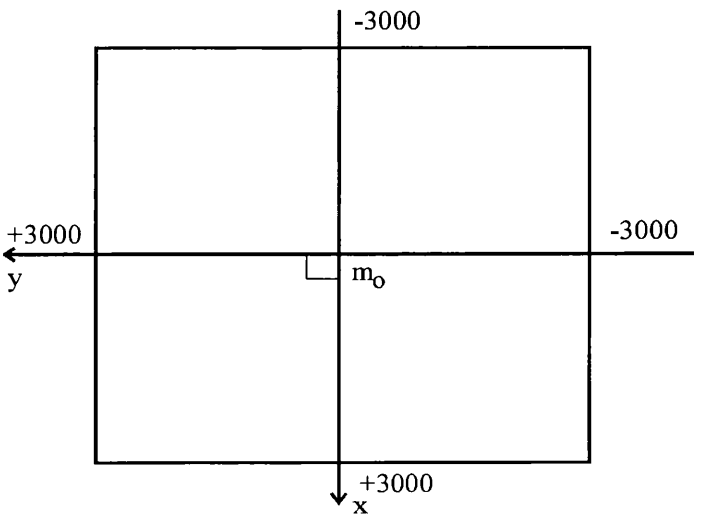

Figure 6.8a Image Coordinate System

where the origin is the central point m_0 of the image;

the y-coordinate is the position corresponding to the detector element number in an individual scan line; and

the x-coordinate is the line corresponding to the scan line number and is proportional to time.

(b) A local terrain coordinate system, with its terrain coordinates (X_L, Y_L, h), (Figure 6.8b).

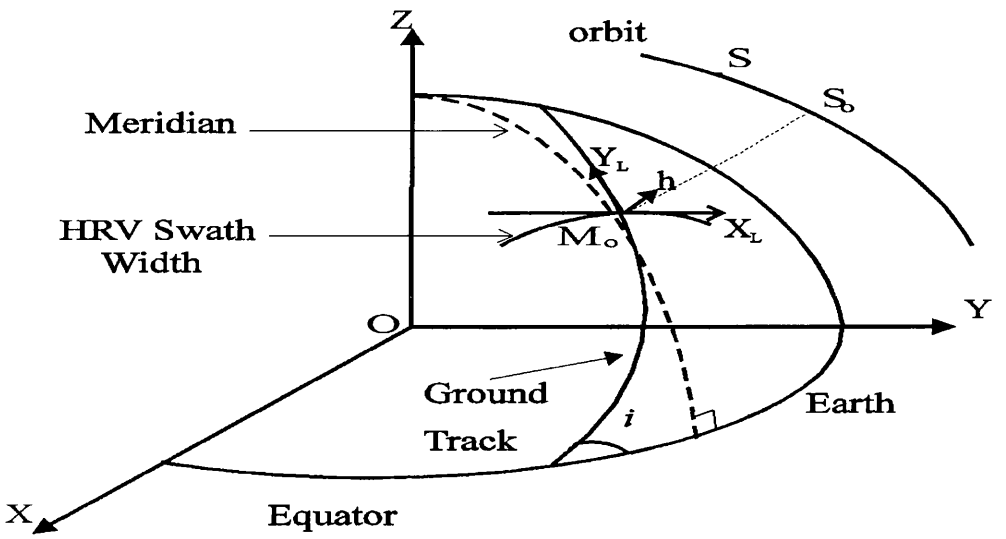

Figure 6.8b Local Terrain Coordinate System

where the origin is centred on M_0, the intersection of the centre line of the scene with the ellipsoid;

the X_L coordinate is the coordinate of the axis tangential to the ellipsoid in the central scan line plane;

the Y_L coordinate is the coordinate of the perpendicular axis in the same plane tangential to the ellipsoid and in the direction of the ascending orbit; and

the h coordinate is the altitude of the ground point.

(c) The Cartographic coordinates (N_C, E_C, h) are defined in a global coordinate system (Figure 6.8c) in which the rectification of the terrain operates.

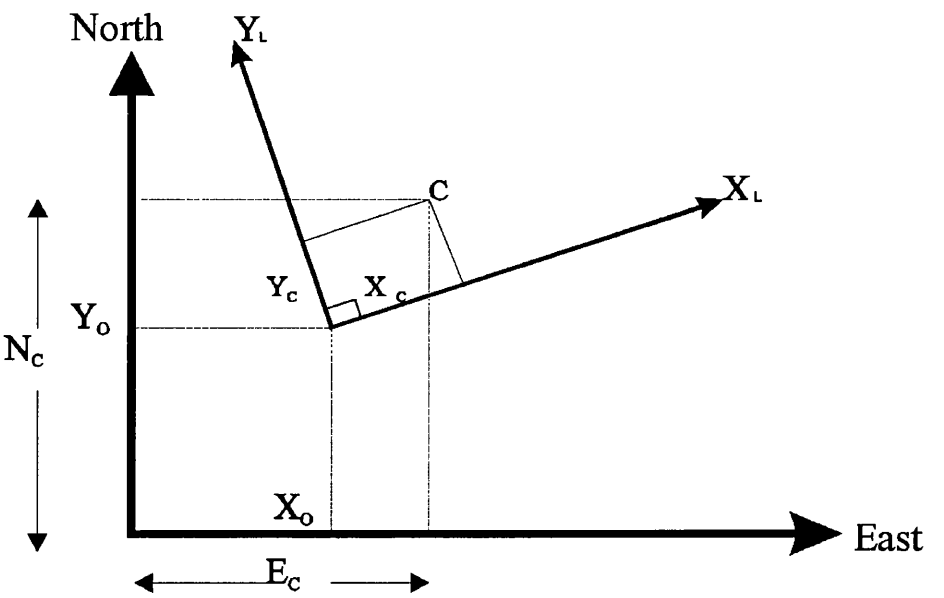

Figure 6.8c Cartographic Coordinate System.

As noted above, a global projection system such as the Universal Transverse Mercator (UTM) would typically form this particular reference system.

6.4.3 Collinearity Equations and the Parameters to be Determined

Because of the close correlation of several of the exterior orientation parameters - e.g. those related to adjacent lines within the SPOT image - it is possible with Toutin's model to combine and integrate several of these parameters into a single term so that only a relatively small number of parameters actually need to be solved. In practice, only eight independent parameters have to be determined with the model (Toutin, 1985). These comprise five terms - two scale factors along the x and y coordinate axes of the image; two levelling factors which are functions of the attitude or rotation angles around the x and y axes; and one factor which is mainly a function of the Earth's rotation - all of which are determined via a least squares solution using the collinearity equations. A further three parameters relate the local terrain (or object) coordinate system to the cartographic projection system.

The actual mathematical expression representing the collinearity equations to go from image cordinates to ground coordinates takes the following form (Toutin, 1985, 1990).

$$P_p + y\,(1 + \delta\,\gamma\,X) - \tau H - H_0 \Delta T^* = 0;$$

$$X + \theta H (\cos\chi)^{-1} + \alpha q\,(Q + \theta\,X - H\,(\cos\chi)^{-1}) - Q\Delta R = 0 \qquad (6.3)$$

where:

$$X = (x - a\,y)\;(1 + h / N_0) + b\,y^2 + c\,x\,y; \text{ and}$$

$$H = h - x^2 / (2N_0)$$

Each individual parameter is given using a mathematical formula (Toutin, 1990) that represents the physical realities of the viewing geometry (satellite, Earth, geographic position of the scene).

P and Q	are scale factors in Y and X respectively;
θ and τ	are a function of levelling angles in X and Y respectively;
α	is a function of the rotation of the Earth;
H_0	is the satellite elevation at the centre line;
N_0	is the normal to the ellipsoid;
χ, $\delta\gamma$, b and c	are the known second-order parameters, which are a function of the satellite, scene centre, and the Earth's centre geometry;
ΔT^* and ΔR	are the non-linear variations in attitude;
p and q	are the image coordinates;
x, y and h	are the ground coordinates in the intermediate reference system.

There are then five unknowns - P, Q, θ, τ, and α, - the two scale factors (P and Q) along the Y and X coordinate axes of the image; the two levelling factors (θ and τ) which are functions of the attitude or rotation angles around the X and Y axes, and the remaining factor, α, which is mainly a function of the Earth's rotation - all of which are determined by means of a least-squares solution using the collinearity equations. This expression gives a direct solution without requiring an iterative procedure. The remaining three parameters constitute the transformation to relate the local terrain coordinate system to the cartographic projection system.

The minimum number of ground control points (GCPs) needed to effect a photogrammetric solution for each image is therefore four (Toutin and Carbonneau, 1989, 1990); any redundancy above that number is taken care of by the least squares solution. In practice, it is normal to use more GCPs than the minimum in order to overcome or minimise the effects of small errors in point identification and measurement and to obtain the best estimate for the values of the exterior orientation

parameters and attitude data. The input to the module comprises the orbital parameters generated by the satellite ephemeris (which are provided from the header file that accompanies the SPOT image data); plus the measured image coordinates (in the form of their row and column pixel values); and the corresponding terrain coordinates (E, N, H) of the ground control points. A quite separate modelling and photogrammetric solution is generated for each of the individual images which go to make up the stereo-pair formed by the overlap of the two cross-track images taken from quite different orbital paths (Fig. 6.2).

In the first instance, these procedures can be regarded as a special form of space resection of a single image based on the measured image points that correspond to the known ground control points (GCPs) - see Figure 6.9.

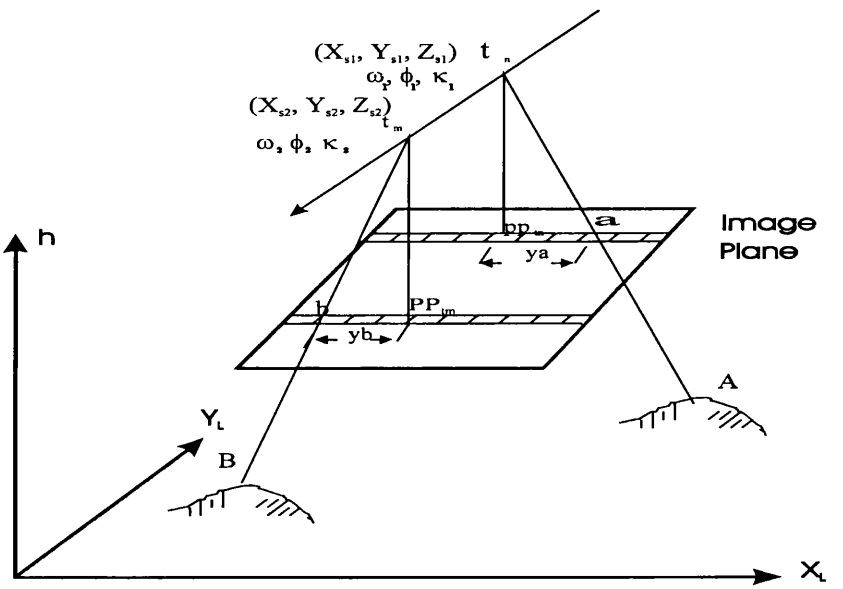

Figure 6.9 Space Resection

Later, in response to a request from the author's supervisor, an absolute orientation program was added to this package which has been fully integrated with EASI/PACE and distributed to other users. This employs space intersection to compute the terrain coordinates of each of the GCPs from the measured image coordinates and the already determined orientation parameters from both images. These computed terrain coordinate values are then compared with the given coordinate values of the GCPs to validate the success (or otherwise) of the whole orientation operation.

6.4.4 Epipolar Geometry

To prepare the stereo-pair to be in a form suitable for image matching, EASI/PACE employs a method of rectifying and resampling the right image to give it a quasi-epipolar geometry. This ensures that the left and the epipolar images are only offset only in the horizontal direction (Figure 6.10).

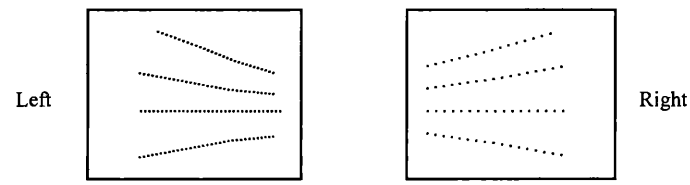

Figure 6.10a Original Images

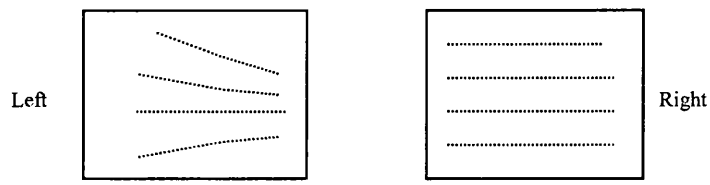

Figure 6.10b Rectified and resampled right image into Epipolar geometry

The epipolar lines employed in this system are used in the search for matching points and to speed up the correlation process. This is important for the next step, the extraction of the DEM.

6.5 ERDAS OrthoMAX Mathematical Model

6.5.1 Introduction

The core software of the OrthoMAX originates and is licensed from an established photogrammetric system supplier, Autometric/Vision International, forming part of software available for its SoftPlotter digital photogrammetric workstation (DPW). In its ERDAS form, it is part of its Imagine remote sensing package. In the standard version sold to the UK higher educational and research communities through the Chest scheme, there is no stereo-viewing and stereo-measuring capability. However these feature can be found in the Professional version – but only at considerably greater cost.

As already mentioned above in Section 6.3.1, whereas there is little alternative in the formulation of the mathematical model used with aerial or space photography, with SPOT imagery, many valid alternatives exist, especially for the modelling of the satellite orbit and the attitude of the platform. The Autometric/Vision geometric and mathematical model of the geometry of SPOT image is basically an orbital parameter model using collinearity equations. This model is similar to the orbital parameter method developed by De Hann (1991,1992) for the orientation of SPOT imagery and is based on the use of specially tailored collinearity equations (Valadan Zoej – personal comunication). The particular model used in OrthoMAX is based on the use of the detailed ephemeris information comprising the position, velocity and attitude values about the satellite that is made available by SPOT Image via the header files of the images. The software needs only first-order corrections to be made to the ephemeris data. This involves determining an image-specific set of changes to the position, velocity and attitude values.

6.5.2 Reference Systems

To relate the image space to the object or ground space, as with EASI/PACE, the solution is based on collinearity equations, but using quite different coordinate systems and utilizing quite different parameters.

1. The 1980 geodetic reference system (GRS 80) is a geocentric system that takes the form of a right-handed set of orthogonal axes with its original at the centre of the Earth's mass O (Figure 6.10).

- The X-axis passes through the zero meridian;
- The Z-axis coincides with the axis of revolution of the reference ellipsoid;
- The Y-axis is perpendicular to the X O Z plane so forming the right-handed set of orthogonal axes with its origin at O.

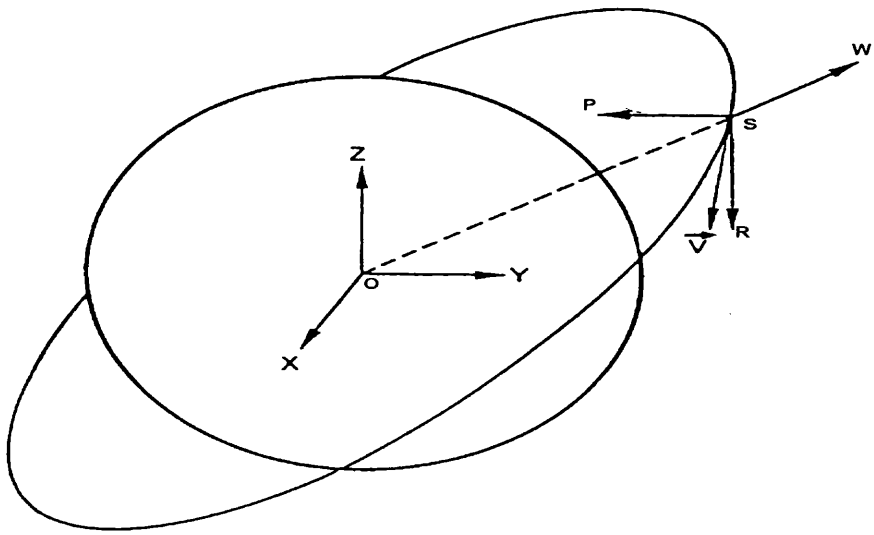

Figure 6.10 Geocentric and Orbital Reference Systems

2. The local orbital reference system is a normal right-handed set of orthogonal axes (SW, SR, SP) with its origin at the satellite's centre of mass (S). The three axes are defined as follows (Figure 6.10)

- Yaw axis SW: its direction is that of the geocentric vector passing through S, but away from the Earth's centre;
- Roll axis SR: it lies in the orbital plane and is perpendicular to the yaw axis, the direction being that of the satellite motion;
- Pitch axis SP: this is perpendicular to both the yaw and roll axes, and to the orbital plane, the direction being that required to form a right handed orthogonal system.

3. The attitude reference system is a normal right-handed set of orthogonal axes rigidly linked to the satellite. The tilts are measured around these axes to give the exact orientation of the HRV instruments with respect to the Earth's surface for the respective positions of the satellite. The satellite's attitude control system tries to align the platform with the target attitude of the satellite and its sensor by applying torques. This takes place under the control of the actual platform attitude which is measured by gyroscopes and tilt sensor that provide the rates of change every 0.125s around the three axes at_1, at_2, and at_3 shown in Figure 6.11.

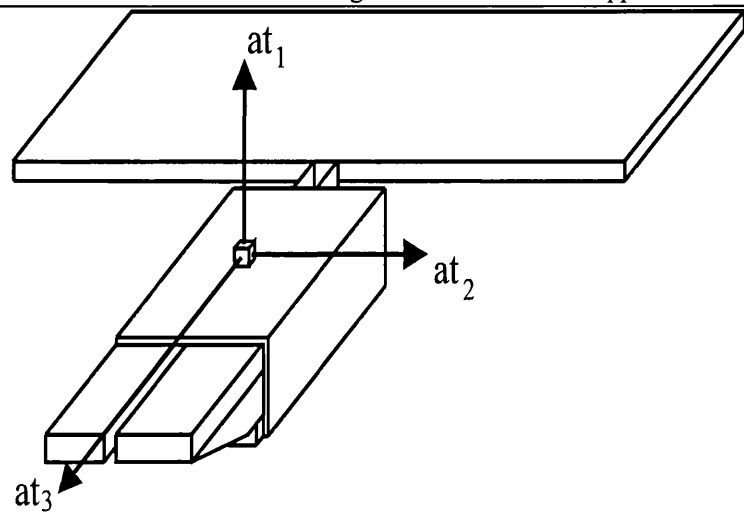

Figure 6.11 Attitude Reference System

4. The look directions. For every detector, the look direction in the attitude reference system is defined by two detector look angles V_x and V_y, which define the viewing direction of the two HRV instruments relative to the local orbital reference system.

6.5.3 Collinearity Equations and Parameters to be Determined

For both sensors, at least six tie points are required on each image to enforce the collinearity conditions. The special form of the collinearity equation joining the image point and its corresponding ground point and passing through the perspective centre is as follows (De Hann 1992).

$$0 = -f\frac{r_{11}(X_i - X_s(t)) + r_{12}(Y_i - Y_s(t)) + r_{13}(Z_i - Z_s(t))}{r_{31}(X_i - X_s(t)) + r_{32}(Y_i - Y_s(t)) + r_{33}(Z_i - Z_s(t))}$$

$$y = -f\frac{r_{21}(X_i - X_s(t)) + r_{22}(Y_i - Y_s(t)) + r_{33}(Z_i - Z_s(t))}{r_{31}(X_i - X_s(t)) + r_{32}(Y_i - Y_s(t)) + r_{33}(Z_i - Z_s(t))} \qquad (6.4)$$

[Since $x = 0$ for a particular line]

Where t is the time of imaging = t_{3000} +1.504ms (row – 3,000).

Equation (6.4) can be reduced to the form:

$$(x\ y\ -f) = \lambda M\ (X_i - X_s(t)) \qquad (6.5)$$

where:

x, y : image coordinates;

f : focal length;

λ : a scale factor;

X_i : the ground coordinate vector of the image point;

X_s : the ground coordinate vector of the projection centre;

M : the total transformation matrix.

The matrix M is further defined as the concatenation of the three separate transformation matrices that go from (1) the geocentric system to the orbital reference system; (2) from there to the attitude reference system ; and (3) from the attitude system to the detector look angles:

$$M = R_b . R_a . R_0 \qquad (6.6)$$

6.5.4 Inverse Transformation of SPOT Level 1B Image to Level 1A Form

Several cubic polynomials are used by the OrthoMAX package to convert the SPOT Level 1B lines and pixels back into their SPOT Level 1A form. These steps are as follows:

- Compute the 1A line number (L) from the 1B line number (l) using the following inverse mapping polynomial:

  $$L = a_0 + a_1 l + a_2 l^2 + a_3 l^3 \qquad (6.7)$$

- Compute the 1A column number (P') corrected for Earth rotation from the 1B column number using the following inverse mapping polynomial:

  $$P' = b_0 + b_1 p + b_2 p^2 + b_3 p^3 \qquad (6.8)$$

- Compute the 1A column number uncorrected for Earth rotation by using the corrected 1A pixel number from the previous step and the uncorrected polynomial and then correcting the previous value:

  $$\Delta P = a_0 + a_1 P' + a_2 p'^2 + a_3 p'^3 \qquad (6.9)$$

In the above equations:

l, p are the line and column values in pixels on the Level 1B image;

L, P are line and column values in pixels on the Level 1A image;

P' is a column number on the Level 1A image corrected for Earth rotation; and

Δ is the correction for Earth rotation.

Unfortunately, as will be seen later in the tests conducted by the author, this procedure does not give the appropriate reverse transformation with the Level 1B data currently produced by the SPOT Image processing facility in France that utilizes a fifth-order polynomial.

6.5.5 Computational Procedure

The computational sequence that implements the space resection and orientation procedure discussed above in Section 6.5.1 begins with the measured line and column coordinates of the image points (in pixels) and the corresponding ground coordinates of these points. In this sequence, all the elements of the collinearity conditions are computed as follows:

- If a Level 1B image is being used, the Level 1B line and column values are converted to their equivalent Level 1A line and column values.
- The viewing angles are computed from the sample number and look angles.
- The time of imaging is computed from the line number.
- The instantaneous vehicle position and velocity are computed by a Lagrange interpolation of the supplied ephemeris data and the position and velocity vector data using the time of imaging as input.
- The local orbital reference frame orientation matrix is computed from the instantaneous position and attitude.
- The attitude reference frame orientation matrix is computed from the given angular drift rates and the line number.
- The attitude matrix is computed using the current values of the angles.
- The total orientation matrix is computed by multiplying together the angular matrix, the attitude reference frame orientation matrix, and the local orbital attitude orientation matrix.

With regard to the OrthoMAX package, this space resection procedure is followed by space intersection: these two operations are implemented together in the form of a bundle adjustment.

6.5.6 Bundle Adjustment

The OrthoMAX software has the capability of carrying out a bundle adjustment procedure to ensure that, for each SPOT stereo-pair, the ground space is accurately mapped into image space and vice-versa, through the mathematical process outlined above using suitably formulated collinearity equations. An estimate of the height precision and efficiency is also obtained in the bundle adjustment carried out with SPOT data. The bundle adjustment procedure can be used to carry out the space triangulation of a strip or block of SPOT stereo-pairs. For the implementation of this procedure, suitable tie points have to be identified and measured on the adjacent images and incorporated in the computational procedure. However, for the author's tests, only single models were used.

The elements utilized in the OrthoMAX bundle adjustment are (i) the unknown parameters to be determined; (ii) the groups of parameters describing the orbit; (iii) the attitude values; and (iv) the image coordinates and ground coordinates of the ground control points. The unknown parameters include the exterior elements of orientation of each image; and the position (X, Y, Z) of the SPOT sensor for each successive projection centre corresponding to each line of the image. Two methods of space resection can be used, the first method is to resect each image individually, while the second method can be applied to photogrammetric procedures utilising a stereo-pair so that both images are resected simultaneously. Each involves an iterative solution rather than the direct solution that is used by Toutin in the EASI/PACE package. Once the elements of exterior orientation of each image have been determined, the only unknowns are the coordinates of each new control point. The values that are actually computed comprise the corrections to be applied to the initial approximations of the terrain coordinates for each ground control point. The solution is then repeated until the magnitude of this correction becomes negligible.

The coordinates of the tie points and the refined coordinates of the ground control points are actually modified during the adjustment process according to the estimated standard deviation values of the coordinates; in fact, even these are treated as unknowns. The known parameters after the space resection has been completed are the elements of

interior orientation, the precision of the various parameters used in the solution - which include those for the exterior orientation elements, the ground control point coordinates, the tie points coordinates, and the image point measurements. The next procedure is known as space intersection where the corresponding rays to the same object point from the stereo-pair must intersect at a point. The procedure requires that the elements of exterior orientation for each image of the stereo-pair be known from the individual space resections.

If the iterative solution fails to converge (3-5 iterations are normal; 10 iterations are the maximum allowable in OrthoMAX) or if it yields unacceptable results, this leads the analyst to examine the residual errors in the coordinates of the control or check points or the changes in the parameters. These residual errors arise after the best fit to all the ground control coordinates, the image coordinate measurements, and exterior parameters. According to the instructions and advice given in the OrthoMAX handbook, the most critical residual error values are those derived from the initial (input) ground coordinates of the ground control points and their adjusted values. If the residual errors exceed the estimated precision (generally twice the precision), the advice is that the input coordinates should be checked for potential blunders. A large residual error may indicate that the estimated precision of the measurements is optimistic - which generally is not harmful; however the error propagation statistics may be biased in some way. By contrast, small residual errors indicate that the estimated precision of the measurements is very pessimistic but will bias the error propagation statistics and may mask other problems. Lack of convergence of the solution can almost always be traced to a bad measurement; to the misidentification of a ground control point on an image; or to poor distribution of control points or a poor initial estimation of the exterior orientation parameters of an image. The final process of bundle adjustment is the bundle adjustment results report of the RMSE values in planimetry and heights. As will be seen later, all this advice is difficult to use considering the results that were actually obtained in the author's tests.

6.6 DMS Mathematical Model

6.6.1 Introduction

As indicated above in Section 6.3, the DMS package takes a quite different approach – that of a two-dimensional interpolative approach – as the basis of its photogrammetric solution to generate maps, DEMs and orthoimages from SPOT stereo-pairs. This is very different to the three-dimensional approach outlined above for both EASI/PACE and OrthoMAX.

6.6.2 Polynomial Approach

Normally the main aim of utilizing a two-dimensional image transformation in photogrammetry is to carry out on image-to-image registration or a simple rectification. The common approach is to use a mathematical formula whose parameters relate the image space to another image or to the object space directly without considering the perspective geometry of the images. Typically the parameters of the transformation model are obtained by using the measured coordinates of a set of ground control points in the image space as observations and transforming them to fit the known coordinates of these ground control points in the object space. Then the computed parameters are substituted back into the transformation model which is then used to compute the planimetric ground coordinates of any other points whose image coordinates have been measured. Polynomial transformations are used widely for this purpose where high positional accuracies are not required.

The DMS approach is quite unusual, if not unique, in that it uses a series of polynomial transformations first to carry out image registration and rectification and then to form a stereo-model from the rectified images. This stereo-model can then be used to generate elevation values either by manual visual measurements or by automatic image matching. The final elevation values are generated through the use of simple parallax formulae rather than the collinearity equations used in full 3D solutions. Once a DEM has been determined, an orthoimage can be generated from the rectified images using the elevation data to carry out the final differential rectification.

As mentioned previously in Section 5.4.3.1, the DMS system can only deal with Level 1B images from which the effects of Earth curvature and rotation and the viewing angle have already been removed. This prior processing allows the use of simple polynomial functions with the DMS package. In the first instance, these are used to carry out image-to-image registration between the two individual images making up the stereo-pair. This is done by fitting the right image to the left image using 4 or 5 individual GCPs used as registration points. Thus the left image acts as a reference image to which the right image is fitted.

In the next stage, the polynomial approach is again followed for the planimetric rectification of both SPOT images forming the stereo-pair. In order to obtain correspondence between the image and map coordinate systems, all the available GCPs should be used, with a minimum of four ground control points (GCPs) whose coordinates should be available in either one of two coordinate systems (Universal Transverse Mercator or a State Plane system) so that they can be used to carry out the image rectification. The procedure requires that the image points should be fitted to the GCPs using a least-squares solution. This yields the correction coefficients in the image domain without any attempt being made to identify the source of any distortion or displacements resulting from the presence of terrain relief or sensor tilt. From the residual errors at the GCPs, the root mean square error in planimetry may be determined.

The polynomial transformations used in DMS are simplified versions (i.e. sub-sets) of the general polynomial transformation which takes the form (Petrie and Kennie 1990)

$X = a_0$ (a constant term)

$+ a_1x + a_2y$ (linear (1st order) terms)

$+ a_3xy + a_4x^2 + a_5y^2$ (quadratic (2nd order) terms)

$+ a_6x^2y + a_7xy^2 + a_8x^3 + a_9y^3$ (cubic (3rd order) terms)

$+ a_{10}x^3y + a_{11}xy^3 + a_{12}x^4 + a_{13}y^4 + a_{14}x^2y^2$ (quartic (4th order) terms)

$+ a_{15}x^3y^2 + a_{16}x^2y^3 + a_{17}x^5 + a_{18}y^5 + a_{19}x^4y + a_{20}xy^4$

$+$ ..... (quintic (5th order) terms)

$Y = b_0$

$+ b_1x + b_2y$

$$+ b_3xy + b_4x^2 + b_5y^2$$

$$+ \ldots \qquad \text{(as above)} \qquad (6.10)$$

$$+ \ldots$$

$$+ b_{15}x^3y^2 + b_{16}x^2y^3 + b_{17}x^5 + b_{18}y^5 + b_{19}x^4y + b_{20}xy^4$$

$$+ \ldots\ldots\ldots\ldots\ldots\ldots\ldots\ldots\ldots\ldots$$

where

X and Y are the ground coordinates of the point;

x and y are the image coordinates of the point; and

a_i and b_i (i =1 to n) are the transformation parameters.

The number of terms of a specific order in these equations will be one greater (i.e. n + 1) than the order of the terms (n). The choice of the order of the polynomial terms (whether 1st, 2nd or 3rd order) used in an image transformation is determined by the degree of accuracy required for particular application, the number of the control points required to achieve this accuracy, and the computational facilities available. As stated by Petrie and El Niweiri (1994) "It is most helpful when deciding which of these terms should actually be used in the transformation of measured image coordinates to terrain coordinates to understand the effects of each term on the transformation and the pattern of distortion or displacement that is modelled or corrected by each term. Those used in DMS are shown in Figure 6.12.

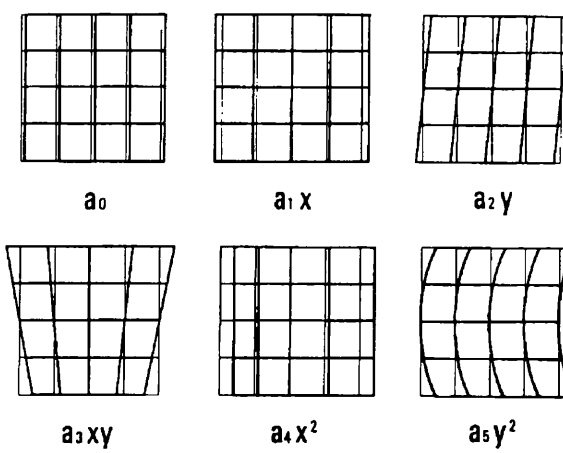

Figure 6.12a The effects of the polynomial terms in X

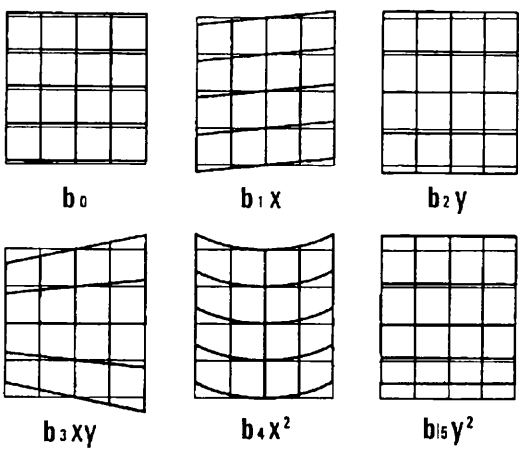

Figure 6.12b The effects of the polynomial terms in Y

In the DMS package only two polynomials - the first-order and the second-order – are provided. The first-order polynomial is the affine transformation which only includes the first three terms of each equation given in Equation (6.10)

$$X = a_0 + a_1 x + a_2 y$$
$$Y = b_0 + b_1 x + b_2 y \qquad (6.11)$$

While the second order polynomial has the following form utilizing the first six terms given in Equation (6.10) for both X and Y:

$$X = a_0 + a_1 x + a_2 y + a_3 x y + a_4 x^2 + a_5 y^2$$
$$Y = b_0 + b_1 x + b_2 y + b_3 x y + b_4 x^2 + b_5 y^2 \qquad (6.12)$$

As is well known, the affine transformation can offer a rotation, a scale change and a translation and is computationally economic. Additional terms are provided with the second-order polynomial by which a more complex warping can be achieved, albeit at the expense of more computational time. The number of GCPs required depends upon the order of the polynomial to be used. The user should be aware that, while the higher order polynomial will result in a more accurate fit in the immediate vicinity of the GCPs, it may introduce new, significant errors in those parts of the image away from the GCPs. But still the order of terms used in DMS is not high – since the third, fourth and fifth order terms of the general polynomial equation are not used.

Normally a batch rectification process will be initiated in DMS to create the two rectified images of the stereopair. The basic geometry of the left image will not be altered although it will be transformed to fit to the GCPs. The right image will be registered and rectified to fit the left image using the parameters determined by the user in the registration process. A least-squares solution of the polynomial equations is then implemented using all available GCPs to yield correction coefficients and to determine the root mean square error (RMSE) values in planimetry indicating the fit between the image and the positions of the ground control points.

As has been mentioned above, height determination can be carried out either by manual measurement or through the use of an image matching (stereocorrelation) technique. In this process, the residual differences in position (i.e. the parallaxes) in the x-direction are

assumed to be the result of relief displacement which can be determined through the measurement process. The differences in x-parallax (i.e. the disparities) can then be used to derive the height differences which, when referenced to one or more GCPs of known elevation, yield the absolute elevations of the DEM (Welch, 1989). The simple equation for the differences in elevation (Δh) between two points is

$$\Delta h = (H/B)\, \Delta p \quad = \Delta p / \tan \alpha_1 + \tan \alpha_2 \qquad (6.13)$$

where H/B = the inverse of the B/H ratio,

$\tan \alpha_1 + \tan \alpha_2 = B/H$

Δp = the difference in parallax between the two points.

When the Δh values are added to the known H coordinates for a control point they yield the absolute elevation values with reference to mean sea level.

6.7 FFI System Mathematical Model

6.7.1 Introduction

As noted previously, the FFI solution has been developed to meet the needs of the Norwegian Defence Research Establishment. It has been devised and implemented by Dr. Bjerke of this Establishment who has an electronics background and has developed a wholly different approach to that employed by mainstream photogrammetrists. The basis of his solution has so far not been published. At the present time, the solution is only able to accept and handle Level 1A SPOT data.

Like the EASI/PACE and OrthoMAX solutions, the mathematical modelling that has been developed for the FFI package is based on the use of the orbital parameter data (- comprising position, height, velocity and attitude data -) that has been measured and recorded on-board the SPOT satellite and telemetered back to the ground receiving station. Of course, this orbital data has only been measured with a certain limited accuracy in terms of achieving a photogrammetric solution that can produce accurate terrain data in the form of a DEM. Nevertheless the orbital data serves as the starting point for the FFI solution. This data is then corrected and refined through the use of ground control points (GCPs) until a correct orientation of the overlapping stereo-images with respect to the ground is achieved. However, instead of carrying out the

modelling and correction of the orbital parameter data using low-order polynomials, the FFI solution utilizes a quite different and highly original approach based on the use of surface mapping functions.

6.7.2 Reference Systems

The basic coordinate systems that have been defined and used by Dr. Bjerke are essentially the same as those that have been discussed above for the modelling and geometry used in the EASI/PACE and OrthoMAX packages and need not be repeated in detail here. They include the following:-

(i) the GRS 80 geocentric system later refined slightly to form the WGS84 system;

(ii) geodetic latitude (ϕ) and longitude(λ);

(iii) the satellite coordinate system with its origin at the instantaneous position (S) of the satellite in space and with its three axes – in the vertical direction (around which the yaw is measured); in the direction of the sensor's linear array (around which the pitch is measured) and in the flight direction (around which the roll is measured); and

(iv) the image coordinate system with x in the flight direction and y in the direction of the linear array - though the origin is (somewhat unusually) placed at the lower left hand corner of the image when viewed from a position above the image.

The FFI system has been devised on the basis that the ground control point (GCP) data will be given in geocentric coordinates within the WGS84 system - which, for all practical purposes, is assumed to be identical to the GRS80 coordinate system that the SPOT system utilizes as its reference coordinate system. Thus, a number of separate transformations have been developed by Dr. Bjerke to cope with fact that the GCP coordinate data might only be available in one or other of two alternative formats - (i) the latitude (ϕ) and longitude (λ) system of geographical coordinates, and (ii) the Universal Transverse Mercator (UTM) projection with its coordinate system of Easting (E), Northing (N) and Height (H) values.

Thus the following transformations (and reverse transformations) have been provided:-

(a) between WGS84 geocentric (X,Y,Z) coordinates and the angular values for geographical or geodetic latitude (ϕ) and longitude (λ) and the associated height value - which can either be the height above the reference ellipsoid or the height above the geoid; and

(b) between geographical latitude (ϕ) and longitude (λ) and the E, N, H coordinates in the UTM system - in which the height values are geoidal, i.e. the values are expected to be the elevations above the mean sea level datum.

It will be seen that there is no direct transformation between coordinates in the WGS84 system and those given in the UTM system. Transformation between those two systems requires the intermediate stage of computing geographical coordinates in latitude and longitude.

6.7.3 Procedure for the Determination of the Orientation of an Individual SPOT Image

For each ground control point, the measured x, y image coordinates and the corresponding set of orbital parameter data (position and height values of the perspective centres and the attitude values) are used to define a direction or vector in the object space. This direction has its origin in the perspective centre S (with coordinates X_S, Y_S, Z_S) for the image line in which the point is located. It takes into account the tilt angle of the linear array sensor at the time of acquisition of the image by the SPOT system. Since the attitude values and the perspective centre coordinate values are only given to a limited accuracy, it will be seen from Figure 6.14 that usually the ray will not pass through the position of the GCP (point P) on the terrain surface.

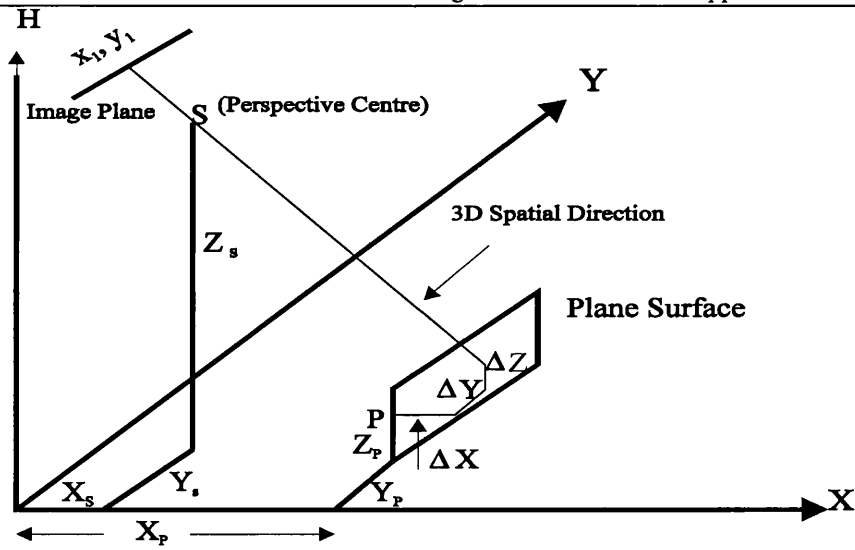

Figure 6.14 Graphic representation of the left image illustrating the method of finding the differences in coordinates (ΔX, ΔY, ΔZ) at each GCP.

The system then computes the amount within the geocentric coordinate system by which the direction has missed the GCP position. This is done by defining the plane at right angles, i.e. normal to the direction of the ray. In principle, this plane is then slid down the ray until it reaches the position where the plane passes through the GCP position. The amount of the miss is given by the differences in the X, Y, Z coordinates between the given coordinates of the GCP and those for the point on the ray direction at which the plane has passed through the GCP. These differences are the values ΔX, ΔY and ΔZ.

This procedure is carried out for each of the GCPs (P_I, P_{II}, ...P_N) that are available within the area of the SPOT stereo-pair. It is implemented first for the left image of the stereo-pair. Thus for the n GCPs that are available, the following set of coordinate difference values will have been generated:-

ΔX_I, ΔY_I, ΔZ_I;

ΔX_{II}, ΔY_{II}, ΔZ_{II};

ΔX_{III}, ΔY_{III}, ΔZ_{III};

.....

.....

ΔX_N; ΔY_N, ΔZ_N.

These values form the basis of two different algorithms that have been devised and developed as alternatives to improve the modelling of the satellite's orbital path from the initial values given by the orbital data supplied in the SPOT header file.

6.7.4 First Algorithm

A mean or average value is calculated by summing all the ΔX values for the left image only and dividing this sum by n, the number of GCPs used ($\sum \Delta X/n$). The same calculation is done for the other two sets of coordinate differences to produce mean values of ΔY and ΔZ. These three mean values are then transferred and applied equally as correction values to all of the successive positions (or perspective centres) of the satellite S_I, S_{II}.....S_N for the left image. Essentially the satellite orbital path is being shifted or displaced to occupy a new set of positions in space. All the successive perspective centres corresponding to each line of the left image only are displaced by an equal amount in ΔX, ΔY and ΔZ.

The same procedure is then applied to the right image of the SPOT stereo-pair and a similar set of correction values is generated which can be applied to each successive perspective centres along the orbital track of the right image.

6.7.4.1 Determination of the Position and Elevation Coordinates of Points on the Ground

Using (i) the x, y coordinate values of the measured image points, (ii) the appropriate orbital parameter data and (iii) the newly corrected X, Y, Z coordinates of the relevant perspective centres, the directions or rays towards each ground control point are re-computed. This is done for each of the two sets of corresponding rays in the left and right images that should intersect or meet in an individual GCP. In practice, they will not intersect, so the minimum miss distance and its direction are computed and the mid-point of the joining vector is then calculated to give the three-dimensional (3D) coordinates (X, Y, Z) of each of the ground control points.

These coordinate values derived from the SPOT stereo-pair can then be compared with the given terrain coordinates values of the GCPs and an accuracy assessment can be carried out by inspection of the individual errors in planimetry and elevation plotted as vectors on a suitable diagram. The use of this vector diagram will reveal the presence of any systematic pattern of errors at the GCPs. Also the diagram will reveal the presence of any GCPs that have been poorly identified and measured on the image. These can either be re-measured or the decision can be taken to discard the offending point. In which case, the whole computational procedure is repeated and a new set of residual errors obtained for each of the GCPs. An overall statement of the accuracy of the procedure can also be obtained by computation of the root mean square error (RMSE) values of the residual errors in X, Y, Z for the whole set of the GCPs available for the stereo-pair. Essentially the procedure described above constitutes the absolute orientation of the stereo-pair to the ground control system.

As will be seen later in Chapter 13, the results of testing the FFI program based on this algorithm using a Level 1A stereo-pair over a test field covering the area around Oslo and Lillestrom gave satisfactory results in terms of geometric accuracy using a set of 28 ground control points (GCPs) derived from the 1:50,000 scale topographic map coverage of the area. The RMSE values of the residual errors at the GCPs were in order of ±10m in planimetry and ± 11m to 12m in height. These results may be regarded as being quite satisfactory given the quality of the GCPs where the accuracy of measuring of the planimetric map data can be estimated to lie between 0.2 to 0.3mm which, at the map scale 1:50,000. is equivalent to 10 to 15m in ground terms. Similarly the height values had been taken from the contours and spot heights shown on these maps and a similar accuracy figure (±10m) can be placed against them. However, later, when more accurate GCPs derived from large scale (1:5,000) maps became available for the Oslo stereo-pair and GCPs measured by high precision GPS sets became available for the Level 1A stereo-pair for scene 122/285 of the Badia area, the geometric accuracy improved only a little. This suggested that there were limitations to the algorithm and that an alternative solution should be developed for use with more accurate control point data. Thus a second algorithm has been devised by Dr. Bjerke to a considerable extent as a result of this experience with the Badia test data.

6.7.5 Second Algorithm

Initially, with this second algorithm, exactly the same procedure is followed for a single image (e.g. the left image) as was done with the first algorithm up to the generation of the error values at the control points, i.e.

ΔX_I, ΔY_I, ΔZ_I; ΔX_{II}, ΔY_{II}, ΔZ_{II}; .....etc, as given at the end of Section 6.6.3 above.

However, instead of deriving the average values of ΔXI, ΔY and ΔZ and applying these as overall corrections to all the successive positions of the perspective centres of the left image (as was done with the first algorithm), the individual ΔX, ΔY and ΔZ values are mapped against each pixel position and the position in space of the corresponding perspective centre. This is done using a special type of surface mapping function originally developed by Goshtasby (1988) for use in 2D image-to-image registration. Here however the function has been developed further by Dr. Bjerke for use with the 3D coordinates generated by the SPOT stereo-pair.

In this method, the individual errors in ΔX, ΔY and ΔZ occurring at all the ground control points are inserted into sets of linear equations having the general form as follows:-

(a) For ΔX,

$$\sum F_i = 0;$$

$$\sum x_i F_i = 0;$$

$$\sum y_i F_i = 0; \qquad (6.14)$$

$$\Delta X_1 = a_0 + a_1 x_1 + a_2 y_1 + \sum_{i=1}^{n} F_i r_{i1}^2 1nr_{i1}^2$$

$$\Delta X_n = a_0 + a_1 x_n + a_2 y_n + \sum_{i=1}^{n} F_i r_{in}^2 1nr_{in}^2$$

(b) For ΔY, the first three equations are the same as those given above for ΔX; however, from the fourth line onwards, the equations are as follows:-

$$\Delta Y_1 = b_0 + b_1 x_1 + b_2 y_1 + \sum_{i=1}^{n} F_i r_{i1}^2 \ln r_{i1}^2$$

$$\text{----------} \qquad (6.15)$$

$$\Delta Y_n = b_0 + b_1 x_n + b_2 y_n + \sum_{i=1}^{n} F_i r_{in}^2 \ln r_{in}^2$$

(c) For ΔZ, again the first three equations are the same as those for ΔX, while, from the fourth line onwards, the equations are as follows:-

$$\Delta Z_1 = c_0 + c_1 x_1 + c_2 y_1 + \sum_{i=1}^{n} F_i r_{i1}^2 \ln r_{i1}^2$$

$$\text{----------} \qquad (6.16)$$

$$\Delta Z_n = c_0 + c_1 x_n + c_2 y_n + \sum_{i=1}^{n} F_i r_{in}^2 \ln r_{in}^2$$

where $r^2 = (x - x_i)^2 + (y - y_i)^2$ – so providing a distance weighted function;

x_i, y_i is the position of the ith control point; and

$f(x, y)$ is the error of the correction value for ΔX or ΔY or ΔZ, at the control point or any other point, as appropriate.

The solution of each set of these simultaneous equations produces numerical values for the coefficients or parameters a_0, a_1, a_2, F_1.....F_n; b_0, b_1, b_2, F_1.....F_n; and c_0, c_1, c_2, F_1.....F_n. (N.B. If for example, n = 14 - i.e. there are 14 GCPs - then there will be n + 3 = 17 equations with 17 unknowns). After the values of the coefficients or parameters have been obtained, when substituted back into the relevant equation, they then define a so-called surface spline which produces a surface passing through all the GCPs. Such a surface represents a mapping function that gives the corrective shift in one of the three coordinate directions, i.e. either in X, Y or Z, at the particular perspective centre S corresponding to any position (*x, y*) measured in the image plane of the left or right image as appropriate. In this way, it can be seen that three quite separate and different mapping functions are generated for ΔX, ΔY and ΔZ respectively and can be used to apply shifts to the particular perspective centre that corresponds to any measured position (with coordinates *x,y*) in the left image. The same procedure is then carried out quite independently for the right image of the SPOT stereo-pair

6.7.5.1 Determination of the Position and Elevation Coordinates of Points on the Ground

Since there is no data redundancy and therefore no least squares solution, the mapping functions in ΔX, ΔY and ΔZ for both the left and right images fit the ground control points (GCPs) exactly. The result after the corrective shifts have been applied to the perspective centres will be a perfect fit of the stereo-model to the GCPs. Of course, this does not mean that there are no errors existing in the ground control points or in the measurements of their positions in the image. Any check on the quality of the final result will have to utilize additional control points that have not been used to calculate the corrective functions and can therefore be utilized as independent check points.

For any other point measured on the two images, e.g. for mapping purposes, the corrective values for that point are derived from the mapping functions for each of the images. The two vector directions or rays from the left and right perspective centres for each measured point then intersect to give the final coordinate values in X, Y and Z for that particular point in the stereo-model.

6.8 Conclusion

In this chapter, the mathematical models and the algorithms used in the systems employed in the present research project have been outlined and discussed. The mathematical models that have been developed and employed in the 3D solutions used in three of the systems - EASI/PACE, OrthoMAX and FFI - are based on the use of orbital parameter data (comprising position, height, velocity and attitude data) that have been measured and recorded on-board the SPOT satellite and telemetered back to the ground receiving station. The initial values of the exterior orientation parameters of the sensors can be derived from the orbital parameters using an orbital model which has the effect of reducing the number of the ground control points required to implement the method. But in general, the satellite ephemeris cannot provide precise exterior orientation parameters. An advantage which can come from utilizing the orbital parameter method is that the object coordinates of the image points can be computed directly in a geocentric coordinate system. This will avoid the effects of the Earth

curvature. Also the position of the projection centre of the sensor (the origin of the image coordinate system) lies on the orbit, thus it becomes a function of the orbital elements and does not inherently include Earth rotation. However differences between the models used by different systems arise from the different orbital elements that are being considered and the number of the unknowns which have to be solved.

There are also a number of differences between the three systems employing a 3D solution. The EASI/PACE and OrthoMAX systems can be considered to be solutions based on the classical approach of analytical photogrammetry employing the well known collinearity equations of photogrammetry which relate corresponding points in the image space and object space through the perspective centre of the imaging sensor. By contrast, the FFI system uses a wholly different and purely mathematical approach to achieving a solution that employs a special type of surface mapping function originally developed for use in 2D image-to-image registration. Dr. Bjerke has then developed this function further to give a unique solution to generate the 3D coordinates from SPOT stereo-pairs.

In case of the fourth system, DMS employs a quite different photogrammetric solution to those that have been adopted by the previous three systems. By contrast, DMS follows a quite different and simpler approach based on the use of 2D polynomial equations which carry out a preliminary rectification of the individual SPOT images making up the stereo-pairs based on a least-squares solution. Therefore it utilizes a simple parallax equation for determination of height from parallaxes that can be measured either manually and visually or by stereocorrelation.

In summary, one can say that the four systems that have been tested in the author's research project form a very good and representative cross-section of the systems that are currently available for digital photogrammetric work to extract DEMs and orthoimages from SPOT stereo-pairs. At the same time, they offer a variety of quite different photogrammetric solutions, which it will be most interesting to test out.

In the next chapter, the procedures which have been adopted for the photogrammetric and remote sensing processing and the experimental procedures employed for the calibration and testing of the systems will be outlined and discussed.

CHAPTER 7: OVERALL STRATEGY, GENERAL CONSIDERATIONS AND EXPERIMENTAL PROCEDURES USED IN THE TESTS

7.1 Introduction

In Chapter 2, a review, summary and analysis of the main published results of tests of geometric accuracy of SPOT stereo-pairs was given. This was followed by Chapter 3 which reviewed the results of tests previously carried out to validate the DEMs that can be extracted from SPOT stereo-pairs. In Chapter 4, the situation regarding surveying and mapping in Jordan was reviewed, since the author has made considerable use of the existing topographic map coverage of Jordan to verify the data extracted from the SPOT stereo-coverage of his test area. In Chapter 5, the application of digital photogrammetric techniques to SPOT stereo-pairs was presented and was followed by a classification of digital photogrammetric workstations and a description of the main characteristics of the systems used in the author's research work. This was followed in Chapter 6 by an account of the mathematical models and photogrammetric solutions applied in the tested systems. These five introductory chapters have given the background to the research project carried out by the author and set the scene for the actual experimental work that he has carried out. The remaining chapters of this dissertation will report on the procedures used and the results obtained during this research work and will conduct an analysis of the results obtained. Before doing so, the strategy adopted and the procedures used to carry out the experimental work on geometric accuracy testing and the validation of the DEMs and orthoimages from SPOT stereo-pairs will be outlined and discussed in the present chapter.

7.2 Overall Strategy and Experimental Requirements

The experimental work carried out during the present research is somewhat different to the other accuracy tests reported by other researchers in terms of

(i) the variety of packages that have been used in the geometric accuracy tests and in the validation of the DEMs and orthoimages;

(ii) the number and the format of the SPOT stereo-pairs used in the tests;

(iii) the location of the test area;

(iv) the quality of the ground control points; and

(v) the methods used in the accuracy testing.

However, in more general terms, the overall strategy that has been employed has followed conventional lines involving the establishment of a high-class test field of ground control points using the latest GPS technology, supplemented by the more innovative use of GPS-derived profiles for DEM testing. In addition to these activities carried out in the field, digitised contour data sets have also been created from the existing topographic map coverage of the test area for the purpose of further validating the DEMs created from the SPOT stereo-pairs.

The methodology and procedures that have then been used for actual testing of the systems have also followed the same general lines used by previous researchers in this field that have been outlined in Chapters 2 and 3. Thus the individual systems have all been tested for the geometric accuracy that could be achieved via an absolute orientation of the SPOT stereo-model and its fit to the ground control points (GCPs). In this respect, it was important to have a dense field of GCPs so that there was a big redundancy in the test data, giving rise to a data sample of a sufficient size in statistical terms for later analysis. In order to satisfy this requirement, one of the stereo-models (122/285) was selected as a special reference model and a dense network of 60 GCPs was established in this particular model. The target accuracy for these reference GCPs was judged to be an RMSE value of ±1m both in position and height - since this is equivalent to 0.1 pixel on a SPOT Pan image and much better than the results got from the previous tests of SPOT stereo-pairs discussed in Chapter 2.

The remaining four stereo-models had smaller numbers of GCPs which still gave rise to some redundancy in the control data and the use of least squares methods in the photogrammetric solutions. As will be seen later in the results Chapters, the use of this quite simple strategy did reveal the many flaws and shortcomings (sometimes of a quite fundamental nature) that were present in the photogrammetric solutions of all of the systems that have been tested.

For the validation (both in terms of accuracy and completeness) of the DEMs and orthoimages that have been generated by all of the tested systems, again the main

procedures that have been used are largely those that have already been described and set out in Chapter 3. They include the fit of the elevation data generated through the use of image matching procedures at the GCPs (as distinct from the values measured visually for absolute orientation purposes). Also the decision was taken to directly measure elevation profiles and so establish cross-sections along the main roads crossing the Project area. This would result in the availability of a reference data set of height values which would allow a direct comparison with the corresponding elevation values determined from the SPOT stereo-pairs. Additionally it was felt that comparisons should be made between the contours generated from the SPOT DEM data and the contours on the existing topographic maps of the area. To this end, there was a need for accurate contours that could be used as a reference data set against which the DEM-derived contours could be compared.

Finally, for the validation of the orthoimages generated by the different systems, their geometric accuracy could be established using the same set of GCPs that had been used for the absolute orientation tests. Here the accuracy requirements were actually much less (equivalent to 0.1mm on a final hard-copy image) than those needed for the initial orientation procedure.

7.2.1 Test Material and Data

A great deal of effort and a very large sum of money has gone into the provision of the material required to carry out the planned programme of tests.

7.2.1.1. SPOT Stereo-images

The test material used in the present research project consists of a block of five SPOT Level 1B Pan stereo-pairs in digital form with a 10m pixel size covering the whole Badia Project area, comprising scenes 122/285; 123/285; 123/286; 124/285 and 124/286. These scenes were provided by the Higher Council of Science and Technology (HCST) in Jordan which is running the Badia Project in collaboration with the Royal Geographic Society (RGS) in London and a number of universities and research organisations in Jordan and the UK. Another SPOT Level 1A Pan stereo-pair for the

reference scene 122/285 has also been acquired for comparative purposes by the Department of Geography and Topographic Science at the University of Glasgow. These SPOT scenes are all of a good image quality in radiometric terms, being cloud-free and also free from the dust and haze that often affects satellite imagery of desert terrain. Also the individual images comprising each stereo-pair have been taken with only a small gap (one to three months) between them, so, over the Project area, there are no difficulties arising from changes in the appearance of the vegetation, cultivated areas and water bodies that might cause problems in forming and viewing the stereo-models and in extracting elevation information from them. The SPOT stereo-pairs have excellent base-height ratios of 0.86 or 0.98 (Table 7.1) which promised good elevation accuracies, especially when the area is so largely devoid of vegetation that might interfere with the heighting process.

Scene No.	Incidence Angle	B/H Ratio
122/285	L 28.2, R 23.7	0.98
123/285	L 25.1, R21.3	0.86
123/286	L 25.1, R21.3	0.86
124/285	L 28.2, R 23.7	0.98
124/286	L 28.2, R 23.7	0.98

Table 7.1 Scene numbers and B/H ratios of the SPOT stereo-pairs

7.2.1.2 Digitised Maps

In addition, the Higher Council for Science and Technology in Jordan (HCST) provided complete topographic map coverage of the test area at 1:50,000 scale in the UTM coordinate system with a contour interval of 20m in hard-copy form. Besides this, the RJGC also made available digitised versions of the existing topographic maps covering the Badia area at 1:250,000 scale together with one sheet at 1:50,000 scale covering part of the reference scene 122/285. These provide contours at intervals of 50m and 10m respectively, which greatly aided the validation of the DEM data generated by the author using the different systems that have been tested.

7.2.2 Establishment of the Badia Test Field

It was very clear from the test results for planimetric and height accuracy reported in Chapters 2 and 3 both for the purpose of geometric accuracy testing and for the

validation of DEMs, that most of these previous tests have used ground control points derived from existing 1:50,000 and 1:25,000 scale topographic maps. Very few of the ground control points provided for these tests were gathered from high precision field surveys undertaken specifically for test purposes. Even when some were provided, they were often used mixed with ground control points derived from existing topographic maps. It was very clear too that the moderate-to-poor results that have often been obtained were due to inadequacies in the GCP data. Indeed, it was obvious that very few test fields have been established specially for this type of accuracy testing. In this respect, the large area of ground covered by individual SPOT images and the even larger area of terrain covered by a block of such images has been a major deterrent to the establishment of high-class test fields for use with satellite imagery.

It is also the case that most of the test materials used in the earlier work of testing SPOT stereo-pairs comprised film diapositives, because of the very limited development of digital photogrammetric systems at that time. As will be clear from the reviews conducted in Chapters 2 and 3, so far, very few geometric accuracy tests have been conducted using digital photogrammetric systems based on the use of digital image data. Now that several digital photogrammetric systems that can handle stereo satellite data are available on the market from commercial remote sensing suppliers, these systems should be tested. However the establishment of a field of accurate ground control points to test these new systems over such a large area is beyond the capability of an individual researcher. This is why it was decided to seek the collaboration of RJGC to establish a very accurate test field in the Badia area. In this respect, the fact that the present author was a former deputy director of RJGC was an important factor in securing this collaboration.

Once this had been done, as discussed above, it was decided to cover the area with 130 ground control points to be distributed with an average of 15 to 20 ground control points for each stereo-pair and with around 60 ground control points for the reference stereo-model 122/285 located in the western part of the Badia area. The selection of the actual number and the location and distribution of the ground control points would of course be controlled by the topography of the area and the distribution of the settlements in the area. After detailed discussions with the RJGC and HCST, the plan was to carry out the

necessary field survey operations employing suitable GPS techniques to establish the control points over a maximum period of three months. In this respect, the author was very fortunate in that the RJGC had just taken delivery of five new geodetic quality GPS sets that could made available for the establishment of the test field.

The area within which the test field is located is called the Northern Badia. It is an area of approximately 12,000 km^2 located in North Eastern Jordan. The area covered by the SPOT imagery is mostly a stony desert area with an old lava flow covering a big part of it. Much of the surface of the lava is covered in boulders and is extremely difficult to access and cross either on foot or in vehicles. However, in many other respects, this desert area is well suited to act as a test field, since it is little developed and has few man-made cultural features. At the same time, there was very little vegetation that could cause problems with measurements or image matching procedures, nor were there rugged mountains and valleys which could result in shadows or steep slopes that again might cause difficulties with image matching.

7.2.3 Systems to be Tested

As noted in Chapters 5 and 6, attention has been focused on the testing of four representative systems (EASI/PACE, OrthoMAX, DMS and FFI) having a variety of different photogrammetric solutions. Obviously on the basis of cost alone, it was impossible to purchase each of these systems for the author's programme of experimental testing. However two of these systems - EASI/PACE and DMS - were already available for use within the Department of Geography and Topographic Science. Access to a third system - OrthoMAX - was available through the good offices of the Macaulay Land Use Research Institute (MLURI) in Aberdeen. In the case of the fourth system, the tests had to be carried out on behalf of the author by Dr. Bjerke in the Division for Electronics of the Norwegian Defence Research Establishment.

To carry out the geometrical accuracy tests and validation of DEMs and orthoimages using the EASI/PACE and DMS packages within the Department, suitable hardware had to be available. For this part of the research project, the author was provided with a PC equipped with a 133 Mhz Pentium processor and fitted with 32 Mbytes RAM and 2

GBytes of hard disk. Later, 4 Gbytes more hard disk storage was added at the request of the present author in order to accommodate the large image data sets that were being used. He also had available a further 2 Gbytes temporary storage on a server located in the University Computer Service. The work on the OrthoMAX system was carried out on Unix-based Sun and SGI graphics workstations at MLURI in Aberdeen.

In addition to the four main image processing systems which have been discussed in the previous chapters, supplementary software systems were needed to carry out certain other image processing and graphics tasks which could not be done on the main systems. These included Adobe Photoshop, CorelDraw and Surfer; other small programs from the Department's software library were needed to carry out transformations (e.g. LINCON), vector plots (e.g. VECTOR), etc.

7.3 Experimental Procedures

As outlined above, three different types of test have been carried out in the present research including

(i) the geometric accuracy tests of SPOT stereo-pairs;

(ii) validation of DEMs; and

(iii) the geometric accuracy tests of the final orthoimages.

The various considerations that affected these procedures will be discussed further in some more detail below.

7.3.1 Geometric Accuracy Tests

In the previously reported results, some of the geometric accuracy tests of planimetry and heights used only a small number of control points; and no independent check points were used to check the accuracy. Furthermore some of these tests reported the geometric accuracy tests of planimetry only. It was resolved to overcome these shortcomings by having a very full data set of highly accurate ground control points that would allow full testing in both planimetry and height.

The published papers giving the results of tests of the geometric accuracy of the data that could be obtained from the SPOT imagery have included tests of individual stereo-models and of strips of SPOT stereo-models that have been measured by space triangulation. In the case of the author's tests, only individual stereo-models have been tested, since, of the four systems tested, only OrthoMAX has the capability of carrying out the space triangulation of SPOT stereo-pairs and it was found that this did not work with recently processed Level 1B stereo-pairs.

In addition, it must be noted that, apart from IGN and CCRS, most of the geometric tests have been carried out by universities and research organisations and most of systems and research software were developed by these organisations. This is not unusual in the initial stages of development of a particular field of activity. However the situation has now changed and a much more stable and mature situation exists with regard to the provision of the software and systems for mapping from SPOT stereo-pairs. Thus, in this research project, the geometric accuracy tests were carried out using variety of commercial digital image processing systems using different solutions.

The individual stereo-models have all been measured singly. For the geometric accuracy tests, different combinations of very accurate control points and check points have been used. Besides the extensive use of RMSE values to give a statistical measure of the overall accuracy in planimetry and height as a further check of the accuracy of fit of the stereomodel to the GCPs, vector plots of the residual values of the individual errors have been used extensively. This allowed the pattern of the residual error values in planimetry and height obtained at the control points and check points after orientation of the stereo-models to be checked graphically in the form of vectors either on the computer screen or as hard-copy plots. This allowed the author to locate any gross errors and decide whether to delete or to re-measure the points concerned. Also it showed immediately whether a systematic pattern of errors was present or whether the error pattern was purely random in nature.

7.3.2 Validation of DEMs

From the review and discussion conducted in Chapter 3, it is quite noticeable how few tests have been carried out into the accuracy of the elevation data that can be extracted from SPOT stereo-pairs and especially from commercially available software packages using digital image data. This is of course due partly to the problems of carrying out such tests over the large area covered by a single SPOT stereo-pair and in finding elevation data of a high quality and density that can be used as a reference data set to allow the validation of the DEM data. From the results of the DEM accuracy tests reported by different researchers, one can say that the accuracy of the DEM as given by the RMSE values varies from a few satisfactory results to mostly poor results.

In the past, the validation of the DEMs extracted from SPOT stereo-pairs has been mainly restricted to two different methods. The first has been the testing of the DEM elevation values at a comparatively small number of check points. The second has been to compare the height values extracted by the DEMs at a large number of grid points over a relatively small area of terrain (typically 1 x 1 or 2 x 2km) with the corresponding height values extracted from the DEMs generated from the contours on existing maps at the same grid interval. This has distinct limitations in that the areas sampled and tested may not be typical of the overall terrain being mapped. Obviously the testing of the DEMs acquired from complete stereo-models would be difficult, but consideration was given by the author as to how to test a larger and more representative sample of elevation data.

In the end, a combination of four methods has been used to validate the DEMs. These are as follows:-

(i) Validation of the DEMs at a set of independent check points that have not used in the orientation procedure. In this method, different combinations of the control points and check points have been used in which some of the available ground control points (GCPs) have been retained purely as check points for the purpose of validating the DEM. In some cases, up to 35 or more very accurate check points have been used to validate the corresponding elevation values in the DEM extracted from the stereo-model. Obviously this will constitute only a small

sample of test data. This particular operation has been supported by vector plots which check the residual errors in height at the control and check points to see if there are any systematic patterns of error in height at the points as a result of the image matching procedure.

(ii) Comparison of the heights given by the contours from the reference map with the corresponding values given by the DEM. This method is similar to the method reported by several previous researchers concerned with the validation of a DEM derived from SPOT stereo-pairs. The main difference between the two methods is that, in the method used by the present author, the contours digitised from 1:250,000 and 1:50,000 scale topographic maps have been superimposed over the DEM extracted from SPOT stereo-pairs and the corresponding height values have been extracted from the DEM for comparative purposes. The use of this procedure eliminates the problems expressed when the reference DEM is extracted from digitised topographic maps by interpolation to provide the elevation values at a given grid interval. The method employed by the present author cuts out this interpolation and so one can validate the DEM extracted from a SPOT stereo-pair through a comparison of the elevations solely along a selected number of the contours of the existing map which had been measured directly using aerial photogrammetric methods.

(iii) The third method is the purely visual comparison of superimposed contours. First of all, the contours extracted from the DEMs at the specified contour interval have been loaded into the EASI/PACE system. Also the contours at the same interval that had been digitised from the existing topographic maps were also loaded and superimposed over the first set of contours. In general, the two sets of contours will not fit exactly due to the errors that are present in both sets of contours. However the comparison offered by this method is still of considerable value; essentially it is a qualitative test that gives an indication of the fit between the two sets of contours.

(iv) The fourth method is another distinctive feature of the validation of the DEMs that has been devised and utilized in the present research project. This method has

employed two terrain profiles measured using kinematic GPS techniques. More than 15,000 individual reference points have been produced by this method. 10% of these have been selected to validate the DEM elevation values at an average distance of 150m or so between each of these selected points measured along the two profile lines.

7.3.3 Geometric Accuracy Tests of Orthoimages

For the orthoimages produced by the different systems, a check of the geometric accuracy of the planimetry of the final product is essential since, for many users, this is one of the most important end-products from the whole procedure. The check has been carried out by measuring quite independently the positions of the ground control points lying within the area of the orthoimage. Then the actual transformation and the subsequent comparison of the transformed measured values with the given coordinate values of the GCPs was executed by a computer program called **LINCON** available from the Department's software library. In this method, no further rectification or fitting should be carried out, so a simple linear conformal (first-order) transformation has been used for the comparison. Once again, vector plots of the residual errors have been generated to see if the residual errors formed a systematic pattern in any part of the orthoimage.

7.4 Conclusion

In this chapter, the overall strategy that has been adopted and the methodology that has been used for the geometric accuracy tests and the validation of DEMs and orthoimages have been discussed. In general, the methods adopted in the present research are those familiar from previous published tests. However, there are some differences, e.g in terms of the quality of the ground control points used in the tests. Except for those carried out by IGN in south east France, very few of the reported tests of SPOT geometric accuracy or validation of DEMs have been able to use a field of very accurate ground control points measured by a full ground survey that has been created specially for this purpose. However establishing a test field in the Badia area was a very expensive task; the estimated cost was £20,000. However it is hoped that this will

provide a control network for other surveying activities associated with the Badia Project and that the high quality test field can be used for further tests of the imagery produced by the forthcoming high-resolution satellites.

In the next chapter, the field survey work carried out to establish the Badia test field will be presented and discussed in some detail. This will include a description of the nature of the test field in terms of its distinctive landscape, followed by a discussion of the methods used and the experience gained during the reconnaissance, observation and fixing of the ground control points and the establishment of the GPS profiles.

CHAPTER 8: FIELD SURVEY WORK CARRIED OUT FOR THE BADIA PROJECT TEST AREA

8.1 Introduction

In the previous chapter, the procedures adopted for the author's experimental work and subsequent data processing have been presented and discussed. In this chapter, the field survey work and measurements carried out to form the ground control network formed part of the experimental work carried out for the author's research project and will be covered in this chapter.

One of the projects within the national development plans mentioned in Section 4.1.2 is the Badia Project being undertaken in the desert region of north-east Jordan. The Badia Project's objective is to undertake inter-disciplinary scientific research which will lead to development activities and environmental improvements in this area. A wide-ranging multi-disciplinary study of this type conducted over a large area requires the integration of a vast amount of spatially located data collected both on the ground and through the use of aerial photography and satellite imagery. All of this data must then be assimilated into a computerised database with facilities for spatial analysis and mapping. In the case of the Badia Project, the resulting geographic information system (GIS) forms a central part of the management and research infrastructure of the project, and, when operational, will be located in the Safawi Field Centre lying at the centre of the Project area and will be linked up with the Royal Jordanian Geographic Centre (RJGC) in Amman.

The Badia Project area has also been short-listed by NASA as a key test site in its wordwide Pathfinder Global Land Cover Test Project; indeed the Badia area is the only site short-listed from the Middle East. Within the Badia Project itself, the need to form a spatial database from SPOT imagery was seen as an essential item to support the research work being undertaken by a large number of field scientists for the Project. Thus the digital elevation data and ortho-images generated from the SPOT stereo-pairs were seen as essential elements of the GIS. Provision of this data became one of the objectives of the author's work, besides the research into the photogrammetric aspects

of his project. For all these reasons, it was necessary to carry out extensive field survey work to establish ground control points for the Badia Project.

In this chapter, first of all, a general discussion will take place regarding the study area. This will be followed by a description of the field work planning; the selection of the control points; an account of the GPS instruments and observations, and the subsequent processing.

8.2 Requirement for Control Points for the SPOT Stereo-Pairs

Obviously to carry out the planned accuracy tests of the SPOT stereo-pairs and the verification or validation of the digital elevation models (DEMs) and orthoimages generated from these, it was necessary to establish a test field of high accuracy ground control points (GCPs) within the Badia Project area.

8.2.1 The Nature of the Field Work.

The main purpose of the field work was to establish a network of ground control points (GCPs) over the Project area utilizing modern methods based on the use of the GPS technique. While conventional observational methods require long periods of angular and /or distance observations to establish these points, the GPS technique is faster and more direct and involves a much lower labour cost, especially when conducted over a large area such as that covered by the Badia Project. Furthermore, it is also possible to use GPS in a mobile or kinematic mode. So the opportunity has been taken to use this method to construct elevation profiles across the test area that can be used to test and verify the quality of the elevation data generated from the SPOT satellite imagery for the whole of the Badia Project area.

8.2.2 The Study Area

The project study area comprises 11,210 sq.km of the north-eastern part of the Badia. This constitutes 15.4% of the total area of the Badia and 12.5% of the total area of Jordan - see Figure 8.1. The study area lies within the boundaries of the Al-Mafraq and

Zarqa Governorates, including 35 villages with a total population of 15,318 people. The climate is that of an arid desert type. In summer (from June to October), hot, dry weather dominates, with very high midday temperatures of about 45°C. Winter lasts from November to March, with an annual precipitation of 30-120 mm and with temperatures dropping to below zero at night. Evaporation is high, and, in general, relative humidity is low. A Field Centre has been established at Safawi village, located 156 km north-east of Amman on the main Baghdad highway, to host the various activities of the Badia research programme. The buildings used for the various activities of the programme were those built for the H5 pumping station on the Iraqi to Haifa oil pipeline in 1934 and had been disused for many years after the pipeline stopped being used during the Arab-Israeli wars. These buildings have now been completely restored and equipped by the Higher Council for Science and Technology (HCST) creating a comfortable base for visiting scientists, post-graduates, trainees, and the programme's permanent staff. The Higher Council also supports the Centre's running costs and contributes substantially towards its programme of scientific research. The author was able to make use of the Field Centre throughout the period of his field work in the area.

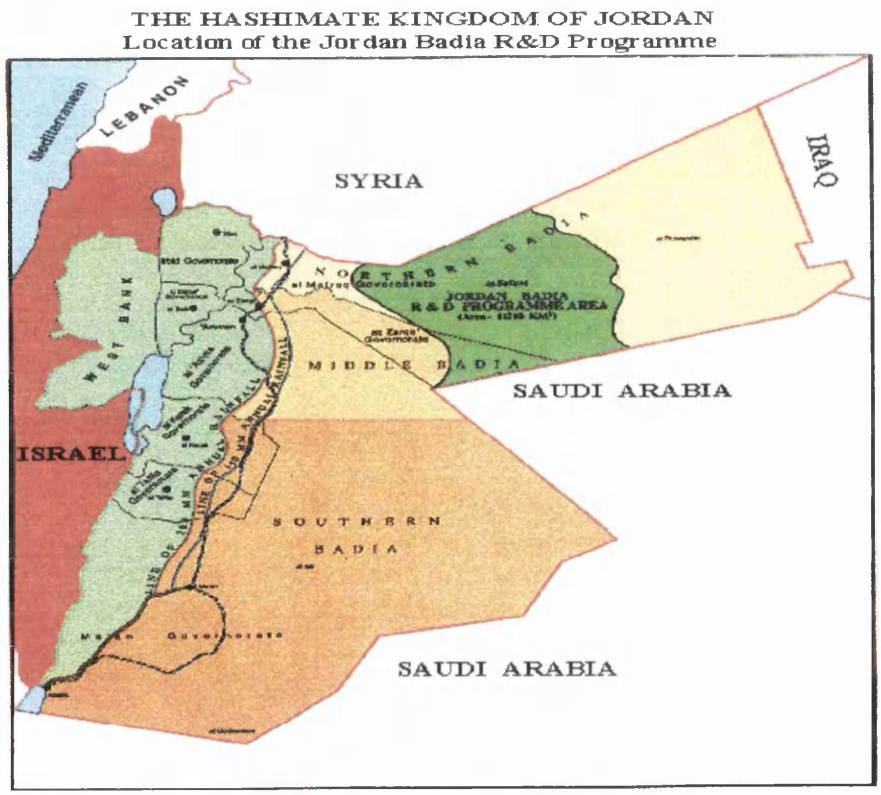

Figure 8.1 Location of the North Badia Area

Safawi village is located in the middle of the project area (Figure 8.2). This village is quite small, and its population consists mainly of the families of the military personnel working in the air base, while others are working in commercial services providing facilities for travellers between Jordan and Baghdad. As mentioned above, there are 35 small settlements mainly concentrated in the north western part of the area, which receives more rainfall. Here fields have been cleaned of basalt boulders and some cultivation takes place, though it is of a marginal nature. Some of these villages such as Um Al-Qutin (the biggest village in the area), Dair Al-Khief, and Mukaftah are located very close to the Syrian boundary. Other villages such as Naiefeh, Manarah, Rahbet Rakad, and Al-Beshrieh are located along the Baghdad highway. Part of the population remains nomadic, travelling with their camel, sheep and goat herds through the Harra desert and into Saudi Arabia. Except for the improved areas created by development projects, the natural vegetation in this area consists of sparse annual grasses. The arable agriculture in this area is limited to the growing of barley.

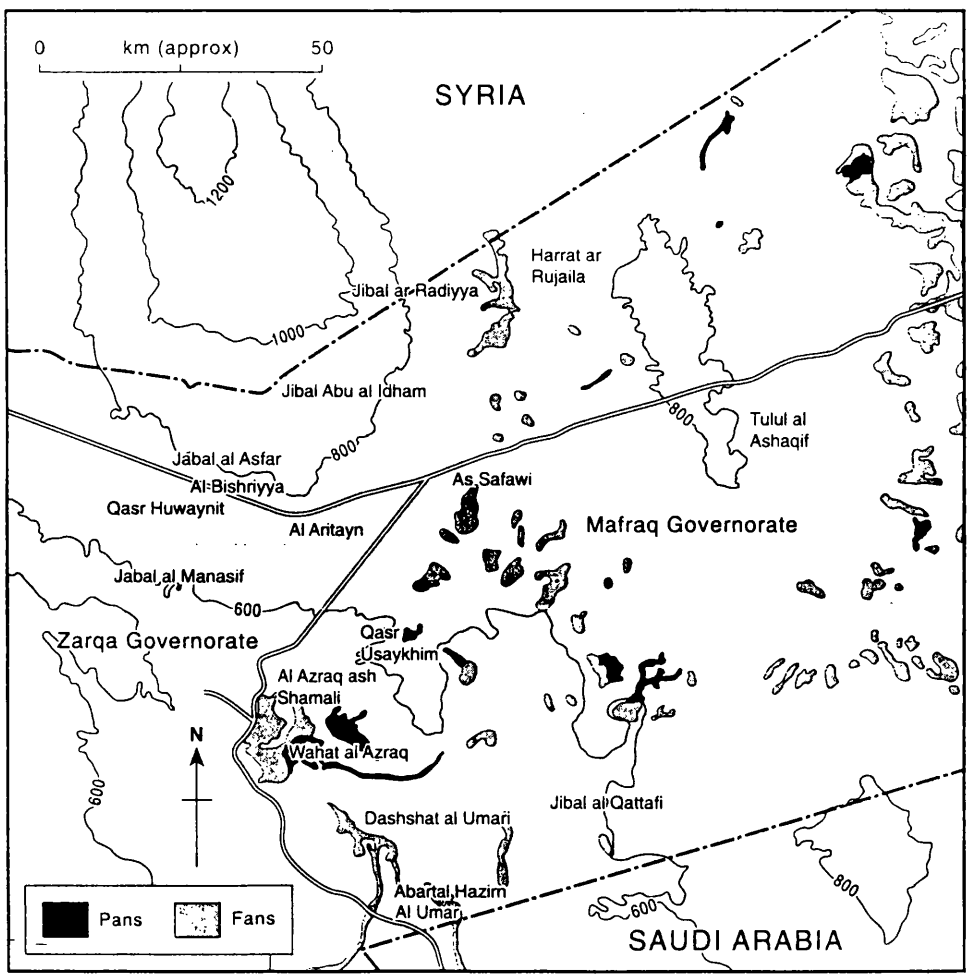

Figure 8.2 Location of the Safawi Field Centre in the North Badia Area

8.2.2.1 Geology of the Project Area

Since the geology of the project area controls so much of this unusual strongly volcanic desert landscape, it is appropriate to outline its geological history. As can be seen clearly on the satellite imagery of the area, the landscape of the area has been strongly affected by volcanic eruptions. Continental basalt flows and tuffs from the Tertiary-Quaternary period cover approximately 11,000 sq.km of the area (Figure 8.3). The resulting basalt plateau is between 50 km and 170 km wide from east and extends 180 km from the Syrian border, through the area east and south of the Azraq basin, into Saudi Arabia. The basalts form part of the major North Arabian Volcanic Province, which extends from the southern rim of the Damascus Basin in Syria, along the eastern margins of the Azraq and Sirhan basins in Jordan and crossing into Saudi Arabia,. Recent studies (Ibrahim, 1992) carried out by the Natural Resources Authority (NRA) of Jordan classified the exposed basalts as one super group, called Harret Ash Shamah which can be further sub-divided into five major groups known as the Asfar, Safawi, Bishriyya, Rimah and Wisad groups. In Jordan, the extension of the Harra Ash Shamah is known locally as Harra El-Jabban. The basaltic cover includes lava flows, major dike systems and volcanic centres of different types, including shield volcanoes and strato-volcanoes. The younger flows are centred on the mountain of Jebal al Arab located across the border in Syria. Considerable amounts of material have erupted from numerous fissures in the terrain surface, with basalt and some tuff being extruded from clusters of isolated cones.

The volcanic rocks of Harra El-Jabban outcrop in different forms such as basaltic flows, volcanic cones, volcanic ridges and basaltic dikes. The basalts of Harra El-Jabban result from six basaltic flows and one eruption of fragmental volcanics (Al-Malabeh, 1993). The thickness of the basalt covering the area generally decreases towards the south. The first three flows in Harra El-Jabban are not exposed. The fourth flow represents the oldest exposed flow in the area. This flow has a thickness that varies between 20m and 60 m. Generally, this flow gives rocks having a dark to medium grey colour.

The fifth flow is exposed over a large area extending to the Jordanian- Saudi Arabian border.Its thickness is estimated to be approximately 25m, with the possibility that the flow is thicker in certain areas, particularly further northwards near the Syrian border. In places, it is exposed a hummocky surface. The surface of this basalt is covered in some places by recent sediments. The last (sixth) flow is restricted markedly in exposure to form three elongated strips each several kilometers in length. Its thickness never exceeds 30m; these basalts are fresh and not covered by any thick sediments.

The volcanicity giving rise to the fifth and the sixth flows was interrupted by an eruptive episode. The resulting volcanos are distributed in chains that mainly have a NNW-SSE or NW-SE direction. The volcanic cones in Harra El-Jabban stand out as peaks in the landscape which otherwise presents a generally plains topography. Since these cones are the most obvious landmarks in the region, the Bedouin inhabitants have given every cone a distinguishing name to facilitate their travelling, to determine their locations, and to orient themselves in the desert. In total, about 80 eruptive centres occur in Harra El-Jabban; these centres are distributed in two volcanic fields - those of (i) Remah and (ii) Ashqaf.

(i) The Remah volcanic field lies in the western part of the Harra. It begins at its western end with the Jebal Makuis volcano located beside the village of Um Al-Qutin, and ends with the Jebal Ashhab volcano located 10 km west of Safawi. The volcanos in this area are distributed over an area of 100 sq.km, Jebal Aritayn which is located in the middle of this field of volcanos, and lies in the middle of the main test area used by the author, is classified as a composite cinder volcano, consisting of two separate contiguous cones occurring along a fissure system trending N-S.

(ii) The Ashqaf volcanic field lies in the eastern part of the Harra; it begins with the Qitar Al Abd volcanic chains in the west and ends with the El-Ashqaf volcanos in the east.

The basaltic ridges are one of the conspicuous volcanic phenomena in Harra El-Jabban. These ridges are called "Al-Khash'a" in Arabic. They can classified into four fields arranged from west to east.

The dike systems are distributed all over the Harra. These systems accompany different basaltic flows and volcanic eruptions. They occupy tensional fractures up to 20 to 90 km in length oriented in a NW-SE direction. An example of the fifth flow dike system is that of Qitar El Abd.

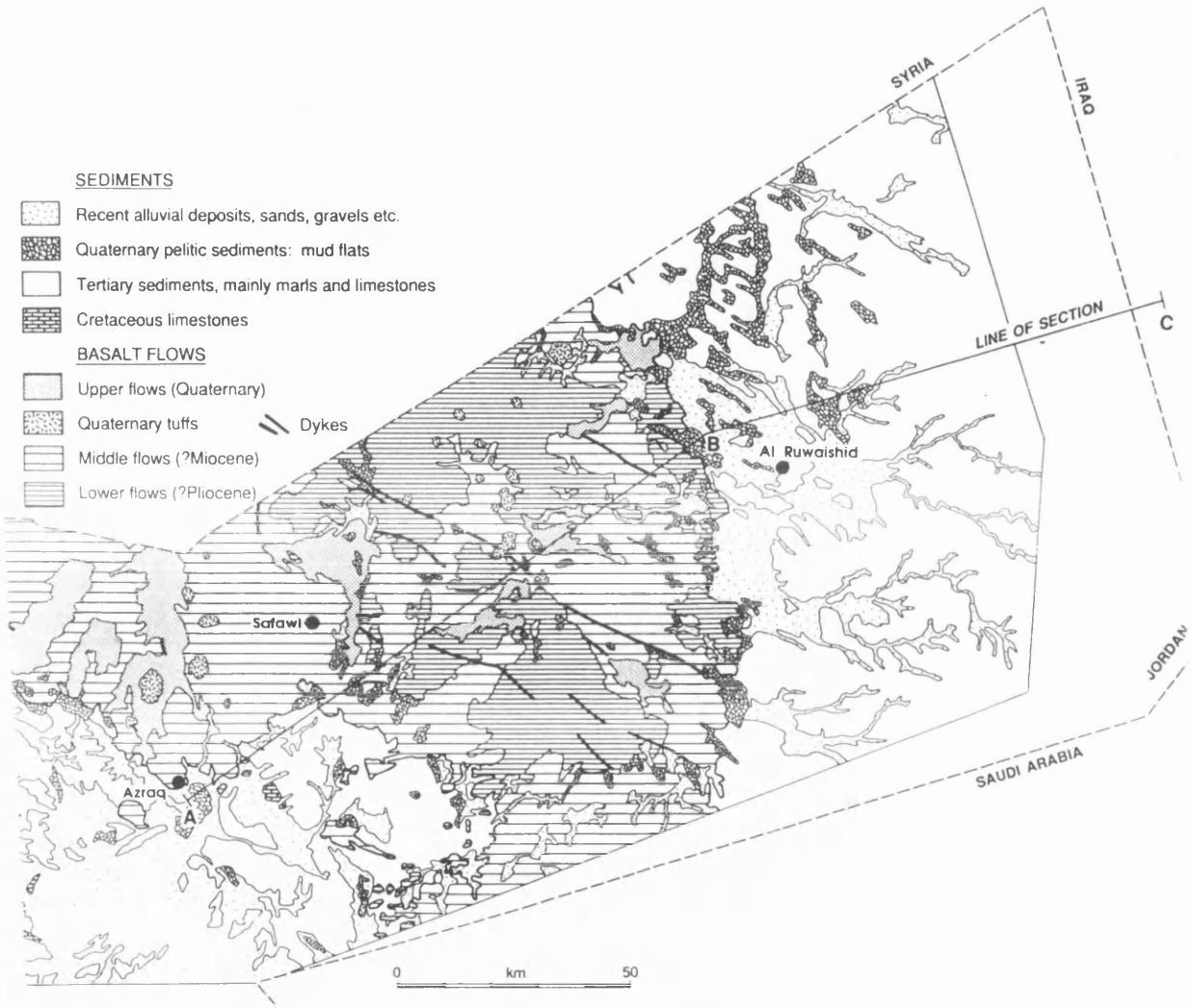

Figure 8.3 Major Geological Divisions of the Badia Area

8.2.2.2 Geomorphology of the Project Area

Basalt boulders of different sizes currently dominate much of the ground surface of the Badia Project area. The different basalt formations discussed in the previous section have a strong influence on the local topography, the drainage network development and the distribution of pans. The whole of the Eastern Badia exhibits major faulting systems.

Block faulting over the central and north-east part of Jordan has contributed to the formation of broad swells and interior drainage basins including the Al-Azraq - Wadi Sirhan Basin.

The overall topography is gently undulating with few sudden breaks of slope, gradients are seldom steep, and, in general, the topography is characterised by gentle concave-convex slopes. The highest ground reaches approximately 1,200m in elevation and occurs in the north-west of the Project area towards the Jebal Addruz (also called Jebal Al-Arab), whereas the lowest part of the area lies at around 400m elevation along the border with Saudi Arabia. The mean altitude is approximately 800m, and occurs in the area around Safawi. The topography is dominated by extensive tracts of gently undulating, low hills introducing elevation differences of 25m to 30m between high points and low points across the landscape within short distances.

In general, there are some topographic variations within the basalt area which depends to a considerable extent on the age and the physical characteristics of specific basalt flows. Generally, the landscape is more rounded, with well developed drainage patterns and a fine colluvial rill network on the older flows. However the areas covered by more recent flows show a more irregular topography with many silt filled depressions.

Beneath the numerous boulders, the ground surface is covered mostly by typical desert pavement - see Figure 8.4. The basalt flows are arranged in sheets. These sheets can be seen along the cliffs bounding the steep-sided wadis. The flat surface of the Harra is occasionally undulating. These undulating areas are restricted into three zones and are mainly associated with the last flow. Sometimes the surface of the basalt is covered either (i) by loose, brownish-coloured, basalt scree, which is known locally as Al-Hamad and results from weathering of the basaltic flows constituting the bedrock, or (ii) by thin to thick soil and clay layers varying from white to yellowish in colour. The size of boulders is controlled by the ground surface geology. In some of the basalt fields, large boulders predominate, while towards the south-east, small, angular, chert fragments are more common. In the western parts of the area, more especially in the north-west, the ground surface is only slightly covered by basalt. As economic

development has begun to influence the Bedouin who inhabit the area, and as they have been encouraged to settle, substantial areas of the western part of the basalt have been cleared of boulders to allow permanent agriculture. Due to the higher amount of rain falling in this western part than in the rest of the Project area, the basalt is often covered by lichen which gives the surface a light grey colour.

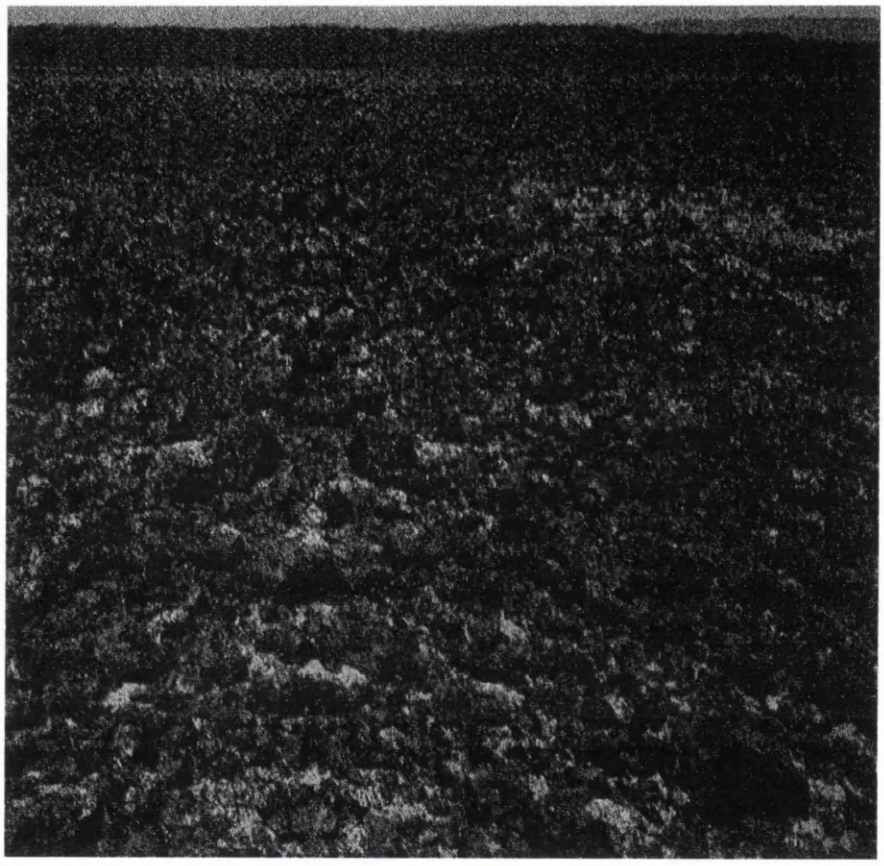

Figure 8.4 . Basalt surface cover.

By contrast, the most southerly part of the Badia area is characterised by wind blown sediment deposits. These aeolian deposits represent the northern margin of an extensive sand sea in Saudi Arabia.

Rainfall is subject to drastic fluctuation both in terms of place and season. The main annual rainfall in Jordan varies from less than 50mm in a year in the desert area of the Badia to more than 600mm in a year over the western heights of Jordan. Individual storms frequently result in wadi floods. Many storms are of high intensity and low duration, resulting in significant runoff and loss of a major potential water resource due to a lack of management and control. The estimated potential evapotranspiration can be in excess of fifty times the mean annual rainfall and the heat energy supplied to the

Earth's surface is far above that required to evaporate all water at or close to the ground surface (Burdon, 1982). About 85% to 92% of the total precipitation that falls in Jordan each year is lost due to evaporation, 5% to 11% disappears through infiltration and 2% to 4% generates runoff.

The surface drainage of the Badia region can be broadly divided into wadi systems, areas of distinct channelized flow, and pans (known locally Qaa or Marab) which are predominately fine-grained sedimentary basins of low relief. In general, infiltration rates are high in wadi channels but decrease rapidly towards the Qaa and towards interfluves. This implies that the runoff from the wadi side slopes will be high, while there will be water storage along the wadi beds and there will be ponding in the Qaa areas. The biggest wadi in the project area is Wadi Rajel, which runs from Jebal Al-Arab in the north (in Syria) to the Al-Azraq basin in the south. The distinct feature of the wadis in the western part of the Badia is that they are running from north to south, while the wadis in the eastern part of the Project area run from south to north.

A distinctive feature of the Badia area is the large number of pans. They represent areas of sediment and water accumulation and storage located in topographic depressions. They can be classified into three groups. The first group are small closed basin pans; these occur in the younger ridged lavas, such as the Bishriyya Group. Associated drainage networks are limited, watersheds are clearly defined and the Qaa represent areas of local sediments accumulated from adjacent slopes. The second group are these pans with distinct wadi inlets and outlets. These features, often referred to locally as Marab, occur where a basin exists along the axis of a wadi. They are characterised by very low angle, fine-gravel fans, which extend from the wadi inlet out into the pan. The third group are large inflow pans with limited outlet drainage. These tend to be pans with the largest catchment areas. They have limited or no outlet drainage. The lowest parts of the pans are characterised by saline deposits.

In general, the area can be divided into a number of units from a geomorphological point of view:

- Volcanic fields in form of isolated volcanos distributed in two parts. The western (Remah) field starts from Jebal Makuis in the west and runs to Jebal Ashhab, 10km west of Safawi. These volcanos are distributed over an area of about 100sq.km. Examples of these are the Jebal Aritayn volcano (which is situated in the middle of this field), Jebal Fahem, and Jebal Remah. In the north-eastern part of the Harra, the Ashqaf volcanic field is distributed over an area of 70sq. km .
- Undulating surfaces mainly associated with the last basaltic flow covering three zones, two in the western part and one in the eastern part of the Harra.
- Flat surfaces with sheets of basalt.
- Flat surfaces of the Al-Hamad in the eastern part of the study area. Here the surface is covered by loose limestone material.
- Rolling topography associated with the southeast part of the study area with blown sediment covering the basalt.
- Pans (Qaa) are scattered throughout the Harra.
- Drainage systems, comprising many meandering wadis that pass through the Harra, in approximately a N-S direction, These wadis are filled with boulders, gravel and silty clays.
- Dikes, which generally occupy tensional fractures 20 to 90km in length oriented with a NW-SE strike. An individual well developed dike system consists of spaced intrusive centres, which are seen as prominent hills such as Qitar El Abd.

Another set of features are the lava-tube caves. These tubes and caves are formed beneath the congealing surface of the basalt flow. They appear normally as big holes that extend as tunnels sometimes several kilometres long (Al-Malabeh, 1993).

Generally speaking, the basaltic area is hard to access either by vehicles or on foot. Very few roads are available in the area; the main paved road is the highway from the Iraqi border to Mafraq which splits at Safawi to pass through Al-Azraq on its way to Amman. The very few other roads are either unpaved roads or rough tracks that have been opened up and used by the nomadic Bedouin people during their seasonal movements to allow water, food, and sheep to be transported from one place to another.

8.2.3 Field Work Planning

Due to the requirements of the research project and the needs for highly accurate ground control points to be provided for the setting up and orientation of the stereo pairs of SPOT imagery, the author arrived in Amman on 17th October 1995 to carry out his field work, bringing with him 5 stereo-pairs of SPOT imagery bought and provided by the Higher Council for Science and Technology (HCST) in Amman. He was provided with full accommodation and a Land Rover and skilled driver to carry out his field work. The first step was to visit the study area; three days were spent in the field carrying out this preliminary reconnaissance and orientation. Comparisons were made between the images and the existing topographic maps which were available and were used for navigation. This preliminary reconnaissance also included the identification and location of some features that could potentially be used as ground control points. At the beginning, only those points located at the intersection of roads were clearly identified; whereas points in the basaltic (Harra) area appeared hard to select and define.

Collaboration with Royal Jordanian Geographic Centre (RJGC) was achieved through an agreement between the Higher Council for Science and Technology (HCST) and the RJGC which had been signed up to provide the author with experienced field surveyors and GPS instruments to carry out the necessary field work. Therefore, after the initial visit and inspection, the author visited RGJC at the end of October 1995 to arrange a suitable date for the skilled surveyors and the GPS receivers to work in the study area. The author was informed that the GPS receivers were not available at this time, since the equipment was being used by other field surveyors in another area. However, the field surveyors would be available in the second half of November. For this reason, the field work was divided into two stages, the first stage being the selection of the ground control points and the marking of these points on the ground and on the images. During the second stage, the surveyors would carry out the observations when the GPS receivers became available. On 18th November 1995, RJGC sent a party of 6 surveyors to the Safawi Field Centre to join up with the author and commence the selection and marking of the ground control points in the study area.

8.2.3.1 Reconnaissance and Selection of the Ground Control Points

The project area is covered by five stereo-pairs of SPOT Pan images with a 10m ground pixel size, comprising scenes 122-285, 123-286, 123-285, 123-286, 124-186 and 124-286. Scene 122-285 was considered as the special test stereo-pair for the geometric accuracy testing; thus it was decided to select around 70 ground control points (GCPs) for this stereo-pair while each of the other four stereo-pairs required 15 ground control points, mainly to achieve the correct absolute orientation of the stereo-pair. The reason why the most westerly scene was selected to be covered by 70 points was that the area is covered by a network of roads and tracks connecting all its small settlements which are concentrated in this area. This meant that the area was easy to access which reduced both the time and the cost of the operation. It also meant that there were plenty of GCP locations that were relatively easy to identify, and plenty of points that could be used as check points. The land surface in this area is covered by a very thin layer of basalt, and the people of this area had already cleaned much of the surface, removing the boulders so that some parts could used for cultivation. By contrast, the southern parts, especially those lying south of the main Baghdad highway were very difficult to access due to the numerous large basaltic boulders existing in the area, for which the surface had not cleaned by the local people. Also there are a number of large pans that were uncrossable. By contrast, the most southerly part of the area comprises an undulating surface and some parts are very easy to access.

8.2.3.2 Selection of the Ground Control Points

In the office in the Safawi Field Centre, preparation for the next day's work started by organising the field survey, which included defining the survey area allocated to each team, and the approximate location and number of points that should be selected. The main work of the author was concentrated on the selection of the control points. It was not an easy task. The author used the original hardcopy SPOT stereo-pairs imaged at 1:400,000 scale for this purpose. These could be viewed either using pocket and mirror stereoscopes, or a magnifier. Enlarged copies of the images at 1:150,000 scale, and topographic maps at 1:50,000 scale were also available and were used to define the

locations of the ground control points and the routes to be taken to arrive at these points. The same procedures were followed every day to select the points and to define the routes to these points and to select alternative points for those areas where the potential points were not well defined either in the field or on the image.

8.2.3.3 Final Location of the Ground Control Points

Fieldwork was conducted from the Safawi Field Centre. Two four-wheel drive Land Rovers with two skilled drivers and six surveyors from Royal Jordanian Geographic Centre were used to carry out the final position-fixing of the GCPs. The team was supervised by the author. The fieldwork started on 19th November 1995 in the western part of the area which is covered by the special SPOT scene 122-285. General navigation in the field was done with the 1:50,000 scale topographic maps and the enlarged 1:150,000 scale copies of the SPOT images.

As mentioned above, the western area is covered by a network of minor roads, some of which showed up on the images; others did not, as they have been constructed since the SPOT images were acquired in 1987. The intersections on the older roads which showed up clearly on the SPOT images were selected as well identified control points at intervals of 5 to 10 km. White and red sprays were used to mark the selected points on the ground. Other points were established in the Qaa (depressions), where a clear and sharp boundary marked the basalt's margin - which shows up in black to grey colours on the SPOT images - from the white colour of the depressions. The ground surface in the Qaa is very flat and reflects the sunlight in bright white colours; thus most of points were selected on the edge of Qaa, or on the edge of black basaltic spots located inside the Qaa. Some other points in the western area were selected at the corners of regular cultivated fields, especially those located in the south-western part of the area. Many points were selected in the middle of small black basaltic spots basaltic present in some depressions. These points were considered to be well identified points and were easy to access. A very few points were identified and selected in the junctions of small valleys. Most of the valleys, especially in the basalts (Harra), do not show any clear and sharp

edges that could be identified and used to position control points. Only three points were selected on the top of a small rounded hill, where the point was clear and easy to select.

In the eastern part of the research area, extending from the Syrian border in the north to the Saudi Arabian border in the south, an undulating surface prevails. In this area, the selection of the points proved to be very difficult except for those points selected at the intersections between the old and new highways to Baghdad. Moving into the area south of the highway in this eastern part, the selection of the GCPs was very difficult, since there is no clear boundary or distinction between the various surface features. But in spite of all these difficulties, a more detailed inspection in this area allowed some points to be selected in the boundary area between small depressions and the limestone bedrock, which was densely covered with angular chert fragments on the ground surface.

Altogether 69 points were fixed in the area of the special test model (122-285) and 14 to 20 points have been selected for each of the other stereo-models. Every point was marked and fixed on the ground, with white and red spray paint marking the actual points and iron poles fixed on the exact locations. In spite of the difficulties experienced in the selection of the GCPs over most of the area, attention was paid to the need to distribute the points in a fairly regular manner over the whole format of the images and to try to ensure that some GCPs were located in the corners of the images (Figure 8.5).

8.2.3.4 Problems

In spite of the careful selection of the ground control points in the office, the author faced further minor problems in the field. Some of these problems related to the provisional points which had been selected in the office. After a big effort (in terms of time and cost) to arrive at these points, some did not show up on the ground as a clear or sharp boundary to enable the survey team to identify their exact location due to disturbance of the features; sometimes it proved impossible to reach some of the points. Rain also caused some problems when accessing some of the points located in the

depressions, in which case, alternative points had to be selected in the same area to keep a good distribution of the points needed for orientation purposes.

The research area is very big and largely uninhabited. During the first stage of the field survey work, there was no radio communication between the Land Rovers. One evening, one of the survey teams did not return back to the Field Centre. The other team then spent the whole night searching for them, but without finding them. The weather was very cold, with the temperature around zero. Next day, in the morning, the airforce personnel at the Safawi air base prepared to send aircraft and helicopters to search for missing team, but just as they were about to do so, a patrol from the border guards found the team. The driver had slept inside the Land Rover and he was in bad condition due to the cold since the car engine was out of order and the heater could not operate. The other two surveyors had left the vehicle when it stopped working, to look for help, hoping that they could find Bedouin people living in the area. Finally, after walking 13km, they did find a Bedouin encampment but the people were unable to help them with the recovery of the vehicle because it was raining. Working in these cold winter conditions was a great challenge and tribute must be paid to the efforts and toughness of the surveyors and drivers who carried out the work to a successful conclusion in these poor conditions.

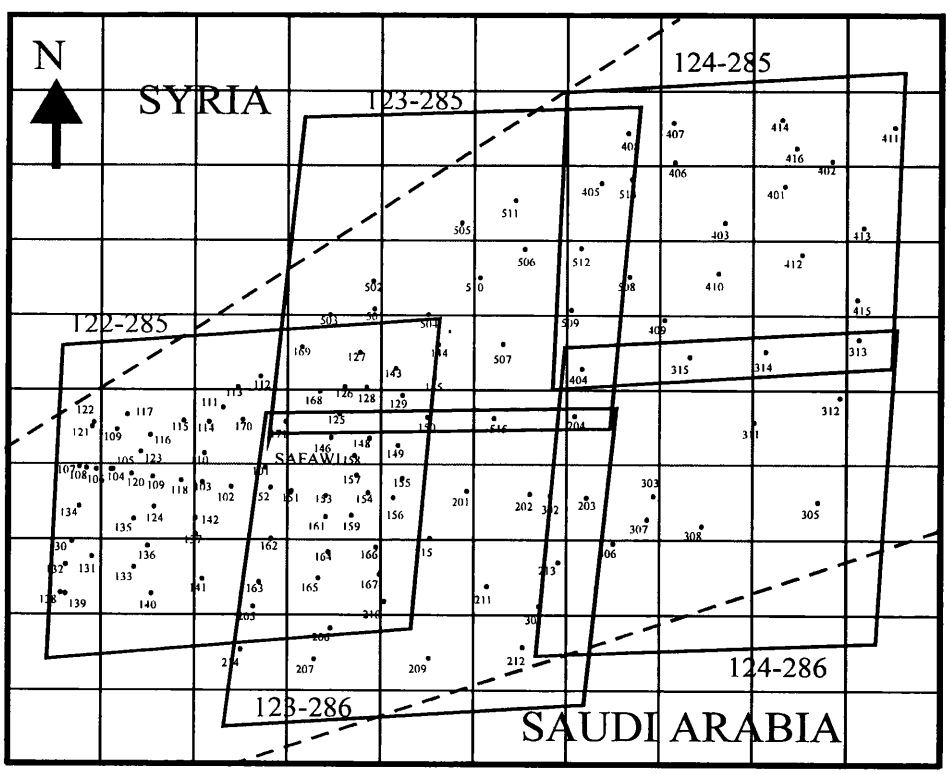

Figure. 8.5. Location of GCPs with respect to the individual SPOT scenes

8.2.4 GPS Instrumentation and Software

Satellite positioning is the term used to describe the determination of the absolute and relative coordinates of points on the Earth's land or sea surfaces by taking and processing measurements from artificial Earth satellites (Cross, 1990). The first applications of this technique took place in the early 1960s, but it was expensive and involved the use of elaborate equipment so that it was only useful for global geodesy. Nowadays relative position can be achieved from satellite measurements with comparative ease and with accuracies ranging from a few metres to a few millimetres. In addition to the high accuracy, satellite positioning has a lot of advantages in that, with suitable equipment and techniques, the derived positions are genuinely three-dimensional. Ground control points can be placed almost anywhere, with the proviso that the location of the points must have clear lines of sight to the satellites being observed. Since the Badia area has no urban development or forest, this last condition could easily be meet.

The Global Positioning System (GPS) is sometimes called NAVSTAR, an acronym derived from the title Navigation Satellite, Timing and Ranging. It is a multi-purpose positioning and navigation system based on the use of 24 satellites arranged in six orbital planes, each with an inclination of 55^{o} to the Equator; a 60^{o} spacing in longitude; an orbital height of about 20,183km and an orbital period of 12 h (Wells, 1987). For most points on the Earth, at least four satellites are in view at any time; often more are visible. Two continuous radio signals named L1 and L2 are transmitted in the L band. Both signals carry a formatted data stream related to the predicted satellite position and its Keplerian elements (Cross, 1990). All of the satellites are tracked by five ground stations which send their data to the main control centre located in Colorado, where the data messages containing the predicted positions for the next day or so are computed for each satellite and sent to the most convenient ground antenna for upload to the satellite. Modulated on the L1 frequency is a C/A code and a P code; on the L2 frequency, there is just the P code. These codes are pseudo-random binary sequences; they are realised by a binary biphase modulation which results in 180^{o} changes of phase of the carrier.

Differential GPS (DGPS) relies on the concept that the errors in the position at one location are similar to those for all locations lying within a given area. By making and recording GPS measurements at a point with known coordinates, these errors can be quantified and corrections can be applied to the observations made at all the other locations lying within the immediate area. These common errors are caused by factors such as clock deviation, selective availability and the changing radio propagation through the atmosphere. If a receiver is placed at a location for which the coordinates are known and accepted, the difference between the known coordinates and the calculated GPS coordinates is the error. The error which has been determined at the base station can be applied to all the other GPS receivers (called rovers or remotes) in the area. Since the sources of the error are constantly changing, it is necessary to continually monitor these changes and to match the error correction data from the base station very closely in time to the data collected by the rover. One way of doing this is to record the data simultaneously at the base station and at the remote with the data sets being processed together at a later time. Nowadays this is a very common practice in survey work and was the method used by the survey team and the author in the Badia area. The other way of doing so is to transmit the correction data from the base station with the corrected position being computed in real-time. This process is called real-time DGPS and is used widely, for example, in navigation, offshore hydrographic surveys, and seismic surveying.

8.2.4.1 GPS Instruments

Five Ashtech Z-12 dual-frequency GPS receivers were bought by the Royal Jordanian Geographic Centre for survey work in 1995, at a total cost of $200,000. The Ashtech Z-12 is a high-class GPS receiver that is designed to make full use of the Navstar global positioning system. It has twelve independent channels and features automatic tracking of all the satellites that are in view. So there is no need for manual or programmed selection of common satellites between survey sites. The system includes the microstrip antenna mounted on a precision machined platform for accurate positioning and centring above the survey mark. Several easy-to-use screens are provided by the receiver's control unit to give the required functionality. Information given in the title of the screen

means that this is for display only, while the use of control means that a screen is being presented that the surveyor can interact with.

(a) Z-12 GPS Receiver Front Panel

The Z-12 receiver is easy to operate in ordinary field use; initially it is just a matter of switching the power on. On the Z-12 GPS receiver's front panel, various keys are provided for controlling the receiver and entering data. These include 9 numbered keys; pressing a particular numbered key calls up a specific screen directly - as shown in Figure 8.6. The numbered keys are also used to enter alphanumeric data such as the antenna height, or site number. Keys such as **c** and **e** are used to cancel the current entry and to enter or save values respectively. Other keys are used to change a numbered screen or sub-screen or to scroll through the different pages or to highlight a field or to flash in a character position in data-entry mode.

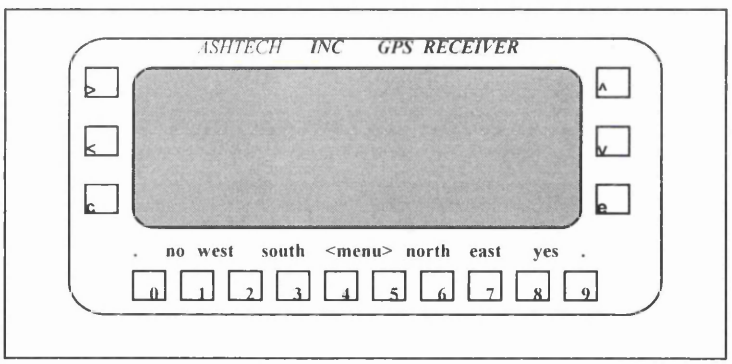

Figure 8.6 Front Panel of the Receiver (Ashtech operating manual).

(b) Z-12 GPS Receiver Back Panel

The Z-12 receiver operates with an input voltage between 10 and 32 VDC from an external power supply. Two power sockets allow the receiver to use two external batteries; a continuous tone indicates that the voltage has dropped below 10 volts when the battery comes close to being discharged. Connections can be made with both the first battery and the second battery but the receiver will operate from whichever battery has the higher charge.

(c) Z-12 GPS Antenna Platform.

The antenna platform can be mounted on a variety of tripods and ranging poles. The geodetic microstrip antenna is seated on a precision machined platform and protected by a weatherproof cover. A low-noise pre-amplifier housed at the base of the antenna provides sufficient gain for a cable up to 30 metres long. Eight dog-legged holes, labelled in the antenna ground plane, allow antenna height measurement using the special sectioned measuring rod to measure through one of these openings.

8.2.5 GPS Observations.

On 25th December 1995, the RJGC observation team arrived at the Safawi Field Centre. The team consisted of six surveyors equipped with three Land Rovers and five Z-12 GPS receivers. The team was provided with full accommodation by the Badia Research and Development Programme at the Safawi Field Centre. The Programme also gave further support by loaning two Land Rovers to the team. The fieldwork started on 26th December. Every day, an observation plan was drawn up for the next day.

As is well known, there are three main methods of surveying using two or more GPS receivers simultaneously. These methods are called the ***Static, Pseudo-Kinematic*** and ***Kinematic*** methods respectively. Collectively they are all employing the relative or differential positioning technique. Static surveying is the most reliable and accurate method, producing coordinate differences for the points to the millimetre level, but this requires the receiver to remain at a site for a relatively long time to get the required redundant observations. The Pseudo-Kinematic survey technique requires the receivers to occupy the points for at least two short periods (5 to 10 minutes), separated by a longer period (1 hour). It does not need to have continuous lock when the receiver is moved to the next point. This method is less accurate than the Static or Kinematic methods due to the short period of data sampling and it can be affected by ionospheric changes between repeat observations. The Kinematic method comprises very rapid surveys of a number of baselines in areas where there is good satellite visibility. At least one receiver is placed at a known stationary base point and one or more rover receivers

are used which move from point to point. This is not as easy to do since lock must be maintained on at least four satellites. Surveying by this method based on the carrier phase of GPS offers first-order control to be established on a series of survey points without the long observation times. Quite often all three methods may be used and combined to form a large GPS survey network.

The method used in the field for the measurement of the ground control points was the Rapid Static technique. Later the kinematic technique was used for the measurement of the GPS profiles used for the checking of the elevation data extracted from the SPOT stereo-pairs. For the fixing of the ground control points, the observational fieldwork started from the western part of the area and then moved steadily to the east. Two of the Ashtech Z-12 GPS receivers occupied two known points or base stations between 9 a.m. and 5 p.m., these points being existing first-order trig points. During the same period, the other three roving receivers occupied different points close to the baseline, carrying out 35 minute sessions of measurements on each point.

8.2.5.1 System Set Up Used for the Rapid Static Technique

The following procedures or steps have been carried out to implement the Rapid Static technique. At each point - whether a known point or an unknown point - the antenna had to be set up over the survey mark (Figure 8.7). No obstacle should be present which prevents line-of-sight reception of the GPS signals. A tripod and a tribrach with an optical plummet was used to set up the GPS set exactly over the ground point. Once the tribrach had been levelled and centred over the survey mark, then the next step involved placing the antenna platform on it with the sign toward the north direction. The next step after this was to connect the antenna through the pre-amplifier to the receiver with an antenna cable. This was followed by the measurement of the antenna height using the Ashtech sectioned precision rod. The final step was to connect the external battery to the power sockets on the receiver's back panel, followed by switching the receiver to the "on" position.

Figure 8.7 Setting up the antenna of GPS Ashtech Z-12 over one of the survey marks.

8.2.5.2 Observations (Operating the Receivers)

The measurement and data collection starts with the receiver being turned to the "on" position. This initiates a self-test. If the receiver detects any problem, it displays an error message and stops. If there are no problems, the receiver displays screen [0]. The screen contrast can be adjusted by pressing the arrow keys. For static surveys, no interaction with the receiver is required. It automatically searches and locks on to all the available satellites; makes the appropriate measurements; computes its position; opens a file and saves all data into this file.

The two primary screens are nos. [4] and [9], which are used for specifying information. With screen [4], entitled mode control (Figure 8.8), the parameter can be changed by pressing key [e] to shift the data-entry mode, and using an arrow key to move the cursor to the desired parameter and either change its value or keep the default values. The receiver is preset to certain default values for the control parameters. Going to screen [9]

by pressing key [9] gives access to the receiver's site and session control screen. With this screen, site information can be entered during data collection.

The first step in the observation sequence is entering a site name. Using screen [9] (Figure 8.9), if the [e] key is pressed to switch to data-entry mode, an alphanumeric conversion table will appear. To enter the site name, one number is typed in at a time where every number corresponds to the letter that is wanted. It is matter of choice to select or allocate any name or number to a specific observation point. The given ground control point numbers start from 101, 201, 301, 401 and 501. Using the arrow keys to correct the cursor position, the cursor jumps to the field where a session identifier can be entered after the fourth character. When the entries are acceptable, then pressing [e] will save the changes in the memory of the GPS set; pressing the [c] key will cancel the changes if something is wrong.

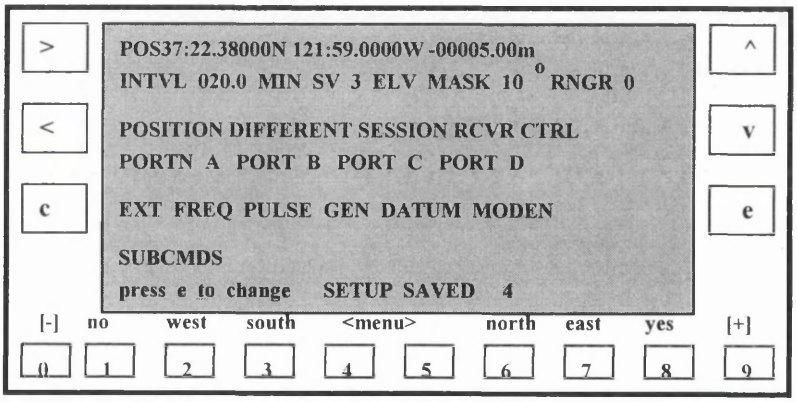

Figure 8.8 Screen [4] (Ashtech Z-12 operating manual).

During the observation, it is possible to press any number of screen keys to jump to and get information. To get sky search information, key [0] is pressed. This screen displays the status of each satellite that the receiver finds, as it performs the sky search. No data can be entered via this screen; it is a display screen only. It shows the number of the satellite that has been located. After it locates the first satellite, the set then reads the satellite time, sets its own internal clock and reports the GPS time. When more satellite data has been collected, it changes the time to GMT. The display also gives the number of each satellite; the channel numbers, the current status of each C/A, P1, P2 code channel; the type of receiver; and the software version number

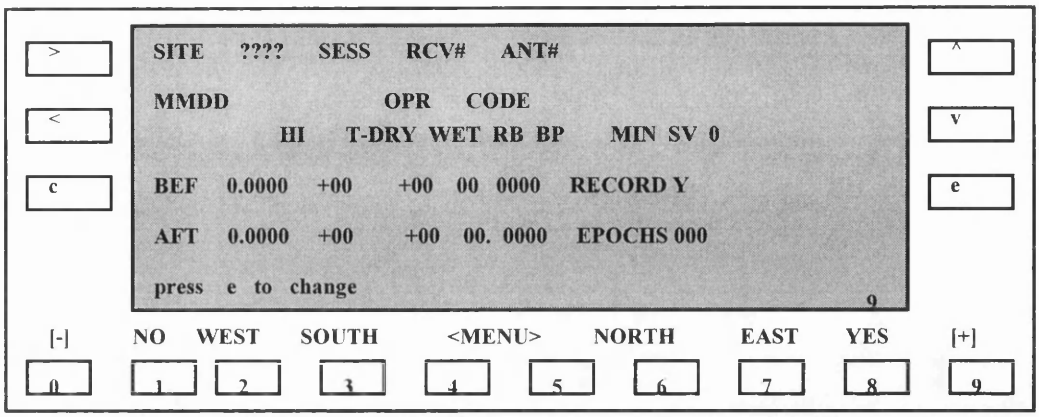

Figure 8.9 Screen [9] (Ashtech Z-12 operating manual).

For orbit information, screen [1] displays the orbital parameters. It displays information such as the elevation and azimuth of each satellite and shows the number of each satellite being tracked, the number of the epoch which is updated every second, and ranges from 0 to 99. If there is any loss of lock, the receiver resets to 0. It shows also the signal-to-noise ratio. When it is less than 20, the signal is weak; when it comes to a value over 50, the signal is adjudged to be strong. On the screen, more information is given that is related to the range of accuracy of each satellite. The accuracy is high when the screen indicates a value of 0; a value over 8 indicates a low accuracy. This screen can be used for display only; it cannot used to enter information - see Figure 8.10.

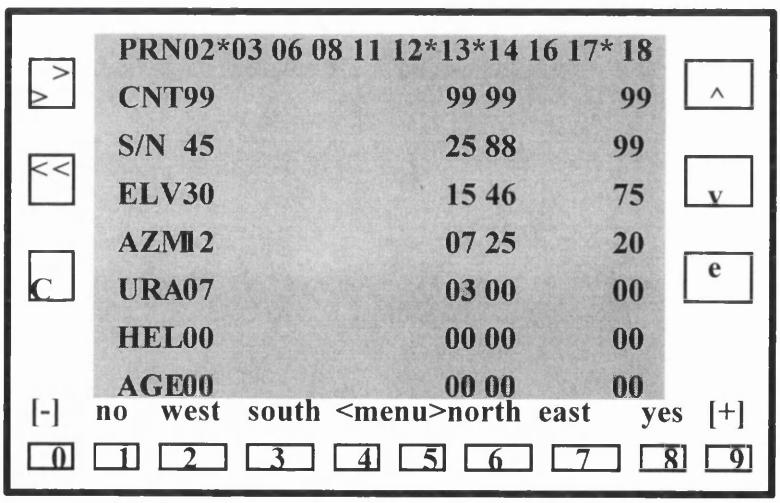

Figure 8.10 Screen [1].

Navigation information can be obtained from screen [2] (- see Figure 8.11), which is related to various components concerned with position. This screen consists of two pages; on the first page, different components show the datum of the displayed position:

the default is WGS-84. The display changes to OLD when the position data is more than 10 seconds old. The screen also displays latitude and longitude in degrees and minutes; the ellipsoidal height of the antenna; the receiver's velocity; and the magnetic variation mode. A dilution of precision in the position may take place since this depends on the relative positions of the satellites. If they are scattered around the sky, the accuracy of a position is better. Any number above 6 indicates a bad position and a dilution of the precision. It shows also the number of satellites currently being used for the position calculation. Screen [2] page 2 shows time-to destination, while Screen [3] shows tracking information, and gives a visual representation of the data recorded for each tracked satellite; it acts only as a display screen.

Mode control is provided by screen [4], where different receiver control parameters such as differential mode; receiver mode; position fit; session programming; pulse generation; datum selection; setting external frequency and modem set-up can be changed. The receiver is programmed to present default values for the control parameters. To change a parameter value, key [e] is pressed to shift to data entry mode.

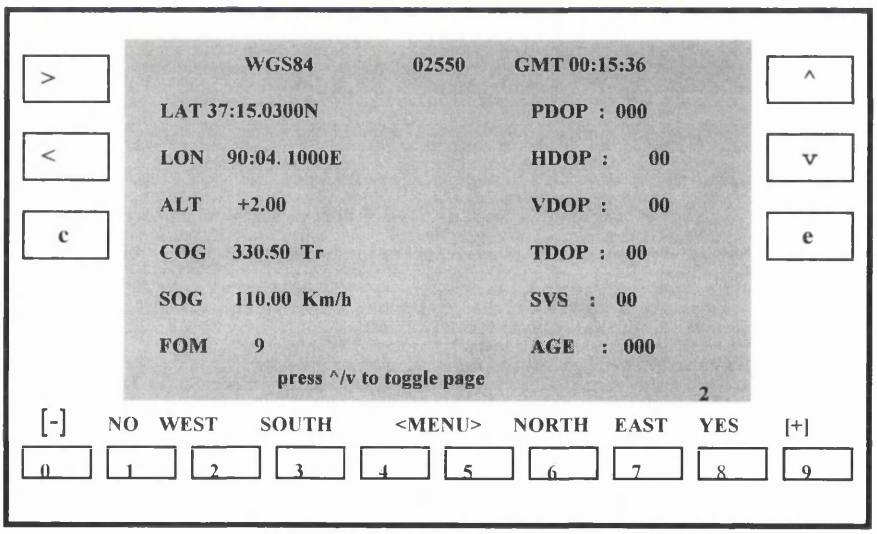

Figure 8.11 Screen [2]

Differential information and range residual/position error appear on screen [5]. Two different displays are available via this screen - page 1 displays differential information, while page 2 displays the range residual and position error information giving the difference between the measured and the calculated range.

Waypoint control is provided via screen [6]. Options allow the user to define a navigation route and to enter the latitude and longitude of each waypoint included in the proposed route. The receiver can compute the distance between the present position and next destination point and display the course to be followed and the time to the next destination point. The first line in the screen will show the route information when screen [6] is invoked. The remaining part of the screen will display a list of records showing the current and next waypoints in the route. Of course, this information concerning waypoints and routes is more appropriate to navigation than to the high precision point location being carried out in the present project.

Satellite selection control appears on screen [7]. On this screen, the user can specify whether to include or omit specific satellites for tracking. Letter Y is associated with a satellite that will be used; N indicates one that will not be used. Other options available for selection include those for the choice of an automatic or manual modes. The receiver can only use the 12 satellites that are displayed on its 12 channels or only the specified satellites.

System control appears on screen [8] which accepts several system-level commands. It shows the files that have been stored in the memory and the site name, It also displays the equivalent hours used to indicate the file size (1 EQHR is equivalent to one hour of data recorded at a 20-second interval for 5 satellites). The standard one megabyte of memory will display 19.5 EQHR when empty.

Site and session control is provided using screen number [9]. On this screen, site information can be entered in order to record which particular site was being occupied. The site name can be entered even during data collection; this will not affect the collection process. Another parameter that can be entered is the identifier of the session. During downloading to the PC, the Hose program of the GPS set takes care that this parameter has been entered while the observed data is being downloaded. Other parameters such as the antenna identifier and receiver serial number; the month and day of the session; the height of the antenna; and other information related to temperature and humidity will be displayed.

The so-called all-in-view information is given by screen [10]. It shows a polar plot of the available satellites and their orbital paths. Screen [10] can be reached by pressing the **[9]** key, then pressing the > arrow key or pressing the **[0]** key first and then pressing the < key three times. It shows any satellite that is visible but has not been locked on to and which satellites have been locked on to. The orbital track of satellite can be shown by pressing the arrow key (Figure 8.12).

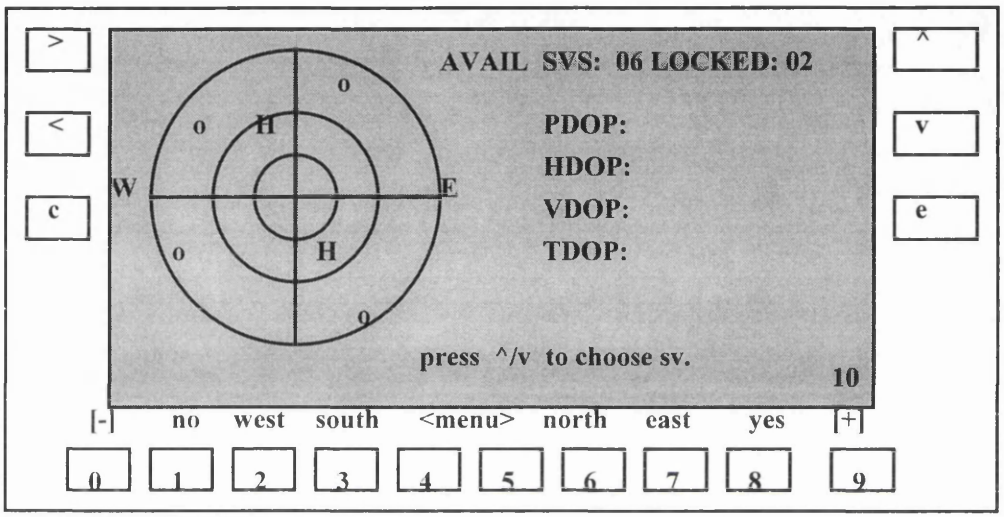

Figure 8.12 Screen [10] (Ashtech Z-12 operating manual).

Visibility information is displayed on screen [11]: it shows the time when each satellite is visible. The screen can be reached by pressing the **[9]** key and the arrow key > twice or pressing **[0]** and < until screen [11] is displayed. It is also gives a bar graph which displays the availability of satellites over a 24 hour period, i.e. 2 to 4 hours before and 20 to 22 hours after the current time. The bar code control screen is number [12]. It permits the observer to input the bar code or keyboard data that can be used to mark a survey site or GIS data point. This screen can be reached by going to screen **[9]** and pressing the > key three times. As mentioned previously, screens [4] and [9] are the screens where the user can change operational parameters and are these that have been used most during the collection for the ground control points in the Badia area.

Generally speaking, every day during the ground control point measurements, the five available receivers were operated in the same way as on the first day, but in another area close to the previous one. This meant that the observations were carried out over

several sessions in static mode and the sessions were connected together by a common (or pivot) geodetic point. Thus the sessions were linked together through pivot sites, these pivot sites being the stations that were common to two or more sessions. If two sessions were to be linked, then the pivot sites had to be occupied in both sessions. The two stationary receivers were located at known first-order geodetic points for enough time to resolve the ambiguities, with the other 3 receivers roving during the same time occupying different ground control points with a 35 minutes observing period on each. During the observations in the Badia area, no fewer than 4 satellites were locked on to, but sometimes as many as 12 satellites were locked on to by the receivers. The net of observed points was also connected and tied into three existing satellite Doppler points.

During the period of the survey, no major problems affected the survey field work. However there were a few minor problems which did not affect the survey procedure. These problems related to the discharge of batteries, in spite of the fact that they had been drained and charged the night before. The solution for this problem was to connect the receiver with the car battery. The discharge of the battery below the 10 volt level closes the file in the receiver, but does not affect the data collected by the receiver, because it is saved by the program, A new file is opened when the second battery is connected to the receiver.

Another problem related to the microwave energy emitted by a military radar station which was being operated in close proximity to one of the first-order trig points and interfered with the operation of the GPS receiver. This problem was solved by requesting the radar station to switch the power off during the observation period.

In total, the observation field work lasted 10 days. At the end of each day's observations, the data collected by the receivers was downloaded to a PC and the data was then processed using the Ashtech Prism software. There was no need to repeat the observations as a result of the processing. Figure 8.13 shows the distribution of the GCPs resulting from the processed GPS data using the Prism software.

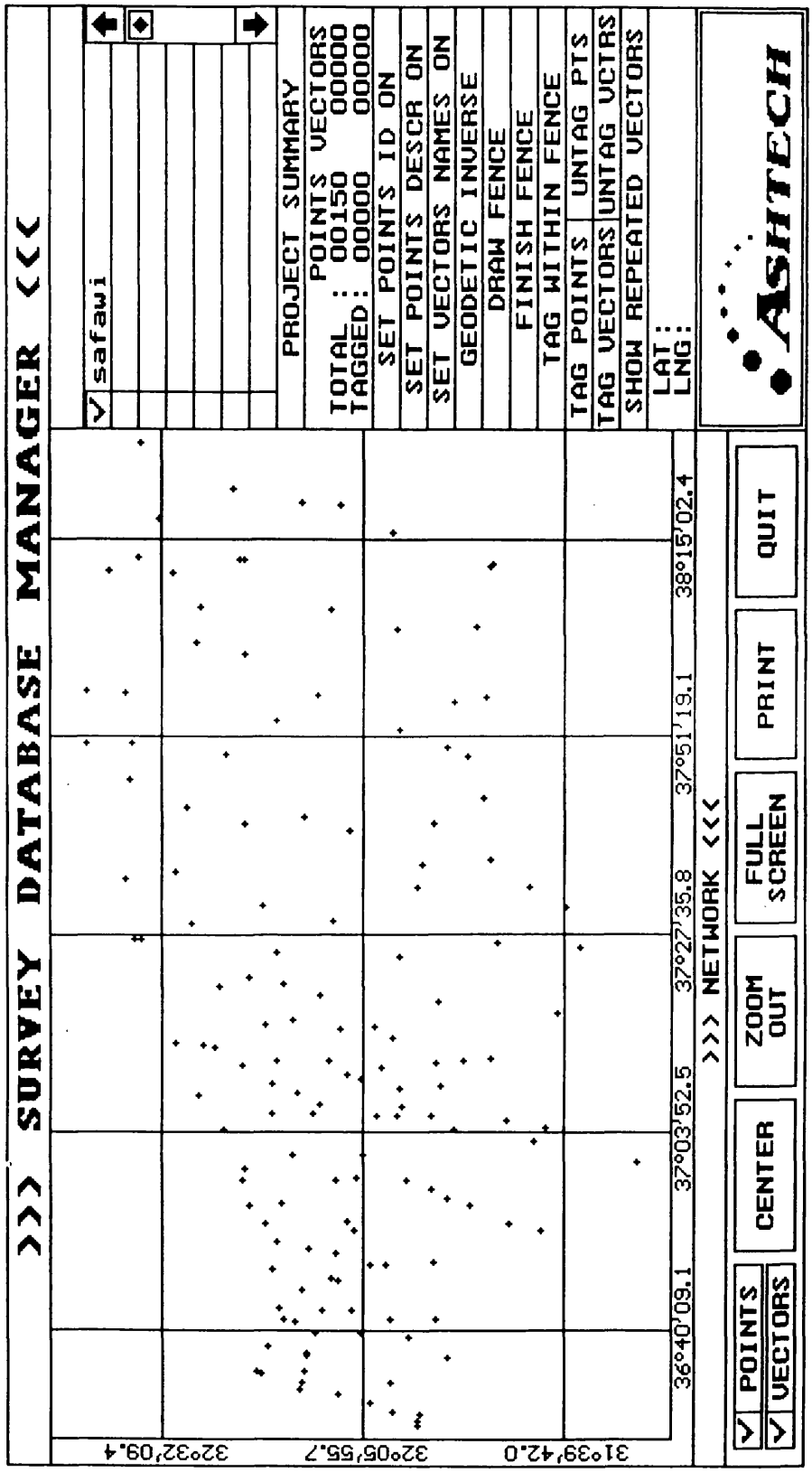

Figure 8.13 Distribution of the GCPs in the Badia Area Processed using the Prism software.

8.2.5.3 GPS Processing and Adjustment

The main purpose of processing the raw data (observations) using the Prism software was of course to obtain the ground control coordinates of each GCP in the WGS 84 (World Geodetic System 1984) geocentric system. The next step was then to carry out the transformation of the WGS 84 coordinates to projection coordinates either in the UTM (Universal Transverse Mercator), or to JTM (Jordan Transverse Mercator) system based on the European Datum 1950 (ED 50).

Processing has been carried out by the RJGC field surveyors using the Prism program module which allows the GPS receiver survey data to be processed to determine the baselines. This program accepts single and dual frequency carrier-phase data (codeless and full-wavelength) as well as code range data. It then calculates the relative positions of the baseline vectors between the stations and gives associated statistical information about the accuracy of the positions. The work started with the survey data files (B, E, S, files) being extracted from the Ashtech receivers using the Prism/Transfer download function. After selecting and employing the processing method that matched the survey-method used, the survey data files were organised into a project site list with site and session-specific information, where the user can change, add to or delete data. This data included site-specific parameters such as antenna height and position which have to be entered by the observer. The computational process combined information in the B-files and E-files to create the raw indifferenced U files (Phase data files) required to process static and pseudo-kinematic survey data. It then formed input parameter files (I-files); output listing files (L-files); vector output files (0-files); and residual plot files (P-files). The process automatically detected and corrected most cycle slips. Residual plots of the receiver's data facilitated the repair of uncorrected cycle slips. Once the Prism software had processed all the data required during a survey session, the possibility existed to pass the processed output data to other Prism program modules for storage or to carry a least squares network adjustment. However, for this particular project, this last process was carried out by the geodetic section of RJGC at its headquarters in Amman.

8.2.6 Observation Accuracy Assessment

As has been mentioned above, the observations with the GPS equipment have been carried out without any major problems. At the end of each day of observation, the data collected by the receivers was downloaded to a PC and then processed using the Ashtech prism software, which meant that, every day, the results of the observations were known to the team and they could plan accordingly for the next day's observation programme. The fixed stations used as the basis for the fixing of the GCPs were mostly first-order geodetic points which have a positional accuracy less than 1m. It was found through the processing that the RMSE values of the residual errors in distance between the fixed stations and the rover points (10 to 70 km) lies in the range from ± 1cm to ± 3cm. For each adjusted position, the standard error were ± 4cm, and the estimated precision was from 0.5 to 2.0 ppm (parts per million) for horizontal position and 0.5 to 1.5 ppm for the vertical value. From this account, it can be concluded that the accuracy of GCPs is less than ± 1m.

8.3 Profiles Along the Old Major Roads

Arising from the good experience of the Royal Jordanian Geographic Centre surveying team in establishing the 130 GPS ground control points (GCPs) over the Badia Test Field in rapid static mode, and the good accuracy which has been obtained from these observations, the RJGC was also asked to carry out the task of establishing profiles along the main roads for an accuracy assessment of the satellite-derived DEMs. The Director-General of RJGC agreed to carry out this additional field survey and the RJGC field survey staff have duly carried out the measurements along the two major old roads in a professional manner.

Based on the 130 ground control points, the survey staff first established 40 points along the roads with a 5km distance between each of the points employing the GPS static survey technique using a static session of 1 hour. For each section of the road, they then extended a kinematic session in a vehicle travelling at a speed of 20 to 25 km/h, using a 2 sec interval between measurements. In this technique, one receiver was held fixed on

each of the known points while the other receivers were mounted on a Toyota Land Cruiser at a height of 2.36m. Based on the computed coordinates of the 40 points, the continuous series of profile points have been computed.

The first profile was measured along 160km of the main old road crossing the Badia area from west to east parallel to the modern highway from Al-Mafraq towards Baghdad. The other profile was measured in a similar manner between Safawi and Al-Azraq which is around 30km in length. More than 15,000 profile points have been measured and recorded by RJGC using this technique and the data was then sent to the author by the Badia Programme office of the Higher Council of Science and Technology (HCST) in Jordan.

8.4 Conclusion

As shown in this chapter, the field work carried out in the difficult terrain of the Badia area has been excuted in a professional manner and to a high standard through several favours. These factors were the following:-

(i) The staff executing the survey work comprised professional field surveyors with extensive experience in carrying out field surveys in desert areas. Indeed some of them had previously shared in the field work carried out to establish the geodetic trig points and in also the maintenance of these points. So they were very familiar with the area and the conditions found there.

(ii) The second positive factor was the availability of four-wheel drive vehicles suitable for work in the very rough and severe terrain.

(iii) The provision and availability of an adequate number of accurate Ashtech dual-frequency GPS instruments.

(iv) The availability of radio telephone communication between the surveyors in the field.

(v) The availability of the enlarged SPOT images and the existing topographic maps of the area which greatly helped the planning of the field survey work, the navigation of the vehicles in the field and the location of the final control points.

(vi) The observation method which has been based on the rapid static method which is a very accurate method.

As a result, the work was carried out smoothly and very successfully. The final results of all these efforts and favourable factors have been the creation of a very accurate test field consisting of 130 ground control points distributed over the whole of a very large area (11,000 sq.km). In addition to the 130 ground control points, the test field has also been supported by the huge number of points provided by the GPS profiles measured along the old main roads crossing the Badia Project area. Establishing a test field of high accuracy ground control points (GCPs) and profiles in the Badia area was essential both for the geometric accuracy tests and for the validation of the DEMs and orthoimages generated from the SPOT stereo-pairs covering the area. Indeed it was the only way to calibrate the systems employed in the present research project. Moreover the test field which has been created, can be considered the only test field of its kind that has been established in the Middle East area.

The next five Chapters (9 to 13) will give the results of the geometric accuracy and validation tests that have been carried out by the author using the four representative systems that have been tested.

CHAPTER 9: GEOMETRIC ACCURACY TESTS OF THE EASI/PACE SYSTEM

9.1 Introduction

In the previous chapter, a general discussion of the experimental procedures and subsequent data processing has been presented. In this chapter, a report will be given on the results of tests of parts of the photogrammetric procedures that are available in the EASI/PACE system that have been carried out with the SPOT stereo-pairs of the Badia area. The problems encountered and the solutions adopted in testing this system will be reported. The results of the extensive tests that have been carried out using the system's space resection and absolute orientation procedures to establish the geometric accuracy of the data that can be extracted from SPOT stereo-imagery using the EASI/PACE software will also be given.

9.2 Ground Control Point Measurements on the Images

For the measurement of the positions of the ground control points on each image, the **GCPWorks** software has been used. The actual measurements of the corresponding image coordinates on the two overlapping images making up each stereo-pair were made monoscopically using Version 6.0.1 of the PCI EASI/PACE system. This runs under the Windows 3.1 Operating System on an ICL/Fujitsu PC equipped with a 133 MHz Pentium processor, 32 Mbytes RAM and 6 Gbytes of hard disk.

As already mentioned, the area covered by SPOT scene 122/285 had been selected as the main test field. The first image of the stereo-pair had been collected on 19th June 1987 with an incidence angle of 23.7° pointing to the right of the nadir direction and the second image on 24th August 1987 with an incidence angle of 28.2° pointing to the left of the nadir direction. Together they produce a stereo-pair with a base-to-height ratio of 0.98. Before the measurements could be carried out, the two scenes forming the stereo-pair had first to be imported to the EASI/PACE environment.

PCI implements the Generic Database (GDB) concept, which allows PCI's Works programs and some PACE programs to access images and other external data files

without requiring specially formatted import and export files. SPOT images can be imported by different programs; one of these is **CDSPOT**, which forms part of the system's satellite DEM and orthorectification package. This program has been used to read into EASI/PACE the images from the CD on which the SPOT data was supplied. The program then automatically creates a PCIDSK file, reads all the requested imagery from CD-ROM, and saves the satellite orbital path information in one or two segments. The **CDSPOT** program also extracts the geographic coordinates and the corresponding pixel and line positions of the scene centre and its four corner points. These values are stored in the so-called orbit segment and can be used as GCPs to be input to the **SMODEL** program for an approximate orientation of the image to the ground. The file parameter is used to specify the name of the PCIDSK file that is being used to hold the imagery and the orbital information that has been read off the CD. This file is created automatically with the dimensions required to hold all of the required data. The orbital parameters receive the segment number which contains all the required orbital position and attitude data. This position and attitude information is needed first as input to the EASI/PACE program called **SMODEL** and later as input to another program called **SORTHO.** SMODEL takes into consideration all the relevant aspects of the image geometry, including the effects of terrain, platform orientation, sensor distortion, Earth curvature and cartographic projection (Cheng and Toutin 1997).

After the two images making up the stereo-pair have been imported, the **GCPWorks** program has been used for the measurements of all of the GCPs that are present on each image. In this program, through the use of the GCPWorks Setup panel (Figure 9.1), the various procedures required for loading the images and setting the other parameters have been selected. Every scene has to be selected as an uncorrected image in order to set up the desired georeferencing system. This is done by inputting all the parameters - including the zone, latitude and ellipsoid - related to the specific projection and coordinate system that is being used for the mapping of the area that has been covered by the stereo-pair and for the final cartographic output that is required by the user. In this research, the coordinate system that has been selected is UTM zone 37, latitude 32° - 40° north based on the European Datum of 1950 (ED 50).

When the first image is selected for the measurements of the GCPs, then two windows are opened - the first for the display of the whole image, while the second is a small window that displays the actual control point location at full resolution with an enlargement of up to 128. All the data related to the GCPs is entered through the keyboard in the particular location in the panel which is used to create, load, save and edit GCPs. This panel is launched by selecting the "**collect GCPs**" step on the main **GCPWorks** control panel. The panel contains several sub-areas. In the GCP editing area, it gives the various options - accept; accept as check point; or delete - that are available. The use of the "**accept**" button will move the GCP down into the GCP list; use of the "**delete**" button will remove the point; while using the "**accept as check point button**" will move the point into the accepted check point list.

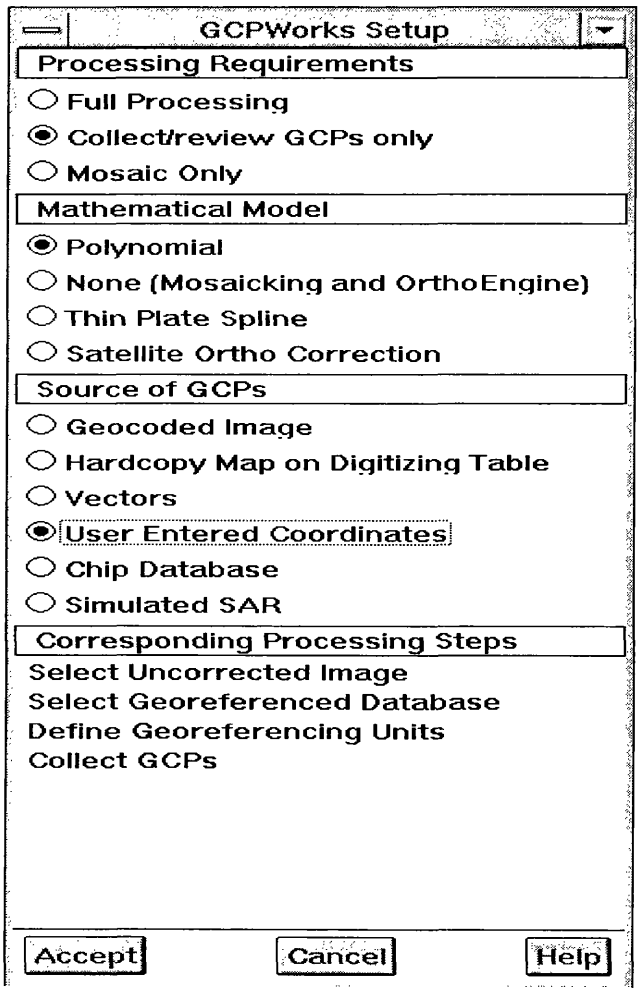

Figure 9.1 GCPWorks Setup panel

Use of the "**save**" button saves the ground control point data as a segment connected with the image file or it can save it separately as a text file. After saving the GCPs as a

segment attached to the file, the user can then check the saved segment by loading the GCPs through selection of the "**load GCPs**" item in the menu of the GCP collection panel.

9.3 Space Resection

After the image coordinates of the GCPs have been measured and collected, the photogrammetric procedures can then be applied to the SPOT satellite images. Forming part of the EASI/PACE satellite orthorectification and DEM extraction package, the **SMODEL** software is used first to carry out the space resection procedure to determine the elements of exterior orientation based on the measured image positions of the known ground control points (GCPs). The model for this operation is generated from the knowledge of the satellite orbit and attitude data derived from the SPOT header file, and the given terrain coordinates of the ground control points. The information that has to be input before running the **SMODEL** program (Figure 9.2) is as follows:

- database file name;
- database ground control segments containing the coordinates of the GCPs;
- the number of the segment containing the orbital data giving the positions and attitude values of the satellite and its sensor;
- the specific segment in the database in which the calculated values will be stored.
- the ellipsoid on which the ground control points have been computed needs to be specified;
- the units in which the results will be given also need to be specified; and
- whether the user wants to modify the GCPs interactively.

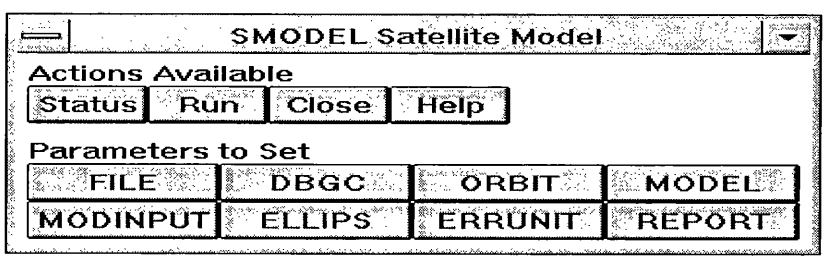

Figure 9.2 SMODEL program parameters

9.3.1 Results of Initial Processing Using SMODEL

In this processing step, each SPOT image is fitted individually to the ground control points via a form of space resection based on the available GCPs. Once the results have been declared, the user is then able to examine and modify the GCPs. When the processing of the image data was undertaken using **SMODEL**, the report showed very large residual errors in planimetry, with an RMSE value of over ± 46.7m for the control points and around ± 90m for the check points. The measurement of the ground control points was repeated several times, but the system reports still showed very large residual errors. Besides the main test model (122/285), it proved to be quite impossible to form any of the other test stereo-models and fit them to the ground control points. To be quite sure about the results, the right image of the main test pair 122/285 was rectified and resampled to epipolar geometry using the **SEPIPRO** program and an epipolar file was created and input to the next module (**SDEM**) for DEM extraction. After the DEM extraction module had performed the processing, it was no surprise to see that (a) a very high RMSE value of ±138.5m for the residual errors in height occurred at the control points, and (b) no DEM had been formed.

9.3.2 Investigation into the Source of Errors

An investigation was made to discover the source of these difficulties concerning the formation of a stereo model in EASI/PACE. The main possibilities were identified as follows:

(i) The GCPs - could there be errors in their coordinate values or were there errors in their identification, either in the field or during their measurement in the system?

(ii) The image data - could it have been badly processed by the suppliers or could it have been corrupted in some way?

(iii) The system - could it contain errors, e.g in the modelling or in the software itself?

(i) The first of these possibilities was quickly eliminated. The main test model 122/285 was tested in the ERDAS OrthoMAX system running on a SUN SparcStation 20 at the

Macaulay Institute for Land Use Research (MLURI) in Aberdeen. This resulted in a good fit of the stereo-model to the GCPs and in the generation of a DEM and an ortho-image. This showed that the GCP coordinate values and the identification and measurements of the GCPs both in the field and in the image processing system had been correctly determined.

(ii) Next came the matter of SPOT image data. The Level 1B images were returned to the supplier, SPOT Image in Toulouse, who pronounced that the images had been correctly processed. However, it then came to light that SPOT Image had changed its processing procedures for the production of Level 1B images in August/September 1995 i.e. at the time of purchase of the images. In particular, a 5th order polynomial had been utilized for the processing instead of the 3rd order polynomial used previously. As will be seen later, this meant that EASI/PACE could not cope either with the three stereo-pairs of the Badia area processed in the old format or with the two processed in the new format.

(iii) To be certain that the processing carried by the author had followed the correct procedure, arrangements were made to repeat the test of the main test stereo-model in the PCI European office in Manchester under the supervision of Richard Selby of PCI. The results achieved with the processing were the same as those carried out by the author at the University of Glasgow. So the images and the GCPs were then sent to PCI in Canada to be processed there. The same results have been obtained there as in the previous tests carried out in Glasgow and Manchester.

Following on from this, faxes were then sent by the PCI company and by Dr. Thierry Toutin of CCRS to Professor Petrie explaining further the problem of handling SPOT Level 1B data. PCI assured us that they tested their program with SPOT Level 1A and 1B data from North American sources and that the accuracy of the results that they had obtained data was about 1/3 of a pixel using Level 1A data and 2/3 of a pixel for Level 1B data. Thus they could not understand why it worked for their Level 1B data and not for the Badia test data. The processing of their Level 1B data had involved the use of a cubic (i.e. 3rd order) polynomial transformation to transform the data back to its Level 1A form, plus a shift due to Earth rotation. According to PCI, the only practical way to

support the 1B data is to convert the data back to its 1A form via a reverse transformation. To carry out this conversion, the transformation coefficients that had been used in the initial conversion from Level 1A to 1B should be made available from SPOT Image.

A further explanation was also forthcoming from the system supplier - to the effect that two different procedures are used to produce Level 1B data. PCI informed us that, in the USA, the Level 1B data is produced direct from Level 0 (raw) data utilizing a parametric solution. Whereas, with the SPOT Image facility in France, a two-stage process is employed with the Level 0 data being converted first to the Level 1A form. This is then converted to Level 1B form utilizing the polynomial transformation mentioned above. After a further investigation of this matter, again as a result of asking PCI for more explanation, it was found that this information was not correct. In fact, in SPOT Image's USA facilities, the same procedure and format is used as that employed in France by SPOT Image, whereas PCI thought that they were using a different format. From the above account, it became obvious that the EASI/PACE software simply did not work with SPOT Level 1B stereo-imagery whatever the processing or format that was being used and solutions had to be found to this major problem revealed by the author's tests over the Badia test field.

9.3.3 Solutions to the Level 1B Processing Problem

Various solutions have been developed independently both at the University of Glasgow and by PCI in Toronto to solve the problems revealed by the tests. In both cases, the procedure has been to convert the Level 1B image back to its Level 1A form.

9.3.3.1 University of Glasgow Solution

While PCI was looking for a solution to this problem, a solution was developed at the University of Glasgow by my research colleague Dr. Valadan Zoej, who, in the course of his research project, had already developed quite independently an analytical photogrammetric solution for use with SPOT stereo-pairs. This is based on his own orbital parameter model and algorithm which is designed to use Level 1A images and to

fit the resulting SPOT stereo-model to the GCPs without producing a DEM or ortho-image. He had also adopted the procedure of converting the Level 1B images back to their Level 1A form. However, since he had no access to the transformation parameters used by SPOT Image to convert the Level 1A image to its Level 1B form, he had to devise his own empirical solution (Valadan Zoej 1997). He did this purely geometrically via a two-step procedure by first transforming the rhomboidal shape of the Level 1B image back to a rectangular image. The resulting image still had too large a size compared with the square shape and dimensions of the equivalent Level 1A image, so a second transformation was then applied to achieve this result (Valadan Zoej and Petrie 1998). Additional corrections were then applied within the bundle adjustment program to ensure that a correct modelling of the attitude parameters was achieved to give a good absolute orientation of the stereo-model and to ensure its fit to the GCPs. The modified bundle adjustment program which implements this solution has been written in the C++ programming language and runs on a 486-based PC.

The image coordinates of all the GCPs present in the five Level 1B stereo-pairs covering the Badia project area were then measured on EASI/PACE by the present author and submitted to Dr. Valadan Zoej to be tested using his program. The residual errors in X,Y,Z at the GCPs for each of the models after absolute orientation are given in Table 9.1 as RMSE values.

Scene No	B/H ratio	No of GCPs	ΔX (m)	ΔY (m)	ΔZ (m)
122/285	0.975	15	±5.0	±5.1	±6.4
123/285	0.858	18	±6.2	±5.7	±8.3
123/286	0.858	20	±6.4	±7.4	±8.1
124/285	0.975	13	±8.0	±8.6	±13.2
124/286	0.975	13	±4.8	±9.0	±3.3

Table 9.1 RMSE Values for the Residual Errors at the GCPs for the Five SPOT Level 1B Stereo-Pairs Covering the Badia Project Area

For the main test stereo-model, 122/285, a further 23 GCPs distributed over the area of the model were measured by the author to be used as independent check points. The RMSE values at these check points in terms of the residual errors in their X, Y and Z coordinates are as follows: $\Delta X = \pm 8.9$m; $\Delta Y = \pm 8.2$m; $\Delta Z = \pm 10.0$m. Vector plots

showed that these errors were random both in extent and direction. This confirmed that the solution devised and developed by Dr. Valadan Zoej was a practical way of overcoming the problems encountered in the processing of the Level 1B imagery of the Badia area using EASI/PACE. It should be said too that this successful test was a great relief to the author and his supervisor and proved the value of having the excellent data of the Badia test field available for experimental work of this kind.

Another aid to devising a solution to the problems experienced with EASI/PACE was provided by the Department of Geography and Topographic Science which purchased a single Level 1A stereo-pair of SPOT images covering the main test area 122/285 to be tested in the systems. When this was tested, good results have also been obtained both with EASI/PACE and with Dr. Valadan Zoej's program. Furthermore a quite straightforward processing could be performed for DEM extraction from the Level 1A stereo-pair using EASI/PACE.

9.3.3.2 PCI Solution

In parallel with the solution developed in Glasgow, a fairly rapid response was received from PCI to solve the problem. As was done in Glasgow, the company acquired the corresponding Level 1A images of the main test model and tested its EASI/PACE software on this model with excellent results. These are shown in Table 9.2, together with the results achieved by PCI with the processing of the corresponding Level 1B stereo-pair. This again highlighted the problems experienced with the processing of the Level 1B stereo-pairs.

SPOT Format	No. of GCPs	ΔX (m)	ΔY (m)	ΔPl (m)	ΔZ (m)
Level 1A	37	±8.3	±5.6	±10.0	±6.4
Level 1B	13	±44.6	±13.9	±46.7	±138.5

Table 9.2 RMSE Values Obtained at the GCPs for Stereo-Pair 122/285

In the meantime, PCI tried to obtain the transformation coefficients from SPOT Image, to solve the problems experienced with the Level 1B stereo-pairs. In particular, with the older Level 1B format, the values were stored in a binary format and could not be read

at all. For this reason, the transformation coefficients had to be provided by SPOT Image in a format that could be read by the EASI/PACE software. After a big effort on the part of its senior staff, PCI obtained the transformation coefficients from SPOT Image in a form that could be read. They then started to fix the problems occurring in EASI/PACE with Level 1B stereo-imagery.

After PCI had modified their system, the first results obtained for the main test area showed much lower residual error values than before, both in planimetry and in height. The substantial modifications that had to be made to the system affected most of satellite ortho and DEM extraction modules. Once this work had been done, then all the modified modules were sent back to Glasgow using the Internet and were loaded into the author's PC. The first three stereo-models 122/285; 124/285 and 124/286 were tested by the author without any difficulties and the corresponding DEMs were extracted from each with very good results. However, when the work started to process the other two stereo-pairs - 123/285 and 123/286 - for the extraction of the DEMs, to everyone's surprise, it was found that the results were still poor and that full DEMs could not be formed. After a further investigation, PCI announced that there were still problems in the software. On investigating these problems, this was when it was found that the five stereo-pairs were not in the same format. The three stereo-pairs that produced DEMs were in the old format using the third-order polynomial, while the other two stereo-pairs that failed to produce DEMs were in the new format using the fifth-order polynomial. So another set of modifications to all the satellite ortho and DEM modules had to be implemented by PCI. As a result of these further modifications made to overcome this difficulty, all of the new modules had to be imported again over the Internet and the two stereo-models with poor results re-processed. The tests of these two stereo-pairs showed good results both in planimetry and height.

To further confirm that the good results that had been obtained - as represented by the very small residual errors in planimetry and height - were indeed correct, all the individual residual errors in planimetry and height have been represented graphically on vector plots. The results of these vector plots in planimetry showed that the errors occurring at the individual control and check points were random both in direction and in amount which confirmed that the new version of the system worked well until this

stage (i.e. space resection and orientation) has been completed. However, only after DEM extraction has been carried out using the image matching procedure, were the values of the elevations obtained for each GCP. So, only then, was it possible to compare these values obtained via the DEM extraction process with the given elevation values for each GCP obtained by the GPS survey. This is when various systematic error patterns started to appear.

The vector plot for stereo-model 122/285 given in Figure 9.3 shows clearly a systematic pattern for the residual errors in height. Inspection of the vector plot for this stereo-pair shows the highly systematic distribution of the individual residual errors occuring at both the control points and the independent check points. By far the majority of points (over 30) have elevation errors in the same (upward) direction. Only a cluster of four or five points located in the lower right corner have errors in the opposite (downward) direction - which, in itself, is also a significantly systematic pattern.

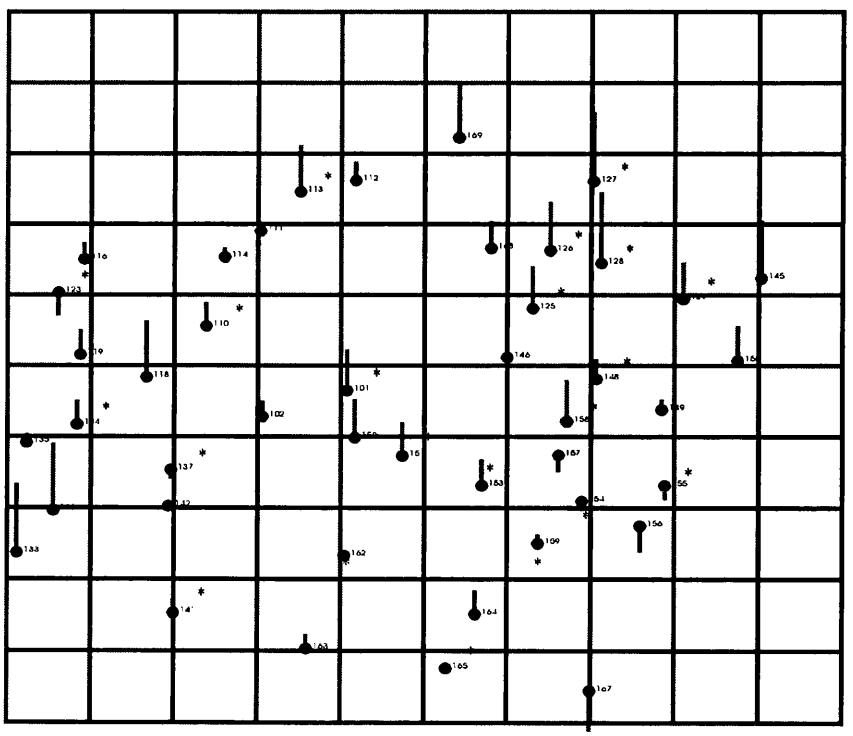

Figure 9.3 Vector plot of the residual errors in height at the control and check points of the Level 1B stereo-pair for scene 122/285
Control points o Check points o*

Another matter that came to light during the intial tests with EASI/PACE was concerned with the lack of provision for stereo-measurements - all the measurements being made monoscopically. Even more serious was the fact that no absolute orientation procedure

had been provided and therefore no declaration of the height values and their fit to the GCPs was made prior to the image matching procedure being carried out. According to Dr. Toutin (Petrie and Toutin, personal communication), facilities for stereo-measurements and a subsequent absolute orientation were both provided on the original version of the software that he had developed at CCRS, but these had not been ported over and implemented by PCI in the EASI/PACE package.

PCI was informed by Professor Petrie about the need for an absolute orientation program. After one month, Dr. Cheng at PCI sent a new program to be added to EASI/PACE which allows the computation of an absolute orientation after the individual analytical space resections of the two SPOT images making up the stereo-pair have been completed using the **SMODEL** routine of EASI/PACE. This absolute orientation routine uses the monoscopically measured image coordinates and the values of the exterior orientation parameters computed from the individual space resections to compute the ground coordinate values of the GCPs. These computed values of the GCPs are then compared with the coordinate values obtained from the GPS-based ground survey to give the residual errors in ΔX, ΔY and ΔZ at each control point or check point. From these, the RMSE values of the residual errors have been calculated. When this new absolute orientation program was tested, the vector plots showed a random distribution of the errors both in planimetry and in heights.

Furthermore, the direct communication between the author and Dr. Cheng using both fax and the Internet allowed further extensive tests of geometric accuracy to be carried out by the author using these programs and gave Dr. Cheng the possibility to modify these programs continuously in a very fast way. Indeed some programs were modified to run faster as the results of the author's tests. In this respect, the following programs have been modified:- **CDSPOT, SMODEL, SEPIPRO, SDEM, SORTHO, SDEMCPY, SDEMMAN, CONTOUR, MSPOT, V6V5VEC,** etc. New programs that have been added to the satellite DEM and orthorectification module as a result of author's experiences are: **SATXYZ** (modified absolute orientation program), **PROFILE** and **VATT** (image exploration). So the consequences of all these problems which have been encountered by the author during his experiemental work were not all negative. The positive side was that it gave the author a lot of insight into the algorithms

used within EASI/PACE and a great deal of practical experience which can be used to overcome the difficulties that he may encounter in the future. The work also showed immediately the value of having a test field with high-quality ground control points that can be used to calibrate a complex piece of software such as the EASI/PACE system.

9.4 Space Resection Accuracy Tests

The detailed results of the space resection and analytical rectification of the individual component images of each of the SPOT Level 1A and Level 1B stereo-pairs of the reference scene 122/285 carried out by the author are shown in Table 9.3. Due to the fact that many more GCPs were available in this stereo-model, several tests were carried out by dividing these ground control points into two groups in different combinations. The first group acted purely as control points for the space resection and analytical rectification, while the second group acted purely as independent check points whose coordinates were not used in the analytical solution to determine the parameters. Both Level 1A and 1B stereo-pairs were tested in this way.

A comparison was made for both the control points and the check points between the given GCP coordinate values determined by the ground survey using differential GPS and the corresponding values derived from the analytical space resection. Inspection of the RMSE values for the residual errors at the check points given in Table 8.3 shows that, for the Level 1B stereo-pair of the reference scene 122/285, as few as five control points can be used to produce a viable solution - albeit with much higher residual errors ocurring at the independent check points. Obviously the best result was achieved at the independent check points when more control points have been used in the solution.

For the Level 1A stereo-pair of the scene 122/285, the best results have been achieved with 12 control points used in the solution and with 36 independent check points. In general, as one would expect, the errors increase with a decrease in the number of control points and an increased number of check points. One notes too that the planimetric accuracy obtained in the space resections of the Level 1A images is slightly better than the accuracy obtained by the space resections carried out on the Level 1B images.

Level	Image	No. of Control Points	Control Points			No. of Check Points	Check Points		
			ΔE (m)	*ΔN* (m)	*ΔPl* (m)		*ΔE* (m)	*ΔN* (m)	*ΔPl* (m)
SPOT 122/285 Level 1A	Left	43	±7.4	±6.4	±9.7	5	±6.4	±5.3	±8.2
	Right		±4.5	±4.3	±6.3		±5.8	±6.8	±9.0
	Left	33	±7.5	±6.4	±9.9	15	±6.6	±6.4	±9.2
	Right		±45	±4.1	±6.1		±5.4	±5.7	±7.8
	Left	23	±4.1	±4.9	±6.4	25	±6.0	±4.7	±7.6
	Right		±4.2	±3.8	±5.7		±5.5	±5.7	±7.9
	Left	12	±4.2	±4.4	±6.0	36	±5.8	±5.2	±7.8
	Right		±4.4	±3.8	±5.8		±5.2	±5.1	±7.2
	Left	5	±5.4	±5.4	±7.6	43	±7.5	±9.6	±12.1
	Right		±6.3	±6.2	±8.8		±10.0	±10.2	±14.5
	Left	48	±5.0	±4.5	±6.7	-	-	-	-
	Right		±4.6	±4.5	±6.4				
SPOT 122/285 Level 1B	Left	43	±5.0	±5.5	±7.4	5	±5.4	±4.9	±7.3
	Right		±5.2	±5.8	±7.8		±5.2	±5.3	±7.5
	Left	33	±4.1	±5.6	±7.0	15	±7.8	±5.4	±9.5
	Right		±4.8	±6.0	±7.7		±7.1	±5.5	±9.0
	Left	23	±4.3	±5.2	±6.8	25	±6.0	±6.1	±8.6
	Right		±5.3	±5.7	±7.8		±5.8	±6.2	±8.5
	Left	13	±3.1	±4.8	±5.7	35	±6.2	±6.1	±8.6
	Right		±3.8	±6.1	±7.2		±6.6	±6.5	±9.3
	Left	5	±5.4	±4.5	±7.0	43	±10.8	±10.8	±15.3
	Right		±3.6	±7.2	±8.0		±9.7	±13.5	±16.7
	Left	48	±4.9	±5.4	±7.3	-	-	-	-
	Right		±5.1	±5.7	±7.7				

Table 9.3 RMSE values for the residual errors in planimetry at the control points and check points during space resection of the stereo-pairs for the reference scene 122/285 over the Badia Test Field.

For the other stereo-pairs covering the Badia test area, the results of the analytical rectification of the individual component images of each of the SPOT Level 1B stereo-pairs in terms of their fit to the whole set of ground control points available for each model and the resulting values of the residual errors in *ΔE* and *ΔN* are set out in Table 9.4. As can seen from this Table, the results for the five SPOT stereo-pairs show a fairly consistent pattern, with an average RMSE value of around ± 4.7m in easting and ±5.8m in northing giving a RMSE value for planimetry (ΔPl) of ± 7.5m - which is well below the single ground pixel value of 10m. The results for the single Level 1A stereo-pair covering Scene 122/285 are only slightly better with an RMSE value for the planimetric accuracy (ΔPl) in the left image of ± 6.7m and ± 6.4m in the right image.

Scene No.	No. of GCPs	Left Image			Right Image		
		ΔE (m)	*ΔN (m)*	*ΔPl (m)*	*ΔE (m)*	*ΔN (m)*	*ΔPl (m)*
122/285 Level 1A	**48**	**±5.0**	**±4.5**	**±6.7**	**±4.6**	**±4.5**	**±6.4**
122/285 Level 1B	**48**	**±4.9**	**±5.4**	**±7.3**	**±5.1**	**±5.7**	**±7.7**
123/285 Level 1B	**23**	**±4.4**	**±4.4**	**±6.2**	**±4.1**	**±5.3**	**±67**
123/286 Level 1B	**29**	**±5.6**	**±5.6**	**±7.9**	**±4.1**	**±5.0**	**±6.5**
124/285 Level 1B	**19**	**±4.3**	**±5.0**	**±6.6**	**±4.9**	**±5.4**	**±7.2**
124/286 Level 1B	**13**	**±4.6**	**±4.6**	**±6.5**	**±4.9**	**±4.8**	**±6.9**

Table 9.4 RMSE Values for the residual errors at the GCPs after space resection for the five SPOT Level 1B stereo-pairs covering the Badia area and the one Level 1A stereo-pair of the reference model

As can be seen in Table 9.5, when using combinations of control points and independent check points, for the other three stereo-pairs - 123/285, 123/286, and 124/285 - where sufficient control points are available, the results from these three stereo-pairs again show an accuracy that is substantially less than one pixel size. These results reflect the fit of each individual stereo-model to the GCPs.

Level of SPOT Images	Image	No. of Control Points	Control Points			No. of Check Points	Check Points		
			ΔE	*ΔN*	*ΔPl*		*ΔE*	*ΔN*	*ΔPl*
123/285 1B	**Left**	**13**	**±4.7**	**±3.8**	**±6.0**	**10**	**±4.7**	**±5.3**	**±7.1**
	Right		**±3.9**	**±6.2**	**±7.3**		**±5.1**	**±4.1**	**±6.6**
123/286 1B	**Left**	**14**	**±5.1**	**±3,9**	**±6.4**	**15**	**±6.3**	**±7.9**	**±10.1**
	Right		**±3.8**	**±3.8**	**±5.4**		**±4.3**	**±6.3**	**±7.6**
124/285 1B	**Left**	**11**	**±4.7**	**±5.8**	**±7.5**	**8**	**±4.3**	**±4.7**	**±6.4**
	Right		**±3.4**	**±5.9**	**±6.8**		**±6.9**	**±5.7**	**±9.0**

Table 9.5 RMSE values of residual errors in planimetry at the control points and check points after space resection for three of the stereo-pairs of SPOT images covering the Badia Test Field

9.5 Absolute Orientation Accuracy Tests

As noted above, the photogrammetric approach used in the EASI/PACE utilizes the monoscopically measured image coordinates of the GCPs and determines the parameters of the exterior orientation via an analytical space resection of each of the individual images making up the stereo-pair. In the following tests using absolute orientation, space intersection has been carried out using the **SATXYZ** routine that was developed by PCI as a result of the author's experimental work. All five Level 1B stereo-pairs covering the Badia area have been processed, in addition to the Level 1A stereo-pair of the reference test scene 122/285.

9.5.1 Accuracy Tests of the Level 1A and 1B Stereo-pairs of the Badia Test Area using Absolute Orientation and All the Available Ground Control Points

Starting with the five Level 1B stereo-pairs for the reference stereo-pair, 122/285, 48 of the available ground control points have been used; all of these points are well identified on the images. The root mean square error (RMSE) values for the residual errors at the GCPs after the absolute orientation were $\Delta Pl = \pm 6.8m$, and $\Delta H = \pm 4.7m$. For the stereo-pair 123/285, 23 ground control points have been used. The RMSE values of the residual errors were $\Delta Pl = \pm 5.7m$, and $\Delta H = \pm 5.8m$. In the case of the stereo-pair 123/286, 29 ground control points were used; the RMSE values of the residual errors were $\Delta Pl = \pm 7.1$ m, and $\Delta H = \pm 4.2m$. For the stereo-pair 124/285, only 19 ground control points have been used; the accuracy obtained in terms of the RMSE values of the residual errors was $\Delta Pl = \pm 6.5$ m, and $\Delta H = \pm 5.4m$. For the stereo-pair 124/286, only 13 ground control points were available, and the accuracy of the results obtained in terms of the RMSE values of the the residual errors was $\Delta Pl = \pm 6.1m$, and $\Delta H = \pm 5.8m$.

Coming finally to the Level 1A stereo-pair for scene 122/285, 47 ground control points were used, and the RMSE values of residual errors obtained were $\Delta Pl = \pm 5.9$ m and $\Delta H = \pm 4.8m$. Table 9.6 summarizes all the results obtained in planimetry and height after absolute orientation for all the stereomodels covering the Badia area and using all the GCPs available for each stereo-model. It will be seen from Table 9.6 that the RMSE values in planimetry of the various stereo-pairs lie in the range $\Delta Pl = \pm 5.7m$ to $\pm 7.1m$, and $\Delta H = \pm 4.2m$ to $\pm 5.8m$ in elevation when all the available GCPs were used for the absolute orientation.

Badia Area Covered by SPOT		Absolute Orientation [All Points]				
Scene No.	B/H ratio	No. of GCPs	Δ E (m)	Δ N (m)	Δ Pl (m)	Δ H (m)
122-285 Level 1B	0.975	48	± 4.7	± 4.9	± 6.8	± 4.7
123-285	0.858	23	± 3.5	± 4.5	± 5.7	± 5.8
123-286	0.858	29	± 4.5	± 5.5	± 7.1	± 4.2
124-285	0.975	19	± 4.1	± 5.0	± 6.5	± 5.4
124-286	0.975	13	± 3.6	± 4.9	± 6.1	± 5.8
122-285 Level 1A	0.975	47	± 4.2	± 4.2	± 5.9	± 4.8

Table 9.6 RMSE values for the residual errors at the GCPs after absolute orientation for the five SPOT Level 1B stereo-pairs covering the Badia Project Area and the one Level 1A stereo-pair.

9.5.2 Accuracy Tests of the Level 1B Stereo-Pair for the Reference Scene 122/285 Using Combinations of Control Points and Check Points

A further detailed set of results for geometric accuracy have been generated for the Level 1B stereo-pair of the main reference model where the largest number of GCPs were available. For these tests, the GCPs were again divided into two groups - control points (used for absolute orientation) and independent check points (used for accuracy checking). The results are summarized in Table 9.7. With 43 control points used in the solution and 5 independent check points, the RMSE values for the residual errors in planimetry and height at the check points were ± 6.7m and ± 6.4m respectively. Increasing the number of independent check points to 15 and using the rest of the GCPs as control points in the solution, the RMSE values of the residual errors at the check points were ± 8.9m in planimetry, and ± 5.3m in height. By increasing the number of check points to 25, the RMSE values of the residual errors at these check points were ± 8.0m in planimetry, and ± 5.8m in height. With 35 check points, the RMSE values of the residual errors at the check points were ±8.4 m in planimetry and ±5.7m in height.

Inspection of the RMSE values for the residual errors at the check points for planimetry and height given in Table 9.7 and shown graphically in Figure 9.4 indicates that the RMSE values of the residual errors lie in the range ± 6.7m to ± 8.7m in planimetry and ± 5.3m to ± 6.4m in height using different combinations of control points and check points - which indicates that the accuracy decreases with a decrease in the number of control points.

	Control Points (m)					Check Points (m)				
Scene No	**No.**	**Δ E**	**Δ N**	**Δ Pl**	**Δ H**	**No.**	**Δ E**	**Δ N**	**Δ Pl**	**Δ H**
122-285 1B	43	± 4.8	± 5.4	± 7.2	± 4.7	5	± 4.9	± 4.6	± 6.7	± 6.4
	33	±4.2	±5.6	±7.0	±4.8	15	±7.3	±5.1	±8.9	±5.3
	23	±4.8	±5.0	±6.9	±4.5	25	±5.3	±6.1	±8.0	±5.8
	13	±3.3	±4.6	±5.7	±3.5	35	±6.0	±5.9	±8.4	±5.7

Table 9.7 RMSE values for the residual errors at the control points and the check points of the Level 1B stereo-pair for scene 122/285

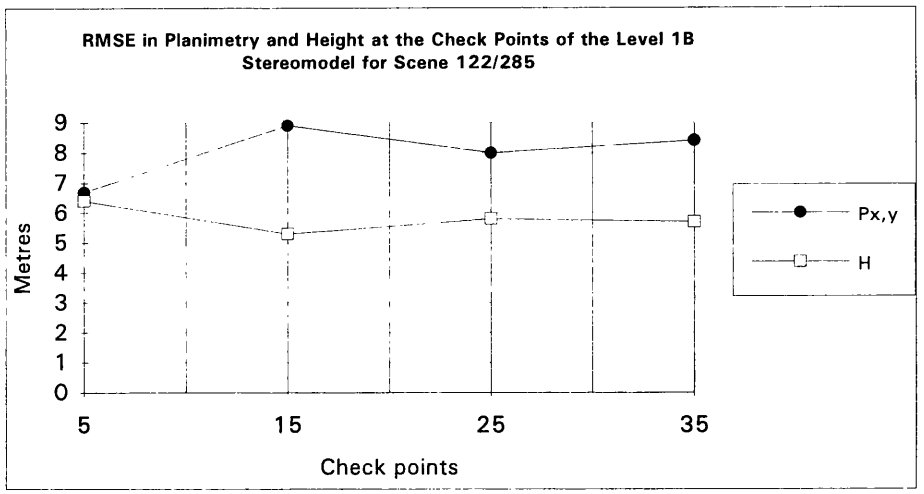

Figure 9.4 Graphical representation of the accuracy of planimetry and height at the check points in the Level 1B stereo-model for the reference scene 122/285

9.5.3 Accuracy Tests of the Other Level 1B Stereo-Models for Scenes 123/285, 123/286 and 124/285

For the stereo-model 123/285, the number of available control points was such that a number could be used as independent check points. The available 23 ground control points were divided into two groups, 13 being used as control points in the solution, while 10 points were kept back for use as independent check points. The RMSE values of the residual errors at the check points were ± 6.9m in planimetry and ± 5.1m in height - see Table 9.8.

For the stereo-model 123/286 - which has quite a big area of overlap with the main reference stereo-pair 122/283 - 29 ground control points were available which meant that some points could be used as independent check points. From these points, 14 control points were used in the solution, while the other 15 points were used as independent check points. The RMSE values of the residual errors obtained at the check points were ± 8.9m in planimetry and ± 6.2m in height - again see Table 9.8.

In case of the stereo-model 124/285, only 19 ground control points are well identified on the images. Of these, 11 control points were used in the solution and the 8 other points were used as independent check points. The RMSE values of the residual errors at the check points were ± 7.2m in planimetry and ±5.2 m in height - see Table 9.8.

	Control Points (m)					Check Points (m)				
Scene No.	**No.**	**Δ E**	**Δ N**	**Δ Pl**	**Δ H**	**No.**	**Δ E**	**Δ N**	**Δ Pl**	**Δ H**
123-285 1B	13	±3.5	±3.8	±5.2	±6.7	10	±4.2	±5.5	±6.9	±5.1
123-286 1B	14	±4.2	±3.9	±5.7	±3.3	15	±4.6	±7.6	±8.9	±6.2
124/285 1B	11	±3.3	±5.9	±6.8	±5.8	8	±5.5	±4.6	±7.2	±5.2

Table 9.8 RMSE values of the residual errors at the control points and the check points of the Level 1B stereo-pairs for scenes 123/285, 123/286 and 124/285

9.5.4 Accuracy Test of the Level 1A Stereo-Pair of the Reference Scene 122/285

Similar tests have been carried out for the main test area using the Level 1A stereo-pair - see the results given in Table 8.9. In the first test with 42 control points used in the solution and using 5 independent check points, the RMSE values of the residual errors at the check points were ± 8.0m in planimetry and ± 5.5m in height. By decreasing the number of control points to 32 and increasing the number of the check points to 15, the RMSE values at the check points became ± 7.9m in planimetry and ± 6.6m in height by which the error values slightly dropped down slightly in planimetry and slightly increased in height. With 22 control points and 25 check points, the RMSE values at the check points were ± 6.7m and ± 6.4m in planimetry and height respectively; this amounted to a slight improvement in accuracy for planimetry and for the heights. With 35 check points, the RMSE value in planimetry was ±6.9m (a slight increase) with ±6.1m in height, again showing a slight decrease. Figure 9.5 shows in graphical form the RMSE values in planimetry and height at the check points.

	Control Points (m)					Check Points (m)				
Scene No.	**No.**	**Δ E**	**Δ N**	**Δ Pl**	**Δ H**	**No.**	**Δ E**	**Δ N**	**Δ Pl**	**Δ H**
122-285 1A	42	±5.1	±6.3	±8.1	±6.1	5	±6.1	±5.3	±8.0	±5.5
	32	±5.2	±6.4	±8.2	±6.0	15	±5.2	±5.9	±7.9	±6.6
	22	±3.8	±4.8	±6.1	±4.1	25	±4.9	±4.6	±6.7	±6.4
	12	±3.9	±4.1	±5.7	±4.6	35	±4.6	±5.1	±6.9	±6.1

Table 9.9 RMSE values of the residual errors at the control points and the check points of the Level 1A stereo-pair for scene 122/285

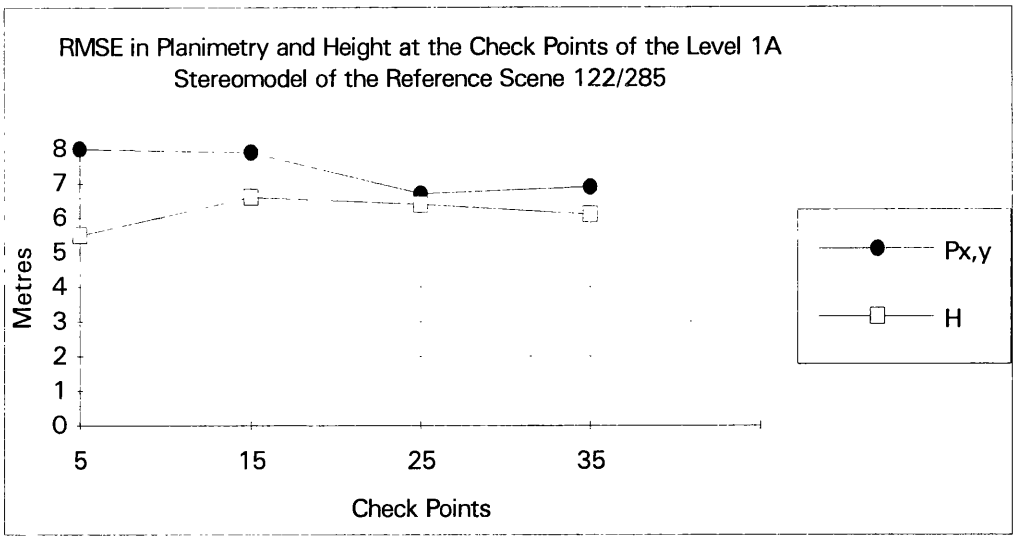

Figure 9.5 Graphical representation of the accuracy in planimetry and height at the check points of the Level 1A stereo-model of the reference scene 122/285

9.5.5 Vector Plots of the Error Values at the Control and Check Points for Model 122/285

Besides the overall RMSE values derived from all the values of the residual errors as a whole, vector plots can be generated to show the extent and the direction of the residual errors at each individual control and check point. These allow the detection of any outliers or gross errors that may be present at individual points. Also they allow the analyst to see if there is any pattern of systematic error present in the stereo-model. Figures 9.6 and 9.7 show the vector plots in planimetry for both the Level 1A and 1B stereo-pairs for the reference scene 122/285. The pattern of errors is random both in extent and direction. This confirms that the final solution adopted in the EASI/PACE system as a result of the author's investigations is correct.

For the residual errors in height of the control and check points, it is clear from Figures 9.8 and 9.9 that the distribution of the errors is random, except in the north-eastern part of the area where a group of four to five points show a systematic error.

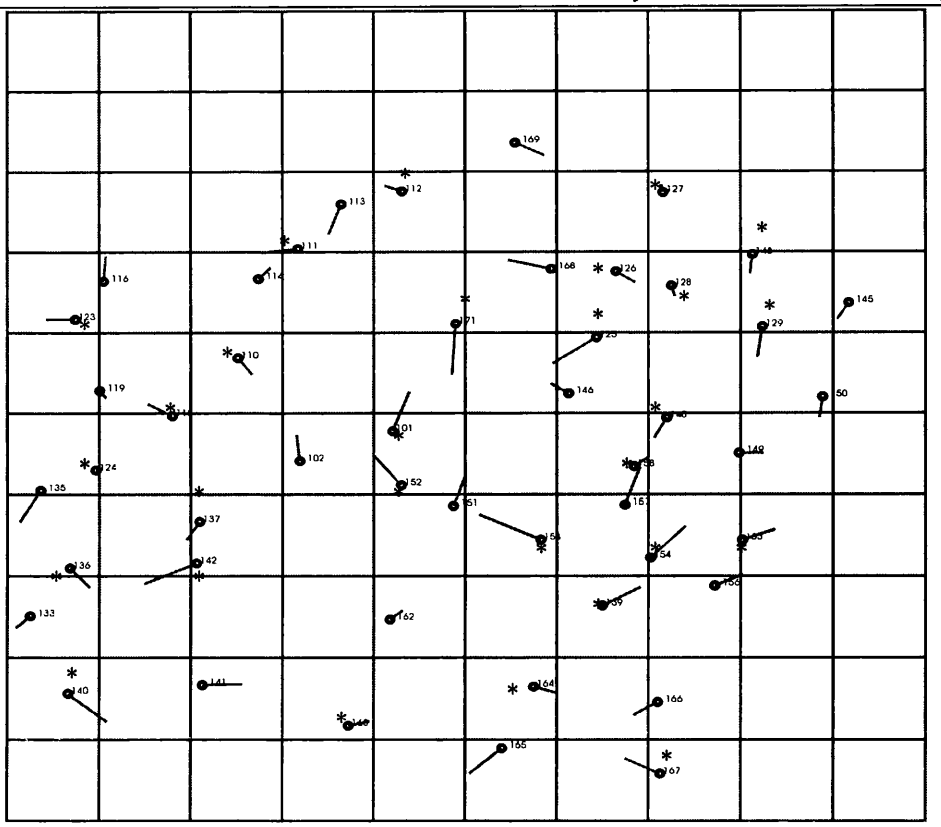

Figure 9.6 Vector plot of the values of the residual errors in planimetry obtained at the control points and check points over the Badia test field for the Level 1B stereo-pair for scene 122/285 Control points o Check points o *

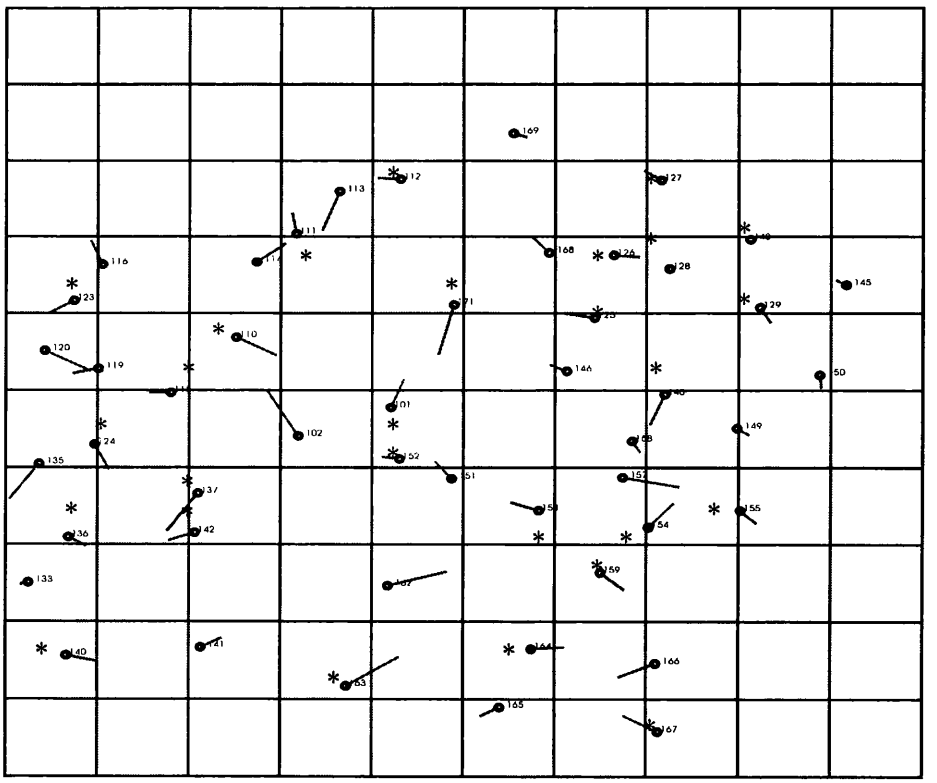

Figure 9.7 Vector plot of the values of the residual errors in planimetry obtained at the control points and check points over the Badia test field for the Level 1A stereo-pair for scene 122/285 Control points o Check points o *

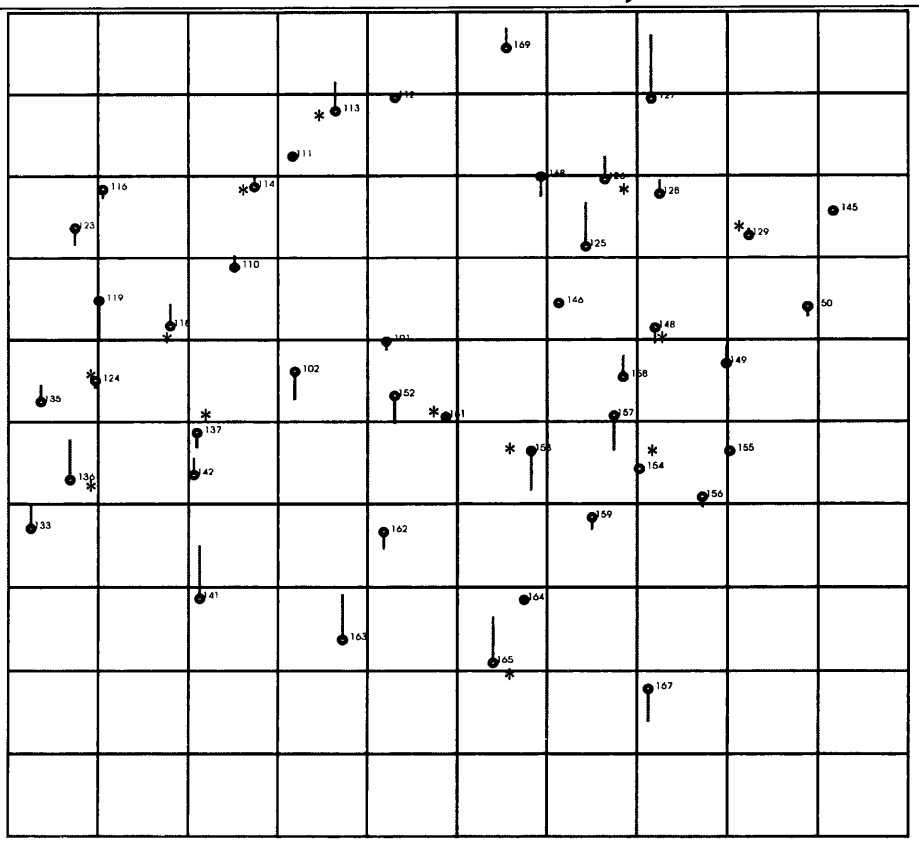

Figure 9.8 Vector plot of the residual errors in height at the control and check points of the Level 1B stereo-pair of scene 122/285 after absolute orientation
Control points o Check points o *

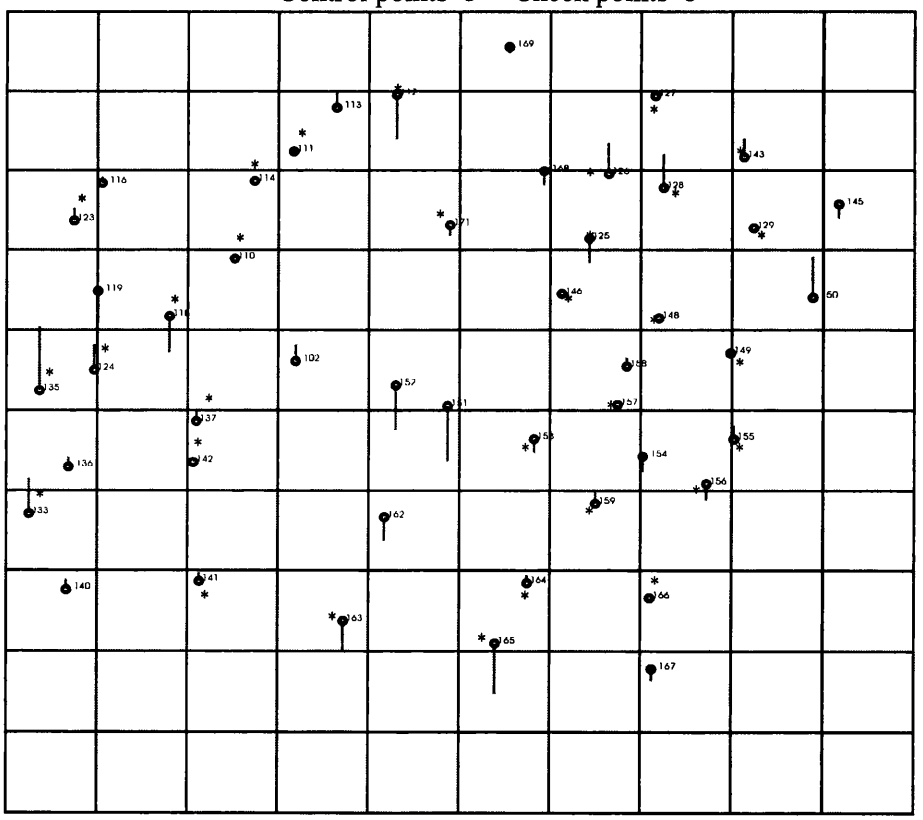

Figure 9.9 Vector plot of the residual errors in height at the control and check points of the Level 1A stereo-pair of scene 122/285 after absolute orientation
Control points o check points o *

9.6 Conclusion

In this chapter, the various problems which have been produced by the EASI/PACE system when carrying out extensive tests of the orientation and formation of the SPOT Level 1B stereo-models have been presented. From the account given in this chapter, it will have been seen that, when the experimental work began, the system simply did not cope with SPOT Level 1B imagery at all. The solutions to the various shortcomings of the system that have been developed both in-house at the University of Glasgow and by PCI have also been presented and discussed.

From the results and the experiences presented in this chapter, the author feels that he can claim immediately that all the work and expense involved in setting up the high accuracy test field in the Badia area for the testing of satellite imagery, including the calibration of the image processing system, have been justified. EASI/PACE was the first system to be tested and the results of the author's tests showed up immediately all the faults and shortcomings of the system, so allowing them to be rectified.

In spite of all the pain caused by this system over a period of more than 6 months, it must be said that PCI responded to the problems highlighted by the author's experimental tests in a fast and serious manner. With the full cooperation between the present author and Dr. Cheng from PCI and the continuous advice from Professor Petrie to PCI on how to solve the problems, virtually all of the problems that have been discovered in the system have been solved. Furthermore the more minor faults which have been introduced later during the modification of the software have been overcome. New programs have been added to the system and the old programs have been extensively modified with great benefit to all users of the system.

In this chapter, part of the image processing procedure has also been discussed, together with the results of an extensive series of geometric accuracy tests using the space resection and absolute orientation routines available in EASI/PACE. These have been carried out using all the Level 1A and 1B stereo-pairs covering the Badia area. As a result of the author's tests, an absolute orientation program has been added to the system to give information regarding the fit of the stereo-model to the GCPs (in particular, the

elevation values) that was not given by space resections of the individual images. From the test results given above, it is apparent that, in terms of geometric accuracy, the modeling of the SPOT orbit and the photogrammetric solution utilized by the EASI/PACE system produces a very acceptable result for topographic mapping at small scales within a fully digital photogrammetric environment. Indeed, as well be seen later in the final concluding chapter, the results obtained are some of the best that have ever been achieved using SPOT Level 1B stereo-pairs.

In the next chapter, the other image processing procedures available in EASI/PACE will be presented. In particular, the methods used to produce DEMs and orthoimages for all the stereo-pairs covering the Badia area will be discussed, followed by those used for the generation of contours at different contour intervals and for DEM, contour and orthoimage mosaicing. Finally this investigation into the photogrammetric aspects of the EASI/PACE system will be completed by the results of an extensive series of tests carried out to validate the accuracy of the DEMs and orthoimages produced by the system. These will be discussed in the next Chapter.

CHAPTER 10: VALIDATION OF DEMs, CONTOURS AND ORTHOIMAGES PRODUCED BY THE EASI/PACE SYSTEM

10.1 Introduction

In the previous chapter, the procedures involved and the problems encountered in the EASI/PACE system concerning the orientation of Level 1B stereo-images have been explained. Moreover, the results of geometric accuracy tests of the SPOT stereo-pairs covering the Badia area using the system's space resection and absolute orientation procedures have been reported. Both of these operations have been made possible through the use of the high quality control points of the Badia test field. In this chapter, the remainder of the photogrammetric image processing steps available for DEM extraction and orthoimage generation within EASI/PACE will be presented, including an account of the mosaicing of the DEMs and orthoimages derived from the SPOT stereo-pairs of the Badia Project Area. Furthermore contours have been generated from the DEM data at different intervals. On completion of these operations, the validation of the DEMs, contours and orthoimages was undertaken employing different types of accuracy and qualitative tests. Again this comprehensive investigation and analysis of the quality of these data sets has been made possible through the availability of the excellent reference data sets available for the Badia area.

10.2 Rectification and Resampling to an Epipolar Geometry

Before image matching can be performed with the EASI/PACE system, the right image needs first to be rectified, while the left image is left unrectified. Thus the rectified right image is transformed and resampled to give it a quasi-epipolar geometry. This ensures that the left image - which has been left unrectified - and the right image are offset only in the horizontal direction. In the EASI/PACE package, the **SEPIPRO** program produces the rectified image from the uncorrected SPOT satellite image and copies the model segment from File 2 (containing the right image) into File **P** (the epipolar file). The production of the image is controlled by the following parameters required as input to this program:-

(i) first specifying the file name within the image data base containing the first SPOT satellite image; then

(ii) specifying the file name within the image data base containing the second SPOT satellite image;

(iii) specifying the file within the image database which will receive the rectified epipolar image; and

(iv) finally specifying the number of binary segments in the first and second files which contain the exterior orientation data created by the SMODEL program. These parameters have been created through the space resection procedure for the left and right images forming part of the exterior orientation and have been generated using the orbital and attitude data and the GCPs.

10.3 Digital Elevation Model (DEM) Extraction

The Level 1A and 1B versions of the main reference stereo-pair and the other four Level 1B stereo pairs have all been processed with a view to creating a DEM for the Badia Project area. To extract a DEM from a stereo-pair, it is necessary to match all the points occurring in an image with the corresponding points existing in the other overlapping image. In this way, the amount of the disparity or parallax that exists in the x-direction due to relief displacement is determined for all the points that are present in the stereo-model. From this information, the corresponding set of elevation values can be calculated. By using the rectified epipolar image, the y-parallax that is likely to be encountered between a pair of left and right stereo-images is reduced to just one image line. Hence, for the extraction of the DEM, the matching procedure can be speeded up since the search for the match is confined to the x-direction - which also helps to improve the reliability of the matching procedure.

The actual procedure involves the matching of the density or grey level values on the two overlapping images comprising the stereo-pair. An area based matching method is used in EASI/PACE to match the pixels in the left image with the corresponding ones in the right image. Thus matching is performed by considering the neighbourhood surrounding a given pixel in the left image (- which forms a template -) and moving this template within a search area in the rectified right image until a position is found which gives the best match. The difference in location between the centre of the template and the original pixel position giving the best match is the disparity. These disparities or

parallax values are converted to elevation values using the exterior orientation parameters determined by the analytical space resection. This produces a regular grid of elevation values which are extracted to form the DEM. The interval between the points on the grid was 20m for all five stereo-pairs tested by the author. The program that is used for DEM extraction is called **SDEM.** The output from the SDEM program is a file with two channels - which are termed "imagery" and "DEM" respectively. The availability of the imagery (which comprises a grey level representation of the elevation data) is useful during the DEM editing carried out to fill in failed values. This program also generates an error report showing the elevation values obtained at each of the input GCPs (which were saved in the satellite modelling segments) and giving the corresponding root mean square error value within the area of the stereo-model where the elevation values were extracted.

In spite of the almost complete lack of cultural detail in this desert area, the results of the image matching carried out using EASI/PACE were good and the procedure has been proven to work well. The matching algorithm worked extremely reliably and produced elevation values for more than 99% of the whole project area. Only a few gaps or holes exist where the correlation has failed in certain shadow areas lacking texture - more especially in the north-western part of the main test area (inside the Syrian boundary) covered by scene 122/285. For the other four stereo-pairs, the maximum number of failed values was 20 pixels in each DEM, out of more than 16 million (4,000 x 4,000) points extracted from each stereo-pair.

10.3.1 DEM Editing

As noted above, it is an unusual situation when the DEM extracted from a SPOT stereo-pair has virtually no failed values. This can only occur in areas with good texture, no shadows, no seasonal changes in the appearance of the respective scenes, no difficult cultural features (e.g. high buildings) and no water surfaces. This is indeed the situation with the five SPOT stereo-pairs covering the Badia Project area. Because the stereo-pair 122/285 covering the main test area has very small holes which lie outside the boundary of Jordan and the exact elevations in these areas were not known, so this area was not edited, for two reasons. The first is that the system lacks the capability to form a 3D

model that can be viewed stereoscopically and be used to measure the exact elevations. The second reason is that, if the author let the system perform editing by simply interpolating height values within the failed area, then the result of this interpolation will not be correct - especially where large holes exist.

In the EASI/PACE system, the DEM editing panel contains a number of functions for modifying DEM data. These include a set of graphical editing tools which are provided to perform functions such as: creating editing masks; interpolating elevations to cover areas with no elevation information; filtering out noisy elevation points; smoothing out irregularities to create a more pleasing elevation model; bulldozing areas/lines of data to a particular elevation; and setting areas (such as lakes) to constant values. However it was not necessary to use these extensively given the excellent situation provided by the Badia test area.

The main editing functions which have actually been used comprise those that define the boundaries of the DEMs. This operation was carried out by specifying two channels, the first for loading the DEM into a 16 or 32-bit real channel into ImageWorks and the second for loading the image of the area in an 8-bit form for the purpose of superimposing the two channels to let the user know the location of the area that is being edited. The DEM editing panel can be invoked by selecting the DEM option from the edit pulldown menu in ImageWorks. The PCT editing panel is opened to select the " **stepped pseudocolour**" table - since this represents the elevation data better. The next step in the procedure involves masking the DEM by first drawing a polygon around the boundary and then setting the area outside the mask to a background (zero) value. Next the cursor is moved to a position outside the mask and the "**fill and cursor**" and "**fill using value**" buttons are pressed after setting the value to zero. Then, by pressing the cursor outside the mask, the boundary of the DEM will be defined and the DEM will appear as a regular shape.

The second editing operation that has been performed was the removal of noise from the DEMs. This editing function is made up of two separate filters. The first filter calculates the average and the variance of the eight elevation values directly surrounding each pixel (excluding failed and background pixels). If the value of the centre pixel is more

than two standard deviations away from the average, it is replaced with the average or mean value. This filter tends to remove small areas of noisy pixels. The second filter counts up the number of failed values directly surrounding each pixel. If there are five or more failed pixels, then the centre pixel is set to a failed value. This tends to grow or increase the failed areas - on the apparent rationale that the pixels adjacent to failed areas tend to have a high probability of being noise.

After this has been done, the interpolate function is then selected to replace the failed values with new elevation values, interpolated from the good elevation values located around the edges of the failed area. The algorithm interpolates elevations linearly between two good values using the rows and columns of the grid of elevation values, and then generates a single value for a particular pixel position based on these row and column values, weighted by their distance from the edge of the failed area. The interpolate function appears to work well for small areas less than 200 pixels - as was the case in the test area. However it should not be used for large failed areas.
The last editing function which has been used was the smooth function, which uses a 3x3 pixel Gaussian smoothing filter. Pixels that have failed or have background values will not be altered and will not be used in the smoothing calculations.

10.3.2 Geocoding the DEM

Since the DEM results extracted from the **SDEM** program are stored in the uncorrected and non-geocoded left hand image file, the **SDEMCPY** program was used to copy the DEM results and transform them into a geocoded form oriented to the UTM coordinate system in order to bring them into a useable framework to carry out the orthorectification of the satellite image using the **SORTHO** program. **SDEMCPY** will automatically create a file with a 16-bit signed channel which preserves the full accuracy of the elevation data.

10.4 Generation of Orthoimages

For the area to be covered by an orthoimage, a suitable digital elevation model (DEM) providing the XYZ coordinate values for all the DEM points must be available. For the

author's research project, the elevations derived from the prior image matching of the SPOT images - which were arranged in a regular grid - were available to represent the terrain. From these points, an elevation value can be derived for each pixel of the orthoimage. Obviously any errors in elevation will create planimetric errors in the orthoimage. Therefore the accuracy of the elevation model has a great influence on the accuracy of the final orthoimage. Either one (i.e. the left or the right) of the original uncorrected images can be transformed into an orthoimage. The correct positions in the digital image are found according to the photogrammetric projection equations using the parameters of the exterior orientation together with the elevation data. Once the orthorectification process has been completed, it is also necessary to find the corresponding grey level value for each pixel in the orthoimage. The relevant value is found through a suitable interpolation or resampling carried out using the grey level values of the pixels adjacent to each particular orthoimage pixel.

Using the **SORTHO** program, all five stereo-models covering the Badia Project area have been used to create orthoimages utilizing the DEMs with elevation values created at 20m intervals. In the input to this program, the particular digital elevation channel that is to be used must be specified. In addition to this, the database input file must be specified; this file should contain the imagery and the relevant exterior orientation segments. Also the output file should be specified; if not, the program will create a new image database and will geocode it such that the orthorectified image will be fitted to the ground control points with the same resolution as the original uncorrected image. The database file name that contains the DEM data also should also be specified, together with the resampling method that is to be used.

Based on the author's experience, one can say that the quality of the final corrected output image and the time required in its calculation is highly dependent on the resampling method chosen. This program offers three of the more popular resampling methods: nearest neighbour, bilinear interpolation, and cubic convolution. For the production of the Badia orthoimages, the cubic convolution method has been used. This method uses the weighted average of the sixteen surrounding pixels in the uncorrected image to give the DN (i.e. grey level) value of the new pixel in the corrected image. It seems to provide a slightly sharper image than the bilinear method.

10.4.1 Othoimage Printed Output

For printing the orthoimages, the **MAPIMA** Module (Figure 10.1) provided in the EASI/PACE system can generate either a black and white grey level image or a colour image from data held in an input PCIDSK file. The image is held as bitmap segments in an output file. A hardcopy image is obtained by running a second printer program available in the EASI/PACE system such as **HPLASER, CANONBJ, EPSON,** etc. which sends the bitmap segments (holding the image) to the specific raster-based printer that has been selected. The type of the image to be printed - i.e. black and white, or colour - can be determined by the capabilities of the output device set by the **MAPDEVIC** parameter. If the output device that has been selected is **HPLASER** (for an HP Laserjet), then a single black and white bitmap segment will be generated; if the selected output device is an **EPSON** or **CANON BJ** colour bubble jet printer, then three separate bitmap segments (for red, green and blue) will be generated.

There are two other basic operations that can be performed by **MAPIMA - CREATE** and **OVERLAY**. These are controlled by the **MAPOPER** parameter. In a **CREATE** operation, a new file containing an image is created. In an **OVERLAY** operation, the image is written, i.e. superimposed, on to an existing map. The parameters specify information about the map when it was created initially. These parameters determine the size of the map, its annotation, etc. During the overlay operation, these parameters are ignored. The parameter **MAPDEVIC** specifies the type of the output device that the map will eventually be printed on.

Figures 10.2 and 10.3 show the orthoimages created for scene 122/285 covering the main test area from both the Level 1A and 1B stereo-pairs. The other orthoimages have been included in Appendix B.

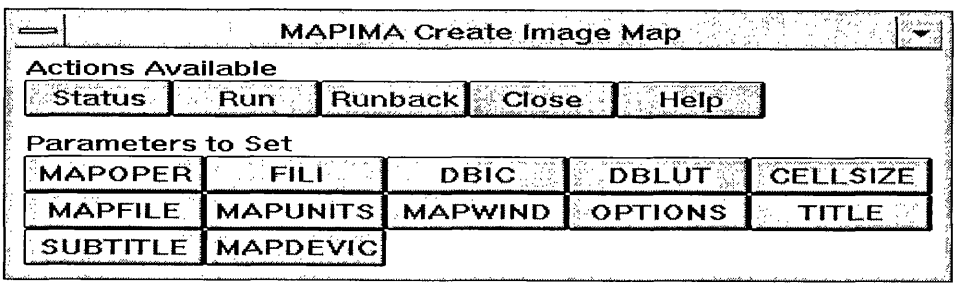

Figure 10.1 MAPIMA program parameters

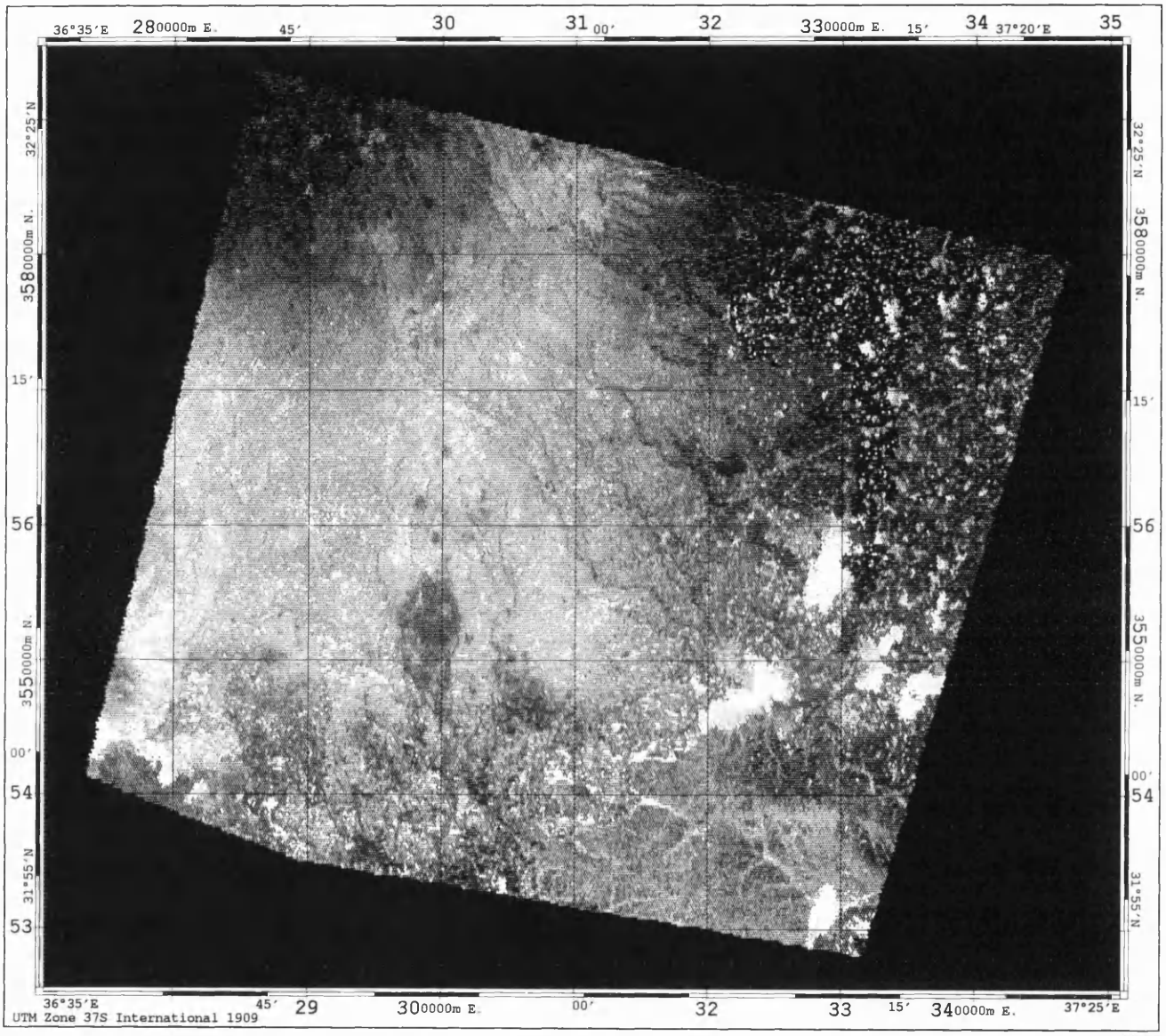

Orthoimage of the Main Test Area Level 1A Scene 122/285

Ground Pixel 20m; Produced by EASI/PACE System

1:500 000 Scale

Kilometres 10 0 10 20 30 40

Miles 10 0 10 20

Figure 10.2 Orthoimage of the main test field produced from the Level 1A stereo-pair of scene 122/285.

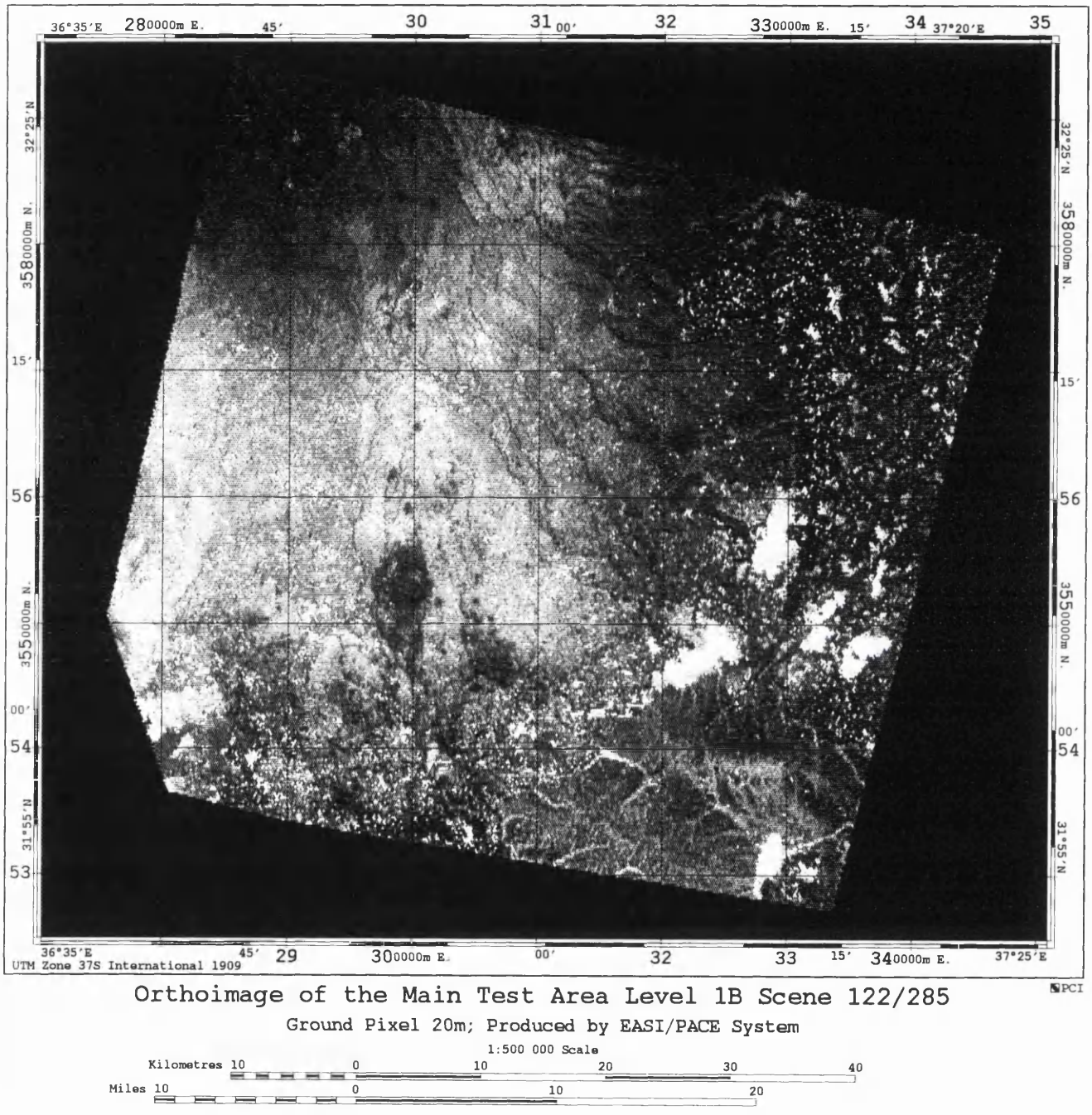

Figure 10.3 Orthoimage of the main test field produced from the Level 1B stereo-pair of scene 122/285.

10.5 Contour Generation

After the extraction of the DEMs for each of the five Level 1B stereo-pairs and the single Level 1A stereo-pair of scene 122/285 covering the main test area, the **CONTOUR** program of EASI/PACE has been used for the generation of contours at both 50m and 20m intervals. When generating contours, the user specifies an integer contour interval and an optional background value for the DEM. If this background value is not specified, the whole input DEM is assumed to have valid DEM data. The **CONTOUR** program then creates the required contours from the DEM using the 16-bit signed integer data, including a new vector segment (or file) containing the contour line data. Each contour line is assigned an integer attribute value which specifies the elevation of the contour. The new vector segment is given a specified segment name and descriptor. This vector segment contains only line structures; if the shape of the DEM is irregular, then those pixels that do not contain valid DEM data are assigned the background value. However elevation contours are not generated wherever the DEM is assigned the background value.

The **CONTOUR** program generates lines at sub-pixel level that are interpolated from the surrounding DEM values, so that the lines appear smooth and curved and will not exhibit a stair-case effect. In general, the interpolation method used in the EASI/PACE system is linear interpolation, e.g. if pixel (1,1) has elevation 0m and pixel (2,1) has an elevation of 100m, the contour for 50m will pass through position (1.5, 1). Figures 10.4 and 10.5 show the contours at a 20m interval that have been extracted from the DEMs of the main test area derived from the Level 1A and Level 1B stereo-pairs respectively for scene 122/285. Figure 10.6 shows the contours from the Level 1B stereo-pair for scene 123/286 with the same contour interval. Other contours extracted from other DEMs are shown in Appendix B.

10.5.1 Contour Output

For the printing or plotting of the contours generated from DEMs or the printing of superimposed contours, the **MAPVEC** module generates black and white or colour line maps from the vector data held in segments in an input PCIDSK file. The resulting

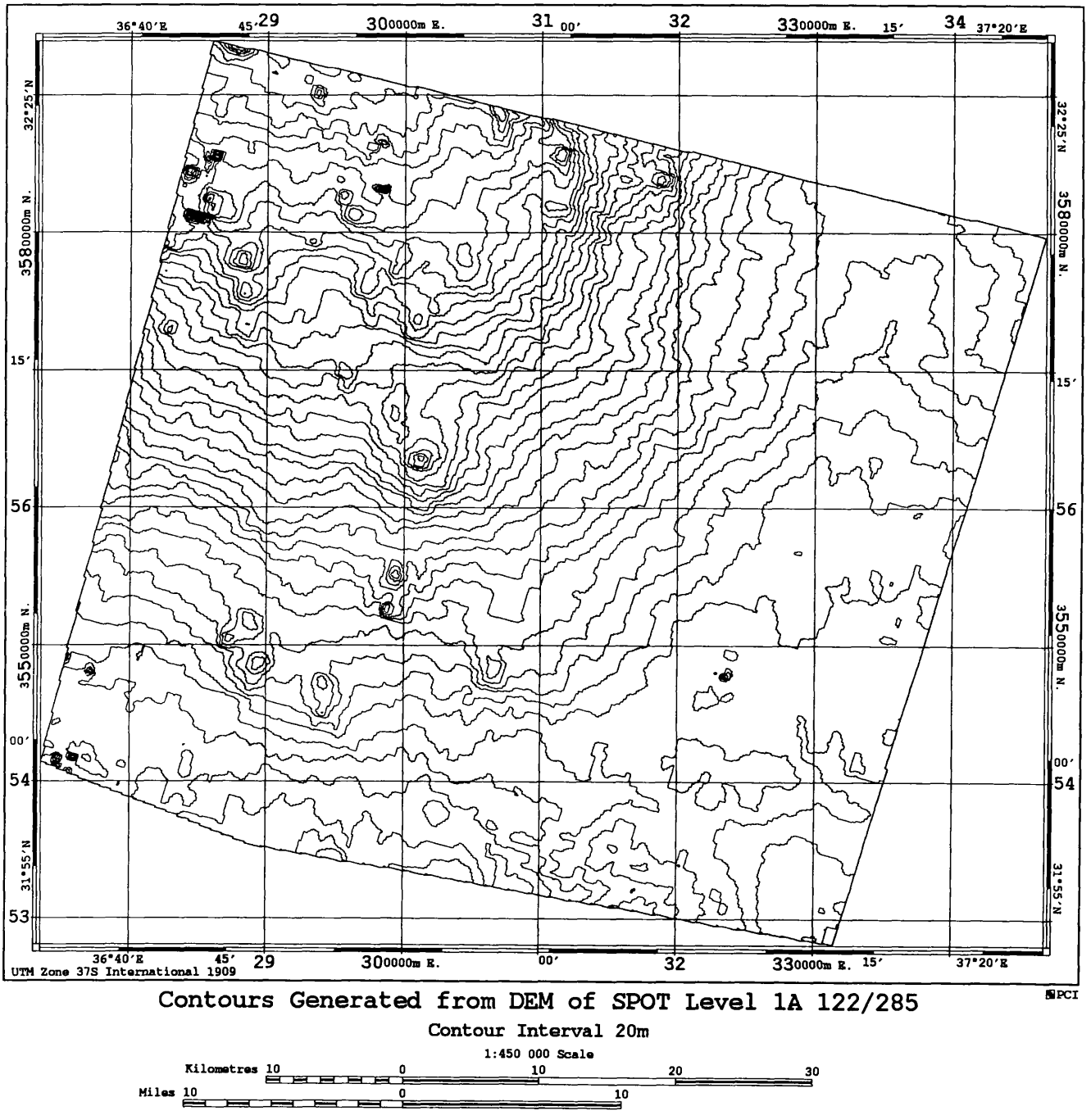

Figure 10.4 Contours generated from the DEM derived from the SPOT Level 1A stereo-pair of the main test area covered by scene 122/285 with a contour interval of 20m.

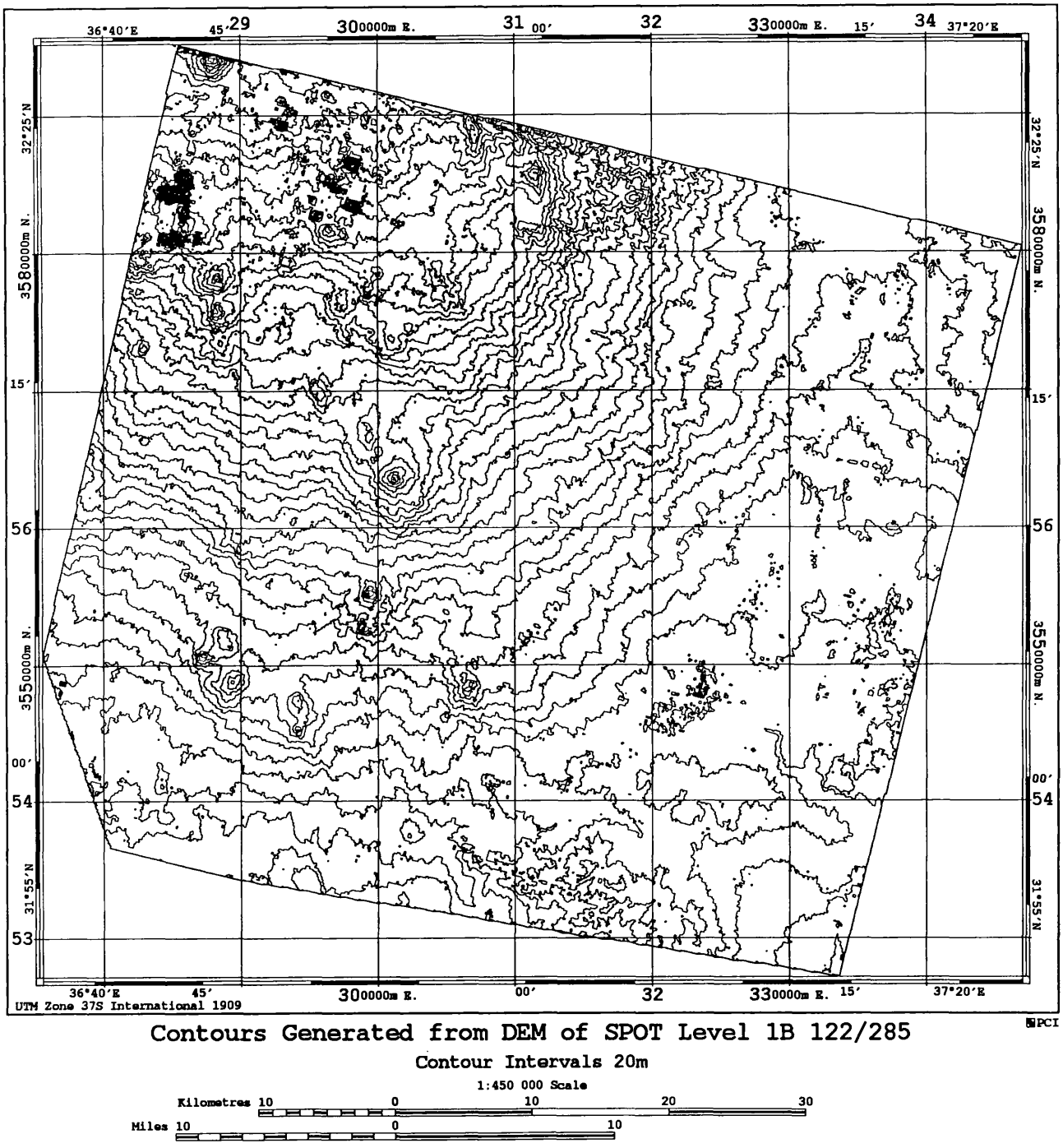

Figure 10.5 Contours generated from the DEM derived from the SPOT Level 1B stereo-pair of the main test area covered by scene 122/285 with a contour interval of 20m.

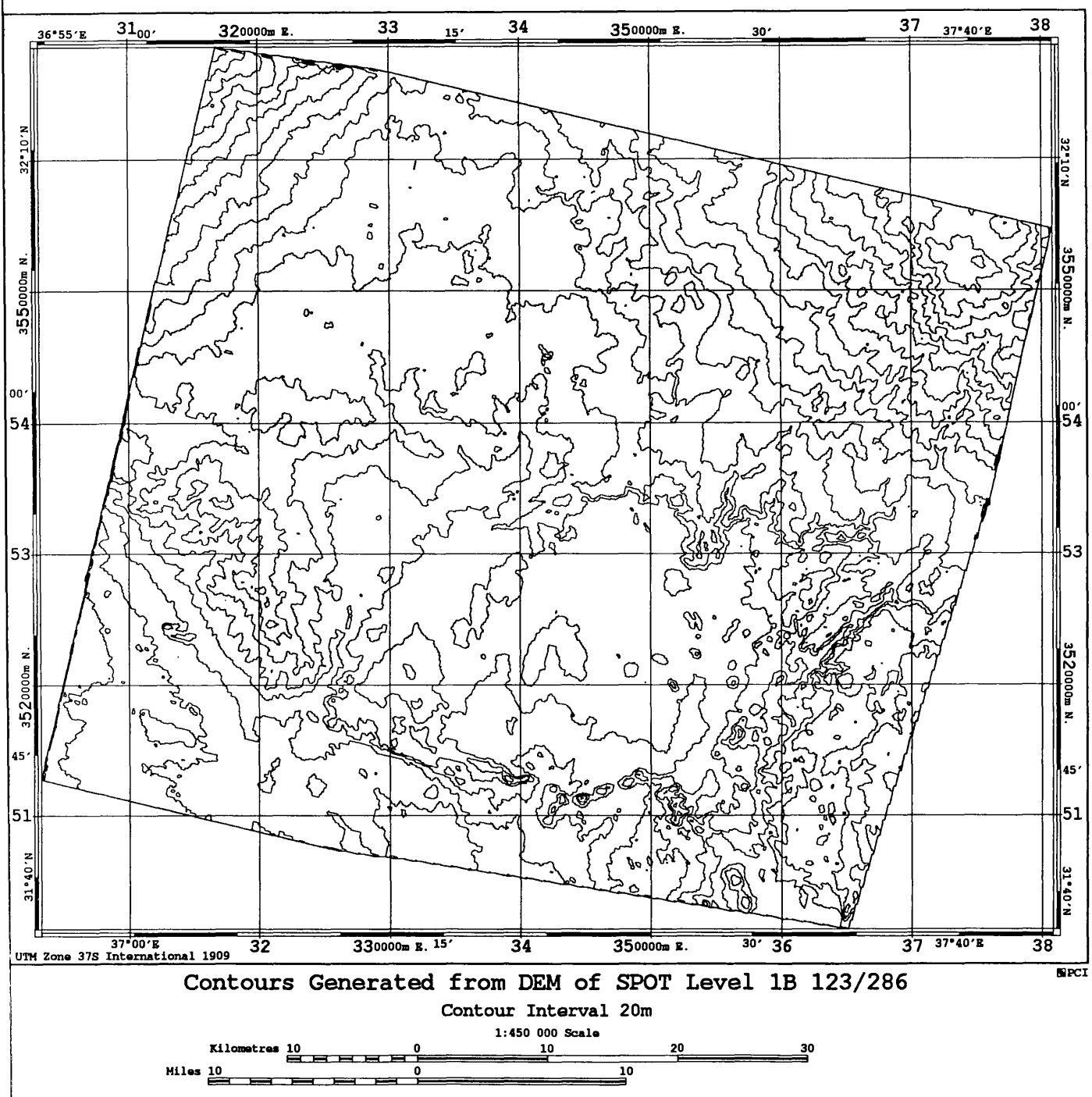

Figure 10.6 Contours generated from the DEM derived from the SPOT Level 1B stereo-pair covered by scene 123/286 with a contour interval of 20m.

raster map is then held as bitmap segments in a second output file. Hardcopy from the maps are obtained by running a second program, such as **HPLASER** or those controlling Canon or Epson bubble-jet printers, which sends the bitmap segments (holding the map) to the corresponding printer. The parameters of the **MAPVEC** module specify the necessary information about the map when it is initially created. This is done by specifying the **MAPOPER** parameter to "create" other parameters that specify the size and scale of the map and how it is to be decorated with labels, annotation, descriptive text etc., together with the actual type of device that the map will eventually be printed on. In the case of an overlay operation, these parameters are ignored, except for a few specific values in the option parameter.

10.6 Generation of a Wire Mesh Perspective View

Most imagery - at least for topographic mapping and remote sensing applications - is taken from high altitudes looking straight down. It is often useful, however, to simulate the view of an observer on the ground looking out over the image at an oblique angle. This is generally known as a perspective view or perspective block diagram and requires that elevation data be available for each pixel in the input imagery. For the generation of such a view, the orthoimage and the DEM should be in a single file. In this research project, a perspective view of the Badia area has been created from an orthoimage with a 10m ground pixel size and a DEM with a 20m grid interval. Another eight-bit channel is needed to put the orthoimage inside the DEM. This requires the copying of the orthoimage to the DEM channel by resampling the orthoimage using the cubic convolution procedure. In the case of a 10m DEM grid being available, a 16-bit channel should be added and the DEM should be copied to the channel of the orthoimage and then resampled using the cubic convolution method.

To create the perspective view, the **PSGIMAG** program has been used. Another program that is available for this type of operation is called **PSGMESH**. This is used to generate the perspective view using a mesh rather than using solids in the manner of the PSGIMAG program. The parameters for these two programs have to be filled with the correct values to be able to run the program. Figure 10.7 shows a representative "fishnet-type" perspective block diagram derived from the DEM and orthoimage

produced from the Level 1B stereo-pair of scene 122/285 forming part of the main test area.

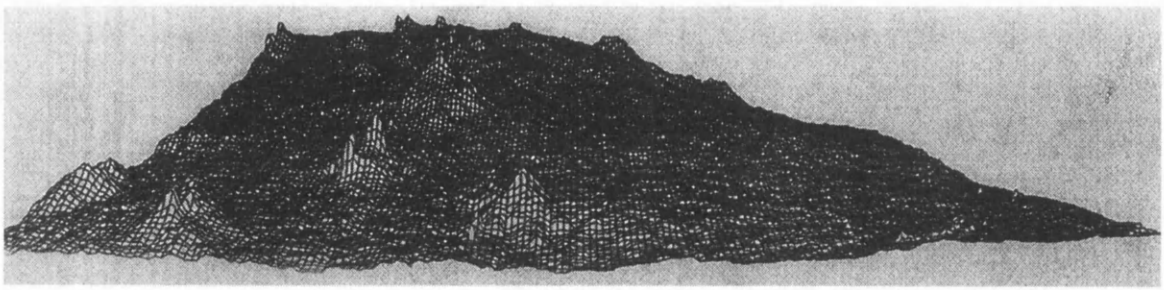

Figure 10.7 A perspective "fishnet-type" block diagram derived from the DEM and orthoimage produced from the Level 1B stereo-pair of scene 122/285.

10.7 Mosaicing of DEMs, Contours and Orthoimages

EASI/PACE provides the possibility to mosaic together the individual DEMs, contour plots and orthoimages generated from the individual stereo-pairs. This mosaicing operation blends several arbitrary shaped images together to form a single large, radiometrically-balanced image so that the boundaries between the original images are not easily seen. Feathering also can be performed along the boundaries and overlaps between uncorrected images, making the seams unnoticeable.

10.7.1 Mosaicing of DEMs

The mosaic area collection panel is used to create, edit, save, and load the mosaic and provide the cutline vectors needed for the mosaicing operation. This panel is launched by selecting the "**select mosaic area**" step on the main control panel in GCPWorks - see Figure 10.8. To carry out the mosaicing of the DEMs, the following six steps have been followed:

(i) The first step was to select the first image to be mosaiced. This image should be considered to be the master image while the other images are considered to be slave images.

(ii) The second step was the creation of the output mosaic file. In this step, an output file has been created which should hold the five mosaiced DEMs. This has been done by inputting the coordinates of the upper left corner of the first DEM and the right lower corner of the last DEM.

(iii) The third step was the selection of the output mosaic file.

(iv) This was followed by the fourth step which defines the mosaic area. In this step, the mosaic cutline vector outlines the area of the uncorrected DEM to be registered during pre-registration and final registration.

(v) In the fifth step, the pre-registration check panel is used to provide an overview or perform chip registration on-screen for the purpose of pre-viewing either the expected registration or the results. This pre-registration panel contains a number of options for the modification of the registration and mosaicing process and a button for performing the overview registration. After pressing the "**register overview**" button, the system carried out the pre-registration into the georeferenced image overview window. After checking that the pre-registration process was successful and being satisfied with the results, then the last step in the processing of disk-to-disk registration was carried out.

(vi) The sixth step employs the disk-to-disk registration panel which is used to perform a final registration from the uncorrected image file to a final (geocoded) output image file. Any number of channels may be registered at once, to produce any desired output file with the appropriate georeferencing type. The disk-to-disk registration panel consists of four sub-areas, the first three of which deal with channel/file mapping selection, while the fourth is used to set the registration option. Once the desired set of registration options has been selected and the desired input/output channel mapping has been established, the "**perform registration**" button located at the bottom of the panel is used to initiate the actual registration.

EASI/PACE also provides a facility called **Blend** which is used to control the distance or width around the mosaic cut line over which blending of the georeferenced and the uncorrected image is performed. Blending implements a form of feathering around the cut line, in which the blend distance determines the distance on either side of the cutline over which the blending is to be carried out. The procedures described above have to be repeated for every DEM added to the previous ones. In this way, the five DEMs

covering the Badia Project area have been mosaiced together, amounting to 530 Mbytes of data using a grid spacing of 20m.

In general, the work required for the mosaicing of the DEMs was carried out smoothly, the system remaining stable during the processing and responding in a very fast manner. No problem was encountered during the whole process. The final DEM mosaic was perfect, with no obvious joins or any differences in the elevation values appearing in the boundary area between the DEMs.

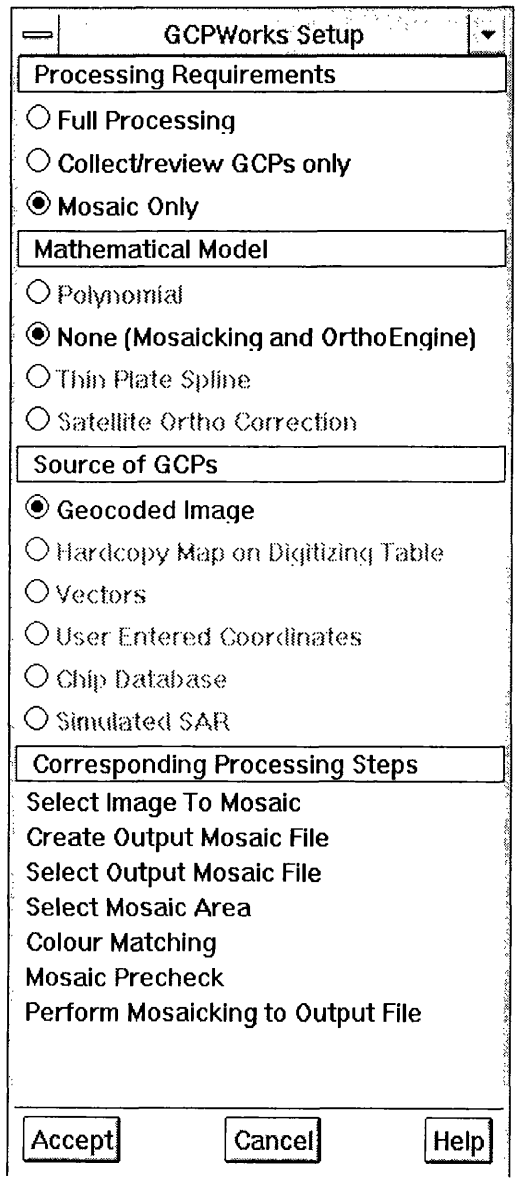

Figure 10.8 GCPWork Setup panel showing the mosaic processing steps.

10.7.2 Merging the Contour Line Plots

As has been stated above in Section 10.5 on contour generation, individual contour plots have been generated from each of the DEMs covering the Badia test area. These contours needed to be merged together to create a single contour plot for the whole Badia area. This allows the analyst or user to see how they fit with each other. The **VECMERG** program has been used for this purpose. This program merges a set of vector segments - in this case, the contours - within the database and saves the merged data set in a new vector segment (or file). The vector segments that have been used as input are not changed. The new database vector segment will be given a specific segment name and segment descriptor. All the vector segments that are specified must be in the same units (such as pixels or in metres in the UTM coordinate system).

The **VECMERG** program running on a PC cannot perform this task due to the huge amount of memory that is required to merge these five sets of contours. To be able to merge the contours required a minimum of 128 RAM memory - which was not available on any PC in the Department. Thus the contour files have been sent to Dr. Cheng in the PCI Company and he processed and merged them using a Unix-based graphics workstation. To achieve this, the data was imported and exported over the Internet through the use of Telnet. Figures 10.9 and 10.10 show the merged contours extracted from the five DEMs covering the whole of the Badia Project area at contour intervals of 20m and 50m respectively.

In general, the system carried out the merging operation in very successful manner, Inspection of the contours in Figures 10.9 and 10.10 shows clearly that the corresponding contours have been connected satisfactorily with each other in the overlapping areas. This helps to confirm that the image matching carried out over the stereo-models was stable for all of the stereo-pairs and reflects the fact that, after all the modifications made to the system, the stereo-models fitted the GCPs well. The only shortcoming in the merging process using a PC is that the user has to divide the area to be merged into small parts and then merge them with each other, which is not too convenient in a big area like that covered by the Badia Project.

10.7.3 Mosaicing of Orthoimages

Basically the same procedures and operations have been used in the mosaicing of the orthoimages as have been employed with the DEMs (in Section 10.7.1) - except that an additional radiometric matching process has been performed for the orthoimages. This comes after the first four steps already discussed in Section 10.7.1 for DEMs. For the fifth step, after the selection of the image and the use of the mosaic cutline vector to define the area to be blended, the colour matching step is used to match the second (slave) orthoimage with the first (master) image - though, in this case, it is grey level values that are being matched. The colour matching panel is used to assign a set of radiometric correction values in the form of a look-up table (LUT) to be used with the uncorrected image. The LUT will be applied to the uncorrected image data during the registration/mosaicing process with the expectation that the transformed data will more closely match the data of the master image. However, since this will rarely happen, the solution is to generate a more appropriate LUT by taking samples from the master image and applying the new LUT to the slave image.

The new LUT is calculated on the basis that should match, as closely as possible, the histograms for the sample areas of the image which have been selected by the analyst. The actual areas to be used for sampling are selected by dragging the red box defined on the display using the left mouse button and placing it over the suitable defined areas selected on the master or any other orthoimage. In the case of the Badia Project area, several samples have been selected from different areas on the master orthoimage and tested until one of these samples matched radiometrically the slave and no obvious differences appeared in grey level value between the two orthoimages when the pre-registration check was applied. The matching LUT is not actually computed until the "**match**" button at the bottom of the panel is selected. At this point, the new LUT is computed based on the current sampling windows. The new LUT is then applied to the uncorrected images (i.e. the slaves) and updated in the "**matching LUTs**" area of the panel. The final registration is then performed. The same process is then repeated for the other orthoimages.

The five orthoimages extracted from the five Level 1B SPOT stereo-pairs imagery have been mosaiced together successfully with no obvious joins along the boundaries. To achieve this good result, considerable time was required to ensure a good match of each of the slave orthoimages with the master. Several tests had to be carried out until all the orthoimages matched well with each other. The final orthoimage mosaic formed a file of 56 Mbytes of data using a pixel size of 20m. Figure 10.11 shows the final orthoimage mosaic for the whole of the Badia Project area.

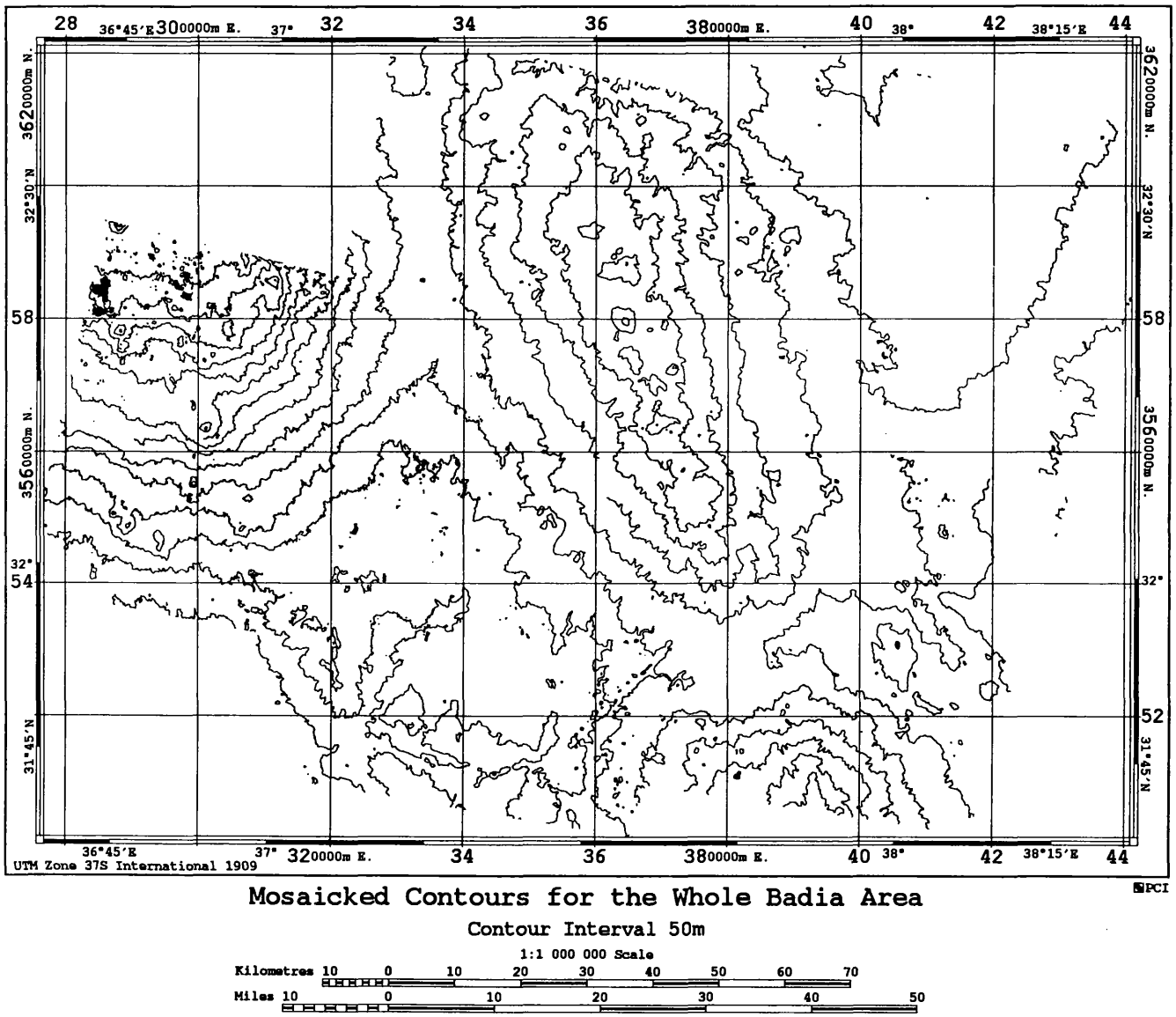

Figure 10.9 Mosaiced contours for the whole Badia Project area at a contour interval of 50m.

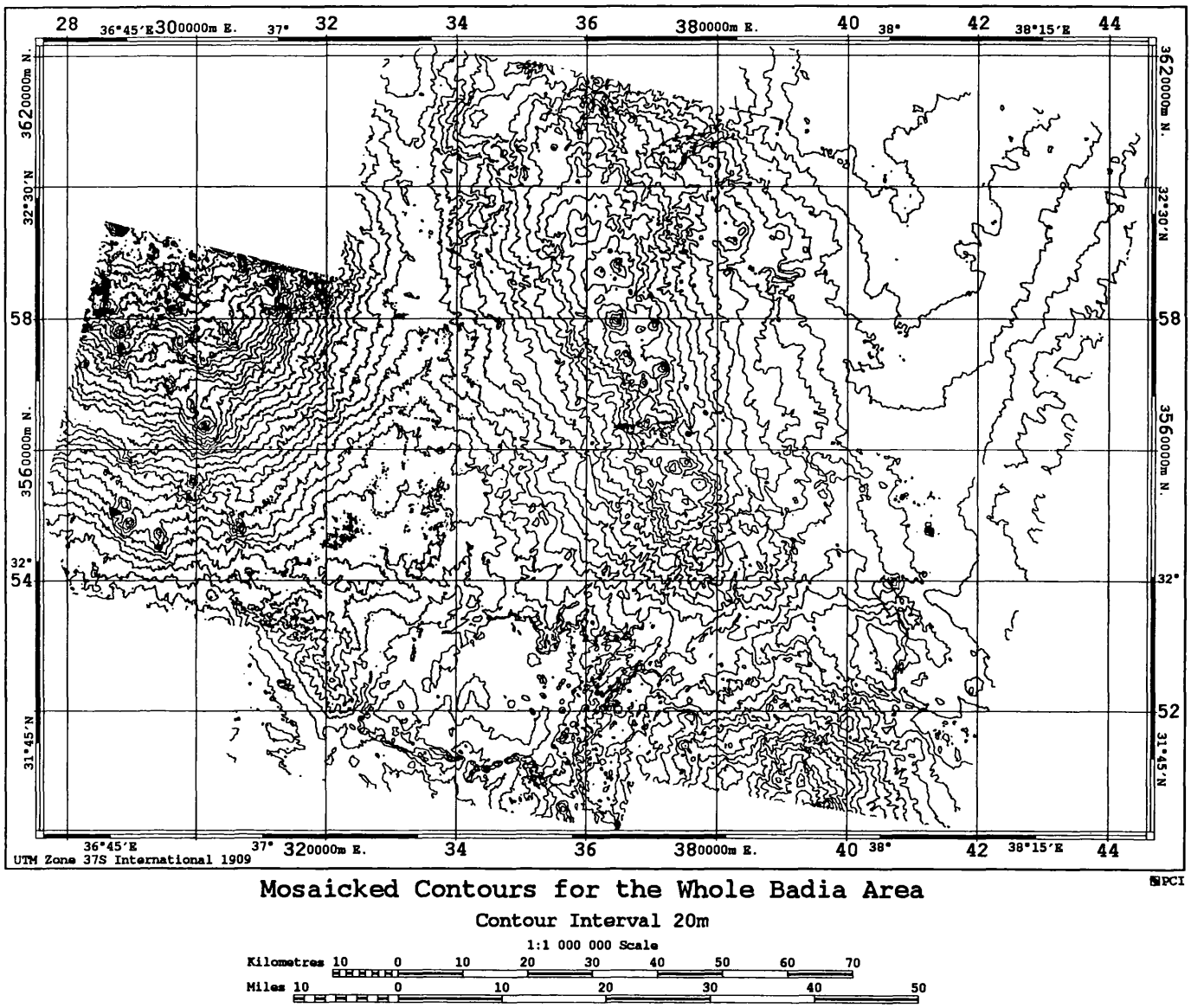

Mosaicked Contours for the Whole Badia Area

Contour Interval 20m

1:1 000 000 Scale

Kilometres 10 0 10 20 30 40 50 60 70

Miles 10 0 10 20 30 40 50

Figure 10.10 Mosaiced contours for the whole Badia Project area at a contour interval of 20m.

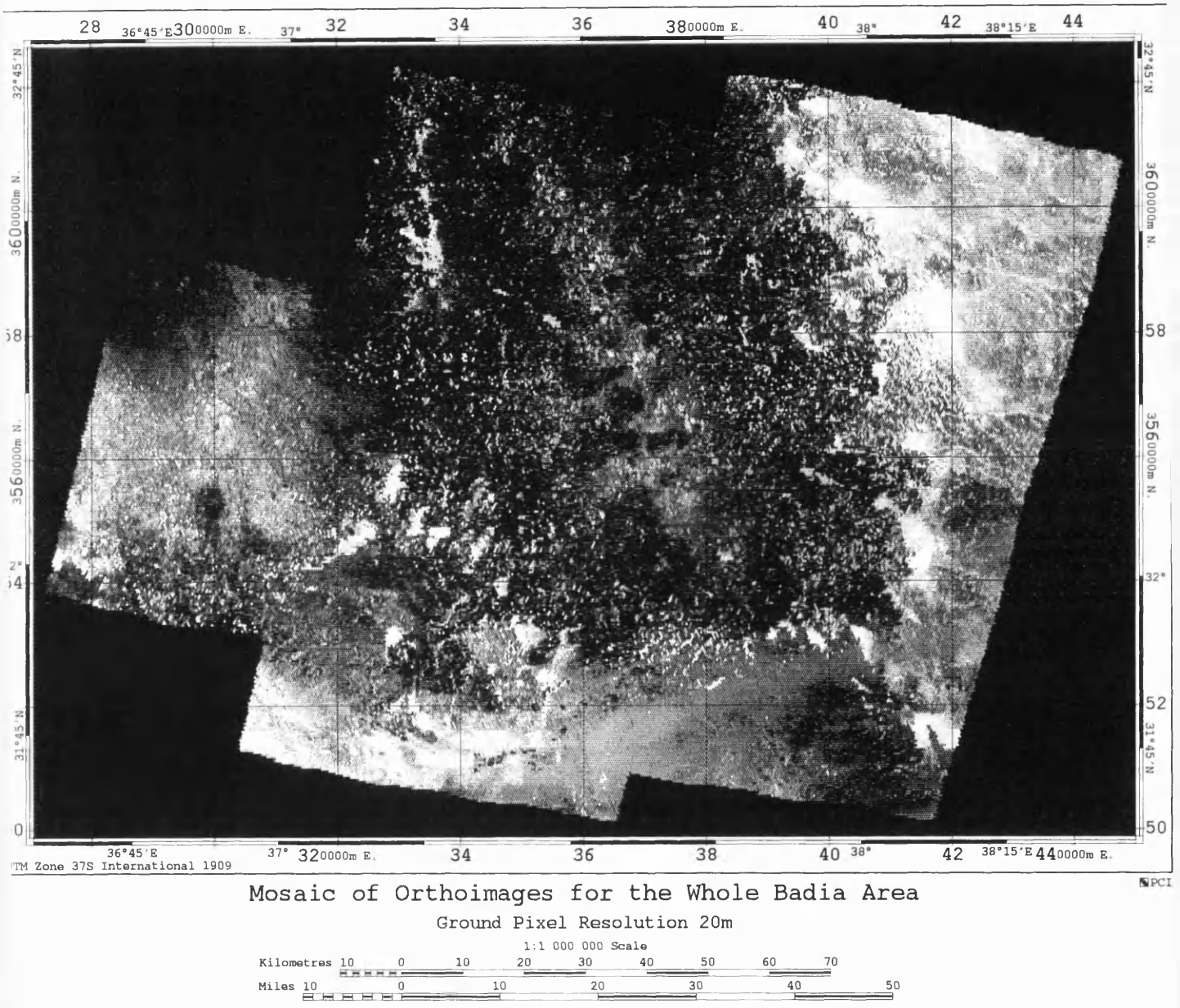

Mosaic of Orthoimages for the Whole Badia Area

Ground Pixel Resolution 20m

1:1 000 000 Scale

Kilometres 10 0 10 20 30 40 50 60 70

Miles 10 0 10 20 30 40 50

Figure 10.11 Orthoimage mosaic for the whole Badia Project area.

10.8 Experience with EASI/PACE

At this stage, having spent quite some time in Sections 10.2 to 10.7 outlining the procedures used, it is worth commenting on the author's overall experience with the

generation of DEMs, contour plots and orthoimages using the EASI/PACE system. In general terms, it is a complex and highly sophisticated system offering a very wide range of options which allow the user to achieve the specific results and products that are required. But this high degree of sophistication and flexibility means that a long and steep learning curve must be negotiated before the user can master the system and actually utilize the many features that it offers. However, of all the various systems tested by the author, it is undoubtelly the most highly developed, even if its complexity makes it difficult for anyone to describe it as being "user friendly". But the final results achieved with the Badia stereo-pairs are very good in terms of the visual or pictorial quality of the product - e.g. the contours run smoothly into one another without obvious breaks and the orthoimage mosaic exhibits a smooth gradation of grey levels between its component images.

10.9 Accuracy Tests of the DEMs of the Badia Test Area

To go further and validate the data quality - more especially in terms of geometric accuracy - of the DEMs extracted from SPOT Level 1A and 1B stereo-pairs for scene 122/285 of the Badia test field, four different methods have been used:-

(i) a comparison of the two sets of superimposed contours;

(ii) a comparison of the height values given by selected contours from the photogrammetrically produced reference map and the corresponding elevation values given by the DEM;

(iii) DEM accuracy reports; and

(iv) comparison of the DEM data with the GPS profiles measured along the main roads.

10.9.1 Comparison of Superimposed Contours

(a) Superimposed Contours at 50m Intervals

In this method, first of all, the contours that have been extracted from the Level 1B DEM at an interval of 50m have been loaded into EASI/PACE using ImageWorks. Also the contours at the same interval (50m) that had been digitised from the 1:250,000 scale topographic map by RJGC were also loaded over the first set of contours to form a map

with two sets of superimposed contours - see Figure 10.12. These contours will not fit exactly due to the errors that are present in both sets of contours. In the case of the contours from the existing map, these errors come both from the original compilation of the map that has been digitised and the errors of the measurements made during the digitising procedure itself. Then, of course, errors are present in the contours extracted from the DEM. These derive both from the accuracy of the DEM elevations themselves arising from the matching algorithm that has been used by the system and from the editing tools and procedures which have been used to correct the DEM - as well as the morphological nature of the area and the contouring procedure itself. In carrying out the test, the present author has considered the digitised contours - which have been produced originally by the aerial photogrammetric method - to be the reference set for the test.

In this method, the test was carried out through a simple visual comparison of the two sets of contours; i.e. essentially it is qualitative test. Inspection of the superimposed contours produced from the Level 1B stereo-pairs in Figure 10.12, shows that more than 90 % of the two sets of contours fit well to each other (to within < 10% of the contour line interval). Minor deviations occur in some parts; these occur mainly in the southern part of the area which is almost flat. More detailed inspection shows that the small lack of fit of the contours occurs in both a positive and a negative manner without any obvious systematic effects - which indicates that the errors are random. In general, the conclusion from the detailed comparison of the two sets of superimposed contour is that the contours generated from the Level 1B DEM by the EASI/PACE system have an excellent fit with the digitised reference contours. This does show that, if the system is provided with excellent data like the Badia image and control data, it can produce an excellent result for the wide contour interval of 50m that is commonly used with small-scale topographic maps such as a 1:250,000 scale series.

The contours extracted from the Level 1A DEM have also been superimposed over the digitised contours using the same procedures as described above; visual inspection again shows an excellent fit of the two sets of contours. Inspection of Figure 10.13 again shows some deviation both in the southern part and in a small part of the north-eastern part of the area. Curiously there is a somewhat less good fit than that of the contours generated from the Level 1B DEM. However the deviation can be estimated to amount

to more or less one-tenth of the contour interval. No individual contour generated from the Level 1A and 1B DEMs has a deviation greater than 20% of the 50m contour interval when compared with the reference set of contours.

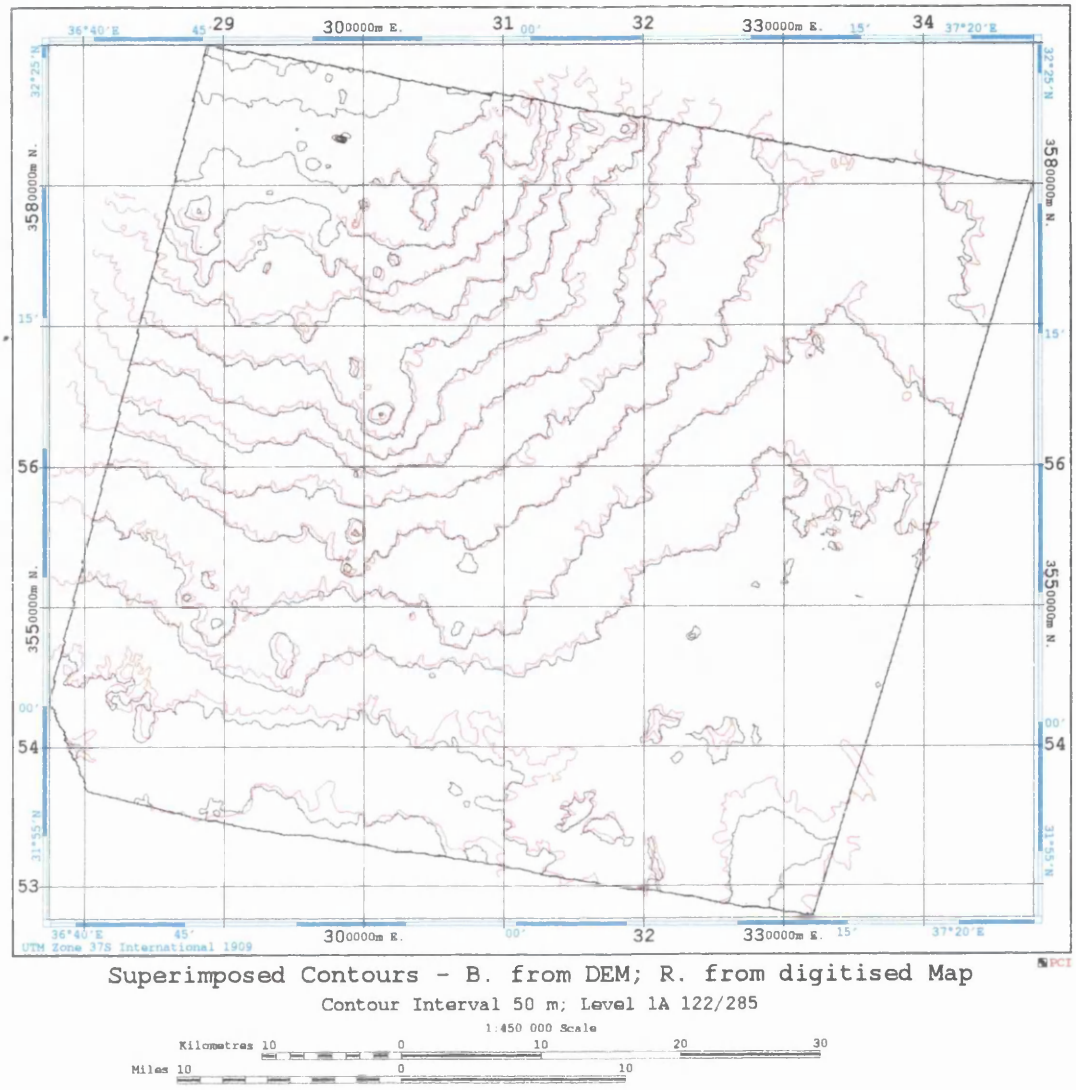

Figure 10.12 Contours at 50m interval extracted from the Level 1A DEM of the main reference stereo-pair for scene 122/285 superimposed over the corresponding digitised contours from the RJGC 1:250,000 scale topographic map.

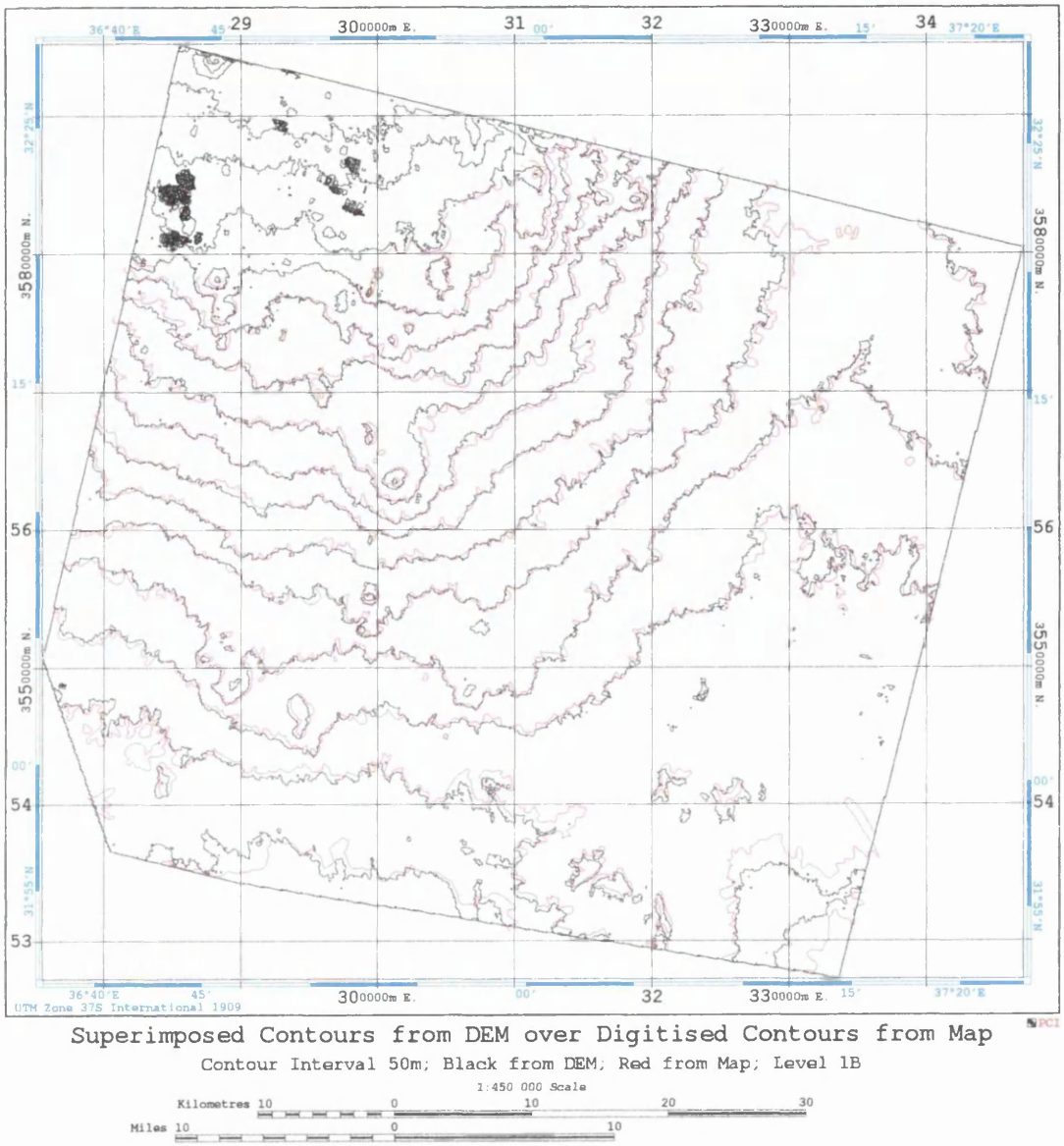

Figure 10.13 Contours at 50m interval extracted from the Level 1B DEM of the main reference stereo-pair for scene 122/285 superimposed over the corresponding digitised contours from the RJGC 1:250,000 scale topographic map.

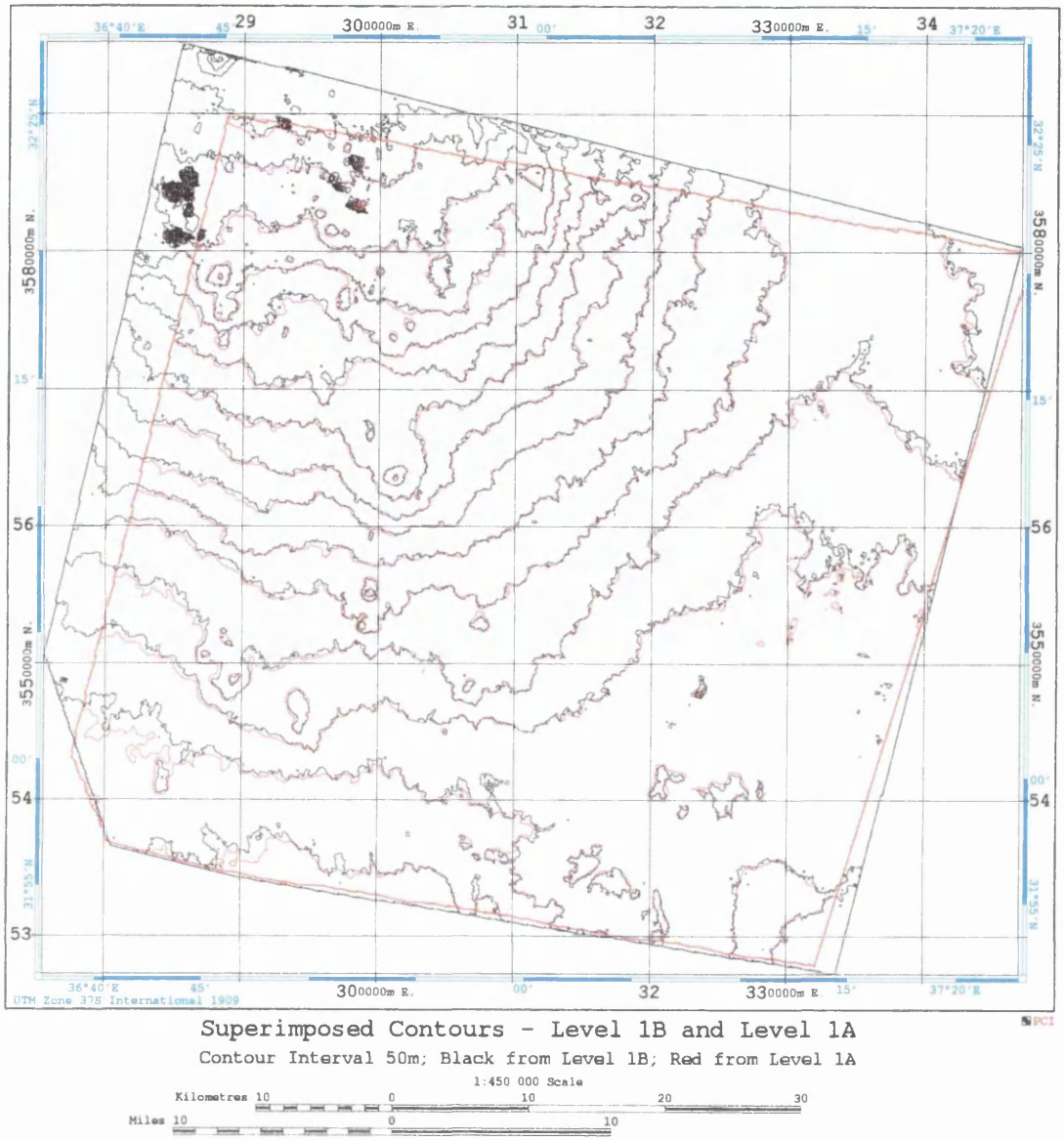

Figure 10.14 Contours at 50m contour interval extracted from the Level 1A and 1B DEMs of the main reference stereo-pair for scene 122/285 superimposed on one another.

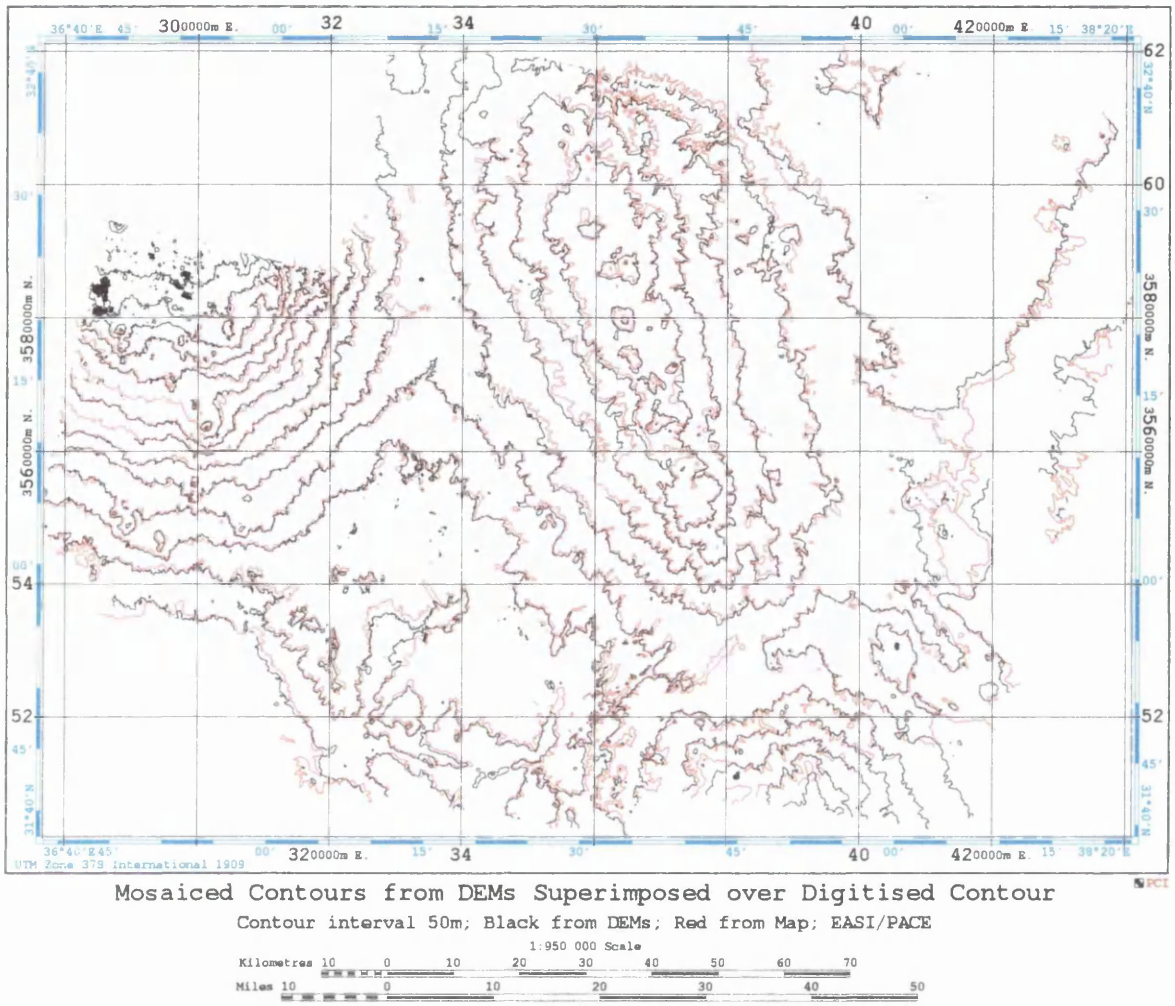

Figure 10.15 Mosaiced contours with a 50m interval extracted from the DEMs of the whole Badia area (given in Red) superimposed on the corresponding digitised contours from the RJGC 1:250,000 scale topographic map (in Black).

Figure 10.14 shows the contours generated from Level 1A and 1B DEMs superimposed on one another. Inspection of this figure shows an excellent fit of the two sets of superimposed contours. Minor deviations occur only in the flat southern part of the area and in local areas along the boundary.

A final inspection concerned the contours of the full DEM that covers the whole Badia area. In this comparison, the mosaiced contours generated from the five individual DEMs covering the Badia area were superimposed over the digitised contours from the

1:250,000 scale topographic map - as shown in Figure 10.15. Once again, the visual inspection shows an excellent fit between the contours - again amounting to less than 10% of the contour line interval. Minor deviations can be seen, more especially in the Al-Hammad area in the eastern part of the area and in the south-western part. Both areas comprise flat terrain.

(b) Superimposed Contours at 10m Intervals

As mentioned above, the same procedures have been followed for a comparison of the contours generated from the Level 1A and 1B DEMs of the reference stereo-pair 122/285 at a 10m contour interval which have been superimposed over the corresponding set of contours digitised from the 1:50,000 scale topographic map. With the latter, the main contour interval is 20m; however the supplementary contours at a 10m interval had also been digitised which gives additional material for the comparison. The title of this 1:50,000 scale map is Dier Al-Khaf. It is located in the extreme north of the DEM for scene 122/285 and covers only part of the SPOT scene.

Inspection of the superimposed contours shown in Figure 10.16. again shows a very good fit to the reference set for both sets of contours generated from the Level 1A and 1B DEMs. Of course, the degree of fit is difficult to judge, especially when the contours are very close to each other in this hilly area, but, in general, a reasonable fit - of the order of 20% of the contour line interval - has been achieved. The other matter which can be seen from the visual inspection is related to the respective shapes of the two sets of contours. The digitised contours show a relatively smooth shape while the contours generated from the DEMs display a more irregular shape with more abrupt changes in direction. It could be that the contours produced from the aerial photos have been smoothed out while they were being measured and compiled, while the contours generated from the DEMs are more irregular since they are produced via automatic procedures without the benefit of human interpretation and editing.

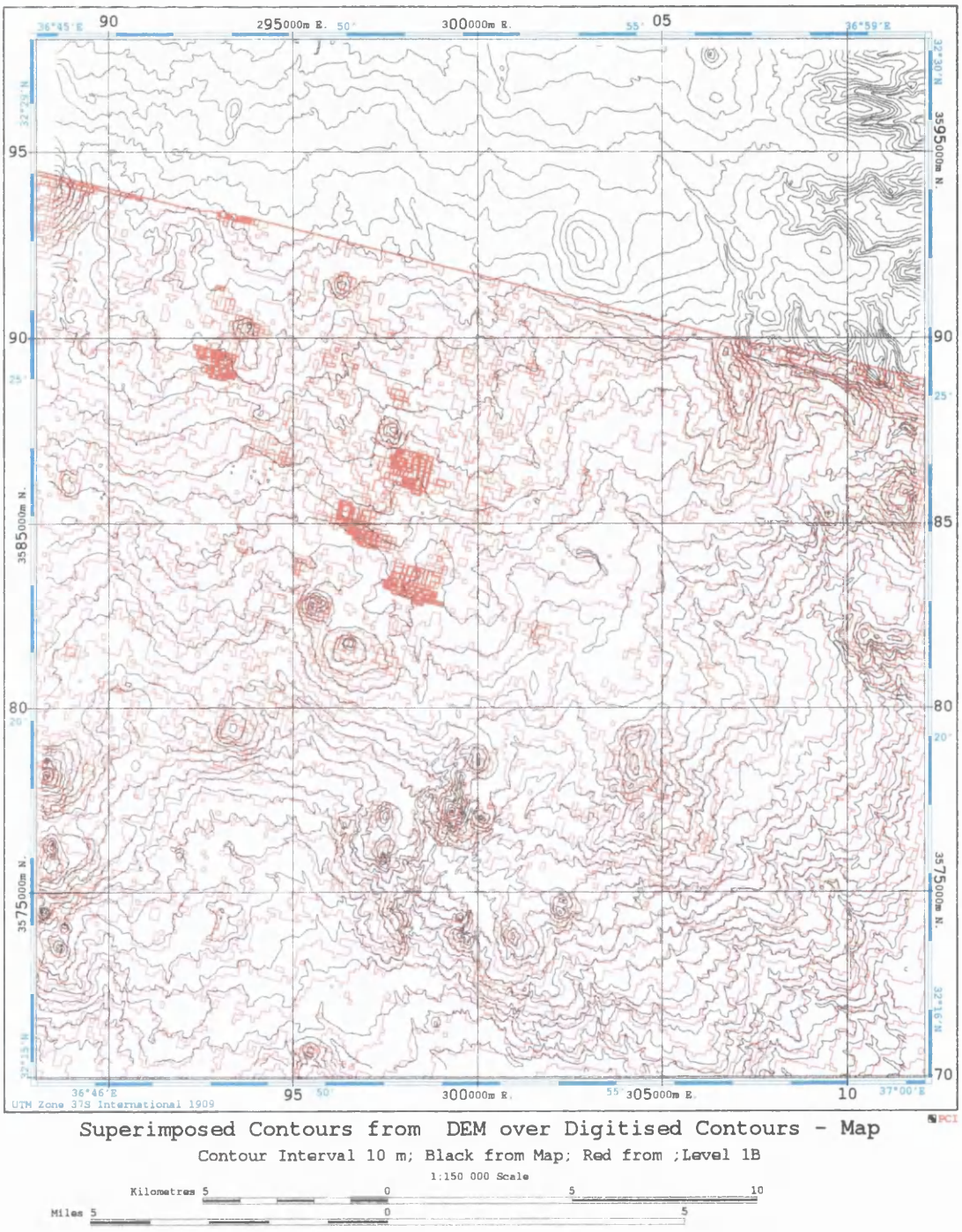

Figure 10.16 Contours at 10m interval extracted from the Level 1B DEM of the main reference stereo-pair for scene 122/285 superimposed over the corresponding digitised contours from the RJGC 1:50,000 scale topographic map.

10.9.2 Comparison of Heights given by the Contours from the Reference Map with the Corresponding Values given by the DEM

In this type of accuracy test, first of all, the DEM should be loaded into ImageWorks using 16-bit data, followed by the superimposition of the file containing the digitised 50m contours. After this had been done, the **VATT** program that is available in EASI/PACE has been used to carry out the test. Before running this program, several parameters need to be specified. These include those related to the input file; the georeference segments; the database input channel; the database input windows and finally, the text file. The program then displays the coordinates and the elevation of the point given by the cursor location when the analyst clicks the cursor. By selecting one of the digitised contours and first placing the cursor at one end of the line, the author then followed the contour line exactly, reading off the corresponding coordinates and elevations given by the DEM on the display sceen whenever there were changes in the shape and direction of the contours. In fact, the elevation values that have been displayed and recorded are the heights on the DEM surface at each successive cursor location. From these readings, the analyst can note the change in the height value given by the DEM to be either negative or positive compared with the elevation value of the contour used as the reference line. In an ideal case, the digitised contours would be perfectly correct and the DEM very accurate, in which case, the heights given at the successive cursor locations should have the same constant value as the reference contour line, but obviously this is not the case.

10.9.2.1 Comparison of DEM Heights with 50m Contours

The first comparison was carried out using the 50m contours from the 1:250,000 scale map for the area covered by the reference scene 122/285. After finishing the first line, the next elevation line was selected and the same procedure was carried out. By this method, five to eight contours at different elevations have been selected, measured and recorded. For the Level 1B DEM, 719 points have been measured and recorded. The RMSE value of the differences in height between the elevations at the measured cursor positions and those given by the digitised contours has been calculated, giving a figure of ± 7m for the Level 1B DEM. The same process has also been carried out for the

DEM extracted from the Level 1A stereo-pair. The RMSE value of the elevation differences obtained for 531 points was ± 8m.

Later the same procedures have also been carried out for the rest of the Level 1B stereo-pairs of the Badia Project area. For the DEM extracted from the Level 1B Stereo-pair 123/286, the RMSE value of the differences in elevation obtained at 403 points along selected contours was ± 6.1m. While for the DEM extracted from stereo-pair 123/285, the RMSE value obtained from the elevation differences at 442 points was ± 8.1m. Finally, with the remaining two Level 1B stereo-pairs, 124/285 and 124/286, the elevation differences at 443 and 410 points respectively gave RMSE values of ±6.3m and ±7.8m.

It can seen from the summary provided in Table 10.1 that the accuracy of the elevation values obtained from Level 1B DEM is slightly better than the accuracy obtained from the Level 1A data. It can be seen also that somewhat better results were obtained from stereo-pairs 123/286 and 124/285: in this respect, one notes that a very big part of these two scenes comprise flat areas. But taken as a whole, the RMSE values are quite remarkably consistent.

DEM	Scene	No. of points	RMSE ΔH
Level 1A	122/285	531	±8.0m
Level 1B	122/285	719	±7.0m
Level 1B	123/285	442	±8.1m
Level 1B	123/286	403	±6.1m
Level 1B	124/285	443	±6.5m
Level 1B	124/286	410	±7.8m

Table 10.1 Comparison of the heights given by the contours from the reference map with the corresponding values given by the DEM.

10.9.2.2 Comparison of DEM Heights with 10m Contours

Another set of accuracy tests have been carried out using the 10m contour data from the 1:50,000 scale map following the same procedures as those described above. In this test, only the contours digitised from the 1:50,000 scale topographic map of Deir Al-Khaf and covering part of the Level 1A and 1B DEMs of the reference scene 122/285 have been tested. For the DEM extracted from the Level 1B stereo-pair for scene 122/285, the

RMSE value of the differences in elevation obtained at 257 points along the selected contours was ± 4.9m. While for the DEM extracted from the Level 1A stereo-pair for scene 122/285, the RMSE value of the differences in elevation at 257 points along selected contours was ± 6.9m. Again in this test, the comparison of the results of the DEM elevation measurements along the corresponding digitised contours show that better results in terms of the RMSE value were obtained with the Level 1B DEM.

10.9.3 DEMs Accuracy at the GCPs

The EASI/PACE system produces a report after the DEM extraction process has been completed and the elevation values calculated. This report declares the accuracy in terms of the RMSE values of the errors in elevation at the control points and check points. In fact, the accuracy that is being quoted here is, to a large extent, that of the matching algorithm that is used in this system. The disparity resulting from the difference in location between the centre of the matching template and the position of the GCP is input to the mathematical model to compute the elevation at the centre of the template. Table 10.2 shows the RMSE values of the differences in elevation at the control points and check points for each of the five Level 1B DEMs in addition to that produced for the Level 1A DEM of the main test area. However, it must be noted that these values were not determined from the measured image coordinate values of the GCPs carried out for the resection procedure, but purely from the disparities generated during the subsequent image matching procedure carried out for the DEM extraction.

For the DEM produced by the Level 1B stereo-pair for scene 122/285, several comparisons were made using different combinations of control and check points for the DEM extraction process. The best accuracy obtained in terms of the RMSE values in elevation was ±3.3m using 15 check points. By increasing the number of check points to 25 and to 35, the RMSE values in height in the DEMs obtained through a comparison of the elevation values derived from the image matching with the given values for these points were ± 3.7m and ± 3.6m respectively. However, in this test, the range of differences in accuracy between 15 to 35 check points is 0.4m, which very small, indeed insignificant.

DEM No.	No. of Points	ΔH (m)	No. of Points	ΔH (m)
122/285 Level 1B	32	±2.4	15	±3.3
	22	±3.8	25	±3.7
	12	±3.7	35	±3.6
	47	±3.7	-	-
122/285 Level 1A	31	±3.8	15	±4.3
	25	±4.0	20	±3.4
	10	±4.5	36	±3.5
123/285 Level 1B	16	±4.7	-	-
	9	±5.8	8	±3.3
123/286 Level 1B	18	±3.9	11	±3.7
	15	±4.9	14	±3.9
	29	±2.6	-	-
124/285 Level 1B	18	±3.2	-	-
	8	±4.8	8	±6.2m
124/286 Level 1B	12	±3.7	-	-

Table 10.2 RMSE values in height at the control and check points in the DEMs obtained through a comparison of the elevation values derived from the image matching technique and the values obtained from the GPS ground survey.

Coming next to the Level 1A DEM produced from the stereo-pair for scene 122/285, three different combinations of control and check points were used for DEM extraction. The RMSE value obtained using 15 check points was ± 4.3m, whereas the RMSE values obtained using 36 check points were ± 3.5m, and ± 3.4m for 20 check points. Thus the RMSE values fall within a range of 0.9m for 15 to 36 check points - which again shows remarkable consistency.

For the Level 1B stereo-pair for scene 123/285, two DEMs have been extracted. In the first test, the RMSE values of the errors in height obtained at the full set of ground control points was ±4.7m. In the second test, using a combination of control and check points, the RMSE value in height using 8 check points was ± 3.3m. For the DEMs produced from the Level 1B stereo-pair for scene 123/286, three separate DEMs have been extracted; two of these DEMs were extracted with different combinations of control and check points. The RMSE values in elevation obtained at 11 and 14 check points were ±3.7 to ± 3.9m respectively, whereas for the full set of 29 ground control points, the RMSE value in elevation was ± 2.6m.

In the case of the DEM produced from the Level 1B stereo-pair for scene 124/285, two DEMs have been extracted. The RMSE value for the elevation errors at the whole set of ground control points used for the first test was ±3.2 m, whereas, for the second test, the

RMSE value for the elevation errors at the check points was ±6.2m. The final test was to carry out a similar check on the DEM produced from Level 1B stereo-pair for scene 124/286. The RMSE value for the errors in height obtained at the control points was ± 3.7m.

In general, inspection of the results in terms of the RMSE values obtained in this way at the check points for all of the individual DEMs covering the Badia area reveal that the accuracy is almost constant. The range in the RMSE values in elevation varies between ±3.3m which resulted from the DEM produced from the Level 1B stereo-pair for scene 122/285 to ±6.2m that resulted from the DEM produced from the Level 1B stereo-pair for scene 124/285. Only one of the Level 1B DEMs - that for scene 124/285 - shows a higher RMSE value compared with the others. This could be caused by the area being flat and featureless and the number of the control points being limited. However, based on the results from these tests, the high accuracy of the height values obtained from the DEMs over the Badia area reflects the very high standard and quality of the ground control points (GCPs) which have been established in the test field, besides the excellent performance of the image matching algorithm used in the EASI/PACE system.

Vector plots of the residual errors in height calculated at the control and check points through image matching when compared with the corresponding elevation values of the GPS points for the Level 1B DEM for scene 122/285 are shown in Figure 10.17. Some kind of systematic error appears especially in the north-eastern part of the vector plot where a group of points all have positive signs. Inspection of the location of these points showed that they are located in a quite dark area of the images where there exists a recent flow of the basaltic lava.

Inspection of the vector plot of the residual errors in elevation of the Level 1A DEM for scene 122/285 given in Figure 10.18 shows that some points display some kind of systematic error in the form of positive signs in the north-eastern part of the vector plot, where again the same kind of basaltic features are occuring.

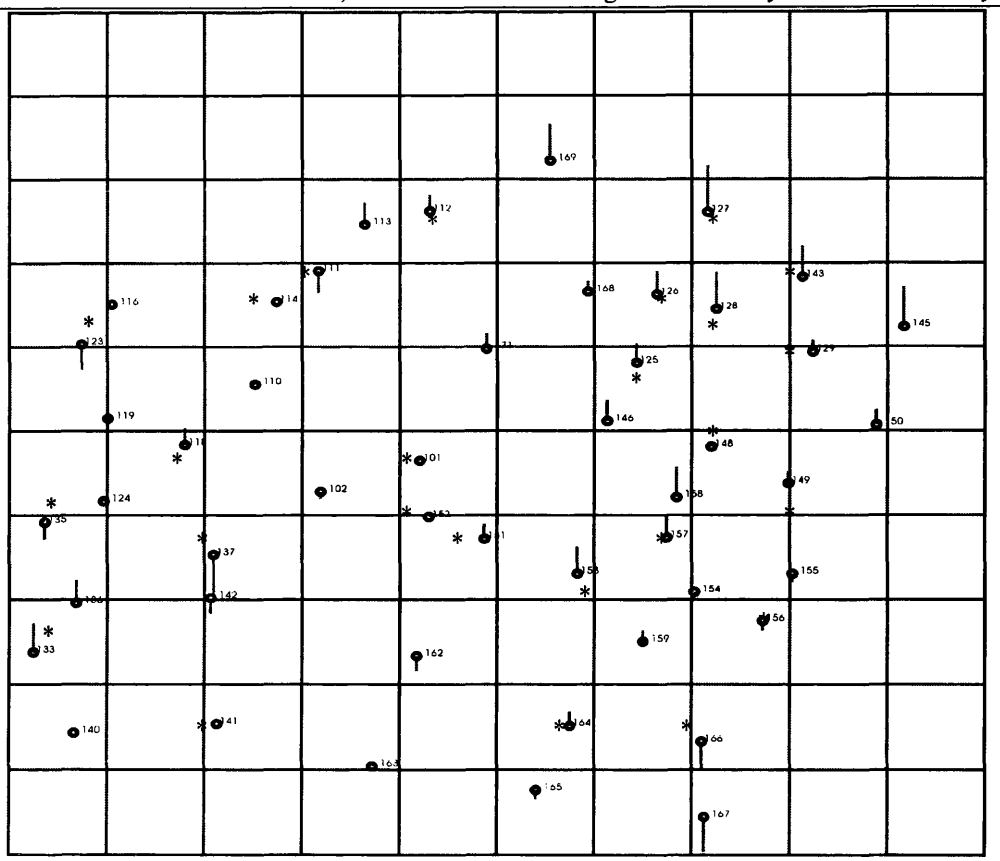

Figure 10.17 Vector plot of the residual errors on height at the control and check points for the Level 1B DEM for scene 122/285 Control points o Check points o *

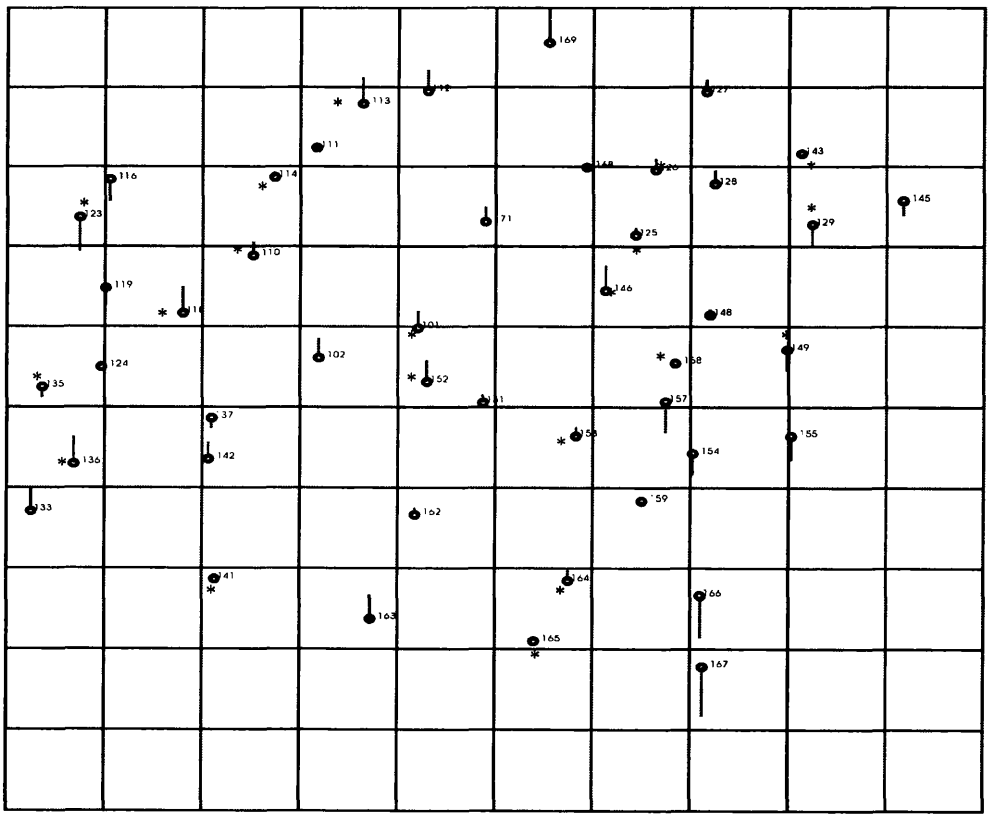

Figure 10.18 Vector plot of the residual errors in height at the control and check points for the Level 1A DEM for scene 122/285 Control points o Check points o *

10.9.4 Accuracy Tests Using the GPS Profiles

For a further validation of the DEM data, accuracy tests have been carried out using two GPS profiles measured by the RJGC surveyors along the main roads of the Badia area. More than 15,000 Differential GPS measurements have been obtained. Of these, a total of 1,248 points have been used to test the accuracy of the DEMs with an average distance of 150m between these points. The 40 GPS points used as base stations were observed in static mode with 1 hour of observations made during each session. The measurements of the rest of the points have been carried out in kinematic mode using a 2 second recording interval in vehicles travelling at speed of 20-25 km/hr. These profiles cross the stereomodels 122/285, 123/285, 123/286 and 124/285. To check the accuracy, the corresponding elevation values measured on the DEMs were extracted. This was done through the coordinates of each point measured by the GPS survey being located in the DEM using the cursor on the display screen.

After recording the elevation values in the DEMs at the positions of all these GPS pofile points, a comparison of the two sets of elevation values was made by finding the differences between the elevation values of each point in the two sets - i.e. the GPS elevation values and the corresponding DEM elevation values. All the differences between the two sets of points were added and the sum divided by the total number of points to give the value of the mean difference between the sets. The mean difference obtained for 1,248 points was 24m - which almost certainly was caused by a datum error. Afterwards, this difference between the two sets of elevations (i.e. the profile elevations and the DEM elevations) was applied to each point. Then the residual difference for each point was squared and added to each other and divided by the number of points, after which, the square root was obtained to get the standard devation. The accuracy in terms of the standard deviation obtained using the profile points which have been selected to check the DEM's accuracy was ± 6.1m. Another test has also been carried out using 528 GPS survey points from the profile data on the Level 1B DEM for the reference scene 122/285 with a standard deviation of ±6.0m.

10.10 Planimetric Accuracy Test of the Orthoimages Produced from the Level 1A and 1B Stereo-Pairs for Scene 122/285

Regarding the geometric accuracy of the final orthoimage, a check was carried out by measuring quite independently on the orthoimage the position of 43 of the GCPs lying within the area of the main test scene, 122/285. These points have been measured using the EASI/PACE system and the transformation and comparison of the transformed measured values and the given coordinate values of the GCPs was executed by a computer program called **LINCON** written in FORTRAN 77 and available from the Department's software library. Using a simple linear conformal (first-order) transformation, the measured x/y image coordinates were transformed into their equivalent E/N terrain coordinates in the UTM system. These were then compared with the corresponding E/N coordinate values derived from the GPS ground survey.

The resulting RMSE values for the Level 1B orthoimage were ±8.7m in ΔE and ±8.8m in ΔN. For the 20m pixel size used to produce the final ortho-image, these give RMSE values of ±0.44 pixel in both the x and y-directions on the orthoimage. The vector plot (Figure 10.19) of the individual residual errors resulting from the comparison showed a completely random distribution with no systematic components. This confirmed the excellent results of the whole process in geometric terms as well as in qualitative terms.

A similar test has been carried out for the orthoimage of the main test area covered by scene 122/285 derived from the Level 1A stereo-pair. The resulting RMSE values for 40 GCPs were ±9.1m in ΔE and ± 9.7m in ΔN. For the 20m pixel size, this gives an RMSE value of ±0.46 pixel and ±0.48 pixel in x and y respectively. A summary of these results is given in Table 10.3.

Orthoimage		No. of GCPs	RMSE in Pixels			RMSE in Metres		
Scene	Level		Δx	Δy	ΔPl	ΔE	ΔN	ΔPl
122/285	1B	43	±0.44	±0.44	±0.6	±8.7	±8.8	±12.3
122/285	1A	40	±0.46	±0.48	±0.67	±9.1	±9.7	±13.3

Table 10.3 Accuracy tests of the orthoimages of the main test field (scene 122/285)

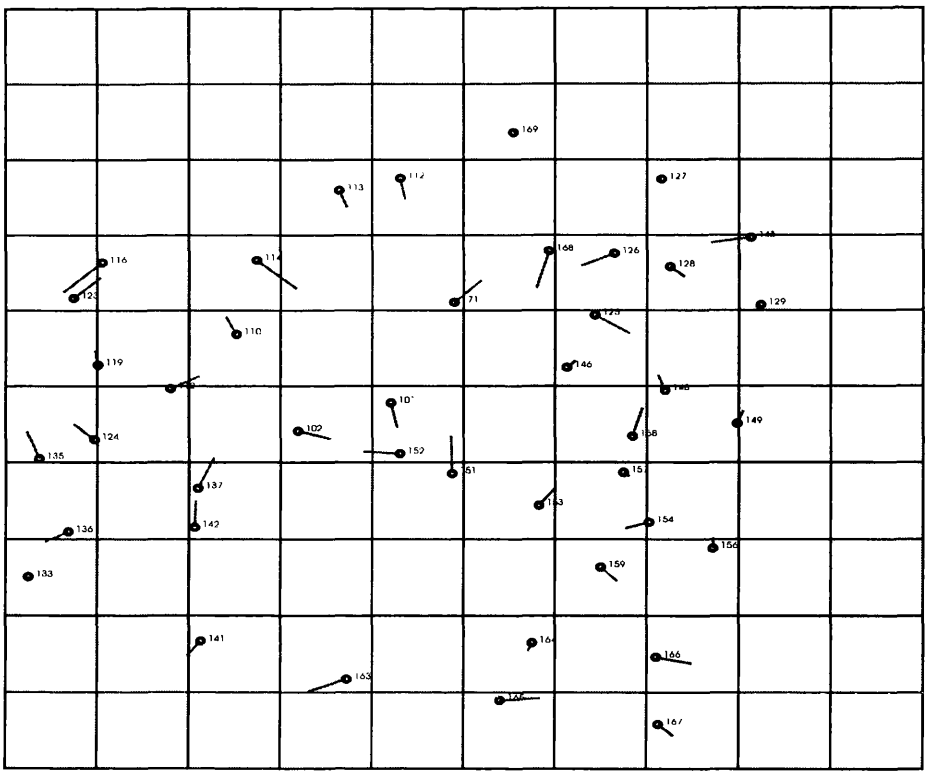

Figure 10.19 Vector plot of the residual errors in planimetry at the GCPs of the orthoimage of the Badia test field (122/285) using a linear conformal transformation.

10.11 Conclusion

In this chapter, the production of the DEMs, contours, and orthoimages, and their merging and mosaicing and the generation of perspective fishnet block diagrams using the EASI/PACE system has been described at some length. In general terms, the work has been carried out quite smoothly with some minor problems related to the availability of memory when merging the contours and in the radiometric matching of the five orthoimages during the mosaicing operation. The first problem has been solved by merging the contours on a workstation belonging to PCI. The final contours showed no evidence of joins or discontinuities along the boundaries between the stereo-models. The second difficulty has been solved by the present author through the testing of several samples and applying the results of this sampling to the orthoimages that were undergoing the mosaicing process. The good result achieved in these tests was seen on the final orthoimage mosaic which displays a smooth grey level appearance with no joins being evident between the images. The system worked in a fast and stable manner throughout the processing without any problem. The visual quality of the final product

can be regarded as excellent. As noted previously, EASI/PACE is a complex sophisticated and flexible image processing system which needs a lot of time and effort to master. Once this has been achieved, it produces results of a high quality.

The second part of this chapter was concerned with the validation of these products - in particular with regard to their geometric accuracy. Tests were devised and excuted to validate the DEMs, contours and orthoimages produced by the EASI/PACE system. Validation of the DEMs has been carried out using four different methods. These include the superimposition of the contours extracted from the DEMs over the digitised contours from the existing RJGC1:250,000 and 1:50,000 scale topographic maps. This test is qualitative since it depends on a visual analysis of the fit between the contours, but a mainly excellent agreement resulted between the respective sets of contours. The second method comprised a comparison between the elevation values given by the existing contours and the corresponding elevation values given by the DEMs. The third test comprised the accuracy reports for the elevation values at the GCPs for the DEMs produced by the system. The results from this test reflect the fact that the image matching technique employed in the system has worked in a thoroughly satisfactory manner to produce an acceptable DEM, contour plot and orthoimage mosaic for a very large area of desert terrain using SPOT Level 1B stereo-imagery. The fourth test has been carried out using the profiles measured by the GPS ground survey. Once again, good agreement was achieved between the two sets of elevation values. In general, all of these tests reflected the relatively high accuracy of the height values contained in the DEMs that are produced by the EASI/PACE system - at least in terms of the requirements of small-scale topographic mapping. This also reflects the high quality of the GCPs and contour data sets established in the Badia test field. Of course, the high quality of the GCPs also revealed that the EASI/PACE system worked very well when supplied with very good quality image data and GCP data.

From the extensive test results contained in Chapters 9 and 10, it would appear that the photogrammetric algorithms used in the EASI/PACE system are capable of producing an acceptable result that may be useful for topographic mapping and map revision at small scales within a fully digital photogrammetric environment - at least within the constraints of the resolution and cross-track geometry of the SPOT stereo-imagery.

The next chapter will report on the experiences and results gained with a similar extensive series of tests carried out using the DMS system which operates on a quite different basis and in a very different manner to that employed in EASI/PACE.

CHAPTER 11: GEOMETRIC ACCURACY TESTS AND VALIDATION OF DEMs, CONTOURS AND ORTHOIMAGES USING DMS SOFTWARE

11.1 Introduction

As discussed in Chapter 6, the DMS system from R-WEL is designed to handle only Level 1B SPOT stereo-pairs for DEM extraction and orthoimage generation. In this chapter, first a discussion of the various image processing steps will be undertaken; then the problems encountered with this system will be discussed; and finally the results of the extensive series of geometric accuracy tests which have been carried out by the author will be presented using combinations of control points and check points taken from the Badia test field. As the account will show, initially it was quite impossible to form a stereo-model and fit it to the ground control points (GCPs), while the errors at the GCPs in planimetry (X/Y) and in elevation (Z) were very large. Satisfactory results have only been achieved after some modules have been modified and other new modules have been added - to a large extent as a result of the author's tests.

Once these modifications had been made, validation of the DEM and orthoimage data produced by DMS could be undertaken. Thus the results of tests of the contours which been generated from the DEMs produced by DMS and superimposed on the contours from the RJGC maps will be presented, together with a comparison of the elevation data derived from the SPOT DEMs with those measured along the profiles using GPS. Finally the mosaicking of the DEMs and the generation of the orthoimages of the test area and their geometric accuracy will be discussed and the results presented.

11.2 Initial Accuracy Test of the Reference Level 1B Stereo-pair for Scene 122/ 285

The two Level 1B images making up the stereo-pair 122/285 have been imported to the DMS environment using the package's **data-raster conversion** routine. This was followed by the application of the global equalization enhancement routine that is available in the package which permits the radiometric enhancement of an image. The image grey level values are assigned to the display levels on the basis of their frequency

of occurrence. In this way, the contrast of the displayed image can be strictly controlled to optimize the viewing parameters that suit the observer. More display values are assigned to the frequently occurring portion of the histogram and hence the radiometric detail is being enhanced. Essentially the image grey level value range is being stretched over a larger portion of the display levels.

Using the Level 1B stereo-pair of scene 122/285 covering the main test area, 40 ground control points have been measured individually on both the left and right images. The next step in the procedure involved the image-to-image registration of the two individual images of the stereo-pair, However the **Registration** option that implements this operation failed to run, and no rectangular box appeared for the registration of the two images. Instead a manual method had to be applied for the registration of the two images. In addition, after running this registration program, no declaration of the residual errors at the GCPs took place. As a result, the author had to escape to another program and run the polynomial coefficient sub-module within the **geocode** module to see the results, and having selected the order of polynomial to be used, it was then possible to fit the images to the GCPs in an approximate way. However, typically the RMSE values in X and Y that were obtained for each of the two component (left and right hand) images making up the stereo-pair were of the order of ±48m with maximum error values of around 90m using the first order terms, and ±34m when the second order terms were used.

The vector plot (Figure 11.1) of the RMSE values of the residual errors at the GCPs showed a pattern of systematic errors occuring in the north-western part of the area covered by the stereo-model. It was clear that these results which have been obtained for the planimetric accuracy of the fit of the images to the GCPs were very poor in absolute terms having regard to both the 10m pixel size of SPOT and to the high quality GCPs which have been obtained by GPS measurements, with an accuracy (σ_{Pl}) of ± 1 to 2m.

In spite of these poor results in terms of the planimetric fit of the stereo-pair to the GCPs, the set of procedures available in DMS have then been used to extract a DEM and to obtain the heights of the terrain points at the required grid spacing interval. When

the DEM file was examined, it was found that the range of elevations did not represent or agree with the range of elevations that were actually present in the area. When the results that had been obtained were compared with the corresponding points on the existing RJGC topographic map at 1:50,000 scale, it was found that the differences in height of some of these points amounted to 300m.

This resulted in an extensive interchange with Professor Welch and Mr. Jordan at the University of Georgia over a period of a year, during which time, the various problems that had been encountered by the author during his tests of the DMS system using the Badia stereo-models were gradually sorted out. Needless to say, this involved numerous alterations to the various programs contained in the SPOT module of the DMS package and the execution of many tests to confirm that the altered programs really did work and solved the difficulties and errors encountered with the program.

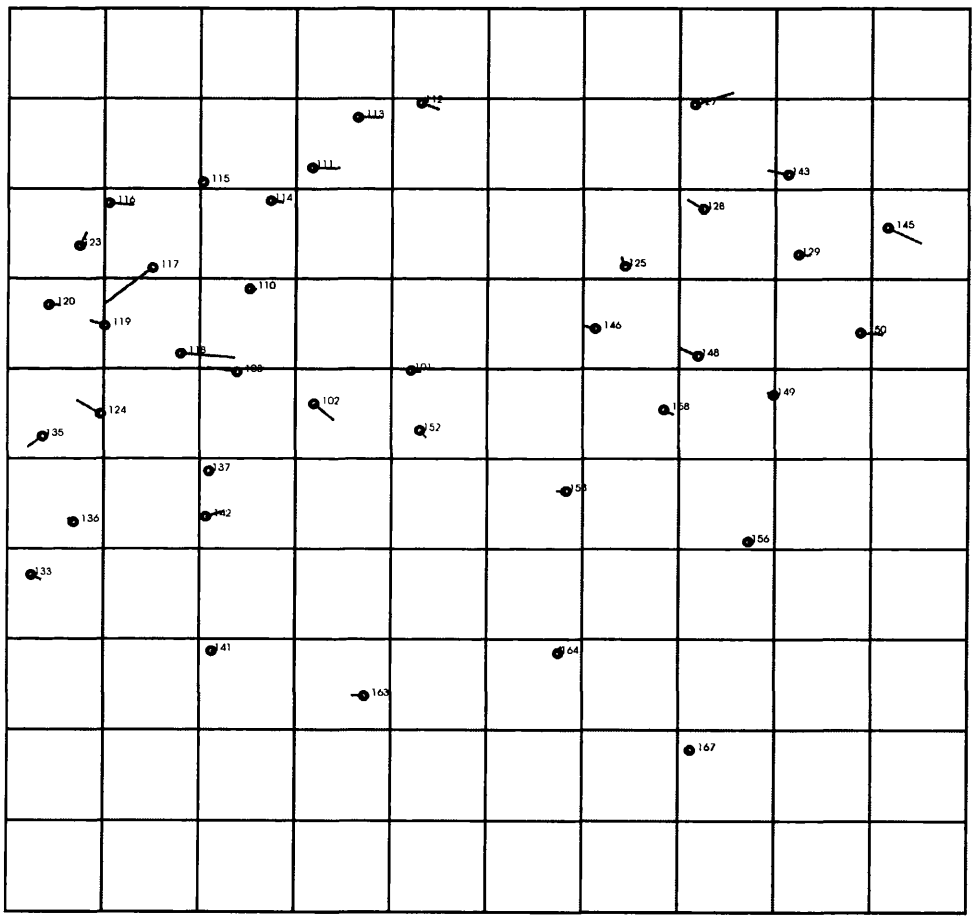

Figure 11.1 Vector plot of the planimetric (X/Y) errors at the ground control points for the SPOT Level 1B stereo-pair of scene 122/285 of the test area

11.2.1 DMS Problems

Based on the author's tests and experiences using DMS with the SPOT stereo-images, besides the major problems with the image-to-image registration outlined above, the following difficulties were presented to Professor Welch and Mr. Jordan for their attention and remedy.

A. Operational Aspects

- One quite troublesome matter that was encountered concerned the measurement of the ground control points (GCPs) on each of the individual SPOT images. The control of the measuring mark or cursor using the mouse was poor and the cursor shook considerably when it was being moved on to the position of the GCP. This caused real uncertainty as to whether the measurement was accurate or not. Moreover, even when taking extreme care during the measurement of the GCP position on the screen, when the mouse button was finally clicked, the cursor pointing moved off the measured position quite noticeably, some times by several pixels, even though the mouse had definitely not been moved. This did not give the user confidence that an accurate pointing was being made to the GCP and could be the source of some of the poor results.
- Next came the combining of the two individually rectified images to form the stereo-model using the so-called **Stereoplotter** module of DMS. The main problem that the present author encountered here was the selection and definition of the area that is common to the two images. It was found that this procedure was extremely difficult to carry out - in particular, finding and ensuring that the centre of each box lies on exactly the same point proved to be extremely difficult. If this was not achieved, then it resulted in an overall lack of correspondence (i.e. a y-parallax) between the two images.
- Another specific complaint about the **SPOTREG** module was that if, during the measurement of a ground control point (GCP), a mistake is made by the operator in the pointing to the GCP, it was impossible to delete the point in question.

B. Accuracy of the Results

- The large dimension of the planimetric errors occuring overall and their systematic nature in parts of the stereo-model was very apparent.
- Most serious of all was the fact that, when the DEM file was examined, the range of elevations did not represent or agree with the range of elevations actually present in the area.
- Furthermore, when the stereo-viewing was implemented with the DEM superimposed on the stereo-model, the vast majority of the grid points were found to be floating well above the terrain surface.

The test images and ground control point data were also sent to the University of Georgia to allow the testing of the modified programs to be carried out in-house.

After two months, a response was received. It came from Mr. Jordan who was assigned the task of investigating and putting right these various problems. His first response included the results of the tests that he had carried out using the modifications that he had made to the software. In particular, he sent the author the results of the test that he had carried out in terms of the planimetric and elevation errors occuring at 22 check points withheld from the solution, together with a DEM created with 100m post (i.e. grid) spacing. His results are given in Table 11.1. The RMSE value of these residual errors in height was ± 8.9m.

Point No.	X	Y	Z	Cal. Z	ΔZ
101	308544.7	3559871	810.3	821.2	+10.9
102	300921.8	3557099	797.7	801.8	+4.1
103	294889.3	3559725	814.2	828.9	+14.7
110	295871.2	3566646	942.6	947.3	+4.7
111	300741.9	3576802	1104.9	1112.1	+7.2
114	297526.4	3574025	1059.9	1064.9	+5
115	292203.0	3575577	1049.7	1050.4	+0.7
117	288243.3	3568402	945.4	952	+6.6
118	290484.4	3561273	848	850.5	+2.5
119	284545.8	3563608	836.7	842.4	+5.7
123	282548.9	3570243	926.5	931.6	+5.1
125	325223.1	3568548	747.5	755.6	+8.1
126	326827.1	3574684	758.2	762.2	+4
146	322957.3	3563359	707.8	712.4	+4.6
148	330976.6	3561085	653.1	667.9	+14.9
151	313517.4	3552940	716.6	740.9	+24.3
152	309233.0	3554859	751.1	760.8	+9.7
157	327583.7	3553037	643.2	646.7	+3.5
158	328329.5	3556594	646.4	655.8	+9.4
168	321496.0	354939	793.9	801.8	+7.9
170	304708.6	3572786	1033.7	1037.1	+3.3
171	313698.7	3569807	886.8	883.3	-3.5

Table 11.1 Errors in elevation at the check points using DMS for the Level 1B stereo-pair of scene 122/285

At this stage, Mr.Jordan did not comunicate to us in Glasgow the methods he used to get this much improved result, where he had had to change the way the images were registered and oriented to ground coordinates. Nor did he mention how many control points he used in this solution and what was the accuracy of fit at the control points. However it was clear from Table 11.1 that all the values of the differences in height at the check points that he had obtained were positive in sign except for one single point that was negative. This gave a strong indication that the modified version of DMS still gave rise to a systematic error in the elevation values of these points.

11.2.2 DMS Modified Version

After another four months, a further modified version of DMS with new program files was received by the author. These included new procedures for creating the SPOT stereomodel and the DEM, and for checking the accuracy of the resulting DEMs and orthoimages. At the same time, Mr. Jordan sent the results of an accuracy test of the DEMs and the orthoimage that he had carried out with the main Level 1B stereo-pair for scene 122/285.

Some of the new programs were designed to implement new procedures for registering SPOT stereo image data and were meant to replace the original **SPOTREG.BAT** and **SPOT_REG.EXE** programs. The new **SPOTREG.BAT** and **SPOT_REG.EXE** programs are simply revisions of the original ones but **SPOTSYNC.EXE** and **SPOT_REL.EXE** were new programs. In addition, four other new programs were supplied. These comprised **POINT2.EXE**, a program for point measurement and transfer; **SPOTCP.EXE** which is a utility program used for merging two CP files into a CPS file and removing relief effects from CPs; **CHKDEM.EXE** which is used to evaluate the accuracy of the correlated DEM against GCPs; and **CHKGCP.EXE** which is used to evaluate the planimetric accuracy of the orthoimages or rectified images. Before describing the new image processing procedures, it is worth mentioning the following results that have been obtained from Mr. Jordan.

Test I

For the SPOT Level 1B stereo-pair of scene 122/285, using the new registration routine, the images were registered to within ±5 m using 6 control points distributed throughout the entire image area. The remainder of the GCPs were withheld from the solution for use as check points. Over a small (2,000 x 2,000 pixel) test area forming part of the stereomodel containing 5 check points, a DEM was created using the **MAP-Stereocorrelation** option in DMS. The results achieved in terms of the RMSE value of the residual errors in height was ±4.5 m.

Test II

The results for a DEM derived from the stereomodel encompassing most of the image area and using 50m post grid spacing and 15x15 correlation matrix are provided in Table 11.2 which gives the data for 6 control points and 21 check points.

Point No	X	Y	Z (m)	Cal. Z (m)	ΔZ (m)
101	308544.7	3559871	810.3	819.6	9.3
103	294889.3	3559725	814.2	823.9	9.7
110	295871.2	3566646	942.6	942.1	-0.5
111	300741.9	3576802	1104.9	1104.2	-0.7
112*	**309287.9**	**3558216**	**1093.7**	**1096.9**	**3.2**
113*	**304306.2**	**3580947**	**1153.9**	**1138.2**	**-15.7**
114	297526.4	3574025	1059.9	1059.2	-0.7
115	292203	3575577	1049.7	1055.5	5.9
116*	**284865.3**	**3573803**	**990.8**	**983.2**	**-7.6**
117	288243.3	3568402	945.4	952.3	6.9
118	290484.4	3561273	848	849	1
119	284545.8	3563608	836.7	839.2	2.5
120*	**280182.8**	**3565344**	**827.5**	**802.5**	**-25**
123	282548.9	3570243	926.5	930.6	4.1
125	325223.1	3568548	747.5	760.8	13.3
126	326827.1	3574684	758.2	762.2	4
127*	**330679.4**	**3582062**	**741.4**	**740.6**	**-0.7**
128*	**331363.3**	**3573362**	**714.6**	**719.9**	**5.3**
146	322957.3	3563359	707.8	721.3	13.5
148	330976.6	3561085	653.1	668.2	15.1
151	313517.4	3552940	716.6	740.5	23.9
152	309233	3554859	751.1	778.1	27
157	327583.7	3553037	643.2	646.6	3.4
158	328329.5	3556594	646.4	657.9	11.5
168	321496	3574939	793.9	797.3	3.4
170	304708.6	3572786	1033.7	1034.9	1.2
171	313698.7	3569807	886.8	890	3.5

Table 11.2 Elevation errors (in metres) at the control and check points (* = control points)

Table 11.2 summarizes the results in elevation at all the GCPs showing an overall RMSE value of ±11m. The RMSE value of the errors in height obtained at the control points only was ±10.6m, while the value for the check points was ±12.1m. Obviously these results received from the supplier were much more encouraging and so testing of the DMS package was resumed by the present author.

11.3 Tests of the New Image Processing Procedures for Registration and DEM Extraction

11.3.1 Measurement of the GCPs

Once the new programs had been received from the software supplier, the Level 1B stereo-pair for scene 122/285 covering the main test area was again selected for a geometric accuracy test and subsequent processing to extract a DEM. According to the new procedures, the routine **POINT2.EXE** was to be used as the first step in the image processing after the two scenes forming the stereo-pair had first been enhanced to maximize their image contrast and improve interpretability by employing the histogram equalization routine to the raw image pixels. This increased the contrast by expanding the range of DN values used to depict the images. The positions of the GCPs on the image were then measured through the new **POINT2.EXE** module. The two images that form the stereo-pair were displayed side-by-side and the control points were measured sequentially on both images. This procedure created two CP files, each file containing the appropriate pixel coordinates and control point numbers for the measured positions of the GCPs on the two images.

11.3.2 Merging the CP Files

Also with the new procedures, another new module called **SPOTCP.EXE** had been created. This merges the two individual SPOT CP files into a single CPS file and removes relief effects from the CPs. It is important at this stage to differentiate between the left and right images of the stereo-pair from the point of view of checking the data integrity.

11.3.3 Registration

In the actual operation of the modified version of DMS with the Badia data, the two images were displayed side-by-side on the computer screen and 35 registration points were identified on each image. The left image has been used as the reference image on to which the right image is to be registered. After the registration points had been

measured and declared, the image-to-image registration solution was adjusted (i.e. improved) by eliminating the less good points. On this basis, 10 points with a mis-registration of more than 10m have been eliminated and the remaining 25 points have been used with an accuracy in registration of ± 6.3m in terms of their RMSE value. Next the area of the output stereo-model was defined on the graphic screen. After this had been done, the stereo-model will be created. The polynomial transformation based on a least squares solution was then implemented to yield correction coefficients and to determine the RMSE value indicating the fit between the image and ground coordinates. From the transformation, the set of coefficients was calculated to provide the first or second order transformation parameters necessary to rectify or geocode any measured image detail and bring it into the reference coordinate system. The file COF contains the transformation parameters necessary to geocode an image and also to relate the vectors to the image.

In practice, the process involved in this step is automated through the use of the batch file that drives it and the COF file that is created in the last step. In this step, two files are produced containing image data that has been rectified and resampled but without the rotation of the images with respect to north. At the end of the process, the fit of the stereo-model to the GCPs should be declared.

However, this did not happen when the present author implemented the procedures. The problem was to discover why the system did not declare this step. So comunication with Mr. Jordan started again. Different solutions were tested to try and run this procedure successfully, but unfortunately they did not succeed. Finally, after more investigation and testing by the author and liaison with Mr. Jordan, the clue to the solution was found. When Mr. Jordan was through fixing the various problems, he used the Windows interface to initiate the process. This creates a file called **BATCH.DAT** that contains 13 parameters. The SPOTSYNC program reads this file to pick out the last parameter and to use it in subsequent steps. When the author used the DOS procedure (since Windows had not responded to some procedures), the BATCH.DAT file was not there. When the author created the BATCH.DAT file with 13 parameters (it needs to be created for every stereo-pair), the final stage of the registration process was successfully implemented and

the results declared. Obviously the new version of DMS supplied to the Department had not been set to generate the requisite file.

11.3.3.1 Planimetric Accuracy and Vector Plot of Stereo-pair 122/285

In the final stage of the registration process, the system declares the residual errors in planimetry at the ground control points in the form of a table - in this case for the second order polynomial (see Appendix C). From the 45 ground control points which have been measured on the images, different combinations of the control points and check points have been used to establish the geometric accuracy in planimetry as shown in Table 11.3.

Scene No.	No. of Control Points	RMSE Values (m)			No. of Check Points	RMSE Values (m)		
		ΔE	ΔN	ΔPl		ΔE	ΔN	ΔPl
122/285 1B	45	±8.4	±7.8	±11.5				
	35	±9.1	±8.0	±12.2	10	±5.6	±7.4	±9.3
	30	±8.7	±7.9	±11.8	15	±8.1	±8.1	±11.5
	25	±8.8	±8.3	±12.1	20	±9.9	±7.4	±12.4
	20	±9.5	±8.5	±12.8	25	±8.7	±8.1	±11.9
	15	±9.4	±9.1	±13.1	30	±8.7	±7.8	±11.6
	10	±8.5	±8.0	±11.9	35	±10.8	±9.1	±13.5

Table 11.3 RMSE values for the residual errors in planimetry at the control points and check points for the SPOT Level 1B stereo-pair for reference scene 122/285

It can be seen from this table, that the accuracy of the planimetry as expressed in RMSE values falls in the range between ± 11.8m to ± 13.1m for the control points and ± 9.3m to ± 13.5m for the check points. The best result of ± 9.3m obtained for the check points occurred when only 10 check points have been used in conjunction with the maximum number (35) of control points. Otherwise for the control points, the results in planimetry do not vary much from ± 11.8m when 30 control points have been used, to ±13.1m with only 15 control points, i.e. only 1.3m over the whole range. While, for the check points the accuracy - as shown in Figure 11.2 - falls in the range 4.3m when from 10 to 35 check points have been used where the accuracy increased with a decrease in the number of check points. From this, it would appear that a quite small number of control points - has few as ten - can be used with DMS and still give satisfactory results.

As can be seen from the vector plot (Figure 11.3), for the Level 1B stereo-pair of scene 122/285, the pattern of the individual residual errors in planimetry is mostly random, with only a few areas where the errors exhibit a slight systematic pattern locally.

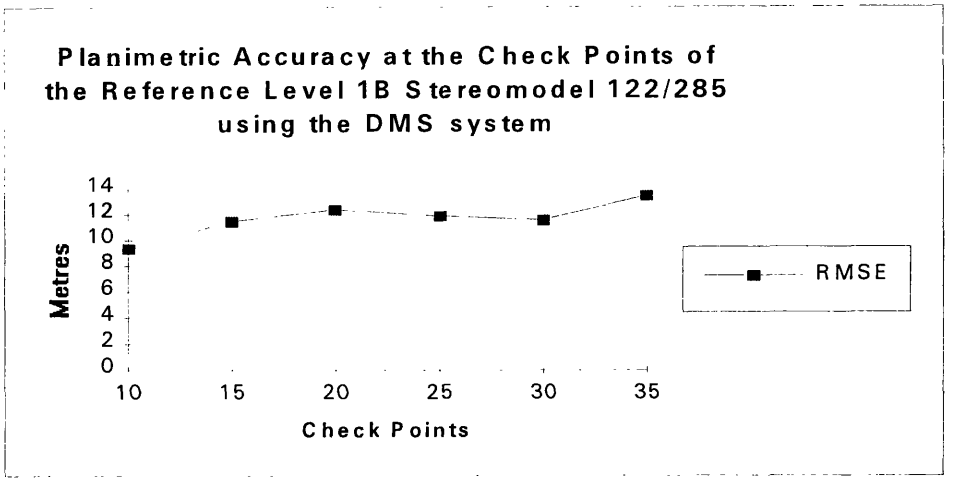

Figure 11.2 Graphic represntation of the accuracy of planimetry at the check points

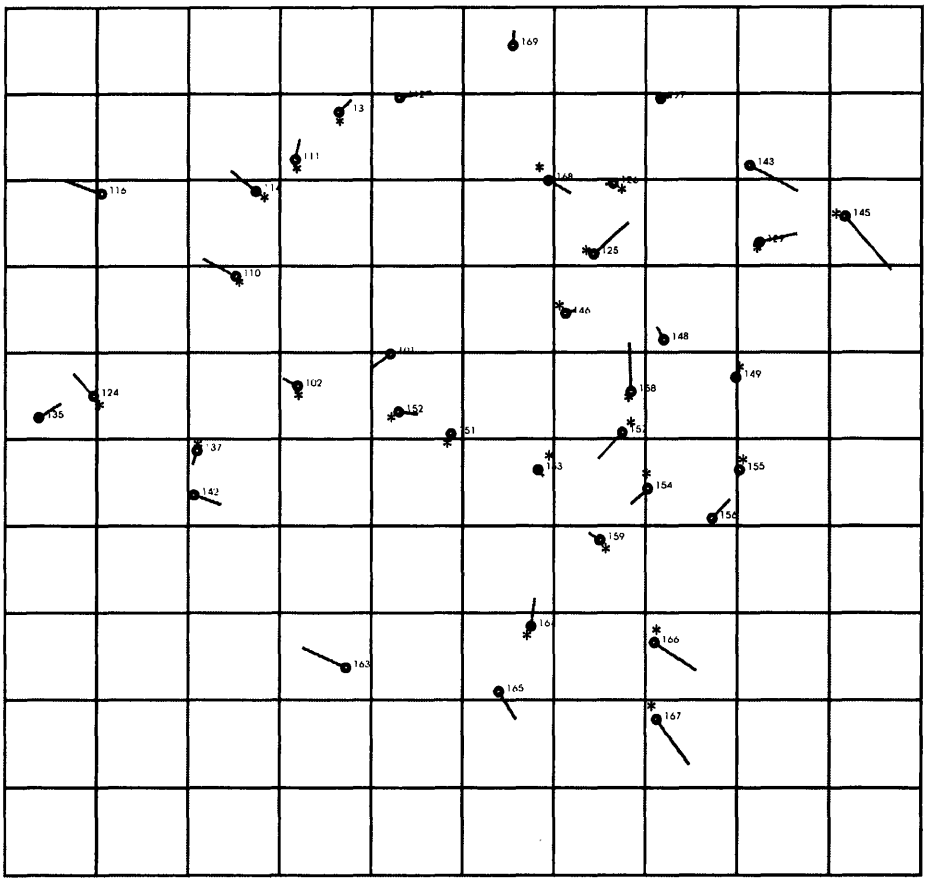

Figure 11.3 Vector plot of the planimetric errors at the control points and check points for the Level 1B stereo-pair for scene 122/285 using DMS
Control points o Check points o *

11.3.3.2 Accuracy Test of Planimetry and Vector plot of the Other Stereo-pairs

For the other stereo-pairs covering the whole Badia area, the same procedures have been followed for their processing. Table 11.4 summarizes the results that have been obtained from the accuracy tests. As can be seen from the Table, the best accuracy in planimetry in terms of the RMSE values obtained at the check points was ±17m where more control points were used in the solution for the Level 1B stereo-model for scene 123/286.

Scene No.	No. of Ground Control Points	RMSE Values at the Control Points (m)			No. of Check points	RMSE Values at the Check Points (m)		
		ΔE	ΔN	ΔPl		ΔE	ΔN	ΔPl
123/285 Level 1B	9	±10.0	±9.3	±13.7	10	±14.5	± 17.6	± 22.8
123/286 Level 1B	13	±10.1	±5.9	±11.7	15	±14.1	± 9.9	± 17.0
124/285 Level 1B	8	±6.0	±8.1	±10.1	8	±18.4	±8.7	±20.3
124/285 Level 1B	16	±10.1	±7.9	±12.8	-	-	-	-
124/286 Level 1B	13	±11.2	±8.5	±14.1	-	-	-	-

Table 11.4 RMSE values for the residual errors in planimetry at the control points and check points for all five SPOT Level 1B stereo-pairs covering the Badia Project area

The vector plots of the individual residual errors at the control and check points for the Level 1B stereo-pairs for scenes 123/285 and 123/286 (Figures 11.4, 11.5) showed that the pattern of residual errors in planimetry is mostly random. The vector plots of the Level 1B stereo-pairs for scenes 124/285 and 124/286 when no check points were used also showed a pattern of residual errors in planimetry that is mostly random (see Figures 11.6 and 11.7).

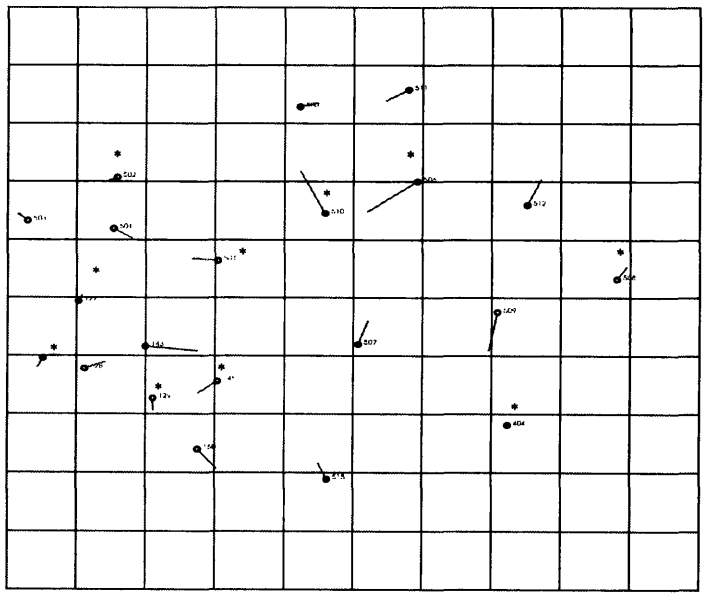

Figure 11.4 Vector plot of the planimetric errors at the control points and check points for the Level 1B stereo-pair for scene 123/285 of the Badia area
Control points o Check points o *

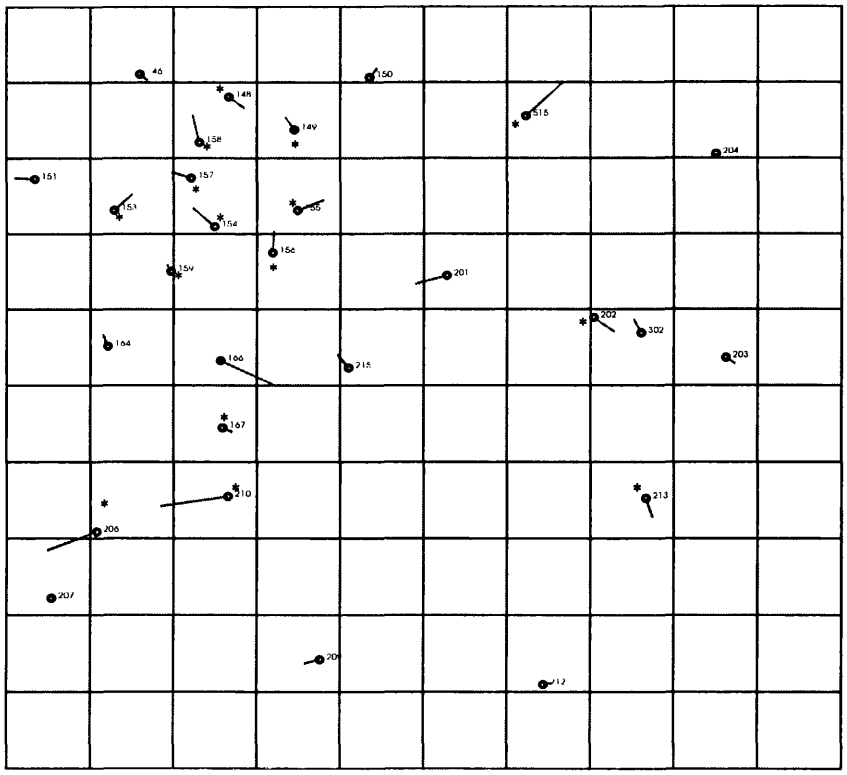

Figure 11.5 Vector plot of the planimetric errors at the control points and check points for the Level 1B stereo-pair for scene 123/286 of the Badia area
Control points o Check points o *

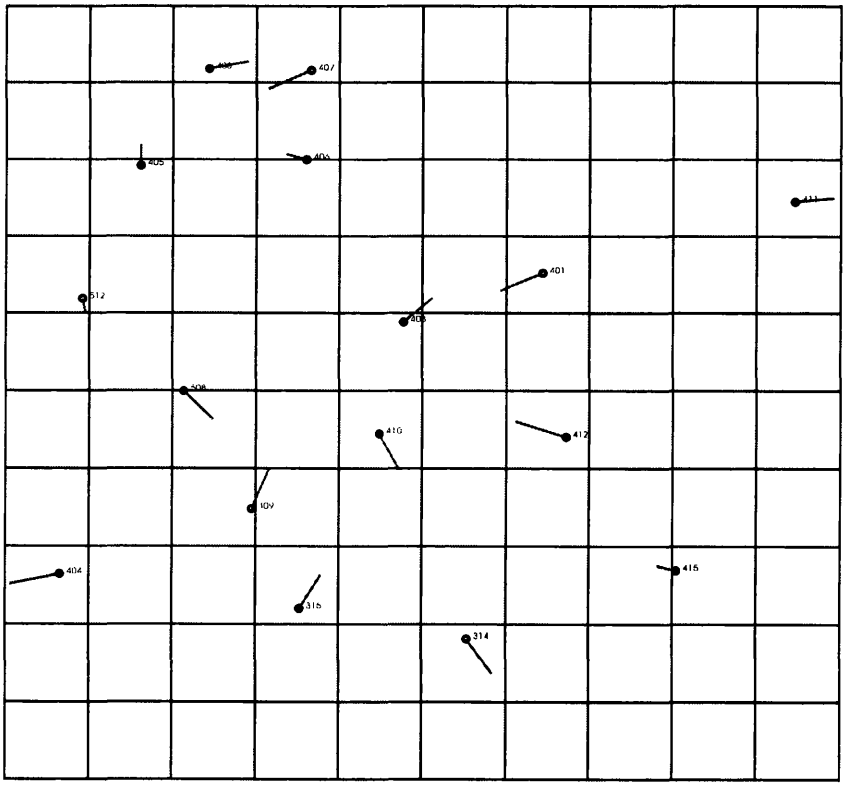

Figure 11.6 Vector plot of the planimetric errors at the ground control points for the Level 1B stereo-pair for scene 124/285

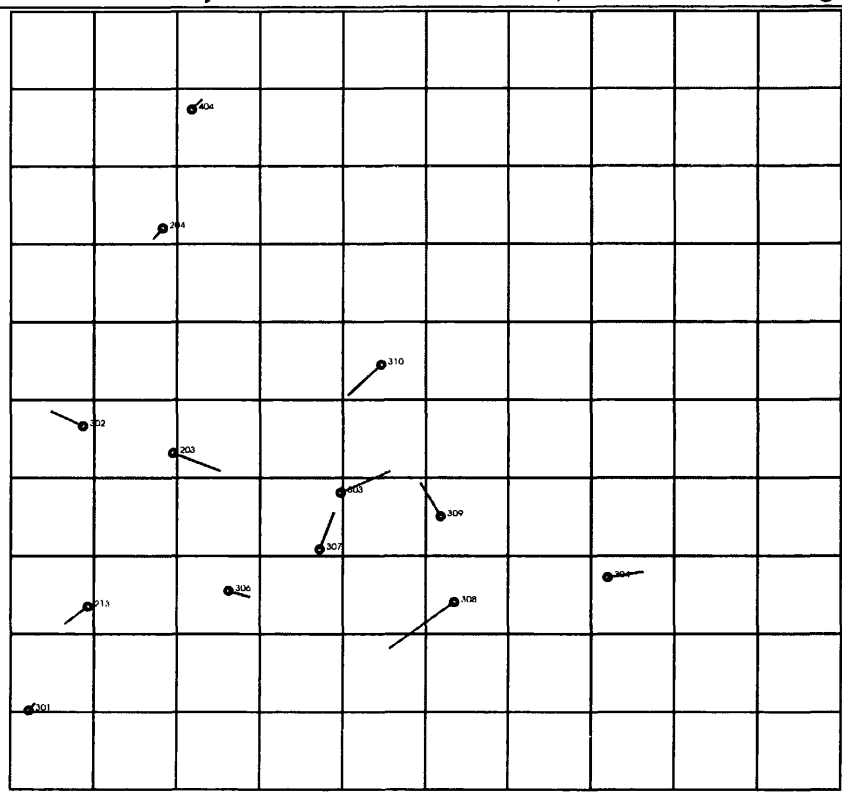

Figure 11.7 Vector plot of the planimetric errors at the ground control points for the Level 1B stereo-pair for scene 124/286

11.3.4 Stereocorrelation

After the registration procedure in which the right image has been registered to the left image, the two image files have been rectified and resampled and a coefficient file has been established, it is advisable for the user to view the stereoimages in 3D using anaglyph spectacles. In this context, it is important first of all to verify that the stereoimage headers contain the correct values for the look angles, the reference elevation and the DN scaling factor. Furthermore it is also important for the user to view the area before the stereocorrelation process is undertaken and to zoom and roam around the stereo-model and see if there is any parallax or want of correspondence between the two images over the whole of its area. In addition, it is very useful to measure spot heights at various positions around the model in order to assess the range of elevation that is present in the area. In this research project, all of the stereo-models were viewed stereoscopically and no y-parallax showed up in the stereo-pairs - which is really quite remarkable having regard to the fact that a 2D polynomial interpolative process has been

used in the photogrammetric solution rather than a more sophisticated 3D solution based on the use of collinearity equations.

After the stereomodels had been checked, the stereocorrelation process has been carried out. As mentioned earlier in Section 6.5.2, the procedure employed for image matching in DMS is based on the rectified and resampled data produced by the preceding stages. The algorithm used employs area correlation. This involves the matching of the density or grey level values on the two images comprising the stereo-pair. The input includes the look angle in degrees for both the left and right images; the name of the file containing the transformation coefficients; the post or grid spacing in pixels; the minimum and maximum anticipated elevation values stated in ground units (metres); the output file name for the DEM; the size of the correlation matrix (between 3 x 3 and 17 x 17 pixels); and the mean elevation value (datum). This last item is very critical; if the correct value is not given, then troubles can result with the final elevation values - as the author can testify. All of the stereo-pairs were processed using the same method, with a post or grid spacing of 10 pixels (100 m) and with a correlation matrix size of 11 x 11 or 13 x 13 pixels. This is quite a large correlation matrix size, but, in general, it was found through experimentation that this size of matrix produces a more accurate DEM than a smaller matrix - though of course, it also takes more processing time to execute than the smaller matrix size.

The program first computes the size of the DEM and then proceeds with the correlation process. The progress of the correlation can be monitored through the "percent completed" bar. In practice, the speed of correlation and the length of time required to complete the task is a function of the DEM cell size; the correlation matrix size; and the range of elevation parallax found in the area. In fact, the process is very efficient and does not take as long to complete as with the other systems that have been tested - only one hour or less being needed to accomplish the correlation of one complete stereo-pair. The report that is produced after the correlation has been completed shows the percentage of successful correlation points and the minimum and maximum elevation values found in the area. Also a report giving the accuracy of the heights obtained at the control points and check points can be obtained using the **CHKDEM.EXE** routine.

In fact, in all of the stereo-pairs, the report showed that 96% and above of the pixels were successfully correlated. However, in general, all the DEMs that were extracted faced some minor problems in correlation usually and inexplicably in the south-eastern part of each of the stereo-pairs.

After extraction of the DEMs, all of them were passed through a low-pass median filter to remove spikes and to smooth the surface. This utilized a threshold value of 3 and a filter template size of 3 x 3 pixels up to 7 x 7 pixels. The degree of smoothing is a function of the size of filter used; as the filter size increases, the smoothing effect increases. In general, a large filter size will correct spikes that spread over a large area (several pixels) whereas a smaller-sized filter will correct individual pixel values. The average value of all the pixels within the filter window is computed for comparison with the central pixel. The median filter with its threshold value then replaces the central pixel elevation value with the median value of its neighbours. This is especially useful in eliminating the large spikes that can occur with a stereocorrelated DEM.

With regard to the automatic extraction of the elevation values for each of Level 1B stereo-pairs using the image matching routines available in DMS, this has proven to work well, in spite of the almost complete lack of cultural detail in this desert area, The matching algorithm has worked reliably and, as noted above, has produced elevation values for more than 96% of the area covered by the DEM.

11.3.5 Orthoimage Generation.

In the DMS system, the orthoimage can be generated by using the DEM derived from the stereo-model and either one of the left or right rectified images which have been produced during the registration process ready for use in the stereocorrelation process. The process available in the DMS system will then automatically produce orthoimages that are free from relief displacement. From the **MAP** application, the item **orthoimage** should be selected. Alternatively from the DOS prompt, the user has to specify **ORTHO.EXE.** When all the parameters that are required have been defined, the system then produces the orthoimage. When all the orthoimages have been produced, they need a further transformation to come into the ground coordinate system - in which case, the

orthoimages can be geocoded and then resampled by one of the standard interpolation methods (i.e. nearest neighbour, bi-linear and cubic convolution) that are available in the DMS system. In fact, all of the orthoimages produced during the author's tests have been resampled using the cubic convolution method with a pixel size of 20m. Figure 11.8 gives an example of the orthoimage produced by DMS for the reference stereomodel for scene 122/285.

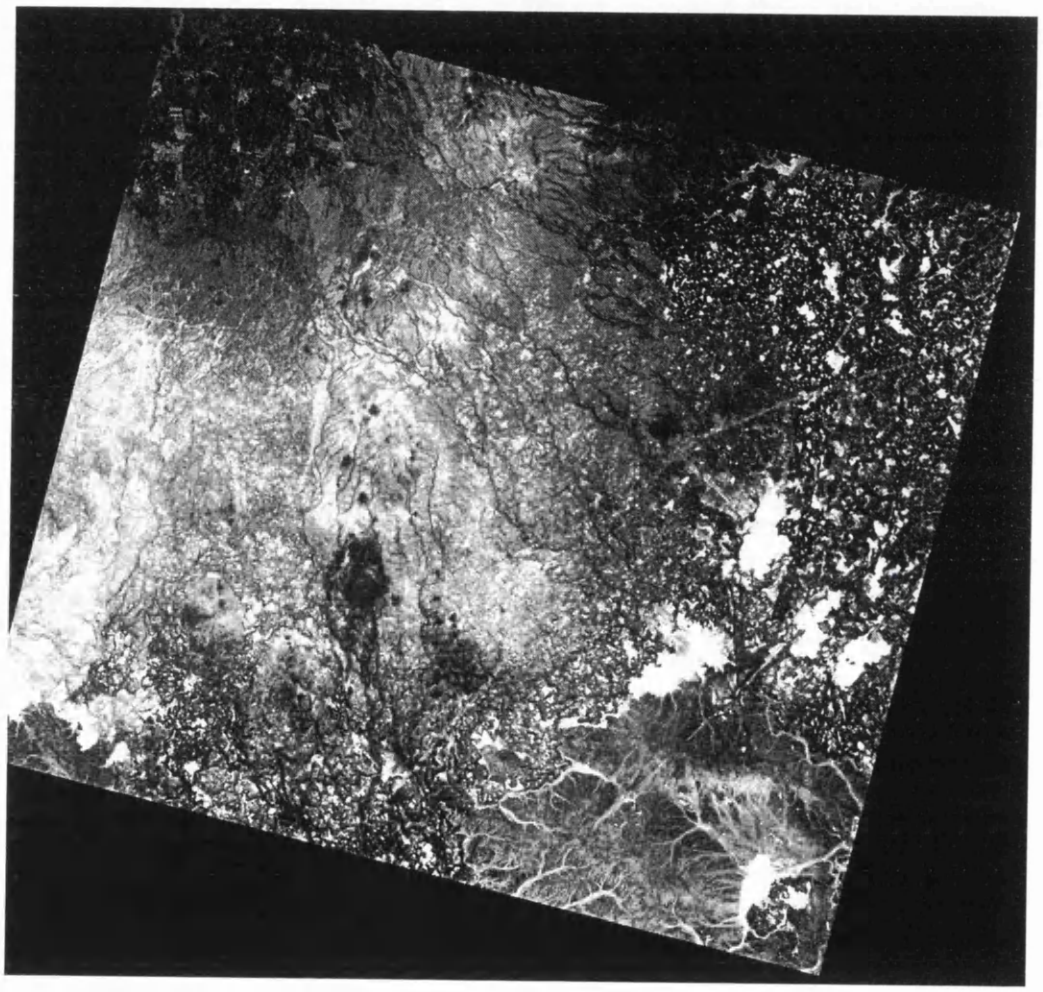

Figure 11.8 Orthoimage of the reference stereomodel for scene 122/285 generated by DMS

11.3.6 Mosaicing of DEMs and Orthoimages

The mosaiced DEMs are generated automatically in the DMS system. The user simply has to respond to the prompts for the input parameters such as the name of the files to be

mosaicked and the output file name before running the **MANAGE** application - **Mosaic program** available in the DMS system. Once this had been done, the five Level 1B DEMs covering the Badia project area have been mosaiced with each other quite automatically in the DMS system without any interaction with the user. In fact, this created a mosaiced DEM with discontinuities along the edges of the individual DEMs which prevented the contour lines in the adjacent models connecting with each other. The frame of each DEM should really be edited by cutting it along the boundary where there is no correlation process, but, in fact, such an editing feature is not available in the DMS system. In summary, it seems that, within DMS, the mosaicked DEMs are overlapped on each other with the possibility of averaging or not averaging the grey values of the overlapped areas depending on the responses given by the user during the input process.

After the five Level 1B DEMs have been mosaiced with each other in DMS, contours have been generated from the mosaiced DEM file using the CONTOUR program in the EASI/PACE system without any problem. This is in contrast with the mosaiced DEM extracted from the EASI/PACE system. In the first case, the size of the file containing the data of mosaiced DEMs is 10Mbytes, whereas, in the second case, the file size for the mosaiced DEMs was around 530Mbytes.

For mosaicing the orthoimages, the same procedures applied for mosaicing the DEMs were applied for mosaicking the orthoimages. The five orthoimages that have been produced for the whole Badia area have been also mosaiced together using the DMS system. From the **MANAGE** application, the **Mosaic** item has again been selected. In response to the program prompts, the user has to enter the name of the destination file which will contain the mosaiced images; the ground X and Y coordinates of the upper left corner; and the name of the files to be mosaiced - which must be geocoded (rectified) in the same coordinate system as the destination file. In response also to the program, the user has the choice to use or not use the equalization histogram - which can be used if these images have not been enhanced previously. Based on the author's experience, the user should not use these histograms in this process. Using the histograms during the mosaicing process will create areas of distinctly different

densities. Once the process has been started, the system automatically mosaics all the images and does not permit the user to use the histogram matching.

After the five orthoimages have been mosaiced together, the orthoimages mosaic has been enhanced using the Adobe Photoshop package. This is a very sophisticated software suite with many options and gave a much more satisfactory result than that achieved using the DMS routines. Figure 11.9 shows the final orthoimage mosaic, it is clear that one of the mosaiced images shows a distinct boundary, while with the others, the boundaries are not seen.

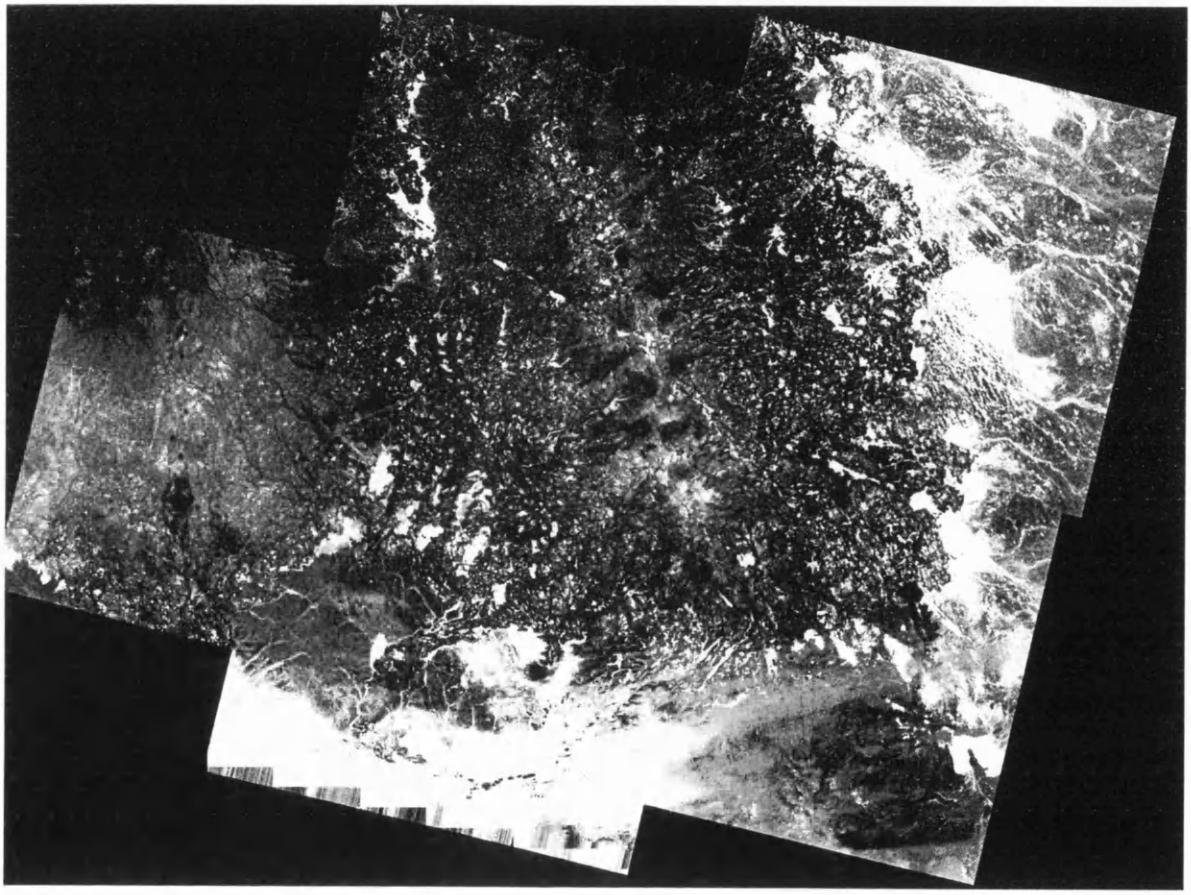

Figure 11.9 Orthoimage mosaic formed from the SPOT stereo-pairs of the Badia area

11.4 Accuracy Tests of the DEMs of the Badia Test Area

To validate the data quality in terms of geometric accuracy of the DEMs extracted from SPOT Level 1B stereo-pairs produced by DMS system, four different methods have been used:-

(i) DEM accuracy reports;

(ii) a comparison of the two sets of superimposed contours;

(iii) a comparison of the height values given by selected contours from the photogrammetrically produced reference map and the corresponding elevation values given by the DEM; and

(iv) comparison of the DEM data with the GPS profiles measured along the main roads

11.4.1 DEMs Accuracy at the GCPs

11.4.1.1 Accuracy of the Elevation Data at the GCPs Extracted from the Level 1B Stereo-pair for Scene 122/285

It will be noted that, with DMS, since there is no absolute orientation of the stereo-pair, no check of the elevation values can be made until the stereo-correlation stage has been completed. Because many more GCPs were available for scene 122/285, different combinations of control and check points have been used for tests of the elevation accuracy. Coming first to the control points, the accuracy of the heights in terms of root mean square error (RMSE) values at the control points in the DEM fall in range from ± 4.4m for 24 control points to ± 5.9m when 14 control points were used. Out of 35 control points, one point exhibited a high residual error, so it has been deleted. From Table 11.5, it is clear that the residual errors in height decrease or increase slightly through increasing or decreasing the number of control points. But the range in the error values is not too big - only one metre in the range from 14 to 34 control points.

Turning next to the check points, the accuracy obtained in terms of the root mean square error (RMSE) values in height in the DEM using different combinations falls between ±5.2 m for 35 check points and ± 6.9 m for 10 check points. From Table 11.5, it is clear that the accuracy decreases with an increase in the number of check points.

As can be seen from the vector plot (Figure 11.10) of the Level 1B stereo pair for Scene 122/285, the pattern of the individual residual errors in heights is mostly random, with

only a few areas where the errors exhibit a slight systematic pattern locally - more noticeably in the south-western part of the area.

Scene No.	No. of Control Points	RMSE in Heights (m) ΔH	No. of Check points	RMSE in Height (m) ΔH
122/285 Level 1B	45	±4.5		
	34	±4.9	10	±6.9
	29	±4.8	15	±6.7
	24	±4.4	20	±6.6
	19	±4.5	25	±6.2
	14	±5.9	30	±5.5
	14	±5.9	35	±5.2

Table 11.5 RMSE values of the residual errors in height at the control points and check points in the DEM produced by DMS for the reference Level 1B stereo-pair for scene 122/285 of the Badia area.

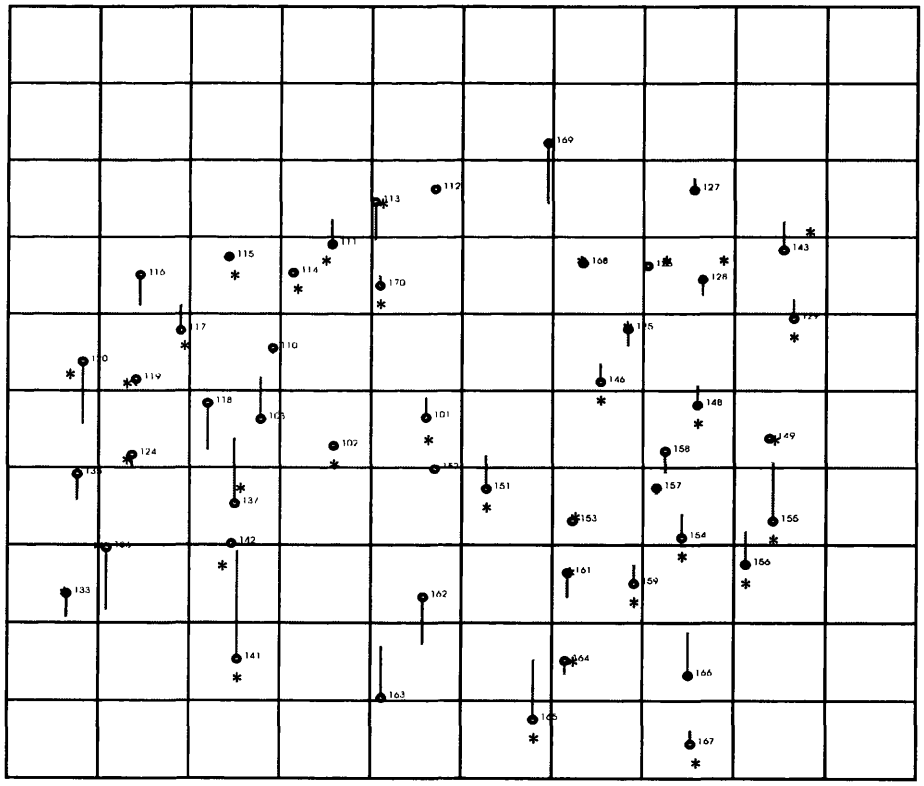

Figure 11.10 Vector plot of the residual errors at the individual control points and check points produced by DMS from the Level 1B stereo-pair for scene 122/285 of the Badia area Control points o Check points o *

11.4.1.2 Accuracy of the Elevation Data at the GCPs Extracted from Other Stereo-pairs of the Badia Area.

The first stereo-pair that has a good number of control points available for test purposes is the Level 1B stereo-pair for scene 123/285. Ten of these points have been used as check points. From the results contained in Table 11.6, it is clear that the range of the RMSE values in height increases both for the control and check points; this range is between ± 10.5m to 15.8m for the control points and between ± 6.6m and ± 10.7m for the check points. These differences in the RMSE values of the height errors shown in the Table 11.6 came after changing the value of the mean terrain elevation of the stereo-model by up to ± 10m. This shows the great sensitivity of the DMS system to the value given to this parameter. As indicated above, it also affects the kind and pattern of systematic errors in height that fall within the area. Some points having a positive sign to the elevation error, may well acquire a negative sign when changing the value of the mean terrain elevation in the stereo-model. Thus care should be taken to put in the correct mean elevation as an input parameter. This can be achieved through the calculation of the mean of the elevations of all the ground control points (GCPs) that have been established in the area.

Scene No.	No. of Control Points	RMSE in Height (m)	No. of Check Points	RMSE in Height (m)
123/285 Level 1B	8	±11.6	10	±6.6
	8	±10.5	10	±8.3
	8	±15.7	10	±10.7
	8	±15.8	10	±10.5

Table 11.6 RMSE values of the residual errors in height at the control points and check points of the Level 1B stereo-pair for scene123/285 lying in the north-western part of the Badia area - using different mean terrain elevation values.

The accuracy of the heights obtained at the GCPs for the stereo-pair for scene 123/286 in terms of their RMSE values falls in the range between ± 4.9m and ± 5.0m for the control points and between ± 5.8m and ±7.0m for the check points (see Table 11.7) - which is a small difference. The differences in the errors in the control points and the check points when the same control and check points are used come simply from changes in the mean elevation value which, as noted above, is one of the input parameters for stereocorrelation. It seems that the user has to try different values of the

mean terrain elevation to get the best results. Not only does this affect the accuracy of the final results but it is also affects the kind and pattern of errors - e.g. whether they are systematic or random in character - simply by changing the value of this parameter.

Scene No.	No. of Control Points (GCPs)	RMSE in Height (m)	No. of Check Points	RMSE in Height (m)
123/286 Level 1B	12	±4.9	15	±7.0
	12	±4.9	18	±6.8
	12	±4.4	18	±5.8
	12	±5.0	18	±6.0

Table 11.7 RMSE values of the residual errors in height for both the control points and check points of the Level 1B stereo-pair for scene 122/286 lying in the south-western part of the Badia area.

For the determination of the accuracy of the heights obtained at the GCPs of the Level 1B stereo pair for scene 124/285 in terms of their RMSE values, again several runs of the stereocorrelation process have been carried out changing the values of the mean terrain elevation of the stereo-model within ± 20m of the mean of the control points. The values obtained fall in the range ±7.5m to ± 18.8m for the 8 control points and between ± 7.0m to ±18.6m for the 8 check points, (see Table 11.8). Yet again, these big differences in the final RMSE values are due solely to the changes in the value of the mean terrain elevation of the stereomodel of the area. In case of using the 16 ground control points, the RMSE value in height was improved to ±5.1m. Finally, for the last stereo-pair for scene 124/286, the accuracy obtained in terms of the RMSE values of the residual errors in height at the 13 control points was ± 7.0m (see also Table 11.8).

Scene No.	No. of Control Points	RMSE in Planimetry and Heights		No. of Check Points	RMSE in Planimetry and Heights	
		Δ Pl (m)	ΔH (m)		Δ Pl (m)	ΔH (m)
124/285 Level 1B	8	±10.1	±13.4	8	±20.3	±12.2
	8	±10.1	±18.8	8	±20.3	±18.6
	8	±10.1	±7.5	8	±20.3	±7.0
	8	±10.1	±8.7	8	±20.3	±11.7
	16	±12.8	±5.1			
124/286 Level 1B	13	±14.1	±7.0			

Table 11.8 RMSE values of the residual errors in planimetry and height of the Level 1B stereo-pair of scene 124/285 located in the north-eastern part of the Badia area using different mean terrain elevation values.

In Figure 11.11. the vector plot of the residual errors in height at the control points and check points for the stereo-pair 123/285 showed random errors, except in the north part of the area where some systematic errors occur in a group of points locally. Vector plots of the residual errors in height at the control and check points in the DEM extracted from the stereo-pair 123/286 also show random errors in the north-western part of the area and systematic errors in the middle (Figure 11.12), where a group of points show a definite pattern of systematic error. Various attempts were made to overcome this matter, but unfortunately, most of the cases showed a pattern of systematic errors over this area.

The vector plot of the residual errors in height at the control points and check points of the stereo-pair 124/285 that is shown in Figure 11.13 displays systematic errors in which all the control and check points showed negative errors. In Figure 11.14, the vector plot shows a much better distribution of the residual errors than the vector plots in Figure 11.13. This has been achieved solely by repeating the stereocorrelation and changing the mean elevation value. Finally the vector plot (Figure 11.15) of the residual errors in height at the ground control points of the stereo-pair for scene 124/286 showed random errors over the whole area.

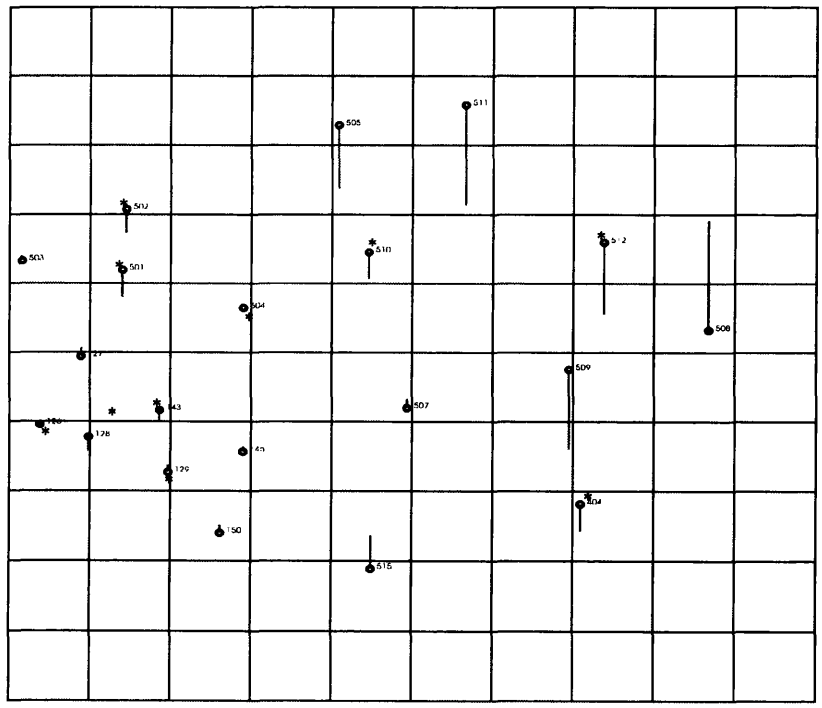

Figure 11.11 Vector plot of the residual errors in height at the control points of the Level 1B stereo-pair for scene 123/285 of the north-western part ofthe Badia area
Control points o Check points o *

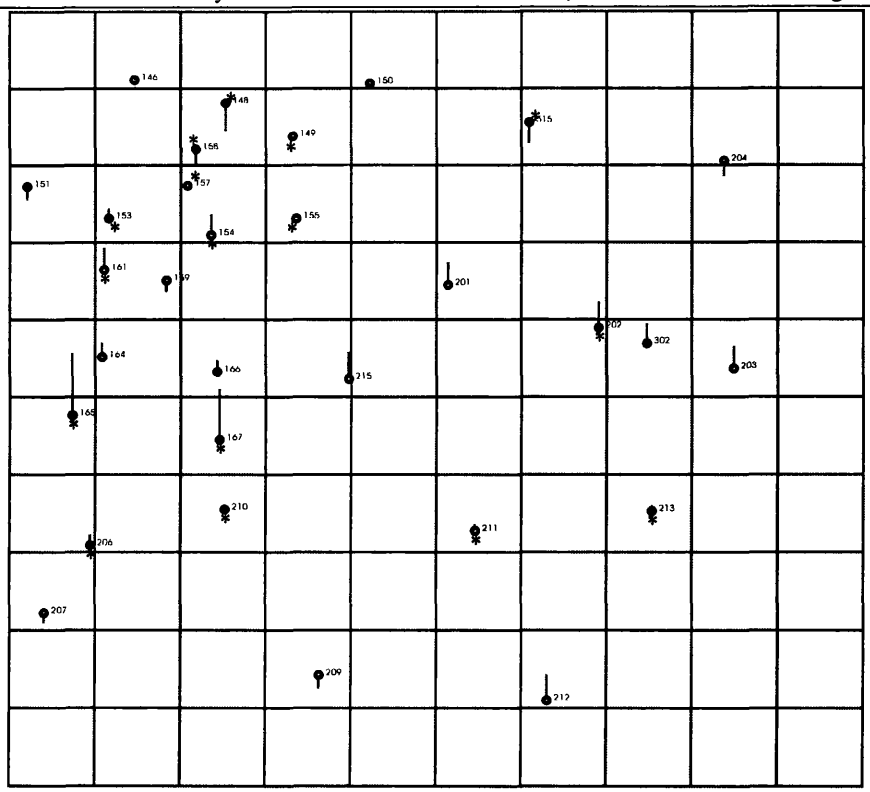

Figure 11.12 Vector plot of the residual errors in height at the control points and check points of the Level 1B stereo-pair for scene 123/286 of the south-western part of the Badia area. Control Points o Check points o *

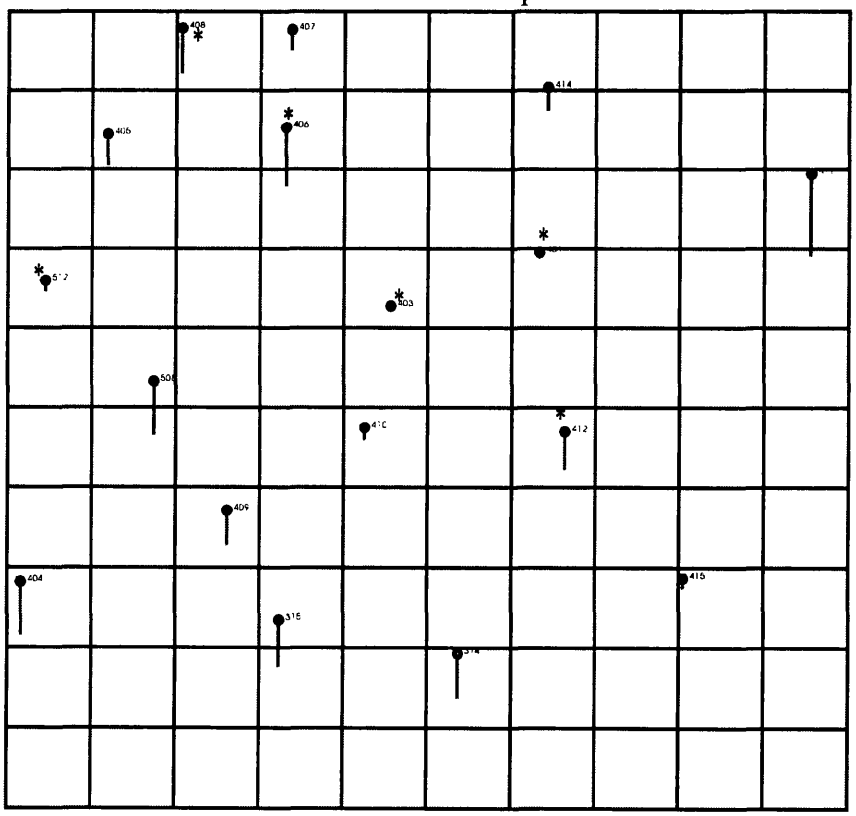

Figure 11.13 Vector plot of the residual errors in height at the control points and check points of the stereo-pair for scene 124/285 of the north-eastern part of the Badia area. Control Points o Check piints o*

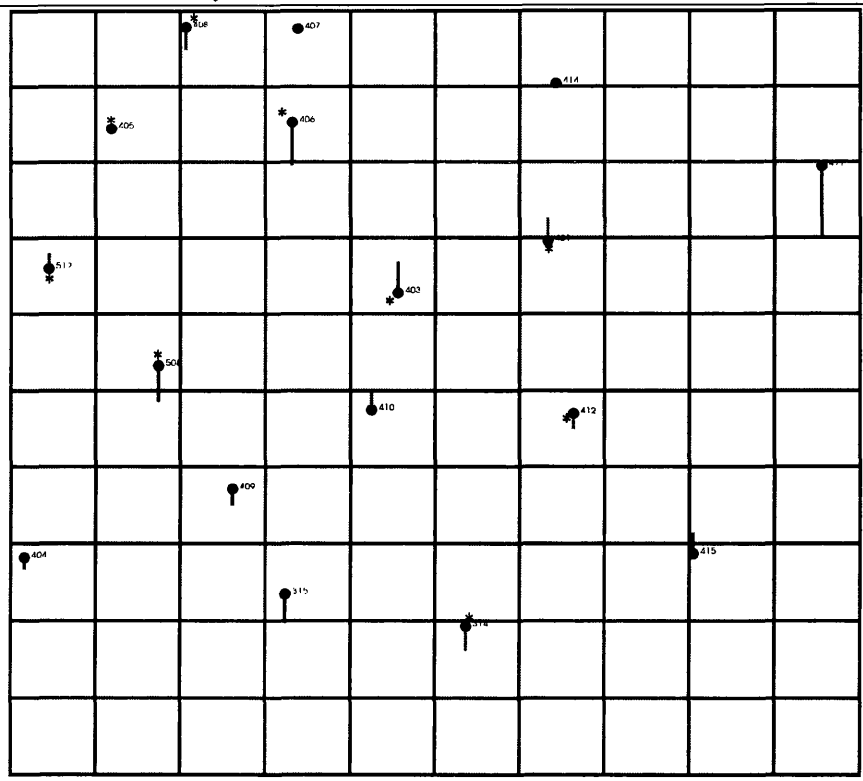

Figure 11.14 Vector plot of the residual errors in height at the control points and check points of the stereo-pair for scene 124/285 of the north-eastern part of the Badia area. control points o Check points o *

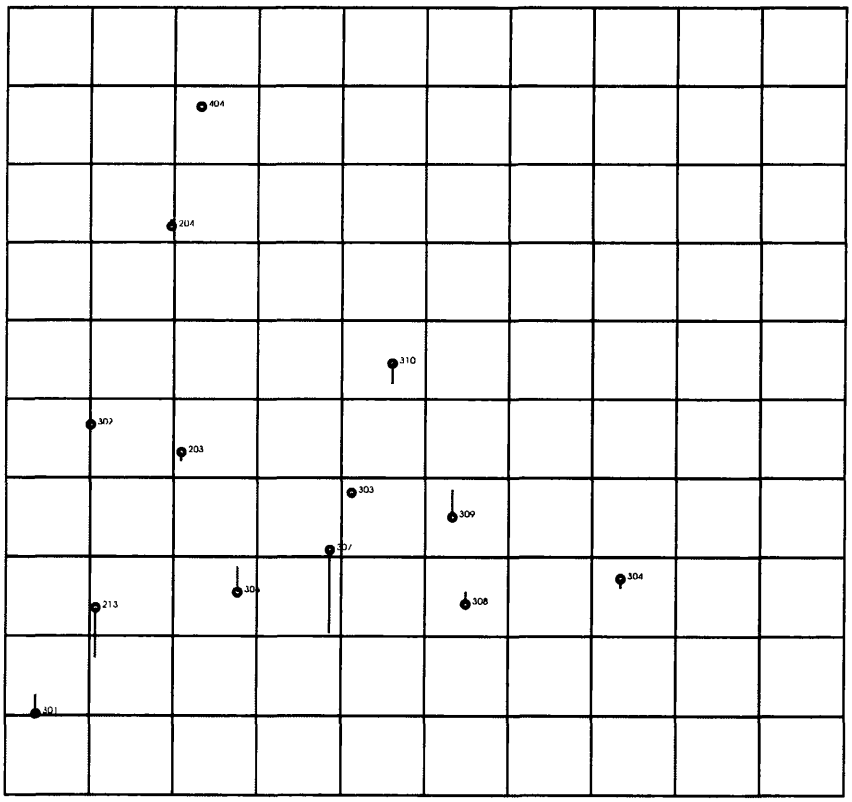

Figure 11.15 Vector plot of the residual errors in height at the ground control points of the stereo-pair for scene 124/286 of the south-eastern part of the Badia area.

11.4.2. Accuracy of Fit of the Contours Derived from DEMs Superimposed over the Digitised Contours Extracted from Existing Topographic Maps

Contours may also be derived from DEM data. However contours cannot be derived from the DEMs inside the DMS environment; instead the DEMs generated by DMS have to be exported to third-party software packages (such as SURFER, EASI/PACE, etc.) to derive the appropriate contours. In this research project, the DEMs have been exported to the EASI/PACE system which was then used to derive contours. New files had to be generated inside EASI/PACE for the DEMs in order to geocode the DEMs and fit them to the correct datum. The SURFER system was not used due to the problem of specifying the correct scale that was encountered in trials with the package.

(a) Superimposed Contours at 50m Intervals

For the reference DEM for scene 122/285, contours have been generated with a 50m contour interval. Contours also have been derived for the other DEMs with a 50m contour interval. DMS generates both 8-bit and 16-bit DEM files that can still be used to display the elevation value at the cursor location on the screen that the DMS system employs. However, it was not possible to import the digitized contours from the RJGC maps into the DMS environment to check the accuracy of the heights by comparing the elevation values provided by the digitized contours from the existing map with the elevation values produced by the SPOT DEM. Thus the contours that have been extracted from the Level 1B DEM at an interval of 50m have been loaded into the EASI/PACE using ImageWorks following the same procedures as those described in Section 10.9.1. In this method, the test was carried out through a simple visual comparison, i.e. the accuracy can only be evaluated by seeing how the superimposed contours fit to each other; such a comparison is more of a qualitative check than a numeric accuracy test.

In Figure 11.16, the contours that have been generated by the DMS system with a 50 m contour interval from the DEM of the reference stereo-pair for scene 122/285 are shown superimposed over the contours digitized from the 1:250,000 scale map having the same contour interval. From Figure 11.16, it is clear that the contours display an excellent agreement in most parts of the stereo-model, whereas, in the lower part of the area, some

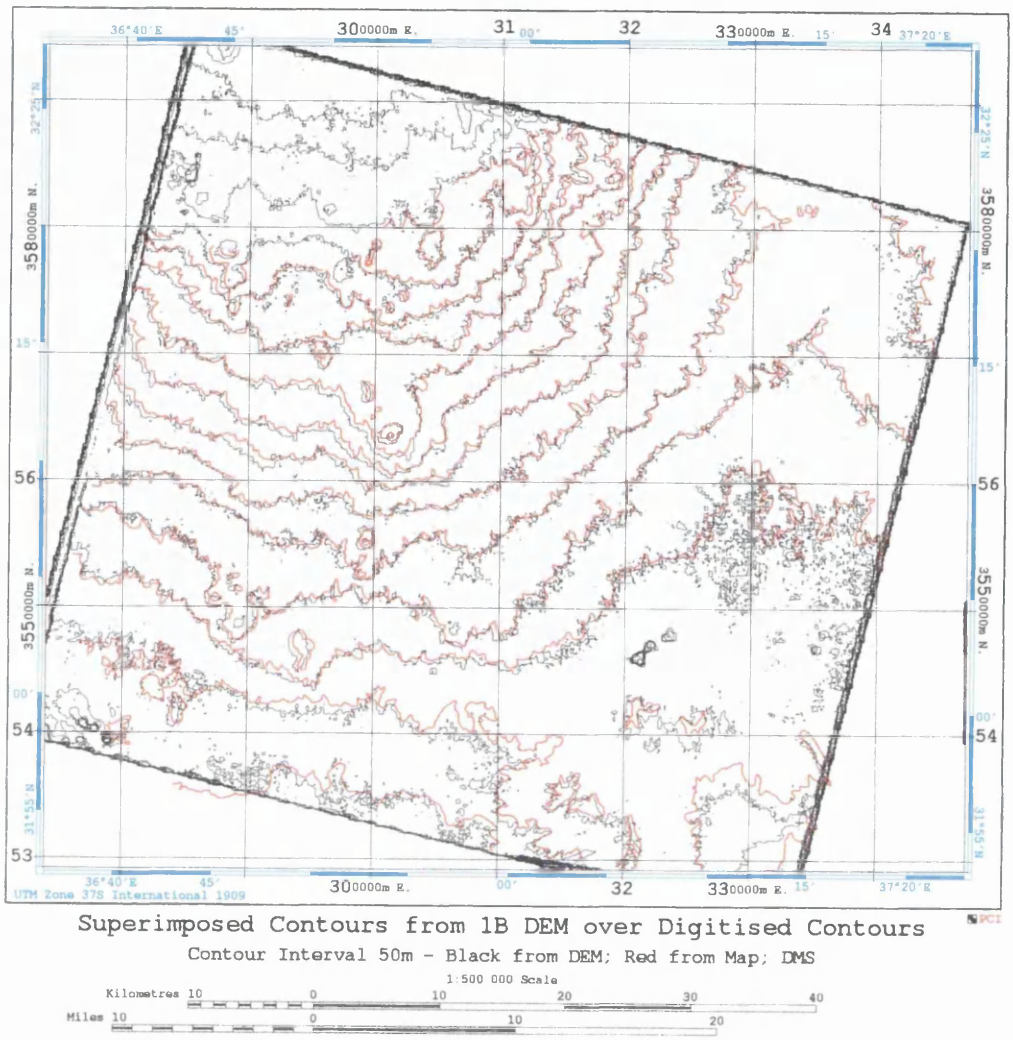

Figure 11.16 Superimposed contours extracted from the DEM of the reference Level 1B stereo-pair for scene 122/285. The contours produced by DMS have been superimposed over the digitised contours from the RJGC 1:250,000 scale topographic map.

some deviation between the contours is evident - amounting to about 15% of the contour interval or less. It can be seen that a great deal of noise is present with large numbers of tiny isolated contours appearing in the eastern part of the stereo-model and around the main contours. These problems have been solved by filtering the DEMs in the EASI/PACE system using ImageWorks. Three procedures available for the editing of DEMs have been implemented in the filtering process after masking the DEM; these were remove noise from the DEM under mask, interpolate under mask and smoothing under mask. The results after filtering are shown in Figure 11.17.

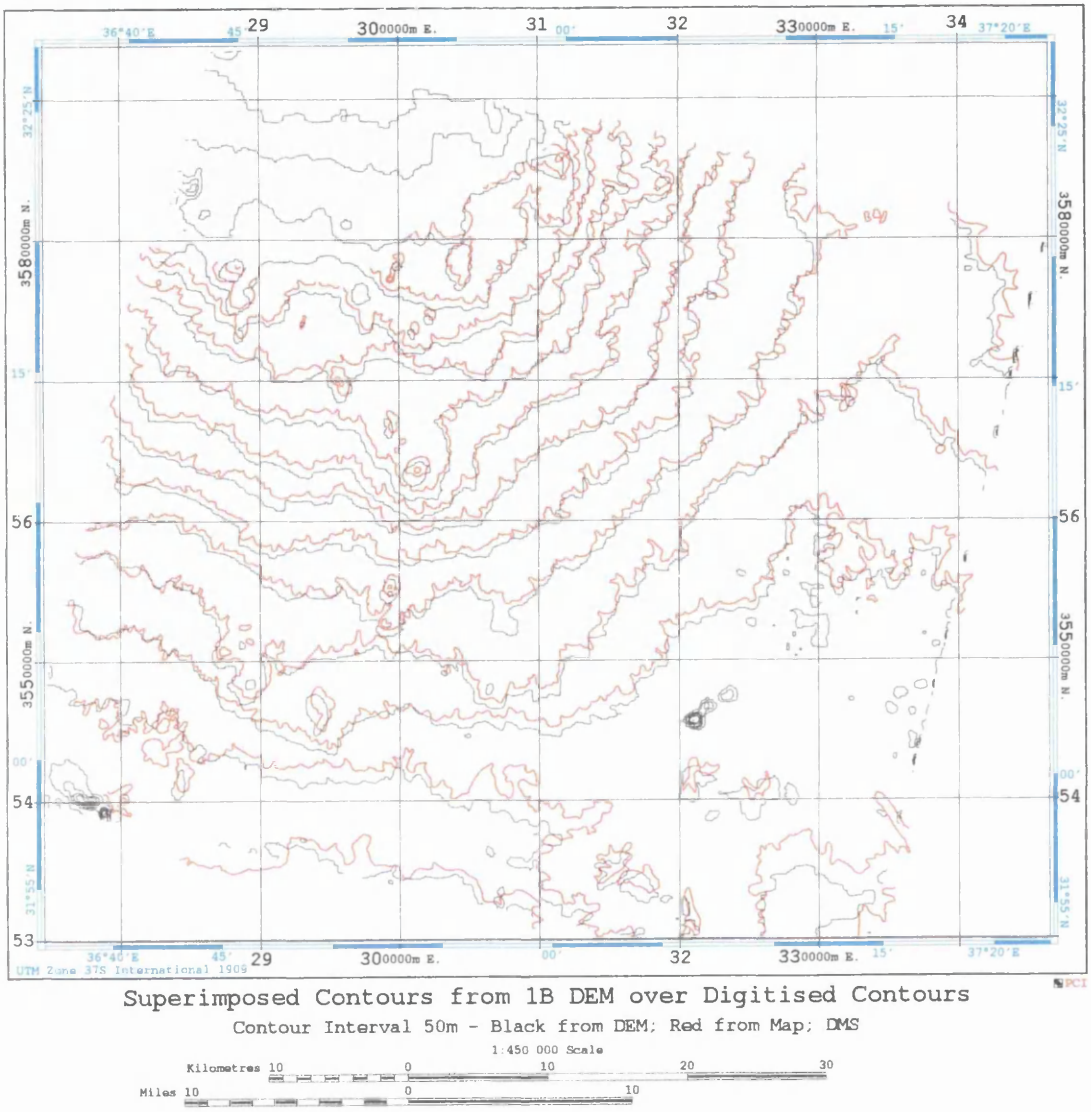

Figure 11.17 Superimposed contours extracted from the DEM of the reference Level 1B stereo-pair for scene 122/285. The contours produced by DMS have been superimposed over the digitised contours from the RJGC 1:250,000 scale topographic map (after filtering).

Another test of fit between the superimposed contours has been carried out using the same GCPs but changing the mean elevation value before carrying out the stereocorrelation. The contours extracted from the new DEM at a 50m interval have been superimposed over the corresponding digitized contours and the result is shown in Figure 11.18. It is clear that the contours have an excellent agreement or fit in the steep terrain but there is a noticeable deviation in the flat areas. This is, of course, due to the

fact that there is only a gentle slope present over this wide area of almost flat terrain. In which case, any small errors in elevation will have a big effect on the planimetric positions of the contours.

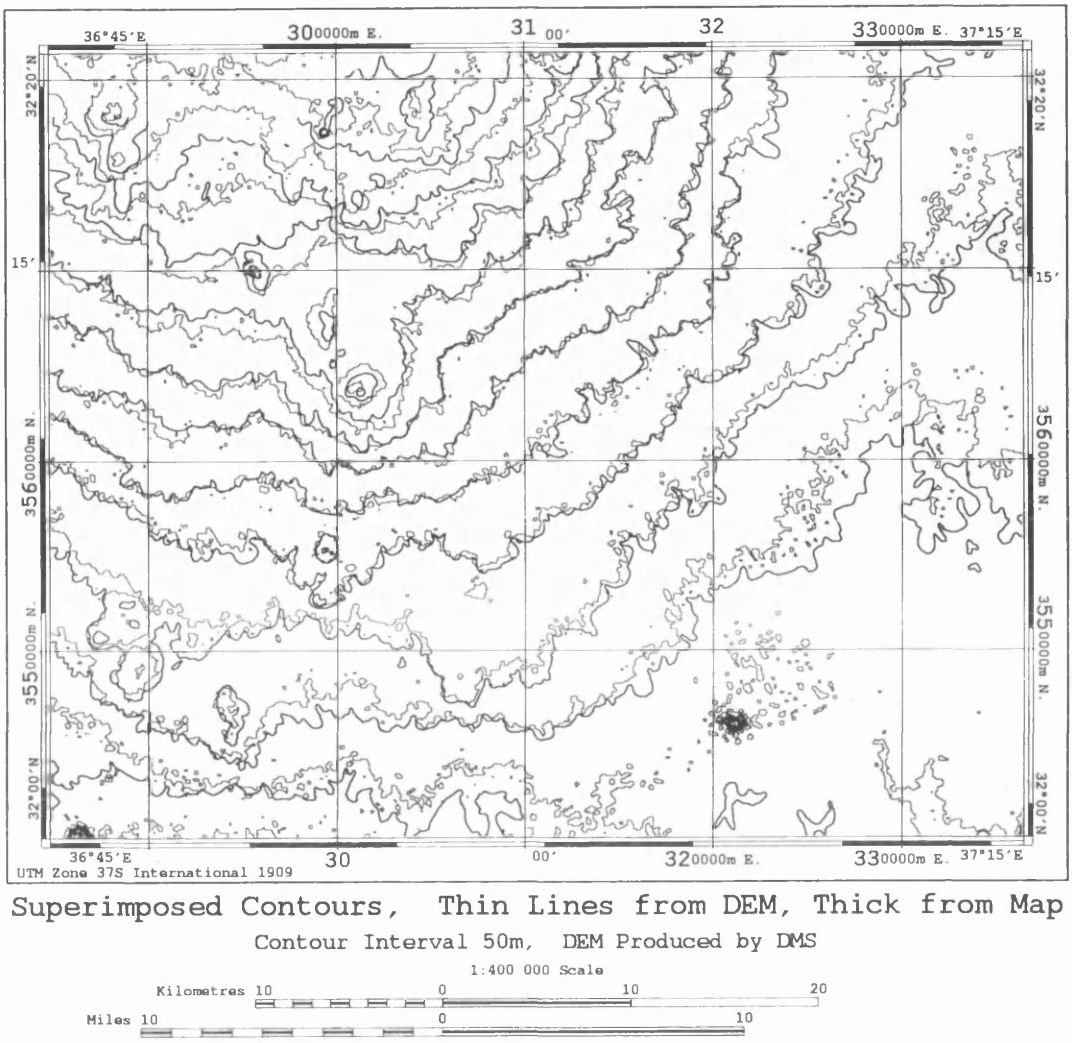

Figure11.18 Superimposed contours extracted from the DEM of part of the Level 1B reference stereo-pair 122/285. The contours produced by DMS at a 50m interval have been superimposed over the corresponding digitised contours from the RJGC 1:250,000 scale topographic map at a same scale as shown in Figure 11.17.

For the other Level 1B stereo-pairs of the Badia area, inspection of the contours generated from the Level 1B DEM for scene 124/286 in the eastern part of the area superimposed over digitised contours from the 1:250,000 scale topographic map as shown in Figure 11.18, displays an excellent fit between the contours in most parts of the area to less than 10% of the contour interval. Minor deviations can be seen, especially in the north-eastern part of the area that comprises flat terrain. Other contours

generated from the other Level 1B DEMs superimposed over digitised contours also show an excellent fit between the respective contours amounting to less than 10% of the contour interval - see Appendix C.

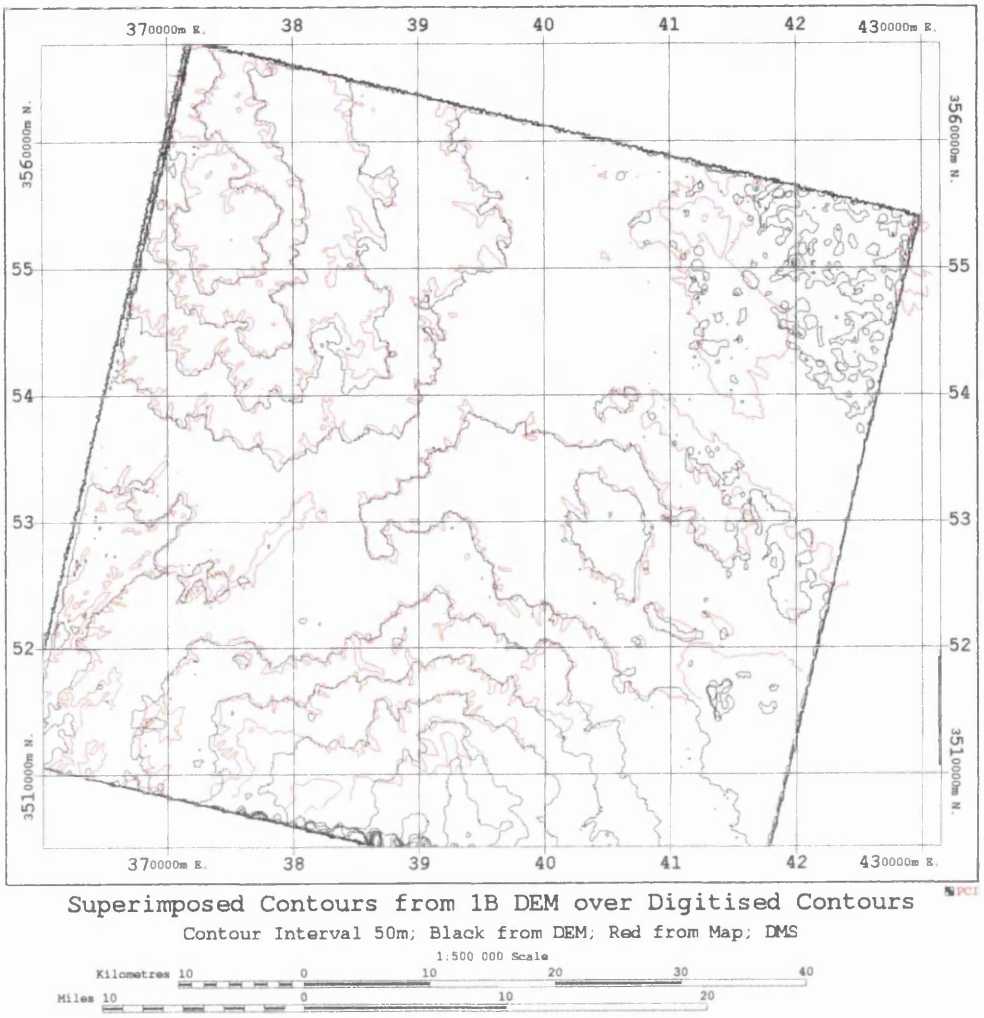

Figure 11.19 Superimposed contours extracted from the DEM Level 1B stereo-pair for scene 124/286. The contours produced by DMS have been superimposed over the digitised contours from the RJGC 1:250,000 scale topographic map.

A final inspection concerned the contours of the full DEM that cover the whole Badia area. In this comparison, the mosaiced contours generated from the five individual DEMS covering the Badia area were superimposed over the digitised contours from the 1:250,000 scale topographic map - as shown in Figure 11.20. Inspection of the fit shows an excellent agreement except in the western DEM where the contours have not been fully generated. Moreover, inspection of the mosaiced contours shows a satisfactory fit along the boundaries.

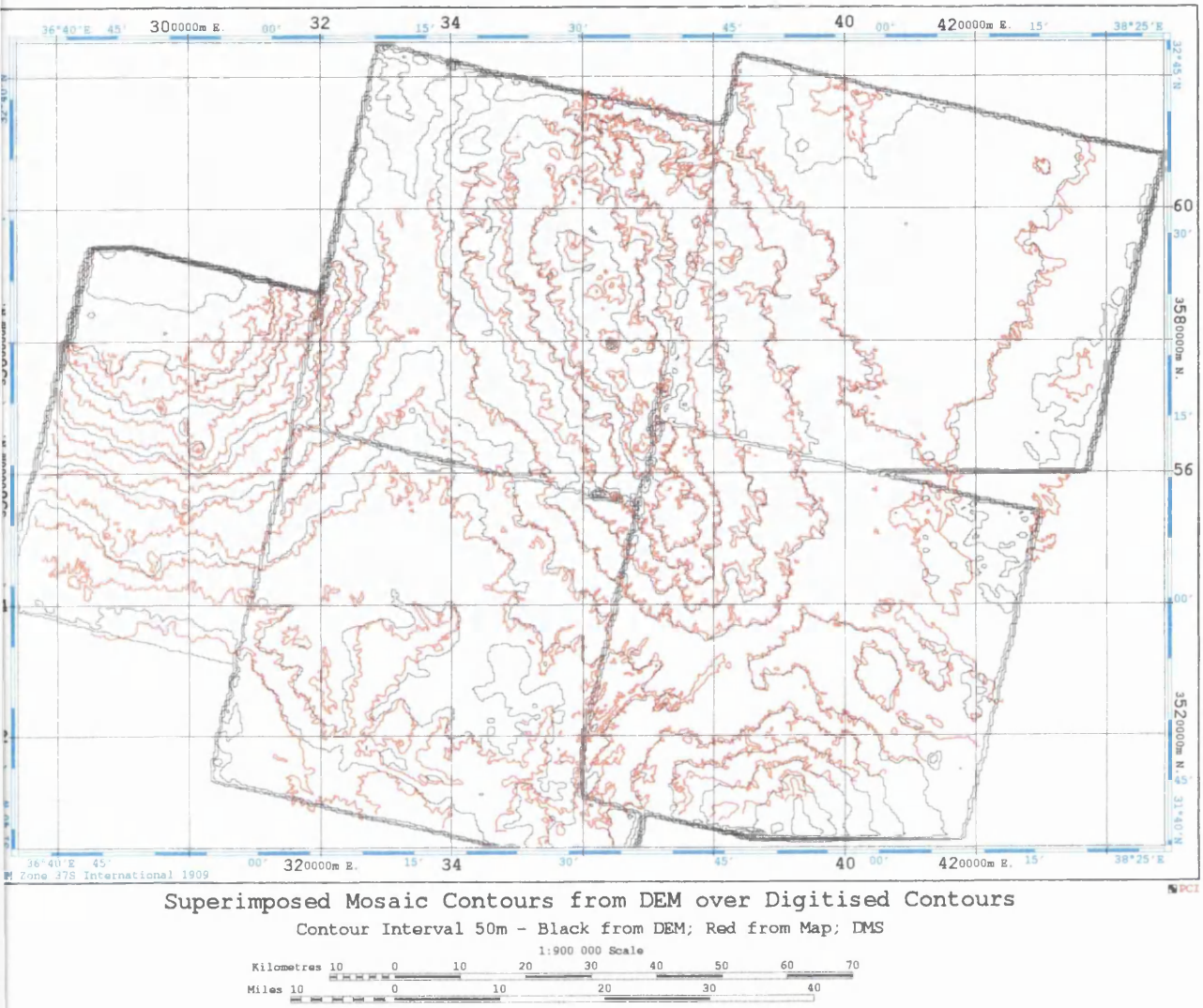

Figure 11.20 Mosaiced contours at a 50m interval extracted from the DEMs produced by DMS superimposed over the digitised contours from the 1:250,000 scale map at an interval of 50m.

(b) Superimposed Contours at 10m Intervals

An inspection of the accuracy of fit of the contours with a 10m interval derived from the DEM for the main reference stereo-model for scene 122/285 superimposed on the digitized contours at the same contour interval derived from the 1:50,000 scale map revealed that the fit is excellent in some parts, but there are some noticeable deviations locally in other parts. Of course, this can be expected knowing that the accuracy of the heights in the DEM is around ± 8m, so a good fit will not occur with the 10m contour interval, while the fit will improve with a 20m interval.

11.4.3 Comparison of Heights given by the Contours from the Reference Map with the Corresponding Values given by the DEM

11.4.3.1 Comparison of DEM Heights with 50m Contours

In this test, the same procedures have been carried out as in Section 10.9.2. The first comparison was made using the reference scene 122/285 covered by 50m contours from the 1:250,000 scale map. For the Level 1B DEM, 589 points have been measured and recorded. The RMSE value of the differences in height between the elevations at the measured cursor position and those given by the digitised contours from the RJGC map have been calculated, giving a figure of ± 9.9m for the Level 1B DEM. The same process has also been carried out for the DEMs generated by DMS for the other Level 1B stereo-pairs of the Badia Project area. For the DEM extracted from the Level 1B stereo-pair 123/285, the RMSE value of the differences in elevation between the two sets obtained at 325 points along selected contours was ±10.8m. While for the DEM extracted from stereo-pair 123/286, the RMSE value obtained from the elevation differences between the two sets at 449 points was ± 12m. Finally, for the remaining two Level 1B stereo-pairs, 124/285 and 124/286, the elevation differences at 297 and 348 points respectively gave RMSE values of ±7.3m and ± 7.8m.

Table 11.9 provids a summary of the accuracy of the elevation values obtained from the Level 1B DEM using this particular test. It can be seen that somewhat lower results were obtained from stereo-pairs 123/285 and 123/286: in this respect, these stereo-pairs are in the new format generated using a fifth order polynomial for the Level 1B processing. Another possible explanation is that these poorer results may be due to the effects of the mean elevation value which is a user input, though this seems less likely.

DEM	Scene	No. of Points	RMSE ΔH (m)
Level 1B	122/285	589	±9.9
Level 1B	123/285	325	±10.8
Level 1B	123/286	449	±12.0
Level 1B	124/285	297	±7.3
Level 1B	124/286	348	±7.8

Table 11.9 Comparison of the heights given by the contours from the reference map with the corresponding values given by the DEM.

11.4.3.2 Comparison of DEM Heights with 10m Contours

Another accuracy test has been carried out using the 10m contour data from the 1:50,000 scale map following the same procedures. In this test, only the contours digitised from the 1:50,000 scale topographic map and covering part of the Level 1B DEM of the reference scene 122/285 have been tested. The RMSE value of the differences in elevation obtained at 220 points along the selected contours was ± 8.1m.

11.4.4 Accuracy Test of the DEMs using the Profiles Measured by GPS

An accuracy test of the DEMs obtained by DMS has been carried out using the profile data that has been measured along 160 km of the old Al-Mafraq-Baghdad main road which lies parallel to the present modern highway. This road appears in four of the stereo-pairs covering the Badia Project area. A second profile had been measured along the old road between Safawi and Al-Azraq which runs parallel to the modern Safawi-Al-Azraq highway that goes on towards Amman. This profile is around 45km long, and appears in two stereo-pairs - the reference stereo-pair 122/285 and stereo-pair 123/286.

More than 15,000 points have been measured along these two profiles and, from these, the author selected 1,248 individual points with an average distance of 150m or less between each of the points. The location of each of the GPS profile points has been measured on the screen and the given heights at all of these GPS points were compared with the corresponding heights extracted from the DEMs for the same locations.

The differences in the elevation values between the values measured by the GPS sets and those for same position derived from the DEMs were calculated. From these differences, the mean difference has been calculated which was consistently around 25.6m. Apparently this is due to datum error. The standard deviation of the points was then calculated from the differences in heights from the mean. The elevation accuracy obtained in terms of the standard deviation was ± 9.3m. For the reference stereo-pair 122/285, 528 GPS points were located and the accuracy obtained in terms of the standard deviation was ± 9.0m.

11.5 Accuracy Test of the Orthoimage of the Reference Stereo-model

To evaluate the accuracy of the orthoimages produced by DMS, a check was carried out by measuring quite independently the positions of 38 GCPs lying within the area of the orthoimage for the main test scene 122/285. Using a simple linear conformal (first-order) transformation, the measured orthoimage coordinates were then transformed into their equivalent UTM terrain coordinates. These were then compared with the corresponding coordinate values derived from the GPS ground survey. The resulting RMSE values of the residual errors in ΔE and ΔN were ± 12.1m and ± 10.6m respectively, which, for the 20m pixel size used to produce the final orthoimage, gives RMSE values of ± 0.6 pixel in the x-direction and ± 0.5 pixel in the y-direction. The vector plot (Figure 11.20) of the individual residual errors resulting from the comparison showed that some kind of small systematic error remained in the south-western and in the north-eastern parts of the area, while the other parts showed a completely random distribution with no systematic components.

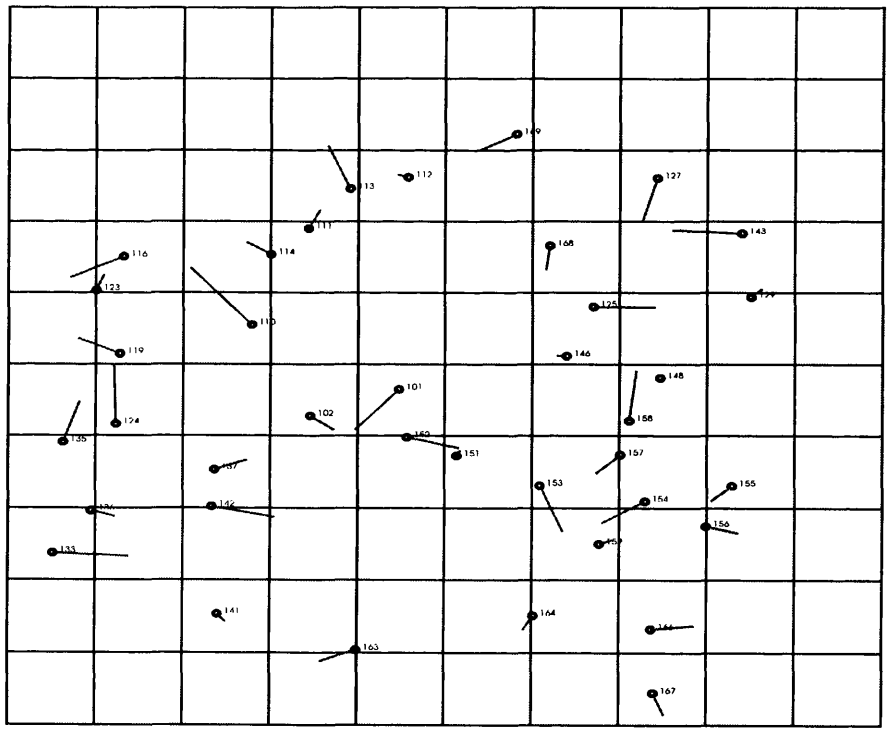

Figure 11.20 Vector plot of the planimetric (X/Y) errors at the check points measured on the orthoimage of the reference Level 1B stereo-model for scene 122/285

11.6 Conclusion

In spite of all many difficulties that were encountered both before and after fixing the system, finally the DMS system gave satisfactory results in terms of geometric accuracy in both planimetry and in heights. The accuracy of the DEM elevation values was less than one pixel size; this has been confirmed both through the accuracy tests using the independent check points and using the GPS profile survey data. It is a really excellent result achieved with the use of a low-cost package and a less sophisticated solution in terms of its photogrammetric procedures than the other systems tested in this project.

With superimposed contours, due to the characteristics of the DMS package, no real quantitative test could be performed. However, from the visual comparison with the contours from the existing RJGC maps, there is a good fit of the contours in most parts and some deviation in the other parts. This is probably due to the deviation of the value of the mean elevation of the area input that is input by the user from the correct mean elevation which is unknown. As the author's tests have shown, this is an extremely sensitive parameter: even a slightly wrong input value has a substantial effect on the final elevation values that are generated by the DEM.

In general, in spite of all the corrections which have been made to the system by modifying or adding new programs as a result of the extensive geometric accuracy tests of the Level 1B SPOT images which have been carried by the present author in collaboration with Mr. Jordan, the system still has several problems related to its lack of stability on the one hand, and the lack of automation of some of the processes on other hand. In addition, some problems are still found in this system, especially in the stereocorrelation process where the system consistently faces a problem over the image matching of the south-eastern part of every stereomodel. Moreover, the automatic process of orthoimage mosaicing without having a full interaction with the user, creates mosaiced orthoimages that are radiometrically unbalanced. In addition, the system faces a certain limitation caused by its inability to generate contours from the extracted DEM and the need to use an external program auch as SURFER or EASI/PACE for this purpose.

Mr. Jordan has explained that the present author was the first user to produce and comprehensively test a full DEM from a SPOT stereo-model using the DMS system. Due to the previous lack of a suitable test field, the system supplier had never been able before to extract and test a full DEM. The system had been tested by the supplier previously on parts of SPOT stereo-pairs amounting to 1,000 x 1,000 pixels, when no problems have been encountered. But the availability of the high accuracy test field of the Badia area brought the underlying problems into the light.

In spite of all of these deficiencies which have largely been put right, the system itself is easy to use and is by far the easiest system to learn of those employed in this research project. In addition, it uses a simple interface, is user friendly and offers very fast processing. Also it produces results of a good accuracy that many users will regard as being adequate, especially since DMS is by far the least expensive of those systems that have been tested. In comparison with other systems, the present author feels that the system is not stable enough (- it crashes quite frequently -) and needs to be developed and refined further. As it stands, the system with its 2D solution is mainly suitable for use over small areas which do not require ultra high accuracy.

In this chapter, the image processing procedures and the tests of the geometric accuracy of planimetry and height produced by the DMS system have been presented and discussed. In addition, tests of the accuracy of the DEMs and orthoimages produced by the DMS system have been carried out. In the next chapter, the tests that have been carried out to establish the geometric accuracy and other characteristics of the OrthoMAX system will be discussed and presented.

CHAPTER 12: GEOMETRIC ACCURACY TESTS AND VALIDATION OF DEMs, CONTOURS AND ORTHOIMAGES USING THE ORTHOMAX SOFTWARE

12.1 Introduction

The various problems that were encountered and revealed as a result of the geometric accuracy tests and the validation of the DEM and orthoimages produced by the EASI/PACE and DMS systems have been discussed in the previous three chapters. In this chapter, the results of conducting a similar series of investigations and experimental tests with the ERDAS OrthoMAX system will be reported and discussed. In course of doing so, a critical account of the photogrammetric and image processing procedures will be presented. Also an assessment of the quality of the DEMs and orthoimages produced by the system will be given following similar procedures to those used with the EASI/PACE and DMS systems.

12.2 Procedures Used in ERDAS OrthoMAX for the Photogrammetric Processing of SPOT Stereo-Pairs

This system was not available in the University of Glasgow. Therefore, in order to carry out the accuracy tests and validation procedures using the five SPOT stereo-pairs of the Badia Project test area, the help of the remote sensing section of MLURI (Macaulay Land Use Research Institute) in Aberdeen was sought and given to carry out an appropriate series of tests. In this respect, on the first trip to Aberdeen, the author and his supervisor travelled with full hope that good results could be obtained from the reference Level 1B stereo-pair for scene 122/285, since we had been given to understand from ERDAS (UK) Ltd that the package was in production use in various establishments in the U.K. In collaboration with Dr. David Miller of MLURI, the main test model was tested using an ERDAS OrthoMAX system, the actual work being done on his Unix-based Sun SparcStation 20 graphics work station.

12.2.1 Pre-Processing Procedures

The first step in the image processing of the SPOT data was of course to import the images into the system. Raw satellite data can be imported from CD-ROM through the system's import/export module, where selection of the type of satellite imagery and file, is made from option parameters. Using the utilities menu, the user must then select the required map projection and coordinate system with the **edit projection** command. In the OrthoMAX package, access is given to over 200 map projections and datums and defined Cartesian co-ordinate systems. From the so-called **Block Tool,** the user is able to set the required reference frame. For this particular Project, the items UTM zone 37 and European datum 1979 were selected. Using the frame editor, the two scenes were imported and an image pyramid was created giving a reduced resolution (RRDS) image of the stereo-pair for fast loading and overview purposes.

12.2.2 Ground Control Point Measurement on the Images

The software provides the capability of carrying out the measurement of the ground control points and tie points in up to three images simultaneously. The system dialogue, which is carried out through the use of suitable prompts, is designed to enable efficient measurement of the ground and tie points occuring within a stereo-model with facilities for any required manipulation - e.g. zooming, contrast adjustment, brightness adjustment, etc. - being available for each of the images either individually or simultaneously. In this system, the two overlapping images appear on the screen side-by-side to try and increase the speed of measuring the control points. The planimetric coordinates and the height of each control point can only be entered once for both images forming the stereo-pair.

To run this program from the system's activities pull-down menu, the user should first select the command for ground control point measurement. After the operator has placed the cursor over the control point location, the arrow keys can be used for the exact positioning of the cursor over the control point, with a zooming factor up to 4x. As the cursor is moved across the image, the x and y image coordinates in pixel values at the bottom of each panel will be updated in real-time. Depressing the left mouse button, a

marker will be placed on the image and the point will be measured. Once a measurement has been made, the x and y image coordinate values will be locked on the display at the foot of the panel. After each measurement, the user can select the next point to be measured. To add tie points (as required for SPOT triangulation), the operator must click on the "**add tie point**" command to invoke the appropriate tie point dialogue - in which case, the user has to enter the ID number and the optional description for the tie point. In addition, there is an **autoplace** button which can be used to semi-automatically locate and measure control and tie points.

12.2.3 Bundle Adjustment Procedures

The actual bundle adjustment procedure can be selected from the **"activities"** pull-down menu that is available in OrthoMAX. This will create the bundle dialogue. The first parameter to be entered is the convergence value which defines the points when the iterative least squares bundle process will be complete. If the maximum adjustment to all the ground control points is less than this value, then the bundle program will stop iterating. The maximum number of iterations that this package will allow is 20 and the default value was set to 10 iterations. The user can then use the **"run"** button to begin the least squares bundle adjustment process. After the bundle adjustment process has been completed, the user can press the "**view results**" button to review the results of the adjustment. This will display a file containing the numbers and the final coordinates of all the control and pass points that were available for each image during the adjustment. Also the residual errors are presented for each iteration including the image residuals, the position residuals for each of the ground control points, and a summary. A **"view propagation"** command is provided for the operator to review the estimated standard deviation values of the coordinates of the exposure stations and the ground control points. Another use of the "**update**" button is to update the a priori image parameters after one adjustment. The actuation of the "**accept**" button saves the results of the current bundle adjustment.

12.2.3.1 Interpretation of the Results

During the first visit to MLURI in Aberdeen, the results of the processing of the main Level 1B stereo-pair for scene 122/285 that have been achieved with the OrthoMAX package in terms of the final RMSE values at the ground control points were X= ±12.5m; Y = ±7.8m - giving an vector of ± 14.7m - and Z = ± 1.0m.

(a) While these results were reasonably satisfactory in a number of respects - e.g. the planimetric errors were not too out of line with expectation - there were still a number of matters that were not clear, more especially the results that being produced by the package's **"View Propagation"** routine. The advice from the supplier was that these are the figures to which particular attention should be paid when trying to assess the accuracy of the final results. In this context, the actual results for the **"Point Standard Deviation (PSD)"** values that were given by the "**View Propagation**" routine for the 49 ground control points (GCPs) used with the stereo-pair when different weighting values were input by the author, were as follows:-

(i) Weight: X = Y = Z = 10m

Points	X(m)	Y(m)	Z(m)
101	7.794	6.912	9.956
102	7.812	6.917	9.530
103	7.845	6.925	9.543
---	-----	-----	-----
---	-----	-----	----
170	7.813	6.916	9.533
171	7.790	6.913	9.527

(ii) Weights: X = 2; Y = 2; Z = 3m

Points	X(m)	Y(m)	Z(m)
101	3.154	3.120	4.756
102	3.154	3.120	4.756
103	3.154	3.120	4.756
---	----	----	----
---	----	----	----
170	3.154	3.120	4.756
171	3.154	3.120	4.756

(iii) Weights: X = 1; Y = 1; Z = 1.5m

Points	X(m)	Y(m)	Z(m)
101	1.633	1.628	2.453
102	1.633	1.628	2.453
103	1.633	1.628	2.453
---	----	----	----
---	----	----	----
170	1.633	1.628	2.453
171	1.633	1.628	2.453

In the first place, the **PSD** values shown are identical for all 49 GCPs for two of the cases [(ii) and (iii)] and virtually identical for the third [case (i)]. On the other hand, their absolute values change quite drastically whenever the one set of weight values is changed for another - in spite of the fact that the same set of input data was being used in all three cases. That is, (a) the same set of measured image coordinate values, and (b) the same set of terrain coordinate values for the GCPs were being used in each of the three cases. Yet the absolute PSD values were completely different.

Furthermore, looking at the **Z (elevation) values,** they change from ± 2.5m for case (iii) [X = Y = 1m; Z = 1.5m] to ± 4.8m for case (ii) [X = Y = 2m] to ± 9.95m for case (iii) [X = Y = Z = 10m]. From this experience, it would appear that any figures can be produced for the standard deviation values using OrthoMAX that one would like by simply altering the weight values - which certainly manages to give the impression that the analytical photogrammetric solution is not stable. This leads on to the further question as to what are the values that should be used for weights when the estimated accuracy of the measurements of position and elevation of the GCPs in the field made by differential GPS is ± 1 metre in X, Y, Z; and the estimated accuracy of the measurements of the image coordinates of these points in the OrthoMAX system is of the order of 0.5 pixel.

(b) Next came the matter of interpreting the output from the **"View Results"** routine of OrthoMAX. This gives a list of the final transformed coordinates at each of the ground control points (GCPs). Associated with these are the values of the corrections that have been made as a result of the last iteration of the bundle adjustment.

However what was missing from the OrthoMAX results were the **differences** between the given coordinate values of check points and the final transformed coordinates. This is, of course, the acid test as to whether the fit of the SPOT stereo-model to the ground control points (GCPs) is good or not. Based on this information, one can then decide whether or not to go on to the next stage of creating the DEM. If the discrepancies between the two sets of coordinates are large, then a detailed inspection will be carried out to locate and eliminate any misidentified or poorly measured points. Instead one only has RMSE values for control points used in the Adjustment.

Thus inspection of the table for **weighting case (i)** [X = Y = Z = 10], showed that the RMSE values are X = ±12.5m; Y = ±7.8m (giving an vector of ±14.7m); and Z = ±1.0m. Until a thorough explanation of the effects of weighting within this adjustment is achieved these figures have little value.

A further inspection of the corresponding tables for **weighting case (ii)** [X = Y = 2m; Z = 3m] showed that the RMSE values drop quite dramatically to X = ±1.05m; Y = ±0.9m (giving a vector of X/Y = ±1m); and Z = ±0.27m. Again such values may not be very helpful.

(c) Which brings up the third matter that came to light during the tests of the stereo-model - that of the **height datum.** The ground control points (GCP) coordinate values have been provided in metres in the Universal Transverse Mercator (UTM) system with height values in metres above Mean Sea Level (MSL). However, when the relevant projection and the datum (European Datum 1979 based on the International Spheroid) were selected within OrthoMAX, inspection of the ground control point editor showed that the height (elevation) values at all the ground control points (GCPs) had been altered by the program by 170 metres or so - without any action on the part of the analyst. At the same time, the X and Y (Easting and Northing) values remain unchanged. One could only presume that this large offset in the Z values was caused by the separation between the Spheroid and the geoid defining the Mean Sea Level (MSL) datum.

All of these points - (a), (b) and (c) - were made to Vision International, the originator of the OrthoMAX package. Also additional remarks were addressed to the company regarding the use of Level 1B SPOT stereo-pairs in processing, and the change of format of Level 1B images by SPOT Image. The response of Mr. Molander, the director of marketing and business development for the Vision softcopy photogrammetry products (OrthoMAX and SoftPlotter) and acting product manager, was as follows:

"A block bundle adjustment by least squares is nothing but a weighted average of the sample data, the image measurements, and the coordinates of the ground control points.

Concerning propagated accuracy and weights, it is true that weights can be massaged to produce nearly any result one wish to see, the statistical measures in the software can be used to measure the validity of various weights and results. A posteriori standard deviation of unit weight, measure the validity of the assumption (weights) and values (system data, measurements, ground coordinates). The least squares adjustment implicitly assumes that the a priori standard deviation of unit weight is 1.0. This figure should be very close to 1.0 for any result to be judged reliable, but values of 0.8-1.5 are considered acceptable. Weights on ground control points drive very heavily the propagated errors. A sigma of 10 m on the ground control produces a sigma of 10m in error propagation. Since the system parameter weights are much lower, then the ground control dominates the propagation. If the ground control sigma's are tightened down to 1m, the propagated errors will be on the order of 1m. Concerning the propagated sigma values are not a judge of the accuracy, but rather are a function of the estimated sigma's for each item (system parameter, ground control points, image sigma's). Image sigma's should be set to around 0.5 pixel and ground sigma's should be set to the known accuracy of the ground control. Listing 10 for sigma, the RMSE values for the final iteration on ground control points are ±12.5, ±7.8, ±1.0 metres for X, Y, Z respectively are very appropriate.

Concerning the changing of the elevation of the ground control UTM coordinates in the software, this matter will be checked.

The change in polynomial order for level 1A-1B mapping polynomials in the CAP 1B format contrasts with our information".

It will be seen that this reply did not really throw much light on the results and statistics produced by the OrthoMAX package. As will seen later, the company's lack of attention to the change in the Level 1B processing was to have considerable repercussions on the final results achieved with the OrthoMAX package.

In spite of all these difficulties, the image matching procedure was then carried out for the extraction of a DEM with a grid interval of 200m to see the final product of OrthoMAX system and to validate the DEM.

12.2.4 DEM Extraction (Stereocorrelation)

The Level 1B stereo-pair of scene 122/285 covering the main test area was processed for DEM extraction. From the file pull-down menus, a new DEM can be defined. This option is only available with the OrthoMAX Elevation Extraction Modules. This function allows a specific imagery source to be selected. The parameters that are to be used are also defined when the **"new"** command is selected within the file pull-down menu, when a **"define new DEM"** dialogue appears on the screen. From the prompt "**source**", either an existing stereo-pair or raw imagery can be selected. Next a new DEM file name is selected. This is followed by the input of the required ground spacing units and the appropriate reference frame. To change this to a different datum or map projection, the operator clicks on the "**Set**" button. This will invoke a reference frame display on the screen showing the list of available datums and map projections. From these, a suitable reference frame can be selected. If the definition of automatic collection parameters is desired, then this is selected within the select **"Set Strategy"** Dialogue. Alternatively the selection of the "**Edit**" pull-down menu invokes an Edit DEM parameters dialogue which can be used to modify the collection parameters of the currently loaded DEM.

The OrthoMAX module provides the capability to generate gridded elevation data from SPOT stereo-pairs. The automatic image matching procedure to produce the DEM is an area-based method based on cross-correlation. During the matching process patches of pixels from the source images are correlated. The primary correlation measure is to employ normilized cross-correlation which takes into account the overall differences in contrast and brightness between the image patches. The algorithm is used a hierarchical approach in which correlation are performed at increasingly higher resolution of imagery. This approach is useful both to speed up the computational process and to compensate for large changes in elevation in the DEM - since it constrains any movement between resolutions to prevent "false fixes" at largely disparate elevation values. The unique aspect that is claimed for Vision algorithm is the simultaneous derivation and use of orthorectified patches of the imagery in the matching process. It will be noticed that, unlike two of the other packages tested during this research project,

no attempt is made to rectify and resample the images and to search along epipolar lines for matches.

Following the collection of the elevation data at each resolution, elevation values for these points which were not successfuly correlated during the automatic process are interpolated by using suitable groups of successfully correlated points in the neighbourhood about each of these points.

12.2.4.1 DEM Stereo Editing in the Professional Version of OrthoMAX

In general to achieve a good DEM, editing tools should be used to edit the DEM. In fact, these editing tools are only available in the so-called professional version of OrthoMAX. However, due to the fact that none of these facilities were available in the version of OrthoMAX that was available at MLURI, so the DEMs produced by this system have been edited in EASI/PACE - e.g. to clean up the area along the boundary of the DEM from spikes and noise. Still it is worth while to mention briefly the methods that are used for editing in the professional version which were inspected during a visit to the facilities of ERDAS (UK) in Cambridge. As will be discussed, a comprehensive set of tools is available.

In the OrthoMAX Professional Module, DEM editing is accomplished via the stereoscopic display of the DEM, where the so-called elevation "posting" or grid height values are represented by crosses located over the stereo-model. The entire DEM view may be toggled on or off by means of the "**show DEM**" button located under the "**View**" pull-down menu. To edit the height of a single point, the point is measured in stereo using the mouse or the arrow keys to place the measuring mark or cursor on the terrain. Alternatively the operator can click on the "**Ht**": window and enter the new point elevation, and then measure the point using the left mouse button. The point nearest the stereo cursor will be assigned either the ground elevation value given by the stereo cursor or the assigned height. The "**equal**" button can be used to set the heights of multiple points to a single elevation, by first drawing a polygon around them. Once the polygon is closed, the next step involves the selection of the "**apply edit**" button to actually apply the changes. The height of the first vertex of the polygon - which can be

set with the terrain-following cursor or manually with the Z-mode, or simply by entering the height value in the "**Ht:text**" field - will be applied to all points lying within the polygon.

The so-called "**face**" button provides the ability to define a planar polygon and adjust all points within the polygon to the height defined by the plane. Like the "**equal**" editing tool, the face tool uses a bounding polygon. With the "**face**" tool, each vertex of the polygon is measured in all three dimensions, and the plane is defined as the best fit plane through these vertices. Once the polygon is closed, the "**Apply Edits**" button can be selected to adjust the enclosed points to the heights defined by the polygon plane. The "**surface**" button provides a routine to fit a surface through a region of DEM points utilising selected interactive measurements. This is implemented by drawing a polygon around the points and then measuring the points inside the polygon by placing the cursor at the desired ground position and elevation through stereoscopic viewing, then applying the "**Edits**" button to fit the surface through the points.

12.2.4.2 Accuracy Test of the Reference Level 1B Stereomodel by Superimposed Contours

To validate the DEM extracted from the main Level 1B stereo-pair of scene 122/285, the only method that was available to the author was to generate contours from the DEM extracted by the OrthoMAX module with a 50m contour interval and to superimpose them on the contours with same contour interval digitised from the existing 1:250,000 scale topographic map in the UTM coordinate system. From Figure 12.1, it is clear there is quite a big difference between the two sets of superimposed contours. The fit is limited to an area of higher relief in some north-western parts, while major deviations appear in the eastern part. It is clear that there is a big shift in the contours extracted from the DEM compared with those from the existing map. This could be explained as the results of a datum error or shift as compared with the European Datum 1979 based on the International Spheroid given to the OrthoMAX system.

This opinion has been confirmed when the file was exported to the EASI/PACE system, and contours have been generated from the DEM and superimposed over the digitised contours.

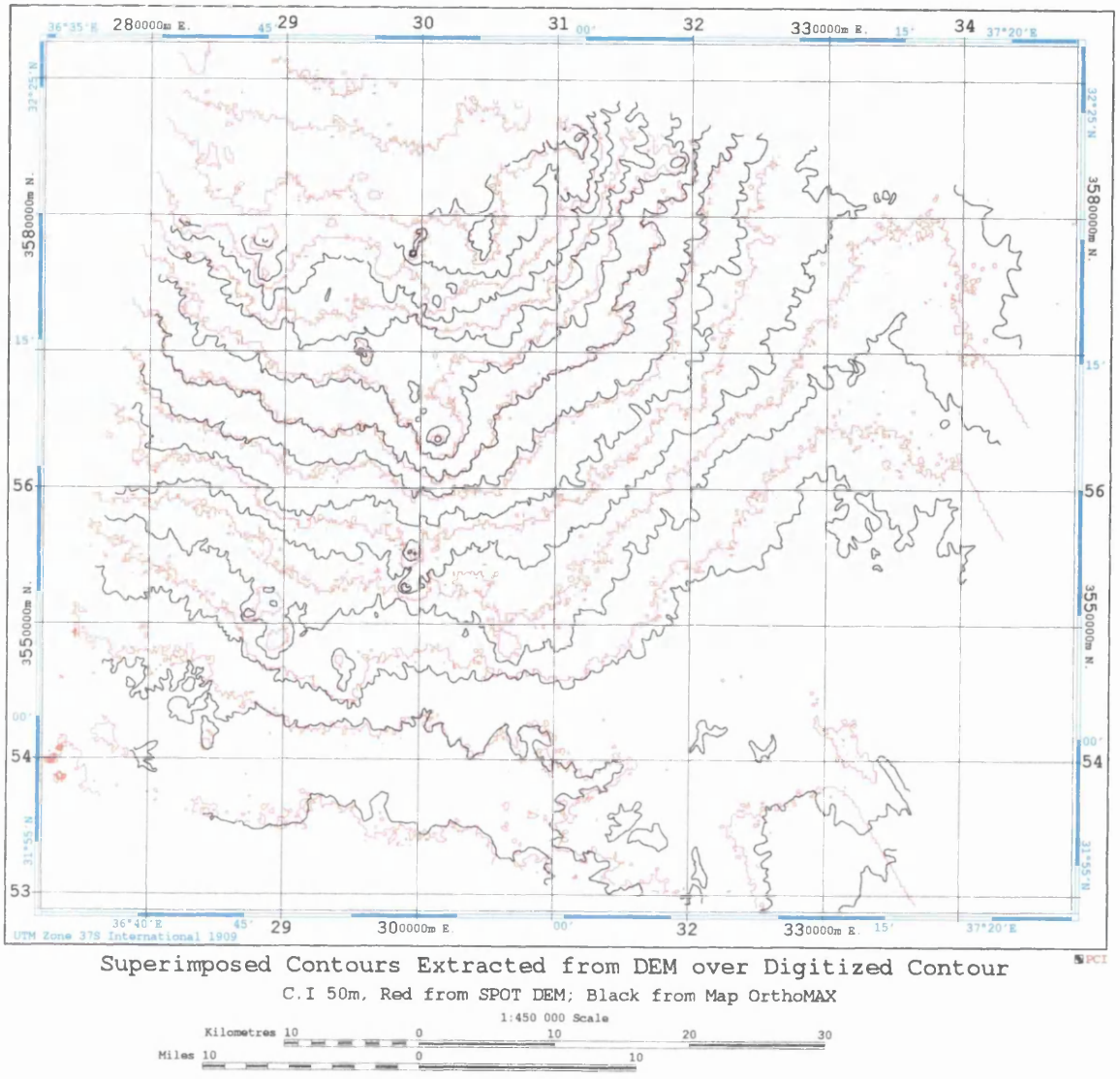

Figure 12.1 Superimposed contours extracted from the DEM of the Level 1B reference stereo-pair of scene 122-285. The contours produced by OrthoMAX have been superimposed over the digitised contours from the RJGC 1:250,000 scale topographic map.

To solve this problem, which clearly showed the shift in the contours, the only solution that was available to the author was to use the **MAS** module (Modify database segments) available in the EASI/PACE system. This has been used to modfiy the segment of the contours to the required georeferencing system, i.e. to the UTM projection system based on European datum 1950. This also required changing the georeference segment of the file to the required georeferencing system using this

program. The inputs to this program were the file name; database segment list; database segment name; database segment description and map unit. As can be seen later in Sections 12.6 and 12.7.2, new contours have been generated from the Level 1B DEM and shown in Figures 12.7 and 12.12.

12.3 Accuracy Tests of the Other Four Stereo-Pairs

To carry out DEM extraction for the rest of the Badia area, further visits have been made to MLURI in Aberdeen. In cooperation with Dr. David Miller, an attempt has been made to process the four remaining Level 1B stereo-pairs. First of all, the stereo-pair 124/285 was processed. The initial step was to change the datum to European 1950 Datum (ED 50), after which 18 ground control points have been measured. The system accepted these ground control points and carried out the orientation successfully. The resulting accuracy report in terms of the RMSE values of the residual errors in planimetry and height after 7 iterations gave ±3.1m, ±4.5m, ±0.016m in X, Y, Z respectively - as shown in Table 12.1. The residual errors in planimetric position are quite acceptable and the vector plot of these errors in planimetry at the individual control points given in Figure 12.2 showed a random error pattern. However that the results in elevation giving RMSE values of ± 0.016m remind us that these RMSE statistics may not useful. Next the processing steps for stereocorrelation and DEM extraction have been performed and the DEM extracted successfully with a 200m grid spacing.

The same procedures have been carried out for the Level 1B stereo-pair of scene 124/286. Due to the limited number of control points available in this area - since a big part of the stereo-pair lies in Saudi Arabia - only 14 ground control points have been used. The orientation process has been carried out without any problems and the results contained in the accuracy report in terms of the RMSE values of the residual errors in planimetry and elevation after 6 iterations gave values of ± 3.4m, ± 3.2m, and ± 0.018m in X, Y, Z respectively. The planimetric errors are possibly useful. Furthermore as shown in Figure.12.3, the vector plot of the errors in planimetry show a quite random patteren of the planimetric errors. However once again, the result in height reminds us that these RMSE values are unlikely to be useful. Stereo correlation was also carried out

for DEM extraction and a DEM was generated with a 200m grid spacing for this stereo model. Table 12.1 summarizes the results which have been achieved for these two models (124/285 and 124/286).

Badia Area	No. of GCPs	ΔX (m)	ΔY (m)	ΔP (m)	ΔH (m)
124/285 Level 1B	18	±3.1	±4.5	±5.5	±0.016
124/286 Level 1B	14	±3.4	±3.2	±4.7	±0.018

Table 12.1 RMSE values at the GCPs.

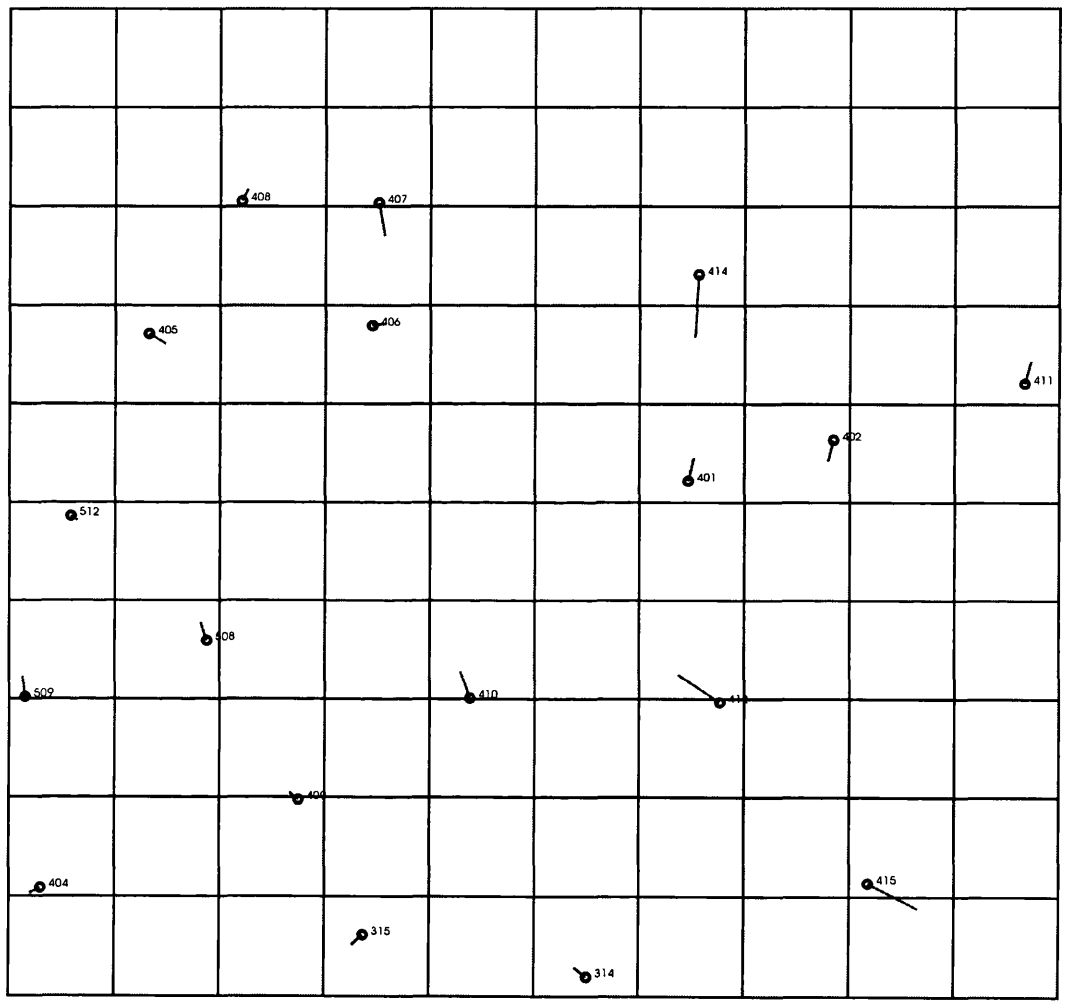

Figure 12.2 Vector plot of the errors in planimetry at the GCPs of the Level 1B stereo-pair for scene 124/285.

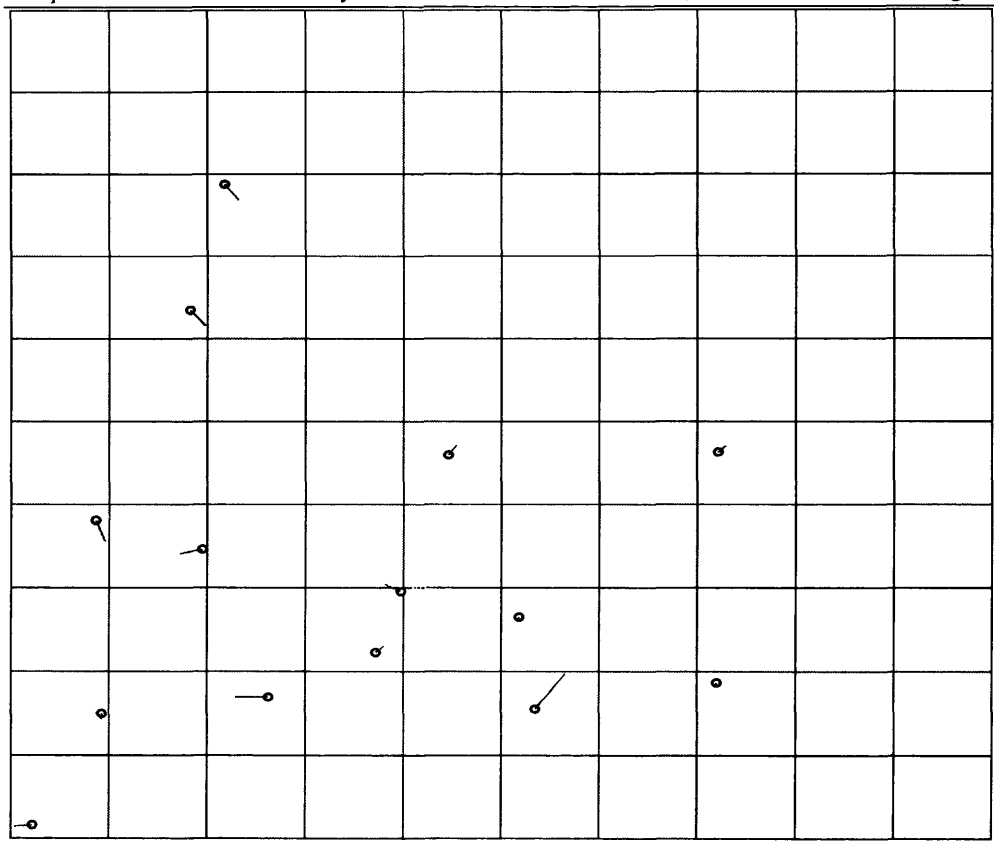

12.3 Vector plot of the errors in planimetry at the GCPs of the Level 1B stereo-pair for scene 124/286.

12.3.1 Problems in Bundle Adjustment for Stereo-Pairs 123/285 and 123/286

The fourth Level 1B stereo-pair for scene 123/285 has also been imported to the processing stage. After carrying out the ground control point measurements and trying to run the bundle adjustment program, the program failed completely. An attempt was made to find methods to run the program but without success. Then the fifth stereo-pair 123/286 was imported and the relevant ground control points have been measured. Again the orientation process did not work when attempts were made to run the program. An attempt was made by Dr. David Miller with Vision International to find a solution for these problems but, to date, no solution has been achieved. In the author's opinion, the difficulty appears to lie in the failure of the OrthoMAX program to cope with the Level 1B images produced by the newer processing method using a 5th order polynomial that has been adopted by SPOT Image.

12.4 Accuracy Tests of the Level 1A and 1B Stereo-models of the Reference Scene 122/285

A third visit was made to MLURI, the main aim of this visit was to test the Level 1A stereo-pair for scene 122/285 and to see how the system behaves with this Level of image, and to try again to solve the problems that had been encountered with the other two Level 1B stereo-pairs 123/285 and 123/286. For the Level 1A stereo-pair for scene 122/285, different numbers of ground control points have been processed. The results of these accuracy tests in terms of the RMSE values in planimetry and elevation obtained are shown in Table 12.2.

Scene	Level	No. of GCPs	ΔX (m)	ΔY (m)	ΔP (m)	ΔH (m)
122/285	1A	47	±3.7	±3.8	±5.3	±1.5
		28	±3.7	±4.0	±5.4	±1.5
		22	±3.9	±4.7	±6.1	±1.2

Table 12.2 RMSE values after bundle adjustment in planimetry and heights at the GCPs of the main test area for the Level 1A stereo-pair 122/285.

The vector plot of the errors in planimetry at the control points shows a random error pattern as shown in Figure 12.4.

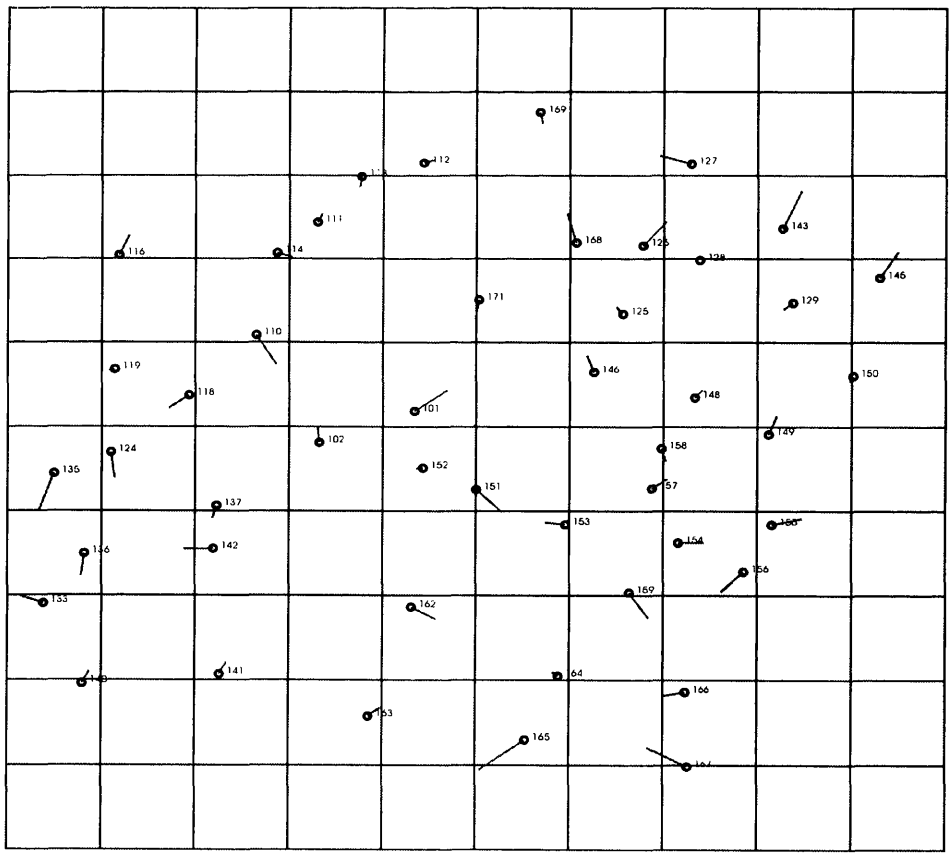

Figure 12.4 Vector plot of the errors in planimetry at the ground control points for the Level 1A stereo-pair for scene 122/285.

Again it is obvious from Table 12.2 that the height error values at the 1.2 to 1.5m level cannot be correct. But the processing was continued for DEM extraction using the system's stereo correlation routines to give elevations at a grid interval of 20m. The DEM extracted from this stereo-pair was later subjected to an accuracy test.

During this third visit, the Level 1B stereo-pair for scene 122/285 was processed again to extract a DEM. Again the gridded DEM was extracted with a 20m grid spacing. Also an accuracy test of the DEM has also been carried out. The accuracy of the bundle adjustment process in terms of RMSE values was ±6.3m in Easting and ±4.7 m in Northing. The vector plot of the error values in planimetry at the control points showed a systematic pattern of errors in the south-western part of the stereo-model and locally in some other parts. In other parts, the vectors show a more random pattern of errors - see Figure 12.5.

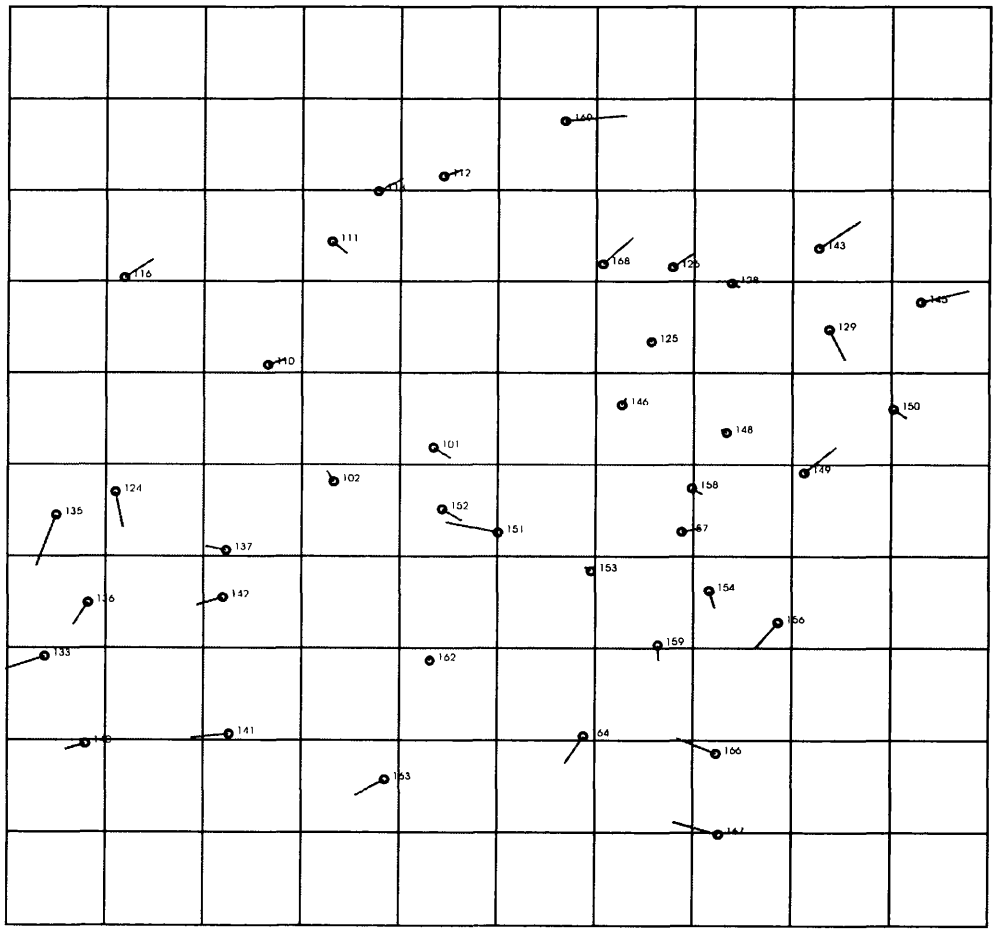

Figure 12.5 Vector plot of the errors in planimetry at the ground control points for the Level 1B stereo-pair for scene 122/285.

12.5 New Format of SPOT Stereo-Pairs 123/285 and 123/286

For the other two stereo-pairs - 123/285 and 123/286 - yet another attempt was made to process them but without success. Since the system was able to process three of the Level 1B stereo-pairs but not the other two, there must be a reason for this. Eventually after discussion with Dr. Cheng of PCI, the author discovered that the five stereo-pairs were not in the same format. SPOT Image changed the format in September 1995; as noted in Chapters 9 and 10, the three of them which have been processed by OrthoMAX without problem are in the old format (using a third order polynomial), while the two others had been produced after the processing (which utilised a fifth order polynomial) was changed - in which case, they will be in the new format. The author informed Dr. David Miller about the possibility of this having caused the problems. Dr. Miller then contacted Vision International directly and they undertook to investigate the idea. Another approach to Vision International about this matter was also made by Professor Petrie (Universty of Glasgow) who asked them to investigate the idea of the images being in two different formats. In reply, Vision International promised to do so as soon as possible. However, up to the time of writing, no positive reply has came from Vision International or from its licensee, ERDAS, nor has any new release of the OrthoMAX software appeared that takes care of the problems encountered by the author.

12.6 Contour Generation

So far, two separate DEMs have been extracted from the Level 1A and Level 1B stereo-pairs of the main test area covered by scene 122/285. In addition, two DEMs have been extracted from the Level 1B stereo-pairs for scenes 124/285 and 124/286. For the DEMs extracted with 20m and 50m post spacing (grid intervals), contours have been generated at intervals of 50m and 10m for the Level 1A and 1B DEMs for the reference stereomodel 122/285 and at a 50m interval for the DEMs extracted from the Level 1B stereo-pairs 124/285 and 124/286. From an initial inspection, it was obvious that these various contour plots really required substantial editing, which would need a lot of time and work to do. Due to the limited period of stay in Aberdeen, these contours had to be left without editing them there. The contours were then exported from the Sun Sparc Station to the server of the MLURI and then exported by ftp to the University of

Glasgow. Unfortunately when these contours files have been imported to the EASI/PACE system to carry out the editing, the process failed, either due to lack of memory or to problems in the data.

To obtain contours suitable for testing, a new set of contours needed to be generated from the DEMs. Once again, this was carried out using the EASI/PACE system. In general, the author takes the view - based on his own experience - that it is not really advisable to process data in a new system that has been processed before by another system. Either this will reduce the accuracy of the data or else the data will not be processed correctly. This was the case with the DEMs generated by OrthoMAX and can be seen in the contours that have been generated by the EASI/PACE system using this data, where it is immediately apparent that the contours have not been correctly generated from the DEMs and give a poor representation of the terrain surface of the area. In particular, a great deal of noise appears to be present with large numbers of tiny isolated contours. Close inspection also shows that the contour lines are far from smooth and exhibit lots of rectangular changes in direction - mostly in the cardinal directions - giving a stepped appearance. Figures 12.6, to 12.9 show the poor quality of the contours at a 50m interval for the Level 1A and 1B DEMs of the reference stereomodel of the main test area and for the other DEMs produced from the Level 1B stereo pairs of scenes 124/285 and 124/286. To improve the quality of the contours and to remove the noise and the tiny isolated contours, the DEM of the reference stereo-model for scene 122/285 and the DEM of the stereo-model 124/286 have been edited in the EASI/PACE system using **ImageWorks** -Edit DEM. Three separate filtering processes have been carried out through editing; these were remove noise, interpolation and smoothing. The results of the filtering process are shown in Figures 12.10 and 12.11.

12.7 Accuracy Test of Heights Contained in the DEMs of the Badia Test Area

To validate the data quality of the DEMs extracted from SPOT Level 1A and 1B stereo-pairs for scene 122/285, four different methods have been used:-

(i) check of the accuracy of the DEM elevation values at the GCPs; and

(ii) the comparison of the two sets of superimposed contours; and

(iii) the comparison of the height values given by the contours from the photogrammetrically produced reference map and the corresponding values given by the DEM; and

(iv) Comparison of the DEM data with the profiles measured by GPS along the main roads.

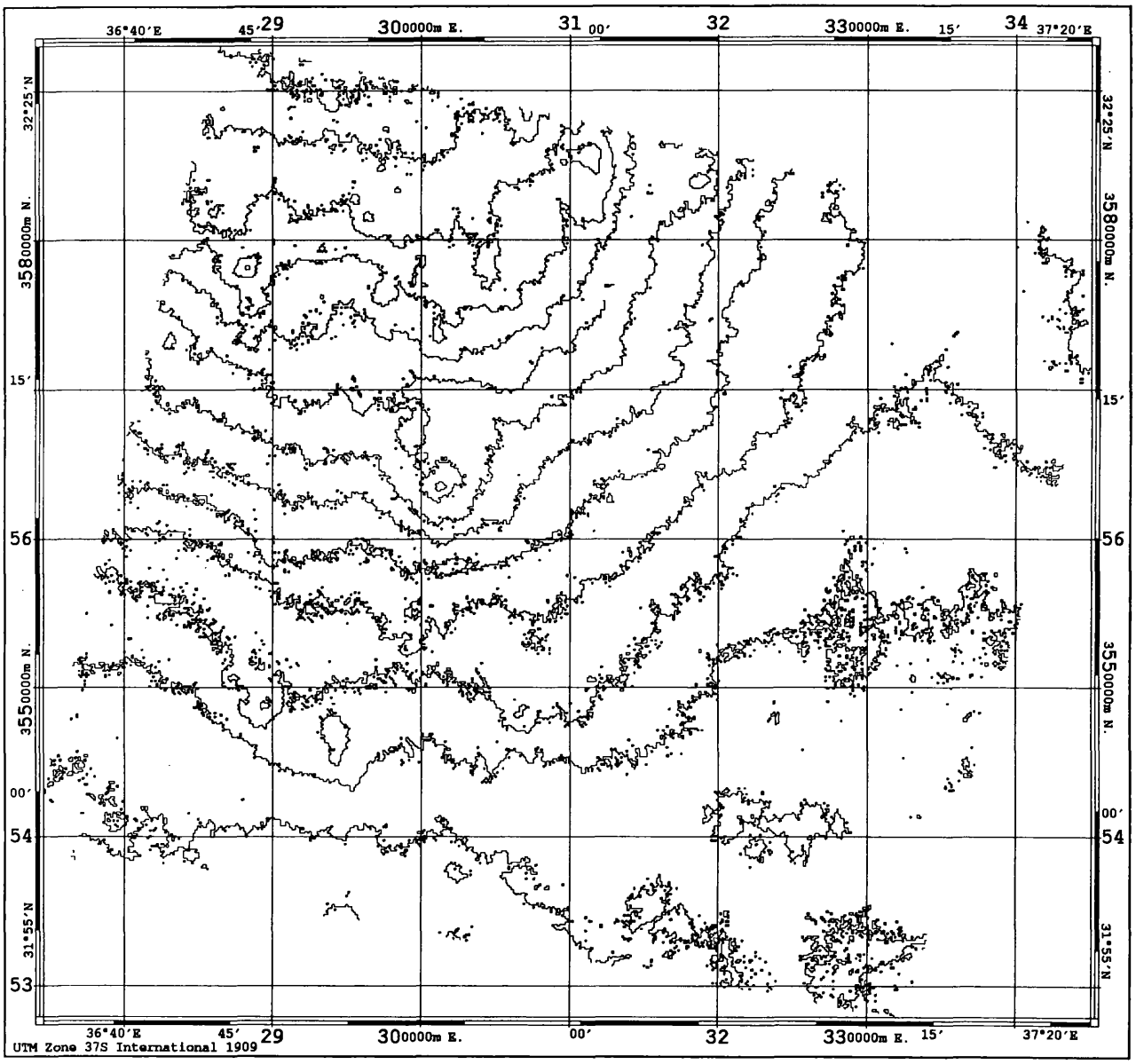

Figure 12.6 Contours generated from the DEM extracted from the Level 1A stereo-pair of the reference stereo-model 122/285 by OrthoMAX at an interval of 50m.

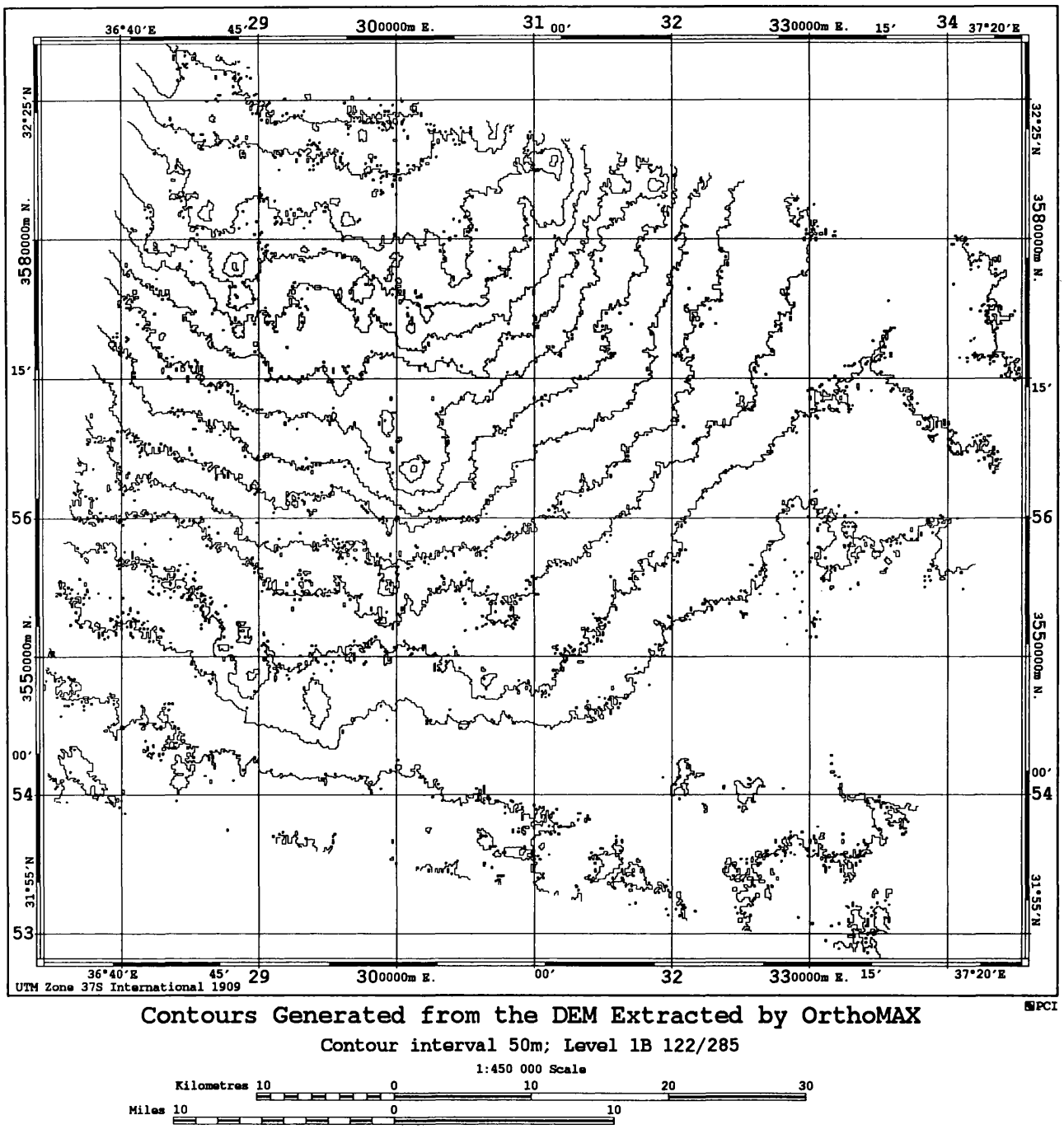

Figure 12.7 Contours generated from the DEM extracted from the Level 1B stereo-pair of the reference stereo-model 122/285 by OrthoMAX at an interval of 50m.

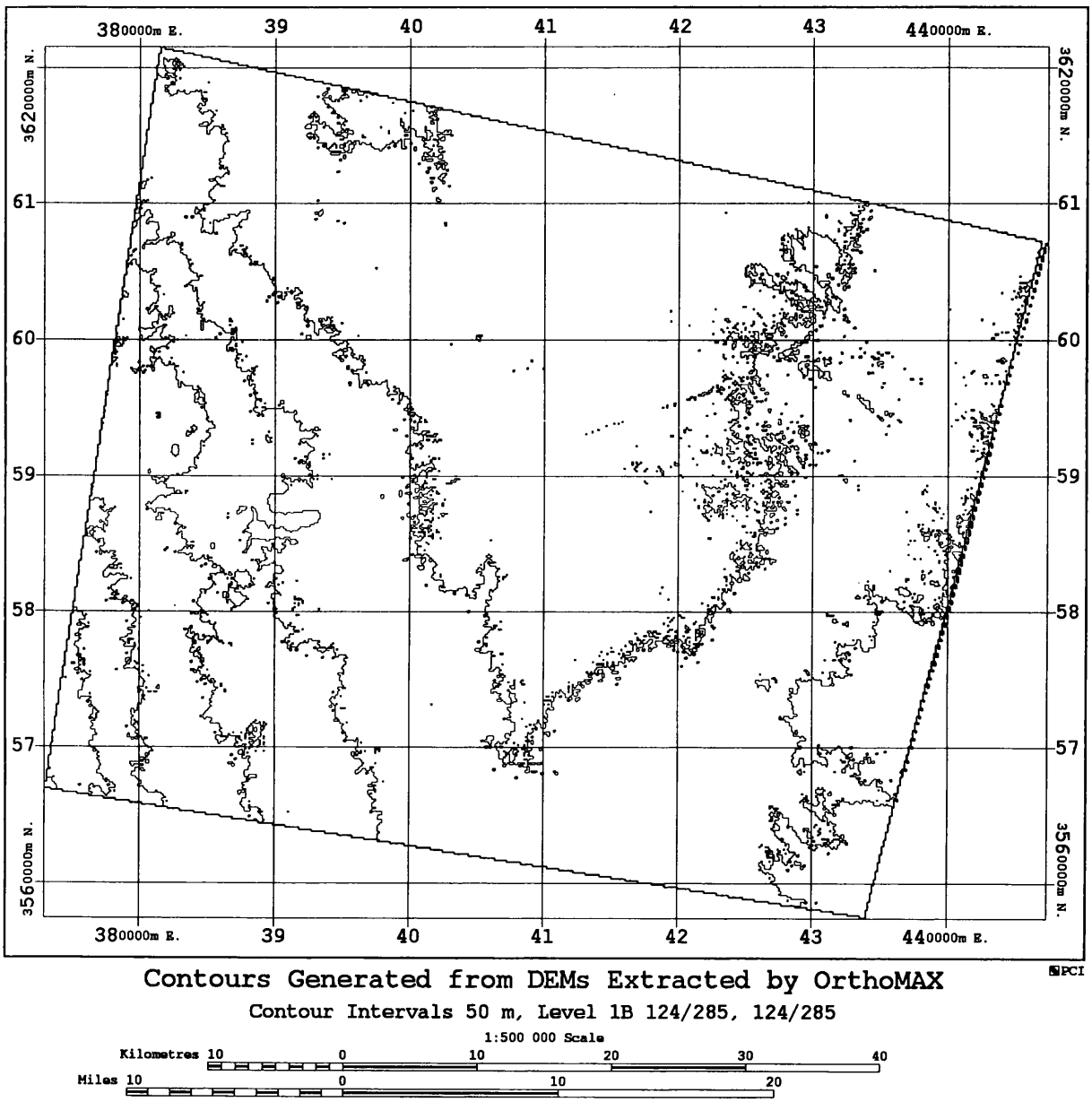

Figure 12.8 Contours generated from the DEM extracted from the Level 1B stereo-pair of scene 124/285 by OrthoMAX at an interval of 50m.

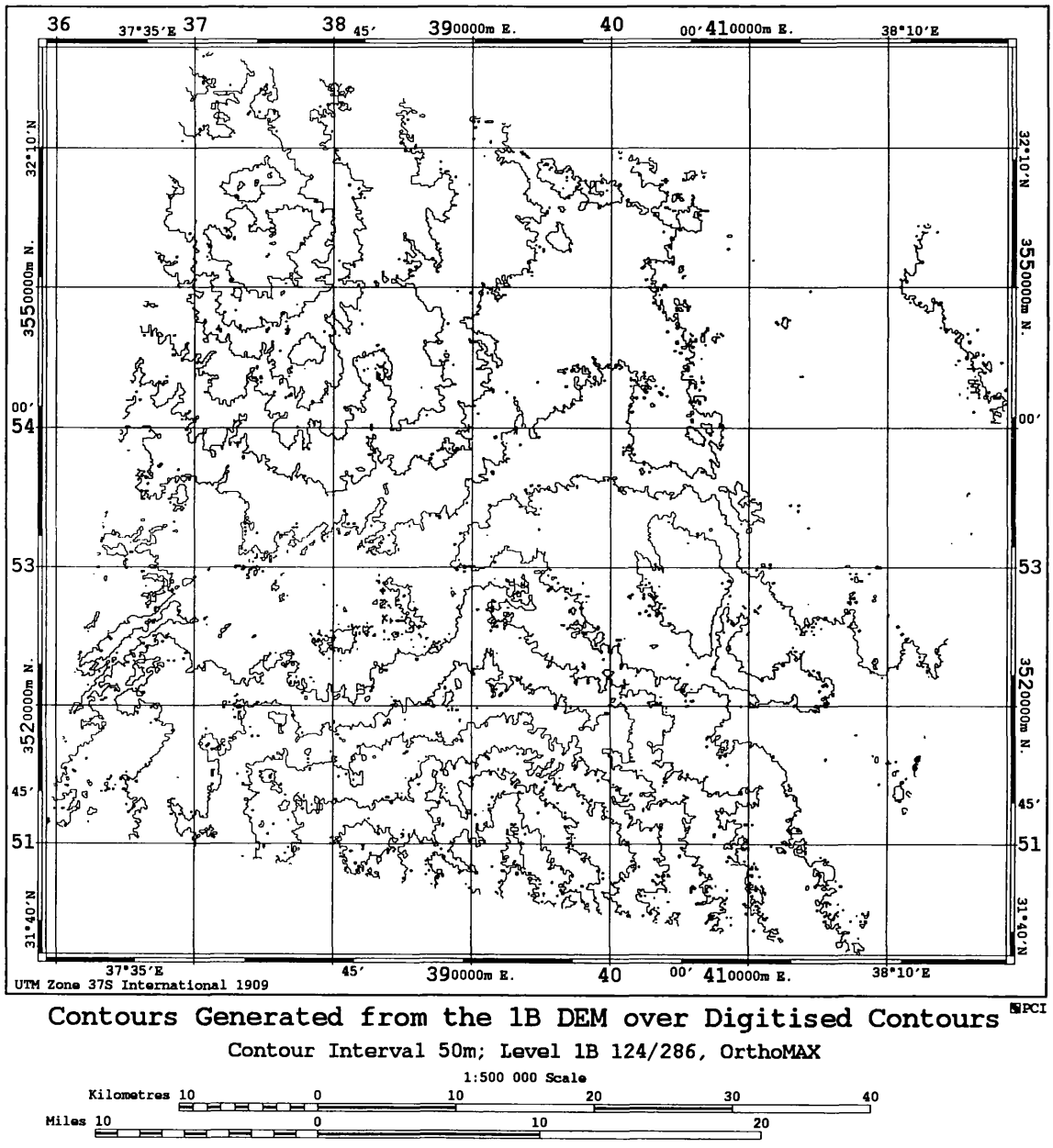

Figure 12.9 Contours generated from the DEM extracted from the Level 1B stereo-pair of scene 124/286 by OrthoMAX at an interval of 50m.

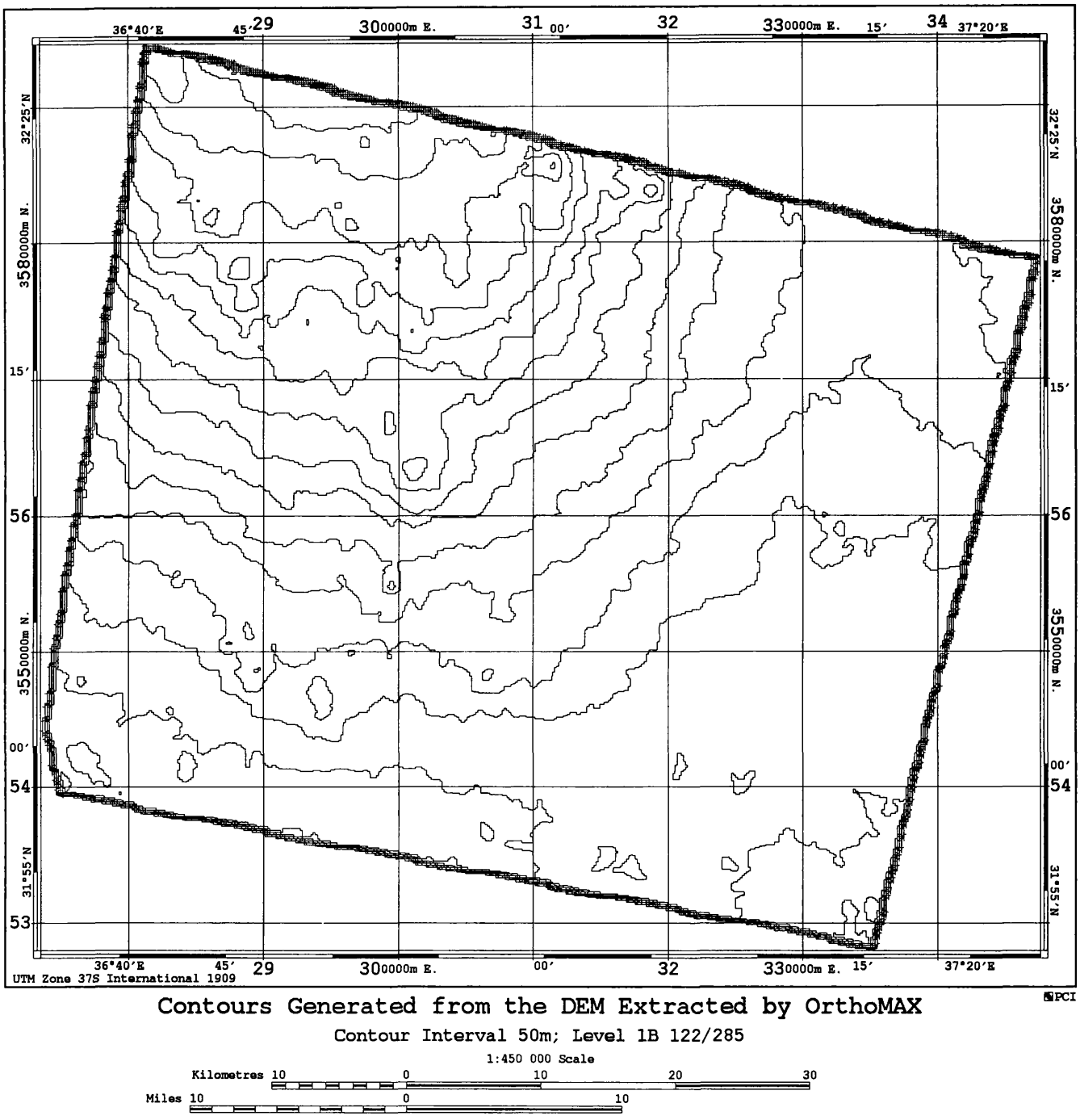

Figure12.10 Contours generated from the DEM extracted from the Level 1B stereo-pair of the reference stereo-model 122/285 by OrthoMAX at an interval of 50m after filtering using the EASI/PACE system.

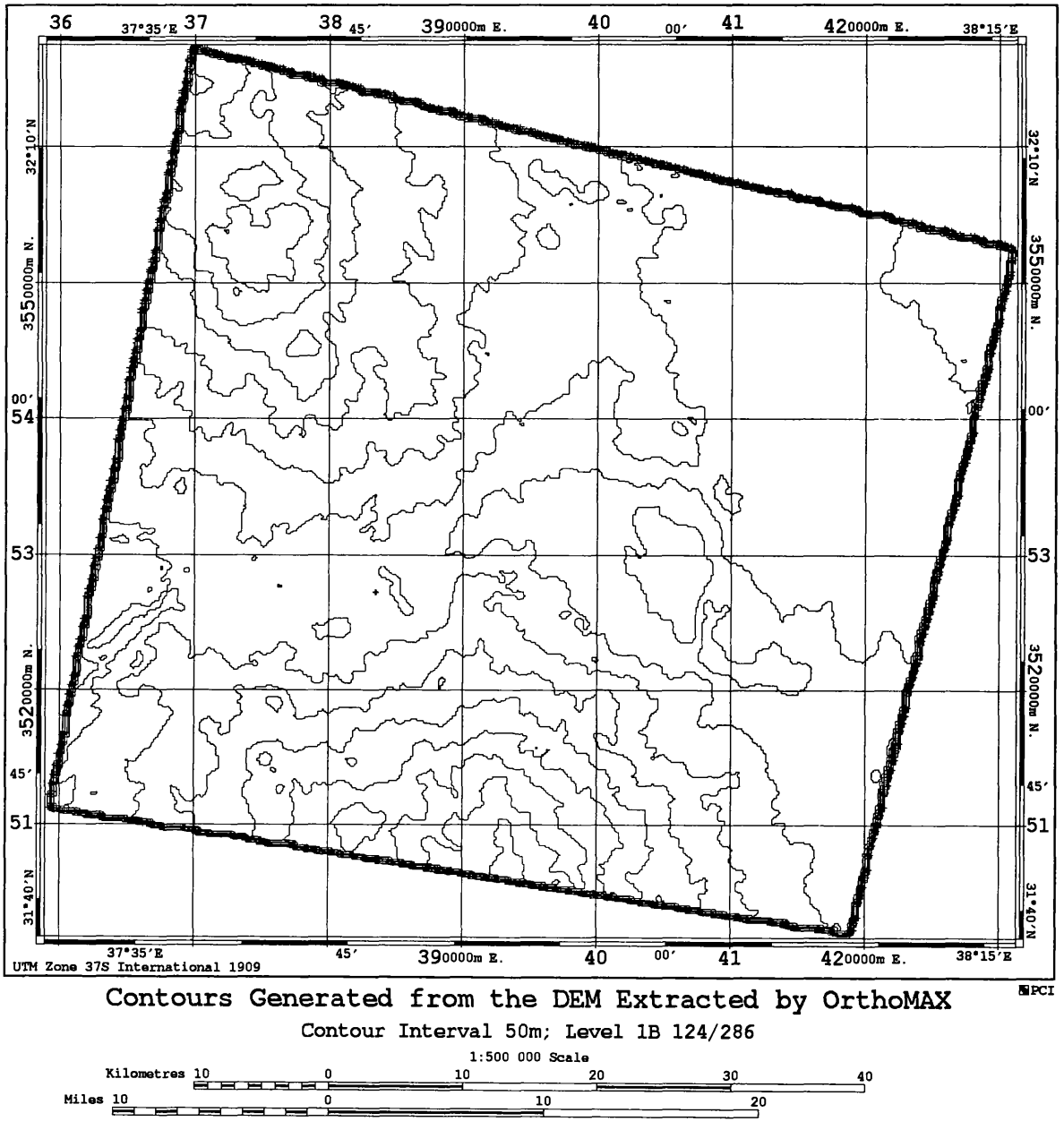

Figure12.11 Contours generated from the DEM extracted from the Level 1B stereo-pair of scene 124/286 by OrthoMAX at an interval of 50m after filtering using the EASI/PACE system.

12.7.1 Accuracy Test of Height at Selected Check Points in the DEM

(a) Accuracy of the Reference Level 1B Stereomodel for Reference Scene 122/285

The DEM extracted from the Level 1B stereo-pair 122/285 has been tested. Since there is no way to use check points during the initial orientation of the SPOT stereo-pair using OrthoMAX, and the final report of the orientation does not contain a list of check points, then the only way is to use some control points in the bundle adjustment solution and to keep other points back as check points to be used later for an accuracy check on elevation using the values got from the DEM. So 28 control points were used for the solution and a total of 25 independent check points have been used to check the accuracy in this way. These check points have never been used as control points for the orientation of the stereomodel. Also it should be said that some of these points were not too well identified and so the given coordinates of these points were used to give the location of these points in the DEM. The accuracy obtained at the check points in terms of the RMSE value in height was ±5.6 m.

(b) Accuracy of the Level 1A Stereomodel for the Reference Scene 122/285

In this accuracy test, 28 control points were measured and were used in the solution of the orientation. The rest of the ground control points that were not used for this purpose were kept apart to be used as check points for an accuracy check of the DEM. As in (a) above, each of these 25 check points have been positioned through the use of its given coordinate values to locate its exact position. Once this had been done, the corresponding elevation value was extracted from the DEM surface. The accuracy obtained at these check points in terms of the RMSE value in height was ± 5.2m.

12.7.2 Comparison of Superimposed Contours

(a) Superimposition of the Level 1A and 1B stereo-pairs over Digitised Contours from Map at 50m Contour Interval

In this test, starting with the Level 1B stereo-pair, only a visual analysis has been carried out. The set of contours extracted from the Level 1B DEM of the reference stereo-model

of scene 122/285 has been superimposed over the digitised contours from the RJGC 1:250,000 scale topographic map. Inspection of the two sets of superimposed contours as shown in Figure 12.12 indicates an excellent fit to each other except for some local areas mostly in the flat southern part of the area which show some deviations with a negative sign. In general, the deviation amounts to around 10% of the contour interval.

The contours extracted from the Level 1B DEMs of the stereo-pairs for the two remaining scenes 124/285 and 124/286 were mosaiced to each other and were superimposed over the digitised contours at 50m interval from the RJGC 1:250,000 scale topographic maps - as shown in Figure 12.13. Inspection of the two sets of contours indicate a good fit to each other. Local deviations can be seen in the eastern part of the area. However, as shown by the contours, this area is almost flat. Inspection of the rest of the area shows an excellent fit with an estimated deviation of less than 10% of the contour interval.

For the contours from the Level 1A DEM of the reference stereo-model of scene 122/285 superimposed on the digitised contours at 50m interval from the RJGC 1:250,000 scale topographic map, the comparison, as shown in Figure 12.14 indicates an excellent fit. Some local deviations occur in the southern part of the area. Inspection of the fit of the contours generated from the Level 1A DEM with the contours generated from Level 1B DEM and superimposed over contours digitised from 1:250,000 scale topographic map, as showed in Figure 12.15, indicate similar results and provide an excellent fit with the digitised contours.

(b) Superimposition of the Level 1A and 1B Stereo-pairs of Scene 122/285 over Digitised Contours from Map at 10m Contour Interval

For this test, contours were generated from the Level 1A and 1B DEMs extracted from the stereo-pairs for scene 122/285 at intervals of 10m and 20m. An attempt was made to superimpose the contours at 10m interval over the digitised contours from the RJGC 1:50,000 scale topographic map at the same contour interval, but the results of the superimposition was not good. This was due to the contours generated at this contour interval not having been filtered or edited which made the contours very close to each-

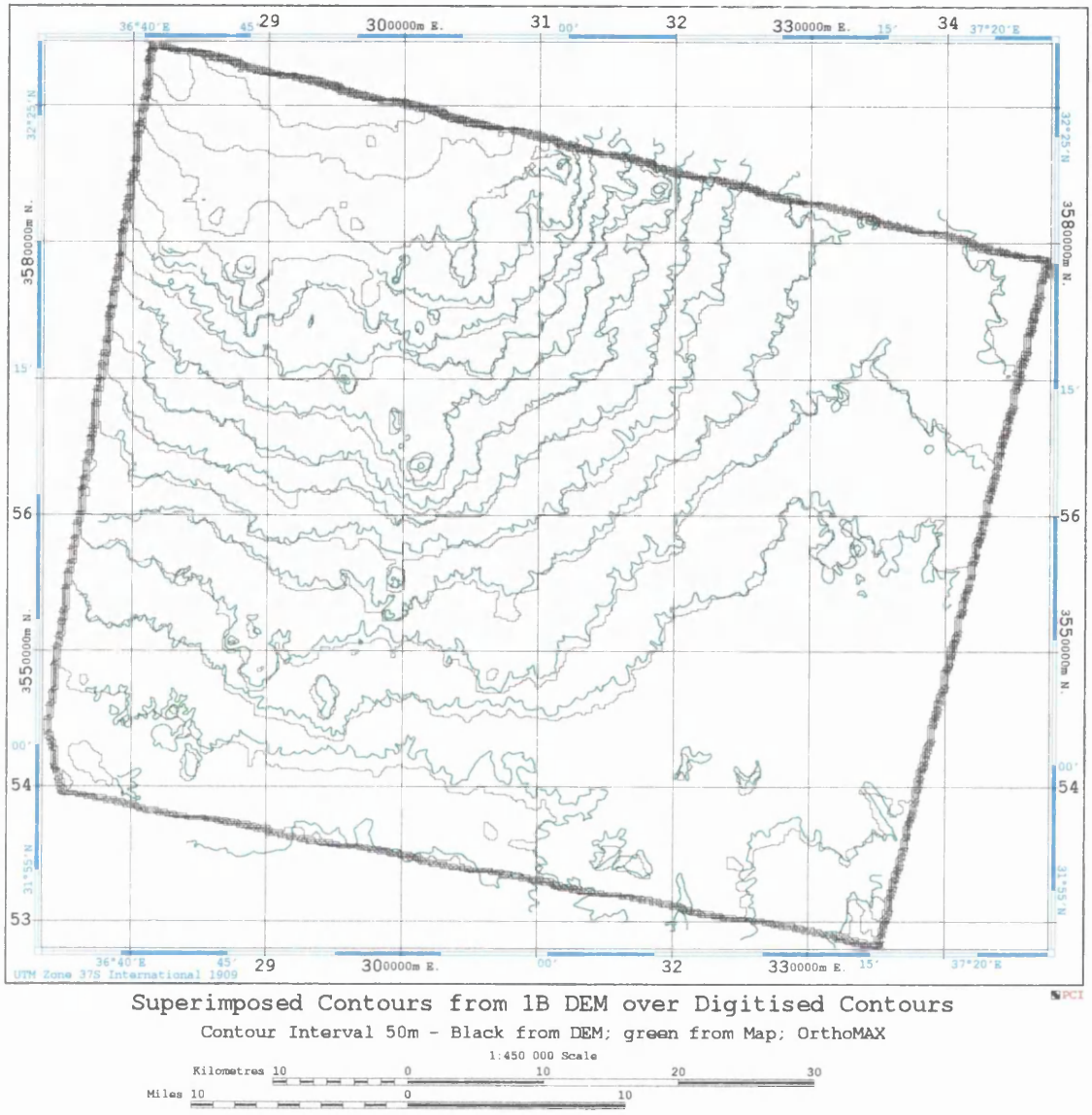

Figure 12.12 Superimposed contours extracted from the DEM of the Level 1B stereopair for scene 122/285. The contours produced by OrthoMAX have been superimposed over the digitised contours from the RJGC 1:250,000 scale topographic map.

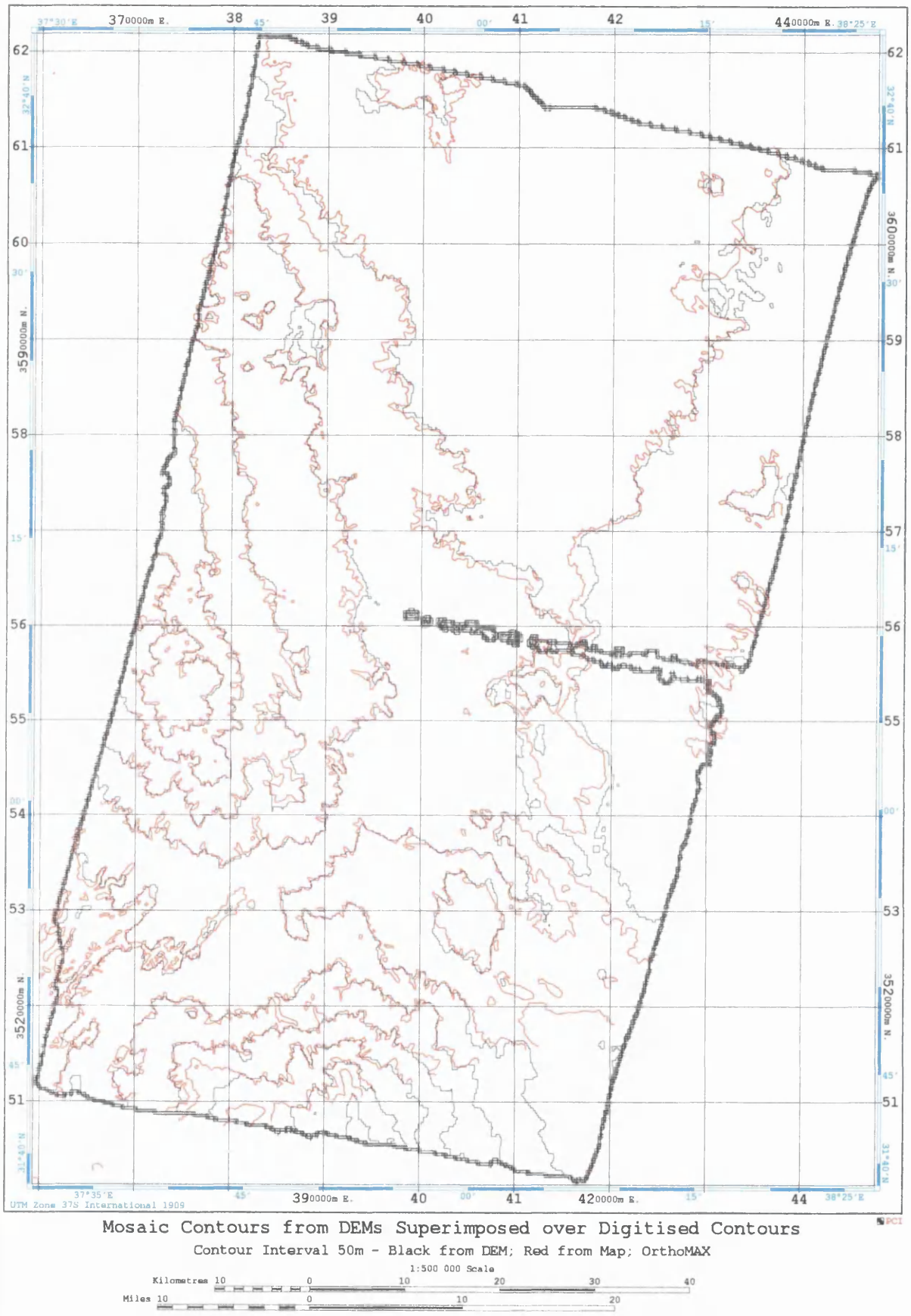

Figure 12.13 Superimposed contours extracted from the DEM of the Level 1B stereopairs for scenes 124/285 and 124/286. The contours produced by OrthoMAX have been superimposed over the digitised contours from the RJGC 1:250,000 scale topographic map

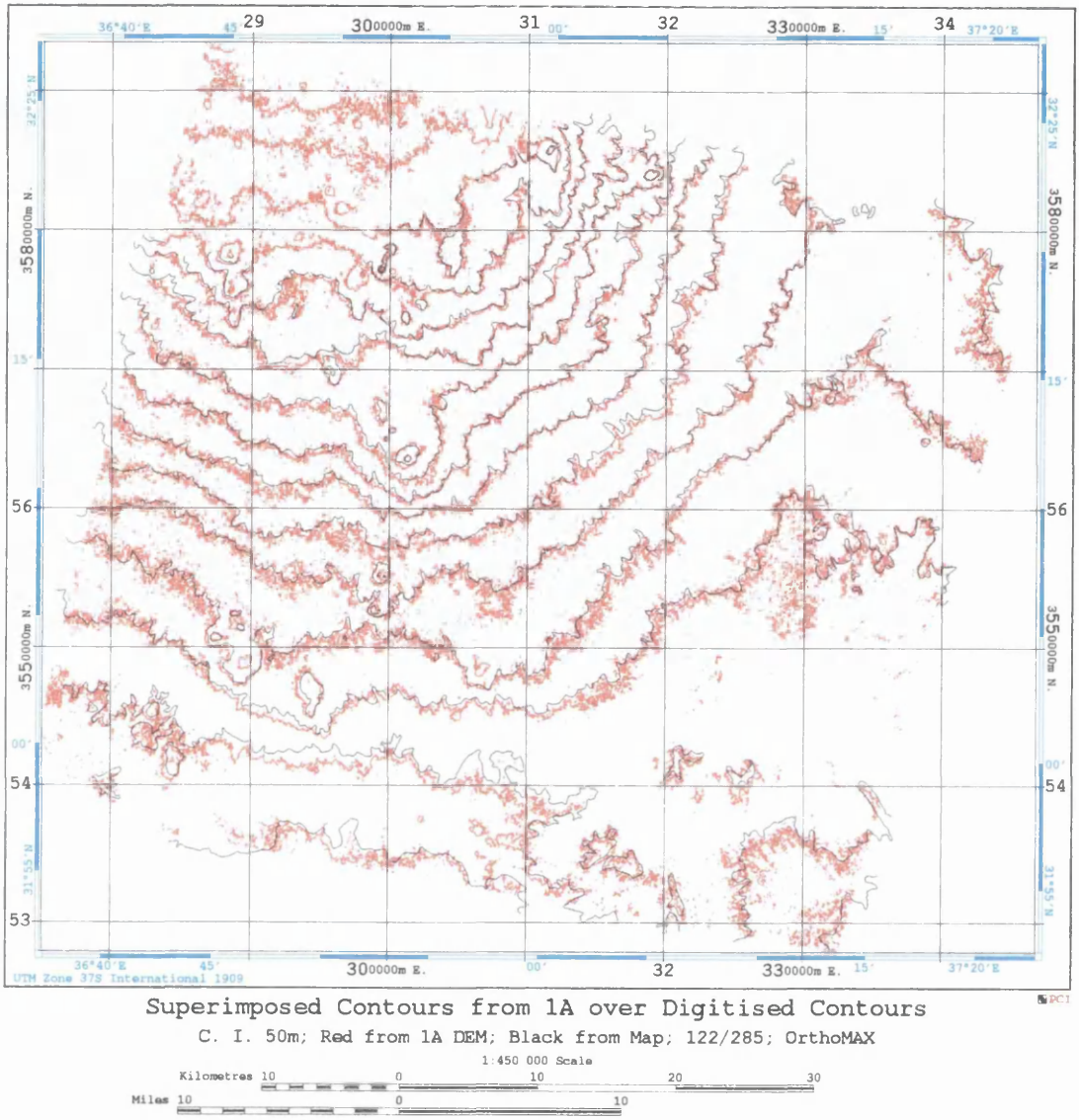

Figure 12.14 Superimposed contours extracted from the DEM of the Level 1A stereopair for scene 122/285. The contours produced by OrthoMAX have been superimposed over the digitised contours from the RJGC 1:250,000 scale topographic map.

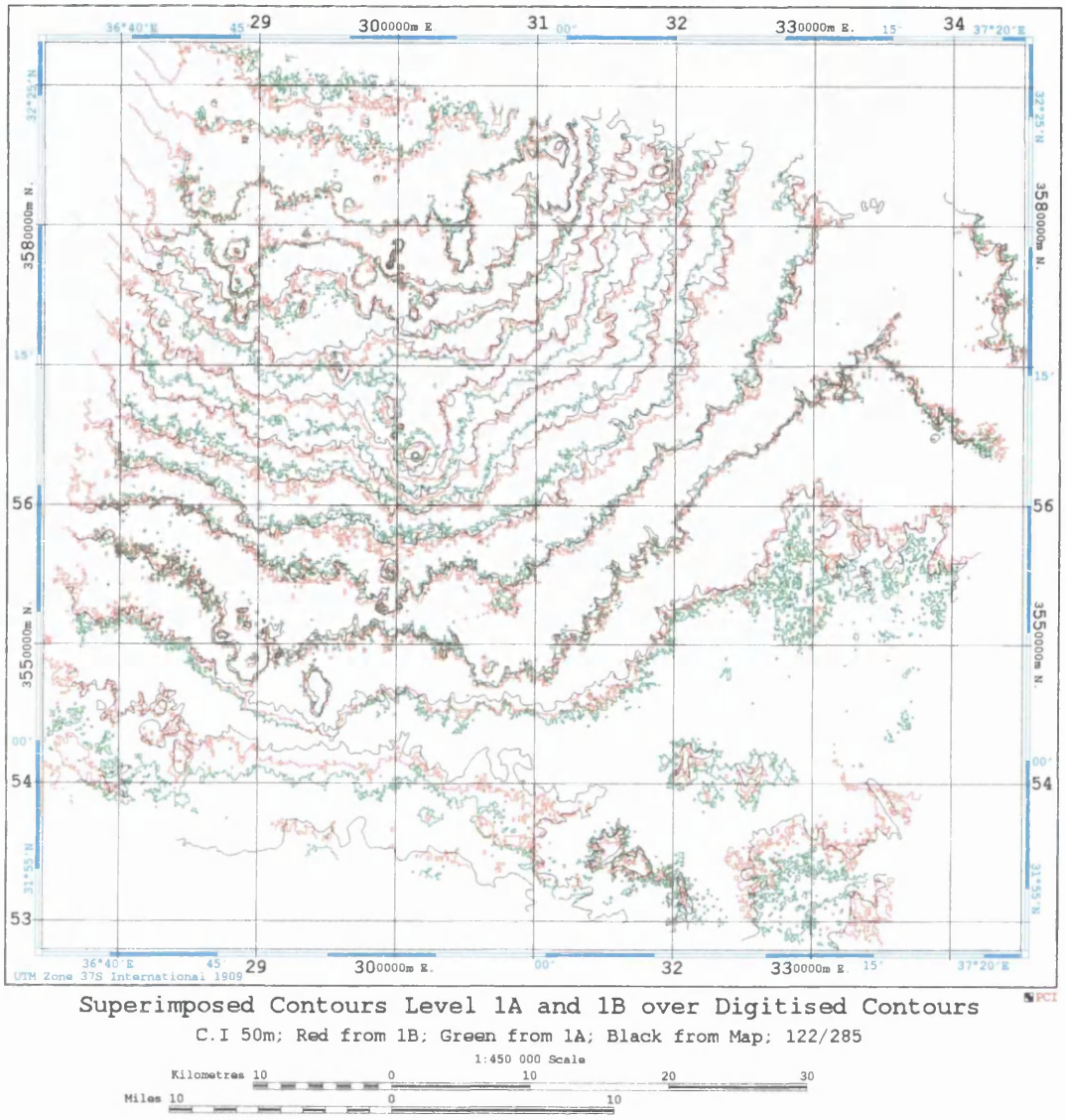

Figure 12.15 Superimposed contours extracted from the DEMs of the Level 1A and 1B stereopairs for scene 122/285. The contours produced by OrthoMAX have been superimposed over the digitised contours from the RGJC 1:250,000 scale topographic map.

other and not readable. The lack of clarity also stemmed from the fact that the main contour lines were surrounded by large numbers of tiny circular features - which appeared to be noise or unwanted artefacts - and requiring several days to edit out these features. To overcome these difficulties, another set of contours was generated from the Level 1A and 1B DEMs at an interval of 20m. Again, the artefacts around the main contours need to be edited and the visual inspection of the accuracy of fit was difficult to judge.

12.7.3 Comparison of Heights given by the Contours from the Reference Map with the Values given by the DEM

(a) Comparison of Heights Along the 50m Contours of the Level 1A and 1B DEMs of the Stereo-Pair for Scene 122/285

In this test, the same method was used as has already been described for the EASI/PACE system. Thus the digitised contours from the 1:250,000 scale map have been superimposed over the DEM. Before loading the DEM into ImageWorks, it should first be converted to 16-bit form. After doing so, then by using the **VATT** Program in EASI/PACE and placing the cursor at one end of the contour line and moving it along the digitised contour to those positions where the contour changes its direction, the program in each case recorded the corresponding coordinates and the heights of all these points from the DEM. These contours have been treated as reference contours, so what had been recorded were the corresponding elevation values of these points measured by the DEM. In this test, five contour lines have been selected, each with a different elevation. The difference between the DEM elevation value at each of these points and the elevation of the contour line in terms of the resulting RMSE value provided a statement of the accuracy of the height of the DEM. The accuracy of the height obtained in this way for the Level 1B DEM for scene 122/285 using 712 points gave an RMSE value of ± 8.9m, as shown in Table 12.3. The same procedures have been applied to the Level 1A DEM of the same reference stereo-pair. The accuracy of the height values obtained for 398 points gave an RMSE value of ±9.2m.

(b) Comparison of Heights Along the 50m Contours of the Level 1B DEMs of the Stereo-Pairs for Scenes 124/285 and 124/286

Similar tests have been also carried out for the other two stereomodels covering the north-eastern and south-eastern parts of the Badia Project area which the OrthoMAX system was able to process without problem. The tests which have been carried out for the DEMs from scenes 124/285 and 124/286 were restricted to the comparison of the reference contours digitised from map with the corresponding values extracted from the DEM due to lack of sufficient control points that could be considered for use as check points. The accuracy achieved in this test in terms of the RMSE value in elevation using 387 check points of the Level 1B DEM for stereo-model 124/285 was ± 5.2m. While the accuracy achieved in the Level 1B DEM for the stereo-model 124/286 in terms of the RMSE value in elevation using 453 points was ± 8.4m.

(c) Comparison of Heights Along the 10m Contours of the Level 1B DEM of the Stereo-Pair for Scene 122/285

The same procedures that have been carried out to test the accuracy of height in the DEM by comparing the reference contours digitised from map at 50m interval with the corresponding values extracted from the DEM have also been carried out for the digitised contours at 10m interval obtained from the 1:50,000 scale topographic map. The DEM accuracy obtained in terms of the RMSE value in elevation using 325 check points along the reference digitised contours from the 1:50,000 scale map was ±8.9 m.

12.7.4 Accuracy Test of the Level 1B DEM of the Reference Stereomodel 122/285 Using GPS Profiles

In this test, the same GPS profile measurements that had been selected to test the accuracy of the elevations contained in the DEMs extracted from the EASI/PACE system have been employed to test the accuracy of the DEM of the Level 1B stereomodel of scene 122/285 obtained from OrthoMAX. A total of 528 GPS points have been used to check the accuracy of the corresponding elevations contained in the DEM. The mean has been computed from the mean of all the errors and therefore is the

estimated elevation of the datum, while the standard deviation has been computed with respect to the mean. The mean of the elevation differences which has been calculated was 22.36m, while the standard deviation was ± 8.4m.

12.8 Overall Summary and Comparison of the Various Tests of Elevation Accuracy

A summary of the results of all these different tests of elevation accuracy achieved with the OrthoMAX package is given in Table 12.3.

Scene	Level	No of Check points	RMSE of Heights ΔH (m)	No. of Check Points	RMSE of the difference between reference contours and DEM values (50m interval) ΔH (m)	No. of Check Points	RMSE of the difference between reference contours and DEM values (10m interval) ΔH (m)	No. of Check points	GPS Profile Δ H (m)
122/285	1B	25	±5.6	712	±8.9	325	±8.9	528	±8.4
122/285	1A	25	±5.2	398	±9.2				
124/285	1B			387	±5.2				
124/286	1B			453	±8.4				

Table 12.3 Overall accuracy tests of DEMs of the stereomodels of the Badia area processed by the OrthoMAX system at the independent check points; a comparison of the difference between the reference contours value with the corresponding values extracted from the DEM and the GPS profile.

It is clear from Table 12.3 that the accuracy of the DEM of the Level 1B stereomodel for the reference scene 122/285 obtained via the GPS profiles has almost the same accuracy as that resulting from the comparison of the reference contours digitised from the 1:250,000 and 1:50,000 scale topographic maps at 50m and 10m intervals with the corresponding values extracted from the DEMs. In each case, the RMSE accuracy lies between ±8.4m to ±8.9m. Going on still further with these comparisons, the RMSE accuracy in elevation lies between the ± 5.6m obtained at the independent check points and the figures of ±8.4m to ±8.9m got from comparisons with the GPS profiles and the digitised contours. The explanation for this appears to be that the accuracy at the independent check points is affected only by the accuracy of the matching process while, for the other tests, the accuracy is affected both by the accuracy of the digitised contours (and the accuracy of the reference topographic maps) and the accuracy of placing the cursor at different positions along the contour lines on the screen. On the other hand,

one can take the view that the accuracy of the profile data which has been acquired using a kinemetic GPS method was very high (± 2 to 3m).

For the DEM produced from the Level 1A stereo-pair for the reference scene 122/285, two DEM accuracy tests have been carried out. In the first test, the same number of check points has been used as for the corresponding Level 1B test and the accuracy obtained in height was an RMSE value of ±5.2m - which is almost the same with only a very slight improvement. For the accuracy obtained in the comparison of the reference contours digitised from the 1:250,000 scale topographic maps at 50m interval with the corresponding value extracted from the DEM, the figure is slightly lower with an RMSE value in elevation of ±9.2m. These small differences compared with these obtained with the Level 1B data do not appear to be significant.

For the other DEMs produced from the Level 1B stereomodels for scenes 124/285 and 124/286, the only test which has been carried out used the comparison of the reference contours digitised from 1:250,000 scale map at 50m interval with the corresponding values extracted from the DEMs. This is due to the flaw in the OrthoMAX system which does not give the accuracy of the elevation values at check points as already discussed in section 12.2.3.1. The accuracy test of the DEM extracted from the stereomodel of scene 124/285 gave an RMSE value in elevation of ±5.2m which is quite good and similar to the accuracy obtained with the Level 1A DEM of the reference stereomodel for scene 122/285. For the DEM produced from the Level 1B stereomodel 124/286, the accuracy obtained in terms of the RMSE value in elevation was ±8.4m which is the same accuracy obtained with the Level 1B DEM of the reference stereomodel for scene 122/285.

12.9 Orthoimage Generation

For every DEM generated from a stereo-pair, the corresponding orthoimage has been generated. During the orthorectification process, the effects of image perspective and relief effects are removed. This requires the input of an image with an accurately known sensor geometry resulting from the initial orientation procedure together with a DEM of the ground surface either in a grid format or in TIN format. With the use of the **Ortho Tool**, the user can select any image used in the bundle adjustment and any DEM to

generate the corresponding digital orthoimage. In this orthorectification process, the effects of elevation upon the image perspective are removed to produce a "geocoded" data set. In any imaging system, each imaged point will have a particular perspective geometry and in order to view each pixel in an orthogonal projection, the effects of terrain relief have to be removed. The DEM is used to model the relief variation present in the image and each pixel in the raw image is rectified and resampled into an orthogonal projection. The accuracy of the resulting orthoimage is based on the accuracy of the initial bundle adjustment, the resolution of the source image and the accuracy of the DEM.

The orthorectification algorithm used by OrthoMAX works in the ground space and projects back from the ground up to the image. A target horizontal ground coordinate is used to interpolate and extract the appropriate height value from the DEM. Then the resulting 3D coordinate set is used to back-project through the corresponding perspective centre into the image space (sometimes called ray-tracing). Bilinear interpolation using the surrounding pixels is used to determine the best grey level or intensity value to be assigned to the resulting output pixel.

12.9.1 Orthorectification Procedures Within OrthoMAX

Within OrthoMAX, an orthorectified image can either be defined, created, opened or deleted using the file pull-down menu. An orthoimage must first be "defined" in terms of its parameters before the actual orthorectification can be performed. To do this, the command **New** is selected from the file pull-down menu to present the appropriate orthoimage dialogue. The current DEM type is then selected from the list of possible available sources, i.e. the appropriate DEM that is to be used for orthorectification is selected. After doing so, the new ortho name will default to correspond to the name of the selected DEM, though this may be changed if required. Next, the **Imagery Block** in which the image that will be used for orthorectification resides is input. Also an orthoimage file name may be inserted into the **New Ortho** name, if the user wants to change the default name. The next step is the selection of the units to be used for the generation of the orthoimage in a specified map reference system. For a change in the reference frame to a different datum or map projection, this will be performed using the

Set-button. Once a DEM has been selected, a default value for the ground spacing will be determined and presented on the display screen. Finally the **OK** button is activated to begin the orthorectifaction process. A status dialogue is then presented indicating the percentage of processing that has been done and both the time elapsed and the estimated time until completion.

In this research, the orthoimages of the stereo-pairs 124/285 and 124/286 have been produced with a pixel spacing of 25m while, for the main test area covered by the Level 1A and Level 1B stereo-pairs for scene 122/285, the production was carried out at a pixel spacing of 20m. Figures 12.16 and 12.17 show examples of the orthoimages produced from the Level 1A and 1B stereo-pairs of the reference stereo-model 122/285 by OrthoMAX.

12.9.2 Orthoimage Mosaic

As mentioned above, the only orthoimages that could be produced using OrthoMAX for the whole Badia Project area were those of the Level 1A and Level 1B stereo-pairs for scene 122/285 in the western part of the area and the two overlapping orthoimages derived from the Level 1B stereo-pairs for scenes 124/285 and 124/286 in the eastern part of the area. So, in this case, the only overlapping stereo-pairs that could be used for mosaicing were the two located in the eastern part of the area. The same problem arose in the mosaicing process as had occurred in EASI/PACE, where an empty area or gap appeared between these two orthoimages. In addition, some distortion was encountered along the boundaries of the DEMs which in turn produced distortions in the boundaries of the orthoimages that required editing to be carried out in these areas.

For the mosaicing process, a contrast match has been performed for each of the two orthoimages to match the slave with the master and to assign a radiometric correction to the slave image. Several tests have been carried out to perform matching without obvious joins along the boundary. A slight difficulty arose from the fact that the two orthoimages are very different in appearance - with dark grey values, prevailing in the western parts of the area (Al-Harrah), while light grey values prevail in the eastern part of the area (Al-Hammad). Figure 12.18 shows the two orthoimages of the eastern part of

the project area mosaiced together. In general, the mosaicing process has been carried out smoothly, except for the matter of the contrast matching process requiring a number of preliminary tests to get a good match of the two images.

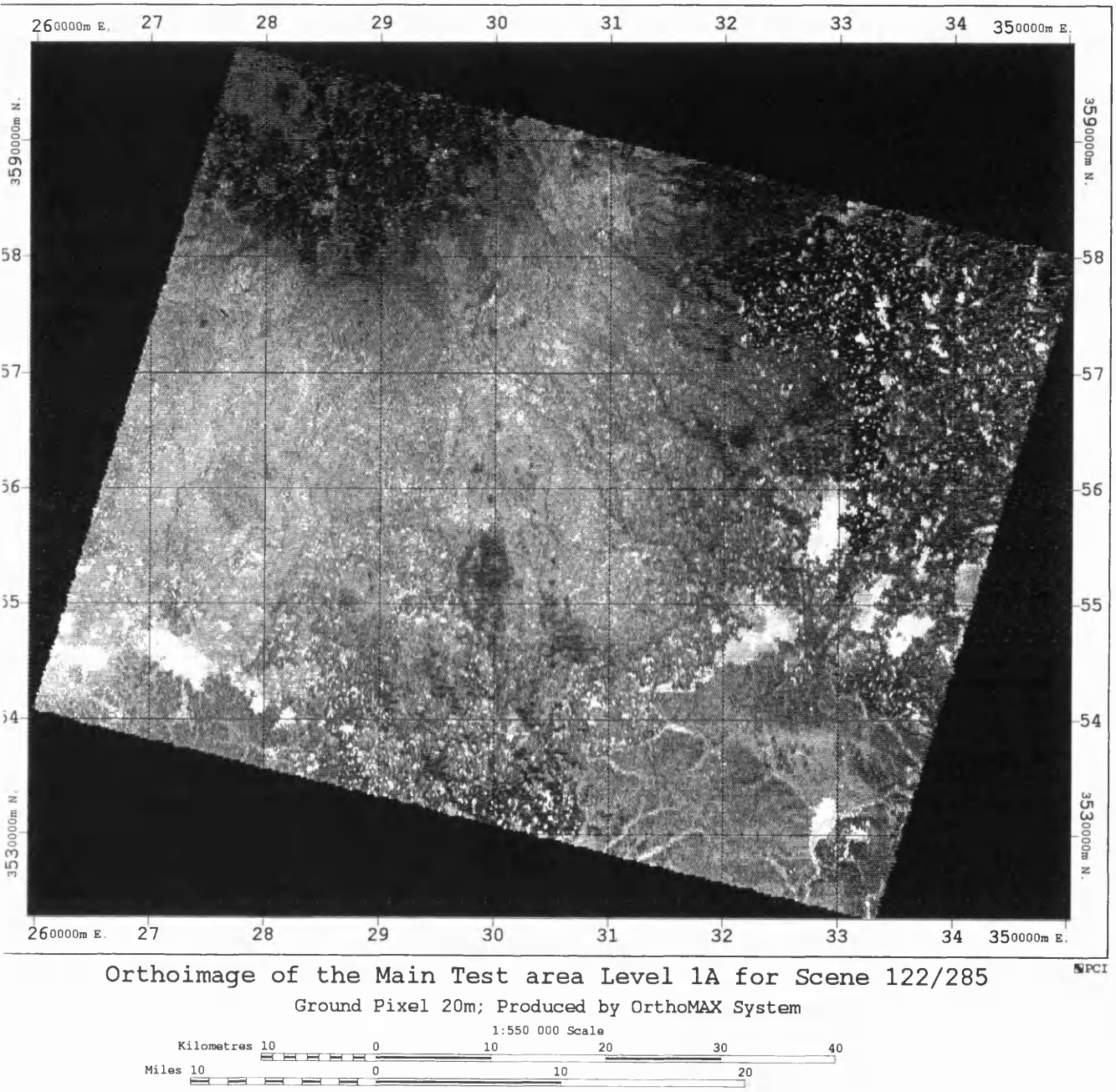

Figure 12.16. Orthoimage Generated by OrthoMAX for the Level 1A stereo-pair for scene 122/285.

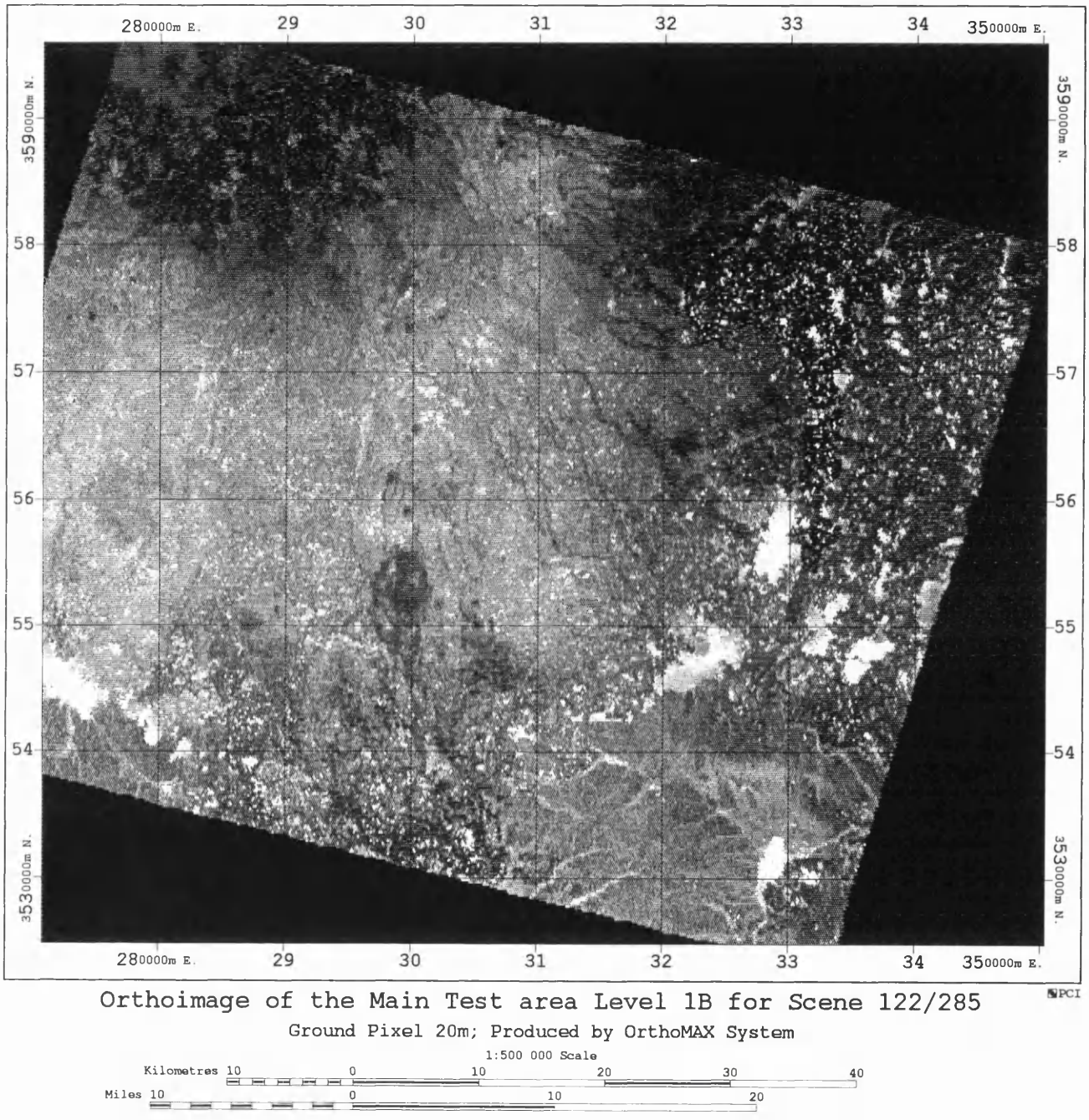

Figure 12.17. Orthoimage Generated by OrthoMAX for the Level 1B stereo-pair for scene 122/285.

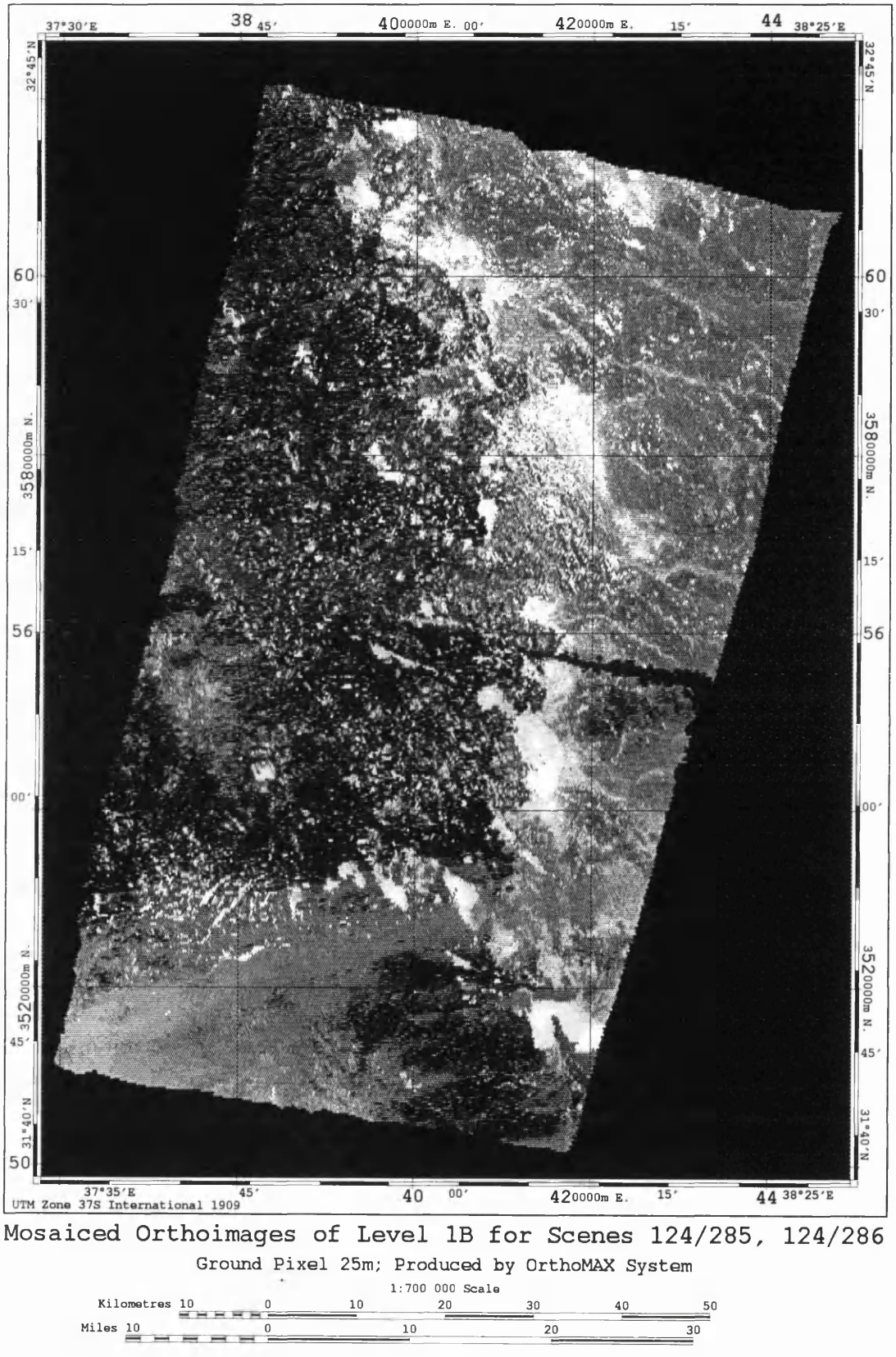

Mosaiced Orthoimages of Level 1B for Scenes 124/285, 124/286

Ground Pixel 25m; Produced by OrthoMAX System

1:700 000 Scale

Kilometres 10 0 10 20 30 40 50

Miles 10 0 10 20 30

Figure 12.18 Mosaic of orthoimages of the Level 1B stereo-pairs for scenes 124/285 and 124/286.

12.9.3 Planimetric Accuracy Test of Orthoimages Produced by OrthoMAX

For the Level 1A orthoimage, an accuracy test has been carried out. The test was carried out by measuring quite independently on the orthoimage the positions of 40 of the GCPs lying within the area of the main test scene 122/285. Using a simple linear conformal (first-order) transformation, the measured image coordinates were then transformed into their equivalent UTM terrain coordinates. These were then compared with the corresponding planimetric coordinate values derived from the GPS ground survey. The locations of the GCPs were measured in **GCPWorks** in EASI/PACE and these image coordinates were then input to the LINCON program - as mentioned previously in the corresponding tests carried out on the orthoimages produced by EASI/PACE and DMS. The resulting RMSE values in ΔE, ΔN and ΔPl were ± 10.5m, ±11.4m and ± 15.5m respectively, which, for the 20m pixel size used to produce the final orthoimage, gives RMSE values of ±0.52 pixel in the x-direction and ± 0.57 pixel in the y-direction. The vector plot of the individual residual errors resulting from the comparison (included as Figure 12.20) showed a completely random pattern with only a few local systematic components. This confirmed the excellent results of the whole process in geometric terms as well as in qualitative terms.

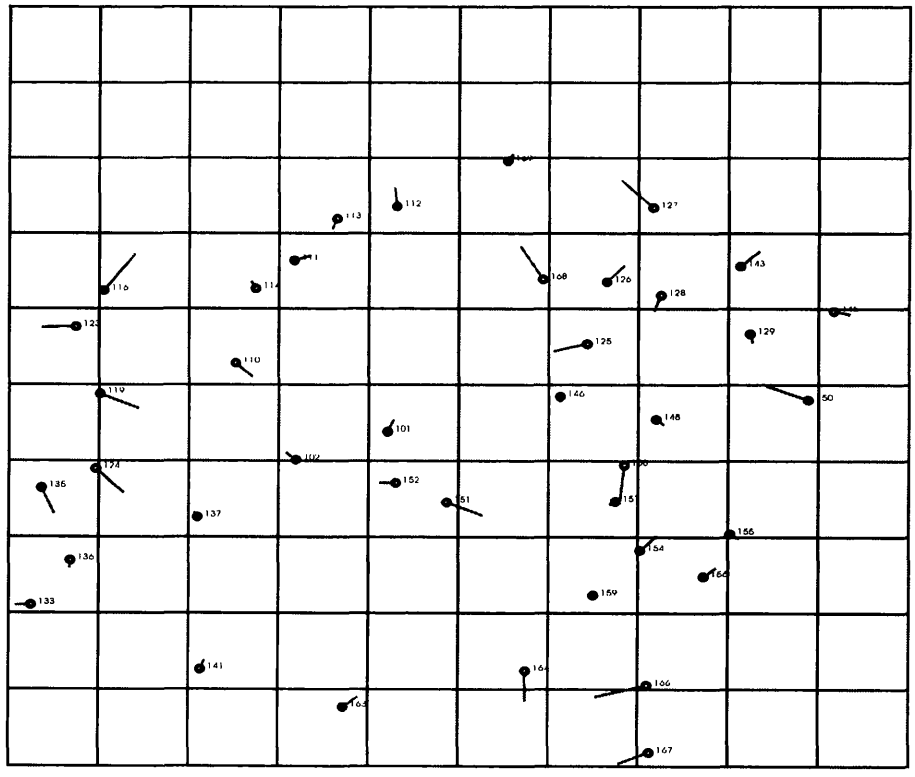

Figure 12.20 Vector plot of the individual planimetric errors at the gound control points for the orthoimage produced by OrthoMAX from the Level 1A stereo-pair for scene 122/285.

Another test of the orthoimage of the Level 1B stereo-pair for reference scene 122/285, resulted in RMSE values for ΔE, ΔN and ΔPl of ±13.4m, ±11.7m and ±17.7m respectively. For the 20m pixel size used to produce the final orthoimage, this gives RMSE values of ±0.67 pixel in the x-direction; ±0.58 pixel in the y-direction; and ± 0.89 pixel in planimetry. The vector plot of the individual residual errors resulting from the comparison - included as Figure 12.21 - showed mainly a random distribution with only local systematic components.

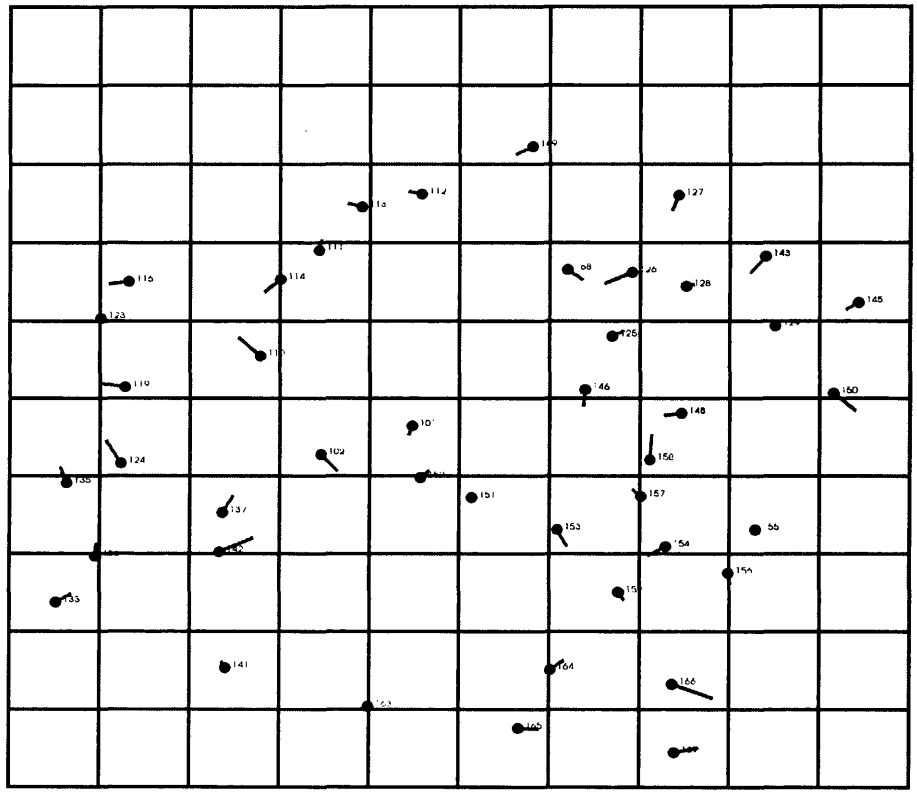

Figure 12.20 Vector plot of the individual planimetric errors at the ground control points for the orthoimage produced by OrthoMAX from the Level 1B stereo-pair of the reference stereomodel 122/285 of the Badia area.

12.10 Conclusion

In this chapter, the experience and results and the various problems encountered during this part of the research project using the OrthoMAX system have been presented. One of the main problems that is very critical in this system which has still not been solved is the declaration of the correct elevation values and the RMSE values in height in the bundle adjustment program. Another problem which is extremely vexatious concerns the inability of users to use check points in the bundle adjustment program. However,

the main problem which has not been solved so far by the system supplier concerns the inability of the system to process SPOT Level 1B stereo-pairs in the new format adopted by SPOT Image. This problem affected this research project directly in terms of the system's inability to process the SPOT Level 1B stereo-pairs 123/285 and 122/286. In spite of all the correspondence with Vision International, supplemented by numerous phone calls, this problem has been not solved. In addition to all of these difficulties, in the version of the system used in this project, there is a lack of a stereoscopic measuring and viewing facility which prevents completely any editing of the DEM extracted from stereo-pair. This affects the final DEM product in terms of its accuracy and data quality, especially since the system produces a marked distortion along the boundary of the final DEM. This required clipping to remove the distortion effects which reduced the area covered by the DEM.

In general, in spite of all of these deficiencies, it can be said that the bundle adjustment has been implemented successfully and the stereomodel was fitted to the ground control points using rigorous photogrammetric methods. DEMs of an adequate quality were then produced by the OrthoMAX system. Also the system can carry out and create geometrically precise orthoimages by performing rectification of SPOT imagery using the DEMs produced after the results of bundle adjustment. In general, the system is not too difficult to learn and to operate; the professional needs only few days' training to operate the system with efficiency.

Coming to the evaluation of the geometric accuracy obtained, the bundle adjustment provided sub-pixel accuracy in planimetry, while the stereocorrelation operation provided an accuracy of height values up to subpixel accuracy in the DEM as measured at the control points and check points. Such an accuracy only can be achieved if the user has very high quality GCPs available. This is the reason why it was necessary for the present research project to establish a first-class test field to carry out the calibration of the system. In general, the mathematical model and programs used in OrthoMAX can accommodate single stereo-pairs for mapping and can perform triangulation for SPOT scenes. However, without the availability of a test field of accurate GCPs such as that set up in the Badia area, no calibration of the system could take place and most of the problems could never have been discovered. With the availablitiy of these accurate

GCPs and the digitized contour data and GPS profiles, the validation of the data quality of the DEMs and orthoimages produced by this system has also been carried out.

In the above account, the photogrammetric and image processing procedures which have been employed in the OrthoMAX system have been given, followed by discussion of the accuracy tests of planimetry and heights of the bundle adjustment and the heights extracted through stereocorrelation. In the next chapter, the image processing procedures and the geometric accuracy tests of the FFI system will be presented and discussed.

CHAPTER 13: GEOMETRIC ACCURACY TESTS AND VALIDATION OF DEMs, CONTOURS AND ORTHOIMAGES GENERATED BY THE FFI SYSTEM

13.1 Introduction

In the previous chapter, the geometric accuracy tests and image processing steps which have been carried out and the problems encountered using the OrthoMAX system have been presented and discussed. The work carried out to validate the DEMs and orthoimages generated by the OrthoMAX system has also been reported. In this chapter, a new system which is not commercially available has been tested employing the Level 1A data of the stereo-pair for scene 122/285. This FFI system became known to the author through the information given on the web site of the Norwegian Defence Research Establishment. As a result, communication started with the developer of the program, Dr. Bjerke, who is a Senior Scientist in the Establishment's Division for Electronics. He was then visited by Professor Petrie. The results of this visit created the opportunity in the present research to cooperate and exchange data for the generation and validation of DEMs. Thus it seemed worthwhile for the author to add the new system to the previous systems for geometric accuracy testing and the validation of the DEMs and orthoimages created by the system.

13.2 Test Material and Data

Arising from Dr. Bjerke's request that he would like to test the Badia Level 1A data, in the first instance, the two images forming the stereo-pair of scene 122/285 were recorded on CD-ROM in TIFF format and sent to him. In addition, the present author provided him with the following data:-

(i) a text file containing the image coordinates in pixels of the ground control points (GCPs) measured by the present author;

(ii) the E, N, H coordinates in the UTM coordinate system of 47 of the GCPs which have been measured during the GPS survey;

(iii) the relevant information on the spheroid and datum used - which is the International Spheroid of 1924 based on the European Datum of 1950;

(iv) the geocentric X, Y, Z coordinates and height of the 47 ground coordinates in the WGS 84 system required by his program; and

(v) a parcel of material containing a hardcopy photographic image of the SPOT scene and diagrams showing the exact locations of the ground control points.

13.3 Orientation and Geometric Accuracy Tests of the Level 1A SPOT Stereo-Pair of Scene 122/285 of the Badia Area

13.3.1 Accuracy Tests of the Space Resections of the Individual SPOT Images

The first results obtained by Dr. Bjerke giving the RMSE values of the residual errors using 45 WGS 84 ground control points in both images are shown in Table 13.1.

Scene No.	Scene	No. of Ground Control Points	RMSE Values of Residual Errors in Planimetry (m)		
			ΔE	ΔN	ΔPl
122/285 1A	Left	45	±16.2	±11.0	±19.6
	Right	45	±12.9	±11.4	±17.2

Table 13.1 RMSE values of the residual errors of the Level 1A stereo-model of scene 122/285 after the space resections of the two individual images had been carried out.

Regarding the RMSE values of the residual errors that were obtained with the Badia data using this system, they were less good than one would expect, having regard to the quality of the GPS control point data and the results obtained with the other systems using the same data. Furthermore they provided purely planimetric accuracy figures for each of the individual SPOT images which did not give any idea about the residual errors in elevation. In this respect, the procedure was not being used to check the fit of the whole stereo-model to the GCPs. So Dr. Bjerke was informed that the use of a full absolute orientation using space intersection is quite essential when carrying out the accuracy testing of SPOT stereo-pairs. The full use of the absolute orientation provides an extra set of geometric conditions (intersecting rays at the GCPs) that need to be fulfilled and so provides a further check, both on the set-up procedure itself and on the interpretation and measurement of the GCPs.

13.3.2 Accuracy Tests of Absolute Orientation

It then came to light that Dr. Bjerke's program could in fact carry out an absolute orientation. The results that he obtained are shown in Table 13.2.

Badia Stereo-Model		ΔE (m)		ΔN (m)		ΔH (m)		ΔR (m)	ΔD (m)
Scene No.	No. of GCPs	Aver.	RMSE	Aver.	RMSE	Aver.	RMSE	RMSE	RMSE
122/285	45	-0.6	±12.3	-4.9	±8.2	-0.8	±13.3	±19.9	±21.5

Table 13.2 Absolute orientation results with Level 1A stereo-pair for scene 122/285.

In his absolute orientation method, Dr. Bjerke is offsetting the orbital path of the satellite by shifting or translating the X, Y, Z coordinates at all the successive perspective centres of each line of the image with a set of average values in ΔX, ΔY, and ΔZ. The use of the value ΔD in the Table is somewhat unusual: it is the closest distance between the corresponding rays from the two satellites pointing at the same physical point on the Earth - in this case, the GCP. In a perfect world with perfect precision, these two rays would intersect in a single point which would represent the position and height of the physical point. Since, in the real world, the precision of the modelling and measurement is not perfect, these rays will generally not intersect, but instead each of them will reach a point at which the distance between them is at a minimum. In fact, ΔD is the 2-D planimetric error vector value that is parallel to the datum plane used for the elevations. Essentially it is the minimum "miss" vector between the two intersecting rays at a certain elevation value. When calculating the final position (E_P, N_P) and height H_P of the physical point P, the midpoint of this vector is used - see Figure 13.1. The value ΔR shown in Table 13.2 is the 3-D vector value derived from the RMSE values of ΔE, ΔN and ΔH, purely by calculation, $\Delta E^2 + \Delta N^2 + \Delta H^2 = \Delta R^2$.

After getting these somewhat disappointing results and investigating the matter, Dr. Bjerke discovered a small error in his algorithm. After fixing the problem, he obtained another set of results but these only showed a small improvement in ΔN - the RMSE values in ΔE and ΔH remained as before - see Table 13.3.

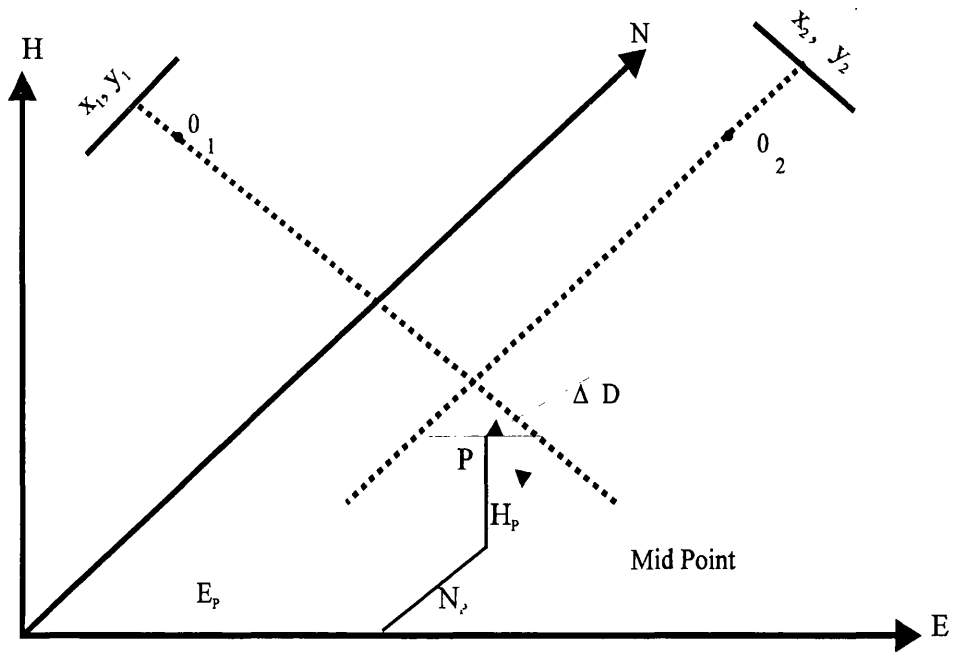

Figure 13.1 ΔD planimetric vector error according to the absolute orientation method employed by Dr. Bjerke.

Scene No.	No. of GCPs	ΔE (m)		ΔN (m)		ΔH (m)		ΔR (m)
		Average	RMSE	Average	RMSE	Average	RMSE	RMSE
122/285	45	0.2	±12.3	0.0	±6.1	-0.1	±13.2	±19.0

Table 13.3 Absolute orientation results with Level 1A stereo-pair 122/285.

In fact, in general, the RMSE values were still very high. Furthermore, the vector plots of the values of the residual errors in planimetry and height showed quite systematic patterns of errors at the individual most GCPs in both planimetry and height (Figure 13.2 a and b). In the case of the planimetric errors, they showed a clear affine scale error between the easting and northing directions. In the case of the heights, the stereo-model appeared to be tilted around an axis running from north-west to south-east across the model.

(a) Planimetry

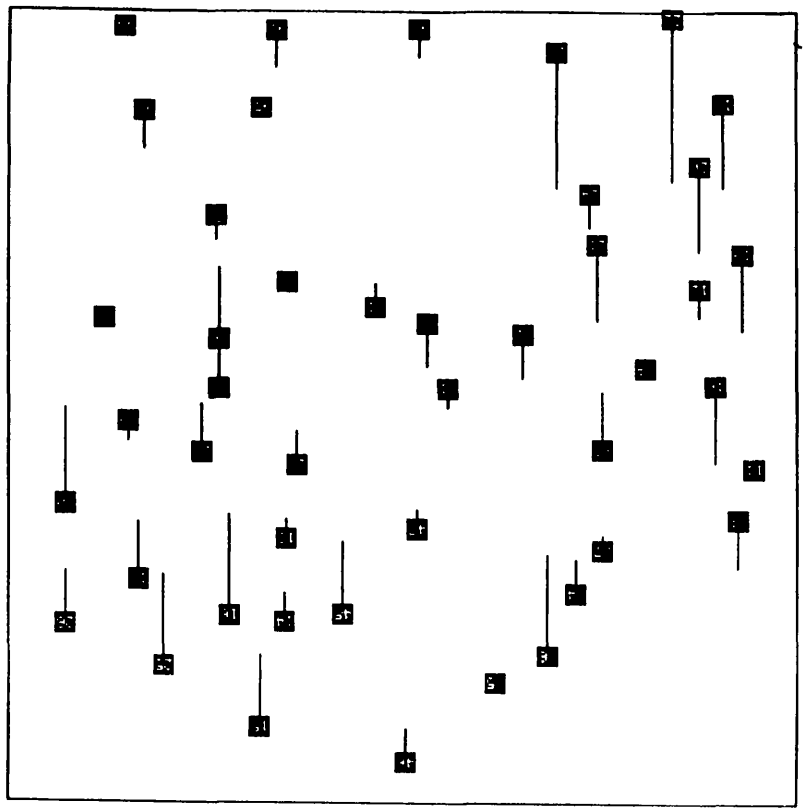

(b) Height

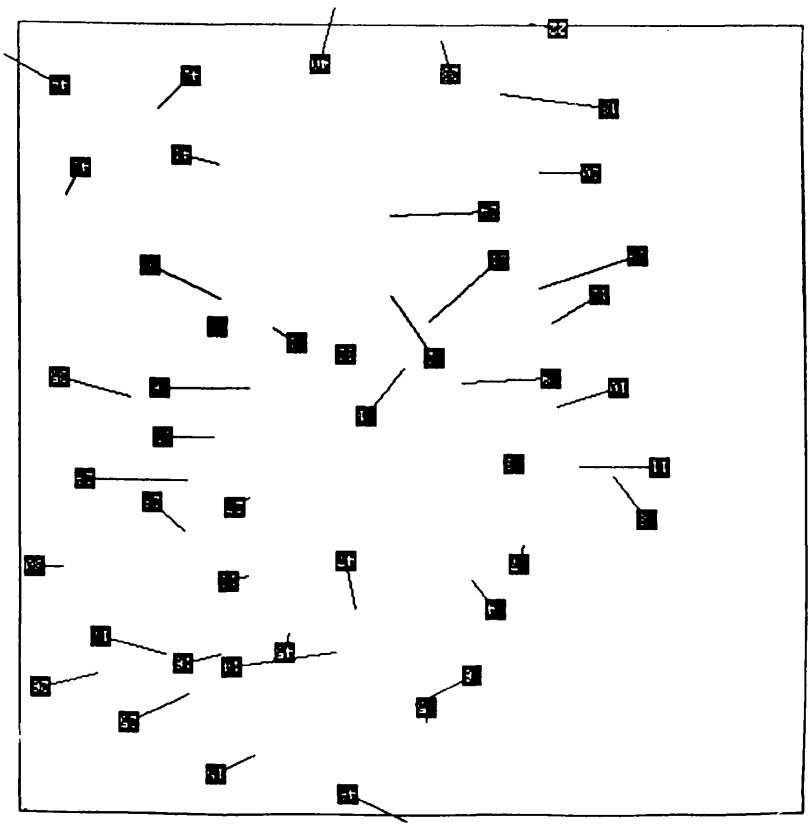

Figure 13.2 a,b Vector plots of the residual errors in planimetry and height at the individual GCPs using the FFI system with its old algorithm.

13.3.3 Accuracy Tests of Absolute Orientation with the New Algorithm

As a result of these tests, Dr. Bjerke devised a completely new algorithm, in which, instead of using an average shift of the perspective centre coordinates, different shifts are produced for each individual centre using a surface mapping function - comprising mapping between the pixel-position and the X, Y, Z errors (- a more detailed description of this new method has been provided in Chapter 6). The result that was then obtained was much better for both the space resection of the individual images as well as for the absolute orientation. Two further tests have been carried out by splitting the GCPs into two roughly equal groups and then interchanging them. The results that were obtained are shown in Table 13.4.

Scene No.	Control Points	Check Points	ΔE (m)		ΔN (m)		ΔH (m)		ΔR (m)
			Aver.	RMSE	Aver.	RMSE	Aver.	RMSE	RMSE
122/285	24	23	2.0	±8.9	-1.1	±6.5	-3.1	±10.1	±14.9
	23	24	0.7	±9.3	1.6	±6.2	-1.4	±10.3	±15.2

Table 13.4 Absolute orientation results at the control and check points using the surface mapping function for the correction of the perspective centres.

Regarding the results shown in Table 13.4., it was obvious that these were much better with the new algorithm - with 3 to 4m improvement in the RMSE values in ΔE and in ΔH being apparent immediately as compared with the values got from the use of the original algorithm.

Figures 13.3 a,b are the vector plots of the residual errors at the individual points in planimetry and height for the 24 check points after absolute orientation using the new algorithm. Then the two groups were switched. Figures 13.4 a,b show the vector plots of the residual errors in planimetry and height using the group of 23 points used as check points. In both figures, a systematic error pattern in planimetry is still very clear along the edges of the stereo-model, while the errors in height are random, except for a small systematic error pattern appearing in local areas.

Figure 13.5 shows graphically the effects of the surface mapping functions in X, Y, Z used with the new algorithm on the left and right images of the Level 1A stereo-pair.

(a) Planimetry

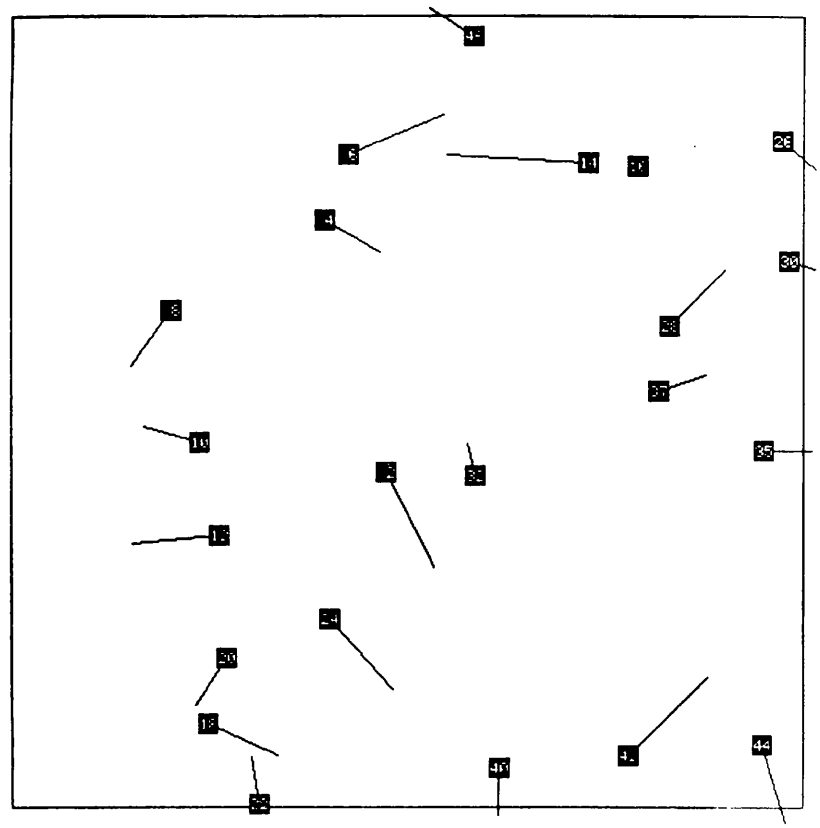

(b) Height

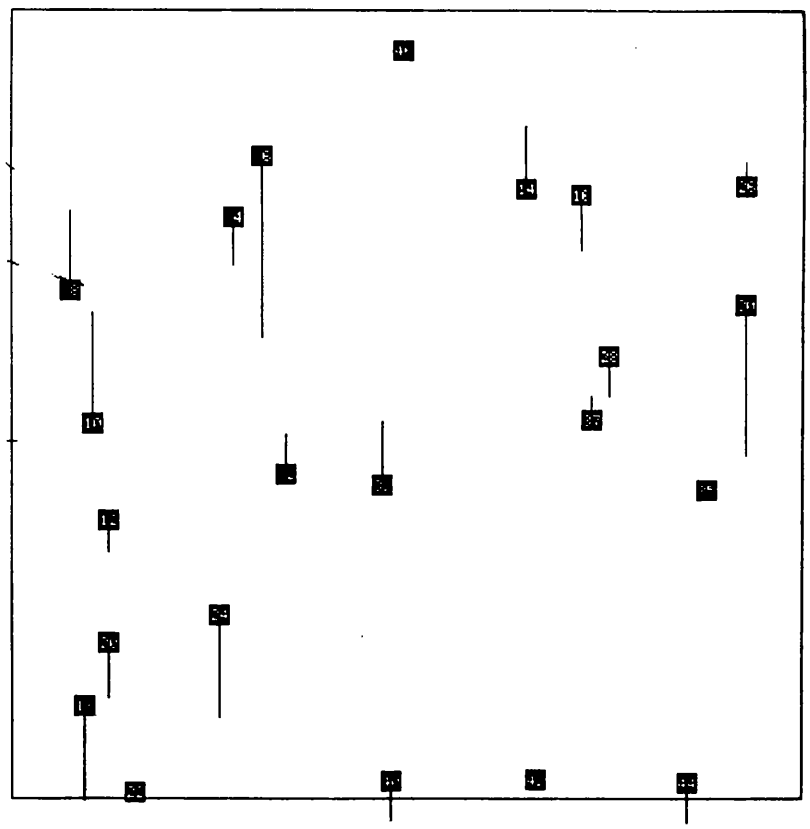

Figure 13.3 a,b Vector plots of the residual errors in planimetry and height at the individual points for the 24 GCPs used as check points during absolute orientation using the new algorithm of the FFI system.

(a) Planimetry

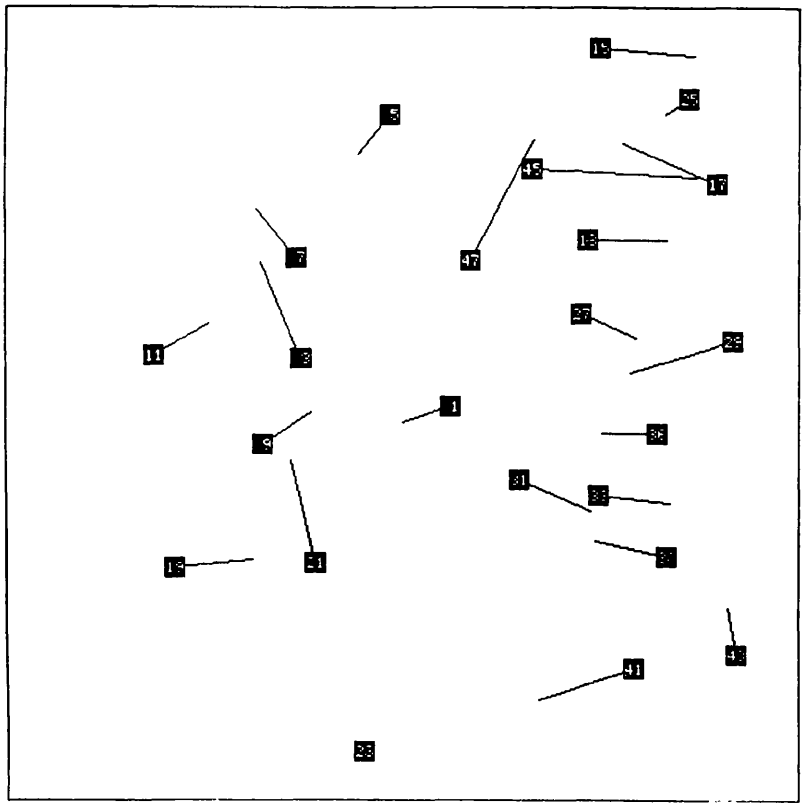

(b) Height

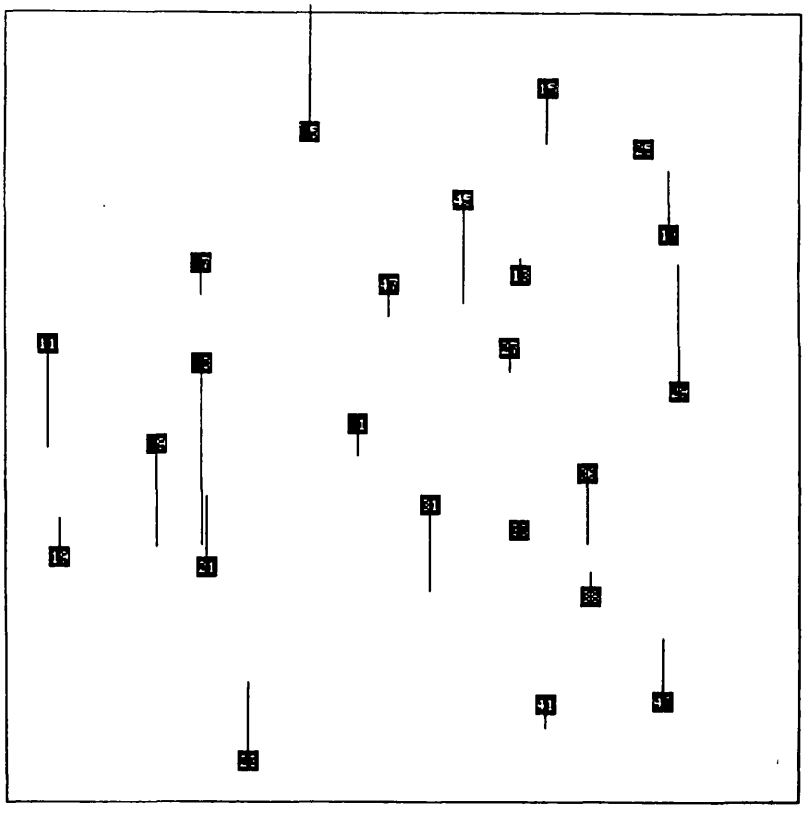

Figure 13.4 a,b Vector plots of the residual errors in planimetry and height at the individual points for the 23 GCPs used as check points during absolute orientation using the new algorithm of the FFI system.

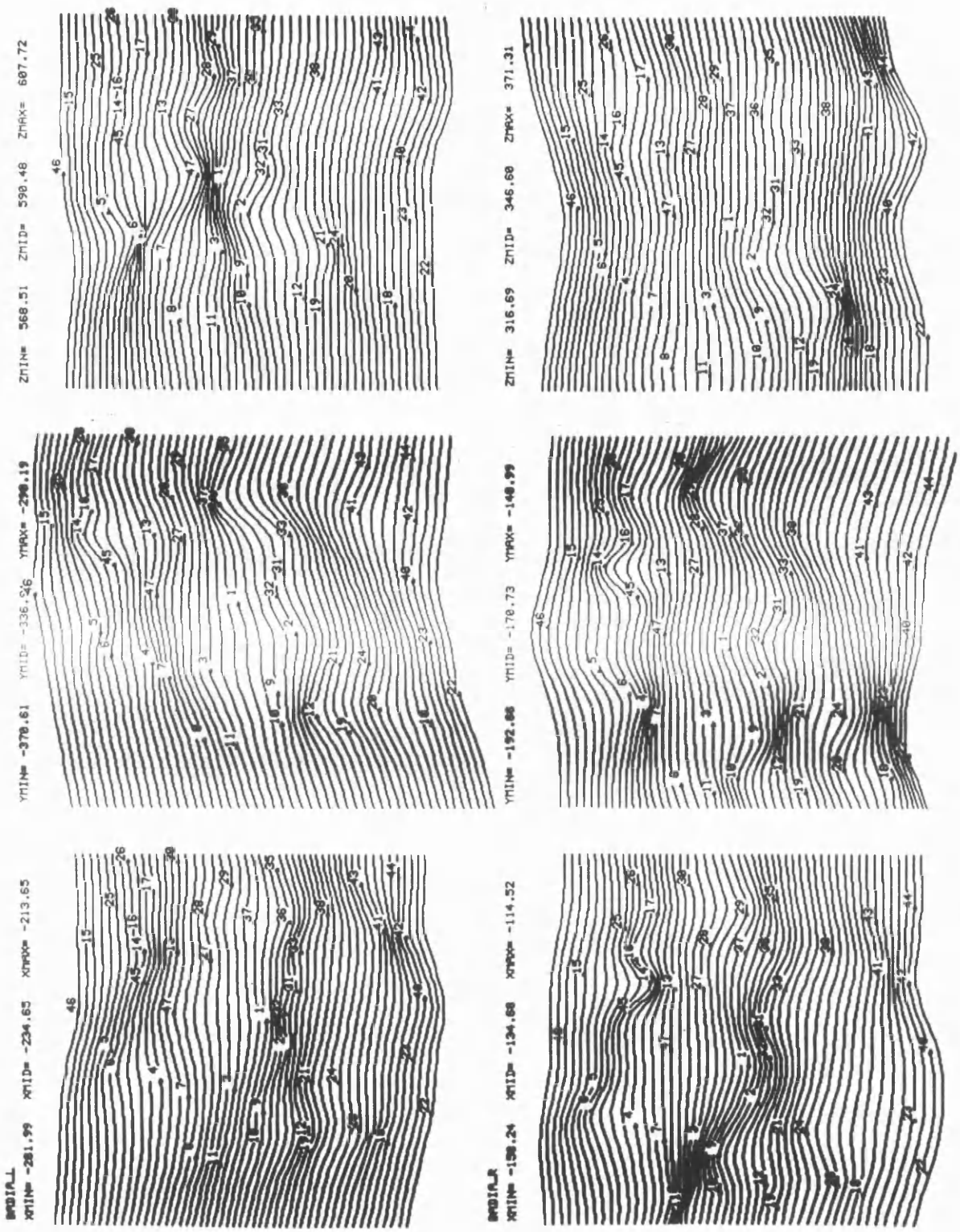

Figure 13.5 The effects of the surface mapping functions on the corrections in X, Y and Z for both the left and right individual images of Level 1A stereo-pair of scene 122/285 using the FFI system.

13.4 DEM Extraction from the Level 1A Stereo-Model of the Reference Scene 122/285

For DEM extraction, the FFI system uses automatic image matching (stereocorrelation) methods in conjunction with a similar surface mapping function to that used for the absolute orientation. The stereo-model is then processed in equal-sized patches of 100 pixels by 100 pixels. The re-sampling is also based on patches of 100 values by 100 values using a 10 metre grid. In this case, the number of files that will be generated by stereocorrelation for a single stereo-model is around 3,000 to 4,000, with a further 3,000 to 4,000 files generated after re-sampling. Thus the estimated time used for the processing of the complete stereo-pair was around 40 hours. The DEM file was then converted by Dr. Bjerke to a text file of coordinates comprising northing, easting and height values. Then this file was written on CD-ROM and sent to the present author for further processing and analysis.

13.5 Reading the DEM File

The DEM text file - amounting to 180 Mbytes of data - has been imported into the EASI/PACE system for checking and display purposes using the **NUMREAD** module. However, the program failed to read the file. The problem was identified by checking the DEM text file against the data format accepted by this program module. This revealed that the program expects the traditional format with the data in the order easting, northing and height and not the format of the FFI DEM text file that utilizes the order northing, easting and height. Using a small conversion program, the problem was solved and the full DEM file was converted to the required format.

13.6 Contour Generation

From the DEM extracted by the FFI system, contours have been generated at intervals of 50m and 20m using the **CONTOUR** module of the EASI/PACE system. Figures 13.6 and 13.7 show these two sets of contours. Inspection shows a very dense pattern of tiny circular features around the main contours which prevent a clear picture being formed of the main contours. These features are presumed to be noise or artefacts of the image

matching procedure used in the FFI system and resulted from the lack of filtering or editing being carried out on the DEM data. To overcome this problem, the Level 1B DEM of the reference stereo-model for scene 122/285 has been filtered in the EASI/PACE system using ImageWorks. Three separate processing procedures have been carried out; these include removing noise, interpolation and smoothing. Figure 13.8 shows the contours at 50m interval after filtering has been carried out.

13.7 Orthoimage Generation

Again using the **SORTHO** module of EASI/PACE, an orthoimage with a pixel size of 10 m has been generated from the DEM using the right image of the stereo-pair. Figure 13.9 shows the orthoimage of the Level 1A stereo-pair for scene 122/285 that has been produced in this way.

13.8 Accuracy Tests of Height in the DEM Produced by the FFI System

To go further and validate the data quality, four different methods have been used to check the accuracy of the height values in the DEM produced by the FFI system as follows:-

(i) DEM accuracy reports;

(ii) a comparison of the two sets of superimposed contours;

(ii) a comparison of the height values given by selected contours from the photogrammetrically produced reference map and the corresponding elevation values given by the DEM; and

(iv) comparison of the DEM data with the GPS profiles measured along the main roads.

13.8.1 Accuracy Test of the Height Values Given by the FFI Produced DEM at the Ground Control Points

In this first test, the result in terms of the RMSE value of the residual errors in height at the 47 ground control points obtained through the stereo-correlation process was ±7.8 m. This result is created purely from the disparities generated during the image matching

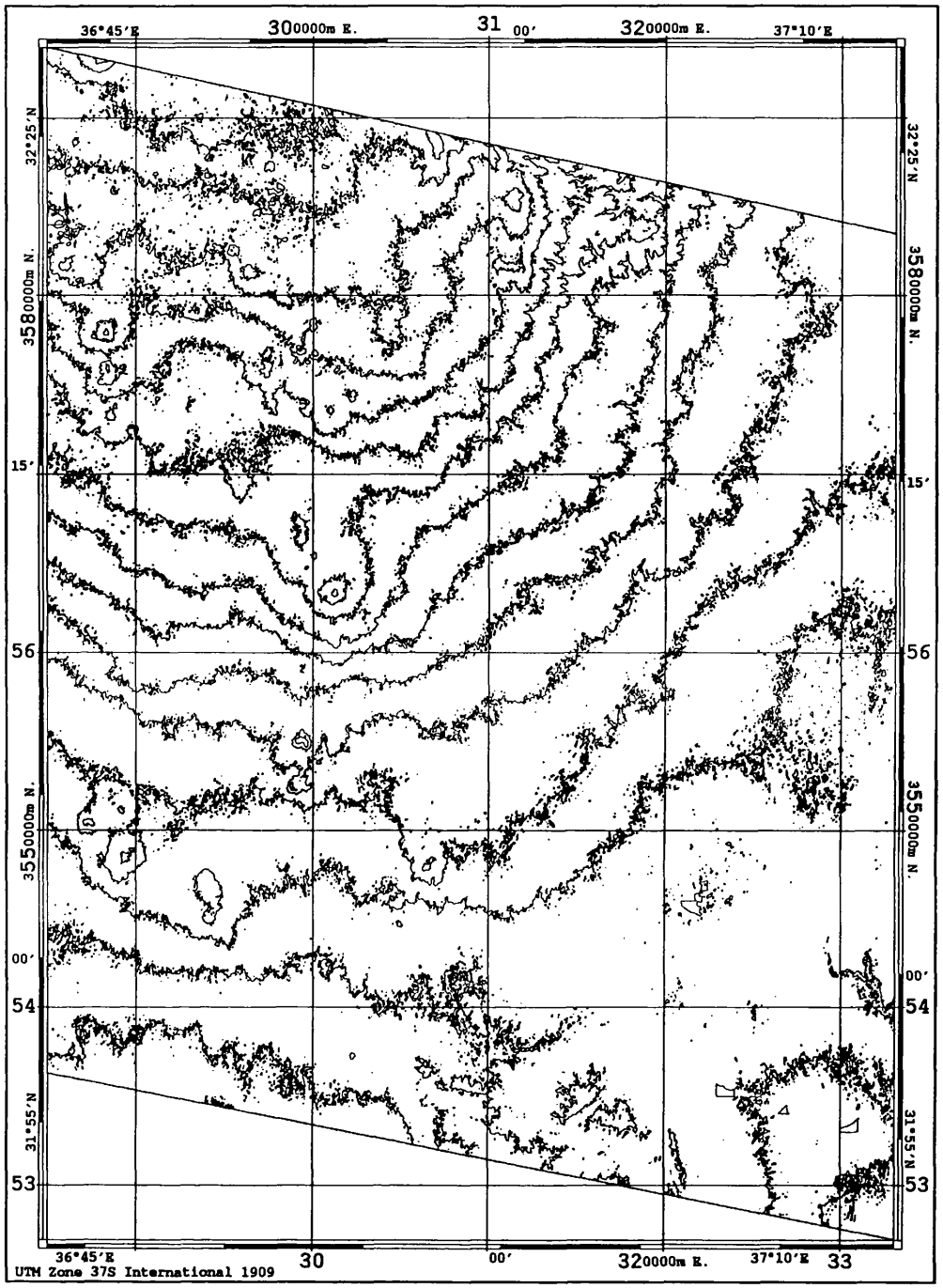

Figure 13.6 Contours at 50 m interval generated from the Level 1A stereo-model for scene 122/285 using the FFI system.

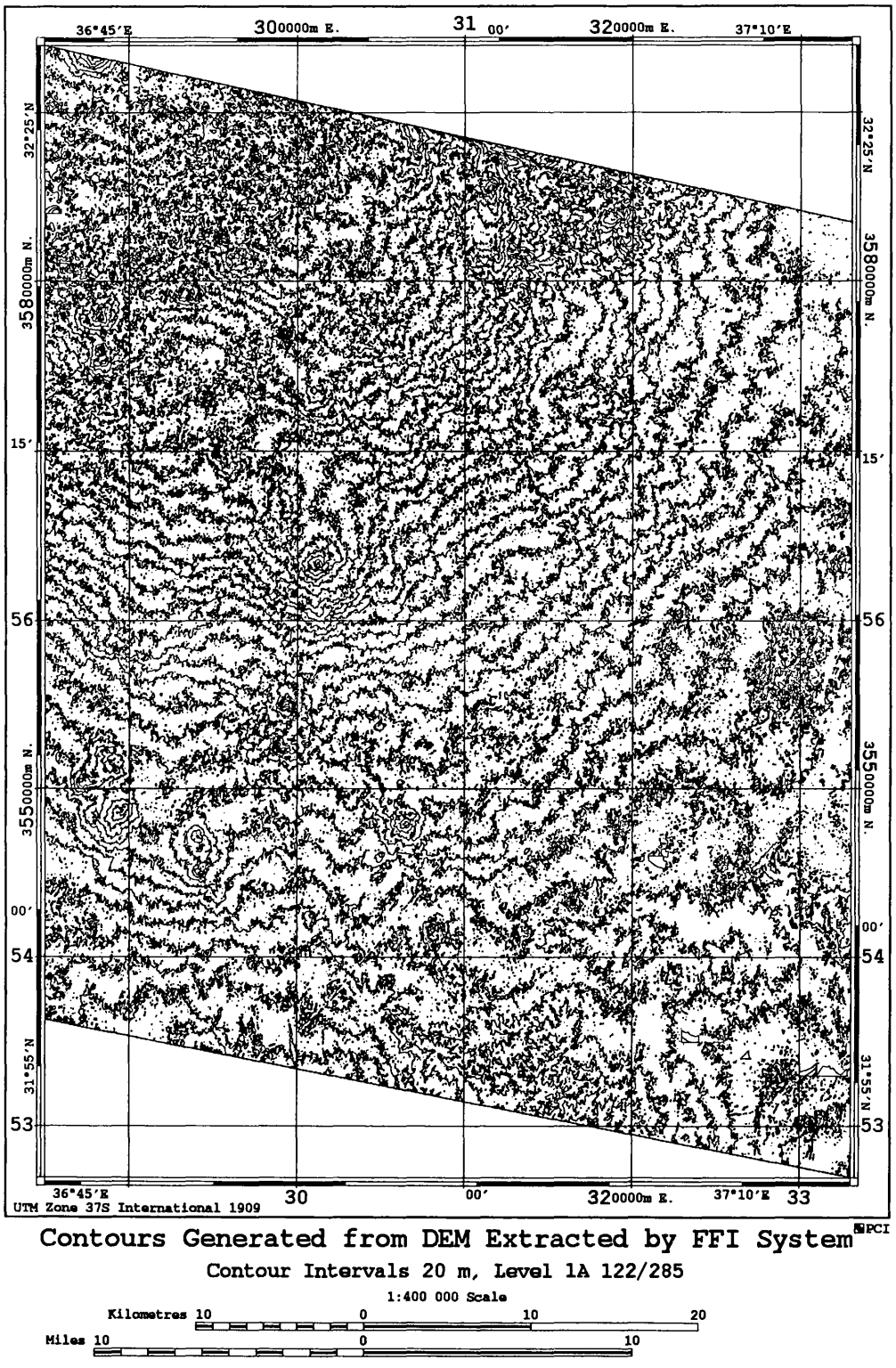

Figure 13.7 Contours at 20 m interval generated from the Level 1A stereo-model for scene 122/285 using the FFI system.

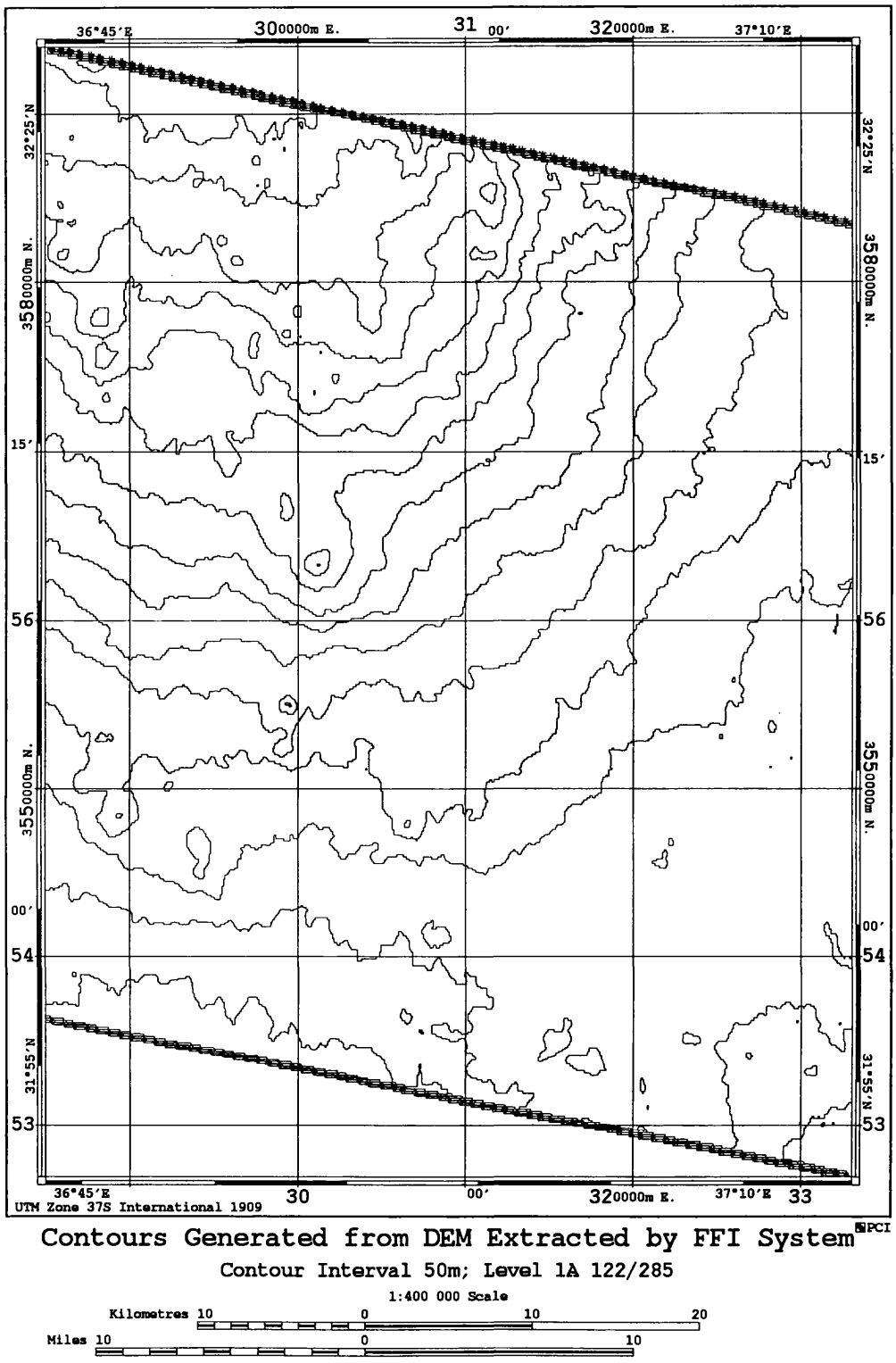

13.8 Contours at 50m interval generated from the Level 1A stereo-model for scene 122/285 using the FFI system after DEM filtering.

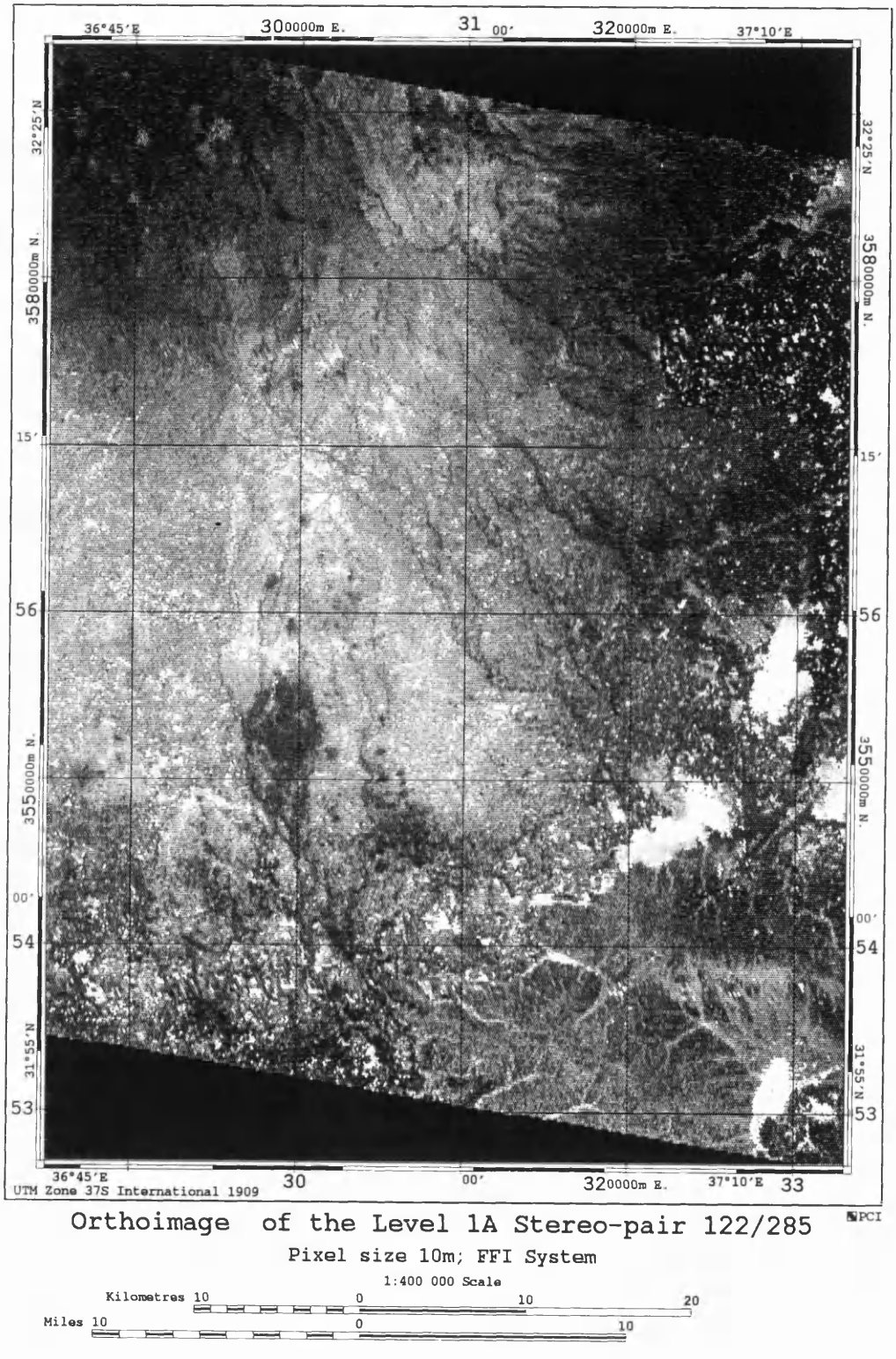

Figure 13.9 Orthoimage generated from the SPOT Level 1A stereo-pair of scene 122/285 using the FFI DEM data covering part of the Badia area.

procedure carried out for DEM extraction by the FFI system. The vector plot of the values of the residual errors at each individual GCP given in Figure 13.10 shows a random error pattern in most parts of the area; a slightly systematic error pattern appeared in some local areas.

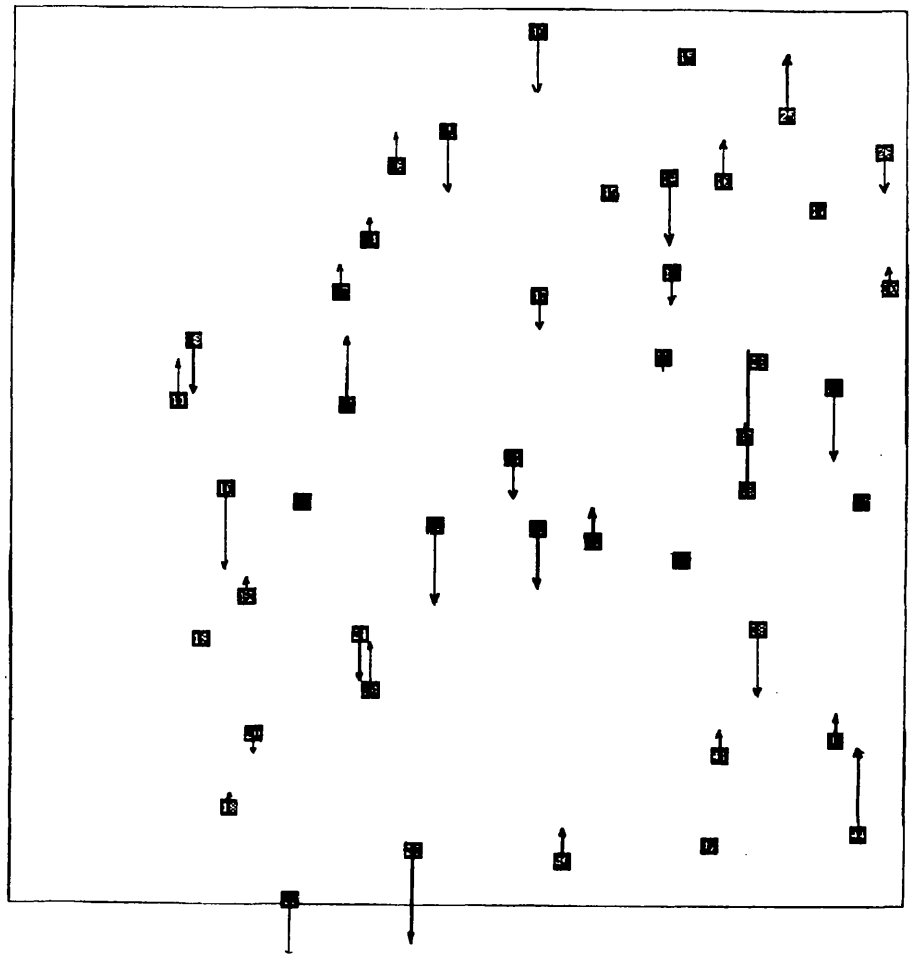

Figure 13.10 Vector plot of the values of the residual errors in height at the ground control points using the DEM data produced by the FFI system.

13.8.2 Accuracy Tests of Heights by Superimposition of Contours.

In this kind of test, a visual comparison of the fit of the contours generated from the DEM superimosed over the digitised contours from the RJGC 1:250,000 scale map has been carried out. The main problem in making this comparison concerns the "noisy" contours produced by the FFI system. Inspection of the accuracy of fit (shown in Figure 13.11) shows a close fit of the two sets of contours. There is some deviation over much of the area, but this deviation not too big - being estimated - at around one-tenth of the contour interval.

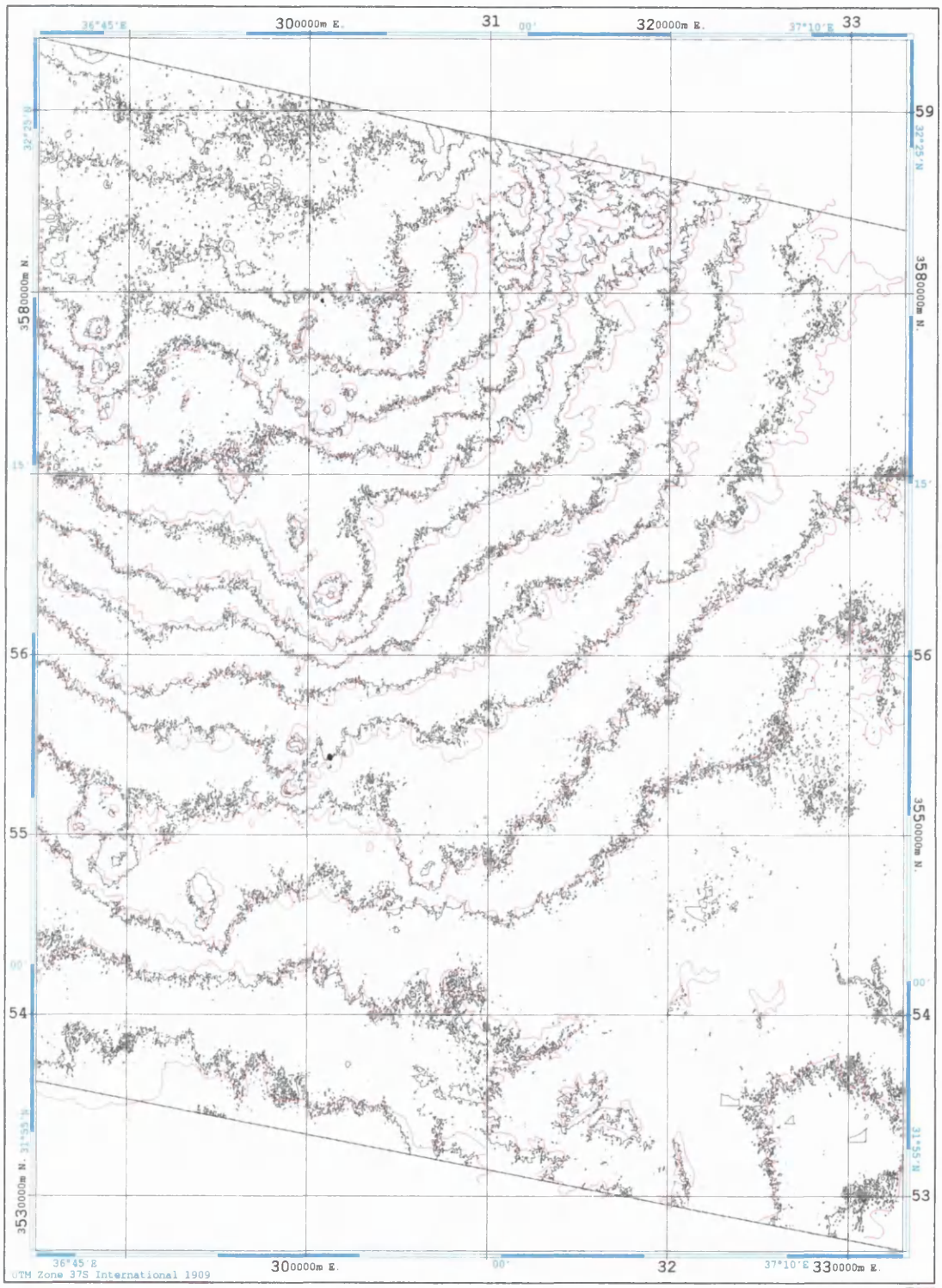

Figure 13.11 Contours extracted from the Badia DEM produced by the FFI package superimposed over the digitised contours from the RJGC topographic map at 1:250,000 scale.

13.8.3 Accuracy Tests of Comparison of the DEM Elevation Values with the Elevation Values given by the RJGC Topographic Map Contours

Two tests of the comparison between the contour values given by the RJGC 1:250,000 and 1:50,000 scale topographic maps and the corresponding elevation values given by the DEM have been carried out. The first test concerned the digitised contours at 50m interval superimposed over the DEM. The result obtained in terms of the RMSE value in height using 761 check points measured on the DEM was ±10.3m. The second test was carried out using the contours at 10m interval superimposed over the DEM and using 417 check points measured by the DEM. The result obtained in terms of the RMSE value in height was ± 9.9m. Table 13.5 summarizes the two sets of test results.

Scene No.	Comparison of the DEM Elevation Value with the Value Given by the Digitised Contours from 1:250,000 Scale RJGC Topographic Map with 50m Contour Interval		Comparison of the DEM Elevation Value with the Value Given by the Digitised Contours from 1:50,000 Scale RJGC Topographic Map with 10m Contour Interval	
122/285	Measured Points	RMSE (m)	Measured Points	RMSE (m)
	761	±10.3	417	±9.9

Table 13.5 Results of the comparison of the DEM elevation values produced by the FFI system with the height values given by the digitised contours from the RJGC topographic maps at 50m and 10m intervals.

13.8.4 Accuracy Test of Heights Produced Using the FFI System Against the GPS Profiles

The same procedures implemented with the DEMs produced by the other systems to test a sample of their height values using the GPS profile data has been followed to test the accuracy of the elevation data in the DEM produced by the FFI system using the measured GPS profile data. The results of the accuracy tests using 366 check points produced an RMSE value of ±8.3m.

13.9 Accuracy Tests of Orthoimage

Regarding the geometric accuracy of the final orthoimage, a check was carried out by measuring quite independently on the orthoimage the position of 27 of the GCPs lying within the area of the Level 1A stereo-pair for the main test scene 122/285. Using a simple linear conformal transformation, the measured image coordinates were then

transformed into their equivalent UTM coordinates. These were then compared with the corresponding coordinate values derived from the GPS ground survey. The resulting RMSE values of the residual errors in ΔE and ΔN were ±7.6 m and ± 5.0 m, respectively, which, for the 10-m pixel size used to produce the final orthoimage, gave RMSE values of ± 0.76 pixel in the x-direction and ± 0.51 pixel in the y-direction on the orthoimage. The vector plot (Figure 13.12) showing the individual residual errors resulting from the comparison showed a systematic pattern only in one or two places but overall it showed a satisfactorily random error distribution.

13.10 Tests of the Orientation and Geometric Accuracy of the SPOT Level 1A Stereo-Pair of the Oslo Test Area Using the FFI System

During the time when Dr. Bjerke was processing the Level 1A stereo-pair for scene 122/285 of the Badia area, he also processed the Level 1A stereo-model of the Oslo area that he used for test purposes with the FFI system. Very large parts of the scenes making up the Oslo stereo-model are covered by water and built-up areas. Also the stereo-pair exhibits a moderate base-to-height ratio of 0.61, but the scenes are of a good quality in radiometric terms.

Dr. Bjerke provided the author with the Oslo stereo-model to be tested in the EASI/PACE system for a further comparison of the results achieved by his system and the EASI/PACE system and to evaluate the mathematical models and algorithm that he had devised and employed in the FFI system.

13.10.1 Accuracy Tests of Space Resection of the Individual SPOT Images Using the FFI System

The first results obtained for the space resection of the individual images making up the Oslo stereo-model running on the FFI system and using the original algorithm are shown in Table 13.6. In this test, a total of 45 ground control points have been used for the space resection and orientation. Of these, 31 control points have been taken from the Statens Kartverk 1:50,000 scale topographic map with an estimated accuracy of ± 20m; while a further 14 control points have been taken from a road-database produced

photogrammetrically from large-scale aerial photographs. These latter points have an estimated accuracy in position and elevation of ± 2m.

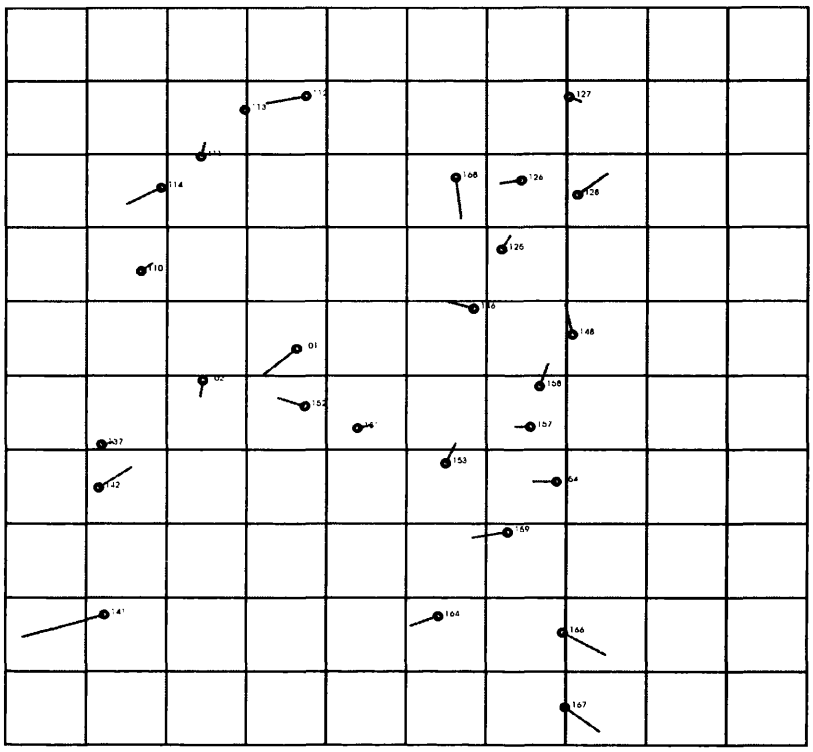

Figure 13.12 Vector plot of the planimetric (X/Y) errors at the ground control points of the ortho-image produced by the Level 1A stereo-model

Level	Scene	No. of Ground Control Points	RMSE Values of Residual Errors in Planimetry (metres)		
			ΔE	ΔN	ΔPl
Oslo 1A	Left	45	±8.5	±12.7	±15.3
	Right	45	±8.0	±7.6	±11.1

Table 13.6 RMSE values of the space resection of the Level 1A stereo-model of the Oslo area using the FFI system.

The results with the Oslo stereo-model were better than one would expect with GCPs extracted from 1:50,000 scale map. However it could be that this is being compensated for in some way by the more accurate points taken from the road database.

13.10.2 Accuracy Tests of Absolute Orientation Using the FFI System

Dr. Bjerke also carried out the absolute orientation of the stereo-model. The results which he obtained are shown in Table 13.7.

Oslo Test Area		ΔE (m)		ΔN(m)		ΔH(m)		ΔR (m)	ΔD (m)
Scene	No. of GCPs	Aver.	RMSE	Aver.	RMSE	Aver.	RMSE	RMSE	RMSE
Oslo 1A	45	-0.6	±7.6	-3.6	±9.7	-1.8	±12.7	±17.7	±10.4

Table 13.7 Absolute orientation results with the Level 1A stereo-pair of the Oslo area using the FFI system.

As can be seen from Table 13.7, the errors in planimetry with the absolute orientation are slightly less than the corresponding errors for the separate images. The correction of the images was carried using the first algorithm by offsetting the orbit of the satellite with an average value.

At this stage, Dr. Bjerke was asked by Professor Petrie to use different combinations of the Oslo GCPs separating the two sets of control point data - since they were of such a different quality in terms of accuracy. The results obtained from these combinations, i.e. the points taken from the map; and those derived from the road database are shown in Table 13.8.

Oslo Stereo-model		ΔE (m)		ΔN (m)		ΔH (m)		ΔR (m)
Control	Check	Aver.	RMSE	Aver.	RMSE	Aver.	RMSE	RMSE
All	All	-0.6	±7.6	-3.6	±9.7	-1.8	±12.7	±17.7
Map	Map	-0.6	±7.7	-3.6	±10.8	-1.8	±13.1	±18.6
Road	Road	-0.7	±4.7	-3.6	±6.7	-1.7	±11.9	±14.5
Map	Road	5.8	±7.5	-4.7	±7.3	0.2	±11.9	±15.8
Road	Map	-7.1	±10.5	-2.5	±10.5	-3.8	±13.5	±20.1

Table 13.8 The results from the absolute orientation using different combinations of GCPs in terms of the RMSE values of the residual errors for the Oslo stereo-pair using the FFI system.

As can be seen from Table 13.8., using the two groups of points - i.e. the map derived points, and the road database points in different combinations - the results given in lines 1, 2 and 3 are for the whole of the particular data set involved with no splitting into control points and check points. Whereas with those given in lines 4 and 5, the GCP data has been split into two groups - the first used as control points, the second group as check points - and the results are given for the check points only.

Inspecting the results where only the map derived data has been used (i.e. in line 2 of the table) and those where only the database points are used (i.e. in line 3 of the table), it is

obvious that the quality of the GCPs in terms of their accuracy is having some effect on the accuracy of the final results in terms of planimetry. So there is some positive influence on the results arising from the better quality of the GCPs. However, what is quite astonishing is the fact that the corresponding RMSE values in height are little different for the respective combinations. For the map-derived points, $\Delta H = \pm 13.1$ m and for road database points, $\Delta H = \pm 11.9$m. So the improvement was very small - only 1.2m - in spite of the big difference in the quality of the control points.

After obtaining these results, Dr. Bjerke found an error in his algorithm, and so he repeated the test. Also 3 road database points were added and three of the map-derived points were deleted, so 28 GCPs derived from the 1:50,000 scale map and 17 GCPs from the road database were used in this second test. The new results are shown in Table 13.9; it is clear from this Table that the results were a little better in terms of the RMSE values for the GCPs derived from the road database, but not elsewhere.

Oslo Stereo-model		ΔE (m)		ΔN (m)		ΔH (m)		ΔR (m)
Control	**Check**	**Aver.**	**RMSE**	**Aver.**	**RMSE**	**Aver.**	**RMSE**	**RMSE**
All	**All**	0.0	±7.5	0.0	±8.5	-0.1	±12.2	±16.7
Map	**Map**	-0.1	±8.0	0.0	±10.0	-0.1	±12.8	±18.1
Road	**Road**	0.0	±5.4	0.0	±4.8	-0.1	±10.7	±12.9
Map	**Road**	5.0	±7.4	-1.8	±5.1	-0.6	±10.9	±14.1
Road	**Map**	-5.1	±9.5	1.8	±10.2	0.5	±12.9	±19.0

Table 13.9 The results from the absolute orientation using different combinations of GCPs in terms of the RMSE values of the residual errors for the Oslo stereo-pair using the FFI system.

Vector plots of the residual values of the errors in planimetry and height for all of the GCPs of the Oslo model are shown in Figure 13.13 a,b. From these, it is very clear that a systematic error pattern prevailed: in particular, the height errors showed a distinct tilt of the stereo-model around an east-west axis.

Another plot showing the errors produced using the road-database points only in conjunction with the old algorithm, also showed a systematic pattern of errors in planimetry in groups of control points as shown in Figure 13.14.

(a) Planimetry

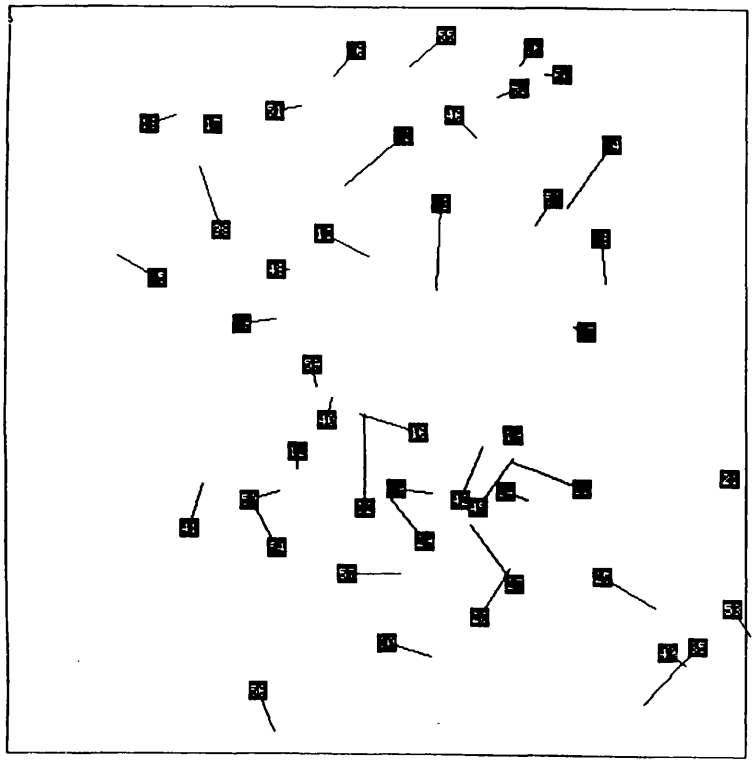

(b) Height

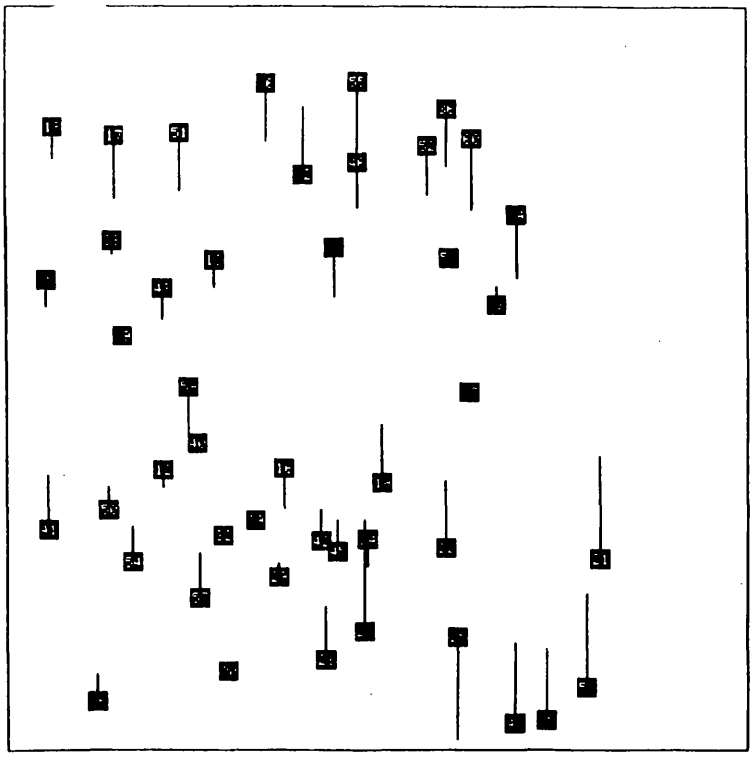

Figure 13.13 a,b Vector plots of the values of the individual residual errors in planimetry and height at the ground control points using the old algorithm of the FFI system.

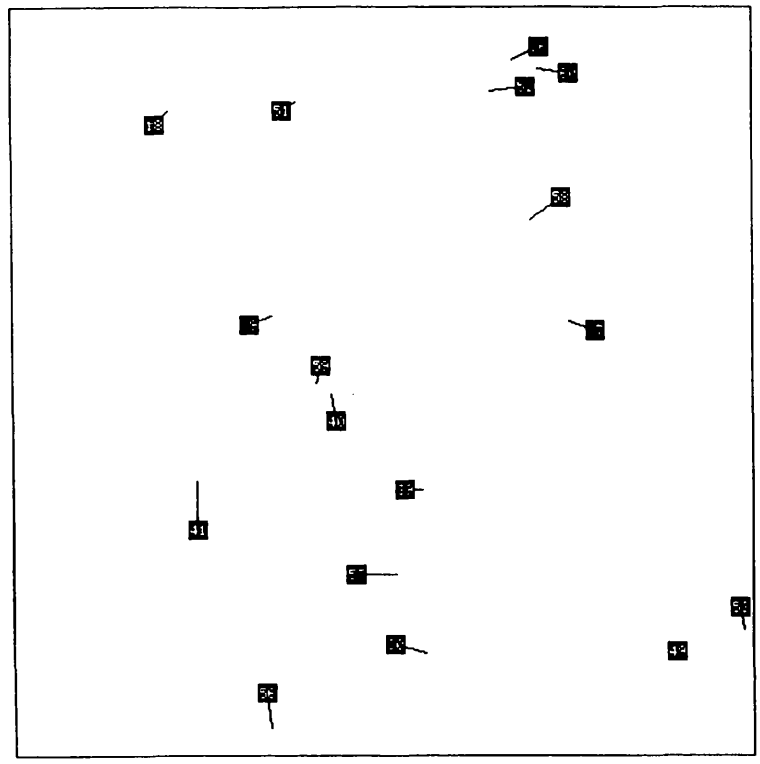

Figure 13.14 Vector plot of the values of the residual errors in planimetry at the ground control points using the road database points only with the old algorithm employed in the FFI system.

Inspection of the vector plot of the values of the residual errors in height as shown in Figure 13.15, also showed a systematic pattern of error.

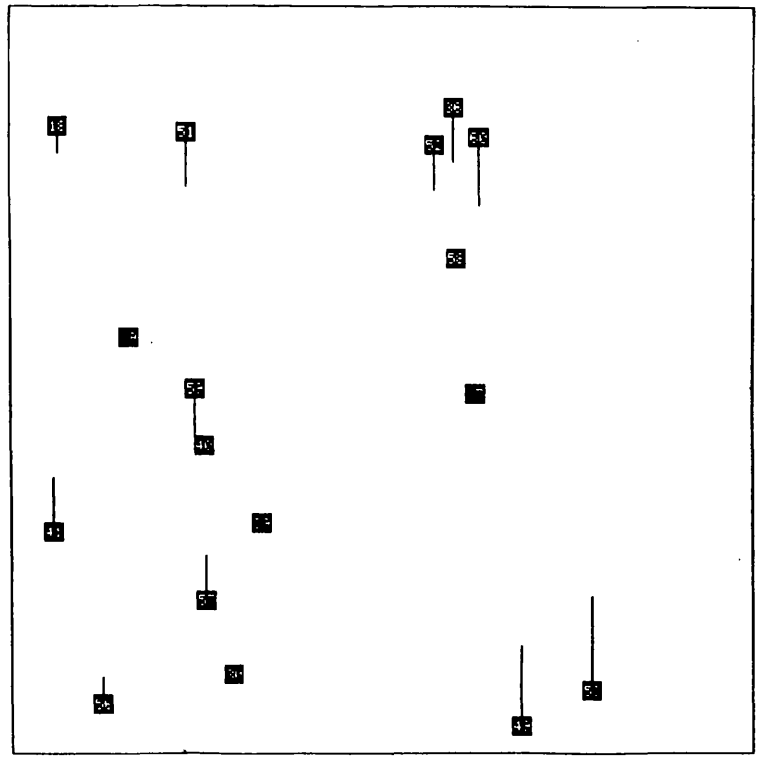

Figure 13.15 Vector plot of the values of the residual errors in height at the control points using the road database points only in the old algorithm employed in the FFI system.

13.10.3 Accuracy Tests of Absolute Orientation with the New Algorithm of the FFI System

Another set of results was obtained using the same Oslo model, but, instead using of employing an average shift of the perspective centres, the X, Y, Z errors have been corrected with the new algorithm using a surface mapping function mapping between the x, y pixel-positions and the X, Y, Z errors at the corresponding perspective centres (see Chapter 6). After this correction, the errors at the GCPs are all Zero to the 4th decimal. The test was carried out by splitting the road database GCPs into two groups (Table 13.10) and using one group as control points and the other as check points - and then interchanging them.

With the new algorithm, some improvement in the RMSE values of the errors in elevation is immediately apparent as compared with the values got from the use of the original algorithm.

Oslo Stereo-model		ΔE (m)		ΔN (m)		ΔH (m)		ΔR (m)
Control	Check	Aver.	RMSE	Aver.	RMSE	Aver.	RMSE	RMSE
9	8	4.3	±5.6	-0.8	±6.0	-2.0	±8.3	±11.7
8	9	-3.5	±3.7	2.8	±8.3	4.9	±7.2	±11.6

Table 13.10 The results from the absolute orientation at the control and check points at the road database points using the surface mapping function for the correction of the perspective centres.

Vector plots of the values of the residual errors in planimetry and height using different combinations of control points and check points showed systematic error patterns in planimetry. Systematic patterns also appear locally in height (Figures 13.16 and 13.17).

13.11 Geometric Accuracy Tests of the Oslo Stereo-Model Using the EASI/PACE System

While the tests of the FFI system using both the Badia and Oslo stereo-models were being carried out, Dr. Bjerke asked the author if he could also test the Oslo stereo-model using the EASI/PACE system for comparative purposes with his own system. This was agreed to and he therefore sent a CD-ROM containing the SPOT stereo-pair of the Oslo area in TIFF format together with a text file containing the measured pixel coordinates and the given ground coordinates of the 45 GCPs available for this area. As noted

above, these control points comprised 28 control points derived from the 1:50,000 scale topographic map and 17 control points from the road database of the area.

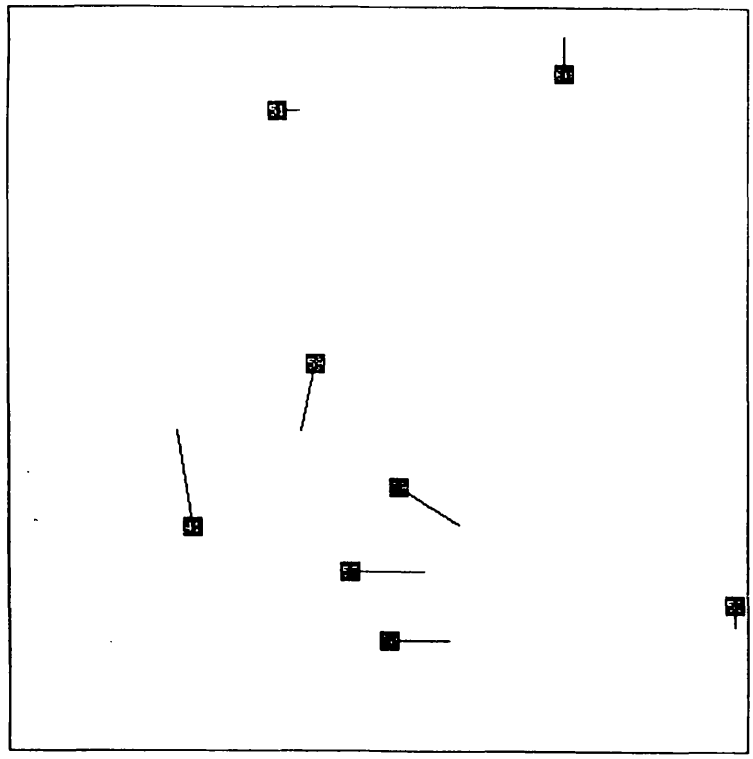

Figure 13.16 Vector plot of the residual errors in planimetry at the check points using the new algorithm of the FFI system.

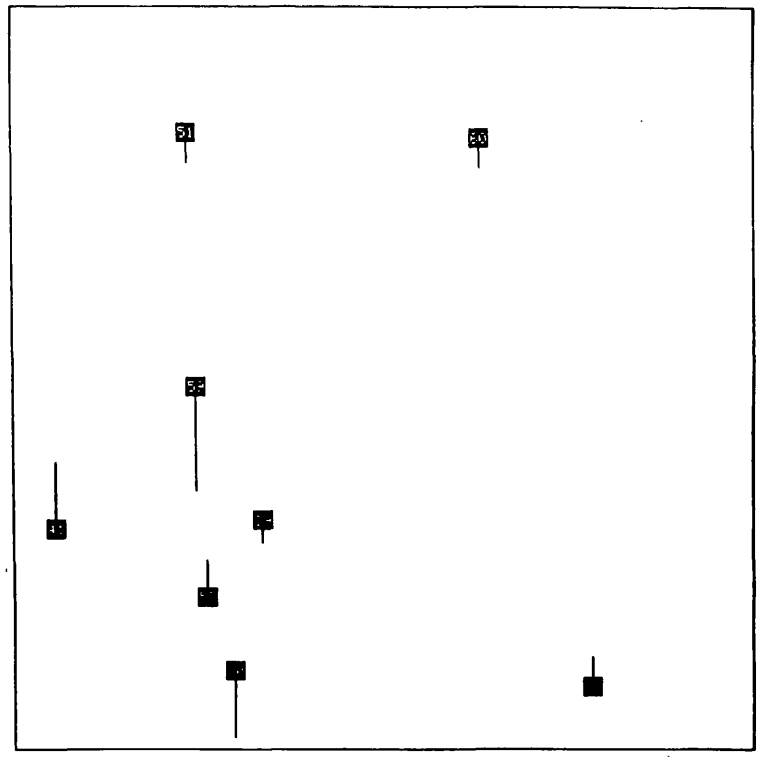

Figure 13.17 Vector plot of the residual errors in height at the check points using the new algorithm of the FFI system.

13.11.1 Space Resection of the Individual SPOT Images of the Oslo Stereo-Model Using EASI/PACE

This test utilised all 45 ground control points (GCPs) available, including both the map-derived points and those originating from the road database. Several tests using different combinations of control points and check points have been carried out for both images using the space resection procedure (the **SMODEL** module) available in the EASI/PACE system. From the results given in Table 13.11, it is clear that the best accuracy achieved with the space resection of the individual SPOT images in planimetry was obtained at the GCPs using only the road database points. In general, the values of the residual errors at the control points and check points are much poorer whenever the map-derived ground control points have been used. The errors at the individual control points and check points from this space resection are shown in Appendix E.

Area	Image	GCPs	RMSE Values at the Control Points			Check Points	RMSE values at the Check Points		
			ΔE (m)	ΔN (m)	ΔPl (m)		ΔE (m)	ΔN (m)	ΔPl (m)
Oslo 1A	Left	45	±7.2	±6.5	±9.7		-	-	-
	Right	(All)	±8.0	±7.4	±10.9		-	-	-
	Left	28	±7.7	±6.6	±10.2	17	±7.9	±9.3	±12.1
	Right	(Map)	±9.3	±7.5	±12.0	(Road)	±6.4	±10.4	±12.2
	Left	26	±7.9	±6.7	±10.4	17	±8.1	±9.1	±12.2
	Right	(Map)	±7.3	±7.5	±10.4	(Road)	±7.3	±10.9	±13.2
	Left	26	±7.9	±6.7	±10.4		-	-	-
	Right	(Map)	±7.3	±7.5	±10.4		-	-	-
	Left	17	±3.6	±4.3	±5.6		-	-	-
	Right	(Road)	±3.0	±4.3	±5.3		-	-	-

Table 13.11 Residual errors after space resection of the individual SPOT images of the Oslo stereo-pair using the EASI/PACE system.

13.11.2 Accuracy Tests of Planimetry and Height of Absolute Orientation of the Oslo Stereo-Model Using EASI/PACE

An absolute orientation using the **SATXYZ** program in the EASI/PACE system has also been carried out for the Oslo stereo-pair. The same combinations of control and check points that had been used in the space resection procedure were also utilized in the absolute orientation (based on space intersection). The plots of the vectors after absolute orientation in Tests 1 and 2 (lines 1 and 2 in Table 13.12) showed that two of the map-derived GCPs had very large residual errors in elevation amounting to 25m and 31m respectively. So these two points have been removed from the data set and all the tests have been repeated with these points deleted. It will be seen that the RMSE value for the

residual errors in elevation at the control points (i.e. the map-derived points) improved markedly after the removal of the two offending points. Whereas for planimetry, very little improvement resulted after removal of the two points.

Area	No. of Control Points	RMSE Values in Planimetry and Height at the Control Points				No. of Check Points	RMSE values in Planimetry and Height at the Check Points			
		ΔE (m)	ΔN (m)	ΔPl (m)	ΔH (m)		ΔE (m)	ΔN (m)	ΔPl (m)	ΔH (m)
Oslo	45 (All)	±7.2	±6.6	±9.8	±8.5					
	28 (Map)	±8.0	±6.8	±10.5	±10.2	17(Road)	±7.4	±9.1	±11.7	±5.4
	26 (Map)	±7.2	±6.9	±10.0	±6.7	17(Road)	±8.1	±9.2	±12.8	±5.6
	17(Road)	±3.1	±4.3	±5.3	±4.4					

Table 13.12 Accuracy tests of the absolute orientation using different combinations of control and check points using the EASI/PACE system.

In Table 13.12, as shown in the first line with all 45 ground control points used in the solution, the RMSE values of the residual errors were ±9.8m in planimetry and ±8.5m in height which is less than one pixel accuracy. When 28 map-derived control points were used in the solution, the RMSE value of the residual errors in elevation at the 17 road database points used as independent check points was ± 5.4m. With line three, when 26 map-derived control points were used in the solution, then the RMSE value of the residual errors at the check points was ± 5.6m, which was a very slight decrease in accuracy. Also the same occurred with the RMSE value of the residual errors in planimetry at the check points with a very slight decrease in accuracy from ±11.7m in the second line (28 control points) to ±12.8 m in the third line when 26 control points were used in the solution. When the road database points only were used in the solution - as shown in the fourth line - the RMSE value of the residual errors improved to ±5.3m and ±4.4m for planimetry and height respectively.

Vector plots of the values of errors of the residuals in planimetry (Figure 13.18) show a mainly random pattern of errors except for a very few points that exhibit a systematic error pattern locally. While the vector plot of the values of the residual errors in height of absolute orientation given in Figure 13.19 showed a completely random distribution both in extent and in direction with no systematic components.

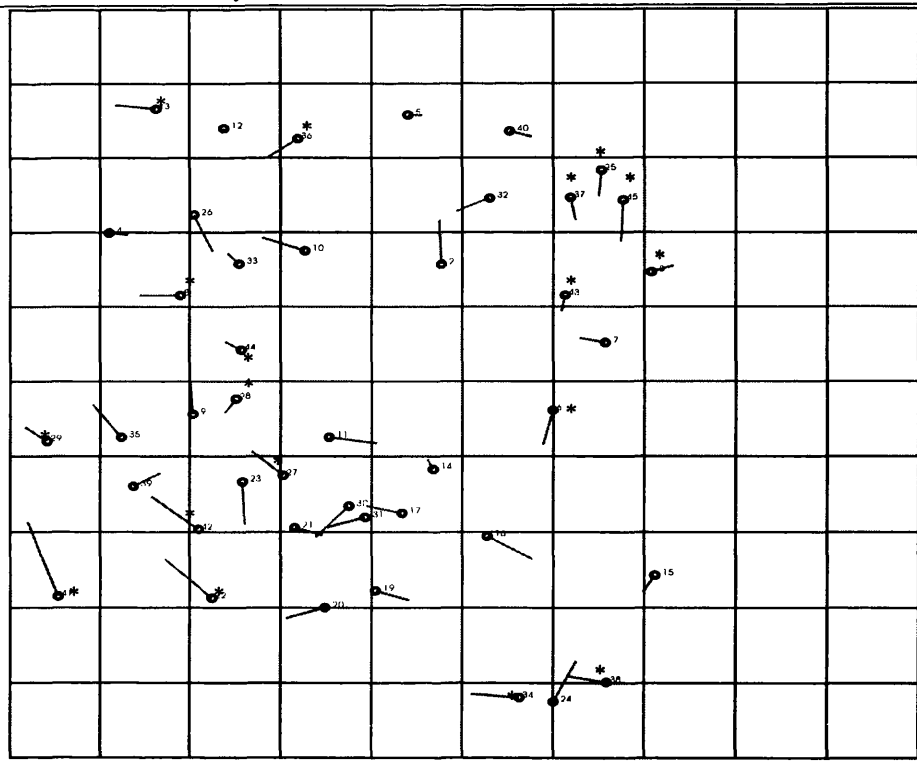

Figure 13. 18 Vector plot of the values of the residual errors in planimetry at the control points and check points after absolute orientation of the Oslo stereo-model using EASI/PACE Control Points Check Points *

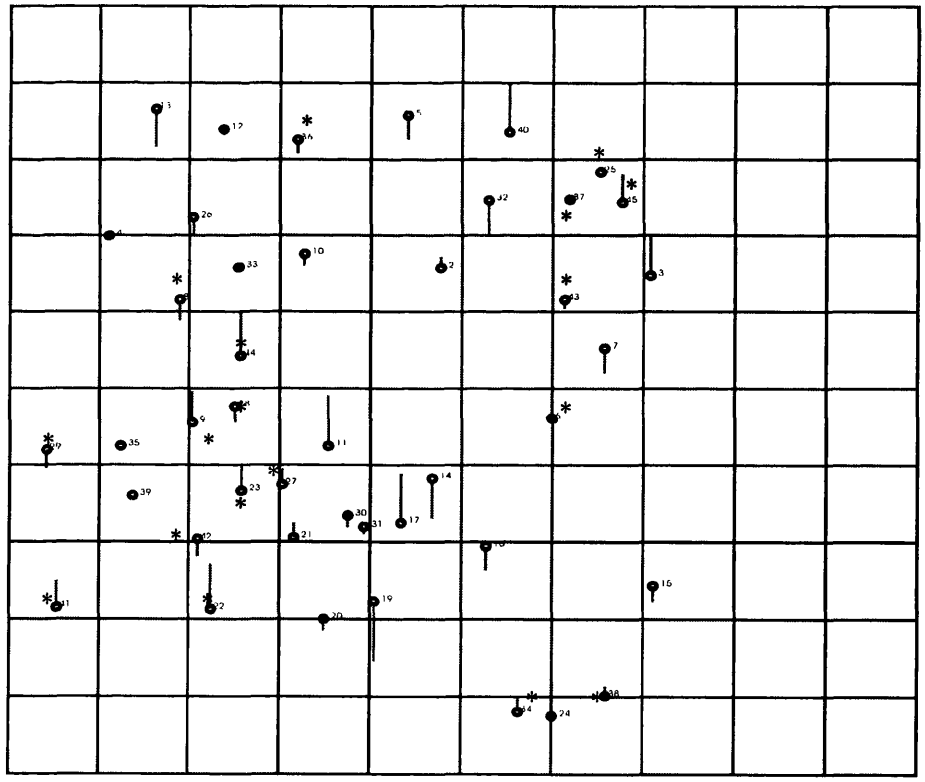

Figure 13.19 Vector plot of the values of the residual errors values in height at the control points and check points after absolute orientation of the Oslo stereomodel using EASI/PACE Control points Check points *

13.11.3 Accuracy Tests of Height in the DEM Produced by Stereocorrelation Using EASI/PACE

Before the stereocorrelation process was carried out, the right image of the Oslo stereo-pair has been rectified and resampled to epipolar geometry. For image matching (stereocorrelation) the **SDEM** module of EASI/PACE has been used. Two DEMs have been extracted, the first one with a 20m grid spacing and the second with a 10m grid spacing. The results of two different tests of the image matching process using the elevation values at the GCPs are shown in Table 13.13. In the first test, the accuracy in terms of the RMSE value for the errors in height obtained at 45 ground control points was ± 6.3m, while, in the second test, the RMSE values obtained from the residual errors at 25 control points was ± 5.8m and at 16 independent check points, ± 7.0m. It is worth mentioning here that these figures resulted from a comparison of the height obtained from the image matching process with the given height values of these points.

Area	Ground Control Points	RMSE Values at the Control Points ΔH (m)	Check Points	RMSE values in Height at the Check Points ΔH (m)
Oslo Stereo-model 1A	45 (All)	±6.3		
	25	±5.8	16	±7.0

Table 13.13 RMSE values in height at the control and check points in the Oslo DEM obtained through a comparison of the elevation values derived from the image matching technique and the values obtained from the maps and road database.

At Dr. Bjerke's request, yet another DEM was extracted with a grid interval of 10m, for a small part of the Oslo stereo-model using EASI/PACE.

13.12 Contours Generated from Oslo DEM by EASI/PACE

Two sets of contours were generated from the Oslo DEM using a 20m spacing between the grid points, in each case, employing the **CONTOUR** program available in the EASI/PACE system. The first set of contours was generated using an interval of 50m. The second set of contours was generated using a 20m interval. These two sets of contours have been sent in hard copy form to Dr. Bjerke to be compared with the contours which can be extracted from the DEM in his system. Also Dr. Bjerke sent a set

of 1:50,000 scale topographic maps covering the Oslo stereo-model to compare the two sets of contours - the contours extracted from Oslo DEM and the contours available in the 1:50,000 scale topographic map. The superimposition of the two sets of the contours showed some kind of fit in some places and some deviations in other places.

13.13 Orthoimage Generation Using EASI/PACE

Using the **SORTHO** module in EASI/PACE system, an orthoimage has been generated from the Oslo stereo-pair with a pixel size of 20m. (Figure 13.22) The right image of the Oslo scene has been selected for processing. Another orthoimage has been generated from part of the Oslo stereo-pair and has been sent to Dr. Bjerke to be compared with the orthoimage generated from the FFI system.

13.14 Conclusion

The FFI system for the processing of SPOT stereo-pairs employs a quite unique and original solution in that it uses surface mapping functions throughout instead of the normal 3D photogrammetric solution employing simple polynomial interpolation for the modelling of the perspective centres and attitude data, followed by the use of specially formulated collinearity equations - as employed for example in the EASI/PACE and OrthoMAX systems. The use of the FFI system is also confined to a small military mapping and intelligence community in Norway and it is not available on a commercial basis like the other systems tested in this research. Nevertheless the availability of the high-quality Badia Test field allowed it to be tested in a way that had not been done before.

The results of this testing again showed up the shortcomings that were present in the system when the tests began. In particular, the use of the high quality Badia data showed that the algorithms originally used in the FFI system allowed only a certain limited geometric accuracy to be achieved using the system. As soon as the Badia test data was used, it was immediately apparent that highly systematic patterns of errors were being produced by the FFI system both in planimetry and height. These had previously been hidden from the originator of the program due to the lower quality of the GCP data

(mainly map-derived) that was available for the test field that was being used in Norway. Once these shortcomings became apparent, Dr. Bjerke immediately devised and implemented alternative strategies and algorithms. These resulted in an immediate and obvious improvement in the accuracy of the results that could be achieved using the FFI package.

Besides the use of the Badia test data, Dr. Bjerke also began to use a much better set of GCP data for his Oslo test field - over which his tests then gave much improved results. With the use of his new algorithms, it was apparent that the FFI package is now capable of producing results that, in terms of geometric accuracy, are comparable to those that are being achieved with the other commercially available packages that have been tested during the author's research project.

In the next chapter, a comparison of the geometric accuracy tests and the validation of the accuracy of the DEMs and orthoimages produced by the various systems will be presented and discussed, including a comparative analysis of the characteristics of the systems employed in the present research and the results achieved both in the tests carried out by the author and, in the past, by other investigators.

CHAPTER 14: COMPARISON OF GEOMETRIC ACCURACY TESTS AND SUBSEQUENT ANALYSIS

14.1 Introduction

In the last five chapters (8, 9, 11, 12 and 13), the results of various geometric accuracy tests that have been carried out on SPOT stereo-models over the Badia test field using four quite different systems have been reported and analysed. In this chapter, a further comparative analysis and discussion will be conducted on the results achieved with these systems with regard to their geometric accuracy in the specific context of topographic mapping. Furthermore, the test results obtained by these systems over the Badia test field will be compared with the results from the geometric accuracy tests reported by other researchers that have been discussed in Chapter 2.

14.2 Limitations in Comparing the Results from Different Systems

As will be obvious from the accounts given in the previous individual chapters, there are quite a number of limitations in carrying out a comparison of the results of the different systems that have been tested by the author over the Badia test field. In the first place, the FFI system can only handle Level 1A SPOT data, while the DMS system only handles Level 1B SPOT data. Only the EASI/PACE and OrthoMAX systems can handle both types of data, and, even then, the OrthoMAX system can only utilize the older type of Level 1B data produced before the change in processing involving the use of a fifth-order polynomial made by SPOT Image in 1995.

Quite apart from the systems' different capabilities in terms of handling the different levels of SPOT data, other matters that limit or curtail an overall comparison arise from the different solutions that have been adopted. Thus the FFI system produces zero errors at the GCPs with its new algorithm using surface mapping functions - since there is no redundancy and therefore no least squares solution. Furthermore, the DMS system produces its planimetric and height results in two quite different steps - since it has quite separate solutions and operations (i) to rectify the planimetry (via the use of its polynomial transformation) and (ii) to generate elevation values (either via stereo-

measurement or image matching). Only the EASI/PACE and OrthoMAX systems generate a conventional absolute orientation - and the former only does so as a result of representations of the author and his supervisor. Nevertheless, notwithstanding these caveats or limitations, it is still interesting to carry out a comparative analysis of the results achieved with the different systems using the Badia test field in terms of their geometric accuracy - on the basis of

(i) the results achieved by the Level 1A and Level 1B forms of the SPOT data;

(ii) the results obtained by the four different systems using the same test data; and

(iii) the results obtained with the Badia data using these different systems in comparison with the results from previous tests of a similar nature carried out by other researchers.

In this context, it will be noted that few of the previous tests had involved the use of SPOT Level 1B data in spite of its obvious popularity with many users.

14.3 Accuracy of the Level 1A and 1B Stereo-Pairs of the Reference Scene 122/285

Several three-dimensional geometric accuracy tests have been carried out on both the Level 1A and 1B stereo-pairs over the Badia test field using the four different systems. Table 14.1 summarises the actual test results of the 3D geometric accuracy achieved in those tests carried out over the reference scene 122/285.

14.3.1 An Overall Comparison of the Results for Level 1A and 1B Stereo-Pairs Obtained by the EASI/PACE and OrthoMAX Systems

The only full comparison that can be made between the results that have been achieved between the Level 1A and 1B stereo-pairs have been those using the absolute orientation program of the EASI/PACE system in different combinations of control points and check points. With the EASI/PACE system, the number of ground control points used in the tests of the Level 1A and 1B stereo-pairs is almost the same, while the range of RMSE values in planimetry at the control points falls between ±5.7m to ± 8.2m for the Level 1A stereo-pair and between ±5.7m to ±7.0m with the Level 1B stereo-pair. At the independent check points, the range of RMSE values with the Level 1A stereo-pair falls

(I) Level 1A - Scene 122/285

A. EASI/PACE	Control Points				Check Points				
No.	ΔE (m)	ΔN(m)	ΔPl (m)	ΔH (m)	No.	ΔE (m)	ΔN(m)	ΔPl (m)	ΔH (m)
47	±4.2	±4.2	±5.9	±4.8	0	-	-	-	-
32	±5.2	±6.4	±8.2	±6.0	15	±5.2	±5.9	±7.9	±6.6
22	±3.8	±4.8	±6.1	±4.1	25	±4.9	±4.6	±6.7	±6.4
12	±3.9	±4.1	±5.7	±4.6	35	±4.6	±5.1	±6.9	±6.1
B. OrthoMAX									
47	±3.7	±3.8	±5.3	±1.5	-	-	-	-	-
28	±3.7	±4.0	±5.4	±1.5	-	-	-	-	-
22	±3.9	±4.7	±6.1	±1.2	-	-	-	-	-
C. FFI									
45	±12.3	±6.1	±13.7	±13.2	-	-	-	-	-
24	-	-	-	-	23	±8.9	±6.5	±11.0	±10.1
23	-	-	-	-	24	±9.3	±6.2	±11.2	±10.3

(II) Level 1B - Scene 122/285

A. EASI/PACE	Control Points				Check Points				
No	ΔE (m)	ΔN (m)	ΔPl (m)	ΔH (m)	No.	ΔE (m)	ΔN (m)	ΔPl (m)	ΔH (m)
45	±4.7	±4.9	±6.8	±4.7	0	-	-	-	-
33	±4.2	±5.6	±7.0	±4.8	15	±7.3	±5.1	±8.9	±5.3
23	±4.8	±5.0	±6.9	±4.5	25	±5.3	±6.1	±8.0	±5.8
13	±3.3	±4.6	±5.7	±3.5	35	±6.0	±5.9	±8.4	±5.7
B. OrthoMAX									
49	±12.5	±7.8	±14.7	±1.0		-	-	-	-
39	±6.3	±4.7	±7.9	±1.3		-	-	-	-
C. DMS									
45	±8.4	±7.8	±11.5	±4.5	-	-	-	-	-
30	±8.7	±7.9	±11.8	±4.8	15	±8.1	±8.1	±11.5	±6.7
20	±9.5	±8.5	±12.8	±4.5	25	±8.7	±8.1	±11.9	±6.2
10	±8.5	±8.0	±11.9	±5.9	35	±10.8	±9.1	±13.5	±5.2

Table 14.1 Results of accuracy tests of the RMSE values of the residual errors in planimetry and height at the control points and check points for the Level 1A and 1B stereo-pairs using the four tested systems.

between ±6.7m to ±7.9m, while for the Level 1B stereo-pair, it falls in the range ±8.0 to ±8.9m. For the height accuracy at the control points using the EASI/PACE system, the best accuracy obtained in terms of RMSE value was ± 3.5m using the Level 1B stereo-pair, while the range of the RMSE values fell between ±3.5m to ±4.8m. For the Level 1A stereo-pair, the best accuracy in terms of the RMSE value was ±4.1m while the range in these values fell between ±4.1 to ±6.0m. These differences are not really very large or significant.

For the OrthoMAX system, the best accuracy achieved in planimetry in terms of RMSE values at the control points for the Level 1A stereo-pair was ±5.3m, which was significantly better than the accuracy obtained with the Level 1B images at ±14.7m using the full GCP data set and of ± 7.9m with a somewhat reduced data set. In general, the planimetric accuracy obtained by the OrthoMAX system at the control points for the

Level 1A stereo-pair is very slightly better than the accuracy obtained by the EASI/PACE system, while the planimetric accuracy obtained using the Level 1B stereo-pair in the EASI/PACE system is much better than the accuracy obtained with Level 1B by the OrthoMAX system. It could be that the OrthoMAX solution for dealing with Level 1B imagery using an inverse polynomial is less sound than that used in EASI/PACE where the actual polynomial coefficient values are extracted directly from the header file. As discussed previously, the height accuracy values (±1.0 to 1.5m) declared by the OrthoMAX system in terms of the root mean square errors resulting from the bundle adjustment program are simply not credible and should be discounted.

From this comparison of the results from the two systems and taking a overall view of these results, it can be seen that, especially using the EASI/PACE system, there is no significant difference in the results (either in planimetry or height) obtained from the Level 1A and 1B stereo-pairs. This is certainly very different to previous published tests, e.g. those by Gugan and Dowman (1988), where the Level 1B results were invariably much poorer than those obtained with the corresponding Level 1A stereo-pairs over the same test field in Cyprus. Moreover, from a general standpoint, the comparison of the results from both sets of data (Level 1A and 1B) shows that both are capable of producting excellent and comparable results - in the order of half-a-pixel (5m) in both planimetry and height - provided high-quality GCP data is used for control purposes.

Although the DMS system is limited to the use of Level 1B stereo-pairs only and, at first sight, it would not appear to have a photogrammetric solution that could produce first-class results, in fact, the results are quite acceptable for many purposes. However it will be noted that the RMSE values at the control points and check points in planimetry are noticeably poorer (12m v. 7m), while in height they are quite close (both circa 5m) to those obtained using EASI/PACE. This latter result is quite astonishing!

14.4 Accuracy Results of the Other Level 1B Stereo-Pairs of the Badia Area

For the other four stereo-pairs of the Badia area, the results of the accuracy tests obtained are summarised in Table 14.2. As will have been apparent from the previous discussion, only the EASI/PACE and DMS packages produced data for all four stereo-

pairs. Because of the inability of OrthoMAX to handle Level 1B imagery processed by SPOT Image using the fifth-order polynomial, the results from the package are limited to only two of the four models (124/285 and 124/286). A further limitation with OrthoMAX concerns the inappropriate (or unbelievable) results in height. Thus the main comparison will be between the EASI/PACE and DMS Systems.

System	Scene No.	No. of Control Points	RMSE Values at Control Points				No. of Check Points	RMSE Values at Check Points			
			ΔE (m)	*ΔN (m)*	*ΔPl (m)*	*ΔH (m)*		*ΔE (m)*	*ΔN (m)*	*ΔPl (m)*	*ΔH (m)*
EASI/PACE	123/285 1B	13	±3.5	±3.8	±5.2	±6.7	10	±4.2	±5.5	±6.9	±5.1
DMS	123/2851 B	9	±10.0	±9.3	±13.7	±11.6	10	±14.5	±17.6	±22.8	±6.6
EASI/PACE	123/286 1B	14	±4.2	±3.9	±5.7	±3.3	15	±4.6	±7.6	±8.9	±6.2
DMS	123/286 1B	13	±10.1	±5.9	±11.7	±4.9	15	±14.1	±9.9	±17.2	±7.0
EASI/PACE	124/285 1B	19	±4.1	±5.0	±6.5	±5.4	0	-	-	-	-
	124/285 1B	11	±3.3	±5.9	±6.8	±5.8	8	±5.5	±4.6	±7.2	±5.2
OrthoMAX	124/285 1B	18	±3.1	±4.5	±5.5	±0.016	-	-	-	-	-
DMS	124/285 1B	16	±10.1	±7.9	±12.8	±5.1	-	-	-	-	-
	124/285 1B	8	±6.0	±8.1	±10.1	±7.5	8	±18.4	±8.7	±20.3	±7.0
EASI/PACE	124/286 1B	13	±3.6	±4.9	±6.1	±5.8	-	-	-	-	-
OrthoMAX	124/286 1B	14	±3.4	±3.2	±4.7	±0.018	-	-	-	-	-
DMS	124/286 1B	13	±11.2	±8.5	±14.1	±7.0	-	-	-	-	-

Table 14.2 Accuracy results in planimetry and height at the control points and check points of the other Level 1B stereo-pairs of the Badia area using the EASI/PACE, OrthoMAX and DMS systems.

Inspection of Table 14.2 makes it clear that, once again, the EASI/PACE system gave much better results at the control and check points in planimetry (in the ratio of roughly 2:1) than the accuracy obtained by the DMS system. It was clear from the tests that DMS system also showed a lower accuracy in planimetry (circa 20m) at the check points when the number of the control points used in the solution was decreased. As for the comparison of the RMSE values in height, the values at the check points for DMS are again only slightly poorer than those obtained with the EASI/PACE system. As far as OrthoMAX is concerned, the RMSE values in planimetry for the two models that could be processed are actually the best of all, being even slightly better than the values obtained with EASI/PACE. With regard to the declared height values, the RMSE values of ±0.016m and ± 0.018m (1/70th of a pixel) cannot be given any credence.

14.5 General Remarks About the Results of the Geometric Accuracy Tests in the Context of Topographic Mapping.

Based on the above discussion, it is perhaps worth analyzing the results in terms of the American National Map Accuracy Standards (NMAS) for topographic mapping. This specifies that 90% of well-defined features included in the map should be within 0.5mm of their correct planimetric positions at a scale of 1:50,000. This translates into a standard error (68%) of ±0.3mm. In which case, the planimetric positional error σ_{Pl} = 0.3mm . map scale number. Thus for 1:50,000 scale mapping, the standard error would be ±15m. It will be seen that the planimetric accuracies achieved in the tests of the SPOT stereo-pairs carried out over the Badia test field mostly lie well within this figure, although the values at the check points got with the DMS system at circa 20m do lie outside this yardstick.

The range of RMSE values at the control points for all of the stereo-models using EASI/PACE fall in the range ±5.2m to ±8.2m which correspond to the planimetric accuracy requirements of maps in the range 1:17,300 to 1:27,300 scales. For OrthoMAX, the corresponding range lies between 1:15,600 to 1:49,000 scale. In the case of the DMS system, the RMSE values correspond to the planimetric accuracy requirements of maps in the scale range 1:33.600 to 1:47,000, while the results generated by the FFI system are equivalent to the requirements of maps at 1:45,600 scale.

Turning next to the American standard for elevation accuracy in a topographic map, this states that 90% of the elevations given by the contours on the map should not be in error by more than half the contour line interval. This immediately begs the question as to what the contour line interval will be for commonly used map scales. Those given by Doyle (1984) and Ghosh (1987) are set out in Table 14.3.

Doyle (1984)		Ghosh (1987)	
Scale	**Contour Interval**	**Scale**	**Contour Interval**
1:25,000	5	1:25,000	10, 20
1:50,000	10	1:50,000	10, 20, 40
1:100,000	20	1:100,000	20, 50
1:250,000	25	1:250,000	

Table 14.3 Scales and contour intervals according to Doyle and Ghosh.

This then brings up the question of the relationship between spot height accuracy (which is what has been measured or determined in the author's tests of the SPOT stereo-pairs) and the contour interval. The general opinion (e.g. Tham 1968) is that the spot height accuracy should be one-third to one-fifth of the minimum contour line interval: or that the minimum contour interval will lie between 3.3 and 5 times that of the spot height accuracy. Taking the best value of ±6m at the check points for the elevation accuracies produced in the author's tests, the corresponding minimum possible contour line interval would be 20 to 30m. According to Doyle (1984), this would only be suitable for mapping at 1:100,000 scale and smaller, while, according to Ghosh (1987), it would be suitable for mapping at 1:50,000 to 1:100,000 scales. depending largely on the specified contour interval, which in turn depends on the type of landscape or terrain that is being mapped, e.g. is it flat, hilly or mountainous.

Of course, while geometric accuracy is a most important factor when carrying out mapping operations from satellite imagery, there are many other factors that have to be taken into consideration, particularly that of the interpretational quality of the imagery which defines the features and therefore the content that can be extracted from a stereo-pair. Thus a major problem which affects the use of satellite imagery for topographic mapping lies in the shortfall in the ground resolution of the satellite images and in the information content of the resulting maps. The 10m pixel size of the SPOT Pan translates to larger values - perhaps to 15 to 20m in terms of ground resolution (Petrie and Liwa 1995). Indeed Naithani (1988) of the Survey of India has assessed the ground resolution of SPOT Pan images as being 28m. Obviously the limitations in the ground resolution of SPOT imagery are reflected in the difficulties experienced in the detection of the smaller objects present on the ground, especially isolated or individual buildings, unsurfaced roads, motorable tracks, footpaths, streams and other drainage features. All of these features have dimensions which are smaller than the ground resolution and may exhibit poor contrast with the surrounding terrain, especially in arid and semi-arid areas.

According to Konecny et al (1982), for the detection and the identification of topographic features for vector line mapping at 1:50,000 scale, a ground pixel size of 3m for monoscopic imaging and 6m for stereoscopic viewing is necessary for a single building. This inability to detect such smaller features or objects means that the map

detail compiled from SPOT Pan satellite imagery (with a ground pixel size of 10m) would then be substantially deficient or incomplete. Indeed 30% of the required detail is the estimate made by Petrie and Liwa (1995) for the shortfall on the basis of their tests carried out in East, Central and Southern Africa. This deficiency will result in the need for a comprehensive field completion procedure to be executed on the ground to locate the missing features, which leads to a substantial additional expense. According to Petrie and Liwa (1995), SPOT Pan data can only supply the data for a preliminary or provisional edition of a 1:50,000 scale topographic map or for rapid and incomplete revision of an existing map at that scale. At present, SPOT data is still substantially deficient in providing the details required for the production of a full or final edition of a new 1:50,000 scale topographic map or making revision of existing maps at that scale.

In summary, the planimetric accuracy of SPOT stereo-pairs can meet the accuracy specifications of maps at a scale of 1:50,000 or even larger. In terms of height accuracy, they can meet the needs of maps at scales of 1:50,000 and smaller where the specified contour interval is 20m or larger. In terms of map content, SPOT data provides only part of the content of a topographic map at a scale of 1:50,000 and a substantial map completion is needed. However, in general terms, SPOT data may be judged to be suitable for producing topographic map at 1:50,000 scale and smaller for large areas of arid and semi-arid terrain having very few cultural features - as is the case over much of Jordan. However those few features - which may be very important in such areas (e.g. the positions of individual buildings or wells) - will need to be added via a thorough ground completion operation.

14.6 Comparative Accuracy Tests of SPOT Level 1B Stereo-Pairs

In general, one of the most distinctive features of this research project are the results obtained using the Level 1B SPOT stereo-pairs. This stands in contrast to the results achieved by previous researchers who have mostly carried out their tests using Level 1A imagery. The extensive accuracy tests carried out during the present research have shown that the accuracies in planimetry and height obtained using SPOT Level 1B stereo-imagery with the new software-based systems can be just as good as the

accuracies obtained from Level 1A stereo-pairs. Very few tests have been carried out till now using Level 1B imagery. In these previous tests, modifications have been made to the mathematical models and software to cope with Level 1B imagery but unfortunately poor results have been obtained. Yet, because of their near-orthographic and map-like geometry, Level 1B images are very popular with many geoscience users - since they are more easily correlated with the existing map coverage of the imaged area. In addition to all of that, Level 1B imagery is cheaper to purchase than the corresponding Level 1A imagery, especially archived imagery obtained prior to 1990.

As a result of the tests undertaken in this research project, it is possible to compare the results which have been achieved using Level 1B SPOT imagery with the results from the other tests carried out by those other researchers concerned with the testing of SPOT imagery. A comparison of these results in terms of RMSE values is given in Table 14.4.

Area	Reported by	Hardware	Software	B/H	Control Points	Check Points	ΔPl (m)	ΔH (m)
South-West Cyprus	Gugan & Dowman (1988)	Kern DSR-1	UCL	0.83	10	15	±31.6 to ±35.8	±15.9 to ±18.9
South Korea	Yeu et al (1992)	Zeiss P2 Planicomp		0.57	13	10	±14.0	±13.8
Badia	Valadan Zoej (1997)	PC	Developed by Valadan Zoej (University of Glasgow)	0.98 to 0.86 0.98	13-20 15	 23	±7.1 to 11.7 ±12.1	±3.3 to ±13.2 ±10.0
Badia	Present author	PC	EASI/PACE	0.98 to 0.86 0.98	11 to 33 13	8-35 -	±6.9 to ±8.9 ±6.1	±5.1 to ±5.8 ±4.8
Badia	Present author	Sun/SGI	OrthoMAX	0.98	14 to 49		±4.7 to ±14.7	±0.016 to ±1.5
Badia	Present author	PC	DMS	0.98 to 0.86 0.98	8-30 13	8-35 -	±11.5 to ±22.8 ±14.1	±5.2 to ±7.0 ±7.0

Table 14.4 Geometric accuracy test results of SPOT Level 1B stereo-pairs

14.6.1 Comparison of Planimetric Accuracy Results

First, for the results obtained by the present research, the best accuracy in terms of the RMSE values obtained at the control points in planimetry was ±4.7m using the OrthoMAX system, followed by the accuracy of ±6.1m obtained by EASI/PACE system, then ±14.1m obtained by the DMS system. Concerning the accuracy at the check points, the best accuracy was ±6.9m obtained by EASI/PACE system, no check

points were used in OrthoMAX, while the best accuracy obtained at the check points using DMS system was ±11.5m. In conclusion, according to the NMAS planimetric accuracy standard, all of the three commercial systems employed in the present research can meet the accuracy specification of maps at 1:50,000 scale or larger at the control points and check points using Level 1B stereo-imagery. In case of the test carried out by Valadan Zoej (1997) using his own software, the planimetric accuracy ranged between ± 7 to ± 12m. These figures are similar to those obtained by the author using the commercially available software packages.

By comparison, the results for planimetry obtained by Gugan and Dowman (1988), gave an RMSE value $> \pm 30$m which corresponds to the accuracy requirements of maps at 1:100,000 scale and smaller. The planimetric accuracy (RMSE = $\pm$ 14.0m) obtained by Yeu et al (1992) is certainly better than those of Gugan and Dowman, but it still does not compare with the results achieved by the author with EASI/PACE and OrthoMAX, being more on a par with those got with DMS.

14.6.2 Comparison of Height Accuracy Results

Concerning the accuracy in height, the best RMSE value obtained at the control points using EASI/PACE was ±4.8m while that at the check points was ± 5.1m. The figures obtained with DMS are only slightly poorer. For height accuracy, with an average accuracy of ± 6m at the check points, the corresponding minimum possible contour line interval would be 20 to 30m. Again these figures are in contrast to those obtained for heights by Gugan and Dowman with an RMSE value of $> \pm 15$m which would point to a possible contour interval of 50 to 60m. Similarly the results achieved by Yeu et al gave an RMSE value for height of ± 13.8m which again points to a minimum contour interval of 50m. According to Doyle and Ghosh, such an interval corresponds to the requirements of 1:250,000 scale mapping.

14.7 Comparative Accuracy Tests of SPOT Level 1A Stereo-pairs

Table 14.5 given below only includes the best accuracy results obtained by the previous researchers which are comparable with the accuracy results obtained over the Badia test area.

Area	Reported	Hardware	Software	For-mat	B/H	GCPs	CHs	ΔPl (m)	ΔH (m)
South France	Rodriguez et al (1988)	Matra Traster Analytical Plotter	IGN	1A		86a	631 215 (a,t,s)	±10.4 ±9.8	±7.1 ±4.3
Aix-en-Provence	Gugan & Dowman (1988)	Kern DSR-1	UCL	1A	0.73 0.73 0.41 0.32	10 s,t 10 10 10 10	20t 62 64 53 20	±17.7 ±15.3	±8.1 ±5.4 ±8.4 ±8.0 ±6.8
Marseille	Konecny et al (1987), Picht (1987)	Zeiss Planicomp Analytical Plotter	Bingo	1A	1	18t	68t	±17.5	±6.5
Cyprus South-west Cyprus	Gugan (1987) Gugan and Dowman (1988)	Kern DSR-1	UCL	1A 1A	0.83	10t 10t	19t 15t	±29.2 ±27.8	±8.8 ±9.4
South-West Cyprus	Ley (1988)	Kern DSR-1 MDA MDA		1A 1A 1A	0.82 0.82 0.82	15 t 6 t 6s	-	±18.1 ±8.8 ±5.6	±7.2 ±6.4 ±4.2
Ottawa Sherbrooke Grenoble	Kratky (1988)	NRC Anaplot I	NRC/CCRS	1A 1A 1A	0.40 0.61 0.94	5 16 5	62 237 12	±7.0 ±7.1 ±10.0	±8.4 ±7.3 ±3.3
Ottawa	Toutin and Carbonneau (1990)		CARTOSPOT	1A	1.0	6	9.2 72	±6.0 ±4.7	±3.5 ±2.8
Irvine California	Cheng & Toutin (1995)		EASI/PACE	1A 1A	0.5	10	10	±4.7	
British Columbia (Canada)	Toutin & Beaudoin (1995)	DVP system	Guichard & Toutin Math-model	1A	0.74	12 t,a	-	±6.2	±3.7
STF (France) STC (China) STU (USA)	Chen (1992)		Group of programs of bundle adjustment	1A	0.96 0.56 0.38	34 25 25	50 32 23	±18.4 ±19.5 ±22.8	±5.0 ±7.8 ±7.1
Tangshan	Zhong (1992)	Chinese-built JX-3	Zhong software	1A	0.5	17 t 17t	40 40	±11.5 ±17.4	±5.7 ±6.9
South Korea	Yeu et al (1992)	Zeiss P2 Planicomp	ERDAS	1 AP 1A	0.57 0.57	13s 13s	10s 10s	±10.1 ±10.8	±11.3 ±6.4
Badia	Valadan Zoej (1997)	PC	Valadan's software	1A	0.98	15s	23	±12.8	±5.6
Badia	Present author	PC	EASI/PACE	1A	0.98	47 12 to 32	- 15 to 35	±5.9 ±6.7 to ±7.9	±4.8 ±6.1 to ±6.6
Badia	Present author	Sun/SGI	OrthoMAX	1A	0.98	47 22-28	-	±5.3 ±5.4 to ±6.1	±1.5 ±1.2 to ±1.5
Badia		PC	FFI	1A	0.98	45 23-24	- 23-24	±13.7 ±11.0 to ±11.2	±13.2 ±10.1 to ±10.3
Oslo	Present Author	PC	EASI/PACE	1A	0.61	45 28 26	 17 17	±9.8 ±11.7 ±12.8	±8.5 ±5.4 ±5.6

Table 14.5 Geometric accuracy test results of SPOT Level 1A imagery reported by different researchers

(s = field survey, t = topgraphic map, a = aerial photograph)

Most of the published results of the geometric accuracy tests of SPOT images over different test areas have been carried out using analytical plotters using SPOT Level 1A raw data in hard-copy form. As shown in Table 14.5, very few tests have been carried out using digital data. In the case of the Badia area, only one Level 1A SPOT stereo-pair - that for the reference scene 122/285 - was available for testing. This stereo-pair has been processed in the EASI/PACE, OrthoMAX and FFI image processing systems. Not only will the Level 1A results be compared with the previously published results but also with the accuracy results obtained from the Level 1B SPOT stereo-pairs covering the Badia area. It is clear from Table 14.5 that the reported tests have been carried out in different locations; with different base-to-height ratios; with different quality and numbers of ground control points and check points; using different software and hardware; and finally with different accuracy results obtained in planimetry and height.

14.7.1 Comparison of Planimetric Accuracy Results

It is very clear that, from the summarized results of the whole series of tests listed in Table 14.5, the best planimetric accuracies obtained at the check points were those reported for the Irvine area by Cheng and Toutin (1995) using EASI/PACE with an RMSE value of ±4.7m, and those reported by Toutin and Carbonneau (1990) with an RMSE value of ± 4.7m for the Ottawa area. These results are virtually identical to the planimetric accuracy results of ± 4.1 to ±4.6m obtained by the author at the control points in the Level 1A SPOT stereo-pair of the Badia area using the EASI/PACE system (which also uses Toutin's modelling and algorithm) and are somewhat better than those (±6.1 to ±6.7m) obtained at the check points using EASI/PACE. The high accuracy obtained is due partly to the high quality of the ground control points used in all of these tests. These have been acquired by ground survey methods for the Ottawa test area while, in the Irvine area, the ground control points have been derived from a very accurate 1:25,000 scale topographic map and the points tested mainly comprised road intersections (personal communication from Dr. Cheng). It should be noted too that the Irvine test was carried out using a single image only - so effectively the result given is that for a space resection, rather than that achieved with the absolute orientation of a single pair. The planimetric accuracy results (RMSE = ±6.2m) reported by Toutin and

Beaudoin (1995) using the DVP system with its stereo-capability over a test area in British Columbia in Canada are also very comparable with the accuracy results achieved over the Badia test area. It should be noted that the mathematical model used as the basis of the photogrammetric solution in all of these systems is that devised by Dr. Toutin, while all the actual systems employed digital data rather than hard copy images. Turning next to the other good planimetric accuracy results, these reported by Rodriguez et al (1988) for the IGN test area in south France, the figures (RMSE of circa $\pm$10m) are not as good as the results obtained during the present research. The accuracy obtained is rather lower at around one pixel size; most probably this is due to the quality of the control points which are a mixture of points derived from topographic maps from photogrammetric measurements on aerial photographs and those fixed by ground survey. In case of the accuracy figures reported by Gugan and Dowman (1988) over the Aix-en-Provence area in south France, the reported accuracy in planimetry (RMSE = $\pm$ 15 to $\pm$17m) is comparatively poor and is not in the same class as those for planimetric accuracy obtained over the Badia test area. Indeed the accuracy obtained is even lower than the accuracy obtained by the author using the DMS system. Much the same can be said regarding the accuracy results in planimetry reported by Konecny et al (1987) and Picht (1987) in the Marseille area. This accuracy is also poorer (RMSE = $\pm$17m) and not really comparable with the results for planimetric accuracy obtained using the present research. This may be due partly to the quality of the ground control points which have been derived from topographic maps.

Coming again to the planimetric accuracy results reported by Gugan (1987) and Gugan and Dowman (1988) for their test area in south-west Cyprus, again comparatively poor results have been obtained. These may have been affected both by the terrain, which is mostly mountainous, and also by the limited quality of the ground control points which have been derived from topographic maps. In case of the planimetric accuracy at the ground control points reported by Ley (1988) over the same area in Cyprus, poor results were obtained using the Kern DSR-1 with UCL's software and ground control points that had been derived from topographic maps. On the other hand, much better accuracy results were reported using the MDA software employing digital image data and ground

control points obtained by ground survey. Indeed the latter accuracy is only slightly lower than the accuracy results obtained in the present research.

14.7.2 Comparison of Height Accuracy Results

For the height accuracy obtained over the Badia test area, the RMSE values obtained at the check points with the EASI/PACE system fall in the range ± 5.5 to ± 6.6m for the Level 1A stereo-pair and ± 5.1 to ± 6.2m for the Level 1B stereo-pair. This accuracy is quite comparable, indeed slightly better, than the results reported by Rodriguez et al (1988) in the accuracy tests carried out in south France using IGN software; and the accuracy reported by Valadan Zoej (1997) carried out using the Badia stereo-model and the ground control points. It is also comparable to the accuracy achieved with the Oslo stereo-model carried out by the present author using the EASI/PACE system; and with the results reported by Ley (1988) in south-west Cyprus. Moreover the height accuracy of the Badia tests is comparable with the accuracy obtained by Kratky (1988) over the Grenoble area.

The very best results in height which have been achieved with Level 1A stereo-pair are those reported by Toutin and Carbonneau (1990), and Toutin and Beaudoin (1995) - which are slightly better than the results obtained in the present research. In fact, it does seem that the mathematical model devised by Toutin plays an important role in all the best results which have been obtained using SPOT stereo-pairs. This modelling was used as the basis of the best results obtained using the EASI/PACE system in the present research; in the Ottawa test where the CARTOSPOT system was used; in the British Columbia test carried out using the DVP; and also the Irvine test where the EASI/PACE system was used in the test.

In general, the height accuracy (at the 0.5 pixel level) obtained by the systems employed in the present research is extremely satisfactory and, in general, they are better than almost all of the accuracy results obtained by researchers other than Toutin, e.g those reported by Gugan and Dowman (1988) in Aix-en Provence; the accuracy results reported by Gugan (1987) and Gugan and Dowman (1988) for south-west Cyprus; and the accuracy results reported by Yeu et al (1992).

14.8 Conclusion.

Based on the results of the tests carried out by the author, the planimetric accuracy obtained by the four systems can meet the requirements of topographic maps at scale 1:50,000 and sometimes larger, while the accuracy of the heights achieved by the systems could correspond to the minimum contour line interval required for 1:50,000 scale maps but more probably those for smaller scales (e.g. 1:100,000). However, what has come out most clearly from all the tests is that the accuracy that can be achieved now with the Level 1B stereo-pairs using certain commercially available systems are quite comparable to those that have been reached with Level 1A stereo-pairs. Till now, only Level 1A stereo-pairs have been used for topographic mapping; now Level 1B stereo-pairs can be considered for the task. The author believes that he can claim some credit for this development, since the testing that he has carried out over the Badia test field has been the foundation for the changes and developments that have taken place in all the systems that have been tested.

Whether mapping at 1:50,000 scale and smaller will be successful or economic will depend largely on the interpretational quality of the imagery which defines the features and therefore the content that can be extracted from SPOT stereo-pairs and is controlled by the ground resolution of the SPOT imagery which may exhibit poor contrast with the surrounding terrain. If there are many features of a small dimension that need to be mapped, then the resulting requirements for field completion may cause the method to be uneconomic.

It was very clear from the results of the accuracy tests reported by other researchers that the quality of the ground control points is a most important factor in achieving good results. Poor results are obtained whenever the ground control points have been derived from topographic maps or from inadequate field survey. The advent of GPS which allows a network of high precision ground control points to be established comparatively rapidly and easily over the large areas of terrain covered by SPOT stereo-pair is an important element in improving the accuracy of the results that can be obtained from SPOT imagery.

Another matter of general interest that comes out of the author's tests and the comparisons with the tests carried out by other researchers is the importance of the mathematical modelling of the SPOT orbital data and the photogrammetric solution that is implemented on the basis of this modelling. Quite clearly those systems (EASI/PACE, CARTOSPOT, DVP, etc) which are based on the modelling developed by Dr. Toutin of CCRS are consistently at the top of the accuracy tests carried out both by the author and by other researchers and experimenters working with Toutin. Another point of general interest in this context is the good performance of the DMS system considering its relatively unsophisticated solution in photogrammetric terms. Although the planimetric accuracy that can be achieved with DMS is not comparable to the solutions based on Toutin's modelling, it is as good as that achieved with many other systems, while the height accuracies achieved with DMS are really very good and better than those achieved with many more sophisticated 3D solutions based on the use of collinearity equations.

This discussion of the suitability of SPOT stereo-imagery for topographic mapping will continued further in the next Chapter (15). This will consider the results achieved during the validation of the DEM elevation data and orthoimages carried out by the author. Comparison will be made between the results achieved using the different systems that have been tested by the author and those achieved by previous researchers.

CHAPTER 15: COMPARATIVE ACCURACY TESTS AND VALIDATION OF THE DEM DATA AND ORTHOIMAGES PRODUCED BY DIFFERENT SYSTEMS

15.1 Introduction

In the previous chapter, the results of the comprehensive series of geometric accuracy tests of SPOT stereo-pairs using different systems that have been carried out during the present research have been discussed and compared with the similar geometric accuracy tests reported by other researchers. Essentially all of these have involved the measurement of comparatively few GCPs (of a very high precision) used as control points and check points after completion of the absolute orientation of the SPOT stereo-pair. In this chapter, the accuracy tests carried out with a view to validating the DEM data extracted from SPOT stereo-pairs that have been carried out in the present research will be evaluated and will be compared with those carried out by several previous researchers. By contrast with the tests carried out on completion of the absolute orientation, the validation of the DEM data involves large number of elevation values often generated by automatic image matching procedures which will be compared mainly with reference data sets of a lower quality (in accuracy terms) than the GCPs involved in the absolute orientation and associated tests described in the previous chapter - although these GCPs have also been included in the validation procedure. This discussion of the quality of the DEM data and its validation will be followed by an analysis of the results of the tests of the planimetric accuracy of the orthoimages generated during the author's experimental work.

15.2 Comparative Height Accuracy Tests of the DEM Data Produced by the Different Systems

Several accuracy tests have been carried out on the elevation data of the DEMs produced from the Level 1A and 1B stereo-models for the reference scene 122/285 and the DEM data extracted from the other stereo-pairs covering the Badia test area using different combinations of control points and check points. These have been produced by each of the four systems that have been tested during the author's research project.

15.2.1 Comparative Height Accuracy of the DEM Data at the Control and Check Points of the Level 1A and 1B Stereo-pairs for the Reference Scene 122/285

For the Level 1A data, the tests were restricted to those produced by the EASI/PACE, OrthoMAX and FFI systems, while for the Level 1B data, the DMS system was added and the FFI system dropped out. The results of the accuracy tests of the elevation data at the high-accuracy GCPs as given by the DEMs produced from the Level 1A and 1B stereo-pairs for the reference scene 122/285 are summarized in Table 15.1.

(I) Level 1A - Scene 122/285

System	Scene/ Format	RMSE of DEMs at the Control Points		RMSE of DEMs at the Check Points	
		No.	Δ H (m)	No.	Δ H (m)
A. EASI/PACE	122/285 1A	31	±3.8	15	±4.3
		25	±4.0	20	±3.4
		10	±4.5	36	±3.5
B. OrthoMAX	122/285 1A	28	-	25	±5.2
C. FFI	122/285 1A	47	±7.8	-	-

(II) Level 1B - Scene 122/285

System	Scene/ Format	RMSE of DEMs at the Control Points		RMSE of DEMs at the Check Points	
		No.	Δ H (m)	No.	Δ H (m)
A. EASI/PACE	122/285 1B	47	±3.7	-	-
		32	±2.4	15	±3.3
		22	±3.8	25	±3.7
		12	±3.7	35	±3.6
B. OrthoMAX	122/285 1B	39	±-1.0	25	±5.6
C. DMS	122/285 1B	45	±4.5	-	-
		29	±4.8	15	±6.7
		19	±4.5	25	±6.2
		14	±5.9	35	±5.2

Table 15.1 Accuracy tests of the elevation values obtained from the DEMs at the control and check points.

15.2.1.1 Comparison of the Level 1A Data

Three separate accuracy tests of the elevation data at the GCPs have been carried out with the Level 1A DEM data from EASI/PACE using different combinations of control points and check points, while a single test was carried out with each of the OrthoMAX and FFI Systems. In each case, the comparison is between the elevation values obtained at these points using the automatic image matching routines of each package with the known high-accuracy values obtained via the GPS field survey.

(i) The best results were obtained using EASI/PACE where the range in the RMSE values using 15 to 36 check points was between ± 3.4 to ± 4.3m (amounting to a range of $\pm$ 0.9m) - which is very small.

(ii) For OrthoMAX, only a single test has been carried out in which the RMSE value in elevation extracted from the DEM using 25 independent check points is ±5.2m - which is only slightly higher.

(iii) In the case of the FFI system, the accuracy of the height in terms of the RMSE value using 47 ground control points was ±7.8 m.

It must be noted that these values were not determined from the measured image coordinate values of GCPs carried out for the resection and orientation procedure, but purely from the disparities generated during the subsequent image matching procedures carried out for the DEM extraction.

15.2.1.2 Comparison of the Level 1B Data

(i) For the accuracy of the elevation values at the 32 control points and 15 independent check points using the EASI/PACE system, the RMSE value obtained at the control points was ±2.4m, while the accuracy obtained at the check points was ±3.3m - which is quite excellent.

(ii) For the DMS system, the RMSE values of the elevations obtained using its stereocorrelation technique at 29 control points and 15 check points were ±4.8m and ±6.7m respectively - which again is a very good result.

(iii) For the accuracy of the elevations obtained at 25 independent check points, the RMSE values obtained by the three systems (EASI/PACE, DMS, and OrthoMAX) were ±3.7m, ±6.2m and ±5.6m respectively.

(iv) The accuracies obtained using the EASI/PACE and DMS systems only at 35 check points were ±3.6m and ±5.2m respectively.

In general, the Level 1B data gave very slightly better results than the Level 1A data, while the overall best results with both the Level 1A and 1B data were obtained by EASI/PACE followed by the OrthoMAX, DMS and FFI systems in that order. Figure 15.1 gives a graphical representation and summary of the accuracy tests of the DEM

height data at 25 check points for the Level 1B stereo-model for the reference scene 122/285 using the different systems. It is especially interesting to note that the elevation values from the DEM produced by OrthoMAX gave quite sensible values at the check points in contrast to those produced at the control points.

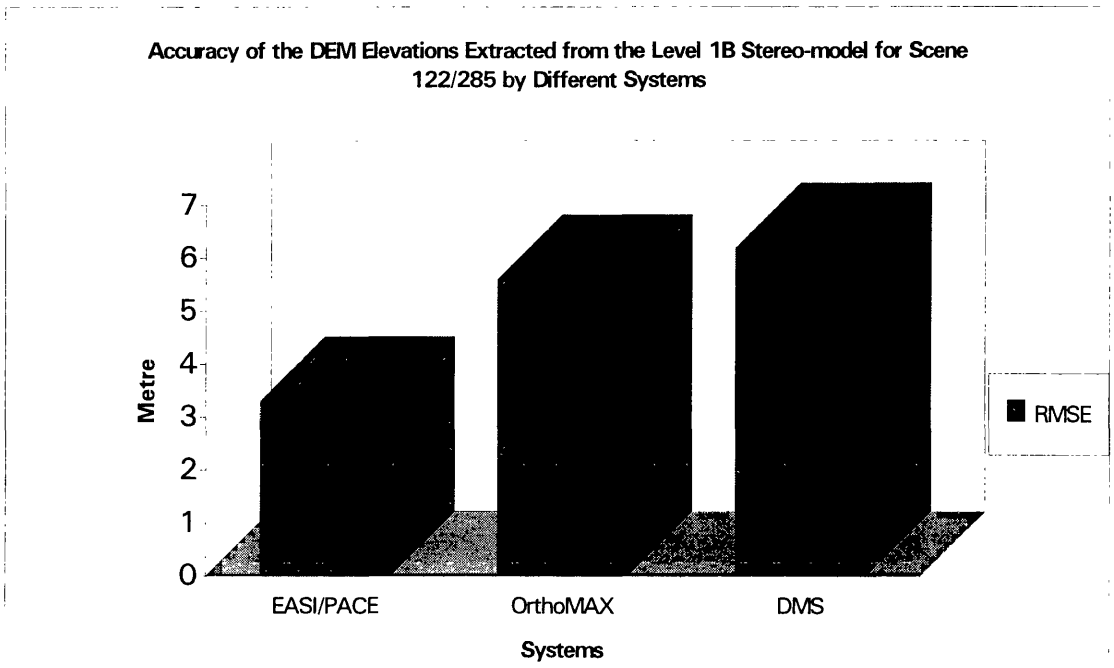

Figure 15.1 Graphical representation of the RMSE values in elevation derived from the DEM height data from different systems using 25 check points.

15.2.2 Comparative Height Accuracy Tests of the DEM Data of the Other Level 1B Stereo-pairs Covering the Badia Area Produced by Different Systems

For the other four Level 1B stereo-pairs covering the Badia test area, the DEMs extracted from these stereo-pairs can be compared fully for only two systems - EASI/PACE and DMS. For the OrthoMAX system, only two DEMs could be extracted and no check points could be used, while for the other two stereo-pairs, the data were in the new format and could not be processed. Given this situation, OrthoMAX has not been included in the comparison.

System	Scene Format	RMSE of Elevation Values at the Control Points		RMSE of Elevation Values at the Check Points	
		No.	Δ H (m)	No.	Δ H (m)
EASI/PACE	123/285	16	±4.7	-	-
		9	±5.9	10	±3.3
DMS	123/285	8	±11.6	10	±6.6
EASI/PACE	123/286	29	±2.6	-	-
		18	±3.9	11	±3.7
		15	±4.9	14	±3.9
DMS	123/286	12	±4.9	15	±7.0
		12	±4.1	18	±5.8
EASI/PACE	124/285	16	±6.0	-	-
		8	±4.8	8	±6.2
DMS	124/285	16	±5.1	-	-
		8	±7.5	8	±7.0
EASI/PACE	124/286	11	±5.8	-	-
DMS	124/286	16	±6.0	-	-

Table 15.2 Accuracy tests of height at the control and check points of the other Level 1B stereo-pairs using the DEM data extracted using the EASI/PACE and DMS systems.

Table 15.2 summarizes the errors in the actual height values obtained with different combinations of control points and check points using the two systems. In general, the RMSE values of the height values at the check points in the four DEMs tested by EASI/PACE system fall in the range between $\pm$ 3.3m and $\pm$ 6.2m. In the case of the DMS system, the RMSE values in height fall within the range $\pm$ 5.8 to $\pm$ 7.0m. Again in these tests, EASI/PACE gave slightly better results than the DMS system.

15.3 Comparison of Accuracy of the Heights Given by the Contours Digitised from the 1:250,000 Scale Topographic Map with the Height Values Given by the DEMs Produced by Different Systems

In this series of accuracy tests, the heights in the six DEMs produced from the Level 1A and 1B stereo-pairs using EASI/PACE; the five Level 1B DEMs produced by the DMS system; the four Level 1A and 1B DEMs produced by the OrthoMAX system; and the single Level 1A DEM produced by the FFI system will be compared with the heights given by the contours digitised from the 1:250,000 scale topographic map.

15.3.1 Accuracy of Height Data in the Level 1A and 1B DEMs of the Stereo-model for the Reference Scene 122/285 as Compared with the Heights Given by the Contours of the 1:250,000 Scale Map

As discussed previously, in this series of accuracy tests, the digitised photogrammetric contours extracted from the existing maps were superimposed over the DEM data and the respective height values were compared for selected contours. This method was applied to the DEMs produced by the four systems employed in the present research. For the reference scene 122/285, the results are summarized in Table 15.3.

System	Scene/Format	Contour Interval	No. of Points Measured	RMSE ΔH (m)
EASI/PACE	1A	50	531	±8.0
OrthoMAX	1A	50	398	±9.2
FFI	1A	50	761	±10.3
EASI/PACE	1B	50	719	±7.0
OrthoMAX	1B	50	712	±8.9
DMS	1B	50	589	±9.9

Table 15.3 Height accuracy in the Level 1A and 1B DEMs produced by the systems by comparison of the height values given by the digitised contours with the height values given by the DEMs.

Inspection of the RMSE values in elevation from all of the systems shows a surprisingly small range of values. Once again, the best result from this particular height accuracy test was obtained using the EASI/PACE system, with OrthoMAX the next best, followed by DMS and FFI. Figure 15.2 gives a graphical representation of the accuracy of the heights in the Level 1A and 1B DEMs produced by the different systems by comparison with the heights given by the digitised contours.

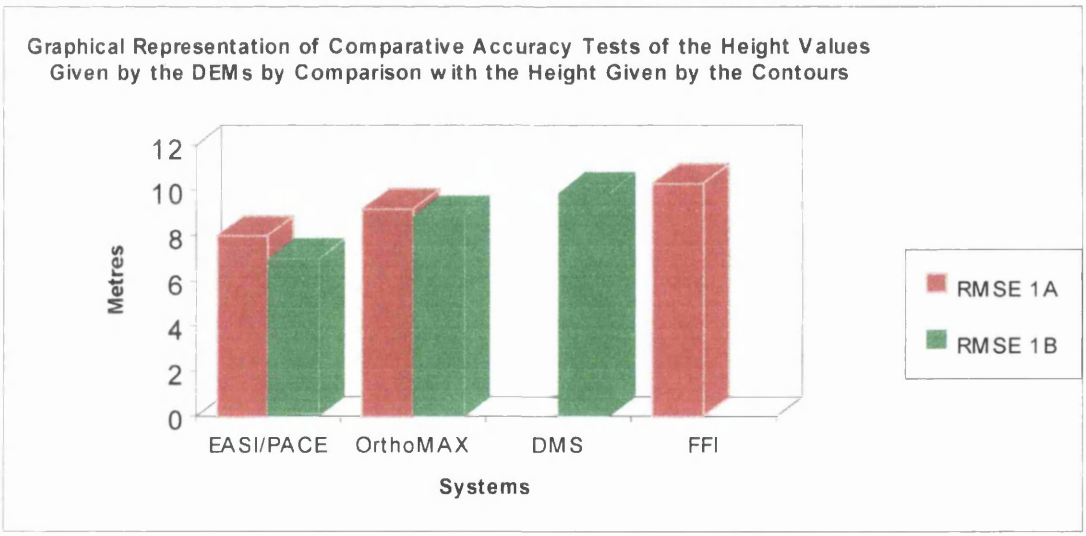

Table 15.2 Graphical representation of the height accuracy in the Level 1A and 1B DEM Data produced by the four systems by comparison with the height values given by the digitised contours.

15.3.2 Accuracy of Height Data of the DEMs Produced from the Other Level 1B Stereo-pairs as Compared with the 50m Contours of the 1:250,000 Scale Map

A summary of the results from the other stereo-pairs is given in Table 15.4. In general, the range of RMSE values in elevation for the data extracted by the EASI/PACE system falls in the range between ±6.1 and ±8.1m; with OrthoMAX, the corresponding range of RMSE values lies between ±5.2 and ±8.4m; while with DMS, the range of RMSE values between ±7.3 and ±12m. These results are not too different to those obtained with the reference scene 122/285.

System	Scene/Format	Contour Interval	No. of Points	RMSE ΔH (m)
EASI/PACE	123/285	50	442	±8.1
DMS	123/285	50	325	±10.8
EASI/PACE	123/286	50	403	±6.1
DMS	123/286	50	449	±12
EASI/PACE	124/285	50	443	±6.5
DMS	124/285	50	279	±7.3
OrthoMAX	124/285	50	387	±5.2
EASI/PACE	124/286	50	410	±7.8
DMS	124/286	50	348	±7.8
OrthoMAX	124/286	50	453	±8.4

Table 15.4 The RMSE values in elevation for the DEMs of the other stereo-pairs covering the Badia area using 50m contours from the 1:250,000 scale map.

Figure 15.3 gives a graphical representation of the height accuracy in the DEMs produced by the systems using a comparison of the heights given by the digitised contours.

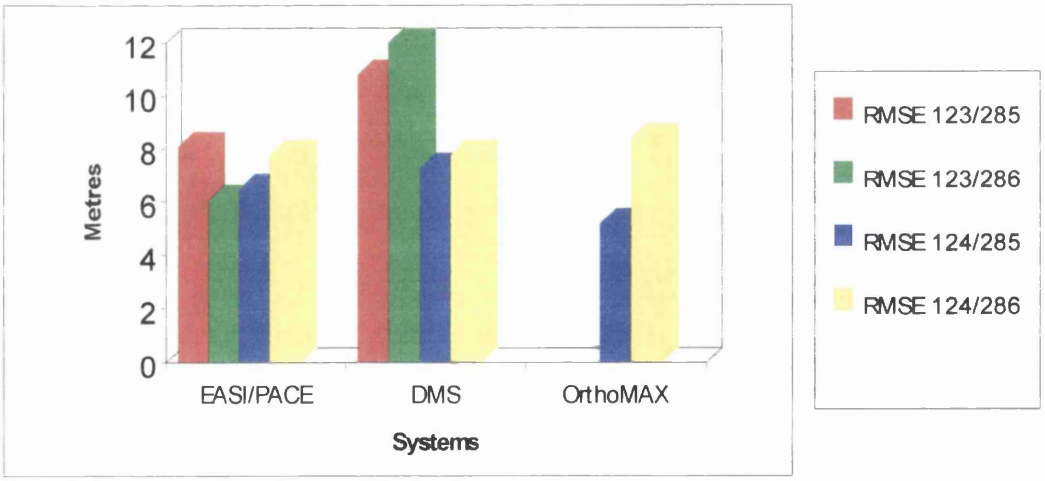

Figure 15.3 Graphical representation of the RMSE values in height in testing the DEMs produced from the other Level 1B stereo-pairs covering the Badia area by comparison with the height values given by the digitised contours as determined by the different systems.

15.3.3 Comparison of the Heights given by the Contours at 10m Interval Digitised from the 1:50,000 Scale Topographic Map with the Corresponding Values given by the Level 1A and 1B DEMs of the Reference Stereo-Pair for Scene 122/285

Another series of height accuracy tests of the DEM elevation data have been carried out using the contours with a 10m contour interval digitised from the 1:50,000 scale map and superimposed over the DEMs. The results in terms of RMSE values are given in Table 15.5. In this test, the best height accuracy obtained with the Level 1B DEM data was that produced by the EASI/PACE system followed by that of the Level 1A DEM produced by EASI/PACE and then by the results obtained from the DEMs produced by the DMS, OrthoMAX and FFI systems respectively in that order. Curiously, some of the results are not very different to those obtained with the contours from the 1:250,000 scale map. This suggests that there was little loss of accuracy in the process of producing the 1:250,000 scale map from the 1:50,000 scale map. However, with EASI/PACE, the results of the validation using the 10m contours are somewhat better than those achieved with the 50m contours - though certainly not five times better as the differences in scale and contour interval might suggest.

System	Format	Contour Interval	No. of Points	RMSE ΔH (m)
EASI/PACE	122/285 1A	10	257	±6.2
	122/285 1B	10	257	±4.9
DMS	122/285 1B	10	220	±8.1
OrthoMAX	122/285 1B	10	325	±8.9
FFI	122/285 1A	10	417	±9.9

Table 15.5 The accuracy of height in the DEMs produced by different systems by comparison of heights given by the digitised 10m contours from the reference map with the height values given by the Level 1A and 1B DEMs.

15.4 Accuracy Tests of Height in the DEMs Produced by the Different Systems Through Comparison with the GPS Profiles

The fourth series of tests of the height accuracy of the various DEM elevation data sets was carried out using the GPS profiles measured along the old main roads crossing the Badia area. The results of these tests of accuracy in height are summarised in Table 15.6. This is the most distinctive set of elevation tests carried out during the present

research, yet it must be said that the results are not too different to those obtained when checking the DEM data against the contours of the existing maps.

System	Scene/ Format	No. of Points	Mean (m)	Standard Deviation Δ H (m)
EASI/PACE	122/285, 123/285, 124/285	1,248	24.0m	±6.1
	122/285 1B	528	24.0m	±6.0
DMS	122/285, 123/285, 124/285	1,248	25.6 m	±9.3
	122/285 1B	528	15.6m	±9.0
OrthoMAX	122/285 1B	528	22.4m	±8.4
FFI	122/285 1A	366	25.9	±8.3

Table 15.6 Height accuracy in the DEMs produced by different systems using GPS profile data.

In general, in this series of tests, the best accuracy obtained in terms of the RMSE value was the ±6.0m obtained by the EASI/PACE system followed by the FFI, OrthoMAX and DMS systems which collectively gave almost the same results with RMSE values of between ± 8 and ± 9m.

15.5 General Remarks About the Results of Accuracy Tests of Height Values of DEM Data

Based on the various summaries and individual discussions given above, it is perhaps worthwhile to attempt an overall analysis of the height accuracy results in terms of the relationship between the various spot height accuracy values which have been determined in the author's tests of the DEMs produced by the SPOT stereo-pairs through image matching (stereocorrelation). Various results have been obtained by the different systems employing the different kinds of test which have been carried out to validate the DEM data. Since the quality of the ground control points and the reference data sets provided by the contours and GPS profiles is the same for all four systems, and the same stereo-pairs have been used, then the main factors responsible for the different results which have been obtained by the systems for the same tests would appear to be:

(i) the mathematical models employed in the system; and

(ii) the matching algorithm employed by each system.

With regard to the matching algorithms, while all the systems employ the area-based algorithm, presumably each system uses a slightly different approach and has its own individual implementation. An overall summary of the actual height accuracy results

obtained by each of the systems in terms of the RMSE values at the check points with the Level 1B stereo-pairs using the four different methods of validation are given in Table 15.7.

Tests Carried Out with Level 1B Stereo-Pairs Only

System	Scene No.	Type of Test	No. of Check Points Tested	RMSE Values ΔH (m)
EASI/PACE	122/285 1B	(1) DEM Values v. GCP Values	15, 25, 35	±3.3, ±3.6, ±3.7
	Other Scenes	-	10, 11, 8	±3.3, ±3.7, ±6.2
	122/285 1B	(2) Comparison with 50m Contours	719	±7.0
	Other Scenes	-	442, 403, 443, 410	±8.1, ±6.1, ±6.5, ±7.8
	122/285 1B	(3) Comparison with 10m Contours	257	±4.9
	122/285	(4) Comparison with GPS Profile Data	528	±6.0
	Other Scenes	-	1,248	±6.1
DMS	122/285 1B	(1) DEM Values v. GCP Values	15, 25, 35	±6.7, ±6.2, ±5.2
	Other Scenes	-	10, 18, 8	±6.6, ±5.8, ±7.0
	122/285 1B	(2) Comparison with 50m Contours	589	±9.9
	Other Scenes	-	325, 449, 279, 348	±10.8, ±12.0, ±7.3, ±7.8
	122/285 1B	(3) Comparison with 10m Contours	220	±8.1
	122/285 1B	(4) Comparison with GPS Profile Data	528	±9.0
	Other Scenes	-	1,248	±9.3
OrthoMAX	122/285 1B	(1) DEM Values v. GCP Values	25	±5.6
	122/285 1B	(2) Comparison with 50m Contours	712	±8.9
	Other Scenes	-	387,453	±5.2, ±8.4
	122/285 1B	(3) Comparison with 10m Contours	325	±8.9
	122/285 1B	(4) Comparison with GPS Profile Data	528	±8.4

Table 15.7 Summary of all the test results carried out with the DEM data from all the Level 1B stereo-pairs using the three systems.

Table 15.8 gives a further more generalised comparison based on the average RMSE values for height accuracy obtained by each of the systems using the four methods of validation.

Type of Test	Scene No.	Average RMSE Values of ΔH (m)		
		EASI/PACE	DMS	OrthoMAX
(1) DEM Values v. GCP Values	**122/285 1B**	±3.5	±6.0	±5.6
	Other Scenes	±4.4	±6.6	-
(2) Comparison with 50m Contours	**122/285 1B**	±7.0	±9.9	±8.9
	Other Scenes	±7.1	±9.5	±6.8
(3) Comparison with 10m Contours	**122/285 1B**	±4.9	±8.1	±8.9
(4) Comparison with GPS Elevation Data	**All Scenes**	±6.0	±9.1	±8.4

Table 15.8 Average RMSE values of height in DEMs at the check points with Level 1B stereo-pairs.

From the summary of the height accuracy results of the DEM elevation data given for the overall series of tests in Table 15.8, the results obtained by the EASI/PACE system at the individual independent check points in terms of the RMSE values using the Level 1B stereo-pair of the reference stereo-model for scene 122/285 was ±3.5m amounting to 0.3 pixel, which is really quite good. For this first method, the GCPs which have been used to check the elevation accuracy can be considered as very accurate spot heights since these points have been measured by GPS in static mode with an accuracy of less

than 1m. Of course, this test could only be carried out using a small number of points. For the other stereo-pairs, the average RMSE value obtained with EASI/PACE was ±4.4m which is also quite good, with quite a small difference between the two sets of results of less than one metre. This confirms the consistency achieved in these results. In case of the third test comparing the height data of the DEM with the values given by the digitized 10m contours using several hundred measured points, the accuracy of height in terms of the average RMSE value was ±4.9m which is almost as good. In this case, the good agreement appeared to be due to the inherent accuracy of the contours digitised from the 1:50,000 scale map. However, as noted previously, this was not the case with the results from the other two systems.

For the second test of comparison of the height data of the DEM with the 50m contours again using several hundred of measured points, the average height accuracy obtained in terms of the RMSE value for the Level 1B stereo-pair of the reference scene 122/285 using EASI/PACE was ±7.0m, while, for the other stereo-pairs, it was ±7.1m, which is almost the same. Of course, this test will be expected to give a rather poorer accuracy value than the previous tests, since one would expect it to be affected by the loss in accuracy involved in the compilation of the 1:250,000 scale map, including the generalisation of the basic 1:50,000 scale map. Other relevant factors could also be the accuracy of digitising the contours and the accuracy of the measurement of the corresponding points carried out by the author.

For the fourth test using the GPS profile data, the accuracy of the height values obtained by the DEMs in the stereomodel of reference scene 122/285 and over the other stereomodels using 1,248 measured GPS points was a standard deviation of ±6.0m. This result is reasonally good, but lies between the average RMSE values obtained in the comparisons with the two sets of digitized contours. However it had been thought when devising this test that the use of the GPS profile data would give a much better result than the comparison with the contours. But, on the evidence of this experience, the GPS profile points measured using the kinematic method do not afford an improved or better validation of the DEM elevation values.

In case of the DMS system, the average RMSE value in height obtained at the check points using the first method comparing the GCP elevation values with the DEM data extracted from the reference stereo-model 122/285 was ±6.0m, while a slightly lower average accuracy of ±6.6m was obtained with the other stereo-pairs. This is quite remarkable given the simple method used to obtain the DEM height data with DMS. Of course, as has been discussed above, the accuracy at a limited number of very accurate check points would be expected to be higher than those obtained using contour and profile data to validate the DEM elevation values.

In the second test using contours with 50m interval, the average height accuracy obtained in the reference stereo-model was ±9.9m while that obtained from the other stereo-pairs was ±9.5m. As one would expect using contour data instead of individually measured spot heights, this was a poorer result than that of the first method. In the third test, a better height accuracy of ±8.1m was obtained in the comparison of the 10m contours than the tests with the 50m contours. This is probably due to the better accuracy of the contours digitised from the 1:50,000 scale map, while, in the previous test, they have been digitised from the 1:250,000 scale map. But the difference is not large.

For the fourth test utilizing the data from the GPS profiles, the result obtained in terms of the standard deviation for all of the stereo-models was ±9.1m, which is slightly better than the results obtained from the second test and poorer than the accuracy obtained from the third test using the contours from the map. Again this was a rather disappointing result - since it had been hoped that the kinematic GPS data would prove to be a better reference set than the contours.

In case of the OrthoMAX system, height accuracy tests were carried out for the independent check points for the reference scene only. The height accuracy obtained in terms of the RMSE value was ±5.6m, which is good. For the second test using the 50m contour data, the height accuracy at the reference stereo-model was ±8.9m which is around 1m better that obtained by the DMS system for the same stereo-model. For the other two stereo-pairs, the average RMSE value in height improved and was equal to

±6.8m. In the third test with the 10m contours, the same height accuracy in terms of an RMSE value of ±8.9m was obtained as in the previous test - which is poorer than the accuracy obtained in DMS system using the same stereo-model. In the fourth test using the GPS profile data, only a slight improvement in the height accuracy was obtained in terms of a standard deviation of ±8.4m.

As a general conclusion, the overall comparison of the four systems showed that the EASI/PACE system gave consistently better results than the other two systems in the four types of validation test employed. This again gives an indication that the mathematical model and photogrammetric solution employed in the EASI/PACE system is somewhat better than those used in the other systems. At the upper limit, the matching algorithm which has been used is giving results of sub-pixel accuracy (0.3 to 0.5 pixel) at the individual spot heights measured by GPS. By comparison, the other two systems, OrthoMAX and DMS, gave similar results in terms of the elevation values provided by their DEMs. The OrthoMAX system gave a slightly better accuracy than DMS; this is hardly what was expected from a system which uses a 3-D solution as compared with the 2-D solution of DMS.

15.6 Overall Comparison of the Height Accuracy of DEMs Investigated and Reported By Different Researchers Using Different Systems Compared to the Height Accuracy of the DEMs of the Badia Test Area.

It is also possible to compare the height accuracy of the DEMs extracted from the SPOT Level 1A and 1B stereo-pairs over the Badia test field with the height accuracy of DEMs achieved by several investigators using different hardware and software systems. In general, it is quite noticeable how few tests have been carried out into the accuracy of elevation data extracted from SPOT stereo-pairs using digital images and automatic image matching techniques as has been done in the present series of tests.

15.6.1 Comparison with Results Obtained Using Analytical Plotters

Table 15.7 and Figure 15.4 summarize the best DEM accuracies obtained by different investigators as set out in Chapter 3: some of the less good results have been omitted from consideration. As can be seen, those included in the Table have mostly been carried out using analytical plotters with manual/visual observation and operator-controlled measurement of the DEM and usually a relatively small number (<200) of measured check points. However Anglerand et al (1992) and Heipke et al (1992) have both used larger samples - of 1,300 and 1,700 points respectively - having utilised image matching techniques in combination with their use of analytical plotters. All of these tests have utilized Level 1A stereo-pairs.

Area	Reported by	Hardware	Software	B/H	No. of Control Points	ΔH (m)	No. of Check Points	S.D ΔH (m)	RMSE ΔH (m)
South-West Cyprus	Gugan and Dowman (1988)	Kern DSR Analytical Plotter	UCL	0.82	10		108		±8.6
Aix-en-Provence	Theodossiou and Dowman (1990)	Kern DSR Analytical Plotter	UCL	0.84 0.91	10 15		185 177	±4.8 ±6.9	±5.7
South-West Sinai	Diefallah (1990)	Wild BC-2 Analytical Plotter	Wild BC-2 software	1.0	20		56		±9.4
Heidelberg **Priorat**	Heipke et al (1992)	Analytical Plotter	HIFI	0.4 0.6	9 9		834 1,300	±10.8 ±8.8	
Mount Fuji	Akiyama (1992)	Zeiss Planicomp Analytical Plotter	Modified BINGO	0.52 0.72 0.52 0.72	32				±5.5 ±5.8 ±9.6 ±6.9
Australia	Priebbenow and Clerici (1988)	Zeiss Planicomp C100 Analytical Plotter	HIFI	0.89	27				±5.4
Sydney	Anglerand et al (1992)	Wild BC2 Analytical Plotter	SATMAP	1.0			1,700		±5 to ±6 ±9.0
Australia **Men**	Trinder et al (1994)		UNSW UCL HAI ERDAS Joanneum				24,505 4,614 7,131 24,523 5,908	±7.4 ±15.1 ±5.2 ±8.9 ±12.1	
Terrey			UNSW UCL HAI ERDAS Joanneum				14,880 2,753 9,247 14,367 3,956	±20.3 ±19.5 ±14.8 ±30.0 ±14.0	
Badg/Lond **Regent**			UNSW UCL HAI ERDAS Joanneum				14,880 2,753 9247 14,367 3,956	±3.8 ±21.1 ±8.6 ±10.5 ±7.6	
			UNSW UCL HAI ERDAS Joanneum				15,612 2,969 15199 15,108 5,073	±2.4 ±2.3 ±5.4 ±4.6 ±4.4	

Table 15.7 The best accuracy results in validation tests of DEMs reported by several investigators employing different hardware and software using Level 1A stereo-pairs

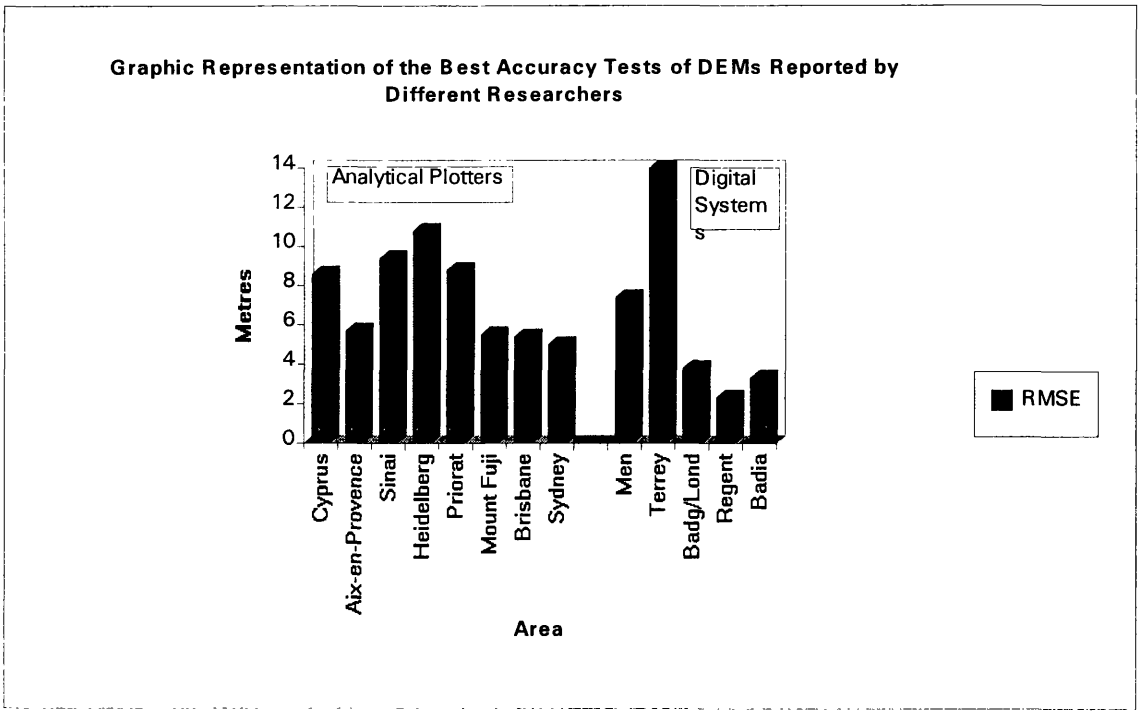

Figure 15.4 Graphic representation of the best results from tests of validation of DEMs reported by other researchers.

Before undertaking a detailed comparison of these results, it should be said that the accuracy of the spot heights obtained by manual/visual measurements carried out in a static mode on an analytical plotter would be expected to be very high - since an experienced professional operator has time to judge the height of the floating mark relative to the terrain surface and to make repetitive measurements of the elevation if required. However the negative side of this procedure is that normally only a comparatively small number of elevations can be measured using such a manual operation to generate the DEM, otherwise the mensuration procedure becomes uneconomic. This means that a large grid interval (or distance) will have to be used between the measured points if the whole stereo-model has to be covered or else the area to be covered will be restricted, say to a 1 x 1 km, 3 x 3 km or 10 x 10 km area, if a greater density of points is required. By contrast, automated stereo-correlation usually involves the measurement of the elevations of huge numbers (hundreds of thousands or millions) of points at high speed. Intrinsically this process might be expected to be less accurate - though this is a matter that needs to be tested and indeed this is being done within the present project.

Attempts have been made to speed up DEM data acquisition with analytical plotters using hardware-based correlators, e.g. as reviewed by Petrie (1990). Thus, for example in the late 1980s, a number of Kern DSR analytical plotters in European universities (Hannover, Stockholm, etc) were fitted with such a device (the VLL correlator). However, they appear to have been used exclusively to produce DEMs from aerial photography: no attempt was ever made to adapt or employ them to measure SPOT stereo-pairs. In this respect, the quasi-epipolar lines that are present in a SPOT stereo-pair - as distinct from the true epipolar lines that are present with aerial photographs - may have been an obstacle to such an application.

Another attempt to measure large numbers of elevation points from space imagery to form a DEM using an analytical plotter was made at the University of Glasgow (Petrie and El-Niweiri 1994). In this case, the terrain elevations were measured on the stereo-model formed from a pair of Metric Camera (MC) photographs of the Red Sea Hills area in Sudan. Instead of measuring individual points in a static mode, the measurements were made continuously by an operator along parallel profiles in a dynamic mode in a Kern DSR instrument using a distance-controlled profiling routine implemented in the control computer. The elevation values were recorded every 400m along each profile. A total of 182,000 elevation points were measured in this way along the 252 profiles required to cover the 110 x 180 km area of the MC stereo-model (El-Niweiri 1988). A deficiency of the method termed out to be the time required - over 40 hours were needed to measure the DEM. In addition to which, the accuracy of the DEM data achieved with 1,389 check points was poor with an overall mean standard deviation value of ±26.8m (Petrie et al 1998).

Coming next to the height accuracy results of the DEM generated from SPOT data reported by Gugan and Dowman (1988) in South West Cyprus, the RMSE in height was ±8.6m. The test area was restricted to a very small area having a 108 point gridded DEM which was then compared with the reference DEM produced from the contours of a 1:50,000 scale map. This accuracy is comparable with the accuracy obtained in the present research with the DMS and OrthoMAX systems in the accuracy tests carried out with 10 and 50m contours and the GPS profiles - while obviously the density of the data acquired using the latter two systems was very much greater.

For the height accuracy results reported by Theodossiou and Dowman (1990) in the Aix-en-Provence area in South France, several blocks of DEM points were measured manually in one of the Kern DSR analytical plotters at UCL from two SPOT stereo-pairs and the results were then compared against the corresponding reference DEMs produced from aerial photographs. The results from two blocks comprising 185 and 177 check points respectively were $\pm$4.8m and $\pm$6.9m in terms of the RMSE values in height. These figures are in the same general range as the results obtained during the present research, but obviously the tests were carried out over quite small areas and only represent a tiny part of the stereo-model. In this particular respect, the results are somewhat different to those obtained during the present research which represent the accuracy of the DEM data collected over a very wide area using automatic image matching procedures. However, the results obtained using the EASI/PACE system during the present research are still better than the UCL results using three different types of accuracy test (i) of the independent check points; (ii) comparison with 10m contours; and (iii) with the GPS profiles. In general, the height accuracies reported by Theodossiou and Dowman are quite good; this appears to be due to the careful manual measurement of individual spot points in the analytical plotters and the very small sample of points that have been measured and used in the DEM validation tests.

In the case of the height accuracy reported by Diefallah (1990) using a Wild BC-2 analytical plotter for his test carried out in South-East Sinai, the RMSE value was $\pm$9.4m which is somewhat higher than that achieved in the validation tests carried out in the present research. Again his comparison is restricted to a very limited number of check points which have been taken from the area's 1:50,000 scale maps. So the lower accuracy may well be related to the quality of the ground control points and the check points used to validate this very low density DEM.

In case of the accuracy test reported by Priebbenow and Clerici (1988) covering the Brisbane metropolian area in Australia, the RMSE value in elevation was $\pm$5.4m for a limited data set of 56 points measured in a Zeiss analytical plotter. Again this represents a very good accuracy and is quite close to the best accuracy figures obtained in the present research. However, the area which has been tested by Priebbenow and Clerici was limited to that covering a 1:25,000 scale map sheet. The elevations were measured

at a 100m interval and elevations at a 25m grid interval were then interpolated and compared with the corresponding data for the same area using controlled aerial photography with elevations interpolated at 25m. The high accuracy obtained seems to be related mainly to the good quality of the control points used in the solution and again to the method of measuring the elevation points manually carried out in a static mode by a professional photogrammetrist using the analytical plotter.

The height accuracy tests reported by Anglerand et al (1992) for another Australian test area using the SATMAP package mounted on a Wild analytical plotter produced RMSE values in height of ± 5.0m to ± 6.0m. These figures give approximately the same accuracy as the best figures obtained in the present research. In these tests, the DEM elevations were compared with the elevation data provided by maps at 1:4,000 scale. Another accuracy figure that was obtained was an RMSE of ± 9.0m which resulted from the comparison between 1,700 points manually observed in the DEM and 9,000 points produced by image matching which certainly has the large sample that is needed for the validation of the DEMs. The RMSE = ± 9.0m is rather less good than the better figures that have been produced for the series of tests carried out over the Badia area, but it certainly lies within the upper limit of the range of RMSE values achieved over the Badia test field.

For the accuracy test reported by Akiyama (1992) in Japan, two test sites, each 3 x 3km in area, were selected in mountainous and flat terrain respectively and measured using a Zeiss analytical plotter and modified BINGO software. The elevation values were measured manually and compared with the corresponding values given by aerial photography. The accuracy results in the flat terrain ranged between RMSE value of ± 5.5 to $\pm$ 5.8m, while the accuracy obtained in the mountainous terrain gave RMSE values ranging between ± 6.9 to $\pm$ 9.6m. This accuracy is quite good in the flat terrain and rather less good in the mountainous terrain, but again only a small number of points within a quite small area have been measured and used in the test.

In case of the accuracy results reported by Heipke et al (1992) in the Heidelberg (Germany) and Priorat (Spain) areas, the results in terms of RMSE values were ± 10.8

and ±8.8m for 834 and 1,300 points respectively. The heights produced by the DEMs were compared with check points having known elevation values. These results are again somewhat poorer than the accuracy obtained by the present research. This is due partly to the relatively poor base-to-height ratio of the two stereo-pairs, and may also be related to one of the stereo-models being covered partly by the cloud.

To summarize this comparison of the results of the DEM validation work conducted over the Badia test area with those achieved elsewhere using SPOT stereo-pairs in an analytical plotter, the following points can be made:-

(i) The use of manual/visual measurements of induvidual spot heights made in an analytical plotter results in a quite restricted number of points forming the DEM. While the sample is small and the distance between the sampled points is large, the accuracy of the individual elevation values measured in this way is high. Notwithstanding these characteristics, the DEM data collected en-mass (3,000 x 3,000 points = 9 million points) in the present series of tests using the automatic image matching techniques available in the new commercial software packages give comparably high accuracies, while, at the same time, they provide a much denser DEM which better represents the terrain and will certainly produce more accurate contouring.

(ii) In the only two tests conducted on analytical plotters using software-based image matching routines - those of Anglerand et al (1992) and Heipke et al (1992) - RMSE values of ±9m were obtained. In very broad terms, these figures are rather less good than the best results (±4 to ±6m) achieved with the systems tested by the author, though they do lie just within the upper range of values achieved during the author's tests.

15.6.2 Comparison with Results Obtained Using Digital Photogrammetric Systems

In the previous section, a comparison with the results obtained using analytical plotters has been made and the results analysed, while in this section, the comparison will be conducted with the results obtained using digital photogrammetric systems. When considering purely digital photogrammetric systems that employ automatic image matching techniques for DEM production from SPOT stereo-pairs, it must be said that,

up till now, most of the published figures for the accuracy of the DEM data have not been too favourable. As pointed out in the review conducted in Chapter 3, in the tests carried out by Brockelbank and Tam (1991) using the LANDSCAN software package, the validation of the DEMs for the DMN and Red Deer stereo-models resulted in RMSE values of ±16.8m and ±11.8m respectively (see Section 3.6.1). For the two tests of the DEM data produced from SPOT stereo-pairs by the STX Corporation, in the tests carried out by Sasowsky et al (1992) and by Bolstad and Stowe (1994), the RMSE figures were no better (see Sections 3.6.2 and 3.6.3). Finally, for the test carried out by Giles and Franklin (1996) using DEM data generated by the HI-VIEW package, the RMSE in elevation of the tested points was ± 21.6m (see Section 3.6.4). It goes virtually without saying that these previously published results achieved using commercially available software employing image matching techniques are not in the same class as the results achieved with the present tests. Whether this is due to the availability of better control data and validation data or whether the systems tested by the author are simply better in terms of their photogrammetric solutions is an open question. In fact, it is one that is difficult to answer since the previous investigators do not appear to have had access to information on the modelling and algorithms that have been employed in the systems used in these tests, nor has this information been published elsewhere for the present author to comment upon.

15.6.2.1 Comparison with the Results of Trinder et al (1994)

The only comparable series of validation tests to those conducted during the present research are those reported by Trinder et al (1994) in Australia. Five systems have been tested using a single Level 1A stereo-pair. Three of these are non-commercial packages (i.e. research software) developed by various universities (UCL, UNSW and the Joanneum Centre at the University of Graz), while the other two are commercially available systems from ERDAS and HAI. The comparisons that will be made in the remaining part of this Section will concentrate on these latter two systems comparing them with the commercially available systems tested by the author.

Some aspects of these tests conducted by Trinder et al are very similar to those that have been carried out in the present research, while other aspects are rather different. With

regard to the ground control points used in the tests reported by Trinder et al, these have been taken from maps at 1:4,000 and 1:25,000 scales while the check points used for the validation of the DEMs' elevation values have been derived from the digitised 1m and 2m contours available on six complete 1:4,000 scale orthophotomaps covering perhaps 25 to 30 sq km of the 3,600 sq km of a complete SPOT stereo-model. By contrast, the ground control points used in the research carried out by the present author have been measured by GPS, while the check points used in the different types of accuracy test used to validate the Badia DEMs came both from GPS profile data measured in kinematic mode and from the elevation values of contours at 10m and 50m intervals digitized from small-scale (1:50,000 and 1:250,000) maps. Thus Trinder's control point data was, if anything, slightly better in terms of its accuracy, while the data available for his DEM validation was of considerably better quality, since it only covered quite small areas of a single SPOT stereo-pair, while the Badia tests were conducted over the wide area covered by five stereo-pairs using rather less accurate reference data.

Other differences are related to the type of test area used as well as its extent. In the case of Trinder's tests, four small areas, each of a different terrain type have been selected, each with different slopes and different vegetation cover, while the tests that have been carried out during the present research comprise a very large area of stony basaltic desert covered by five stereo-pairs which has no vegetation cover and does not have areas with markedly different slope steepness. Yet another difference between the two methods is that, in the method used for the validation of the DEMs reported by Trinder, thousands of check points were used. These were derived from a high-density reference DEM produced from contours where the heights were interpolated at the same grid interval as the DEM generated from the SPOT stereo-pair. In the case of the Badia tests, the check points were restricted to just over one thousand points measured by GPS in kinematic mode along profiles together with another several hundred points measured directly along the photogrammetrically measured contours produced with a 10m interval together with their reduced-scale version at a 50m interval.

As noted above, the results reported by Trinder constitute the most comprehensive test in terms of the number of check points used to validate the accuracy of DEMs extracted from SPOT stereo-pairs. Comparing his results with those achieved over the Badia test

field, ERDAS is the only system that is common to the two sets of tests and can be compared. However, even here, it is not certain that the two packages are the same, since ERDAS used a different package prior to licensing OrthoMAX from Vision International. The ERDAS software has been tested in four areas having different slope steepness. The best results achieved by Trinder gave a standard deviation of $\pm$4.6m in height using 15,108 check points in the Regent area which is a suburban and residential area with slopes less than 5%. In the Men area of undulating to steep terrain of 10 to 15% with little vegetation cover, the accuracy obtained was $\pm$8.9m. While in the Badg/Lond area with slopes up to 15% with sparse trees, the accuracy obtained in terms of standard deviation was $\pm$10.5m. Finally in the Terry area of very steep slopes of 10% to 50% and heavy vegetation cover, the accuracy obtained was $\pm$30m. In summary, it can be said that the accuracy obtained by Trinder and his colleagues using ERDAS over four different test areas range in accuracy between $\pm$4.6m to $\pm$30m in terms of standard deviations. Most of these results are somewhat poorer than the results obtained by the present research except for the Regent area which almost flat. By comparison, the OrthoMAX system gave a standard deviation = $\pm$8.4m in height over the Badia area using 528 check points using the GPS profile data while, at the independent check points, the accuracy obtained was an RMSE = $\pm$5.2m. However, it must also be remembered that Trinder's test field in the Sydney area had many trees and some areas of steep slope, whereas the Badia test field is virtually free of vegetation and has few steep slopes of the type encountered by Trinder et al.

In the case of the EASI/PACE system, the accuracy obtained over the Badia area gave a standard devation of $\pm$6.0m using 1,248 check points from the GPS profile data. Most of the other tests reported by Trinder carried out using the four other systems showed a somewhat poorer accuracy than that obtained during the present research except for the Regent area which again gave slightly better results than those obtained in the present research. However it would be true to say that some of the very best results achieved with Trinder's tests are those produced by the HAI software. As shown in Table 15.7, this produced standard deviations in the range ±5.2m (Men); ±5.4m (Regent); ±8.6m (Badg/Lond) to ±14.6m (Terrey). Leaving aside the last area (which is steep and wooded), these results lie in the same range as those achieved by the EASI/PACE,

OrthoMAX and DMS systems tested over the Badia area. It was a great pity that the present author did not have access to the SOCET SET software that has been developed from the HAI package. For all the superior quality of the data available to Trinder et al for validation purposes, this does not appear to have played a significient role in the quality of the final results. In other words, the Badia results do not appear to have been burdened by having slightly poorer reference data for validation purposes.

Of course, some other very good results have been achieved by the university-developed research software also tested by Trinder et al - as shown in Table 15.7. However, so far, these have not been packaged and made available commercially and their use appears to be restricted to the university research groups who have developed these packages. It is difficult therefore to judge how robust this software would be if it was released to be used by the various communities who are interested in generating DEMs from SPOT stereo-pairs.

In general, the accuracy tests reported by Trinder et al (1994) appear to have been affected by (i) the quite different mathematical models employed in the systems used in their tests; (ii) the very different image matching algorithms employed by the tested systems; and (iii) the varied nature of the terrain used as the test area, especially the presence of vegetation and steep slopes. While the differences in the accuracy in the present author's research appear to be related mainly to the mathematical models employed by the systems, since basically the four systems employ the same image matching algorithm. Also the Badia test field has not been burdened either with dense vegetation cover or with steep slopes.

15.7 Planimetric Accuracy Results of the Ortho-images of the Level 1A and 1B Stereo-Models of the Reference Scene 122/285 of the Badia Test Field

A test of the planimetric accuracy of the final ortho-images has been carried out for the reference stereo-model using both the Level 1A and 1B stereo-pairs with the different systems and using a simple linear conformal transformation for this comparison of the image positions of the GCPs measured on the ortho-images with the high accuracy

coordinates obtained in the field using GPS. A summary of the results is given in Table 15.8.

System	SPOT Format	Pixel Size	No. of Check points	RMSE in Pixels			RMSE in Metres		
				Δx	Δ y	ΔPl	Δ X	Δ Y	ΔPl
EASI/PACE	122/285 1A	20	40	±0.46	±0.48	±0.67	±9.1	±9.7	±13.3
	122/285 1B	20	43	±0.44	±0.44	±0.60	±8.7	±8.8	±12.3
OrthoMAX	122/285 1A	20	40	±0.52	±0.57	±0.77	±10.5	±11.4	±15.5
	122/285 1B	20	43	±0.67	±0.58	±0.89	±13.4	±11.7	±17.7
DMS	122/285 1B	20	38	±060	±0.53	±0.80	±12.1	±10.6	±16.0
FFI	122/285 1A	10	27	±0.76	±0.51	±0.91	±7.6	±5.0	±9.1

Table 15. 8 Accuracy tests of the ortho-images produced from the Level 1A and 1B stereomodels for the reference scene122/285 by the various systems.

As will be seen from this table, a 20m pixel has been used to produce orthoimages with the EASI/PACE OrthoMAX and DMS systems; whereas a 10m pixel has been used with the FFI system.

(i) The accuracy obtained at the 40 check points in terms of the RMSE value gave ΔPl = ±13.3m for the ortho-image produced by the EASI/PACE system using the Level 1A stereo-pair for scene 122/285. In the case of the ortho-image produced by the Level 1B stereo-pair with the EASI/PACE system, again employing a linear conformal transformation and 43 check points, gave an RMSE of ΔPl = ±12.3m. As can be seen from Table 15.8, the RMSE values in Δx and Δy are less than half-a-pixel with both Levels of imagery.

(ii) In the case of the OrthoMAX system, the accuracy of the ortho-image produced from the Level 1A stereo-pair for scene 122/285 using 40 check points and a linear conformal transformation gave an RMSE of ΔPl = ±15.5m, while the accuracy of the Level 1B orthoimage using 43 check points gave an RMSE of ΔPl = ±17.7m.

(iii) For the DMS system, the accuracy of the ortho-image produced from the Level 1B stereo-pair for scene 122/285 using 38 check points and employing the linear conformal transformation gave an RMSE of ΔPl = ±16.0m.

(iv) For the accuracy test of the ortho-image of 10m pixel size produced by the FFI system from the Level 1A stereo-pair of scene 122/285, 27 ground control points have been measured. The accuracy obtained using the linear conformal transformation was an RMSE values of ΔPl = ± 9.1m.

In general, two systems - EASI/PACE and FFI - produced ortho-images that satisfy the accuracy requirements of maps at 1:50,000 scale, while the other two systems satisfy the accuracy requirements of topographic maps at scales slightly smaller than 1:50,000. However, it could well be that the better geometric accuracy of the ortho-images produced by EASI/PACE system was helped by the better accuracy of its DEM which was more accurate than the DEMs generated by the other systems. In case of the FFI system, the geometric accuracy of the ortho-image appears to have been affected mainly by the DEM being produced at a 10m grid interval in accordance with which the ortho-image has also been produced using a 10m pixel size. But, in general terms, the planimetric accuracy of all the orthoimages can be viewed as being satisfactory for mapping purposes at scales of 1:50,000 and smaller.

15.8 Conclusion

In this chapter, an overview of the accuracy tests concerned with the validation of the DEMs extracted from the SPOT stereo-pairs covering the Badia area using different systems and using different types of reference material has been presented and discussed. In general, the validation of the DEMs carried out in the present research can be considered (along with that of Trinder et al) to be the most extensive series of tests carried out so far and covering by far the largest test area. Four different types of accuracy test have been carried out to validate the DEMs. From the results of these four different tests, the EASI/PACE system shows a better accuracy and consistency in terms of the resulting elevation values than the other systems, followed at not too great a distance by the OrthoMAX system and then the DMS system. This helps to confirm the finding put forward in the previous chapter that the mathematical model employed in the EASI/PACE system appears to be somewhat better than these used in the other systems in terms of the resulting DEM elevation accuracy. In addition to that, and in spite of the fact that all of the systems are using basically the same matching algorithm, it does seem that the matching algorithm employed in the EASI/PACE system has also worked extremely reliably and well. In terms of the accuracies being achieved with the DEM from the different Levels of SPOT imagery, it is clear that the results obtained from the Level 1B stereo-pairs are slightly better than the results obtained from the single Level 1A stereo-pair that was tested.

In many ways, this represents a considerable step forward since Level 1B stereo-pairs have never previously been considered as being suitable for the extraction of DEMs and the generation of ortho-images. The newly developed software packages that have just become available with commercial digital photogrammetric systems now offer the chance for a much wider group of users - especially those working in the geosciences in remote areas - to make use of SPOT stereo-pairs, whereas previously they could not contemplate doing so. The author feels that he can claim to have contributed substantially to this development via the testing that he has carried out during his research project which resulted in many modifications being made to all of these packages, which simply were not operational when his testing started.

In the case of the height accuracy of the DEMs reported by other researchers, most of the accuracy tests have been carried out using analytical plotters which are not available to potential users outside the main mapping community. The main characteristic of this method is that, in practical terms, it is restricted to producing the DEM of a quite small area with a high density of measured points of a comparatively high elevation accuracy. It is also affected by the time that has to be spent in measuring the elevation points in the stereo-model manually and visually which limits the number of points that can be extracted. However, the DEM accuracy that can be expected from this method is very high due to the manual/visual measurement of the elevation points.

In case of the DEMs produced from the new digital photogrammetric systems using automated image matching techniques, very large numbers of elevation points can now be extracted from the SPOT stereo-pairs over very large and inaccessible areas. In spite of certain limitations in accuracy, this data might well satisfy the needs of many users. However, the accuracy that can be achieved using this automated method might be expected to be lower than the first method of measuring a limited number of points manually. But the results obtained by the validation process during the author's tests have shown that the accuracy of the elevation points obtained using the current image matching software can be in the same order of accuracy as that achieved using an analytical plotter. Of course, this may not always be the case, but certainly in suitable terrain such as the Badia area without vegetation cover and lacking large areas of water, the image matching appears to work well and the accuracy of the elevation points that

can be obtained is as high as that available from analytical plotters. By contrast, in very difficult terrain with vegetation cover, the image matching will not work so well and the final result may be expected to be poorer. Of course, other factors such as the base-to-height ratio of the stereo-pair may also play a role in the final accuracy of the DEM. From the experience gained from the series of tests carried out in the present research, it was found that, once the many shortcomings or defects in the original software had been removed, the quality of the ground control points and the mathematical models are the main factors affecting the final accuracy. All of the matching algorithms that have been developed seem to work well in the open terrain that suits their use.

However, it is important to note that, although these new developments will open the door to the use of SPOT stereo-pairs by a new group of users, there is still a need for them to have quite a good basic knowlege about photogrammetry and what is possible and what is not possible using these new systems - otherwise all that will happen is a repetition of the poor results that were produced from the first generation of these digital systems (as discussed in Section 15.6.2) that has caused considerable disillusion among potential users. Furthermore, the need to acquire an adequate number of high quality GCPs placed in suitable locations for orientation purposes is a matter that needs to be emphasized to potential users.

CHAPTER 16 : CONCLUSIONS AND RECOMMENDATIONS

16.1 Introduction

As indicated in the introduction to this dissertation (i.e. in Chapter 1), there is an increasing demand in developing countries for topographic maps at the standard scales of 1:50,000, 1:100,000 and 1:200,000 used for national coverage. For more developed countries that already have complete coverage, there is still the need to update their maps at these scales. To help to satisfy both of these requirements and to increase the rate of mapping and map revision at medium and small scales, images from the SPOT series of satellites have been used by a few national mapping organisations for these purposes. Almost exclusively, these organisations have used analytical plotters and hard-copy Level 1A images for the purpose, utilizing the classical methods of stereo-plotting of the planimetric detail and contours carried out by an operator. Although the capability of handling SPOT stereo-pairs has been developed for the new digital photogrammetric systems, till now, there has been no application of these systems for this purpose by national mapping organisations. These new developments with digital photogrammetric systems feature highly automated methods based on the use of image matching methods for the extraction of DEMs and ortho-images from SPOT stereo-pairs. These are now being offered by several well known commercial suppliers of remote sensing image processing systems in competition with similar products from the well established mainstream photogrammetric system suppliers.

However, with exception of those reported by Trinder et al (1994), the few published results achieved with older digital systems have been poor, especially in terms of their height accuracy. Thus there is a need for further tests to calibrate some of these new commercial systems both in terms of the overall geometric accuracy that they can achieve and the validation of the DEMs and ortho-images generated by them for mapping purposes. An extensive programme of such tests has been carried out during this research project using the two major types of SPOT image - the Level 1A and 1B products - that are offered by SPOT Image. Quite apart from the possibilities that the new highly automated digital systems offer to the main national mapping agencies, there is potentially a large market for such systems among the geoscience, geophysical and

geoexploration communities. They are concerned either with scientific work (e.g. geological research and mapping) or with the location of mineral or oil and gas deposits that can be exploited commercially. Much of this work takes place in remote and sparsely populated areas which are either unmapped or poorly mapped or else, access to the existing maps of these areas is restricted for security reasons. For this community - which is well used to utilizing remotely sensed satellite data in its work - the advent of digital photogrammetric systems capable of producing DEMs and ortho-images from SPOT data using automated methods is a major attraction. Especially this is the case when the resulting data are also in a form that can be easily incorporated into a geographic information system (GIS) or a geological or geophysical data processing package.

16.2 Research Summary

In this research project, six main objectives have been set out in the introduction (Chapter 1). These comprise the following:

1. Establishing a test area capable of being recognised as an international test field of the highest quality suitable for geometric accuracy testing and the validation of DEMs and ortho-images generated from satellite imagery of all types.
2. Calibration of the software packages from each of the main remote sensing system suppliers with a particular emphasis on the use of SPOT Level 1B stereo-pairs.
3. Carrying out geometric accuracy tests of the planimetry and heights in stereo-models after the absolute orientation of the SPOT stereo-pairs, based on different mathematical models and using different software packages and different numbers of control points and check points.
4. The execution of experimental tests to validate the DEMs and ortho-images generated from SPOT stereo-pairs by the various systems by comparison with the reference data sets given by aerial photogrammetry and GPS profiles.
5. The production of a digital terrain model and ortho-image mosaic for the whole of the large area covered by the Badia Project. This is intended to form part of the topographic database for a GIS covering the Project area. The DEMs generated would also be made available to other researchers in some British universities and

other researchers in Jordanian Universities who are studying the geology, geomorphology, soils and hydrology of the Badia area. In this respect, it was also hoped to carry out a terrain analysis of the area in collaboration with a geomorphologist from the University of Durham.

6. The results of the research work would also provide important information as to the possibilities of undertaking medium and small-scale topographic mapping and map revision in Jordan from satellite imagery.

16.3 Overall Conclusions and Recommendations

The detailed investigations carried out in this research project have all been documented, discussed and analyzed in the previous chapters and there is no need to repeat these in this final chapter. However it seems pertinent to make some concluding remarks on these investigations giving an overview that attempts to summarize the results from the large number of geometric accuracy tests and the validation of the DEMs and orthoimages that have been carried out during the efforts to calibrate the systems employed in this research project. As will be seen, most of the stated objectives of this research project have been achieved successfully; though some objectives could not be achieved due mainly to the series of flaws that were found to be present in the systems employed in this research work. A detailed discussion as to whether each of the six research objectives stated above was reached will be given in the six sections (16.3.1 to 16.3.6) that follow together the recommendations that can be made as a result of the author's research project.

16.3.1 Badia Test Field

As noted in Chapter 1, the first main objective was to establish a very accurate test field in the Badia area that was capable of properly testing and calibrating the systems being used to establish the geometric accuracy of SPOT stereo-pairs and for the validation of the DEM data and ortho-images generated from these pairs. In the author's opinion, such a test field has been successfully established. This can be seen and evaluated both from the results given by the surveyors and geodesists who undertook the work in collaboration with the author and through the extensive series of accuracy tests which

have been carried out using the SPOT stereo-images. At no time during the author's experimental work has there been any sign (e.g. in the form of gross errors or systematic error patterns) that there were any errors or shortcomings in the ground control point locations or coordinate values. This is also reflected in the quality of the final results achieved both in the geometric accuracy tests and in the validation of the DEMs and orthoimages obtained using different systems.

This test field is the one of the few test fields established anywhere in the world for the specific purpose of testing satellite imagery over a large area of terrain. Furthermore, it is also the only test field of its type that has been established in the Middle East and, in this sense, this area can be considered as an international test field. In spite of the high cost of establishing this test field, the information and the advantages that can be gained from its use can be considered to be very high at both the international and the local levels. At the international level, the test area has already been listed as a Pathfinder site by NASA due to the specific type of terrain and the wide area that it covers. It should also satisfy the needs and the recommendations of the CEOS Working Group on Calibration and Validation (WGCV) which is trying to establish a series of controlled test sites in different parts of the world. Each of these sites should have a network of very accurate control points required for the calibration of different systems, together with data sets suitable for the validation of the terrain height data contained in the DEMs produced from different types of imagery and for the testing of the different algorithms and matching techniques used to produce DEM data. At the local level, the results which have been obtained in the present research have encouraged the RJGC to look into the possibilities of undertaking the task of map revision using satellite mapping techniques - which is now a matter of great current interest (General Director of RJGC - personal communication).

At the moment, the main shortcoming of the Badia test field is that it is not completely covered by digitised map data at 1:50,000 scale with 10m contours. This limited the area for which the DEM data could be validated and caused the author to use the data from the 1:250,000 scale map series with its 50m contour interval for the validation of the remaining data. However this matter is currently being addressed and recently the

digitizing and verification of several more 1:50,000 scale sheets has been completed. Before too long, the whole of the test field will be covered with this type of data.

Another slightly disappointing outcome from the author's tests has been the fact that the elevation profile data produced through the use of real-time kinematic (RTK) GPS techniques appears to be no better in terms of its use as a reference data set than the digitized 10m contours produced photogrammetrically from aerial photography when used to validate the DEM data generated from the SPOT stereo-pairs. Given the accuracy figures that have appeared in surveying publications, it was expected that the GPS profiles would be of a superior quality. However, a somewhat similar experience has just been reported from a newly established test field in Australia so this is a matter which needs to be investigated further. The author plans to do so in collaboration with the surveying and geodesy staff of the RJGC on his return to Jordan.

The longer term advantages of the Badia test field are that it can be used as a test site for other pushbroom scanners employing CCD linear array sensors. In particular, images from the Indian IRS-1C and 1-D satellites (which with their cross-track coverage are in many ways similar to SPOT, but have a higher resolution) have now come onto the international market and certain system suppliers (e.g. PCI and LH Systems) have now produced software that will allow DEM and ortho-image data to be extracted from their stereo-imagery. This software needs to be tested, especially now that new receiving stations are being established in Greece and Dubai that will ensure IRS coverage of the Middle East. When IRS stereo-coverage has been acquired for the Badia Project area, it is hoped to carry out a similar series of tests over the test site.

The Japanese JERS OPS is another satellite having along-track stereo-coverage that needs to be tested and indeed coverage of the Badia area has recently been completed for this satellite and is now available for testing. Needless to say, the imagery that will be generated by the forthcoming high resolution satellites such as IKONOS-1 and QuickBird are other obvious candidates for testing. Moreover, the test field is of a quality that can be used successfully for the geometric accuracy testing and validation of DEM produced from satellite radar interferometry. Indeed this kind of work has been suggested previously to the author by Professor Petrie and it is hoped carry it out during

the new Shuttle Radar Topography Mission (SRTM) expected next year. A proposal to carry out this kind of work is currently under discussion with JPL and the appropriate software is being produced by ERDAS and PCI. Once again, the Badia test field would be an extremely suitable site for the calibration of these systems and it can be strongly recommended to fulfil this role.

16.3.2 Calibration of the Systems Using SPOT Level 1A and 1B Stereo Models

In contrast to most of the accuracy tests reported by other researchers which have been carried out using Level 1A SPOT images, a unique aspect of this research has been the availability of a block of five SPOT Pan Level 1B stereo-pairs with a 10-m pixel size covering the whole of the Badia Project area. In addition to which, a single Level 1A stereo-pair for the reference scene 122/285 was also purchased for comparative purposes. The individual images comprising each stereo-pair had been taken with only a small time gap (one to three months) between them, so there were no difficulties arising from changes in the appearance of the vegetation and hydrology in the area, which made them ideal for test purposes. Furthermore, all of these SPOT stereo-pairs possess an excellent base-to-height ratio (0.86 to 0.98). With these excellent stereo-images and the very good quality of the ground control points that have been established in this very accurate test field, the necessary conditions have been created for the calibration of the various systems that have been tested. In fact, the author intended to test several other systems that have been placed on the market, but some limitations have occurred partly due to the fundamental flaws that showed up in two of the systems which have been tested, while others were not available for various other reasons.

In fact, a total of six systems have actually been tested during this research using the SPOT Level 1B imagery. At first, the results of the initial tests of all these systems were disappointing. In the case of the EASI/PACE system, it was found that this system did not accept Level 1B stereo-pairs in spite of the fact that PCI advertised and publicised the fact that the system would accept Level 1B imagery. All of this only came to light as a result of the tests carried out over the Badia test field by the author. As a result, extensive modifications to the system have been carried out by the PCI company in collaboration with the present author. In case of the DMS system, while it did accept the

SPOT Level 1B stereo-pairs, initially the system did not work properly as shown by the tests carried out by the author. So once again, collaboration with the system supplier was necessary and resulted in extensive modifications of the system by adding new programs. Indeed the author was the first user who has successfully produced a full DEM from a SPOT stereo-pair using the DMS system. In the case of the OrthoMAX system, it would only accept SPOT Level 1B imagery in its old format only, and was not capable of dealing with the new format of Level 1B imagery. Other problems - most notably the improbable height values given by the system's absolute orientation - have been found in the system and both ERDAS and Vision International have been informed of these flaws in the system. Apparently this system has recently (in April 1998) been modified as a result of the author's findings but this was too late for the present author to carry out the tests of the stereo-models with the new SPOT Level 1B format.

Other systems, e.g. TNT-mips from MicroImages and the VirtuoZo system, have also been tested. In the case of TNT-mips, this system was made available to the present author by the European agent, Nigel Press Associates. Extensive tests have been carried out with this system without getting any worthwhile results. The author has informed the supplier directly that the system not coping with Level 1B stereo-pairs. Now, under pressure from Nigel Press Associates, MicroImages are now trying to fix the system. The VirtuoZo system was made available to the present author by Survey Development Services (SDS) who are the European agents for the system. The results of the tests showed that the system was not operational even during the initial tests carried out using the Level 1A stereo-pairs. The author has been informed by the agents that the faults that have been uncovered in this system have now been fixed, but again this development has come too late to be able to test and calibrate the system. In the case of the FFI system, this only copes with Level 1A stereo imagery. However, yet again, the series of tests that have been carried out with this system gave results with both the Badia and Norwegian data that revealed fundamental problems in the system. As a result, new algorithms have been adopted for use in the system.

From this discussion mentioned above, the author feels that can claim to have contributed very substantially to the calibration and further development of digital photogrammetric systems that can handle SPOT stereo-pairs through the programme of

testing that he has carried out during his research project. Indeed his work has resulted in many modifications - often of a fundamental nature - being made to these packages. Also, in spite of the considerable effort, pain, cost and time caused by this difficult and time-consuming calibration work, the author feels that the results obtained in this particular aspect of his research project have been very successful. Furthermore he has been able to show that good results can be obtained by the systems using Level 1B stereo-pairs after the modifications brought about through the author's programme of experimental testing using this type of imagery. As pointed out above, this will give the geocience, geophysical and geoexploration communities the capability to deal with Level 1B imagery (which is in widespread use in this sector) and to produce DEMs and ortho-images from it.

Needless to say, an obvious recommendation that can be made on the basis of the author's experience is that the calibration of new systems designed to handle satellite stereo-imagery for mapping applications should be carried out by an independent organisation over a first-class test field such as that covering the Badia Project area. On the basis of the author's experience, the system suppliers and software houses working in this particular area have simply not been rigorous or thorough enough in their testing and validation procedures prior to releasing their software for sale to the user communities.

16.3.3 Gemetric Accuracy Test Results of Planimetry and Height of Level 1A and 1B SPOT Stereo-Pairs of the Badia Test Area Using Different Systems.

In the present research, the geometric accuracy tests that have been carried out on SPOT Level 1A and 1B stereo-pairs and the results obtained by each system have been reported and discussed in the individual relevant Chapters (9, 11, 12, and 13). Moreover, the results of the extensive series of geometric accuracy tests obtained by the systems have been analyzed and compared with one another and with the previously reported geometric accuracy tests in Chapter 14. From this extensive experimental work, some general conclusions can be reached.

In broad terms, based on the results of series of tests carried out by the author, the planimetric accuracy obtained by the four systems that were fully tested can meet the planimetric accuracy requirements of topographic maps at the scale 1:50,000 and sometimes larger. In the case of the corresponding height accuracy requirements, the results obtained would correspond to the minimum contour line interval required for 1:50,000 scale maps in some circumstances, but more often they are more comparable with the contour intervals required for smaller (e.g. 1:100,000 or 1:200,000) scale maps. However, besides these accuracy issues that have been addressed during this project, whether the SPOT imagery will actually be used by national mapping agencies for 1:50,000 scale mapping will depend to a considerable extent on the interpretation quality of the imagery since this defines the various types of feature that can actually be resolved and identified and therefore the content that can be extracted from SPOT stereo-pairs. This is controlled by the ground resolution of the SPOT imagery which is a considerably larger figure (?15 to 18m) than the ground pixel size of 10m (Petrie and Liwa 1995).

One of the most interesting results that has come out from the extensive series of accuracy tests is that the results of geometric accuracy achieved with the Level 1B stereo-pairs are comparable to those obtained from Level 1A stereo-pairs; indeed they are even slightly better, especially in heights. Furthermore the accuracy results obtained from the Level 1B stereo-pairs can be considered to be among the best results obtained so far by any researcher and are in sharp contrast to those previously reported by other researchers using Level 1B imagery. Previously only Level 1A stereo-pairs have been used for topographic mapping purposes and are those preferred by the photogrammetric community due to the poor results obtained and reported previously from Level 1B tests. Now based on the excellent geometric accuracy results obtained by the author over the Badia area, one can say that Level 1B can be considered, indeed recommended, for the same task.

Indeed, going on with this discussion regarding the actual or potential use of Level 1B stereo-pairs, very few results had been published regarding the accuracy that can be achieved using this format, in spite of the fact that this type of imagery is very popular and widespread use among the geoscience and geophysical communities. At the same

time, the reported results from the few tests of geometric accuracy using Level 1B imagery was very poor. This appears to have been due to the early attempts either to use the mathematical models which had been originally developed for use with Level 1A stereo-pairs or to modify these systems in an approximate manner or a non-rigorous way to cope with Level 1B imagery. However now that better modelling has been achieved with the current systems, excellent results have been achieved by the author with the EASI/PACE and OrthoMAX systems due partly to the high quality of the ground control points and partly to the modified mathematical models employed by the systems. Concerning the results of the accuracy tests obtained by the systems employed in the present research, one can also say that, the importance of the mathematical model employed by each individual system is very clear and appears to be one of the main factors responsible for the different results achieved with the accuracy tests. This proves that the SPOT modules of the new generation of digital photogrammetric systems can give excellent results in terms of geometric accuracy and are quite comparable with the accuracies which can be obtained using analytical plotters, especially if high quality ground control points are used. Certainly the solutions adopted by these systems produce results which will be acceptable to a wide spectrum of users concerned with topographic base mapping at small scales within a fully digital photogrammetric environment.

In the case of the tests of Level 1A SPOT stereo-pairs reported by other researchers, most of the reported results carried out in analytical plotters using SPOT data in hard-copy form. Now however, comparable results are starting to be obtained from digital photogrammetric systems. In this respect, the mathematical model developed by Toutin and implemented in a number of different systems (EASI/PACE, CARTOSPOT, DVP, etc) has had a positive effect in the results achieved both in the author's tests and in those carried out by Toutin and his collaborators. With regard to other influences on the final results, the main system parameter that is influencing the heighting accuracy of the stereo imagery is the mirror viewing angle which determines the base-to-height ratio. As is well known, the use of a larger base-to-height ratio gives better results in terms of heighting accuracy. In the case of the Badia imagery, large ratios were available and no doubt had a favourable influence on the good results that have been achieved.

The geometric accuracy obtained in the Badia tests is quite comparable with the best results obtained using analytical plotters carried out in south France; indeed they are even slightly better, It is clear that the best accuracy figures obtained from all tests have invariably utilized ground control points obtained from high quality ground survey. In this respect, the widespread availability of GPS now makes it much easier for users to provide good quality GCPs over the huge areas covered by SPOT scenes than was the case previously. It is also quite clear that the results where the control points have been derived from existing maps are considerably worse than those derived from aerial photographs or from high-precision ground survey (Dowman (1991)). In this context, it should be noted that, in the OEEPE tests reported by Dowman et al (1991), some models could not obtain a solution without quite a substantial minimum number of control points (the range was between 4 and 14!!). Thus different solutions required a different minimum number of control points. Having regard to the large number of ground control points available for the Badia area, this has not been an issue during the present tests. Nor has this matter been investigated further in the accuracy tests carried out in the present research. As noted above, different results have been obtained by the systems in spite of the same ground control points having been used to set up the stereo-models - which points more to the influence of the different modelling.

Turning lastly to consider the geometric accuracy results achieved by individual systems, in the case of the EASI/PACE system, after modification, the mathematical model and the photogrammetric solution adopted by PCI to enable the system to handle single stereo-pairs gave a better accuracy in height for both the Level 1A and 1B stereo-pairs than the accuracy obtained by the other systems. For the OrthoMAX system using the mathematical model and programs that can accommodate single stereo-pairs and triangulation of SPOT scenes, the several tests of single stereo-pairs show better accuracy in planimetry than the other systems, While the FFI system gave slightly better results in planimetry than the DMS system. However one of the most interesting points that has emerged from the tests is the performance of the DMS system. Notwithstanding its quite simple and non-rigorous photogrammetric solution, the height accuracies achieved are really very good and will be acceptable to many users, especially since it is a very low-cost system.

16.3.4 Validation of DEMs and Orthoimages

The validation of the DEMs in terms of their elevation accuracy has been carried out in the present research using four different data sets allowing different types of accuracy test to be carried out. While the reported accuracy tests carried out by other researchers have mostly been restricted to very small areas of the DEMs, and usually to using one single validation method and a small number of points, the accuracy tests carried out by the present author have utilized samples taken from the whole of the high-density DEMs describing the very large area of terrain covered by the five SPOT stereo-pairs. For the overall accuracy of the DEMs generated over the Badia test field, Figure 16.1 gives a graphical representation of all the height accuracy values for the DEMs produced by the different systems that have been tested and validated in the present research.

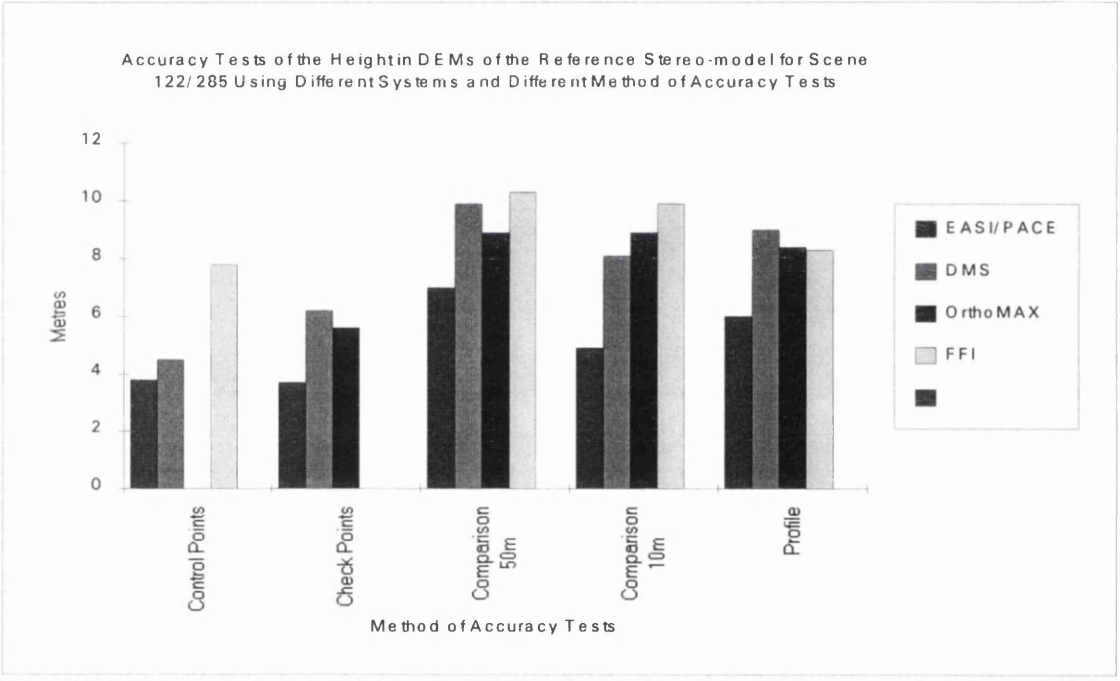

Figure 16. 1 Accuracy tests of height in the DEMs of the reference stereo-model 122/285 using different systems and different method of accuracy

In general, from the extensive series of validation tests which have been carried out on both the Level 1A and 1B SPOT stereo-pairs, it can be said that the Level 1B DEMs show a very slightly better accuracy than the DEMs produced from the Level 1A stereo-pair. Also the best accuracy figures were obtained using the EASI/PACE system corresponding to the height accuracy requirements for a 20m contour interval. Again this points to the finding that the mathematical model and the photogrammetric solution

adopted by the EASI/PACE system are the best of those tested. These results correspond to the requirements of 1:50,000 scale mapping in certain areas but not in those areas that need a 10m contour interval. Slightly less good are the results obtained by the OrthoMAX, DMS and FFI systems. But certainly the results obtained by the three commercially available systems will be of great interest to those concerned with mineral and oil and gas exploration in remote areas who may not be quite so concerned with absolute elevation accuracy as the topographic mapping community, especially if no real alternative exists. However, the results are also highly relevant to those in mapping organisations concerned with the image mapping of large areas of arid and semi-arid terrain.

Since the area-based image matching algorithm employed by all the tested systems was the same in each case, again this suggests that the main factor affecting the accuracy was the mathematical models employed by these systems. It has also been shown that the matching algorithms employed by all of these systems work very well over rather featureless desert terrain such as the Badia area where there were very few gaps or holes left in the DEMs and the pattern of the residual errors is mostly random. Indeed, it must be made clear that, because it is an area of stony desert with reasonably good texture and little vegetation, the Badia test area is especially suited to the automatic generation of DEM data from SPOT stereo-pairs. However, the results obtained in the present research can be classified as excellent, and since the RMSE values are consistently well below the one pixel level over the whole extent of the large area covered, they are certainly as good as, if not better than, the accuracy results obtained by other researchers. In fact, only Trinder et al (1994) have produced any comparable results for DEMs generated using automatic image matching techniques on a DPW and these have only been validated for certain limited areas. However Professor Trinder and his group have been able to test the effects of vegetation and slope on elevation accuracy in a way that has not been possible over the desert terrain of the Badia Project area.

It was noted in Chapter 3 how few tests have been carried out into the accuracy of the validation of the DEM data that can be extracted from SPOT stereo-pairs. Moreover, most of the validation tests have been carried out on analytical plotters using different kinds of hardware and software with the DEMs measured manually in static mode; and

few tests have been carried out using digital photogrammetric systems with the capability of automatic image matching. Another important point which should be mentioned here is that the validation of the DEMs reported by other researchers only cover very small parts of the DEMs, e.g. a few thousand pixels or small areas of 1 x 1km or 2 x 2 km, etc., while the validation of the DEMs carried out in the present research constitutes a much more extensive test covering the full DEMs extracted from five SPOT stereo-pairs covering the whole Badia area, in addition to the Level 1A DEM extracted from the stereomodel for reference scene 122/285.

As a general conclusion, taken together, the accuracy of the DEMs obtained by Professor Trinder in his tests of specific small areas of varied terrain type and the accuracy obtained by the present author over a very much larger area of desert terrain have proved that digital photogrammetric systems using automated image matching techniques are capable of generating DEMs with a very high accuracy by the standards possible with SPOT stereo-pairs and sometimes with an even better accuracy than that which can be obtained by analytical plotters where the DEM can be produced by measuring the points manually and visually in a static mode. The automated matching method is much faster and the cost of the data acquisition is much reduced. However, this is only true provided several conditions are met. These include (i) a high quality of the ground control points used for orientation of the stereo-model; (ii) the use of a good mathematical model by the system; (iii) the use of a very good matching algorithm; and (iv) images of a good radiometric quality with sparse vegetation cover and few water bodies.

As for the geometric (i.e. planimetric) accuracy of the ortho-images produced by the various systems, the final results obtained by all the systems display a sub-pixel accuracy. The best accuracy of the individual ortho-images was produced by the FFI system, though this took place when the DEM extracted by this system had a 10m grid interval and the ortho-image had a corresponding pixel size of 10m. With a 20m DEM and ortho-image, the order was EASI/PACE, DMS and the OrthoMAX system. Taking an overall view, the tests show the excellent results of the whole process in geometric terms.

16.3.5 DEM Extraction and Generation of Digital Orthoimages and Contours for the Badia Project

The individual DEMs and orthoimages produced by the EASI/PACE, DMS and OrthoMAX systems have been successfully mosaiced and have formed a single seamless DEM and orthoimage covering the whole of the Badia Project area. In each case, the merging operation went fairly smoothly and there were no obvious joins visible between the individual components of the DEMs and the orthoimages. Only one individual orthoimage produced by DMS system showed slight discrepancies at the joins. This can be related to the use of its automatic mosaicing process without any interaction with the user.

Contours with different contour intervals have also been successfully extracted from the DEMs. Only two of the systems - EASI/PACE and OrthoMAX - can actually generate contours internally within the system. The other two systems needed third party software to generate contours from the DEMs. The individual contours generated from the individual DEMs have been merged together to check the accuracy of elevation points at the boundaries between the individual DEMs. Several attempts have been made by the author to merge the contours extracted from the five DEMs on his PC, but unfortunately the merging operation did not succeed due to the limitations in the memory of the computer used for the tests. To solve these problems, the merging operation had to be done by PCI using a large Unix workstation.

In conclusion, the DEMs and the orthoimages extracted from SPOT Level 1B stereo-pairs of the whole Badia area have been made available to the Jordan Badia Research Project programme and have been passed on to other researchers in geology, geomorphology, and hydrology in Jordanian universities. The data sets have also been supplied to various researchers in British universities through the Centre for Overseas Research and Development (CORD) of University of Durham which is heavily involved in the Badia Project. Finally the data sets provided by the present author have been incorporated in the overall GIS of the Badia Project set up by HCST, in which they form an important part of the topographic database.

One of the stated objectives of the present research was to carry out a terrain analysis of the Badia area with collaboration of a geomorphologist in the University of Durham. In fact, this objective has not been achieved due to the many flaws encountered in the systems during the period of carrying the present research. It took such a time to identify these and have them corrected and to re-test the systems that the analysis has not been done due to lack of time. However it is hoped to do so in the near future.

16.3.6 The Potential Contribution of SPOT Images and Other Satellite Images to Topographic Mapping in Jordan

It can be said from the results of the various tests of SPOT images carried out during the present research that potentially the SPOT sensor is capable of acquiring images from which 1:50,000 scale topographic maps or smaller can be produced or revised to a reasonable standard at least in terms of accuracy - with the proviso that this of course depends on the quality of the ground control points, the base-to-height ratio, the quality of the images and the system employed in photogrammetric processing. But, in fact, the present SPOT data with its 10m ground pixel size is still substantially deficient in providing the details required for the production of a full or final edition of a new 1:50,000 scale map or for the comprehensive revision of an existing published map at that scale. In order to overcome these deficiencies, an additional comprehensive field completion is necessary. But, in fact, 90% of Jordan is desert and mostly lacks population and cultural details, and has very long boundaries with four countries along which a no flying zone operates. Thus mapping from SPOT satellite can be used to help solve some of Jordan's mapping problems by producing new small-scale maps or, more probably, using them for the revision of the existing available maps. However, these problems cannot all be solved only using SPOT imagery; in particular, other satellite imagery with similar geometric characteristics but better resolution can be used, such as that provided by the Indian IRS-1C and IRS-1D satellites. The resulting images have a 5m ground pixel size but they have only been launched relatively recently. Furthermore the imaging has only just become available for non-Indian users and has not yet been properly tested. However, with its similar geometry and considerably improved ground resolution to that of SPOT imagery, it may be expected to provide still more mapping capability than SPOT. Thus an obvious recommendation is to use the Badia test field to

carry out further tests of the IRS imagery, both for the international mapping communities in general and for the RJGC in particular.

Other commercial satellites are now under construction to take still higher resolution images of the Earth's surface. These include the three main American programmes - the QuickBird satellites from EarthWatch; IKONOS-1 from Space Imaging; and OrbView from the Orbital Sciences Corporation, all of which will offer stereo-imagery with a 1m ground pixel size. Currently there is considerable anxiety among the mapping community that not all of these satellites will be successful - given the recent demise of SPOT-3 and the loss of NASA's Landsat 6 and Clark satellites and Early Bird from EarthWatch before they became operational. However, if the new satellites are launched successfully and they do come into routine operation, undoubtedly this will lead to a large expansion in the use of satellite images for topographic mapping purposes. These satellites will not only have a superior ground resolution but they have a different geometry with flexible pointing of the sensor for which completely new algorithms and software need to be developed. This is a matter which has been addressed by my research colleague, Dr. Valadan Zoej (1997). Of course, any decision to use these high resolution images for mapping purposes and for the production of medium-scale topographic mapping and map revision will also be a matter of cost. As have been indicated in Section 16.3.1, the possibility of using satellite imagery for mapping in Jordan is now under active consideration largely as a result of the author's activities in this area. In this context, the presence of the test field that has been established in the Badia area will offer an excellent opportunity for the new types of imagery and the new systems required to handle these images to be tested in Jordanian conditions, which are similar to these existing in much of South West Asia and North East Africa. It is strongly recommended that this should be done.

16.4 Final Remarks

This research has given the author the opportunity to become familiar with different digital photogrammetric and remote sensing systems and has given him experience with these state-of-the-art systems which will be invaluable in his future career as a university lecturer. Furthermore the extensive series of experimental tests carried out in

this research have greatly reinforced the knowledge of the author in the field of photogrammetry and topographic mapping in general and have also taught him how to deal with and overcome the many problems that have been encountered in the present research. In doing so, he has been able to establish the geometric accuracy of SPOT stereo-pairs produced by these systems and to validate the DEMs and orthoimages - especially for Level 1B imagery - which had not been done before. The results of this research are reflected in the vastly improved systems that are now able to deal with SPOT Level 1B stereo-pairs. The author hopes that the result of his work in calibrating and testing these systems and in validating the data which are produced by them will be of considerable value to the topographic mapping community, and for others who are engaged in scientific activities in geology, geomorphology, hydrology, environmental monitoring and global change research. Hopefully, too, this research project will be regarded as having contributed substantially to promoting the use of satellite linear array imagery in the topographic mapping of extensive areas of arid and semi-arid terrain and for its use in scientific activities in other fields. Undoubtedly too, his work has helped to provide users with new corrected versions of systems as a direct result of them having been calibrated by the author. Besides this, the establishment of the Badia test site is an important contribution to the international group which is trying to establish a series of controlled test sites in different parts of the world for use with satellite imagery. Equally important will be its contribution to the mapping of Jordan since the author plans to continue to use the test field that he has created for this purpose.

REFERENCES

Abdalla, A. E., 1980. The Potential of Remotely Sensed Satellite Data for Topographic Mapping of Sudan at Small Scales. Unpublished M.Sc. Thesis, University of Glasgow, 116 pages.

Akiyama, M., 1992. Topographic Mapping Method Using SPOT Imagery. International Archives of Photogrammetry & Remote Sensing, 29 (B4): 336-341.

Al-Malabeh, A., 1993. The Volcanology, Mineralogy and Geochemistry of Selected Pyroclastic Cones from Ne-Jordan and their Evaluation for Possible Industrial Applications. Ph.D. Dissertation, Den Naturwissenschaftlichen Fakultaten der Friedrich-Alexander-Universitat, Erlangen-Nurnberg: 6-47.

Al-Rousan, N., Cheng, P., Petrie, G., Toutin, Th. and Valadan Zoej, M. J., 1997. Automated DEM Extraction and Orthoimage Generation from SPOT Level 1B Imagery. Photogrammetric Engineering & Remote Sensing, 63 (8): 965-974.

Anglerand, C. Becek, K. and Trinder, J. C., 1992. DEM Determination from SPOT. International Archives of Photogrammetry & Remote Sensing, 29 (B4): 969-973.

Ashtech Z-12 GPS Receiver Operating Manual, 1994. 195 pages.

Atilola, O., 1992. Mapping with Satellite Imagery: The Nigerian Experience. International Archives of Photogrammetry & Remote Sensing, 29 (B4): 116-121.

Bolstad, P. V. and Stowe, T., 1994. An Evaluation of DEM Accuracy: Elevation, Slope, and Aspect. Photogrammetric Engineering & Remote Sensing, 60 (11): 1327-1332.

Brockelbank, D. C. and Tam, A. P., 1991. Stereo Elevation Determination Techniques for SPOT Imagery. Photogrammetric Engineering & Remote Sensing, 57 (8): 1065-1073.

Burdon, D. J., 1982. Hydrological Consideration in the Middle East. Quarterly Journal of Engineering Geology, 15: 71-82.

Chen, Y., 1992. The Simultaneous Adjustment for SPOT Image using Orbit Data and a Few Control Points. International Archives of Photogrammetry & Remote Sensing, 29 (B3): 67-71.

Cheng, P. and Toutin, Th., 1995. High Accuracy Data Fusion of Satellite and Airphoto Images. Technical Papers, ASPRS Annual Convention: 453-464.

Cheng, P. and Stohr, C., 1996. Automated Digital Elevation Model Extraction of a Landfill Site Using Stereo Aerial Photos. Presented Paper, ASPRS Annual Convention, Baltimore, 13 pages.

Cheng, P. and Toutin, T., 1997. On-Site Interactive GPS and Geometric Modeling: A Winning Combination. Earth Observation Magazine, : 35-37.

Cross, P. A., 1990. Satellite Position-Fixing Systems for Land and Offshore Engineering Surveying. In Engineering Surveying Technology, (Eds. T.J.M. Kennie and G. Petrie): 111-145.

De Haan, A., 1991. Contribution of Politecnico di Milano to OEEPE Test on Triangulation with SPOT Data. OEEPE Test of Triangulation of SPOT Data, OEEPE Official Publication, (26): 93-107.

De Haan, A., 1992. An Analysis of the Precision of a DEM Obtained from SPOT Data. International Archives of Photogrammetry & Remote Sensing, 29 (B4): 440-447.

Deifallah, M. A. M., 1990. Heighting Accuracy of SPOT Imagery. International Archives of Photogrammetry & Remote Sensing, 28 (B4): 402-413.

Diefallah, M. A. M., 1992 (a). Testing Accuracy of SPOT Imageries. International Archives of Photogrammetry & Remote Sensing. 29 (B2): 38-42.

Diefallah, M. A. M., 1992 (b). Stereoscopic Accuracy of SPOT Imageries. International Archives of Photogrammetry & Remote Sensing, 29 (B4): 285-288.

Deren, L. and Jiayu, C., 1988. Bundle Adjustment of SPOT Imagery. International Archives of Photogrammetry & Remote Sensing, 27 (B4): 449-455.

Dowman, I. J., Gugan, D. J., Muller, J. P., O'Neill, M. and Paramananda, V., 1987. Digital Processing of SPOT Data. Fast Processing of Photogrammetric Data, ISPRS WG II/2 : 318-329.

Dowman, I. J., Neto, F. and Veillet, I., 1991. Description of Test and Summary Results. OEEPE Test of Triangulation of SPOT Data, OEEPE Official Publication, (26): 19-41.

Dowman, I. J., 1993. Test Sites for Evaluation of DEMs from Satellite Data: A Report from CEOS Working Group on Calibration and Validation Sub Group On Terrain Mapping. Proccedings, Workshop and Conference, "International Mapping from Space", ISPRS WG IV/2, University of Hannover: 129-135.

Doyle, F. J., 1984. Surveying and Mapping with Space Data. ITC Journal, 1984-4: 314-321.

El-Manadili, Y. and Novak, K.,1996. Precision Rectification of SPOT Imagery Using the Direct Linear Transformation Model. Photogrammetric Engineering & Remote Sensing, 62 (1): 67-72.

El-Niweiri, A. E. H., 1988. Geometric Accuracy Testing, Evaluation and Applicability of Space Imagery to the Small Scale Topographic Mapping of the Sudan. Ph.D Dissertation, University of Glasgow, (2 Vols): 380 pages.

Fukushima, Y., 1988. Generation of DTM Using SPOT Image Near Mt. Fuji by Digital Image Correlation. International Archives of Photogrammetry & Remote Sensing, 27 (B3): 225-234.

Galtier, B., 1986. The Potential of SPOT for Topographic Mapping. Proceedings of the Twentieth International Symposium on Remote Sensing of the Environment: 403-409.

Ganguly, P. K., 1991. Mathematical Modelling for Mapping from SPOT. M.Sc. Thesis, ITC, Netherlands. 89 pages.

Ghosh, S. K., 1987. Photo-Scale, Map-Scale and Contour Intervals in Topographic Mapping. Photogrammetria, 42(2): 34-50.

Giles, P. T. and Franklin, S. E., 1996. Comparison of Derivative Topographic Surfaces of a DEM Generated from Stereoscopic SPOT Images with Field Measurements. Photogrammetric Engineering & Remote Sensing, 62 (10): 1165-1171.

Goshtasby, A., 1988. Registration of Images with Geometric Distortions. IEEE Transactions on Geoscience & Remote Sensing, 26 (1): 60-64.

Gugan, D. J., 1987. Topographic Mapping from SPOT Imagery. Ph.D Dissertation, University College London: 253 pages.

Gugan, D. J. and Dowman, I. J., 1988. Accuracy and Completeness of Topographic Mapping from SPOT Imagery. Photogrammetric Record, 12 (72): 787-796.

Guichard, H., 1983. Etude Theoretique de la Precision dans l'Exploitation Cartographique d'un Satellite a Defilement: Application a SPOT. Bulletin de la Societe Francaise de Photogrammetrie et de Teledetection, 90 (1983-2): 15-26.

Hartley, W. S., 1988. Topographic Mapping with SPOT 1 Data: A Practical Approach by the Ordnance Survey. Photogrammetric Record, 12 (72): 833-846.

Heipke, C. and Kornus, W., 1991. Nonsemantic Photogrammetric Processing of Digital Imagery - The Example of SPOT Stereo Scene. Digital Photogrammetric Systems:86-102.

Heipke, C., Kornus, W., Strunz, G., Thiemann, R. and Colomina, I., 1992. Automatic Photogrammetric Processing of SPOT Imagery for Point Determination, DTM Generation and Orthoprojection. International Archives of Photogrammetry & Remote Sensing, 29 (B4): 465-471.

Ibrahim, K. M., 1992. The Geological Framework for the Harrat As-haam Basaltic Supergroup and its Volcanotectonic Evolution. Natural Resources Authority, Amman.

Imhof, E., 1982. Cartographic Relief Presentation. Walter de Gruyter, Berlin.

Jacobsen, K., 1990. Cartographic Potential of Space Images. Proceedings, ISPRS Commission II Symposium "Progress in Data Processing and Analysis", Dresden: 127-134a.

Jacobsen, K., 1993. Comparative Analysis of the Potential of Satellite Images for Mapping. Proceedings, Workshop and Conference, "International Mapping from Space", ISPRS WG IV/2: 107-116.

Kihlblom, U.G., 1992. Map Production from Satellite Data. Proceedings, First International Conference on Surveying & Mapping, Tehran. Paper No. 12:167-183.

Kölbl, O., 1996. Survey on the Application of Digital Photogrammetric Workstations. Proceedings of the OEEPE Workshop on "Application of Digital Photogrammetric Workstations", Lausanne, Switzerland.

Kruck, E., 1987. BINGO Bundle Adjustment Program for SPOT Data. Seminar on Photogrammetric Mapping from SPOT Imagery, Hannover. 18 pages.

Konecny, G., Schuhr, W. and Wu, J., 1982. Investigation of Interpretability of Images by Different Sensors and Platforms for Small Scale Mapping. Proceedings ISPRS Commission IV Symposium, Crystal City:373-387.

Konecny, G., 1987. Geometric Evaluation of SPOT Imagery. Seminar on Photogrammetric Mapping from SPOT Imagery, Hannover: 20-53.

Konecny, G., Lohmann, P., Engel, H. and Kruck, E., 1987. Evaluation of SPOT Imagery on Analytical Photogrammetric Instruments. Photogrammetric Engineering & Remote Sensing, 53 (9): 1223-1230.

Konecny, G., 1995. Current Status and Future Possibilities for Topographic Mapping from Space. EARSeL Advances in Remote Sensing, 4 (2): 1-18.

Kratky, V., 1987. Rigorous Stereophotogrammetric Treatment of SPOT Images. SPOT-1 Utilisation des Images, Bilan, Resultats, CNES, Paris: 1195-1204.

Kratky, V., 1988 (a). Universal Photogrammetric Approach to Geometric Processing of SPOT Images. International Archives of Photogrammetry & Remote Sensing, 27 (B3): 180-189.

Kratky, V., 1988 (b). Rigorous Photogrammetric Processing of SPOT Image at CCM Canada. Proceedings of the International Symposium on Topographic Applications of SPOT Data, Canada: 35-49.

Kruck, E., 1987. BINGO Bundle Adjustments Program for SPOT Data. Seminar on Photogrammetric Mapping from SPOT Imagery, Hannover. 18 pages.

Lauritson, L. and Howard, B. A., 1993. The Role of the Committee on Earth Observation Satellites (CEOS) Working Group on Data (WGD) in the Coordination of International Remote Sensing Activities. Proceedings of the 25th International Symposium on Remote Sensing & Global Environmental Change, Graz, Austria: I-429 to I-439.

Ley, R. G., 1988. Some Aspects of Height Extraction From SPOT Imagery. Photogrammetric Record, 12 (72): 823-832.

Madani, M., 1996. Intergraph Integrated Digital Photogrammetry System, Proceedings of the OEEPE Workshop on the Application of Digital Photogrammetric Workstations, Lausanne, Switzerland, 11 pages.

Murray, K. J. and Farrow, J. E., 1988. Experiences Producing Small Scale Line Mapping from SPOT Imagery. International Archives of Photogrammetry & Remote Sensing, 27 (B11): 407-421.

Murray, K. J. and Gilbert, E.V., 1990. Small Scale Line Mapping from SPOT Imagery. Proceedings of the Twenty-Third International Symposium on Remote Sensing of Environment, Vol. (II): 1149-1158.

Murray, K. J., and Newby, P. R. T., 1990. Mapping from SPOT Imagery at the Ordnance Survey. International Archives of Photogrammetry & Remote Sensing, 28 (B4): 430-438.

Naithani, K. K., 1988. Can Satellite Imagery Ever Replace Aerial Photography?- a Photogrammetric View. International Archives of Photogrammetry and Remote Sensing, 27 (B4): 274-279. [also published in ITC Journal, 1990-1: 29-31].

Novak, K., 1992. Rectification of Digital Imagery. Photogrammetric Engineering & Remote Sensing, 58 (3): 339-344.

Pattyn, F., 1992. Topographic Mapping with SPOT in Polar Region. International Archives of Photogrammetry & Remote Sensing, 29 (B4): 472-475.

Petrie, G., 1970. Some Considerations Regarding Mapping from Earth Satellites. Photogrammetric Record, 6 (36): 590-624.

Petrie, G. and Kennie, T. J. M., 1990. Modelling, Interpolation and Contouring Procedures. Chapter 8 in Terrain Modelling in Surveying and Civil Engineering (Eds. G. Petrie and T. J. M. Kennie): 122-127.

Petrie, G., 1990. The Impact of Analytical Photogrammetric Instrumentation on DEM Data Acquisition and Processing. Chapter 5 in Terrain Modelling in Surveying and Civil Engineering (Eds. G. Petrie and T. J. M. Kennie): 49 -72.

Petrie, G. and El-Niweiri, A. E. H., 1994. Comparative Testing of Space Images for Small-Scale Topographic Mapping of Sudan. ITC Journal, 1994-2: 95-112.

Petrie, G. and Liwa, E. J., 1995. Comparative Tests of Small Scale Aerial Photography and SPOT Satellite Imagery for Topographic Mapping and Map Revision in Eastern, Central and Southern Africa. ITC Journal, 1995-1: 43-55.

Petrie, G., 1997(a). The Current Situation in Africa Regarding Topographic Mapping and Map Revision from Satellite Images. ITC Journal, 1997-1: 49-63.

Petrie, G., 1997(b). Developments in Digital Photogrammetric Systems for Topographic Mapping and GIS/LIS Applications. ITC Journal, 1997-2: 121-135.

Petrie, G., Al-Rousan, N., El-Niweiri, A. E. H., Li, Z., and Valadan Zoej, M. J., 1998. Topographic Mapping of Arid and Semi-arid Areas in the Red Sea Region from Stereo Space Imagery. EARSeL Advances in Remote Sensing, (5): 11-30.

Picht, G., 1987. Processing of SPOT Images with BINGO. Seminar on Photogrammetric Mapping from SPOT Imagery, Hannover: 1-7.

Priebbenow, R. J. and Clerici, E., 1988. Cartographic Applications of SPOT Imagery. International Archives of Photogrammetry & Remote Sensing, 27 (B4): 289-297.

Priebbenow, R. J., 1991. Triangulation of SPOT Imagery at the Department of Lands, Queensland. OEEPE Test of Triangulation of SPOT Data, OEEPE Official Publication, (26): 109-128.

Radhadevi, P. V. and Ramachandran, R., 1994. Orbital Attitude Modelling of SPOT Imagery with a Single Ground Control Point. Photogrammetric Record, 14 (84): 973-982.

Rodriguez, V., Gigord, P., de Gaujac, A. C. and Munier, P., 1988. Evaluation of the Stereoscopic Accuracy of the SPOT Satellite. Photogrammetric Engineering & Remote Sensing, 54 (2): 217-221.

Sasowsky, K. C., Petersen, G. W. and Evans, B. M., 1992. Accuracy of SPOT Digital Elevation Model and Derivatives: Utility for Alaska's North Slope. Photogrammetric Engineering and Remote Sensing, 58 (6): 815-824.

Shibasaki, R., Murai, S., and Okuda, T., 1988. SPOT Imagery Orientation with Auxiliary Satellite Position and Attitude Data. International Archives of Photogrammetry & Remote Sensing, 27 (B9): 125-132.

Tham, P., 1968. Aerial Map Accuracy in Photogrammetry - European Standard Error V. American C-factor. Svensk Landmateritidskrift, (2): 12pp.

Theodossiou, E. L. and Dowman, I. J., 1990. Heighting Accuracy of SPOT. Photogrammetric Engineering & Remote Sensing, 56 (12): 1643-1649.

Toutin, Th., 1985. Analyse Mathematique pour des Possibilites Cartographiques du Systeme SPOT. XYZ Revue de l'Association Francais de Topographie, 25: 53-66.

Toutin, Th., 1986. Etude Mathematique Pour la Rectification d'Images SPOT-HRV. Proceedings of the 18th International Congress of Surveying, Toronto, Canada: 379-395.

Toutin, Th. and Carbonneau, Y., 1989. La Multi-Stereoscopie pour les Corrections d'Images SPOT-HRV, Canadian Journal of Remote Sensing, 15 (2): 110-119.

Toutin, Th. and Carbonneau, Y., 1990. Multi-Stereoscopy for the Correction of SPOT-HRV Images. International Archives of Photogrammetry & Remote Sensing, 28 (B4): 298-313.

Toutin, Th., 1995. Multi-Source Data Fusion with an Integrated and Unified Geometric Modelling. EARSeL - Advances in Remote Sensing, 4 (2): 118-129.

Toutin, Th. and Beaudoin, M., 1995. Real-Time Extraction of Planimetric and Altimetric Features from Digital Stereo SPOT Data Using a Digital Video Plotter. Photogrammetric Engineering & Remote Sensing, 61 (1): 63-68.

Trinder, J. C., Vuillemin, A., and Donnelly, B. F., 1994. A Study of Procedures and Tests on DEM Software for SPOT Images. International Archives of Photogrammetry & Remote Sensing, 30 (B4): 449-456.

Valadan Zoej, M. J., 1997. Photogrammetric Evaluation of Space Linear Array Imagery for Medium Scale Topographic Mapping. Ph.D Dissertation, University of Glasgow, (2Vols): 303 pages.

Valadan Zoej, M. J. and Petrie, G., 1998. Mathematical Modelling and Accuracy Testing of SPOT Level 1B Stereopairs. Photogrammetric Record, 16(91): 67-82.

Veillet, I., 1990. Block Adjustment of SPOT Images for Large Area Topographic Mapping. International Archives of Photogrammetry & Remote Sensing, 28 (3-2): 926-936.

Walker, A. S. and Petrie, G., 1996. Digital Photogrammetric Workstations, 1992-96. International Archives of Photogrammetry & Remote Sensing, 31 (B2): 384-395.

Welch, R., 1989. Desktop Mapping with Personal Computers. Photogrammetric Engineering & Remote Sensing, 55 (11): 1651-1662.

Wells, D., 1987. Global Positioning System. Guide to GPS Positioning, Canadian GPS Associates: 15 chapters.

Westin, T., 1990. Precision Rectification of SPOT Imagery. Photogrammetric Engineering & Remote Sensing, 56 (2): 247-253.

Westin, T., 1991. Pass Processing and Extrapolation of SPOT Image Geometry. Photogrammetric Record, 13 (78): 923-929.

Yeu, B. M., Lee, H. J. and Sohn, D. J., 1992 (a). Accuracy Improvement of Three Dimensional Positioning Using Spot Imagery. International Archives of Photogrammetry & Remote Sensing, 29 (B4): 372-377.

Yeu, B. M., Cho, G. S., Yom, J. H., and Kwon, H., 1992 (b). Accuracy Evaluation By GCP Acquisition Method in Bundle Adjustment for SPOT Imagery. International Archives of Photogrammetry & Remote Sensing, 29 (B4): 412-417.

Zhong, Y., 1992. Analytical Stereomapping Using SPOT Imagery. International Archives of Photogrammetry & Remote Sensing, 29 (B4): 280-284.

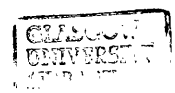

SYSTEM CALIBRATION, GEOMETRIC ACCURACY TESTING AND VALIDATION OF DEM AND ORTHOIMAGE DATA EXTRACTED FROM SPOT STEREO-PAIRS USING COMMERCIALLY AVAILABLE IMAGE PROCESSING SYSTEMS

BY

NAIEF MAHMOUD Al-ROUSAN

Volume II

A Thesis Submitted for

the Degree of Doctor of Philosophy (Ph.D.)

of the Faculty of Science at the University of Glasgow

in Photogrammetry and Remote Sensing

Topographic Science, July 1998

APPENDIX A : CONTROL POINTS AND PROFILE DATA

A.1 Introduction

In this Appendix, a list of the coordinate values of the ground control points (GCPs) in the Universal Transverse Mercator (UTM), Jordan Transverse Mercator (JTM) and WGS 84 coordinate systems will be given. A total of 130 control points have been measured over the Badia Test Field using Ashtech 12 GPS sets in conjunction with the rapid static method. The accuracy of these points is less than 1m both in planimetry and height. Most of these ground control points are well identified on the SPOT scenes. A few of these points were not used in the tests due to the location of these points being outside the overlap area. Some others are not well identified, but these points have been used as check points to check the accuracy of some DEMs.

The list of GCP coordinate values is followed by a listing of the coordinates of the profile data measured over the Badia Test Field using GPS and implementing the kinemetic survey method. A total of 1,248 points have been selected from the more than 15,000 points that have been measured.

A.2 Ground Control Points in the UTM and JTM Coordinate Systems

	UTM		JTM		Elevation
GCP No.	X (M)	Y (m)	X (m)	Y (m)	H (m)
101	308544.669	3559870.413	497154.456	558775.473	810.299
102	300921.813	3557098.576	489586.502	555863.304	797.659
103	294889.283	3559724.891	483508.095	558376.322	814.225
104	276368.542	3567281.994	464856.798	565584.977	792.794
105	275909.483	3567412.505	464395.577	565706.868	793.612
106	272854.459	3568141.362	461328.791	566378.429	782.278
107	269357.578	3569585.173	457807.184	567754.261	798.697
108	270787.186	3568859.895	459249.386	567058.043	802.285
109	277989.322	3576770.680	466299.834	575098.380	958.301
110	295871.199	3566645.391	484360.850	565311.670	942.609
111	300741.906	3576801.496	489039.974	575553.662	1104.942
112	309287.944	3582167.164	497481.995	581076.475	1093.675
113	304306.158	3580947.261	492525.194	579764.051	1153.919
114	297526.394	3574024.390	485877.79	572717.905	1059.898
115	292203.029	3575576.658	480528.118	574170.136	1049.674
116	284865.279	3573802.547	473227.303	572260.133	990.834
117	288243.343	3568402.170	476704.171	566925.575	945.384
118	290484.381	3561272.389	479076.662	559841.191	847.957
119	284545.790	3563607.619	473097.804	562064.789	836.672
120	280182.758	3565344.286	468704.886	563719.348	827.529
121	273255.862	3579468.813	461518.794	577706.598	935.309
122	272832.538	3578575.593	461112.395	576806.012	917.056

123	282548.934	3570242.780	470978.559	568659.153	926.492
124	284233.497	3556247.451	472922.415	554702.821	705.601
125	325223.139	3568548.152	513664.965	567760.026	747.516
126	326827.076	3574684.140	515153.992	573923.750	758.239
127	330679.379	3582061.38	518867.277	581370.401	741.388
128	331363.258	3573362.330	519713.293	572686.972	714.602
129	338783.514	3569542.050	527202.450	569006.153	720.909
130	266312.232	3552051.811	455089.473	550177.195	594.239
131	270209.389	3547506.987	459068.436	545707.389	587.040
132	264522.576	3546922.248	453395.987	545017.709	590.026
133	278850.432	3542817.332	467791.193	541180.426	589.206
134	268539.408	3560147.298	457165.022	558308.977	688.535
135	279715.010	3554356.652	468441.518	552729.225	666.974
136	282128.565	3547222.124	470985.964	545643.419	611.143
137	292705.709	3551481.912	481478.587	550096.936	708.999
138	262874.639	3540614.135	451865.809	538683.136	655.033
139	263912.148	3540146.147	452911.305	538234.628	642.082
140	281962.207	3535718.276	471032.423	534142.858	553.364
141	292955.156	3536500.414	482005.129	535127.592	541.520
142	292450.809	3547659.920	481294.638	546272.150	675.238
143	337967.500	3576238.202	526261.841	575685.126	716.597
144	347383.779	3579711.577	535610.701	579333.319	779.810
145	345745.961	3571770.952	534121.449	571364.171	767.193
146	322957.330	3563359.228	511496.531	562530.803	707.785
148	330976.637	3561084.712	519555.354	560406.169	653.063
149	336884.040	3557833.686	525521.310	557265.918	644.062
150	343633.169	3563012.343	532172.279	562568.537	701.709
151	313517.357	3552939.957	502253.711	551940.233	716.645
152	309232.993	3554858.615	497935.541	553778.608	751.130
153	320665.358	3549829.657	509456.587	548963.676	629.794
154	329681.641	3548198.349	518499.916	547500.020	625.959
155	337166.622	3549815.308	525952.58	549255.172	631.489
156	334923.978	3545629.419	523788.159	545029.004	628.161
157	327583.703	3553036.651	516312.991	552297.798	643.164
158	328329.544	3556593.364	516992.574	555867.141	646.406
159	325744.302	3543781.439	514645.705	543011.707	633.968
161	320261.404	3544824.900	509145.482	543953.312	625.724
162	308314.302	3542497.549	497246.263	541405.826	603.401
163	304905.635	3532800.617	494018.248	531650.165	536.498
164	320102.158	3536358.836	509142.839	535487.482	627.516
165	317474.332	3530715.452	506620.179	529797.747	605.417
166	330238.048	3534946.041	519301.255	534262.373	594.120
167	330419.432	3528361.542	519604.065	527683.376	596.827
168	321495.980	3574939.058	509820.061	574079.151	793.943
169	318580.572	3586702.722	506686.041	585783.896	954.594
170	304708.586	3572785.441	493079.725	571613.423	1033.718
171	313698.694	3569807.342	502121.463	568804.11	886.812
201	350511.732	3543351.815	539413.852	543040.56	655.899
202	363798.985	3539196.598	552775.267	539131.969	713.740
203	375648.127	3535240.030	564695.820	535394.941	741.806
204	374762.966	3555431.940	563436.843	555568.047	902.724
205	303176.076	3527297.357	492390.949	526117.487	516.260
206	319060.961	3518167.941	508437.264	517284.257	567.414
207	315011.730	3511658.373	504509.187	510702.824	548.856
209	339189.029	3505650.727	528788.458	505140.688	542.238
210	330884.735	3521647.174	520192.888	520979.762	588.409

211	352931.099	3519576.851	542271.346	519315.644	597.818
212	359260.860	3503218.918	548900.109	503077.265	660.695
213	368483.733	3521471.342	557786.251	521495.971	727.430
214	299720.949	3517738.582	489113.342	516499.531	510.720
215	341769.760	3534241.107	530842.512	533770.575	622.585
301	363529.165	3512142.368	553003.980	512077.396	697.499
302	368042.453	3537681.931	557046.047	537695.988	732.539
303	389811.485	3531696.745	578923.424	532113.463	670.323
304	412380.125	3524083.206	601632.534	524916.070	684.115
305	424243.652	3520779.049	613557.913	521830.125	681.542
306	380363.203	3522860.289	569638.719	523103.456	714.052
307	388019.908	3526598.320	577225.981	526982.267	719.408
308	399431.413	3521857.765	588724.467	522452.082	706.520
309	398273.582	3529545.628	587424.959	530118.554	668.093
310	393224.459	3543170.438	582124.177	543649.751	725.155
311	412469.892	3543418.895	601365.194	544254.486	698.739
312	430904.572	3544300.681	619785.337	545477.721	741.237
313	435885.029	3557066.897	624529.723	558338.252	759.954
314	416258.305	3559482.397	604855.836	560389.267	699.456
315	400242.739	3562606.112	588781.666	563215.264	711.367
401	423468.985	3597161.777	611363.370	598206.487	681.681
402	433833.480	3600300.880	621670.198	601540.548	703.665
403	410179.891	3592074.527	598168.776	592869.689	665.684
404	377215.883	3566138.906	565690.424	566319.352	850.916
405	384893.052	3608353.782	572576.845	608673.792	685.835
406	400814.650	3608976.602	588486.005	609596.141	654.517
407	401283.792	3618271.293	588780.046	618899.597	641.467
408	391498.267	3618422.804	578991.957	618866.551	659.520
409	395605.635	3572832.728	583954.165	573355.343	716.005
410	407856.019	3580587.08	596059.795	581338.38	679.687
411	447605.402	3604587.983	635363.996	606087.216	744.812
412	425744.588	3580252.558	613955.858	581338.113	698.453
413	439091.463	3582964.999	627253.918	584300.451	727.561
414	424195.557	3612833.260	611795.365	613893.176	672.817
415	436331.853	3566523.583	624800.696	567804.780	740.422
416	426680.656	3605366.552	614421.255	606472.452	682.940
501	334515.315	3591456.239	522526.233	590833.993	733.624
502	334878.665	3598065.913	522765.581	597448.409	733.676
503	325159.131	3592448.592	513154.600	591650.770	790.749
504	345777.044	3587347.841	533861.636	586937.586	806.769
505	354648.088	3607149.131	542359.131	606900.491	893.160
506	367447.341	3597536.126	555336.478	597529.719	870.331
507	361030.760	3576489.309	549314.825	576366.528	923.003
508	389053.182	3584947.778	577175.733	585347.487	733.406
509	376121.014	3580644.755	564325.161	580803.102	847.942
510	357454.622	3593416.772	545422.839	593223.762	952.471
511	366460.883	3609365.020	554127.948	609338.133	855.089
512	379350.760	3594484.798	567295.529	594702.028	791.595
513	391427.103	3607512.265	579126.289	607955.240	661.859
515	357684.029	3559195.208	546290.788	559013.493	765.688
601	354816.355	3605916.027	542550.543	605670.824	635.354

A.3 Ground Control Points in the WGS 84 Coordinate System

No.	X(m)	Y (m)	Z (m)
101	4318773.513	3250831.450	3375556.086
102	4324553.455	3245707.772	3373078.595
110	4323771.214	3238572.537	3381150.459
111	4316703.038	3239106.844	3389906.357
112	4309259.145	3244071.971	3394573.388
113	4312842.514	3240563.249	3393494.440
114	4319782.561	3237466.606	3387480.982
115	4322367.094	3232713.304	3388696.162
116	4327519.767	3227451.604	3387035.359
118	4329206.256	3236049.753	3376460.821
119	4331836.867	3230543.383	3378325.645
120	4333757.496	3226488.486	3379710.775
123	4330358.885	3226774.719	3383949.644
124	4334982.840	3232695.064	3372020.590
125	4304957.612	3261100.391	3383120.490
126	4301437.545	3260312.912	3388338.087
127	4296002.969	3260868.593	3394618.343
128	4299182.768	3264324.291	3387262.204
129	4296229.636	3271479.225	3384137.373
133	4343710.262	3232845.540	3360482.400
135	4338478.219	3229716.937	3370316.942
136	4339922.139	3233992.226	3364287.356
137	4331810.173	3241020.953	3368135.553
140	4344721.496	3237667.429	3354499.466
141	4337719.276	3246133.985	3355350.421
142	4333519.528	3242078.771	3364874.869
143	4293946.271	3268580.446	3389785.784
145	4291067.634	3276255.730	3386138.963
146	4308466.103	3261028.124	3378675.956
148	4304468.360	3268109.211	3376837.451
149	4302191.702	3273865.941	3374162.050
150	4295951.179	3277493.987	3378666.769
151	4318544.163	3257045.623	3369715.735
152	4320386.649	3253025.396	3371291.914
153	4315407.707	3263703.765	3367143.218
154	4310560.200	3271303.790	3365889.601
155	4305323.646	3276766.127	3367366.771
156	4308421.679	3276389.727	3363786.417
157	4309865.115	3268114.849	3369968.736
158	4307941.190	3267516.260	3372993.658
159	4314802.504	3269747.132	3362093.296
163	4331968.237	3256846.507	3352407.226
164	4321301.257	3267751.904	3355711.084
165	4325210.253	3267537.905	3350870.170
166	4315665.731	3276228.556	3354641.431
167	4318262.329	3278564.509	3349055.642
168	4304613.437	3256025.272	3388494.184
169	4301608.191	3249835.389	3398474.264
170	4315908.211	3243568.198	3386539.131
171	4311565.682	3251621.389	3384085.893
201	4299823.746	3289481.828	3362073.570
202	4293408.454	3301382.645	3358737.222

203	4287757.534	3312054.263	3355522.535
204	4280083.606	3304696.822	3372720.550
205	4335267.617	3257294.621	3347696.478
206	4329362.491	3272942.681	3340215.060
207	4334484.052	3271882.136	3334609.345
209	4322155.294	3293001.110	3329838.615
210	4320726.460	3281158.827	3343353.980
211	4308069.219	3299273.646	3341887.188
212	4310910.645	3309717.535	3328079.620
213	4297816.449	3310980.371	3343744.651
214	4341284.491	3257723.522	3339516.078
215	4308914.280	3285596.378	3354214.933
301	4304665.470	3310151.682	3335741.774
303	4280423.365	3324344.739	3352614.270
304	4269583.082	3344614.109	3346338.899
305	4263568.067	3355013.932	3343609.273
306	4289915.371	3319870.384	3345041.265
307	4283657.603	3324656.892	3348293.526
308	4278536.021	3335197.006	3344358.706
309	4276071.874	3331712.129	3350860.575
310	4273627.263	3323232.766	3362411.018
311	4261585.284	3338252.883	3362763.036
312	4249793.963	3352433.121	3363653.793
313	4241432.066	3352072.754	3374512.065
314	4252598.853	3335852.040	3376404.726
315	4261243.828	3322238.079	3378933.289
401	4232436.612	3328806.825	3408292.359
402	4224689.835	3335874.936	3411014.429
403	4242802.656	3320095.857	3403897.782
404	4274103.321	3303012.159	3381783.618
405	4251661.003	3294722.857	3417419.883
406	4241532.174	3307013.097	3418071.834
407	4237333.771	3304217.347	3425897.055
408	4243337.946	3296484.515	3425948.564
409	4259875.412	3315161.521	3387549.055
410	4249040.038	3322155.399	3394185.694
411	4214336.430	3345219.028	3414720.481
412	4238083.351	3336308.444	3394037.810
413	4228663.568	3345861.027	3396421.042
414	4225418.480	3324059.036	3421503.678
415	4237223.812	3349240.410	3382510.821
416	4227008.698	3328545.511	3415232.803
505	4270935.753	3271403.957	3416184.008
506	4267068.847	3284743.761	3408216.649
507	4279823.845	3286813.884	3390399.063
508	4258900.046	3305938.051	3397738.380
509	4268751.830	3297269.538	3394037.109
510	4274992.006	3278298.397	3404669.539
511	4262716.511	3279950.238	3418169.702
512	4260953.375	3295112.386	3405726.798
513	4247959.682	3300135.487	3416759.499

A.4 GPS Profile Points Compared with the Corresponding Elevation Values Measured in the DEMs Produced by the Different Systems

PROGRAM: PRISM v2.1.00 Apr 15 1997
CREATED FROM: Point File SEC-01G.PTS

SYSTEM:	UTMN	Univ. Transverse Merc. (N)
DATUM:	WGS84	World Geodetic Sys. 1984□
ELLIPSOID:	WGS84	World Geodetic Sys. 1984
SEMI-MAJOR AXIS:		6,378,137.000m
INVERSE FLATTENING:		298.2572236
PROJECTION:	TM83	Transverse Mercator
ZONE:	ZN37 37	Zone37 - 36 E to 42 E
UNITS:	METER	METER

The listings of the height values from each of the different systems are given under the headings EASI/PACE, DMS, OrthoMAX and FFI

POINT	NORTHING	EASTING	HEIGHT	SITE	EASI (H)	DMS(H)	OrthoMAX	FFI
00009	3563004.720	322685.040	731.809	SS01	710.000	712.200		
00122	3563096.047	322788.810	730.880	????	714.000	708.200		
00131	3563157.854	322892.727	730.476	????	709.000	708.200		
00140	3563215.787	322989.174	730.155	????	709.000	700.200		
00149	3563274.855	323087.889	730.225	????	709.000	696.200		
00160	3563335.201	323187.210	731.061	????	709.000	708.200		
00171	3563396.838	323288.611	731.541	????	713.000	708.200		
00181	3563453.087	323384.172	731.165	????	713.000	708.200		
00192	3563499.000	323484.372	729.421	????	710.000	708.200		
00204	3563569.981	323588.037	727.655	????	710.000	708.200		
00214	3563630.035	323688.478	727.927	????	708.000	696.200		
00223	3563684.169	323785.677	728.548	????	708.000	704.200		
00233	3563733.733	323893.032	729.018	????	708.000	700.200		
00244	3563782.119	324006.364	729.501	????	706.000	704.200		
00252	3563818.125	324093.049	729.418	????	706.000	708.200		
00261	3563861.872	324196.817	728.573	????	703.000	704.200		
00269	3563901.617	324291.925	728.297	????	707.000	700.200		
00278	3563943.888	324394.491	729.482	????	707.000	700.200		
00287	3563986.885	324497.042	730.881	????	707.000	704.200		
00296	3564030.007	324600.247	732.285	????	707.000	704.200		
00305	3564073.007	324703.477	733.668	????	707.000	708.200		
00314	3564117.199	324808.895	734.059	????	712.000	704.200		
00322	3564155.931	324903.266	733.442	????	712.000	708.200		
00330	3564196.438	325002.819	732.784	????	712.000	708.200		
00339	3564241.927	325110.870	732.135	????	712.000	708.200		
00348	3564283.825	325212.092	731.553	????	712.000	708.200		
00358	3564333.552	325330.052	730.883	????	711.000	708.200		
00366	3564374.682	325429.140	730.298	????	711.000	708.200		
00374	3564416.106	325528.495	729.693	????	710.000	708.200		
00383	3564461.618	325638.543	729.500	????	710.000	708.200		
00392	3564507.598	325748.366	730.494	????	710.000	708.200		
00400	3564549.607	325847.970	731.775	????	711.000	708.200		
00409	3564596.362	325958.247	733.498	????	711.000	704.800		
00418	3564642.420	326068.657	735.219	????	711.000	708.200		
00427	3564686.331	326177.394	736.314	????	713.000	708.200		
00437	3564734.849	326294.121	735.650	????	712.000	708.200		
00446	3564779.473	326401.136	734.694	????	712.000	708.200		
00455	3564824.098	326508.442	733.697	????	712.000	708.200		
00464	3564868.252	326614.312	733.150	????	707.000	704.200		
00473	3564911.314	326716.809	732.763	????	707.000	708.200		
00483	3564955.447	326822.665	732.274	????	706.000	708.200		
00493	3565000.469	326929.581	731.219	????	706.000	704.200		
00503	3565045.515	327036.246	730.203	????	706.000	708.200		
00513	3565089.904	327143.467	729.194	????	702.000	700.200		
00571	3565111.314	327196.206	728.744	????	702.000	704.200		

ASHTECH POINTS FILE
PROGRAM: PRISM v2.1.00 Apr 15 1997
CREATED FROM: Point File SEC-02G.PTS

POINT	NORTHING	EASTING	HEIGHT	SITE	EASI	DMS	OrthoMAX	FFI
00027	3565114.916	327206.903	726.246	SS02	702.000	704.200	698.000	699.000
00088	3565161.735	327318.384	728.147	????	702.000	708.200	698.000	696.000
00097	3565207.073	327427.288	727.758	????	704.000	700.200	701.000	691.000
00106	3565252.749	327536.909	727.403	????	704.000	696.200	694.000	689.000
00115	3565299.544	327649.061	726.103	????	699.000	696.200	696.000	687.000
00124	3565345.631	327758.597	723.829	????	699.000	696.200	694.000	690.000
00133	3565390.225	327867.233	721.468	????	693.000	696.200	694.000	690.000
00142	3565433.914	327972.025	720.289	????	693.000	696.200	693.000	695.000
00152	3565481.391	328083.306	720.230	????	695.000	684.300	689.000	686.000
00162	3565523.460	328188.698	720.138	????	695.000	692.300	693.000	686.000
00172	3565569.304	328296.713	719.849	????	695.000	696.200	692.000	681.000
00183	3565616.133	328408.875	718.299	????	694.000	696.200	693.000	678.000
00194	3565664.706	328524.766	716.549	????	694.000	696.200	692.000	687.000
00205	3565713.653	328640.805	714.830	????	692.000	688.300	691.000	683.000
00216	3565760.403	328752.915	714.759	????	691.000	680.300	690.000	678.000
00227	3565809.380	328871.005	716.719	????	691.000	688.300	688.000	678.000
00237	3565857.839	328987.250	718.885	????	691.000	696.200	688.000	682.000
00247	3565905.374	329099.850	720.486	????	691.000	700.200	690.000	681.000
00258	3565952.314	329213.177	719.728	????	690.000	684.300	689.000	685.000
00268	3566000.601	329328.941	717.857	????	694.000	696.200	692.000	678.000
00278	3566048.813	329444.518	715.478	????	689.000	696.200	687.000	678.000
00289	3566098.201	329562.618	712.131	????	689.000	692.300	683.000	680.000
00300	3566146.509	329678.597	708.620	????	689.000	688.300	682.000	674.000
00312	3566198.514	329799.941	707.302	????	686.000	684.300	680.000	673.000
00321	3566244.535	329909.573	707.320	????	685.000	684.300	682.000	674.000
00339	3566336.248	330131.769	707.312	????	683.000	676.300	675.000	677.000
00350	3566391.051	330259.875	707.302	????	681.000	680.300	679.000	683.000
00361	3566435.118	330381.689	707.632	????	681.000	672.400	684.000	677.000
00372	3566469.870	330502.830	708.343	????	683.000	676.300	684.000	677.000
00382	3566501.705	330615.781	708.971	????	685.000	684.300	681.000	675.000
00392	3566534.654	330730.866	709.657	????	685.000	684.300	687.000	672.000
00402	3566571.331	330858.358	710.541	????	687.000	684.300	684.000	671.000
00411	3566603.859	330973.502	711.464	????	687.000	684.300	684.000	679.000
00421	3566640.425	331100.504	712.337	????	686.000	684.300	684.000	680.000
00431	3566675.541	331223.857	712.021	????	686.000	684.300	686.000	680.000
00441	3566708.404	331338.727	711.632	????	687.000	684.300	684.000	679.000
00451	3566740.819	331452.783	711.290	????	687.000	688.300	690.000	678.000
00462	3566774.656	331571.104	710.924	????	687.000	688.300	682.000	680.000
00473	3566808.759	331689.834	710.575	????	687.000	688.300	682.000	680.000
00485	3566843.950	331807.539	710.566	????	687.000	684.300	681.000	680.000
00491	3566852.185	331844.852	710.622	????	687.000	684.300	687.000	681.000

ASHTECH POINTS FILE
PROGRAM: PRISM v2.1.00 Apr 15 1997
CREATED FROM: Point File SEC-03G.PTS

POINT	NORTHING	EASTING	HEIGHT	SITE	EASI	DMS	OrthoMAX	FFI
00132	3566883.282	331951.316	711.431	????	687.000	684.300	687.000	680.000
00143	3566917.992	332072.865	712.282	????	687.000	684.300	683.000	683.000
00154	3566951.892	332191.631	712.312	????	687.000	684.300	679.000	682.000
00165	3566985.435	332308.352	711.395	????	687.000	684.300	679.000	677.000
00176	3567019.772	332425.953	710.857	????	686.000	684.300	682.000	674.000
00186	3567051.675	332540.714	712.397	????	687.000	684.300	683.000	685.000

00197	3567086.862	332663.616	714.782	????	689.000	684.300	687.000	681.000
00207	3567120.521	332778.033	716.534	????	689.000	696.200	691.000	685.000
00216	3567152.762	332889.826	717.783	????	689.000	688.300	689.000	684.000
00226	3567185.225	333003.563	719.091	????	689.000	692.300	689.000	
00236	3567219.560	333118.429	719.319	????	689.000	688.300	684.000	
00245	3567253.331	333228.182	718.549	????	689.000	692.300	690.000	
00256	3567291.432	333349.344	717.727	????	694.000	696.200	688.000	
00267	3567328.176	333465.446	716.979	????	689.000	696.200	681.000	
00278	3567365.233	333582.406	716.217	????	689.000	696.200	695.000	
00289	3567402.336	333699.342	715.714	????	689.000	692.300	695.000	
00301	3567440.749	333820.186	716.266	????	689.000	688.300	684.000	
00311	3567477.496	333936.129	716.661	????	687.000	684.300	690.000	
00321	3567515.634	334055.983	715.217	????	687.000	696.200	689.000	
00330	3567551.841	334168.719	713.143	????	688.000	692.300	679.000	
00339	3567587.618	334282.803	710.942	????	686.000	688.300	682.000	
00349	3567626.862	334404.643	709.782	????	686.000	676.300	679.000	
00359	3567663.002	334518.791	709.810	????	684.000	684.300	679.000	
00369	3567698.435	334632.414	709.823	????	684.000	684.300	681.000	
00379	3567734.474	334745.561	709.874	????	686.000	688.300	685.000	
00390	3567773.839	334869.949	709.908	????	686.000	684.300	682.000	
00400	3567809.705	334982.767	709.940	????	685.000	684.300	684.000	
00410	3567845.839	335095.045	710.168	????	687.000	684.300	683.000	
00421	3567883.300	335212.393	711.533	????	687.000	688.300	683.000	
00432	3567919.438	335325.719	713.412	????	687.000	684.300	684.000	
00444	3567966.432	335449.286	715.048	????	687.000	684.300	677.000	
00455	3568021.125	335565.609	715.348	????	689.000	688.300	685.000	
00466	3568079.991	335682.199	715.536	????	690.000	696.200	689.000	
00477	3568138.842	335798.131	715.820	????	690.000	696.200	686.000	
00487	3568192.256	335902.944	716.070	????	690.000	696.200	686.000	
00498	3568250.196	336016.408	716.719	????	690.000	696.200	688.000	
00510	3568312.682	336138.943	717.637	????	694.000	696.200	694.000	
00520	3568365.524	336243.073	718.395	????	695.000	696.200	698.000	
00531	3568423.318	336359.990	719.215	????	698.000	696.200	691.000	
00542	3568472.878	336479.793	720.132	????	698.000	700.200	691.000	
00552	3568509.743	336590.023	720.981	????	699.000	700.200	690.000	
00570	3568529.024	336651.130	721.401	????	699.000	700.200	683.000	

ASHTECH POINTS FILE
PROGRAM: PRISM v2.1.00 Apr 15 1997
CREATED FROM: Point File SEC-04G.PTS

POINT	NORTHING	EASTING	HEIGHT	SITE	EASI	DMS	OrthoMAX	FFI
00012	3568528.160	336677.414	719.128	SS04	699.000	700.200	683.000	
00125	3568564.936	336791.127	722.213	????	699.000	704.200	693.000	
00135	3568605.285	336917.021	723.621	????	698.000	712.200	695.000	
00152	3568673.307	337127.374	727.587	????	704.000	704.200	702.000	
00162	3568710.055	337245.954	729.760	????	704.000	708.200	703.000	
00172	3568747.663	337364.285	731.462	????	707.000	708.200	699.000	
00181	3568781.866	337471.133	732.958	????	707.000	708.200	700.000	
00191	3568819.333	337589.385	734.598	????	707.000	716.100	705.000	
00201	3568856.942	337707.397	736.239	????	711.000	716.100	707.000	
00211	3568894.506	337825.536	737.872	????	712.000	716.100	709.000	
00221	3568932.383	337943.116	739.538	????	712.000	716.100	711.000	
00231	3568969.414	338057.125	741.125	????	715.000	716.100	708.000	
00241	3569004.985	338170.473	742.713	????	720.000	716.100	715.000	
00251	3569040.945	338285.274	743.732	????	720.000	724.100	715.000	
00261	3569079.089	338404.782	743.204	????	722.000	716.100	710.000	
00272	3569118.519	338529.442	742.628	????	722.000	720.100	714.000	

00283	3569155.960	338644.082	743.488	????	723.000	736.000	714.000
00293	3569192.563	338759.920	745.790	????	722.000	720.100	715.000
00304	3569231.375	338883.474	748.396	????	722.000	728.100	719.000
00315	3569269.514	339003.756	750.693	????	726.000	728.100	723.000
00326	3569308.315	339124.980	751.420	????	726.000	728.100	723.000
00337	3569345.416	339241.498	751.677	????	727.000	728.100	723.000
00349	3569384.190	339363.280	752.170	????	727.000	728.100	721.000
00359	3569419.953	339475.080	752.837	????	734.000	728.100	726.000
00368	3569455.384	339586.655	753.450	????	734.000	728.100	726.000
00378	3569492.891	339703.079	754.169	????	734.000	736.000	725.000
00389	3569530.585	339821.823	754.903	????	734.000	736.000	725.000
00399	3569566.872	339936.674	755.577	????	734.000	736.000	727.000
00410	3569602.222	340052.779	756.127	????	734.000	736.000	724.000
00422	3569641.242	340174.605	756.551	????	734.000	736.000	727.000
00432	3569679.604	340291.438	756.555	????	735.000	736.000	728.000
00442	3569717.282	340409.581	756.607	????	735.000	736.000	728.000
00453	3569754.925	340528.169	756.630	????	736.000	736.000	729.000
00464	3569792.387	340645.432	756.687	????	736.000	736.000	728.000
00475	3569829.696	340762.499	756.740	????	737.000	736.000	733.000
00486	3569867.631	340881.952	756.759	????	737.000	736.000	732.000
00496	3569904.643	340997.820	757.216	????	737.000	736.000	731.000
00506	3569942.145	341114.373	759.011	????	738.000	736.000	724.000
00517	3569971.622	341207.672	760.453	????	732.000	736.000	724.000

ASHTECH POINTS FILE
PROGRAM: PRISM v2.1.00 Apr 15 1997
CREATED FROM: Point File SEC-05G.PTS

POINT	NORTHING	EASTING	HEIGHT	SITE	EASI	DMS	OrthoMAX	FFI
00013	3569971.892	341181.397	758.010	SS05	738.000	732.200		
00127	3570005.686	341299.991	762.403	????	742.000	732.000		
00137	3570028.152	341413.554	764.024	????	742.000	732.200		
00146	3570050.304	341521.189	764.540	????	742.000	732.200		
00155	3570072.909	341630.307	764.794	????	740.000	732.200		
00165	3570096.048	341741.537	765.054	????	740.000	739.200		
00176	3570120.647	341859.905	765.871	????	744.000	743.300		
00187	3570144.767	341976.529	766.897	????	744.000	743.400		
00198	3570168.923	342093.570	767.906	????	747.000	743.400		
00208	3570191.200	342200.716	768.779	????	747.000	743.400		
00219	3570216.643	342322.742	768.913	????	747.000	743.400		
00235	3570253.987	342503.020	768.850	????	747.000	743.400		
00244	3570277.783	342618.044	768.811	????	747.000	743.400		
00253	3570301.256	342728.824	768.909	????	747.000	743.400		
00264	3570326.010	342850.074	769.001	????	747.000	743.400		
00274	3570350.286	342967.852	769.076	????	748.000	743.400		
00283	3570372.705	343075.510	769.175	????	748.000	744.800		
00293	3570396.929	343191.786	770.050	????	747.000	743.400		
00304	3570421.709	343311.767	772.066	????	749.000	743.400		
00314	3570445.130	343423.326	773.272	????	750.000	743.400		
00324	3570469.592	343542.353	772.969	????	750.000	743.400		
00334	3570493.461	343656.951	772.783	????	752.000	743.400		
00344	3570518.704	343777.117	773.318	????	752.000	743.400		
00354	3570541.858	343890.286	773.890	????	752.000	754.600		
00364	3570567.117	344000.818	774.749	????	754.000	754.600		
00375	3570609.503	344119.588	775.390	????	754.000	754.600		
00386	3570670.087	344234.519	776.810	????	758.000	754.600		
00397	3570740.145	344351.492	779.125	????	757.000	754.600		
00408	3570809.369	344467.565	780.691	????	759.000	754.600		

00419	3570880.164	344586.354	780.126	????	759.000	754.600
00431	3570951.150	344704.803	780.612	????	758.000	754.600
00442	3571021.238	344822.233	782.000	????	761.000	754.600
00455	3571093.995	344943.984	783.444	????	761.000	754.600
00468	3571166.052	345065.159	784.893	????	762.000	754.600
00479	3571225.331	345186.268	786.532	????	762.000	756.000
00488	3571263.656	345297.291	788.236	????	770.000	756.000
00498	3571300.128	345414.514	789.817	????	770.000	760.200
00508	3571336.416	345527.930	791.259	????	770.000	763.000
00519	3571374.982	345650.387	791.931	????	770.000	765.800
00530	3571413.163	345770.107	792.546	????	769.000	767.200
00542	3571449.825	345886.137	793.074	????	769.000	765.800

ASHTECH POINTS FILE
PROGRAM: PRISM v2.1.00 Apr 15 1997
CREATED FROM: Point File SEC-06G.PTS
UNITS: METER METER

POINT	NORTHING	EASTING	HEIGHT	SITE	EASI	DMS	OrthoMAX	FFI
00033	3571450.943	345889.562	790.708	SS06	769.000	765.800		
00118	3571485.611	345997.108	792.666	????	769.000	765.800		
00131	3571525.165	346121.162	791.790	????	771.000	765.800		
00141	3571560.074	346231.065	791.059	????	771.000	767.200		
00151	3571596.686	346346.415	791.544	????	771.000	767.200		
00161	3571633.472	346462.043	792.370	????	771.000	767.200		
00172	3571671.679	346581.866	793.207	????	772.000	767.200		
00182	3571708.700	346698.525	793.398	????	772.000	767.200		
00193	3571746.022	346815.333	793.151	????	771.000	767.200		
00203	3571781.960	346928.973	792.809	????	771.000	767.200		
00214	3571819.680	347047.501	792.447	????	771.000	767.200		
00226	3571857.905	347167.922	793.517	????	771.000	767.200		
00238	3571894.662	347283.223	795.882	????	771.000	767.200		
00250	3571931.583	347399.252	798.247	????	774.000	767.200		
00262	3571970.385	347521.088	800.597	????	774.000	767.200		
00273	3572007.040	347636.261	800.687	????	774.000	767.200		
00283	3572041.542	347744.176	800.368	????	779.000	767.200		
00294	3572079.902	347865.584	799.902	????	778.000	767.200		
00305	3572118.172	347984.524	799.422	????	778.000	767.200		
00316	3572155.381	348101.833	798.993	????	778.000	765.800		
00326	3572191.527	348215.073	798.851	????	780.000	765.800		
00336	3572228.571	348332.147	799.804	????	780.000	778.300		
00347	3572265.095	348446.510	800.916	????	782.000	778.300		
00358	3572302.622	348563.973	802.051	????	780.000	779.700		
00368	3572339.488	348680.123	803.255	????	785.000	777.000		
00378	3572376.552	348796.583	804.585	????	785.000	778.300		
00387	3572410.658	348903.955	805.843	????	785.000	788.100		
00398	3572448.326	349022.016	807.270	????	785.000	779.800		
00409	3572486.171	349140.153	808.773	????	785.000	779.700		
00420	3572523.583	349260.228	809.393	????	787.000	778.300		
00431	3572562.220	349377.741	808.980	????	784.000	778.300		
00442	3572599.477	349495.295	808.446	????	785.000	777.000		
00453	3572637.066	349612.619	808.009	????	785.000	778.300		
00464	3572674.665	349730.389	807.589	????	782.000	778.300		
00474	3572710.024	349840.597	807.469	????	782.000	778.300		
00484	3572745.463	349952.216	808.028	????	782.000	778.300		
00494	3572780.996	350063.197	808.662	????	785.000	778.300		
00505	3572820.085	350184.433	809.395	????	785.000	779.700		
00515	3572855.149	350295.343	809.690	????	785.000	779.700		

00525	3572891.177	350408.392	809.428	????	785.000	778.300
00535	3572926.184	350518.340	809.162	????	786.000	779.700
00546	3572964.792	350638.988	808.917	????	786.000	778.300
00557	3573000.660	350751.645	810.056	????	788.000	778.300

ASHTECH POINTS FILE
PROGRAM: PRISM v2.1.00 Apr 15 1997
CREATED FROM: Point File SEC-07G.PTS
UNITS: METER METER

POINT	NORTHING	EASTING	HEIGHT	SITE	EASI	DMS	OrthoMAX	FFI
00012	3573003.879	350761.899	808.004	SS07	788.000	778.300		
00123	3573042.411	350882.625	812.432	????	788.000	778.300		
00132	3573079.544	350998.797	814.423	????	789.000	779.700		
00143	3573118.148	351119.617	815.653	????	793.000	789.500		
00154	3573155.379	351236.115	816.824	????	794.000	789.500		
00163	3573192.192	351351.706	818.043	????	794.000	789.500		
00172	3573227.853	351462.500	819.944	????	794.000	790.900		
00182	3573266.691	351584.443	822.067	????	796.000	789.500		
00191	3573301.987	351695.510	823.993	????	796.000	790.900		
00200	3573335.526	351812.300	824.259	????	800.000	790.900		
00209	3573366.162	351928.171	823.643	????	800.000	790.900		
00219	3573397.274	352046.936	824.011	????	800.000	790.900		
00229	3573427.892	352163.568	824.903	????	803.000	796.500		
00239	3573458.273	352279.105	825.829	????	803.000	800.700		
00249	3573488.384	352393.722	826.794	????	805.000	802.100		
00259	3573519.146	352511.800	827.708	????	805.000	802.100		
00268	3573548.120	352621.325	828.294	????	806.000	802.100		
00277	3573578.025	352735.283	827.792	????	806.000	802.100		
00285	3573604.865	352837.699	827.228	????	806.000	800.700		
00295	3573636.099	352956.356	826.590	????	807.000	802.100		
00305	3573664.877	353066.021	826.800	????	807.000	802.100		
00316	3573695.645	353183.094	827.352	????	807.000	802.100		
00327	3573726.513	353300.246	827.938	????	807.000	802.100		
00338	3573757.564	353418.911	828.547	????	808.000	802.100		
00348	3573786.893	353529.621	829.134	????	808.000	802.100		
00358	3573816.131	353641.792	829.414	????	807.000	802.100		
00368	3573846.740	353758.380	829.008	????	807.000	803.500		
00378	3573877.544	353875.414	828.604	????	811.000	802.100		
00388	3573908.447	353992.638	828.256	????	809.000	803.500		
00398	3573938.952	354109.074	828.810	????	809.000	803.500		
00408	3573970.124	354226.593	829.532	????	808.000	802.100		
00419	3574002.059	354347.110	829.931	????	808.000	802.100		
00429	3574030.926	354458.550	829.830	????	807.000	802.100		
00439	3574060.317	354570.941	829.788	????	807.000	802.100		
00449	3574089.936	354683.637	829.763	????	807.000	802.100		
00459	3574119.149	354795.002	829.831	????	809.000	802.100		
00470	3574137.513	354865.380	830.701	????	808.000	802.100		

ASHTECH POINTS FILE
PROGRAM: PRISM v2.1.00 Apr 15 1997
CREATED FROM: Point File SEC-08G.PTS

POINT	NORTHING	EASTING	HEIGHT	SITE	EASI	DMS	OrthoMAX	FFI
00009	3574137.298	354865.421	828.966	SS08	808.000	802.100		
00120	3574166.699	354976.013	833.080	????	817.000	802.100		
00130	3574197.591	355094.290	835.640	????	817.000	802.100		

00139	3574225.500	355200.612	837.971	????	817.000	803.500
00149	3574256.505	355318.845	840.551	????	819.000	814.700
00159	3574287.684	355437.626	843.131	????	819.000	813.300
00169	3574318.847	355556.630	845.729	????	825.000	814.700
00179	3574350.422	355675.950	848.165	????	825.000	814.700
00188	3574382.512	355787.223	849.630	????	828.000	813.300
00198	3574419.488	355903.374	851.083	????	835.000	823.100
00208	3574457.109	356018.074	852.540	????	835.000	824.500
00218	3574495.993	356136.753	854.125	????	835.000	824.500
00228	3574534.584	356253.748	855.618	????	835.000	825.900
00238	3574571.356	356365.441	858.347	????	839.000	825.900
00249	3574608.645	356478.549	862.352	????	839.000	825.900
00260	3574645.909	356591.643	866.373	????	844.000	835.700
00270	3574684.381	356708.887	870.554	????	852.000	835.700
00280	3574723.242	356825.857	874.814	????	858.000	835.700
00290	3574761.391	356943.325	877.745	????	858.000	835.700
00299	3574797.927	357054.155	879.515	????	858.000	841.300
00310	3574838.616	357177.803	881.528	????	862.000	846.900
00320	3574875.015	357288.243	884.137	????	862.000	848.300
00331	3574913.488	357404.358	889.058	????	865.000	851.000
00342	3574950.846	357517.978	893.913	????	873.000	858.000
00352	3574988.925	357633.753	897.505	????	879.000	859.400
00362	3575029.773	357757.862	899.982	????	879.000	860.800
00372	3575068.997	357876.657	899.402	????	873.000	860.800
00381	3575105.457	357988.068	896.620	????	873.000	856.600
00392	3575143.833	358103.451	895.750	????	873.000	855.200
00402	3575182.291	358219.845	897.920	????	875.000	859.400
00413	3575220.484	358337.059	902.772	????	875.000	859.400
00423	3575258.158	358451.900	906.077	????	884.000	858.000
00433	3575295.683	358565.620	907.429	????	884.000	870.600
00443	3575331.702	358676.186	908.586	????	885.000	872.000
00454	3575371.730	358797.113	909.788	????	885.000	880.400
00464	3575400.621	358911.584	910.250	????	883.000	883.200
00473	3575418.425	359024.324	908.448	????	883.000	883.300
00483	3575435.532	359145.085	905.341	????	883.000	876.200
00493	3575452.024	359263.356	904.393	????	883.000	855.200
00502	3575466.796	359369.737	906.063	????	883.000	862.200
00511	3575482.927	359486.033	910.263	????	889.000	872.000
00520	3575498.696	359597.698	914.603	????	889.000	872.000
00529	3575514.355	359710.599	918.523	????	901.000	874.800
00538	3575529.942	359823.400	922.145	????	901.000	884.600
00547	3575545.840	359940.129	925.031	????	901.000	881.800

ASHTECH POINTS FILE
PROGRAM: PRISM v2.1.00 Apr 15 1997
CREATED FROM: Point File SEC-09G.PTS
UNITS: METER METER

POINT	NORTHING	EASTING	HEIGHT	SITE	EASI	DMS	OrthoMAX	FFI
00010	3575552.582	359989.586	922.768	SS09	902.000	881.000		
00122	3575569.555	360111.666	926.380	????	902.000	884.600		
00132	3575585.795	360228.760	927.141	????	908.000	883.200		
00143	3575602.590	360350.081	928.197	????	908.000	895.800		
00152	3575617.793	360460.089	929.346	????	908.000	895.800		
00161	3575634.166	360577.572	931.839	????	911.000	902.800		
00170	3575650.370	360694.312	935.215	????	911.000	908.400		
00179	3575665.855	360806.280	938.261	????	919.000	905.600		
00188	3575680.141	360918.872	940.219	????	919.000	907.000		

00198	3575697.071	361035.675	941.719	????	914.000	905.600
00207	3575714.879	361146.305	941.500	????	922.000	905.600
00216	3575729.079	361262.759	940.328	????	920.000	907.000
00233	3575763.027	361478.216	940.692	????	920.000	918.200
00243	3575791.475	361594.830	942.546	????	922.000	918.200
00253	3575823.408	361708.077	944.350	????	922.000	918.200
00263	3575855.683	361821.664	945.899	????	925.000	918.200
00273	3575888.712	361938.528	946.804	????	925.000	918.200
00283	3575922.061	362056.175	947.655	????	929.000	918.200
00293	3575955.546	362174.740	948.537	????	929.000	918.200
00303	3575989.897	362296.067	949.422	????	929.000	919.600
00312	3576021.470	362407.864	950.456	????	932.000	923.700
00322	3576054.728	362525.340	953.191	????	932.000	925.100
00332	3576089.506	362648.711	956.497	????	938.000	927.900
00342	3576123.694	362769.204	959.693	????	938.000	929.300
00352	3576157.057	362887.304	962.803	????	942.000	929.300
00362	3576189.328	363000.142	965.839	????	942.000	930.700
00373	3576223.515	363120.870	969.018	????	945.000	929.300
00383	3576261.493	363247.304	971.116	????	947.000	934.900
00392	3576293.597	363369.395	969.462	????	947.000	939.100
00401	3576326.843	363487.680	967.298	????	947.000	940.500
00410	3576358.315	363597.723	965.125	????	947.000	941.900
00419	3576391.962	363715.609	960.687	????	941.000	940.500
00429	3576424.713	363832.107	955.658	????	941.000	940.500
00438	3576458.854	363950.518	952.120	????	937.000	940.500
00448	3576492.507	364071.475	950.998	????	937.000	940.500
00458	3576525.900	364188.831	950.017	????	932.000	937.700
00467	3576557.379	364300.111	949.585	????	932.000	934.700
00477	3576591.521	364420.238	949.577	????	932.000	929.300
00487	3576625.198	364540.247	949.545	????	932.000	937.700
00497	3576659.701	364660.623	949.552	????	932.000	934.900
00507	3576693.931	364781.455	949.549	????	934.000	929.300
00517	3576728.397	364902.779	949.520	????	934.000	929.300
00527	3576762.742	365024.310	949.519	????	929.000	934.900
00538	3576789.829	365120.080	949.501	????	929.000	941.900

ASHTECH POINTS FILE
PROGRAM: PRISM v2.1.00 Apr 15 1997
CREATED FROM: Point File SEC-10G.PTS
UNITS: METER METER

POINT	NORTHING	EASTING	HEIGHT	SITE	EASI	DMS	OrthoMAX	FFI
00120	3576823.853	365239.137	949.470	????	930.000	932.100		
00130	3576857.376	365357.866	949.450	????	930.000	929.300		
00140	3576891.191	365476.807	949.429	????	933.000	929.300		
00150	3576924.734	365594.582	949.414	????	933.000	930.700		
00160	3576957.952	365712.599	949.398	????	933.000	930.700		
00170	3576991.789	365832.077	949.025	????	933.000	930.700		
00180	3577026.574	365954.747	948.214	????	930.000	930.700		
00190	3577061.276	366077.452	947.369	????	929.000	929.300		
00200	3577095.167	366196.475	947.630	????	929.000	921.000		
00210	3577127.611	366311.072	948.331	????	930.000	918.200		
00220	3577159.938	366425.553	948.849	????	930.000	918.000		
00230	3577194.132	366544.048	948.390	????	928.000	918.200		
00240	3577228.090	366665.227	947.855	????	928.000	918.200		
00250	3577262.971	366788.585	947.323	????	927.000	919.600		
00259	3577293.890	366897.342	946.862	????	929.000	918.200		
00269	3577328.264	367018.215	946.334	????	929.000	918.200		

00279	3577362.221	367137.514	947.309	????	926.000	918.200
00289	3577394.447	367251.637	949.650	????	926.000	918.200
00300	3577428.665	367372.119	951.836	????	929.000	918.200
00310	3577462.075	367489.515	952.246	????	929.000	918.200
00320	3577495.334	367606.787	952.361	????	927.000	918.200
00331	3577531.939	367735.437	952.475	????	927.000	918.200
00341	3577565.014	367852.480	952.500	????	933.000	918.200
00352	3577594.930	367983.047	952.614	????	933.000	918.200
00363	3577616.304	368114.337	952.764	????	930.000	918.200
00373	3577635.700	368234.144	952.838	????	930.000	918.200
00383	3577654.991	368354.349	952.828	????	930.000	916.800
00393	3577674.172	368476.432	951.290	????	927.000	916.800
00403	3577693.086	368595.976	949.045	????	927.000	916.800
00413	3577711.912	368713.788	946.843	????	924.000	916.800
00423	3577729.709	368828.180	945.574	????	924.000	918.200
00434	3577749.090	368949.843	946.137	????	924.000	918.200
00444	3577767.053	369061.528	946.678	????	924.000	916.800
00455	3577786.534	369185.436	947.237	????	926.000	918.200
00466	3577805.995	369309.485	947.801	????	926.000	919.600
00477	3577824.503	369427.868	948.513	????	931.000	918.200
00489	3577843.927	369550.025	949.455	????	931.000	918.200
00501	3577863.005	369672.150	950.403	????	931.000	918.200
00513	3577881.894	369791.676	951.355	????	932.000	918.200
00525	3577901.774	369917.009	952.345	????	932.000	918.200
00540	3577921.933	370043.108	953.293	????	934.000	918.200

ASHTECH POINTS FILE
PROGRAM: PRISM v2.1.00 Apr 15 1997
CREATED FROM: Point File SEC-11G.PTS
UNITS: METER METER

POINT	NORTHING	EASTING	HEIGHT	SITE	EASI	DMS	OrthoMAX	FFI
00004	3577920.680	370034.004	951.077	SS11	934.000	918.200		
00073	3577942.406	370159.781	954.190	????	934.000	918.200		
00077	3577960.197	370274.445	954.951	????	932.000	918.200		
00081	3577979.147	370391.870	955.753	????	932.000	918.200		
00085	3577997.417	370510.824	956.480	????	931.000	918.200		
00089	3578017.426	370633.384	955.409	????	931.000	918.200		
00093	3578036.476	370752.832	953.065	????	925.000	918.200		
00097	3578055.694	370875.449	950.639	????	925.000	918.200		
00101	3578075.329	370999.159	948.230	????	924.000	918.200		
00105	3578095.775	371127.458	945.691	????	924.000	918.200		
00109	3578115.444	371253.279	943.193	????	924.000	918.200		
00113	3578132.775	371369.983	940.811	????	920.000	912.600		
00117	3578149.731	371477.223	938.941	????	920.000	905.600		
00122	3578167.923	371592.147	937.607	????	914.000	907.000		
00129	3578186.075	371706.488	936.301	????	914.000	907.000		
00139	3578206.170	371831.062	934.751	????	910.000	907.000		
00148	3578224.754	371953.169	931.883	????	910.000	907.000		
00156	3578242.400	372064.072	928.994	????	905.000	905.600		
00165	3578260.695	372180.548	925.965	????	905.000	905.000		
00175	3578281.240	372309.288	922.674	????	900.000	898.600		
00184	3578300.646	372431.004	920.449	????	900.000	895.800		
00193	3578318.870	372546.277	918.688	????	900.000	894.400		
00202	3578337.377	372663.494	916.860	????	898.000	984.400		
00211	3578355.891	372780.026	915.058	????	898.000	894.400		
00221	3578376.338	372908.956	913.292	????	893.000	894.400		
00231	3578396.147	373033.709	912.332	????	893.000	891.600		

00241	3578415.641	373156.565	911.375	????	890.000	884.600
00251	3578435.182	373279.833	910.299	????	890.000	886.000
00261	3578454.885	373404.638	909.003	????	888.000	884.600
00270	3578473.158	373519.637	907.199	????	888.000	884.600
00279	3578491.808	373636.991	905.186	????	886.000	879.000
00288	3578510.347	373754.419	903.182	????	886.000	873.400
00297	3578528.661	373870.610	902.038	????	886.000	873.400
00307	3578548.282	373993.561	901.961	????	882.000	872.000
00316	3578566.526	374109.071	901.888	????	882.000	872.000
00326	3578585.523	374229.347	901.663	????	876.000	872.000
00335	3578604.947	374351.458	900.793	????	874.000	872.000
00343	3578623.533	374467.719	899.980	????	874.000	869.000
00351	3578642.359	374586.545	898.985	????	874.000	863.600
00359	3578662.173	374711.329	896.123	????	866.000	859.400
00367	3578681.237	374833.470	892.800	????	866.000	860.800
00376	3578700.232	374953.806	889.500	????	863.000	860.300
00384	3578709.426	375011.097	887.974	????	863.000	860.800

ASHTECH POINTS FILE
PROGRAM: PRISM v2.1.00 Apr 15 1997
CREATED FROM: Point File SEC-12G.PTS
UNITS: METER METER

POINT	NORTHING	EASTING	HEIGHT	SITE	EASI	DMS	OrhoMAX	FFI
00007	3578709.368	375016.985	885.889	SS12	863.000	859.400		
00218	3578731.224	375135.610	886.428	????	863.000	859.400		
00229	3578768.008	375254.486	885.315	????	859.000	859.400		
00240	3578816.294	375370.244	883.870	????	859.000	859.400		
00252	3578869.479	375496.079	882.927	????	859.000	860.800		
00263	3578918.378	375611.760	882.349	????	858.000	860.800		
00274	3578969.021	375731.420	881.530	????	856.000	848.300		
00284	3579016.141	375842.915	880.668	????	856.000	853.800		
00295	3579068.924	375967.723	879.526	????	856.000	846.900		
00306	3579120.636	376089.894	876.941	????	852.000	848.300		
00316	3579168.830	376203.396	874.235	????	852.000	848.300		
00327	3579219.783	376323.765	872.336	????	852.000	848.300		
00338	3579270.665	376443.754	870.715	????	847.000	835.700		
00349	3579318.806	376557.567	869.327	????	844.000	835.700		
00360	3579367.694	376672.871	868.503	????	844.000	837.100		
00371	3579418.172	376791.847	867.568	????	841.000	837.100		
00382	3579470.636	376915.491	866.306	????	841.000	837.100		
00393	3579523.390	377040.050	865.039	????	841.000	837.100		
00404	3579575.586	377163.182	863.783	????	838.000	835.700		
00415	3579624.310	377278.242	862.672	????	838.000	835.700		
00426	3579674.397	377396.191	862.019	????	835.000	837.100		
00437	3579723.779	377512.761	861.239	????	835.000	834.300		
00448	3579774.754	377632.955	859.726	????	831.000	831.500		
00459	3579827.405	377756.975	858.115	????	831.000	824.500		
00469	3579875.338	377870.307	856.643	????	832.000	824.500		
00480	3579926.323	377990.403	855.104	????	831.000	824.500		
00493	3579983.355	378123.525	854.613	????	830.000	824.500		
00504	3580031.401	378238.235	854.373	????	830.000	824.500		
00515	3580081.636	378356.680	852.712	????	826.000	824.500		
00526	3580133.881	378479.732	850.007	????	826.000	824.500		
00537	3580185.337	378600.893	847.371	????	819.000	824.500		
00549	3580236.978	378722.729	846.238	????	818.000	824.500		
00560	3580287.955	378842.889	846.245	????	818.000	824.500		
00569	3580331.680	378945.593	846.282	????	819.000	824.500		

00580	3580382.260	379064.754	845.461	????	819.000	821.700
00591	3580432.517	379183.327	843.135	????	815.000	811.900
00602	3580482.865	379301.542	840.876	????	814.000	813.300
00614	3580535.226	379424.419	839.053	????	811.000	813.300
00626	3580585.310	379542.944	837.298	????	811.000	806.000
00639	3580637.737	379664.997	835.038	????	811.000	802.100
00650	3580666.626	379733.000	832.967	????	808.000	802.100

ASHTECH POINTS FILE
PROGRAM: PRISM v2.1.00 Apr 15 1997
CREATED FROM: Point File SEC-13G.PTS
UNITS: METER METER

POINT	NORTHING	EASTING	HEIGHT	SITE	EASI	DMS	OrthoMAX	FFI
00019	3580663.282	379726.026	830.802	SS13	808.000	812.200		
00135	3580714.671	379846.670	828.680	????	804.000	810.600		
00145	3580764.031	379962.766	824.399	????	798.000	805.900		
00156	3580815.103	380081.757	821.787	????	798.000	801.200		
00167	3580865.784	380202.814	821.375	????	793.000	802.800		
00178	3580918.683	380326.907	821.110	????	793.000	802.800		
00189	3580970.488	380449.238	820.838	????	795.000	802.800		
00200	3581023.306	380573.308	820.590	????	795.000	802.800		
00210	3581073.337	380691.324	820.477	????	795.000	802.800		
00220	3581123.702	380809.940	820.308	????	791.000	793.300		
00231	3581177.602	380936.693	818.712	????	791.000	793.300		
00241	3581226.260	381051.531	817.247	????	788.000	793.300		
00252	3581277.349	381171.573	816.807	????	790.000	793.300		
00263	3581329.414	381294.434	816.723	????	786.000	793.300		
00273	3581377.954	381408.476	816.634	????	786.000	793.300		
00283	3581419.155	381525.087	814.785	????	783.000	791.700		
00293	3581440.427	381650.901	812.907	????	783.000	790.100		
00302	3581441.429	381764.794	811.647	????	783.000	783.800		
00311	3581440.130	381876.437	810.239	????	780.000	782.300		
00321	3581438.654	382002.625	809.533	????	780.000	782.300		
00330	3581437.868	382118.116	810.050	????	780.000	782.300		
00339	3581436.974	382232.415	810.568	????	780.000	782.300		
00348	3581436.161	382347.901	810.908	????	779.000	782.300		
00357	3581436.017	382465.767	810.084	????	779.000	782.300		
00367	3581434.086	382588.168	808.878	????	778.000	780.700		
00376	3581433.138	382704.330	807.763	????	779.000	782.300		
00385	3581431.059	382823.441	806.969	????	778.000	774.400		
00394	3581429.984	382939.992	806.621	????	776.000	774.400		
00403	3581428.854	383056.575	806.277	????	776.000	780.700		
00412	3581428.247	383172.271	806.131	????	776.000	782.300		
00422	3581427.248	383296.606	806.781	????	776.000	780.700		
00431	3581426.669	383406.422	807.458	????	776.000	783.800		
00441	3581425.287	383528.889	808.093	????	776.000	782.300		
00450	3581423.888	383640.649	808.214	????	777.000	774.400		
00460	3581422.200	383761.540	807.903	????	777.000	771.200		
00470	3581420.470	383884.438	807.023	????	777.000	771.200		
00480	3581420.236	384007.119	806.050	????	777.000	783.800		
00490	3581418.939	384127.373	805.908	????	777.000	783.800		
00501	3581418.074	384255.973	806.028	????	775.000	776.000		
00511	3581416.590	384375.097	804.438	????	775.000	772.800		
00521	3581415.542	384474.300	802.126	????	771.000	772.800		
00525	3581415.388	384491.286	801.717	????	771.000	772.800		

ASHTECH POINTS FILE

PROGRAM: PRISM v2.1.00 Apr 15 1997
CREATED FROM: Point File SEC-14G.PTS
UNITS: METER METER

POINT	NORTHING	EASTING	HEIGHT	SITE	EASI	DMS	OrthoMAX	FFI
00096	3581414.194	384617.702	799.071	????	771.000	771.000		
00105	3581413.397	384733.404	798.294	????	767.000	771.200		
00115	3581412.390	384854.030	798.707	????	767.000	771.200		
00125	3581410.678	384972.006	799.081	????	768.000	768.100		
00135	3581410.205	385090.474	799.218	????	768.000	763.400		
00145	3581408.594	385216.823	797.892	????	765.000	760.200		
00154	3581407.584	385330.993	796.232	????	765.000	766.500		
00164	3581406.535	385456.992	794.531	????	766.000	771.200		
00173	3581405.661	385568.291	794.473	????	766.000	772.800		
00183	3581403.991	385686.615	795.475	????	766.000	771.200		
00192	3581403.187	385802.940	795.754	????	765.000	771.200		
00202	3581401.958	385927.707	795.824	????	765.000	771.200		
00212	3581400.812	386052.404	795.890	????	767.000	772.800		
00222	3581399.709	386176.949	795.947	????	767.000	771.200		
00231	3581398.549	386288.907	796.203	????	770.000	772.800		
00241	3581397.540	386412.360	798.244	????	770.000	771.200		
00250	3581395.318	386525.578	800.482	????	772.000	772.800		
00260	3581393.756	386648.895	802.746	????	772.000	771.200		
00269	3581394.056	386767.689	803.210	????	772.000	772.800		
00278	3581393.043	386883.427	802.213	????	773.000	772.800		
00288	3581392.470	387004.054	801.381	????	773.000	772.800		
00298	3581404.608	387124.344	800.332	????	772.000	771.200		
00308	3581438.072	387241.742	799.187	????	772.000	771.200		
00319	3581495.085	387365.131	797.625	????	769.000	774.400		
00330	3581552.997	387482.713	797.295	????	769.000	768.100		
00341	3581609.138	387596.156	797.608	????	768.000	771.200		
00352	3581665.793	387710.131	797.894	????	768.000	772.800		
00363	3581724.982	387829.935	797.897	????	768.000	771.200		
00374	3581787.714	387954.652	797.361	????	771.000	771.200		
00384	3581843.076	388069.688	796.817	????	771.000	771.200		
00394	3581899.130	388183.909	796.218	????	768.000	772.800		
00405	3581961.172	388309.319	795.211	????	768.000	772.800		
00415	3582018.278	388425.192	793.345	????	765.000	763.400		
00426	3582078.877	388547.408	791.336	????	765.000	761.800		
00437	3582139.424	388669.606	789.329	????	758.000	761.800		
00448	3582200.337	388791.072	787.389	????	758.000	763.400		
00459	3582255.650	388905.836	784.528	????	752.000	757.100		
00483	3582377.263	389150.023	775.362	????	746.000	749.200		
00492	3582408.389	389214.665	772.947	????	746.000	739.700		

ASHTECH POINTS FILE
PROGRAM: PRISM v2.1.00 Apr 15 1997
CREATED FROM: Point File SEC-15G.PTS
UNITS: METER METER

POINT	NORTHING	EASTING	HEIGHT	SITE	EASI	DMS	OrthoMAX	FFI
00114	3582467.407	389333.405	770.078	????	746.000	741.300		
00124	3582522.789	389444.890	768.542	????	738.000	741.300		
00135	3582582.597	389566.001	766.867	????	739.000	741.300		
00145	3582639.574	389681.009	764.270	????	734.000	742.900		
00156	3582702.046	389806.729	761.312	????	734.000	736.600		
00167	3582763.421	389927.815	761.011	????	730.000	730.300		

00177	3582817.186	390042.057	762.980	????	734.000	731.900
00189	3582879.559	390169.144	765.303	????	734.000	722.400
00200	3582941.876	390292.098	764.671	????	730.000	727.100
00212	3583002.900	390412.359	760.771	????	730.000	724.000
00222	3583058.236	390527.866	755.941	????	724.000	731.900
00233	3583117.606	390648.850	750.923	????	726.000	722.400
00244	3583175.343	390765.335	747.237	????	720.000	720.800
00255	3583233.542	390883.205	746.157	????	720.000	722.400
00265	3583292.177	391001.560	745.460	????	720.000	720.800
00275	3583351.002	391119.937	744.809	????	717.000	720.800
00285	3583408.939	391237.733	744.477	????	717.000	720.800
00296	3583468.401	391358.514	745.972	????	720.000	720.800
00306	3583527.143	391477.467	747.628	????	720.000	719.300
00316	3583582.884	391590.105	747.502	????	720.000	720.800
00326	3583641.997	391709.637	745.783	????	717.000	720.800
00336	3583699.907	391826.514	744.485	????	717.000	720.800
00346	3583755.947	391940.192	743.789	????	717.000	720.800
00357	3583817.768	392064.673	743.075	????	715.000	719.300
00367	3583876.264	392182.455	742.337	????	716.000	719.300
00378	3583933.408	392303.231	741.585	????	715.000	711.400
00389	3583984.720	392425.055	740.241	????	715.000	711.400
00399	3584024.565	392547.294	737.463	????	715.000	711.400
00408	3584061.798	392659.814	734.885	????	711.000	711.400
00419	3584103.756	392786.460	734.232	????	711.000	709.000
00431	3584146.158	392915.081	735.358	????	707.000	709.800
00440	3584183.803	393029.075	734.699	????	707.000	711.400
00450	3584225.660	393156.376	733.311	????	708.000	709.800
00459	3584262.121	393266.131	732.135	????	708.000	709.800
00469	3584302.580	393388.468	731.044	????	708.000	709.800
00479	3584341.318	393505.048	731.929	????	708.000	709.800
00488	3584378.678	393619.702	733.168	????	709.000	709.800
00499	3584415.792	393734.021	733.030	????	707.000	709.800

ASHTECH POINTS FILE
PROGRAM: PRISM v2.1.00 Apr 15 1997
CREATED FROM: Point File SEC-16G.PTS
UNITS: METER METER

POINT	NORTHING	EASTING	HEIGHT	SITE	EASI	DMS	OrthoMAX	FFI
00121	3584456.545	393856.874	731.956	????	707.000	709.800		
00131	3584496.499	393977.369	732.549	????	710.000	709.800		
00140	3584533.526	394091.182	734.740	????	710.000	709.800		
00150	3584573.630	394214.260	737.611	????	712.000	709.800		
00160	3584638.320	394329.960	739.045	????	712.000	709.000		
00173	3584748.320	394446.029	737.873	????	713.000	709.800		
00187	3584868.172	394565.327	737.072	????	713.000	709.800		
00200	3584979.740	394676.820	736.259	????	711.000	709.800		
00214	3585100.076	394796.695	735.453	????	711.000	709.800		
00228	3585220.362	394916.566	734.614	????	709.000	709.800		
00242	3585340.605	395036.496	733.771	????	710.000	709.800		
00256	3585461.419	395156.842	732.935	????	710.000	709.800		
00270	3585580.687	395275.404	732.195	????	707.000	700.400		
00284	3585698.074	395392.376	731.842	????	707.000	700.400		
00298	3585814.559	395509.334	731.526	????	705.000	698.800		
00312	3585933.494	395627.429	730.623	????	705.000	698.800		
00326	3586059.010	395752.419	728.338	????	702.000	700.400		
00340	3586178.977	395872.218	727.560	????	702.000	700.400		
00354	3586296.712	395989.644	727.334	????	703.000	700.400		

00369	3586422.620	396115.280	727.105	????	703.000	700.400
00383	3586540.620	396232.949	726.864	????	703.000	700.400
00397	3586665.015	396356.782	724.787	????	702.000	700.400
00410	3586778.362	396469.830	723.228	????	699.000	700.400
00425	3586903.449	396594.348	724.250	????	702.000	700.400
00438	3587014.291	396705.173	724.111	????	702.000	700.400
00451	3587131.919	396822.360	721.339	????	697.000	700.400
00465	3587254.333	396944.022	718.906	????	697.000	700.400
00478	3587369.618	397058.799	718.842	????	694.000	689.300
00490	3587469.442	397178.674	718.748	????	694.000	689.300
00500	3587519.922	397299.410	719.013	????	694.000	689.300
00510	3587562.153	397421.780	718.937	????	695.000	689.300
00521	3587601.071	397544.702	718.678	????	695.000	689.300
00533	3587640.271	397662.566	718.376	????	693.000	689.300

ASHTECH POINTS FILE
PROGRAM: PRISM v2.1.00 Apr 15 1997
CREATED FROM: Point File SEC-17G.PTS
UNITS: METER METER

POINT	NORTHING	EASTING	HEIGHT	SITE	EASI	DMS	OrthoMAX	FFI
00125	3587686.641	397798.537	716.736	????	693.000	689.300		
00135	3587726.211	397916.671	715.111	????	692.000	689.300		
00145	3587764.603	398031.634	714.618	????	692.000	689.300		
00156	3587804.493	398151.181	715.116	????	692.000	689.300		
00167	3587844.566	398270.488	715.617	????	689.000	689.300		
00178	3587884.884	398390.801	716.118	????	691.000	689.300		
00189	3587925.814	398513.346	716.585	????	691.000	689.300		
00198	3587963.731	398626.518	716.002	????	687.000	689.300		
00207	3588002.273	398741.840	714.995	????	687.000	689.300		
00216	3588040.446	398856.282	713.973	????	687.000	684.600		
00225	3588078.799	398970.700	712.941	????	687.000	679.900		
00235	3588119.806	399092.859	711.844	????	687.000	687.800		
00245	3588160.102	399214.024	710.847	????	687.000	678.300		
00255	3588200.555	399334.286	710.973	????	687.000	678.300		
00265	3588241.471	399456.886	712.220	????	689.000	678.300		
00275	3588282.714	399579.825	713.557	????	689.000	686.200		
00284	3588320.349	399692.147	714.371	????	687.000	686.200		
00294	3588362.329	399817.438	713.955	????	685.000	678.300		
00304	3588405.060	399941.378	712.428	????	685.000	679.900		
00314	3588445.755	400067.155	710.734	????	685.000	679.900		
00324	3588486.283	400188.651	710.074	????	685.000	679.900		
00333	3588523.409	400299.370	709.894	????	685.000	679.900		
00343	3588564.201	400421.067	709.704	????	685.000	679.900		
00353	3588604.593	400540.669	709.523	????	684.000	679.900		
00363	3588644.860	400661.007	709.321	????	684.000	679.900		
00373	3588685.393	400782.648	709.133	????	684.000	679.900		
00383	3588726.306	400905.463	708.755	????	684.000	679.900		
00392	3588764.040	401017.143	708.175	????	684.000	679.900		
00402	3588805.648	401141.904	707.483	????	684.000	679.900		
00412	3588847.457	401267.019	706.791	????	685.000	679.900		
00422	3588888.904	401390.586	706.384	????	683.000	679.900		
00432	3588928.975	401510.691	706.384	????	684.000	679.900		
00442	3588969.347	401630.746	706.373	????	684.000	679.900		
00452	3589009.795	401752.042	706.342	????	684.000	679.900		
00462	3589050.193	401873.196	705.967	????	683.000	679.900		
00473	3589092.895	402000.292	705.292	????	683.000	679.900		
00484	3589134.510	402125.792	704.610	????	681.000	679.900		

00494	3589172.576	402239.463	704.022	????	681.000	679.900
00506	3589209.210	402349.657	703.813	????	681.000	679.900

ASHTECH POINTS FILE
PROGRAM: PRISM v2.1.00 Apr 15 1997
CREATED FROM: Point File SEC-18G.PTS

POINT	NORTHING	EASTING	HEIGHT	SITE	EASI	DMS	OrthoMAX	FFI
00121	3589249.256	402467.832	703.824	????	681.000	675.100		
00130	3589287.310	402582.110	703.812	????	680.000	678.300		
00139	3589325.031	402695.094	703.809	????	680.000	678.300		
00149	3589366.261	402818.344	703.686	????	679.000	673.600		
00159	3589406.708	402939.103	703.421	????	680.000	668.800		
00169	3589446.822	403058.843	703.171	????	680.000	670.400		
00179	3589486.568	403177.623	702.917	????	679.000	668.800		
00189	3589526.424	403297.401	702.654	????	679.000	668.800		
00199	3589566.675	403417.141	702.359	????	678.000	670.400		
00209	3589607.536	403539.302	701.789	????	678.000	670.400		
00219	3589648.323	403661.349	701.204	????	677.000	668.800		
00229	3589688.640	403781.887	700.683	????	677.000	668.800		
00239	3589729.131	403902.553	700.224	????	675.000	668.800		
00249	3589768.738	404023.004	699.804	????	675.000	668.800		
00259	3589810.040	404144.323	699.325	????	674.000	668.800		
00269	3589851.149	404267.590	698.791	????	674.000	668.800		
00279	3589892.053	404389.384	698.335	????	673.000	668.800		
00289	3589931.523	404507.735	698.055	????	673.000	668.800		
00299	3589971.446	404627.094	697.829	????	673.000	668.800		
00309	3590012.046	404747.789	697.546	????	672.000	668.800		
00319	3590052.532	404868.762	697.173	????	672.000	668.800		
00329	3590092.964	404990.201	696.753	????	671.000	668.800		
00339	3590133.975	405112.807	696.161	????	671.000	665.700		
00349	3590175.285	405235.744	695.557	????	671.000	661.000		
00359	3590216.243	405357.726	695.216	????	671.000	661.000		
00369	3590255.729	405476.230	695.271	????	670.000	659.400		
00379	3590295.737	405595.050	695.316	????	670.000	659.400		
00389	3590336.587	405717.519	694.974	????	670.000	661.000		
00399	3590377.017	405838.568	694.537	????	670.000	659.400		
00409	3590416.365	405956.675	694.106	????	670.000	659.400		
00419	3590456.014	406074.904	693.689	????	670.000	659.400		
00429	3590495.891	406194.714	693.242	????	670.000	659.400		
00439	3590535.909	406313.317	692.988	????	699.000	659.400		
00449	3590575.020	406430.309	692.987	????	669.000	659.400		
00459	3590613.692	406545.892	692.970	????	668.000	659.400		
00469	3590652.959	406663.051	692.936	????	668.000	659.400		
00479	3590693.073	406783.046	692.907	????	668.000	659.400		
00488	3590728.800	406890.365	692.877	????	669.000	659.400		
00500	3590769.022	407011.248	692.860	????	669.000	659.400		

ASHTECH POINTS FILE
PROGRAM: PRISM v2.1.00 Apr 15 1997
CREATED FROM: Point File SEC-19G.PTS
UNITS: METER METER

POINT	NORTHING	EASTING	HEIGHT	SITE	EASI	DMS	OrthoMAX	FFI
00085	3590810.176	407133.360	692.819	????	668.000	659.400		
00095	3590850.040	407252.232	692.648	????	668.000	659.400		
00105	3590889.449	407370.444	692.181	????	667.000	659.400		

00115	3590929.432	407489.617	691.722	????	667.000	659.400
00125	3590968.894	407608.307	691.298	????	666.000	659.400
00135	3591009.051	407727.929	690.856	????	666.000	659.400
00145	3591049.353	407848.200	690.368	????	665.000	659.400
00155	3591089.512	407968.577	689.921	????	665.000	659.400
00165	3591129.740	408088.495	689.495	????	664.000	659.400
00175	3591169.687	408207.946	689.020	????	664.000	659.400
00185	3591209.872	408327.737	688.568	????	664.000	657.800
00195	3591250.066	408447.972	688.125	????	662.000	657.800
00205	3591290.366	408568.647	687.602	????	662.000	654.700
00214	3591327.149	408678.258	687.152	????	662.000	649.900
00224	3591367.410	408799.304	686.755	????	662.000	648.400
00233	3591403.165	408905.657	686.894	????	663.000	648.400
00243	3591442.894	409024.038	687.010	????	663.000	648.400
00253	3591482.192	409139.674	687.320	????	663.000	648.400
00264	3591529.656	409266.884	687.241	????	663.000	649.900
00274	3591575.732	409382.627	687.023	????	663.000	648.400
00285	3591623.679	409503.268	686.959	????	663.000	659.400
00296	3591670.834	409622.143	686.911	????	663.000	657.800
00309	3591717.100	409740.651	686.845	????	663.000	659.400
00327	3591763.519	409860.170	686.843	????	663.000	659.400
00340	3591813.853	409984.215	687.127	????	663.000	659.400
00352	3591866.209	410115.635	687.784	????	663.000	657.800
00362	3591912.983	410233.459	688.357	????	663.000	659.400
00372	3591960.617	410354.430	688.368	????	663.000	657.800
00382	3592009.238	410476.504	688.007	????	664.000	657.800
00392	3592056.524	410595.510	687.770	????	664.000	659.400
00402	3592101.911	410709.669	688.625	????	664.000	657.800
00412	3592146.704	410822.882	689.715	????	664.000	657.800
00422	3592194.150	410942.762	690.845	????	664.000	659.400
00433	3592244.043	411068.093	691.182	????	666.000	659.400
00443	3592290.723	411185.900	691.216	????	667.000	659.400
00453	3592339.187	411308.162	691.231	????	667.000	657.800
00463	3592387.578	411430.183	691.234	????	667.000	659.400
00473	3592436.165	411552.746	691.283	????	666.000	657.800
00484	3592483.142	411671.962	691.291	????	666.000	657.800

ASHTECH POINTS FILE
PROGRAM: PRISM v2.1.00 Apr 15 1997
CREATED FROM: Point File SEC-20G.PTS
UNITS: METER METER

POINT	NORTHING	EASTING	HEIGHT	SITE	EASI	DMS	OrthoMAX	FFI
00048	3592494.921	411701.219	688.969	SS20	666.000	657.800		
00127	3592543.632	411823.491	691.357	????	666.000	657.800		
00137	3592593.024	411948.223	691.351	????	666.000	657.800		
00147	3592638.777	412074.566	691.406	????	668.000	659.400		
00157	3592681.715	412202.623	691.515	????	668.000	657.800		
00167	3592723.819	412328.683	692.006	????	668.000	659.400		
00178	3592769.861	412466.300	692.542	????	668.000	659.400		
00188	3592811.564	412590.405	692.960	????	671.000	659.400		
00198	3592852.594	412713.108	693.062	????	671.000	659.400		
00209	3592896.114	412842.844	693.204	????	670.000	659.400		
00220	3592941.250	412978.168	693.317	????	670.000	659.400		
00231	3592987.666	413115.357	693.402	????	670.000	659.400		
00241	3593028.890	413240.288	693.417	????	670.000	659.400		
00252	3593073.665	413373.839	693.475	????	672.000	659.400		
00262	3593115.643	413498.820	693.516	????	672.000	659.400		

00271	3593152.894	413610.856	693.531	????	672.000	659.400
00281	3593194.711	413735.479	693.583	????	672.000	659.400
00291	3593236.161	413859.193	693.791	????	672.000	659.400
00302	3593281.324	413994.118	694.186	????	672.000	659.400
00312	3593322.753	414117.979	694.257	????	672.000	659.400
00322	3593364.849	414243.785	694.085	????	672.000	661.000
00333	3593410.423	414379.848	694.237	????	672.000	659.400
00344	3593455.282	414513.428	694.678	????	672.000	659.400
00355	3593500.400	414648.307	695.136	????	673.000	659.400
00366	3593545.873	414784.233	695.492	????	673.000	659.400
00377	3593592.108	414921.248	695.707	????	673.000	659.400
00396	3593671.556	415158.535	696.031	????	673.000	659.400
00406	3593713.390	415283.783	696.215	????	674.000	657.800
00417	3593758.228	415419.870	696.458	????	674.000	662.500
00428	3593802.380	415550.427	696.563	????	674.000	668.800
00440	3593849.031	415690.518	695.926	????	674.000	659.400
00451	3593893.347	415820.772	694.968	????	673.000	659.400
00462	3593938.937	415957.925	693.945	????	673.000	659.400
00474	3593985.444	416097.734	693.709	????	672.000	659.400
00486	3594032.398	416236.961	693.626	????	671.000	659.400
00498	3594080.145	416380.531	693.527	????	671.000	659.400

ASHTECH POINTS FILE
PROGRAM: PRISM v2.1.00 Apr 15 1997
CREATED FROM: Point File SEC-21G.PTS
UNITS: METER METER

POINT	NORTHING	EASTING	HEIGHT	SITE	EASI	DMS	OrthoMAX	FFI
00120	3594125.912	416517.130	693.417	????	670.000	659.400		
00130	3594167.318	416640.813	693.509	????	670.000	659.400		
00140	3594210.096	416768.748	693.614	????	671.000	661.000		
00150	3594250.869	416890.135	693.695	????	671.000	659.400		
00160	3594291.462	417011.442	693.811	????	671.000	659.400		
00171	3594336.260	417145.066	693.899	????	671.000	659.400		
00182	3594381.600	417280.272	694.098	????	672.000	659.400		
00193	3594427.170	417416.456	694.393	????	672.000	657.800		
00203	3594468.838	417540.033	694.927	????	671.000	657.800		
00214	3594513.465	417673.055	695.940	????	671.000	662.500		
00225	3594559.107	417809.738	696.549	????	672.000	659.400		
00235	3594603.074	417937.215	697.000	????	672.000	659.400		
00245	3594644.223	418064.773	697.158	????	674.000	659.400		
00255	3594687.122	418192.891	697.487	????	674.000	659.400		
00265	3594730.074	418320.435	697.769	????	674.000	659.400		
00277	3594777.590	418461.450	697.698	????	674.000	659.400		
00289	3594824.281	418601.062	697.642	????	675.000	661.000		
00301	3594869.880	418738.820	698.169	????	675.000	659.400		
00312	3594911.781	418863.997	698.786	????	675.000	659.400		
00323	3594954.732	418991.050	698.926	????	675.000	670.400		
00334	3594996.747	419119.707	698.993	????	675.000	672.000		
00346	3595044.779	419260.957	698.646	????	675.000	665.700		
00357	3595088.130	419390.889	698.278	????	675.000	659.400		
00368	3595131.760	419520.382	697.989	????	675.000	661.000		
00380	3595178.548	419659.891	698.080	????	674.000	659.400		
00391	3595220.888	419787.445	698.164	????	674.000	656.200		
00401	3595260.336	419905.073	698.235	????	674.000	661.000		
00412	3595305.286	420039.333	698.316	????	674.000	661.000		
00424	3595349.876	420172.369	698.431	????	674.000	656.200		
00436	3595395.566	420309.308	698.511	????	674.000	659.400		

00447	3595439.297	420440.103	698.608	????	675.000	662.500	
00459	3595486.916	420581.677	698.705	????	675.000	659.400	
00470	3595530.333	420711.681	698.788	????	675.000	661.000	
00481	3595575.030	420845.195	698.866	????	675.000	659.400	
00491	3595619.020	420976.367	699.015	????	675.000	661.000	
00509	3595659.898	421097.620	699.260	????	675.000	656.200	

ASHTECH POINTS FILE
PROGRAM: PRISM v2.1.00 Apr 15 1997
CREATED FROM: Point File SEC-25G.PTS
UNITS: METER METER

POINT	NORTHING	EASTING	HEIGHT	SITE	EASI	DMS	OrthoMAX	FFI
00565	3563997.544	283171.303	857.925	????	829.000	827.500	834.000	
00575	3563949.526	283293.307	856.914	????	829.000	827.500	836.000	
00587	3563898.156	283424.969	857.863	????	833.000	831.500	830.000	
00599	3563845.963	283558.604	855.552	????	826.000	831.500	842.000	
00612	3563794.753	283689.346	856.207	????	833.000	831.500	837.000	
00624	3563744.196	283819.393	860.962	????	833.000	835.500	824.000	

ASHTECH POINTS FILE
PROGRAM: PRISM v2.1.00 Apr 15 1997
CREATED FROM: Point File SEC-26G.PTS
UNITS: METER METER

POINT	NORTHING	EASTING	HEIGHT	SITE	EASI	DMS	OrthoMAX	FFI
00008	3563682.374	283979.345	862.429	SS26	841.000	843.500	842.000	
00125	3563625.158	284124.671	868.627	????	841.000	839.500	840.000	
00137	3563577.357	284249.047	865.762	????	833.000	839.500	840.000	
00148	3563527.286	284376.350	864.139	????	833.000	831.500	833.000	
00160	3563476.820	284505.896	861.065	????	829.000	827.500	836.000	
00170	3563432.523	284618.911	860.482	????	829.000	827.500	832.000	
00181	3563384.195	284743.284	859.641	????	829.000	831.500	828.000	
00193	3563331.762	284877.813	854.960	????	818.000	819.600	824.000	
00204	3563280.467	285009.082	849.661	????	822.000	819.600	829.000	
00215	3563229.119	285141.681	846.991	????	822.000	819.600	827.000	
00227	3563176.587	285275.517	848.222	????	820.000	823.600	818.000	
00238	3563126.810	285402.310	847.843	????	820.000	819.600	816.000	
00250	3563074.911	285533.818	847.619	????	819.000	823.600	825.000	
00262	3563023.965	285665.453	847.891	????	819.000	823.600	821.000	
00273	3562975.361	285790.089	851.179	????	821.000	819.600	835.000	
00286	3562923.393	285923.076	850.934	????	821.000	823.600	830.000	
00298	3562871.789	286054.298	851.792	????	824.000	823.600	822.000	
00310	3562820.425	286187.187	855.586	????	824.000	835.500	830.000	
00321	3562773.838	286306.159	858.597	????	826.000	835.500	838.000	
00333	3562724.436	286435.059	858.216	????	831.000	835.500	838.000	
00345	3562670.279	286571.059	864.177	????	831.000	831.500	839.000	
00357	3562620.083	286697.540	867.543	????	836.000	835.500	846.000	
00369	3562568.829	286825.688	863.298	????	836.000	827.500	831.000	
00381	3562514.228	286967.618	862.964	????	825.000	831.500	828.000	
00392	3562462.987	287100.037	858.647	????	825.000	827.500	830.000	
00404	3562406.242	287244.780	856.729	????	828.000	827.500	823.000	
00414	3562360.501	287363.296	857.557	????	828.000	827.500	826.000	
00425	3562311.393	287491.677	856.592	????	827.000	827.500	829.000	
00437	3562260.436	287623.648	854.826	????	823.000	827.500	826.000	
00449	3562207.002	287763.138	859.336	????	826.000	827.500	828.000	
00461	3562156.686	287892.575	858.132	????	826.000	831.500	835.000	

00473	3562105.831	288024.040	856.369	????	827.000	827.500	829.000
00485	3562051.948	288159.110	852.566	????	824.000	827.500	834.000
00496	3562005.305	288282.175	850.828	????	823.000	823.600	828.000
00508	3561955.345	288411.316	855.007	????	823.000	819.600	830.000
00522	3561903.441	288543.555	854.192	????	823.000	827.500	827.000
00535	3561855.489	288665.822	854.498	????	823.000	827.500	834.000
00547	3561806.041	288792.435	854.244	????	828.000	831.500	836.000
00559	3561755.624	288923.086	857.450	????	828.000	827.500	836.000
00572	3561700.414	289060.669	859.457	????	832.000	831.500	825.000
00584	3561651.044	289191.579	861.529	????	832.000	835.500	838.000

ASHTECH POINTS FILE
PROGRAM: PRISM v2.1.00 Apr 15 1997
CREATED FROM: Point File SEC-27G.PTS
UNITS: METER METER

POINT	NORTHING	EASTING	HEIGHT	SITE	EASI	DMS	OrthoMAX	FFI
00009	3561636.289	289229.018	860.783	SS27	834.000	835.500	835.000	838.000
00126	3561584.441	289361.209	864.294	????	834.000	835.500	842.000	846.000
00140	3561529.456	289491.117	864.808	????	839.000	839.500	837.000	840.000
00153	3561447.434	289616.244	864.904	????	838.000	839.500	841.000	840.000
00165	3561368.597	289745.254	864.408	????	840.000	839.500	841.000	845.000
00176	3561295.545	289867.123	865.849	????	840.000	843.500	845.000	840.000
00190	3561218.795	289997.161	869.568	????	838.000	839.500	843.000	842.000
00202	3561172.372	290130.257	865.898	????	838.000	839.500	845.000	837.000
00214	3561129.212	290269.544	865.269	????	841.000	839.500	847.000	838.000
00224	3561105.609	290393.831	868.564	????	841.000	843.500	847.000	845.000
00235	3561089.146	290522.961	870.004	????	841.000	847.400	841.000	846.000
00247	3561077.911	290658.061	868.003	????	839.000	839.500	841.000	844.000
00260	3561028.239	290783.699	869.727	????	839.000	835.500	842.000	850.000
00272	3560976.329	290916.148	870.948	????	846.000	847.400	845.000	849.000
00283	3560926.690	291043.529	872.491	????	843.000	843.500	844.000	850.000
00294	3560876.089	291172.086	874.270	????	843.000	847.400	850.000	851.000
00305	3560825.475	291303.225	872.549	????	843.000	851.400	849.000	846.000
00317	3560771.607	291440.685	869.753	????	842.000	839.500	846.000	852.000
00330	3560717.932	291579.395	868.747	????	841.000	839.500	839.000	840.000
00341	3560669.311	291703.646	867.868	????	835.000	839.500	839.000	850.000
00352	3560620.223	291829.745	864.393	????	835.000	839.500	847.000	837.000
00364	3560566.513	291967.814	864.660	????	835.000	835.500	845.000	840.000
00377	3560513.507	292101.737	864.610	????	835.000	839.500	843.000	841.000
00390	3560461.765	292235.788	864.205	????	838.000	839.500	840.000	840.000
00402	3560413.200	292359.124	864.236	????	831.000	831.500	837.000	840.000
00414	3560364.937	292482.538	861.650	????	826.000	831.500	831.000	835.000
00427	3560309.785	292624.896	859.052	????	826.000	827.500	832.000	837.000
00439	3560256.698	292758.751	855.904	????	829.000	827.500	831.000	830.000
00467	3560229.116	292833.443	854.248	????	829.000	831.500	831.000	829.000
00593	3560178.902	292961.171	852.380	????	825.000	831.500	834.000	828.000
00613	3560088.409	293193.360	853.484	????	829.000	831.500	831.000	821.000
00624	3560038.669	293321.622	856.074	????	829.000	831.500	835.000	832.000
00636	3559983.602	293461.774	855.684	????	832.000	827.500	835.000	832.000
00648	3559931.302	293597.801	857.491	????	832.000	839.500	838.000	830.000
00660	3559881.966	293727.411	856.645	????	826.000	835.500	837.000	839.000
00674	3559825.835	293867.822	853.718	????	826.000	823.600	828.000	831.000
00686	3559779.047	293987.103	851.906	????	818.000	819.600	829.000	835.000
00700	3559725.015	294126.112	846.693	????	818.000	819.600	820.000	826.000
00713	3559672.043	294261.964	841.574	????	821.000	819.600	823.000	819.000
00725	3559620.955	294393.415	838.465	????	812.000	811.600	818.000	817.000
00737	3559568.567	294526.852	838.637	????	811.000	819.600	814.000	812.000

00750	3559517.378	294664.248	838.998	????	811.000	819.600	818.000	815.000

ASHTECH POINTS FILE
PROGRAM: PRISM v2.1.00 Apr 15 1997
CREATED FROM: Point File SEC-28G.PTS
UNITS: METER METER

POINT	NORTHING	EASTING	HEIGHT	SITE	EASI	DMS	OrthoMAX	FFI
00014	3559501.039	294705.860	838.538	SS28	811.000	807.700	818.000	818.000
00122	3559445.252	294839.824	833.953	????	813.000	807.700	815.000	811.000
00134	3559393.261	294972.787	831.749	????	813.000	807.700	816.000	809.000
00148	3559339.765	295110.453	831.190	????	805.000	807.700	809.000	808.000
00160	3559290.389	295239.689	830.159	????	805.000	811.600	812.000	815.000
00172	3559241.806	295362.611	828.400	????	803.000	807.700	808.000	807.000
00184	3559188.556	295499.309	828.281	????	803.000	807.700	808.000	809.000
00196	3559135.712	295633.766	827.968	????	806.000	807.700	808.000	814.000
00208	3559084.310	295764.719	828.650	????	799.000	799.700	812.000	804.000
00220	3559035.421	295891.184	829.349	????	801.000	807.700	810.000	803.000
00237	3558962.786	296077.776	825.497	????	800.000	807.700	812.000	800.000
00249	3558914.254	296201.432	825.190	????	800.000	803.700	812.000	799.000
00262	3558859.022	296338.647	825.620	????	801.000	807.700	810.000	800.000
00273	3558810.130	296468.889	827.768	????	801.000	807.000	803.000	798.000
00285	3558758.863	296600.460	827.284	????	805.000	799.700	801.000	801.000
00298	3558705.425	296738.758	827.345	????	805.000	807.700	810.000	797.000
00310	3558654.304	296868.767	825.290	????	802.000	803.700	802.000	801.000
00322	3558603.372	296999.026	823.796	????	802.000	795.700	801.000	795.000
00334	3558551.976	297130.254	822.877	????	796.000	799.700	801.000	799.000
00346	3558500.163	297263.483	821.602	????	796.000	799.700	805.000	785.000
00359	3558448.032	297396.951	822.085	????	802.000	799.700	796.000	799.000
00370	3558395.623	297532.187	822.165	????	802.000	799.700	795.000	799.000
00381	3558342.827	297668.650	820.070	????	804.000	799.700	808.000	790.000
00392	3558294.282	297793.276	822.094	????	794.000	799.700	798.000	798.000
00404	3558243.394	297924.881	823.165	????	798.000	799.700	808.000	788.000
00417	3558189.371	298063.720	824.870	????	798.000	807.700	814.000	800.000
00429	3558136.653	298199.282	824.013	????	802.000	803.700	809.000	795.000
00442	3558084.197	298333.239	828.851	????	802.000	803.700	811.000	793.000
00455	3558030.299	298470.946	831.787	????	808.000	799.700	811.000	798.000
00467	3557980.305	298600.320	832.293	????	808.000	811.600	806.000	798.000
00481	3557923.537	298745.772	834.059	????	810.000	807.000	814.000	803.000
00494	3557872.923	298875.893	835.497	????	810.000	811.600	812.000	806.000
00516	3557819.677	299015.725	836.571	????	815.000	811.600	817.000	807.000
00563	3557768.512	299147.526	838.220	????	809.000	815.600	816.000	806.000
00577	3557715.717	299281.271	838.674	????	813.000	807.700	815.000	806.000
00592	3557661.569	299421.148	836.830	????	813.000	807.700	813.000	806.000
00607	3557609.638	299555.165	834.521	????	810.000	803.700	810.000	804.000
00706	3557559.235	299685.066	833.199	SS29	810.000	799.700	818.000	803.000
00719	3557506.641	299820.040	832.107	SS29	804.000	803.700	808.000	796.000
00733	3557451.583	299958.619	830.900	SS29	804.000	803.700	808.000	803.000
00815	3557399.754	300110.658	825.148	????	795.000	803.700	812.000	779.000

ASHTECH POINTS FILE
PROGRAM: PRISM v2.1.00 Apr 15 1997
CREATED FROM: Point File SEC-29G.PTS
UNITS: METER METER

POINT	NORTHING	EASTING	HEIGHT	SITE	EASI	DMS	OrthoMAX	FFI
00023	3558783.586	305799.860	841.803	SS30	810.000	811.600	808.000	810.000

00359	3558704.506	305557.224	840.734	????	813.000	819.000	823.000	807.000
00370	3558662.306	305421.910	840.975	????	813.000	815.600	822.000	807.000
00381	3558617.838	305284.014	843.566	????	813.000	807.700	820.000	808.000
00393	3558567.898	305127.419	846.455	????	813.000	819.600	822.000	811.000
00404	3558522.614	304983.435	843.956	????	814.000	819.600	821.000	806.000
00414	3558484.337	304863.288	842.202	????	814.000	819.600	821.000	806.000
00424	3558443.973	304735.029	838.328	????	814.000	807.700	817.000	805.000
00436	3558389.202	304588.807	836.248	????	811.000	811.600	815.000	797.000
00448	3558308.685	304446.935	834.291	????	799.000	811.600	814.000	800.000
00460	3558219.530	304304.496	827.726	????	799.000	799.700	800.000	801.000
00471	3558138.701	304176.723	829.136	????	804.000	807.700	817.000	792.000
00484	3558063.321	304023.961	831.076	????	802.000	807.700	812.000	792.000
00497	3558002.054	303869.694	833.433	????	805.000	807.700	807.000	803.000
00509	3557945.952	303729.564	832.466	????	805.000	803.700	806.000	797.000
00521	3557887.253	303581.964	830.080	????	801.000	799.700	800.000	790.000
00532	3557831.521	303442.766	827.139	????	801.000	799.700	797.000	795.000
00544	3557798.673	303296.292	826.423	????	798.000	795.700	806.000	804.000
00554	3557807.578	303159.192	824.363	????	798.000	807.700	805.000	783.000
00567	3557817.497	302986.784	823.563	????	798.000	811.600	821.000	784.000
00579	3557812.570	302834.230	824.025	????	798.000	803.700	812.000	792.000
00590	3557794.798	302694.300	824.088	????	798.000	807.700	808.000	786.000
00601	3557749.444	302549.044	824.007	????	800.000	799.700	801.000	788.000
00613	3557700.185	302393.814	824.868	????	800.000	795.700	800.000	783.000
00624	3557656.009	302255.294	825.982	????	799.000	807.700	809.000	793.000
00636	3557606.383	302097.792	820.345	????	799.000	803.700	803.000	785.000
00649	3557554.958	301936.628	818.989	????	793.000	791.700	801.000	786.000
00660	3557511.113	301798.767	820.044	????	791.000	799.700	802.000	785.000
00672	3557461.800	301645.305	821.233	????	791.000	799.700	804.000	788.000
00684	3557412.484	301490.766	820.695	????	793.000	787.800	793.000	783.000
00695	3557366.918	301349.368	821.640	????	793.000	799.700	799.000	794.000
00708	3557337.917	301184.359	825.983	????	802.000	799.700	798.000	794.000
00720	3557338.453	301032.102	829.492	????	802.000	803.700	812.000	797.000
00731	3557338.678	300883.188	826.987	????	802.000	799.700	800.000	798.000
00742	3557339.386	300742.863	826.014	????	802.000	803.700	800.000	797.000
00754	3557340.227	300592.031	824.866	????	802.000	795.700	800.000	795.000
00767	3557335.432	300447.947	827.153	????	801.000	799.700	805.000	795.000
00781	3557319.863	300308.400	832.173	????	801.000	799.700	804.000	781.000

ASHTECH POINTS FILE
PROGRAM: PRISM v2.1.00 Apr 15 1997
CREATED FROM: Point File SEC-31G.PTS
UNITS: METER METER

POINT	NORTHING	EASTING	HEIGHT	SITE	EASI	DMS	OrthoMAX	FFI
00012	3562048.575	317409.936	779.670	SS32	759.000	767.000	762.000	
00129	3562016.556	317268.570	783.977	????	763.000	755.900	767.000	
00143	3561981.582	317114.194	787.035	????	763.000	767.000	768.000	
00155	3561950.711	316975.085	789.921	????	768.000	767.900	770.000	
00168	3561919.451	316838.498	789.307	????	768.000	767.900	772.000	
00182	3561885.118	316682.967	790.425	????	768.000	767.000	769.000	
00195	3561851.632	316533.216	789.981	????	768.000	763.900	767.000	
00207	3561819.385	316392.101	787.378	????	768.000	763.900	769.000	
00220	3561786.051	316238.954	791.780	????	771.000	779.800	771.000	
00232	3561752.546	316088.604	793.500	????	771.000	775.800	774.000	
00243	3561722.340	315952.932	794.622	????	771.000	767.900	776.000	
00255	3561689.752	315805.105	793.203	????	771.000	775.800	774.000	
00267	3561655.613	315656.230	791.153	????	769.000	767.900	774.000	
00279	3561624.221	315512.781	791.968	????	769.000	767.900	772.000	

00289	3561593.993	315377.287	793.067	????	770.000	767.900	771.000
00301	3561557.694	315214.175	792.820	????	771.000	767.900	769.000
00314	3561525.598	315068.938	792.763	????	771.000	767.900	771.000
00326	3561494.727	314934.805	792.380	????	765.000	763.900	771.000
00338	3561463.366	314794.662	793.333	????	765.000	763.900	770.000
00350	3561433.286	314652.229	797.068	????	773.000	783.800	774.000
00365	3561397.883	314493.839	797.566	????	773.000	779.800	778.000
00379	3561365.564	314351.179	800.183	????	776.000	779.800	780.000
00393	3561333.788	314206.862	801.213	????	776.000	779.800	779.000
00406	3561302.999	314065.308	800.163	????	774.000	771.800	777.000
00420	3561267.285	313910.869	800.161	????	785.000	787.800	792.000
00433	3561235.766	313763.872	806.971	????	785.000	787.800	791.000
00446	3561200.481	313609.763	810.490	????	782.000	783.800	786.000
00458	3561169.321	313469.287	807.005	????	782.000	787.800	786.000
00472	3561133.843	313310.382	805.597	????	778.000	787.800	786.000
00484	3561101.334	313166.570	804.500	????	778.000	787.800	789.000
00497	3561065.792	313011.227	805.124	????	778.000	787.800	783.000
00509	3561024.547	312871.717	802.599	????	777.000	779.800	781.000
00521	3560978.753	312726.532	801.575	????	777.000	783.800	779.000
00533	3560933.289	312581.649	803.863	????	779.000	783.800	782.000
00545	3560887.134	312434.363	808.009	????	779.000	783.800	790.000
00557	3560842.709	312294.080	811.549	????	787.000	787.800	791.000
00569	3560797.255	312152.197	811.778	????	787.000	799.700	795.000
00581	3560750.921	312006.338	812.820	????	787.000	803.700	796.000
00593	3560711.593	311879.615	813.949	????	787.000	799.700	802.000
00607	3560664.437	311732.357	815.342	????	794.000	803.700	800.000

ASHTECH POINTS FILE
PROGRAM: PRISM v2.1.00 Apr 15 1997
CREATED FROM: Point File SEC-33G.PTS
UNITS: METER METER

POINT	NORTHING	EASTING	HEIGHT	SITE	EASI	DMS	OrthoMAX	FFI
00012	3558720.206	318562.822	737.162	SS33	721.000	732.000	725.000	714.000
00126	3558867.350	318696.355	737.675	????	717.000	732.000	717.000	720.000
00141	3559008.528	318827.127	736.150	????	716.000	728.100	719.000	729.000
00163	3559166.554	318967.731	735.602	????	716.000	724.100	716.000	711.000
00179	3559316.593	319110.887	735.320	????	716.000	724.100	720.000	708.000
00185	3559374.338	319162.817	735.880	????	715.000	724.100	717.000	704.000
00201	3559526.895	319306.071	734.983	????	715.000	724.100	717.000	704.000
00219	3559683.820	319452.264	732.253	????	714.000	724.100	716.000	704.000
00236	3559841.034	319596.724	729.871	????	714.000	716.100	713.000	702.000
00254	3560001.689	319744.227	735.362	????	713.000	716.100	712.000	704.000
00272	3560159.423	319890.761	735.180	????	713.000	712.200	714.000	714.000
00289	3560312.310	320033.477	740.347	????	715.000	720.100	717.000	710.000
00306	3560468.571	320177.688	735.388	????	719.000	712.200	717.000	709.000
00323	3560623.389	320321.697	737.023	????	714.000	720.100	717.000	712.000
00342	3560788.072	320470.529	730.703	????	718.000	716.100	718.000	700.000
00361	3560949.905	320621.049	735.081	????	711.000	712.200	709.000	704.000
00378	3561104.610	320761.632	736.824	????	714.000	716.100	713.000	705.000
00396	3561267.901	320911.626	731.256	????	714.000	712.200	709.000	701.000
00414	3561432.178	321062.093	733.614	????	708.000	716.100	711.000	702.000
00432	3561595.074	321210.666	734.681	????	715.000	716.100	710.000	698.000
00450	3561757.999	321359.239	729.547	????	712.000	716.100	712.000	699.000
00467	3561909.930	321503.122	725.750	????	708.000	708.200	704.000	692.000
00486	3562073.861	321653.814	726.909	????	708.000	708.200	704.000	700.000
00504	3562235.460	321801.756	733.199	????	708.000	708.200	706.000	708.000
00522	3562397.946	321954.674	733.438	????	714.000	716.100	710.000	696.000

00537	3562527.320	322072.701	728.973	????	710.000	716.100	710.000	709.000
00570	3562839.816	322243.689	731.223	????	712.000	708.200	707.000	697.000
00630	3562945.650	322393.931	730.926	????	712.000	716.100	708.000	701.000
00642	3562989.801	322541.107	732.633	????	712.000	716.100	711.000	706.000
00666	3563004.103	322685.051	731.824	????	710.000	712.200	710.000	704.000

ASHTECH POINTS FILE
PROGRAM: PRISM v2.1.00 Apr 15 1997
CREATED FROM: Point File SEC-34G.PTS
UNITS: METER METER

POINT	NORTHING	EASTING	HEIGHT	SITE	EASI	DMS	OrthoMAX	FFI
00012	3554325.565	314720.871	729.825	SS34	710.000	724.100	719.000	710.000
00132	3554505.028	314861.233	731.759	????	711.000	728.100	719.000	710.000
00151	3554685.023	315005.926	731.756	????	709.000	716.100	720.000	703.000
00171	3554871.086	315154.255	728.778	????	709.000	720.100	715.000	707.000
00192	3555065.682	315306.628	726.827	????	705.000	716.100	714.000	705.000
00211	3555264.210	315461.725	726.272	????	704.000	716.100	713.000	708.000
00230	3555459.536	315615.609	721.092	????	702.000	716.100	714.000	697.000
00249	3555643.563	315764.179	724.094	????	702.000	708.000	705.000	708.000
00267	3555822.405	315906.884	729.028	????	708.000	716.100	712.000	705.000
00286	3556002.775	316051.507	734.539	????	713.000	720.100	708.000	708.000
00304	3556175.417	316197.199	735.607	????	713.000	728.100	722.000	712.000
00321	3556331.926	316341.880	735.935	????	713.000	732.000	720.000	711.000
00337	3556485.952	316496.662	731.614	????	713.000	724.100	717.000	706.000
00356	3556651.083	316645.575	728.463	????	711.000	724.100	712.000	706.000
00376	3556805.292	316792.736	737.096	????	713.000	716.100	711.000	713.000
00394	3556965.288	316940.592	735.626	????	713.000	720.100	717.000	721.000
00412	3557129.279	317092.427	733.147	????	711.000	720.100	714.000	711.000
00429	3557288.804	317238.214	735.271	????	715.000	712.200	717.000	715.000
00447	3557454.232	317392.848	736.229	????	711.000	716.100	720.000	715.000
00464	3557613.223	317538.047	732.067	????	716.000	720.100	721.000	708.000
00481	3557773.298	317687.399	731.753	????	709.000	716.100	717.000	704.000
00498	3557935.653	317837.601	727.806	????	710.000	720.100	716.000	697.000
00514	3558094.746	317981.327	726.891	????	708.000	716.100	718.000	709.000
00530	3558248.503	318125.445	728.127	????	708.000	712.200	719.000	705.000
00547	3558404.528	318269.338	731.181	????	713.000	716.100	716.000	711.000
00564	3558556.364	318410.528	735.736	????	715.000	720.100	720.000	714.000
00581	3558698.783	318542.787	738.077	????	721.000	732.000	721.000	714.000

ASHTECH POINTS FILE
PROGRAM: PRISM v2.1.00 Apr 15 1997
CREATED FROM: Point File SEC-35G.PTS
UNITS: METER METER

POINT	NORTHING	EASTING	HEIGHT	SITE	EASI	DMS	OrthoMAX	FFI
00025	3549265.997	311263.660	721.241	SS35	707.000	704.200	711.000	689.000
00148	3549462.179	311397.356	722.256	????	699.000	708.200	708.000	695.000
00167	3549657.440	311533.848	722.393	????	702.000	704.200	706.000	694.000
00188	3549871.426	311681.428	722.601	????	698.000	704.200	706.000	693.000
00208	3550068.357	311820.651	718.235	????	697.000	708.200	702.000	680.000
00227	3550266.175	311958.238	722.106	????	697.000	704.200	699.000	695.000
00248	3550466.928	312109.864	720.483	????	699.000	704.200	700.000	691.000
00268	3550649.487	312249.741	723.226	????	699.000	700.200	700.000	696.000
00286	3550841.257	312396.505	723.887	????	701.000	708.200	713.000	702.000
00304	3551026.242	312537.652	726.049	????	702.000	708.200	701.000	695.000
00323	3551222.311	312687.851	728.493	????	703.000	720.100	714.000	705.000

00341	3551409.239	312830.369	730.503	????	706.000	716.100	721.000	714.000
00360	3551603.786	312978.903	734.297	????	708.000	716.100	716.000	713.000
00380	3551808.254	313135.329	727.879	????	703.000	724.100	707.000	705.000
00400	3552007.217	313286.851	729.399	????	703.000	692.300	711.000	709.000
00419	3552212.658	313431.789	731.816	????	703.000	704.200	716.000	709.000
00489	3552895.202	313578.932	735.792	????	711.000	724.100	722.000	713.000
00506	3553077.334	313725.271	728.804	????	710.000	724.100	720.000	721.000
00525	3553262.260	313872.662	730.731	????	710.000	728.100	720.000	713.000
00542	3553444.123	314021.824	729.611	????	707.000	720.100	714.000	708.000
00561	3553634.829	314171.117	733.519	????	715.000	712.200	714.000	719.000
00580	3553824.078	314320.985	738.999	????	712.000	720.100	725.000	727.000
00599	3554009.264	314467.050	733.343	????	712.000	732.000	722.000	713.000
00616	3554180.295	314604.950	732.723	????	712.000	720.100	720.000	711.000

ASHTECH POINTS FILE
PROGRAM: PRISM v2.1.00 Apr 15 1997
CREATED FROM: Point File SEC-36G.PTS
UNITS: METER METER

POINT	NORTHING	EASTING	HEIGHT	SITE	EASI	DMS	OrthoMAX	FFI
00029	3544163.981	307734.016	646.363	SS36	634.000	628.600	627.000	622.000
00150	3544352.381	307885.779	652.605	????	627.000	632.600	632.000	624.000
00168	3544536.068	308036.047	660.149	????	631.000	632.600	636.000	620.000
00186	3544728.076	308182.603	662.193	????	638.000	640.500	640.000	628.000
00204	3544918.376	308333.394	664.687	????	646.000	644.500	646.000	639.000
00218	3545039.900	308478.801	665.771	????	650.000	644.500	647.000	640.000
00233	3545176.699	308620.986	667.085	????	650.000	644.500	652.000	641.000
00251	3545346.137	308772.596	670.389	????	661.000	644.500	648.000	645.000
00267	3545497.078	308910.929	672.608	????	661.000	656.400	654.000	641.000
00284	3545660.254	309047.701	676.789	????	670.000	652.500	651.000	650.000
00304	3545848.973	309165.080	683.045	????	674.000	660.400	659.000	659.000
00324	3546032.347	309281.173	694.593	????	676.000	664.400	672.000	669.000
00343	3546214.123	309427.037	698.134	????	666.000	676.300	673.000	673.000
00360	3546376.373	309559.096	696.259	????	669.000	676.300	676.000	674.000
00379	3546563.476	309704.563	700.704	????	676.000	676.300	676.000	675.000
00407	3546859.920	309851.602	705.222	????	679.000	688.300	681.000	679.000
00464	3547545.227	309998.523	719.172	????	691.000	700.200	700.000	696.000
00482	3547706.810	310149.809	720.841	????	696.000	704.200	697.000	703.000
00500	3547862.895	310302.692	721.923	????	698.000	696.200	702.000	693.000
00520	3548049.269	310450.827	723.910	????	698.000	708.200	706.000	696.000
00541	3548270.400	310594.667	726.815	????	703.000	708.200	710.000	708.000
00562	3548498.281	310743.222	727.915	????	706.000	708.200	712.000	706.000
00583	3548725.121	310890.351	729.087	????	708.000	704.200	707.000	693.000
00603	3548944.483	311037.577	727.778	????	700.000	716.100	710.000	701.000
00623	3549150.144	311182.328	727.469	????	707.000	712.200	707.000	694.000

ASHTECH POINTS FILE
PROGRAM: PRISM v2.1.00 Apr 15 1997
CREATED FROM: Point File SEC-37G.PTS
UNITS: METER METER

POINT	NORTHING	EASTING	HEIGHT	SITE	EASI	DMS	OrthoMAX	FFI
00017	3539737.538	303916.309	623.831	SS37	599.000	600.700	594.000	579.000
00121	3539783.246	304157.151	624.112	????	608.000	604.700	601.000	597.000
00131	3539806.155	304299.039	622.171	????	609.000	600.700	600.000	593.000
00143	3539869.849	304443.748	623.396	????	609.000	588.900	599.000	599.000
00157	3539985.826	304590.043	623.645	????	610.000	604.700	599.000	603.000

00170	3540089.805	304721.844	624.125	????	610.000	604.700	603.000	602.000
00185	3540215.232	304880.381	623.173	????	609.000	604.700	606.000	598.000
00199	3540333.828	305022.987	623.040	????	611.000	604.700	604.000	595.000
00214	3540476.847	305162.480	621.700	????	611.000	604.700	602.000	596.000
00230	3540620.191	305301.084	622.359	????	608.000	604.700	605.000	604.000
00246	3540772.057	305446.728	622.445	????	611.000	604.700	612.000	600.000
00263	3540924.649	305594.357	625.179	????	599.000	604.700	614.000	603.000
00281	3541100.297	305741.645	626.381	????	602.000	604.700	612.000	595.000
00300	3541287.488	305891.850	624.915	????	600.000	604.700	613.000	609.000
00318	3541470.756	306038.013	623.981	????	600.000	604.700	614.000	596.000
00337	3541659.783	306189.824	625.108	????	600.000	604.700	621.000	602.000
00356	3541846.986	306335.274	627.039	????	604.000	604.700	619.000	600.000
00392	3542279.373	306482.004	635.392	????	606.000	612.700	612.000	612.000
00454	3543011.634	306624.967	640.078	????	617.000	620.600	623.000	621.000
00467	3543092.059	306762.790	641.990	????	618.000	628.600	622.000	610.000
00480	3543168.803	306910.216	641.152	????	617.000	624.600	621.000	618.000
00498	3543332.545	307051.680	645.183	????	617.000	624.600	624.000	618.000
00516	3543505.616	307193.384	644.893	????	620.000	624.600	624.000	618.000
00534	3543683.678	307338.861	644.966	????	621.000	624.600	626.000	619.000
00553	3543863.522	307485.788	645.132	????	623.000	632.600	629.000	617.000
00573	3544046.475	307636.024	646.839	????	622.000	632.600	628.000	615.000

ASHTECH POINTS FILE
PROGRAM: PRISM v2.1.00 Apr 15 1997
CREATED FROM: Point File SEC-38G.PTS
UNITS: METER METER

POINT	NORTHING	EASTING	HEIGHT	SITE	EASI	DMS	OrthoMAX	FFI
00001	3535388.108	299796.861	577.617	SS38	552.000	557.000	556.000	539.000
00145	3535488.947	299942.733	584.796	????	556.000	557.000	558.000	554.000
00171	3535705.266	300188.283	588.090	????	558.000	560.900	566.000	560.000
00182	3535737.748	300334.295	589.259	????	565.000	564.900	570.000	556.000
00193	3535767.157	300478.041	589.450	????	565.000	576.900	570.000	559.000
00206	3535843.375	300620.423	588.798	????	563.000	564.900	558.000	562.000
00224	3536025.775	300769.876	588.076	????	561.000	564.900	565.000	557.000
00243	3536205.643	300923.820	588.394	????	564.000	564.900	570.000	562.000
00256	3536304.717	301064.671	589.275	????	561.000	580.800	571.000	559.000
00270	3536416.304	301205.001	590.363	????	561.000	572.900	568.000	554.000
00288	3536590.863	301354.143	588.698	????	562.000	564.900	572.000	557.000
00306	3536757.840	301494.481	590.323	????	562.000	572.900	571.000	565.000
00324	3536925.359	301637.423	595.209	????	570.000	580.800	573.000	567.000
00343	3537095.054	301780.610	600.674	????	571.000	584.800	573.000	566.000
00362	3537266.518	301924.517	610.392	????	580.000	580.800	584.000	584.000
00380	3537443.961	302074.785	615.993	????	588.000	592.800	593.000	586.000
00396	3537601.143	302213.295	616.980	????	590.000	604.700	605.000	576.000
00413	3537759.575	302357.216	611.999	????	594.000	592.800	599.000	576.000
00482	3537907.897	302492.376	609.452	????	587.000	592.800	594.000	572.000
00498	3538066.364	302638.109	607.853	????	585.000	588.800	588.000	576.000
00515	3538226.011	302783.540	605.283	????	578.000	588.800	583.000	572.000
00531	3538388.716	302930.557	601.600	????	577.000	584.800	583.000	570.000
00548	3538555.785	303083.590	603.250	????	577.000	572.900	580.000	570.000
00564	3538723.279	303222.334	602.889	????	578.000	588.800	579.000	571.000
00580	3538893.981	303363.461	604.531	????	576.000	592.800	585.000	581.000
00593	3539035.397	303480.453	610.276	????	586.000	584.800	587.000	585.000
00610	3539212.143	303624.360	611.322	????	586.000	592.800	589.000	585.000
00633	3539498.656	303768.838	616.422	????	590.000	592.800	591.000	596.000
00657	3539735.077	303911.631	625.998	????	599.000	600.700	594.000	602.000

APPENDIX B: RESULTS FROM TESTS OF THE EASI/PACE SYSTEM

B.1 Introduction
B.2 Accuracy Results in Planimetry after Space Resection for all SPOT Scenes of the Badia Area Using the SMODEL Program of the EASI/PACE System
- B.2.1 SPOT Level 1B Stereo-pair for Reference Scene 122/285
- B.2.2 SPOT Level 1A Stereo-pair for Reference Scene 122/285
- B.2.3 Level 1B Stereo-model of Scene 123/285
- B.2.4 Level 1B Stereo-model of Scene 123/286
- B.2.5 Level 1B Stereo-model of Scene 124/285
- B.2.6 Level 1B Stereo-model of Scene 124/286

B.3 Accuracy Results of Absolute Orientation
- B.3.1 The Results of Absolute Orientation of the Level 1B Stereo-pair for Reference Scene 122/285
- B.3.2 The Results of Absolute Orientation of the Level 1A Stereo-pair for Reference Scene 122/285
- B.3.3 The Results of Absolute Orientation of the Level 1B Stereo-pair for Scene 123/285
- B.3.4 The Results of Absolute Orientation of the Level 1B Stereo-pair for Scene 123/286
- B.3.5 The Results of Absolute Orientation of the Level 1B Stereo-pair for Scene 124/285
- B.3.6 The Results of Absolute Orientation of the Level 1B Stereo-pair for Scene 124/286

B.4 DEM Accuracy Results
- B.4.1 DEM Accuracy Results of the Level 1B Reference Stereo-model for Scene 122/285
- B.4.2 DEM Accuracy Results of the Level 1A Reference Stereo-model for Scene 122/285
- B.4.3 DEM Accuracy Results of the Level 1B Stereo-pair for Scene 123/285
- B.4.4 DEM Accuracy Results of the Level 1B Stereo-pair for Scene 123/286
- B.4.5 DEM Accuracy Results of the Level 1B Stereo-pair for Scene 124/285
- B.4.6 DEM Accuracy Results of the Level 1B Stereo-pair for Scene 124/286

B.5 Vector Plots of Planimetry and Height
- B.5.1 Vector Plots of the Residual Errors in Planimetry and Height of the Level 1B Stereo-model for Scene 123/285
- B.5.2 Vecor Plots of the Residual Errors in Planimetry and Height of the Level 1B Stereo-model for Scene 123/286
- B.5.3 Vector Plots of the Residual Errors in Planimetry and Height of the Level 1B Stereo-model for Scene 124/285
- B.5.4 Vector Plots of the Residual Errors in Planimetry and Height of the Level 1B Stereo-model for Scene 124/286

B.6 Orthoimage Generation and Orthoimage Accuracy Results
- B.6.1 Accuracy Results of Orthoimages
- B.6.2 Vector Plots of the Planimetric Errors of Orthoimages Generated from the Level 1A and 1B Stereo-pairs of the Reference Scene 122/285
- B.6.3 Orthoimages Generated from SPOT Images

B.7 Contours Generated from DEMs
- B.7.1 Contours Generated from the DEMs Superimposed over the Digitized Contours from the 1:250,000 Scale Map at a Contour Interval of 50m.

APPENDIX B: RESULTS FROM TESTS OF THE EASI/PACE SYSTEM

B.1 Introduction

In this Appendix, the accuracy results after the space resection of the individual SPOT Level 1A and 1B images using the **SMODEL** program of the EASI/PACE system over the Badia Test Field are presented first in Appendix B2. These are followed by the results of the absolute orientations using space intersection which are given in Appendix B3. The accuracy results achieved during the tests of the DEM data against the GCP data are presented in Appendix B4 in different combinations of both control and check points. These accuracy results in planimetry and height are then followed by the vector plots of the residual values at the control and check points which are included in Appendix B5. In Appendix B6, the results of the accuracy tests of the orthoimages generated from the Level 1A and 1B stereo-models for the reference scene are also presented, in addition to a vector plot of the residual errors in planimetry of the orthoimages. The contours extracted from DEMs are also presented in Appendix B.7 including their superimposition on the reference set of contours.

B.2 Accuracy Results in Planimetry After Space Resection for all SPOT Scenes of the Badia Area Using the SMODEL Program of the EASI/PACE System

B.2.1 SPOT Level 1B Stereo-pair for Reference Scene 122/285

The following are the results of the space resection giving the planimetric accuracy of the left image of the Level 1B stereo-model for reference scene 122/285 using 43 control points and 5 check points

SMODEL Satellite Model Calculation V6.0 EASI/PACE 13:14 22-SEP-97

Report File : D:\SWEST\TEST\5CHL.TXT

Using GCPs stored in the GCP segment :

GCPID	CALCULATED GCP		RESIDUAL (Metre)		
	X	Y	ΔX	ΔY	Vector
101	308540.02	3559864.89	4.65	5.52	7.22
102	300921.99	3557088.57	-0.18	10.01	10.01
110	295864.76	3566650.52	6.44	-5.13	8.24
113	304305.10	3580952.00	1.06	-4.74	4.86
111	300751.48	3576802.35	-9.57	-0.85	9.61

114	297519.99	3574019.15	6.40	5.24	8.27
116	284867.78	3573796.42	-2.50	6.13	6.62
119	284541.99	3563607.42	3.80	0.20	3.81
124	284230.85	3556244.53	2.65	2.92	3.94
135	279720.82	3554364.82	-5.81	-8.17	10.02
133	278854.91	3542819.46	-4.48	-2.13	4.95
136	282121.59	3547226.70	6.97	-4.58	8.34
141	292951.51	3536498.62	3.65	1.79	4.06
142	292458.74	3547668.60	-7.93	-8.68	11.76
137	292709.32	3551487.64	-3.61	-5.73	6.77
167	330424.54	3528361.29	-5.11	0.25	5.12
165	317478.05	3530719.93	-3.72	-4.48	5.83
164	320097.44	3536363.34	4.72	-4.50	6.52
162	308310.87	3542494.84	3.43	2.70	4.36
159	325743.46	3543774.06	0.84	7.38	7.43
153	320672.80	3549826.75	-7.44	2.91	7.99
151	313513.79	3552930.04	3.57	9.92	10.55
152	309235.87	3554858.27	-2.88	0.35	2.90
157	327580.13	3553022.96	3.57	13.69	14.15
158	328326.02	3556589.79	3.52	3.57	5.02
148	330981.61	3561091.49	-4.97	-6.78	8.40
146	322963.25	3563354.77	-5.92	4.46	7.41
149	336877.84	3557833.59	6.20	0.10	6.20
150	343636.49	3563019.90	-3.32	-7.56	8.25
125	325226.73	3568556.82	-3.59	-8.67	9.38
129	338784.79	3569544.03	-1.28	-1.98	2.36
145	345751.31	3571776.49	-5.35	-5.54	7.70
126	326819.67	3574686.40	7.41	-2.26	7.75
128	331361.63	3573364.56	1.63	-2.23	2.76
168	321498.46	3574938.18	-2.48	0.88	2.63
127	330678.54	3582055.65	0.84	5.73	5.80
169	318579.62	3586701.85	0.95	0.87	1.29
118	290490.98	3561266.33	-6.60	6.06	8.96
156	334918.01	3545626.66	5.97	2.76	6.58
155	337158.76	3549812.33	7.86	2.98	8.41
140	281956.60	3535718.10	5.61	0.18	5.61
166	330244.81	3534951.38	-6.76	-5.34	8.62
171	313696.98	3569814.58	1.71	-7.24	7.44
		RMS	±4.96	±5.52	±7.42

RESIDUAL ERRORS AT CHECK POINTS:

GCPID	CALCULATED CHECK POINT		ERRORS (Metre)		
	X	Y	ΔX	ΔY	Vector
-112	309290.89	3582164.18	-2.95	2.98	4.19
-123	282556.56	3570239.41	-7.63	3.37	8.34
-163	304900.07	3532800.23	5.57	0.39	5.59
-154	329677.16	3548191.50	4.48	6.85	8.19
-143	337968.16	3576243.38	-0.66	-5.18	5.22
		RMS	±5.44	±4.85	±7.29

N02 (2 X ellipsoid normal) : 0.1276894858944160D+08
aa (Unknown tied to Earth rotation) : 0.5365589970720992D-01
ALPHA (IFOV) : 0.1200000000000000D-04

bb (Unknown of 2nd order) : 0.9635876951825774D-09
C0 (Scene centre column) : 0.3000000000000000D+04
cc (Unknown of 2nd order): 0.2804298974764739D-08
COSKHI (Parameter): 0.9999937558689350D+00
DELGAM (Unknown of 2nd order): 0.3270781780345786D-08
GAMMA (Scene orient. rel. to the North): 0.2433856189529862D+00
K_1 (Cross track scale function): 0.1426692568891696D-05
L0 (Scene centre row): 0.3000000000000000D+04
P (Along track scale function): 0.1001815384965296D+02
Q (Satellite-Scene centre dist): 0.1050577334300622D+07
TAU (Levelling angle along track dir): 0.3533890080154706D-02
THETA (Levelling angle across track dir): 0.5357750689609079D+00
THETAS (THETA/COS_KHI): 0.5357784144315494D+00
X0 (Carto coord of scene centre): 0.3045057210917524D+06
Y0 (Carto coord of scene centre): 0.3560746146690248D+07
DELH (Radar parameter in H dir.): 0.0000000000000000D+00
COEFY2 (Radar parameter in Y2 dir.): 0.0000000000000000D+00

EARTH ELLIPSOID USED : E004

The following are the results of the space resection giving the planimetric accuracy of the right image of the Level 1B stereo-model for reference scene 122/285 using 43 control points and 5 check points:

SMODEL Satellite Model Calculation V6.0 EASI/PACE 12:58 22-SEP-97

Report File : D:\SWEST\TEST\5CHR.TXT

Using GCPs stored in the GCP segment :

GCPID	CALCULATED GCP		RESIDUAL (Metre)		
	X	Y	ΔX	ΔY	Vector
101	308544.50	3559864.80	0.17	5.61	5.61
102	300924.47	3557097.13	-2.66	1.45	3.03
110	295868.76	3566648.80	2.44	-3.41	4.19
113	304307.34	3580947.21	-1.18	0.05	1.18
111	300748.37	3576800.54	-6.46	0.96	6.53
116	284862.15	3573790.30	3.13	12.25	12.65
124	284232.52	3556254.16	0.98	-6.71	6.78
135	279720.06	3554364.91	-5.05	-8.26	9.68
136	282125.76	3547222.21	2.80	-0.09	2.81
133	278857.16	3542811.77	-6.73	5.56	8.73
141	292949.87	3536491.97	5.29	8.44	9.96
142	292459.71	3547661.70	-8.90	-1.78	9.08
137	292704.47	3551492.32	1.24	-10.41	10.48
151	313512.72	3552943.46	4.64	-3.50	5.81
152	309239.05	3554864.24	-6.06	-5.62	8.26
146	322961.51	3563355.17	-4.18	4.06	5.83
148	330974.69	3561089.21	1.95	-4.50	4.90
158	328330.95	3556599.30	-1.41	-5.94	6.10
157	327581.09	3553041.79	2.61	-5.14	5.76
164	320103.49	3536352.88	-1.33	5.96	6.11
159	325733.42	3543786.69	10.88	-5.25	12.08
167	330420.54	3528352.84	-1.11	8.70	8.77
162	308304.93	3542493.03	9.37	4.52	10.40
165	317482.57	3530710.74	-8.24	4.71	9.50
156	334924.87	3545634.43	-0.89	-5.01	5.09

145	345745.87	3571763.94	0.09	7.01	7.01
129	338785.66	3569544.79	-2.15	-2.74	3.49
125	325233.00	3568552.99	-9.86	-4.84	10.98
150	343633.70	3563014.39	-0.53	-2.05	2.12
149	336881.35	3557835.77	2.69	-2.08	3.40
126	326820.80	3574680.23	6.28	3.91	7.40
128	331363.50	3573354.67	-0.24	7.66	7.66
168	321494.08	3574929.96	1.90	9.10	9.30
127	330688.82	3582055.96	-9.44	5.42	10.88
169	318574.43	3586710.29	6.14	-7.57	9.75
118	290487.09	3561278.95	-2.71	-6.56	7.10
119	284541.97	3563611.78	3.82	-4.16	5.65
171	313691.11	3569809.53	7.58	-2.19	7.89
140	281956.00	3535713.46	6.20	4.81	7.85
155	337159.00	3549818.36	7.62	-3.06	8.21
166	330243.89	3534947.02	-5.84	-0.98	5.92
114	297524.74	3574015.84	1.65	8.55	8.71
153	320669.84	3549836.58	-4.48	-6.92	8.24
		RMS	± 5.19	±5.82	7.80

RESIDUAL ERRORS AT CHECK POINTS:

GCPID	CALCULATED CHECK POINT		ERRORS (Metre)		
	X	Y	ΔX	ΔY	Vector
-112	309288.56	3582163.05	-0.62	4.11	4.16
-123	282553.10	3570243.12	-4.17	-0.34	4.18
-163	304908.47	3532790.85	-2.83	9.77	10.17
-154	329672.66	3548198.81	8.98	-0.46	8.99
-143	337965.58	3576237.07	1.92	1.13	2.23
		RMS	±5.24	±5.34	±7.48

N02 (2 X ellipsoid normal) : 0.1276894614656886D+08
aa (Unknown tied to Earth rotation) : 0.6160900121450223D-01
ALPHA (IFOV) : 0.1200000000000000D-04
bb (Unknown of 2nd order) : 0.1003265514513486D-07
C0 (Scene centre column) : 0.3000000000000000D+04
cc (Unknown of 2nd order): -.4986760190496625D-08
COSKHI (Parameter): 0.9999449434080690D+00
DELGAM (Unknown of 2nd order): -.1393479130891412D-07
GAMMA (Scene orient. rel. to the North): 0.1634972812408024D+00
K_1 (Cross track scale function): 0.1412007907772972D-05
L0 (Scene centre row): 0.3000000000000000D+04
P (Along track scale function): 0.9978256313747972D+01
Q (Satellite-Scene centre dist): 0.9772044311696800D+06
TAU (Levelling angle along track dir): 0.1049391624774306D-01
THETA (Levelling angle across track dir): -.4433961378760061D+00
THETAS (THETA/COS_KHI): -.4434205511003419D+00
X0 (Carto coord of scene centre): 0.3123402161617218D+06
Y0 (Carto coord of scene centre): 0.3560448721603012D+07
DELH (Radar parameter in H dir.): 0.0000000000000000D+00
COEFY2 (Radar parameter in Y2 dir.): 0.0000000000000000D+00

The following are the results of the space resection giving the planimetric accuracy of the left image of the Level 1B stereomodel for reference scene 122/285 using 33 control points and 15 check points:

SMODEL Satellite Model Calculation V6.0 EASI/PACE 13:15 22-SEP-97

Report File : D:\SWEST\TEST\15CHL.TXT

Using GCPs stored in the GCP segment :

GCPID	CALCULATED GCP		RESIDUAL (Metre)		
	X	Y	ΔX	ΔY	Vector
101	308540.93	3559865.26	3.74	5.15	6.37
102	300923.58	3557089.32	-1.77	9.26	9.43
110	295867.02	3566650.99	4.18	-5.60	6.98
113	304306.54	3580951.34	-0.38	-4.08	4.10
114	297522.13	3574019.13	4.26	5.26	6.77
116	284871.77	3573797.24	-6.49	5.31	8.38
119	284545.82	3563608.80	-0.03	-1.18	1.18
124	284234.64	3556246.38	-1.14	1.07	1.57
136	282125.42	3547228.97	3.14	-6.85	7.54
141	292953.68	3536500.62	1.48	-0.21	1.49
137	292711.79	3551489.07	-6.08	-7.16	9.39
167	330423.78	3528361.45	-4.35	0.09	4.35
165	317477.88	3530720.60	-3.55	-5.15	6.26
162	308311.65	3542495.94	2.65	1.60	3.09
159	325743.08	3543774.30	1.22	7.14	7.24
153	320672.84	3549827.23	-7.48	2.43	7.87
151	313514.24	3552930.51	3.12	9.45	9.95
157	327579.83	3553023.10	3.87	13.55	14.09
148	330981.29	3561091.47	-4.65	-6.76	8.20
149	336877.23	3557833.35	6.81	0.34	6.82
150	343635.65	3563019.17	-2.48	-6.83	7.27
125	325226.71	3568556.71	-3.57	-8.56	9.27
129	338784.16	3569543.45	-0.65	-1.40	1.54
145	345750.40	3571775.45	-4.44	-4.50	6.32
128	331361.43	3573364.31	1.83	-1.98	2.70
168	321498.79	3574938.07	-2.81	0.99	2.98
127	330678.53	3582055.35	0.85	6.03	6.09
169	318580.23	3586701.30	0.34	1.42	1.46
156	334917.31	3545626.54	6.67	2.88	7.26
155	337158.04	3549812.11	8.58	3.20	9.15
140	281960.03	3535720.55	2.17	-2.28	3.15
166	330244.16	3534951.57	-6.11	-5.53	8.24
171	313697.60	3569814.46	1.09	-7.12	7.20
		RMS	±4.13	±5.62	±6.98

RESIDUAL ERRORS AT CHECK POINTS:

GCPID	CALCULATED CHECK POINT		ERRORS (Metre)		
	X	Y	ΔX	ΔY	Vector
-112	309291.96	3582163.52	-4.02	3.64	5.42
-111	300753.26	3576802.02	-11.35	-0.52	11.37
-123	282560.85	3570240.57	-11.92	2.21	12.12

-135	279725.23	3554367.02	-10.22	-10.37	14.56
-133	278859.03	3542821.95	-8.60	-4.62	9.76
-142	292461.15	3547670.16	-10.34	-10.24	14.55
-163	304900.96	3532801.70	4.68	-1.08	4.80
-164	320097.20	3536363.83	4.96	-4.99	7.04
-154	329676.70	3548191.61	4.94	6.74	8.36
-152	309236.67	3554858.81	-3.68	-0.19	3.68
-158	328325.75	3556589.90	3.79	3.46	5.14
-146	322963.33	3563354.89	-6.00	4.34	7.40
-126	326819.69	3574686.19	7.39	-2.05	7.67
-118	290493.88	3561267.38	-9.50	5.01	10.74
-143	337967.70	3576242.85	-0.20	-4.65	4.65
		RMS	±7.80	±5.38	±9.48

N02 (2 X ellipsoid normal) : 0.1276894858944160D+08
aa (Unknown tied to Earth rotation) : 0.5359530336018570D-01
ALPHA (IFOV) : 0.1200000000000000D-04
bb (Unknown of 2nd order) : 0.9635876951825774D-09
C0 (Scene centre column) : 0.3000000000000000D+04
cc (Unknown of 2nd order): 0.2804298974764739D-08
COSKHI (Parameter): 0.9999998566776746D+00
DELGAM (Unknown of 2nd order): 0.3270781780345786D-08
GAMMA (Scene orient. rel. to the North): 0.2434544961198061D+00
K_1 (Cross track scale function): 0.1428008795570822D-05
L0 (Scene centre row): 0.3000000000000000D+04
P (Along track scale function): 0.1001809997279491D+02
Q (Satellite-Scene centre dist): 0.1050479411876798D+07
TAU (Levelling angle along track dir): -.5353921107768744D-03
THETA (Levelling angle across track dir): 0.5367927528677048D+00
THETAS (THETA/COS_KHI): 0.5367928298021014D+00
X0 (Carto coord of scene centre): 0.3045086861861590D+06
Y0 (Carto coord of scene centre): 0.3560749685893636D+07
DELH (Radar parameter in H dir.): 0.0000000000000000D+00
COEFY2 (Radar parameter in Y2 dir.): 0.0000000000000000D+00

EARTH ELLIPSOID USED : E004

The following are the results of the space resection giving the planimetric accuracy of the right image of the Level 1B stereo-model for reference scene 122/285 using 33 control points and 15 check points:

SMODEL Satellite Model Calculation V6.0 EASI/PACE 13:01 22-SEP-97

Report File : D:\SWEST\TEST\15CHR.TXT

Using GCPs stored in the GCP segment :

GCPID	CALCULATED GCP		RESIDUAL (Metre)		
	X	Y	ΔX	ΔY	Vector
101	308545.77	3559865.08	-1.10	5.33	5.44
102	300926.35	3557097.64	-4.54	0.94	4.64
110	295870.84	3566649.42	0.36	-4.03	4.05
113	304308.40	3580947.42	-2.24	-0.16	2.24
116	284865.17	3573791.46	0.11	11.09	11.09
124	284235.95	3556255.51	-2.45	-8.06	8.42
136	282129.53	3547223.60	-0.97	-1.48	1.77

141	292952.82	3536492.78	2.34	7.63	7.98
137	292707.16	3551493.18	-1.45	-11.27	11.36
151	313513.82	3552943.60	3.54	-3.64	5.08
148	330974.72	3561089.19	1.92	-4.48	4.87
157	327581.43	3553041.66	2.27	-5.01	5.50
159	325734.02	3543786.38	10.28	-4.94	11.41
167	330421.23	3528352.05	-1.80	9.49	9.66
162	308306.61	3542493.32	7.69	4.23	8.78
165	317483.85	3530710.37	-9.52	5.08	10.79
156	334925.02	3545633.92	-1.04	-4.50	4.62
145	345744.97	3571763.51	0.99	7.44	7.50
129	338785.12	3569544.62	-1.61	-2.57	3.03
125	325233.12	3568553.13	-9.98	-4.98	11.16
150	343633.11	3563013.94	0.06	-1.60	1.60
149	336881.18	3557835.51	2.86	-1.82	3.39
128	331363.25	3573354.84	0.01	7.49	7.49
168	321494.29	3574930.29	1.69	8.77	8.93
127	330688.43	3582056.34	-9.05	5.04	10.36
169	318574.53	3586710.67	6.04	-7.95	9.98
119	284545.21	3563613.02	0.58	-5.40	5.43
171	313691.82	3569809.74	6.87	-2.40	7.28
140	281959.92	3535714.64	2.29	3.63	4.30
155	337158.98	3549817.90	7.64	-2.59	8.07
166	330244.47	3534946.43	-6.42	-0.39	6.43
114	297526.51	3574016.33	-0.12	8.06	8.06
153	320670.61	3549836.61	-5.25	-6.95	8.72
		RMS	±4.79	±5.97	±7.66

RESIDUAL ERRORS AT CHECK POINTS:

GCPID	CALCULATED CHECK POINT		ERRORS (Metre)		
	X	Y	ΔX	ΔY	Vector
-112	309289.27	3582163.27	-1.33	3.89	4.11
-111	300749.80	3576800.88	-7.89	0.62	7.92
-123	282556.42	3570244.42	-7.49	-1.64	7.66
-135	279723.98	3554366.47	-8.97	-9.82	13.30
-133	278861.30	3542813.20	-10.87	4.13	11.62
-142	292462.48	3547662.54	-11.67	-2.62	11.96
-163	304910.56	3532791.14	-4.92	9.48	10.68
-152	309240.37	3554864.49	-7.38	-5.87	9.44
-146	322961.88	3563355.33	-4.55	3.90	6.00
-158	328331.19	3556599.24	-1.65	-5.88	6.11
-164	320104.51	3536352.54	-2.35	6.30	6.72
-154	329673.00	3548198.53	8.64	-0.18	8.64
-126	326820.73	3574680.47	6.35	3.67	7.34
-118	290489.78	3561279.85	-5.40	-7.46	9.21
-143	337964.96	3576237.12	2.54	1.08	2.76
		RMS	±7.14	±5.50	±9.01

N02 (2 X ellipsoid normal) : 0.1276894614656886D+08
aa (Unknown tied to Earth rotation) : 0.6152842889270040D-01
ALPHA (IFOV) : 0.1200000000000000D-04
bb (Unknown of 2nd order) : 0.1003265514513486D-07
C0 (Scene centre column) : 0.3000000000000000D+04

cc (Unknown of 2nd order): -.498676019049625D-08
COSKHI (Parameter): 0.9999688172932528D+00
DELGAM (Unknown of 2nd order): -.1393479130891412D-07
GAMMA (Scene orient. rel. to the North): 0.1635457411779394D+00
K_1 (Cross track scale function): 0.1411561904014367D-05
L0 (Scene centre row): 0.3000000000000000D+04
P (Along track scale function): 0.9978450839660936D+01
Q (Satellite-Scene centre dist): 0.9771479878152280D+06
TAU (Levelling angle along track dir): 0.7897362262126905D-02
THETA (Levelling angle across track dir): -.4429314446274692D+00
THETAS (THETA/COS_KHI): -.4429452568595190D+00
X0 (Carto coord of scene centre): 0.3123419077508956D+06
Y0 (Carto coord of scene centre): 0.3560450908017059D+07
DELH (Radar parameter in H dir.): 0.0000000000000000D+00
COEFY2 (Radar parameter in Y2 dir.): 0.0000000000000000D+00

EARTH ELLIPSOID USED : E004

The following are the results of the space resection giving the planimetric accuracy of the left image of the Level 1B stereo-model for reference scene 122/285 using 23 control points and 25 check points:

SMODEL Satellite Model Calculation V6.0 EASI/PACE 13:17 22-SEP-97

Report File : D:\SWEST\TEST\25CHL.TXT

Using GCPs stored in the GCP segment :

GCPID	CALCULATED GCP		RESIDUAL (Metre)		
	X	Y	ΔX	ΔY	Vector
102	300923.26	3557087.99	-1.45	10.59	10.68
110	295865.97	3566649.18	5.23	-3.79	6.46
113	304304.97	3580948.97	1.19	-1.71	2.08
116	284869.78	3573795.64	-4.50	6.91	8.25
119	284544.48	3563607.60	1.31	0.02	1.31
124	284233.76	3556245.62	-0.26	1.83	1.84
136	282124.97	3547228.31	3.59	-6.19	7.16
142	292461.08	3547669.05	-10.27	-9.13	13.74
163	304901.94	3532800.94	3.70	-0.32	3.71
167	330424.69	3528361.26	-5.26	0.28	5.27
165	317478.91	3530719.73	-4.58	-4.28	6.27
162	308312.24	3542495.33	2.06	2.21	3.02
159	325743.60	3543774.26	0.70	7.18	7.21
154	329677.04	3548192.05	4.60	6.30	7.80
158	328325.82	3556590.51	3.72	2.85	4.69
146	322963.15	3563355.15	-5.82	4.08	7.11
150	343635.18	3563020.61	-2.01	-8.27	8.51
145	345749.59	3571776.94	-3.63	-5.99	7.01
168	321498.12	3574938.26	-2.14	0.80	2.28
169	318578.93	3586700.91	1.64	1.81	2.44
155	337158.17	3549813.05	8.45	2.26	8.75
140	281960.20	3535719.56	2.01	-1.28	2.38
171	313696.96	3569813.49	1.73	-6.15	6.38
	RMS		±4.32	±5.20	±6.76

RESIDUAL ERRORS AT CHECK POINTS:

GCPID	CALCULATED CHECK POINT		ERRORS (Metre)		
	X	Y	ΔX	ΔY	Vector
-101	308540.66	3559864.14	4.01	6.27	7.44
-112	309290.53	3582161.70	-2.59	5.46	6.05
-111	300751.79	3576799.72	-9.88	1.78	10.04
-114	297520.70	3574016.96	5.69	7.43	9.36
-123	282558.96	3570239.22	-10.03	3.56	10.64
-135	279724.24	3554366.47	-9.23	-9.82	13.48
-133	278858.65	3542821.19	-8.22	-3.86	9.08
-141	292954.24	3536499.79	0.92	0.62	1.11
-137	292711.52	3551487.97	-5.81	-6.06	8.39
-164	320098.02	3536363.20	4.14	-4.36	6.01
-153	320673.20	3549827.27	-7.84	2.39	8.20
-151	313514.39	3552929.82	2.97	10.14	10.57
-152	309236.66	3554857.85	-3.67	0.77	3.75
-157	327580.03	3553023.53	3.67	13.12	13.62
-148	330981.18	3561092.38	-4.54	-7.67	8.92
-149	336877.13	3557834.52	6.91	-0.83	6.96
-125	325226.32	3568557.04	-3.18	-8.89	9.44
-129	338783.62	3569544.72	-0.11	-2.67	2.67
-126	326819.07	3574686.83	8.01	-2.69	8.45
-128	331360.88	3573365.40	2.38	-3.07	3.88
-127	330677.67	3582056.64	1.71	4.74	5.04
-118	290492.94	3561265.91	-8.56	6.48	10.74
-156	334917.61	3545627.17	6.37	2.25	6.75
-166	330244.90	3534951.68	-6.85	-5.64	8.87
-143	337966.98	3576244.41	0.52	-6.20	6.23
		RMS	±6.01	±6.09	±8.56

N02 (2 X ellipsoid normal) : 0.1276894858944160D+08
aa (Unknown tied to Earth rotation) : 0.5355562532080279D-01
ALPHA (IFOV) : 0.1200000000000000D-04
bb (Unknown of 2nd order) : 0.9635876951825774D-09□
C0 (Scene centre column) : 0.3000000000000000D+04
cc (Unknown of 2nd order): 0.2804298974764739D-08
COSKHI (Parameter): 0.9999711415717454D+00
DELGAM (Unknown of 2nd order): 0.3270781780345786D-08
GAMMA (Scene orient. rel. to the North): 0.2434443350806968D+00
K_1 (Cross track scale function): 0.1426931419294016D-05
L0 (Scene centre row): 0.3000000000000000D+04
P (Along track scale function): 0.1001860072528468D+02
Q (Satellite-Scene centre dist): 0.1050514279920580D+07
TAU (Levelling angle along track dir): -.7597325518356084D-02
THETA (Levelling angle across track dir): 0.5358891876208492D+00
THETAS (THETA/COS_KHI): 0.5359046529868288D+00
X0 (Carto coord of scene centre): 0.3045089583206273D+06
Y0 (Carto coord of scene centre): 0.3560754274334869D+07
DELH (Radar parameter in H dir.): 0.0000000000000000D+00
COEFY2 (Radar parameter in Y2 dir.): 0.0000000000000000D+00

EARTH ELLIPSOID USED : E004

The following are the results of the space resection giving the planimetric accuracy of the right image of the Level 1B stereo-model for reference scene 122/285 using 23 control points and 25 check points:

SMODEL Satellite Model Calculation V6.0 EASI/PACE 13:02 22-SEP-97

Report File : D:\SWEST\TEST\25CHR.TXT

Using GCPs stored in the GCP segment :

GCPID	CALCULATED GCP		RESIDUAL (Metre)		
	X	Y	ΔX	ΔY	Vector
102	300925.63	3557097.83	-3.82	0.75	3.89
110	295870.39	3566648.49	0.81	-3.10	3.20
113	304309.14	3580945.27	-2.98	1.99	3.58
116	284864.92	3573789.62	0.36	12.93	12.94
124	284234.64	3556255.51	-1.14	-8.06	8.14
136	282127.56	3547224.37	1.00	-2.25	2.46
142	292460.80	3547663.41	-9.99	-3.49	10.58
163	304908.71	3532793.71	-3.07	6.91	7.57
146	322963.41	3563355.99	-6.08	3.24	6.89
158	328332.94	3556600.67	-3.40	-7.31	8.06
154	329674.42	3548200.61	7.22	-2.26	7.56
159	325734.71	3543788.62	9.59	-7.18	11.98
167	330421.62	3528355.55	-2.19	5.99	6.38
162	308305.60	3542495.18	8.70	2.37	9.02
165	317482.88	3530713.30	-8.55	2.15	8.82
145	345749.62	3571764.18	-3.66	6.77	7.70
150	343637.08	3563015.29	-3.91	-2.95	4.89
168	321496.32	3574929.92	-0.34	9.14	9.14
169	318576.89	3586709.04	3.68	-6.32	7.31
119	284544.32	3563612.22	1.47	-4.60	4.83
171	313692.72	3569809.25	5.97	-1.91	6.26
140	281957.09	3535716.31	5.12	1.97	5.48
155	337161.43	3549820.09	5.20	-4.79	7.06
		RMS	±5.29	±5.67	±7.75

RESIDUAL ERRORS AT CHECK POINTS:

GCPID	CALCULATED CHECK POINT		ERRORS (Metre)		
	X	Y	ΔX	ΔY	Vector
-101	308545.70	3559865.29	-1.03	5.12	5.22
-112	309290.46	3582161.32	-2.52	5.84	6.36
-111	300750.12	3576799.02	-8.21	2.48	8.58
-123	282555.92	3570242.91	-6.99	-0.13	7.00
-135	279722.48	3554366.57	-7.47	-9.92	12.41
-133	278858.93	3542814.22	-8.50	3.11	9.05
-141	292950.49	3536494.74	4.67	5.67	7.34
-137	292705.73	3551493.72	-0.02	-11.81	11.81
-151	313513.79	3552944.64	3.57	-4.68	5.89
-152	309240.09	3554865.20	-7.10	-6.58	9.68
-148	330977.03	3561090.38	-0.39	-5.67	5.69
-157	327582.88	3553043.31	0.82	-6.66	6.71
-164	320104.14	3536355.12	-1.98	3.72	4.22
-156	334926.94	3545636.33	-2.96	-6.91	7.52

-129	338788.78	3569545.33	-5.27	-3.28	6.21
-125	325235.15	3568553.42	-12.01	-5.27	13.12
-149	336884.03	3557837.13	0.01	-3.44	3.44
-126	326823.29	3574680.37	3.79	3.77	5.34
-128	331366.27	3573355.07	-3.01	7.26	7.85
-127	330691.89	3582055.91	-12.51	5.47	13.65
-118	290488.84	3561279.35	-4.46	-6.96	8.27
-143	337968.91	3576237.37	-1.41	0.83	1.64
-166	330245.22	3534949.49	-7.18	-3.45	7.96
-114	297526.54	3574014.67	-0.15	9.72	9.72
-153	320671.15	3549838.29	-5.79	-8.64	10.40
		RMS	±5.81	±6.21	±8.51

N02 (2 X ellipsoid normal) : 0.1276894614656886D+08
aa (Unknown tied to Earth rotation) : 0.6167515890688459D-01
ALPHA (IFOV) : 0.1200000000000000D-04
bb (Unknown of 2nd order) : 0.1003265514513486D-07
C0 (Scene centre column) : 0.3000000000000000D+04
cc (Unknown of 2nd order): -.4986760190496625D-08
COSKHI (Parameter): 0.9999862029090534D+00
DELGAM (Unknown of 2nd order): -.1393479130891412D-07
GAMMA (Scene orient. rel. to the North): 0.1634951572122334D+00
K_1 (Cross track scale function): 0.1410480920263302D-05
L0 (Scene centre row): 0.3000000000000000D+04
P (Along track scale function): 0.9977983926603864D+01
Q (Satellite-Scene centre dist): 0.9772043614810852D+06
TAU (Levelling angle along track dir): 0.5253070814568002D-02
THETA (Levelling angle across track dir): -.4419852382604846D+00
THETAS (THETA/COS_KHI): -.4419913364551512D+00
X0 (Carto coord of scene centre): 0.3123432988739257D+06
Y0 (Carto coord of scene centre): 0.3560453174175469D+07
DELH (Radar parameter in H dir.): 0.0000000000000000D+00
COEFY2 (Radar parameter in Y2 dir.): 0.0000000000000000D+00

EARTH ELLIPSOID USED : E004

The following are the results of the space resection giving the planimetric accuracy of the left image of the Level 1B stereo-model for reference scene 122/285 using 13 control points and 35 check points:

SMODEL Satellite Model Calculation V6.0 EASI/PACE 13:18 22-SEP-97

Report File : D:\SWEST\TEST\35CHL.TXT

Using GCPs stored in the GCP segment :

GCPID	CALCULATED GCP		RESIDUAL (Metre)		
	X	Y	ΔX	ΔY	Vector
102	300924.64	3557089.38	-2.83	9.20	9.63
113	304305.86	3580950.94	0.30	-3.68	3.69
116	284869.46	3573797.51	-4.18	5.04	6.54
119	284544.59	3563609.18	1.20	-1.56	1.97
136	282125.63	3547229.53	2.93	-7.41	7.96
167	330424.80	3528362.73	-5.37	-1.19	5.50
162	308313.84	3542496.38	0.46	1.16	1.25
154	329676.88	3548193.06	4.76	5.29	7.11
158	328325.62	3556591.36	3.92	2.00	4.40

145	345747.21	3571777.91	-1.25	-6.96	7.07
168	321498.13	3574939.12	-2.15	-0.06	2.15
169	318578.93	3586702.01	1.64	0.71	1.79
140	281961.65	3535720.82	0.56	-2.54	2.60
		RMS	±3.05	±4.75	±5.65

RESIDUAL ERRORS AT CHECK POINTS:

GCPID	CALCULATED CHECK POINT		ERRORS (Metre)		
	X	Y	ΔX	ΔY	Vector
-101	308541.92	3559865.45	2.75	4.96	5.67
-110	295866.95	3566650.87	4.25	-5.48	6.94
-112	309291.27	3582163.41	-3.33	3.75	5.02
-111	300752.71	3576801.66	-10.80	-0.16	10.80
-114	297521.55	3574018.85	4.84	5.54	7.35
-123	282558.53	3570240.99	-9.60	1.79	9.76
-124	284234.10	3556246.93	-0.60	0.52	0.79
-135	279724.21	3554367.76	-9.20	-11.11	14.43
-133	278859.36	3542822.47	-8.93	-5.14	10.30
-141	292956.09	3536500.87	-0.93	-0.46	1.04
-142	292462.52	3547670.33	-11.71	-10.41	15.67
-137	292712.79	3551489.27	-7.08	-7.36	10.21
-163	304903.95	3532802.01	1.69	-1.39	2.19
-165	317480.48	3530721.08	-6.15	-5.63	8.33
-164	320099.22	3536364.48	2.94	-5.64	6.36
-159	325744.02	3543775.40	0.28	6.04	6.05
-153	320673.86	3549828.22	-8.50	1.44	8.62
-151	313515.60	3552930.97	1.76	8.99	9.16
-152	309238.01	3554859.09	-5.02	-0.47	5.05
-157	327580.01	3553024.47	3.69	12.18	12.73
-148	330980.59	3561093.16	-3.95	-8.45	9.32
-146	322963.34	3563356.02	-6.01	3.21	6.81
-149	336875.90	3557835.39	8.14	-1.70	8.32
-150	343633.05	3563021.59	0.12	-9.25	9.25
-125	325226.26	3568557.91	-3.12	-9.76	10.24
-129	338782.11	3569545.53	1.40	-3.48	3.75
-126	326818.68	3574687.58	8.40	-3.44	9.08
-128	331360.04	3573366.05	3.22	-3.72	4.92
-127	330676.64	3582057.15	2.74	4.23	5.04
-118	290493.75	3561267.48	-9.37	4.91	10.58
-156	334916.85	3545628.31	7.13	1.11	7.22
-155	337157.02	3549814.10	9.60	1.21	9.68
-166	330244.89	3534952.95	-6.84	-6.91	9.72
-143	337965.37	3576245.02	2.13	-6.82	7.14
-171	313697.80	3569814.79	0.90	-7.44	7.50
		RMS	±6.15	±6.05	±8.63

N02 (2 X ellipsoid normal) : 0.1276894858944160D+08
aa (Unknown tied to Earth rotation) : 0.5350883085495415D-01
ALPHA (IFOV) : 0.1200000000000000D-04
bb (Unknown of 2nd order) : 0.9635876951825774D-09
C0 (Scene centre column) : 0.3000000000000000D+04
cc (Unknown of 2nd order): 0.2804298974764739D-08
COSKHI (Parameter): 0.9999930083049316D+00

DELGAM (Unknown of 2nd order): 0.3270781780345786D-08□
GAMMA (Scene orient. rel. to the North): 0.2434406685144686D+00
K_1 (Cross track scale function): 0.1424277419866320D-05
L0 (Scene centre row): 0.3000000000000000D+04
P (Along track scale function): 0.1001822522183523D+02
Q (Satellite-Scene centre dist): 0.1050535909183496D+07
TAU (Levelling angle along track dir): -.3739456750578671D-02
THETA (Levelling angle across track dir): 0.5336963287473624D+00
THETAS (THETA/COS_KHI): 0.5337000602154414D+00
X0 (Carto coord of scene centre): 0.3045076819430264D+06
Y0 (Carto coord of scene centre): 0.3560752986456130D+07
DELH (Radar parameter in H dir.): 0.0000000000000000D+00
COEFY2 (Radar parameter in Y2 dir.): 0.0000000000000000D+00

EARTH ELLIPSOID USED : E004

The following are the results of the space resection giving the planimetric accuracy of the right image of the Level 1B stereo-model for reference scene 122/285 using 13 control points and 35 check points:

SMODEL Satellite Model Calculation V6.0 EASI/PACE 13:04 22-SEP-97

Report File : D:\SWEST\TEST\35CHR.TXT

Using GCPs stored in the GCP segment :

GCPID	CALCULATED GCP		RESIDUAL (Metre)		
	X	Y	ΔX	ΔY	Vector
102	300928.15	3557098.77	-6.34	-0.19	6.34
113	304309.87	3580946.03	-3.71	1.23	3.91
116	284864.41	3573791.40	0.87	11.15	11.19
136	282129.47	3547226.14	-0.91	-4.02	4.12
158	328333.39	3556602.39	-3.85	-9.03	9.82
154	329675.21	3548202.00	6.43	-3.65	7.40
167	330423.48	3528356.04	-4.05	5.50	6.83
162	308309.11	3542496.02	5.19	1.53	5.41
145	345746.03	3571766.80	-0.07	4.15	4.15
168	321496.43	3574931.88	-0.45	7.18	7.19
169	318576.47	3586710.94	4.10	-8.22	9.19
119	284544.83	3563614.00	0.96	-6.38	6.45
140	281960.40	3535717.53	1.81	0.75	1.96
		RMS	±3.83	±6.10	±7.21

RESIDUAL ERRORS AT CHECK POINTS:

GCPID	CALCULATED CHECK POINT		ERRORS (Metre)		
	X	Y	ΔX	ΔY	Vector
-101	308547.96	3559866.24	-3.29	4.17	5.31
-110	295871.90	3566649.51	-0.70	-4.12	4.18
-112	309291.02	3582162.35	-3.08	4.81	5.71
-111	300751.07	3576799.82	-9.16	1.68	9.31
-123	282555.42	3570244.86	-6.49	-2.08	6.81
-124	284235.81	3556257.39	-2.31	-9.94	10.20
-135	279723.19	3554368.72	-8.18	-12.07	14.59

-133	278860.96	3542815.94	-10.53	1.39	10.63
-141	292954.52	3536495.69	0.64	4.72	4.76
-142	292463.78	3547664.51	-12.97	-4.59	13.75
-137	292708.34	3551494.91	-2.63	-13.00	13.27
-163	304913.15	3532794.27	-7.51	6.35	9.84
-151	313516.29	3552945.59	1.07	-5.63	5.73
-152	309242.69	3554866.11	-9.70	-7.49	12.25
-146	322964.17	3563357.69	-6.84	1.54	7.01
-148	330976.77	3561092.39	-0.13	-7.68	7.68
-157	327583.70	3553044.83	0.00	-8.18	8.18
-164	320107.22	3536355.58	-5.06	3.26	6.02
-159	325736.46	3543789.61	7.84	-8.17	11.32
-165	317486.68	3530713.49	-12.35	1.96	12.50
-156	334926.90	3545637.77	-2.92	-8.35	8.85
-129	338786.72	3569547.74	-3.21	-5.69	6.53
-125	325235.33	3568555.27	-12.19	-7.12	14.12
-150	343634.30	3563017.67	-1.13	-5.33	5.45
-149	336882.89	3557839.21	1.15	-5.52	5.64
-126	326822.82	3574682.55	4.26	1.59	4.55
-128	331365.21	3573357.48	-1.95	4.85	5.22
-127	330690.32	3582058.67	-10.94	2.71	11.27
-118	290490.37	3561280.64	-5.99	-8.25	10.19
-171	313694.00	3569810.44	4.69	-3.10	5.62
-143	337966.57	3576240.13	0.93	-1.93	2.14
-155	337160.68	3549821.83	5.94	-6.52	8.82
-166	330246.70	3534950.34	-8.65	-4.30	9.66
-114	297527.53	3574015.59	-1.13	8.80	8.87
-153	320673.09	3549839.54	-7.74	-9.88	12.55
		RMS	±6.61	±6.47	±9.25

N02 (2 X ellipsoid normal) : 0.1276894614656886D+08
aa (Unknown tied to Earth rotation) : 0.6154297503614443D-01
ALPHA (IFOV) : 0.1200000000000000D-04
bb (Unknown of 2nd order) : 0.1003265514513486D-07
C0 (Scene centre column) : 0.3000000000000000D+04
cc (Unknown of 2nd order): -.4986760190496625D-08
COSKHI (Parameter): 0.9999995755848566D+00
DELGAM (Unknown of 2nd order): -.1393479130891412D-07
GAMMA (Scene orient. rel. to the North): 0.1635114334930211D+00
K_1 (Cross track scale function): 0.1413710332612023D-05
L0 (Scene centre row): 0.3000000000000000D+04
P (Along track scale function): 0.9978420293693206D+01
Q (Satellite-Scene centre dist): 0.9771789863365456D+06
TAU (Levelling angle along track dir): 0.9213201546556574D-03
THETA (Levelling angle across track dir): -.4450566411304784D+00
THETAS (THETA/COS_KHI): -.4450568300193368D+00
X0 (Carto coord of scene centre): 0.3123434773093872D+06
Y0 (Carto coord of scene centre): 0.3560458008572557D+07
DELH (Radar parameter in H dir.): 0.0000000000000000D+00
COEFY2 (Radar parameter in Y2 dir.): 0.0000000000000000D+00

EARTH ELLIPSOID USED : E004

The following are the results of the space resection giving the planimetric accuracy of the left image of the Level 1B stereo-model for reference scene 122/285 using 5 control points and 43 check points:

SMODEL Satellite Model Calculation V6.0 EASI/PACE 18:10 22-SEP-97

Report File : D:\SWEST\TEST\43CHR.TXT□

Using GCPs stored in the GCP segment :

GCPID	CALCULATED GCP		RESIDUAL (Metre)		
	X	Y	ΔX	ΔY	Vector
102	300928.09	3557102.73	-6.28	-4.15	7.52
116	284863.75	3573793.77	1.53	8.78	8.91
141	292952.17	3536503.12	2.99	-2.71	4.04
150	343632.51	3563006.20	0.66	6.14	6.17
169	318579.47	3586710.78	1.10	-8.06	8.14
		RMS	±3.62	±7.15	±8.01

RESIDUAL ERRORS AT CHECK POINTS:

GCPID	CALCULATED CHECK POINT		ERRORS (Metre)		
	X	Y	ΔX	ΔY	Vector
-101	308547.29	3559866.99	-2.62	3.42	4.31
-110	295864.21	3566656.57	6.99	-11.18	13.19
-112	309293.64	3582162.74	-5.70	4.42	7.22
-113	304312.75	3580947.37	-6.59	-0.11	6.59
-111	300753.90	3576802.83	-11.99	-1.33	12.06
-123	282561.57	3570259.07	-12.64	-16.29	20.62
-124	284234.90	3556275.27	-1.40	-27.82	27.85
-135	279729.37	3554394.55	-14.36	-37.90	40.53
-136	282131.81	3547240.73	-3.25	-18.61	18.89
-133	278863.15	3542831.54	-12.72	-14.21	19.07
-142	292473.98	3547681.09	-23.17	-21.17	31.39
-137	292708.93	3551503.25	-3.22	-21.34	21.59
-163	304892.99	3532777.72	12.65	22.90	26.17
-151	313510.84	3552951.68	6.52	-11.72	13.41
-152	309241.17	3554866.46	-8.18	-7.84	11.33
-146	322963.18	3563354.73	-5.85	4.50	7.38
-148	330975.11	3561086.54	1.53	-1.83	2.39
-158	328331.02	3556596.72	-1.48	-3.36	3.68
-157	327580.69	3553038.71	3.01	-2.06	3.64
-164	320097.63	3536350.61	4.53	8.23	9.39
-154	329671.27	3548194.21	10.37	4.14	11.17
-159	325731.80	3543782.28	12.50	-0.84	12.52
-167	330423.83	3528338.18	-4.40	23.36	23.77
-162	308305.82	3542496.66	8.48	0.89	8.52
-165	317480.10	3530707.16	-5.77	8.29	10.10
-156	334922.33	3545627.21	1.65	2.21	2.76
-145	345745.51	3571755.22	0.45	15.73	15.74
-129	338786.07	3569539.31	-2.56	2.74	3.75
-125	325239.37	3568549.48	-16.23	-1.33	16.28
-149	336872.67	3557836.71	11.37	-3.02	11.77
-126	326823.54	3574679.62	3.54	4.52	5.74
-128	331365.59	3573353.14	-2.33	9.19	9.48
-168	321495.84	3574920.80	0.14	18.26	18.26
-127	330692.30	3582056.14	-12.92	5.24	13.94
-118	290515.14	3561286.22	-30.76	-13.83	33.72
-119	284549.36	3563627.17	-3.57	-19.55	19.87

-171	313693.62	3569822.22	5.07	-14.88	15.72
-143	337965.78	3576225.03	1.72	13.17	13.29
-140	281955.44	3535731.18	6.77	-12.90	14.57
-155	337156.07	3549819.96	10.55	-4.65	11.53
-166	330240.40	3534939.86	-2.35	6.18	6.61
-114	297523.18	3574014.01	3.21	10.38	10.87
-153	320676.38	3549838.31	-11.02	-8.65	14.01
		RMS	±9.71	±13.51	±16.63

N02 (2 X ellipsoid normal) : 0.1276894614656886D+08
aa (Unknown tied to Earth rotation) : 0.6117160762836060D-01
ALPHA (IFOV) : 0.1200000000000000D-04
bb (Unknown of 2nd order) : 0.1003265514513486D-07
C0 (Scene centre column) : 0.3000000000000000D+04
cc (Unknown of 2nd order): -.4986760190496625D-08
COSKHI (Parameter): 0.9998182033291074D+00
DELGAM (Unknown of 2nd order): -.1393479130891412D-07
GAMMA (Scene orient. rel. to the North): 0.1640238020419734D+00
K_1 (Cross track scale function): 0.1412193839395294D-05
L0 (Scene centre row): 0.3000000000000000D+04
P (Along track scale function): 0.9980348810187024D+01
Q (Satellite-Scene centre dist): 0.9771106867826802D+06
TAU (Levelling angle along track dir): -.1907072405318443D-01
THETA (Levelling angle across track dir): -.4433057379759212D+00
THETAS (THETA/COS_KHI): -.4433863441372046D+00
X0 (Carto coord of scene centre): 0.3123464077897017D+06
Y0 (Carto coord of scene centre): 0.3560472901798993D+07
DELH (Radar parameter in H dir.): 0.0000000000000000D+00
COEFY2 (Radar parameter in Y2 dir.): 0.0000000000000000D+00

EARTH ELLIPSOID USED : E004

The following are the results of the space resection giving the planimetric accuracy of the right image of the Level 1B stereo-model for reference scene 122/285 using 5 control points and 43 check points:

SMODEL Satellite Model Calculation V6.0 EASI/PACE 18:11 22-SEP-97

Report File : D:\SWEST\TEST\43CHL.TXT

Using GCPs stored in the GCP segment :

GCPID	CALCULATED GCP		RESIDUAL (Metre)		
	X	Y	ΔX	ΔY	Vector
102	300930.27	3557091.41	-8.46	7.17	11.09
116	284865.46	3573802.65	-0.18	-0.10	0.21
141	292949.79	3536504.81	5.37	-4.40	6.94
150	343633.85	3563011.94	-0.68	0.40	0.79
169	318576.61	3586705.79	3.96	-3.07	5.01
		RMS	±5.40	±4.48	±7.02

RESIDUAL ERRORS AT CHECK POINTS:

GCPID	CALCULATED CHECK POINT		ERRORS (Metre)		
	X	Y	ΔX	ΔY	Vector
-101	308546.88	3559855.79	-2.21	14.62	14.79
-110	295872.29	3566656.05	-1.09	-10.66	10.72
-112	309300.12	3582165.33	-12.18	1.83	12.32
-113	304316.67	3580960.34	-10.51	-13.08	16.78
-111	300760.01	3576805.85	-18.10	-4.35	18.61
-114	297527.83	3574024.12	-1.44	0.27	1.46
-123	282558.87	3570253.23	-9.94	-10.45	14.42
-119	284545.73	3563619.53	0.06	-11.91	11.91
-124	284234.81	3556256.63	-1.31	-9.18	9.27
-135	279723.03	3554379.42	-8.02	-22.77	24.15
-133	278858.16	3542832.38	-7.73	-15.05	16.92
-136	282125.53	3547238.78	3.03	-16.66	16.93
-142	292474.71	3547672.78	-23.90	-12.86	27.14
-137	292716.30	3551494.10	-10.59	-12.19	16.14
-163	304907.64	3532799.43	-2.00	1.19	2.32
-167	330435.07	3528349.23	-15.64	12.31	19.90
-165	317493.07	3530721.43	-18.74	-5.98	19.67
-164	320102.42	3536357.02	-0.26	1.82	1.84
-162	308318.45	3542494.04	-4.15	3.50	5.43
-159	325737.53	3543769.61	6.77	11.83	13.63
-154	329674.58	3548181.04	7.06	17.31	18.70
-153	320692.31	3549816.96	-26.95	12.70	29.79
-151	313521.43	3552928.07	-4.07	11.89	12.57
-152	309250.11	3554846.99	-17.12	11.63	20.70
-157	327583.76	3553017.69	-0.06	18.96	18.96
-158	328329.66	3556584.98	-0.12	8.38	8.38
-148	330984.65	3561086.77	-8.01	-2.06	8.27
-146	322969.28	3563352.05	-11.95	7.18	13.94
-149	336877.87	3557826.94	6.17	6.75	9.15
-125	325242.94	3568553.93	-19.80	-5.78	20.63
-129	338786.81	3569546.43	-3.30	-4.38	5.49
-145	345749.08	3571768.72	-3.12	2.23	3.84
-126	326825.49	3574684.15	1.59	-0.01	1.59
-128	331365.81	3573361.30	-2.55	1.03	2.75
-168	321515.83	3574933.07	-19.85	5.99	20.73
-127	330683.58	3582054.00	-4.20	7.38	8.49
-118	290497.18	3561274.47	-12.80	-2.08	12.96
-156	334917.47	3545618.43	6.51	10.99	12.77
-155	337157.57	3549804.34	9.05	10.97	14.23
-140	281955.03	3535737.31	7.18	-19.04	20.34
-166	330250.18	3534944.69	-12.13	1.35	12.21
-143	337970.08	3576238.90	-2.58	-0.69	2.67
-171	313707.02	3569825.18	-8.33	-17.84	19.68
	RMS		±10.80	±10.78	±15.26

N02 (2 X ellipsoid normal) : 0.1276894858944160D+08
aa (Unknown tied to Earth rotation) : 0.5314697867272841D-01
ALPHA (IFOV) : 0.1200000000000000D-04
bb (Unknown of 2nd order) : 0.9635876951825774D-09
C0 (Scene centre column) : 0.3000000000000000D+04
cc (Unknown of 2nd order): 0.2804298974764739D-08
COSKHI (Parameter): 0.9999581869764726D+00
DELGAM (Unknown of 2nd order): 0.3270781780345786D-08
GAMMA (Scene orient. rel. to the North): 0.2438273302593856D+00

K_1 (Cross track scale function): 0.1415537208043065D-05
L0 (Scene centre row): 0.3000000000000000D+04
P (Along track scale function): 0.1001939249008895D+02
Q (Satellite-Scene centre dist): 0.1050762594007146D+07
TAU (Levelling angle along track dir): -.9145014616387742D-02
THETA (Levelling angle across track dir): 0.5264437067467133D+00
THETAS (THETA/COS_KHI): 0.5264657198702445D+00
X0 (Carto coord of scene centre): 0.3045092109733536D+06
Y0 (Carto coord of scene centre): 0.3560759978104392D+07
DELH (Radar parameter in H dir.): 0.0000000000000000D+00
COEFY2 (Radar parameter in Y2 dir.): 0.0000000000000000D+00

EARTH ELLIPSOID USED : E004

The following are the results of the space resection giving the planimetric accuracy of the left image of the Level 1B stereo-model for reference scene 122/285 using 48 ground control points:

SMODEL Satellite Model Calculation V6.0 EASI/PACE 13:14 22-SEP-97

EARTH ELLIPSOID USED : E004

SMODEL Satellite Model Calculation V6.0 EASI/PACE 13:20 22-SEP-97

Report File : D:\SWEST\TEST\48GRL.TXT

Using GCPs stored in the GCP segment :

GCPID	CALCULATED GCP		RESIDUAL (Metre)		
	X	Y	ΔX	ΔY	Vector
101	308540.35	3559865.13	4.32	5.28	6.82
102	300922.19	3557088.86	-0.38	9.72	9.73
110	295864.37	3566650.93	6.83	-5.54	8.79
112	309290.48	3582164.51	-2.54	2.65	3.67
113	304304.64	3580952.49	1.52	-5.23	5.45
111	300751.01	3576802.85	-9.10	-1.35	9.20
114	297519.43	3574019.63	6.96	4.76	8.43
116	284866.19	3573796.87	-0.91	5.68	5.75
123	282554.92	3570239.83	-5.99	2.95	6.68
119	284540.84	3563607.77	4.95	-0.15	4.95
124	284229.97	3556244.76	3.53	2.69	4.43
135	279719.64	3554365.05	-4.63	-8.40	9.59
133	278854.34	3542819.76	-3.91	-2.43	4.60
136	282121.01	3547226.94	7.55	-4.82	8.96
141	292952.15	3536498.86	3.01	1.55	3.39
142	292458.91	3547668.88	-8.10	-8.96	12.08
137	292709.31	3551487.92	-3.60	-6.01	7.00
163	304901.26	3532800.49	4.38	0.13	4.38
167	330425.70	3528361.79	-6.27	-0.25	6.27
165	317479.49	3530720.37	-5.16	-4.92	7.13
164	320098.65	3536363.71	3.51	-4.87	6.00
162	308311.75	3542495.04	2.55	2.50	3.57
159	325744.28	3543774.29	0.02	7.15	7.15
154	329677.71	3548191.63	3.93	6.72	7.79
153	320673.44	3549826.84	-8.08	2.82	8.56
151	313514.41	3552930.23	2.95	9.73	10.17
152	309236.38	3554858.49	-3.39	0.13	3.39
157	327580.57	3553023.02	3.13	13.63	13.99

158	328326.31	3556589.78	3.23	3.58	4.82
148	330981.68	3561091.40	-5.04	-6.69	8.38
146	322963.41	3563354.73	-6.08	4.50	7.57
149	336877.84	3557833.57	6.20	0.12	6.20
150	343636.14	3563019.90	-2.97	-7.56	8.12
125	325226.72	3568556.75	-3.58	-8.60	9.31
129	338784.46	3569543.92	-0.95	-1.87	2.09
145	345750.70	3571776.44	-4.74	-5.49	7.25
126	326819.40	3574686.22	7.68	-2.08	7.96
128	331361.31	3573364.33	1.95	-2.00	2.80
168	321498.23	3574938.06	-2.25	1.00	2.46
127	330677.90	3582055.29	1.48	6.09	6.27
169	318579.02	3586701.81	1.55	0.91	1.80
118	290490.45	3561266.70	-6.07	5.69	8.32
156	334918.47	3545626.87	5.51	2.55	6.07
155	337158.99	3549812.46	7.63	2.85	8.14
140	281956.68	3535718.44	5.52	-0.16	5.53
166	330245.75	3534951.74	-7.70	-5.70	9.58
143	337967.60	3576243.11	-0.10	-4.91	4.91
171	313697.04	3569814.76	1.65	-7.41	7.60
		RMS	±4.89	±5.39	±7.28

N02 (2 X ellipsoid normal) : 0.1276894858944160D+08
aa (Unknown tied to Earth rotation) : 0.5363312075719852D-01
ALPHA (IFOV) : 0.1200000000000000D-04
bb (Unknown of 2nd order) : 0.9635876951825774D-09
C0 (Scene centre column) : 0.3000000000000000D+04
cc (Unknown of 2nd order): 0.2804298974764739D-08
COSKHI (Parameter): 0.9999835960497840D+00
DELGAM (Unknown of 2nd order): 0.3270781780345786D-08
GAMMA (Scene orient. rel. to the North): 0.2433727724098199D+00
K_1 (Cross track scale function): 0.1425292943788772D-05
L0 (Scene centre row): 0.3000000000000000D+04
P (Along track scale function): 0.1001785456902927D+02
Q (Satellite-Scene centre dist): 0.1050626430758457D+07
TAU (Levelling angle along track dir): 0.5727888591640930D-02
THETA (Levelling angle across track dir): 0.5346324425253502D+00
THETAS (THETA/COS_KHI): 0.5346412127531877D+00
X0 (Carto coord of scene centre): 0.3045045350681888D+06
Y0 (Carto coord of scene centre): 0.3560744880741218D+07
DELH (Radar parameter in H dir.): 0.0000000000000000D+00
COEFY2 (Radar parameter in Y2 dir.): 0.0000000000000000D+00

EARTH ELLIPSOID USED : E004

The following are the results of the space resection giving the planimetric accuracy of the right image of the Level 1B stereo-model for reference scene 122/285 using 48 ground control points:

SMODEL Satellite Model Calculation V6.0 EASI/PACE 13:06 22-SEP-97

Report File : D:\SWEST\TEST\48GR.TXT

Using GCPs stored in the GCP segment :

GCPID	CALCULATED GCP		RESIDUAL (Metre)		
	X	Y	ΔX	ΔY	Vector
101	308544.42	3559865.20	0.25	5.21	5.22
102	300924.28	3557097.56	-2.47	1.02	2.67
110	295868.43	3566649.18	2.77	-3.79	4.69
112	309288.36	3582163.33	-0.42	3.83	3.85
113	304307.07	3580947.59	-0.91	-0.33	0.97
111	300748.06	3576800.93	-6.15	0.57	6.18
116	284861.65	3573790.49	3.63	12.06	12.60
123	282552.58	3570243.28	-3.65	-0.50	3.68
124	284232.08	3556254.38	1.42	-6.93	7.07
135	279719.58	3554365.07	-4.57	-8.42	9.58
136	282125.33	3547222.50	3.23	-0.38	3.25
133	278856.72	3542812.11	-6.29	5.22	8.18
141	292949.66	3536492.49	5.50	7.92	9.64
142	292459.43	3547662.14	-8.62	-2.22	8.90
137	292704.17	3551492.71	1.54	-10.80	10.91
163	304908.50	3532791.49	-2.86	9.13	9.57
151	313512.79	3552943.89	4.57	-3.93	6.03
152	309239.01	3554864.67	-6.02	-6.05	8.54
146	322961.70	3563355.34	-4.37	3.89	5.85
148	330975.10	3561089.33	1.54	-4.62	4.87
158	328331.32	3556599.52	-1.78	-6.16	6.41
157	327581.47	3553042.09	2.23	-5.44	5.87
164	320103.83	3536353.56	-1.67	5.28	5.54
154	329673.14	3548199.19	8.50	-0.84	8.54
159	325733.84	3543787.20	10.46	-5.76	11.94
167	330421.22	3528353.61	-1.79	7.93	8.13
162	308304.96	3542493.54	9.34	4.01	10.16
165	317482.90	3530711.52	-8.57	3.93	9.43
156	334925.51	3545634.84	-1.53	-5.42	5.63
145	345746.60	3571763.90	-0.64	7.05	7.07
129	338786.21	3569544.79	-2.70	-2.74	3.84
125	325233.20	3568553.10	-10.06	-4.95	11.21
150	343634.44	3563014.47	-1.27	-2.13	2.48
149	336881.94	3557835.92	2.10	-2.23	3.06
126	326820.99	3574680.21	6.09	3.93	7.25
128	331363.82	3573354.60	-0.56	7.73	7.75
168	321494.15	3574929.99	1.83	9.07	9.25
127	330689.04	3582055.74	-9.66	5.64	11.19
169	318574.36	3586710.29	6.21	-7.57	9.79
118	290486.71	3561279.29	-2.33	-6.90	7.29
119	284541.50	3563612.00	4.29	-4.38	6.13
171	313691.06	3569809.82	7.63	-2.48	8.02
143	337966.04	3576236.92	1.46	1.28	1.94
140	281955.64	3535713.95	6.57	4.32	7.86
155	337159.67	3549818.67	6.95	-3.36	7.72
166	330244.50	3534947.64	-6.46	-1.60	6.65
114	297524.40	3574016.22	1.99	8.17	8.41
153	320670.08	3549836.95	-4.72	-7.29	8.69
		RMS	±5.13	±5.69	±7.66

N02 (2 X ellipsoid normal) : 0.1276894614656886D+08
aa (Unknown tied to Earth rotation) : 0.6161954689063980D-01
ALPHA (IFOV) : 0.1200000000000000D-04
bb (Unknown of 2nd order) : 0.1003265514513486D-07
C0 (Scene centre column) : 0.3000000000000000D+04

cc (Unknown of 2nd order): -.4986760190496625D-08
COSKHI (Parameter): 0.9999286657543668D+00
DELGAM (Unknown of 2nd order): -.1393479130891412D-07
GAMMA (Scene orient. rel. to the North): 0.1634891918669837D+00
K_1 (Cross track scale function): 0.1411831624717314D-05
L0 (Scene centre row): 0.3000000000000000D+04
P (Along track scale function): 0.9978022327325518D+01
Q (Satellite-Scene centre dist): 0.9772240303497886D+06
TAU (Levelling angle along track dir): 0.1194503070075891D-01
THETA (Levelling angle across track dir): -.4432311102818642D+00
THETAS (THETA/COS_KHI): -.4432627300943327D+00
X0 (Carto coord of scene centre): 0.3123401495790800D+06
Y0 (Carto coord of scene centre): 0.3560447933124138D+07
DELH (Radar parameter in H dir.): 0.0000000000000000D+00
COEFY2 (Radar parameter in Y2 dir.): 0.0000000000000000D+00

EARTH ELLIPSOID USED : E004

B.2.2 SPOT Level 1A Stereo-pair for Reference Scene 122/285

The following are the results of the space resection giving the planimetric accuracy of the left image of the Level 1A stereo-model for reference scene 122/285 using 43 control points and 5 check points:

SMODEL Satellite Model Calculation V6.0 EASI/PACE 13:28 22-SEP-97

Report File : D:\SWEST\TEST\5CHLA.TXT

Using GCPs stored in the GCP segment :

GCPID	CALCULATED GCP		RESIDUAL (Metre)		
	X	Y	ΔX	ΔY	Vector
101	308540.45	3559860.71	3.55	9.70	10.33
102	300930.45	3557083.21	-8.63	15.37	17.63
110	295860.28	3566650.55	10.92	-5.16	12.08
113	304310.44	3580960.32	-4.28	-13.06	13.74
111	300742.74	3576794.36	-0.83	7.14	7.18
114	297518.25	3574017.86	8.15	6.53	10.44
116	284868.52	3573793.13	-3.25	9.42	9.96
119	284553.34	3563607.45	-7.55	0.17	7.55
118	290490.71	3561271.09	-6.33	1.30	6.46
124	284230.01	3556253.62	3.48	-6.17	7.09
135	279723.84	3554365.66	-8.83	-9.01	12.62
136	282124.66	3547222.82	3.90	-0.70	3.96
133	278853.86	3542815.78	-3.43	1.55	3.76
140	281955.07	3535718.47	7.14	-0.20	7.14
142	292458.80	3547661.24	-7.99	-1.32	8.10
137	292714.82	3551492.93	-9.11	-11.02	14.30
163	304892.20	3532790.62	13.44	10.00	16.75
162	308298.61	3542492.25	15.69	5.30	16.56
146	322961.71	3563356.17	-4.38	3.06	5.34
148	330980.16	3561093.64	-3.52	-8.93	9.60
158	328327.03	3556596.36	2.52	-2.99	3.91
157	327568.41	3553039.17	15.29	-2.51	15.50
151	313522.29	3552933.71	-4.93	6.24	7.96

152	309238.07	3554857.38	-5.08	1.24	5.23
159	325738.17	3543786.95	6.13	-5.51	8.25
153	320673.29	3549826.35	-7.93	3.31	8.59
164	320093.90	3536358.45	8.26	0.38	8.27
167	330430.14	3528356.72	-10.71	4.83	11.75
166	330249.13	3534950.64	-11.09	-4.60	12.00
165	317480.71	3530718.54	-6.38	-3.08	7.09
125	325230.50	3568545.84	-7.36	2.32	7.72
149	336880.43	3557835.16	3.61	-1.47	3.90
126	326819.06	3574683.67	8.02	0.47	8.03
168	321499.57	3574932.95	-3.59	6.11	7.08
127	330682.67	3582056.57	-3.29	4.81	5.83
145	345747.93	3571768.73	-1.97	2.22	2.97
169	318575.67	3586703.15	4.90	-0.43	4.92
171	313702.46	3569823.19	-3.77	-15.85	16.29
150	343632.29	3563016.19	0.88	-3.84	3.94
120	280170.65	3565348.60	12.11	-4.31	12.85
155	337162.40	3549819.11	4.23	-3.81	5.69
143	337966.25	3576237.00	1.25	1.20	1.73
128	331362.48	3573361.00	0.78	1.33	1.54
		RMS	±7.36	±6.36	±9.73

RESIDUAL ERRORS AT CHECK POINTS:

GCPID	CALCULATED CHECK POINT		ERRORS (Metre)		
	X	Y	ΔX	ΔY	Vector
-112	309293.54	3582166.60	-5.60	0.57	5.63
-123	282556.00	3570244.99	-7.07	-2.21	7.41
-141	292950.37	3536495.94	4.78	4.47	6.55
-154	329675.06	3548190.13	6.58	8.22	10.53
-129	338779.76	3569546.21	3.75	-4.16	5.61
		RMS	±6.36	±5.25	±8.24

N02 (2 X ellipsoid normal) : 0.1276894858944160D+08
aa (Unknown tied to Earth rotation) : 0.5363356281734311D-01
ALPHA (IFOV) : 0.1200000000000000D-04
bb (Unknown of 2nd order) : 0.9637452434055284D-09
C0 (Scene centre column) : 0.3000000000000000D+04
cc (Unknown of 2nd order): 0.2800395867240290D-08
COSKHI (Parameter): 0.9999939712577718D+00
DELGAM (Unknown of 2nd order): 0.3290999296140512D-08
GAMMA (Scene orient. rel. to the North): 0.2434218474939870D+00
K_1 (Cross track scale function): 0.1428660487260507D-05
L0 (Scene centre row): 0.3000000000000000D+04
P (Along track scale function): 0.1001820410535049D+02
Q (Satellite-Scene centre dist): 0.1050524186535993D+07
TAU (Levelling angle along track dir): 0.3472404569484749D-02
THETA (Levelling angle across track dir): 0.5373774260519958D+00
THETAS (THETA/COS_KHI): 0.5373806657815081D+00
X0 (Carto coord of scene centre): 0.3045110274878860D+06
Y0 (Carto coord of scene centre): 0.3560754333340650D+07
DELH (Radar parameter in H dir.): 0.0000000000000000D+00
COEFY2 (Radar parameter in Y2 dir.): 0.0000000000000000D+00

EARTH ELLIPSOID USED : E004

The following are the results of the space resection giving the planimetric accuracy of the right image of the Level 1A stereo-model for reference scene 122/285 using 43 control points and 5 check points:

SMODEL Satellite Model Calculation V6.0 EASI/PACE 13:46 22-SEP-97

Report File : D:\SWEST\TEST\5CHRA.TXT

Using GCPs stored in the GCP segment :

GCPID	CALCULATED GCP		RESIDUAL (Metre)		
	X	Y	ΔX	ΔY	Vector
101	308537.84	3559862.94	6.83	7.47	10.12
102	300927.93	3557097.84	-6.12	0.74	6.17
110	295871.29	3566643.96	-0.09	1.43	1.43
113	304309.66	3580948.96	-3.51	-1.70	3.90
111	300744.33	3576793.91	-2.42	7.59	7.97
114	297518.21	3574019.27	8.18	5.12	9.65
156	334927.83	3545634.51	-3.86	-5.10	6.39
116	284865.18	3573799.84	0.10	2.71	2.71
166	330242.58	3534948.41	-4.53	-2.37	5.11
124	284231.74	3556251.12	1.76	-3.67	4.07
135	279719.55	3554358.71	-4.54	-2.06	4.98
133	278858.00	3542813.18	-7.57	4.16	8.63
136	282123.65	3547221.69	4.92	0.43	4.94
163	304902.83	3532795.93	2.81	4.69	5.46
142	292461.11	3547662.44	-10.30	-2.52	10.60
137	292706.24	3551486.92	-0.54	-5.01	5.03
140	281956.38	3535716.62	5.83	1.66	6.06
146	322962.79	3563358.15	-5.46	1.07	5.56
148	330978.94	3561091.33	-2.31	-6.61	7.01
158	328328.49	3556591.25	1.06	2.12	2.37
157	327576.20	3553032.77	7.51	3.88	8.45
159	325742.87	3543783.73	1.43	-2.29	2.70
151	313514.18	3552941.33	3.18	-1.37	3.46
152	309230.09	3554853.58	2.90	5.03	5.81
164	320099.45	3536358.55	2.71	0.29	2.72
165	317473.21	3530717.69	1.12	-2.24	2.51
162	308311.62	3542491.32	2.68	6.23	6.78
167	330421.16	3528358.95	-1.73	2.59	3.11
149	336878.56	3557833.13	5.48	0.55	5.50
150	343636.90	3563015.48	-3.73	-3.14	4.88
125	325226.48	3568550.06	-3.34	-1.91	3.85
145	345739.96	3571772.65	6.00	-1.70	6.23
126	326825.29	3574677.48	1.79	6.66	6.90
127	330683.00	3582059.55	-3.62	1.83	4.06
168	321497.56	3574935.14	-1.58	3.92	4.23
169	318576.43	3586711.27	4.14	-8.55	9.50
128	331370.12	3573363.44	-6.86	-1.11	6.95
118	290482.60	3561280.10	1.78	-7.71	7.92
119	284542.90	3563615.65	2.89	-8.03	8.53
153	320673.57	3549831.42	-8.21	-1.76	8.40
171	313697.98	3569813.33	0.71	-5.99	6.03
143	337966.69	3576231.55	0.81	6.66	6.71
155	337162.92	3549817.28	3.71	-1.98	4.20

RMS ±4.52 ±4.33 ±6.26

RESIDUAL ERRORS AT CHECK POINTS:

GCPID	CALCULATED CHECK POINT X	Y	ERRORS (Metre) ΔX	ΔY	Vector
-112	309284.99	3582169.67	2.95	-2.51	3.87
-123	282553.80	3570241.07	-4.87	1.71	5.16
-141	292954.29	3536492.58	0.87	7.83	7.88
-154	329673.10	3548196.21	8.54	2.14	8.80
-129	338778.05	3569552.61	5.46	-10.56	11.89

RMS ± 5.83 ±6.83 ±8.98

N02 (2 X ellipsoid normal) : 0.1276894614656886D+08
aa (Unknown tied to Earth rotation) : 0.6150762049743955D-01
ALPHA (IFOV) : 0.1200000000000000D-04
bb (Unknown of 2nd order) : 0.1003199597018114D-07
C0 (Scene centre column) : 0.3000000000000000D+04
cc (Unknown of 2nd order): -.4982705245390573D-08
COSKHI (Parameter): 0.9999880088477170D+00
DELGAM (Unknown of 2nd order): -.1394416529022841D-07
GAMMA (Scene orient. rel. to the North): 0.1635694493148104D+00
K_1 (Cross track scale function): 0.1416250204142132D-05
L0 (Scene centre row): 0.3000000000000000D+04
P (Along track scale function): 0.9978714411351202D+01
Q (Satellite-Scene centre dist): 0.9771860887795118D+06
TAU (Levelling angle along track dir): 0.4897217162443542D-02
THETA (Levelling angle across track dir): -.4474626088394470D+00
THETAS (THETA/COS_KHI): -.4474679744960710D+00
X0 (Carto coord of scene centre): 0.3123370205047688D+06
Y0 (Carto coord of scene centre): 0.3560440722719716D+07
DELH (Radar parameter in H dir.): 0.0000000000000000D+00
COEFY2 (Radar parameter in Y2 dir.): 0.0000000000000000D+00

EARTH ELLIPSOID USED : E004

The following are the results of the space resection giving the planimetric accuracy of the left image of the Level 1A stereo-model for reference scene 122/285 using 33 control points and 15 check points:

SMODEL Satellite Model Calculation V6.0 EASI/PACE 13:30 22-SEP-97

Report File : D:\SWEST\TEST\15CHLA.TXT

Using GCPs stored in the GCP segment :

GCPID	CALCULATED GCP X	Y	RESIDUAL (Metre) ΔX	ΔY	Vector
102	300930.44	3557082.37	-8.63	16.21	18.36
110	295860.14	3566649.10	11.06	-3.71	11.66
113	304310.00	3580957.50	-3.84	-10.24	10.94
111	300742.37	3576791.87	-0.47	9.63	9.64

116	284868.44	3573792.19	-3.17	10.36	10.83
119	284553.45	3563607.27	-7.66	0.35	7.67
124	284230.29	3556254.18	3.20	-6.73	7.46
135	279724.20	3554366.69	-9.19	-10.03	13.61
133	278854.25	3542816.84	-3.82	0.49	3.85
140	281955.42	3535719.28	6.78	-1.01	6.86
142	292458.99	3547661.24	-8.18	-1.32	8.28
163	304892.36	3532790.79	13.28	9.82	16.52
162	308298.73	3542492.26	15.57	5.29	16.44
146	322961.74	3563356.14	-4.41	3.09	5.38
158	328327.02	3556596.61	2.53	-3.25	4.12
157	327568.37	3553039.30	15.33	-2.64	15.56
152	309238.05	3554856.66	-5.06	1.95	5.42
159	325738.05	3543786.77	6.25	-5.33	8.22
153	320673.32	3549826.41	-7.96	3.25	8.60
167	330429.82	3528356.36	-10.38	5.19	11.61
166	330248.91	3534950.54	-10.86	-4.50	11.76
165	317480.57	3530717.98	-6.24	-2.53	6.73
149	336880.33	3557835.62	3.71	-1.94	4.19
168	321499.60	3574932.69	-3.62	6.37	7.33
127	330682.78	3582057.08	-3.40	4.30	5.49
145	345747.66	3571768.85	-1.70	2.11	2.71
169	318575.56	3586702.05	5.01	0.67	5.06
171	313702.32	3569821.94	-3.63	-14.60	15.04
150	343632.06	3563016.51	1.11	-4.16	4.31
120	280170.82	3565348.85	11.94	-4.57	12.78
155	337162.20	3549819.40	4.42	-4.09	6.02
143	337966.25	3576237.56	1.25	0.64	1.41
128	331362.52	3573361.38	0.74	0.95	1.20
		RMS	±7.54	±6.41	±9.90

RESIDUAL ERRORS AT CHECK POINTS:

GCPID	CALCULATED CHECK POINT		ERRORS (Metre)		
	X	Y	ΔX	ΔY	Vector
-101	308540.39	3559859.73	3.61	10.68	11.28
-112	309293.19	3582164.24	-5.25	2.93	6.01
-114	297517.96	3574015.73	8.44	8.66	12.09
-123	282556.02	3570244.53	-7.09	-1.75	7.30
-118	290490.73	3561270.40	-6.35	1.99	6.66
-136	282125.04	3547223.78	3.53	-1.66	3.90
-141	292950.68	3536496.50	4.47	3.92	5.95
-137	292714.99	3551492.82	-9.28	-10.91	14.32
-148	330980.17	3561094.05	-3.53	-9.34	9.99
-151	313522.27	3552933.16	-4.91	6.79	8.38
-154	329674.96	3548190.25	6.68	8.10	10.50
-164	320093.76	3536357.96	8.40	0.87	8.44
-125	325230.49	3568545.69	-7.35	2.47	7.76
-129	338779.64	3569546.49	3.87	-4.44	5.89
-126	326819.09	3574683.70	7.99	0.44	8.00
		RMS	±6.58	±6.37	±9.15

N02 (2 X ellipsoid normal) : 0.1276894858944160D+08
aa (Unknown tied to Earth rotation) : 0.5359236700059900D-01

ALPHA (IFOV) : 0.1200000000000000D-04
bb (Unknown of 2nd order) : 0.9637452434055284D-09
C0 (Scene centre column) : 0.3000000000000000D+04
cc (Unknown of 2nd order): 0.2800395867240290D-08
COSKHI (Parameter): 0.9999845225963268D+00
DELGAM (Unknown of 2nd order): 0.3290999296140512D-08
GAMMA (Scene orient. rel. to the North): 0.2434591818358131D+00
K_1 (Cross track scale function): 0.1428374171614490D-05
L0 (Scene centre row): 0.3000000000000000D+04
P (Along track scale function): 0.1001865810642614D+02
Q (Satellite-Scene centre dist): 0.1050521398394850D+07
TAU (Levelling angle along track dir): -.5563769047257053D-02
THETA (Levelling angle across track dir): 0.5371238735731324D+00
THETAS (THETA/COS_KHI): 0.5371321869848162D+00
X0 (Carto coord of scene centre): 0.3045125799314475D+06
Y0 (Carto coord of scene centre): 0.3560760634612845D+07
DELH (Radar parameter in H dir.): 0.0000000000000000D+00
COEFY2 (Radar parameter in Y2 dir.): 0.0000000000000000D+00

EARTH ELLIPSOID USED : E004

The following are the results of the space resection giving the planimetric accuracy of the right image of the Level 1A stereo-model for reference scene 122/285 using 33 control points and 15 check points:

SMODEL Satellite Model Calculation V6.0 EASI/PACE 13:47 22-SEP-97

Report File : D:\SWEST\TEST\15CHRA.TXT

Using GCPs stored in the GCP segment :

GCPID	CALCULATED GCP		RESIDUAL (Metre)		
	X	Y	ΔX	ΔY	Vector
102	300926.43	3557097.80	-4.62	0.78	4.69
110	295869.70	3566643.56	1.50	1.83	2.36
113	304307.92	3580947.73	-1.76	-0.47	1.82
111	300742.60	3576792.89	-0.70	8.61	8.64
156	334928.08	3545634.60	-4.10	-5.18	6.61
116	284863.90	3573799.59	1.38	2.96	3.26
166	330242.54	3534948.55	-4.49	-2.51	5.15
124	284230.56	3556251.80	2.93	-4.35	5.24
135	279718.54	3554359.62	-3.53	-2.97	4.61
133	278856.89	3542814.26	-6.45	3.07	7.15
163	304901.56	3532796.58	4.08	4.03	5.74
142	292459.67	3547662.94	-8.86	-3.02	9.37
140	281955.08	3535717.68	7.12	0.60	7.15
146	322962.11	3563358.22	-4.78	1.01	4.88
158	328328.20	3556591.43	1.35	1.94	2.36
157	327575.86	3553032.93	7.84	3.72	8.68
159	325742.43	3543783.85	1.87	-2.41	3.05
152	309228.77	3554853.57	4.22	5.05	6.58
165	317472.32	3530717.87	2.02	-2.42	3.15
162	308310.41	3542491.77	3.89	5.78	6.97
167	330421.16	3528359.02	-1.73	2.52	3.06
149	336878.90	3557833.26	5.14	0.43	5.16
150	343637.70	3563015.39	-4.53	-3.04	5.46
145	345740.80	3571772.36	5.17	-1.41	5.36

127	330682.72	3582059.60	-3.34	1.78	3.79
168	321496.72	3574935.01	-0.74	4.05	4.12
169	318575.30	3586710.67	5.27	-7.95	9.54
128	331369.91	3573363.50	-6.66	-1.17	6.76
119	284541.65	3563615.89	4.14	-8.27	9.25
153	320672.85	3549831.68	-7.50	-2.02	7.76
171	313696.69	3569812.88	2.01	-5.54	5.89
143	337966.93	3576231.56	0.57	6.64	6.66
155	337163.33	3549817.38	3.29	-2.07	3.89
		RMS	±4.51	±4.05	±6.06

RESIDUAL ERRORS FOR CHECK POINTS:

GCPID	CALCULATED CHECK POINT		ERRORS (Metre)		
	X	Y	ΔX	ΔY	Vector
-101	308536.46	3559862.76	8.21	7.66	11.23
-112	309283.40	3582168.60	4.55	-1.44	4.77
-114	297516.54	3574018.46	9.85	5.93	11.50
-123	282552.63	3570241.09	-3.70	1.69	4.06
-136	282122.49	3547222.67	6.07	-0.55	6.10
-141	292952.89	3536493.47	2.26	6.94	7.30
-137	292704.81	3551487.33	0.89	-5.42	5.49
-148	330978.82	3561091.50	-2.18	-6.79	7.13
-154	329672.94	3548196.37	8.70	1.98	8.92
-151	313513.03	3552941.37	4.33	-1.41	4.55
-164	320098.67	3536358.67	3.48	0.16	3.49
-129	338778.37	3569552.53	5.15	-10.48	11.67
-125	325225.86	3568550.00	-2.72	-1.85	3.29
-126	326824.75	3574677.42	2.32	6.72	7.11
-118	290481.14	3561280.13	3.24	-7.74	8.39
		RMS	±5.36	±5.65	±7.79

N02 (2 X ellipsoid normal) : 0.1276894614656886D+08
aa (Unknown tied to Earth rotation) : 0.6150782368686633D-01
ALPHA (IFOV) : 0.1200000000000000D-04
bb (Unknown of 2nd order) : 0.1003199597018114D-07
C0 (Scene centre column) : 0.3000000000000000D+04
cc (Unknown of 2nd order): -.4982705245390573D-08
COSKHI (Parameter): 0.9999997969847144D+00
DELGAM (Unknown of 2nd order): -.1394416529022841D-07
GAMMA (Scene orient. rel. to the North): 0.1635815618120656D+00
K_1 (Cross track scale function): 0.1415185822729887D-05
L0 (Scene centre row): 0.3000000000000000D+04
P (Along track scale function): 0.9978827402483556D+01
Q (Satellite-Scene centre dist): 0.9772147237281130D+06
TAU (Levelling angle along track dir): 0.6372053787477521D-03
THETA (Levelling angle across track dir): -.4465021018453984D+00
THETAS (THETA/COS_KHI): -.4465021924921686D+00
X0 (Carto coord of scene centre): 0.3123370793268016D+06
Y0 (Carto coord of scene centre): 0.3560443762990342D+07
DELH (Radar parameter in H dir.): 0.0000000000000000D+00
COEFY2 (Radar parameter in Y2 dir.): 0.0000000000000000D+00

EARTH ELLIPSOID USED : E004

The following are the results of the space resection giving the planimetric accuracy of the left image of the Level 1A stereo-model for reference scene 122/285 using 23 control points and 25 check points:

SMODEL Satellite Model Calculation V6.0 EASI/PACE 13:31 22-SEP-97

Report File : D:\SWEST\TEST\25CHLA.TXT

Using GCPs stored in the GCP segment :

GCPID	CALCULATED GCP		RESIDUAL (Metre)		
	X	Y	ΔX	ΔY	Vector
102	300921.65	3557096.46	0.17	2.11	2.12
110	295870.98	3566648.61	0.22	-3.22	3.23
113	304303.77	3580948.41	2.39	-1.14	2.65
116	284866.75	3573792.64	-1.47	9.90	10.01
119	284552.49	3563607.92	-6.70	-0.30	6.71
124	284229.88	3556255.05	3.62	-7.60	8.42
136	282125.18	3547224.70	3.39	-2.58	4.26
140	281956.33	3535719.97	5.88	-1.70	6.12
142	292459.46	3547661.74	-8.65	-1.82	8.84
163	304907.22	3532795.71	-1.59	4.90	5.15
162	308314.32	3542490.48	-0.02	7.07	7.07
146	322962.11	3563356.92	-4.78	2.31	5.31
158	328327.93	3556597.46	1.61	-4.09	4.40
154	329676.39	3548190.93	5.25	7.42	9.09
159	325739.66	3543787.24	4.64	-5.80	7.43
167	330425.49	3528358.46	-6.06	3.09	6.80
168	321499.20	3574933.51	-3.22	5.55	6.42
127	330682.21	3582058.37	-2.83	3.01	4.13
145	345747.90	3571769.92	-1.94	1.04	2.20
169	318574.29	3586702.65	6.28	0.07	6.29
171	313698.24	3569815.42	0.46	-8.08	8.10
150	343632.80	3563017.55	0.37	-5.20	5.22
155	337163.65	3549820.22	2.98	-4.92	5.75
		RMS	±4.11	±4.94	±6.43

RESIDUAL ERRORS AT CHECK POINTS:

GCPID	CALCULATED CHECK POINT		ERRORS (Metre)		
	X	Y	ΔX	ΔY	Vector
-101	308541.50	3559867.17	2.50	3.24	4.09
-112	309291.83	3582164.19	-3.89	2.98	4.90
-111	300741.05	3576791.68	0.85	9.82	9.86
-114	297516.72	3574015.66	9.67	8.73	13.03
-156	334932.82	3545627.02	-8.84	2.40	9.16
-118	290490.17	3561270.78	-5.78	1.61	6.00
-135	279710.49	3554361.83	4.52	-5.18	6.87
-133	278854.55	3542817.74	-4.12	-0.41	4.14
-141	292951.95	3536497.10	3.21	3.32	4.62
-137	292703.08	3551486.99	2.63	-5.08	5.72
-148	330980.87	3561095.04	-4.23	-10.33	11.16
-157	327578.90	3553037.70	4.80	-1.04	4.92

-151	313523.04	3552933.54	-5.68	6.41	8.57
-152	309238.57	3554856.98	-5.57	1.63	5.81
-153	320674.48	3549827.05	-9.13	2.61	9.49
-164	320095.70	3536358.18	6.46	0.66	6.49
-166	330245.75	3534952.94	-7.71	-6.90	10.34
-165	317482.80	3530718.08	-8.47	-2.63	8.87
-125	325230.59	3568546.49	-7.45	1.66	7.64
-149	336881.31	3557836.62	2.73	-2.94	4.01
-129	338779.95	3569547.56	3.57	-5.51	6.56
-126	326818.86	3574684.67	8.22	-0.53	8.24
-123	282556.91	3570245.19	-7.97	-2.41	8.33
-143	337966.16	3576238.83	1.34	-0.63	1.48
-128	331362.48	3573362.51	0.78	-0.18	0.80
		RMS	±5.96	±4.68	±7.58

N02 (2 X ellipsoid normal) : 0.1276894858944160D+08
aa (Unknown tied to Earth rotation) : 0.5352945041400659D-01
ALPHA (IFOV) : 0.1200000000000000D-04
bb (Unknown of 2nd order) : 0.9637452434055284D-09
C0 (Scene centre column) : 0.3000000000000000D+04
cc (Unknown of 2nd order): 0.2800395867240290D-08
COSKHI (Parameter): 0.9999546319761454D+00
DELGAM (Unknown of 2nd order): 0.3290999296140512D-08
GAMMA (Scene orient. rel. to the North): 0.2434648488161476D+00
K_1 (Cross track scale function): 0.1427915603482260D-05
L0 (Scene centre row): 0.3000000000000000D+04
P (Along track scale function): 0.1001885740229547D+02
Q (Satellite-Scene centre dist): 0.1050571994889178D+07
TAU (Levelling angle along track dir): -.9525871238670426D-02
THETA (Levelling angle across track dir): 0.5367552224329751D+00
THETAS (THETA/COS_KHI): 0.5367795750615413D+00
X0 (Carto coord of scene centre): 0.3045130362304477D+06
Y0 (Carto coord of scene centre): 0.3560764148768852D+07
DELH (Radar parameter in H dir.): 0.0000000000000000D+00
COEFY2 (Radar parameter in Y2 dir.): 0.0000000000000000D+00

EARTH ELLIPSOID USED : E004

The following are the results of the space resection giving the planimetric accuracy of the right image of the Level 1A stereo-model for reference scene 122/285 using 23 control points and 25 check points:

SMODEL Satellite Model Calculation V6.0 EASI/PACE 13:49 22-SEP-97

Report File : D:\SWEST\TEST\25CHRA.TXT

Using GCPs stored in the GCP segment :

GCPID	CALCULATED GCP		RESIDUAL (Metre)		
	X	Y	ΔX	ΔY	Vector
102	300927.03	3557097.27	-5.21	1.31	5.37
110	295870.67	3566642.01	0.53	3.39	3.43
113	304307.81	3580944.85	-1.65	2.41	2.93
116	284866.85	3573796.90	-1.57	5.65	5.87
124	284233.57	3556250.89	-0.07	-3.44	3.44

136	282125.72	3547222.72	2.84	-0.59	2.90
163	304902.30	3532798.65	3.33	1.97	3.87
142	292461.18	3547663.29	-10.37	-3.37	10.91
140	281957.99	3535719.12	4.22	-0.85	4.30
146	322962.71	3563356.67	-5.38	2.56	5.95
158	328329.44	3556590.46	0.10	2.90	2.90
154	329674.55	3548196.33	7.09	2.02	7.37
159	325743.69	3543784.46	0.62	-3.02	3.08
162	308311.00	3542492.74	3.30	4.81	5.84
167	330423.46	3528361.23	-4.03	0.31	4.04
150	343640.75	3563013.25	-7.58	-0.91	7.63
129	338780.36	3569549.86	3.15	-7.81	8.42
145	345743.72	3571769.25	2.24	1.70	2.81
168	321496.98	3574932.23	-1.00	6.83	6.90
169	318575.12	3586706.76	5.45	-4.03	6.78
119	284544.58	3563614.25	1.21	-6.63	6.74
171	313696.63	3569810.95	2.07	-3.61	4.16
155	337165.91	3549816.91	0.71	-1.60	1.75
		RMS	±4.23	±3.80	±5.68

RESIDUAL ERRORS AT CHECK POINTS:

GCPID	CALCULATED CHECK POINT		ERRORS (Metre)		
	X	Y	ΔX	ΔY	Vector
-101	308536.63	3559861.94	8.04	8.47	11.68
-112	309283.10	3582165.50	4.84	1.66	5.12
-111	300742.87	3576790.40	-0.97	11.10	11.14
-114	297517.22	3574016.19	9.17	8.20	12.30
-156	334930.46	3545634.69	-6.48	-5.27	8.35
-123	282556.06	3570238.67	-7.12	4.11	8.22
-166	330244.64	3534949.99	-6.59	-3.95	7.68
-135	279722.44	3554358.74	-7.43	-2.09	7.72
-133	278860.59	3542814.74	-10.15	2.59	10.48
-141	292954.39	3536495.01	0.76	5.40	5.45
-137	292706.32	3551487.25	-0.62	-5.33	5.37
-148	330980.23	3561089.95	-3.59	-5.24	6.35
-157	327577.11	3553032.41	6.60	4.25	7.84
-151	313513.34	3552941.22	4.01	-1.26	4.21
-152	309229.04	3554853.26	3.96	5.35	6.65
-164	320099.57	3536360.29	2.58	-1.45	2.96
-165	317473.16	3530720.18	1.17	-4.73	4.87
-149	336881.16	3557831.89	2.88	1.80	3.40
-125	325226.43	3568547.85	-3.30	0.30	3.31
-126	326825.34	3574674.53	1.74	9.61	9.77
-127	330683.54	3582055.71	-4.16	5.67	7.03
-128	331370.98	3573360.58	-7.72	1.75	7.92
-118	290482.92	3561278.98	1.46	-6.60	6.75
-153	320673.65	3549831.66	-8.29	-2.00	8.53
-143	337968.65	3576228.13	-1.15	10.07	10.14
		RMS	±5.54	±5.68	±7.93

N02 (2 X ellipsoid normal) : 0.1276894614656886D+08
aa (Unknown tied to Earth rotation) : 0.6155355622239747D-01
ALPHA (IFOV) : 0.1200000000000000D-04

bb (Unknown of 2nd order) : 0.1003199597018114D-07
C0 (Scene centre column) : 0.3000000000000000D+04
cc (Unknown of 2nd order): -.4982705245390573D-08
COSKHI (Parameter): 0.9999980637017012D+00
DELGAM (Unknown of 2nd order): -.1394416529022841D-07
GAMMA (Scene orient. rel. to the North): 0.1635677896187948D+00
K_1 (Cross track scale function): 0.1411991307680660D-05
L0 (Scene centre row): 0.3000000000000000D+04
P (Along track scale function): 0.9977626008598992D+01
Q (Satellite-Scene centre dist): 0.9772005820580334D+06
TAU (Levelling angle along track dir): 0.1967894266837156D-02
THETA (Levelling angle across track dir): -.4434409554069670D+00
THETAS (THETA/COS_KHI): -.4434418140425972D+00
X0 (Carto coord of scene centre): 0.3123394421602938D+06
Y0 (Carto coord of scene centre): 0.3560441397873663D+07
DELH (Radar parameter in H dir.): 0.0000000000000000D+00
COEFY2 (Radar parameter in Y2 dir.): 0.0000000000000000D+00

EARTH ELLIPSOID USED : E004

The following are the results of the space resection giving the planimetric accuracy of the left image of the Level 1A stereo-model for reference scene 122/285 using 12 control points and 36 check points:

SMODEL Satellite Model Calculation V6.0 EASI/PACE 13:33 22-SEP-97

Report File : D:\SWEST\TEST\35CHLA.TXT

Using GCPs stored in the GCP segment :

GCPID	CALCULATED GCP		RESIDUAL (Metre)		
	X	Y	ΔX	ΔY	Vector
102	300923.93	3557097.61	-2.12	0.97	2.33
113	304306.09	3580950.20	0.07	-2.94	2.94
116	284866.01	3573794.94	-0.73	7.61	7.65
119	284552.19	3563609.83	-6.40	-2.21	6.77
136	282125.21	3547226.11	3.35	-3.99	5.21
140	281957.25	3535721.02	4.96	-2.74	5.67
154	329676.79	3548192.02	4.86	6.33	7.97
167	330425.43	3528359.46	-6.00	2.08	6.35
168	321500.74	3574934.84	-4.76	4.22	6.36
145	345745.97	3571771.80	-0.01	-0.85	0.85
169	318576.07	3586704.25	4.50	-1.53	4.75
150	343630.88	3563019.29	2.28	-6.94	7.31
		RMS	±4.15	±4.36	±6.02

RESIDUAL ERRORS AT CHECK POINTS:

GCPID	CALCULATED CHECK POINT		ERRORS (Metre)		
	X	Y	ΔX	ΔY	Vector
-101	308543.98	3559868.27	0.02	2.14	2.14
-110	295872.66	3566650.19	-1.46	-4.80	5.02
-112	309294.19	3582165.88	-6.25	1.29	6.38
-111	300743.13	3576793.45	-1.23	8.05	8.14

-114	297518.46	3574017.44	7.93	6.95	10.55
-156	334932.21	3545628.29	-8.23	1.13	8.31
-118	290491.19	3561272.36	-6.81	0.03	6.81
-124	284229.75	3556256.69	3.75	-9.23	9.97
-135	279709.50	3554363.60	5.51	-6.95	8.87
-133	278854.35	3542819.16	-3.91	-1.83	4.32
-141	292954.04	3536497.82	1.12	2.60	2.83
-142	292461.21	3547662.81	-10.40	-2.89	10.79
-137	292704.68	3551488.16	1.02	-6.25	6.33
-163	304909.86	3532796.21	-4.22	4.40	6.10
-162	308316.76	3542491.17	-2.45	6.38	6.83
-146	322963.53	3563358.06	-6.20	1.17	6.31
-148	330981.16	3561096.28	-4.52	-11.57	12.42
-158	328328.60	3556598.59	0.94	-5.23	5.31
-157	327579.68	3553038.78	4.02	-2.13	4.55
-151	313525.38	3552934.46	-8.02	5.49	9.72
-152	309241.06	3554857.96	-8.06	0.66	8.09
-159	325740.72	3543788.19	3.59	-6.75	7.64
-153	320676.07	3549827.95	-10.71	1.71	10.85
-164	320097.55	3536358.92	4.61	-0.08	4.61
-166	330245.82	3534953.96	-7.77	-7.92	11.09
-165	317484.94	3530718.70	-10.61	-3.25	11.10
-125	325231.87	3568547.74	-8.73	0.41	8.74
-149	336880.53	3557838.03	3.51	-4.35	5.59
-129	338779.24	3569549.14	4.27	-7.09	8.27
-126	326819.90	3574686.02	7.18	-1.88	7.42
-127	330682.67	3582059.86	-3.29	1.52	3.62
-171	313700.57	3569816.71	-1.87	-9.37	9.56
-123	282555.80	3570247.46	-6.86	-4.68	8.31
-155	337162.64	3549821.60	3.98	-6.30	7.45
-143	337965.61	3576240.43	1.89	-2.22	2.92
-128	331362.89	3573363.90	0.37	-1.57	1.62
		RMS	±5.81	±5.20	±7.79

N02 (2 X ellipsoid normal) : 0.1276894858944160D+08
aa (Unknown tied to Earth rotation) : 0.5347452270106707D-01
ALPHA (IFOV) : 0.1200000000000000D-04
bb (Unknown of 2nd order) : 0.9637452434055284D-09
C0 (Scene centre column) : 0.3000000000000000D+04
cc (Unknown of 2nd order): 0.2800395867240290D-08
COSKHI (Parameter): 0.9999676695577860D+00
DELGAM (Unknown of 2nd order): 0.3290999296140512D-08
GAMMA (Scene orient. rel. to the North): 0.2434699529910903D+00□
K_1 (Cross track scale function): 0.1423098893335570D-05
L0 (Scene centre row): 0.3000000000000000D+04
P (Along track scale function): 0.1001890016669827D+02
Q (Satellite-Scene centre dist): 0.1050639610242654D+07
TAU (Levelling angle along track dir): -.8041394178591699D-02
THETA (Levelling angle across track dir): 0.5327733857233986D+00
THETAS (THETA/COS_KHI): 0.5327906110794622D+00
X0 (Carto coord of scene centre): 0.3045118816474870D+06
Y0 (Carto coord of scene centre): 0.3560764936777392D+07
DELH (Radar parameter in H dir.): 0.0000000000000000D+00
COEFY2 (Radar parameter in Y2 dir.): 0.0000000000000000D+00

EARTH ELLIPSOID USED : E004

The following are the results of the space resection giving the planimetric accuracy of the right image of the Level 1A stereo-model for reference scene 122/285 using 12 control points and 36 check points:

SMODEL Satellite Model Calculation V6.0 EASI/PACE 13:50 22-SEP-97

Report File : D:\SWEST\TEST\35CHRA.TXT

Using GCPs stored in the GCP segment :

GCPID	CALCULATED GCP		RESIDUAL (Metre)		
	X	Y	ΔX	ΔY	Vector
102	300927.67	3557097.17	-5.85	1.40	6.02
113	304308.31	3580944.66	-2.16	2.60	3.38
116	284867.75	3573797.18	-2.47	5.37	5.91
136	282126.78	3547222.95	1.78	-0.83	1.97
140	281959.05	3535718.75	3.15	-0.47	3.19
154	329674.09	3548197.01	7.55	1.34	7.67
167	330422.77	3528360.72	-3.33	0.83	3.44
150	343639.66	3563015.07	-6.49	-2.73	7.04
145	345742.58	3571771.40	3.38	-0.45	3.41
168	321497.05	3574933.71	-1.07	5.35	5.45
169	318575.32	3586708.19	5.26	-5.47	7.59
119	284545.54	3563614.55	0.25	-6.94	6.94
		RMS	±4.35	±3.76	±5.75

RESIDUAL ERRORS AT CHECK POINTS:

GCPID	CALCULATED CHECK POINT		ERRORS (Metre)		
	X	Y	Δ X	ΔY	Vector
-101	308537.06	3559862.03	7.61	8.38	11.32
-110	295871.40	3566641.87	-0.20	3.52	3.53
-112	309283.50	3582165.75	4.44	1.41	4.66
-111	300743.47	3576790.16	-1.56	11.34	11.44
-114	297517.90	3574015.99	8.50	8.40	11.95
-156	334929.69	3545635.37	-5.72	-5.95	8.25
-123	282557.00	3570239.06	-8.07	3.72	8.88
-166	330244.03	3534949.94	-5.98	-3.90	7.14
-124	284234.57	3556251.31	-1.08	-3.86	4.01
-135	279723.51	3554359.29	-8.50	-2.64	8.90
-133	278861.69	3542814.79	-11.26	2.54	11.54
-163	304902.80	3532798.15	2.83	2.47	3.76
-141	292955.25	3536494.70	-0.10	5.71	5.71
-142	292462.04	3547663.13	-11.23	-3.21	11.68
-137	292707.17	3551487.20	-1.47	-5.29	5.49
-146	322962.67	3563357.81	-5.34	1.42	5.52
-148	330979.82	3561091.44	-3.19	-6.72	7.44
-158	328329.13	3556591.59	0.42	1.77	1.82
-157	327576.80	3553033.27	6.91	3.38	7.69
-159	325743.38	3543784.66	0.92	-3.22	3.35
-151	313513.60	3552941.36	3.76	-1.41	4.01
-152	309229.44	3554853.31	3.55	5.31	6.39
-164	320099.46	3536359.84	2.69	-1.01	2.87
-165	317473.13	3530719.38	1.20	-3.93	4.11

-162	308311.42	3542492.65	2.88	4.90	5.69
-149	336880.42	3557833.40	3.62	0.29	3.63
-129	338779.61	3569551.83	3.90	-9.78	10.53
-125	325226.32	3568549.20	-3.18	-1.05	3.35
-126	326825.20	3574676.30	1.87	7.84	8.06
-127	330683.30	3582058.20	-3.92	3.18	5.05
-128	331370.64	3573362.62	-7.39	-0.29	7.39
-118	290483.78	3561278.97	0.60	-6.58	6.61
-153	320673.63	3549832.19	-8.27	-2.53	8.65
-171	313696.91	3569811.43	1.78	-4.09	4.46
-143	337968.02	3576230.56	-0.52	7.64	7.66
-155	337165.07	3549817.94	1.55	-2.63	3.05
		RMS	±5.18	±5.06	±7.24

N02 (2 X ellipsoid normal) : 0.1276894614656886D+08
aa (Unknown tied to Earth rotation) : 0.6153012556962834D-01
ALPHA (IFOV) : 0.1200000000000000D-04
bb (Unknown of 2nd order) : 0.1003199597018114D-07
C0 (Scene centre column) : 0.3000000000000000D+04
cc (Unknown of 2nd order): -.4982705245390573D-08
COSKHI (Parameter): 0.9999939349577670D+00
DELGAM (Unknown of 2nd order): -.1394416529022841D-07
GAMMA (Scene orient. rel. to the North): 0.1635727265769140D+00
K_1 (Cross track scale function): 0.1412507672907602D-05
L0 (Scene centre row): 0.3000000000000000D+04
P (Along track scale function): 0.9978374685140528D+01
Q (Satellite-Scene centre dist): 0.9771664990154232D+06
TAU (Levelling angle along track dir): -.3482842922241457D-02
THETA (Levelling angle across track dir): -.4438882515067630D+00
THETAS (THETA/COS_KHI): -.4438909437240836D+00
X0 (Carto coord of scene centre): 0.3123400954028176D+06
Y0 (Carto coord of scene centre): 0.3560445993335902D+07
DELH (Radar parameter in H dir.): 0.0000000000000000D+00
COEFY2 (Radar parameter in Y2 dir.): 0.0000000000000000D+00

EARTH ELLIPSOID USED : E004

The following are the results of the space resection giving the planimetric accuracy of the left image of the Level 1A stereo-model for reference scene 122/285 using 5 control points and 43 check points:

SMODEL Satellite Model Calculation V6.0 EASI/PACE 13:39 22-SEP-97

Report File : D:\SWEST\TEST\43CHLA.TXT

Using GCPs stored in the GCP segment :

GCPID	CALCULATED GCP		RESIDUAL (Metre)		
	X	Y	ΔX	ΔY	Vector
102	300930.20	3557089.29	-8.39	9.29	12.52
116	284865.53	3573804.10	-0.25	-1.56	1.58
141	292949.79	3536505.26	5.37	-4.84	7.23
169	318576.58	3586705.08	3.99	-2.36	4.64
150	343633.89	3563012.87	-0.72	-0.53	0.89
		RMS	±5.38	±5.43	±7.64

RESIDUAL ERRORS AT CHECK POINTS:

GCPID	CALCULATED CHECK POINT		ERRORS (Metre)		
	X	Y	ΔX	ΔY	Vector
-101	308540.88	3559864.66	3.12	5.75	6.54
-110	295859.16	3566657.58	12.04	-12.19	17.13
-112	309293.57	3582169.33	-5.63	-2.16	6.03
-113	304309.91	3580963.81	-3.75	-16.55	16.97
-111	300741.90	3576799.09	0.00	2.40	2.40
-114	297517.09	3574023.84	9.30	0.55	9.32
-123	282552.78	3570257.09	-3.85	-14.31	14.81
-119	284550.74	3563619.09	-4.95	-11.47	12.49
-118	290489.07	3561280.35	-4.69	-7.96	9.24
-124	284227.69	3556266.00	5.81	-18.55	19.44
-135	279720.88	3554379.82	-5.87	-23.17	23.90
-136	282122.36	3547235.98	6.21	-13.85	15.18
-133	278851.20	3542829.83	-0.77	-12.50	12.52
-140	281953.11	3535731.10	9.10	-12.82	15.72
-142	292457.86	3547670.36	-7.05	-10.44	12.60
-137	292713.81	3551501.98	-8.10	-20.06	21.64
-163	304892.72	3532796.16	12.91	4.46	13.66
-162	308299.28	3542496.97	15.02	0.58	15.03
-146	322963.10	3563357.61	-5.77	1.62	5.99
-148	330981.80	3561093.52	-5.17	-8.81	10.21
-158	328328.58	3556596.60	0.97	-3.24	3.38
-157	327569.91	3553039.36	13.79	-2.71	14.05
-151	313523.19	3552936.68	-5.83	3.28	6.69
-152	309238.64	3554861.32	-5.64	-2.71	6.26
-154	329676.54	3548189.65	5.10	8.69	10.08
-159	325739.55	3543786.98	4.75	-5.54	7.30
-153	320674.59	3549828.12	-9.23	1.53	9.36
-164	320095.09	3536359.35	7.07	-0.51	7.09
-167	330431.30	3528355.00	-11.87	6.55	13.55
-166	330250.42	3534949.44	-12.38	-3.40	12.83
-165	317481.80	3530719.87	-7.47	-4.42	8.68
-125	325231.98	3568546.68	-8.84	1.47	8.96
-149	336882.06	3557833.55	1.98	0.13	1.99
-129	338781.53	3569544.19	1.99	-2.14	2.92
-126	326820.61	3574684.49	6.46	-0.35	6.47
-168	321500.84	3574934.80	-4.86	4.26	6.46
-127	330684.41	3582057.19	-5.04	4.19	6.55
-145	345749.64	3571764.85	-3.68	6.11	7.13
-171	313703.17	3569825.74	-4.48	-18.39	18.93
-120	280167.26	3565362.07	15.50	-17.79	23.59
-155	337163.88	3549817.04	2.75	-1.73	3.24
-143	337968.12	3576235.68	-0.62	2.52	2.59
-128	331364.20	3573361.06	-0.94	1.27	1.58
		RMS	±7.49	±9.56	±12.14

N02 (2 X ellipsoid normal) : 0.1276894858944160D+08
aa (Unknown tied to Earth rotation) : 0.5336741654396450D-01
ALPHA (IFOV) : 0.1200000000000000D-04
bb (Unknown of 2nd order) : 0.9637452434055284D-09

C0 (Scene centre column) : 0.3000000000000000D+04
cc (Unknown of 2nd order): 0.2800395867240290D-08
COSKHI (Parameter): 0.9999742075239458D+00
DELGAM (Unknown of 2nd order): 0.3290999296140512D-08
GAMMA (Scene orient. rel. to the North): 0.2437012421023022D+00
K_1 (Cross track scale function): 0.1426237897888333D-05
L0 (Scene centre row): 0.3000000000000000D+04
P (Along track scale function): 0.1001841308825610D+02
Q (Satellite-Scene centre dist): 0.1050702004813601D+07
TAU (Levelling angle along track dir): -.7182405441951518D-02
THETA (Levelling angle across track dir): 0.5354929303699120D+00
THETAS (THETA/COS_KHI): 0.5355067424147426D+00
X0 (Carto coord of scene centre): 0.3045116206072771D+06
Y0 (Carto coord of scene centre): 0.3560768308854738D+07
DELH (Radar parameter in H dir.): 0.0000000000000000D+00
COEFY2 (Radar parameter in Y2 dir.): 0.0000000000000000D+00

EARTH ELLIPSOID USED : E004

The following are the results of the space resection giving the planimetric accuracy of the right image of the Level 1A stereo-model for reference scene 122/285 using 5 control points and 43 check points:

SMODEL Satellite Model Calculation V6.0 EASI/PACE 13:54 22-SEP-97

Report File : D:\SWEST\TEST\43CHRA.TXT

Using GCPs stored in the GCP segment :

GCPID	CALCULATED GCP		RESIDUAL (Metre)		
	X	Y	ΔX	ΔY	Vector
102	300931.93	3557091.59	-10.12	6.98	12.29
116	284864.95	3573799.30	0.33	3.24	3.26
141	292949.06	3536506.71	6.10	-6.30	8.77
150	343633.65	3563009.48	-0.48	2.86	2.90
169	318576.41	3586709.51	4.16	-6.79	7.96
		RMS	±6.27	±6.19	±8.81

RESIDUAL ERRORS AT CHECK POINTS:

GCPID	CALCULATED CHECK POINT		ERRORS (Metre)		
	X	Y	ΔX	ΔY	Vector
-101	308541.77	3559863.90	2.90	6.51	7.13
-110	295880.01	3566650.33	-8.81	-4.94	10.10
-112	309292.13	3582168.68	-4.19	-1.51	4.45
-113	304329.03	3580945.85	-22.87	1.41	22.91
-111	300752.67	3576796.03	-10.77	5.46	12.07
-114	297526.92	3574023.32	-0.53	1.07	1.19
-120	280190.89	3565363.32	-8.89	-19.03	21.01
-123	282563.90	3570253.39	-14.97	-10.61	18.34
-166	330241.82	3534948.24	-3.77	-2.20	4.37
-124	284241.49	3556265.69	-7.99	-18.24	19.91
-135	279729.62	3554375.78	-14.61	-19.13	24.07
-133	278867.99	3542831.56	-17.55	-14.23	22.60

-136	282133.43	3547238.41	-4.86	-16.28	16.99
-163	304907.97	3532794.71	-2.33	5.90	6.35
-142	292472.68	3547673.44	-21.87	-13.52	25.71
-137	292716.90	3551506.36	-11.20	-24.45	26.89
-140	281958.21	3535740.43	4.00	-22.16	22.51
-146	322965.99	3563358.09	-8.66	1.14	8.73
-148	330979.73	3561089.61	-3.10	-4.90	5.79
-158	328329.78	3556590.49	-0.23	2.87	2.88
-154	329673.43	3548195.49	8.21	2.85	8.69
-157	327577.48	3553032.34	6.22	4.31	7.57
-159	325734.16	3543785.79	10.14	-4.35	11.03
-151	313535.31	3552939.80	-17.95	0.15	17.95
-152	309236.10	3554857.61	-3.11	1.00	3.27
-164	320101.86	3536360.89	0.30	-2.05	2.08
-165	317488.82	3530728.61	-14.48	-13.16	19.57
-162	308307.73	3542498.82	6.57	-1.27	6.69
-167	330416.07	3528359.79	3.36	1.75	3.79
-149	336880.07	3557829.45	3.97	4.24	5.81
-129	338776.96	3569547.49	6.55	-5.44	8.52
-125	325229.38	3568548.64	-6.24	-0.48	6.26
-145	345736.65	3571764.93	9.31	6.02	11.09
-126	326826.68	3574675.55	0.40	8.59	8.60
-127	330685.19	3582056.32	-5.81	5.06	7.71
-168	321510.06	3574937.88	-14.08	1.18	14.13
-128	331371.58	3573360.51	-8.32	1.82	8.52
-118	290506.59	3561287.57	-22.21	-15.18	26.90
-119	284552.75	3563628.28	-6.96	-20.66	21.80
-153	320676.60	3549833.38	-11.24	-3.72	11.84
-171	313703.73	3569813.75	-5.04	-6.41	8.15
-143	337966.33	3576226.59	1.17	11.61	11.67
-155	337153.74	3549816.48	12.88	-1.17	12.94
		RMS	±10.39	±10.18	±14.54

N02 (2 X ellipsoid normal) : 0.1276894614656886D+08
aa (Unknown tied to Earth rotation) : 0.6114350492000482D-01□
ALPHA (IFOV) : 0.1200000000000000D-04
bb (Unknown of 2nd order) : 0.1003199597018114D-07
C0 (Scene centre column) : 0.3000000000000000D+04
cc (Unknown of 2nd order): -.4982705245390573D-08
COSKHI (Parameter): 0.9999555095117016D+00
DELGAM (Unknown of 2nd order): -.1394416529022841D-07
GAMMA (Scene orient. rel. to the North): 0.1639464919342436D+00
K_1 (Cross track scale function): 0.1419062602437032D-05
L0 (Scene centre row): 0.3000000000000000D+04
P (Along track scale function): 0.9978124302459210D+01
Q (Satellite-Scene centre dist): 0.9770286920092828D+06
TAU (Levelling angle along track dir): -.9433287611412966D-02
THETA (Levelling angle across track dir): -.4498917145248539D+00
THETAS (THETA/COS_KHI): -.4499117313174714D+00
X0 (Carto coord of scene centre): 0.3123425118735866D+06
Y0 (Carto coord of scene centre): 0.3560454561948154D+07
DELH (Radar parameter in H dir.): 0.0000000000000000D+00
COEFY2 (Radar parameter in Y2 dir.): 0.0000000000000000D+00

EARTH ELLIPSOID USED : E004

The following are the results of the space resection giving the planimetric accuracy of the left image of the Level 1A stereo-model for reference scene 122/285 using 48 ground control points:

SMODEL Satellite Model Calculation V6.0 EASI/PACE 13:34 22-SEP-97

Report File : D:\SWEST\TEST\48GRLA.TXT

Using GCPs stored in the GCP segment :

GCPID	CALCULATED GCP		RESIDUAL (Metre)		
	X	Y	ΔX	ΔY	Vector
101	308540.96	3559868.28	3.04	2.13	3.72
102	300921.05	3557097.52	0.77	1.06	1.30
110	295871.11	3566650.59	0.09	-5.20	5.20
112	309292.65	3582167.21	-4.71	-0.04	4.71
113	304304.74	3580952.10	1.42	-4.84	5.05
111	300741.82	3576794.99	0.09	6.50	6.50
114	297517.35	3574018.54	9.05	5.85	10.77
116	284867.54	3573794.16	-2.26	8.38	8.68
156	334931.72	3545626.03	-7.74	3.39	8.45
119	284552.55	3563608.41	-6.76	-0.79	6.81
118	290490.00	3561271.85	-5.62	0.54	5.65
124	284229.37	3556254.55	4.12	-7.10	8.21
135	279709.96	3554360.78	5.05	-4.13	6.53
136	282124.17	3547223.67	4.40	-1.55	4.66
133	278853.41	3542816.62	-2.97	0.71	3.06
140	281954.75	3535719.10	7.46	-0.82	7.51
141	292950.17	3536496.37	4.99	4.04	6.42
142	292458.38	3547661.81	-7.57	-1.89	7.80
137	292702.21	3551487.20	3.50	-5.29	6.34
163	304905.23	3532795.24	0.41	5.38	5.39
162	308312.77	3542490.21	1.53	7.34	7.50
146	322961.48	3563356.51	-4.15	2.72	4.96
148	330980.14	3561093.85	-3.51	-9.14	9.79
158	328327.03	3556596.51	2.51	-3.14	4.02
157	327577.89	3553036.90	5.82	-0.25	5.82
151	313522.06	3552933.95	-4.71	6.01	7.63
152	309237.73	3554857.70	-4.74	0.91	4.83
154	329675.24	3548190.07	6.40	8.28	10.46
159	325738.35	3543786.84	5.95	-5.40	8.04
153	320673.27	3549826.48	-7.91	3.18	8.53
164	320094.09	3536358.27	8.06	0.57	8.08
167	330423.80	3528358.07	-4.37	3.47	5.58
166	330244.22	3534952.26	-6.17	-6.22	8.76
165	317480.96	3530718.28	-6.63	-2.83	7.21
125	325230.21	3568546.21	-7.07	1.94	7.33
149	336880.59	3557835.20	3.45	-1.51	3.76
129	338779.73	3569546.42	3.78	-4.37	5.78
126	326818.69	3574684.16	8.39	-0.02	8.39
168	321499.09	3574933.50	-3.11	5.56	6.37
127	330682.26	3582057.20	-2.88	4.18	5.08
145	345748.00	3571768.82	-2.04	2.13	2.95
169	318574.89	3586703.86	5.68	-1.13	5.79
171	313698.17	3569816.83	0.53	-9.49	9.51
150	343632.50	3563016.18	0.67	-3.84	3.89

123	282557.49	3570246.11	-8.56	-3.33	9.18
155	337162.71	3549818.97	3.91	-3.66	5.36
143	337966.09	3576237.39	1.41	0.81	1.63
128	331362.23	3573361.43	1.03	0.90	1.36
		RMS	±5.04	±4.45	±6.73

N02 (2 X ellipsoid normal) : 0.1276894858944160D+08
aa (Unknown tied to Earth rotation) : 0.5359724374755200D-01
ALPHA (IFOV) : 0.1200000000000000D-04
bb (Unknown of 2nd order) : 0.9637452434055284D-09
C0 (Scene centre column) : 0.3000000000000000D+04
cc (Unknown of 2nd order): 0.2800395867240290D-08
COSKHI (Parameter): 0.9999975463042280D+00
DELGAM (Unknown of 2nd order): 0.3290999296140512D-08
GAMMA (Scene orient. rel. to the North): 0.2434426594713537D+00
K_1 (Cross track scale function): 0.1428763683023221D-05
L0 (Scene centre row): 0.3000000000000000D+04
P (Along track scale function): 0.1001837141708696D+02
Q (Satellite-Scene centre dist): 0.1050547623303068D+07
TAU (Levelling angle along track dir): 0.2215267389244760D-02
THETA (Levelling angle across track dir): 0.5374909573470051D+00
THETAS (THETA/COS_KHI): 0.5374922761895307D+00
X0 (Carto coord of scene centre): 0.3045108307361226D+06
Y0 (Carto coord of scene centre): 0.3560755797002928D+07
DELH (Radar parameter in H dir.): 0.0000000000000000D+00
COEFY2 (Radar parameter in Y2 dir.): 0.0000000000000000D+00

EARTH ELLIPSOID USED : E004

The following are the results of the space resection giving the planimetric accuracy of the right image of the Level 1A stereo-model for reference scene 122/285 using 48 ground control points:

SMODEL Satellite Model Calculation V6.0 EASI/PACE 13:51 22-SEP-97

Report File : D:\SWEST\TEST\48GRRA.TXT

Using GCPs stored in the GCP segment :

GCPID	CALCULATED GCP		RESIDUAL (Metre)		
	X	Y	ΔX	ΔY	Vector
101	308538.13	3559862.93	6.54	7.49	9.94
102	300928.04	3557098.07	-6.22	0.51	6.25
110	295871.18	3566644.03	0.02	1.36	1.36
112	309285.17	3582168.99	2.78	-1.82	3.32
113	304309.72	3580948.42	-3.57	-1.16	3.75
111	300744.31	3576793.57	-2.40	7.93	8.28
114	297518.11	3574019.08	8.29	5.31	9.84
156	334928.60	3545634.38	-4.62	-4.96	6.78
116	284864.60	3573799.97	0.68	2.58	2.66
123	282553.16	3570241.37	-4.22	1.41	4.45
166	330243.35	3534948.67	-5.30	-2.63	5.92
124	284231.28	3556251.78	2.22	-4.33	4.87
135	279718.92	3554359.53	-3.91	-2.88	4.86
133	278857.46	3542814.35	-7.03	2.99	7.64
136	282123.18	3547222.66	5.38	-0.54	5.41
163	304903.19	3532796.78	2.45	3.84	4.55

141	292954.29	3536493.60	0.86	6.82	6.87
142	292461.02	3547663.15	-10.21	-3.23	10.71
137	292706.13	3551487.50	-0.42	-5.59	5.61
140	281956.03	3535717.91	6.18	0.37	6.19
146	322963.32	3563357.75	-5.99	1.48	6.17
148	330979.59	3561090.83	-2.95	-6.12	6.79
158	328329.13	3556590.93	0.42	2.43	2.47
154	329673.80	3548196.11	7.84	2.24	8.16
157	327576.85	3553032.57	6.86	4.08	7.98
159	325743.55	3543783.83	0.75	-2.39	2.51
151	313514.61	3552941.41	2.75	-1.46	3.11
152	309230.42	3554853.70	2.57	4.92	5.55
164	320100.10	3536358.97	2.06	-0.13	2.07
165	317473.85	3530718.33	0.48	-2.88	2.92
162	308312.00	3542491.82	2.31	5.73	6.18
167	330421.97	3528359.40	-2.54	2.14	3.32
149	336879.29	3557832.62	4.75	1.07	4.87
150	343637.66	3563014.69	-4.49	-2.34	5.07
129	338778.75	3569551.71	4.76	-9.66	10.77
125	325227.02	3568549.46	-3.88	-1.31	4.10
145	345740.72	3571771.56	5.25	-0.61	5.28
126	326825.82	3574676.67	1.26	7.47	7.57
127	330683.54	3582058.45	-4.16	2.93	5.08
168	321498.00	3574934.43	-2.02	4.63	5.05
169	318576.76	3586710.28	3.81	-7.56	8.46
128	331370.71	3573362.58	-7.46	-0.25	7.46
118	290482.34	3561280.46	2.04	-8.07	8.32
119	284542.39	3563616.08	3.40	-8.46	9.12
153	320674.13	3549831.45	-8.78	-1.79	8.96
171	313698.32	3569812.92	0.37	-5.58	5.59
143	337967.35	3576230.48	0.15	7.73	7.73
155	337163.68	3549816.99	2.94	-1.68	3.39
		RMS	±4.56	±4.51	±6.42

N02 (2 X ellipsoid normal) : 0.1276894614656886D+08
aa (Unknown tied to Earth rotation) : 0.6149921574756038D-01
ALPHA (IFOV) : 0.1200000000000000D-04
bb (Unknown of 2nd order) : 0.1003199597018114D-07
C0 (Scene centre column) : 0.3000000000000000D+04
cc (Unknown of 2nd order): -.4982705245390573D-08
COSKHI (Parameter): 0.9999883686406552D+00
DELGAM (Unknown of 2nd order): -.1394416529022841D-07
GAMMA (Scene orient. rel. to the North): 0.1635820957162182D+00
K_1 (Cross track scale function): 0.1416505124654800D-05
L0 (Scene centre row): 0.3000000000000000D+04
P (Along track scale function): 0.9978402055002860D+01
Q (Satellite-Scene centre dist): 0.9772114243784246D+06
TAU (Levelling angle along track dir): 0.4823186142110299D-02
THETA (Levelling angle across track dir): -.4477345286178873D+00
THETAS (THETA/COS_KHI): -.4477397364396548D+00
X0 (Carto coord of scene centre): 0.3123371905618657D+06
Y0 (Carto coord of scene centre): 0.3560440702914638D+07
DELH (Radar parameter in H dir.): 0.0000000000000000D+00
COEFY2 (Radar parameter in Y2 dir.): 0.0000000000000000D+00

EARTH ELLIPSOID USED : E004

B.2.3 Level 1B Stereo-model of Scene 123/285

The following are the results of the space resection giving the planimetric accuracy of the left image of the Level 1B stereo-model for scene 123/285 using 23 ground control points.

SMODEL Satellite Model Calculation V6.0 EASI/PACE 17:13 30-NOV-97

Report File : F:\NWEST\SML23.TXT

Using GCPs stored in the GCP segment :

GCPID	CALCULATED GCP		RESIDUAL (Metre)		
	X	Y	ΔX	ΔY	Vector
126	326825.47	3574687.42	1.61	-3.28	3.65
127	330680.86	3582055.02	-1.48	6.36	6.53
128	331358.68	3573357.91	4.58	4.42	6.36
129	338783.09	3569551.33	0.42	-9.28	9.29
143	337968.98	3576232.63	-1.48	5.57	5.76
145	345750.65	3571770.59	-4.69	0.36	4.71
150	343638.09	3563012.84	-4.92	-0.50	4.95
204	374759.04	3555431.95	3.93	-0.01	3.93
404	377213.38	3566137.86	2.50	1.05	2.71
405	384886.88	3608359.09	6.17	-5.31	8.14
501	334509.99	3591459.66	5.33	-3.42	6.33
502	334881.29	3598066.28	-2.63	-0.37	2.66
503	325158.26	3592446.43	0.87	2.16	2.33
504	345783.42	3587347.46	-6.38	0.38	6.39
505	354645.29	3607154.64	2.80	-5.51	6.18
506	367452.88	3597537.64	-5.54	-1.51	5.74
507	361022.77	3576490.39	7.99	-1.08	8.06
508	389063.08	3584945.72	-9.90	2.06	10.11
509	376118.54	3580637.32	2.47	7.44	7.84
510	357454.68	3593419.35	-0.06	-2.58	2.58
511	366462.69	3609356.48	-1.81	8.54	8.73
512	379349.26	3594486.90	1.50	-2.10	2.58
515	357685.29	3559198.59	-1.26	-3.38	3.60
		RMS	±4.39	±4.39	±6.21

N02 (2 X ellipsoid normal) : 0.1276912505510508D+08
aa (Unknown tied to Earth rotation) : 0.5473845578797543D-01
ALPHA (IFOV) : 0.1200000000000000D-04
bb (Unknown of 2nd order) : 0.1547234124871933D-08
C0 (Scene centre column) : 0.3000000000000000D+04
cc (Unknown of 2nd order): 0.2344598665768838D-08
COSKHI (Parameter): 0.9999310905007358D+00
DELGAM (Unknown of 2nd order): 0.2195832222367986D-08
GAMMA (Scene orient. rel. to the North): 0.2330038797778100D+00
K_1 (Cross track scale function): 0.1392282723913940D-05
L0 (Scene centre row): 0.3000000000000000D+04
P (Along track scale function): 0.1001198783368329D+02
Q (Satellite-Scene centre dist): 0.9977636180559318D+06
TAU (Levelling angle along track dir): -.1174024043172606D-01
THETA (Levelling angle across track dir): 0.4487087608120689D+00

THETAS (THETA/COS_KHI): 0.4487396832389408D+00□
X0 (Carto coord of scene centre): 0.3547862894650264D+06
Y0 (Carto coord of scene centre): 0.3588954203948740D+07
DELH (Radar parameter in H dir.): 0.0000000000000000D+00
COEFY2 (Radar parameter in Y2 dir.): 0.0000000000000000D+00

EARTH ELLIPSOID USED : E004

The following are the results of the space resection giving the Planimetric accuracy of the right image of the Level 1B stereo-model for scene 123/285 using 23 ground control points:

SMODEL Satellite Model Calculation V6.0 EASI/PACE 17:27 30-NOV-97

Report File : F:\NWEST\SMR23.TXT

Using GCPs stored in the GCP segment :

GCPID	CALCULATED GCP		RESIDUAL (Metre)		
	X	Y	ΔX	ΔY	Vector
126	326820.18	3574684.88	6.90	-0.74	6.93
127	330681.08	3582054.92	-1.70	6.46	6.68
128	331364.68	3573359.51	-1.42	2.82	3.16
129	338785.49	3569544.29	-1.98	-2.24	2.99
143	337973.10	3576235.26	-5.60	2.94	6.33
145	345747.18	3571772.27	-1.22	-1.32	1.79
150	343636.27	3563021.55	-3.10	-9.21	9.72
168	321499.09	3574933.98	-3.11	5.08	5.95
404	377212.12	3566129.70	3.76	9.21	9.95
405	384889.88	3608363.19	3.17	-9.41	9.93
501	334509.17	3591456.67	6.15	-0.43	6.17
502	334878.69	3598063.56	-0.03	2.35	2.35
503	325157.10	3592450.16	2.03	-1.57	2.57
504	345780.05	3587354.97	-3.01	-7.13	7.74
505	354650.59	3607152.72	-2.50	-3.59	4.37
506	367450.41	3597535.97	-3.07	0.16	3.07
507	361031.18	3576494.01	-0.42	-4.70	4.72
508	389057.10	3584943.65	-3.92	4.13	5.69
509	376125.51	3580638.65	-4.50	6.11	7.59
510	357456.63	3593409.71	-2.01	7.06	7.34
511	366455.06	3609363.12	5.82	1.90	6.13
512	379350.72	3594484.33	0.04	0.47	0.47
515	357674.29	3559203.54	9.74	-8.33	12.81
		RMS	±4.09	±5.31	±6.70

N02 (2 X ellipsoid normal) : 0.1276912524384488D+08
aa (Unknown tied to Earth rotation) : 0.6142686816895547D-01
ALPHA (IFOV) : 0.1200000000000000D-04
bb (Unknown of 2nd order) : 0.9555266451507780D-08
C0 (Scene centre column) : 0.3000000000000000D+04
cc (Unknown of 2nd order): -.4567067108441230D-08
COSKHI (Parameter): 0.9999947775780074D+00
DELGAM (Unknown of 2nd order): -.1299393025456174D-07
GAMMA (Scene orient. rel. to the North): 0.1629273024794038D+00
K_1 (Cross track scale function): 0.1411276652662097D-05
L0 (Scene centre row): 0.3000000000000000D+04
P (Along track scale function): 0.9980521777377792D+01

Q (Satellite-Scene centre dist): 0.9464307737434374D+06
TAU (Levelling angle along track dir): -.3231861043851342D-02
THETA (Levelling angle across track dir): -.4040228989701307D+00
THETAS (THETA/COS_KHI): -.4040250089592230D+00
X0 (Carto coord of scene centre): 0.3554589077629054D+06
Y0 (Carto coord of scene centre): 0.3589081375980201D+07

DELH (Radar parameter in H dir.): 0.0000000000000000D+00

COEFY2 (Radar parameter in Y2 dir.): 0.0000000000000000D+00

EARTH ELLIPSOID USED : E004

The following are the results of the space resection giving the planimetric accuracy of the left image of the Level 1B stereo-model for scene 123/285 using 13 control points and 10 check points:

1
SMODEL Satellite Model Calculation V6.0 EASI/PACE 19:15 30-NOV-97

Report File : F:\NWEST\SML10.TXT

Using GCPs stored in the GCP segment :

GCPID	CALCULATED GCP		RESIDUAL (Metre)		
	X	Y	ΔX	ΔY	Vector
128	331359.23	3573358.79	4.03	3.54	5.36
150	343639.68	3563013.12	-6.51	-0.78	6.55
204	374759.04	3555431.61	3.93	0.33	3.94
404	377213.28	3566137.46	2.60	1.45	2.97
405	384886.74	3608358.40	6.31	-4.62	7.82
502	334881.29	3598067.11	-2.63	-1.20	2.89
503	325157.25	3592447.80	1.88	0.79	2.04
505	354647.01	3607154.34	1.08	-5.21	5.32
507	361024.68	3576489.93	6.08	-0.62	6.11
508	389061.51	3584945.31	-8.33	2.47	8.69
510	357456.76	3593418.89	-2.14	-2.12	3.01
511	366464.37	3609355.84	-3.49	9.18	9.82
515	357686.82	3559198.43	-2.79	-3.22	4.26
		RMS	± 4.68	±3.78	±6.02

RESIDUAL ERRORS AT CHECK POINTS:

GCPID	CALCULATED CHECK POINT		ERRORS (Metre)		
	X	Y	ΔX	ΔY	Vector
-126	326825.54	3574688.54	1.54	-4.40	4.66
-127	330681.05	3582055.97	-1.67	5.41	5.66
-129	338784.39	3569551.80	-0.88	-9.75	9.79
-143	337970.04	3576233.17	-2.54	5.03	5.63
-145	345752.34	3571770.73	-6.38	0.22	6.38
-501	334510.22	3591460.46	5.10	-4.22	6.62
-504	345784.92	3587347.58	-7.88	0.26	7.88
-506	367454.51	3597537.00	-7.17	-0.87	7.22
-509	376119.07	3580636.75	1.94	8.01	8.24
-512	379349.65	3594486.25	1.11	-1.45	1.82

RMS ±4.68 ±5.31 ±7.08

N02 (2 X ellipsoid normal) : 0.1276912505510508D+08
aa (Unknown tied to Earth rotation) : 0.5470645885858067D-01
ALPHA (IFOV) : 0.1200000000000000D-04
bb (Unknown of 2nd order) : 0.1547234124871933D-08
C0 (Scene centre column) : 0.3000000000000000D+04
cc (Unknown of 2nd order): 0.2344598665768838D-08
COSKHI (Parameter): 0.9999263042623562D+00
DELGAM (Unknown of 2nd order): 0.2195832222367986D-08
GAMMA (Scene orient. rel. to the North): 0.2330324847792860D+00
K_1 (Cross track scale function): 0.1389423917413054D-05
L0 (Scene centre row): 0.3000000000000000D+04
P (Along track scale function): 0.1001189047564485D+02
Q (Satellite-Scene centre dist): 0.9977783513986306D+06
TAU (Levelling angle along track dir): -.1214116016178060D-01
THETA (Levelling angle across track dir): 0.4459629376295647D+00
THETAS (THETA/COS_KHI): 0.4459958056194458D+00
X0 (Carto coord of scene centre): 0.3547859397009568D+06
Y0 (Carto coord of scene centre): 0.3588954811431424D+07
DELH (Radar parameter in H dir.): 0.0000000000000000D+00
COEFY2 (Radar parameter in Y2 dir.): 0.0000000000000000D+00

EARTH ELLIPSOID USED : E004

The following are the results of the space resection giving the planimetric accuracy of the right image of the Level 1B stereo-model for scene 123/285 using 13 control points and 10 check points:

SMODEL Satellite Model Calculation V6.0 EASI/PACE 19:07 30-NOV-97

Report File : F:\NWEST\SMR10.TXT

Using GCPs stored in the GCP segment :

GCPID	CALCULATED GCP		RESIDUAL (Metre)		
	X	Y	ΔX	ΔY	Vector
128	331364.40	3573359.28	-1.14	3.05	3.25
150	343637.54	3563020.95	-4.37	-8.61	9.65
168	321497.45	3574934.15	-1.47	4.91	5.12
404	377213.81	3566128.98	2.07	9.93	10.14
405	384890.70	3608362.38	2.35	-8.60	8.92
502	334877.80	3598063.54	0.86	2.37	2.52
503	325155.14	3592450.43	3.99	-1.84	4.39
505	354651.66	3607152.70	-3.57	-3.57	5.05
507	361033.30	3576493.68	-2.54	-4.37	5.06
508	389057.69	3584942.75	-4.51	5.03	6.76
510	357458.35	3593409.64	-3.73	7.13	8.05
511	366456.51	3609362.85	4.37	2.17	4.88
515	357676.34	3559202.81	7.69	-7.60	10.81

RMS ±3.88 ±6.19 ±7.30

RESIDUAL ERRORS AT CHECK POINTS:

GCPID CALCULATED CHECK POINT ERRORS (Metre)

	X	Y	ΔX	ΔY	Vector
-126	326819.31	3574684.85	7.77	-0.71	7.80
-127	330680.37	3582054.85	-0.99	6.53	6.61
-129	338786.19	3569543.87	-2.68	-1.82	3.24
-143	337973.46	3576234.92	-5.96	3.28	6.80
-145	345748.46	3571771.83	-2.50	-0.88	2.65
-501	334508.52	3591456.59	6.80	-0.35	6.80
-504	345780.92	3587354.76	-3.88	-6.92	7.93
-506	367452.11	3597535.63	-4.77	0.50	4.80
-509	376127.19	3580638.04	-6.18	6.72	9.14
-512	379352.08	3594483.68	-1.32	1.12	1.73
		RMS	±5.10	±4.12	±6.56

N02 (2 X ellipsoid normal) : 0.1276912524384488D+08
aa (Unknown tied to Earth rotation) : 0.6140240308305889D-01
ALPHA (IFOV) : 0.1200000000000000D-04
bb (Unknown of 2nd order) : 0.9555266451507780D-08
C0 (Scene centre column) : 0.3000000000000000D+04
cc (Unknown of 2nd order): -.4567067108441230D-08
COSKHI (Parameter): 0.9999995368929078D+00
DELGAM (Unknown of 2nd order): -.1299393025456174D-07
GAMMA (Scene orient. rel. to the North): 0.1629364604551665D+00
K_1 (Cross track scale function): 0.1412974073904739D-05
L0 (Scene centre row): 0.3000000000000000D+04
P (Along track scale function): 0.9980553650646988D+01
Q (Satellite-Scene centre dist): 0.9464793411693468D+06
TAU (Levelling angle along track dir): -.9624005547575354D-03
THETA (Levelling angle across track dir): -.4058209790463731D+00
THETAS (THETA/COS_KHI): -.4058211669850338D+00□
X0 (Carto coord of scene centre): 0.3554586319951188D+06
Y0 (Carto coord of scene centre): 0.3589079437383786D+07
DELH (Radar parameter in H dir.): 0.0000000000000000D+00
COEFY2 (Radar parameter in Y2 dir.): 0.0000000000000000D+00

EARTH ELLIPSOID USED : E004

B.2.4 Level 1B Stereo-model of Scene 123/286

The following are the results of the space resection giving the planimetric accuracy of the left image of the Level 1B stereo-model for scene 123/286 using 29 ground control points:

SMODEL Satellite Model Calculation V6.0 EASI/PACE 20:18 30-NOV-97

Report File : D:\SOUTHWM\SML29.TXT

Using GCPs stored in the GCP segment :

GCPID	CALCULATED GCP		RESIDUAL(Metre)		
	X	Y	ΔX	ΔY	Vector
146	322958.55	3563355.16	-1.22	4.07	4.25
148	330979.19	3561090.44	-2.55	-5.73	6.27
149	336876.29	3557832.20	7.75	1.49	7.89
150	343638.82	3563009.39	-5.65	2.95	6.38

151	313520.29	3552938.76	-2.93	1.20	3.17
153	320672.94	3549837.20	-7.58	-7.54	10.69
154	329676.70	3548195.96	4.94	2.39	5.49
156	334926.62	3545623.06	-2.64	6.36	6.88
157	327576.11	3553030.73	7.59	5.92	9.63
158	328330.87	3556586.24	-1.33	7.12	7.24
159	325737.62	3543784.61	6.68	-3.17	7.39
164	320094.44	3536367.22	7.72	-8.38	11.40
165	317482.08	3530709.90	-7.75	5.55	9.53
166	330243.89	3534953.54	-5.84	-7.50	9.51
167	330427.82	3528358.39	-8.39	3.15	8.97
201	350517.16	3543345.31	-5.43	6.51	8.48
202	363803.01	3539201.46	-4.03	-4.86	6.31
203	375644.08	3535241.48	4.05	-1.45	4.30
204	374759.06	3555430.75	3.91	1.19	4.09
206	319056.35	3518174.25	4.61	-6.31	7.81
207	315007.47	3511654.89	4.26	3.48	5.50
209	339187.31	3505658.15	1.72	-7.42	7.62
210	330877.81	3521645.15	6.93	2.02	7.22
211	352939.64	3519570.54	-8.54	6.31	10.62
212	359257.03	3503213.98	3.83	4.94	6.25
213	368487.54	3521463.49	-3.81	7.85	8.73
215	341773.16	3534245.04	-3.40	-3.93	5.19
302	368042.87	3537691.62	-0.42	-9.69	9.69
515	357676.50	3559201.75	7.53	-6.54	9.97
		RMS	±5.55	±5.63	±7.91

N02 (2 X ellipsoid normal) : 0.1276879105096307D+08
aa (Unknown tied to Earth rotation) : 0.5508632642706943D-01
ALPHA (IFOV) : 0.1200000000000000D-04
bb (Unknown of 2nd order) : 0.1465086180891859D-08
C0 (Scene centre column) : 0.3000000000000000D+04
cc (Unknown of 2nd order): 0.2394160614173618D-08
COSKHI (Parameter): 0.9999337323608888D+00
DELGAM (Unknown of 2nd order): 0.2275588505921620D-08
GAMMA (Scene orient. rel. to the North): 0.2327242099215111D+00
K_1 (Cross track scale function): 0.1395602289059510D-05
L0 (Scene centre row): 0.3000000000000000D+04
P (Along track scale function): 0.1001582121339909D+02
Q (Satellite-Scene centre dist): 0.9977633195053264D+06
TAU (Levelling angle along track dir): -.1151296893014486D-01
THETA (Levelling angle across track dir): 0.4518873123924546D+00
THETAS (THETA/COS_KHI): 0.4519172598823406D+00
X0 (Carto coord of scene centre): 0.3386642397053779D+06
Y0 (Carto coord of scene centre): 0.3534462360787262D+07
DELH (Radar parameter in H dir.): 0.0000000000000000D+00
COEFY2 (Radar parameter in Y2 dir.): 0.0000000000000000D+00

EARTH ELLIPSOID USED : E004

The following are the results of the space resection giving the planimetric accuracy of the right image of the Level 1B stereo-model for scene 123/286 using 29 ground control points:

SMODEL Satellite Model Calculation V6.0 EASI/PACE 20:03 30-NOV-97

Report File : D:\SOUTHWM\SMR29.TXT

Using GCPs stored in the GCP segment :

GCPID	CALCULATED GCP		RESIDUAL (Metre)		
	X	Y	ΔX	ΔY	Vector
146	322955.45	3563357.06	1.88	2.17	2.87
148	330981.30	3561092.81	-4.66	-8.10	9.35
149	336876.25	3557833.33	7.79	0.36	7.79
150	343639.97	3563008.24	-6.80	4.10	7.94
151	313523.51	3552935.44	-6.15	4.52	7.63
153	320667.96	3549836.03	-2.60	-6.37	6.88
154	329681.27	3548194.59	0.37	3.76	3.78
156	334925.40	3545623.63	-1.42	5.79	5.96
157	327575.35	3553028.68	8.35	7.97	11.54
158	328327.79	3556589.35	1.75	4.01	4.38
159	325742.90	3543780.88	1.40	0.56	1.51
164	320097.73	3536363.83	4.43	-4.99	6.68
165	317476.65	3530717.75	-2.32	-2.30	3.26
166	330242.13	3534955.66	-4.08	-9.62	10.45
167	330425.97	3528368.53	-6.54	-6.99	9.57
201	350513.73	3543345.01	-2.00	6.81	7.10
202	363799.15	3539194.22	-0.17	2.38	2.38
203	375645.73	3535241.95	2.40	-1.92	3.08
204	374761.55	3555431.22	1.42	0.72	1.59
206	319062.04	3518166.77	-1.08	1.17	1.60
207	315005.18	3511653.56	6.55	4.81	8.13
209	339187.23	3505651.24	1.80	-0.51	1.87
210	330882.03	3521649.64	2.71	-2.47	3.67
211	352932.94	3519567.92	-1.84	8.93	9.12
212	359260.93	3503217.41	-0.07	1.51	1.51
213	368485.49	3521472.98	-1.76	-1.64	2.41
215	341772.66	3534245.93	-2.90	-4.82	5.62
302	368044.77	3537684.00	-2.32	-2.07	3.11
515	357678.19	3559202.97	5.84	-7.76	9.71
		RMS	±4.05	±5.02	±6.45

N02 (2 X ellipsoid normal) : 0.1276879123813404D+08
aa (Unknown tied to Earth rotation) : 0.6192359196329110D-01
ALPHA (IFOV) : 0.1200000000000000D-04
bb (Unknown of 2nd order) : 0.9476012600555214D-08
C0 (Scene centre column) : 0.3000000000000000D+04
cc (Unknown of 2nd order): -.4555609185968758D-08
COSKHI (Parameter): 0.9998732458409010D+00
DELGAM (Unknown of 2nd order): -.1291214870478763D-07
GAMMA (Scene orient. rel. to the North): 0.1633280574399707D+00
K_1 (Cross track scale function): 0.1411976874337382D-05
L0 (Scene centre row): 0.3000000000000000D+04
P (Along track scale function): 0.9979142443786058D+01
Q (Satellite-Scene centre dist): 0.9463141149594770D+06
TAU (Levelling angle along track dir): -.1592345836166880D-01
THETA (Levelling angle across track dir): -.4044187027220019D+00
THETAS (THETA/COS_KHI): -.4044699709730534D+00
X0 (Carto coord of scene centre): 0.3429874326127838D+06
Y0 (Carto coord of scene centre): 0.3534510879284113D+07
DELH (Radar parameter in H dir.): 0.0000000000000000D+00
COEFY2 (Radar parameter in Y2 dir.): 0.0000000000000000D+00

EARTH ELLIPSOID USED : E004

The following are the results of the space resection giving the planimetric accuracy of the left image of the Level 1B stereo-model for scene 123/286 using 14 control points and 15 check points:

1

SMODEL Satellite Model Calculation V6.0 EASI/PACE 20:49 30-NOV-97

Report File : D:\SOUTHWM\SM15CHL.TXT

Using GCPs stored in the GCP segment :

GCPID	CALCULATED GCP		RESIDUAL (Metre)		
	X	Y	ΔX	ΔY	Vector
146	322956.72	3563356.37	0.61	2.86	2.92
149	336876.43	3557832.93	7.61	0.76	7.65
150	343639.34	3563009.74	-6.17	2.60	6.70
151	313517.71	3552940.87	-0.35	-0.91	0.98
154	329676.69	3548197.34	4.95	1.01	5.06
165	317481.73	3530712.49	-7.40	2.96	7.97
166	330244.69	3534955.40	-6.64	-9.36	11.47
202	363804.36	3539202.49	-5.38	-5.89	7.98
203	375644.39	3535242.69	3.74	-2.66	4.59
204	374759.90	3555431.15	3.07	0.79	3.17
207	315008.04	3511658.25	3.69	0.12	3.69
210	330879.41	3521647.53	5.33	-0.36	5.34
212	359258.98	3503216.78	1.88	2.14	2.85
213	368488.66	3521465.40	-4.93	5.94	7.71
		RMS	±5.13	±3.88	±6.43

RESIDUAL ERRORS AT CHECK POINTS:

GCPID	CALCULATED CHECK POINT		ERRORS (Metre)		
	X	Y	ΔX	ΔY	Vector
-148	330978.52	3561091.29	-1.88	-6.58	6.84
-153	320671.62	3549838.93	-6.26	-9.27	11.18
-156	334927.28	3545624.35	-3.30	5.07	6.04
-157	327575.56	3553032.03	8.14	4.62	9.36
-158	328330.17	3556587.38	-0.63	5.98	6.02
-159	325737.48	3543786.35	6.82	-4.91	8.40
-164	320094.08	3536369.49	8.08	-10.65	13.37
-167	330429.04	3528360.52	-9.61	1.02	9.66
-201	350518.67	3543346.28	-6.94	5.54	8.88
-206	319057.01	3518177.20	3.95	-9.26	10.07
-209	339189.79	3505660.95	-0.76	-10.22	10.24
-211	352941.61	3519572.49	-10.51	4.36	11.38
-215	341774.77	3534246.59	-5.01	-5.48	7.42
-302	368043.97	3537692.71	-1.52	-10.78	10.88
-515	357678.92	3559206.85	5.11	-11.64	12.71
		RMS	±6.28	±7.89	±10.09

N02 (2 X ellipsoid normal) : 0.1276879105096307D+08
aa (Unknown tied to Earth rotation) : 0.5506315068927042D-01
ALPHA (IFOV) : 0.1200000000000000D-04

bb (Unknown of 2nd order) : 0.1465086180891859D-08
C0 (Scene centre column) : 0.3000000000000000D+04
cc (Unknown of 2nd order): 0.2394160614173618D-08
COSKHI (Parameter): 0.9999553135363998D+00
DELGAM (Unknown of 2nd order): 0.2275588505921620D-08
GAMMA (Scene orient. rel. to the North): 0.2327298248021000D+00
K_1 (Cross track scale function): 0.1392967781909528D-05
L0 (Scene centre row): 0.3000000000000000D+04
P (Along track scale function): 0.1001525590922433D+02
Q (Satellite-Scene centre dist): 0.9978236197079092D+06
TAU (Levelling angle along track dir): -.9454042426253964D-02
THETA (Levelling angle across track dir): 0.4494612485849160D+00
THETAS (THETA/COS_KHI): 0.4494813343162009D+00
X0 (Carto coord of scene centre): 0.3386639302315127D+06
Y0 (Carto coord of scene centre): 0.3534463101136000D+07
DELH (Radar parameter in H dir.): 0.0000000000000000D+00
COEFY2 (Radar parameter in Y2 dir.): 0.0000000000000000D+00

EARTH ELLIPSOID USED : E004

The following are the results of the space resection giving the planimetric accuracy of the right image of the Level 1B stereo-model for scene 123/286 using 14 control points and 15 check points:

SMODEL Satellite Model Calculation V6.0 EASI/PACE 20:55 30-NOV-97

Report File : D:\SOUTHWM\SM15CHR.TXT

Using GCPs stored in the GCP segment :

GCPID	CALCULATED GCP		RESIDUAL (Metre)		
	X	Y	ΔX	ΔY	Vector
146	322959.08	3563358.78	-1.75	0.45	1.80
149	336875.99	3557834.79	8.05	-1.10	8.13
150	343638.57	3563010.13	-5.40	2.21	5.83
151	313514.74	3552936.63	2.62	3.33	4.24
154	329682.17	3548195.71	-0.53	2.64	2.69
165	317480.05	3530718.21	-5.72	-2.76	6.35
166	330242.37	3534956.33	-4.32	-10.29	11.16
202	363798.18	3539194.36	0.80	2.24	2.38
203	375647.61	3535240.85	0.52	-0.82	0.97
204	374761.21	3555432.22	1.76	-0.28	1.78
207	315008.22	3511653.32	3.51	5.05	6.15
210	330881.63	3521649.99	3.11	-2.82	4.20
212	359260.90	3503216.13	-0.04	2.79	2.79
213	368486.32	3521471.98	-2.59	-0.64	2.67
		RMS	±3.81	±3.78	±5.36

RESIDUAL ERRORS AT CHECK POINTS:

GCPID	CALCULATED CHECK POINT		ERRORS (Metre)		
	X	Y	ΔX	ΔY	Vector
-148	330982.50	3561094.35	-5.86	-9.64	11.28
-153	320671.65	3549836.99	-6.29	-7.33	9.66
-156	334925.06	3545624.74	-1.08	4.68	4.80
-157	327577.03	3553029.97	6.67	6.68	9.44

-158	328329.47	3556590.72	0.07	2.64	2.64
-159	325744.54	3543781.93	-0.24	-0.49	0.54
-164	320100.60	3536364.59	1.56	-5.75	5.96
-167	330425.88	3528369.08	-6.45	-7.54	9.93
-201	350511.84	3543345.82	-0.11	6.00	6.00
-206	319064.23	3518166.84	-3.27	1.10	3.45
-209	339185.90	3505650.67	3.13	0.06	3.13
-211	352931.69	3519567.40	-0.59	9.45	9.46
-215	341771.16	3534246.61	-1.40	-5.50	5.67
-302	368044.58	3537683.80	-2.13	-1.87	2.83
-515	357675.89	3559204.63	8.14	-9.42	12.46
		RMS	±4.29	±6.32	±7.64

N02 (2 X ellipsoid normal) : 0.1276879123813404D+08
aa (Unknown tied to Earth rotation) : 0.6187042432091943D-01
ALPHA (IFOV) : 0.1200000000000000D-04
bb (Unknown of 2nd order) : 0.9476012600555214D-08
C0 (Scene centre column) : 0.3000000000000000D+04
cc (Unknown of 2nd order): -.4555609185968758D-08
COSKHI (Parameter): 0.9999488914880220D+00
DELGAM (Unknown of 2nd order): -.1291214870478763D-07
GAMMA (Scene orient. rel. to the North): 0.1633757397695449D+00
K_1 (Cross track scale function): 0.1406748289955272D-05
L0 (Scene centre row): 0.3000000000000000D+04
P (Along track scale function): 0.9979362940846996D+01
Q (Satellite-Scene centre dist): 0.9462628643293562D+06
TAU (Levelling angle along track dir): -.1011063107476273D-01
THETA (Levelling angle across track dir): -.3990873938220970D+00
THETAS (THETA/COS_KHI): -.3991077916274460D+00
X0 (Carto coord of scene centre): 0.3429885472962325D+06
Y0 (Carto coord of scene centre): 0.3534507409611608D+07
DELH (Radar parameter in H dir.): 0.0000000000000000D+00
COEFY2 (Radar parameter in Y2 dir.): 0.0000000000000000D+00

EARTH ELLIPSOID USED : E004

B.2.5 Level 1B Stereo-model of Scene 124/285

The following are the results of the space resection giving the planimetic accuracy of the left image of the Level 1B stereo-model for scene 124/285 using 19 ground control points:

SMODEL Satellite Model Calculation V6.0 EASI/PACE 11:56 30-NOV-97

Report File : F:\NEAST\SM19L.TXT

Using GCPs stored in the GCP segment :

GCPID	CALCULATED GCP		RESIDUAL (Metre)		
	X	Y	ΔX	ΔY	Vector
512	379349.73	3594486.35	1.03	-1.55	1.86
314	416265.72	3559480.17	-7.42	2.23	7.75
315	400246.29	3562610.50	-3.55	-4.39	5.64
401	423466.58	3597156.85	2.40	4.93	5.48
402	433827.81	3600308.07	5.67	-7.19	9.16

403	410185.55	3592076.57	-5.66	-2.04	6.02
404	377212.47	3566146.87	3.41	-7.96	8.66
405	384890.81	3608353.06	2.24	0.72	2.35
406	400812.87	3608972.95	1.78	3.65	4.06
407	401290.47	3618274.88	-6.68	-3.59	7.59
408	391503.43	3618422.66	-5.16	0.14	5.16
409	395601.36	3572838.77	4.28	-6.04	7.40
410	407849.43	3580578.26	6.59	8.82	11.01
411	447602.41	3604587.85	2.99	0.13	3.00
412	425742.61	3580255.70	1.98	-3.14	3.71
413	439092.95	3582968.06	-1.49	-3.06	3.40
415	436334.60	3566516.86	-2.75	6.72	7.26
508	389055.76	3584944.27	-2.58	3.51	4.36
509	376118.09	3580636.65	2.92	8.11	8.62
		RMS	±4.28	±5.02	±6.60

N02 (2 X ellipsoid normal) : 0.1276912543258554D+08
aa (Unknown tied to Earth rotation) : 0.5349868694600560D-01
ALPHA (IFOV) : 0.1200000000000000D-04
bb (Unknown of 2nd order) : 0.9986427203142418D-09
C0 (Scene centre column) : 0.3000000000000000D+04
cc (Unknown of 2nd order): 0.2923029958928500D-08
COSKHI (Parameter): 0.9998881954464700D+00
DELGAM (Unknown of 2nd order): 0.3228840787888254D-08
GAMMA (Scene orient. rel. to the North): 0.2344391853326867D+00
K_1 (Cross track scale function): 0.1424443184804403D-05
L0 (Scene centre row): 0.3000000000000000D+04
P (Along track scale function): 0.1001178392105594D+02
Q (Satellite-Scene centre dist): 0.1050279645565782D+07
TAU (Levelling angle along track dir): -.1495481907031171D-01
THETA (Levelling angle across track dir): 0.5334703216779185D+00
THETAS (THETA/COS_KHI): 0.5335299727583176D+00
X0 (Carto coord of scene centre): 0.4037795585208274D+06
Y0 (Carto coord of scene centre): 0.3588367444823811D+07
DELH (Radar parameter in H dir.): 0.0000000000000000D+00
COEFY2 (Radar parameter in Y2 dir.): 0.0000000000000000D+00

EARTH ELLIPSOID USED : E004

The following are the results of the space resection giving the planimetric accuracy of the right image of the Level 1B stereo-model for scene 124/285 using 19 ground control points:

SMODEL Satellite Model Calculation V6.0 EASI/PACE 12:22 30-NOV-97

Report File : F:\NEAST\SM19R.TXT

Using GCPs stored in the GCP segment :

GCPID	CALCULATED GCP		RESIDUAL (Metre)		
	X	Y	ΔX	ΔY	Vector
509	376122.31	3580637.55	-1.30	7.21	7.33
314	416259.50	3559476.17	-1.20	6.23	6.35
315	400238.56	3562607.32	4.18	-1.21	4.35
401	423467.04	3597159.69	1.94	2.09	2.86
402	433828.39	3600306.50	5.09	-5.62	7.59

403	410187.38	3592076.93	-7.49	-2.40	7.87
404	377218.03	3566142.06	-2.15	-3.15	3.81
405	384886.05	3608361.41	7.00	-7.63	10.35
406	400810.56	3608980.71	4.09	-4.11	5.80
407	401283.05	3618264.57	0.74	6.72	6.76
408	391506.66	3618419.77	-8.39	3.04	8.93
409	395605.95	3572831.67	-0.31	1.06	1.10
410	407856.86	3580579.38	-0.84	7.70	7.75
411	447607.63	3604581.47	-2.23	6.51	6.88
412	425737.33	3580259.13	7.26	-6.57	9.79
413	439098.41	3582966.59	-6.95	-1.59	7.13
512	379345.49	3594492.21	5.27	-7.41	9.10
415	436330.16	3566528.38	1.69	-4.80	5.09
508	389059.58	3584943.85	-6.40	3.93	7.51
		RMS	±4.87	±5.35	±7.23

N02 (2 X ellipsoid normal) : 0.1276912543258554D+08
aa (Unknown tied to Earth rotation) : 0.6064056413061297D-01
ALPHA (IFOV) : 0.1200000000000000D-04
bb (Unknown of 2nd order) : 0.1007842864142168D-07
C0 (Scene centre column) : 0.3000000000000000D+04
cc (Unknown of 2nd order): -.5011511327000720D-08
COSKHI (Parameter): 0.9999409454454752D+00
DELGAM (Unknown of 2nd order): -.1398269406935534D-07
GAMMA (Scene orient. rel. to the North): 0.1545330048841036D+00
K_1 (Cross track scale function): 0.1417237990005702D-05
L0 (Scene centre row): 0.3000000000000000D+04
P (Along track scale function): 0.9973308765879590D+01
Q (Satellite-Scene centre dist): 0.9771347851309254D+06
TAU (Levelling angle along track dir): -.1086828285400932D-01
THETA (Levelling angle across track dir): -.4482810686003843D+00
THETAS (THETA/COS_KHI): -.4483075432026382D+00
X0 (Carto coord of scene centre): 0.4112122828893856D+06
Y0 (Carto coord of scene centre): 0.3588447187125666D+07
DELH (Radar parameter in H dir.): 0.0000000000000000D+00
COEFY2 (Radar parameter in Y2 dir.): 0.0000000000000000D+00

EARTH ELLIPSOID USED : E004

The following are the results of the space resection giving the planimetric accuracy of the left image of the Level 1B stereo-model for scene 124/285 using 11 control points and 8 check points:

SMODEL Satellite Model Calculation V6.0 EASI/PACE 12:55 30-NOV-97

Report File : F:\NEAST\SM8CHL.TXT

Using GCPs stored in the GCP segment :

GCPID	CALCULATED GCP		RESIDUAL (Metre)		
	X	Y	ΔX	ΔY	Vector
512	379350.92	3594485.02	-0.16	-0.22	0.27
314	416264.55	3559481.75	-6.25	0.65	6.28
315	400245.47	3562611.68	-2.73	-5.57	6.21
402	433828.17	3600307.04	5.31	-6.16	8.14
404	377212.36	3566147.52	3.52	-8.61	9.30
407	401292.17	3618272.19	-8.38	-0.90	8.42
410	407849.27	3580578.29	6.75	8.79	11.08

411	447602.88	3604586.66	2.52	1.32	2.85
413	439092.59	3582968.25	-1.13	-3.25	3.44
415	436333.61	3566518.14	-1.76	5.44	5.72
509	376118.71	3580636.26	2.30	8.50	8.81
		RMS	±4.68	±5.79	±7.45

RESIDUAL ERRORS AT CHECK POINTS:

GCPID	CALCULATED CHECK POINT		ERRORS (Metre)		
	X	Y	ΔX	ΔY	Vector
-401	423466.91	3597155.93	2.07	5.85	6.21
-403	410185.86	3592075.83	-5.97	-1.30	6.11
-405	384892.51	3608350.81	0.54	2.97	3.01
-406	400814.14	3608970.91	0.51	5.69	5.72
-408	391505.41	3618419.80	-7.14	3.00	7.74
-409	395601.10	3572839.19	4.54	-6.46	7.89
-412	425742.21	3580255.96	2.38	-3.40	4.14
-508	389056.22	3584943.75	-3.04	4.03	5.05
		RMS	±4.26	±4.71	±6.35

N02 (2 X ellipsoid normal) : 0.1276912543258554D+08
aa (Unknown tied to Earth rotation) : 0.5357347949437816D-01
ALPHA (IFOV) : 0.1200000000000000D-04
bb (Unknown of 2nd order) : 0.9986427203142418D-09
C0 (Scene centre column) : 0.3000000000000000D+04
cc (Unknown of 2nd order): 0.2923029958928500D-08
COSKHI (Parameter): 0.9998931238101376D+00
DELGAM (Unknown of 2nd order): 0.3228840787888254D-08
GAMMA (Scene orient. rel. to the North): 0.2344177723267538D+00
K_1 (Cross track scale function): 0.1424819802458081D-05
L0 (Scene centre row): 0.3000000000000000D+04
P (Along track scale function): 0.1001124966285065D+02
Q (Satellite-Scene centre dist): 0.1050241563525641D+07□
TAU (Levelling angle along track dir): -.1462144494119852D-01
THETA (Levelling angle across track dir): 0.5337565398248635D+00
THETAS (THETA/COS_KHI): 0.5338135917876505D+00
X0 (Carto coord of scene centre): 0.4037799716343598D+06
Y0 (Carto coord of scene centre): 0.3588366616214892D+07
DELH (Radar parameter in H dir.): 0.0000000000000000D+00
COEFY2 (Radar parameter in Y2 dir.): 0.0000000000000000D+00

EARTH ELLIPSOID USED : E004

The following are the results of the space resection giving the planimetric accuracy of the right image of the Level 1B stereo-model for scene 124/285 using 11 control points and 8 check points:

SMODEL Satellite Model Calculation V6.0 EASI/PACE 12:53 30-NOV-97

Report File : F:\NEAST\8CHR.TXT

Using GCPs stored in the GCP segment :

GCPID	CALCULATED GCP		RESIDUAL (Metre)		
	X	Y	ΔX	ΔY	Vector
509	376123.02	3580638.53	-2.01	6.23	6.54
314	416259.28	3559476.04	-0.98	6.36	6.43
315	400239.21	3562607.37	3.53	-1.26	3.75
402	433828.65	3600307.92	4.83	-7.04	8.54
404	377218.55	3566142.27	-2.67	-3.36	4.29
407	401285.33	3618267.37	-1.54	3.92	4.22
410	407857.91	3580580.21	-1.89	6.87	7.12
411	447606.58	3604583.09	-1.18	4.89	5.03
413	439097.20	3582967.41	-5.74	-2.41	6.23
512	379346.58	3594494.02	4.18	-9.22	10.13
415	436328.38	3566528.55	3.47	-4.97	6.06
		RMS	±3.43	±5.86	±6.79

RESIDUAL ERRORS AT CHECK POINTS:

GCPID	CALCULATED CHECK POINT		ERRORS (Metre)		
	X	Y	ΔX	ΔY	Vector
-401	423467.98	3597161.04	1.00	0.74	1.25
-403	410188.76	3592078.28	-8.87	-3.75	9.63
-405	384887.62	3608364.20	5.43	-10.42	11.75
-406	400812.59	3608983.05	2.06	-6.45	6.77
-408	391508.71	3618422.87	-10.44	-0.06	10.44
-409	395606.97	3572832.24	-1.33	0.49	1.42
-412	425737.33	3580259.80	7.26	-7.24	10.25
-508	389060.86	3584945.08	-7.68	2.70	8.14
		RMS	±6.93	±5.67	±8.95

N02 (2 X ellipsoid normal) : 0.1276912543258554D+08
aa (Unknown tied to Earth rotation) : 0.6063645897262410D-01
ALPHA (IFOV) : 0.1200000000000000D-04
bb (Unknown of 2nd order) : 0.1007842864142168D-07
C0 (Scene centre column) : 0.3000000000000000D+04
cc (Unknown of 2nd order): -.5011511327000720D-08
COSKHI (Parameter): 0.9998632558602648D+00
DELGAM (Unknown of 2nd order): -.1398269406935534D-07
GAMMA (Scene orient. rel. to the North): 0.1545572404145815D+00
K_1 (Cross track scale function): 0.1418925652301465D-05
L0 (Scene centre row): 0.3000000000000000D+04
P (Along track scale function): 0.9973720402196856D+01
Q (Satellite-Scene centre dist): 0.9770967293512112D+06□
TAU (Levelling angle along track dir): -.1653917732474228D-01
THETA (Levelling angle across track dir): -.4497334853037478D+00
THETAS (THETA/COS_KHI): -.4497949921330043D+00
X0 (Carto coord of scene centre): 0.4112130880277202D+06
Y0 (Carto coord of scene centre): 0.3588452257794381D+07
DELH (Radar parameter in H dir.): 0.0000000000000000D+00
COEFY2 (Radar parameter in Y2 dir.): 0.0000000000000000D+00

EARTH ELLIPSOID USED : E004

B.2.6 Level 1B Stereo-model of Scene 124/286

The following are the results of the space resection giving the planimetric accuracy of the left image of the Level 1B stereo-model for scene 124/286 using 13 ground control points:

SMODEL Satellite Model Calculation V6.0 EASI/PACE 14:07 30-NOV-97

Report File : F:\SEAST\SM01L.TXT

Using GCPs stored in the GCP segment :

GCPID	CALCULATED GCP		RESIDUAL (Metre)		
	X	Y	ΔX	ΔY	Vector
203	375653.54	3535237.50	-5.41	2.53	5.98
204	374758.17	3555430.13	4.80	1.81	5.13
213	368475.51	3521471.82	8.22	-0.48	8.23
301	363527.94	3512134.70	1.22	7.67	7.77
302	368046.21	3537687.86	-3.76	-5.93	7.02
303	389807.91	3531702.81	3.57	-6.07	7.04
304	412378.08	3524083.56	2.04	-0.35	2.07
306	380367.33	3522862.46	-4.13	-2.17	4.67
308	399438.02	3521864.41	-6.61	-6.65	9.37
309	398276.10	3529544.48	-2.52	1.15	2.77
310	393220.81	3543164.76	3.65	5.68	6.75
311	412467.18	3543413.71	2.71	5.19	5.85
404	377219.65	3566141.28	-3.77	-2.37	4.45
		RMS	±4.60	±4.62	±6.52

N02 (2 X ellipsoid normal) : 0.1276879142530591D+08
aa (Unknown tied to Earth rotation) : 0.5423727976089168D-01
ALPHA (IFOV) : 0.1200000000000000D-04
bb (Unknown of 2nd order) : 0.9161108633548356D-09
C0 (Scene centre column) : 0.3000000000000000D+04
cc (Unknown of 2nd order): 0.2976408323151684D-08
COSKHI (Parameter): 0.9999222246154352D+00
DELGAM (Unknown of 2nd order): 0.3308567873473560D-08
GAMMA (Scene orient. rel. to the North): 0.2338551826193556D+00□
K_1 (Cross track scale function): 0.1436807312123696D-05
L0 (Scene centre row): 0.3000000000000000D+04
P (Along track scale function): 0.1001396396927323D+02
Q (Satellite-Scene centre dist): 0.1050097117595433D+07
TAU (Levelling angle along track dir): -.1247272696899114D-01
THETA (Levelling angle across track dir): 0.5436755112618616D+00
THETAS (THETA/COS_KHI): 0.5437177991227832D+00
X0 (Carto coord of scene centre): 0.3876267006206769D+06
Y0 (Carto coord of scene centre): 0.3533820862469972D+07
DELH (Radar parameter in H dir.): 0.0000000000000000D+00
COEFY2 (Radar parameter in Y2 dir.): 0.0000000000000000D+00

EARTH ELLIPSOID USED : E004

The following are the results of the space resection giving the planimetric accuracy of the right image of the Level 1B stereo-model for scene 124/286 using 13 ground control points:

SMODEL Satellite Model Calculation V6.0 EASI/PACE 13:32 30-NOV-97

Report File : F:\SEAST\SM01R.TXT

Using GCPs stored in the GCP segment :

GCPID	CALCULATED GCP		RESIDUAL (Metre)		
	X	Y	ΔX	ΔY	Vector
203	375642.56	3535236.73	5.57	3.30	6.48
204	374760.49	3555433.72	2.48	-1.78	3.06
213	368478.16	3521473.51	5.57	-2.17	5.97
301	363537.17	3512142.61	-8.01	-0.24	8.01
302	368039.39	3537685.38	3.06	-3.45	4.61
303	389812.01	3531694.54	-0.53	2.20	2.27
304	412376.96	3524089.33	3.16	-6.12	6.89
306	380370.69	3522862.69	-7.49	-2.40	7.87
308	399427.66	3521845.46	3.75	12.30	12.86
309	398271.90	3529550.15	1.68	-4.52	4.82
310	393222.89	3543166.15	1.57	4.29	4.57
311	412476.78	3543421.86	-6.89	-2.96	7.50
404	377219.81	3566137.37	-3.93	1.54	4.22
		RMS	±4.92	±4.83	±6.89

N02 (2 X ellipsoid normal) : 0.1276879161247868D+08
aa (Unknown tied to Earth rotation) : 0.6214270824816540D-01
ALPHA (IFOV) : 0.1200000000000000D-04
bb (Unknown of 2nd order) : 0.9999311799882858D-08
C0 (Scene centre column) : 0.3000000000000000D+04
cc (Unknown of 2nd order): -.5001919893741090D-08
COSKHI (Parameter): 0.9999795021217042D+00
DELGAM (Unknown of 2nd order): -.1390076591053546D-07
GAMMA (Scene orient. rel. to the North): 0.1544996402736130D+00
K_1 (Cross track scale function): 0.1405608086158252D-05
L0 (Scene centre row): 0.3000000000000000D+04
P (Along track scale function): 0.9973214088468616D+01
Q (Satellite-Scene centre dist): 0.9774226243888534D+06
TAU (Levelling angle along track dir): -.6402891309003059D-02
THETA (Levelling angle across track dir): -.4375418909657108D+00
THETAS (THETA/COS_KHI): -.4375508598299838D+00
X0 (Carto coord of scene centre): 0.3992570253896461D+06
Y0 (Carto coord of scene centre): 0.3533859437088152D+07
DELH (Radar parameter in H dir.): 0.0000000000000000D+00
COEFY2 (Radar parameter in Y2 dir.): 0.0000000000000000D+00

EARTH ELLIPSOID USED : E004

B.3 Accuracy Results of Absolute Orientation

B.3.1 The Results of Absolute Orientation of Level 1B Stereo-pair for Reference Scene 122/285

The following are the results of the absolute orientation using space intersection carried out for the Level 1B stereo-pair for the reference scene 122/285 using 48 ground control points:

Calculated				Errors (metres)		
GCPID	X	Y	Z	ΔX	ΔY	ΔZ
101	308542.52	3559864.57	806.2	2.2	5.8	4.1
102	300922.43	3557088.80	797.2	-0.6	9.8	0.5
110	295866.66	3566650.33	938.1	4.5	-4.9	4.5
112	309289.58	3582164.75	1095.4	-1.6	2.4	-1.7
113	304306.45	3580952.02	1150.4	-0.3	-4.8	3.5
111	300749.80	3576803.16	1107.3	-7.9	-1.7	-2.4
114	297522.34	3574018.87	1054.1	4.1	5.5	5.8
116	284864.69	3573797.26	993.9	0.6	5.3	-3.1
123	282553.54	3570240.18	929.3	-4.6	2.6	-2.8
119	284540.83	3563607.77	836.7	5.0	-0.2	0.0
124	284230.14	3556244.72	705.3	3.4	2.7	0.3
135	279719.68	3554365.04	666.9	-4.7	-8.4	0.1
133	278856.32	3542819.24	585.2	-5.9	-1.9	4.0
136	282123.63	3547226.26	605.8	4.9	-4.1	5.3
141	292951.60	3536499.01	542.6	3.6	1.4	-1.1
142	292459.92	3547668.62	673.2	-9.1	-8.7	2.0
137	292706.32	3551488.69	714.9	-0.6	-6.8	-5.9
163	304906.06	3532799.25	527.4	-0.4	1.4	9.1
167	330424.17	3528362.19	599.5	-4.7	-0.6	-2.7
165	317482.36	3530719.62	600.2	-8.0	-4.2	5.2
164	320102.63	3536362.67	620.3	-0.5	-3.8	7.3
162	308308.40	3542495.91	609.7	5.9	1.6	-6.3
159	325737.16	3543776.14	646.9	7.1	5.3	-12.9
154	329674.37	3548192.49	632.0	7.3	5.9	-6.0
153	320670.55	3549827.59	635.1	-5.2	2.1	-5.3
151	313512.13	3552930.82	720.9	5.2	9.1	-4.3
152	309237.15	3554858.29	749.7	-4.2	0.3	1.5
157	327578.95	3553023.44	646.1	4.7	13.2	-2.9
158	328327.98	3556589.35	643.4	1.6	4.0	3.0
148	330978.33	3561092.27	659.1	-1.7	-7.6	-6.1
146	322962.46	3563354.98	709.5	-5.1	4.3	-1.8
149	336879.87	3557833.05	640.4	4.2	0.6	3.6
150	343635.83	3563019.98	702.3	-2.7	-7.6	-0.5
125	325230.64	3568555.73	740.3	-7.5	-7.6	7.2
129	338785.34	3569543.69	719.3	-1.8	-1.6	1.6
145	345749.86	3571776.65	768.7	-3.9	-5.7	-1.5
126	326820.94	3574685.82	755.4	6.1	-1.7	2.8
128	331363.78	3573363.69	710.1	-0.5	-1.4	4.5
168	321496.97	3574938.39	796.3	-1.0	0.7	-2.4
127	330683.89	3582053.74	730.4	-4.5	7.6	11.0
169	318575.72	3586702.67	960.9	4.8	0.1	-6.3
118	290487.43	3561267.48	854.0	-3.0	4.9	-6.1
156	334921.50	3545626.08	622.8	2.5	3.3	5.4
155	337158.68	3549812.54	632.1	7.9	2.8	-0.6
140	281956.68	3535718.44	553.4	5.5	-0.2	0.0
166	330245.56	3534951.79	594.5	-7.5	-5.7	-0.3
143	337967.46	3576243.15	716.9	0.0	-4.9	-0.3
171	313694.49	3569815.42	891.6	4.2	-8.1	-4.8
	RMS Error :			±4.7	±4.9	±4.8

The following are the results of the absolute orientation using space intersection carried out for the Level 1B stereo-pair for the reference scene 122/285 using 43 control points and 5 check points:

Calculated				Errors (metres)		
GCPID	X	Y	Z	ΔX	ΔY	ΔZ
101	308542.42	3559864.28	805.7	2.3	6.1	4.6
102	300922.45	3557088.45	796.8	-0.6	10.1	0.9
110	295867.02	3566649.94	938.1	4.2	-4.6	4.5
113	304306.80	3580951.57	1150.6	-0.6	-4.3	3.3
111	300750.17	3576802.69	1107.5	-8.3	-1.2	-2.6
114	297522.78	3574018.44	1054.4	3.6	6.0	5.5
116	284865.73	3573796.95	995.0	-0.4	5.6	-4.2
119	284541.63	3563607.51	837.4	4.2	0.1	-0.7
124	284230.80	3556244.54	705.7	2.7	2.9	-0.1
135	279720.52	3554364.90	667.6	-5.5	-8.2	-0.6
133	278856.83	3542818.96	585.3	-6.4	-1.6	3.9
136	282124.14	3547226.05	606.0	4.4	-3.9	5.2
141	292951.42	3536498.65	541.7	3.7	1.8	-0.2
142	292460.00	3547668.28	672.8	-9.2	-8.4	2.5
137	292706.48	3551488.37	714.6	-0.8	-6.5	-5.6
167	330423.31	3528361.60	599.0	-3.9	-0.1	-2.2
165	317481.56	3530719.04	599.0	-7.2	-3.6	6.4
164	320101.93	3536362.20	619.4	0.2	-3.4	8.2
162	308307.99	3542495.58	608.8	6.3	2.0	-5.4
159	325736.58	3543775.82	646.4	7.7	5.6	-12.4
153	320670.16	3549827.42	634.6	-4.8	2.2	-4.8
151	313511.83	3552930.53	720.3	5.5	9.4	-3.7
152	309236.95	3554857.99	749.1	-4.0	0.6	2.1
157	327578.58	3553023.36	646.0	5.1	13.3	-2.8
158	328327.67	3556589.37	643.4	1.9	4.0	3.0
148	330978.09	3561092.38	659.4	-1.5	-7.7	-6.3
146	322962.30	3563355.01	709.5	-5.0	4.2	-1.7
149	336879.56	3557833.15	641.0	4.5	0.5	3.1
150	343635.57	3563020.13	703.3	-2.4	-7.8	-1.6
125	325230.55	3568555.84	740.5	-7.4	-7.7	7.0
129	338785.21	3569543.93	720.2	-1.7	-1.9	0.7
145	345749.71	3571776.90	770.0	-3.8	-5.9	-2.8
126	326820.98	3574686.07	755.8	6.1	-1.9	2.4
128	331363.77	3573364.01	710.7	-0.5	-1.7	3.9
168	321497.05	3574938.54	796.6	-1.1	0.5	-2.6
127	330684.08	3582054.23	731.2	-4.7	7.1	10.2
169	318576.04	3586702.77	961.4	4.5	0.0	-6.8
118	290487.88	3561267.13	854.2	-3.5	5.3	-6.2
156	334920.97	3545625.91	622.9	3.0	3.5	5.2
155	337158.22	3549812.47	632.4	8.4	2.8	-1.0
140	281956.84	3535718.04	552.9	5.4	0.2	0.5
166	330244.83	3534951.38	594.1	-6.8	-5.3	0.0
171	313694.49	3569815.22	891.5	4.2	-7.9	-4.7
		RMS Error :		±4.8	±5.4	±4.7

	Calculated			Errors (metres)		
CHKID	X	Y	Z	ΔX	ΔY	ΔZ
-112	309289.87	3582164.44	1095.6	-1.9	2.7	-2.0

-123	282554.61	3570239.91	930.5	-5.7	2.9	-4.0
-163	304905.52	3532798.83	526.2	0.1	1.8	10.3
-154	329673.88	3548192.33	631.8	7.8	6.0	-5.9
-143	337967.47	3576243.56	717.8	0.0	-5.4	-1.3
		RMS Error :	±4.9	±4.6	±6.4	

The following are the results of the absolute orientation using space intersection carried out for the Level 1B stereo-pair for the reference scene 122/285 using 33 control points and 15 check points:

Calculated				Errors (metres)		
GCPID	X	Y	Z	ΔX	ΔY	ΔZ
101	308543.53	3559864.61	805.4	1.1	5.8	4.9
102	300924.22	3557089.16	796.4	-2.4	9.4	1.2
110	295869.18	3566650.45	938.4	2.0	-5.1	4.2
-112	309290.66	3582163.84	1096.2	-2.7	3.3	-2.5
113	304307.96	3580950.99	1151.2	-1.8	-3.7	2.8
-111	300751.71	3576802.41	1108.0	-9.8	-0.9	-3.0
114	297524.70	3574018.49	1054.8	1.7	5.9	5.1
116	284869.20	3573797.88	996.1	-3.9	4.7	-5.2
-123	282558.41	3570241.17	931.5	-9.5	1.6	-5.0
119	284545.19	3563608.95	837.9	0.6	-1.3	-1.3
124	284234.47	3556246.42	705.9	-1.0	1.0	-0.3
-135	279724.75	3554367.14	668.0	-9.7	-10.5	-1.0
-133	278861.06	3542821.45	585.1	-10.6	-4.1	4.1
136	282128.04	3547228.33	605.9	0.5	-6.2	5.3
141	292954.10	3536500.52	540.7	1.1	-0.1	0.8
-142	292462.66	3547669.78	672.3	-11.9	-9.9	3.0
137	292709.11	3551489.73	714.2	-3.4	-7.8	-5.2
-163	304907.18	3532800.16	524.8	-1.5	0.5	11.7
167	330423.46	3528361.53	597.4	-4.0	0.0	-0.6
165	317482.29	3530719.51	597.4	-8.0	-4.1	8.0
-164	320102.47	3536362.53	618.0	-0.3	-3.7	9.6
162	308309.32	3542496.52	607.8	5.0	1.0	-4.4
159	325736.79	3543775.86	645.3	7.5	5.6	-11.3
-154	329673.91	3548192.30	631.0	7.7	6.1	-5.0
153	320670.64	3549827.77	633.8	-5.3	1.9	-4.0
151	313512.67	3552930.90	719.6	4.7	9.1	-2.9
-152	309238.07	3554858.46	748.5	-5.1	0.2	2.6
157	327578.67	3553023.39	645.3	5.0	13.3	-2.1
-158	328327.72	3556589.41	642.9	1.8	4.0	3.6
148	330977.95	3561092.29	659.1	-1.3	-7.6	-6.0
-146	322962.53	3563355.09	709.2	-5.2	4.1	-1.5
149	336879.21	3557832.86	640.6	4.8	0.8	3.5
150	343634.83	3563019.37	703.1	-1.7	-7.0	-1.4
125	325230.60	3568555.75	740.4	-7.5	-7.6	7.1
129	338784.58	3569543.34	720.2	-1.1	-1.3	0.7
145	345748.72	3571775.86	770.1	-2.8	-4.9	-2.9
-126	326820.90	3574685.89	756.0	6.2	-1.8	2.2
128	331363.50	3573363.80	710.9	-0.2	-1.5	3.7
168	321497.26	3574938.44	796.8	-1.3	0.6	-2.8
127	330683.82	3582054.04	731.7	-4.4	7.3	9.7
169	318576.28	3586702.28	962.0	4.3	0.4	-7.5
-118	290490.68	3561268.17	854.3	-6.3	4.2	-6.4
156	334920.80	3545625.68	622.0	3.2	3.7	6.2
155	337157.92	3549812.14	631.7	8.7	3.2	-0.2
140	281960.63	3535720.41	552.2	1.6	-2.1	1.2
166	330244.95	3534951.37	592.7	-6.9	-5.3	1.4

-143	337966.84	3576243.06	718.1	0.7	-4.9	-1.5
171	313695.12	3569815.08	891.5	3.6	-7.7	-4.7
		RMS Error :	±5.3	±5.4	±5.3	

1

The following are the results of the absolute orientation using space intersection carried out for the Level 1B stereo-pair for the reference scene 122/285 using 23 control points and 25 check points:

Calculated				Errors (metres)		
GCPID	X	Y	Z	ΔX	ΔY	ΔZ
-101	308543.24	3559863.54	805.4	1.4	6.9	4.9
102	300923.56	3557087.92	797.1	-1.7	10.7	0.6
110	295868.36	3566648.63	937.9	2.8	-3.2	4.7
-112	309290.60	3582161.68	1093.6	-2.7	5.5	0.1
113	304307.54	3580948.37	1148.9	-1.4	-1.1	5.0
-111	300751.09	3576799.88	1106.3	-9.2	1.6	-1.4
-114	297523.96	3574016.20	1053.5	2.4	8.2	6.4
116	284868.06	3573796.04	994.3	-2.8	6.5	-3.5
-123	282557.22	3570239.62	930.0	-8.3	3.2	-3.6
119	284544.04	3563607.71	837.5	1.7	-0.1	-0.9
124	284233.32	3556245.73	706.5	0.2	1.7	-0.9
-135	279723.44	3554366.66	668.6	-8.4	-10.0	-1.6
-133	278859.52	3542820.98	587.5	-9.1	-3.7	1.8
136	282126.70	3547227.91	607.7	1.9	-5.8	3.5
-141	292952.89	3536500.11	544.1	2.3	0.3	-2.6
142	292461.56	3547668.94	674.3	-10.8	-9.0	0.9
-137	292708.09	3551488.77	715.7	-2.4	-6.9	-6.7
163	304906.32	3532799.91	528.3	-0.7	0.7	8.2
167	330423.64	3528361.51	598.7	-4.2	0.0	-1.9
165	317481.82	3530719.05	600.2	-7.5	-3.6	5.3
-164	320102.28	3536362.20	619.8	-0.1	-3.4	7.7
162	308308.79	3542496.13	609.9	5.5	1.4	-6.5
159	325737.16	3543775.77	645.5	7.1	5.7	-11.6
154	329674.67	3548192.60	630.2	7.0	5.7	-4.2
-153	320670.94	3549827.79	633.9	-5.6	1.9	-4.1
-151	313512.56	3552930.25	720.0	4.8	9.7	-3.4
-152	309237.76	3554857.60	749.1	-4.8	1.0	2.1
-157	327579.46	3553023.66	644.2	4.2	13.0	-1.0
158	328328.65	3556589.85	641.3	0.9	3.5	5.1
-148	330979.13	3561092.86	656.7	-2.5	-8.2	-3.7
146	322963.23	3563355.13	707.6	-5.9	4.1	0.2
-149	336880.72	3557833.68	637.7	3.3	0.0	6.4
150	343636.87	3563020.22	698.8	-3.7	-7.9	3.0
-125	325231.53	3568555.82	738.0	-8.4	-7.7	9.5
-129	338786.46	3569544.05	715.9	-2.9	-2.0	5.0
145	345751.07	3571776.60	764.6	-5.1	-5.6	2.6
-126	326822.08	3574686.12	752.7	5.0	-2.0	5.5
-128	331364.98	3573364.44	707.2	-1.7	-2.1	7.4
168	321498.07	3574938.27	794.0	-2.1	0.8	-0.1
-127	330685.51	3582054.80	727.1	-6.1	6.6	14.3
169	318577.05	3586701.35	958.1	3.5	1.4	-3.5
-118	290489.66	3561266.67	854.5	-5.3	5.7	-6.5
-156	334921.85	3545626.18	620.7	2.1	3.2	7.5
155	337159.23	3549812.80	629.6	7.4	2.5	1.9
140	281959.03	3535719.83	555.7	3.2	-1.6	-2.3
-166	330245.35	3534951.57	593.3	-7.3	-5.5	0.8
-143	337968.85	3576243.97	713.3	-1.3	-5.8	3.3

171	313695.22	3569813.89	890.1	3.5	-6.6	-3.3
		RMS Error :		±5.0	±5.1	±5.1

The following are the space results of the absolute orientation using space intersection carried out for the Level 1B stereo-pair for the reference scene 122/285 using 13 control points and 35 check points:

Calculated				Errors (metres)		
GCPID	X	Y	Z	ΔX	ΔY	ΔZ
102	300925.52	3557089.16	796.0	-3.7	9.4	1.7
113	304308.48	3580950.31	1148.8	-2.3	-3.1	5.1
116	284867.69	3573797.94	994.4	-2.4	4.6	-3.6
119	284544.31	3563609.25	837.2	1.5	-1.6	-0.6
136	282127.92	3547228.98	606.5	0.6	-6.9	4.6
167	330424.87	3528362.71	596.7	-5.4	-1.2	0.1
162	308311.44	3542496.96	607.9	2.9	0.6	-4.5
154	329674.97	3548193.53	629.4	6.7	4.8	-3.4
158	328328.64	3556590.63	640.9	0.9	2.7	5.5
145	345747.86	3571777.75	766.0	-1.9	-6.8	1.2
168	321498.05	3574939.14	794.1	-2.1	-0.1	-0.2
169	318576.72	3586702.54	958.8	3.9	0.2	-4.2
140	281961.43	3535720.87	553.8	0.8	-2.6	-0.4
		RMS Error :		±3.3	±4.6	±3.5

	Calculated			Errors (metres)		
CHKID	X	Y	Z	ΔX	ΔY	ΔZ
-101	308545.03	3559864.70	804.4	-0.4	5.7	5.9
-110	295869.65	3566650.23	937.3	1.6	-4.8	5.3
-112	309291.31	3582163.40	1093.6	-3.4	3.8	0.1
-111	300752.15	3576801.80	1106.0	-10.2	-0.3	-1.1
-114	297524.96	3574018.03	1053.2	1.4	6.4	6.7
-123	282556.74	3570241.43	930.2	-7.8	1.4	-3.7
-124	284233.97	3556246.96	705.9	-0.5	0.5	-0.3
-135	279723.70	3554367.89	668.0	-8.7	-11.2	-1.1
-133	278860.85	3542822.11	586.2	-10.4	-4.8	3.0
-141	292955.89	3536500.92	541.9	-0.7	-0.5	-0.4
-142	292463.82	3547670.02	672.7	-13.0	-10.1	2.5
-137	292710.05	3551489.93	714.4	-4.3	-8.0	-5.4
-163	304909.66	3532800.64	525.8	-4.0	0.0	10.7
-165	317484.72	3530720.05	597.7	-10.4	-4.6	7.7
-164	320104.60	3536363.19	617.7	-2.4	-4.3	9.8
-159	325738.31	3543776.78	644.3	6.0	4.7	-10.3
-153	320672.23	3549828.61	632.8	-6.9	1.0	-3.0
-151	313514.43	3552931.26	718.8	2.9	8.7	-2.2
-152	309239.76	3554858.66	747.8	-6.8	0.0	3.3
-157	327579.75	3553024.53	643.6	4.0	12.1	-0.5
-148	330978.61	3561093.63	656.6	-2.0	-8.9	-3.6
-146	322963.63	3563355.94	707.2	-6.3	3.3	0.5
-149	336879.36	3557834.56	637.9	4.7	-0.9	6.2
-150	343634.23	3563021.31	699.6	-1.1	-9.0	2.1
-125	325231.46	3568556.65	737.9	-8.3	-8.5	9.6
-129	338784.43	3569544.97	716.8	-0.9	-2.9	4.1
-126	326821.49	3574686.90	753.1	5.6	-2.8	5.2

-128	331363.83	3573365.14	707.7	-0.6	-2.8	6.9
-127	330683.88	3582055.41	728.1	-4.5	6.0	13.3
-118	290490.83	3561268.18	853.8	-6.4	4.2	-5.8
-156	334921.38	3545627.21	620.1	2.6	2.2	8.0
-155	337158.18	3549813.82	629.4	8.4	1.5	2.1
-166	330246.22	3534952.63	591.7	-8.2	-6.6	2.4
-143	337966.61	3576244.72	714.4	0.9	-6.5	2.2
-171	313696.33	3569815.14	889.6	2.4	-7.8	-2.8
	RMS Error :			±6.0	±5.9	±5.7

B.3.2 The Results of Absolute Orientation of the Level 1A Stereo-pair for Reference Scene 122/285

The following are the results of the absolute orientation using space intersection carried out for the Level 1A stereo-pair for reference scene 122/285 using 48 ground control points:

Calculated				Errors (metres)		
GCPID	X	Y	Z	ΔX	ΔY	ΔZ
102	300924.62	3557096.62	790.8	-2.8	2.0	6.9
110	295871.90	3566650.39	941.1	-0.7	-5.0	1.5
112	309288.69	3582168.21	1101.3	-0.7	-1.0	-7.6
113	304307.72	3580951.35	1148.1	-1.6	-4.1	5.8
111	300743.30	3576794.62	1102.1	-1.4	6.9	2.9
114	297517.75	3574018.44	1059.1	8.6	5.9	0.8
116	284865.63	3573794.65	994.7	-0.4	7.9	-3.9
156	334929.03	3545626.71	632.9	-5.0	2.7	-4.8
119	284546.92	3563609.83	848.0	-1.1	-2.2	-11.4
118	290485.42	3561273.01	857.1	-1.0	-0.6	-9.1
124	284230.65	3556254.23	703.0	2.8	-6.8	2.6
135	279714.49	3554359.64	657.8	0.5	-3.0	9.2
136	282123.86	3547223.75	611.8	4.7	-1.6	-0.6
133	278855.68	3542816.05	584.6	-5.2	1.3	4.6
140	281955.57	3535718.89	551.7	6.6	-0.6	1.6
141	292952.61	3536495.75	536.8	2.5	4.7	4.7
142	292459.64	3547661.49	672.8	-8.8	-1.6	2.5
137	292704.21	3551486.69	705.1	1.5	-4.8	3.9
163	304904.05	3532795.54	538.7	1.6	5.1	-2.2
162	308312.24	3542490.34	604.4	2.1	7.2	-1.0
146	322962.36	3563356.28	706.2	-5.0	2.9	1.6
148	330980.21	3561093.83	652.9	-3.6	-9.1	0.1
158	328328.83	3556596.05	643.2	0.7	-2.7	3.3
157	327577.84	3553036.91	643.2	5.9	-0.3	-0.1
151	313517.37	3552935.14	725.4	0.0	4.8	-8.8
152	309234.41	3554858.54	757.4	-1.4	0.1	-6.3
154	329673.78	3548190.44	628.6	7.9	7.9	-2.6
159	325741.56	3543786.03	628.2	2.7	-4.6	5.8
153	320673.21	3549826.49	629.9	-7.9	3.2	-0.1
164	320097.30	3536357.46	621.7	4.9	1.4	5.8
167	330422.66	3528358.36	598.8	-3.2	3.2	-2.0
166	330244.18	3534952.27	594.2	-6.1	-6.2	-0.1
165	317477.17	3530719.24	612.3	-2.8	-3.8	-6.9
125	325228.17	3568546.73	751.3	-5.0	1.4	-3.8
149	336880.19	3557835.30	644.8	3.9	-1.6	-0.7
129	338778.59	3569546.71	722.9	4.9	-4.7	-2.0
126	326823.38	3574682.97	749.6	3.7	1.2	8.6
168	321498.45	3574933.66	795.1	-2.5	5.4	-1.2
127	330682.82	3582057.05	740.3	-3.4	4.3	1.0

145	345743.59	3571769.93	774.9	2.4	1.0	-7.7
169	318575.21	3586703.77	954.0	5.4	-1.1	0.6
171	313698.72	3569816.69	885.8	0.0	-9.4	1.1
150	343635.59	3563015.40	696.3	-2.4	-3.1	5.4
123	282555.95	3570246.50	929.6	-7.0	-3.7	-3.1
155	337163.50	3549818.77	630.1	3.1	-3.5	1.4
143	337967.59	3576237.01	713.9	-0.1	1.2	2.7
128	331366.73	3573360.30	706.4	-3.5	2.0	8.2
		RMS Error :		±4.2	±4.2	±4.8

The following are the results of the absolute orientation using space intersection carried out for the Level 1A stereo-pair for reference scene 122/285 using 42 control points and 5 check points:

Calculated				Errors (metres)		
GCPID	X	Y	Z	ΔX	ΔY	ΔZ
102	300927.69	3557083.91	803.0	-5.9	14.7	-5.3
110	295866.54	3566648.95	930.3	4.7	-3.6	12.3
113	304311.31	3580960.10	1152.2	-5.2	-12.8	1.7
111	300743.66	3576794.12	1103.1	-1.8	7.4	1.8
114	297518.17	3574017.88	1060.1	8.2	6.5	-0.2
116	284866.33	3573793.69	995.3	-1.1	8.9	-4.5
119	284547.52	3563608.93	848.4	-1.7	-1.3	-11.8
118	290485.86	3561272.33	857.6	-1.5	0.1	-9.6
124	284231.18	3556253.33	703.3	2.3	-5.9	2.3
135	279722.53	3554366.00	669.6	-7.5	-9.3	-2.7
136	282124.35	3547222.90	611.8	4.2	-0.8	-0.6
133	278856.21	3542815.19	584.5	-5.8	2.1	4.7
140	281955.97	3535718.24	551.6	6.2	0.0	1.8
142	292459.91	3547660.96	673.1	-9.1	-1.0	2.2
137	292711.22	3551493.85	716.1	-5.5	-11.9	-7.1
163	304897.23	3532789.34	527.1	8.4	11.3	9.4
162	308305.58	3542490.48	590.3	8.7	7.1	13.1
146	322962.10	3563356.07	707.1	-4.8	3.2	0.7
148	330979.78	3561093.74	653.7	-3.1	-9.0	-0.7
158	328328.43	3556596.00	643.9	1.1	-2.6	2.5
157	327573.41	3553037.89	634.1	10.3	-1.2	9.0
151	313517.23	3552935.00	726.1	0.1	5.0	-9.4
152	309234.38	3554858.32	758.1	-1.4	0.3	-7.0
159	325741.13	3543786.20	628.6	3.2	-4.8	5.3
153	320672.90	3549826.44	630.5	-7.5	3.2	-0.7
164	320096.93	3536357.68	622.0	5.2	1.2	5.5
167	330424.92	3528358.05	606.0	-5.5	3.5	-9.2
166	330245.79	3534951.49	600.0	-7.7	-5.4	-5.9
165	317476.81	3530719.53	612.5	-2.5	-4.1	-7.1
125	325227.90	3568546.50	752.3	-4.8	1.7	-4.8
149	336879.65	3557835.36	645.4	4.4	-1.7	-1.4
126	326823.12	3574682.63	750.8	4.0	1.5	7.5
168	321498.30	3574933.28	796.3	-2.3	5.8	-2.4
127	330682.53	3582056.61	741.6	-3.1	4.8	-0.3
145	345743.00	3571769.98	775.8	3.0	1.0	-8.7
169	318575.22	3586703.26	955.4	5.4	-0.5	-0.8
171	313701.25	3569823.50	889.1	-2.6	-16.2	-2.3
150	343634.97	3563015.50	697.0	-1.8	-3.2	4.7
155	337162.92	3549818.98	630.6	3.7	-3.7	0.9
143	337967.14	3576236.78	715.0	0.4	1.4	1.6
128	331366.36	3573360.01	707.5	-3.1	2.3	7.1

RMS Error : ±5.1 ±6.3 ±6.1

Calculated				Error (metres)		
CHKID	X	Y	Z	ΔX	ΔY	Δ Z
-112	309288.90	3582167.78	1102.6	-1.0	-0.6	-8.9
-123	282555.41	3570245.14	927.7	-6.5	-2.4	-1.2
-141	292952.77	3536495.33	536.9	2.4	5.1	4.6
-154	329673.31	3548190.57	629.1	8.3	7.8	-3.1
-129	338778.08	3569546.64	723.9	5.4	-4.6	-3.0

RMS Error : ±6.1 ±5.3 ±5.5

The following are the results of the absolute orientation using space intersection carried out for the Level 1A stereo-pair for reference scene 122/285 using 32 control points and 15 check points:

Calculated				Errors (metres)		
GCPID	X	Y	Z	ΔX	ΔY	ΔZ
102	300926.86	3557083.22	804.5	-5.0	15.4	-6.9
110	295865.58	3566647.81	931.9	5.6	-2.4	10.7
113	304310.02	3580957.50	1153.9	-3.9	-10.2	0.0
111	300742.46	3576791.85	1104.8	-0.6	9.6	0.2
116	284865.60	3573792.86	996.6	-0.3	9.7	-5.8
119	284546.92	3563608.82	849.8	-1.1	-1.2	-13.2
124	284230.73	3556254.08	704.7	2.8	-6.6	0.9
135	279722.21	3554367.16	671.0	-7.2	-10.5	-4.0
133	278855.86	3542816.46	586.0	-5.4	0.9	3.2
140	281955.49	3535719.27	553.2	6.7	-1.0	0.1
142	292459.23	3547661.18	674.8	-8.4	-1.3	0.5
163	304896.62	3532789.78	528.5	9.0	10.8	8.0
162	308304.98	3542490.77	591.7	9.3	6.8	11.7
146	322961.74	3563356.14	707.8	-4.4	3.1	0.0
158	328328.27	3556596.31	644.1	1.3	-2.9	2.3
157	327573.21	3553038.14	634.4	10.5	-1.5	8.7
152	309233.58	3554857.73	759.5	-0.6	0.9	-8.4
159	325740.81	3543786.11	629.0	3.5	-4.7	5.0
153	320672.52	3549826.60	631.2	-7.2	3.1	-1.5
167	330424.70	3528357.58	605.8	-5.3	4.0	-9.0
166	330245.62	3534951.32	599.9	-7.6	-5.3	-5.8
165	317476.16	3530719.03	613.4	-1.8	-3.6	-8.0
149	336879.82	3557835.75	645.0	4.2	-2.1	-0.9
168	321497.85	3574933.10	797.2	-1.9	6.0	-3.2
127	330682.49	3582057.15	741.9	-3.1	4.2	-0.5
145	345743.38	3571769.86	774.7	2.6	1.1	-7.5
169	318574.54	3586702.29	956.5	6.0	0.4	-1.9
171	313700.39	3569822.40	890.5	-1.7	-15.1	-3.6
150	343635.38	3563015.71	695.9	-2.2	-3.4	5.8
155	337163.09	3549819.19	629.9	3.5	-3.9	1.5
143	337967.32	3576237.30	714.7	0.2	0.9	1.9
128	331366.34	3573360.47	707.7	-3.1	1.9	6.9

RMS Error : ±5.2 ±6.4 ±6.0

Calculated				Errors (metres)		
CHKID	X	Y	Z	ΔX	ΔY	ΔZ
-112	309287.76	3582165.52	1104.1	0.2	1.6	-10.4
-114	297517.05	3574015.95	1061.7	9.3	8.4	-1.8
-123	282554.80	3570244.82	929.0	-5.9	-2.0	-2.5
-118	290485.07	3561271.74	859.2	-0.7	0.6	-11.2
-136	282123.97	3547224.04	613.3	4.6	-1.9	-2.1
-141	292952.18	3536496.14	538.6	3.0	4.3	2.9
-137	292710.49	3551493.89	717.8	-4.8	-12.0	-8.8
-148	330979.73	3561094.16	653.8	-3.1	-9.4	-0.8
-151	313516.54	3552934.53	727.3	0.8	5.4	-10.7
-154	329673.17	3548190.67	629.1	8.5	7.7	-3.2
-164	320096.39	3536357.34	622.8	5.8	1.5	4.8
-125	325227.55	3568546.39	752.9	-4.4	1.8	-5.4
-129	338778.26	3569546.82	723.4	5.3	-4.8	-2.5
-126	326822.86	3574682.80	751.3	4.2	1.3	6.9
		RMS Error :		±5.2	±5.9	±6.6

The following are the results of the absolute orientation using space intersection carried out for the Level 1A stereo-pair for reference scene 122/285 using 22 control points and 25 check points:

Calculated				Errors (metres)		
GCPID	X	Y	Z	ΔX	ΔY	ΔZ
102	300924.40	3557095.83	792.4	-2.6	2.7	5.3
110	295871.56	3566648.48	941.5	-0.4	-3.1	1.1
113	304306.27	3580947.83	1149.1	-0.1	-0.6	4.8
116	284866.48	3573792.70	991.4	-1.2	9.8	-0.5
119	284548.08	3563608.93	845.6	-2.3	-1.3	-8.9
124	284232.17	3556254.53	701.0	1.3	-7.1	4.6
136	282125.71	3547224.58	610.1	2.9	-2.5	1.1
140	281957.31	3535719.75	551.4	4.9	-1.5	1.9
142	292460.25	3547661.56	673.7	-9.4	-1.6	1.5
163	304904.37	3532796.37	541.8	1.3	4.2	-5.3
162	308312.38	3542490.93	607.0	1.9	6.6	-3.6
146	322962.49	3563356.83	707.1	-5.2	2.4	0.7
158	328329.56	3556597.08	643.5	0.0	-3.7	2.9
154	329674.79	3548191.30	628.8	6.8	7.1	-2.8
159	325742.22	3543786.65	629.4	2.1	-5.2	4.6
167	330424.07	3528358.79	599.3	-4.6	2.8	-2.5
168	321498.18	3574933.75	795.8	-2.2	5.3	-1.9
145	345745.61	3571770.44	771.2	0.3	0.5	-4.0
169	318574.34	3586702.64	954.5	6.2	0.1	0.1
171	313697.91	3569815.50	887.4	0.8	-8.2	-0.6
150	343637.81	3563016.39	693.0	-4.6	-4.0	8.7
155	337165.32	3549819.84	628.6	1.3	-4.5	2.9
		RMS Error :		±3.8	±4.8	±4.1

Calculated				Errors (metres)		
CHKID	X	Y	Z	ΔX	ΔY	ΔZ
-112	309287.25	3582165.24	1102.5	0.7	1.9	-8.8
-111	300742.18	3576791.42	1102.7	-0.3	10.1	2.2

-114	297517.00	3574015.60	1059.3	9.4	8.8	0.6
-156	334930.64	3545627.52	632.0	-6.7	1.9	-3.8
-118	290485.82	3561271.78	856.5	-1.4	0.6	-8.6
-135	279716.70	3554360.41	654.4	-1.7	-3.8	12.6
-133	278857.88	3542816.98	582.5	-7.4	0.3	6.7
-141	292953.47	3536496.75	538.6	1.7	3.7	2.9
-137	292704.77	3551486.60	705.7	0.9	-4.7	3.3
-148	330981.10	3561094.99	652.6	-4.5	-10.3	0.4
-157	327578.52	3553037.78	643.8	5.2	-1.1	-0.7
-151	313517.12	3552934.91	727.6	0.2	5.1	-11.0
-152	309234.00	3554858.03	759.7	-1.0	0.6	-8.6
-153	320673.57	3549827.26	631.5	-8.2	2.4	-1.7
-164	320097.63	3536357.73	624.0	4.5	1.1	3.5
-166	330245.49	3534953.00	594.6	-7.4	-7.0	-0.5
-165	317477.37	3530719.34	615.3	-3.0	-3.9	-9.8
-125	325228.22	3568547.04	751.8	-5.1	1.1	-4.3
-149	336881.78	3557836.52	643.2	2.3	-2.8	0.8
-126	326823.49	3574683.60	749.8	3.6	0.5	8.5
-123	282557.19	3570245.13	925.9	-8.3	-2.3	0.6
-143	337968.75	3576238.24	712.0	-1.3	0.0	4.6
-128	331367.37	3573361.38	705.8	-4.1	0.9	8.8

RMS Error : ±4.9 ±4.6 ±6.4

The following are the results of the absolute orientation using space intersection carried out for the Level 1A stereo-pair for the reference scene 122/285 using 12 control points and 35 check points:

Calculated				Errors (Metres)		
GCPID	X	Y	Z	ΔX	ΔY	Δ Z
102	300925.96	3557097.14	793.7	-4.1	1.4	3.9
113	304307.87	3580949.79	1150.4	-1.7	-2.5	3.5
116	284866.72	3573794.77	989.4	-1.4	7.8	1.5
119	284548.55	3563610.67	844.0	-2.8	-3.0	-7.4
136	282126.37	3547225.84	608.8	2.2	-3.7	2.3
140	281958.44	3535720.74	551.0	3.8	-2.5	2.4
154	329674.76	3548192.50	629.6	6.9	5.9	-3.6
167	330423.83	3528359.83	599.7	-4.4	1.7	-2.8
168	321498.93	3574935.26	797.3	-3.0	3.8	-3.4
145	345744.11	3571772.24	770.5	1.8	-1.3	-3.3
169	318575.29	3586704.44	956.1	5.3	-1.7	-1.5
150	343636.34	3563018.01	692.1	-3.2	-5.7	9.6

RMS Error : ±3.9 ±4.1 ±4.6

Calculated				Errors (metres)		
CHKID	X	Y	Z	ΔX	ΔY	ΔZ
-110	295872.96	3566650.12	942.0	-1.8	-4.7	0.6
-112	309288.77	3582167.13	1104.1	-0.8	0.0	-10.5
-111	300743.72	3576793.31	1103.8	-1.8	8.2	1.1
-114	297518.41	3574017.45	1060.0	8.0	6.9	-0.1
-156	334930.00	3545628.80	632.1	-6.0	0.6	-3.9
-118	290486.93	3561273.35	856.5	-2.5	-1.0	-8.5
-124	284232.72	3556256.00	699.6	0.8	-8.5	6.0
-135	279716.80	3554361.91	652.1	-1.8	-5.3	14.9

-133	278858.44	3542818.21	580.9	-8.0	-0.9	8.3
-141	292955.04	3536497.59	539.6	0.1	2.8	2.0
-142	292461.67	3547662.70	674.3	-10.9	-2.8	0.9
-137	292706.11	3551487.83	706.2	-0.4	-5.9	2.8
-163	304906.00	3532797.11	543.8	-0.4	3.5	-7.3
-162	308313.84	3542491.85	608.9	0.5	5.7	-5.5
-146	322963.13	3563358.15	708.5	-5.8	1.1	-0.7
-148	330981.00	3561096.32	653.3	-4.4	-11.6	-0.3
-158	328329.71	3556598.33	644.4	-0.2	-5.0	2.0
-157	327578.75	3553038.99	644.8	4.9	-2.3	-1.7
-151	313518.44	3552936.08	729.6	-1.1	3.9	-13.0
-152	309235.53	3554859.24	761.6	-2.5	-0.6	-10.5
-159	325742.61	3543787.75	630.5	1.7	-6.3	3.4
-153	320674.32	3549828.36	633.0	-9.0	1.3	-3.2
-164	320098.53	3536358.69	625.7	3.6	0.1	1.8
-166	330245.31	3534954.08	595.0	-7.3	-8.0	-0.9
-165	317478.51	3530720.20	617.2	-4.2	-4.8	-11.7
-125	325228.75	3568548.47	753.3	-5.6	-0.3	-5.7
-149	336881.02	3557837.92	643.2	3.0	-4.2	0.9
-129	338779.15	3569549.16	721.1	4.4	-7.1	-0.2
-126	326823.87	3574685.09	750.9	3.2	-1.0	7.3
-127	330683.22	3582059.74	740.4	-3.8	1.6	1.0
-171	313699.27	3569817.01	889.3	-0.6	-9.7	-2.5
-123	282557.28	3570247.12	923.4	-8.3	-4.3	3.0
-155	337164.45	3549821.18	628.3	2.2	-5.9	3.2
-143	337968.09	3576239.85	712.1	-0.6	-1.6	4.5
-128	331367.28	3573362.88	706.6	-4.0	-0.5	8.0
	RMS Error :		±4.6	±5.1	±6.1	

B.3.3 The Results of Absolute Orientation of the Level 1B Stereo-pair for Scene 123/285

The following are the results of the absolute orientation using space intersection carried out for the Level 1B stereo-pair for scene 123/285 using 23 ground control points:

Calculated				Errors (metres)		
GCPID	X	Y	Z	ΔX	ΔY	ΔZ
126	326823.22	3574687.89	763.7	3.9	-3.7	-5.5
127	330680.98	3582054.99	741.1	-1.6	6.4	0.3
128	331361.41	3573357.34	708.0	1.9	5.0	6.6
129	338784.93	3569550.94	716.6	-1.4	-8.9	4.3
143	337970.74	3576232.26	712.4	-3.2	5.9	4.2
145	345748.77	3571770.99	771.5	-2.8	0.0	-4.3
150	343636.36	3563013.20	705.7	-3.2	-0.9	-4.0
404	377213.41	3566137.85	850.9	2.5	1.1	0.1
405	384888.08	3608358.84	683.3	5.0	-5.1	2.5
501	334509.87	3591459.69	733.9	5.4	-3.4	-0.3
502	334880.31	3598066.48	736.1	-1.7	-0.6	-2.4
503	325157.41	3592446.60	792.9	1.7	2.0	-2.1
504	345781.05	3587347.96	812.3	-4.0	-0.1	-5.5
505	354647.80	3607154.12	887.4	0.3	-5.0	5.8
506	367451.74	3597537.88	872.8	-4.4	-1.7	-2.5
507	361026.78	3576489.55	914.1	4.0	-0.2	8.9
508	389059.97	3584946.39	739.8	-6.8	1.4	-6.4
509	376122.27	3580636.53	840.0	-1.3	8.2	7.9
510	357456.61	3593418.94	948.1	-2.0	-2.2	4.4
511	366458.36	3609357.39	864.8	2.5	7.6	-9.7

512	379350.32	3594486.68	789.3	0.4	-1.9	2.3
515	357679.07	3559199.90	779.4	5.0	-4.7	-13.7
		RMS Error :		±3.5	±4.5	±5.8

The following are the results of the absolute orientation using space intersection carried out for the Level 1B stereo-pair for scene 123/285 using 13 control points and 10 check points:

Calculated				Error (metres)		
GCPID	X	Y	Z	ΔX	ΔY	ΔZ
128	331361.65	3573358.29	708.8	1.6	4.0	5.8
150	343637.89	3563013.49	705.8	-4.7	-1.2	-4.1
404	377214.30	3566137.24	848.8	1.6	1.7	2.2
405	384888.47	3608358.04	682.1	4.6	-4.3	3.7
502	334879.97	3598067.38	736.9	-1.3	-1.5	-3.2
503	325156.07	3592448.04	793.7	3.1	0.6	-3.0
505	354649.16	3607153.89	888.2	-1.1	-4.8	5.0
507	361028.78	3576489.07	913.9	2.0	0.2	9.1
508	389059.67	3584945.70	737.2	-6.5	2.1	-3.8
510	357458.45	3593418.54	948.6	-3.8	-1.8	3.8
511	366459.91	3609356.77	865.1	1.0	8.3	-10.0
515	357680.96	3559199.66	778.7	3.1	-4.5	-13.0
		RMS Error :		±3.5	±3.8	±6.7

Calculated				Errors (metres)		
CHKID	X	Y	Z	ΔX	ΔY	ΔZ
-126	326822.96	3574689.07	764.6	4.1	-4.9	-6.3
-127	330680.83	3582056.01	741.9	-1.5	5.4	-0.5
-129	338786.00	3569551.47	717.1	-2.5	-9.4	3.8
-143	337971.54	3576232.86	713.0	-4.0	5.3	3.6
-145	345750.31	3571771.15	771.9	-4.4	-0.2	-4.7
-501	334509.77	3591460.56	734.7	5.6	-4.3	-1.1
-504	345782.30	3587348.13	812.9	-5.3	-0.3	-6.1
-506	367453.38	3597537.24	872.8	-6.0	-1.1	-2.5
-509	376123.41	3580635.84	838.7	-2.4	8.9	9.3
-512	379351.22	3594485.92	788.2	-0.5	-1.1	3.4
		RMS Error :		±4.2	±5.5	±5.1

B.3.4 The Results of Absolute Orientation of the Level 1B Stereo-pair for Scene 123/286

The following are the results of the absolute orientation using space intersection carried out for the Level 1B stereo-pair for scene 123/286 using 29 ground control points:

Calculated				Errors (metres)		
GCPID	X	Y	Z	ΔX	ΔY	ΔZ
146	322956.93	3563355.50	711.7	0.4	3.7	-3.9

148	330979.98	3561090.27	651.2	-3.3	-5.6	1.9
149	336876.17	3557832.22	644.3	7.9	1.5	-0.3
150	343639.52	3563009.24	700.1	-6.3	3.1	1.6
151	313522.10	3552938.38	712.2	-4.7	1.6	4.5
153	320670.74	3549837.66	635.1	-5.4	-8.0	-5.4
154	329679.06	3548195.46	620.4	2.6	2.9	5.5
156	334925.98	3545623.20	629.7	-2.0	6.2	-1.5
157	327575.96	3553030.76	643.5	7.7	5.9	-0.4
158	328329.10	3556586.61	650.6	0.4	6.8	-4.2
159	325740.54	3543784.00	627.1	3.8	-2.6	6.9
164	320096.35	3536366.82	622.9	5.8	-8.0	4.6
165	317478.78	3530710.59	613.3	-4.4	4.9	-7.9
166	330242.83	3534953.76	596.6	-4.8	-7.7	-2.5
167	330425.90	3528358.79	601.3	-6.5	2.7	-4.4
201	350515.44	3543345.68	659.7	-3.7	6.1	-3.8
202	363801.76	3539201.73	716.4	-2.8	-5.1	-2.6
203	375644.94	3535241.30	740.1	3.2	-1.3	1.8
204	374760.37	3555430.47	900.0	2.6	1.5	2.7
206	319059.84	3518173.52	559.2	1.1	-5.6	8.3
207	315006.54	3511655.09	551.1	5.2	3.3	-2.2
209	339188.03	3505658.00	540.7	1.0	-7.3	1.6
210	330879.46	3521644.80	584.6	5.3	2.4	3.8
211	352936.40	3519571.22	604.8	-5.3	5.6	-6.9
212	359258.77	3503213.61	657.1	2.1	5.3	3.6
213	368485.31	3521463.96	732.0	-1.6	7.4	-4.6
215	341772.82	3534245.11	623.3	-3.1	-4.0	-0.7
302	368044.78	3537691.21	728.6	-2.3	-9.3	4.0
515	357677.25	3559201.59	764.0	6.8	-6.4	1.6
	RMS Error :			±4.5	±5.5	±4.2

The following are the results of the absolute orientation using space intersection carried out for the Level 1B stereo-pair for scene 123/286 using 14 ground control points and 15 check points:

Calculated				Errors (metres)		
GCPIDS	X	Y	Z	ΔX	ΔY	ΔZ
146	322957.61	3563356.18	705.6	-0.3	3.0	2.2
149	336876.04	3557833.01	645.0	8.0	0.7	-0.9
150	343638.92	3563009.83	702.7	-5.8	2.5	-1.0
151	313516.75	3552941.08	719.0	0.6	-1.1	-2.4
154	329679.52	3548196.73	619.3	2.1	1.6	6.7
165	317480.41	3530712.77	608.6	-6.1	2.7	-3.2
166	330243.48	3534955.66	596.9	-5.4	-9.6	-2.8
202	363801.94	3539203.01	718.9	-3.0	-6.4	-5.2
203	375646.40	3535242.25	737.7	1.7	-2.2	4.1
204	374760.50	3555431.02	901.5	2.5	0.9	1.3
207	315008.63	3511658.12	547.4	3.1	0.2	1.4
210	330880.29	3521647.34	586.4	4.4	-0.2	2.0
212	359260.12	3503216.53	658.3	0.7	2.4	2.4
213	368486.62	3521465.84	731.6	-2.9	5.5	-4.2
	RMS Error :			±4.2	±3.9	±3.4

Calculated				Errors (metres)		
CHKID	X	Y	Z	ΔX	ΔY	ΔZ
-148	330980.15	3561090.94	649.2	-3.5	-6.2	3.9
-153	320671.84	3549838.88	629.3	-6.5	-9.2	0.5
-156	334926.16	3545624.59	630.8	-2.2	4.8	-2.6
-157	327576.48	3553031.83	641.0	7.2	4.8	2.2
-158	328329.52	3556587.51	648.0	0.0	5.8	-1.5
-159	325741.32	3543785.52	624.8	3.0	-4.1	9.2
-164	320097.67	3536368.72	618.9	4.5	-9.9	8.6
-167	330426.64	3528361.03	602.4	-7.2	0.5	-5.5
-201	350515.19	3543347.03	663.6	-3.5	4.8	-7.7
-206	319061.51	3518176.23	556.7	-0.6	-8.3	10.7
-209	339188.89	3505661.14	544.2	0.1	-10.4	-2.0
-211	352936.91	3519573.51	608.0	-5.8	3.3	-10.1
-215	341772.94	3534246.98	626.7	-3.2	-5.9	-4.1
-302	368045.31	3537692.42	729.7	-2.9	-10.5	2.8
-515	357677.58	3559207.14	768.6	6.5	-11.9	-3.0
	RMS Error :			±4.6	±7.6	±6.2

B.3.5 The Results of Absolute Orientation of the Level 1B Stereo-pair for Scene 124/285

The following are the results of the absolute orientation using space intersection carried out for the Level 1B stereo-pair for Scene 124/285 using 19 ground control points:

Calculated				Errors (metres)		
GCPID	X	Y	Z	ΔX	ΔY	ΔZ
512	379347.20	3594486.87	796.8	3.6	-2.1	-5.2
314	416262.83	3559480.78	704.7	-4.5	1.6	-5.3
315	400242.66	3562611.26	718.2	0.1	-5.1	-6.9
401	423466.55	3597156.86	681.7	2.4	4.9	-0.1
402	433828.31	3600307.97	702.8	5.2	-7.1	0.9
403	410186.51	3592076.37	663.9	-6.6	-1.8	1.8
404	377215.75	3566146.18	844.3	0.1	-7.3	6.6
405	384887.76	3608353.70	692.1	5.3	0.1	-6.2
406	400810.97	3608973.34	658.2	3.7	3.3	-3.7
407	401287.77	3618275.44	646.8	-4.0	-4.2	-5.3
408	391505.33	3618422.26	655.7	-7.1	0.5	3.8
409	395604.48	3572838.12	710.0	1.2	-5.4	6.0
410	407853.26	3580577.46	672.5	2.8	9.6	7.2
411	447606.10	3604587.07	738.4	-0.7	0.9	6.4
412	425739.37	3580256.38	704.3	5.2	-3.8	-5.8
413	439096.20	3582967.37	721.8	-4.7	-2.4	5.7
415	436330.81	3566517.66	747.0	1.0	5.9	-6.6
508	389057.77	3584943.85	729.4	-4.6	3.9	4.0
509	376120.14	3580636.23	843.8	0.9	8.5	4.2
	RMS Error :			±4.1	±5.0	±5.4

The following are the results of the absolute orientation using space intersection carried out for the Level 1B stereo-pair for scene 124/285 using 11 control points and 8 check points:

Calculated				Errors (metres)		
GCPID	X	Y	Z	ΔX	ΔY	ΔZ
512	379348.03	3594485.62	797.5	2.7	-0.8	-5.9
314	416262.38	3559482.20	703.4	-4.1	0.2	-3.9
315	400242.74	3562612.26	716.5	0.0	-6.1	-5.2
402	433828.35	3600307.00	703.3	5.1	-6.1	0.3
404	377216.00	3566146.76	843.6	-0.1	-7.8	7.3
407	401289.25	3618272.80	647.2	-5.5	-1.5	-5.7
410	407853.63	3580577.37	671.5	2.4	9.7	8.2
411	447605.39	3604586.12	740.4	0.0	1.9	4.4
413	439095.29	3582967.68	722.8	-3.8	-2.7	4.7
415	436329.47	3566519.02	747.6	2.4	4.6	-7.2
509	376120.66	3580635.85	844.0	0.3	8.9	4.0
		RMS Error :		±3.3	±5.9	±5.8

Calculated				Errors (metres)		
CHKID	X	Y	Z	ΔX	ΔY	ΔZ
-401	423466.95	3597155.92	681.6	2.0	5.9	0.1
-403	410187.16	3592075.56	663.2	-7.3	-1.0	2.4
-405	384888.90	3608351.57	693.2	4.2	2.2	-7.4
-406	400812.16	3608971.32	658.4	2.5	5.3	-3.9
-408	391506.76	3618419.52	656.8	-8.5	3.3	2.7
-409	395604.87	3572838.39	708.7	0.8	-5.7	7.3
-412	425739.15	3580256.60	704.0	5.4	-4.0	-5.5
-508	389058.46	3584943.28	729.0	-5.3	4.5	4.4
		RMS Error :		±5.5	±4.6	±5.2

B.3.6 The Results of Absolute Orientation of the Level 1B Stereo-pair for Scene 124/286

The following are the results of the absolute orientation using space intersection carried out for the Level 1B stereo-pair for scene 124/286 using 13 ground control points:

Calculated				Errors (metres)		
GCPID	X	Y	Z	ΔX	ΔY	ΔZ
203	375648.17	3535238.65	752.2	0.0	1.4	-10.4
204	374759.12	3555429.93	900.9	3.8	2.0	1.9
213	368476.84	3521471.53	724.9	6.9	-0.2	2.6
301	363531.96	3512133.84	689.6	-2.8	8.5	7.9
302	368043.18	3537688.50	738.5	-0.7	-6.6	-6.0
303	389811.02	3531702.15	664.5	0.5	-5.4	5.8
304	412376.90	3524083.82	686.2	3.2	-0.6	-2.1
306	380369.18	3522862.07	710.5	-6.0	-1.8	3.5
308	399434.51	3521865.16	712.9	-3.1	-7.4	-6.4
309	398273.34	3529545.07	673.1	0.2	0.6	-5.0
310	393221.86	3543164.53	723.2	2.6	5.9	2.0
311	412471.66	3543412.75	690.7	-1.8	6.2	8.0
404	377220.21	3566141.16	849.8	-4.3	-2.3	1.1
		RMS Error :		±3.6	±4.9	±5.8

B.4 DEM Accuracy Results

B.4.1 DEM Accuracy Results of the Level 1B Stereo-model for Reference Scene 122/285

The following are the DEM accuracy results of the Level 1B stereo-pair for reference scene 122/285 using 32 ground control points and 15 check points:

DBIW(1) = 144 DBIW(2) = 60
DBIW(3) = 7601 DBIW(4) = 5891

RMS Error Report on DEM file

GCP No.	Image Pixel	Image Line	Input Elev.	Calc. Elev.	Diff Elev
101	2161	1497	810.3	809.0	1.3
102	1824	1724	797.7	797.0	0.7
110	1467	1321	942.6	944.0	-1.4
113	1710	525	1154.0	1153.0	1.0
114	1462	943	1060.0	1060.0	0.0
116	848	1107	990.8	991.0	-0.2
119	951	1605	836.7	838.0	-1.3
124	1022	1966	705.6	705.0	0.6
136	1026	2429	611.1	603.0	8.1
141	1679	2819	541.5	538.0	3.5
137	1491	2094	709.0	715.0	-6.0
167	3598	2762	596.8	598.0	-1.2
165	2941	2804	605.4	605.0	0.4
162	2354	2343	603.4	603.0	0.4
159	3186	2071	634.0	632.0	2.0
153	2866	1838	629.8	628.0	1.8
151	2484	1774	716.6	713.0	3.6
157	3164	1600	643.2	643.0	0.2
148	3232	1167	653.1	653.0	0.1
149	3557	1254	644.1	644.0	0.1
150	3825	921	701.7	702.0	-0.3
125	2865	874	747.5	746.0	1.5
129	3511	663	720.9	721.0	-0.1
145	3824	471	767.2	764.0	3.2
128	3104	567	714.6	712.0	2.6
168	2608	610	793.9	794.0	-0.1
127	2967	154	741.4	742.0	-0.6
169	2329	74	954.6	953.0	1.6
156	3609	1870	628.2	631.0	-2.8
155	3667	1640	631.5	633.0	-1.5
166	3509	2445	594.1	597.0	-2.9
171	2294	952	886.8	885.0	1.8

No. of GCP Points within DBIW window : 32
Root Mean Sq. Error in elevation (m) : ± 2.4

Check Pt.	Image Pixel	Image Line	Input Elev.	Calc. Elev.	Diff Elev
-112	1936	406	1094.0	1095.0	-1.0
-111	1586	769	1105.0	1109.0	-4.0
-123	777	1307	926.5	932.0	-5.5

-135	824	2111	667.0	669.0	-2.0
-133	920	2682	589.2	583.0	6.2
-142	1524	2283	675.2	675.0	0.2
-163	2303	2854	536.5	533.0	3.5
-164	3001	2498	627.5	624.0	3.5
-154	3323	1809	626.0	629.0	-3.0
-152	2254	1732	751.1	749.0	2.1
-158	3157	1418	646.4	643.0	3.4
-146	2817	1154	707.8	704.0	3.8
-126	2869	558	758.2	757.0	1.2
-118	1269	1647	848.0	845.0	3.0
-143	3390	348	716.6	717.0	-0.4

No. of Check Points within DBIW window : 15
Root Mean Sq. Error in elevation (m) : ± 3.3

The following are the DEM accuracy results of the Level 1B stereo-pair for scene 122/285 using 22 ground control points and 25 check points:

DBIW reset to :
DBIW(1) = 144 DBIW(2) = 60
DBIW(3) = 7601 DBIW(4) = 5891

RMS Error Report on DEM file

GCP No.	Image Pixel	Image Line	Input Elev.	Calc. Elev.	Diff Elev
102	1824	1724	797.7	799.0	-1.3
110	1467	1321	942.6	943.0	-0.4
113	1710	525	1154.0	1150.0	4.0
116	848	1107	990.8	990.0	0.8
119	951	1605	836.7	838.0	-1.3
124	1022	1966	705.6	705.0	0.6
136	1026	2429	611.1	607.0	4.1
142	1524	2283	675.2	679.0	-3.8
163	2303	2854	536.5	538.0	-1.5
167	3598	2762	596.8	603.0	-6.2
162	2354	2343	603.4	607.0	-3.6
159	3186	2071	634.0	633.0	1.0
154	3323	1809	626.0	628.0	-2.0
158	3157	1418	646.4	641.0	5.4
146	2817	1154	707.8	704.0	3.8
150	3825	921	701.7	699.0	2.7
145	3824	471	767.2	761.0	6.2
168	2608	610	793.9	792.0	1.9
127	2967	154	741.4	734.0	7.4
169	2329	74	954.6	948.0	6.6
155	3667	1640	631.5	633.0	-1.5
171	2294	952	886.8	884.0	2.8

No. of GCP Points within DBIW window : 22
Root Mean Sq. Error in elevation (m) : ±3.8

Check Pt.	Image Pixel	Image Line	Input Elev.	Calc. Elev.	Diff Elev
-101	2161	1497	810.3	810.0	0.3
-112	1936	406	1094.0	1091.0	3.0
-111	1586	769	1105.0	1109.0	-4.0
-114	1462	943	1060.0	1060.0	0.0

-123	777	1307	926.5	931.0	-4.5
-135	824	2111	667.0	670.0	-3.0
-133	920	2682	589.2	585.0	4.2
-141	1679	2819	541.5	542.0	-0.5
-137	1491	2094	709.0	716.0	-7.0
-165	2941	2804	605.4	609.0	-3.6
-164	3001	2498	627.5	626.0	1.5
-153	2866	1838	629.8	627.0	2.8
-151	2484	1774	716.6	714.0	2.6
-152	2254	1732	751.1	751.0	0.1
-157	3164	1600	643.2	642.0	1.2
-148	3232	1167	653.1	652.0	1.1
-149	3557	1254	644.1	642.0	2.1
-125	2865	874	747.5	744.0	3.5
-129	3511	663	720.9	716.0	4.9
-126	2869	558	758.2	754.0	4.2
-128	3104	567	714.6	708.0	6.6
-118	1269	1647	848.0	845.0	3.0
-156	3609	1870	628.2	631.0	-2.8
-166	3509	2445	594.1	600.0	-5.9
-143	3390	348	716.6	710.0	6.6

No. of Check Points within DBIW window : 25
Root Mean Sq. Error in elevation (m) : ± 3.7

The following are the DEM accuracy results of the Level 1B stereo-pair for reference scene 122/285 using 12 ground control points and 35 check points:

DBIW reset to :
DBIW(1) = 144 DBIW(2) = 60
DBIW(3) = 7601 DBIW(4) = 5891

RMS Error Report on DEM file

GCP No.	Image Pixel	Image Line	Input Elev.	Calc. Elev.	Diff Elev
102	1824	1724	797.7	796.0	1.7
113	1710	525	1154.0	1150.0	4.0
116	848	1107	990.8	990.0	0.8
119	951	1605	836.7	837.0	-0.3
136	1026	2429	611.1	605.0	6.1
167	3598	2762	596.8	599.0	-2.2
162	2354	2343	603.4	603.0	0.4
154	3323	1809	626.0	626.0	0.0
158	3157	1418	646.4	641.0	5.4
145	3824	471	767.2	761.0	6.2
168	2608	610	793.9	793.0	0.9
169	2329	74	954.6	949.0	5.6

No. of GCP Points within DBIW window : 12
Root Mean Sq. Error in elevation (m) : ± 3.7

Check Pt.	Image Pixel	Image Line	Input Elev.	Calc. Elev.	Diff Elev
-101	2161	1497	810.3	808.0	2.3
-110	1467	1321	942.6	942.0	0.6
-112	1936	406	1094.0	1092.0	2.0
-111	1586	769	1105.0	1108.0	-3.0

-114	1462	943	1060.0	1059.0	1.0
-123	777	1307	926.5	932.0	-5.5
-124	1022	1966	705.6	704.0	1.6
-135	824	2111	667.0	669.0	-2.0
-133	920	2682	589.2	583.0	6.2
-141	1679	2819	541.5	540.0	1.5
-142	1524	2283	675.2	676.0	-0.8
-137	1491	2094	709.0	715.0	-6.0
-163	2303	2854	536.5	534.0	2.5
-165	2941	2804	605.4	605.0	0.4
-164	3001	2498	627.5	623.0	4.5
-159	3186	2071	634.0	631.0	3.0
-153	2866	1838	629.8	624.0	5.8
-151	2484	1774	716.6	713.0	3.6
-152	2254	1732	751.1	749.0	2.1
-157	3164	1600	643.2	640.0	3.2
-148	3232	1167	653.1	652.0	1.1
-146	2817	1154	707.8	703.0	4.8
-149	3557	1254	644.1	642.0	2.1
-150	3825	921	701.7	699.0	2.7
-125	2865	874	747.5	744.0	3.5
-129	3511	663	720.9	717.0	3.9
-126	2869	558	758.2	754.0	4.2
-128	3104	567	714.6	709.0	5.6
-127	2967	154	741.4	735.0	6.4
-118	1269	1647	848.0	844.0	4.0
-156	3609	1870	628.2	629.0	-0.8
-155	3667	1640	631.5	632.0	-0.5
-166	3509	2445	594.1	597.0	-2.9
-143	3390	348	716.6	711.0	5.6
-171	2294	952	886.8	884.0	2.8

No. of Check Points within DBIW window : 35
Root Mean Sq. Error in elevation (m) : ±3.6

The following are the DEM accuracy results of the Level 1B stereo-pair for reference scene 122/285 using 47 ground control points:

DBIW reset to :
DBIW(1) = 144 DBIW(2) = 60
DBIW(3) = 7601 DBIW(4) = 5891

RMS Error Report on DEM file

GCP No.	Image Pixel	Image Line	Input Elev.	Calc. Elev.	Diff Elev
101	2161	1498	810.3	807.0	3.3
102	1824	1724	797.7	797.0	0.7
110	1467	1321	942.6	939.0	3.6
112	1936	406	1094.0	1092.0	2.0
113	1710	525	1154.0	1149.0	5.0
111	1586	769	1105.0	1106.0	-1.0
114	1462	943	1060.0	1059.0	1.0
116	848	1107	990.8	990.0	0.8
123	777	1307	926.5	929.0	-2.5
119	951	1605	836.7	833.0	3.7
124	1022	1966	705.6	703.0	2.6
135	824	2111	667.0	667.0	0.0
133	920	2682	589.2	581.0	8.2

136	1026	2429	611.1	604.0	7.1
141	1678	2819	541.5	538.0	3.5
142	1524	2283	675.2	675.0	0.2
137	1491	2094	709.0	712.0	-3.0
163	2303	2854	536.5	535.0	1.5
167	3598	2762	596.8	606.0	-9.2
165	2941	2803	605.4	606.0	-0.6
164	3001	2498	627.5	626.0	1.5
162	2354	2343	603.4	604.0	-0.6
159	3185	2071	634.0	635.0	-1.0
154	3323	1809	626.0	631.0	-5.0
153	2867	1838	629.8	626.0	3.8
151	2484	1774	716.6	716.0	0.6
152	2254	1732	751.1	747.0	4.1
157	3164	1600	643.2	645.0	-1.8
158	3157	1418	646.4	646.0	0.4
148	3232	1167	653.1	655.0	-1.9
146	2817	1154	707.8	705.0	2.8
149	3557	1254	644.1	649.0	-4.9
150	3825	921	701.7	705.0	-3.3
125	2866	874	747.5	746.0	1.5
129	3511	663	720.9	723.0	-2.1
145	3824	471	767.2	769.0	-1.8
126	2869	558	758.2	756.0	2.2
128	3104	567	714.6	713.0	1.6
168	2609	610	793.9	794.0	-0.1
127	2967	154	741.4	740.0	1.4
169	2328	74	954.6	951.0	3.6
118	1269	1647	848.0	842.0	6.0
156	3609	1870	628.2	634.0	-5.8
155	3667	1640	631.5	638.0	-6.5
166	3510	2444	594.1	603.0	-8.9
143	3390	348	716.6	719.0	-2.4
171	2294	952	886.8	886.0	0.8

No. of GCP Points within DBIW window : 47
Root Mean Sq. Error in elevation (m) : ±3.7

B.4.2 DEM Accuracy Results of the Level 1A Stereo-model for Reference Scene 122/285

The following are the DEM accuracy results of the Level 1A stereopair for scene 122/285 using 31 ground control points and 15 check points:

DBIW reset to :
DBIW(1) = 129 DBIW(2) = 60
DBIW(3) = 5742 DBIW(4) = 5880

RMS Error Report on DEM file

GCP No.	Image Pixel	Image Line	Input Elev.	Calc. Elev.	Diff Elev
102	1424	1721	797.7	797.0	0.7
110	1121	1319	942.6	946.0	-3.4
113	1281	524	1154.0	1152.0	2.0
111	1192	768	1105.0	1110.0	-5.0
116	612	1105	990.8	996.0	-5.2
119	718	1602	836.7	843.0	-6.3
124	790	1962	705.6	709.0	-3.4

135	636	2108	667.0	672.0	-5.0
133	738	2677	589.2	588.0	1.2
142	1208	2279	675.2	680.0	-4.8
163	1850	2850	536.5	536.0	0.5
162	1868	2339	603.4	603.0	0.4
146	2180	1152	707.8	704.0	3.8
158	2455	1415	646.4	646.0	0.4
157	2467	1597	643.2	647.0	-3.8
152	1764	1729	751.1	750.0	1.1
159	2504	2067	634.0	634.0	0.0
153	2247	1835	629.8	628.0	1.8
167	2849	2757	596.8	604.0	-7.2
166	2768	2440	594.1	602.0	-7.9
165	2345	2799	605.4	607.0	-1.6
149	2756	1252	644.1	647.0	-2.9
168	1995	609	793.9	795.0	-1.1
127	2255	153	741.4	740.0	1.4
145	2927	470	767.2	767.0	0.2
169	1753	74	954.6	952.0	2.6
171	1762	950	886.8	885.0	1.8
120	526	1571	827.5	837.0	-9.5
155	2856	1637	631.5	635.0	-3.5
143	2590	347	716.6	715.0	1.6
128	2379	566	714.6	712.0	2.6

No. of GCP Points within DBIW window : 31
Root Mean Sq. Error in elevation (m) : ±3.8

Check Pt.	Image Pixel	Image Line	Input Elev.	Calc. Elev.	Diff Elev
-101	1681	1495	810.3	808.0	2.3
-112	1456	405	1094.0	1096.0	-2.0
-114	1100	942	1060.0	1062.0	-2.0
-123	563	1305	926.5	938.0	-11.5
-118	975	1644	848.0	847.0	1.0
-136	813	2425	611.1	608.0	3.1
-141	1354	2814	541.5	542.0	-0.5
-137	1173	2091	709.0	717.0	-8.0
-148	2502	1165	653.1	653.0	0.1
-151	1946	1771	716.6	715.0	1.6
-154	2599	1806	626.0	631.0	-5.0
-164	2379	2494	627.5	625.0	2.5
-125	2206	873	747.5	750.0	-2.5
-129	2696	662	720.9	725.0	-4.1
-126	2196	557	758.2	758.0	0.2

No. of Check Points within DBIW window : 15
Root Mean Sq. Error in elevation (m) : ± 4.3

The following are the DEM accuracy results of the Level 1A stereo-pair for scene 122/285 using 10 ground control points and 36 check points:

DBIW reset to :
DBIW(1) = 128 DBIW(2) = 60
DBIW(3) = 5744 DBIW(4) = 5880

RMS Error Report on DEM file

GCP No.	Image Pixel	Image Line	Input Elev.	Calc. Elev.	Diff Elev
102	1423	1721	797.7	801.0	-3.3
113	1281	524	1154.0	1153.0	1.0
116	612	1105	990.8	989.0	1.8
119	718	1602	836.7	838.0	-1.3
136	813	2425	611.1	606.0	5.1
154	2599	1806	626.0	632.0	-6.0
167	2849	2757	596.8	606.0	-9.2
168	1995	609	793.9	794.0	-0.1
145	2927	470	767.2	764.0	3.2
169	1753	74	954.6	950.0	4.6

No. of GCP Points within DBIW window : 10
Root Mean Sq. Error in elevation (m) : ±4.4

Check Pt.	Image Pixel	Image Line	Input Elev.	Calc. Elev.	Diff Elev
-101	1681	1495	810.3	809.0	1.3
-110	1121	1319	942.6	945.0	-2.4
-112	1456	405	1094.0	1096.0	-2.0
-111	1192	768	1105.0	1111.0	-6.0
-114	1100	942	1060.0	1061.0	-1.0
-156	2821	1867	628.2	631.0	-2.8
-118	975	1644	848.0	845.0	3.0
-124	790	1962	705.6	706.0	-0.4
-135	636	2108	667.0	669.0	-2.0
-133	738	2677	589.2	582.0	7.2
-141	1354	2814	541.5	541.0	0.5
-142	1208	2279	675.2	680.0	-4.8
-137	1173	2091	709.0	718.0	-9.0
-163	1850	2849	536.5	536.0	0.5
-162	1868	2339	603.4	608.0	-4.6
-146	2180	1152	707.8	708.0	-0.2
-148	2502	1165	653.1	653.0	0.1
-158	2455	1415	646.4	646.0	0.4
-157	2467	1597	643.2	647.0	-3.8
-151	1946	1771	716.6	715.0	1.6
-152	1764	1729	751.1	753.0	-1.9
-159	2504	2067	634.0	634.0	0.0
-153	2247	1835	629.8	632.0	-2.2
-164	2379	2494	627.5	627.0	0.5
-166	2768	2440	594.1	602.0	-7.9
-165	2345	2799	605.4	610.0	-4.6
-125	2206	873	747.5	750.0	-2.5
-149	2756	1252	644.1	645.0	-0.9
-129	2696	662	720.9	724.0	-3.1
-126	2196	557	758.2	757.0	1.2
-127	2255	153	741.4	739.0	2.4
-171	1762	951	886.8	885.0	1.8
-123	563	1305	926.5	931.0	-4.5
-155	2856	1637	631.5	634.0	-2.5
-143	2590	347	716.6	715.0	1.6
-128	2379	566	714.6	712.0	2.6

No. of Check Points within DBIW window : 36
Root Mean Sq. Error in elevation (m) : ±3.4

B.4.3 DEM Accuracy Results of the Level 1B Stereo-model for Scene 123/285

The following are the DEM accuracy results of the Level 1B stereo-pair for scene 123/285 using 16 ground control points:

DBIW reset to :
DBIW(1) = 131 DBIW(2) = 60
DBIW(3) = 7252 DBIW(4) = 5890

RMS Error Report on DEM file

GCP No.	Image Pixel	Image Line	Input Elev.	Calc. Elev.	Diff Elev
1	667	2519	758.2	758.0	0.2
2	769	2116	741.4	741.0	0.4
3	902	2532	714.6	713.0	1.6
4	1308	2631	720.9	725.0	-4.1
5	1622	2443	767.2	770.0	-2.8
6	1619	2893	701.7	710.0	-8.3
8	3222	2354	850.9	856.0	-5.1
9	3103	210	685.8	674.0	11.8
10	847	1614	733.6	730.0	3.6
11	788	1289	733.7	730.0	3.7
12	381	1674	790.8	786.0	4.8
13	1444	1684	806.8	807.0	-0.2
14	2315	2036	923.0	927.0	-4.0
16	1946	1254	952.5	952.0	0.5
17	2198	374	855.1	851.0	4.1
18	2996	949	791.6	788.0	3.6

No. of GCP Points within DBIW window : 16
Root Mean Sq. Error in elevation (m) : ±4.7

The following DEM accuracy results of the Level 1B stereopair for scene 123/285 using 9 control points and 10 check points:

DBIW reset to :
DBIW(1) = 131 DBIW(2) = 60
DBIW(3) = 7252 DBIW(4) = 5890

RMS Error Report on DEM file

GCP No.	Image Pixel	Image Line	Input Elev.	Calc. Elev.	Diff Elev
126	667	2519	758.2	758.0	0.2
150	1619	2893	701.7	705.0	-3.3
404	3222	2354	850.9	855.0	-4.1
405	3103	210	685.8	674.0	11.8
502	788	1289	733.7	728.0	5.7
503	381	1674	790.8	787.0	3.8
510	1946	1254	952.5	948.0	4.5
511	2198	374	855.1	851.0	4.1
512	2996	949	791.6	784.0	7.6

No. of GCP Points within DBIW window : 9
Root Mean Sq. Error in elevation (m) : ±5.9

Check Pt.	Image Pixel	Image Line	Input Elev.	Calc. Elev.	Diff Elev
-127	769	2116	741.4	739.0	2.4
-128	902	2532	714.6	712.0	2.6
-129	1308	2631	720.9	723.0	-2.1
-143	1190	2316	716.6	714.0	2.6
-145	1622	2443	767.2	769.0	-1.8
-501	847	1614	733.6	727.0	6.6
-504	1444	1684	806.8	808.0	-1.2
-507	2315	2036	923.0	923.0	0.0
-509	3001	1661	847.9	851.0	-3.1
-515	2348	2916	765.7	771.0	-5.3

No. of Check Points within DBIW window : 10
Root Mean Sq. Error in elevation (m) : ±3.3

B.4.4 DEM Accuracy Results of the Level 1B Stereo-model for Scene 123/286

The following are the DEM accuracy results of the Level 1B stereo-pair for scene 123/286 using 18 ground control points and 11 check points:

DBIW reset to :
DBIW(1) = 123 DBIW(2) = 60
DBIW(3) = 7269 DBIW(4) = 5890

RMS Error Report on DEM file

GCP No.	Image Pixel	Image Line	Input Elev.	Calc. Elev.	Diff Elev
146	764	278	707.8	711.0	-3.2
148	1179	295	653.1	655.0	-1.9
149	1504	386	644.1	647.0	-2.9
150	1774	56	701.7	708.0	-6.3
151	425	893	716.6	715.0	1.6
157	1107	727	643.2	642.0	1.2
159	1124	1198	634.0	633.0	1.0
165	872	1929	605.4	610.0	-4.6
166	1444	1576	594.1	596.0	-1.9
201	2336	933	655.9	656.0	-0.1
202	3032	982	713.7	719.0	-5.3
203	3656	1038	741.8	742.0	-0.2
204	3383	66	902.7	899.0	3.7
207	971	2885	548.9	546.0	2.9
210	1629	2216	588.4	593.0	-4.6
212	3226	2785	660.7	668.0	-7.3
213	3466	1791	727.4	733.0	-5.6
215	2014	1477	622.6	628.0	-5.4

No. of GCP Points within DBIW window : 18
Root Mean Sq. Error in elevation (m) : ±3.9

Check Pt.	Image Pixel	Image Line	Input Elev.	Calc. Elev.	Diff Elev
-153	807	962	629.8	636.0	-6.2
-154	1264	938	626.0	628.0	-2.0
-156	1550	1002	628.2	631.0	-2.8
-158	1102	545	646.4	646.0	0.4
-164	935	1624	627.5	629.0	-1.5

-167	1530	1894	596.8	603.0	-6.2
-206	1093	2521	567.4	568.0	-0.6
-209	2217	2898	542.2	549.0	-6.8
-211	2727	2062	597.8	601.0	-3.2
-302	3257	1006	732.5	733.0	-0.5
-515	2504	79	765.7	766.0	-0.3

No. of Check Points within DBIW window : 11
Root Mean Sq. Error in elevation (m) : ± 3.7

The following are the DEM accuracy results of the Level 1B stereo-pair for scene 123/286 using 15 ground control points and 14 check points:

DBIW reset to :
DBIW(1) = 123 DBIW(2) = 60
DBIW(3) = 7269 DBIW(4) = 5890

RMS Error Report on DEM file

GCP No.	Image Pixel	Image Line	Input Elev.	Calc. Elev.	Diff Elev
146	764	278	707.8	708.0	-0.2
149	1504	386	644.1	643.0	1.1
150	1774	56	701.7	705.0	-3.3
151	425	893	716.6	708.0	8.6
154	1264	938	626.0	620.0	6.0
165	873	1929	605.4	603.0	2.4
166	1444	1575	594.1	591.0	3.1
201	2336	933	655.9	655.0	0.9
203	3656	1038	741.8	743.0	-1.2
204	3383	66	902.7	903.0	-0.3
207	971	2885	548.9	537.0	11.9
210	1629	2216	588.4	587.0	1.4
212	3226	2785	660.7	667.0	-6.3
213	3466	1791	727.4	733.0	-5.6
302	3257	1006	732.5	734.0	-1.5

No. of GCP Points within DBIW window : 15
Root Mean Sq. Error in elevation (m) : ±4.9

Check Pt.	Image Pixel	Image Line	Input Elev.	Calc. Elev.	Diff Elev
-148	1179	295	653.1	652.0	1.1
-153	807	962	629.8	631.0	-1.2
-156	1550	1002	628.2	628.0	0.2
-157	1106	727	643.2	639.0	4.2
-158	1102	545	646.4	642.0	4.4
-159	1124	1198	634.0	629.0	5.0
-164	935	1624	627.5	621.0	6.5
-167	1530	1894	596.8	595.0	1.8
-202	3032	982	713.7	719.0	-5.3
-206	1093	2521	567.4	559.0	8.4
-209	2217	2898	542.2	542.0	0.2
-211	2727	2062	597.8	597.0	0.8
-215	2014	1477	622.6	620.0	2.6
-515	2503	79	765.7	766.0	-0.3

No. of Check Points within DBIW window : 14
Root Mean Sq. Error in elevation (m) : ± 3.9

The following are the DEM accuracy results of the Level 1B stereo-pair for scene 123/286 using 29 ground control points:

DBIW reset to :
DBIW(1) = 123 DBIW(2) = 60
DBIW(3) = 7269 DBIW(4) = 5890

RMS Error Report on DEM file

GCP No.	Image Pixel	Image Line	Input Elev.	Calc. Elev.	Diff Elev
1	764	278	707.8	712.0	-4.2
2	1179	295	653.1	654.0	-0.9
3	1504	386	644.1	644.0	0.1
4	1774	56	701.7	701.0	0.7
5	425	893	716.6	715.0	1.6
6	808	962	629.8	632.0	-2.2
7	1264	938	626.0	624.0	2.0
8	1550	1002	628.2	629.0	-0.8
9	1106	727	643.2	642.0	1.2
10	1102	545	646.4	644.0	2.4
11	1124	1197	634.0	631.0	3.0
12	935	1624	627.5	628.0	-0.5
13	873	1929	605.4	607.0	-1.6
14	1444	1575	594.1	593.0	1.1
15	1530	1894	596.8	596.0	0.8
16	2336	933	655.9	654.0	1.9
17	3032	982	713.7	718.0	-4.3
18	3656	1038	741.8	743.0	-1.2
19	3383	66	902.7	901.0	1.7
20	1093	2521	567.4	563.0	4.4
21	971	2885	548.9	544.0	4.9
22	2217	2898	542.2	545.0	-2.8
23	1629	2216	588.4	590.0	-1.6
24	2727	2062	597.8	597.0	0.8
25	3226	2785	660.7	666.0	-5.3
26	3466	1791	727.4	732.0	-4.6
27	2014	1477	622.6	620.0	2.6
28	3257	1006	732.5	732.0	0.5
29	2503	79	765.7	764.0	1.7

No. of GCP Points within DBIW window : 29
Root Mean Sq. Error in elevation (m) : ±2.6

B.4.5 DEMs Accuracy Results of the Level 1B Stereo-model for Scene 124/285

The following are the DEM accuracy results of the Level 1B stereo-pair for scene 124/285 using 18 ground control points:

DBIW reset to :
DBIW(1) = 135 DBIW(2) = 60
DBIW(3) = 7619 DBIW(4) = 5891□

RMS Error Report on DEM file

GCP No.	Image Pixel	Image Line	Input Elev.	Calc. Elev.	Diff Elev
1	2894	2763	699.5	704.0	-4.5

2	2079	2797	711.4	713.0	-1.6
3	2807	846	681.7	683.0	-1.3
4	3276	572	703.7	702.0	1.7
5	2219	1247	665.7	664.0	1.7
6	920	2892	850.9	846.0	4.9
7	799	750	685.8	688.0	-2.2
8	1566	534	654.5	655.0	-0.5
9	1481	76	641.5	643.0	-1.5
10	1004	183	659.5	659.0	0.5
11	1735	2353	716.0	717.0	-1.0
12	2240	1834	679.7	680.0	-0.3
14	3115	1642	698.4	699.0	-0.6
15	3734	1355	727.6	734.0	-6.4
16	3791	2188	740.4	749.0	-8.6
17	1276	1840	733.4	734.0	-0.6
18	699	2200	847.9	846.0	1.9
19	693	1489	791.6	794.0	-2.4

No. of GCP Points within DBIW window : 18
Root Mean Sq. Error in elevation (m) : ±3.2

The following are the DEM accuracy results of the Level 1B stereo-pair for scene 124/285 using 13 ground control points:

DBIW reset to :
DBIW(1) = 135 DBIW(2) = 60
DBIW(3) = 7619 DBIW(4) = 5891

RMS Error Report on DEM file

GCP No.	Image Pixel	Image Line	Input Elev.	Calc. Elev.	Diff Elev
1	2894	2763	699.5	703.0	-3.5
2	2079	2797	711.4	712.0	-0.6
3	2807	846	681.7	683.0	-1.3
4	2220	1247	665.7	662.0	3.7
5	920	2892	850.9	843.0	7.9
6	799	750	685.8	688.0	-2.2
7	1566	534	654.5	654.0	0.5
8	1003	183	659.5	661.0	-1.5
9	1735	2353	716.0	714.0	2.0
10	2240	1834	679.7	680.0	-0.3
12	1276	1840	733.4	732.0	1.4
13	699	2200	847.9	849.0	-1.1
14	693	1489	791.6	793.0	-1.4

No. of GCP Points within DBIW window : 13
Root Mean Sq. Error in elevation (m) : ± 2.9

The following are the DEM accuracy results of the Level 1B stereo-pair for scene 124/285 using 11 ground control points:

DBIW reset to :
DBIW(1) = 135 DBIW(2) = 60
DBIW(3) = 7619 DBIW(4) = 5891

RMS Error Report on DEM file

GCP No.	Image Pixel	Image Line	Input Elev.	Calc. Elev.	Diff Elev
1	2894	2763	699.5	708.0	-8.5
2	2079	2796	711.4	716.0	-4.6
3	2807	846	681.7	687.0	-5.3
4	920	2892	850.9	842.0	8.9
5	799	750	685.8	685.0	0.8
6	1566	534	654.5	655.0	-0.5
7	1004	183	659.5	658.0	1.5
8	1735	2353	716.0	718.0	-2.0
9	2240	1834	679.7	682.0	-2.3
11	3791	2188	740.4	753.0	-12.6
12	693	1489	791.6	790.0	1.6

No. of GCP Points within DBIW window : 11
Root Mean Sq. Error in elevation (m) : ±5.8

The following are the DEM accuracy results of the Level 1B stereo-pair for scene 124/285 using 8 ground control points and 8 check points:

DBIW reset to :
DBIW(1) = 135 DBIW(2) = 60
DBIW(3) = 7619 DBIW(4) = 5891

RMS Error Report on DEM file

GCP No.	Image Pixel	Image Line	Input Elev.	Calc. Elev.	Diff Elev
314	2895	2763	699.5	696.0	3.5
315	2079	2796	711.4	708.0	3.4
404	921	2892	850.9	845.0	5.9
407	1481	76	641.5	636.0	5.5
410	2240	1835	679.7	673.0	6.7
415	3791	2188	740.4	745.0	-4.6
509	698	2200	847.9	847.0	0.9
512	693	1488	791.6	797.0	-5.4

No. of GCP Points within DBIW window : 8
Root Mean Sq. Error in elevation (m) : ±4.8

Check Pt.	Image Pixel	Image Line	Input Elev.	Calc. Elev.	Diff Elev
-401	2807	847	681.7	673.0	8.7
-403	2220	1248	665.7	655.0	10.7
-405	799	750	685.8	688.0	-2.2
-406	1566	534	654.5	649.0	5.5
-408	1004	183	659.5	657.0	2.5
-409	1735	2353	716.0	713.0	3.0
-412	3116	1643	698.4	691.0	7.4
-508	1276	1840	733.4	730.0	3.4

No. of Check Points within DBIW window : 8
Root Mean Sq. Error in elevation (m) : ±6.2

B.4.6 DEM Accuracy Results of the Level 1B Stereo-model for Scene 124/286

The following are the DEM accuracy results of the Level 1B stereo-pair for scene 124/286 using 18 ground control points:

DBIW reset to :
DBIW(1) = 139 DBIW(2) = 60
DBIW(3) = 7613 DBIW(4) = 5891

RMS Error Report on DEM file

GCP No.	Image Pixel	Image Line	Input Elev.	Calc. Elev.	Diff Elev
1	3270	1689	684.1	684.0	0.1
2	2519	1587	668.1	670.0	-1.9
3	2083	1580	670.3	672.0	-1.7
4	1031	2837	697.5	702.0	-4.5
5	1727	2120	714.1	720.0	-5.9
6	1164	2325	727.4	731.0	-3.6
7	954	1541	732.5	735.0	-2.5
8	1353	1572	741.8	744.0	-2.2
9	1080	600	902.7	902.0	0.7
10	2116	983	725.2	724.0	1.2
11	3050	748	698.7	690.0	8.7
12	1073	51	850.9	851.0	-0.1

No. of GCP Points within DBIW window : 12
Root Mean Sq. Error in elevation (m) : ±3.7

B.5 Vector Plots of Planimetry and Heights

B.5.1 Vector Plots of the Residual Errors in Planimetry and Heights of the Level 1B Stereo-model for Scene 123/285

(a) Vector plot of the residual errors in planimetry and heights at the individual ground control points using 23 GCPs are given in Figures B.1, B.2

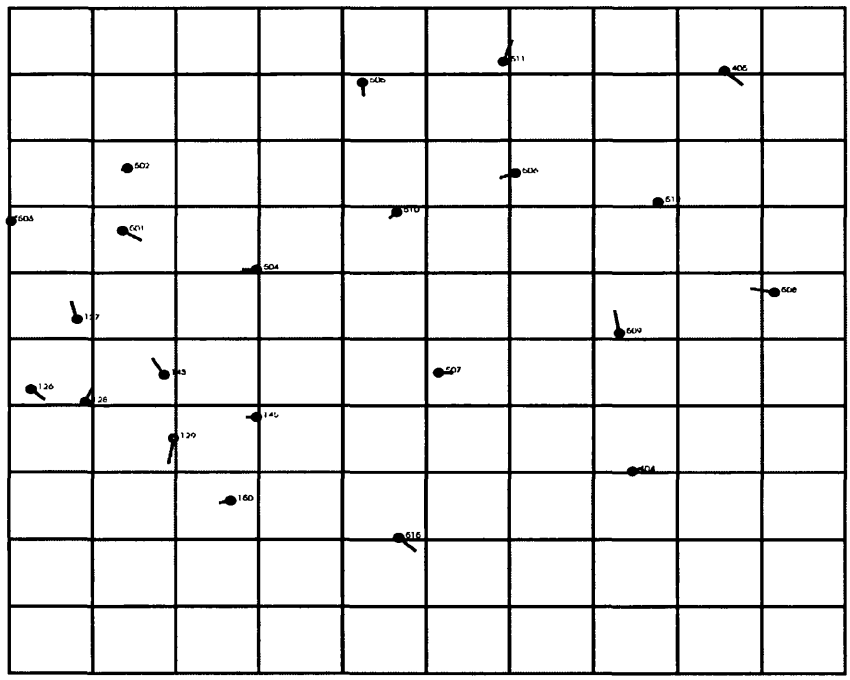

Figure B.1 Vector plot of the residual errors in planimetry at the ground control points of the Level 1B stereo-pair for scene 123/285 after absolute orientation.

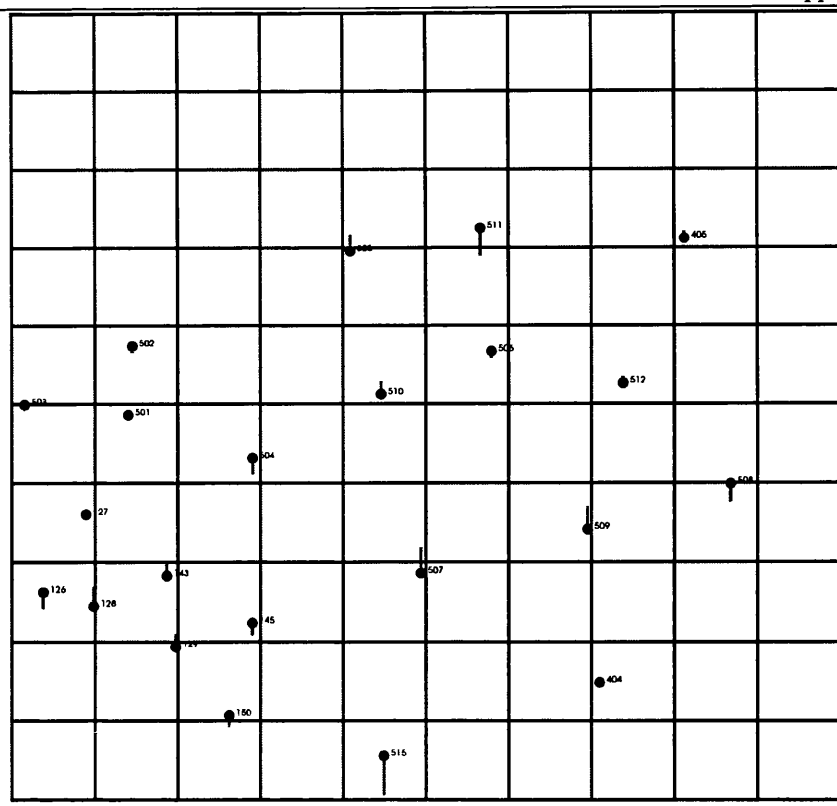

Figure B.2 Vector plot of the residual errors in heights at the ground control points of the Level 1B stereo-model for scene 123/286 after absolute orientation.

(b) Vector plot of the residual errors in height using 10 check points and 13 GCPs is given in Figure B.3.

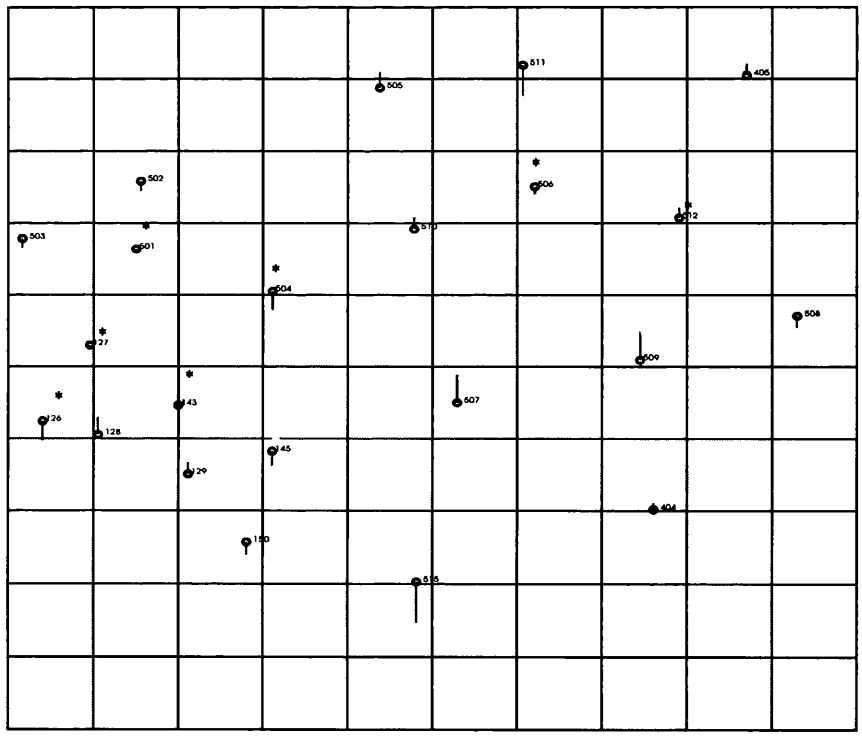

Figure B.3 Vector plot of the residual errors in height at the control points and check points of the Level 1B stereo-pair for scene 123/285 after absolute orientation
Control points o Check points o *

B.5.2 Vector Plots of the Residual Errors in Planimetry and Height of the Level 1B Stereo-model for Scene 123/286

(a) Vector plot of the residual errors in planimetry using 29 ground control points is given in Figure B.4.

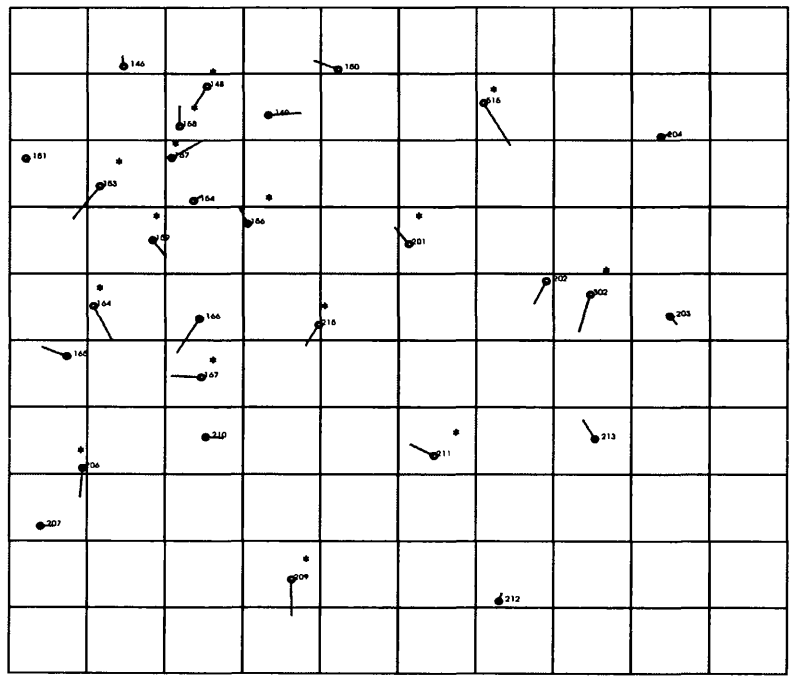

Figure B.4 Vector plot of the residual errors in planimetry at the control and check points of the Level 1B stereo-pair for scene 123/286 after absolute orientation Control points o Check points o *

(b) Vector plot of the residual errors in height using 15 check points and 14 ground control points is given in Figure B.5

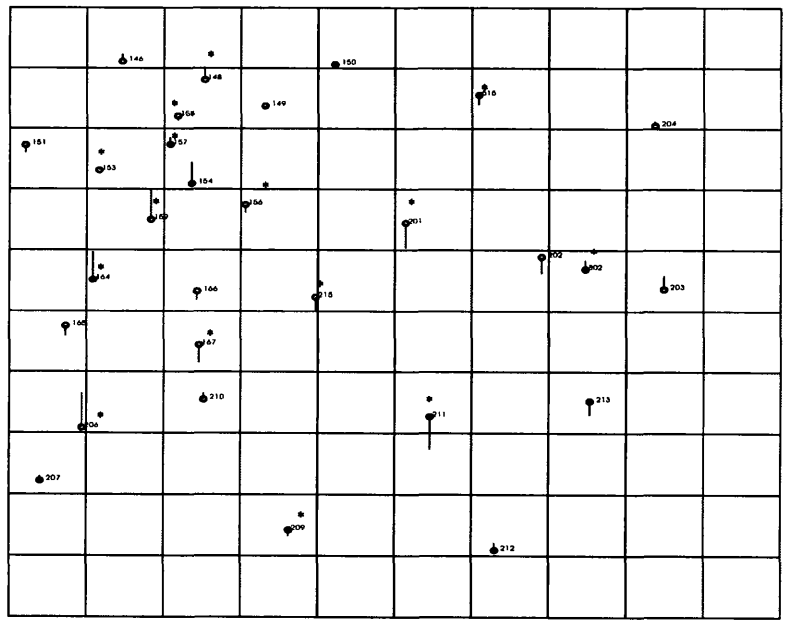

Figure B.5 Vector plots of the residual errors in height at the control points and check points of the Level 1B stereo-pair for scene 123/286
Control points o Check points o *

B.5.3 Vector Plots of the Residual Errors in Planimetry and Heights of the Level 1B Stereo-model for Scene 124/285

(a) Vector plot of the residual errors in planimetry using 19 ground control points is given in Figure B.6

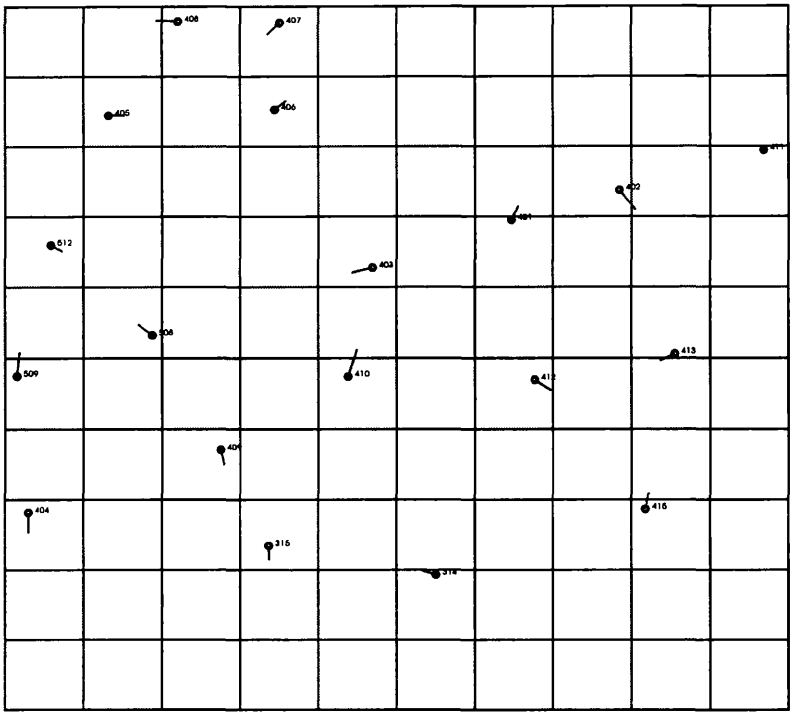

Figure B.6 Vector plots of the residual errors in planimetry at the ground control points of the Level 1B stereo-pair for scene 124/285.

(a) Vector plot of the residual errors in height using 19 ground control points is given in Figure B.7

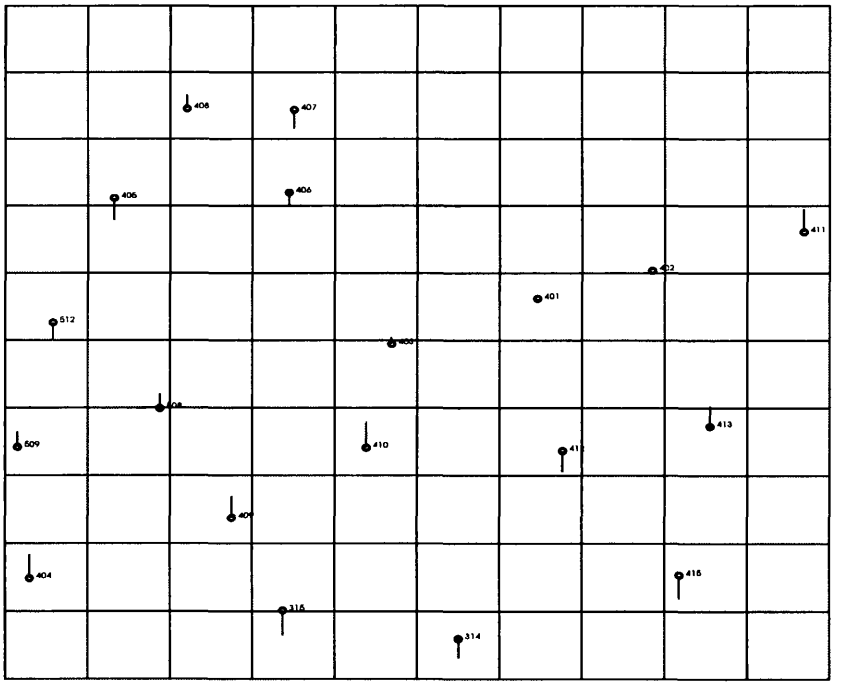

Figure B.7 Vector plot of the residual errors in height at the ground control points of the Level 1B stereo-pair for scene 124/285 after absolute orientation.

B.5.4 Vector Plots of the Residual Errors in Planimetry and Height of the Level 1B Stereo-model for Scene 124/286

(a) Vector plot the residual errors of planimetry using 13 ground control points is given in Figure B.8

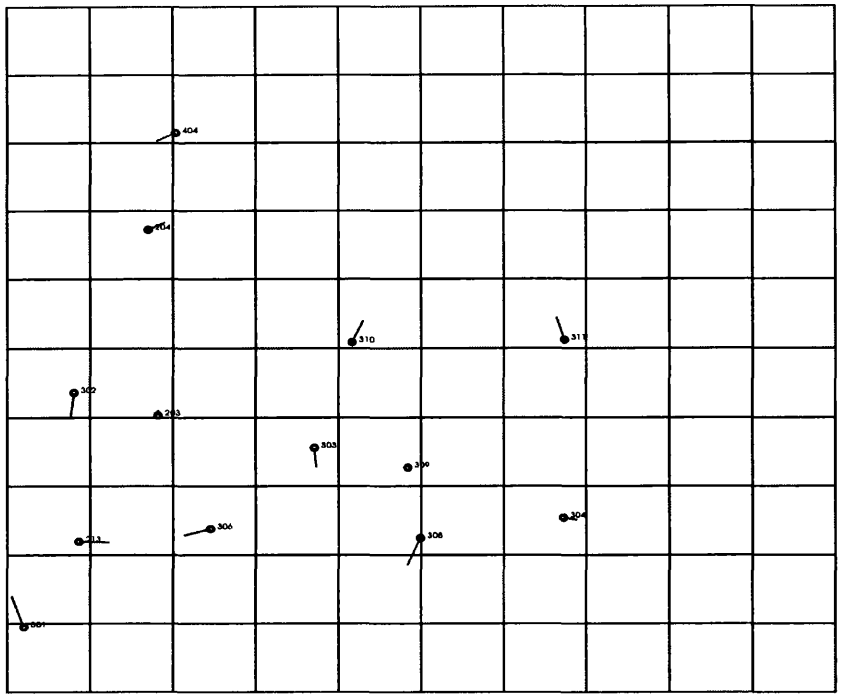

Figure B.8 Vector plots of the residual errors in planimetry at the ground control points of the Level 1B stereo-pair for scene 124/286 after absolute orientation.

(b) Vector plot of the residual errors in heights using 13 ground control points is given in Figure B.9.

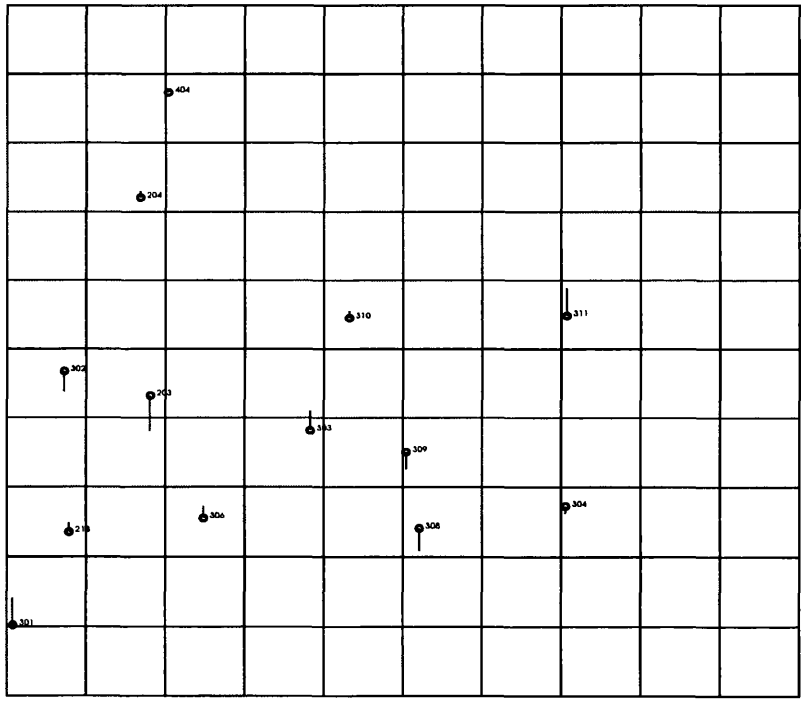

Figure B.9 Vector plots of the residual errors in height at the ground control points of the Level 1B stereo-pair for scene 124/286 after absolute orientation.

B.6 Orthoimage Generation and Orthoimage Accuracy Results

B.6.1 Accuracy Results of Orthoimages

(a) Accuracy Result of Orthoimage of the Level 1A Stereo-model for Reference Scene 122/285 Level 1A Using Linear Conformal Transformation

No.	E (m)	N (m)	ΔE (m)	ΔN (m)
101	308545.	3559870.	-9.066	-11.383
102	300922.	3557099.	21.678	-10.626
110	295871.	3566645.	8.432	1.848
111	300742.	3576802.	11.287	1.442
112	309288.	3582167.	4.118	-1.136
113	304306.	3580947.	-3.550	-1.317
114	297526.	3574024.	-2.182	-20.037
116	284865.	3573803.	-5.419	-18.117
119	284546.	3563608.	-0.747	5.509
124	284233.	3556247.	-9.901	13.126
135	279715.	3554357.	-3.647	3.284
133	278850.	3542817.	-2.432	0.027
136	282129.	3547222.	-8.687	-6.852
146	322957.	3563359.	0.287	-3.149
125	325223.	3568548.	22.492	7.005
127	330679.	3582061.	8.091	-9.191
148	330977.	3561085.	0.057	6.253
154	329682.	3548198.	-16.867	3.670
167	330419.	3528362.	8.157	-9.429
163	304906.	3532801.	-16.193	-14.624
158	328330.	3556593.	-0.965	10.972
157	327584.	3553037.	-5.870	8.826
151	313517.	3552940.	10.482	-1.474
164	320102.	3536359.	-8.211	-10.683
166	330238.	3534946.	7.356	-5.199
141	292955.	3536500.	-13.748	-11.114
129	338784.	3569542.	1.64	-6.03
159	325744.	3543781.	2.33	2.83
126	326827.	3574684.	9.96	11.10
168	321496.	3574939.	-12.50	22.26
145	345746.	3571771.	9.20	-2.04
156	334924.	3545629.	7.17	5.90
169	318581.	3586703.	3.24	4.86
137	292706.	3551482.	-1.90	3.26
128	331363.	3573362.	-3.77	-10.71
152	309233.	3554859.	-9.34	0.12
123	282549.	3570243.	-18.97	-0.58
150	343633.	3563012.	-23.58	9.18
155	337167.	3549815.	4.83	-3.12
143	337967.	3576238.	10.58	10.25

RMSE E = ±9.14m; RMSE N = ±9.69m; RMSE x = ± 0.46 Pixel; RMSE y = ±0.48 Pixel

(b) Accuracy Result of Orthoimage of the Level 1B Stereo-model Reference 122/285 Using Linear Conformal Transformation

The residuals in E and N for control points are as follows:

No.	E (m)	N (m)	Δ E(m)	ΔN (m)
101	308544.669	3559870.413	-2.982	-12.439
102	300921.813	3557098.576	-14.001	4.559
110	295871.199	3566645.391	2.589	-8.926
112	309287.944	3582167.164	-4.246	8.440
113	304306.158	3580947.261	-5.791	6.817
111	300741.806	3576801.496	-3.062	7.436
114	297526.394	3574024.390	14.136	13.392
116	284865.279	3573802.547	12.615	14.864
118	290484.381	3561272.389	-13.361	-5.272
119	284545.790	3563607.619	-1.085	-6.225
124	284233.497	3556247.451	6.564	-6.440
135	279715.010	3554356.652	3.074	-11.318
136	282128.565	3547222.124	8.521	7.432
133	278850.432	3542817.332	-0.625	5.914
141	292955.156	3536500.414	6.318	10.190
163	304905.635	3532800.617	17.487	8.881
166	330238.048	3534946.041	-11.294	4.325
167	330419.432	3528361.542	-2.511	7.545
165	317474.332	3530715.452	-13.855	1.327
164	320102.158	3536358.836	4.240	5.693
146	322957.330	3563359.228	-3.238	-4.471
158	328329.544	3556593.364	-2.814	-14.793
157	327583.703	3553036.651	-0.899	1.504
159	325744.302	3543781.439	-4.634	7.607
154	329681.641	3548198.349	11.864	3.075
153	320665.358	3549829.657	-4.850	-7.770
156	334923.978	3545629.419	2.703	-5.224
151	313517.357	3552939.957	1.039	-18.056
152	309232.993	3554858.615	15.132	-0.627
142	292450.809	3547659.920	-0.799	-11.098
137	292705.709	3551481.912	-7.441	-13.368
148	330976.637	3561084.712	4.015	-9.190
125	325223.139	3568548.152	-14.010	7.390
129	338783.514	3569542.050	2.990	-0.933
149	336884.040	3557833.686	-0.628	-7.662
168	321495.980	3574939.058	4.454	16.452
126	326827.076	3574684.140	13.248	3.734
128	331363.258	3573362.330	-5.939	2.437
143	337967.500	3576238.202	16.423	-0.598
127	330679.379	3582061.380	0.100	-2.723
169	318580.572	3586702.722	-3.227	-4.982
171	313698.694	3569807.342	-12.066	-12.244
123	282548.934	3570242.780	-14.154	-9.927

RMSE E = ±8.7m; RMSE N = ±8.8m ; RMSE x = ±0.44 Pixel; RMSE y =± 0.44 Pixel

B.6.2 Vector Plots of the Planimetric Errors of Orthoimages Generated from Level 1A and 1B Stereo-pairs of the Reference Scene 122/285.

(a) Vector Plot of the Planimetric Errors in the Level 1A Orthoimage Using 40 Check Points

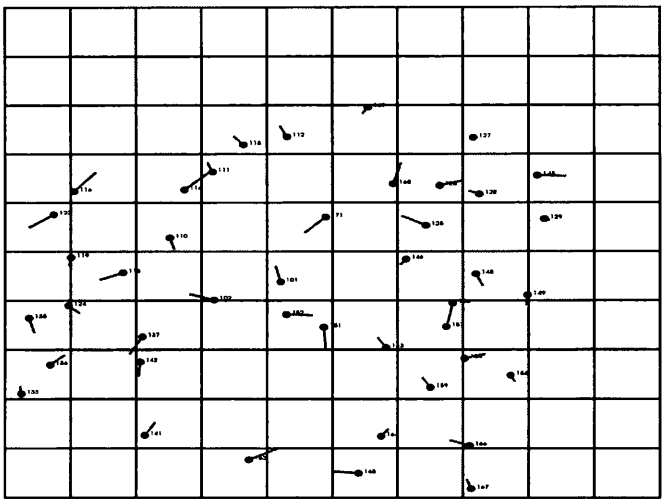

Figure B.10 Vector plot of the residual errors in planimetry at the ground control points in the orthoimage of the Level 1A stereo-pair for reference scene 122/285.

(b) Vector Plot of the Planimetric Errors in the Level 1B Orthoimage Using 43 Check Points

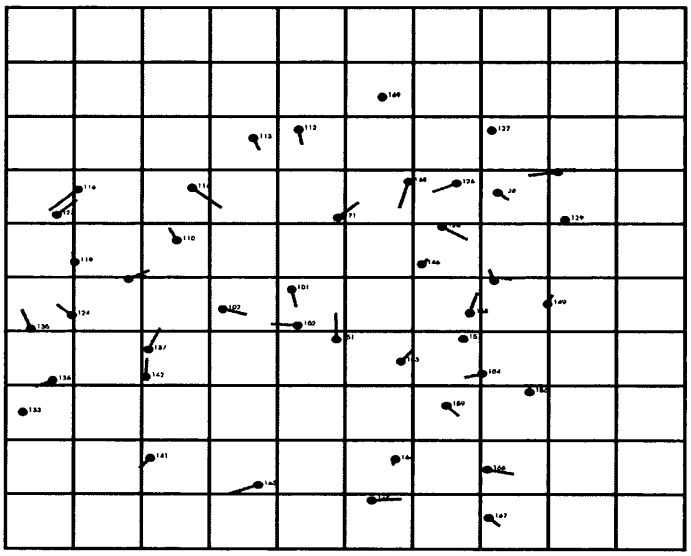

Figure B.11 Vector plot of the residual errors in planimetry at the GCPs in the orthoimage of the Level 1B stereo-model for the reference scene 122/285.

B.6.3 Orthoimages Generated from SPOT Images

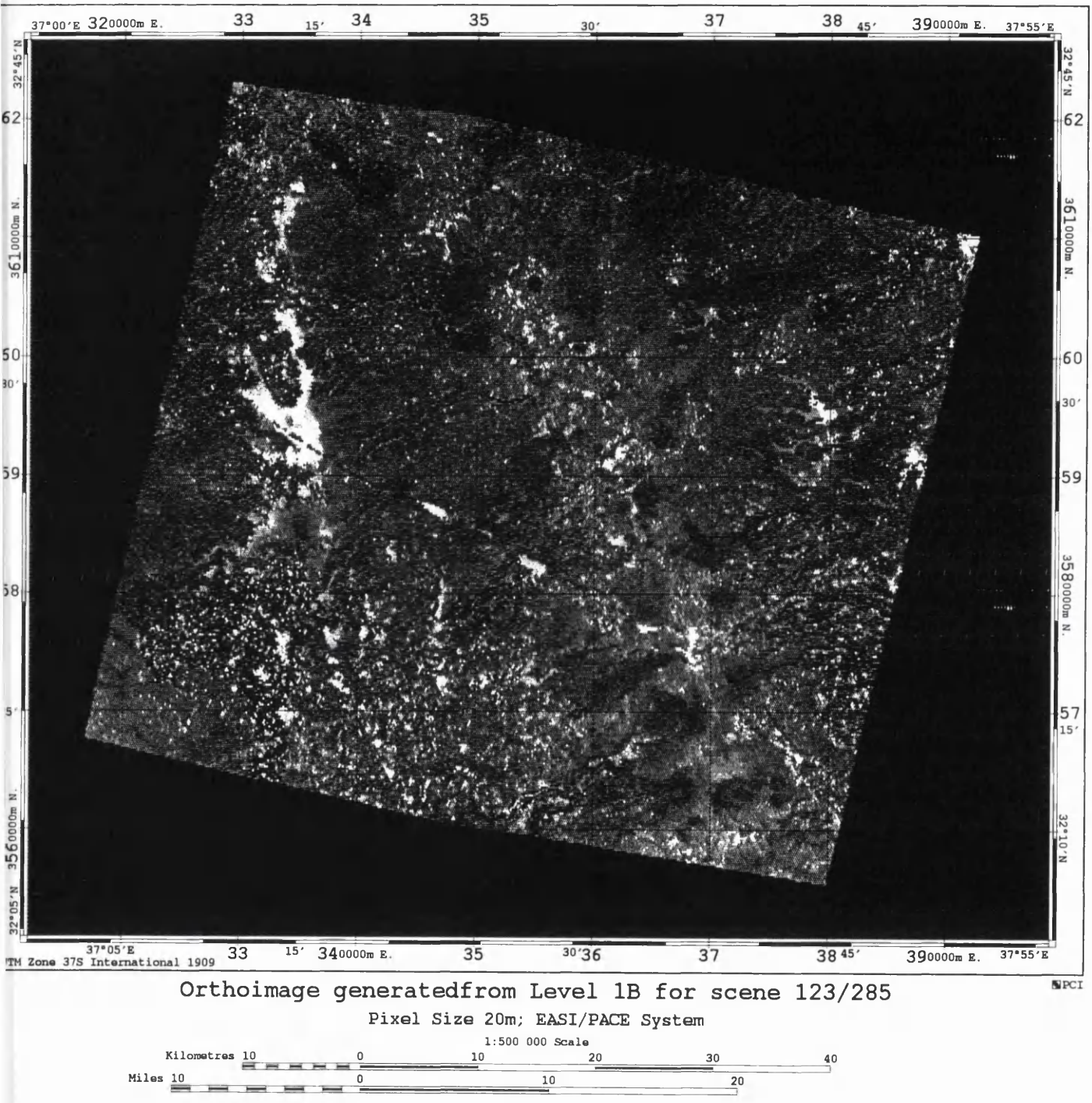

Orthoimage generatedfrom Level 1B for scene 123/285

Pixel Size 20m; EASI/PACE System

1:500 000 Scale

Kilometres 10 0 10 20 30 40

Miles 10 0 10 20

Figure B.12 Orthoimage Generated from Level the 1B stereo-pair for Scene 123/285.

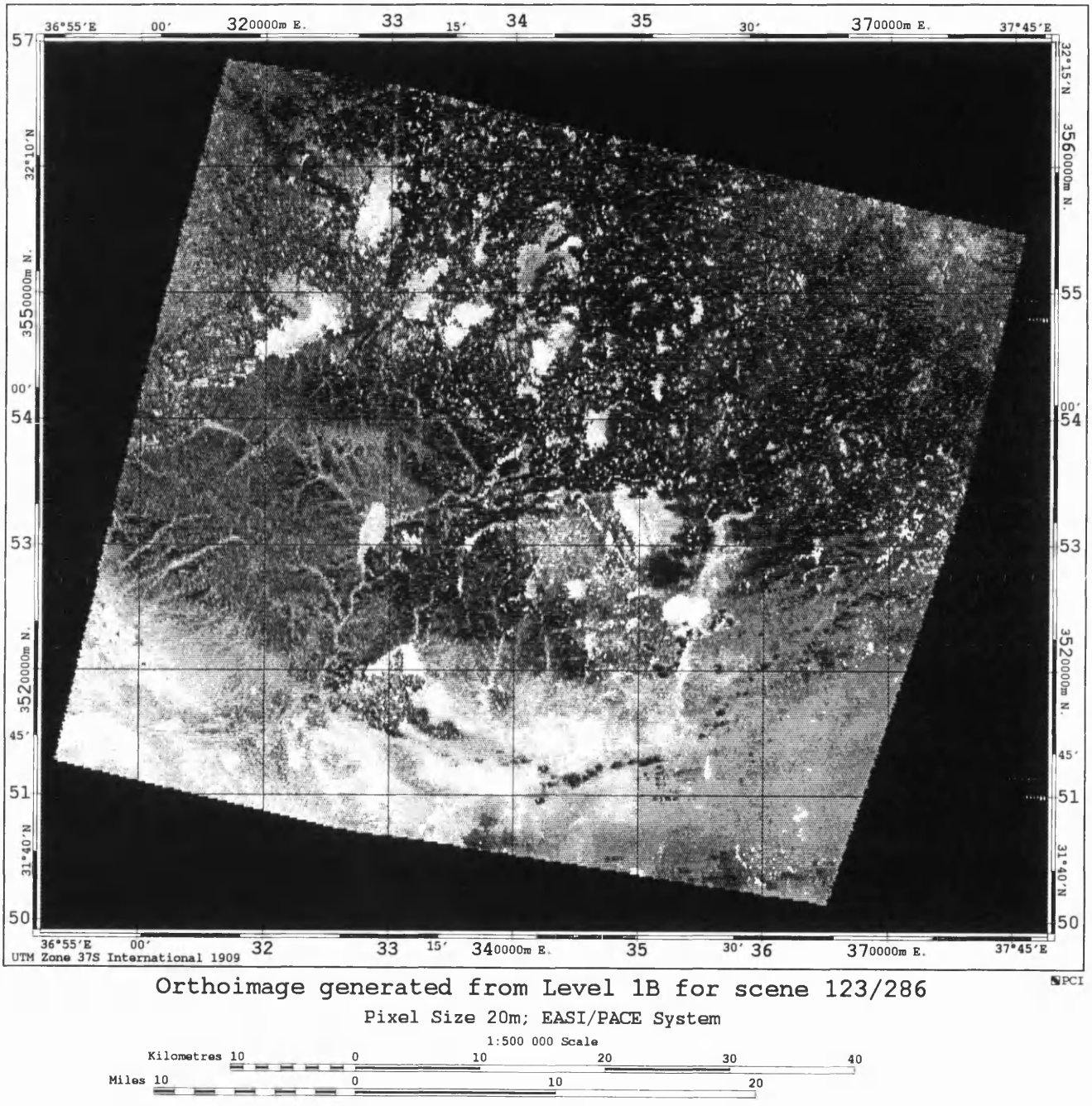

Figure B.13 Orthoimage Generated from the Level 1B stereo-pair for Scene 123/286.

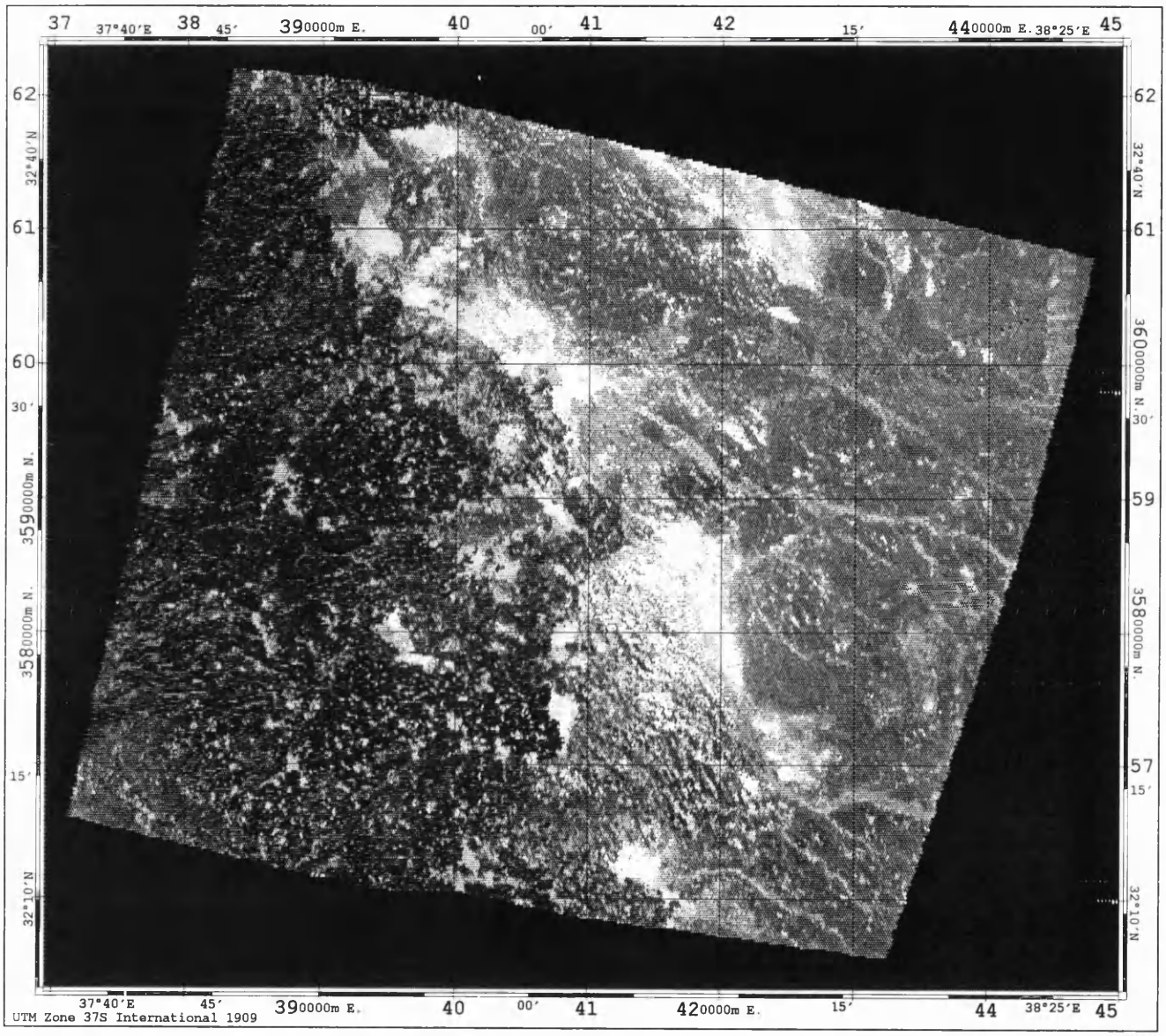

Orthoimage Generated from Level 1B for Scene 124/285

Pixel Size 20m; EASI/PACE System

1:500 000 Scale

Kilometres 10 0 10 20 30 40

Miles 10 0 10 20

Figure B.14 Orthoimage Generated from the Level 1B stereo-pair for Scene 124/285.

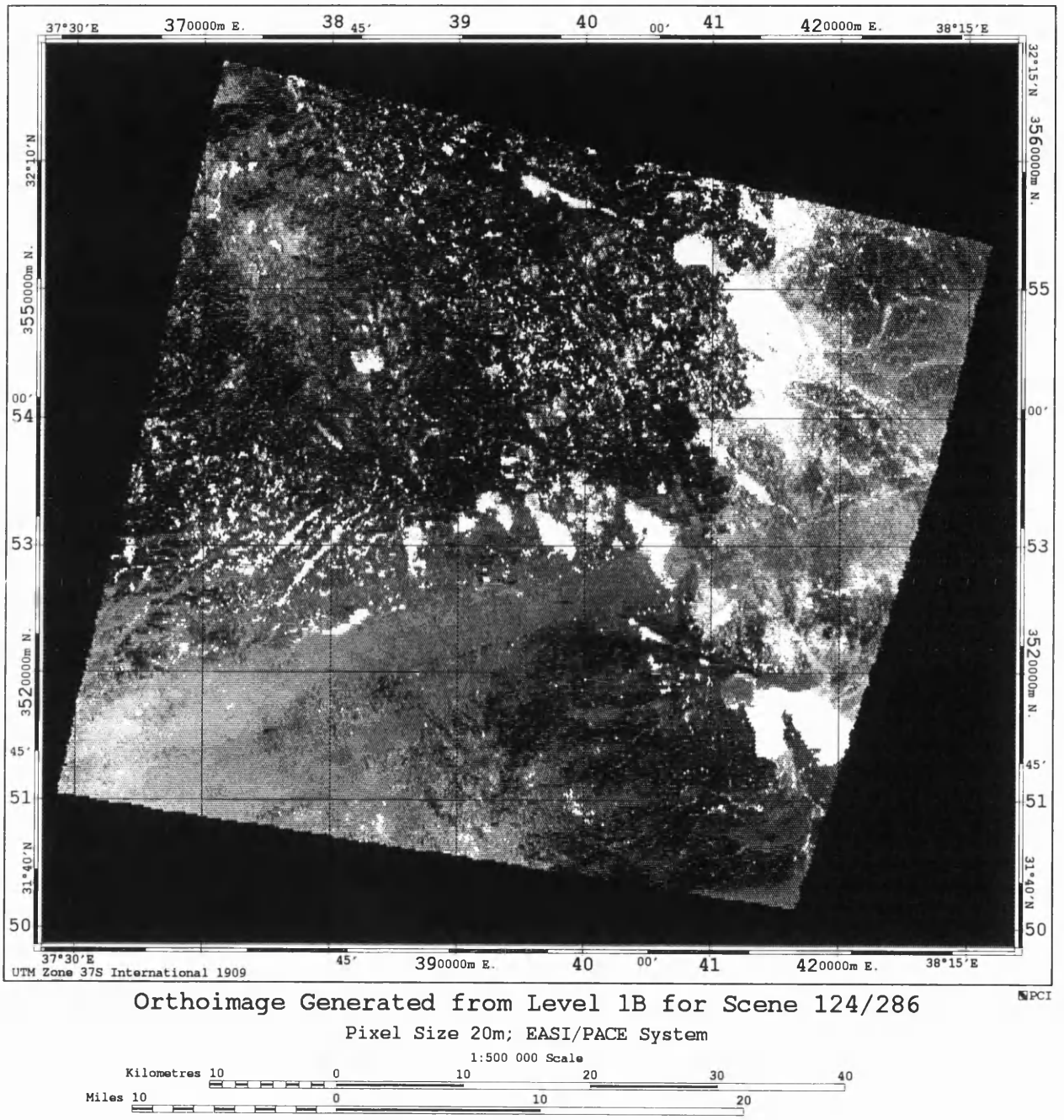

Figure B.15 Orthoimage Generated from the Level 1B stereo-pair for Scene 124/286.

B.7 Contours Generated from DEMs

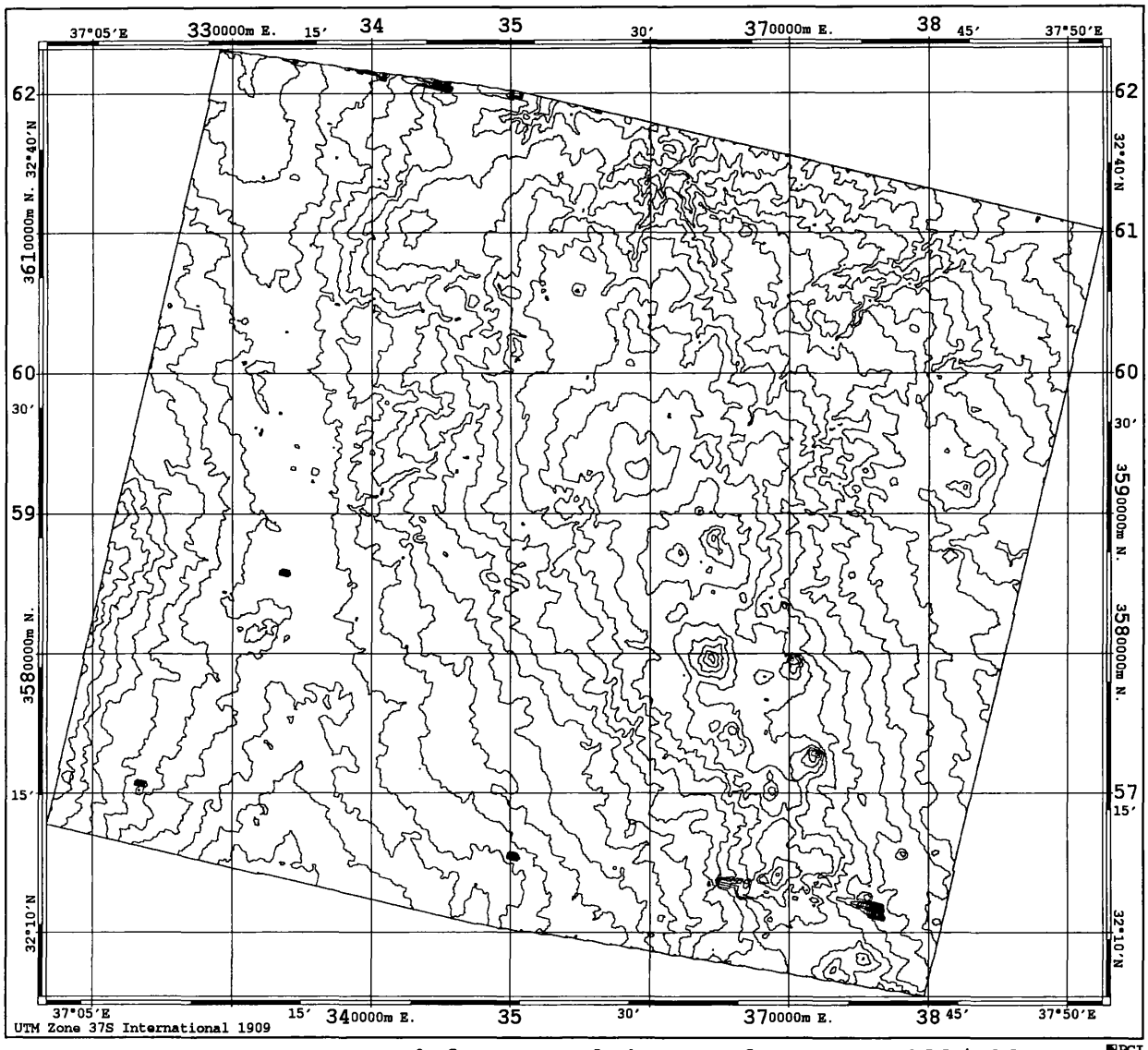

Contours Generated from Level 1B DEM for Scene 123/285

Contour Interval 20m; EASI/PACE System

1:500 000 Scale

Kilometres 10 0 10 20 30 40

Miles 10 0 10 20

Figure B.16 Contours at 20m Interval Generated from the Level 1B DEM for Scene 123/285.

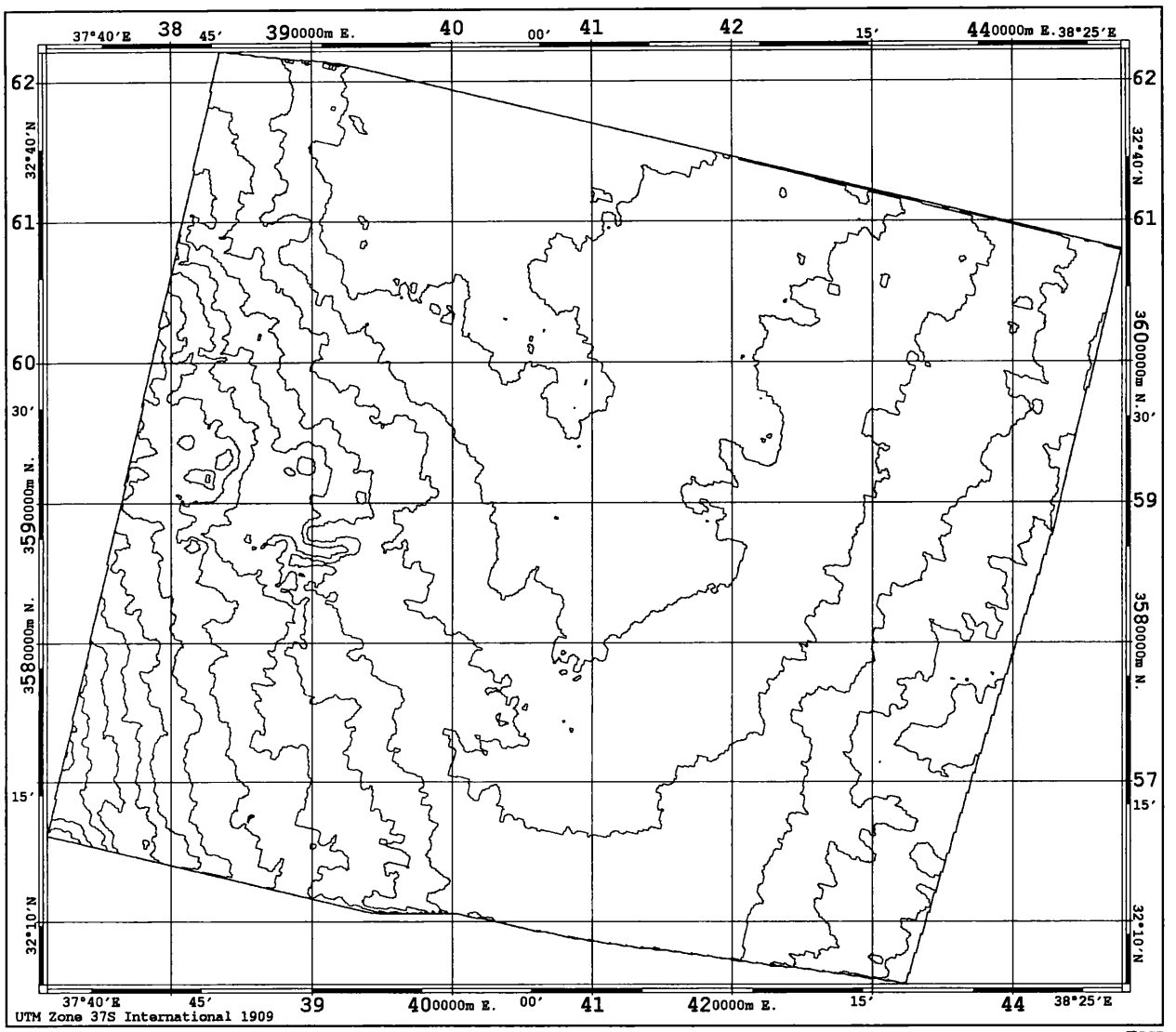

Figure B.17 Contours at 20m Interval Generated from the Level 1B DEM for Scene 124/285.

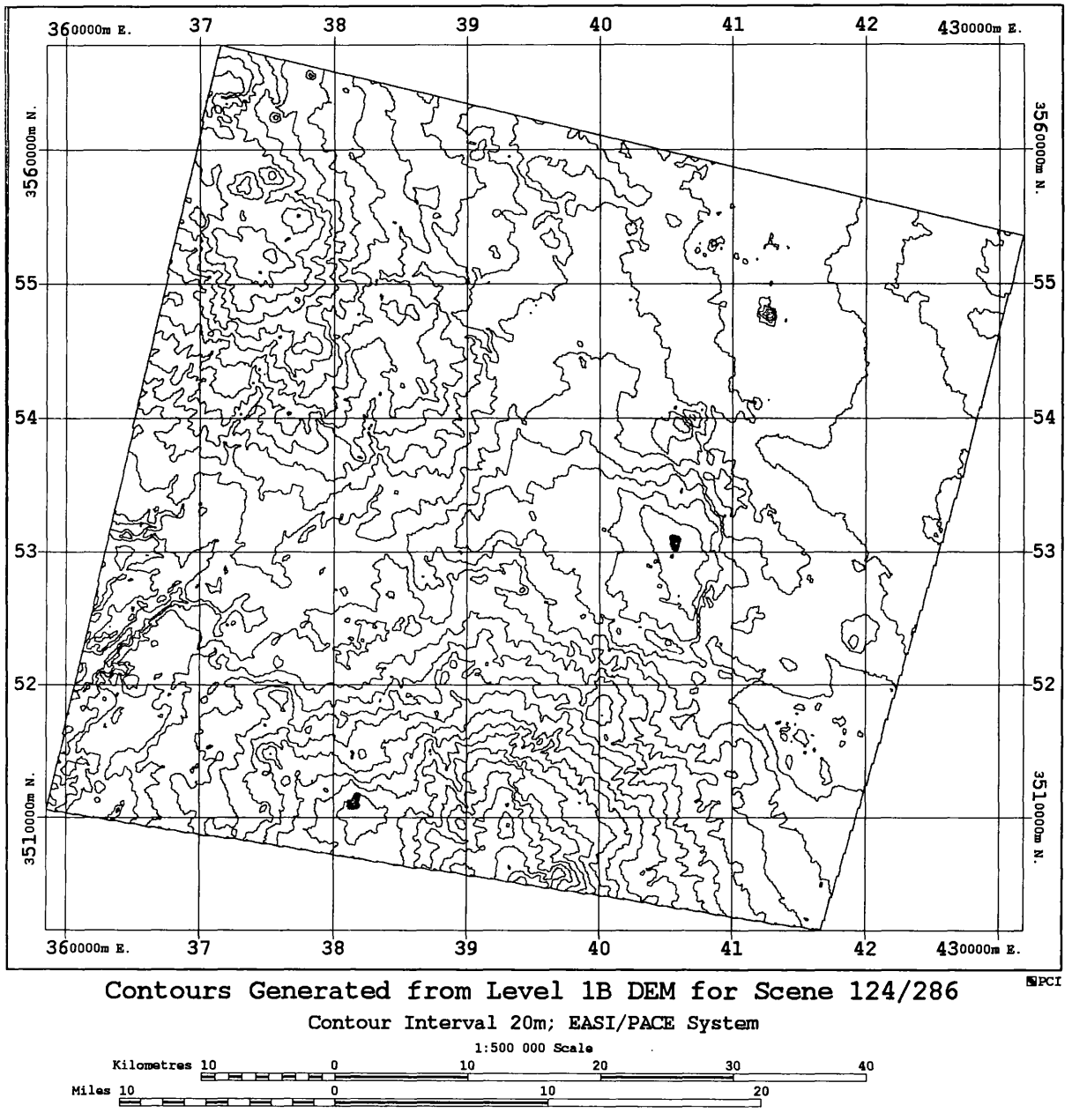

Figure B.18 Contours at 20m Interval Generated from the Level 1B DEM for Scene 124/286.

B.7.1 Contours Generated from the DEMs Superimposed over the Digitized Contours from the 1:250,000 Scale Map at Contour Interval 50m.

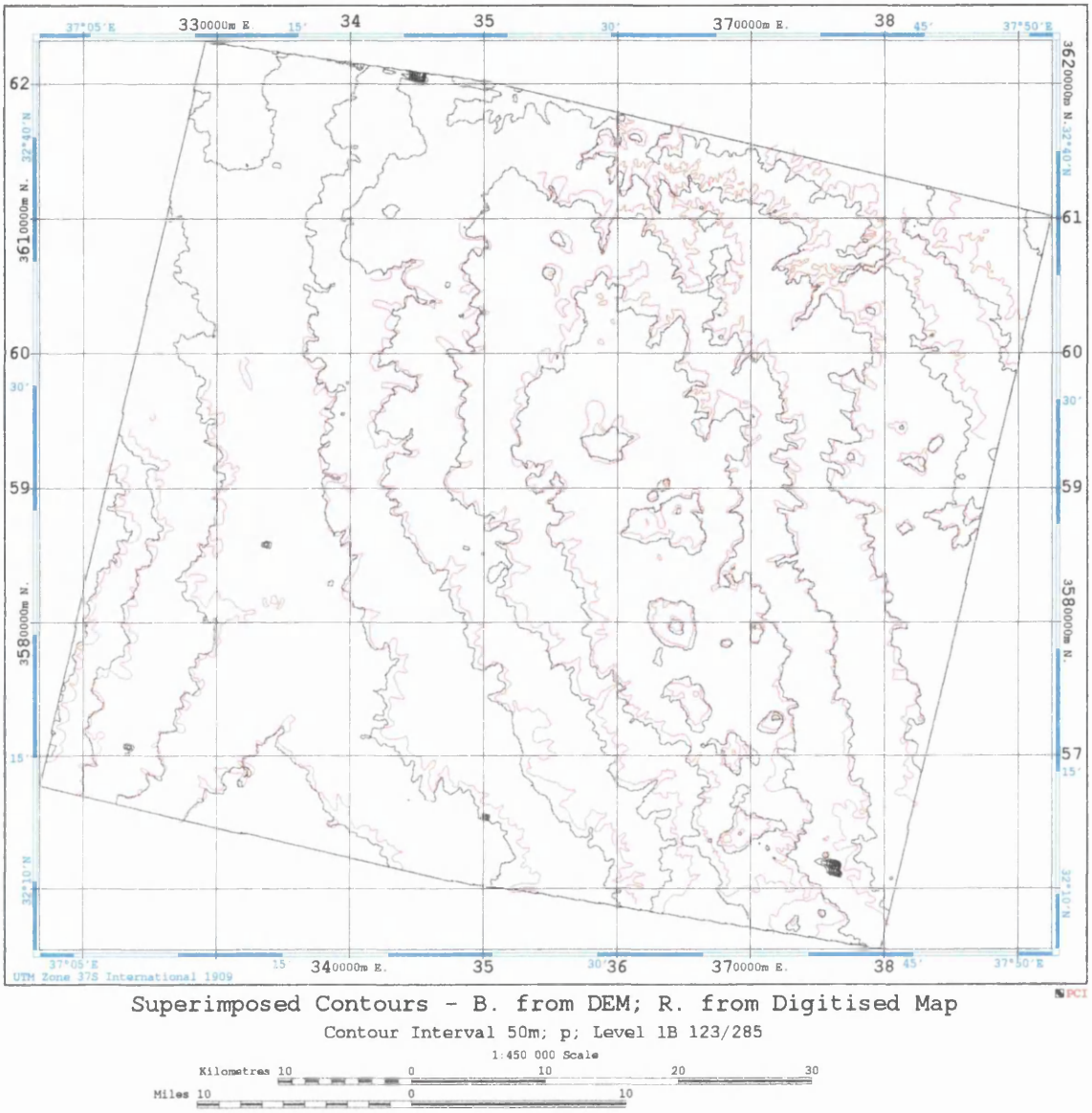

Figure B.19 Contours from the Level 1B DEM for Scene 123/285 Superimposed over the Digitised Contours from the 1:250,000 Scale Map at 50m Interval.

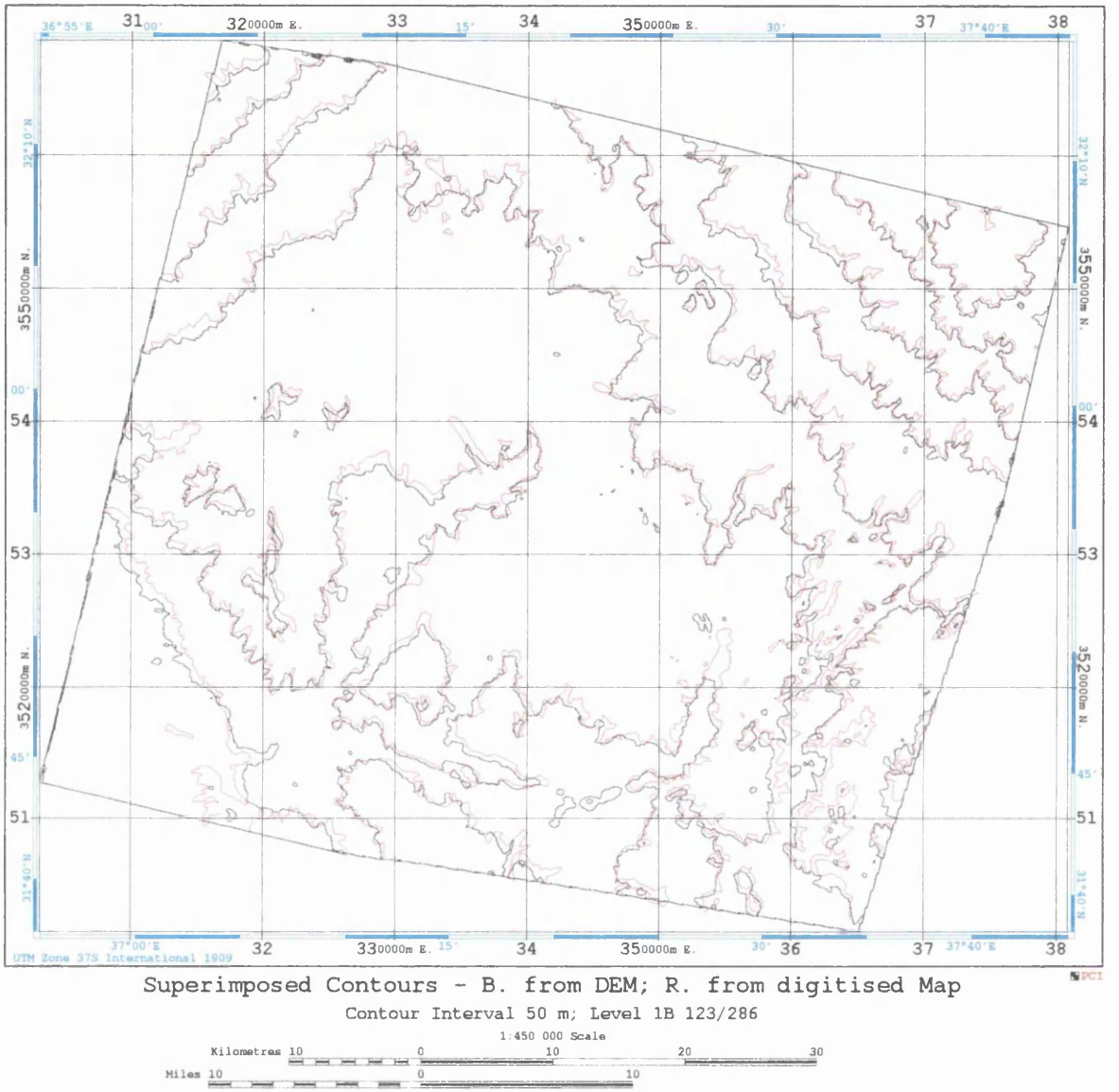

Figure B.20 Contours from the Level 1B DEM for Scene 123/286 Superimposed over the Digitised Contours from the 1:250,000 Scale Map at 50m Interval.

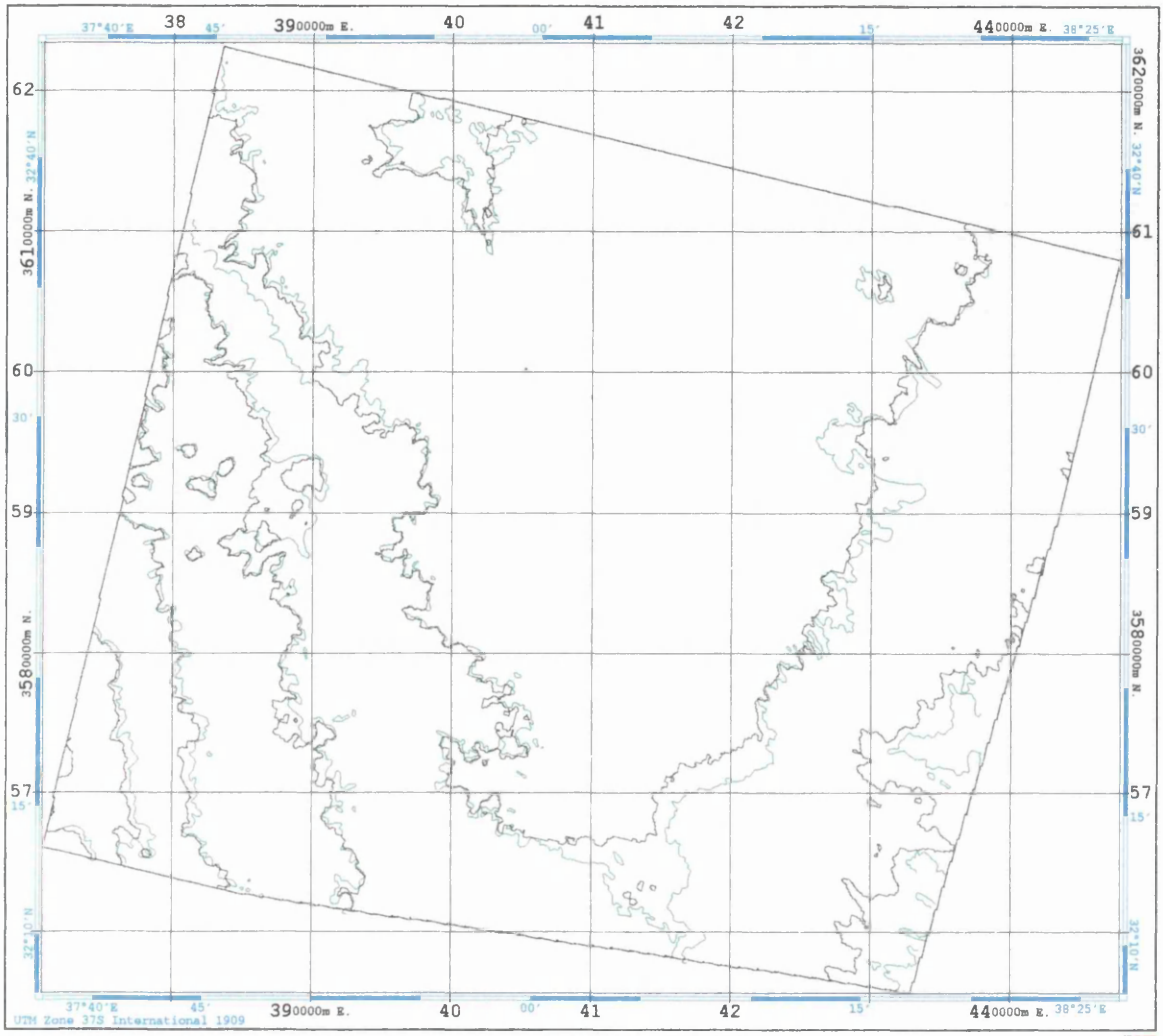

Superimposed Contours from DEM over Digitised Contours

C.I. 50m; Black from DEM; Green from Map; Level 1B 124/285

1:450 000 Scale

Kilometres 10 0 10 20 30

Miles 10 0 10

Figure B.21 Contours from the Level 1B DEM for Scene 124/285 Superimposed over the Digitised Contours from the 1:250,000 Scale Map at 50m Interval.

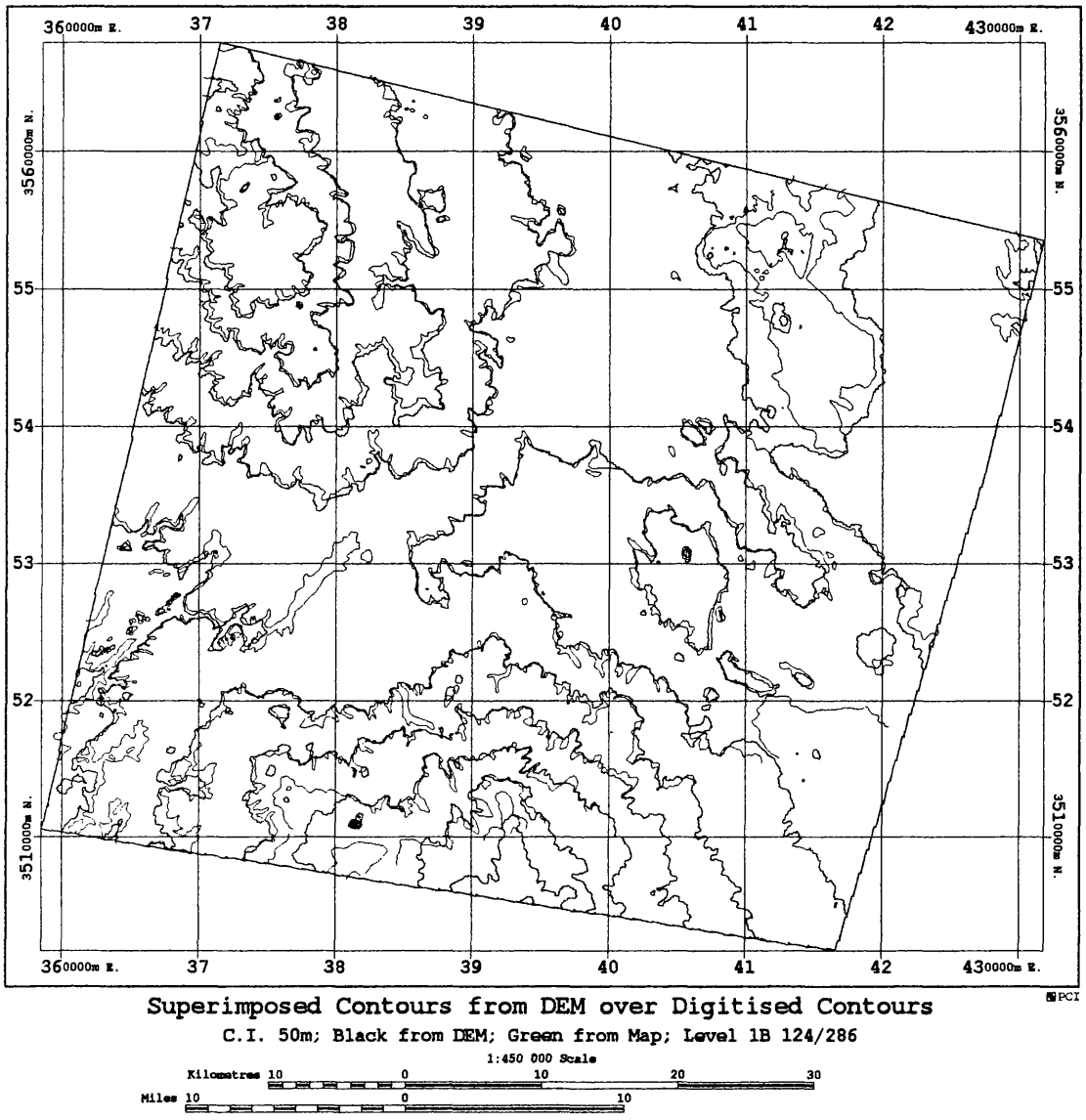

Figure B.22 Contours from the Level 1B DEM for Scene 124/286 Superimposed over the Digitised Contours from the 1:250,000 Scale Map at 50m Interval.

APPENDIX C: RESULTS FROM TESTS OF THE DMS SYSTEM

C.1 Introduction
C.2 Accuracy Results in Planimetry of the SPOT Stereo-models over the Badia Area
C.2.1 Accuracy Results of the Level 1B Stereo-model for Reference Scene 122/285
C.3 Accuracy Results in Height for the DEMs Extracted from SPOT Stereo-pairs over the Badia Area
C.3.1 Accuracy Results in Height in the DEM of the Level 1B Stereo-model for the Reference Scene 122/285
C.3.2 Accuracy Results in Height in the DEM of the Level 1B Stereo-model for the Reference Scene123/285 Using Different Combinations of Control and Check Points
C.3.3 Accuracy Results in Height in the DEM of the Level 1B Stereo-model for Scene123/286
C.3.4 Accuracy Results in Height in the DEM of the Level 1B Stereo-model for Scene 124/285
C.3.5 Accuracy Results in Height in the DEM of the Level 1B Stereo-model for Scene 124/286
C.4 Comparison of Superimposed Contours
C.5 Orthoimage Generation
C.6 Accuracy Results in Planimetry of the Orthoimage of the Reference Scene 122/285 at the Individual GCPs

APPENDIX C: RESULTS FROM TESTS OF DMS SYSTEM

C.1 Introduction

In this Appendix, the accuracy results in planimetry of the SPOT Level 1B stereo-pairs using different combinations of control points and check points are presented Appendix C.2. These are followed in Appendix C.3 by the accuracy results achieved during the tests of the DEM data which again are presented in different combinations of control and check points. In Appendix C.4, the results of comparison of superimposed contours also presented, followed by the rest of orthoimages covering the Badia area and generated by DMS system given in Appendix C.5. In Appendix C.6, the results of the accuracy tests of the orthoimage of the reference scene also included.

C. 2 Accuracy Results in Planimetry of SPOT Level 1B Stereopairs over the Badia Area

The following are the results of the tests of the planimetric accuracy of the SPOT Level 1B stereo-model of the reference scene 122/285 using 10 control points and 35 check points:

Desktop Mapping System (DMS) - Geocode Module

```
Image control point filename.....: SPOTREG.CP
Ground control point filename....: E:\WEL10\WEST.GCP
Coefficient filename.............: E:\WEL10\WESTL.COF
```

Point	S	True-X	True-Y	Est-X	Est-Y	Image-X	Image-Y	Error-XY
101	H	308544.7	3559870.4	308537.0	3559850.6	3088.25	2880.50	21.3
102	H	300921.8	3557098.6	300929.2	3557090.1	2415.87	3331.75	11.2
110	I	295871.2	3566645.4	295861.7	3566643.2	1693.61	2527.25	9.8
111	H	300741.9	3576801.5	300746.3	3576804.2	1923.57	1424.00	5.1
112	I	309287.9	3582167.2	309300.3	3582167.5	2625.38	697.50	12.3
113	H	304306.2	3580947.3	304312.3	3580949.4	2170.24	936.00	6.5
114	H	297526.4	3574024.4	297519.6	3574026.1	1676.99	1771.25	7.0
116	I	284865.3	3573802.5	284856.1	3573797.4	452.41	2099.00	10.5
118	H	290484.4	3561272.4	290491.1	3561269.5	1301.33	3178.00	7.3
119	H	284545.8	3563607.6	284549.7	3563597.5	668.12	3095.50	10.8
124	H	284233.5	3556247.5	284229.6	3556256.7	813.83	3815.25	10.0
125	H	325223.1	3568548.2	325232.2	3568554.0	4499.95	1633.50	10.8
126	H	326827.1	3574684.1	326817.2	3574679.8	4506.45	1001.00	10.8
127	I	330679.4	3582061.4	330673.8	3582068.9	4703.22	191.25	9.3
128	H	331363.3	3573362.3	331365.0	3573363.4	4979.69	1019.00	2.0
129	H	338783.5	3569542.1	338787.2	3569549.6	5792.07	1210.00	8.4
133	H	278850.4	3542817.3	278863.1	3542812.3	616.58	5249.00	13.6
135	I	279715.0	3554356.7	279729.0	3554367.8	422.11	4107.00	17.9
136	H	282128.6	3547222.1	282133.2	3547222.6	827.90	4742.25	4.6
137	H	292705.7	3551481.9	292705.9	3551470.4	1752.55	4075.25	11.5
140	I	281962.2	3535718.3	281955.9	3535715.2	1088.28	5863.25	7.0
141	H	292955.2	3536500.4	292942.6	3536501.7	2136.56	5522.25	12.6
142	H	292450.8	3547659.9	292463.1	3547653.2	1820.98	4451.50	14.0
143	H	337967.5	3576238.2	337945.7	3576234.3	5549.54	581.75	22.2
145	I	345746.0	3571771.0	345749.1	3571761.4	6414.71	827.50	10.1
146	H	322957.3	3563359.2	322957.2	3563350.2	4404.32	2193.25	9.0
148	H	330976.6	3561084.7	330965.8	3561084.7	5236.48	2220.00	10.9
149	H	336884.0	3557833.7	336872.2	3557832.6	5888.27	2393.25	11.9
150	H	343633.2	3563012.3	343636.6	3563017.2	6420.11	1727.00	5.9
151	H	313517.4	3552940.0	313514.9	3552927.8	3738.47	3432.25	12.4
152	I	309233.0	3554858.6	309239.9	3554845.0	3277.10	3349.25	15.3
153	H	320665.4	3549829.7	320662.0	3549818.9	4507.45	3561.75	11.3
154	H	329681.6	3548198.3	329665.1	3548189.4	5420.94	3503.00	18.8
155	H	337166.6	3549815.3	337153.4	3549815.1	6108.79	3164.75	13.2
156	H	334924.0	3545629.4	334918.9	3545641.9	5992.47	3623.75	13.5
157	H	327583.7	3553036.7	327566.1	3553019.1	5100.71	3084.75	24.9
158	I	328329.5	3556593.4	328321.3	3556607.6	5087.56	2718.25	16.5
159	H	325744.3	3543781.4	325730.3	3543783.8	5145.13	4025.50	14.2
163	H	304905.6	3532800.6	304880.0	3532819.2	3384.91	5592.25	31.7
164	H	320102.2	3536358.8	320093.5	3536376.2	4776.50	4880.50	19.4
165	H	317474.3	3530715.5	317469.4	3530716.9	4658.30	5493.25	5.2
166	I	330238.0	3534946.0	330240.6	3534946.4	5796.29	4775.00	2.5
167	H	330419.4	3528361.5	330414.9	3528365.3	5972.13	5410.00	5.9
168	H	321496.0	3574939.1	321500.9	3574927.2	3984.29	1105.25	12.8
169	H	318580.6	3586702.7	318575.5	3586714.4	3416.83	32.75	12.7

Status key: I=In O=Out H=Hold

Desktop Mapping System (DMS) - Geocode Module

```
Total points=          45                              Pixels    Ground
Used in solution=      10          RMSE solution       ±1.19     ±11.94
Withheld for checking= 35          RMSE check          ±1.35     ±13.54

Coefficients  (2nd order polynomial)
     9.697      -2.403      0.00000     -0.00000     -0.00000   285515.692
    -2.417      -9.721      0.00000      0.00000      0.00000  3595288.196
     0.098      -0.032     -0.00000      0.00000     -0.00000    72113.513
    -0.020      -0.107      0.00000      0.00000     -0.00000   371997.772
```

The following are the results of the tests of the planimetric accuracy of the SPOT Level 1B stereo-model of the reference scene 122/285 using 15 control points and 30 check points:

Desktop Mapping System (DMS) - Geocode Module

```
Image control point filename.....: SPOTREG.CP
Ground control point filename....: E:\WEL10\WEST.GCP
Coefficient filename.............: E:\WEL10\WESTL.COF
```

Point	S	True-X	True-Y	Est-X	Est-Y	Image-X	Image-Y	Error-XY
101	H	308544.7	3559870.4	308541.6	3559853.6	3088.25	2880.50	17.0
102	H	300921.8	3557098.6	300933.3	3557092.9	2415.87	3331.75	12.8
110	I	295871.2	3566645.4	295862.2	3566645.5	1693.61	2527.25	9.0
111	H	300741.9	3576801.5	300747.1	3576803.3	1923.57	1424.00	5.5
112	I	309287.9	3582167.2	309302.9	3582163.5	2625.38	697.50	15.4
113	H	304306.2	3580947.3	304313.9	3580946.3	2170.24	936.00	7.8
114	H	297526.4	3574024.4	297519.5	3574026.5	1676.99	1771.25	7.2
116	I	284865.3	3573802.5	284850.6	3573798.0	452.41	2099.00	15.4
118	I	290484.4	3561272.4	290490.8	3561272.2	1301.33	3178.00	6.4
119	H	284545.8	3563607.6	284546.0	3563600.1	668.12	3095.50	7.6
124	H	284233.5	3556247.5	284227.9	3556258.9	813.83	3815.25	12.7
125	H	325223.1	3568548.2	325235.4	3568555.9	4499.95	1633.50	14.5
126	H	326827.1	3574684.1	326819.9	3574679.4	4506.45	1001.00	8.6
127	I	330679.4	3582061.4	330676.3	3582064.1	4703.22	191.25	4.1
128	H	331363.3	3573362.3	331366.9	3573363.5	4979.69	1019.00	3.8
129	H	338783.5	3569542.1	338787.0	3569551.1	5792.07	1210.00	9.7
133	H	278850.4	3542817.3	278864.1	3542809.5	616.58	5249.00	15.7
135	I	279715.0	3554356.7	279725.6	3554369.5	422.11	4107.00	16.6
136	H	282128.6	3547222.1	282133.9	3547222.1	827.90	4742.25	5.3
137	H	292705.7	3551481.9	292709.4	3551471.9	1752.55	4075.25	10.7
140	I	281962.2	3535718.3	281962.0	3535708.1	1088.28	5863.25	10.2
141	H	292955.2	3536500.4	292952.3	3536496.0	2136.56	5522.25	5.2
142	H	292450.8	3547659.9	292467.8	3547653.4	1820.98	4451.50	18.2
143	H	337967.5	3576238.2	337945.9	3576232.8	5549.54	581.75	22.3
145	I	345746.0	3571771.0	345746.0	3571761.9	6414.71	827.50	9.1
146	H	322957.3	3563359.2	322961.1	3563353.2	4404.32	2193.25	7.1
148	H	330976.6	3561084.7	330968.4	3561088.1	5236.48	2220.00	8.9
149	H	336884.0	3557833.7	336873.3	3557836.2	5888.27	2393.25	11.0
150	I	343633.2	3563012.3	343634.5	3563020.3	6420.11	1727.00	8.1
151	H	313517.4	3552940.0	313521.4	3552930.4	3738.47	3432.25	10.3
152	I	309233.0	3554858.6	309245.7	3554847.7	3277.10	3349.25	16.7
153	H	320665.4	3549829.7	320668.7	3549821.1	4507.45	3561.75	9.2
154	H	329681.6	3548198.3	329670.3	3548191.5	5420.94	3503.00	13.2
155	H	337166.6	3549815.3	337155.7	3549817.9	6108.79	3164.75	11.2
156	H	334924.0	3545629.4	334923.0	3545643.5	5992.47	3623.75	14.1
157	I	327583.7	3553036.7	327570.9	3553022.2	5100.71	3084.75	19.4
158	I	328329.5	3556593.4	328325.2	3556611.0	5087.56	2718.25	18.2
159	H	325744.3	3543781.4	325737.8	3543784.2	5145.13	4025.50	7.1
163	I	304905.6	3532800.6	304893.5	3532811.8	3384.91	5592.25	16.5
164	H	320102.2	3536358.8	320104.7	3536372.5	4776.50	4880.50	13.9
165	H	317474.3	3530715.5	317483.4	3530708.9	4658.30	5493.25	11.2
166	I	330238.0	3534946.0	330249.7	3534942.5	5796.29	4775.00	12.2
167	H	330419.4	3528361.5	330426.6	3528356.5	5972.13	5410.00	8.7
168	H	321496.0	3574939.1	321504.2	3574926.8	3984.29	1105.25	14.7
169	I	318580.6	3586702.7	318579.3	3586706.8	3416.83	32.75	4.2

Status key: I=In O=Out H=Hold

Desktop Mapping System (DMS) - Geocode Module

```
Total points=          45
Used in solution=      15
Withheld for checking= 30
```

	Pixels	Ground
RMSE solution	1.31	13.08
RMSE check	1.16	11.62

Coefficients (2nd order polynomial)

9.703	-2.405	-0.00000	-0.00000	-0.00000	285509.464
-2.416	-9.712	0.00000	-0.00000	0.00000	3595274.921
0.099	-0.026	0.00000	0.00000	-0.00000	61367.487
-0.020	-0.098	-0.00000	0.00000	-0.00000	356025.151

The following are the results of the tests of the planimetric accuracy of the SPOT Level 1B stereo-model of the reference scene 122/285 using 25 control points and 20 check points:

Desktop Mapping System (DMS) - Geocode Module

```
Image control point filename.....: SPOTREG.CP
Ground control point filename....: E:\WEL10\WEST.GCP
Coefficient filename.............: E:\WEL10\WESTL.COF
```

Point	S	True-X	True-Y	Est-X	Est-Y	Image-X	Image-Y	Error-XY
101	H	308544.7	3559870.4	308536.8	3559857.1	3088.25	2880.50	15.5
102	I	300921.8	3557098.6	300928.5	3557096.4	2415.87	3331.75	7.0
110	I	295871.2	3566645.4	295859.8	3566647.8	1693.61	2527.25	11.6
111	H	300741.9	3576801.5	300746.9	3576804.3	1923.57	1424.00	5.8
112	I	309287.9	3582167.2	309302.6	3582164.0	2625.38	697.50	14.9
113	H	304306.2	3580947.3	304314.4	3580946.8	2170.24	936.00	8.3
114	I	297526.4	3574024.4	297519.3	3574027.7	1676.99	1771.25	7.9
116	I	284865.3	3573802.5	284854.8	3573797.1	452.41	2099.00	11.8
118	I	290484.4	3561272.4	290488.2	3561274.4	1301.33	3178.00	4.3
119	H	284545.8	3563607.6	284545.8	3563601.0	668.12	3095.50	6.6
124	H	284233.5	3556247.5	284225.6	3556260.6	813.83	3815.25	15.3
125	I	325223.1	3568548.2	325231.4	3568557.6	4499.95	1633.50	12.5
126	H	326827.1	3574684.1	326816.2	3574680.4	4506.45	1001.00	11.5
127	I	330679.4	3582061.4	330673.4	3582063.6	4703.22	191.25	6.4
128	H	331363.3	3573362.3	331363.5	3573363.9	4979.69	1019.00	1.6
129	I	338783.5	3569542.1	338785.1	3569550.3	5792.07	1210.00	8.4
133	H	278850.4	3542817.3	278860.5	3542810.9	616.58	5249.00	11.9
135	I	279715.0	3554356.7	279723.9	3554370.5	422.11	4107.00	16.4
136	H	282128.6	3547222.1	282130.2	3547224.0	827.90	4742.25	2.5
137	I	292705.7	3551481.9	292704.8	3551475.0	1752.55	4075.25	7.0
140	I	281962.2	3535718.3	281958.0	3535709.7	1088.28	5863.25	9.5
141	H	292955.2	3536500.4	292948.4	3536498.8	2136.56	5522.25	6.9
142	I	292450.8	3547659.9	292463.1	3547656.6	1820.98	4451.50	12.7
143	H	337967.5	3576238.2	337943.2	3576231.7	5549.54	581.75	25.1
145	I	345746.0	3571771.0	345745.6	3571759.1	6414.71	827.50	11.8
146	I	322957.3	3563359.2	322957.1	3563355.5	4404.32	2193.25	3.7
148	H	330976.6	3561084.7	330966.2	3561089.1	5236.48	2220.00	11.4
149	H	336884.0	3557833.7	336873.7	3557835.9	5888.27	2393.25	10.5
150	I	343633.2	3563012.3	343635.7	3563018.2	6420.11	1727.00	6.4
151	H	313517.4	3552940.0	313517.2	3552933.8	3738.47	3432.25	6.2
152	I	309233.0	3554858.6	309241.0	3554851.3	3277.10	3349.25	10.8
153	H	320665.4	3549829.7	320666.6	3549823.5	4507.45	3561.75	6.2
154	I	329681.6	3548198.3	329671.6	3548192.2	5420.94	3503.00	11.8
155	H	337166.6	3549815.3	337159.4	3549816.9	6108.79	3164.75	7.4
156	H	334924.0	3545629.4	334927.6	3545642.6	5992.47	3623.75	13.6
157	I	327583.7	3553036.7	327569.7	3553023.6	5100.71	3084.75	19.1
158	I	328329.5	3556593.4	328323.3	3556612.5	5087.56	2718.25	20.1
159	I	325744.3	3543781.4	325739.4	3543785.3	5145.13	4025.50	6.2
163	I	304905.6	3532800.6	304892.7	3532814.1	3384.91	5592.25	18.7
164	H	320102.2	3536358.8	320107.4	3536373.5	4776.50	4880.50	15.6
165	H	317474.3	3530715.5	317487.9	3530709.4	4658.30	5493.25	14.8
166	I	330238.0	3534946.0	330257.9	3534941.1	5796.29	4775.00	20.5
167	H	330419.4	3528361.5	330439.4	3528353.6	5972.13	5410.00	21.5
168	I	321496.0	3574939.1	321500.4	3574928.3	3984.29	1105.25	11.6
169	I	318580.6	3586702.7	318578.7	3586706.4	3416.83	32.75	4.1

Status key: I=In O=Out H=Hold

Desktop Mapping System (DMS) - Geocode Module

```
Total points=          45
Used in solution=      25                          Pixels      Ground
Withheld for checking= 20      RMSE solution         1.21       12.08
                               RMSE check            1.24       12.38

Coefficients  (2nd order polynomial)
      9.694      -2.412     0.00000     0.00000     0.00000  285528.231
     -2.412      -9.709    -0.00000    -0.00000     0.00000 3595267.831
      0.095      -0.020    -0.00000    -0.00000     0.00000   51514.648
     -0.019      -0.096    -0.00000    -0.00000    -0.00000  353883.092
```

The following are the results of the tests of the planimetric accuracy of the SPOT Level 1B stereo-model of the reference scene 122/285 using 30 control points and 15 check points:

Desktop Mapping System (DMS) - Geocode Module

```
Image control point filename.....: SPOTREG.CP
Ground control point filename....: E:\WEL10\WEST.GCP
Coefficient filename.............: E:\WEL10\WESTL.COF
```

Point	S	True-X	True-Y	Est-X	Est-Y	Image-X	Image-Y	Error-XY
101	H	308544.7	3559870.4	308538.0	3559855.1	3088.25	2880.50	16.7
102	I	300921.8	3557098.6	300929.6	3557094.7	2415.87	3331.75	8.7
110	I	295871.2	3566645.4	295859.5	3566646.6	1693.61	2527.25	11.7
111	H	300741.9	3576801.5	300744.5	3576804.5	1923.57	1424.00	4.0
112	I	309287.9	3582167.2	309300.2	3582165.6	2625.38	697.50	12.4
113	I	304306.2	3580947.3	304311.3	3580947.9	2170.24	936.00	5.2
114	H	297526.4	3574024.4	297517.2	3574027.3	1676.99	1771.25	9.6
116	I	284865.3	3573802.5	284851.1	3573797.0	452.41	2099.00	15.2
118	H	290484.4	3561272.4	290488.7	3561273.3	1301.33	3178.00	4.5
119	I	284545.8	3563607.6	284545.7	3563600.2	668.12	3095.50	7.4
124	I	284233.5	3556247.5	284227.0	3556260.0	813.83	3815.25	14.1
125	I	325223.1	3568548.2	325234.3	3568556.6	4499.95	1633.50	14.0
126	H	326827.1	3574684.1	326819.3	3574680.8	4506.45	1001.00	8.5
127	I	330679.4	3582061.4	330676.7	3582066.4	4703.22	191.25	5.7
128	H	331363.3	3573362.3	331367.6	3573364.2	4979.69	1019.00	4.7
129	I	338783.5	3569542.1	338790.5	3569550.0	5792.07	1210.00	10.6
133	I	278850.4	3542817.3	278863.7	3542812.8	616.58	5249.00	14.0
135	I	279715.0	3554356.7	279725.9	3554370.5	422.11	4107.00	17.6
136	H	282128.6	3547222.1	282132.8	3547224.6	827.90	4742.25	4.9
137	I	292705.7	3551481.9	292706.3	3551474.1	1752.55	4075.25	7.8
140	I	281962.2	3535718.3	281960.2	3535712.9	1088.28	5863.25	5.7
141	I	292955.2	3536500.4	292948.5	3536500.3	2136.56	5522.25	6.6
142	H	292450.8	3547659.9	292464.5	3547656.1	1820.98	4451.50	14.2
143	I	337967.5	3576238.2	337948.9	3576233.2	5549.54	581.75	19.3
145	I	345746.0	3571771.0	345752.8	3571759.9	6414.71	827.50	13.0
146	I	322957.3	3563359.2	322959.5	3563353.7	4404.32	2193.25	6.0
148	H	330976.6	3561084.7	330969.2	3561087.1	5236.48	2220.00	7.9
149	I	336884.0	3557833.7	336876.5	3557833.6	5888.27	2393.25	7.5
150	H	343633.2	3563012.3	343640.6	3563016.9	6420.11	1727.00	8.7
151	I	313517.4	3552940.0	313518.0	3552931.5	3738.47	3432.25	8.5
152	H	309233.0	3554858.6	309242.0	3554849.2	3277.10	3349.25	13.0
153	I	320665.4	3549829.7	320666.7	3549821.0	4507.45	3561.75	8.7
154	H	329681.6	3548198.3	329671.1	3548189.4	5420.94	3503.00	13.8
155	I	337166.6	3549815.3	337159.5	3549814.0	6108.79	3164.75	7.3
156	I	334924.0	3545629.4	334926.0	3545639.7	5992.47	3623.75	10.5
157	H	327583.7	3553036.7	327570.7	3553021.0	5100.71	3084.75	20.4
158	I	328329.5	3556593.4	328325.2	3556610.0	5087.56	2718.25	17.2
159	I	325744.3	3543781.4	325737.4	3543782.8	5145.13	4025.50	7.0
163	I	304905.6	3532800.6	304889.3	3532815.0	3384.91	5592.25	21.7
164	H	320102.2	3536358.8	320102.9	3536372.3	4776.50	4880.50	13.5
165	I	317474.3	3530715.5	317481.1	3530709.5	4658.30	5493.25	9.1
166	I	330238.0	3534946.0	330251.3	3534939.3	5796.29	4775.00	14.9
167	H	330419.4	3528361.5	330428.7	3528353.0	5972.13	5410.00	12.6
168	I	321496.0	3574939.1	321502.4	3574928.6	3984.29	1105.25	12.3
169	I	318580.6	3586702.7	318577.4	3586709.9	3416.83	32.75	7.8

Status key: I=In O=Out H=Hold

Desktop Mapping System (DMS) - Geocode Module

```
Total points=          45
Used in solution=      30
Withheld for checking= 15
```

	Pixels	Ground
RMSE solution	1.17	11.75
RMSE check	1.15	11.50

Coefficients (2nd order polynomial)

9.699	-2.405	0.00000	-0.00000	-0.00000	285512.378
-2.412	-9.712	-0.00000	0.00000	0.00000	3595272.573
0.098	-0.025	-0.00000	0.00000	-0.00000	61267.403
-0.021	-0.099	-0.00000	0.00000	-0.00000	358402.630

The following are the results of the tests of the planimetric accuracy of the SPOT Level 1B stereo-model of the reference scene 122/285 using 35 control points and 10 check points:

Desktop Mapping System (DMS) - Geocode Module

```
Image control point filename.....: SPOTREG.CP
Ground control point filename....: E:\WEL10\WEST.GCP
Coefficient filename.............: E:\WEL10\WESTL.COF
```

Point	S	True-X	True-Y	Est-X	Est-Y	Image-X	Image-Y	Error-XY
101	H	308544.7	3559870.4	308538.3	3559855.9	3088.25	2880.50	15.8
102	I	300921.8	3557098.6	300929.5	3557095.2	2415.87	3331.75	8.4
110	I	295871.2	3566645.4	295860.0	3566646.6	1693.61	2527.25	11.2
111	H	300741.9	3576801.5	300745.4	3576803.8	1923.57	1424.00	4.2
112	I	309287.9	3582167.2	309300.7	3582164.4	2625.38	697.50	13.1
113	I	304306.2	3580947.3	304312.1	3580946.8	2170.24	936.00	6.0
114	I	297526.4	3574024.4	297518.1	3574026.9	1676.99	1771.25	8.7
116	I	284865.3	3573802.5	284852.0	3573796.3	452.41	2099.00	14.7
118	I	290484.4	3561272.4	290488.6	3561273.3	1301.33	3178.00	4.3
119	H	284545.8	3563607.6	284545.6	3563599.9	668.12	3095.50	7.7
124	I	284233.5	3556247.5	284225.9	3556259.6	813.83	3815.25	14.3
125	I	325223.1	3568548.2	325234.6	3568557.3	4499.95	1633.50	14.7
126	H	326827.1	3574684.1	326819.2	3574680.7	4506.45	1001.00	8.6
127	I	330679.4	3582061.4	330675.8	3582065.1	4703.22	191.25	5.2
128	I	331363.3	3573362.3	331367.3	3573364.4	4979.69	1019.00	4.5
129	I	338783.5	3569542.1	338790.2	3569550.8	5792.07	1210.00	11.0
133	I	278850.4	3542817.3	278859.8	3542811.1	616.58	5249.00	11.3
135	I	279715.0	3554356.7	279724.2	3554369.7	422.11	4107.00	16.0
136	H	282128.6	3547222.1	282130.1	3547223.6	827.90	4742.25	2.2
137	I	292705.7	3551481.9	292705.2	3551474.1	1752.55	4075.25	7.9
140	I	281962.2	3535718.3	281955.3	3535710.7	1088.28	5863.25	10.3
141	H	292955.2	3536500.4	292945.2	3536499.1	2136.56	5522.25	10.1
142	I	292450.8	3547659.9	292462.9	3547655.9	1820.98	4451.50	12.7
143	I	337967.5	3576238.2	337947.9	3576233.0	5549.54	581.75	20.2
145	I	345746.0	3571771.0	345751.8	3571760.5	6414.71	827.50	12.0
146	I	322957.3	3563359.2	322960.0	3563354.8	4404.32	2193.25	5.2
148	H	330976.6	3561084.7	330969.6	3561088.6	5236.48	2220.00	8.1
149	I	336884.0	3557833.7	336877.0	3557835.6	5888.27	2393.25	7.2
150	I	343633.2	3563012.3	343640.7	3563018.6	6420.11	1727.00	9.8
151	I	313517.4	3552940.0	313518.2	3552932.7	3738.47	3432.25	7.3
152	I	309233.0	3554858.6	309242.1	3554850.1	3277.10	3349.25	12.5
153	H	320665.4	3549829.7	320667.1	3549822.6	4507.45	3561.75	7.3
154	I	329681.6	3548198.3	329671.7	3548191.5	5420.94	3503.00	12.1
155	I	337166.6	3549815.3	337160.3	3549816.5	6108.79	3164.75	6.4
156	H	334924.0	3545629.4	334926.8	3545642.1	5992.47	3623.75	13.0
157	I	327583.7	3553036.7	327571.3	3553022.8	5100.71	3084.75	18.6
158	I	328329.5	3556593.4	328325.8	3556611.8	5087.56	2718.25	18.8
159	I	325744.3	3543781.4	325737.8	3543784.7	5145.13	4025.50	7.3
163	I	304905.6	3532800.6	304886.9	3532814.5	3384.91	5592.25	23.3
164	I	320102.2	3536358.8	320102.4	3536373.4	4776.50	4880.50	14.6
165	H	317474.3	3530715.5	317479.9	3530709.9	4658.30	5493.25	7.9
166	I	330238.0	3534946.0	330251.6	3534941.2	5796.29	4775.00	14.4
167	I	330419.4	3528361.5	330428.7	3528354.4	5972.13	5410.00	11.7
168	I	321496.0	3574939.1	321502.6	3574928.4	3984.29	1105.25	12.5
169	I	318580.6	3586702.7	318577.0	3586707.8	3416.83	32.75	6.2

Status key: I=In O=Out H=Hold

Desktop Mapping System (DMS) - Geocode Module

```
Total points=          45                                  Pixels     Ground
Used in solution=      35          RMSE solution             1.22      12.17
Withheld for checking= 10          RMSE check                0.93       9.26

Coefficients  (2nd order polynomial)
      9.698       -2.405      0.00000      -0.00000       0.00000  285514.287
     -2.412       -9.710      -0.00000     -0.00000       0.00000 3595269.302
      0.097       -0.026      -0.00000      0.00000       0.00000   62773.967
     -0.020       -0.097      -0.00000     -0.00000      -0.00000  354493.150
```

The following are the results of the tests of the planimetric accuracy of the SPOT Level 1B stereo-model of the reference scene 122/285 using 45 ground control points:

Desktop Mapping System (DMS) - Geocode Module

```
Image control point filename.....: SPOTREG.CP
Ground control point filename....: E:\WEL10\WEST.GCP
Coefficient filename.............: E:\WEL10\WESTL.COF
```

Point	S	True-X	True-Y	Est-X	Est-Y	Image-X	Image-Y	Error-XY
101	I	308544.7	3559870.4	308539.6	3559857.7	3088.25	2880.50	13.7
102	I	300921.8	3557098.6	300930.6	3557097.0	2415.87	3331.75	8.9
110	I	295871.2	3566645.4	295860.2	3566647.8	1693.61	2527.25	11.2
111	I	300741.9	3576801.5	300745.2	3576804.8	1923.57	1424.00	4.6
112	I	309287.9	3582167.2	309300.8	3582165.3	2625.38	697.50	12.9
113	I	304306.2	3580947.3	304311.8	3580947.7	2170.24	936.00	5.6
114	I	297526.4	3574024.4	297517.8	3574027.8	1676.99	1771.25	9.3
116	I	284865.3	3573802.5	284850.2	3573795.7	452.41	2099.00	16.6
118	I	290484.4	3561272.4	290488.8	3561274.2	1301.33	3178.00	4.8
119	I	284545.8	3563607.6	284545.0	3563600.0	668.12	3095.50	7.6
124	I	284233.5	3556247.5	284226.1	3556260.1	813.83	3815.25	14.7
125	I	325223.1	3568548.2	325235.8	3568558.2	4499.95	1633.50	16.2
126	I	326827.1	3574684.1	326820.4	3574681.4	4506.45	1001.00	7.2
127	I	330679.4	3582061.4	330676.9	3582065.3	4703.22	191.25	4.6
128	I	331363.3	3573362.3	331368.5	3573364.6	4979.69	1019.00	5.7
129	I	338783.5	3569542.1	338791.0	3569550.0	5792.07	1210.00	10.9
133	I	278850.4	3542817.3	278860.6	3542811.4	616.58	5249.00	11.8
135	I	279715.0	3554356.7	279724.1	3554369.7	422.11	4107.00	15.9
136	I	282128.6	3547222.1	282130.8	3547224.2	827.90	4742.25	3.1
137	I	292705.7	3551481.9	292706.2	3551475.6	1752.55	4075.25	6.4
140	I	281962.2	3535718.3	281956.5	3535711.4	1088.28	5863.25	8.9
141	I	292955.2	3536500.4	292946.5	3536500.7	2136.56	5522.25	8.6
142	I	292450.8	3547659.9	292464.0	3547657.4	1820.98	4451.50	13.5
143	I	337967.5	3576238.2	337949.0	3576232.4	5549.54	581.75	19.4
145	I	345746.0	3571771.0	345752.3	3571758.4	6414.71	827.50	14.0
146	I	322957.3	3563359.2	322961.2	3563355.9	4404.32	2193.25	5.1
148	I	330976.6	3561084.7	330970.4	3561088.9	5236.48	2220.00	7.5
149	I	336884.0	3557833.7	336877.2	3557834.8	5888.27	2393.25	6.9
150	I	343633.2	3563012.3	343640.7	3563016.7	6420.11	1727.00	8.7
151	I	313517.4	3552940.0	313519.4	3552934.4	3738.47	3432.25	5.9
152	I	309233.0	3554858.6	309243.4	3554852.0	3277.10	3349.25	12.3
153	I	320665.4	3549829.7	320667.9	3549823.8	4507.45	3561.75	6.4
154	I	329681.6	3548198.3	329671.7	3548191.5	5420.94	3503.00	12.0
155	I	337166.6	3549815.3	337159.7	3549815.2	6108.79	3164.75	6.9
156	I	334924.0	3545629.4	334926.0	3545641.1	5992.47	3623.75	11.9
157	I	327583.7	3553036.7	327571.9	3553023.3	5100.71	3084.75	17.8
158	I	328329.5	3556593.4	328326.5	3556612.3	5087.56	2718.25	19.1
159	I	325744.3	3543781.4	325737.8	3543785.0	5145.13	4025.50	7.4
163	I	304905.6	3532800.6	304887.7	3532816.0	3384.91	5592.25	23.6
164	I	320102.2	3536358.8	320102.3	3536374.0	4776.50	4880.50	15.2
165	I	317474.3	3530715.5	317479.5	3530710.4	4658.30	5493.25	7.2
166	I	330238.0	3534946.0	330250.1	3534940.2	5796.29	4775.00	13.4
167	I	330419.4	3528361.5	330426.3	3528352.8	5972.13	5410.00	11.1
168	I	321496.0	3574939.1	321503.7	3574929.5	3984.29	1105.25	12.3
169	I	318580.6	3586702.7	318577.4	3586708.5	3416.83	32.75	6.6

Status key: I=In O=Out H=Hold

Desktop Mapping System (DMS) - Geocode Module

			Pixels	Ground
Total points=	45			
Used in solution=	45	RMSE solution	1.15	11.50
Withheld for checking=	0	RMSE check	0.00	0.00

Coefficients (2nd order polynomial)

9.701	-2.404	0.00000	-0.00000	-0.00000	285508.814

The following are the results of the planimetric accuracy of the Level 1B stereo-model for scene 123/285.

Desktop Mapping System (DMS) - Geocode Module

Image control point filename.....: SPOTREG.CP
Ground control point filename....: E:\WELNW\NW.GCP
Coefficient filename.............: E:\WELNW\TESTLL.COF

Point	S	True-X	True-Y	Est-X	Est-Y	Image-X	Image-Y	Error-XY
126	H	326827.1	3574684.1	326825.6	3574681.7	948.94	4779.50	2.8
127	I	330679.4	3582061.4	330688.5	3582061.2	1155.44	3972.00	9.1
128	H	331363.3	3573362.3	331381.5	3573372.3	1423.12	4802.00	20.8
129	H	338783.5	3569542.1	338783.3	3569537.8	2233.02	5004.75	4.3
145	I	345746.0	3571771.0	345733.3	3571759.8	2859.23	4628.25	16.9
150	I	343633.2	3563012.3	343636.7	3563014.3	2856.79	5528.00	4.1
404	H	377215.9	3566138.9	377195.0	3566162.9	6056.37	4448.00	31.8
502	H	334878.7	3598065.9	334870.4	3598052.9	1194.03	2318.50	15.4
503	I	325159.1	3592448.6	325151.9	3592450.6	376.97	3088.00	7.5
504	H	345777.0	3587347.8	345769.0	3587334.3	2502.77	3111.00	15.7
508	I	389053.2	3584947.8	389060.8	3584951.6	6775.16	2345.00	8.5
512	H	379350.8	3594484.8	379372.4	3594511.1	5608.69	1637.50	34.0
509	I	376121.0	3580644.8	376106.3	3580629.9	5613.71	3064.50	20.9
501	H	334515.3	3591456.2	334537.6	3591446.1	1314.02	2969.50	24.5
510	H	357454.6	3593416.8	357460.7	3593434.5	3500.16	2247.50	18.8
506	O	367447.3	3597536.1	367432.1	3597497.2	4376.70	1622.00	41.8
505	I	354648.1	3607149.1	354658.2	3607144.6	2909.58	977.00	11.1
143	H	337967.5	3576238.2	337953.0	3576207.7	1998.23	4374.50	33.7
507	I	361030.8	3576489.3	361042.9	3576508.9	4241.52	3813.00	23.0
511	I	366460.9	3609365.0	366452.9	3609368.4	4005.55	488.50	8.7

Status key: I=In O=Out H=Hold

			Pixels	Ground
Total points=	20			
Used in solution=	9	RMSE solution	1.37	13.66
Withheld for checking=	10	RMSE check	2.28	22.81

Coefficients (2nd order polynomial)

9.740	-2.306	-0.00000	0.00000	-0.00000	328593.117
-2.305	-9.722	0.00000	-0.00000	0.00000	3623346.294
0.116	-0.019	0.00000	-0.00000	-0.00000	40482.119
-0.022	-0.095	-0.00000	-0.00000	-0.00000	355567.835

The following are the results of the planimetric accuracy of the Level 1B stereo-model for scene 123/286

Desktop Mapping System (DMS) - Geocode Module

```
Image control point filename.....: SPOTREG.CP
Ground control point filename....: F:\WELSW\SW.GCP
Coefficient filename.............: F:\WELSW\TESTL.COF
```

Point	S	True-X	True-Y	Est-X	Est-Y	Image-X	Image-Y	Error-XY
146	I	322957.3	3563359.2	322961.3	3563355.7	788.15	501.75	5.3
148	H	330976.6	3561084.7	330984.7	3561078.3	1622.37	538.00	10.3
149	H	336884.0	3557833.7	336879.3	3557841.1	2271.51	716.75	8.8
150	I	343633.2	3563012.3	343637.4	3563017.8	2810.05	57.25	7.0
151	I	313517.4	3552940.0	313506.9	3552940.7	108.95	1732.75	10.5
153	H	320665.4	3549829.7	320674.9	3549839.4	878.66	1869.00	13.6
154	H	329681.6	3548198.3	329670.3	3548199.1	1792.55	1821.00	11.4
155	H	337166.6	3549815.3	337153.2	3549821.4	2483.80	1490.50	14.7
156	H	334924.0	3545629.4	334924.8	3545642.0	2363.44	1948.50	12.6
157	H	327583.7	3553036.7	327573.6	3553040.1	1476.30	1398.50	10.7
158	H	328329.5	3556593.4	328325.8	3556609.3	1466.91	1034.00	16.3
159	H	325744.3	3543781.4	325742.3	3543785.3	1512.21	2341.00	4.3
164	I	320102.2	3536358.8	320099.5	3536365.9	1134.50	3193.00	7.5
165	O	317474.3	3530715.5	317319.5	3530719.6	994.49	3806.50	154.9
166	I	330238.0	3534946.0	330265.9	3534932.3	2157.42	3098.00	31.0
167	H	330419.4	3528361.5	330424.5	3528359.2	2324.79	3734.00	5.6
201	I	350511.7	3543351.8	350495.8	3543346.3	3933.26	1812.50	16.9
202	H	363799.0	3539196.6	363788.4	3539188.6	5324.48	1910.25	13.2
203	I	375648.1	3535240.0	375653.2	3535236.5	6572.01	2021.00	6.2
204	I	374763.0	3555431.9	374763.6	3555429.3	6019.23	76.50	2.7
206	H	319061.0	3518167.9	319035.6	3518157.6	1451.90	4989.50	27.4
207	I	315011.7	3511658.4	315012.4	3511659.6	1210.50	5714.75	1.4
209	I	339189.0	3505650.7	339180.9	3505648.5	3701.47	5743.00	8.4
210	H	330884.7	3521647.2	330849.9	3521641.7	2521.39	4378.00	35.2
211	O	352931.1	3519576.9	352957.9	3519521.9	4723.10	4074.50	61.1
212	I	359260.9	3503218.9	359265.2	3503219.8	5713.08	5516.50	4.4
213	H	368483.7	3521471.3	368487.3	3521460.4	6191.27	3527.50	11.6
215	I	341769.8	3534241.1	341763.9	3534249.0	3292.90	2899.25	9.8
515	H	357684.0	3559195.2	357665.2	3559214.1	4265.03	103.25	26.7
302	I	368042.5	3537681.9	368038.8	3537689.8	5773.28	1958.00	8.7

Status key: I=In O=Out H=Hold

			Pixels	Ground
Total points=	30			
Used in solution=	13	RMSE solution	1.18	11.77
Withheld for checking=	15	RMSE check	1.70	16.97

Coefficients (2nd order polynomial)

9.719	-2.319	-0.00000	0.00000	0.00000	316464.177
-2.308	-9.735	0.00000	0.00000	0.00000	3570058.823
0.092	-0.017	0.00000	-0.00000	0.00000	42222.814
-0.020	-0.105	-0.00000	0.00000	-0.00000	367979.475

The following are the results of the planimetric accuracy of the Level 1B stereo-model for scene 124/285.

Desktop Mapping System (DMS) - Geocode Module

Image control point filename.....: SPOTREG.CP
Ground control point filename....: E:\WELNEM\NE.GCP
Coefficient filename.............: E:\WELNEM\TESTL.COF

Point	S	True-X	True-Y	Est-X	Est-Y	Image-X	Image-Y	Error-XY
314	H	416258.3	3559482.4	416273.0	3559465.3	4591.82	5477.50	22.6
315	I	400242.7	3562606.1	400253.0	3562613.5	2960.77	5543.50	12.6
401	H	423469.0	3597161.8	423440.3	3597158.5	4417.65	1645.00	28.9
403	H	410179.9	3592074.5	410174.9	3592084.8	3243.98	2447.00	11.4
404	I	377215.9	3566138.9	377209.3	3566130.1	636.62	5736.00	11.0
405	I	384893.1	3608353.8	384900.2	3608360.1	402.11	1450.50	9.6
406	H	400814.7	3608976.6	400805.8	3608980.2	1937.61	1021.00	9.5
407	I	401283.8	3618271.3	401277.7	3618266.0	1766.28	106.50	8.0
408	H	391498.3	3618422.8	391525.1	3618424.8	811.94	317.50	26.9
409	I	395605.6	3572832.7	395606.9	3572844.9	2272.05	4656.50	12.3
410	I	407856.0	3580587.1	407850.7	3580574.9	3284.80	3620.50	13.3
411	I	447605.4	3604588.0	447608.5	3604591.4	6597.77	359.00	4.6
412	H	425744.6	3580252.6	425716.0	3580257.9	5030.86	3236.00	29.1
414	O	424195.6	3612833.3	424195.2	3612903.5	4124.59	95.50	70.3
415	I	436331.9	3566523.6	436328.1	3566520.5	6379.96	4325.00	4.8
508	H	389053.2	3584947.8	389056.8	3584937.4	1353.67	3632.50	11.0
509	O	376121.0	3580644.8	376121.7	3580602.2	194.70	4354.00	42.6
512	H	379350.8	3594484.8	379353.3	3594478.7	186.13	2929.50	6.6

Status key: I=In O=Out H=Hold

			Pixels	Ground
Total points=	18			
Used in solution=	8	RMSE solution	1.01	10.05
Withheld for checking=	8	RMSE check	2.03	20.30

Coefficients (2nd order polynomial)

9.698	-2.343	0.00000	0.00000	0.00000	384392.845
-2.312	-9.717	-0.00000	-0.00000	-0.00000	3623388.252
0.088	-0.002	-0.00000	-0.00000	0.00000	9862.704
-0.022	-0.092	-0.00000	-0.00000	-0.00000	351107.610

The following are the results of the planimetric accuracy of the Level 1B stereo-model for scene 124/286.

Desktop Mapping System (DMS) - Geocode Module

```
Image control point filename.....: SPOTREG.CP
Ground control point filename....: F:\WELSE\SE.GCP
Coefficient filename.............: F:\WELSE\TESTLL.COF
```

Point	S	True-X	True-Y	Est-X	Est-Y	Image-X	Image-Y	Error-XY
203	I	375648.1	3535240.0	375664.2	3535233.5	1134.15	3090.50	17.4
204	I	374763.0	3555431.9	374759.6	3555427.9	576.66	1146.50	5.3
301	I	363529.2	3512142.4	363531.4	3512145.1	492.13	5618.00	3.5
302	I	368042.5	3537681.9	368031.7	3537687.2	334.58	3028.25	12.0
303	I	389811.5	3531696.7	389828.2	3531704.4	2595.19	3106.75	18.4
304	I	412380.1	3524083.2	412392.2	3524085.2	4971.73	3328.50	12.2
306	I	380363.2	3522860.3	380370.5	3522858.1	1879.56	4186.75	7.6
307	I	388019.9	3526598.3	388024.8	3526611.7	2537.56	3644.50	14.2
308	I	399431.4	3521857.8	399409.3	3521841.1	3757.19	3846.75	27.7
309	I	398273.6	3529545.6	398266.0	3529557.7	3467.27	3121.00	14.3
310	I	393224.5	3543170.4	393213.2	3543159.3	2659.78	1912.75	15.9
213	I	368483.7	3521471.3	368475.9	3521465.1	755.36	4596.75	10.1
404	I	377215.9	3566138.9	377219.5	3566142.7	567.30	47.25	5.3

Status key: I=In O=Out H=Hold

			Pixels	Ground
Total points=	13			
Used in solution=	13	RMSE solution	1.41	14.11
Withheld for checking=	0	RMSE check	0.00	0.00

Coefficients (2nd order polynomial)

9.709	-2.323	-0.00000	-0.00000	0.00001	371822.287
-2.324	-9.730	0.00000	0.00000	0.00000	3567920.109
0.077	-0.025	0.00000	-0.00000	0.00000	53093.764
-0.008	-0.107	0.00000	0.00000	-0.00000	369797.914

C.3.1 Accuracy Results in Height in the DEM of the Level 1B Stereo-model for the Reference Scene 122/285

In this section, the corresponding results in elevation at the ground control points derived from the image matching operation of the DMS system are presented.

No.	X (m)	Y (m)	GCP- H (m)	Cal. H (m)	Δ H (m)
- 101	308544.7	3559871	810.299	814.1334	3.834412
102	300921.8	3557099	797.659	797.2563	-.4026489
110	295871.2	3566646	942.609	941.6378	-.9711914
-111	300741.9	3576802	1104.942	1108.525	3.583374
112	309287.9	3582167	1093.675	1093.406	-.2687988
113	304306.2	3580947	1153.919	1147.248	-6.670532
114	297526.4	3574025	1059.898	1060.591	.6934814
116	284865.3	3573803	990.834	985.591	-5.242981
118	290484.4	3561273	847.957	840.1382	-7.818787
-119	284545.8	3563608	836.672	835.5515	-1.120544
124	284233.5	3556248	705.601	703.7303	-1.870667
125	325223.1	3568548	747.516	744.7488	-2.767151
-126	326827.1	3574684	758.239	757.0544	-1.184631
127	330679.4	3582062	741.388	741.1438	-.2442017
128	331363.3	3573362	714.602	711.9664	-2.635559
129	338783.5	3569542	720.909	723.8526	2.943604
133	278850.4	3542817	589.206	585.2552	-3.950745
135	279715	3554357	666.974	662.7118	-4.262207
-136	282128.6	3547222	611.143	601.184	-9.958984
137	292705.7	3551482	708.999	718.5498	9.550781
-141	292955.2	3536501	541.52	558.9075	17.38751
142	292450.8	3547660	675.238	674.8821	-.355835
143	337967.5	3576238	716.597	713.1241	-3.4729
146	322957.3	3563359	707.785	709.9274	2.142395
-148	330976.6	3561085	653.063	655.0425	1.979553
149	336884	3557834	644.062	642.3881	-1.673889
151	313517.3	3552940	716.645	723.8874	7.242371
152	309233	3554859	751.13	752.0717	.9416504
-153	320665.3	3549830	629.794	629.5698	-.2241821
154	329681.7	3548198	625.959	630.2473	4.288269
155	337166.6	3549815	631.489	640.4308	8.941772
-156	334924	3545630	628.161	632.8251	4.664063
157	327583.7	3553037	643.164	641.5046	-1.659363
158	328329.5	3556593	646.406	642.3149	-4.091064
159	325744.3	3543782	633.968	633.9988	3.082275
162	308314.3	3542498	603.401	597.4194	-5.981628
163	304905.6	3532801	536.498	543.2672	6.769165
164	320102.2	3536359	627.516	627.5605	4.449463
-165	317474.3	3530716	605.417	601.5588	-3.858215
166	330238.1	3534946	594.12	601.184	7.064026
167	330419.4	3528362	596.827	592.1012	-4.72583
168	321496	3574939	793.943	793.632	-.3110352
169	318580.6	3586703	954.594	944.1272	-10.4668
103	294889.3	3559725	814.225	820.4595	6.234497

RMSE = 10 Check Points = ±6.87m
RMSE = 34 Control Points = ±4.88 m

No.	X (m)	Y (m)	GCP- H (m)	Cal. H (m)	Δ H (m)
- 101	308544.7	3559871	810.299	814.0666	3.767578
102	300921.8	3557099	797.659	799.4015	1.742493

110	295871.2	3566646	942.609	941.6377	-.9713135
-111	300741.9	3576802	1104.942	1108.836	3.893677
112	309287.9	3582167	1093.675	1093.406	-.2687988
-113	304306.2	3580947	1153.919	1148.019	-5.899536
114	297526.4	3574025	1059.898	1060.591	.6934814
116	284865.3	3573803	990.834	985.8342	-4.999817
118	290484.4	3561273	847.957	841.0826	-6.874329
-119	284545.8	3563608	836.672	835.4727	-1.199341
124	284233.5	3556248	705.601	703.7303	-1.870728
125	325223.1	3568548	747.516	744.7489	-2.76709
-126	326827.1	3574684	758.239	757.3791	-.8599243
127	330679.4	3582062	741.388	741.7089	.3209229
-128	331363.3	3573362	714.602	712.1135	-2.488464
129	338783.5	3569542	720.909	724.2396	3.330627
133	278850.4	3542817	589.206	583.437	-5.768982
135	279715	3554357	666.974	662.7118	-4.262207
-136	282128.6	3547222	611.143	601.184	-9.958984
137	292705.7	3551482	708.999	719.3288	10.32977
-141	292955.2	3536501	541.52	560.3114	18.79138
142	292450.8	3547660	675.238	675.0341	-.2039185
-143	337967.5	3576238	716.597	712.1172	-4.479736
146	322957.3	3563359	707.785	710.515	2.72998
-148	330976.6	3561085	653.063	656.2426	3.179565
149	336884	3557834	644.062	642.2025	-1.859497
-151	313517.3	3552940	716.645	723.8668	7.221741
152	309233	3554859	751.13	751.8848	.7547607
-153	320665.3	3549830	629.794	628.951	-.8430176
154	329681.7	3548198	625.959	630.2493	4.290283
155	337166.6	3549815	631.489	641.889	10.39996
-156	334924	3545630	628.161	635.1322	6.971191
157	327583.7	3553037	643.164	641.6326	-1.531372
158	328329.5	3556593	646.406	642.6936	-3.712402
159	325744.3	3543782	633.968	633.9988	3.076172
162	308314.3	3542498	603.401	600.0218	-3.379211
163	304905.6	3532801	536.498	539.8132	3.315186
164	320102.2	3536359	627.516	628.1443	.6283569
-165	317474.3	3530716	605.417	601.8675	-3.5495
166	330238.1	3534946	594.12	601.184	7.064026
-167	330419.4	3528362	596.827	599.7198	2.892761
168	321496	3574939	793.943	793.8802	-6.280518
169	318580.6	3586703	954.594	943.8842	-10.70984
103	294889.3	3559725	814.225	819.8613	5.636292

RMSE 15 Check Points = ±6.72m
RMSE 29 Control Points = ±4.84m

No.	X (m)	Y (m)	GCP- H (m)	Cal. H (m)	Δ H (m)
- 101	308544.7	3559871	810.299	814.3302	4.031189
102	300921.8	3557099	797.659	797.419	-.2399902
110	295871.2	3566646	942.609	941.6378	-.9711914
-111	300741.9	3576802	1104.942	1108.224	3.281494
112	309287.9	3582167	1093.675	1093.406	-.2687988
113	304306.2	3580947	1153.919	1147.12	-6.798462
114	297526.4	3574025	1059.898	1060.591	.6934814
116	284865.3	3573803	990.834	985.6864	-5.147583
118	290484.4	3561273	847.957	840.7546	-7.202332
-119	284545.8	3563608	836.672	835.4331	-1.238892
-124	284233.5	3556248	705.601	703.7303	-1.870728
125	325223.1	3568548	747.516	744.7488	-2.767151

-126	326827.1	3574684	758.239	757.0994	-1.139648
127	330679.4	3582062	741.388	740.3472	-1.040833
-128	331363.3	3573362	714.602	712.0392	-2.562744
129	338783.5	3569542	720.909	723.5642	2.655212
-133	278850.4	3542817	589.206	582.3095	-6.896484
135	279715	3554357	666.974	662.7118	-4.262207
-136	282128.6	3547222	611.143	601.184	-9.958984
137	292705.7	3551482	708.999	717.2589	8.259827
-141	292955.2	3536501	541.52	559.7868	18.26678
142	292450.8	3547660	675.238	674.8645	-.3734741
-143	337967.5	3576238	716.597	713.7886	-2.80835
146	322957.3	3563359	707.785	710.1738	2.388794
-148	330976.6	3561085	653.063	654.6647	1.601746
-149	336884	3557834	644.062	642.7035	-1.358521
-151	313517.3	3552940	716.645	724.2396	7.594604
152	309233	3554859	751.13	752.5403	1.410278
-153	320665.3	3549830	629.794	629.8804	8.642578
154	329681.7	3548198	625.959	630.5969	4.637878
-155	337166.6	3549815	631.489	639.0623	7.573242
-156	334924	3545630	628.161	636.3384	8.177368
157	327583.7	3553037	643.164	641.2756	-1.888428
158	328329.5	3556593	646.406	642.2025	-4.203491
159	325744.3	3543782	633.968	633.9988	3.082275
162	308314.3	3542498	603.401	600.7426	-2.658447
163	304905.6	3532801	536.498	540.5639	4.065918
-164	320102.2	3536359	627.516	629.8755	2.359497
-165	317474.3	3530716	605.417	601.184	-4.232971
166	330238.1	3534946	594.12	601.184	7.064026
-167	330419.4	3528362	596.827	592.5548	-4.272217
168	321496	3574939	793.943	792.7977	-1.145325
169	318580.6	3586703	954.594	944.0893	-10.5047
103	294889.3	3559725	814.225	819.3256	5.100647
170	304708.6	3572786	1033.718	1037.086	3.367798
117	288243.3	3568402	945.384	949.2573	3.873352
120	280182.8	3565344	827.529	818.2147	-9.314331
115	292203	3575577	1049.674	1049.745	7.141113
161	320261.4	3544825	625.724	622.6371	-3.086853

RMSE = 20 Check Points = ±6.62 m
RMSE = 24 Control Points = ±4.35 m

No.	X (m)	Y (m)	GCP- H (m)	Cal. H (m)	Δ H (m)
-101	308544.7	3559871	810.299	814.3302	4.031189
-102	300921.8	3557099	797.659	797.419	-.2399902
110	295871.2	3566646	942.609	941.6378	-.9711914
-111	300741.9	3576802	1104.942	1108.224	3.281494
112	309287.9	3582167	1093.675	1093.406	-.2687988
-113	304306.2	3580947	1153.919	1147.12	-6.798462
-114	297526.4	3574025	1059.898	1060.591	.6934814
116	284865.3	3573803	990.834	985.6864	-5.147583
118	290484.4	3561273	847.957	840.7546	-7.202332
-119	284545.8	3563608	836.672	835.4331	-1.238892
-124	284233.5	3556248	705.601	703.7303	-1.870728
125	325223.1	3568548	747.516	744.7488	-2.767151
-126	326827.1	3574684	758.239	757.0994	-1.139648
127	330679.4	3582062	741.388	740.3472	-1.040833
-128	331363.3	3573362	714.602	712.0392	-2.562744
129	338783.5	3569542	720.909	723.5642	2.655212
-133	278850.4	3542817	589.206	582.3095	-6.896484

135	279715	3554357	666.974	662.7118	-4.262207
-136	282128.6	3547222	611.143	601.184	-9.958984
-137	292705.7	3551482	708.999	717.2589	8.259827
-141	292955.2	3536501	541.52	559.7868	18.26678
142	292450.8	3547660	675.238	674.8645	-.3734741
-143	337967.5	3576238	716.597	713.7886	-2.80835
-146	322957.3	3563359	707.785	710.1738	2.388794
-148	330976.6	3561085	653.063	654.6647	1.601746
-149	336884	3557834	644.062	642.7035	-1.358521
-151	313517.3	3552940	716.645	724.2396	7.594604
152	309233	3554859	751.13	752.5403	1.410278
-153	320665.3	3549830	629.794	629.8804	8.642578
154	329681.7	3548198	625.959	630.5969	4.637878
-155	337166.6	3549815	631.489	639.0623	7.573242
-156	334924	3545630	628.161	636.3384	8.177368
157	327583.7	3553037	643.164	641.2756	-1.888428
158	328329.5	3556593	646.406	642.2025	-4.203491
159	325744.3	3543782	633.968	633.9988	3.082
162	308314.3	3542498	603.401	600.7426	-2.658447
163	304905.6	3532801	536.498	540.5639	4.065918
-164	320102.2	3536359	627.516	629.8755	2.359497
-165	317474.3	3530716	605.417	601.184	-4.232971
166	330238.1	3534946	594.12	601.184	7.064026
-167	330419.4	3528362	596.827	592.5548	-4.272217
-168	321496	3574939	793.943	792.7977	-1.145325
169	318580.6	3586703	954.594	944.0893	-10.5047
103	294889.3	3559725	814.225	819.3256	5.100647

RMSE = 25 Check Points = ±6.17 m
RMSE = 19 Control Points = ±4.46 m

No.	X (m)	Y (m)	GCP- H (m)	Cal. H (m)	Δ H (m)
- 101	308544.7	3559871	810.299	813.636	3.337036
-102	300921.8	3557099	797.659	797.4047	-.2542725
110	295871.2	3566646	942.609	941.6377	-.9713135
-111	300741.9	3576802	1104.942	1109.039	4.096924
112	309287.9	3582167	1093.675	1093.406	-.2686768
-113	304306.2	3580947	1153.919	1147.643	-6.276001
-114	297526.4	3574025	1059.898	1060.591	.6934814
116	284865.3	3573803	990.834	985.7764	-5.057556
118	290484.4	3561273	847.957	840.2907	-7.66626
-119	284545.8	3563608	836.672	835.5515	-1.120544
-124	284233.5	3556248	705.601	703.7303	-1.870667
-125	325223.1	3568548	747.516	744.7488	-2.767151
-126	326827.1	3574684	758.239	757.6559	-.5831299
127	330679.4	3582062	741.388	743.3879	1.999878
-128	331363.3	3573362	714.602	711.934	-2.667969
-129	338783.5	3569542	720.909	724.2396	3.330566
-133	278850.4	3542817	589.206	585.3611	-3.84491
135	279715	3554357	666.974	662.7118	-4.262207
-136	282128.6	3547222	611.143	601.184	-9.958984
-137	292705.7	3551482	708.999	719.6789	10.67987
-141	292955.2	3536501	541.52	558.997	17.47699
-142	292450.8	3547660	675.238	674.8452	-.3928223
-143	337967.5	3576238	716.597	711.938	-4.658997
-146	322957.3	3563359	707.785	710.8815	3.096497
-148	330976.6	3561085	653.063	656.3298	3.266846
-149	336884	3557834	644.062	643.3354	-.7266235
-151	313517.3	3552940	716.645	722.153	5.507935

152	309233	3554859	751.13	751.6517	.5216675
-153	320665.3	3549830	629.794	629.6371	-.1569214
-154	329681.7	3548198	625.959	629.8958	3.936829
-155	337166.6	3549815	631.489	641.0673	9.578308
-156	334924	3545630	628.161	633.5637	5.402649
157	327583.7	3553037	643.164	642.1122	-1.051819
158	328329.5	3556593	646.406	642.9	-3.506042
-159	325744.3	3543782	633.968	633.9988	3.082275
162	308314.3	3542498	603.401	595.7617	-7.639282
163	304905.6	3532801	536.498	544.8345	8.336548
-164	320102.2	3536359	627.516	625.2529	-2.263062
165	317474.3	3530716	605.417	605.5135	9.655762
-166	330238.1	3534946	594.12	601.184	7.064026
-167	330419.4	3528362	596.827	599.038	2.210999
-168	321496	3574939	793.943	795.0916	1.148621
169	318580.6	3586703	954.594	944.6187	-9.975342
103	294889.3	3559725	814.225	821.1403	6.915344

RMSE = 30 Check Points = ±5.52m
RMSE = 14 Control Points = ±5.9 m

No.	X (m)	Y (m)	GCP- H (m)	Cal. H (m)	Δ H (m)
- 101	308544.7	3559871	810.299	813.636	3.337036
-102	300921.8	3557099	797.659	797.4047	-.2542725
110	295871.2	3566646	942.609	941.6377	-.9713135
-111	300741.9	3576802	1104.942	1109.039	4.096924
112	309287.9	3582167	1093.675	1093.406	-.2686768
-113	304306.2	3580947	1153.919	1147.643	-6.276001
-114	297526.4	3574025	1059.898	1060.591	.6934814
116	284865.3	3573803	990.834	985.7764	-5.057556
118	290484.4	3561273	847.957	840.2907	-7.66626
-119	284545.8	3563608	836.672	835.5515	-1.120544
-124	284233.5	3556248	705.601	703.7303	-1.870667
-125	325223.1	3568548	747.516	744.7488	-2.767151
-126	326827.1	3574684	758.239	757.6559	-.5831299
-127	330679.4	3582062	741.388	743.3879	1.999878
-128	331363.3	3573362	714.602	711.934	-2.667969
-129	338783.5	3569542	720.909	724.2396	3.330566
-133	278850.4	3542817	589.206	585.3611	-3.84491
135	279715	3554357	666.974	662.7118	-4.262207
-136	282128.6	3547222	611.143	601.184	-9.958984
-137	292705.7	3551482	708.999	719.6789	10.67987
-141	292955.2	3536501	541.52	558.997	17.47699
-142	292450.8	3547660	675.238	674.8452	-.3928223
-143	337967.5	3576238	716.597	711.938	-4.658997
-146	322957.3	3563359	707.785	710.8815	3.096497
-148	330976.6	3561085	653.063	656.3298	3.266846
-149	336884	3557834	644.062	643.3354	-.7266235
-151	313517.3	3552940	716.645	722.153	5.507935
152	309233	3554859	751.13	751.6517	.5216675
-153	320665.3	3549830	629.794	629.6371	-.1569214
-154	329681.7	3548198	625.959	629.8958	3.936829
-155	337166.6	3549815	631.489	641.0673	9.578308
-156	334924	3545630	628.161	633.5637	5.402649
157	327583.7	3553037	643.164	642.1122	-1.051819
158	328329.5	3556593	646.406	642.9	-3.506042
-159	325744.3	3543782	633.968	633.9988	3.082275
162	308314.3	3542498	603.401	595.7617	-7.639282
163	304905.6	3532801	536.498	544.8345	8.336548

-164	320102.2	3536359	627.516	625.2529	-2.263062
-165	317474.3	3530716	605.417	605.5135	9.655762
166	330238.1	3534946	594.12	601.184	7.064026
-167	330419.4	3528362	596.827	599.038	2.210999
-168	321496	3574939	793.943	795.0916	1.148621
169	318580.6	3586703	954.594	944.6187	-9.975342
103	294889.3	3559725	814.225	821.1403	6.915344
-170	304708.6	3572786	1033.718	1035.399	1.680542
-117	288243.3	3568402	945.384	949.5799	4.195923
-120	280182.8	3565344	827.529	817.3456	-10.18335
-115	292203	3575577	1049.674	1050.186	.5119629
-161	320261.4	3544825	625.724	621.6932	-4.030762

RMSE = Check Points 35 = ±5.17m
RMSE = Control Points 14 = ±5.9 m

C.3.2 Accuracy Results in Height in the DEM of the Level 1B Stereo-model for Scene 123/285

No.	X (m)	Y (m)	GCP- H (m)	Cal. H (m)	Δ H (m)
- 126	326827.1	3574684	758.239	764.1753	5.936279
127	330679.4	3582062	741.388	750.8002	9.41217
-128	331363.3	3573362	714.602	716.3984	1.796448
-129	338783.5	3569542	720.909	727.8657	6.956665
-143	337967.5	3576238	716.597	724.8156	8.218628
145	345746	3571771	767.193	773.7346	6.541626
150	343633.2	3563012	701.709	706.5195	4.810486
-404	377215.9	3566139	850.916	850.5487	-.3673096
-501	334515.3	3591456	733.624	727.8332	-5.790833
-502	334878.7	3598066	733.676	729.2853	-4.390686
503	325159.1	3592449	790.749	796.9183	6.169312
-504	345777	3587348	806.769	810.1146	3.345642
505	354648.1	3607149	893.16	876.1805	-16.97943
507	361030.8	3576489	923.003	924.72	1.717041
508	389053.2	3584948	733.406	714.8646	-18.54138
509	376121	3580645	847.942	832.3364	-15.60559
-510	357454.6	3593417	952.471	939.2606	-13.21045
-515	357684	3559195	765.688	772.4736	6.785645

RMSE = 10 Check Points = ±6.63 m
RMSE = 8 Control Points = ±11.57 m

No.	X (m)	Y (m)	GCP- H (m)	Cal. H (m)	Δ H (m)
- 126	326827.1	3574684	758.239	759.7683	1.529297
127	330679.4	3582062	741.388	748.0244	6.636414
-128	331363.3	3573362	714.602	714.2617	-.340332
-129	338783.5	3569542	720.909	724.5366	3.627625
-143	337967.5	3576238	716.597	721.413	4.815979
145	345746	3571771	767.193	771.5122	4.319214
150	343633.2	3563012	701.709	702.6755	.9664917
-404	377215.9	3566139	850.916	846.5198	-4.396179
-501	334515.3	3591456	733.624	726.1542	-7.469788
-502	334878.7	3598066	733.676	727.4605	-6.215515
503	325159.1	3592449	790.749	795.0000	4.250977
-504	345777	3587348	806.769	806.8126	.0435791
-505	354648.1	3607149	893.16	872.9521	-20.20789
506	367447.3	3597536	870.331	850.9554	-19.37561
507	361030.8	3576489	923.003	922.5052	-.4978027

508	389053.2	3584948	733.406	712.1091	-21.29688
509	376121	3580645	847.942	829.3841	-18.55792
- 510	357454.6	3593417	952.471	940.8391	-11.6319
515	357684	3559195	765.688	768.2361	2.548096

RMSE = 10 Check Points = ±8.34m
RMSE = 8 Check Points = ±10.50m

No.	X (m)	Y (m)	GCP- H (m)	Cal. H (m)	Δ H (m)
-126	326827.1	3574684	758.239	758.5139	.2749023
127	330679.4	3582062	741.388	745.7914	4.403381
-128	331363.3	3573362	714.602	711.2587	-3.343323
-129	338783.5	3569542	720.909	722.3005	1.391479
-143	337967.5	3576238	716.597	713.2084	-3.388611
145	345746	3571771	767.193	769.4189	2.225952
150	343633.2	3563012	701.709	684.3041	-17.40485
-404	377215.9	3566139	850.916	849.3311	-1.5849
-501	334515.3	3591456	733.624	725.0016	-8.622375
-502	334878.7	3598066	733.676	725.0472	-8.628784
503	325159.1	3592449	790.749	793.0466	2.297546
-504	345777	3587348	806.769	801.6714	-5.097595
505	354648.1	3607149	893.16	866.2665	-26.89349
507	361030.8	3576489	923.003	919.4051	-3.5979
508	389053.2	3584948	733.406	736.4424	3.036438
509	376121	3580645	847.942	817.8763	-30.06567
-510	357454.6	3593417	952.471	940.8558	-11.61523
-512	379350.8	3594485	791.595	765.0108	-26.58417

RMSE = 10 Check Points = ±10.21 m
RMSE = 8 Control Points = ±15.74m

No.	X (m)	Y (m)	GCP- H (m)	Cal. H (m)	Δ H (m)
-126	326827.1	3574684	758.239	759.0684	.8293457
127	330679.4	3582062	741.388	744.5552	3.167175
-128	331363.3	3573362	714.602	709.3417	-5.260315
-129	338783.5	3569542	720.909	723.5636	2.654602
-143	337967.5	3576238	716.597	712.5851	-4.011902
145	345746	3571771	767.193	769.1394	1.946411
150	343633.2	3563012	701.709	704.6215	2.912537
-404	377215.9	3566139	850.916	841.236	-9.680054
-501	334515.3	3591456	733.624	723.7029	-9.921082
-502	334878.7	3598066	733.676	725.073	-8.603027
503	325159.1	3592449	790.749	792.6272	1.878174
-504	345777	3587348	806.769	805.5913	-1.177673
505	354648.1	3607149	893.16	870.224	-22.93597
506	367447.3	3597536	870.331	845.7262	-24.6048
507	361030.8	3576489	923.003	919.8	-3.203003
509	376121	3580645	847.942	819.1459	-28.79608
-510	357454.6	3593417	952.471	942.695	-9.776001
-512	379350.8	3594485	791.595	765.5336	-26.0614

RMSE = 10 Check Points = ±10.45m
RMSE = 8 Control Points = ±15.80m

C.3.3 Accuracy Results in Height in the DEM of the Level 1B Stereo-model for Scene 123/286

No.	X (m)	Y (m)	GCP- H (m)	Cal. H (m)	Δ H (m)
146	322957.3	3563359	707.785	709.8377	2.052734
-148	330976.6	3561085	653.063	650.1398	-2.923218
-149	336884	3557834	644.062	639.66	-4.401978
150	343633.2	3563012	701.709	697.953	-3.755981
151	313517.3	3552940	716.645	718.8905	2.245483
-153	320665.3	3549830	629.794	638.2561	8.462097
-154	329681.7	3548198	625.959	627.6549	1.695923
-155	337166.6	3549815	631.489	638.0724	6.583374
-156	334924	3545630	628.161	635.9289	7.767883
-157	327583.7	3553037	643.164	639.4728	-3.691162
-158	328329.5	3556593	646.406	640.0278	-6.378174
-159	325744.3	3543782	633.968	638.2561	4.288086
161	320261.4	3544825	625.724	626.3724	.6483765
164	320102.2	3536359	627.516	638.256	10.74005
165	317474.3	3530716	605.417	614.7474	9.330383
166	330238.1	3534946	594.12	602.605	8.484985
-167	330419.4	3528362	596.827	612.3496	15.52258
201	350511.7	3543352	655.899	662.0235	6.124512
-202	363799	3539197	713.74	716.3713	2.631287
204	374763	3555432	902.724	901.415	-1.30896
-206	319061	3518168	567.414	567.6921	.2780762
207	315011.7	3511658	548.856	545.5632	-3.292847
209	339189	3505651	542.238	545.5632	3.325195
-210	330884.8	3521647	588.409	602.4346	14.02557
211	352931.1	3519577	597.818	601.1799	3.361877
212	359260.9	3503219	660.695	662.0235	1.328491
-213	368483.7	3521471	727.43	729.0291	1.59906
215	341769.8	3534241	622.585	626.6575	4.072449
-515	357684	3559195	765.688	763.7373	-1.950684
302	368042.4	3537682	732.539	733.0217	.482666

RMSE = 15 Check Points = ±6.97m
RMSE = 12 Control Points = ±4.92 m

No.	X (m)	Y (m)	GCP- H (m)	Cal. H (m)	Δ H (m)
146	322957.3	3563359	707.785	709.8377	2.052734
-148	330976.6	3561085	653.063	650.1398	-2.923218
-149	336884	3557834	644.062	639.66	-4.401978
150	343633.2	3563012	701.709	697.953	-3.755981
151	313517.3	3552940	716.645	718.8905	2.245483
-153	320665.3	3549830	629.794	638.2561	8.462097
-154	329681.7	3548198	625.959	627.6549	1.695923
-155	337166.6	3549815	631.489	638.0724	6.583374
-156	334924	3545630	628.161	635.9289	7.767883
-157	327583.7	3553037	643.164	639.4728	-3.691162
-158	328329.5	3556593	646.406	640.0278	-6.378174
-159	325744.3	3543782	633.968	638.2561	4.288086
-161	320261.4	3544825	625.724	626.3724	.6483765
164	320102.2	3536359	627.516	638.256	10.74005
-165	317474.3	3530716	605.417	614.7474	9.330383
166	330238.1	3534946	594.12	602.605	8.484985
-167	330419.4	3528362	596.827	612.3496	15.52258
201	350511.7	3543352	655.899	662.0235	6.124512
-202	363799	3539197	713.74	716.3713	2.631287
204	374763	3555432	902.724	901.415	-1.30896

-206	319061	3518168	567.414	567.6921	.2780762
207	315011.7	3511658	548.856	545.5632	-3.292847
209	339189	3505651	542.238	545.5632	3.325195
-210	330884.8	3521647	588.409	602.4346	14.02557
-211	352931.1	3519577	597.818	601.1799	3.361877
212	359260.9	3503219	660.695	662.0235	1.328491
-213	368483.7	3521471	727.43	729.0291	1.59906
215	341769.8	3534241	622.585	626.6575	4.072449
-515	357684	3559195	765.688	763.7373	-1.950684
302	368042.4	3537682	732.539	733.0217	.482666

RMSE = 18 Check Points = ±6.84m
RMSE = 12 Control Points = ±4.92m

No.	X (m)	Y (m)	GCP- H (m)	Cal. H (m)	Δ H (m)
146	322957.3	3563359	707.785	708.8657	1.080688
-148	330976.6	3561085	653.063	646.2319	-6.831055
-149	336884	3557834	644.062	643.3342	-.7277832
150	343633.2	3563012	701.709	701.2766	-.432373
151	313517.3	3552940	716.645	713.3001	-3.34491
-153	320665.3	3549830	629.794	632.3478	2.553772
-154	329681.7	3548198	625.959	631.1394	5.18042
-155	337166.6	3549815	631.489	631.9767	.4876709
-157	327583.7	3553037	643.164	643.1629	-1.098633
-158	328329.5	3556593	646.406	642.4493	-3.956665
-159	325744.3	3543782	633.968	631.1394	-2.828613
-161	320261.4	3544825	625.724	631.1394	5.415405
164	320102.2	3536359	627.516	631.1394	3.623413
-165	317474.3	3530716	605.417	620.6093	15.19226
166	330238.1	3534946	594.12	597.0728	2.952759
-167	330419.4	3528362	596.827	609.0963	12.26923
201	350511.7	3543352	655.899	661.4583	5.559265
-202	363799	3539197	713.74	720.0074	6.267395
203	375648.1	3535240	741.806	747.3668	5.56073
204	374763	3555432	902.724	898.938	-3.78595
-206	319061	3518168	567.414	570.0558	2.641846
207	315011.7	3511658	548.856	546.3175	-2.538513
209	339189	3505651	542.238	538.9591	-3.27887
-210	330884.8	3521647	588.409	588.9962	.5871582
-211	352931.1	3519577	597.818	599.4392	1.621216
212	359260.9	3503219	660.695	667.0057	6.31073
-213	368483.7	3521471	727.43	728.8358	1.405823
215	341769.8	3534241	622.585	629.1277	6.542725
-515	357684	3559195	765.688	760.5104	-5.177612
302	368042.4	3537682	732.539	737.3472	4.808167

RMSE = 18 Check Points = ±5.75 m
RMSE = 12 Control Points = ±4.40m

No.	X (m)	Y (m)	GCP- H (m)	Cal. H (m)	Δ H (m)
146	322957.3	3563359	707.785	703.7443	-4.040649
-148	330976.6	3561085	653.063	640.8042	-12.25879
-149	336884	3557834	644.062	637.7799	-6.282104
150	343633.2	3563012	701.709	696.6494	-5.059631
151	313517.3	3552940	716.645	708.9705	-7.6745
-153	320665.3	3549830	629.794	627.8796	-1.914429
-154	329681.7	3548198	625.959	626.5588	.5997925
-155	337166.6	3549815	631.489	627.0837	-4.405273

156	334924	3545630	628.161	626.5588	-1.602234
-157	327583.7	3553037	643.164	637.5104	-5.653564
-158	328329.5	3556593	646.406	636.8605	-9.545532
-159	325744.3	3543782	633.968	626.5588	-7.409241
-161	320261.4	3544825	625.724	626.5588	.8347778
164	320102.2	3536359	627.516	626.5588	-.9572144
-165	317474.3	3530716	605.417	616.0978	10.68085
166	330238.1	3534946	594.12	592.8044	-1.315552
-167	330419.4	3528362	596.827	602.891	6.063965
201	350511.7	3543352	655.899	656.3651	.4661255
-202	363799	3539197	713.74	714.6985	.9585571
203	375648.1	3535240	741.806	742.6463	.840271
204	374763	3555432	902.724	893.1173	-9.606689
-206	319061	3518168	567.414	566.1678	-1.246216
207	315011.7	3511658	548.856	542.2027	-6.65332
209	339189	3505651	542.238	534.5649	-7.673035
-210	330884.8	3521647	588.409	584.4354	-3.973572
-211	352931.1	3519577	597.818	593.2403	-4.577698
212	359260.9	3503219	660.695	661.3809	.6858521
-213	368483.7	3521471	727.43	724.5818	-2.848145
215	341769.8	3534241	622.585	624.36	1.774963
-515	357684	3559195	765.688	755.7883	-9.899719
302	368042.4	3537682	732.539	731.6946	-.8443604

RMSE = 18 Check Points = ±6.03m
RMSE = 12 Control Points =± 5.03m

C.3.4 Accuracy Results in Height in the DEM of the Level 1B Stereo-model for Scene 124/285

No.	X (m)	Y (m)	GCP- H (m)	Cal. H (m)	Δ H (m)
-314	416258.3	3559483	699.456	685.5538	-13.90216
315	400242.8	3562606	711.367	696.7029	-14.66406
-401	423469	3597162	681.681	679.6633	-2.0177
-403	410179.9	3592075	665.684	665.8069	.1228638
404	377215.9	3566139	850.916	834.2524	-16.66357
405	384893.1	3608354	685.835	675.7966	-10.03839
-406	400814.7	3608977	654.517	635.9717	-18.54535
407	401283.8	3618271	641.467	634.8231	-6.643921
-408	391498.3	3618423	659.52	645.1342	-14.38586
409	395605.6	3572833	716.005	705.1094	-10.89557
410	407856	3580587	679.687	675.7966	-3.890381
411	447605.4	3604588	744.812	718.9446	-25.86743
-412	425744.6	3580253	698.453	686.4058	-12.04718
415	436331.8	3566524	740.422	737.1878	-3.234192
-508	389053.2	3584948	733.406	716.5963	-16.80969
-512	379350.8	3594485	791.595	788.1115	-3.483521

RMSE = 8 Check Points = ±12.19m
RMSE = 8 Control Points = ±13.36m

No.	X (m)	Y (m)	GCP- H (m)	Cal. H (m)	Δ H (m)
-314	416258.3	3559483	699.456	678.6359	-20.82007
315	400242.8	3562606	711.367	689.1842	-22.1828
-401	423469	3597162	681.681	672.773	-8.90802
-403	410179.9	3592075	665.684	659.0692	-6.614868
404	377215.9	3566139	850.916	833.3432	-17.57281
405	384893.1	3608354	685.835	669.8458	-15.98926

-406	400814.7	3608977	654.517	628.3136	-26.20343
407	401283.8	3618271	641.467	627.3811	-14.08588
-408	391498.3	3618423	659.52	638.2011	-21.31891
409	395605.6	3572833	716.005	698.2732	-17.73181
410	407856	3580587	679.687	668.0878	-11.59924
411	447605.4	3604588	744.812	711.7244	-33.08759
-414	424195.6	3612833	672.817	658.3922	-14.4248
415	436331.8	3566524	740.422	731.3771	-9.044922
-508	389053.2	3584948	733.406	710.2806	-23.12537
-512	379350.8	3594485	791.595	780.1776	-11.41736

RMSE = 8 Check Points =±18.56m
RMSE = 8 Control points =±18.79m

No.	X (m)	Y (m)	GCP- H (m)	Cal. H (m)	Δ H (m)
- 314	416258.3	3559483	699.456	693.4308	-6.025208
315	400242.8	3562606	711.367	704.2201	-7.146912
-401	423469	3597162	681.681	687.432	5.750977
-403	410179.9	3592075	665.684	673.4134	7.72937
404	377215.9	3566139	850.916	848.0933	-2.822693
405	384893.1	3608354	685.835	684.4376	-1.397461
-406	400814.7	3608977	654.517	643.7115	-10.80548
407	401283.8	3618271	641.467	642.796	1.328979
-408	391498.3	3618423	659.52	653.8645	-5.655518
409	395605.6	3572833	716.005	711.9682	-4.036804
410	407856	3580587	679.687	684.4376	4.750549
411	447605.4	3604588	744.812	727.0319	-17.78009
-412	425744.6	3580253	698.453	694.5302	-3.922852
414	424195.6	3612833	672.817	673.0076	.1905518
415	436331.8	3566524	740.422	745.5837	5.161682
-508	389053.2	3584948	733.406	724.4942	-8.911804
-512	379350.8	3594485	791.595	795.4056	3.810669

RMSE = 8 Check Points = ±6.96 m
RMSE = 8 Control Points = ±7.45m

No.	X (m)	Y (m)	GCP- H (m)	Cal. H (m)	Δ H (m)
- 314	416258.3	3559483	699.456	678.2881	-21.16791
315	400242.8	3562606	711.367	715.5428	4.175842
-401	423469	3597162	681.681	698.0805	16.39948
-403	410179.9	3592075	665.684	678.1913	12.50732
404	377215.9	3566139	850.916	852.2062	1.290222
405	384893.1	3608354	685.835	688.7684	2.93335
-406	400814.7	3608977	654.517	658.7762	4.259155
407	401283.8	3618271	641.467	648.0756	6.608643
-408	391498.3	3618423	659.52	666.9816	7.461548
409	395605.6	3572833	716.005	710.5646	-5.44043
410	407856	3580587	679.687	684.2798	4.592773
-411	447605.4	3604588	744.812	736.0339	-8.778076
412	425744.6	3580253	698.453	705.7581	7.305115
415	436331.8	3566524	740.422	760.059	19.63702
-508	389053.2	3584948	733.406	729.8799	-3.526062
-512	379350.8	3594485	791.595	800.8528	9.257813

RMSE = 8 Check Points = ±11.71m
RMSE = 8 Control Points = ±8.68m

No.	X (m)	Y (m)	GCP- H (m)	Cal. H (m)	Δ H (m)
314	416258.3	3559483	699.456	705.6066	6.150574

315	400242.8	3562606	711.367	708.5964	-2.77063
401	423469	3597162	681.681	691.7586	10.07758
403	410179.9	3592075	665.684	674.6085	8.9245
404	377215.9	3566139	850.916	850.2242	-.6917725
405	384893.1	3608354	685.835	686.4376	.6025391
406	400814.7	3608977	654.517	655.7139	1.196838
407	401283.8	3618271	641.467	644.8237	3.35675
408	391498.3	3618423	659.52	663.6443	4.124268
409	395605.6	3572833	716.005	711.5054	-4.499573
410	407856	3580587	679.687	677.9212	-1.765808
411	447605.4	3604588	744.812	747.3936	2.581604
412	425744.6	3580253	698.453	695.4296	-3.023376
415	436331.8	3566524	740.422	747.5464	7.12439
508	389053.2	3584948	733.406	727.553	-5.852966
512	379350.8	3594485	791.595	797.9393	6.344299

RMSE = 16 Ground Control Points = ±5.13M

No.	X (m)	Y (m)	GCP- H (m)	Cal. H (m)	Δ H (m)
314	416258.3	3559483	699.456	705.6066	6.150574
315	400242.8	3562606	711.367	708.5964	-2.77063
401	423469	3597162	681.681	691.7586	10.07758
403	410179.9	3592075	665.684	674.6085	8.9245
404	377215.9	3566139	850.916	850.2242	-.6917725
405	384893.1	3608354	685.835	686.4376	.6025391
406	400814.7	3608977	654.517	655.7139	1.196838
407	401283.8	3618271	641.467	644.8237	3.35675
408	391498.3	3618423	659.52	663.6443	4.124268
409	395605.6	3572833	716.005	711.5054	-4.499573
410	407856	3580587	679.687	677.9212	-1.765808
411	447605.4	3604588	744.812	747.3936	2.581604
412	425744.6	3580253	698.453	695.4296	-3.023376
415	436331.8	3566524	740.422	747.5464	7.12439
508	389053.2	3584948	733.406	727.553	-5.852966
509	376121	3580645	847.942	797.9393	-50.00275
512	379350.8	3594485	791.595	797.9393	6.344299

RMSE = 17 control Points = ±13.11m

C.3.5 Accuracy Results in Heights in the DEM of the Level 1B of Stereo-model for Scene 124/286

No.	X (m)	Y (m)	GCP- H (m)	Cal. H (m)	Δ H (m)
203	375648.1	3535240	741.806	739.7092	-2.096802
204	374763	3555432	902.724	904.3557	1.631653
301	363529.2	3512142	697.499	701.8351	4.336121
302	368042.4	3537682	732.539	725.407	-7.132019
303	389811.5	3531697	670.323	669.0719	-1.251099
304	412380.1	3524083	684.115	681.9328	-2.18219
306	380363.2	3522860	714.052	719.7937	5.741699
307	388019.9	3526598	719.408	701.0957	-18.31232
308	399431.4	3521858	706.52	709.2896	2.769592
309	398273.6	3529546	668.093	674.2635	6.170471
310	393224.5	3543171	725.155	720.573	-4.582031
213	368483.7	3521471	727.43	716.4059	-11.02405
404	377215.9	3566139	850.916	850.6333	-.2827148

RMSE = 13 Gound Control Points = ±7.01m

C.6 Accuracy Results in Planimetry of Orthoimage of the Reference Scene 122/285 at the Individual GCPs

No.	x	y	Δx	Δy
101	1760.813	-1766.813	0.761	0.852
102	1380.813	-1904.938	-0.422	0.301
110	1126.688	-1426.063	1.054	-1.196
111	1371.438	-918.938	-0.203	-0.394
112	1798.375	-650.875	0.188	-0.060
113	1549.062	-711.063	0.380	-0.918
114	1210.031	-1057.969	0.424	-0.267
116	576.375	-1069.875	0.923	0.443
119	560.687	-1578.938	0.716	-0.326
123	461.625	-1247.125	-0.134	-0.343
124	545.812	-1946.063	0.034	-1.272
135	320.187	-2041.063	-0.287	-0.864
136	441.062	-2398.813	-0.407	0.121
133	278.063	-2619.063	-1.305	0.069
141	982.312	-2934.938	-0.153	0.161
142	957.937	-2376.938	-1.089	0.223
137	970.125	-2185.375	-0.561	-0.207
125	2596.625	-1331.875	-1.063	0.007
127	2868.063	-656.938	0.247	0.885
129	3273.875	-1281.875	-0.192	-0.180
143	3231.625	-947.125	1.197	-0.075
146	2482.125	-1591.375	0.170	0.000
148	2883.375	-1705.125	-0.031	0.071
151	2010.375	-2112.375	-0.071	-0.124
152	1796.938	-2016.813	-0.902	0.227
153	2368.188	-2268.938	-0.400	0.956
155	3192.625	-2268.875	0.360	0.309
156	3081.438	-2478.063	-0.569	0.150
157	2713.312	-2107.938	0.423	0.388
158	2751.125	-1928.625	-0.120	-1.054
154	2817.937	-2349.938	0.751	0.450
159	2622.063	-2570.813	-0.237	-0.088
163	1579.187	-3119.937	0.623	0.238
164	2339.563	-2941.938	0.170	0.301
166	2847.375	-3012.125	-0.755	-0.081
167	2855.937	-3341.937	-0.193	0.454
168	2409.063	-1012.812	0.060	0.512
169	2262.625	-424.375	0.608	0.330

RMSE = 0.6 in x and 0.5 in y in Pixel

No.	X (m)	Y (m)	ΔX (m)	ΔY (m)
101	308544.669	3559870.413	-15.216	-17.041
102	300921.813	3557098.576	8.433	-6.024
110	295871.199	3566645.391	-21.075	23.920
111	300741.906	3576801.496	4.059	7.868
112	309287.944	3582167.164	-3.755	1.195
113	304306.158	3580947.261	-7.600	18.351
114	297526.394	3574024.390	-8.477	5.326
116	284865.279	3573802.547	-18.457	-8.869
119	284545.790	3563607.619	-14.313	6.521
123	282548.934	3570242.780	2.689	6.848
124	284233.497	3556247.451	-0.659	25.436
135	279715.010	3554356.652	5.757	17.274
136	282128.565	3547222.124	8.151	-2.421

133	278850.432	3542817.332	26.103	-1.383
141	292955.156	3536500.414	3.060	-3.212
142	292450.809	3547659.920	21.791	-4.460
137	292705.709	3551481.912	11.220	4.133
125	325223.139	3568548.152	21.243	-0.152
127	330679.379	3582061.380	-4.950	-17.711
129	338783.514	3569542.050	3.819	3.596
143	337967.500	3576238.202	-23.946	1.489
146	322957.330	3563359.228	-3.414	-0.011
148	330976.637	3561084.712	0.602	-1.421
151	313517.357	3552939.957	1.414	2.486
152	309232.993	3554858.615	18.033	-4.544
153	320665.358	3549829.657	7.989	-19.110
155	337166.622	3549815.308	-7.216	-6.178
156	334923.978	3545629.419	11.365	-2.997
157	327583.703	3553036.651	-8.462	-7.746
158	328329.544	3556593.364	2.403	21.084
154	329681.641	3548198.349	-15.024	-8.992
159	325744.302	3543771.439	4.740	1.772
163	304905.635	3532800.617	-12.466	-4.741
164	320102.158	3536358.836	-3.394	-6.000
166	330238.048	3534946.041	15.081	1.631
167	330419.432	3528361.542	3.843	-9.071
168	321495.980	3574939.058	-1.204	-10.243
169	318580.572	3586702.722	-12.165	-6.604

RMSE = ± 12.1 m in Easting and ± 10.6m in Northing

C.4 Comparison of Superimposed Contours

The following are contours generated from the DEMs superimposed over the digitised contours from the RJGC 1:250,000 scale maps for the rest of stereo-models.

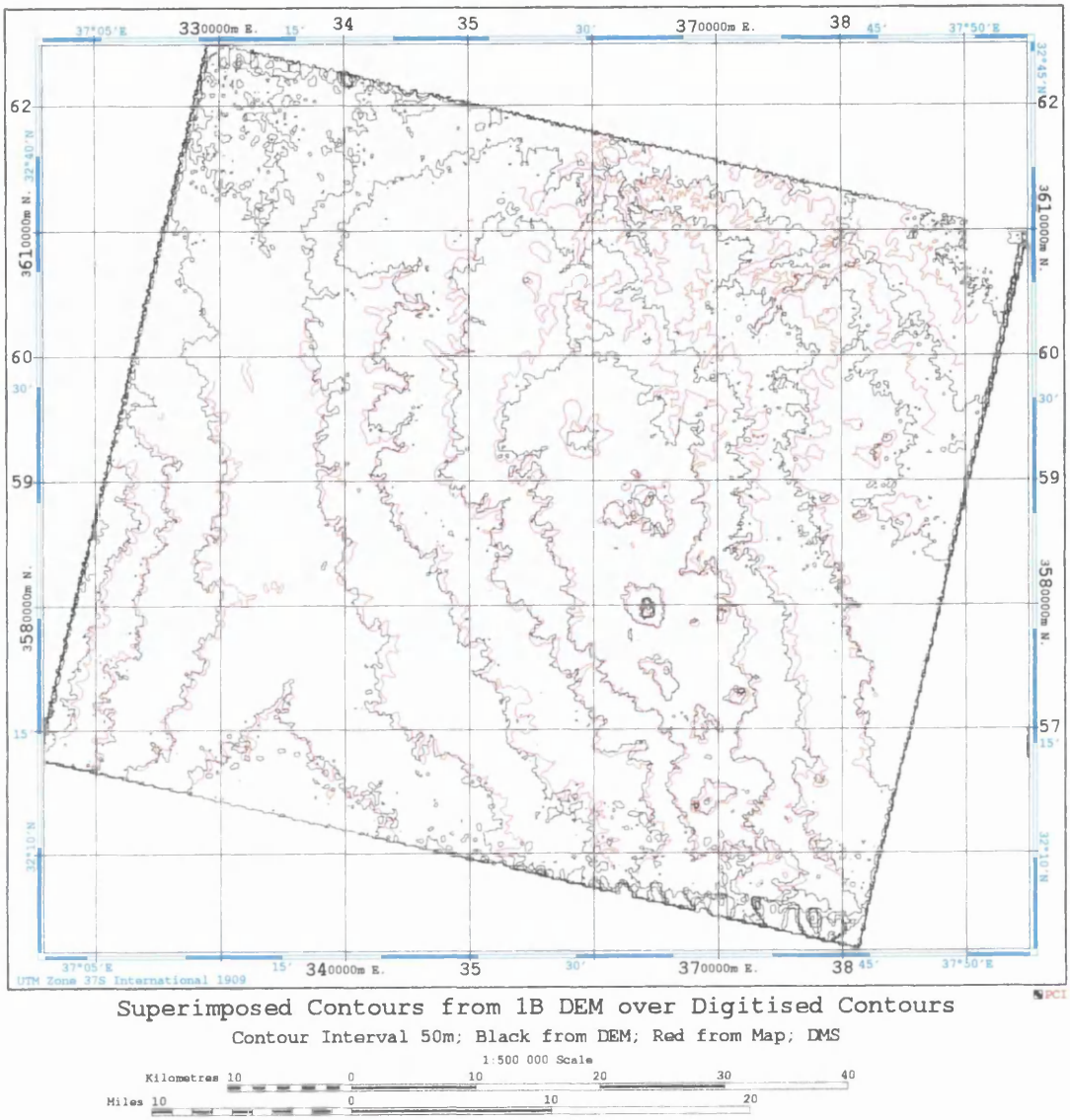

Figure C.1 Contours at 50m interval extracted from the DEM of the Level 1B stereo-model for scene 123/285 superimposed over the corresponding digitised contours from the RJGC 1:250,000 scale map.

The contours extracted from the DEM at a 50m interval have been superimposed over the corresponding digitised contours and the result is shown in Figure C.1. It is clear that the contours have an excellent agreement or fit in most parts of the area to less than 10% of the contour interval. Minor deviations can be seen especially in the north-eastern part.

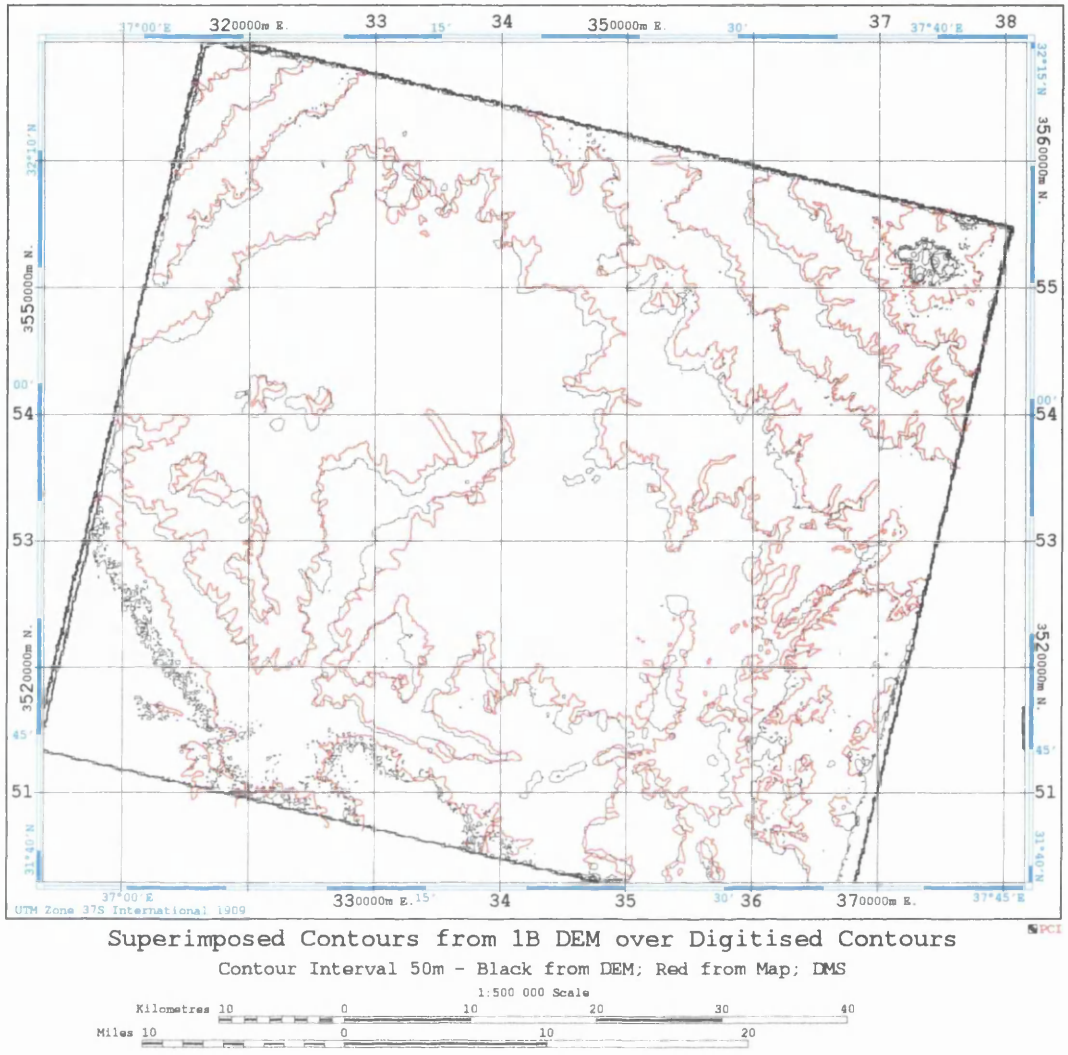

Figure C.2 Contours at 50m interval extracted from the DEM of the Level 1B stereo-model for scene 123/286 superimposed over the corresponding digitised contours from the RJGC 1:250,000 scale map.

Inspection of the fit of the superimposed contours as shown in Figure C.2 shows an excellent agreement except in the south-west part of the DEM where the minor deviation can be seen.

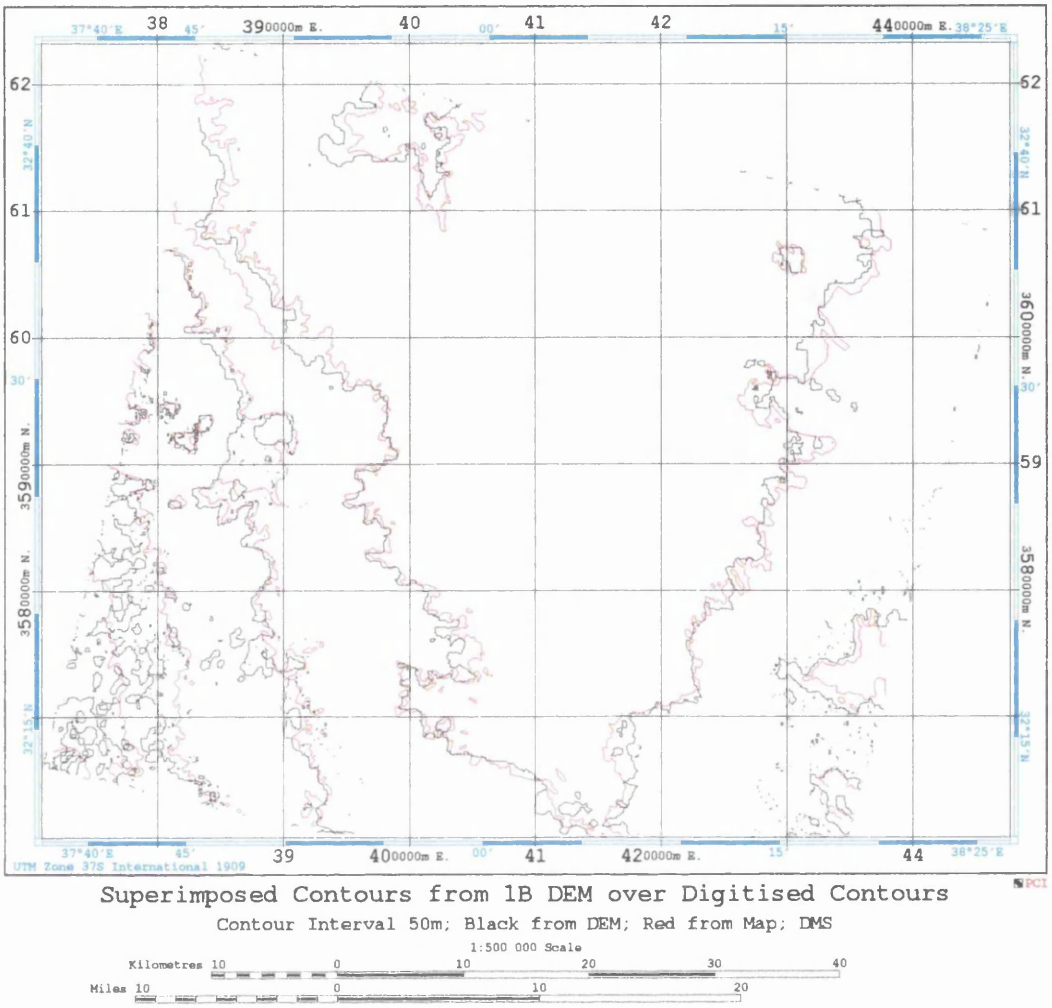

Figure C.3 Contours at 50m interval extracted from the DEM of the Level 1B stereo-model for scene 124/285 superimposed over the corresponding digitised contours from the RJGC 1:250,000 scale map.

Inspection of the fit between the superimposed contours shown in Figure C.3 displays some kind of fit between the contours in most parts of the area, but some deviations can be seen, especially in the south-western part of the area.

C.5 Orthoimage Generation

The following are the rest of the orthoimages generated from SPOT stereo-pairs of the Badia area. Radiometric enhancements have been carried out using the Adobe Photoshop package.

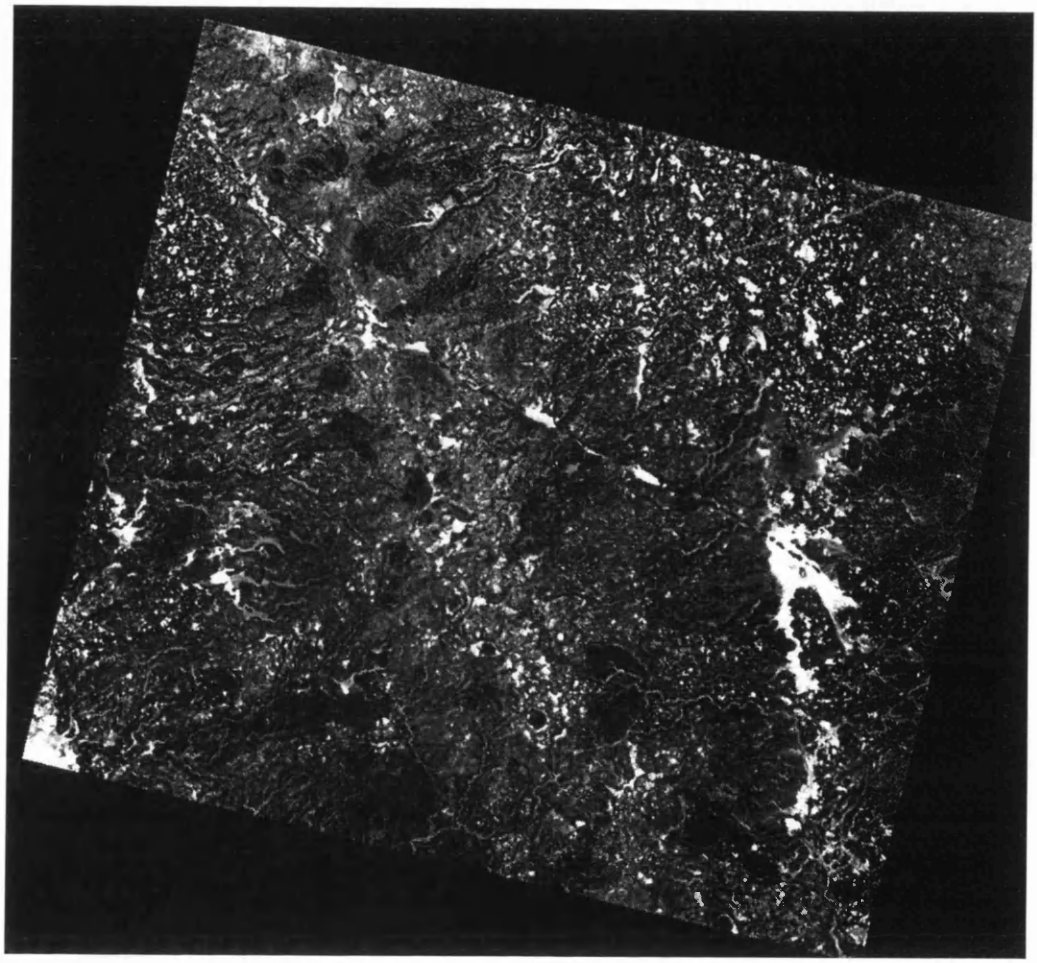

Figure C.4 Orthoimage generated from Level 1B SPOT stereo-pair for scene 123/285 by the DMS system.

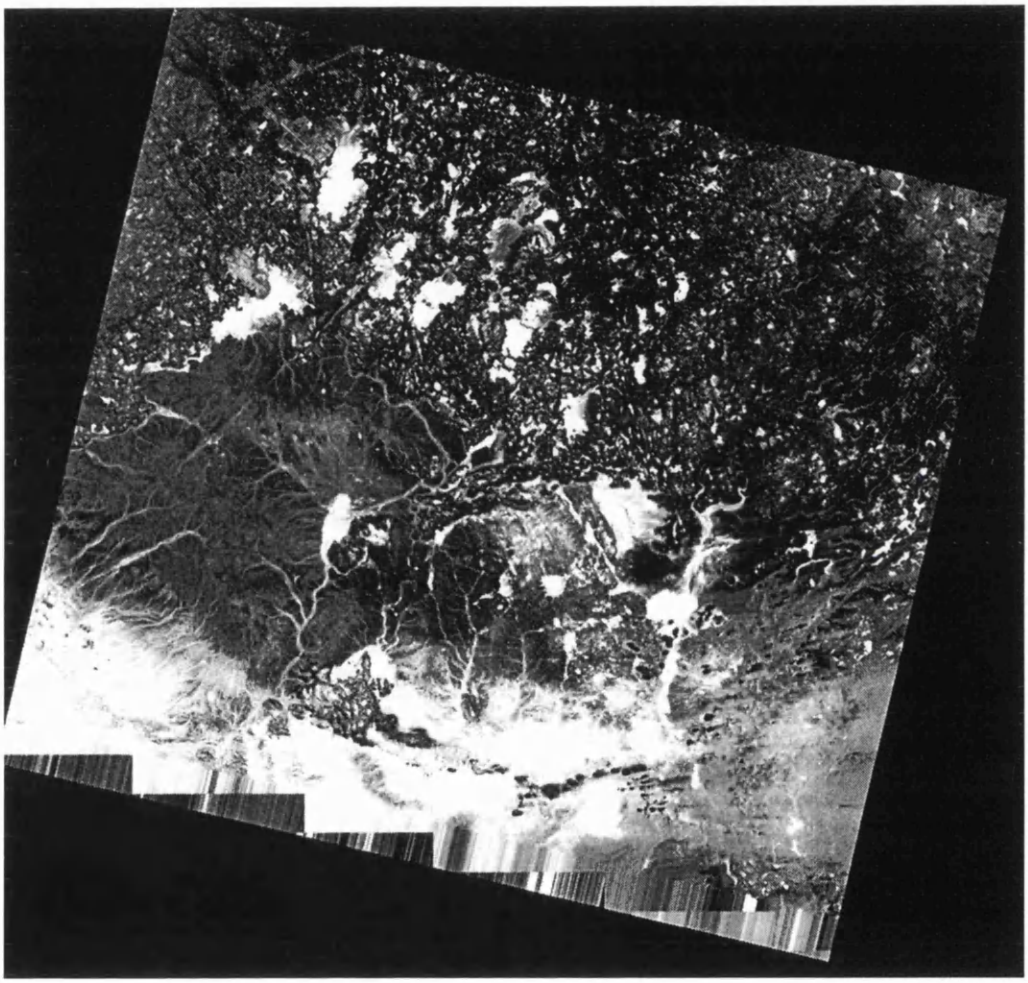

Figure C.5 Orthoimage generated from Level 1B SPOT stereo-pair for scene 123/286 by the DMS system.

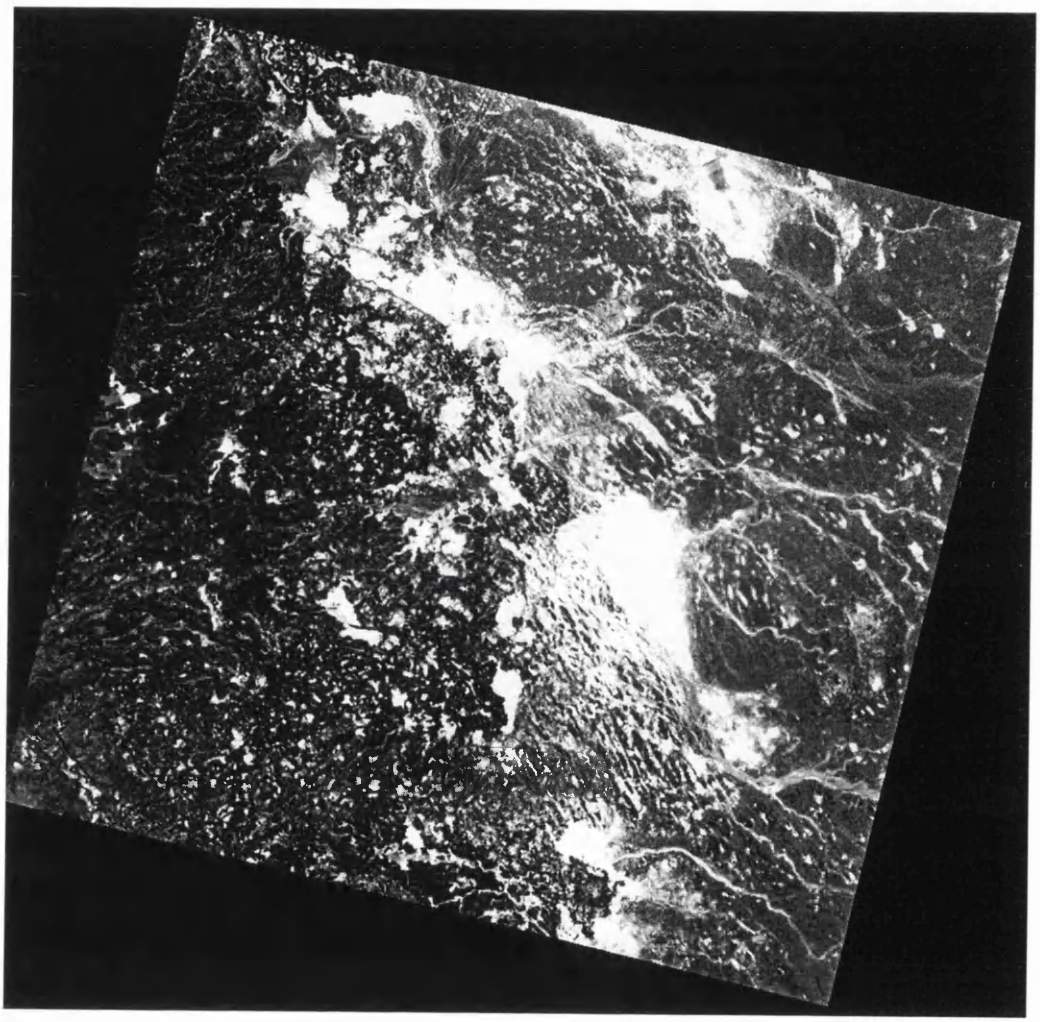

Figure C.6 Orthoimage generated from Level 1B SPOT stereo-pair for scene 124/285 by the DMS system.

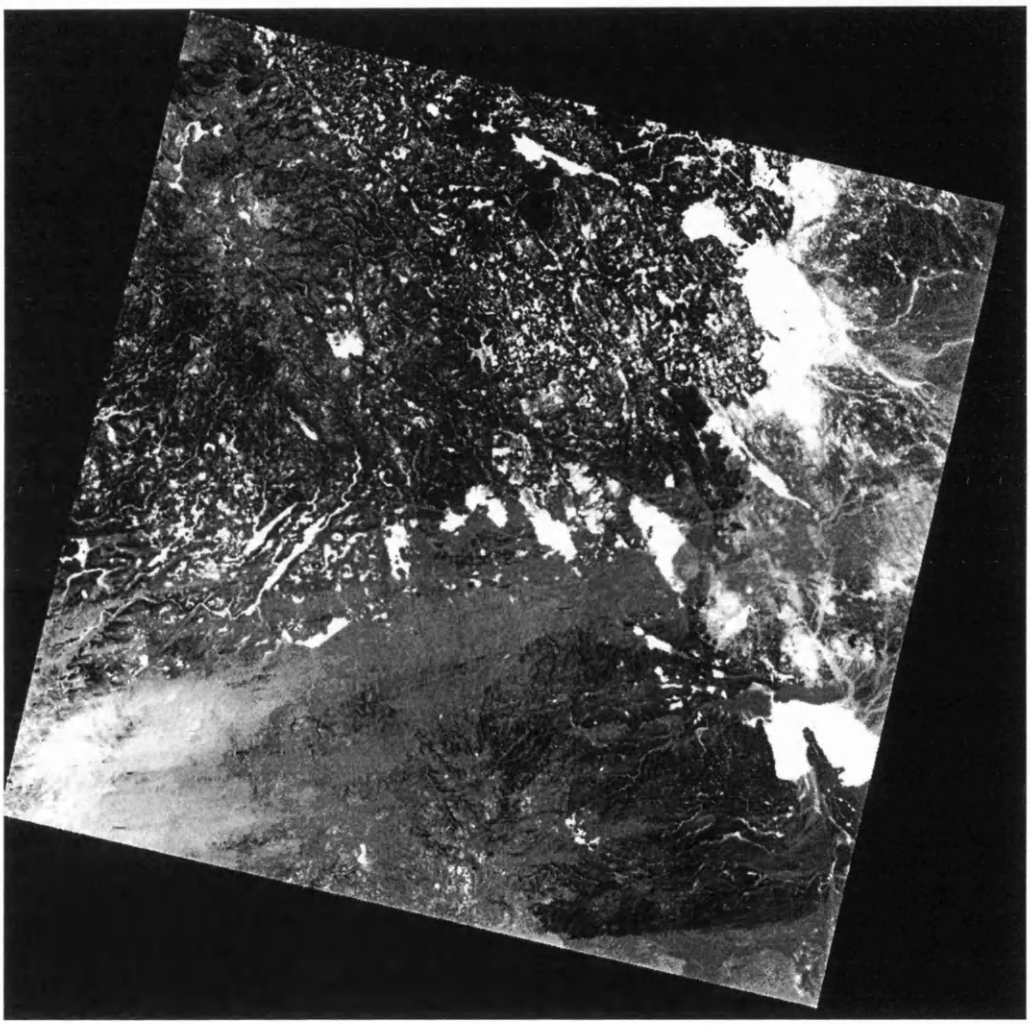

Figure C.7 Orthoimage generated from Level 1B SPOT stereo-pair for scene 124/286 by the DMS system.

C.6 Accuracy Results in Planimetry of the Orthoimage of the Reference Scene 122/285 at the Individual GCPs

No.	x	y	Δx	Δy
101	1760.813	-1766.813	0.761	0.852
102	1380.813	-1904.938	-0.422	0.301
110	1126.688	-1426.063	1.054	-1.196
111	1371.438	-918.938	-0.203	-0.394
112	1798.375	-650.875	0.188	-0.060
113	1549.062	-711.063	0.380	-0.918
114	1210.031	-1057.969	0.424	-0.267
116	576.375	-1069.875	0.923	0.443
119	560.687	-1578.938	0.716	-0.326
123	461.625	-1247.125	-0.134	-0.343
124	545.812	-1946.063	0.034	-1.272
135	320.187	-2041.063	-0.287	-0.864
136	441.062	-2398.813	-0.407	0.121
133	278.063	-2619.063	-1.305	0.069
141	982.312	-2934.938	-0.153	0.161
142	957.937	-2376.938	-1.089	0.223
137	970.125	-2185.375	-0.561	-0.207
125	2596.625	-1331.875	-1.063	0.007
127	2868.063	-656.938	0.247	0.885
129	3273.875	-1281.875	-0.192	-0.180
143	3231.625	-947.125	1.197	-0.075
146	2482.125	-1591.375	0.170	0.000
148	2883.375	-1705.125	-0.031	0.071
151	2010.375	-2112.375	-0.071	-0.124
152	1796.938	-2016.813	-0.902	0.227
153	2368.188	-2268.938	-0.400	0.956
155	3192.625	-2268.875	0.360	0.309
156	3081.438	-2478.063	-0.569	0.150
157	2713.312	-2107.938	0.423	0.388
158	2751.125	-1928.625	-0.120	-1.054
154	2817.937	-2349.938	0.751	0.450
159	2622.063	-2570.813	-0.237	-0.088
163	1579.187	-3119.937	0.623	0.238
164	2339.563	-2941.938	0.170	0.301
166	2847.375	-3012.125	-0.755	-0.081
167	2855.937	-3341.937	-0.193	0.454
168	2409.063	-1012.812	0.060	0.512
169	2262.625	-424.375	0.608	0.330

RMSE = ± 0.6 in x and ± 0.5 in y in Pixel

No.	X (m)	Y (m)	ΔX (m)	ΔY (m)
101	308544.669	3559870.413	-15.216	-17.041
102	300921.813	3557098.576	8.433	-6.024
110	295871.199	3566645.391	-21.075	23.920
111	300741.906	3576801.496	4.059	7.868
112	309287.944	3582167.164	-3.755	1.195
113	304306.158	3580947.261	-7.600	18.351
114	297526.394	3574024.390	-8.477	5.326
116	284865.279	3573802.547	-18.457	-8.869
119	284545.790	3563607.619	-14.313	6.521
123	282548.934	3570242.780	2.689	6.848
124	284233.497	3556247.451	-0.659	25.436
135	279715.010	3554356.652	5.757	17.274
136	282128.565	3547222.124	8.151	-2.421

133	278850.432	3542817.332	26.103	-1.383
141	292955.156	3536500.414	3.060	-3.212
142	292450.809	3547659.920	21.791	-4.460
137	292705.709	3551481.912	11.220	4.133
125	325223.139	3568548.152	21.243	-0.152
127	330679.379	3582061.380	-4.950	-17.711
129	338783.514	3569542.050	3.819	3.596
143	337967.500	3576238.202	-23.946	1.489
146	322957.330	3563359.228	-3.414	-0.011
148	330976.637	3561084.712	0.602	-1.421
151	313517.357	3552939.957	1.414	2.486
152	309232.993	3554858.615	18.033	-4.544
153	320665.358	3549829.657	7.989	-19.110
155	337166.622	3549815.308	-7.216	-6.178
156	334923.978	3545629.419	11.365	-2.997
157	327583.703	3553036.651	-8.462	-7.746
158	328329.544	3556593.364	2.403	21.084
154	329681.641	3548198.349	-15.024	-8.992
159	325744.302	3543771.439	4.740	1.772
163	304905.635	3532800.617	-12.466	-4.741
164	320102.158	3536358.836	-3.394	-6.000
166	330238.048	3534946.041	15.081	1.631
167	330419.432	3528361.542	3.843	-9.071
168	321495.980	3574939.058	-1.204	-10.243
169	318580.572	3586702.722	-12.165	-6.604

RMSE = ± 12.1 m in Easting and ± 10.6m in Northing

APPENDIX D: RESULTS FROM TESTS OF THE ORTHOMAX SYSTEM

D.1 Orthoimage Accuracy Results at the Individual GCPs of the Level 1A and 1B Stereo-pair for Reference Scene 122/285

(a) Level 1A

The following are the accuracy results in planimetry achieved with the orthoimage generated from the Level 1A stereo-pair of reference scene 122/285 using a linear conformal transformation to fit the image points to the GCPs.

No.	x	y	Δx	Δy (pixel)
101	2458.	-1934.	-0.18	-0.41
102	2077.	-2072.	0.28	-0.25
110	1824.	-1594.	-0.49	0.46
111	2067.	-1087.	-0.47	-0.17
112	2495.	-819.	0.04	-0.64
113	2246.	-879.	0.13	0.35
114	1907.	-1226.	0.13	-0.25
116	1273.	-1238.	-0.87	-1.21
119	1257.	-1746.	-1.09	0.48
124	1242.	-2114.	-0.79	0.81
135	1016.	-2208.	-0.36	0.85
133	974.	-2786.	0.43	0.01
136	1137.	-2565.	0.02	0.27
146	3179.	-1759.	-0.01	0.20
125	3293.	-1499.	0.95	0.25
127	3566.	-825.	0.89	-0.92
148	3579.	-1872.	-0.23	0.18
154	3514.	-2517.	-0.49	-0.49
167	3553.	-3508.	0.87	0.37
163	2276.	-3287.	-0.42	-0.34
158	3447.	-2096.	0.12	1.25
157	3410.	-2275.	0.16	0.09
151	2706.	-2279.	-1.01	0.43
164	3036.	-3108.	-0.01	1.00
166	3544.	-3179.	1.44	0.38
141	1678.	-3102.	-0.13	-0.33
129	3970.	-1449.	-0.08	0.30
159	3318.	-2738.	-0.12	-0.14
126	3372.	-1193.	-0.50	-0.55
168	3106.	-1181.	0.62	-1.11
145	4318.	-1338.	-0.46	0.10
156	3777.	-2646.	-0.36	-0.30
169	2960.	-592.	-0.16	-0.24
137	1666.	-2353.	0.09	-0.16
128	3599.	-1258.	0.19	0.54
152	2493.	-2184.	0.47	-0.01
123	1159.	-1415.	0.95	0.03
150	4214.	-1777.	1.18	-0.46
155	3889.	-2436.	-0.24	0.16
143	3929.	-1115.	-0.53	-0.51

RMSE = ± 0.52 in x and ± 0.57 in y (pixels)

No.	X (m)	Y (m)	ΔX (m)	ΔY (m)
101	308545.	3559870.	3.56	8.26
102	300922.	3557099.	-5.68	5.08
110	295871.	3566645.	9.82	-9.22
111	300742.	3576802.	9.31	3.36
112	309288.	3582167.	-0.80	12.90
113	304306.	3580947.	-2.66	-7.05
114	297526.	3574024.	-2.52	4.92
116	284865.	3573803.	17.40	24.27
119	284546.	3563608.	21.70	-9.59
124	284233.	3556247.	15.71	-16.16
135	279715.	3554357.	7.14	-17.02
133	278850.	3542817.	-8.65	-0.29
136	282129.	3547222.	-0.48	-5.40
146	322957.	3563359.	0.20	-4.04
125	325223.	3568548.	-18.97	-5.01
127	330679.	3582061.	-17.71	18.50
148	330977.	3561085.	4.67	-3.55
154	329682.	3548198.	9.72	9.84
167	330419.	3528362.	-17.37	-7.32
163	304906.	3532801.	8.35	6.70
158	328330.	3556593.	-2.45	-25.00
157	327584.	3553037.	-3.29	-1.78
151	313517.	3552940.	20.12	-8.55
164	320102.	3536359.	0.13	-19.93
166	330238.	3534946.	-28.79	-7.70
141	292955.	3536500.	2.63	6.49
129	338784.	3569542.	1.64	-6.03
159	325744.	3543781.	2.33	2.83
126	326827.	3574684.	9.96	11.10
168	321496.	3574939.	-12.50	22.26
145	345746.	3571771.	9.20	-2.04
156	334924.	3545629.	7.17	5.90
169	318581.	3586703.	3.24	4.86
137	292706.	3551482.	-1.90	3.26
128	331363.	3573362.	-3.77	-10.71
152	309233.	3554859.	-9.34	0.12
123	282549.	3570243.	-18.97	-0.58
150	343633.	3563012.	-23.58	9.18
155	337167.	3549815.	4.83	-3.12
143	337967.	3576238.	10.58	10.25

RMSE ± 10.5m in Easting and ± 11.4m in Northing

(b) Level 1B

The corresponding set of values for the orthoimage generated from the Level 1B stereo-pair of reference scene 122/285 are as follows:

No.	X (m)	Y (m)	Δ X (m)	ΔY (m)
101	308545.	3559870.	-3.064	-9.243
102	300922.	3557099.	14.291	-16.180
110	295871.	3566645.	-18.561	17.895

111	300742.	3576801.	2.421	11.053
112	309288.	3582167.	-11.439	2.774
113	304306.	3580947.	-12.383	3.484
114	297526.	3574024.	-13.795	-12.580
116	284865.	3573803.	-16.543	-2.419
123	282549.	3570243.	-0.792	7.702
119	284546.	3563608.	-19.971	3.749
124	284233.	3556247.	-12.629	22.671
125	325223.	3568548.	9.990	5.344
126	326827.	3574684.	-22.937	-10.863
127	330679.	3582061.	-5.261	-14.939
128	331363.	3573362.	6.945	1.443
143	337968.	3576238.	-13.039	-16.737
129	338784.	3569542.	-3.889	2.989
145	345746.	3571771.	-10.930	-7.036
146	322957.	3563359.	-1.317	-16.642
148	330977.	3561085.	-14.693	-2.198
150	343633.	3563012.	19.166	-16.891
157	327584.	3553037.	-6.844	7.616
158	328330.	3556593.	1.654	24.552
151	313517.	3552940.	-1.852	0.357
152	309233.	3554859.	7.800	7.410
153	320665.	3549830.	8.430	-16.782
154	329682.	3548198.	-15.562	-9.453
155	337167.	3549815.	-0.230	4.872
156	334924.	3545629.	1.713	-11.399
159	325744.	3543781.	4.781	-8.180
164	320102.	3536359.	11.930	9.048
166	330238.	3534946.	34.618	-13.576
167	330419.	3528362.	20.912	4.605
163	304906.	3532801.	1.524	-9.021
141	292955.	3536500.	-3.713	6.909
133	278850.	3542817.	13.206	8.582
136	282129.	3547222.	0.814	13.284
135	279715.	3554357.	-5.106	16.071
142	292451.	3547660.	28.705	13.799
137	292706.	3551482.	9.432	16.792
168	321496.	3574939.	13.168	-9.914
169	318581.	3586703.	-14.520	-8.024
165	317474.	3530715.	17.566	-0.925

RMSE = ± 13.4m in Easting and ± 11.7m in Northing

RMSE = ± 0.67 in x; 0.58 in y (pixels)

APPENDIX E: RESULTS FROM TESTS OF THE EASI/PACE SYSTEM OVER THE OSLO TEST AREA

E. 1 Results from the Space Resection of Individual SPOT Images

E.1.1 First Test

E.1.2 Second Test

E.1.3 Third Test

E.1.4 Fourth Test

E.1.5 Fifth Test

E.2 Accuracy Results of Absolute Orientation of the Oslo Stereo-model

E.2.1 First Test Using 45 Ground Control Points

E.2.1 Second Test Using 28 Control Points and 17 Check Points

E.2.3 Third Test Using 26 Ground Control Points Derived from Map

E.2.4 Fourth Test Using 17 Road Database Ground Control Points

E.3 Accuracy Results of Height in DEM

E.3.1 Accuracy Results of Height in DEM at 43 Ground Control Points

E.3.2 Accuracy Results of Height in DEM at 25 Control Points and 16 Check Points

E.3.3 Accuracy Results of Height in DEM at 16 Road Database Ground Control Points

E.5 Accuracy Test of the Orthoimage Generated by the Level 1A Stereo-pair at the Individual GCPs

E. 1 Results From the Space Resection of Individual SPOT Images

E.1.1 First Test

The following are the results of the space resection giving the planimetric accuracy of the left image of the Level 1A stereo-model for the reference scene 122/285 using 45 ground control points

SMODEL Satellite Model Calculation V6.0 EASI/PACE 19:57 18-OCT-97

Report File : E:\OSLO\SMA.TXT

Using GCPs stored in the GCP segment :

GCPID	CALCULATED GCP		RESIDUAL (Metre)		
	X	Y	ΔX	ΔY	Vector
1	619257.47	6677240.62	2.53	9.38	9.72
2	620349.77	6671008.62	0.23	16.38	16.38
3	636531.09	6670284.53	8.91	5.47	10.45
4	594698.88	6673954.65	11.12	-4.65	12.06
5	617818.09	6685036.35	1.91	3.65	4.12
6	628968.34	6657273.04	0.46	-8.74	8.75
7	633017.67	6663624.92	-7.67	5.08	9.20
8	600277.99	6668081.73	-8.09	-2.73	8.53
9	601245.46	6656922.21	4.54	7.79	9.02
10	609860.34	6672274.89	-10.34	5.11	11.53
11	611722.75	6654752.92	17.25	-2.92	17.49
12	603656.81	6683790.81	3.19	-0.81	3.29
13	598377.82	6685611.42	-7.42	1.28	7.53
14	619743.16	6651785.66	-3.16	4.34	5.37
15	636779.54	6642003.89	0.46	-3.89	3.91
16	623908.22	6645606.07	11.78	-6.07	13.25
17	617343.93	6647750.40	-3.93	-0.40	3.95
18	623143.74	6638377.68	-3.74	2.32	4.40
19	615283.61	6640581.89	6.39	-1.89	6.66
20	611408.51	6639015.76	-8.51	-5.76	10.27
21	609089.45	6646405.32	10.55	-5.32	11.81
22	602737.99	6639901.51	-5.99	5.69	8.26
23	605075.13	6650645.52	4.87	-15.52	16.27
24	629026.62	6630269.06	13.38	10.94	17.28
25	632701.13	6679837.34	-1.63	-2.24	2.77
26	601317.67	6675659.89	7.33	-9.89	12.31
27	608194.17	6651216.99	-5.07	6.11	7.94
28	604586.83	6658350.68	-1.23	-7.38	7.48
29	589875.86	6654394.17	-0.06	-2.67	2.67
30	613267.63	6648401.55	-7.63	-11.55	13.84
31	614499.20	6647365.33	-9.20	-5.33	10.63
32	624101.89	6677219.04	-11.89	0.96	11.92
33	604800.07	6671045.97	-0.07	4.03	4.03
34	626391.85	6630644.74	-7.05	-0.84	7.10
35	595642.18	6654754.05	-2.18	5.95	6.34
36	609340.15	6682804.97	-6.65	-4.37	7.96
37	630350.19	6677280.48	0.61	-2.38	2.46
38	633118.40	6632085.97	-3.70	0.83	3.79
39	596588.80	6650226.14	11.20	-1.14	11.26
40	625651.95	6683497.29	8.05	2.71	8.49
41	590706.29	6640058.70	0.11	12.10	12.10
42	601692.63	6646248.17	-10.33	5.93	11.91
43	629942.13	6668091.03	-1.63	-1.03	1.93

44	604998.32	6662952.63	1.48	-0.83	1.70
45	634356.07	6677035.81	0.83	-7.71	7.75
		RMS	±7.15	±6.50	±9.66

N02 (2 X ellipsoid normal) : 0.1278845814253259D+08
aa (Unknown tied to Earth rotation) : 0.2988344713345168D-01
ALPHA (IFOV) : 0.1200000000000000D-04
bb (Unknown of 2nd order) : 0.6576045830144635D-08
C0 (Scene centre column) : 0.3000000000000000D+04
cc (Unknown of 2nd order): -.3438413378293570D-09
COSKHI (Parameter): 0.9996572313223574D+00
DELGAM (Unknown of 2nd order): -.4084609461756581D-08
GAMMA (Scene orient. rel. to the North): 0.3473814450091974D+00
K_1 (Cross track scale function): 0.1378371351639592D-05
L0 (Scene centre row): 0.3000000000000000D+04
P (Along track scale function): 0.1001484675057122D+02
Q (Satellite-Scene centre dist): 0.9114750751570446D+06
TAU (Levelling angle along track dir): -.2618950147561706D-01
THETA (Levelling angle across track dir): 0.3150678003886048D+00
THETAS (THETA/COS_KHI): 0.3151758327920358D+00
X0 (Carto coord of scene centre): 0.6096123693450196D+06
Y0 (Carto coord of scene centre): 0.6659686193449231D+07
DELH (Radar parameter in H dir.): 0.0000000000000000D+00
COEFY2 (Radar parameter in Y2 dir.): 0.0000000000000000D+00

EARTH ELLIPSOID USED : E012

The following are the results of the space resection giving the planimetric accuracy of the right image of the Level 1A stereo-model for the reference scene 122/285 using 45 ground control points

SMODEL Satellite Model Calculation V6.0 EASI/PACE 20:51 18-OCT-97

Report File : E:\OSLO\SMB.TXT

Using GCPs stored in the GCP segment :

GCPID	CALCULATED GCP		RESIDUAL (Metre)		
	X	Y	ΔX	ΔY	Vector
1	619241.89	6677244.86	18.11	5.14	18.83
2	620352.47	6671010.85	-2.47	14.15	14.37
3	636536.17	6670285.61	3.83	4.39	5.82
4	594700.64	6673953.88	9.36	-3.88	10.13
5	617817.18	6685038.43	2.82	1.57	3.23
6	628969.90	6657269.60	-1.10	-5.30	5.42
7	633014.56	6663631.37	-4.56	-1.37	4.76
8	600276.24	6668082.64	-6.34	-3.64	7.31
9	601248.43	6656917.04	1.57	12.96	13.06
10	609860.23	6672276.46	-10.23	3.54	10.83
11	611729.11	6654751.47	10.89	-1.47	10.98
12	603658.81	6683788.74	1.19	1.26	1.73
13	598376.22	6685610.54	-5.82	2.16	6.21
14	619737.95	6651793.82	2.05	-3.82	4.34
15	636775.56	6642007.20	4.44	-7.20	8.46
16	623902.55	6645606.11	17.45	-6.11	18.48
17	617348.78	6647748.03	-8.78	1.97	9.00

18	623162.96	6638373.13	-22.96	6.87	23.97
19	615274.77	6640590.22	15.23	-10.22	18.34
20	611404.88	6639017.62	-4.88	-7.62	9.04
21	609090.67	6646407.97	9.33	-7.97	12.27
22	602741.47	6639898.05	-9.47	9.15	13.17
23	605077.61	6650643.83	2.39	-13.83	14.04
24	629028.07	6630265.98	11.93	14.02	18.41
25	632701.33	6679835.71	-1.83	-0.61	1.93
26	601316.47	6675655.88	8.53	-5.88	10.36
27	608195.21	6651216.35	-6.11	6.75	9.11
28	604583.45	6658348.26	2.15	-4.96	5.40
29	589872.98	6654395.23	2.82	-3.73	4.67
30	613264.24	6648401.96	-4.24	-11.96	12.68
31	614499.53	6647377.36	-9.53	-17.36	19.80
32	624096.68	6677216.11	-6.68	3.89	7.73
33	604803.37	6671050.42	-3.37	-0.42	3.39
34	626388.98	6630637.20	-4.18	6.70	7.89
35	595642.91	6654755.20	-2.91	4.80	5.62
36	609340.18	6682802.74	-6.68	-2.14	7.01
37	630351.28	6677281.85	-0.48	-3.75	3.78
38	633115.89	6632081.85	-1.19	4.95	5.09
39	596588.61	6650232.09	11.39	-7.09	13.41
40	625660.06	6683495.52	-0.06	4.48	4.48
41	590707.13	6640057.58	-0.73	13.22	13.24
42	601688.33	6646248.07	-6.03	6.03	8.53
43	629939.63	6668089.20	0.87	0.80	1.18
44	605002.87	6662945.05	-3.07	6.75	7.41
45	634359.53	6677033.31	-2.63	-5.21	5.84
		RMS	±8.02	±7.37	±10.89

N02 (2 X ellipsoid normal) : 0.1278845814253259D+08
aa (Unknown tied to Earth rotation) : 0.3606714020959381D-01
ALPHA (IFOV) : 0.1200000000000000D-04
bb (Unknown of 2nd order) : 0.1220535059449868D-07
C0 (Scene centre column) : 0.3000000000000000D+04□
cc (Unknown of 2nd order): -.3280176034502756D-08
COSKHI (Parameter): 0.9996679702061812D+00
DELGAM (Unknown of 2nd order): -.1504103343773206D-07
GAMMA (Scene orient. rel. to the North): 0.2101659178306366D+00
K_1 (Cross track scale function): 0.1379999169478435D-05
L0 (Scene centre row): 0.3000000000000000D+04
P (Along track scale function): 0.9973253225546216D+01
Q (Satellite-Scene centre dist): 0.9025409985649916D+06
TAU (Levelling angle along track dir): -.2577577283937458D-01
THETA (Levelling angle across track dir): -.3018667677975638D+00
THETAS (THETA/COS_KHI): -.3019670298482243D+00
X0 (Carto coord of scene centre): 0.6212448485022273D+06
Y0 (Carto coord of scene centre): 0.6660015983471520D+07
DELH (Radar parameter in H dir.): 0.0000000000000000D+00
COEFY2 (Radar parameter in Y2 dir.): 0.0000000000000000D+00

EARTH ELLIPSOID USED : E012

E.1.2 Second Test

The following are the results of the space resection giving the planimetric accuracy of the left image of the Level 1A stereo-model for the reference scene 122/285 using 28 control points and 17 check points:

SMODEL Satellite Model Calculation V6.0 EASI/PACE 15:00 19-OCT-97

Report File : E:\OSLO\SM17CH.TXT

Using GCPs stored in the GCP segment :

GCPID	CALCULATED GCP		RESIDUEAL (Metre)		
	X	Y	ΔX	ΔY	Vector
1	619257.74	6677243.79	2.26	6.21	6.61
2	620349.87	6671011.91	0.13	13.09	13.09
3	636531.33	6670289.90	8.67	0.10	8.67
4	594705.50	6673950.98	4.50	-0.98	4.60
5	617818.55	6685040.33	1.45	-0.33	1.48
7	633018.23	6663628.82	-8.23	1.18	8.32
9	601248.59	6656920.07	1.41	9.93	10.03
10	609862.07	6672276.00	-12.07	4.00	12.72
11	611723.91	6654753.19	16.09	-3.19	16.41
12	603660.76	6683791.71	-0.76	-1.71	1.87
14	619744.07	6651786.25	-4.07	3.75	5.53
15	636783.12	6642005.45	-3.12	-5.45	6.28
16	623909.58	6645606.77	10.42	-6.77	12.43
17	617345.25	6647749.33	-5.25	0.67	5.29
18	623145.88	6638376.30	-5.88	3.70	6.95
19	615284.93	6640581.42	5.07	-1.42	5.27
20	611410.28	6639013.22	-10.28	-3.22	10.77
21	609091.28	6646402.93	8.72	-2.93	9.20
23	605077.30	6650643.73	2.70	-13.73	13.99
24	629030.19	6630268.36	9.81	11.64	1 5.22
26	601321.46	6675661.03	3.54	-11.03	11.58
30	613269.14	6648399.72	-9.14	-9.72	13.35
31	614500.66	6647363.65	-10.66	-3.65	11.26
32	624101.45	6677224.07	-11.45	-4.07	12.15
33	604802.76	6671046.72	-2.76	3.28	4.28
35	595646.83	6654749.80	-6.83	10.20	12.28
39	596593.10	6650221.00	6.90	4.00	7.97
40	625651.19	6683503.54	8.81	-3.54	9.49
		RMS	±7.71	±6.61	±10.15

RESIDUAL ERRORS FOR CHECK POINTS:

GCPID	CALCULATED CHECK POINT		ERRORS (Metre)		
	X	Y	ΔX	ΔY	Vector
-6	628969.01	6657276.23	-0.21	-11.93	11.93
-8	600282.24	6668079.03	-12.34	-0.03	12.34
-13	598383.86	6685610.98	-13.46	1.72	13.56
-22	602740.84	6639896.40	-8.84	10.80	13.96

-25	632700.29	6679844.14	-0.79	-9.04	9.08
-27	608195.85	6651215.92	-6.75	7.18	9.85
-28	604589.61	6658347.86	-4.01	-4.56	6.07
-29	589882.66	6654386.99	-6.86	4.51	8.21
-34	626395.02	6630643.39	-10.22	0.51	10.23
-36	609342.47	6682806.63	-8.97	-6.03	10.81
-37	630349.56	6677286.26	1.24	-8.16	8.26
-38	633122.61	6632085.67	-7.91	1.13	7.99
-41	590712.19	6640048.88	-5.79	21.92	22.67
-42	601695.66	6646243.76	-13.36	10.34	16.89
-43	629942.06	6668095.58	-1.56	-5.58	5.80
-44	605001.08	6662950.63	-1.28	1.17	1.74
-45	634355.45	6677042.49	1.45	-14.39	14.46
		RMS	±7.86	±9.25	±12.13

N02 (2 X ellipsoid normal) : 0.1278845814253259D+08
aa (Unknown tied to Earth rotation) : 0.2990732086524938D-01
ALPHA (IFOV) : 0.1200000000000000D-04
bb (Unknown of 2nd order) : 0.6576045830144635D-08
C0 (Scene centre column) : 0.3000000000000000D+04
cc (Unknown of 2nd order): -.3438413378293570D-09
COSKHI (Parameter): 0.9998678530928198D+00
DELGAM (Unknown of 2nd order): -.4084609461756581D-08
GAMMA (Scene orient. rel. to the North): 0.3472364501051330D+00
K_1 (Cross track scale function): 0.1383398865250155D-05
L0 (Scene centre row): 0.3000000000000000D+04
P (Along track scale function): 0.1001638034326101D+02
Q (Satellite-Scene centre dist): 0.9112678721605116D+06
TAU (Levelling angle along track dir): -.1625872725669739D-01
THETA (Levelling angle across track dir): 0.3213506359275918D+00
THETAS (THETA/COS_KHI): 0.3213931070326752D+00
X0 (Carto coord of scene centre): 0.6096144713809474D+06
Y0 (Carto coord of scene centre): 0.6659683538320132D+07
DELH (Radar parameter in H dir.): 0.0000000000000000D+00
COEFY2 (Radar parameter in Y2 dir.): 0.0000000000000000D+00

EARTH ELLIPSOID USED : E012

The following are the results of the space resection giving the planimetric accuracy of the right image of the Level 1A stereo-model for the reference scene 122/285 using 28 control points and 17 check points:

SMODEL Satellite Model Calculation V6.0 EASI/PACE 15:01 19-OCT-97

Report File : E:\OSLO\SM17CHB.TXT

Using GCPs stored in the GCP segment :

GCPID	CALCULATED GCP		RESIDUAL (Metre)		
	X	Y	ΔX	ΔY	Vector
1	619242.78	6677246.70	17.22	3.30	17.54
2	620353.31	6671012.80	-3.31	12.20	12.64
3	636537.11	6670289.21	2.89	0.79	2.99
4	594705.20	6673950.38	4.80	-0.38	4.82
5	617818.20	6685041.61	1.80	-1.61	2.41

7	633015.52	6663633.40	-5.52	-3.40	6.49
9	601251.17	6656914.01	-1.17	15.99	16.03
10	609862.01	6672276.77	-12.01	3.23	12.44
11	611730.56	6654750.42	9.44	-0.42	9.45
12	603661.82	6683790.16	-1.82	-0.16	1.82
14	619739.00	6651792.50	1.00	-2.50	2.69
15	636777.67	6642007.31	2.33	-7.31	7.67
16	623903.70	6645604.96	16.30	-4.96	17.04
17	617349.94	6647744.67	-9.94	5.33	11.28
18	623164.26	6638369.42	-24.26	10.58	26.47
19	615276.06	6640588.14	13.94	-8.14	16.14
20	611406.36	6639012.93	-6.36	-2.93	7.00
21	609092.31	6646403.54	7.69	-3.54	8.46
23	605079.71	6650640.71	0.29	-10.71	10.71
24	629029.93	6630263.73	10.07	16.27	19.13
26	601319.68	6675657.89	5.32	-7.89	9.52
30	613265.58	6648397.85	-5.58	-7.85	9.63
31	614500.81	6647373.36	-10.81	-13.36	17.19
32	624097.32	6677220.00	-7.32	0.00	7.32
33	604805.85	6671051.09	-5.85	-1.09	5.95
35	595646.58	6654750.10	-6.58	9.90	11.89
39	596591.98	6650225.47	8.02	-0.47	8.03
40	625660.58	6683500.86	-0.58	-0.86	1.04

RMS ±9.30 ±7.54 ±11.98

RESIDUAL ERRORS AT CHECK POINTS:

GCPID	CALCULATED CHECK POINT		ERRORS (Metre)		
	X	Y	X	Y	Vector
-6	628970.88	6657271.16	-2.08	-6.86	7.17
-8	600279.43	6668079.16	-9.53	-0.16	9.53
-13	598380.39	6685611.32	-9.99	1.38	10.09
-22	602743.72	6639890.55	-11.72	16.65	20.36
-25	632701.84	6679841.19	-2.34	-6.09	6.52
-27	608196.97	6651213.85	-7.87	9.25	12.14
-28	604585.73	6658343.72	-0.13	-0.42	0.44
-29	589877.88	6654387.03	-2.08	4.47	4.93
-34	626390.64	6630633.98	-5.84	9.92	11.51
-36	609342.20	6682804.07	-8.70	-3.47	9.37
-37	630351.82	6677286.16	-1.02	-8.06	8.13
-38	633118.05	6632080.08	-3.35	6.72	7.51
-41	590711.32	6640045.11	-4.92	25.69	26.15
-42	601690.81	6646241.67	-8.51	12.43	15.06
-43	629940.37	6668092.15	0.13	-2.15	2.15
-44	605005.17	6662941.64	-5.37	10.16	11.49
-45	634360.16	6677038.60	-3.26	-10.50	10.99

RMS ±6.43 ±10.37 ±12.21

N02 (2 X ellipsoid normal) : 0.1278845814253259D+08
aa (Unknown tied to Earth rotation) : 0.3615439144847024D-01
ALPHA (IFOV) : 0.1200000000000000D-04
bb (Unknown of 2nd order) : 0.1220535059449868D-07
C0 (Scene centre column) : 0.3000000000000000D+04
cc (Unknown of 2nd order): -.3280176034502756D-08

COSKHI (Parameter): 0.9999536804327340D+00
DELGAM (Unknown of 2nd order): -.1504103343773206D-07
GAMMA (Scene orient. rel. to the North): 0.2100156909742872D+00
K_1 (Cross track scale function): 0.1377140387922372D-05
L0 (Scene centre row): 0.3000000000000000D+04
P (Along track scale function): 0.9974997036387514D+01
Q (Satellite-Scene centre dist): 0.9024909029255728D+06
TAU (Levelling angle along track dir): -.9625256954302362D-02
THETA (Levelling angle across track dir): -.2984784422741537D+00
THETAS (THETA/COS_KHI): -.2984922683068540D+00
X0 (Carto coord of scene centre): 0.6212457564503327D+06
Y0 (Carto coord of scene centre): 0.6660013486373032D+07
DELH (Radar parameter in H dir.): 0.0000000000000000D+00
COEFY2 (Radar parameter in Y2 dir.): 0.0000000000000000D+00

EARTH ELLIPSOID USED : E012

E.1.3 Third Test

The following are the results of the space resection giving the planimetric accuracy of the left image of the Level 1A stereo-model for the reference scene 122/285 using 26 control points and 17 check points:

SMODEL Satellite Model Calculation V6.0 EASI/PACE 15:28 19-OCT-97

Report File : E:\OSLO\SM26GA.TXT

Using GCPs stored in the GCP segment :

GCPID	CALCULATED GCP		RESIDUAL (Metre)		
	X	Y	ΔX	ΔY	Vector
2	620349.65	6671011.34	0.35	13.66	13.66
3	636531.36	6670288.90	8.64	1.10	8.71
4	594705.33	6673950.49	4.67	-0.49	4.69
5	617817.96	6685039.57	2.04	0.43	2.08
7	633018.40	6663627.94	-8.40	2.06	8.64
9	601248.70	6656920.03	1.30	9.97	10.05
10	609861.79	6672275.57	-11.79	4.43	12.59
11	611724.06	6654753.09	15.94	-3.09	16.23
12	603660.32	6683791.31	-0.32	-1.31	1.35
14	619744.35	6651785.83	-4.35	4.17	6.03
15	636784.17	6642004.76	-4.17	-4.76	6.33
16	623910.14	6645606.39	9.86	-6.39	11.75
17	617345.59	6647748.81	-5.59	1.19	5.71
19	615285.52	6640581.46	4.48	-1.46	4.71
20	611410.82	6639013.06	-10.82	-3.06	11.24
21	609091.59	6646402.66	8.41	-2.66	8.82
23	605077.53	6650643.72	2.47	-13.72	13.95
24	629031.42	6630268.03	8.58	11.97	14.73
26	601321.26	6675661.14	3.74	-11.14	11.76
30	613269.41	6648399.24	-9.41	-9.24	13.19
31	614500.97	6647363.17	-10.97	-3.17	11.42
32	624101.10	6677223.45	-11.10	-3.45	11.62
33	604802.57	6671046.63	-2.57	3.37	4.24
35	595647.00	6654749.73	-7.00	10.27	12.42
39	596593.32	6650220.80	6.68	4.20	7.89
40	625650.69	6683502.87	9.31	-2.87	9.74

RMS ±7.88 ±6.72 ±10.36

RESIDUAL ERRORS AT CHECK POINTS:

GCPID	CALCULATED CHECK POINT		ERRORS (Metre)		
	X	Y	ΔX	ΔY	Vector
-6	628969.31	6657275.67	-0.51	-11.37	11.39
-8	600282.07	6668078.53	-12.17	0.47	12.18
-13	598383.48	6685610.62	-13.08	2.08	13.25
-22	602741.25	6639896.13	-9.25	11.07	14.42
-25	632699.97	6679843.32	-0.47	-8.22	8.23
-27	608196.08	6651215.86	-6.98	7.24	10.05
-28	604589.60	6658347.35	-4.00	-4.05	5.69
-29	589882.86	6654386.66	-7.06	4.84	8.56
-34	626396.13	6630643.01	-11.33	0.89	11.37
-36	609341.96	6682806.00	-8.46	-5.40	10.04
-37	630349.26	6677285.43	1.54	-7.33	7.49
-38	633123.90	6632085.16	-9.20	1.64	9.35
-41	590712.57	6640048.32	-6.17	22.48	23.31
-42	601695.94	6646243.51	-13.64	10.59	17.27
-43	629942.04	6668094.85	-1.54	-4.85	5.09
-44	605000.98	6662950.12	-1.18	1.68	2.05
-45	634355.24	6677041.65	1.66	-13.55	13.65

RMS ±8.05 ±9.12 ±12.16

N02 (2 X ellipsoid normal) : 0.1278845814253259D+08
aa (Unknown tied to Earth rotation) : 0.2989660254630713D-01
ALPHA (IFOV) : 0.1200000000000000D-04
bb (Unknown of 2nd order) : 0.6576045830144635D-08
C0 (Scene centre column) : 0.3000000000000000D+04
cc (Unknown of 2nd order): -.3438413378293570D-09
COSKHI (Parameter): 0.9999102112111102D+00
DELGAM (Unknown of 2nd order): -.4084609461756581D-08
GAMMA (Scene orient. rel. to the North): 0.3472325523131136D+00
K_1 (Cross track scale function): 0.1383787271069959D-05
L0 (Scene centre row): 0.3000000000000000D+04
P (Along track scale function): 0.1001617386062007D+02
Q (Satellite-Scene centre dist): 0.9112772324414908D+06
TAU (Levelling angle along track dir): -.1340155837040395D-01
THETA (Levelling angle across track dir): 0.3219128970679672D+00
THETAS (THETA/COS_KHI): 0.3219418038326264D+00
X0 (Carto coord of scene centre): 0.6096143808258316D+06
Y0 (Carto coord of scene centre): 0.6659682657622444D+07
DELH (Radar parameter in H dir.): 0.0000000000000000D+00
COEFY2 (Radar parameter in Y2 dir.): 0.0000000000000000D+00

EARTH ELLIPSOID USED : E012

The following are the results of the space resection giving the planimetric accuracy of the right image of the Level 1A stereo-model for the reference scene 122/285 using 26 control points and 17 check points:

SMODEL Satellite Model Calculation V6.0 EASI/PACE 16:53 06-NOV-97

Report File : E:\OSLO\SM17CHB.TXT

Using GCPs stored in the GCP segment :

GCPID	CALCULATED GCP		RESIDUAL (Metre)		
	X	Y	ΔX	ΔY	Vector
2	620351.63	6671012.46	-1.63	12.54	12.64
3	636536.85	6670288.05	3.15	1.95	3.70
4	594704.62	6673950.07	5.38	-0.07	5.38
5	617814.75	6685041.49	5.25	-1.49	5.46
7	633015.88	6663632.23	-5.88	-2.23	6.29
9	601251.49	6656913.88	-1.49	16.12	16.19
10	609860.22	6672276.67	-10.22	3.33	10.75
11	611730.76	6654750.20	9.24	-0.20	9.25
12	603659.08	6683790.45	0.92	-0.45	1.03
14	619739.94	6651791.69	0.06	-1.69	1.69
15	636781.92	6642005.61	-1.92	-5.61	5.93
16	623905.75	6645603.99	14.25	-3.99	14.79
17	617351.45	6647743.56	-11.45	6.44	13.14
19	615278.13	6640587.68	11.87	-7.68	14.14
20	611408.72	6639012.08	-8.72	-2.08	8.97
21	609093.76	6646402.77	6.24	-2.77	6.82
23	605080.54	6650640.45	-0.54	-10.45	10.47
24	629034.86	6630262.28	5.14	17.72	18.45
26	601317.72	6675658.67	7.28	-8.67	11.32
30	613266.89	6648396.83	-6.89	-6.83	9.71
31	614502.28	6647372.31	-12.28	-12.31	17.39
32	624094.88	6677219.78	-4.88	0.22	4.89
33	604804.27	6671051.43	-4.27	-1.43	4.50
35	595647.67	6654749.77	-7.67	10.23	12.78
39	596593.58	6650224.80	6.42	0.20	6.42
40	625657.33	6683500.79	2.67	-0.79	2.79
		RMS	±7.26	±7.50	±10.44

RESIDUAL ERRORS AT CHECK POINTS:

GCPID	CALCULATED CHECK POINT		ERRORS (Metre)		
	X	Y	ΔX	ΔY	Vector
-6	628971.64	6657270.30	-2.84	-6.00	6.64
-8	600278.86	6668078.70	-8.96	0.30	8.97
-13	598378.02	6685611.67	-7.62	1.03	7.69
-22	602746.19	6639889.51	-14.19	17.69	22.68
-25	632699.61	6679840.69	-0.11	-5.59	5.59
-27	608197.66	6651213.55	-8.56	9.55	12.83
-28	604585.99	6658342.95	-0.39	0.35	0.53
-29	589879.87	6654386.19	-4.07	5.31	6.69
-34	626395.25	6630632.48	-10.45	11.42	15.47
-36	609339.28	6682804.04	-5.78	-3.44	6.73
-37	630349.82	6677285.58	0.98	-7.48	7.55
-38	633123.34	6632078.36	-8.64	8.44	12.08
-41	590714.91	6640043.43	-8.51	27.37	28.66
-42	601692.54	6646240.85	-10.24	13.25	16.74
-43	629939.67	6668091.40	0.83	-1.40	1.63
-44	605004.84	6662941.04	-5.04	10.76	11.88

-45	634358.50	6677037.96	-1.60	-9.86	9.98
		RMS	±7.34	±10.92	±13.16

N02 (2 X ellipsoid normal) : 0.1278845814253259D+08
aa (Unknown tied to Earth rotation) : 0.3602092334589838D-01
ALPHA (IFOV) : 0.1200000000000000D-04
bb (Unknown of 2nd order) : 0.1220535059449868D-07
C0 (Scene centre column) : 0.3000000000000000D+04
cc (Unknown of 2nd order): -.3280176034502756D-08
COSKHI (Parameter): 0.9999837045824788D+00
DELGAM (Unknown of 2nd order): -.1504103343773206D-07□
GAMMA (Scene orient. rel. to the North): 0.2100269457744368D+00
K_1 (Cross track scale function): 0.1374839390324890D-05
L0 (Scene centre row): 0.3000000000000000D+04
P (Along track scale function): 0.9974883273892482D+01
Q (Satellite-Scene centre dist): 0.9025600323593596D+06
TAU (Levelling angle along track dir): -.5708908098895577D-02
THETA (Levelling angle across track dir): -.2955874360180536D+00
THETAS (THETA/COS_KHI): -.2955922528172293D+00
X0 (Carto coord of scene centre): 0.6212459636979026D+06
Y0 (Carto coord of scene centre): 0.6660012095117809D+07
DELH (Radar parameter in H dir.): 0.0000000000000000D+00
COEFY2 (Radar parameter in Y2 dir.): 0.0000000000000000D+00

EARTH ELLIPSOID USED : E012

E.1.4 Fourth Test

The following are the results of the space resection giving the planimetric accuracy of the left image of the Level 1A stereo-model for the reference scene 122/285 using 26 control points:

SMODEL Satellite Model Calculation V6.0 EASI/PACE 14:08 21-OCT-97

Report File : E:\OSLO\SM26GMA.TXT

Using GCPs stored in the GCP segment :

GCPID	CALCULATED GCP		RESIDUAL (Metre)		
	X	Y	ΔX	ΔY	Vector
2	620349.65	6671011.34	0.35	13.66	13.66
3	636531.36	6670288.90	8.64	1.10	8.71
4	594705.33	6673950.49	4.67	-0.49	4.69
5	617817.96	6685039.57	2.04	0.43	2.08
7	633018.40	6663627.94	-8.40	2.06	8.64
30	613269.41	6648399.24	-9.41	-9.24	13.19
9	601248.70	6656920.03	1.30	9.97	10.05
10	609861.79	6672275.57	-11.79	4.43	12.59
11	611724.06	6654753.09	15.94	-3.09	16.23
12	603660.32	6683791.31	-0.32	-1.31	1.35
31	614500.97	6647363.17	-10.97	-3.17	11.42
14	619744.35	6651785.83	-4.35	4.17	6.03
15	636784.17	6642004.76	-4.17	-4.76	6.33
16	623910.14	6645606.39	9.86	-6.39	11.75
17	617345.59	6647748.81	-5.59	1.19	5.71
19	615285.52	6640581.46	4.48	-1.46	4.71

20	611410.82	6639013.06	-10.82	-3.06	11.24
21	609091.59	6646402.66	8.41	-2.66	8.82
32	624101.10	6677223.45	-11.10	-3.45	11.62
23	605077.53	6650643.72	2.47	-13.72	13.95
24	629031.42	6630268.03	8.58	11.97	14.73
33	604802.57	6671046.63	-2.57	3.37	4.24
26	601321.26	6675661.14	3.74	-11.14	11.76
40	625650.69	6683502.87	9.31	-2.87	9.74
39	596593.32	6650220.80	6.68	4.20	7.89
35	595647.00	6654749.73	-7.00	10.27	12.42
		RMS	±7.88	±6.72	±10.36

N02 (2 X ellipsoid normal) : 0.1278845814253259D+08
aa (Unknown tied to Earth rotation) : 0.2989660254630708D-01
ALPHA (IFOV) : 0.1200000000000000D-04
bb (Unknown of 2nd order) : 0.6576045830144635D-08
C0 (Scene centre column) : 0.3000000000000000D+04
cc (Unknown of 2nd order): -.3438413378293570D-09
COSKHI (Parameter): 0.9999102112111102D+00
DELGAM (Unknown of 2nd order): -.4084609461756581D-08
GAMMA (Scene orient. rel. to the North): 0.3472325523131136D+00
K_1 (Cross track scale function): 0.1383787271069960D-05
L0 (Scene centre row): 0.3000000000000000D+04
P (Along track scale function): 0.1001617386062007D+02
Q (Satellite-Scene centre dist): 0.9112772324414908D+06
TAU (Levelling angle along track dir): -.1340155837040404D-01
THETA (Levelling angle across track dir): 0.3219128970679680D+00
THETAS (THETA/COS_KHI): 0.3219418038326271D+00
X0 (Carto coord of scene centre): 0.6096143808258316D+06
Y0 (Carto coord of scene centre): 0.6659682657622444D+07
DELH (Radar parameter in H dir.): 0.0000000000000000D+00
COEFY2 (Radar parameter in Y2 dir.): 0.0000000000000000D+00

EARTH ELLIPSOID USED : E012

The following are the results of the space resection giving the planimetric accuracy of the right image of the Level 1A stereo-model for the reference scene 122/285 using 26 control points:

SMODEL Satellite Model Calculation V6.0 EASI/PACE 14:03 21-OCT-97

Report File : E:\OSLO\SM26GMB.TXT

Using GCPs stored in the GCP segment :

GCPID	CALCULATED GCP		RESIDUAL (Metre)		
	X	Y	ΔX	ΔY	Vector
2	620351.63	6671012.46	-1.63	12.54	12.64
3	636536.85	6670288.05	3.15	1.95	3.70
4	594704.62	6673950.07	5.38	-0.07	5.38
5	617814.75	6685041.49	5.25	-1.49	5.46
32	624094.88	6677219.78	-4.88	0.22	4.89
7	633015.88	6663632.23	-5.88	-2.23	6.29
33	604804.27	6671051.43	-4.27	-1.43	4.50
9	601251.49	6656913.88	-1.49	16.12	16.19

10	609860.22	6672276.67	-10.22	3.33	10.75
11	611730.76	6654750.20	9.24	-0.20	9.25
12	603659.08	6683790.45	0.92	-0.45	1.03
30	613266.89	6648396.83	-6.89	-6.83	9.71
14	619739.94	6651791.69	0.06	-1.69	1.69
15	636781.92	6642005.61	-1.92	-5.61	5.93
16	623905.75	6645603.99	14.25	-3.99	14.79
17	617351.45	6647743.56	-11.45	6.44	13.14
19	615278.13	6640587.68	11.87	-7.68	14.14
20	611408.72	6639012.08	-8.72	-2.08	8.97
21	609093.76	6646402.77	6.24	-2.77	6.82
35	595647.67	6654749.77	-7.67	10.23	12.78
23	605080.54	6650640.45	-0.54	-10.45	10.47
24	629034.86	6630262.28	5.14	17.72	18.45
39	596593.58	6650224.80	6.42	0.20	6.42
26	601317.72	6675658.67	7.28	-8.67	11.32
40	625657.33	6683500.79	2.67	-0.79	2.79
31	614502.28	6647372.31	-12.28	-12.31	17.39
		RMS	±7.26	±7.50	±10.44

N02 (2 X ellipsoid normal) : 0.1278845814253259D+08
aa (Unknown tied to Earth rotation) : 0.3602092334589840D-01
ALPHA (IFOV) : 0.1200000000000000D-04
bb (Unknown of 2nd order) : 0.1220535059449868D-07
C0 (Scene centre column) : 0.3000000000000000D+04
cc (Unknown of 2nd order): -.3280176034502756D-08
COSKHI (Parameter): 0.9999837045824788D+00
DELGAM (Unknown of 2nd order): -.1504103343773206D-07
GAMMA (Scene orient. rel. to the North): 0.2100269457744368D+00
K_1 (Cross track scale function): 0.1374839390324890D-05
L0 (Scene centre row): 0.3000000000000000D+04
P (Along track scale function): 0.9974883273892482D+01
Q (Satellite-Scene centre dist): 0.9025600323593596D+06
TAU (Levelling angle along track dir): -.5708908098895511D-02
THETA (Levelling angle across track dir): -.2955874360180534D+00
THETAS (THETA/COS_KHI): -.2955922528172290D+00
X0 (Carto coord of scene centre): 0.6212459636979026D+06
Y0 (Carto coord of scene centre): 0.6660012095117809D+07
DELH (Radar parameter in H dir.): 0.0000000000000000D+00
COEFY2 (Radar parameter in Y2 dir.): 0.0000000000000000D+00

EARTH ELLIPSOID USED : E012

E.1.5 Fifth Test

The following are the results of the space resection giving the planimetric accuracy of the left image of the Level 1A stereo-model for the reference scene 122/285 using 17 control points:

SMODEL Satellite Model Calculation V6.0 EASI/PACE 13:45 21-OCT-97

Report File : E:\OSLO\SM17G.TXT

Using GCPs stored in the GCP segment :

GCPID	CALCULATED GCP		RESIDUAL (Metre)		
	X	Y	ΔX	ΔY	Vector

45	634354.47	6677029.85	2.43	-1.75	2.99
44	604994.58	6662952.76	5.22	-0.96	5.31
43	629940.03	6668086.91	0.47	3.09	3.12
42	601688.26	6646251.17	-5.96	2.93	6.64
6	628965.97	6657270.67	2.83	-6.37	6.97
41	590701.02	6640063.48	5.38	7.32	9.08
8	600274.19	6668081.87	-4.29	-2.87	5.16
25	632699.50	6679831.26	0.00	3.84	3.84
27	608190.41	6651218.80	-1.31	4.30	4.50
38	633115.85	6632086.33	-1.15	0.47	1.24
37	630348.31	6677275.01	2.49	3.09	3.97
13	598374.65	6685609.87	-4.25	2.83	5.10
36	609337.26	6682801.88	-3.76	-1.28	3.98
22	602733.47	6639905.14	-1.47	2.06	2.53
34	626388.74	6630646.32	-3.94	-2.42	4.62
29	589871.17	6654397.66	4.63	-6.16	7.71
28	604582.91	6658351.42	2.69	-8.12	8.55
		RMS	±3.64	±4.27	±5.61

N02 (2 X ellipsoid normal) : 0.1278845814253259D+08
aa (Unknown tied to Earth rotation) : 0.2993127233449764D-01
ALPHA (IFOV) : 0.1200000000000000D-04
bb (Unknown of 2nd order) : 0.6576045830144635D-08
C0 (Scene centre column) : 0.3000000000000000D+04
cc (Unknown of 2nd order): -.3438413378293570D-09
COSKHI (Parameter): 0.9997620507942910D+00
DELGAM (Unknown of 2nd order): -.4084609461756581D-08
GAMMA (Scene orient. rel. to the North): 0.3474435497443455D+00
K_1 (Cross track scale function): 0.1378494042082652D-05
L0 (Scene centre row): 0.3000000000000000D+04
P (Along track scale function): 0.1001327799014653D+02
Q (Satellite-Scene centre dist): 0.9115382995536038D+06
TAU (Levelling angle along track dir): -.2181899000407529D-01
THETA (Levelling angle across track dir): 0.3154929404147840D+00
THETAS (THETA/COS_KHI): 0.3155680295767689D+00
X0 (Carto coord of scene centre): 0.6096086301863962D+06
Y0 (Carto coord of scene centre): 0.6659685554649151D+07
DELH (Radar parameter in H dir.): 0.0000000000000000D+00
COEFY2 (Radar parameter in Y2 dir.): 0.0000000000000000D+00

EARTH ELLIPSOID USED : E012

The following are the results of the space resection giving the planimetric accuracy of the right image of the Level 1A stereo-model for the reference scene 122/285 using 17 control points:

SMODEL Satellite Model Calculation V6.0 EASI/PACE 13:52 21-OCT-97

Report File : E:\OSLO\SM17GB.TXT

Using GCPs stored in the GCP segment :

GCPID	CALCULATED GCP		RESIDUAL (Metre)		
	X	Y	X	Y	Vector
45	634357.99	6677029.35	-1.09	-1.25	1.66
44	604998.61	6662946.78	1.19	5.02	5.16
43	629937.17	6668087.57	3.33	2.43	4.12

42	601683.26	6646253.70	-0.96	0.40	1.04
6	628967.35	6657270.45	1.45	-6.15	6.32
41	590704.81	6640063.74	1.59	7.06	7.24
8	600273.14	6668083.59	-3.24	-4.59	5.61
25	632699.16	6679831.49	0.34	3.61	3.63
27	608189.22	6651221.32	-0.12	1.78	1.78
38	633116.69	6632086.67	-1.99	0.13	1.99
37	630348.71	6677278.30	2.09	-0.20	2.10
13	598374.64	6685608.67	-4.24	4.03	5.85
36	609336.36	6682800.34	-2.86	0.26	2.87
22	602736.10	6639904.78	-4.10	2.42	4.76
34	626386.96	6630643.47	-2.16	0.43	2.20
29	589871.56	6654399.35	4.24	-7.85	8.92
28	604579.08	6658350.83	6.52	-7.53	9.96
		RMS	±3.02	±4.32	±5.27

N02 (2 X ellipsoid normal) : 0.1278845814253259D+08
aa (Unknown tied to Earth rotation) : 0.3611933271730150D-01
ALPHA (IFOV) : 0.1200000000000000D-04
bb (Unknown of 2nd order) : 0.1220535059449868D-07
C0 (Scene centre column) : 0.3000000000000000D+04
cc (Unknown of 2nd order): -.3280176034502756D-08
COSKHI (Parameter): 0.9998139778382702D+00
DELGAM (Unknown of 2nd order): -.1504103343773206D-07
GAMMA (Scene orient. rel. to the North): 0.2102072678883982D+00
K_1 (Cross track scale function): 0.1373199144543332D-05
L0 (Scene centre row): 0.3000000000000000D+04
P (Along track scale function): 0.9971122708781452D+01
Q (Satellite-Scene centre dist): 0.9027010969589874D+06
TAU (Levelling angle along track dir): -.1929114205920085D-01
THETA (Levelling angle across track dir): -.2933568241456258D+00
THETAS (THETA/COS_KHI): -.2934114051694916D+00
X0 (Carto coord of scene centre): 0.6212416725826942D+06
Y0 (Carto coord of scene centre): 0.6660015861875497D+07
DELH (Radar parameter in H dir.): 0.0000000000000000D+00
COEFY2 (Radar parameter in Y2 dir.): 0.0000000000000000D+00

EARTH ELLIPSOID USED : E012

E.2 Accuracy Results of Absolute Orientation of the Oslo Stereo-model

E.2.1 First Test Using 45 Ground Control Points

Calculated				Errors (metres)		
GCPID	X	Y	Z	ΔX	ΔY	ΔZ
1	619249.60	6677242.76	164.5	10.4	7.2	-25.5
2	620350.78	6671008.34	181.8	-0.8	16.7	3.2
3	636533.51	6670283.86	111.7	6.5	6.1	7.3
4	594699.75	6673954.42	230.9	10.2	-4.4	3.1
5	617817.41	6685036.53	177.2	2.6	3.5	-2.2
6	628969.65	6657272.68	183.5	-0.9	-8.4	4.0
7	633015.18	6663625.61	126.5	-5.2	4.4	-7.5
8	600277.13	6668081.96	180.1	-7.2	-3.0	-2.9
9	601247.51	6656921.66	266.1	2.5	8.3	6.9
10	609860.12	6672274.95	220.7	-10.1	5.0	-0.7
11	611725.99	6654752.04	242.6	14.0	-2.0	10.4
12	603657.97	6683790.51	294.9	2.0	-0.5	4.1

13	598377.28	6685611.56	343.9	-6.9	1.1	-1.9
14	619739.53	6651786.66	172.3	0.5	3.3	-11.3
15	636777.00	6642004.60	189.3	3.0	-4.6	-7.3
16	623905.45	6645606.84	190.4	14.6	-6.8	-8.4
17	617346.63	6647749.66	92.6	-6.6	0.3	8.4
18	623154.02	6638374.82	70.0	-14.0	5.2	31.0
19	615278.26	6640583.36	282.7	11.7	-3.4	-16.7
20	611406.57	6639016.29	176.1	-6.6	-6.3	-6.1
21	609089.71	6646405.25	153.2	10.3	-5.2	0.8
22	602740.08	6639900.94	105.3	-8.1	6.3	6.8
23	605076.55	6650645.14	251.3	3.4	-15.1	4.7
24	629027.90	6630268.70	209.3	12.1	11.3	3.7
25	632701.48	6679837.25	178.4	-2.0	-2.1	1.1
26	601317.70	6675659.88	435.9	7.3	-9.9	0.1
27	608194.80	6651216.82	241.7	-5.7	6.3	2.0
28	604585.63	6658351.00	121.2	0.0	-7.7	-4.0
29	589874.54	6654394.52	182.3	1.3	-3.0	-4.6
30	613265.99	6648402.00	106.2	-6.0	-12.0	-5.2
31	614497.74	6647365.73	105.6	-7.7	-5.7	-4.6
32	624099.82	6677219.61	208.6	-9.8	0.4	-6.6
33	604801.04	6671045.72	327.7	-1.0	4.3	3.3
34	626391.56	6630644.82	173.5	-6.8	-0.9	-0.9
35	595642.42	6654753.98	257.2	-2.4	6.0	0.8
36	609340.47	6682804.88	205.9	-7.0	-4.3	1.1
37	630350.55	6677280.38	155.6	0.3	-2.3	1.1
38	633117.78	6632086.14	194.5	-3.1	0.7	-1.8
39	596588.02	6650226.35	185.6	12.0	-1.4	-2.6
40	625656.09	6683496.16	202.8	3.9	3.8	13.2
41	590706.76	6640058.57	4.4	-0.4	12.2	1.6
42	601690.72	6646248.69	150.4	-8.4	5.4	-6.3
43	629941.18	6668091.29	165.2	-0.7	-1.3	-2.9
44	605001.37	6662951.81	132.6	-1.6	0.0	10.2
45	634358.17	6677035.23	170.7	-1.3	-7.1	6.4
	RMS Error :			±7.2	±6.6	± 8.5

E.2.2 Second Test Using 28 Control Points and 17 Check Points

Calculated				Errors (metres)		
GCPIDS	X	Y	Z	ΔX	ΔY	ΔZ
2	620350.48	6671011.08	182.4	-0.5	13.9	2.6
3	636534.31	6670287.96	110.2	5.7	2.0	8.8
4	594705.11	6673950.56	234.8	4.9	-0.6	-0.8
5	617816.23	6685040.12	180.7	3.8	-0.1	-5.7
7	633016.53	6663628.54	124.6	-6.5	1.5	-5.6
9	601250.78	6656919.37	266.0	-0.8	10.6	7.0
10	609860.96	6672275.83	222.7	-11.0	4.2	-2.7
11	611727.68	6654751.95	241.4	12.3	-1.9	11.6
12	603659.90	6683791.44	300.4	0.1	-1.4	-1.4
14	619741.43	6651786.76	170.1	-1.4	3.2	-9.1
15	636782.90	6642005.17	185.6	-2.9	-5.2	-3.6
16	623908.32	6645606.97	187.5	11.7	-7.0	-5.5
17	617349.19	6647747.66	89.8	-9.2	2.3	11.2
19	615281.14	6640582.85	279.5	8.9	-2.9	-13.5
20	611409.99	6639013.32	172.6	-10.0	-3.3	-2.6

21	609092.65	6646402.33	150.6	7.3	-2.3	3.4
23	605079.41	6650643.13	249.9	0.6	-13.1	6.1
24	629034.12	6630267.16	205.2	5.9	12.8	7.8
26	601320.05	6675661.52	440.2	5.0	-11.5	-4.2
30	613268.54	6648399.51	103.7	-8.5	-9.5	-2.7
31	614500.41	6647363.34	102.7	-10.4	-3.3	-1.7
32	624098.60	6677224.24	209.9	-8.6	-4.2	-7.9
33	604802.81	6671046.56	330.2	-2.8	3.4	0.8
35	595647.35	6654749.62	256.8	-7.4	10.4	1.2
39	596593.00	6650220.90	184.1	7.0	4.1	-1.1
40	625654.20	6683501.76	204.9	5.8	-1.8	11.1
		RMS Error :	±7.2	±6.9	±6.7	

Calculated				Error (metres)		
CHKID	X	Y	Z	ΔX	ΔY	ΔZ
-6	628971.28	6657275.05	181.6	-2.5	-10.7	5.9
-8	600280.65	6668078.98	182.1	-10.7	0.0	-4.9
-13	598381.03	6685611.38	350.7	-10.6	1.3	-8.7
-22	602744.44	6639895.13	101.8	-12.4	12.1	10.3
-25	632700.17	6679843.25	178.9	-0.7	-8.2	0.6
-27	608197.18	6651215.51	240.1	-8.1	7.6	3.6
-28	604588.51	6658347.69	120.8	-2.9	-4.4	-3.6
-29	589881.66	6654387.04	181.9	-5.9	4.5	-4.2
-34	626397.25	6630642.65	169.3	-12.5	1.2	3.3
-36	609341.01	6682806.30	210.2	-7.5	-5.7	-3.2
-37	630349.54	6677285.34	155.9	1.3	-7.2	0.8
-38	633124.67	6632084.91	190.5	-10.0	1.9	2.2
-41	590714.34	6640047.77	0.0	-7.9	23.0	6.0
-42	601694.74	6646243.88	148.0	-12.4	10.2	-3.9
-43	629941.35	6668095.07	164.4	-0.9	-5.1	-2.1
-44	605003.90	6662949.20	133.1	-4.1	2.6	9.7
-45	634357.42	6677040.96	170.5	-0.5	-12.9	6.6
		RMS Error :	±8.1	±9.2	±5.6	

E.2.3 Third Test Using 26 Ground Control Points Derived from Map

Calculated				Errors (metres)		
GCPID	X	Y	Z	ΔX	ΔY	ΔZ
2	620350.48	6671011.08	182.4	-0.5	13.9	2.6
3	636534.31	6670287.96	110.2	5.7	2.0	8.8
4	594705.11	6673950.56	234.8	4.9	-0.6	-0.8
5	617816.23	6685040.12	180.7	3.8	-0.1	-5.7
7	633016.53	6663628.54	124.6	-6.5	1.5	-5.6
9	601250.78	6656919.37	266.0	-0.8	10.6	7.0
10	609860.96	6672275.83	222.7	-11.0	4.2	-2.7
11	611727.68	6654751.95	241.4	12.3	-1.9	11.6
12	603659.90	6683791.44	300.4	0.1	-1.4	-1.4
14	619741.43	6651786.76	170.1	-1.4	3.2	-9.1
15	636782.90	6642005.17	185.6	-2.9	-5.2	-3.6
16	623908.32	6645606.97	187.5	11.7	-7.0	-5.5
17	617349.19	6647747.66	89.8	-9.2	2.3	11.2

19	615281.14	6640582.85	279.5	8.9	-2.9	-13.5
20	611409.99	6639013.32	172.6	-10.0	-3.3	-2.6
21	609092.65	6646402.33	150.6	7.3	-2.3	3.4
23	605079.41	6650643.13	249.9	0.6	-13.1	6.1
24	629034.12	6630267.16	205.2	5.9	12.8	7.8
26	601320.05	6675661.52	440.2	5.0	-11.5	-4.2
30	613268.54	6648399.51	103.7	-8.5	-9.5	-2.7
31	614500.41	6647363.34	102.7	-10.4	-3.3	-1.7
32	624098.60	6677224.24	209.9	-8.6	-4.2	-7.9
33	604802.81	6671046.56	330.2	-2.8	3.4	0.8
35	595647.35	6654749.62	256.8	-7.4	10.4	1.2
39	596593.00	6650220.90	184.1	7.0	4.1	-1.1
40	625654.20	6683501.76	204.9	5.8	-1.8	11.1

RMS Error : ±7.2 ±6.9 ±6.7

E.2.4 Fourth Test Using 17 Road Database Ground Control Points

Calculated				Errors (metres)		
GCPID	X	Y	Z	ΔX	ΔY	ΔZ
45	634356.33	6677029.30	171.4	0.6	-1.2	5.7
44	604997.21	6662952.01	133.9	2.6	-0.2	8.9
43	629938.53	6668087.35	166.9	2.0	2.7	-4.6
42	601685.67	6646251.91	152.7	-3.4	2.2	-8.6
6	628966.74	6657270.45	185.2	2.1	-6.2	2.3
41	590702.77	6640062.99	0.0	3.6	7.8	6.0
8	600273.54	6668082.05	179.5	-3.6	-3.1	-2.3
25	632699.31	6679831.31	180.1	0.2	3.8	-0.6
27	608189.58	6651219.03	246.4	-0.5	4.1	-2.7
38	633116.30	6632086.20	191.4	-1.6	0.6	1.3
37	630348.06	6677275.08	157.5	2.7	3.0	-0.8
13	598374.83	6685609.82	341.4	-4.4	2.9	0.6
36	609337.07	6682801.94	207.7	-3.6	-1.3	-0.7
22	602734.78	6639904.76	107.8	-2.8	2.4	4.3
34	626388.30	6630646.45	173.9	-3.5	-2.5	-1.3
29	589871.18	6654397.66	177.7	4.6	-6.2	0.0
28	604581.25	6658351.89	122.8	4.3	-8.6	-5.6

RMS Error : ±3.1 ±4.3 ±4.4

E.3 Accuracy Results of Height in DEM

E.3.1 Accuracy Results of Heights in DEM at 43 Ground Control Points

DBIW resized to :
DBIW(1) = 694 DBIW(2) = 97
DBIW(3) = 5094 DBIW(4) = 5831

RMS Error Report on DEM file

GCP No.	Image Pixel	Image Line	Input Elev.	Calc. Elev.	Diff Elev
1	1617	512	139.0	158.0	-19.0
2	1768	786	185.0	190.0	-5.0
3	2461	545	119.0	123.0	-4.0
4	623	1084	234.0	241.0	-7.0
5	1425	170	175.0	184.0	-9.0
6	2361	1284	187.5	186.0	1.5

7	2424	917	119.0	133.0	-14.0
8	962	1265	177.2	187.0	-9.8
9	1194	1772	273.0	275.0	-2.0
10	1302	905	220.0	222.0	-2.0
11	1677	1696	253.0	253.0	0.0
12	842	469	299.0	303.0	-4.0
13	584	473	342.0	357.0	-15.0
14	2064	1699	161.0	171.0	-10.0
16	2342	1918	182.0	184.0	-2.0
17	2029	1929	101.0	102.0	-1.0
18	2429	2270	101.0	110.0	-9.0
19	2065	2300	266.0	273.0	-7.0
20	1926	2440	170.0	167.0	3.0
21	1704	2132	154.0	154.0	0.0
22	1543	2545	112.1	115.0	-2.9
23	1463	2001	256.0	259.0	-3.0
24	2811	2551	213.0	218.0	-5.0
25	2142	161	179.5	181.0	-1.5
26	881	891	436.0	439.0	-3.0
27	1586	1921	243.7	237.0	6.7
28	1310	1648	117.2	129.0	-11.8
29	748	2084	177.7	181.0	-3.3
30	1846	1968	101.0	102.0	-1.0
31	1916	1995	101.0	100.0	1.0
32	1823	430	202.0	207.0	-5.0
33	1108	1048	331.0	328.0	3.0
34	2694	2578	172.6	170.0	2.6
35	991	1969	258.0	260.0	-2.0
36	1101	419	207.0	209.0	-2.0
37	2085	321	156.7	158.0	-1.3
39	1107	2165	183.0	187.0	-4.0
40	1784	109	216.0	221.0	-5.0
41	1026	2743	6.0	11.0	-5.0
42	1392	2265	144.1	148.0	-3.9
43	2221	760	162.3	166.0	-3.7
44	1251	1425	142.8	144.0	-1.2
45	2258	265	177.1	177.0	0.1

No. of GCP Points within DBIW window : 43
Root Mean Sq. Error in elevation (m) : ±6.3m

E.3.2 Accuracy Results of Height in DEM at 25 Control Points and 16 Check Points

DBIW resized to :
DBIW(1) = 694 DBIW(2) = 97
DBIW(3) = 5094 DBIW(4) = 5831

RMS Error Report on DEM file

GCP No.	Image Pixel	Image Line	Input Elev.	Calc. Elev.	Diff Elev
2	1768	786	185.0	191.0	-6.0
3	2461	545	119.0	121.0	-2.0
4	623	1084	234.0	244.0	-10.0
5	1425	170	175.0	186.0	-11.0
7	2424	917	119.0	131.0	-12.0
9	1194	1772	273.0	275.0	-2.0
10	1302	905	220.0	225.0	-5.0
11	1677	1696	253.0	251.0	2.0

12	842	469	299.0	307.0	-8.0
14	2064	1699	161.0	170.0	-9.0
16	2342	1918	182.0	181.0	1.0
17	2029	1929	101.0	100.0	1.0
19	2065	2300	266.0	274.0	-8.0
20	1926	2440	170.0	167.0	3.0
21	1704	2132	154.0	153.0	1.0
23	1463	2001	256.0	259.0	-3.0
24	2811	2551	213.0	214.0	-1.0
26	881	891	436.0	445.0	-9.0
30	1846	1968	101.0	101.0	0.0
31	1916	1995	101.0	99.0	2.0
32	1823	430	202.0	208.0	-6.0
33	1108	1048	331.0	331.0	0.0
35	991	1969	258.0	260.0	-2.0
39	1107	2165	183.0	187.0	-4.0
40	1784	109	216.0	222.0	-6.0

No. of GCP Points within DBIW window : 25
Root Mean Sq. Error in elevation (m) : ±5.8m

Check Pt.	Image Pixel	Image Line	Input Elev.	Calc. Elev.	Diff Elev
-6	2361	1284	187.5	185.0	2.5
-8	962	1265	177.2	188.0	-10.8
-13	584	473	342.0	362.0	-20.0
-22	1543	2545	112.1	110.0	2.1
-25	2142	161	179.5	182.0	-2.5
-27	1586	1921	243.7	237.0	6.7
-28	1310	1648	117.2	127.0	-9.8
-29	748	2084	177.7	180.0	-2.3
-34	2694	2578	172.6	166.0	6.6
-36	1101	419	207.0	214.0	-7.0
-37	2085	321	156.7	158.0	-1.3
-41	1026	2743	6.0	6.0	0.0
-42	1392	2265	144.1	145.0	-0.9
-43	2221	760	162.3	166.0	-3.7
-44	1251	1425	142.8	144.0	-1.2
-45	2258	265	177.1	175.0	2.1

No. of Check Points within DBIW window : 16
Root Mean Sq. Error in elevation (m) : ± 7.0m

E.3.3 Accuracy Results of Height in DEM at 16 Road Database Ground Control Points

DBIW resized to :
DBIW(1) = 693 DBIW(2) = 97
DBIW(3) = 5091 DBIW(4) = 5831

RMS Error Report on DEM file

GCP No.	Image Pixel	Image Line	Input Elev.	Calc. Elev.	Diff Elev
45	2258	265	177.1	174.0	3.1
44	1251	1425	142.8	147.0	-4.2
43	2221	760	162.3	168.0	-5.7
42	1392	2265	144.1	150.0	-5.9
6	2361	1284	187.5	189.0	-1.5
41	1026	2743	6.0	5.0	1.0

8	962	1265	177.2	187.0	-9.8
25	2142	161	179.5	183.0	-3.5
27	1586	1921	243.7	243.0	0.7
37	2085	321	156.7	159.0	-2.3
13	584	473	342.0	350.0	-8.0
36	1101	419	207.0	211.0	-4.0
22	1543	2545	112.1	118.0	-5.9
34	2694	2578	172.6	172.0	0.6
29	748	2084	177.7	172.0	5.7
28	1310	1648	117.2	127.0	-9.8

No. of GCP Points within DBIW window : 16
Root Mean Sq. Error in elevation (m) : ±5.3m

E.4 Accuracy Test of the Orthoimage Generated by the Level 1A Stereo-pair at the Individual GCPs

No.	x	y	Δ x	Δy (Pixels)
101	2353.938	-3413.812	0.900	0.754
102	1592.625	-3690.625	0.070	0.495
110	1088.125	-2735.375	-0.330	-0.243
111	1574.938	-1719.813	-0.114	-0.436
112	2428.188	-1184.063	1.093	0.218
113	1931.125	-1305.625	0.074	-0.155
114	1252.375	-1998.375	0.949	0.493
125	4022.625	-2545.125	-0.238	-0.430
126	4182.188	-1932.188	0.596	0.094
127	4568.312	-1194.688	-0.334	0.141
128	4637.125	-2063.625	-0.826	-0.648
146	3795.125	-3064.125	0.698	-0.200
148	4597.375	-3290.875	0.198	-0.901
151	2852.375	-4105.875	-0.413	-0.104
152	2422.875	-3913.875	0.751	-0.253
153	3566.875	-4416.375	-0.281	-0.611
154	4467.375	-4580.125	0.650	-0.011
157	4257.875	-4096.375	0.428	-0.019
158	4333.125	-3740.125	-0.232	-0.677
137	771.562	-4251.562	-0.339	-0.068
142	746.625	-4633.125	-0.909	-0.624
141	793.875	-5750.125	2.200	0.656
159	4073.375	-5021.875	0.972	0.164
164	3509.438	-5764.063	0.769	0.279
166	4524.750	-5905.750	-1.174	0.657
167	4542.625	-6564.125	-0.953	0.719
168	3649.938	-1907.813	-0.151	1.237
118	553.250	-3272.250	-4.056	-0.525

RMSE = ± 0.76 in x and ±0.51 in y (pixels)

No	E (m)	N (m)	Δ E (m)	Δ N (m)
101	308544.669	3559870.314	-9.001	-7.537
102	300921.813	3557098.576	-0.696	-4.950
110	295871.199	3566645.391	3.304	2.432
111	300741.906	3576801.496	1.140	4.357
112	309287.944	3582167.164	-10.932	-2.192
113	304306.158	3580947.261	-0.737	1.540
114	297526.394	3574024.390	-9.482	-4.933
125	325223.139	3568548.152	2.374	4.293
126	326827.076	3574684.140	-5.965	-0.947
127	330679.397	3582061.380	3.336	-1.422
128	331363.258	3573362.330	8.254	6.481
146	322957.330	3563359.228	-6.986	2.000
148	330976.637	3561084.712	-1.986	9.015

151	313517.357	3552939.957	4.132	1.044
152	309232.993	3554858.615	-7.513	2.534
153	320665.358	3549829.657	2.805	6.116
154	329681.641	3548198.349	-6.503	0.112
157	327583.703	3553036.651	-4.287	0.196
158	328329.544	3556593.364	2.320	6.770
137	292705.709	3551481.912	3.400	0.686
142	292450.809	3547659.920	9.097	6.243
141	292955.156	3536500.414	-21.995	-6.554
159	325744.302	3543781.439	-9.727	-1.632
164	320102.158	3536358.836	-7.698	-2.784
166	330238.048	3534946.041	11.739	-6.563
167	330419.432	3528361.542	9.529	-7.177
168	321495.980	3574939.058	1.506	-12.377
118	290484.381	3561272.389	40.571	5.249

RMSE = ±7.6 m in Easting and ± 5.0m in Northing